ON THE EVOLUTION OF TYPE II STARS

F. HOYLE* AND M. SCHWARZSCHILD†

Princeton University Observatory

Received February 4, 1955

ABSTRACT

The evolution of the stars in globular clusters has been followed from the main sequence to the top of the red giant branch. In the initial phases the relevant models consist of partially degenerate isothermal helium cores and radiative hydrogen envelopes. These models show the well-known turnoff from the main sequence in the Hertzsprung-Russell diagram of globular clusters. The helium core steadily increases in mass because of the hydrogen-burning. When the core has reached approximately 20 per cent of the total stellar mass, the envelope has reached an appreciable extent, and it is found necessary to take into account explicitly the photospheric boundary condition and the hydrogen convection zone. During the subsequent phases this convection zone steadily deepens while the luminosity increases; the star evolves in the Hertzsprung-Russell diagram along the observed red giant sequence. During these phases the internal temperature steadily rises so that the carbon cycle can keep in balance with the increasing luminosity. At the top of the red giant sequence the temperature in the hydrogen-burning shell at the edge of the core reaches about 40,000,000°, while the helium core reaches approximately 50 per cent of the stellar mass.

The model sequence thus computed appears to be in satisfactory agreement with the observations in globular clusters. In addition, the difference between the red giants of population I and population II can, it seems, be explained by the difference in the metal abundance of the two populations if this abundance difference is taken account of in the photospheric boundary condition; for the relevant evolution phases, a larger metal content produces a larger extent of the envelope and hence later spectral types.

It is estimated that near the top of the red giant sequence the more and more rapid contraction of the core will heat the center until it reaches the temperature necessary to start helium-burning. The onset of this process is believed to terminate the red giant sequence by eliminating the degeneracy in the core. Preliminary computations suggest that this change in the stellar model will rather suddenly lower the luminosity and put the star on the beginning of the horizontal branch in the Hertzsprung-Russell diagram.

I. INTRODUCTION

The aim of the present paper is to consider the evolution of type II stars, with particular reference to the color-magnitude diagrams of the stars of globular clusters. This means that we are concerned with stars of mass a little above that of the sun, say from 1.1 $M_\odot$ to 1.2 $M_\odot$. The time required for the evolution of such stars is of the order of five billion years. Although, as just stated, we are largely concerned with stars of type II, we shall also discuss reasons for the observed differences between the giants of populations I and II.

Perhaps it should be emphasized at the outset that the present work has been undertaken by way of a preliminary reconnaissance of the problem. Our aim has been to discover the physics underlying the color-magnitude diagrams in question rather than to arrive at a finally accepted standard of precision in the mathematical calculations. That is to say, we have not hesitated to make mathematical simplifications where we have had reason to believe that approximation was not likely to affect the final results to a serious extent.

The sketch shown in Figure 1 illustrates the general characteristics of the problem. The stars of the clusters M3 and M92, as observed by Arp, Baum, and Sandage (1953), lie close to the curve of Figure 1. The evolutionary problem will be considered in the following form: to find the track in the color-magnitude diagram along which a star of a definite mass evolves. Such a track presumably starts on the main sequence, leads up-

* Normally at St. John's College, Cambridge.

† This work was supported in part by funds of the Eugene Higgins Trust allocated to Princeton University.

ward and to the right, makes an excursion through the region of the red giants and supergiants, returns to the left, and finally drops into the white dwarf region.

Such an evolutionary track is not identical with the line occupied by the stars of a cluster in the color-magnitude diagram. The latter line is the locus for stars of various masses at one time, while an evolutionary track is the locus for stars of the same mass at various times. This difference, however, is in practice rather small, as can be seen from a preliminary analysis by Sandage (1954). All the stars in globular clusters which are now observed between points M and P of Figure 1 have started their evolution within a short section of the main sequence, have therefore nearly the same masses, and are evolving along a tight family of tracks which closely hug the observed sequence in the color-magnitude diagram. We shall therefore ignore these small differences except in so far as we

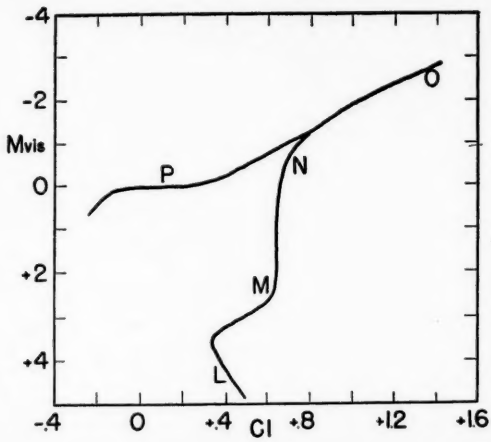

FIG. 1.—Schematic Hertzsprung-Russell diagram for globular clusters

shall use $1.1\odot$ for the masses of stars between points L and M and $1.2\odot$ for stars from M to P.

Reference to Figure 1 enables the whole evolutionary track to be divided into four portions, L–M, M–N, N–O, and O–P. This division brings out the point that in each of these portions appreciably different physical conditions are operative within the stars. More precisely, those physical approximations that can be validly used between L and M cannot all be used between M and N, and so on. We shall discuss the four portions in the sequence in which the stars evolve through them.

In the following it will be found that evolution from L to M differs from that from M to N in the envelope solutions, not in the core solutions, which are common to the whole length of track from L to N. For this reason we shall devote the next section to some general remarks about the core alone.

II. GENERAL REMARKS ABOUT THE DEVELOPMENT OF THE CORE DURING EVOLUTION FROM L TO M

The evolution of the innermost parts of a star depends mainly on two issues: on whether during the early phases of the evolution the main source of opacity within the star is by electron scattering or by free-free transitions, yielding the Kramers opacity formula, and on whether the main process of energy generation is the proton-proton chain or the carbon-nitrogen cycle. The simplest case to treat is the combination of opac-

ity by free-free transitions and energy generation by the carbon-nitrogen cycle. It is known that in this case the star initially has a convective core containing about 14 per cent of the total mass. As the star ages, helium is produced in the core. Recent work by Sweet (1950) and Mestel (1953) on the effects of stellar rotation suggests that mixing outside the convective core is a quite negligible process. Hence the composition of the core is gradually changed from hydrogen to helium, but outside the core the material retains its original composition. Only after all the hydrogen of the core has been used up and the energy generation is then forced to occur outside the core, does the helium gradually become displaced outward in the star.

The question now arises as to what happens to the central regions of a star when the hydrogen there becomes exhausted. Initially, there is a temperature gradient within the core. This temperature gradient cannot persist for more than a short fraction of the time of evolution of the star. Once nuclear-energy generation in the core ceases, gravitation becomes the only source of energy that is available to maintain an appreciable temperature gradient within the core. But it can be shown that, for a star similar in mass to the sun, gravitation cannot supply sufficient energy to maintain an appreciable temperature gradient for more than a small percentage of the time of about five billion years that is required for the early stages of the evolution of the star. In an evolutionary sequence computed by Sandage and Schwarzschild (1952), gravitational contraction of the core seemed to raise the central temperature appreciably. This was caused by two factors: first, in the computed sequence, evolutionary changes occurred at inappropriately great speeds—for reasons we will discuss in Section VI—and, second, electron conduction at incipient degeneracy was ignored. If both factors are corrected, the inference is inescapable for the early evolutionary phases: once the core runs out of hydrogen, an appreciable temperature gradient cannot be maintained within it. The core must become isothermal. This conclusion does not, however, apply to more advanced and much more rapid evolutionary stages, which we shall discuss in a later section.

Models with isothermal, nondegenerate cores were first investigated by Schönberg and Chandrasekhar (1942). Subsequently, Gamov and Keller (1945) pointed out the possible importance of degeneracy in such cores, and models with partially degenerate, isothermal cores have since been computed in detail by Harrison (1946), Hayashi (1949), and Schwarzschild, Rabinowitz, and Härm (1953). We shall essentially follow the procedure of the last-mentioned paper.

After the isothermal core has developed, the star's energy is supplied by a shell surrounding the core. Because of the strong dependence of the energy production on temperature, the effective thickness of the energy-producing shell is only a small fraction of the radius of the core. This being so, it is possible to approximate the integrations by assuming that the energy production occurs in a layer of negligible thickness surrounding the core. So long as the appropriate boundary condition is used in fitting core and envelope together, this approximation can scarcely lead to any appreciable error.

It will be recalled that all this discussion depends on the main energy production being by the carbon-nitrogen cycle. In our problem this is the case by the time that the evolution has carried the star to the neighborhood of the point M of Figure 1 and in the subsequent parts of the evolutionary track. But it is not correct for the early part of the evolution near L. Yet we shall use the structural model just proposed, namely, an isothermal core with the possibility of central degeneracy surrounded by an energy-producing shell of negligible thickness, even in the early part of the evolution. Although this cannot be considered a finally satisfactory approximation, it seems adequate in the present reconnaissance.

III. EQUATIONS FOR THE PORTION L–M OF THE EVOLUTIONARY TRACK

It will be useful to begin with an explicit list of our assumptions.

SIMPLIFYING ASSUMPTIONS

1. Radiation pressure is neglected.
2. Relativistic degeneracy is neglected.
3. No mixing occurs in the envelope, so that the core has a constant composition of essentially pure helium and the envelope a constant composition predominantly of hydrogen. There is an abrupt transition between the material of the core and that of the envelope.
4. The mean molecular weight in the core is taken to be $\frac{4}{3}$, which is correct for helium in the nondegenerate part of the core but which exaggerates the pressure in the degenerate parts, the exaggeration in the case of extreme degeneracy being by a factor of 1.5.
5. The abundance of the heavy elements (i.e., elements other than hydrogen and helium) is assumed to be so low that they do not contribute to the opacity.
6. The envelope is divided into two parts, an outer part, in which the free-free transitions of *H* and *He* determine the opacity, and an inner zone, in which the opacity is taken as arising from free electron scattering. No intermediate zones of mixed opacity have been introduced—the opacity formula is switched abruptly from free-free transitions to electron scattering at an appropriate interface, the opacity being kept continuous. The criterion for the switch is that the two sources of opacity become equal at the interface.
7. Whenever energy production by thermonuclear reactions occurs in a shell, the thickness of the shell is neglected. Hence the energy flux is taken to jump discontinuously at the shell. It will also be assumed that the flux is constant outside the shell.
8. The envelope will be assumed to satisfy the conditions of radiative equilibrium. This assumption applies only to the evolution from *L* to *M* (Fig. 1). This assumption will be dropped when we come to consider the later stages of the evolution.
9. The boundary condition that the temperature and density shall tend to zero at the surface of the star is used.

NOTATION

Subscripts will be used with the following meanings: *i* for quantities in the core, *e* for quantities in the envelope, *c* for central values, 1 for values at the interface between core and envelope, and *s* for values at the interface where the opacity formula switches. All other symbols have their usual meanings.

BASIC EQUATIONS AND DEFINITIONS

Mechanical equilibrium:

$$\frac{dP}{dr} = -\rho \frac{GM_r}{r^2}, \qquad \frac{dM_r}{dr} = 4\pi r^2 \rho . \tag{1}$$

Equation of state:

In degenerate material

$$P = \frac{8\pi}{3h^3} (2mkT)^{3/2} kTF_{3/2}(\psi) , \tag{2}$$

$$\rho = \frac{4\pi}{h^3} (2mkT)^{3/2} \mu_i H F_{1/2}(\psi) , \tag{3}$$

with

$$F_\nu(\psi) = \int_0^\infty \frac{u^\nu}{e^{u-\psi}+1}\, du \tag{4}$$

and

$$\mu_i = 1.333 .$$

In nondegenerate material

$$P = \frac{k}{\mu H} \rho T , \tag{5}$$

with

$$\mu = \mu_i = 1.333 \text{ in the core} \quad \text{and} \quad \mu = \mu_e = 0.533 \text{ in the envelope} . \tag{6}$$

Thermal equilibrium:

Radiative equilibrium in the envelope,

$$\frac{dT}{dr} = -\frac{3}{4ac}\frac{\kappa\rho}{T^3}\frac{L_r}{4\pi r^2}, \tag{7}$$

with

$$\kappa = 3.68 \times 10^{22}(1+X)\frac{\rho}{T^{3.5}} \tag{8}$$

for free-free transitions, and with

$$\kappa = 0.19(1+X) \tag{9}$$

for electron scattering.

In the isothermal core,

$$\frac{dT}{dr} = 0. \tag{10}$$

Nuclear-energy production:

$$L = 4\pi\int_0^R \epsilon\rho r^2 dr, \tag{11}$$

with

$$\epsilon_{pp} = 0.5X^2\rho\left(\frac{T}{15\times 10^6}\right)^4 \tag{12}$$

for the proton-proton chain, and with

$$\epsilon_{CN} = 600X\frac{X_{CN}}{0.01}\rho\left(\frac{T}{20\times 10^6}\right)^{15} \tag{13}$$

for the carbon-nitrogen cycle,

$$\epsilon = \epsilon_{pp} + \epsilon_{CN} . \tag{14}$$

The composition of the stellar material initially is

$$X = 0.9, \qquad \mu = \mu_e = 0.533 . \tag{15}$$

This is the composition in the envelope.

Comments:

The value of X_{CN} will be stated when results are presented. The coefficient in equation (13) requires the slowest reaction in the carbon cycle to be the formation of N^{13} from C^{12}. Our value of the coefficient is close to that adopted by W. A. Fowler (1954). The form we have adopted for equation (13) will enable the energy generation to be calculated in the portion of the evolution from M to O, where temperatures appreciably above 20×10^6° K have to be considered and where the exponent 15 is perhaps more appropriate than the somewhat higher value that would be more appropriate for the range $10\text{–}20 \times 10^6$° K, as considered by Fowler.

Homology invariants:

$$U = \frac{d\log M_r}{d\log r} = \frac{4\pi r^3}{M_r}\rho, \tag{16}$$

$$V = \frac{-d\log P}{d\log r} = \frac{\rho}{P}\frac{GM_r}{r}, \tag{17}$$

$$n+1=\frac{d\log P}{d\log T}=\frac{16\pi a\,cG}{3}\frac{T^4}{\kappa P}\frac{M_r}{L} \qquad \text{in envelope} \tag{18}$$

$$=\infty \quad \text{in isothermal core}. \tag{19}$$

TRANSFORMATION FOR THE ISOTHERMAL CORE

Temperature throughout the core:

$$T_1. \tag{20}$$

Nondimensional independent variable ξ:

$$r=\frac{h^{3/2}}{4\pi\mu_i H}(2mkT_1)^{-1/4}(2mG)^{-1/2}\xi. \tag{21}$$

Expression for M_r, *derived from* (1), (2), *and* (3):

$$M_r=\frac{h^{3/2}}{4\pi\mu_i^2H^2}(2mkT_1)^{3/4}(2mG)^{-3/2}\left(-\xi^2\frac{d\psi}{d\xi}\right). \tag{22}$$

Basic differential equation, derived from (1), (2), *and* (3):

$$\frac{1}{\xi^2}\frac{d}{d\xi}\left(\xi^2\frac{d\psi}{d\xi}\right)=-F_{1/2}(\psi). \tag{23}$$

Conditions at center:

$$\psi=\psi_c, \qquad \frac{d\psi}{d\xi}=0 \text{ at } \xi=0. \tag{24}$$

Homology invariants, from (16), (17), *and* (19):

$$U=\frac{F_{1/2}(\psi)\,\xi^3}{(-\xi^2 d\psi/d\xi)}, \qquad V=\frac{F_{1/2}(\psi)}{F_{3/2}(\psi)}\frac{3}{2\xi}\left(-\xi^2\frac{d\psi}{d\xi}\right), \qquad n+1=\infty. \tag{25}$$

Numerical forms of (2), (3), (21), (22):

$$\begin{aligned} P&=8.96\times10^{17}\left(\frac{T_1}{20\times10^6}\right)^{5/2}F_{3/2}(\psi),\\ \rho&=1086\left(\frac{T_1}{20\times10^6}\right)^{3/2}F_{1/2}(\psi),\\ r&=1.166\times10^{9}\left(\frac{T_1}{20\times10^6}\right)^{-1/4}\xi,\\ M_r&=0.01090M_\odot\left(\frac{T_1}{20\times10^6}\right)^{3/4}\left(-\xi^2\frac{d\psi}{d\xi}\right). \end{aligned} \tag{26}$$

TRANSFORMATION FOR THE RADIATIVE ENVELOPE

Nondimensional variables:

$$P=p\frac{GM^2}{4\pi R^4}, \qquad T=t\frac{\mu_e H}{k}\frac{GM}{R}, \qquad M_r=qM, \qquad r=xR. \tag{27}$$

Basic differential equations, from (1), (5), (7), (8), *and* (9):

$$\frac{dp}{dx}=-\frac{pq}{tx^2}, \qquad \frac{dq}{dx}=\frac{px^2}{t}, \tag{28}$$

$$\frac{dt}{dx} = -C_{Kr}\frac{p^2}{x^2 t^{8.5}} \text{ for free-free transitions, } (x > x_s), \tag{29}$$

$$\frac{dt}{dx} = -C_{El}\frac{p}{x^2 t^4} \text{ for electron scattering, } (x < x_s), \tag{30}$$

with

$$C_{Kr} = \frac{3}{4ac}\frac{3.68\times 10^{20}(1+X)}{(4\pi)^3}\left(\frac{k}{\mu_e HG}\right)^{7.5}\frac{LR^{0.5}}{M^{5.5}} = 10^{-5.8146}\frac{L}{L_\odot}\left(\frac{R}{R_\odot}\right)^{0.5}\left(\frac{M_\odot}{M}\right)^{5.5}, \tag{31}$$

and with

$$C_{El} = \frac{3}{4ac}\frac{0.19(1+X)}{(4\pi)^2}\left(\frac{k}{\mu_e HG}\right)^4\frac{L}{M^3} = 10^{-3.9741}\frac{L}{L_\odot}\left(\frac{M_\odot}{M}\right)^3. \tag{32}$$

Continuity of opacity at x_s, from (29) and (30):

$$C_{El} = C_{Kr}\frac{p_s}{t_s^{4.5}}. \tag{33}$$

Condition at surface:

$$q = 1, \quad t = 0, \quad p = 0 \quad \text{at} \quad x = 1. \tag{34}$$

Homology invariants:

$$U = \frac{px^3}{qt}, \quad V = \frac{q}{xt}, \tag{35}$$

$$n+1 = \frac{q}{C_{Kr}}\frac{t^{8.5}}{p^2} \quad \text{for} \quad x > x_s, \tag{36}$$

$$n+1 = \frac{q}{C_{El}}\frac{t^4}{p} \quad \text{for} \quad x < x_s. \tag{37}$$

FITTING CONDITIONS

Fitting of homology invariants at x_1, from (16), (17), (18):

$$\frac{U_{1i}}{U_{1e}} = \frac{\mu_{1i}}{\mu_{1e}} = 2.5, \quad \frac{V_{1i}}{V_{1e}} = \frac{\mu_{1i}}{\mu_{1e}} = 2.5 \tag{38}$$

$$(n+1)_{1e} \text{ must be finite.} \tag{39}$$

Fitting of M_r at x_1, from (22) and third equation of (27):

$$M_{r1i} = q_{1e}M. \tag{40}$$

Fitting of r at x_1, from (21) and fourth equation of (27):

$$r_{1i} = x_{1e}R. \tag{41}$$

Fitting of opacity at x_s:

L as computed from equation (31) $= L$ as computed from equation (32). (42)

Energy production in thin shell at x_1, from (11), (12), (13), and (14):

For thin shell, from equations (17) and (18),

$$P \approx P_1 \left(\frac{r}{r_1}\right)^{-V_{1e}}, \qquad T \approx T_1 \left(\frac{r}{r_1}\right)^{-V_{1e}/(n+1)_{1e}}.$$

Hence, for the proton-proton chain,

$$L_{pp} \approx 0.5 X^2 \rho_{1e}^2 \left(\frac{T_1}{15 \times 10^6}\right)^4 \frac{4\pi r_1^3}{V_{1e}[2+2/(n+1)_{1e}]-3}, \tag{43}$$

and, for carbon cycle,

$$L_{CN} \approx 600 X \frac{X_{CN}}{0.01} \rho_{1e}^2 \left(\frac{T_1}{20 \times 10^6}\right)^{15} \frac{4\pi r_1^3}{V_{1e}[2+13/(n+1)_{1e}]-3}. \tag{44}$$

Total luminosity:

$$L = L_{pp} + L_{CN}. \tag{45}$$

Equations (1)–(45) already contain the mathematics of the problem, but it may be useful to add a few qualitative remarks about the equations. Specification of ψ_c and T_1 determines the interior solution completely, as regards both the homology variables and the physical variables. Specification of the luminosity and radius of the star, L and R—the mass M being considered as given—together with the surface boundary condition, determines the envelope solution in both the homology variables and the physical variables for $x \geq x_s$: this follows because equation (31) determines C_{Kr}, and equations (27)–(30) then determine all the variables, as functions of x in the case of the homology variables and as functions of r in the case of the physical variables. A knowledge of the physical variables then determines x_s, the point at which we switch the opacity from the Kramers form to the electron-scattering form. Hence the whole envelope is determined. To the four quantities so introduced, namely, ψ_c, T_1, L, and R, we must now add two more, x_1 and ξ_1, which determine the points in both the core and the envelope integrations at which fitting is to take place. This makes a total of six quantities, one more than the number of fitting conditions (38), (40), (41), and (45). The problem is therefore indeterminate unless one of the six quantities is given *ab initio*. The physical meaning of this indeterminacy is that a unique solution cannot be obtained unless the fraction q_1 of the total mass contained in the core is given. If q_1 is specified, the problem becomes determinate, since a knowledge of q_1 enables x_1 to be read off from the envelope solution. The six quantities ψ_c, T_1, L, R, x_1, and ξ_1 are therefore immediately reduced to five unknowns, which can be determined from the five fitting conditions.

IV. RESULTS FOR THE EVOLUTION FROM L TO M

In practice it is desirable to proceed by a different method, but one equivalent to that just explained. We start by specifying q_1 and by making guesses for T_1 and x_s. A single-parameter family of envelope solutions can then be obtained with C_{Kr} as the free parameter, the value of x_1 being known for each member of the family (since q_1 is specified). The core solutions are likewise represented by a single-parameter family, a family in which ψ_c represents the free parameter. A knowledge of q_1, together with the guessed value of T_1, determines ξ_1 for each member of the family of core solutions, in accordance with condition (40). Two unknowns still remain: C_{Kr} for the envelope solution and ψ_c for the core solution. These are determined by the two fitting conditions contained in (38). Then equation (41) fixes R, and equation (31) thereupon gives L.

This procedure leaves two conditions that, in general, remain unsatisfied, equations (42) and (45). It is only to be expected that two such conditions will remain, since x_s and T_1 are determinate quantities that do not have to be guessed at the outset. This problem may be met in the following way. We start by guessing x_s and T_1 as shrewdly as we can.

A trial solution is then made in accordance with the method of the previous paragraph. Then equations (42) and (45) are used to obtain better values of x_s and T_1, and the process is then repeated. This iterative method has the double merit of converging quickly and of allowing one to work entirely in terms of one-parameter families of solutions—a one-parameter family for the core and a one-parameter family for the envelope. Although the iterative determination of x_s and T_1 greatly eases the computational work,

TABLE 1

MODELS WITH PARTIALLY DEGENERATE EXHAUSTED CORES (c TO 1) AND RADIATIVE ENVELOPES (1 TO SURFACE)
($M = 1.1\ M_\odot$)

	$[-\xi^2(d\psi/d\xi)]_1$						
	12.5	15.0	17.5	20.0	22.5	25.0	27.5
$T_c \times 10^{-6}$	16.2	17.0	17.8	18.6	19.5	20.0	20.0
ψ_c	+ 1.28	+ 3.55	+ 5.54	+ 7.86	+10.3	+11.4	+12.6
log C	− 5.58	− 5.32	− 5.05	− 4.75	− 4.44	− 4.05	− 3.58
U_{1s}	0.50	0.32	0.19	0.12	0.08	0.06	0.04
V_{1s}	1.14	1.50	1.97	2.52	3.01	3.43	3.73
$(n+1)_{1s}$	2.21	2.86	3.23	3.71	4.10	3.95	3.39
log x_1	− 1.21	− 1.36	− 1.57	− 1.84	− 2.22	− 2.85	− 4.10
log q_1	− 0.98	− 0.88	− 0.80	− 0.72	− 0.66	− 0.60	− 0.57
log t_1	+ 0.17	+ 0.30	+ 0.48	+ 0.75	+ 1.10	+ 1.72	+ 2.96
log p_1	+ 2.55	+ 3.00	+ 3.70	+ 4.73	+ 6.05	+ 8.45	+13.35
log x_s	− 0.64	− 0.81	− 1.00	− 1.23	− 1.46	− 1.77	− 2.04
log p_s	+ 1.58	+ 2.05	+ 2.58	+ 3.20	+ 3.91	+ 5.00	+ 6.45
log t_s	− 0.18	− 0.03	+ 0.14	+ 0.33	+ 0.54	+ 0.83	+ 1.21
$q_1 = M_{r1}/M$	+ 0.11	+ 0.13	+ 0.16	+ 0.19	+ 0.22	+ 0.25	+ 0.27
log $R/R_\odot$	+ 0.07	+ 0.17	+ 0.33	+ 0.59	+ 0.91	+ 1.52	+ 2.76
log $L/L_\odot$	+ 0.45	+ 0.66	+ 0.85	+ 1.02	+ 1.17	+ 1.25	+ 1.10
log ρ_c	+ 3.17	+ 3.66	+ 3.94	+ 4.18	+ 4.37	+ 4.45	+ 4.51
log ρ_{1s}	+ 1.89	+ 1.91	+ 1.95	+ 1.92	+ 1.93	+ 1.88	+ 1.82
log T_{eff}	+ 3.84	+ 3.84	+ 3.80	+ 3.72	+ 3.60	+ 3.31	+ 2.66
Bol. cor.	+ 0.05	+ 0.05	+ 0.06	+ 0.10	+ 1.04	.....	.....
M_{vis}	+ 3.55	+ 3.03	+ 2.56	+ 2.18	+ 2.74	.....	.....
CI	+ 0.26	+ 0.26	+ 0.36	+ 0.65	+ 1.36	.....	.....

this is still very far from being easy, as can be realized from the circumstance that each change of x_s changes the envelope family.

The physical reason why an iterative method works well in the present case is that the stellar model is rather insensitive to the initial values assigned to x_s and T_1.

First and second approximations have been calculated by the iterative method. We have not proceeded to a third approximation for the reason that when really high accuracy is demanded, some of our physical approximations would first have to be improved.

Consequently, the results shown in Table 1 represent only a second approximation. The values there given probably exhibit the correct general trend, however; but too much reliance on exact values would be unwise. Before considering the comparison of our results with observation, it is worth noting that the run of the values of T_1 in the various models corresponds to the energy-generation process changing from being almost wholly due to the proton-proton chain in the first model to being almost wholly due to the car-

bon cycle in the other models. A value $X_{CN} = 0.0005$ was used for the concentration of carbon and nitrogen. This is about the amount that seems appropriate for a type II star. The accuracy of the switch from Kramers opacity to free-electron opacity is as good as our neglect of a combined opacity warrants.

The results are plotted in a color-magnitude diagram in Figure 2. The numbers attached to the calculated points give the fraction of the total mass present in the exhausted core. The shaded area in Figure 2 is that occupied by the stars of the globular clusters M3 (Sandage 1953) and M92 (Arp, Baum, and Sandage 1953). Color indices have been derived on the system used by Sandage (1953). This was done by a rather complex procedure. The calculated effective temperatures of our models were first used to estimate

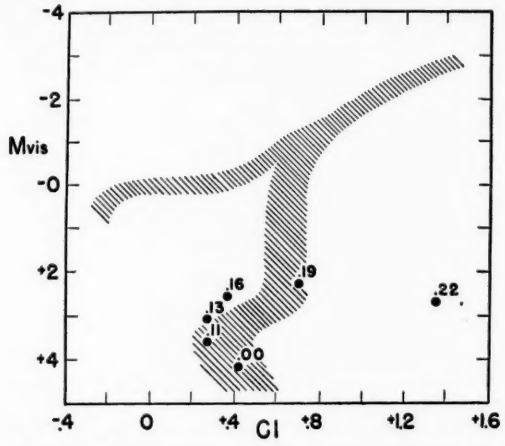

FIG. 2.—Hertzsprung-Russell diagram for models with isothermal cores and radiative envelopes. The numbers give the fraction of the mass in the core. The shaded area indicates the observed sequences in globular clusters.

spectral class in accordance with the work of Keenan and Morgan (1951). Then the color index used by Johnson and Morgan, denoted by $B - V$, was read off from the tables of Johnson and Morgan (1953). These values of $B - V$ were next used to calculate an international color index $P - V$ by means of the equation

$$P - V = -0.176 + 1.090\,(B - V)\,. \tag{46}$$

Finally, the color index, CI, used by Sandage was obtained from $P - V$, using the relation

$$P - V = 0.92CI + 0.05\,. \tag{47}$$

Although the stage of the argument where spectral classes are read off against effective temperatures really refers to main-sequence stars only, the final result of effective temperatures against color index should be the same for all stars, whether of the main sequence or not.

One of the points in Figure 2, the point 0.000, does not represent a calculated model from Table 1. This point is the estimated starting point of the evolutionary sequence, its position being fixed at a magnitude of +4.1 on the main sequence. The magnitude of +4.1 was arrived at by the argument that we are now concerned with stars of mass 1.1$\odot$, and from the mass-luminosity formula (as applied to main-sequence stars). We

should expect that such stars would initially have a luminosity exceeding the present luminosity of the sun by about the factor of $(1.1)^{5.5}$.

The results are satisfactory, in that they show the turn of the evolutionary sequence as it comes off the main sequence. There is, however, a marked tendency of our calculated points to lie to the left and above the mean of the distribution of the stars of the globular clusters (leaving aside a consideration of the $q_1 = 0.22$ point for the moment). This is presumably a reflection of the approximations made in the foregoing discussion. Perhaps the most important of these was our assumption concerning the evolution of the core. We have supposed, even in the early phases of evolution when energy generation is largely by the proton-proton chain, that the material of the star is sharply divided in composition at the core boundary. This does not become well satisfied until energy generation by the carbon cycle becomes dominant. Consequently, the model we have used is an idealization. Since, moreover, it is very likely the nature of the model that produces the initial movement to the left in the color-magnitude diagram, it is clear that our idealization of the problem may very well have exaggerated this movement. Other factors that may also contribute to the excess bulge to the left in our calculated sequence are: (i) The neglect of the combined contributions of free-free transitions and of electron scattering to the opacity probably causes luminosities to be somewhat exaggerated. A reduction of luminosities would produce a lesser bulge to the left. (ii) Our calculations are made for $\mu_e = 0.533$, corresponding to about 90 per cent hydrogen and 10 per cent helium (heavier elements being present in small traces), this being regarded as the initial composition of the material of the star. If μ_e were effectively equal to 0.5, corresponding to very little initial helium, the luminosities would be reduced, and the bulge to the left would again be reduced.

It may also be noted that the observed stars in globular clusters are not all stars of the same mass, especially in the region of the turnoff from the main sequence. The turnoff for smaller masses than that used here, $1.1\odot$, would lie to the right and below the points of Figure 2. It would be possible to argue that stars near the 0.19 point of Figure 2 are of mass $1.1\odot$ but that stars at the turnoff are of lower mass and hence appear more to the right in the diagram.

It is considered that a combination of some, or of all, of these factors could readily explain the difference between our calculated values and the mean of the observed distributions of stars.

V. THE AGES OF THE GLOBULAR CLUSTERS

Before we go on to discuss the much more serious discrepancy shown by the $q_1 = 0.22$ point, it is of interest to estimate the time required for the evolution from the initial point of the sequence to the $q_1 = 0.19$ point. Since the conversion of 1 gm of hydrogen into helium yields about 6.2×10^{18} ergs, it follows that the time required to burn dm grams of stellar material is $6.2 \times 10^{18}\, X dm/L$. Hence the time required for evolution along our sequence up to the $q_1 = 0.19$ point is

$$6.2 \times 10^{18} X \int_0^{0.19M} \frac{dm}{L} = 6.2 \times 10^{18} XM \int_0^{0.19} \frac{dq_1}{L}. \tag{48}$$

The actual evaluation of this integral is done very simply by plotting $1/L$ as a function of q_1 in accordance with the results shown in Table 1. The integral is then just the area under the portion of the curve from $q_1 = 0$ to $q_1 = 0.19$. Putting $X = 0.9$, $M = 1.1\odot$, this gives a time of 6.2×10^9 years. This value is in satisfactory agreement with a recent estimate by Sandage (1953). An earlier value by Sandage and Schwarzschild (1952) turns out to be an underestimate, caused by the neglect of the lower luminosities at the earliest evolution phases.

Caution must be exercised in interpreting this result, since error in the calculation of L for the early part of the sequence must affect the result to an important degree. Never-

theless, we can say that the ages of the globular clusters must be of this general order of magnitude. The justification for taking the age as being equal to the time of evolution to the $q_1 = 0.19$ point is twofold. One is that the time required for the remainder of the evolution beyond this point is short compared to 6.2×10^9 years. Second, the stars now near the $q_1 = 0.19$ point presumably followed an evolutionary track that bulged to the left of the stars that are now turning off the main sequence—and this is just what our calculated points do. Under these circumstances it therefore seems more appropriate to calculate the time of evolution to the 0.19 point rather than to the 0.13 point, for instance.

VI. THE REASON WHY THE LATER MODELS OF TABLE 1 FAIL

We now come to the critical problem of the failure of our calculated point $q_1 = 0.22$ to follow the observed distribution of the stars of the globular clusters. The calculated evolutionary track, after leaving the 0.19 point, moves rapidly to the right without appreciable increase in luminosity (the apparent decrease in magnitude for the 0.22 point in Fig. 2 is due to a bolometric correction). This tendency is so marked that the next model in the sequence, that for $q_1 = 0.25$ in Table 1, lies so far to the right that it cannot be marked at all within the usual range of color index. This rapid swing to the right agrees with the results obtained by other authors using different interior models (Hoyle and Lyttleton 1949; Sandage and Schwarzschild 1952). It arises from one of the simplifications introduced earlier, which ceases to be a valid approximation. The simplification is that given as assumption No. 9 in our list. Radiative-envelope solutions integrated to the mathematical boundary condition of zero pressure and temperature at the surface of the star cease to give a satisfactory expression of the actual physical boundary condition. The invalidity of the usual simple surface condition was already suspected by Gardiner (1951) for red giants. The importance of using the accurate surface conditions was recently shown in detail by Osterbrock (1953) for red dwarfs.

The actual physical surface condition may be put into the following form:

$$T \to T_{\text{eff}}, \qquad \rho \to \frac{\mu HGM}{kT\kappa R^2} \qquad \text{as} \qquad r \to R. \tag{49}$$

The quantity $R^2kT/\mu HGM$ appearing in (49) may be interpreted as the scale height at the surface. The significance of (49), so far as T is concerned, is clear. The condition on ρ expresses the requirement that radiation must be able to escape from the star at $r = R$; the photosphere of the star is reached (it is also an implicit requirement that ρ shall exceed $\mu GHM/kT\kappa r^2$ for $r < R$, although, so far as we are aware, this is a condition that is invariably satisfied if [49] is satisfied). Reference to the dimensionless variables q, t, and p shows that the boundary conditions should, strictly speaking, not be

$$t = 0, \qquad p = 0 \qquad \text{at} \qquad x = 1,$$

but

$$t = t_p, \qquad p = p_p \qquad \text{at} \qquad x = 1,$$

where t_p and p_p are to be such that (49) is satisfied. It has usually been argued, however, that the values of t_p and p_p required to satisfy (49) are so little different from zero that $t = 0$, $p = 0$, at $x = 1$, can be used as a mathematical idealization. That is to say, it is argued that the envelope solutions corresponding to the idealized mathematical conditions differ negligibly in the interior of the star from the solutions that satisfy (49). This assumption is valid if T and ρ rise to the values required by (49) for x only slightly less than unity. It is not sufficient that t and p should rise above t_p and p_p for x only slightly less than unity, since p may rise to p_p, not through ρ rising to the value required by (49) but through t becoming much larger than t_p. In all cases of which we are aware this requirement is satisfied for T, that is, T always rises in the mathematically idealized solu-

tion to T_{eff} for values of x only very slightly less than 1. The situation is different for ρ, as we shall now see.

For x close to 1 the mathematical idealized solutions give

$$\log \rho = -2.8641 + 3.25 \log\left(\frac{1}{x} - 1\right) - 0.5 \log C_{Kr} + \log \frac{M}{M_\odot} - 3 \log \frac{R}{R_\odot}. \quad (50)$$

This equation follows by putting $\rho \propto T^{3.25}$ and $M_r = M$ in the physical equations (1) and (7), with κ given by equation (8). The value of C_{Kr} determines the constant of proportionality in $\rho \propto T^{3.25}$. Since we shall consider the behavior of ρ at the surface in detail in a later section, it is sufficient here to quote a result—that, in order to satisfy (49), $\log \rho$ must not be much different from -7.5, ρ being in grams per cubic centimeter. Putting $M = 1.1\odot$, $\log \rho = -7.5$ in equation (50), we can work a value of x for each of the models given in Table 1. This table is revealing in showing that the mathematical idealization is a good approximation for the first few models but is thoroughly bad for the last two models and may even be inadequate for $q_1 = 0.22$ and $q_1 = 0.19$.

TABLE 2

DISTANCE AT WHICH PHOTOSPHERIC DENSITY IS REACHED IN MODELS OF TABLE 1

q_1.....	0.11	0.13	0.16	0.19	0.22	0.25	0.27
x.....	0.995	0.993	0.989	0.980	0.956	0.839	0.240

Stated in more physical terms, our present result means that, for the late models of Table 1, the density falls too soon as the surface is approached, too soon in the sense that the density falls to the photospheric value before T has fallen to T_{eff}—radiation escapes before the temperature has fallen to its surface value.

The situation can be restated in terms of the value possessed by the density at the place where T has fallen to T_{eff}. This can be calculated in the following way. Near the surface the temperature is given by

$$\log T = \log\left(\frac{1}{x} - 1\right) + 6.4624 + \log \frac{M}{M_\odot} - \log \frac{R}{R_\odot}. \quad (51)$$

This equation is obtained by putting $\rho \propto T^{3.25}$ and $M_r = M$ in equation (1). We now put $T = T_{\text{eff}}$ in equation (51) and proceed to eliminate x between equations (50) and (51). The resulting equation with $M = 1.1\odot$ gives ρ (all this refers to the idealized mathematical case, of course). In this way the values given in Table 3 were worked out. These values are all too low, since, as stated earlier, the physical boundary condition (49) turns out (in a later section) to require $\log \rho$ to be near -7.5 at the surface.

TABLE 3

DENSITY AT POINT WHERE $T = T_{\text{eff}}$ IN MODELS OF TABLE 1

q_1.....	0.11	0.13	0.16	0.19	0.22	0.25
$\log \rho$....	−8.64	−8.75	−8.90	−9.32	−9.78	−10.73

A further circumstance makes the discrepancy still worse. It is well known that, for stars of the range of effective temperatures under consideration, there must be a convection zone immediately below the photosphere. In this convection zone, hydrogen is in a critical stage of ionization. Now ρ declines with T in this hydrogen convection zone at a

rate that is considerably faster than $T^{3.25}$. This means that when the necessary allowance is made for the unstable hydrogen zone, the values of log ρ come out even smaller than the results given in Table 3. It may be added that the hydrogen convection zone is such a thin surface shell that it has been customary until recently to omit consideration of it from investigation on stellar interiors. But we now see how this zone can become important, not through its size, but through its effect on the photospheric value of ρ.

These considerations raise the very serious question as to how the stars adjust their photospheric densities so that the surface boundary condition (49) is satisfied. The solution to the problem appears to be obtained by an extension of convection from the shallow surface zone considered in the previous paragraph down to great depths below the photosphere. Thus, below the ionization zone, convection requires $\rho \propto T^{3/2}$, giving a much slower decline of ρ with T than the $\rho \propto T^{3.25}$ relation that arises in the case of radiative equilibrium. We think that a star can adjust its photospheric density to the required value by adopting a structure with a sizable outer convection zone, the parameter of adjustment being the depth of this convection zone. As an extreme, we may note that if the convection zone were to extend right through to the core, the surface density would be of the order of

$$\rho_1 \left(\frac{T_{\text{eff}}}{T_1}\right)^{3/2},$$

which, for log $\rho_1 \approx 2$, log $T_1 \approx 7.30$, and log $T_{\text{eff}} \approx 3.75$ (as representative values), gives a surface value of log ρ of -3.3. Even allowing for the possible effect of the unstable hydrogen zone, this is much too high a photospheric density. It follows, therefore, that the star can indeed find a solution to its problem; if there is no extended ionization zone, the photospheric density comes out too low; if the convection zone goes right through to the core, the photospheric density comes out too high, so some intermediate case may be expected to give the correct value.

The important question now to be considered is what effect such an extended convection zone has on the structure of the star. The results arrived at show that the effect is small for models up to $q_1 = 0.19$ in Table 1 but that thereafter the effect is so large that the models calculated for q_1 greater than 0.19 must be abandoned.

VII. EQUATIONS FOR THE PORTION M–N OF THE EVOLUTIONARY TRACK

We have to alter our former equations in such a way as to include an outer convection zone, in which

$$P = KT^{2.5}, \tag{52}$$

where the value of K is determined so as to satisfy the surface condition (49). The details of how this was done will emerge at a later stage. Equation (52) takes the place of the radiative equation (7). With the same definitions (27) of the nondimensional variables, the equations for the convection zone can be transformed to

$$\frac{dp}{dx} = -\frac{pq}{tx^2}, \qquad \frac{dq}{dx} = \frac{px^2}{t}, \qquad p = Et^{2.5}, \tag{53}$$

where

$$E = 4\pi KG^{1.5}\left(\frac{\mu H}{k}\right)^{2.5} M^{0.5}R^{1.5}. \tag{54}$$

The quantity E can be used as the convection parameter, equally as well as K. This we shall often do in the following work.

Surface boundary condition:

$$q = 1, \qquad p = 0 \qquad \text{at} \qquad x = 1. \tag{55}$$

Radiative zone:
Equations as before.

Fitting between convective and radiative zones:
p, x, q, t, and dt/dx to be continuous. Use subscript 2 to denote quantities at this interface.

Fitting between radiative zone and exhausted core:
As before.

Exhausted core:
Equations as before.

The logic of determining a solution of the equations for a specified q_1 is essentially the same as before. We are regarding E (or K) as being determined by the surface condition (49). The envelope solution is then determinate if L and R are given—the mass again being taken as fixed. In particular, the value of x, namely, x_2, at which the convection zone ends and the radiative zone begins, is determined by the last of the fitting conditions at x_2, and x_s is determined by condition (42) as before. The radiative solution is accordingly determinate if L and R are specified. We therefore have four parameters: L and R determining the envelope solution and ψ_c and T_1 determining the core solution. The given value of q_1 determines x_1, while ξ_1 has again to be introduced as an additional parameter, yielding a total of five parameters to be determined by the same five remaining fitting conditions as before.

For practical reasons it turns out to be advantageous to depart from this simple logical method of determining stellar models, however. Instead of using the surface condition to introduce E at the outset (which is difficult to do because R and T_{eff} are not known until the end of the determination of a model), we preferred to regard the interior solutions as functions of two variables q_1 and E. That is to say, when all fitting conditions are taken care of, we still have two degrees of freedom in the interior solutions. One of the degrees of freedom, q_1, refers to the stage of evolution that the star has reached, while the other freedom, E, is then available to satisfy the surface condition (49). This procedure was first applied by Osterbrock (1953).

Even so, the arithmetical work was found to be so heavy that it seemed desirable, always remembering that the present investigation is only a preliminary reconnaissance, to introduce an approximation into the calculations. To understand the nature of this approximation, it will be necessary once more to transform the equations for the radiative zone. The reader who is not particularly interested in the computational details may wish to skip the consideration of this transformation and instead to proceed directly to the results contained in Table 4.

A COMPUTATIONAL APPROXIMATION

A transformation of the equations of the radiative zone is obtained by introducing the quantities q_0 and x_0 and by defining starred variables in accordance with

$$p = p^* \frac{q_0^2}{x_0^4}, \qquad t = t^* \frac{q_0}{x_0}, \qquad q = q^* q_0, \qquad x = x^* x_0. \tag{56}$$

Equations (28), (29), and (30), when written in terms of starred variables, take the form

$$\frac{dp^*}{dx^*} = \frac{-p^* q^*}{t^* x^{*2}}, \qquad \frac{dq^*}{dx^*} = \frac{p^* x^{*2}}{t^*}, \tag{57}$$

$$\frac{dt^*}{dx^*} = -C^*_{Kr} \frac{p^{*2}}{x^{*2} t^{*8.5}} \qquad \text{for} \quad x^* > x^*_s, \tag{58}$$

$$\frac{dt^*}{dx^*} = -C^*_{El}\frac{p^*}{x^{*2}p^{*4}} \qquad \text{for} \qquad x^* < x^*_s, \tag{59}$$

with

$$C^*_{Kr} = C_{Kr}\frac{x_0^{0.5}}{q_0^{5.5}}, \qquad C^*_{El} = C_{El}q_0^{-3}. \tag{60}$$

The fitting conditions at the interface between the convective zone and the radiative zone can be expressed in terms of starred variables:

$$U^*_2 = \frac{p^*_2 x^{*3}_2}{t^*_2 q^*_2} = \frac{p_2 x_2^3}{t_2 q_2} = U_2, \tag{61}$$

$$V^*_2 = \frac{q^*_2}{t^*_2 x^*_2} = \frac{q_2}{t_2 x_2} = V_2, \tag{62}$$

$$\begin{aligned}(n+1)^*_2 &= C^*_{Kr}\frac{p^{*2}_2}{x^*_2 t^{*9.5}_2} = (n+1)_2 = 2.5 \qquad \text{if} \qquad x^*_2 > x^*_s \\ &= C^*_{El}\frac{p^*_2}{x^*_2 t^{*5}_2} = (n+1)_2 = 2.5 \qquad \text{if} \qquad x^*_2 < x^*_s .\end{aligned} \tag{63}$$

Now the starred solution is not determinate when x_2 and E are specified, as was the unstarred solution. Indeed, two further conditions have to be imposed to make the starred solution determinate: this simply reflects the arbitrariness of x_0 and q_0. We now impose the additional conditions on the starred solution,

$$q^* = 1, \qquad p^* = 0, \qquad t^* = 0 \qquad \text{at} \qquad x^* = 1. \tag{64}$$

This has the enormous computational advantage of allowing the same family of solutions to be used for the starred variables as was formerly used in obtaining the models of Table 1. But one crucial point remains: the starred solution is now overconstrained. Instead of introducing two conditions, (64) has introduced three conditions. With all the conditions (64), there is, in general, no starred solution at all. Striking out one of the conditions in (64) would lose the whole point of the present procedure, which is to use the same family of radiative solutions as were formerly employed, while striking out one of the conditions (61), (62), or (63) would introduce a measure of physical inaccuracy. Experience in other problems has shown, however, that failure to satisfy (63) does not introduce important errors, and this is the simplification that we have resorted to.

Even with this simplification, the fitting problem is still awkward: it must be remembered that three adjustments have now to be made, the switch between convective and radiative zones, the opacity switch, and the fit to the exhausted core. It was found best to work from a starred solution as a starting point, working both inward and outward from such a solution, the fitting at the core proceeding in essentially the same fashion as in the case of the models of Table 1, while the fitting to the convective zone determined x_2 and related C^*_{Kr} to E. The quantities T_1 and x_s were again determined by a method of successive approximations. It was found sufficiently accurate, energy generation being now by the carbon cycle, to use $T_1 = 20 \times 10^6$° K throughout the evolution from M to N (see Fig. 1). When later we come to consider evolution from N to O it will be found that $T_1 = 20 \times 10^6$° K is no longer a good approximation. Care was taken that x_s was adjusted with reasonable accuracy.

The procedure just outlined has two degrees of freedom, q_1 and a second parameter which may conveniently be taken as C^*_{Kr} in the actual computations. Since, however, E is determined when q_1 and C^*_{Kr} are specified, we can equally well regard q_1 and E as the two degrees of freedom, and this is more convenient for the purposes of discussion.

VIII. INTERIOR RESULTS FOR THE PORTION M–N OF THE EVOLUTIONARY TRACK

A set of actual solutions is given in Table 4. The variables used in preparing this table are the original unstarred variables defined in equation (27). The approximation just

TABLE 4

MODELS WITH PARTIALLY DEGENERATE EXHAUSTED CORES (c TO 1), RADIATIVE INTERMEDIATE ZONES (1 TO 2), AND CONVECTIVE ENVELOPES (2 TO SURFACE) ($M = 1.2\ M_\odot$, $T_1 = 20 \times 10^6$° K)

	$[-\xi^2(d\psi/d\xi)]_1$						
	25.0	25.0	25.0	27.5	27.5	27.5	30.0
E	25.3	20.0	17.0	23.9	20.0	18.9	23.1
$\log C_{Kr}$	− 5.00	− 4.60	− 4.50	− 5.00	− 4.75	− 4.50	− 5.25
ψ_c	+11.6	+11.4	+11.3	+12.7	+12.6	+12.5	+14.8
U_{1e}	0.031	0.045	0.049	0.022	0.027	0.033	0.010
V_{1e}	3.06	3.26	3.31	3.38	3.50	3.61	3.70
$(n+1)_{1e}$	3.93	3.93	3.93	3.96	3.96	3.96	3.99
$\log x_1$	− 1.75	− 1.93	− 2.01	− 2.02	− 2.34	− 2.45	− 2.41
$\log q_1$	− 0.64	− 0.64	− 0.64	− 0.60	− 0.60	− 0.60	− 0.56
$\log l_1$	+ 0.61	+ 0.75	+ 0.80	+ 0.84	+ 1.11	+ 1.28	+ 1.29
$\log p_1$	+ 3.72	+ 4.64	+ 4.94	+ 4.49	+ 5.90	+ 6.55	+ 5.95
U_2	0.53	0.70	0.59	0.34	0.58	0.60	0.076
V_2	1.91	3.19	3.68	1.90	2.28	2.88	2.00
$(n+1)_2$	3.18	3.87	3.96	3.24	3.74	3.86	3.59
$\log x_2$	− 0.68	− 0.40	− 0.28	− 0.79	− 0.58	− 0.46	− 1.17
$\log q_2$	− 0.48	− 0.20	− 0.14	− 0.49	− 0.35	− 0.23	− 0.54
$\log l_2$	− 0.08	− 0.31	− 0.48	+ 0.02	− 0.13	− 0.23	+ 0.33
$\log p_2$	+ 1.21	+ 0.53	+ 0.04	+ 1.43	+ 1.02	+ 0.70	+ 2.20
$\log x_s$	(− 0.47)	− 0.75	− 0.87	(− 0.43)	− 0.72	− 0.82	(− 0.27)
$\log l_s$	(− 0.22)	− 0.08	− 0.04	(− 0.19)	− 0.007	+ 0.01	(− 0.18)
$\log p_s$	(+ 0.78)	+ 1.38	+ 1.73	(+ 0.72)	+ 1.50	+ 1.64	(+ 0.62)
$q_1 = M_{r1}/M$	0.23	0.23	0.23	0.25	0.25	0.25	0.28
$x_2 = r_2/R$	0.21	0.40	0.52	0.16	0.26	0.35	0.068
$\log R/R_\odot$	+ 0.48	+ 0.62	+ 0.67	+ 0.71	+ 0.98	+ 1.15	+ 1.16
$\log L/L_\odot$	+ 1.68	+ 1.44	+ 1.01	+ 1.98	+ 1.67	+ 1.47	+ 2.25
$\log \rho_c$	+ 4.46	+ 4.46	+ 4.44	+ 4.52	+ 4.51	+ 4.51	+ 4.62
$\log \rho_1$	+ 1.42	+ 1.78	+ 1.88	+ 1.27	+ 1.60	+ 1.57	+ 0.93
$\log T_{eff}$	+ 3.94	+ 3.81	+ 3.68	+ 3.90	+ 3.69	+ 3.55	+ 3.74
Bol. cor.	+ 0.35	+ 0.05	+ 0.13	+ 0.20	+ 0.12	+ 1.53	+ 0.08
M_{vis}	+ 0.78	+ 1.13	+ 2.24	− 0.12	+ 0.58	+ 2.48	− 0.92
CI	− 0.01	+ 0.34	+ 0.85	+ 0.09	+ 0.79	+ 1.47	+ 0.56

discussed shows itself in the entries in Table 4 for $(n + 1)_2$. These are calculated on the radiative side of the interface at x_2. The correct value should be 2.5, as set out in equation (63).

These interior solutions have been plotted in Figure 3, using the same color indices as before. It is to be emphasized that these solutions do not yet represent stellar models. Before we obtain a stellar model, the surface condition (49) must be satisfied. The points of Figure 3 show where a star would lie if the surface condition were satisfied. So far, our interior solutions have two degrees of freedom, E and q_1. This is why the points in Figure 3 scatter over the diagram instead of being confined to a sequence.

Suppose, then, that we take a section of the color-magnitude diagram corresponding to a given magnitude. Then a whole set of interior solutions can be obtained, yielding this magnitude but corresponding to different T_{eff}. This fixing of the magnitude may be thought of as fixing one of the two degrees of freedom, leaving one degree of freedom that

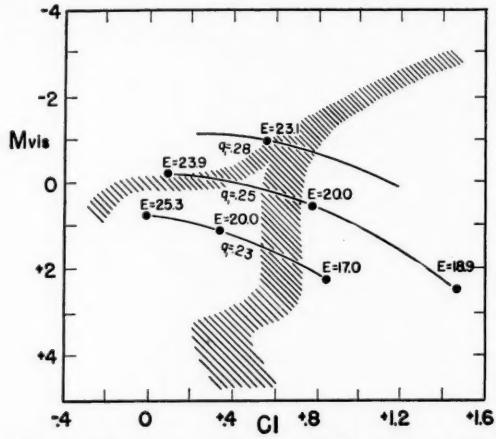

FIG. 3.—Hertzsprung-Russell diagram for mathematical models with convective envelopes and arbitrary E values.

allows T_{eff} to be varied. Now, as T_{eff} varies in such a case, E also varies. But it turns out that E varies only very slowly. This slow variation of E with T_{eff} is very different from the variation of E with T_{eff} (at a fixed magnitude) as given by the surface condition. In Section X we shall find that the surface condition gives a very steep variation of E with T_{eff} (at a fixed magnitude). We could therefore imagine plotting two curves at a fixed magnitude of E with T_{eff}, one curve from the interior solution and one from the surface condition. Because E varies slowly along one curve and steeply along the other, the two curves intersect at a well-determined value of T_{eff}. This is the value of T_{eff} for the stellar model. Since this procedure can be carried out for all magnitudes from M to N (Fig. 1), an evolutionary sequence is thereby obtained, so that the stars follow a definite sequence corresponding to the one remaining degree of freedom, which is conveniently represented by the parameter q_1. The actual determination of the evolutionary sequence must await the detailed consideration of the surface condition given in Section X.

IX. THE INTERIOR CONDITIONS FOR THE PORTION N–O OF THE EVOLUTIONARY TRACK

Before dealing with the surface condition, it is convenient, however, to give some consideration to the interior solutions for the portion N–O (Fig. 1) of the evolutionary

track. Then when we come to the details of the surface condition, it will be found possible to determine stellar models for the portion M–N of the evolutionary track and for the portion N–O, both from the same analysis.

An attempt to prolong the interior solutions beyond the point N of the evolutionary track soon shows that the approximation $T_1 = 20 \times 10^6\,^\circ$ K can no longer be used. As q_1 rises above 0.3, the density of material in the energy-producing shell falls extremely low *if the approximation* $T_1 = 20 \times 10^6\,^\circ$ *K continues to be used*, as is shown by the values in Table 5, which were obtained by using this approximation. Such a decrease in the

TABLE 5

DENSITIES IN ENERGY-PRODUCING SHELL

q_1	0.3010	0.3020	0.3021
ρ_{1e}	2.934	0.1460	0.0537

density of the burning shell must, of course, be compensated for by an increase in temperature, so that the carbon cycle can keep up with the necessary rate of energy production. Before as much as 30 per cent of the star becomes converted to helium, the temperature in both the core and the energy-producing shell must rise above $20 \times 10^6\,^\circ$ K. Stellar models for the portion N–O of the evolutionary track may be defined as the portion of the evolution where the core begins to warm up. Along the portion L–M there was some degree of heating of the core, from about $13 \times 10^6\,^\circ$ K to about $20 \times 10^6\,^\circ$ K. This rise was occasioned mainly by the proton-proton chain's being the main source of energy production for stellar models near L. Once the carbon cycle becomes the main source of energy production, as it is near M, the value of T_1 stays nearly constant at $20 \times 10^6\,^\circ$ K until the neighborhood at N is reached. Then a further stage of heating sets in.

Again, for the purpose of a preliminary reconnaissance, we shall make certain approximations, but whereas our approximations previously required T_1 to be constant (from M to N, that is), in the present case we shall treat the variation of T_1 carefully. Our present approximations will concern certain structural characteristics of the stellar models. These are to put both $(n+1)_{1e}$ and V_{1e} equal to 4. These approximations are based partly on the experience with the values found for $(n+1)_{1e}$ and V_{1e} in the earlier models of the evolutionary sequence (cf. Table 4) and partly on the fact that $n+1$ and V approach 4 when the center is approached in any centrally condensed solution in radiative equilibrium with electron-scattering opacity. That, in fact, at N the radiative zone approaches the center closely is shown by the small value of x_1 for the last model in Table 4.

The formal statement of our analysis goes as follows:

Approximation:

$$V_{1c} \approx 4\,, \qquad (n+1)_{1c} \approx 4 \tag{65}$$

$$V_{1i} \approx 10 \text{ from } (38)\,. \tag{66}$$

Relation for L from (18), using (65):

$$L = \frac{a\,c}{3}\,\frac{4\pi G}{0.19\,(1+X)}\,\frac{T_1^4}{P_1}\,M_{r_1}\,. \tag{67}$$

Energy generation from (44), with $X_{CN} = 0.005$, $X = 0.9$:

$$L = 60\pi\,\rho_{1e}^2\left(\frac{T_1}{20\times 10^6}\right)^{15} r_1^3\,. \tag{68}$$

Solution for T_1 from (67) and (68), using P_1, ρ_1, and r_1 from (26):

$$\left(\frac{T_1}{20\times 10^6}\right)^{15} = 0.0064\,\frac{(-\xi^2 d\psi/d\xi)_1}{\xi_1^3 F_{1/2}^3(\psi_1)}. \tag{69}$$

Procedure for computation:

Determine nondimensional quantities by interpolation in the core solutions at the point where $V_i = 10$. This gives ξ_1 and ψ_1. Then T_1 is given by equation (69), and P_1, ρ_{1i}, r_1, and M_{r_1} follow from equation (26). L is given by substituting these quantities in equation (67). The use of different core solutions gives different q_1's. This is the free parameter. Results are given in Table 6. They show a strong increase in core temperature, T_1, with core mass, q_1.

TABLE 6

MODELS FOR PARTIALLY DEGENERATE EXHAUSTED CORES AND HYDROGEN-BURNING SHELLS
(Temperature and Luminosity as Functions of Core Mass; $M = 1.2M_\odot$)

	$[-\xi^2(d\psi/d\xi)]_1$							
	27.0	28.0	29.0	30.0	31.0	32.0	33.0	34.0
ψ_c	+14.8	+15.7	+16.5	+17.4	+18.2	+19.0	+19.8	+20.6
$\log F_{1/2}(\psi_c)$	+ 1.58	+ 1.62	+ 1.65	+ 1.68	+ 1.72	+ 1.74	+ 1.77	+ 1.79
$\log \xi_1$	+ 0.44	+ 0.45	+ 0.46	+ 0.48	+ 0.49	+ 0.50	+ 0.52	+ 0.53
$\log F_{1/2}(\psi_1)$	− 0.98	− 1.21	− 1.49	− 1.75	− 2.01	− 2.25	− 2.51	− 2.75
$T_1\times 10^{-6}$	22.7	25.1	28.4	32.0	35.9	40.0	44.9	50.0
$q_1 = M_{r1}/M$	0.27	0.30	0.34	0.39	0.44	0.49	0.55	0.61
$\log L/L_\odot$	+ 1.56	+ 1.91	+ 2.32	+ 2.72	+ 3.10	+ 3.47	+ 3.85	+ 4.20
$\log r_1$	+ 9.50	+ 9.50	+ 9.51	+ 9.50	+ 9.50	+ 9.49	+ 9.50	+ 9.50
$\log \rho_c$	+ 4.70	+ 4.80	+ 4.92	+ 5.03	+ 5.14	+ 5.23	+ 5.34	+ 5.43
$\log \rho_{1e}$	+ 2.14	+ 1.97	+ 1.78	+ 1.59	+ 1.41	+ 1.24	+ 1.05	+ 0.88

The dependence of $L/L_\odot$ on q_1, as given by Table 6, is important in relation to our later discussion of the physical boundary conditions at the surface of the star. It will be noticed that the present analysis does not give $R/R_\odot$. We have seen that, until the surface condition is applied, the interior solutions have two degrees of freedom. One parameter is q_1. The second parameter may be taken as E, or, if it is more convenient, as $R/R_\odot$. What is implied by the present results is that $L/L_\odot$ is determined by q_1 almost independently of the second parameter. We shall see that, in contrast with this situation, the surface condition relates $L/L_\odot$ to $R/R_\odot$ almost independently of q_1. The situation may be expressed as follows:

Interior of the star:

$L/L_\odot$ determined by q_1, almost independently of $R/R_\odot$.

Surface condition:

$R/R_\odot$ determined by $L/L_\odot$, almost independently of q_1 .

The importance of these considerations is that they emphasize the advantage of dividing the problem into two parts, an interior investigation of the sort already given and an investigation of the surface condition now to be given.

X. A DISCUSSION OF THE SURFACE CONDITION

INFORMATION FROM THE INTERIOR

Although formally the interior solutions have two degrees of freedom, which we now take to be E and q_1, the value of E is closely determined when q_1 is specified, provided that we introduce the condition that R shall be within reasonable limits. Obviously absurd values of R are obtained if E is varied (for given q_1) outside a rather narrow range. The points marked in Figure 3 refer to nearly the same values of q_1. These points demonstrate how small changes in E produce very large variations in R.

It will be convenient in relation to later work to consider how E varies with q_1, imposing the condition that E must always be chosen so as to give a reasonable value for R. This can be done by running convective-envelope solutions for various values of E right in to $x = 0$. The value taken by q when $x = 0$ will not be zero in such a case but represents an approximation for q_1. This procedure depends on two points: (i) q changes little between $x = x_1$ and $x = 0$ when a convective solution is thus run to the center of the star, provided that R takes a reasonable value; (ii) the value of q at $x = x_1$ is much the same whether an entirely convective envelope or an envelope with separate convective and radiative zones is used. Point ii explains why an entirely convective envelope may be used to relate E and q_1, while i dispenses with the necessity of determining x_1 by allowing q_1 to be estimated from the connective value of q at $x = 0$. For any reasonable R this procedure gives an association between E and q_1, that is probably correct to within 10 per cent.

Some results are given in Table 7, these results being subject to the condition that

TABLE 7

FRACTION OF MASS IN CORE AS FUNCTION OF E

E	8	16	22	24
q_1	0.67	0.443	0.306	0.270

R takes reasonable values (i.e., such values as lead to values of T_{eff} between 2000° and 10,000° K). This approximate relationship of E to q_1, obtained simply from requiring R to lie within reasonable limits, greatly assists the application of the surface condition.

GENERAL STRUCTURE OF ATMOSPHERE

We divide the atmosphere into three regions: (1) an upper photospheric region with isothermal equilibrium; (2) a lower photospheric region in which energy flow is predominantly by radiation (convection may occur in this region but is unable to convey the whole energy flux); and (3) a convection zone in which the energy flow is predominantly by convection. The convection is divided into two parts, a thin outer shell in which the ionization of hydrogen is incomplete and the deeper zone that runs into the interior solution.

The interface between the first two regions is the photosphere, defined by an optical depth of $\frac{2}{3}$. At the photosphere $T_p = T_{\text{eff}}$ and $r_p = R$.

The interface between the lower photospheric region and the convection zone is defined as the depth at which convection can first manage to convey the whole energy flux.

Notation:

Subscript p for photospheric values.

Subscript a for values at the interface between the lower photospheric region and the convection zone.

Subscript b for values at a depth such that the ionization of hydrogen is effectively complete, which can be regarded as the start of the interior solution.

GENERAL EQUATIONS IN ATMOSPHERE

Definitions:

$\theta = 5040/T$; y = fraction of hydrogen that is ionized; g = acceleration due to gravity; P_e = electron pressure; and I = ionization potential of hydrogen.

Opacity by H^-:

$$\log \kappa = \log P_e - 2.800 + 1.55\theta \,. \tag{70}$$

Hydrogen ionization:

$$\log \frac{y}{1-y} = -13.53\,\theta + \tfrac{5}{2}\log T - 0.48 - \log P_e \,. \tag{71}$$

Electron pressure:

$$P_e = y\,\frac{k}{H}\,\rho T \,. \tag{72}$$

From (70), (71), and (72), when y is small:

$$\log \kappa = \tfrac{1}{2}\log \rho - 5.215\,\theta + \tfrac{7}{4}\log T + 0.918 \,. \tag{73}$$

These analytical formulae represent κ to within 5 per cent accuracy for the range of ρ and T that is important in the present analysis (Chandrasekhar and Münch 1946).

UPPER PHOTOSPHERIC REGION

Optical depth:

$$\int_{r_p}^{\infty} \kappa \rho\, dr = \tfrac{2}{3} \,. \tag{74}$$

From isothermal equilibrium with $\mu = 1$:

$$\rho = \rho_p \exp\Big[-\frac{gH}{kT_{\text{eff}}} (r - r_p) \Big] \,, \tag{75}$$

applicable for points near photosphere.

From (74) and (75), and for $\kappa \propto \rho^{1/2}$ as given by (73):

$$\kappa_p \rho_p \frac{kT_{\text{eff}}}{gH} = 1 \,, \tag{76}$$

or, using (73) at the photosphere for κ_p and after some reduction,

$$\rho_p^{3/2} = 10^{-4.396}\,\frac{g}{g_\odot}\,T_{\text{eff}}^{-11/4}\,10^{5.215\theta_p} \,. \tag{77}$$

LOWER PHOTOSPHERIC REGION

Equilibrium equations:

$$\frac{d}{dr}(\rho T) = -\frac{gH}{k}\,\rho \,, \tag{78}$$

$$\frac{dT}{dr} = -\frac{3}{16}\,\frac{\kappa \rho}{T^3}\,T_{\text{eff}}^4 \,. \tag{79}$$

ρT relation, given by dividing (78) by (79) and using (73) for κ:

$$(\rho T)^{3/2} - (\rho_p T_{\text{eff}})^{3/2} = 10^{-3.493}\,\frac{g}{g_\odot}\,T_{\text{eff}}^{-4} \int_{T_{\text{eff}}}^{T} T^{7/4}\,10^{5.215\theta}\,dT \,, \tag{80}$$

or with

$$10^{5.215\theta} \approx 10^{5.215\theta_p}\left(\frac{T}{T_{\rm eff}}\right)^{-a}, \qquad a = \frac{5.215\,\theta_p}{\log e} = 12.02\,\theta_p,$$

$$(\rho T)^{3/2} = (\rho_p T_{\rm eff})^{3/2} + 10^{-3.493}\,\frac{g}{g_\odot}\,\frac{10^{5.215\theta_p}}{12.02\,\theta_p - 2.75}\,T_{\rm eff}^{-5/4}\left[1-\left(\frac{T_{\rm eff}}{T}\right)^{12.02\theta_p-2.75}\right]. \tag{81}$$

Value of ρT at interface with region of effective convection, from (81) and (77):

$$(\rho_a T_a)^{3/2} = \frac{g}{g_\odot}\,T_{\rm eff}^{-5/4}\cdot 10^{5.215\theta_p}\left(10^{-4.396} + \frac{10^{-3.493}}{12.02\,\theta_p - 2.75}\right). \tag{82}$$

The physical basis of the present results is readily intelligible. Immediately below the photosphere the term in $(T_{\rm eff}/T)^{12.02\theta_p-2.75}$ in equation (81) can be neglected. This arises from the behavior of κ, which increases very rapidly with T because of the increasing ionization of hydrogen. This causes the value of dT/dr required to transport the flux in accordance with equation (79) to increase sharply, so sharply that equation (78) requires $d\rho/dr$ to become negative. Indeed, the large value of dT/dr requires T to increase so steeply that ρT remains nearly constant, as is implied by equation (81). Evidently, then, result (81) depends on the large increase of κ with increasing T. This means that (81) remains valid even if other sources of opacity other than H^- become important as T rises. Result (81) would hold a fortiori in such a case. This is the reason why our use of the opacity formula (73) at depths below the photosphere cannot lead to appreciable error.

THE ONSET OF EFFECTIVE CONVECTION

The condition for convective stability,

$$\frac{d\log\rho}{d\log T} > \frac{1}{\gamma - 1}, \tag{83}$$

is flagrantly violated when equation (81) is satisfied. Hence it is clear that much of the region that we have called "the lower photosphere" must be convectively unstable. It might therefore seem questionable whether the equation of radiative transfer (79) should be used in this region. Our procedure is correct, however, so long as even the most violent convective motions remain inadequate to transport the energy flux. The most rapid convective velocity may be taken equal to the velocity of sound, which for largely un-ionized hydrogen may be taken as $(5kT/3H)^{1/2}$. Under conditions of violent convective instability, such as must occur when equation (81) is satisfied, velocities of the order of the velocity of sound may well be attained. The average convective flux of energy may then be written as

$$\beta\rho\left[Iy + \frac{5}{2}\,\frac{kT}{H}\,(1+y)\right]\left(\frac{5kT}{3H}\right)^{1/2}, \tag{84}$$

where β is an efficiency factor less than 1. If $\beta = 1$, then (84) gives the maximum rate of transport of energy in upward-moving columns of material. In taking an average flux, account has, however, to be taken of the fact that upward-moving material does not cover the whole surface of the star. There must be columns of downward-moving material, and these must not only occupy probably about 50 per cent of the surface area of the star but also carry energy downward. The downward currents therefore demand a value of β appreciably less than 1. Convective theory at the present time is not sufficiently well developed for any certain value of β to be specified under the extreme superadiabatic conditions implied by (81). In the following work we shall use a value $\beta = 0.3$ corresponding to a 30 per cent convective efficiency. This conjecture seems adequate for

our purpose, since the results obtained are not particularly sensitive to the value adopted for β—the general features of our results would remain for other values of β. The only important point is that having once decided on a value of β for a particular model of the evolutionary sequence, we should stick to it throughout.

The formal conditions that determine the onset of convection are the following:

Convective velocity:

$$\left(\frac{5}{3}\frac{kT_a}{H}\right)^{1/2}.$$

Convective flux equal to total flux:

$$\beta\rho_a\left[Iy_a+\frac{5}{2}\frac{kT_a}{H}(1+y_a)\right]\left(\frac{5}{3}\frac{kT_a}{H}\right)^{1/2}=\frac{ac}{4}T_{\text{eff}}^4. \tag{85}$$

Efficiency coefficient:

$$\beta\approx 0.3\,. \tag{86}$$

Solving for T_a in terms of T_{eff} from equation (71), after eliminating P_e by equation (72), ρ_a by equation (82), and y_a by equation (85), we have

$$T_a\approx 10{,}000^\circ\text{K}, \tag{87}$$

with an error of less than 5 per cent for the range of T_{eff} of interest.

Solving for ρ_a from equation (82) with $T_a = 10{,}000^\circ$ K and $12.02\theta_p - 2.75 \approx 8$, gives us

$$\rho_a^{3/2}=\frac{g}{g_\odot}T_{\text{eff}}^{-5/4}10^{-10.10+5.215\theta_p}. \tag{88}$$

Eliminating ρ_a from equation (85) by means of equation (82) gives

$$12.94y_a+2.06\,(1+y_a)\;=10^{-15.0607}\left(\frac{g}{g_\odot}\right)^{-2/3}T_{\text{eff}}^{29/6}10^{-3.48\theta_p}. \tag{89}$$

Equation (89) determines y_a in terms of T_{eff} and R (R and M determine g). It turns out that, in the cases of interest, y_a is appreciably less than unity. Hence there must follow a convective region in which y_a rises to values close to 1. This region is not included in the interior solution. So, before we can join the present investigation to that of the interior, we must give some consideration to this hydrogen convection zone.

An important point may, however, be mentioned at this stage. Although conditions near the photosphere and in the hydrogen ionization zone have an important bearing on the structure of the star, their depth is very small compared with R. Consequently, in discussing these outermost regions, we can use T as variable instead of r. This is just what was done when equation (78) was divided by equation (79). It is only the variation of ρ and y with T that is important in these outermost regions. A discussion of the dependence on r would only yield the additional information that their depth was very small compared to R.

THE HYDROGEN IONIZATION ZONE

The entropy per unit mass is constant throughout the hydrogen ionization zone. This condition applied at the top (a) of the zone and at the bottom (b) gives

$$13.53\,[\theta_a(1+y_a)-\theta_b(1+y_b)]+\tfrac{5}{2}(y_a-y_b)\log e+2\log\frac{y_a(1-y_b)}{y_b(1-y_a)}=0. \tag{90}$$

Approximations:

y_a sufficiently small for $\log(1-y_a)\approx -y_a\log e$.

Zone sufficiently deep for $y_b\approx 1$.

$\rho - T$ relation from equations (71), (72), and (90):

$$\frac{\rho_b}{T_b^{3/2}} = \left(\frac{\rho_a}{T_a^{3/2}}\right)^{1/2} 10^{-3.66-y_a(6.765\theta_a+1.75\log e)}. \tag{91}$$

THE FITTING OF THE ATMOSPHERE TO THE INTERIOR

From equation (52), applied at bottom (b) of the hydrogen ionization zone, one obtains:

$$K = \frac{k}{\mu_e H}\frac{\rho_b}{T_b^{3/2}}. \tag{92}$$

Finally, the parameter E is obtained from equation (54); eliminating $\rho_b/T_b^{1.5}$ by equation (91), with T_a given by equation (87), ρ_a by equation (88), and y_a by equation (89), and g by GM/R^2, gives

$$\log E = 1.56 - \tfrac{5}{12}\log\frac{M}{M_\odot} + \tfrac{5}{6}\log\frac{R}{R_\odot} - \tfrac{5}{12}\log T_{\text{eff}} + 1.74\,\theta_p \\ - 10^{-15.62}\left(\frac{M}{M_\odot}\right)^{-2/3}\left(\frac{R}{R_\odot}\right)^{4/3} T_{\text{eff}}^{29/6}\, 10^{-3.48\theta_p}. \tag{93}$$

With a very slight approximation the main result of this section can now be derived.

At the beginning of the present section it was seen that, for reasonable R, the interior solution determines E to within a close margin when q_1 is specified. Not only this, but E as given by the interior considerations varies by only a moderate factor (about 3) over a considerable range of q_1. This suggests that we adopt some typical value for E, say,

$$E \approx 15 \text{ for all } q_1. \tag{94}$$

The error in E is then always less than a factor of 2. The corresponding error in equation (93) is very small, since only $\log E$ appears in this equation. From equations (93) and (94) we obtain

$$0.38 - \tfrac{5}{12}\log\frac{M}{M_\odot} + \tfrac{5}{6}\log\frac{R}{R_\odot} - \tfrac{5}{12}\log T_{\text{eff}} + 1.74\,\theta_p \\ = 10^{-15.62}\left(\frac{M}{M_\odot}\right)^{-2/3}\left(\frac{R}{R_\odot}\right)^{4/3} T_{\text{eff}}^{29/6}\, 10^{-3.48\theta_p}. \tag{95}$$

With M specified as $1.2\odot$ in the present investigation, equation (95) can now be solved for $R/R_\odot$ when T_{eff} is specified. Since

$$L = \pi a\, cR^2 T_{\text{eff}}^4, \tag{96}$$

this means that L is also given when T_{eff} is specified. Hence we obtain a relation between L and T_{eff}, thereby determining a unique track for our stellar models in the color-magnitude diagram.

At first sight it might seem that the evolutionary track from M to O (Fig. 1) is entirely a product of the surface condition. This is not correct, however, since our realization that the approximation $E \approx 15$ could be used for all q_1 depended on the interior investigation. But, granted this, it can then be said that the form of the evolutionary track is determined by the surface condition.

One proviso must be mentioned concerning equation (95). Solutions of this equation can evidently be accepted only if y_a, according to equation (89), is >0. This restriction is not trivial, as will be seen below.

XI. RESULTS FOR THE PORTION M–O OF THE EVOLUTIONARY TRACK

Equation (95) yields the results given in Table 8. Values of L are calculated from equation (96), values of y_a from equation (89). Equations (71) and (72) give T_a; equation (82) gives ρ_a; and equation (77) gives ρ_p. Finally, y_p is obtained from equations (71) and (72).

The approximation $T_a \approx 10{,}000°$ K is seen to be a good one: it will be recalled that T_a enters (85) and (91) only in a rather insensitive way. The values of the color index were obtained by the method already described, using equations (46) and (47), except that some slight smoothing was used to remove irregularities in the plot of color index against T_{eff}. The values of q_1 were obtained from the interior results, which, as we have seen, give

TABLE 8

MODELS FOR RED GIANTS OF POPULATION II

($M = 1.2M_\odot$)

	log T_{eff}							
	+3.738	+3.724	+3.710	+3.688	+3.670	+3.660	+3.645	+3.612
$R/R_\odot$	3.58	5.83	9.14	17.7	30.2	39.9	61.8	163.
log $L/L_\odot$	+ 1.028	+ 1.394	+ 1.728	+ 2.215	+ 2.606	+ 2.810	+ 3.130	+ 3.840
Bol. cor.	+ 0.08	+ 0.09	+ 0.10	+ 0.12	+ 0.15	+ 0.23	+ 0.50	+ 1.0
M_{pv}	+ 2.2	+ 1.3	+ 0.5	− 0.7	− 1.7	− 2.1	− 2.6	− 3.9
CI	+ 0.57	+ 0.62	+ 0.69	+ 0.81	+ 0.93	+ 1.00	+ 1.11	+ 1.30
q_1	0.22	0.25	0.29	0.33	0.37	0.40	0.44	0.55
y_a	0.068	0.124	0.178	0.259	0.326	0.362	0.417	0.541
T_a(° K)	9,480	9,960	10,200	10,500	10,600	10,700	10,800	10,850
log ρ_a	− 7.33	− 7.50	− 7.63	− 7.83	− 7.96	− 8.03	− 8.14	− 8.36
log ρ_p	− 7.26	− 7.42	− 7.54	− 7.72	− 7.83	− 7.89	− 7.98	− 8.19
log y_p	− 3.99	− 4.14	− 4.30	− 4.58	− 4.83	− 4.97	− 5.20	− 5.74

a close relation between $L/L_\odot$ and q_1; so that, with $L/L_\odot$ obtained from equation (96), corresponding values of q_1 could be obtained from a plot of $L/L_\odot$ against q_1 (as given by Table 6). The circles in Figure 4 represent our results in the color-magnitude diagram, the numbers attached to the points representing the corresponding values of q_1.

The agreement between our results and the observed giant branches of the globular clusters is thought to be satisfactory, with the exception of the topmost point, $q_1 = 0.55$. This stellar model will be discussed in the following section, with special reference to the cause of this discrepancy.

A second approximation could now be calculated, with the results in Table 8 being used to give better values of T_a and E. Thus with q_1 and R given by Table 8, values of E could be obtained from the interior solutions. Then, with T_a as given in Table 8, a second approximation could be calculated in the same way. This has not been done, since it is known that a second approximation would give results that were only very slightly different from those in Table 8. Such a degree of refinement as would be implied by a second approximation would indeed be illusory on account of other sources of uncertainty—the behavior of the efficiency factor in equation (85), for instance, which may change somewhat with T_{eff}.

A critical point must now be mentioned. When in the foregoing work we wrote $T_p = T_{\text{eff}}$ and $\theta_p = 5040/T_p$, we were assuming that the ionization temperature of the photosphere is equal to T_{eff}. This is almost certainly not strictly correct: the ionization

temperature may be expected to be somewhat different from and probably lower than T_{eff}. This may well account for our calculated sequence lying at the right-hand border of the observed sequences of the globular-cluster stars, for if ionization temperatures are lower than effective temperatures, our procedure would lead to color indices that were too large. This point will be raised again in Section XIII.

It remains in this section to discuss an incomplete feature of the present calculations. It might seem that if the sequence of models were prolonged at low luminosities to smaller q_1 (higher T_{eff}), the sequence would continue at color indices in the range +0.5 to +0.6 down to the main sequence, in distinction to the observed sequence which branches sharply left at about the $q_1 = 0.22$ model. This would mean that our present models would differ from those that were calculated earlier in the paper for the portion L–M of

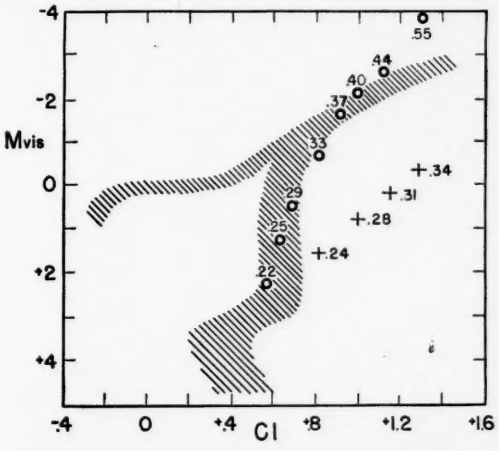

FIG. 4.—Hertzsprung-Russell diagram for models with convective envelopes. The circles refer to type II giants (negligible metal content) and the crosses to type I giants (solar metal content).

the evolutionary track. The question would then arise as to which method of calculation was the correct one.

Actually, this dilemma does not occur because equation (85) with $\beta \approx 0.3$—on which equation (95) is based—breaks down for models earlier than about $q_1 = 0.20$. Equation (85) with (86) represents essentially an extreme value for the convective flux which should be a good approximation in the later models, with their low photospheric densities and temperatures. At the higher densities and temperatures shown by Table 8 for $q_1 \approx 0.2$, however, the convection currents will be able to carry the necessary flux without reaching velocities equal to that of sound. The extreme equation (85) should then be replaced by the usual equations for the convective velocities and the resulting flux (Biermann 1948), which could be formally represented by a reduced β in equation (85). That, in fact, equation (85) breaks down just about at $q_1 = 0.20$ is shown by the values of y_a, which become negative for $q_1 < 0.2$—a physical impossibility caused by substituting a false decrease in y_a for the neglected decrease in β.

It is therefore clear that the model sequence given in Table 8 must be terminated at about $q_1 = 0.20$. For earlier models ($q_1 < 0.2$) it seems highly likely that convection in the envelope plays only a minor role, so that there the models of Table 1 may be trusted. We may then interpret the turn in the observed sequence at M (Fig. 1) as caused by convection in the envelope becoming a determining factor for the radius of the star.

XII. THE METAL CONTENT OF TYPE II STARS

The highest of the points marked in Figure 4 has moved distinctly away from the observed sequence of stars. Calculations for still larger color indices show an even greater divergence from the observed sequence. An explanation for this discrepancy between calculation and observation is therefore required. Although some measure of uncertainty is attached to the bolometric correction, it seems unlikely that an explanation of the discrepancy can be sought in these terms. Indeed, the bolometric correction of 1 mag. adopted for the last model in Table 8 would already seem to be an exaggeration—a correction of perhaps 0.6 mag. would be more appropriate, and this would increase the discrepancy even more.

The present suggestion is that the assumption made throughout the previous two sections—that the supply of free electrons at the photosphere comes essentially from the ionization of hydrogen—ceases to be valid at the top of the evolutionary track. Sooner or later, with decreasing T_{eff}, the supply of free electrons from metal atoms must come to exceed the supply from hydrogen. When this happens, the form of the evolutionary track is considerably altered, as we shall see. The value of T_{eff} at which the contribution of the metals becomes important evidently depends on the concentration of metal atoms in the material of the star. That a small metal abundance suffices to affect the last model of Table 8 is indicated by the very low ionization of hydrogen, y_p, in the photosphere of that model.

In the present section we shall invert the argument of the previous paragraph. We shall assume the correctness of this explanation of the discrepancy between the last model of Table 8 and the observed sequences, and we shall calculate the concentration of metals that is required to overcome the discrepancy. Having regard to the probable exaggeration of the bolometric correction in Table 8 (for the last model), we shall carry through the calculation on the supposition that the effect of metals is to reduce the luminosity of the last model by 1 mag.

In computing the changes produced in the last model by the change in luminosity ($\Delta \log L = -0.4$), we shall work from the bottom of the atmosphere upward and take care to use only those equations from the previous sections which are basic to the lower regions, i.e., in which no use has yet been made of any equations for the photosphere which here have to be changed because of the metal content. From equation (96) we obtain $\Delta \log R = -0.2$; from equation (54), with $E \approx 15$, we get $\Delta \log K = +0.3$; and from equation (92), therefore, $\Delta \log (\rho_b / T_b^{3/2}) = +0.3$. By solving equation (91), equation (85) with (86), and equation (71) with (72) simultaneously for y_a, ρ_a, and θ_a, we have $\Delta y_a = -0.09$, $\log \rho_a = +0.10$, and $\Delta\theta_a = +0.01$. Finally, with $\Delta \log g = +0.4$, equation (81) gives $\Delta \log \rho_p = -0.12$. The application of the last equation might here seem unjustified, since it is based on an opacity coefficient for which the free electrons were taken to come purely from hydrogen, not the metals. This is, on the present supposition, wrong at p (the photosphere); but it is correct—with a large margin—at a, as is shown by the high value of y_a in the last column of Table 8. To assume it correct for the entire region from a to p does seem, therefore, a reasonable approximation.

We now come to the photosphere. Here equations (70) and (71), of course, hold as before; but equation (72) must be replaced by

$$P_e = (A^{-1} + y) \frac{k}{H} \rho T , \tag{97}$$

where A, as usual, is the ratio of hydrogen atoms to metal atoms. Equation (76) is little affected by this change (at most by a factor of 1.33) and may therefore be used as it stands. We may now complete our computation of A as follows. Equation (76) gives $\Delta \log \kappa_p = +0.52$; equation (70) gives $\Delta \log P_{e_p} = +0.52$; equation (71) yields $\Delta \log y_p = -0.52$; and equation (97) gives $\Delta \log (A^{-1} + y_p) = +0.64$. The last two values—in comparison with $\log y_p = -5.74$ and $A^{-1} = 0$ for the last model of Table 8—

result in $\log y_p = -6.26$ and $\log (A^{-1} + y_p) = -5.10$ or

$$A = 135{,}000 . \tag{98}$$

This result may be compared with the A value of population I, which is usually given as 8000. Our value is seventeen times larger. That the A value of population II is, in fact, larger (less metals) than that of population I had already been found from spectrographic data (Schwarzschild, Spitzer, and Wildt 1951). For the extreme population II to which the globular clusters belong, a factor of about 17 is, by order of magnitude, in agreement with the spectrographic data of Chamberlain and Aller (1951) on subdwarfs. This encouraging agreement should, however, not be taken as too weighty, since our computations are, by their very character, still very inaccurate.

Two additional points may be noted. First, a metal abundance as given by equation (98) will noticeably change the last model of Table 8, as we have seen, but will hardly affect even the next to the last model, as can be seen from the steep rise of the photospheric hydrogen ionization, y_p, between these two models. Second, the modification of the last model by the metals lowers the luminosity and therefore, according to Table 6, lowers the mass in the core to $q_1 = 0.49$.

XIII. THE GIANT SEQUENCE OF POPULATION I

The red giants of population I differ from those in globular clusters by being generally 2 or even 3 mag. fainter than the latter. It is tempting to assume that this difference arises from the difference between the populations in metal content. To investigate this possibility we shall here interrupt the main topic of this paper—the evolution of stars in globular cluster—and repeat the calculations of Section XI with a metal content appropriate for population I.

Those equations of Section X which express basic physical relations hold as before, except that equation (72) has to be replaced by equation (97). In applying equation (97) to the photosphere and using $A = 10^4$, y can be ignored as long as $\log T_{\text{eff}} < 3.7$. This can be seen from the y_p values of Table 8. Thus equation (77) has to be replaced by

$$\rho_p^2 = A \frac{g}{g_\odot} T_{\text{eff}}^{-2} 10^{-8.59-1.55\theta_p} . \tag{99}$$

Next, in the lower photospheric region we have to integrate equation (78) divided by equation (79). Here κ and hence $(A^{-1} + y)$ appear in the denominator of the integrand. We shall divide the integral at the temperature T_q, where $y = A^{-1}$. At the lower temperatures we shall use $y = 0$, which overestimates the integrand, while at the higher temperatures we shall use $y = \infty$, which underestimates the integrand. The two errors—and particularly their sum—seem to be tolerably small. We then obtain, in place of equation (82),

$$\rho_a T_a = \alpha \rho_p T_{\text{eff}} , \tag{100}$$

with

$$\alpha^2 = 1 + \frac{32}{3}\left(4 + \frac{1.55}{\log e}\,\theta_p\right)^{-1}\left[\left(\frac{T_q}{T_{\text{eff}}}\right)^4 \cdot 10^{1.55(\theta_p - \theta_q)} - 1\right] . \tag{101}$$

For T_q, guided by the y_p-values of Table 8, we here use $\log T_q = 3.738$.

In the still lower layers, hydrogen is sufficiently ionized that it supplies most of the free electrons, and the metal admixture has no further effect. With the foregoing changes, we finally obtain, in place of equation (95)—again with $T_a \approx 10{,}000°$ and $\beta = 0.3$,

$$-\log E + \tfrac{1}{2}\log \alpha + \tfrac{1}{4}\log A + \tfrac{3}{4}\log \frac{M}{M_\odot} + \log \frac{R}{R_\odot} + 0.73 - 0.39\theta_p$$
$$= \alpha^{-1} A^{-1/2} \left(\frac{M}{M_\odot}\right)^{-1/2} \frac{R}{R_\odot} T_{\text{eff}}^4 10^{-14.053+0.775\theta_p} . \tag{102}$$

To apply this equation, we may take, as before, $E \approx 15$ and $M = 1.1\ M_\odot$. Furthermore, $A \approx 10^4$ appropriate for population I. Equation (102)—with α given by equation (101)—then contains nothing but R and $T_{\rm eff}$, so that R can be solved for as a function of $T_{\rm eff}$. After this, L follows from equation (96), ρ_p from equation (99), ρ_a from equation (100), and y_a from equation (85).

The results of this computation are given in Table 9 for four values of $T_{\rm eff}$ from 4900° to 4100°. The four models are represented by crosses in Figure 4. Before discussing these results, we should emphasize once more the great numerical uncertainties which are still inherent in these calculations. In particular, the characteristics of convective-energy transport in stellar envelopes is still far from well known. Here this uncertainty

TABLE 9

MODELS FOR RED GIANTS OF POPULATION I
($M = 1.1 M_\odot$)

	log $T_{\rm eff}$			
	+3.688	+3.660	+3.636	+3.612
α	1.70	2.21	2.77	3.46
log $R/R_\odot$	+0.78	+1.06	+1.27	+1.48
log $L/L_\odot$	+1.270	+1.638	+2.042	+2.366
log ρ_p	−7.55	−7.85	−8.09	−8.32
log ρ_a	−7.63	−7.85	−8.01	−8.17
y_a	0.12	0.14	0.24	0.31
log $T_{\rm eff}$	+3.688	+3.660	+3.636	+3.612
Bol. cor.	+0.12	+0.23	+0.6	+0.9
$M_{\rm vis}$	+1.6	+0.8	+0.2	−0.3
CI	+0.81	+1.00	+1.17	+1.30

appears in the efficiency coefficient β: if β is lowered by a factor of 2, the brightness of the last model in Table 9 is lowered by 2 mag. In spite of these uncertainties, it appears fairly safe, however, to judge the relative effects of the metal content from these computations.

Figure 4 shows that the introduction of a metal content appropriate for population I has, in fact, lowered the brightness—for a fixed effective temperature—by 2–3 mag. and has placed the two last models of Table 9 right in the region of the observed red giants of population I. It seems safe to conclude that it is probably the difference in metal content that causes the difference in absolute magnitude of the red giants in the two stellar populations.

As we have seen, only in the photospheric regions does the metal content play a critical role. There it greatly affects the extent of the tenuous envelope, i.e., the radius of the star. However, it affects the structure of the deep interior hardly at all. In particular, we have derived the mass-luminosity relation—here represented by the L-q_1 relation of Table 6—without any reference to the details of the photospheric regions.

We have not carried the detailed computations to effective temperatures below 4000°, since a number of complications would arise there. First, at lower temperatures the most common metals are no longer fully ionized, so that the number of free electrons would soon fall below A^{-1}. This does not introduce a difficulty in principle but an appreciable complication in the computations. Second, H^- may no longer be the only effective source of opacity, but atomic lines and molecular bands may start to contribute noticeably. Finally, the bolometric corrections rise steeply, and so does their uncertainty.

XIV. THE TIP OF THE GIANT SEQUENCE

The luminosity L increases with q_1 along the giant branch up to values of about 0.5. The question that evidently arises is why L does not go on increasing as q_1 rises above 0.5. What is it that determines the top of the sequence? We shall discuss this problem first from a qualitative point of view.

It will be recalled that T_1, the temperature of the core, rises along the giant branch between N and O of Figure 1. Our models still continue to maintain an isothermal condition within the core, however, the rise of temperature being what is required to provide the increasing degree of energy generation.

A deviation from these models comes when an isothermal condition is no longer maintained within the core, even as an approximation. Because of the gravitational energy that is constantly being released as new material is added to the core, it is clear that a temperature gradient must be set up, to such a degree that the flux of energy out of the core equals in order of magnitude the rate of release of gravitational energy. Now the rate at which material is added to the core evidently depends on L, since the rate of conversion of hydrogen into helium is $(6.2 \times 10^{18})^{-1} L$ gm/sec, L being in ergs per second (1 gm of hydrogen converted to helium yields 6.2×10^{18} ergs). The rate at which gravitational energy is released is roughly proportional to the rate at which helium is added to the core, so that the rate of release of gravitational energy is roughly proportional to L. Clearly, then, for a sufficiently large L the temperature gradients inside the core will become so large that we can no longer ignore the temperature difference between the center and the surface of the core.

It is emphasized in relation to these remarks that the energy released by gravitation does not make an important contribution to L, which is still almost wholly maintained by hydrogen-burning. The importance of gravitational energy is that it serves to raise the temperature within the core. The effect of the rise of temperature is not an immediate one, however. So long as the material of the central body of the core remains degenerate, a rise in temperature makes only a slight difference to the dependence of pressure on density and hence only a slight difference to the general structure of the core. It is true that a temperature gradient in the outer nondegenerate part of the core has some effect on the density within the hydrogen-burning shell and for this reason has some slight effect on the whole star. But, by and large, the effects are small so long as the inner part of the core remains degenerate. It therefore appears that a really marked deviation from the models discussed is contingent on the core's assuming a nondegenerate structure, even in its inner part. The question now arises as to how this can happen.

For a sufficient rise in temperature within the core, energy begins to be generated at its center through the conversion of helium to carbon (Salpeter 1952). This occurs at densities of the order of 10^5 gm/cm^3 (the present case) when the temperature rises to a value close to and a little in excess of $10^{8\circ}$ K—say, to a temperature of $1.2 \times 10^{8\circ}$ K. The relevant process depends on a resonance level of the C^{12} nucleus at about 7.68 mev above ground level (Hoyle 1954). Resonance in this level requires the energy generation to depend on T approximately as $\exp[-36/T]$, where T is in units of $10^{8\circ}$ K. Under these circumstances we have a situation similar to that envisaged by L. Mestel (1952) in his study of white dwarfs. In nondegenerate matter a state of balance is always reached between the generation of energy and the outflow of energy. This is because in nondegenerate matter expansion implies cooling, and contraction, heating. Thus if energy production were to exceed the outward flux, there would be an expansion followed by cooling and by a fall in the energy production. This would continue until a balance was reached. A deficiency of energy production leads to shrinkage, to a rise in temperature, and to increased energy production, with again a trend toward a state of balance.

All this is altered when the material is degenerate. Expansion of degenerate material implies heating, not cooling, and contraction implies cooling, not heating. This means

that when energy production occurs in degenerate material, there is no natural balancing process. If energy production is inadequate to balance the outward flux, the shrinkage that occurs is accompanied by cooling and by a further falling-behind of the energy generation. If energy production exceeds the outward flux, the expansion that occurs is accompanied by heating and by an increasing excess of energy production. The situation in this case is unstable, with the energy generation increasing more and more. The instability ends in such a case only when the temperature has risen sufficiently for the material to become nondegenerate, at which stage the balancing process discussed earlier can come into operation (provided that, by the time this stage is reached, the star is not in a state of wholesale explosion).

Returning now to the heating of the helium core by the release of gravitational energy, we see that, although the immediate effect of raising the inner temperature of the core does not modify the structure of the star very much, sooner or later a drastic situation will arise. This happens when the inner temperature becomes high enough for the energy generation through helium-burning to exceed the outward flow of energy within the core. This must arise because the energy generation rises much more steeply with temperature than does the outward flux, so that eventually (for a value of T near $1.2 \times 10^{8\,\circ}$ K) the energy generation becomes dominant. Then an instability of energy generation occurs along the lines discussed. That is to say, the core assumes a nondegenerate structure. We believe that it is this change that ends the ascent of stars up the giant branch of the evolutionary sequence.

We must now pass to a quantitative consideration of these matters, our problem being to decide at what stage of the evolutionary sequence the temperature in the core rises to about $1.2 \times 18^{8\,\circ}$ K. The transition to a nondegenerate core may be regarded as occurring when this stage is reached. Our problem then is to find the value of L (and hence of q_1 and T_{eff}) at which appreciable helium-burning sets in at the center of the core.

Near the center of the core where the matter is highly degenerate, we may expect the outward flux of energy to be transported by electron conduction, not by radiation (or convection). Indeed, the conductivity of highly degenerate matter is so great that such material must always be in a nearly isothermal condition, otherwise the flow of energy would be extremely large. Consequently, the main decline of temperature must occur outside the highly degenerate matter, where the outward flux is carried by radiation. It is in this region that the temperature falls from its inner, nearly isothermal, value to the value appropriate for the hydrogen-burning shell. Subject to the following plausible assumption, the energy transfer in this region can be readily estimated: that the temperature gradient is of the order of $-T_c/r$ at the place where the opacity is highest, T_c being the central temperature and r the distance from the center at which the opacity is highest in the radiative zone of the core. Since the temperature of the hydrogen-burning shell is to be much lower than T_c for the case of interest ($T_c \approx 1.2 \times 10^{8\,\circ}$ K), it follows that the mean temperature gradient for the whole core is of the order of $-T_c/r_1$, and this we may expect to be of the order of $-T_c/r$, where r is the distance from the center to the place in the nondegenerate material where the opacity is highest. Now this occurs where the material is first nondegenerate, since the density is then highest. We shall define this as the place at which the pressure is equal to twice what the pressure would be if the density were maintained and the temperature were just equal to zero. This occurs at $\psi = 4$ in the core solution; and at $\psi = 4$ we have

$$F_{1/2}(\psi) = 5.77\,, \qquad F_{3/2}(\psi) = 17.65\,.$$

The value of ξ at which ψ falls to 4 is not independent of ψ_0, however. But fortunately the dependence is a weak one. Thus, for $\psi_0 = 20$, which is a representative value for the top of the giant sequence, $\xi = 1.65$ at $\psi = 4$, while for $\psi_0 = 10$, $\xi = 1.54$ and for $\psi_0 = 100$, $\xi = 1.34$, both at $\psi = 4$. Using values for $\psi_0 = 20$ and denoting quantities at $\psi = 4$

by the subscript g, we have

$$\rho_g = 6.26 \times 10^3 \left(\frac{T_c}{20 \times 10^6}\right)^{3/2}, \tag{103}$$

$$P_g = 1.58 \times 10^{19} \left(\frac{T_c}{20 \times 10^6}\right)^{5/2}, \tag{104}$$

$$r_g = 1.92 \times 10^9 \left(\frac{T_c}{20 \times 10^6}\right)^{-1/4}. \tag{105}$$

Since there is little change in temperature within the highly degenerate part of the core, we can put $T = T_c$ at $\psi = 4$. Then we obtain

$$L_g = 4\pi r_g \frac{4ac}{3} \frac{T_c^4}{0.19\rho_g}, \tag{106}$$

where the temperature gradient has been put equal to $-T_c/r_g$, and L_g represents the flux at r_g and hence represents the energy flux out of the core. Substituting for ρ_g and r_g from equations (103) and (104), we obtain

$$L_g = 10^{16.564} T_c^{9/4}. \tag{107}$$

The next step is to estimate the rate of release of gravitational energy. Then, by using this for L_g, an estimate for T_c is obtained. The result gives a value of T_c that depends on the position of the star on the evolutionary sequence.

Consider a time interval $\delta\tau$. The gravitational energy released in this time interval is (Sandage and Schwarzschild 1952)

$$\delta\left[-4\pi\int_0^{r_g} r^2\left(\frac{3}{2}P - \frac{G\rho M_r}{r}\right)dr\right] - P_g\delta\left[\frac{4\pi}{3}r_g^3\right] + \frac{kT_c}{\mu_i H}\left[\left(\frac{\gamma}{\gamma-1} - V_i\right)\delta M_r\right]_g, \tag{108}$$

where γ is the ratio of specific heats, equal to $\frac{5}{3}$ in our work, and δ refers to the change in the various quantities r_g, M_{r_g}, and V_{ig} occurring in the time interval $\delta\tau$. After some reduction, equation (108) can be shown to give

$$\delta\left\{M_r \frac{kT_c}{\mu_i H}\left[-\frac{1}{3}\left(\frac{\xi^3 F_{3/2}[\psi]}{-\xi^2[d\psi/d\xi]}\right) + \tfrac{1}{2}B(\xi)\right]\right\}_g + \frac{kT_c}{\mu_i H}\left[\left(\frac{\gamma}{\gamma-1} - V_i\right)\delta M_r - U_i M_r \frac{\delta r}{r}\right]_g, \tag{109}$$

where

$$B(\xi) = \frac{1}{-\xi^2(d\psi/d\xi)}\int_0^{\xi} F_{1/2}(\psi)\left(-\xi^2\frac{d\psi}{d\xi}\right)\xi\, d\xi.$$

An estimate has been made for equation (109) by using the step from $q_1 = 0.55$ to $q_1 = 0.61$ in Table 6. The result was an energy release of about 2.7×10^{48} ergs.

This is the total energy release for the whole step. To find the average rate of release of gravitational energy, which we denote by L_g, we must divide equation (109) by $\delta\tau$. Since the outflow of energy within the core is small compared with the total luminosity L of the star (this will be seen from values given later), the following equation may be used to estimate $\delta\tau$:

$$\delta\tau = 6 \times 10^{18}\delta q_1 \frac{M}{\bar{L}}, \tag{110}$$

where $\bar{L}$ is the total luminosity of the star averaged over the step in q_1. Dividing the

energy yield of 2.7×10^{48} ergs, as given by equation (109), by $\delta\tau$, as given by equation (110), we obtain

$$L_g \approx 3 \times 10^{-3} \bar{L} . \tag{111}$$

The precise value of the numerical coefficient in formula (111) is dependent on the particular step in q_1 from 0.55 to 0.61. But this coefficient is only slowly varying when the step in q_1 is changed. So we can use this present value of the coefficient as a suitable approximation for other steps. The value of $\bar{L}$, on the other hand, is sensitive to q_1, as the values in Table 6 show. Consequently, the appropriate value of $\bar{L}$ must be used for values of q_1 outside the range 0.55–0.61, but the coefficient in relation (111) can be retained.

Now relations (107) and (111) give

$$T_c \approx 2.7 \times 10^6 \left(\frac{\bar{L}}{L_\odot}\right)^{4/9}, \tag{112}$$

this equation being applicable for $\bar{L}$ large enough for T_c to rise appreciably above T_1.

We can now invert the problem. By putting $T_c = 1.2 \times 10^8$° K in relation (112), we can calculate the average luminosity of the star at the onset of helium-burning. The result is

$$\log \frac{\bar{L}}{L_\odot} \approx 3.70 ,$$

the corresponding value of q_1 being about 0.52, a value close to the range of q_1 used in the foregoing computations. For greater accuracy, an interative method with respect to q_1 might be used; but, in view of our other assumptions, this degree of refinement is not warranted here.

Our present result suggests that the top of the giant sequence, whether of the type II or the type I giants of mass $\approx 1.2\odot$, should occur at a luminosity about 5000 times greater than that of the sun. This gives

$$M_{pv} = -4.6 + \text{bolometric correction} . \tag{113}$$

The difference between the largest M_{pv} of type I and type II giants would therefore seem to lie, not in the bolometric luminosities, but in a notable difference of bolometric correction, the correction being about 3 mag. at the tip of the type I sequence and about 1 mag. at the tip of the type II sequence. The difference arises from the difference in color index, which is due to a difference in the concentration of metals relative to hydrogen in in the original material from which the two types of stars were formed.

The present work requires the upper limit of the giant branch to be about the same in all globular clusters (there will be slight differences of M_{pv} arising from different bolometric corrections). This is in very good agreement with the observed situation. The only feature of our results that does not agree well with observation is that the value of M_{pv} given by (113) would seem to be too bright by about $\frac{3}{4}$ mag. Unless the bolometric correction at the tip of the sequence should turn out to be somewhat larger than 1 mag., this seems a real discrepancy in the theory, although perhaps not a serious one. Indeed, some such discrepancy is to be expected, since the derivation of equation (106) was based on an order-of-magnitude argument only.

Result (112) establishes a point that was assumed in calculating models for the portion L–N (Fig. 1) of the evolutionary track, that the core could be regarded as isothermal for these early models. We see that T_c does not rise appreciably above T_1 until the upper part of the giant branch is reached.

XV. A TENTATIVE DISCUSSION OF THE PORTION O–P OF THE EVOLUTIONARY TRACK

It is necessary now to consider stellar models with a nondegenerate core. These models differ from those that have hitherto been considered, in that they possess a double energy

source, due to helium-burning in the core and to hydrogen-burning in a shell surrounding the core. It will be sufficient to take the envelope as radiative throughout, as was done in Section III. If the models obtained turn out to be in the color-magnitude diagram to the left of the giant sequence, as worked out for type II stars, then the surface condition may be adjudged unimportant. If, on the other hand, the models obtained should turn out to be to the right of the giant sequence, then the neglect of the surface condition is inappropriate. In such a case the stars must be placed on the giant sequence at the same luminosity (approximately) as is given by our present calculations. The situation is that we trust the present models to give L as a function of q_1 correctly, but we trust the present models to give R as a function of q_1 only if the resulting position in the color magnitude is to the left of the giant sequence; otherwise we place the star on the giant sequence at the calculated L.

On account of the sensitive dependence of helium-burning on temperature, the helium core must possess an inner convective zone. We denote the value of quantities at the interface between this zone and an outer radiative part of the core by the subscript d. Dimensionless variables for the hydrogen envelope are again given by equation (27), and dimensionless variables for the core are given by replacing μ_e in equation (27) by μ_i ($\mu_e = 0.533$, $\mu_i = 1.333$). The equations for the dimensionless variables take the following forms:

$$0 < x < 1: \qquad \frac{dp}{dx} = -\frac{pq}{tx^2}, \qquad \frac{dq}{dx} = \frac{px^2}{t}, \tag{114}$$

$$0 < x < x_d: \qquad \frac{d \log p}{d \log t} = 2.5, \tag{115}$$

$$x_d < x < x_1: \qquad \frac{dt}{dx} = -{}^*C_{El}\frac{p}{t^4x^2}, \tag{116}$$

$$x_1 < x < x_s: \qquad \frac{dt}{dx} = -C_{El}\frac{p}{t^4x^2}, \tag{117}$$

$$x_s < x < 1: \qquad \frac{dt}{dx} = -C_{Kr}\frac{p^2}{t^{8.5}x^2}. \tag{118}$$

The subscript to the constant ${}^*C_{El}$ implies that the opacity in the region $x_d < x < x_1$ is taken as due essentially to electron scattering.

We show, first, that the problem is determinate. The boundary conditions at the center are

$$q = 0 \quad \text{and} \quad \frac{dp}{dx} = 0 \quad \text{at} \quad x = 0. \tag{119}$$

There are two disposable constants for equations (114) and (115), the central values of t and $p - p_c$ and t_c, say. For the moment we also regard x_d as a disposable constant. Then with p_c, t_c, and x_d all specified, a solution for $0 < x < x_1$ can be obtained from equations (115) and (116), where x_1 is fixed by the requirement that q shall take some assigned value q_1. The transition from equation (116) to equation (117) for specified x_d is made with the fitting condition that the physical variables and their derivatives are to be continuous. This requires the continuity of the dimensionless variables and their derivatives. The value of ${}^*C_{El}$ is given by the continuity of dt/dx.

Next equations (114), (117), and (118) can be integrated inward from the boundary condition

$$p = 0, \quad q = 1, \quad t = 0 \quad \text{at} \quad x = 1, \tag{120}$$

provided that values of x_s and C_{Kr} are specified. The fitting condition at x_s are that the variables, both physical and dimensionless, and their derivatives be continuous. The

value of $^*C_{El}$ is determined by the continuity of dt/dx. Since we are regarding q_1 as given, six quantities remain to be determined; five of the quantities are those already mentioned—p_c, t_c, x_d, C_{Kr}, and x_s—and the sixth is R, which is required to permit a conversion from the dimensionless variables to the physical variables. Fitting at x_1 supplies three conditions, and three other conditions are given by certain physical requirements. We take the conditions at x_1 first. The continuity of p and t at x_1 gives two conditions. A third

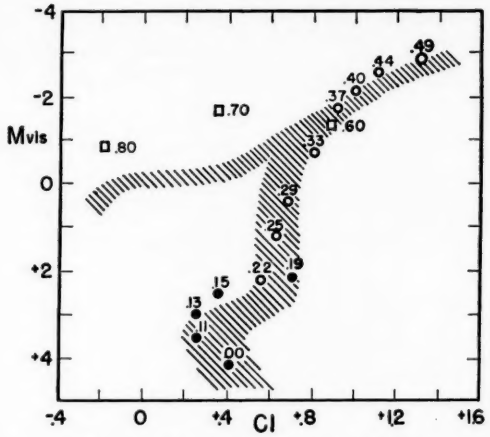

FIG. 5.—Hertzsprung-Russell diagram for entire sequence of models following the evolution of type II stars. The numbers give the fraction of the mass in which the hydrogen is burned out.

condition is that the envelope solution has a value q_1 at x_1. The three physical conditions are as follows:

(i) The energy generation in the core due to the burning of helium must equal the outward flux, L_{core}, say, as determined by

$$^*C_{El} = -\frac{0.57}{4ac}\left(\frac{k}{\mu_i HG}\right)^4 \frac{1}{(4\pi)^2}\frac{L_{\text{core}}}{M^3}, \tag{121}$$

with $\mu_i = 1.333$.

(ii) The energy production in the hydrogen shell must equal $L_{\text{total}}-L_{\text{core}}$, where L_{tota} is determined by

$$C_{El} = -\frac{0.57\,(1+X)}{4ac}\left(\frac{k}{\mu_e HG}\right)^4 \frac{1}{(4\pi)^2}\frac{L_{\text{total}}}{M^3}, \tag{122}$$

with $x = 0.9$, $\mu_e = 0.533$.

(iii) The opacity from electron scattering must equal the opacity from free-free transitions at $x = x_s$.

In our numerical work we proceeded in much the same way as in the earlier investigations. That is to say, values of T_c, T_1, and x_s were guessed, and a check-back at the end of the calculations was made with requirements i, ii, and iii. The situation concerning T_c is highly favorable; for, since energy production by helium-burning depends so sensitively on the temperature, the value of T_c can be accurately guessed at the outset as being close to $1.0 \times 10^{8\,\circ}$ K. In the hydrogen-burning shell we took $T_1 = 20 \times 10^{6\,\circ}$ K. This proved to be a sufficiently good guess for the calculation of a second approximation to be unnecessary. The value of x_s was adjusted with reasonable accuracy. Results are given in Table 10. The points marked by squares in Figure 5 represent these stellar models.

The results, while not good, are not entirely discouraging. The first model for $q_1 = 0.60$ seems to give a clear indication that the assumption of a nondegenerate structure by the core forces a star down the giant branch. The other two models, for $q_1 = 0.70$ and $q_1 = 0.80$, show a marked movement to the left in the diagram, although at about 1 mag. above the observed horizontal branch. A deviation of our models from the observed sequence is only to be expected, however, since the model for $q_1 = 0.80$ and probably also that for $q_1 = 0.70$ already deviate from the physical evolution of a star in an important respect. A comparison of L_{core} with L_{total} shows that for $q_1 = 0.60$ the energy generation in the core is comparable to the energy generation in the shell. Now the energy yield from the conversion of 1 gm of helium into carbon is about 6×10^{17} ergs, which is only about one-tenth the energy yielded by the conversion of 1 gm of hydrogen into helium. Hence q_1 cannot increase as much as from 0.60 to 0.70 before all the helium is consumed—if we accept the values of L_{core} and L_{total} given in Table 10, that is. It appears, therefore, that

TABLE 10

MODELS WITH HELIUM-BURNING IN CONVECTIVE CORE (*c* TO *d*), RADIATIVE ZONE IN HELIUM (*d* TO 1), HYDROGEN-BURNING SHELL (AT 1), AND RADIATIVE ENVELOPE (1 TO SURFACE)

($M = 1.2M_\odot$; $T_c = 100 \times 10^6$; $T_2 = 20 \times 10^6$)

	$q_1 = M_{r1}/M$		
	0.60	0.70	0.80
θ_d	0.658	0.657	0.657
ξ_d	1.565	1.566	1.568
$\log x_d$	− 2.70	− 2.44	−1.87
$\log q_d$	− 0.73	− 0.66	−0.60
$\log t_d$	+ 2.04	+ 1.84	+1.34
$\log p_d$	+ 9.38	+ 8.42	+6.29
$(n+1)_{1i}$	14.6	11.5	7.8
U_{1e}	0.076	0.084	0.11
V_{1e}	3.53	3.58	3.72
$(n+1)_{1e}$	3.91	3.90	3.89
$\log x_1$	− 2.29	− 2.03	−1.49
$\log q_1$	− 0.22	− 0.15	−0.10
$\log t_1$	+ 1.52	+ 1.32	+0.82
$\log p_1$	+ 7.06	+ 6.18	+4.23
$\log C_{\text{BI}}$	− 1.76	− 1.64	−1.62
$\log x_s$	− 0.39	− 0.53	−0.58
$\log p_s$	− 1.20	0.00	+0.25
$\log t_s$	− 0.55	− 0.26	−0.19
$\log R/R_\odot$	+ 1.39	+ 1.19	+0.69
$\log L/L_\odot$	+ 2.44	+ 2.55	+2.57
$\log \rho_c$	+ 3.58	+ 3.16	+3.03
$\log \rho_{1e}$	+ 1.11	+ 1.04	+1.09
$L_{\text{hyd}}/L_{\text{hel}}$	0.96	0.55	0.05
$\log T_{\text{eff}}$	+ 3.67	+ 3.80	+4.06
Bol. cor.	+ 0.14	+ 0.05	+0.85
M_{vis}	− 1.33	− 1.70	−0.94
CI	+ 0.88	+ 0.35	−0.19

the type of model considered here can remain valid for only a very brief space of the evolution. After only a short time helium must become exhausted at the very center of the star, and helium-burning must also become confined to a shell. We should therefore consider the following model: (*a*) inner core of carbon, possibly degenerate, and in a nearly isothermal condition; (*b*) energy production by helium-burning in a shell surrounding the inner carbon core; (*c*) a nondegenerate helium zone with outward energy flux; (*d*) energy production by hydrogen-burning in a shell surrounding the helium zone; (*e*) an outer hydrogen envelope. Such a model would be complicated to integrate, especially as the solutions for the envelope should include the opacity switch and possibly also an outer convection zone. A numerical consideration of such a complex model has been judged as outside the scope of the present paper, particularly as there is no guaranty that the outcome will continue the evolution very much further. If it should turn out that when the helium-burning passes from an inner convective zone to a shell, the ratio $L_{\text{core}}/L_{\text{total}}$ remains of order unity, then such a model, with all its complexity, can represent only a short-lived phase in the existence of a star. Soon, for the reason already given, the helium of the core will become entirely converted to carbon, and the core will presumably return to a degenerate condition.

The present work is therefore seen to leave uncertain the models for the evolutionary stages after onset of helium-burning. Evidently a thorough investigation is required before the stars can be satisfactorily traced along the horizontal branch of the color-magnitude diagram.

XVI. CONCLUSIONS

The results obtained have all been collected together in Figure 5. We have used dots to denote the models without an outer convection zone (Secs. III and IV), circles for the results of Sections X and XI, including the surface condition and the outer convection zone, and squares for the helium-burning models. For the type II stars a ratio of metal atoms to hydrogen atoms of 1/135,000 was used, as compared with a ratio of 1/10,000 for type I stars.

Along the portion of the track denoted by the dots, soon after leaving the main sequence the star must develop an outer convection zone in order to meet the physical boundary condition at the surface of the star. The run to the right of the dots is accompanied by an increasing strength of convection near the surface of the star. Eventually, however, the convection currents approach the speed of sound. Further evolution along the sequence of the dots is then impossible. When this stage is reached, the convection zone can be made to reach only to a depth adequate to meet the surface boundary condition if the radius of the star is steadily increased at a nearly constant surface temperature (this is for type II stars). The evolution follows the circles.

Throughout this evolution the star possesses a partially degenerate isothermal core surrounded by a shell in which hydrogen-burning occurs. The temperature in this hydrogen-burning shell remains near $20 \times 10^{6\,\circ}$ K until $\log L/L_{\odot}$ has risen to about 2.0. At this stage the core begins to evolve in such a way that the density in the shell tends to decrease. This effect, together with the necessity of providing energy at an increasing rate, forces the temperature in the energy-producing shell to values that are substantially higher than have hitherto been associated with the operation of the carbon cycle. A rise to a temperature of $40 \times 10^{6\,\circ}$ K or even $50 \times 10^{6\,\circ}$ K occurs on the giant branch.

This rise in temperature does not in itself affect the isothermal condition within the core. A change from isothermal conditions within the core is not due to any rise in temperature that may be required to operate the carbon cycle but to the release of gravitational energy within the core. The rate of this release becomes greater as the luminosity of the star rises, since the greater the luminosity, the greater the rate of hydrogen-burning and hence the greater the rate at which material is added to the helium core. Toward the top of the giant branch the rate of release of gravitational energy becomes sufficient to maintain a considerable temperature difference between the center of the star and the

hydrogen-burning shell. The setting-up of a considerable temperature gradient is aided by the high opacity of material just outside the degenerate portion of the core.

Eventually the temperature at the center of the core rises high enough for the release of energy by helium-burning to become important. This happens at a central temperature of about 1.2×10^8° K. The core then possesses an instability that causes the energy generation by helium-burning to increase until the core expands quite suddenly to a nondegenerate structure. We then have a stellar model with a double energy source—helium-burning within the core and hydrogen-burning in a shell surrounding the core. Computations indicate that the two sources of energy are of approximately comparable importance. The total luminosity declines in this stage, and the stars evolve toward the left in the color-magnitude diagram. The indications of our calculations are represented by the squares in Figure 5. It is emphasized, however, that at this stage of our work the physical basis of the stellar models is exposed to criticism. Consequently, these latter results are at best only an indication of a trend. A program for improving these models was suggested earlier.

The fraction q_1 of the mass of the star contained in the core is marked in Figure 5 at the various calculated points. The time required for evolution from q_1 to $q_1 + dq_1$ is proportional to dq_1/L. An inspection of Figure 5 shows that the rate of evolution speeds up very considerably. A star spends most of its life on, or near, the main sequence. The ages of the stars of the globular clusters were estimated at about 6×10^9 years. Some uncertainty was, however, attached to this calculation: so far as the accuracy of our physical approximations is concerned, it would scarcely be surprising if a more complete theory should give an age as low as 4×10^9 years or as high 8×10^9 years.

The evolution of the stars along the giant branch is determined in part by the interior conditions within the star and in part by the surface boundary conditions. These two factors operate in such a way that the luminosity is determined essentially by the internal conditions, while the radius is determined by the surface condition. The difference between the giant sequences of type I and type II stars is due to surface conditions that differ because of the different concentrations of metal atoms in the two types of star. The drastic difference between the two sequences emphasizes the importance of the surface condition.

The incidence of helium-burning in the core would seem to determine the top of the giant sequence. This occurs when L becomes so large that the rate of release of gravitational energy is sufficient to raise the temperature at the center of the core to a value somewhat in excess of 10^8° K. The critical value of L calculated earlier was $\log L/L_\odot = 3.70$, the precise numerical value being exposed to some error, since our estimate contained approximations. The theory requires the same value of L at the top of the sequence, irrespective of the metal content of a star—the value of L should be the same for both type I and type II giants.

Helium-burning within the core is important because it creates an instability in the core, causing it to assume a nondegenerate structure. It is this that apparently induces a marked fall in the value of L, taking the star to the region of the horizontal branch. The instability would seem to be a sudden one, causing a nearly discontinuous jump from the top of the giant sequence to the point of entry into the horizontal branch.

It is emphasized that our main aims in this paper have been to explore the physical reasons that underlie the remarkable evolution of the type II stars. While we believe that our work possesses sufficient arithmetical accuracy for this purpose, it is clear that very considerable improvements in the calculation remain to be made. Whether the improvements would best be made by the methods we have used is perhaps open to doubt. When methods that are designed in the first place as a simplified representation of the problem become as complicated as we have found them to be in this investigation, it is perhaps an indication that an entirely new line of attack is desirable. In this case we feel that the new line may turn out to be a fully automatic representation, using large electri-

cal machines. Our method of using several one-parameter families of solutions, plus fitting conditions, plus a surface boundary condition, plus iteration, may no longer give the best way of breaking down the problem.

As a final remark, a warning must be issued against using the results of this paper by analogy to stars of markedly different mass. Our results are calculated for stars with masses 1.1 to 1.2 times that of the sun. They can presumably be extrapolated somewhat out of this range, but any appreciable change, say to stars of $2.5\odot$, will very likely lead to serious errors. This is because the nature of the degenerate core is certainly going to be different in stars of larger masses.

We acknowledge with great pleasure the extensive contributions which Mr. R. Härm has made to this work.

REFERENCES

Arp, H. C., Baum, W. A., and Sandage, A. R. 1953, *A.J.*, **58**, 4.
Biermann, L. 1948, *Zs. f. Ap.*, **25**, 135.
Chamberlain, J. W., and Aller, L. A. 1951, *Ap. J.*, **114**, 52.
Chandrasekhar, S., and Münch, G. 1946, *Ap. J.*, **104**, 446.
Fowler, W. A. 1954, *Mémoires in −8° de la Société royale des Sciences de Liège*, 4th ser. **13**, Fasc. III, 88.
Gamov, G., and Keller, G. 1945, *Rev. Mod. Phys.*, **17**, 125.
Gardiner, J. G. 1951, *M.N.*, **111**, 102.
Harrison, M. H. 1946, *Ap. J.*, **103**, 193.
Hayashi, M. 1949, *Phys. Rev.*, **75**, 1619.
Hoyle, F. 1954, *Ap. J. Supplement Series*, **1**, 121.
Hoyle, F., and Lyttleton, R. A. 1949, *M.N.*, **109**, 614.
Johnson, H. L., and Morgan, W. W. 1953, *Ap. J.*, **117**, 313.
Keenan, P. C., and Morgan, W. W. 1951, "Classification of Stellar Spectra," in *Astrophysics*, ed. J. A. Hynek, chap. i, p. 12.
Mestel, L. 1952, *M.N.*, **112**, 583.
———. 1953, *ibid.*, **113**, 716.
Osterbrock, D. E. 1953, *Ap. J.*, **118**, 529.
Salpeter, E. E. 1952, *Ap. J.*, **115**, 326.
Sandage, A. R. 1953, *A.J.*, **58**, 61.
———. 1954, *Mémoires in −8° de la Société royale des Sciences de Liège*, 4th ser., **13**, Fasc. III, 254.
Sandage, A. R., and Schwarzschild, M. 1952, *Ap. J.*, **116**, 463.
Schönberg, M., and Chandrasekhar, S. 1942, *Ap. J.*, **96**, 161.
Schwarzschild, M., Rabinowitz, I., and Härm, R. 1953, *Ap. J.*, **118**, 326.
Schwarzschild, M., Spitzer, L., and Wildt, R. 1951, *Ap. J.*, **114**, 398.
Sweet, P. A. 1950, *M.N.*, **110**, 548.

STUDIES IN GALACTIC STRUCTURE. II. LUMINOSITY CLASSIFICATION FOR 1270 BLUE GIANT STARS

W. W. MORGAN, A. D. CODE, AND A. E. WHITFORD
Yerkes and Washburn Observatories
Received May 2, 1955

ABSTRACT

Two-dimensional spectral classification on the MK system is given for 1270 stars of early type. The catalogue includes 118 southern stars classified from spectrograms obtained at the Radcliffe Observatory. Photoelectric colors are listed for 71 per cent of the stars; of these colors, 386 are of stars not previously measured. The new colors include those of 102 southern stars obtained at the Radcliffe and Cape Observatories.

An observing program of spectroscopic parallaxes of early-type stars was begun in 1942 with the Yerkes 40-inch refractor and a small spectrograph giving a dispersion of around 100 A/mm at $H\delta$. The plan was to obtain spectrograms of all O–B5 stars in the *Henry Draper Catalogue* north of declination $-20°$. This program was later supplemented by the addition of the "OB stars" in the catalogue of Nassau and Morgan (1951).

In the years following, spectrograms of most of the *HD* stars were obtained, together with around two-thirds of the Nassau-Morgan list. The remainder of the latter were taken by W. A. Hiltner and S. L. Sharpless with two low-dispersion cameras attached to the 82-inch McDonald Cassegrain spectrograph. The observers who had the principal share in the 40-inch observing were E. Margaret Burbidge, Douglas Duke, Merle Tuberg Gold, Marjorie Hall Harrison, L. R. Henrich, W. W. Morgan, Nancy G. Roman, and S. L. Sharpless.

The selection for inclusion in Tables 1 and 2 is approximately that defined by Morgan (1951) for the OB group. However, in the case of the Nassau-Morgan list, all observed stars have been given, including those which proved to lie outside the OB limits. There are three exceptions to this rule: HD 196604 (Am), HD 227144 (A7), and BD+37°4368 (K3 III); these stars have been omitted. The last-named lies considerably outside the galactic-latitude limit of the Nassau-Morgan survey and may be an error in the earlier catalogue.

The spectrograms were classified on the MK system (Johnson and Morgan 1953) by Morgan. Since the present catalogue (Table 1) contains the majority of all early-type stars classified on this system, the latter can be considered to be defined by the present results for the high-luminosity stars of early type.

Color indices on the C_1 system of Stebbins, Huffer, and Whitford (1940) were determined for a number of the stars by Code and Whitford with the 15-inch refractor at Madison and the 60-inch reflector at Mount Wilson. These observations supplement the data of the "1332 B stars" catalogue. Photoelectric magnitudes on the International photovisual system were also determined for many of the same stars. The photometric results will be discussed in detail at a later time.

The data are listed in Table 1. The columns give: 1, a running number; an asterisk refers to a note; 2, the name of the star. The *HD* number or the *BD* number are preferred, except in the case of the O-association described by Johnson and Morgan (1954). This has been named VI Cygni, and the designation of the stars corresponds to the published map. The anonymous stars are numbered according to the catalogue of Nassau and Morgan.

Columns 3 and 4 give the position for 1900, and column 5 the spectral type on the MK system. Columns 6 and 7 give the visual magnitude and the color on the C_1 system. The two-decimal magnitudes are from the *Revised Harvard Photometry;* the one-decimal magnitudes are photoelectric measures by Stebbins, Huffer, and Whitford (1940) or the magnitudes of Code and Whitford corrected by +0.1 mag. to reduce them to the Harvard visual system. If a weight is given after the color, the photometry is by Code and Whitford; if no weight is listed, the color and magnitude have been taken from the "1332 B stars."

Total interstellar absorptions and corrected distance moduli have not been included for two reasons: there are some ambiguities in the systemic chracteristics of certain color systems, and a revised calibration of the luminosity classes is now being carried out. A comparison of the present photometric data with other published results will not be given here.

Certain features of the notation in column 5 should be described. A colon (:) at any position in the spectral classification denotes uncertainty in the part of the type immediately preceding the colon. Occasionally a luminosity class is inclosed in parentheses in the case of some Be stars; this indicates a probably greater uncertainty, due to the possibility that spectral peculiarities may affect the luminosity classification. An "(e)" indicates that the star is almost certain to have $H\alpha$ in emission, from the appearance of $H\beta$, although no definite emission is observed at the latter position. A luminosity class followed by a question mark is uncertain, usually because of spectral peculiarities; in such cases the absolute magnitude of the star may not correspond to what might be deduced from the luminosity class.

Table 2 is similar in form to Table 1; however, some of the notation is not the same. The magnitudes are on the International photovisual system; that is, they are systematically brighter by 0.1 mag. than those of Table 1. All the magnitudes and colors in Table 2 are due to A. D. Code and T. E. Houck. The observations were made at the Radcliffe and Cape Observatories; the spectra were obtained with the Radcliffe reflector. Details of the observations will be published at a later time, together with a comparison of the photometry with that of other observers.

The spectral types of Table 2 are of somewhat lower accuracy than those in Table 1; this is principally due to a less favorable distribution of standard stars. In addition, there may be minor systematic differences in the classification.

We wish to thank the observers who obtained the spectrograms at Yerkes and McDonald. The photometry and spectrograms obtained in South Africa were the result of a grant to two of us (A. E. Whitford and A. D. Code) by the National Science Foundation. We also wish to express our thanks to the directors of the Radcliffe, Cape, and Mount Wilson Observatories for making their facilities available. One of us (W. W. Morgan) is indebted to Dr. D. L. Harris for help in the completion of the investigation.

REFERENCES

Johnson, H. L., and Morgan, W. W. 1953, *Ap. J.*, **117**, 313.
———. 1954, *ibid.*, **119**, 344.
Morgan, W. W. 1951, *Pub. Obs. U. Michigan*, **10**, 33.
Nassau, J. J., and Morgan, W. W. 1951, *Ap. J.*, **113**, 141.
Stebbins, Joel, Huffer, C. M., and Whitford, A. E. 1940, *Ap. J.*, **91**, 20.

TABLE 1

OB STARS

No	Star	R.A. 1900	Decl. 1900	MK	m	C_1
1	+60°2668	$0^h\ 00^m.8$	+60° 19'	B1 III	9.1	+0.06 (1)
2	108	0.9	+63 7	08 fp	7.36	.00
3	+59°2829	1.6	+60 4	B0: IV:pne		
4	593	5.3	+59 6	B1 V	6.70	- .14
5	1070	9.9	+59 15	A5 II:	8.1	+ .12 (3)
6	1337	12.5	+50 53	09 III	6.12	- .20
7	1383	12.9	+61 10	B1 II	7.8	- .02
8	+62°49	13.5	+63 1	B0.5 III		
9	1544	14.6	+61 31	B0 III:	8.5	- .06
10	+61°39	14.8	+61 54	B0.5 IV	9.0	.00
11	+63°33	16.3	+64 3	B1 V		
12	+60°39	16.4	+61 11	09 V		
13	1743	16.6	+61 38	B0 III	8.7	- .03
14	1810	17.4	+61 41	B0 IV	8.4	- .05
15	+61°74	20.3	+62 0	09 Vnn		
16	+62°79	20.8	+62 53	09.5 IV		
17	+60°51	21.0	+60 52	A2 Ib		
18	+63°48	21.0	+63 52	B1 (III:)nne		
19	236419	22.3	+60 4	B2 III		
20	+55°81	22.7	+55 51	B1.5: V:nn(e)		
21	2451	23.2	+61 57	B0.5 IV	8.9	- .12
22	2619	24.7	+64 43	B0.5 III	8.4	+ .11 (3)
23	+61°105	25.7	+61 53	09 V		
24	2905	27.3	+62 23	B1 Ia	4.24	- .09
25	2928	27.5	+61 59	A0 Iab		+ .06 (1)
26	+63°61	27.8	+63 27	B1 Iab		
27	3191	30.1	+60 55	B1 IV:nn	8.7	+ .04
28	+60°73	31.4	+60 49	B1 Ib		
29	Anon #1	34.2	+60 25	09 IV		
30	+63°70	34.9	+63 22	B0 Ib		
31	3940	36.9	+63 45	A1 Ia	7.40	+ .23
32	+61°153	37.1	+61 41	A0 Ib		
33	+64°76	38.9	+64 43	B1 Ib		
34	4613	43.0	+65 2	B1 II	8.9	+ .14 (3)
35	Anon #2	43.8	+60 27	B2: V:pnne		
36	4694	43.9	+64 5	B3 Ia	8.5	+ .26 (2)
37	4717	44.2	+62 37	A0 Ib	8.2	+ .18
38	+60°114	44.3	+60 22	B2 (III:)pe		
39	+61°175	44.6	+61 50	B3 II		
40	4768	$0^h\ 44^m.6$	+59° 7'	B5 Ib	7.9	+0.06

TABLE 1 (CONTINUED)

No	Star	R.A. 1900	Decl. 1900	MK	m	C_1
41	4841	$0^h\ 45^m.4$	+63° 14'	B5 Ia	7.07	+0.14
42	+63°102	46.3	+64 8	B1 II		
43	5005 br	47.0	+56 5	06	7.9	- .12
44	5005 ft	47.0	+56 5	09		
45	Anon #3	47.5	+60 16	B2: IVnn		
46	5394	50.7	+60 11	B0 IV:e	2.25	- .11
47	236589	52.1	+55 54	B1 II	9.0	
48	5551	52.2	+63 11	B1.5 Ib	7.7	+ .13
49	5552	52.2	+61 24	B1 Ia	9.1	+ .17 (2)
50	5689	53.5	+63 5	06	9.3	- .04
51	5776	54.3	+62 30	A0 Ib	8.2	+ .09 (1)
52	+62°183	54.9	+62 55	B1 V:p		
53	6182	57.8	+61 18	B1 Ibp	8.4	+ .07
54	6675	1 2.4	+69 10	B0.5 III	7.1	- .06
55	+60°180	5.8	+60 47	B0:: pe		
56	7103	6.2	+61 21	B3 Ib	8.4	+ .15
57	236664	7.5	+58 33	B0.5 V		
58	7252	7.7	+60 21	B1 V	7.26	- .10
59	7694	11.7	+54 54	B1 V	7.41	- .18
60	236689	12.3	+57 51	B1.5 (V)pe	10.6	- .07 (1)
61	+57°243	12.5	+57 41	B0: IV:e	9.8	+ .04 (1)
62	+57°252	13.3	+57 43	B1 IV		
63	7902	13.6	+57 40	B6 Ib	7.2	+ .03
64	7927	13.8	+57 42	F0 Ia	5.25	
65	+64°156	17.0	+65 5	B0.5 III		
66	+62°246	18.3	+62 16	B5 Ia		
67	236740	20.9	+59 46	B3 Ia	7.8	+ .06 (1)
68	8768	21.4	+62 45	09.5 IV	9.0	+ .02
69	8965	23.3	+59 44	B0.5 V	7.26	- .04
70	+61°277	23.9	+62 13	B0 IV:nn		
71	236762	24.5	+59 13	B1.5 III		
72	9105	24.6	+62 51	B5 Iab	7.46	+ .16
73	236768	25.2	+58 52	B1: nnV:p		
74	+60°261	25.9	+60 37	07		
75	9311	26.6	+60 10	B5 Ib	7.26	+ .07
76	+59°273	26.9	+60 7	B2 III		
77	+60°279	29.9	+60 28	B2 II		
78	+59°286	29.9	+59 26	B1 III:n		
79	236810	31.8	+60 4	B2 III	8.6	-0.04 (1)
80*	Anon #4	$1^h\ 32^m.2$	+57° 39'	06 fp		

TABLE 1 (CONTINUED)

No	Star	R.A. 1900	Decl. 1900	MK	m	C_1
81	236815	$1^h\ 32^m.8$	+59° 54'	B0.5 III	8.4	-0.07 (1)
82	+57°359	32.8	+57 20	B1: V:		
83	10063	33.3	+55 17	B8 Iab	7.5	- .04 (3)
84	10125	33.9	+63 40	O9.5 Ib	8.5	- .03
85	+61°312	36.0	+61 57	B1 III		
86	+62°297	36.1	+63 6	B1 Ib		
87	+55°393	37.6	+55 40	B1 V		
88	+60°331	38.8	+60 43	B8 Iab		
89	+60°333	39.0	+60 43	B5 Iab		
90	+60°339	39.3	+60 45	B6 Iab		
91	+60°343	39.4	+60 45	B2 II		
92	232522	39.6	+54 51	B1 II	8.5	- .16 (1)
93	10756	40.1	+60 10	B8 Ia	7.71	
94	10898	41.9	+57 58	B2 Ib	7.4	- .01
95	+63°247	42.1	+63 49	B0 III		
96	+54°395	45.2	+54 58	B0 IV:p		- .04 (1)
97	236894	45.4	+57 57	O8 V	9.2	- .04 (1)
98	232552	45.8	+54 51	B0 pe	8.2	+ .01
99	+63°253	46.3	+63 42	B0 III		
100	+54°404	46.6	+54 37	B1 III		
101	11554	48.4	+57 24	B1 Vpe	9.5	.00
102	+55°441	49.3	+56 3	B1 (V)pe		
103*	+63°261	50.3	+63 32	B pnne		
104	11831	51.1	+59 54	A2 Ia	8.2	+ .25 (3)
105	+58°343	52.0	+58 26	B2 III		
106	+58°351	53.6	+58 29	B1 III		
107	12301	55.6	+63 54	B8 Ib	5.62	+ .05
108	12302	55.6	+59 12	B1: V:pe	8.1	- .05
109	12323	55.8	+55 8	O9 V	9.0	- .12 (3)
110	232588	57.1	+54 38	B1.5 III	8.7	- .14 (1)
111	236935	57.2	+58 0	B1: V:ne		
112	12509	57.6	+63 54	B1 III	7.2	- .03 (3)
113	12567	58.1	+63 49	B0.5 III	9.5	.00 (1)
114	12727	59.6	+56 34	B2 III	9.1	- .11 (3)
115	12856	$2\ 0.9$	+56 38	B0 pe	8.6	- .06
116	12867	1.0	+57 14	B1 V	9.5	- .08 (3)
117	12882	1.1	+64 33	B6 Ia	7.54	- .01
118	12953	1.7	+57 57	A1 Ia	5.90	+ .06
119	12993	2.1	+57 27	O5	9.1	- .05 (4)
120	13051	$2^h\ 2^m.6$	+56° 31'	B1 IV::	8.7	-0.07

TABLE 1 (CONTINUED)

No	Star	R.A. 1900	Decl. 1900	MK	m	C_1
121	+63°300	$2^h\ 3^m.0$	+63° 36'	B pe		
122	13267	4.6	+57 11	B5 Ia	6.36	-0.01
123	13268	4.6	+55 41	O8 Vnn	8.1	- .12
124	13338	5.3	+57 28	B1 V	9.3	- .03 (4)
125	+57°513	5.6	+57 38	B1 III		
126	+57°515	5.7	+57 13	B1: pe		
127	13402	5.9	+59 4	B0.5 I	8.2	+ .11 (4)
128	13476	6.6	+58 6	A3 Iab	6.50	+ .16
129	13494	6.7	+56 6	B1 III	9.4	- .05 (4)
130	13544	7.1	+53 27	B0.5 IV		
131	13561	7.3	+56 2	B0.5 V:p?	8.9	- .10 (4)
132	+54°490	7.3	+54 35	B1 V		
133	13590	7.6	+63 34	B2 III		+ .02
134	13621	7.8	+54 51	B1 V	8.2	- .13 (4)
135	13659	8.1	+56 28	B1 Ib	8.8	+ .07 (4)
136	13716	8.6	+57 18	B0.5 III	8.4	- .06
137	13744	8.9	+57 50	A0 Iab	7.8	+ .20
138	13745	8.9	+55 32	B0 III	7.96	- .09
139	13758	9.0	+57 17	B1 V	9.2	+ .01 (4)
140	13831	9.7	+56 17	B0 IIIp?	7.9	- .14
141	13841	9.8	+56 34	B2 Ib	7.21	- .07
142	13854	9.9	+56 36	B1 Iab	6.42	- .04
143	13866	10.0	+56 15	B2 Ib	7.4	- .06
144	+56°473	10.0	+56 39	B1 II:		
145	13890	10.2	+56 19	B1 III:pe	8.6	- .02 (3)
146	13900	10.3	+56 26	B1 IV		
147	+56°482	10.7	+56 43	B1 III?p	9.7	- .03 (2)
148	+56°484	10.8	+56 26	B0: V:ne		
149	13969	10.8	+56 38	B1 IV:	8.7	- .08
150	14010	11.1	+63 58	B9 Ia	7.05	+ .10
151	14014	11.1	+55 46	B0.5 V	8.9	- .08 (3)
152	+56°493	11.2	+56 24	B1 V:pe:		
153	14052	11.4	+56 45	B1 Ib	8.3	+ .03 (1)
154	14053	11.4	+56 33	B1 II	8.3	- .07
155	14092	11.7	+56 18	B1 V	9.4	- .04 (3)
156	14134	12.1	+56 40	B3 Ia	6.66	+ .03
157	14143	12.2	+56 43	B2 Ia	6.66	+ .06
158	14162	12.4	+56 41	B0.5 V		
159	14250	13.2	+56 39	B0.5 V:n		
160	14302	$2^h\ 13^m.6$	+55° 52'	B1 II-III	8.4	-0.04

TABLE 1 (CONTINUED)

	No	Star	R.A. 1900	Decl. 1900	MK	m	C_1	
	161	14322	$2^h\ 13^m.8$	+55° 27'	B8 Ib	6.84	0.00	
	162	14331	13.9	+55 22	B0 III	8.5	- .11	(2)
	163	14357	14.1	+56 25	B2 II	8.6	+ .04	(2)
(4)	164	14422	14.7	+56 56	B1 V:pe	10.5	+ .10	(3)
	165	14433	14.8	+56 47	A1 Ia	6.54	+ .13	
	166	14434	14.8	+56 27	06	8.4	- .09	
(4)	167	14442	14.9	+59 6	05.5	9.3	+ .04	
	168	14443	14.9	+56 42	B2 Ib			
(4)	169	14489	15.3	+55 23	A2 Ia	5.22	+ .04	
	170	14501	15.4	+57 42	B3 V:n	9.5	+ .02	(3)
(4)	171	14520	15.6	+56 38	B2 II	9.2	- .09	(1)
	172	+56°589	15.7	+57 2	B1 III			
	173	14535	15.8	+56 47	A2 Iap?	7.46	+ .21	
(4)	174	14542	15.9	+56 56	B8 Ia	6.95	+ .17	
(4)	175	14605	16.5	+56 8	B0.5 (V)pe	10.2	+ .15	
	176	14633	16.7	+41 2	08 V	7.3	- .30	
	177	+56°606	17.7	+57 2	B1 II			
	178	14818	18.2	+56 10	B2 Ia	6.24	+ .06	
(4)	179	14899	19.2	+56 47	B8 Ib	7.5	+ .04	(3)
	180	14947	19.5	+58 25	06 f	8.04		
	181	14956	19.6	+57 14	B2 Ia	7.32	+ .16	
	182	15137	21.2	+52 6	09.5 V	7.9	- .15	(1)
	183	15316	22.8	+57 22	A3 Iab	7.30	+ .30	
	184	15325	22.9	+56 48	B1 IV			
(3)	185	+60°493	23.3	+60 43	B0.5 Ia			
	186	+62°411	23.9	+62 58	B1 Ib-II			
(2)	187	+60°497	24.3	+61 10	07	9.0	+ .12	(1)
	188	+60°498	24.5	+61 6	09 V	9.5	+ .22	(1)
	189	15497	24.6	+57 15	B6 Ia	7.20	+ .26	
	190	+60°501	24.9	+61 2	06.5	8.0	+ .10	(1)
(3)	191	15548	25.0	+56 13	B1 V			
	192	15558	25.1	+61 1	06	7.82	+ .12	
(1)	193	15570	25.2	+60 56	05 f		+ .20	
	194	15571	25.2	+56 59	B1 II:		+ .02	
(3)	195	15620	25.6	+57 31	B8 Iab			
	196	15629	25.7	+61 5	05	8.9	+ .12	(2)
	197	15642	25.8	+54 54	B0 III:	8.6	- .18	
	198	15690	26.3	+57 5	B1.5 Ib		+ .18	
	199	+60°512	$26^m.4$	+60 57	06	9.2	+ .15	(1)
	200	15752	$2^h\ 26^m.8$	+57° 58'	B0 III	8.8	+0.09	

TABLE 1 (CONTINUED)

No	Star	R.A. 1900	Decl. 1900	MK	m	C_1
201	15785	2^h $27^m.2$	+60° 6'	B1 Iab	8.41	+0.08
202	+62°419	27.2	+63 8	B0: V?	9.9	+ .01 (1)
203	+62°424	28.4	+62 30	08	9.0	+ .06 (1)
204	16243	31.3	+57 23	B2 II:	8.4	+ .11
205	16310	32.0	+58 38	B1 II:	8.2	+ .14 (2)
206	16429	33.1	+60 51	09.5 III	7.9	+ .20 (1)
207	16691	37.5	+56 28	05 f	8.9	+ .07 (2)
208	16778	36.3	+59 24	A2 Ia	7.71	+ .39
209	16779	36.3	+57 24	B2 Ib		
210	16808	36.7	+57 53	B0.5 Ib		
211*	16832	36.9	+56 14	B0 p	7.54	+ .25
212	17088	39.5	+57 19	B9 Ia		
213	17114	39.7	+58 55	B1 V		+ .28
214	17145	40.0	+57 15	B8 Ia	6.4	+ .28 (2)
215	17378	42.2	+56 40	A5 Ia		
216	237007	42.7	+59 59	B0 V	7.11	+ .01
217	17505	43.4	+60 1	07	8.2	.00 (3)
218	17520	43.5	+59 59	08 V	8.6	+ .25 (1)
219	17603	44.4	+56 38	07 f:		
220	+59°562	45.7	+60 3	08 V		
221	+60°586	46.4	+60 14	07	8.5	- .02 (1)
222	17857	47.0	+63 43	B8 Ib	7.78	+ .16
223	+60°594	49.1	+60 59	09 V	9.5	+ .02 (1)
224	18076	49.2	+58 41	B0 II-III		
225	+60°596	49.3	+60 15	B1 V:n	9.7	+ .01 (1)
226	18326	51.6	+60 10	08	7.91	+ .05
227	+51°659	51.7	+51 42	B0 IIInn	7.00	- .08
228	18352	51.9	+60 53	B1 V		.00
229	18409	52.4	+62 19	09 Ib		
230	237056	55.0	+57 13	B0.5: V:pe		
231	19243	3 0.7	+62 0	B1 V:e	6.54	+ .06
232	19820	6.2	+59 11	09 IV	7.09	+ .09
233	237090	7.2	+59 33	B0.5 IV:nn		
234	237091	7.3	+59 33	B1: V:pnne		
235	+51°704	9.2	+51 38	B1 V:nn		
236	+51°710	11.7	+51 39	B5 Ib		
237	237121	12.7	+58 30	B0.5 V		
238	+49°916	17.0	+49 17	B3 p shell	10.7	+ .19 (1)
239	20898	$17^m.1$	+60 8	B2 III	8.1	+ .06 (2)
240	20959	3^h $17^m.8$	+59° 5'	B3 III	8.1	0.00 (2)

TABLE 1 (CONTINUED)

No	Star	R.A. 1900	Decl. 1900	MK	m	C_1
241	21212	$3^h\ 20.^m3$	+62° 9'	B2 V:e	8.3	+0.11
242	21291	21.0	+59 36	B9 Ia	4.42	+ .06
243	21389	21.9	+58 32	A0 Ia	4.76	+ .13
244	21483	22.7	+30 2	B3 III	7.06	+ .11
245	21856	26.3	+35 6	B1 V	5.80	- .14
246	22253	29.9	+56 23	B0.5 III	6.79	- .04
247	22951	36.0	+33 39	B0.5 V	5.04	- .10
248	23180	38.0	+31 58	B1 III	3.94	- .08
249	23675	41.9	+52 21	B0.5 III	6.76	+ .08
250	23800	42.9	+52 11	B1 IV	6.87	+ .01
251	24131	45.5	+34 3	B1 V	5.73	- .08
252	24398	47.8	+31 35	B1 Ib	2.91	- .04
253	24431	48.1	+52 21	O9 IV-V	6.70	.00
254	24432	48.1	+48 45	B3 II	7.02	+ .09
255	24534	49.1	+30 45	O pe (var)	var	+ .04
256	+55°837	50.2	+55 38	B2 Ib		
257	24760	51.1	+39 43	B0.5 V	2.96	- .20
258	Anon #7	51.2	+56 56	O7.5		
259	+56°864	51.2	+56 57	O6 nn		
260	+56°866	51.4	+56 49	O9 V		
261	237204	52.4	+56 37	B0.5 V		
262	24912	52.5	+35 30	O7	4.05	- .14
263	+55°838	52.9	+55 12	B3 Ib		
264	232874	54.5	+53 27	B0.5 V		
265	237211	55.3	+56 15	O9.5 I?p		
266	237213	56.5	+55 43	B3 Ia		
267	25348	56.6	+53 3	B1 Vpnne	8.4	- .04
268	25443	57.4	+61 48	B0.5 III	6.75	+ .02
269	25517	58.1	+44 0	B1 V	9.3	- .01
270	25638	59.1	+62 4	B0 II-III	7.0	+ .08
271	25914	4 1.2	+56 50	B6 Ia	8.1	+ .13
272	232947	17.5	+53 11	B0 Ia		
273	+51°921	17.7	+51 49	B0 II		
274	28446	24.1	+53 42	B0 III	5.86	- .08
275	28497	24.5	-13 17	B1 Vn	5.50	- .15
276	29248	31.3	- 3 33	B2 III	4.12	- .22
277	232999	37.0	+50 20	B1 IV		
278	30614	44.1	+66 10	O9.5 Ia	4.38	- .14
279	30836	45.9	+ 5 26	B2 III	3.78	- .20
280	31237	$4^h\ 49.^m0$	+ 2° 17'	B2 III	3.87	-0.21

TABLE 1 CONTINUED)

No	Star	R.A. 1900	Decl. 1900	MK	m	C_1	
281	31327	4^h $49^m.7$	+36° 1'	B2 Ib	6.18	+0.08	
282	+30°748	51.9	+30 32	B1.5 V			
283	31726	53.1	-14 24	B1 V	5.87	- .20	
284	+43°1168	55.0	+43 42	B9 Iab			
285	+40°1189	5 3.3	+40 33	B2: III:nn			
286	33203	3.5	+37 11	B2 II: + K?	6.17	+ .21	
287	33357	4.6	+42 2	B1: (V)ne		- .09	(3)
288	33461	5.3	+41 6	B2: V:nne	7.9	- .05	
289	33604	6.3	+40 5	B2 V:pe	7.32	- .12	
290	34078	9.7	+34 12	09.5 V	5.81	- .07	
291	34085	9.7	- 8 19	B8 Ia	0.34	- .13	
292	34656	14.0	+37 20	07	6.71	- .06	
293	+39°1264	14.2	+39 14	B2 V			
294	34816	15.0	-13 17	B0.5 IV	4.29	- .22	
295	34921	15.8	+37 35	B0 IV:pe	7.39	- .01	
296	242908	16.0	+33 25	05	9.1	- .04	(2)
297	242926	16.1	+33 13	06	9.3	.00	(2)
298	242935	16.2	+33 19	08	9.3	- .05	(2)
299	34989	16.4	+ 8 20	B1 V	5.71	- .18	
300	35149	17.6	+ 3 27	B1 V	4.99	- .20	
301	35215	18.1	+30 6	B1 V	9.11	- .12	(1)
302	35345	19.0	+35 33	B1 Vpe	8.4	- .03	
303	35347	19.0	+29 32	B1: (V:)e		- .12	(1)
304	35395	19.3	+20 30	B0.5 III:	6.83	+ .02	
305	+42°1286	19.3	+42 57	B0.5 V			
306	35411	19.4	- 2 29	B0.5 V	3.44	- .22	
307	35439	19.6	+ 1 45	B1 V:pe	4.73	- .16	
308	35468	19.8	+ 6 16	B2 III	1.70	- .24	
309	+42°1288	20.1	+42 14	B8 Ib			
310	35600	20.8	+30 7	B9 Ib	5.72	- .02	
311	35619	21.0	+34 41	07	8.5	- .02	
312	35633	21.1	+34 27	B0.5 IV	7.9	- .01	
313	35653	21.2	+33 52	B0.5 V	7.50	- .04	
314	+34°1058	21.9	+34 34	08 nn			
315	35921	23.0	+35 18	09.5 III	6.71	- .02	
316	35952	23.2	+35 53	B5 II-III	9.1	+ .01	(3)
317	+35°1141	23.3	+35 8	B0.5: V:n			
318	+39°1328	25.1	+40 0	09 III?			
319	36212	$25^m.1$	+34 48	B3 II	7.9	- .05	(3)
320	36280	5^h $25^m.5$	+34° 52'	B0.5 IVn	9.0	-0.12	

TABLE 1 (CONTINUED)

No	Star	R.A. 1900	Decl. 1900	MK	m	C_1	
321	36371	5^h $26^m.2$	+32° 7'	B5 Iab	4.88	0.00	
322	36483	26.9	+36 24	09.5 III	8.4	+ .04	
323	36485	26.9	- 0 22	B2 V	6.87		
324	36486	26.9	- 0 22	09.5 II	2.48	- .23	
325	36512	27.1	- 7 23	B0 V	4.64	- .18	
326	36547	27.4	+23 16	B1 III	9.0	.00	
327	36591	27.6	- 1 40	B1 V	5.30	- .20	
328	+35°1169	27.6	+35 45	B1: V:pe			
329	36695	28.5	- 1 14	B1 V	5.37	- .21	
330	36822	29.3	+ 9 25	B0 IV	4.53	- .18	
331	36861	29.6	+ 9 52	08	3.66	- .22	
332	36879	29.7	+21 20	06	7.5	- .06	
333	36959	30.1	- 6 5	B1 V	5.58		
334	36960	30.1	- 6 5	B0 Vp	4.67	- .24	
335	37017	30.4	- 4 34	B2 V	6.54	- .14	
336	37018	30.4	- 4 54	B2 III	4.65	- .19	
337	37022	30.4	- 5 27	06 p	5.36	- .02	
338*	245310	30.4	+21 8	B2 : III::nnep			
339	37032	30.5	+34 45	B0.5 V	8.1	- .06	(2)
340	37041	30.5	- 5 29	09.5 Vp	5.17	- .16	
341	37043	30.5	- 5 59	09 III	2.87	- .23	
342	37128	31.1	- 1 16	B0 Ia	1.75	- .20	
343	245493	31.1	+33 53	B2: V:p(e)			
344	37303	32.5	- 6 0	B1 V	5.75	- .24	
345	37468	33.7	- 2 39	09.5 V	3.78	- .16	
346	37490	33.9	+ 4 4	B3 IIIe	4.54	- .17	
347	37614-5	34.7	+38 8	B2 III	8.?	- .12	(1)
348	37737	35.7	+36 9	B0 II:	8.1	- .02	(3)
349	37742	35.7	- 2 0	09.5 Ib	2.05	- .22	(3)
350	37767	35.9	+36 6	B3 V	9.1	- .15	(1)
351	+34°1150	36.5	+34 18	B2 V			
352	+37°1292	36.9	+37 57	B3 V:p(e)			
353	38010	37.5	+25 24	B1 V:pe	6.86	- .09	
354	38017	37.6	+30 53	B3 II		+ .16	(1)
355	246901	38.3	+33 29	B1: + G5:Ib:			
356	38131	38.4	+35 8	B0.5 V	8.3	- .06	(2)
357	+34°1162	38.4	+34 2	B2 V:nn			
358	38191	38.9	+21 25	B1: (V)n(e)	8.6	-0.05	
359	+36°1261	41.7	+36 12	B2 III?p?			
360	38658	5^h $42^m.3$	+28° 17'	B3 II			

TABLE 1 (CONTINUED)

No	Star	R.A. 1900	Decl. 1900	MK	m	C_1
361	38666	5^h $42^m.3$	-32° 20'	09.5 V	5.20	
362	38708	42.6	+29 6	B3: p(e)	8.4	-0.13 (1)
363	38771	43.0	- 9 42	B0.5 Ia	2.20	- .16
364	38909	44.0	+31 2	B3 II-III	8.2	- .16 (1)
365	39136	45.4	+32 13	B3 III		- .11 (1)
366	248587	46.5	+19 7	A0 Iab		
367	248893	48.0	+22 6	B0 II-III		
368	248894	48.0	+20 51	08:V:nn		
369	39680	49.0	+13 49	06: pe		- .13 (1)
370	39712	49.2	+30 41	B2 IV	8.2	- .13 (2)
371	39746	49.4	+27 42	B1 II	7.1	- .06
372	39970	50.9	+24 14	A0 Ia	6.02	+ .06
373	40003	51.1	+23 25	B3 Ib		+ .25 (1)
374	40111	51.8	+25 57	B1 Ib	4.90	- .16
375	249695	52.2	+30 12	B1: V:pnne		
376	40297	52.8	+27 33	A0 Ib	7.4	- .04 (1)
377	249845	53.0	+32 53	B2: V:nn		
378	250028	53.8	+25 6	B2: V:pnne		
379	250163	54.4	+19 11	B1.5: V:pne		
380	40589	54.7	+27 35	B9 Iab:	6.1	- .05 (1)
381	250289	55.0	+23 20	B2 III:e		
382	250290	55.0	+23 18	B3 Ib		
383	40893	56.7	+31 2	B0 IV		
384	40894	56.7	+28 40	B2 V	7.6	- .22 (4)
385	41117	58.0	+20 8	B2 Ia	4.71	- .02
386	251117	58.7	+28 46	B0 IV	9.3	- .19 (2)
387	251311	59.4	+23 1	B1.5: IV:n	8.8	
388	41398	59.8	+28 56	B2 Ib	7.45	- .02
389	251726	6 1.0	+19 2	B1 V:e		
390	251847	1.4	+23 45	B1 IV		
391	41690	1.6	+21 53	B1 V	7.8	- .04
392	252321	3.1	+23 54	B1 V		
393	41997	3.2	+15 44	O7		
394	42087	3.7	+23 8	B2.5 Ib	5.76	- .05
395	42088	3.7	+20 31	O6	7.40	- .13
396	42379	5.3	+21 36	B1 II	7.6	.00
397	42400	5.4	+20 56	B5 II	6.86	- .03
398	253049	5.8	+20 10	B2 IV		
399	253214	$6^m.4$	+20 7	B1.5: V:nn	9.4	+0.02
400	253247	6^h $6^m.5$	+18° 3'	B1 V		

TABLE 1 (CONTINUED)

No	Star	R.A. 1900	Decl. 1900	MK	m	C_1
401	253659	6^h $8^m.1$	+16° 33'	B0.5: V:nne		
402	42896	8.2	+20 13	B1: V:nn		
403	43078	9.2	+22 20	B0 IV	8.9	+0.03
404	43112	9.4	+13 53	B1 V	5.81	- .27
405	254042	9.8	+24 6	B0.5: IV:nn		
406	43384	10.8	+23 46	B3 Iab	6.26	+ .01
407	254577	11.8	+22 26	B0.5 II-III		
408	43582	11.9	+22 41	B0 IIIn	8.9	+ .01 (2)
409	254699	12.3	+23 36	B1 V		
410	254755	12.5	+22 43	O9 V:p?		
411	43703	12.6	+23 3	B1 IV:p?	8.9	+ .04
412	43753	12.9	+23 2	B0.5 III	8.1	- .03
413	43818	13.2	+23 30	B0 II	7.03	.00
414	43836	13.3	+23 19	A0 II	7.03	+ .11
415	43837	13.3	+20 37	B2 Ibp?	8.6	+ .13 (1)
416	255055	13.6	+23 20	O9 V:p		
417	43907	13.7	+22 9	B1 V:p?	8.7	- .04 (2)
418	44139	15.1	+22 13	B0.5 V		
419	44458	16.8	-11 44	B1 Vpe	5.49	- .09
420	256035	16.9	+22 55	O9 V:p		
421	44506	17.0	-34 6	B1.5 V:	5.60	
422	44597	17.5	+20 27	O9 V		- .04 (1)
423	44637	17.7	+15 9	B2 V:pe	8.1	.00
424	256276	17.7	+22 27	B1.5: V:nn		
425	256413	18.1	+19 58	B5 III		
426	44743	18.3	-17 54	B1 II-III	1.99	- .18
427	44811	18.8	+19 45	O7.5 V		- .03 (1)
428	44965	19.6	+11 45	B3 II		
429	45166	20.8	+ 8 3	B pe	9.7	- .15
430	45314	21.6	+14 57	O9? pe	7.09	- .06
431	257971	23.1	+11 22	B0.5 III		
432	45626	23.4	- 4 23	B7 pe shell		
433*	45910	25.2	+ 5 57	B2: III:pe	6.70	.00
434	45995	25.6	+11 19	B2 V:nne	5.83	- .16
435	46056	26.0	+ 4 54	O8	7.96	- .06
436	46149	26.6	+ 5 6	O8	7.66	- .09
437	46150	26.6	+ 5 0	O6	6.80	- .04
438	46202	26.9	+ 5 3	O9 V	8.16	- .10
439	46223	27.0	+ 4 53	O5	7.14	- .04
440	46300	6^h $27^m.5$	+ 7° 24'	A0 Ib	4.50	-0.13

TABLE 1 (CONTINUED)

No	Star	R.A. 1900	Decl. 1900	MK	m	C_1
441	46328	$6^h\ 27.^m6$	-23° 21'	B0.5 IV	4.35	-0.21
442	259431	27.6	+10 24	B6 pe	8.9	- .11
443	259440	27.6	+ 5 52	B0: pe		
444	259597	28.1	+ 8 24	B0.5: V:nne	8.6	- .16
445	46484	28.6	+ 4 44	B1 V	7.65	
446	46485	28.6	+ 4 36	08	8.4	.00
447	46559	29.0	+ 2 28	B8 I		
448	46573	29.1	+ 2 36	07	8.5	- .02
449	46660	29.5	+11 12	B1 V		
450	46711	29.8	+ 2 51	B3 II		
451	46783	30.2	+ 9 56	B9 Ib	7.92	
452	46847	30.5	+ 2 47	B0 III:p		
453	46883	30.7	+10 22	B0.5: V	8.1	+ .05
454	46966	31.1	+ 6 10	08		- .16
455	47129	32.0	+ 6 13	08	6.06	- .12
456	47240	32.5	+ 5 3	B1 Ib	6.16	- .06
457	47360	33.1	+ 4 43	B0.5 V		
458	47359	33.1	+ 4 58	B0.5 V(pe)	8.81	
459	47382	33.2	+ 4 42	B0 III		
460	47417	33.4	+ 7 0	B0 IV		- .10
461	47432	33.5	+ 1 42	09.5 II	6.13	- .05
462	47761	35.1	- 4 36	B2 V:pe	8.4	- .06
463	-0°1385	35.2	- 0 16	08		
464	47839	35.5	+ 9 59	07	4.68	- .25
465	47887	35.7	+ 9 34	B2 III:	7.02	- .21
466	48099	36.6	+ 6 27	06	6.20	- .18
467	48279	37.5	+ 1 49	08	7.4	- .02
468	48282	37.5	-10 24	B3 III		
469	48434	38.3	+ 4 2	B0 III	5.78	- .15
470	48615	39.2	+12 11	B1 V		
471	48663	39.4	+12 21	B1 V		
472	48691	39.5	+ 0 42	B0.5 IV		
473	+0°1576	39.7	+ 0 43	09 III:		
474	49330	42.8	+ 0 53	B0: pnne	8.79	
475	49567	43.9	+ 1 6	B3 II-III	6.06	- .19
476	49585	44.0	+ 0 12	B0.5: (V)nn		
477	49787	45.0	- 5 24	B1 V:pe	7.30	- .14
478	49977	45.9	-14 0	B1.5: V:pne	8.1	- .05
479	49992	$46.^m0$	- 5 13	B1: pne		
480	50064	$6^h\ 46.^m4$	+ 0° 25'	B6: Ia	8.3	+0.22 (2)

TABLE 1 (CONTINUED)

No	Star	R.A. 1900	Decl. 1900	MK	m	C_1
481	50083	6^h $46^m.5$	+ 5° 13'	B2: V:nne	6.76	-0.11
482	50091	46.5	-13 7	B3 pe shell	8.6	- .13
483	50696	49.2	+ 0 18	B1: (V)nne		
484	50707	49.2	-20 6	B1 IV	4.66	- .20
485	50891	50.0	- 3 34	B0: pe		
486	51193	51.3	- 3 40	B1 V:nn	8.4	- .16 (1)
487	51283	51.6	-22 49	B3 II-III	5.26	
488	51309	51.7	-16 55	B3 II	4.39	
489	51452	52.3	- 4 4	B0: III:nn		
490	51480	52.4	-10 41	P Cyg	6.97	+ .02
491	51756	53.5	- 2 53	B0.5 IV	7.3	- .14 (1)
492	52089	54.7	-28 50	B2 II	1.63	
493	52244	55.3	-16 3	B2: III:pne		
494	52266	55.4	- 5 40	O9 V	6.97	- .16
495	52382	55.9	- 9 4	B1 Ib	6.36	- .05
496*	52504	56.4	- 3 0	B1: V:	9.5	- .18 (1)
497	52533	56.5	- 2 59	O9 V		
498	+0°1769	57.3	+ 0 39	B3 III		
499	52918	57.9	- 4 6	B1 V	4.89	- .20
500	53032	58.4	- 2 36	B6: (IV:)	9.5	- .19 (1)
501	53138	58.8	-23 41	B3 Ia	3.12	
502	53367	59.7	-10 18	B0 IV:e	7.01	+ .06
503	53428	59.9	- 8 42	B2 Ib	8.6	+ .04
504	53649	7^h 0.7	- 8 52	B0.5 III		
505	53667	0.8	- 8 34	B0.5 III	7.7	- .06
506	53754	1.1	- 8 39	B1 II		
507	53755	1.1	-10 30	B0 V:	6.5	- .16 (1)
508	53756	1.1	-12 40	B2 IV	7.20	
509	53974	2.0	-11 8	B0.5 IV	5.28	- .12
510	53975	2.0	-12 14	O8	6.40	- .19
511	54439	3.7	-11 42	B2 IIIn		
512	54464	3.8	- 3 54	B2: (V)pe		
513	54493	3.9	-12 43	B2 III	7.00	
514	-0°1618	3.9	- 0 52	B1 V:ne		
515	54662	4.6	-10 11	O6	6.20	- .15
516	54764	5.0	-16 4	B1 II	6.03	-0.09 (2)
517	54786	5.1	-15 56	B0: pe		
518	54879	5.5	-11 39	O9.5 V		
519	54911	5.6	-15 31	B2 II	7.03	
520	55036	7^h $6^m.2$	- 4° 32'	A3 Ib		

TABLE 1 (CONTINUED)

No	Star	R.A. 1900	Decl. 1900	MK	m	C_1	
521	55538	$7^h\ 8^m.2$	-15° 19'	B2 III	7.8	-0.15	
522	55606	8.5	- 1 54	B1: V:pnne	8.72		
523	55879	9.7	-10 8	B0 IV	5.99	- .23	
524	56310	11.4	-16 3	B1 V	6.79		
525	56847	13.6	-15 27	B7 Ib? shell?	8.9	- .03	
526	57060	14.5	-24 23	07 f(var)	4.90v	- .23	
527	57061	14.5	-24 47	09 III	4.40	- .25	
528	57386	15.9	- 8 15	B1.5: V:pnne			
529	57682	17.2	- 8 48	09 V	6.17	- .20	
530	58350	20.1	-29 6	B5 Ia	2.43		
531	58439	20.5	-18 49	A2 Ib	6.27		
532	58644	21.4	- 8 54	B2 IV			
533	58978	22.8	-22 53	B0 IV?pe	5.48	- .22	
534	59075	23.2	-18 17	B8 I:			
535	59094	23.3	-15 53	B2 V:nne			
536	59612	25.6	-22 49	A5 Ib	4.80		
537	60308	28.7	-15 14	B2 Iab	8.30	+ .05	
538	60325	28.8	-14 7	B1 V	6.24	- .14	
539	60848	31.4	+17 7	08 V:pe	7.2	- .22	
540	60855	31.4	-14 16	B2 IV:e?	5.57	- .16	
541	61068	32.3	-19 29	B2 III	5.7	- .23	(2)
542	61347	33.7	-13 38	09 Ib	8.6	- .08	
543	62532	39.3	-17 42	B1: V:pnne			
544	63462	43.9	-25 42	B0 V:pe	4.59	- .18	
545	64993	51.4	-23 48	B1 III	7.5	- .14	
546	66665	59.5	+ 6 29	B1 V	7.6	- .21	
547	66811	8 0.1	-39 43	O5 f	2.27		
548	76510	51.5	-13 31	B1 V	8.0	- .23	
549	87737	10 1.9	+17 15	A0 Ib	3.58	- .15	
550	91316	27.5	+ 9 49	B1 Ib	3.85	- .20	
551	93521	42.7	+38 6	09 Vp	6.89	- .26	
552	104337	11 55.7	-19 6	B1.5 V	5.28		
553	116658	13 19.9	-10 38	B1 V	1.21	- .23	
554	119608	39.1	-17 26	B1 Ib	7.32		
555	143018	15 52.8	-25 50	B1 V	3.00	- .24	
556	143275	54.4	-22 20	B0 V	2.54	- .21	
557	144217	59.6	-19 32	B0.5 V	2.90	- .20	
558	144470	16 1.0	-20 24	B1 V	4.13	- .17	
559	147165	$15^m.1$	-25 21	B1 III	3.08	- .10	
560	149363	$16^h\ 29^m.1$	- 5° 56'	B0.5 III	7.9	-0.14	

TABLE 1 (CONTINUED)

No	Star	R.A. 1900	Decl. 1900	MK	m	C_1	
561	149438	16^h $29^m.7$	-28° 1'	B0 V	2.91	-0.26	
562	149757	31.7	-10 22	09.5 V	2.70	- .13	
563	149881	32.4	+14 40	B0.5 III	6.59	- .19	
564	151890	45.1	-37 53	B1.5 V	3.09		
565	154445	17 0.4	- 0 45	B1 V	5.62	- .11	
566	157857	20.7	-10 55	07 f	7.43	- .12	
567	158661	25.4	-17 3	B0.5 Ib	8.2	- .06	
568	159176	28.1	-32 31	07	5.71	- .10	
569	159864	31.8	-17 46	B0.5 II	8.6	- .02	
570	160186	33.4	-18 21	B0.5 V	9.0	- .09	
571	160233	33.7	+ 4 24	B1 V			
572	161961	43.4	- 2 9	B0.5 III	7.9	- .04	
573	162064	44.0	-19 52	B0 Ia	8.98	+ .16	
574	163800	52.9	-22 30	08	6.92	.00	
575	163892	53.4	-22 27	09 IV	7.14	- .04	
576	164002	53.9	-22 33	B0.5 V	7.15	- .13	
577	164188	54.9	-15 48	B0.5 IV	8.7	+ .05	
578	164353	55.6	+ 2 56	B5 Ib	3.92	- .12	
579	164359	55.6	-22 7	B0 III	7.4	- .10	
580	164384	55.7	-23 10	B1.5: V:nn	8.4	- .14	
581	164402	55.8	-22 46	B0 Ib	5.73	- .14	
582	164438	56.0	-19 6	09 IV	7.28	+ .02	
583	164492	56.3	-23 1	07	6.91	+ .03	
584	164514	56.4	-22 54	A5 Ia	7.28	+ .36	(2)
585	164581	56.7	-20 44	B1 V	6.85	- .10	(2)
586	164637	57.0	-22 43	B0.5 III	6.57	- .16	
587	164794	57.7	-24 22	05	5.86	- .15	
588	164816	57.8	-24 19	B0 V	7.1	- .14	
589	164833	57.9	-22 50	B0 III	6.86	- .14	
590	164844	58.0	-22 34	B1 V	8.0	- .16	
591	164883	58.1	-22 30	B0 V	7.1	- .14	
592	-22°4543	58.2	-22 29	B1 V:n	9.0	- .15	(2)
593	164906	58.3	-24 24	B1 IV:pe	7.5	- .06	
594	165049	59.0	-15 22	B2 III	8.07	+ .09	
595	165052	59.0	-24 24	07	6.79	- .09	
596	165174	59.6	+ 1 55	B0.5 III	6.09	- .12	
597	165285	18 0.1	-19 58	B0.5 V:nne	8.73	+ .02	
598	165319	0.3	-14 12	B0 Ia	8.2	+ .11	
599	-17°5020	$0^m.7$	-17 13	B0 III	9.5	+ .14	(2)
600	165516	18^h $1^m.2$	-21° 27'	B0.5 Ib	6.22	-0.09	

TABLE 1 (CONTINUED)

No	Star	R.A. 1900	Decl. 1900	MK	m	C_1	
601	165783	18^h $2^m.6$	-19° 52'	B1: V	8.38	-0.01	(2)
602	165784	2.6	-21 28	A2 Ia	6.58	+ .28	(2)
603	165832	2.8	-19 24	B5 III		- .04	(2)
604	165921	3.2	-24 1	O7.5 nn(V)	7.4	- .08	
605	166125	4.1	-14 12	B3 II-III	9.1	+ .09	
606	166167	4.3	-21 20	B9 Ib		+ .13	(2)
607	166188	4.4	-18 13	B2 V:pe	9.0	+ .09	
608	166286	4.8	-16 46	B1 II	7.58	- .01	
609	166287	4.8	-16 50	B0.5 III	7.6	- .03	
610	166304	4.9	-16 44	B1 V	9.1	- .04	
611	166331	5.1	+10 45	B1 V	9.3	- .12	
612	166418	5.4	-16 44	B0 II	8.2	+ .07	
613	166443	5.5	-20 44	B1 V:e	8.8	- .08	
614	166524	5.9	-18 25	B0 ?Vpe		+ .09	(2)
615	166539	6.0	-15 37	B0 IV	8.7	- .04	
616	166540	6.0	-16 55	B0.5 IV	8.0	- .04	
617	166546	6.0	-20 27	O9.5 III	7.17	- .13	
618	166566	6.1	-15 42	B1 II	7.9	- .02	
619	166568	6.1	-18 45	B1.5 (V)pe	9.0	- .05	
620	166569	6.1	-19 5	B1 II		+ .06	(2)
621	166586	6.2	-15 7	B0 V			
622	166628	6.4	-19 28	B3 Ia	7.14	+ .16	
623	166689	6.7	-16 24	B1 Ib-II	7.34	- .09	
624	166716	6.8	-15 25	B0 II-III	7.95	- .08	(1)
625	166734	6.9	-10 46	O8 f	8.8	+ .39	
626	166787	7.1	-19 47	B0.5 Ib-II	8.4	+ .10	
627	166803	7.2	-15 13	B0.5 III	7.9	- .03	
628	166922	7.7	-19 20	B2 III			
629	166937	7.8	-21 5	B8 Iap	4.01	- .04	(2)
630	166965	7.9	-19 2	B3 II	8.8	+ .03	
631	167224	9.1	-18 59	B3 II	7.9	- .10	
632	167263	9.3	-20 25	O9 II	6.02	- .14	
633	167264	9.3	-20 46	B0 Ia	5.42	- .13	
634	167287	9.4	-19 1	B1 Ib	7.0	- .09	
635	167330	9.6	-12 34	O9 I-II	8.4	+ .13	
636	167336	9.6	-18 24	B0 II	8.9	+ .10	
637	167356	9.7	-18 42	A0 Ia	6.08	- .05	(2)
638	-20°5060	9.7	-20 23	B0: IV::pe	var	- .04	(2)
639	167375	$9^m.8$	-18 59	B1 IV			
640	167411	18^h $10^m.0$	-18° 17'	B0 II	7.9	-0.03	

TABLE 1 (CONTINUED)

No	Star	R.A. 1900	Decl. 1900	MK	m	C_1	
641	167451	$18^h\ 10^m.2$	-13° 36'	B0.5 Ib	8.7	+0.17	
642	167497	10.4	-14 20	B2 II		+ .12	(1)
643	167543	10.6	-14 40	B2 III	8.8	+ .04	
644	167633	11.0	-16 33	O6	8.2	- .04	
645	167659	11.1	-19 0	O8	7.3	- .05	
646	167771	11.6	-18 30	O8	6.37	- .11	
647	167791	11.7	-16 16	B5 III		- .05	(2)
648	167838	11.9	-15 28	B5 Ia	6.64	+ .08	
649	-12°4970	12.1	-12 32	B0.5 Ia	8.8	+ .35	(2)
650	-12°4982	12.5	-12 13	B0 II	9.3	+ .17	(2)
651	-11°4586	12.5	-11 21	O8 (I?)	9.5	+ .34	(2)
652	167971	12.5	-12 17	O8 f	7.34	+ .23	
653	168015	12.7	-13 25	B1 V		+ .04	(2)
654	168021-br	12.7	-18 39	B0 Ib	6.9	- .03	
655	168075	12.9	-13 50	O7		+ .07	(2)
656	168076	12.9	-13 50	O5		+ .08	(1)
657	168080	12.9	-18 12	B0.5 II	9.2	- .12	
658	168112	13.1	-12 8	O5.5	8.5	+ .19	
659	168137	13.2	-13 51	O8 V		+ .05	(2)
660	168183	13.4	-14 2	B0 III	8.2	.00	
661	168229	13.6	-18 16	B0.5: V:pe		- .06	(2)
662	168418	14.4	-17 2	B2 III	9.6	+ .03	
663	168444	14.6	-14 53	O8 V	8.86	+ .12	
664	168461	14.7	-12 13	O8			
665	168488	14.8	-17 42	B0.5 II		+ .05	(2)
666	168489	14.8	-17 48	B0 III		+ .01	(2)
667	168504	14.9	-14 0	O8		+ .08	(2)
668	168552	15.2	-17 11	B3 Ib	8.3	+ .04	
669	168571	15.3	-17 26	B1 Ib-II	8.0	+ .13	
670	168607	15.5	-16 25	B9 Ia+:p		+ .65	(2)
671	168625	15.6	-16 25	B8 Ia+?		+ .57	(2)
672	-20°5108	16.4	-20 7	B0.5 II	9.3	+ .10	(2)
673	168814	16.6	-14 26	A2 Ib	7.26	+ .17	(2)
674	168897	17.0	-17 30	B1.5 V:pne		- .01	(2)
675	168917	17.1	-14 25	O9 V:		+ .05	(2)
676	168936	17.2	-17 43	A2 II		- .08	(2)
677	169034	17.6	-13 39	B5 Ia	8.6	+ .45	
678	-9°4713	18.4	- 9 57	B2: V:pne	8.9	+ .05	(1)
679	169226	18.6	-12 15	Cont + e		+ .55	(2)
680	169227	$18^h\ 18^m.6$	-12° 17'	B1.5 Ia		+ .46	(2)

TABLE 1 (CONTINUED)

No	Star	R.A. 1900	Decl. 1900	MK	m	C_1	
681	-14°5037	$18^h\ 19^m.3$	-14° 42'	B1.5 Ia(+?)	8.4	+0.55	(1)
682	169419	19.4	-17 35	B0 II-III	9.5	+ .11	
683	169454	19.6	-14 2	B1 Ia+	6.84	+ .29	
684	169515	19.9	-12 45	Cont+e		+ .42	(2)
685	169582	20.2	- 9 49	O5 f		+ .12	(2)
686	169673	20.7	-15 41	B1 II	7.17	- .12	(1)
687	169727	21.0	-13 43	O6	9.5	+ .21	
688	169753	21.1	- 9 15	B3 Ib	7.8	+ .20	
689	169754	21.1	-11 25	B0.5 Ia	9.0	+ .36	
690	169755	21.1	-14 34	O8 V	9.4	+ .12	
691	170061	22.4	-14 47	B0: nne	9.4	+ .05	
692	170159	22.9	-13 4	B0.5 Ib	8.6	+ .11	
693	-8°4617	23.8	- 8 38	O8.5 (V)	9.4	+ .39	(2)
694	170452	24.4	-13 1	O9: V			
695	170453	24.4	-14 17	B1 II-III	9.2	+ .03	
696	170604	25.2	-16 39	B0.5 II	8.4	- .07	
697	170700	25.7	-14 11	B1 II	8.8	- .04	
698	170716	25.8	-12 24	B0.5 Ib	9.6	+ .03	
699	-11°4667	26.7	-11 22	B1: V:pe	9.7	+ .26	(1)
700	170938	26.9	-15 46	B1 Ia	8.1	+ .28	
701	171012	27.3	-18 26	B0.5 Ia	6.98	+ .06	
702	171198	28.3	-12 20	O7:	9.7	+ .12	
703	171305	29.0	- 4 53	B1 V	8.60	+ .09	(2)
704	171432	29.7	-18 38	B1 Ia	7.1	- .03	
705	171589	30.6	-14 12	O7 f	8.3	- .03	
706	172175	33.6	- 7 57	O6 f	9.7	+ .13	
707	172252	34.1	-11 58	B0 V:e	9.6	+ .21	
708	172275	34.2	- 7 27	O6		+ .21	(2)
709	172367	34.7	- 7 20	B0 V	9.6	+ .06	
710	172488	35.4	- 8 49	B0.5 V		+ .12	(2)
711	172510	35.5	-14 51	B1 V	8.81	- .02	
712	172527	35.6	- 4 11	A0 Ib		+ .29	(2)
713	173011	38.1	-11 36	B0.5 V			
714	173198	39.0	- 1 39	B1 V			
715	173219	39.1	- 7 13	B1: V:pne	7.9	- .07	
716	173438	40.2	- 4 42	B0.5 Ia	8.6	+ .20	
717	173637	41.2	- 8 2	B1 IV	9.0	+ .01	
718	173783	42.0	- 9 25	O9 I		+ .09	(2)
719	173987	43.2	- 6 34	B0.5 Iab	9.0	- .01	
720	174513	$18^h\ 45^m.7$	- 7° 54'	B1 V:pne	8.6	-0.13	

TABLE 1 (CONTINUED)

No	Star	R.A. 1900	Decl. 1900	MK	m	C_1	
721	-0°3584	$18^h\ 49^m.2$	- 0° 41'	08			
722	175514	50.6	+ 9 13	08: Vnn	9.0	+0.08	
723	175754	51 7	-19 17	08 f	7.03	- .20	(2)
724	175876	52.3	-20 33	06	6.73	- .20	(2)
725	177284	58.9	- 2 10	B0.5 p	9.2	- .10	
726	+2°3771	59.2	+ 2 58	B0 III	9.3	+ .16	(1)
727	177812	19 1.1	+ 3 6	B1 Ib	8.9	+ .14	
728	178129	2.3	+ 3 17	B3 Ia	7.8	+ .07	
729	180968	13.5	+22 51	B0.5 IV	5.40	- .12	
730	+14°3887	17.0	+14 42	B ep	10.0	+ .63	(1)
731	+14°3898	18.8	+15 2	B0 III	9.5	+ .21	(1)
732	+22°3687	20.5	+22 35	B2 (V)pe	9.4	+ .15	(1)
733	183143	23.0	+18 5	B7 Ia	6.93	+ .38	
734	183561	25.1	+26 30	B2 III		- .05	(3)
735	184279	28.6	+ 3 34	B0.5 IV	6.78	- .19	
736	184915	31.5	- 7 15	B0.5 III	5.04	- .14	
737	184943	31.7	+23 38	B8 Ia			
738	185418	33.9	+17 2	B0.5 V	7.42	- .10	
739	185859	36.1	+20 15	B0.5 Ia	6.44	+ .04	
740	+28°3434	37.4	+28 55	B1 Ibp	8.5	- .06	(1)
741	+28°3438	38.2	+28 46	B2 IV	9.0	- .14	(1)
742	+23°3745	38.6	+23 13	B0.5 Ib	8.8	+ .17	(2)
743	+23°3747	38.9	+23 12	B1 III	10.3	+ .15	(2)
744	+22°3782	39.0	+23 3	07	9.3	+ .12	(2)
745	+23°3759	41.0	+23 48	B0 II	8.8	+ .22	(1)
746	+23°3761	41.2	+24 4	B0 II:	8.9	+ .17	(1)
747	186745-6	41.2	+23 41	B8 Ia	7.01	+ .34	(4)
748	+23°3762	41.4	+23 44	B0.5 III:nn	9.3	+ .22	(1)
749	+22°3800	41.5	+22 57	B2 III:n	9.6	+ .01	(1)
750	186841	41.7	+23 50	B1 Ia		+ .25	(4)
751	186980	42.4	+31 52	07.5	7.28	- .11	
752	186994	42.5	+44 43	B0 III	7.3	- .22	
753	+27°3512	42.6	+28 0	07	8.8	- .06	(1)
754	+24°3881	42.9	+24 36	06 f	9.1	+ .18	(1)
755	+27°3513	42.9	+27 47	A2 Ia	8.3	+ .04	(1)
756	187320	44.3	+19 24	B2 III	7.5	- .10	
757	187399	44.7	+29 10	B7 Ia?e		- .04	(3)
758	187459	45.0	+33 12	B0.5 Ib	6.35	- .06	
759	+28°3485	45.0	+28 33	B2 V:n	9.0	- .10	(1)
760	225985	$19^h\ 45^m.7$	+32° 43'	B1 V:pe shell	9.2	-0.08	(4)

TABLE 1 (CONTINUED)

No	Star	R.A. 1900	Decl. 1900	MK	m	C_1	
761	+22°3836	19h 46.9	+22° 35'	B1 II	9.2	+0.08	(1)
762	187851	47.0	+27 27	B2 V:nn		- .07	(4)
763	187879	47.2	+40 20	B1 IV:	5.62	- .14	
764	187982-3	47.8	+24 44	A1 Iab	5.67	+ .22	(4)
765	188001	47.9	+18 25	08 f	6.29	- .10	
766	188209	49.0	+46 46	09.5 III	5.51	- .17	
767	188252	49.2	+47 41	B2 III	5.70	- .18	
768	+27°3550	50.0	+28 5	B9 Ia	9.0	+ .34	(1)
769	188439	50.1	+47 34	B0.5 IIIp	6.15	- .19	
770	226868	54.6	+34 56	B0 Ib	9.0	+ .27	(2)
771	227018	56.1	+35 2	07	9.1	+ .05	(4)
772	189779	56.6	+29 37	B2 III		- .09	(4)
773	189957	57.6	+41 43	B0 III	7.73	- .14	(4)
774	190066	58.1	+21 52	B1 Iab	6.55	- .06	
775	227245	58.6	+35 24	07	10.0	+ .11	(1)
776	+28°3598	59.1	+28 25	B0 III:np	9.5	+ .36	(1)
777	190429 br	59.8	+35 45	05 f		- .06	(2)
778	190429 ft	59.8	+35 45	09.5 Ibp			
779	+25°4083	59.9	+25 59	B1 III	9.0	+ .15	(1)
780	190467 20	0.0	+36 8	B5 II:n	8.2	- .04	
781	+31°3921	0.4	+31 52	B1 Ib	8.7	+ .08	(1)
782	227460	0.6	+35 59	B0.5: V	9.9	+ .28	
783	190603	0.7	+31 56	B1.5 Ia+?	5.69	+ .13	
784	190864	1.9	+35 19	06	7.8	- .07	
785	227611	2.0	+35 37	B0 pe	8.7	+ .01	
786	190916	2.2	+41 0	B9 Iab	7.62	+ .08	(3)
787	190918	2.2	+35 31	09.5 I+WR	7.01	+ .01	(2)
788	190919	2.2	+35 24	B1 Ib	7.30	.00	
789	+35°3955	2.2	+35 32	B1 Ib	7.3	- .04	
790	+35°3956	2.3	+35 29	B0.5 V	7.9	- .05	
791	227634	2.3	+35 29	B0 Ib	8.0	- .03	
792	190967	2.4	+35 6	B1 Ib-II	7.92	- .01	
793	190991	2.5	+39 47	B0 IVp		- .07	(3)
794	227696	2.8	+35 27	B0.5 IV:	8.3	- .04	
795	227704	2.9	+34 38	B0 III	8.7	+ .03	(3)
796	191139	3.3	+36 7	B0.5 III	8.3	- .11	
797	227757	3.5	+36 4	09 V	9.3	- .05	(3)
798	191201	3.6	+35 26	B0 III	7.12	- .07	
799	191243	3.8	+34 8	B5 Ib	6.07	- .06	(3)
800*	227836	20h 4.3	+35° 50'	B2:: pne	9.6	+0.02	

TABLE 1 (CONTINUED)

No	Star	R.A. 1900	Decl. 1900	MK	m	C_1
801	191395	20^h $4^m.6$	+39° 28'	B0.5 V:	8.4	-0.11
802	191396	4.6	+37 50	B0.5 II		
803	227877	4.6	+35 10	B1: IV:nn	9.2	- .08
804	191423	4.7	+42 19	09 V:		- .06 (4)
805	191456	4.9	+36 23	B0.5 III		- .10 (3)
806	227902	4.9	+37 13	B1 V	9.3	.00 (3)
807	191473	5.0	+36 57	B0 IV		
808	191495	5.1	+35 14	B0 V	8.12	- .11
809	191566	5.5	+35 11	B0.5 IV	7.7	- .05
810	191611	5.7	+36 12	B0.5 III		
811	191612	5.7	+35 26	08	7.8	- .02
812	191639	5.8	- 9 9	B1 V	6.45	- .14
813	228041	6.2	+35 12	B0.5 V:e	9.2	+ .03
814	228053	6.3	+36 24	B1 II	8.9	+ .07
815	191781	6.6	+45 6	B0 Ibp	9.25	+ .16 (3)
816	228101	6.9	+37 10	B1 V	8.5	- .08 (3)
817	228104	6.9	+35 35	B1: IV:pe	9.1	.00
818	191877	7.0	+21 35	B1 Ib	6.11	- .12
819	191917	7.2	+35 39	B1 III	7.8	- .11
820	191978	7.5	+41 4	08	8.2	- .06
821	192001	7.6	+41 50	09.5 IV		+ .02 (3)
822	192079	8.0	+37 16	B0 IV		+ .05 (3)
823	228263	8.4	+37 21	B1 V	9.6	- .06 (3)
824	192281	9.0	+39 58	05 f	7.47	+ .07
825	228368	9.5	+34 43	07	8.6	+ .10 (3)
826	192422	9.7	+38 28	B0.5 Ib	7.10	+ .05
827	+32°3749	9.8	+32 15	B0: pe		
828	228456	10.3	+36 30	B2 IV		
829	192539	10.3	+31 41	B2 III	7.38	- .04
830	192639	10.8	+37 3	08 f	7.02	+ .03
831	192660	10.9	+40 1	B0 Ia	7.72	+ .16 (3)
832	228548	11.4	+39 40	B0 pe	10.3	+ .19
833	228587	11.7	+36 19	B1 II	10.3	+ .27 (1)
834	228602	11.8	+36 32	B1 III	10.1	+ .13 (1)
835	192832	11.9	+42 6	B5 Ia		+ .31 (3)
836	228690	12.8	+37 37	B0.5 V	9.4	.00 (3)
837	+37°3859	12.8	+37 20	B1 IV		
838	193007	12.9	+37 20	B0.5 II		
839	193009	12.9	+32 4	B1 V:pnne	7.02	- .06
840	+37°3862	20^h $12^m.9$	+37° 20'	B0 V:	9.5	+0.05 (3)

TABLE 1 (CONTINUED)

No	Star	R.A. 1900	Decl. 1900	MK	m	C_1
841	193032	$20^h\ 13^m.0$	+38° 35'	B0 III		+0.02 (3)
842	228712	13.1	+40 34	B0.5 Ia	8.8	+ .42 (3)
843	193076	13.3	+37 22	B0.5 II		+ .02 (4)
844	193117	13.5	+40 32	09.5 II		+ .16 (3)
845	193182	13.8	+39 16	A: shell	6.56	- .17 (3)
846	193183	13.8	+37 55	B1.5 Ib	7.12	+ .08
847	228766	13.8	+37 0	06 f or WR		
848	228779	14.0	+34 30	09.5 Ib	9.1	+ .52 (1)
849	193237	14.1	+37 43	P Cyg	4.88	+ .06
850	+30°3980	14.4	+30 30	B9 Ib-II		
851	193322	14.6	+40 25	08	5.82	- .07
852	228841	14.8	+38 34	07.5 p	9.1	+ .10
853	228854	15.0	+36 2	08:	8.9	+ .29 (1)
854	228860	15.1	+36 39	B0.5 IV	9.9	+ .16 (1)
855	193426	15.1	+39 54	B9 Ia		+ .44 (3)
856	193427	15.1	+39 5	B1 V		
857	193443	15.2	+37 57	09 III	7.4	+ .03
858	193444	15.2	+37 31	B0.5 V		+ .11 (3)
859	228882	15.4	+40 23	B0.5 Ia	9.4	+ .41 (1)
860	193514	15.5	+38 57	07 f	7.29	+ .10
861	193516	15.5	+37 28	B2: III:	9.1	+ .08
862	228913	15.8	+35 54	B0.5 III:nn	10.1	+ .15 (1)
863	228919	15.9	+40 8	B1 IV	9.9	+ .25 (1)
864	193595	15.9	+38 44	07		+ .03 (3)
865	193610	16.0	+42 41	A0: Ib:		+ .32 (3)
866	193611	16.0	+38 1	B0 Vp		+ .12 (2)
867	228928	16.0	+40 20	B2 Ib:nn	10.1	+ .26 (1)
868	228929	16.0	+39 36	B0.5 Ib	9.8	+ .43 (1)
869	228943	16.1	+38 17	B0 II:	9.4	+ .27 (1)
870	193634	16.2	+38 1	B3 III		+ .02 (3)
871	193682	16.5	+37 30	05		+ .11 (5)
872	228969	16.5	+38 21	B2 II:	9.6	+ .15 (1)
873	228989	16.7	+38 23	09 Vnn	9.8	+ .22 (1)
874	193793	17.1	+43 32	05 + WR	6.83	+ .07 (3)
875	193794	17.1	+39 2	B0 V		+ .15 (3)
876	229033	17.2	+37 25	B0 II-III	8.9	+ .21 (1)
877	229049	17.4	+38 42	B2 III:p	9.8	+ .18 (1)
878	193855	17.4	+38 42	B2 III		.00 (3)
879	229059	17.5	+37 5	B1.5 Iap	8.9	+ .61 (2)
880	193945	$20^h\ 17^m.9$	+40° 52'	B0 Vnn		+0.17 (3)

TABLE 1 (CONTINUED)

No	Star	R.A. 1900	Decl. 1900	MK	m	C_1
						+0.36 (3)
881	193946	$20^h\ 17^m.9$	+39 30'	B1 Ib		
882	+45°3149	17.9	+45 43	B1 V		
883	194009	18.2	+38 18	B3 II		
884	229108	18.3	+39 8	B0.5 Ib	9.6	+ .26 (1)
885	229115	18.4	+34 55	B2 IV	10.1	+ .17 (1)
						+ .29 (3)
886	194057	18.4	+44 30	B1 Ib		- .09 (3)
887	194092	18.6	+40 39	B0.5 III		
888	194094	18.6	+38 23	B0 V		+ .39 (3)
889	194153	18.9	+37 48	B1 Iab		+ .42 (1)
890	229153	19.0	+37 39	B0 I	9.2	
891	229159	19.2	+38 53	B1.5 Ib		- .11 (3)
892	194194	19.2	+40 23	B2 III		+ .14 (2)
893	194205	19.3	+39 2	B2 III		
894	229171	19.4	+38 8	B0.5 III:n		+ .34 (2)
895	229196	19.7	+40 34	05	8.7	
896	194279	19.7	+40 26	B1.5 Ia	7.05	+ .33
897	194280	19.7	+38 37	B0 Ib		+ .24 (2)
898	+36°4048	19.8	+36 59	B0 Ib		
899	229202	19.8	+39 50	08 V:	9.7	+ .27 (1)
900	229214	20.0	+36 12	B1 Ib		
901	194334	20.0	+38 34	07.5 V		+ .25 (1)
902	229221	20.1	+38 11	B pe	9.6	+ .28
903	229227	20.2	+38 8	B0 II		
904	229232	20.3	+38 47	05 f	9.6	+ .24 (1)
905	229234	20.3	+38 12	09.5 III		
906	229238	20.4	+38 13	B0 I		
907	229239	20.4	+38 11	B0 II		
908	194649	21.7	+39 54	06.5		+ .35 (2)
909	194779	22.4	+41 1	B3 II	7.66	.00
910	+39°4189	22.7	+39 18	B2 p?e?		
911	194839	22.8	+41 3	B0.5 Ia	7.45	+ .34
912	+38°4098	23.8	+38 27	B9 Ib		
913	+40°4179	24.1	+40 16	08 V:		
914	+37°3945	24.6	+38 2	B0 II:nn		
915	+40°4185	24.7	+40 18	B0 V:		
916	195213	24.9	+40 28	07		+ .26 (1)
917	195229	25.0	+41 40	B0.5 III		- .07 (3)
918	195407	26.0	+36 39	B0 IV:pe	7.72	.00
919	+46°2948	$26^m.1$	+46 20	B1 V:nne		
920	195592	$20^h\ 27^m.2$	+43° 59'	09.5 Ia	7.15	+0.30

TABLE 1 (CONTINUED)

No	Star	R.A. 1900	Decl. 1900	MK	m	C_1	
921	VI Cyg 1	$20^h\ 27^m.5$	+41° 10'	09 V?			
922	VI Cyg 2	27.7	+41 10	B1 Ib?			
923	VI Cyg 3	28.0	+40 52	09?			
924	VI Cyg 4	28.6	+41 06	08			
925	VI Cyg 5	28.8	+40 58	07 f			
926	VI Cyg 6	29.2	+41 05	08 (V)			
927	195965	29.3	+47 53	B0 V	6.82	-0.15	
928	VI Cyg 9	29.6	+40 55	05 f			
929	VI Cyg 7	29.7	+41 00	06 f			
930	VI Cyg 8A	29.7	+40 58	06 f			
931	VI Cyg 8B	29.7	+40 58	08?			
932	VI Cyg 8C	29.7	+40 58	06?			
933	VI Cyg 8D	29.7	+40 58	09?			
934	+37°3976	29.9	+37 56	B1.5 Vn			
935	VI Cyg 10	30.2	+41 12	09.5 Ia			
936	VI Cyg 11	30.6	+41 16	06 f			
937	+45°3216	30.5	+45 19	08			
938	+36°4145	32.5	+37 4	09 V			
939	+47°3162	36.8	+47 44	B1 Ib-II			
940	197345	38.0	+44 55	A2 Ia	1.33	- .10	
941	+42°3835	38.6	+42 50	09 p?			
942	197460	38.8	+36 2	B0.5 Ib	8.2	+ .01	
943	+35°4258	42.3	+35 11	B0.5 Vn			
944	235350	42.3	+50 49	B0.5 IV	9.4	+ .17	(2)
945	+45°3260	42.3	+45 59	09 V			
946	198478	45.5	+45 45	B3 Ia	4.89	+ .05	
947	198479	45.5	+45 16	B1 III	8.52	+ .04	(1)
948	198512	45.7	+53 52	B1 Vpnne	7.95	- .04	
949	+44°3594	45.7	+45 3	B1: V:pne			
950	198781	47.6	+63 40	B0.5 V	6.38	- .14	
951	198820	47.9	+32 28	B3 III	6.35	- .15	
952	198846	48.1	+34 17	B0 IV	7.1	- .13	
953	198895	48.4	+55 7	B1 V	8.26	+ .14	
954	198931	48.6	+44 3	B1 Vnne:		+ .15	(1)
955	+47°3211	49.7	+47 33	B0 II-III			
956	+37°4092	49.8	+37 48	B1 III			
957	199140	50.1	+28 8	B2 III	6.44	- .18	
958	199216	50.7	+49 9	B1 II	7.13	+ .11	
959	199478	52.4	+47 2	B8 Ia	5.76	+0.09	
960	+42°3914	$20^h\ 52^m.7$	+42° 44'	B0 III:			

TABLE 1 (CONTINUED)

	No	Star	R.A. 1900	Decl. 1900	MK	m	C_1	
	961	199579	$20^h\ 53^m.1$	+44° 33'	O6	6.01	-0.12	
	962	+45°3341	53.6	+46 9	B1 II			
	963	+44°3655	54.9	+44 45	B1 IV			
	964	200120	56.4	+47 8	B1 IV:e	4.86	- .22	
	965	+45°3360	57.1	+45 51	B3 V			
	966	200310	57.6	+45 46	B1 V	5.24	- .20	
	967	200776	21 0.4	+45 56	B1 IV:p		- .12	(2)
	968	200857	1.0	+54 51	B3 III	7.16	+ .16	
	969	201345	3.9	+33 0	O9 p	7.76	- .22	
	970	201795	6.8	+38 33	B1 V	7.7	- .13	
	971	201819	7.0	+35 53	B1 Vp	6.40	- .18	
	972	202124	8.8	+44 7	O9.5 Ib	7.83	- .05	
	973	202214	9.3	+59 35	B0 V	5.65	- .08	
	974	202253	9.5	+43 28	B2 III	7.70	- .06	
	975	202347	10.1	+45 12	B1 V	7.47	- .16	
	976	202349	10.1	+37 21	B0.5 V	7.34	- .17	
	977	+41°4064	12.4	+42 7	B3: pnn shell			
	978	202850	13.5	+38 59	B9 Iab	4.28	- .05	
	979	203025	14.6	+58 10	B2 III	6.41	- .02	
	980	203064	14.8	+43 31	O8	5.06	- .16	
	981	203374	16.7	+61 25	B0 IVpe	6.64	+ .01	
	982	203938	20.2	+46 44	B0.5 IV	7.10	+ .13	
	983	+43°3913	21.3	+44 0	B1.5 V:pnne			
(2)	984	204116	21.4	+54 57	B1 Ve	7.96	+ .09	
	985	204172	21.7	+36 14	B0 Ib	5.84	- .19	
	986	204710	25.4	+44 29	B8 Ib	6.90	.00	(2)
(1)	987	204722	25.5	+43 54	B2 V:nn(e)	7.52	- .10	
	988	204827	26.1	+58 18	B0 V	8.3	+ .15	
	989	205021	27.4	+70 7	B2 III	3.32	- .25	
	990	205139	28.3	+60 1	B1 II	5.52	- .08	
	991	205196	28.6	+57 4	B0 Ib	7.36	+ .15	
	992	+47°3487	32.1	+47 28	B pe			
(1)	993	+48°3437	32.7	+48 54	B1 Iab			
	994	206165	35.2	+61 38	B2 Ib	4.87	+ .02	
	995	206183	35.3	+56 32	B0 V	7.6	- .11	
	996	206259	35.8	+51 54	B3 III	7.48	- .10	(2)
	997	206267	35.9	+57 2	O6	5.64	- .06	
	998	+49°3591	36.7	+50 3	O7.5			
	999	206773	39.3	+57 17	B0 V:pe	6.98	-0.05	
	1000	+28°4177	$21^h\ 40^m.6$	+29° 6'	B1 III			

TABLE 1 (CONTINUED)

No	Star	R.A. 1900	Decl. 1900	MK	m	C_1
1001	239758	$21^h\ 41^m.5$	+58° 36'	B2 III:nn	9.5	+0.04 (2)
1002	207198	42.2	+61 59	09 II	5.97	+ .03
1003	+49°3615	42.2	+49 50	B1 V:		
1004	207260	42.6	+60 40	A2 Ia	4.46	+ .16
1005	207308	42.9	+61 50	B0.5 V	7.6	- .01
1006	207329	43.1	+51 39	B1.5 Ib?e	7.45	+ .03
1007	207330	43.1	+48 51	B3 III	4.26	- .16
1008	207538	44.6	+59 14	B0 V	7.03	+ .03
1009	207673	45.6	+40 40	A2 Ib	6.49	+ .13
1010	207793	46.5	+52 14	B0.5 III	6.56	+ .06
1011	+47°3588	48.9	+47 32	B1.5 V		
1012	208218	49.7	+62 13	B1 III:	6.76	+ .01
1013	208220	49.7	+43 1	B1 IVe	9.8	- .24
1014	208392	50.9	+62 8	B1 IV:	7.10	.00
1015	208501	51.5	+56 8	B8 Ib	6.01	+ .26
1016	235673	54.1	+52 19	O7	9.2	- .02 (2)
1017	208905	54.3	+60 49	B1 Vp?	6.90	- .07
1018	235679	55.0	+53 59	B2 Ia?p?	8.9	+ .07 (2)
1019	209008	55.1	+ 6 14	B3 III	5.99	- .16
1020	209145	56.1	+59 50	B1 V	7.96	+ .02 (2)
1021	209339	57.6	+62 0	B0 IV	6.48	- .12
1022	209481	58.7	+57 31	O9 V	5.50	- .12
1023	209678	22 0.1	+52 43	B2 I		+ .07 (3)
1024	+51°3239	0.3	+51 37	B2 V		
1025	209900	1.6	+53 1	A0 Ib-II		+ .06 (2)
1026	209975	2.1	+61 48	O9.5 Ib	5.17	- .12
1027	+49°3735	2.2	+49 25	B1.5 V:nn(e)		
1028	210072	2.7	+54 46	B2 V		+ .03 (1)
1029	210221	3.8	+52 49	A3 Ib	6.50	+ .07 (2)
1030	+52°3122	5.0	+52 29	B1 V:		
1031	210478	5.6	+60 30	B1 V	7.26	- .10 (1)
1032	210809	7.9	+51 56	O9 Ib	7.6	- .06
1033	210839	8.1	+58 56	O6 f	5.19	- .04
1034	+52°3135	8.5	+53 12	B3 II:		
1035	239886	8.9	+56 46	B9 Iab	8.9	+ .36 (2)
1036	239895	9.8	+57 10	B8 Ia	8.7	+0.34 (2)
1037	+53°2833	12.5	+53 40	B1 III		
1038	+54°2726	13.1	+54 58	B1 II		
1039	235781	13.2	+53 9	B6 Ib		
1040	+53°2837	$22^h\ 13^m.3$	+53° 42'	B2 III:		

TABLE 1 (CONTINUED)

No	Star	R.A. 1900	Decl. 1900	MK	m	C_1	
1041	235783	$22^h\ 13^m.4$	+53° 59'	B1 Ib			
1042	211853	15.0	+55 37	B0: I:+WR			
1043	+53°2843	15.0	+53 46	08			
1044	235795	15.2	+51 37	B1: V:nne			
1045	211880	15.2	+62 43	B0.5 V		+0.10	(1)
1046	211971	15.9	+59 38	A2 Ib	7.16	+ .35	(2)
1047	212044	16.4	+51 21	B1: V:pnne	7.08	- .16	
1048	235813	18.5	+54 18	B0 III			
1049	212455	19.3	+54 44	B5 Iab	8.0	+ .09	
1050	235825	19.6	+54 44	09 V			
1051	+54°2764	20.2	+54 53	B1 Ib			
1052	212827	22.0	+53 16	A0 II			
1053	+54°2775	22.3	+54 57	B1 V			
1054	+52°3210	23.0	+53 8	B1 V			
1055	+53°2885	23.2	+53 40	B2 III			
1056	213023	23.5	+63 14	09 V:			
1057	213087	23.9	+64 37	B0.5 Ib	5.66	+ .01	
1058	213405	26.0	+64 36	B0.5 V	8.0	+ .04	
1059	+54°2790	26.1	+54 16	B0 IVn			
1060	213470-1	26.5	+56 43	A3 Ia	6.73	+ .14	(2)
1061	235874	28.9	+50 42	B3 III			
1062	214080	30.7	-16 54	B1 Ib	6.69		
1063	214168	31.4	+39 7	B1 Ve	5.83	- .14	
1064	214419	32.9	+56 23	07 +WR	8.92		
1065	240010	34.6	+55 19	B1: IV:pnne			
1066	214680	34.8	+38 32	09 V	4.91	- .23	
1067	214993	37.0	+39 43	B2 III	5.18	- .20	
1068	215191	38.4	+37 17	B1 V	6.22	- .14	
1069	+55°2795	38.8	+55 49	B1 III			
1070	+53°2964	39.3	+53 33	B2 IV:pnne			
1071	+54°2847	40.3	+55 13	B1 II?nn			
1072	215605	41.3	+57 20	B2: IV:nne			
1073	240047	41.4	+56 55	B2 III			
1074	215733	42.2	+16 43	B1 II	7.2	- .18	
1075	+55°2808	42.4	+55 56	B2 III			
1076	215806	42.7	+57 46	B0 Ib			
1077	215835	42.9	+57 33	06 n		- .01	(2)
1078	215836	42.9	+55 54	B1 II			
1079	216014	$44^s.2$	+64 32	B0.5 V:nn	6.83	+ .05	
1080	216044	$22^h\ 44^m.5$	+54° 36'	B0 II	8.6	-0.08	

TABLE 1 (CONTINUED)

No	Star	R.A. 1900	Decl. 1900	MK	m	C_1
1081	216092	22^h $44^m.9$	+47° 24'	B1 V:		
1082	216411	47.6	+58 28	B1 Ia	7.16	+0.15
1083	216438	47.8	+53 11	B1 II	8.6	- .13
1084	216532	48.6	+61 54	08	8.4	+ .06
1085	216658	49.6	+61 36	B0 V	9.1	+ .19
1086	216711	50.0	+62 4	B1 V	9.2	+ .16
1087	+55°2840	51.0	+55 51	07.5 p		
1088	+56°2903	51.7	+57 3	B0.5: IV:		
1089	216898	51.8	+61 46	08	8.3	+ .09
1090	216927	52.0	+58 22	B9 Ia	8.7	+ .26
1091	+63°1907	52.5	+63 56	B1 Ia		
1092	217035	52.6	+62 19	B0 V	7.76	+ .05
1093	217061	52.8	+62 5	B1 V	9.0	+ .19
1094	217086	53.0	+62 12	06	7.70	+ .17 (2)
1095	217297	54.7	+63 10	B1.5 V	7.36	+ .01
1096	217312	54.8	+62 32	B0 IV		+ .05 (2)
1097	217490	56.0	+59 5	B0.5 Ia		+ .22 (2)
1098	240160	57.4	+56 27	09		
1099	+56°2929	57.5	+56 30	B2 V:nn		
1100	+56°2930	57.9	+57 0	B1 IV		
1101	240165	58.0	+56 39	09.5 V		
1102	240168	58.2	+56 4	B1 III		
1103	240171	58.5	+56 36	B1 V		
1104	217919	59.0	+63 10	B0 IV:n		+ .14 (2)
1105	218066	23 0.0	+62 51	B1: V:		+ .02 (1)
1106	218195	1.0	+57 43	08		
1107	218323	2.0	+63 46	B0.5 II		
1108	218342	2.1	+62 41	B0 IV	7.46	+ .10
1109	218376	2.4	+58 53	B0.5 IV	4.93	- .18
1110	236044	2.7	+54 13	B1 V		
1111	+55°2899	2.7	+55 27	B1 IIIp		
1112	218915	6.7	+52 31	09 I	7.06	- .10
1113	219188	8.9	+ 4 27	B0.5 III	6.93	- .14
1114	219287	9.6	+58 51	B0 Ia		+ .36 (2)
1115	+63°1962	12.8	+63 15	B1 III		
1116	+63°1964	13.1	+63 35	B0 II		
1117	240250	13.6	+59 19	B9 Iab		
1118	+62°2210	14.3	+62 57	B9 Ia		
1119	220116	16.1	+57 43	B0.5 Vpe		+0.16 (2)
1120	+60°2522	23^h $16^m.2$	+60° 39'	07 f		

TABLE 1 (CONTINUED)

No	Star	R.A. 1900	Decl. 1900	MK	m	C_1	
1121	+60°2525	23^h $17^m.3$	+60° 19'	B0 III-IV			
1122	220770	21.4	+60 53	A5 Ib		+0.19	(2)
1123	+60°2542	22.6	+60 50	A2 Ib			
1124	+60°2582	30.9	+60 22	B8 Iab			
1125	222568	36.6	+67 48	B1 IV	8.1	+ .03	
1126	+61°2509	39.0	+61 36	B0.5 Ib			
1127	+60°2615	39.9	+61 7	B0.5 Ib			
1128	+62°2296	42.5	+62 40	B3 Ia?			
1129	+61°2526	42.9	+61 29	B2 Ib			
1130	+62°2299	43.2	+62 50	08			
1131	+61°2529	43.6	+61 26	B1 Ib			
1132	223385	44.0	+61 40	A3 Ia+	5.61	+ .24	
1133	+62°2313	47.1	+62 45	B3 Ib			
1134	+61°2550	47.4	+61 34	B0 IV			
1135	223924	48.6	+56 16	B1.5 V	8.3	- .15	
1136	+61°2559	48.7	+61 52	09 V			
1137	223960	48.9	+60 18	A0 Ia+	6.98	+ .21	
1138	223987	49.2	+61 3	B1 Ib	7.56	+ .08	
1139	224055	49.7	+61 17	B3 Ia	7.16	+ .20	
1140	224151	50.5	+56 53	B0.5 II	6.05	- .06	
1141	224257	51.3	+55 26	B0 IV		- .16	(2)
1142	+66°1661	52.5	+67 0	09 V	8.8	+ .41	(2)
1143	224424	52.7	+59 9	B1 Iab	8.4	+ .21	
1144	224436	52.8	+56 32	B1 II		- .04	(2)
1145	240464	53.7	+59 43	09 V			
1146	224572	53.9	+55 12	B1 V	4.93	- .17	
1147	224599	54.1	+59 29	B0.5: V:pnne	9.7	- .04	
1148	224905	56.6	+59 54	B1 Vn	8.5	- .08	
1149	+66°1675	57.1	+66 51	07			
1150	225094	58.3	+63 5	B3 Ia	6.26	+ .02	
1151	225146	58.8	+60 33	B0 Ibp	8.6	- .02	
1152	225160	23^h $58^m.9$	+61° 40'	08 f	8.2	-0.04	

TABLE 2

SOUTHERN OB STARS

No	Star	R.A. 1900	Decl. 1900	MK	m	C_1
1153	62150	$7^h\ 37^m.4$	-32° 24'	B3 Ia	7.7	+0.09 (3)
1154	62483	39.0	-52 57	B2 II	8.2	- .16 (2)
1155	63578	44.5	-46 22	B1 V	5.2	- .20 (6)
1156	68450	8 7.3	-36 59	B0 II	6.5	- .14 (1)
1157	68761	8.7	-36 41	B0.5 III	6.6	- .17 (3)
1158	69106	10.3	-36 38	B0.5 II	7.2	- .17 (2)
1159	69425	11.8	-36 49	B1: V:pe	9.1	- .06 (1)
1160	69464	12.0	-35 19	O7 f	8.9	+ .01 (1)
1161	70930	19.5	-48 10	B1 V	4.8	- .20 (std)
1162	71304	21.5	-43 59	O9 II?	8.2	+ .12 (2)
1163	72554	28.4	-45 47	B1 III	8.3	+ .03 (1)
1164	73882	35.5	-40 4	O8 (V)	7.3	+ .06 (3)
1165	75821	47.1	-46 10	B0 III	5.1	- .22 (7)
1166	75860	47.4	-43 23	B1.5 Iab	7.7	+ .23 (6)
1167	76968	54.3	-50 22	B0 II	7.1	- .09 (3)
1168	77581	58.3	-40 10	B0.5 Ib	6.9	+ .10 (3)
1169	78958	9 5.9	-43 29	B0.5 II	9.1	+ .20 (3)
1170	80077	12.5	-49 33	B2 Iape	7.7	+ .53 (7)
1171	81370	20.0	-52 19	B0 IV:	8.8	- .08 (3)
1172	83043	30.6	-53 12	B1 V:pe	8.6	- .12 (1)
1173	83597	34.5	-53 14	B1 Vpe	9.3	- .08 (1)
1174	85871	49.6	-54 54	B1 V	6.6	- .19 (2)
1175	88115	10 4.5	-62 10	B1 III	8.4	- .14 (2)
1176	90087	18.8	-59 16	O9.5 V	8.0	- .12 (1)
1177	91452	28.4	-63 26	B0 I?	7.7	- .06 (1)
1178	91651	29.8	-59 37	O9 Vp?	8.9	- .14 (3)
1179	-57°3340	31.7	-57 41	B0.5 V	8.8	- .13
1180	91943	31.8	-57 41	B0.5 Ib	6.8	- .10 (2)
1181	-57°3346	31.9	-57 42	B1 II	7.7	- .09
1182	-57°3348	32.0	-57 42	B0.5 V	9.3	- .15
1183	91969	32.0	-57 43	B0 Ib	6.6	- .13 (2)
1184	92850	38.1	-56 29	B0 Ib	8.1	- .10 (3)
1185	93130	40.2	-59 21	O6		
1186	93160	40.3	-59 3	O7	7.4	- .05 (1)
1187	93190	40.5	-58 46	B0: IV:pe	8.6	+ .03
1188	-59°3291	40.6	-59 26	O9.5 III		
1189*	93206	40.6	-59 28	B0 Ib:		- .06 (std)
1190	93222	40.7	-59 34	O7	8.2	- .10
1191	-59°3300	40.8	-59 16	O6	8.7	- .02
1192	93250	$10^h\ 40^m.9$	-59° 3'	O5	7.4	-0.05

TABLE 2 (CONTINUED)

No	Star	R.A. 1900	Decl. 1900	MK	m	C_1
1193	93403	$10^h\ 41^m.9$	-58° 53'	O5 (f)	7.3	-0.02 (2)
1194	94909	52.2	-57 1	B0 Ib	7.3	+ .09 (2)
1195	94963	52.6	-61 11	O8 f	7.1	- .16 (3)
1196	95275	54.9	-54 21	O9 V	8.6	- .15 (3)
1197	95461	56.0	-58 50	B0.5 Iab		+ .06 (2)
1198	95731	57.8	-58 50	B1 Ib	9.1	- .04 (2)
1199	96248	11 00.7	-59 19	B1 Iab	6.6	- .02 (std)
1200	96670	3.0	-59 20	O8	7.4	- .06 (2)
1201	96880	4.2	-58 52	B1 Ib	7.6	+ .10 (2)
1202	96917	4.4	-56 31	O9 II:	7.1	- .09 (2)
1203	97522	8.2	-64 40	B1 Ib-II	7.8	+ .01 (2)
1204	97848	10.2	-58 29	O9 IV	8.7	- .13 (2)
1205	97913	10.6	-58 38	B0 (I?)p:	8.9	- .11 (2)
1206	97966	10.9	-58 52	O7.5	8.9	- .11 (2)
1207	98614	15.6	-59 1	B1 III	8.5	- .08 (1)
1208	98733	16.5	-59 37	B1 Ib	8.0	- .05 (4)
1209	99546	22.0	-58 53	O8		- .15 (2)
1210	99857	24.1	-65 56	B1 Ib	7.5	- .07 (3)
1211	99953	24.8	-63 00	B2 Ia	6.5	+ .01 (3)
1212	100099	25.9	-63 16	O9.5 V?	8.1	- .08 (3)
1213	100199	26.6	-62 23	B1 Ibp	8.1	- .11 (1)
1214	100276	27.2	-60 03	B1 Ib	7.2	- .11 (3)
1215	100943	31.9	-61 6	B5 Ia	7.2	- .08 (2)
1216	102997	46.3	-61 17	B5 Ia	6.6	+ .01 (2)
1217	104200	54.9	-55 44	B1 III	7.7	- .18 (1)
1218	104631	57.8	-61 36	B1 II	6.8	- .09 (1)
1219	104705	58.3	-62 8	B0.5 III	7.9	- .13 (2)
1220	105056	12 0.6	-69 1	B0 I:pe	7.5	- .10 (2)
1221	106068	7.1	-62 23	B9 Ia	6.0	+ .01 (2)
1222	108639	23.6	-60 15	B0 III:p?	7.9	- .09 (2)
1223	109399	29.2	-72 10	B1 Ib	7.7	- .13 (4)
1224	109978	33.8	-61 53	O9 IV	8.8	+ .07 (4)
1225	110360	36.4	-60 6	O7	9.3	- .06 (4)
1226	110639	38.4	-60 50	B1 Ib-II	8.4	+ .19 (4)
1227	110660	38.5	-63 30	B1 V	10.0	+ .12 (3)
1228	110863	40.0	-60 0	B1 Vp	9.1	+ .02 (3)
1229	110984	40.8	-60 38	B0 IV	9.0	+ .10 (2)
1230	111558	44.9	-69 6	B8 Ia	7.3	- .06 (1)
1231	112147	49.2	-58 28	B0: IV:pe	9.2	.00 (3)
1232	112272	$12^h\ 50^m.4$	-63° 49'	B0.5 Ia	7.4	+0.25 (4)

TABLE 2 (CONTINUED)

No	Star	R.A. 1900	Decl. 1900	MK	m	C_1
1233	112784	$12^h\ 54^m.0$	-60° 3'	09.5 III	8.3	-0.10 (6)
1234	113163	56.6	-60 12	B5 IV	7.8	.00 (5)
1235	113421	58.4	-59 17	B1 III:	9.4	- .04 (2)
1236	113422	58.4	-61 10	B1 Ia	8.3	+ .26 (3)
1237	113511	59.1	-63 31	B0 III:	9.1	+ .05 (3)
1238	113659	13 0.1	-64 33	09 IV	8.1	- .14
1239	113904	1.7	-64 46	B0 I:+WR	5.5	- .16
1240	114011	2.4	-60 39	B1.5 Ia(+)	9.3	+ .24 (3)
1241	114340	4.8	-59 13	B1 Ia+		+ .12 (2)
1242	114441	5.4	-54 49	B2 IVpe	8.1	- .06 (1)
1243	114478	5.6	-62 17	B1 II	8.7	+ .10 (1)
1244	114737	7.3	-63 3	09 V		
1245	114800	7.7	-62 41	B2 Vpe	7.9	- .08 (3)
1246	114886	8.3	-63 3	09: V		
1247	115363	11.6	-63 10	B1 Ia+	7.8	+ .16 (2)
1248	115842	14.6	-55 17	B0.5 Iab	6.1	+ .01 (std)
1249	116849	21.2	-65 46	B1: V:pe	9.2	- .07 (1)
1250	116852	21.2	-78 20	09 III	8.5	- .18 (3)
1251	117111	23.0	-64 59	B1 Vpe		- .09 (2)
1252	117216	23.7	-64 37	B1 V:	10.3	.00 (1)
1253	117856	27.9	-62 50	B0 Ib	7.4	- .04 (1)
1254	118571	32.6	-60 29	B0 IV:	8.8	- .14 (2)
1255	119646	39.3	-61 57	B2 Ib-II	6.6	- .07 (6)
1256	120678	45.8	-62 14	O pe	7.8	- .05 (1)
1257	123056	14 0.3	-59 59	09.5 V	8.2	- .07 (1)
1258	125241	13.0	-60 26	09 I	8.5	-0.03 (1)
1259	150168	16 34.1	-49 27	B1 II		
1260	152217	46.9	-41 6	B0 III		
1261	152245	47.1	-40 22	B0 III		
1262	152246	47.1	-40 55	09: III:		
1263	152268	47.3	-40 49	B0 III		
1264	152291	47.4	-40 29	B0 III:pn(e)		
1265	152405	48.0	-40 22	B0 Ib:		
1266	152407	48.0	-40 56	08? f		
1267	152622	49.3	-40 20	B0 III:n		
1268	152623	49.3	-40 31	08 V		
1269	152667	49.6	-40 40	B0 Ia?p		
1270	152723	$16^h\ 49^m.9$	-40° 22'	06		

NOTES TO TABLES

80 Type may be O6+WR.
103 Type may be Ap nne.
211 Luminosity class V at λ 4650; *Ib* at λ 4100.
338 Spectrum of preceding star; following star, gG8.
433 Shell.
496 Two-line binary; $\Delta m \sim 0.5$.
800 Shell; sharp absorption lines of *Fe* II.
1189 Light-variable: 6.3–6.5 mag.

STELLAR SPECTRA IN MILKY WAY REGIONS. III. A REGION IN CEPHEUS-LACERTA

S. W. McCuskey
Warner and Swasey Observatory, Case Institute of Technology
Received March 25, 1955

ABSTRACT

Spectra and photographic magnitudes are given for 4222 stars in LF4, an area of 16.9 square degrees in Cepheus-Lacerta at R.A. 22^h22^m, dec. $+53°.8$ (1945). Blue-red color indices for 1764 early-type stars are also listed. Identification charts are presented in Figure 1*a*–Figure 1*m*. Table 1 presents the observational data.

The Milky Way to the south of the galactic plane in Cepheus and Lacerta is reasonably smooth and free of obvious obscuration. Region LF4 of the observational program of the Warner and Swasey Observatory lies in this area, centered at R.A. 22^h22^m; dec. $+53°.8$ (1945); $l = 70°$, $b = -3°$. In the northwestern half of the circular area the star clouds are quite bright, while in the southeasterly part of the field the stellar population is less. This effect is shown more strikingly on the Ross and Calvert *Atlas of the Milky Way*, print No. 19, than on our long-exposure plates. On this print the center of LF4 is situated 14.3 cm from the left-hand side and 11.8 cm from the bottom. The present paper deals with the observational data obtained for a study of the galactic structure and changes in the luminosity function in LF4. An analysis of the data has been published elsewhere (McCuskey 1951). In general, the pattern of the present paper follows those published for Regions LF1, LF3b, and LF2 (McCuskey 1949; Nassau and MacRae 1949; McCuskey and Seyfert 1950).

Sectional charts covering the area are given in Figure 1*a*–Figure 1*m*, where the star numbers progress approximately in order of right ascension in each zone of declination, after the fashion of the *BD* numbering scheme. An index to the sectioning is indicated on the first part of the chart. Approximate 1950 co-ordinates are shown on the charts and serve for identification purposes only. The area covered is 16.9 square degrees.

Table 1 gives the observational data for this field. While an attempt has been made to obtain the spectra of all stars brighter than $m_{pg} = 12.5$, there were many cases where overlapping spectra made classification uncertain. On the other hand, some stars fainter than 12.5 are included. Altogether, Table 1 contains 4222 entries, listed in zones of declination.

Column 1 gives the serial number of a star for identification on the charts of Figure 1. An asterisk following the number indicates that it is a *BD* star, while an "R" refers to the remarks at the end of the table. The *BD* numbers corresponding to the numbers in our catalogue are given for those stars which are included in the "Remarks."

The apparent photographic magnitudes given in column 2 were determined from plates taken with the Schmidt-type telescope. For the early-type stars these were measured in the Eichner photometer, as well as by estimate with a graduated scale of stellar images. Magnitudes for the remaining stars were measured only with the graduated scale. The resulting probable errors of a final magnitude determined by photometer and by scale were ± 0.04 and ± 0.07 mag., respectively.

A photoelectric check has recently been made of the sequence stars in LF4 and a few stars in the outlying parts of the field. Six of the sequence stars, ranging from $m_{pg} = 8$ to $m_{pg} = 12$ were measured on three nights with the photocell by Dr. Victor Blanco, to whom I am much indebted for the observations. Details of our photocell equipment

and of the color system have been indicated elsewhere (MacRae, Harris, and Rogerson 1952). These measures indicate that a correction of +0.02 mag. should be made to the zero point of the m_{pg} given in column 2 to reduce them to the P system of Stebbins, Whitford, and Johnson (1950). Field errors were negligible.

Column 3 gives the red color indices for 1764 stars, principally of early type, in LF4. Photored magnitudes for these were measured with the Eichner photometer, a final magnitude having a probable error of ±0.03. The red indices, therefore, have an internal probable error of ±0.05 mag. The effective wave length of the Eastman 103*a*-E plates and No. 22 Wratten filter used for the red magnitudes is about λ 6200. A calibration sequence for the red photometry was established by polar comparison, the NPS magnitudes (slightly revised) provided by Nassau and Burger (1946) serving as standards.

The photoelectric observations mentioned also provided a check on the color system. The relation R.I. = $1.33(P - V)$ was used to compute red indices, and we found for six stars an average systematic difference between these and the catalogue values of 0.01 mag. Our catalogued colors are too blue by this amount. The red indices listed in column 3 thus appear to be free of serious systematic error.

Spectral types and luminosity classes are listed in column 4. These have been observed on three to six plates taken with the 24–36-inch Burrell telescope. While most of the classification was done on plates taken with the 4° prism (dispersion 283 A/mm at $H\gamma$), resolution of certain overlapping spectra was accomplished on plates taken with the 2° prism.

The nomenclature for luminosity class is that of Morgan, Keenan, and Kellman (1943). Criteria for such classification most appropriate for our spectra have been published by Nassau and van Albada (1947). For all stars brighter than $m_{pg} = 11.0$ and of spectral class F0 and later, an attempt has been made to subdivide the stars into four luminosity classes: I (supergiants), III (giants), IV (subgiants), and V (dwarfs). Fainter stars of classes G2 and later have been designated simply as III or V, the resolution of the spectra being insufficient for more detailed separation.

High-luminosity objects of early type are designated by the class OB, following the work of Nassau and Morgan (1951). Early-type stars of lesser luminosity but having decidedly weak hydrogen for their class have been designated by "Bi" in the "Remarks."

INTERESTING OBJECTS IN LF4

Mention should be made of certain stars and clusters which make LF4 an interesting region for study.

1. *BD+55°2721 = HD 211853.*—Beals (*Pub. Dom. Ap. Obs. Victoria*, **4**, 286, 1930) proposes O7 + OW7 as a classification for this star. With the exception of λ 4686, emission is weak on our spectra. There is a trace of absorption on properly exposed plates.

2. *Nova Lacerta 1936.*—Our +55°83. Here N_1 and N_2 are the dominant emission features in the spectrum; $H\beta$ is in emission and rather strong. There appear to be broad but weak emission features at λλ 4387, 4550, and 4800.

3. *Compact cluster of early B stars.*—The brightest member is No. 55°293 in our list. There appear to be about six stars in the group. The star BD+55°2736 appears to lie in the cluster.

4. *HD 213049.*—Just north of our No. +55°441. Very strong emission at λ 4686 and broad but weaker emission bands throughout. Beals (*op. cit.*) proposes OW8 as a type.

5. *NGC 7245.*—Cluster of faint stars. No. 54°252 of our list is in the cluster. Shapley (*Star Clusters*, Appendix B) gives approximate diameter 3′; 40 stars; magnitude of fifth star, 13.

6. *NGC 7296.*—A cluster of B5–B8 stars, including Nos. 52°712 and 52°713 of our list.

7. *IC 1442.*—A very loose cluster surrounding our No. 53°290.

8. *Emission object.*—Midway between our Nos. 54°209 and 54°169. $H\beta$, $H\gamma$, and $H\delta$ in emission. Very faint.

9. *Variables.*—Several variable stars are included in the field. Among them, spectral types can be assigned as given in the accompanying table. The information, except for

Star	LF4 No.	Variation	Range (Mag.)	Spectrum
AB Cephei.....	Edge	Long period (?)	13–15.5	Me
RW Cephei.....	55°299	Irregular	8.4–9.1	M01a
SU Lacertae.....	Near 55°449	M (313 days)	10.4–16	M5e:
AW Lacertae.....	54°369	E (β Lyrae)	10.3–11.0	B2:
TW Lacertae.....	54°850	E (Algol)	11.5–13.3	A2
CP Lacertae.....	55°83	Nova (1936)	1.9–[16	.....
WZ Lacertae.....	Near 53°348	LP (287 days)	13.6–14.8	M
SV Lacertae.....	Near 53°917	M (305 days)	12.6–[16.5	Me
RZ Lacertae.....	52°914	Constant	8.9	B8

spectral type, is taken from B. V. Kukarkin and P. P. Parenago, *General Catalogue of Variable Stars* (Moscow: Academy of Sciences, U.S.S.R., 1948).

REFERENCES

McCuskey, S. W. 1949, *Ap. J.*, **109**, 426.
———. 1951, *ibid.*, **113**, 672.
McCuskey, S. W., and Seyfert, C. K. 1950, *Ap. J.*, **112**, 90.
MacRae, D. A., Harris, D. L., and Rogerson, J. 1952, *A.J.*, **57**, 19.
Morgan, W. W., Keenan, P. C., and Kellman, E. 1943, *An Atlas of Stellar Spectra* (Chicago: University of Chicago Press).
Nassau, J. J., and van Albada, G. B. 1947, *Ap. J.*, **106**, 20.
Nassau, J. J., and Burger, V. 1946, *Ap. J.*, **103**, 25.
Nassau, J. J., and MacRae, D. A. 1949, *Ap. J.*, **110**, 478.
Nassau, J. J., and Morgan, W. W. 1951, *Pub. U. Michigan Obs.*, **10**, 43.
Stebbins, J., Whitford, A. E., and Johnson, H. L. 1950, *Ap. J.*, **112**, 469.

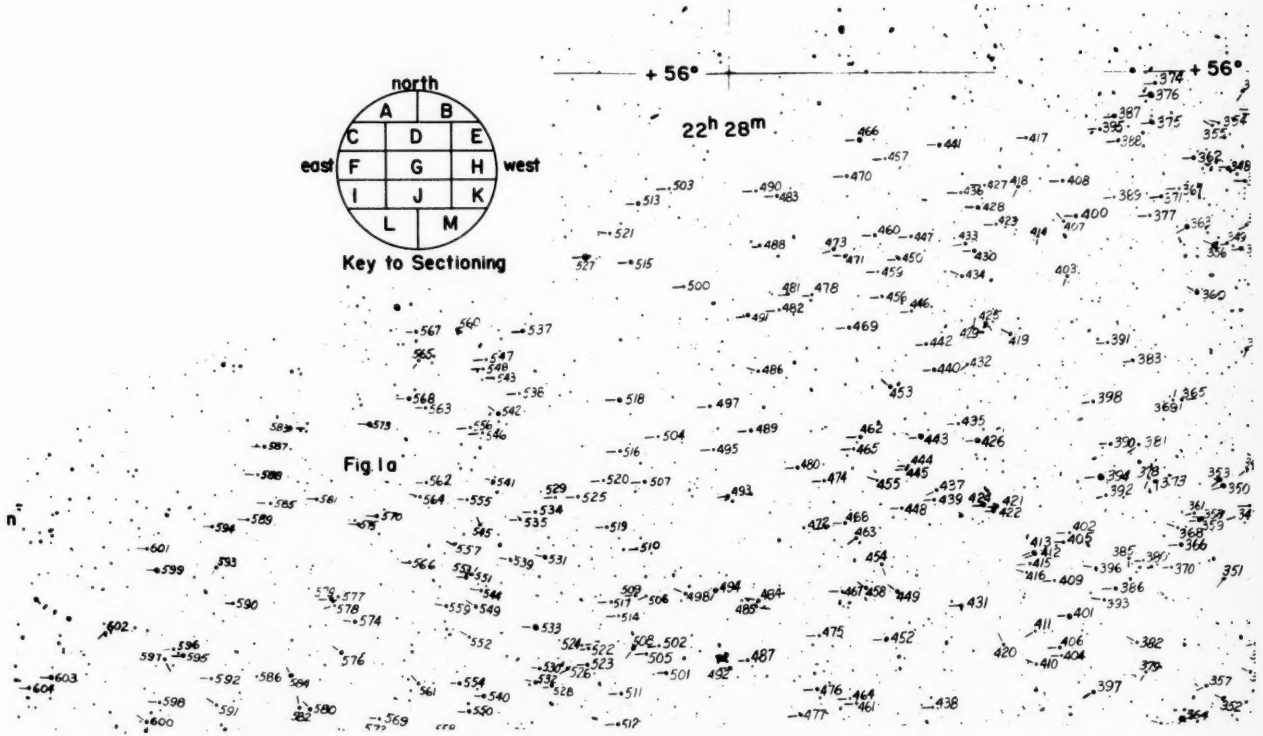

FIG. 1*a*.—Identification chart for LF4

FIG. 1a.—Identification chart for LF4

FIG. 1b.—Identification chart for LF4

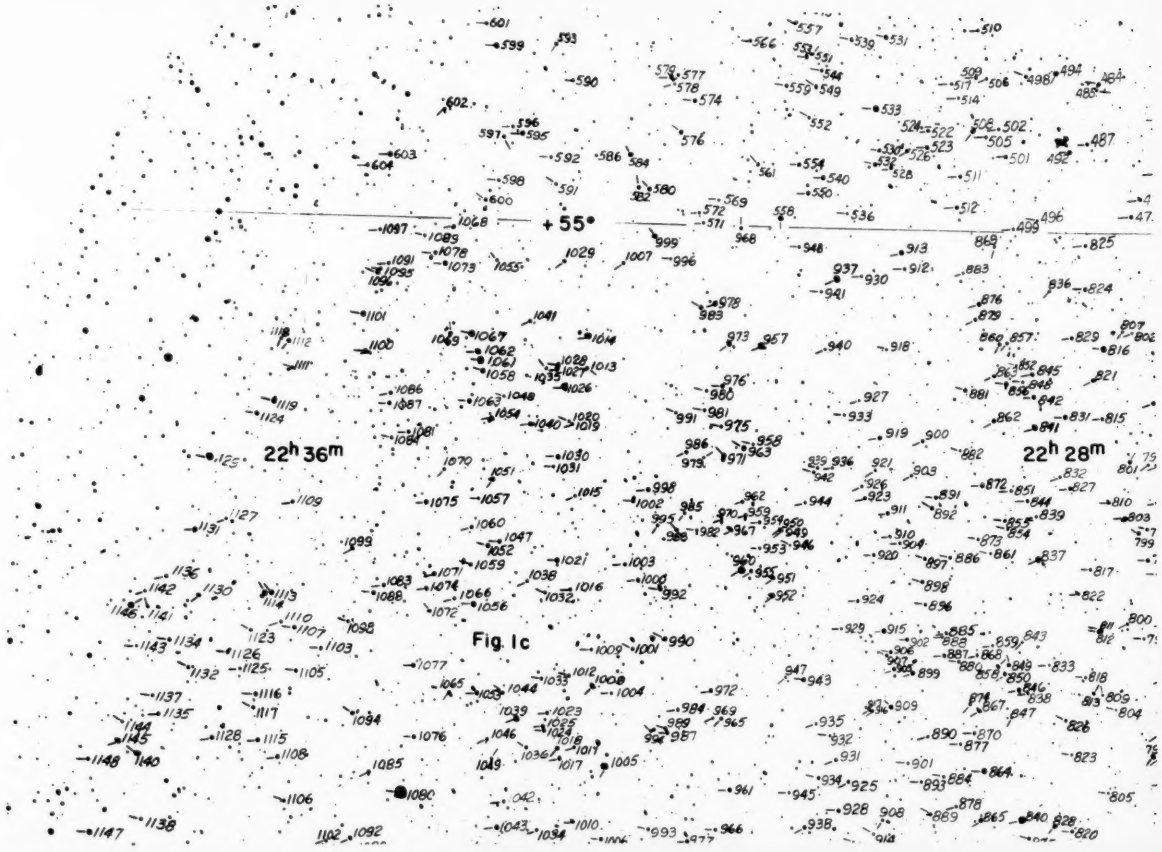

FIG. 1c.—Identification chart for LF4

FIG. 1c.—Identification chart for LF4

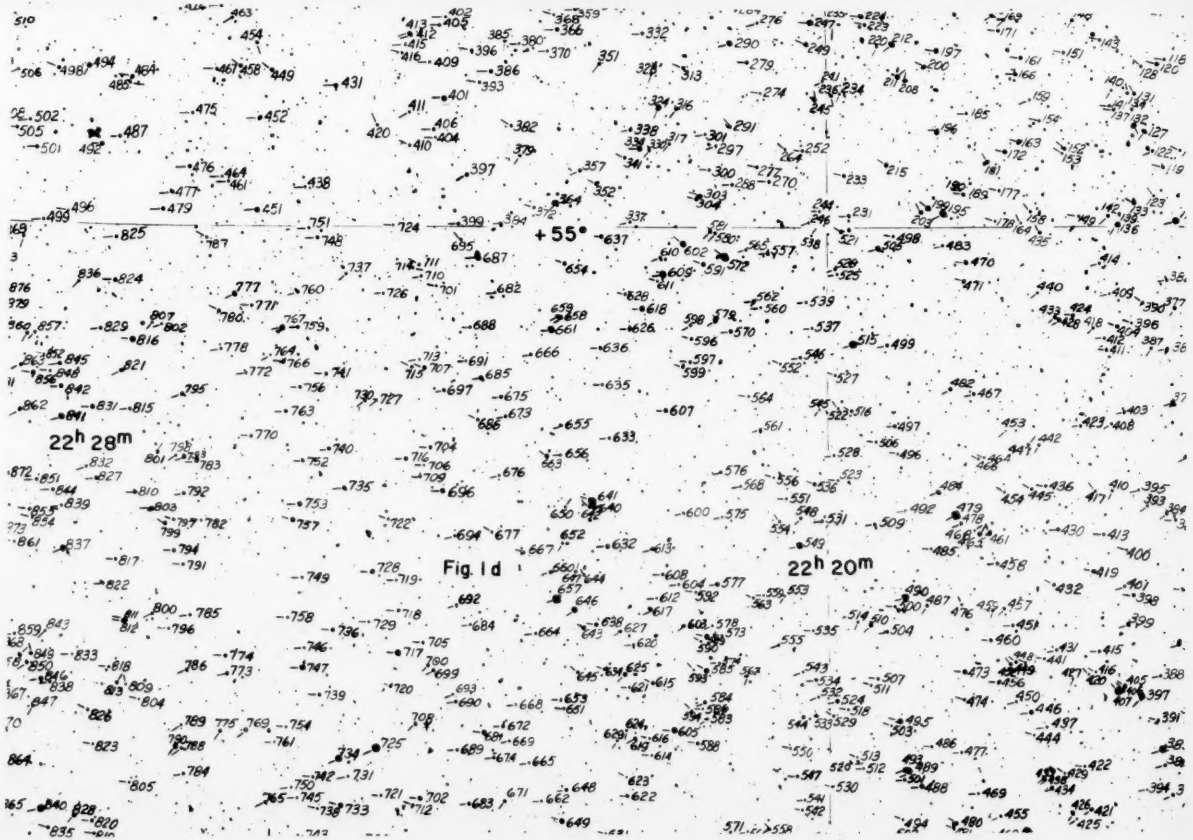

FIG. 1*d*.—Identification chart for LF4

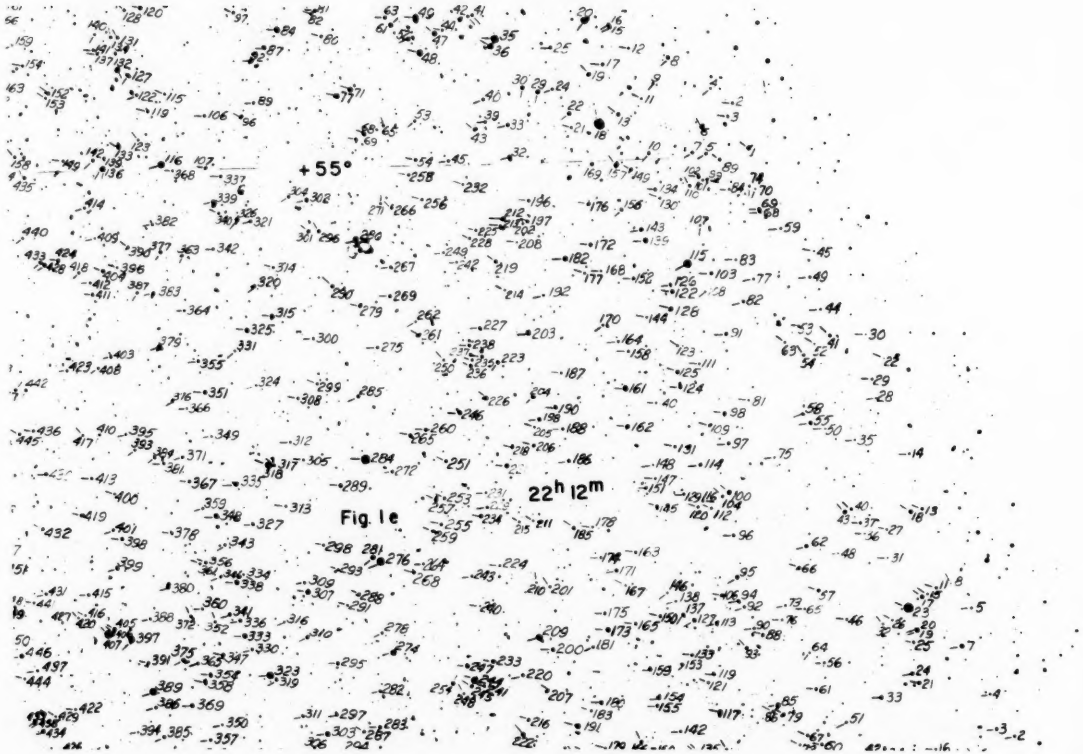

FIG. 1e.—Identification chart for LF4

FIG. 1e.—Identification chart for LF4

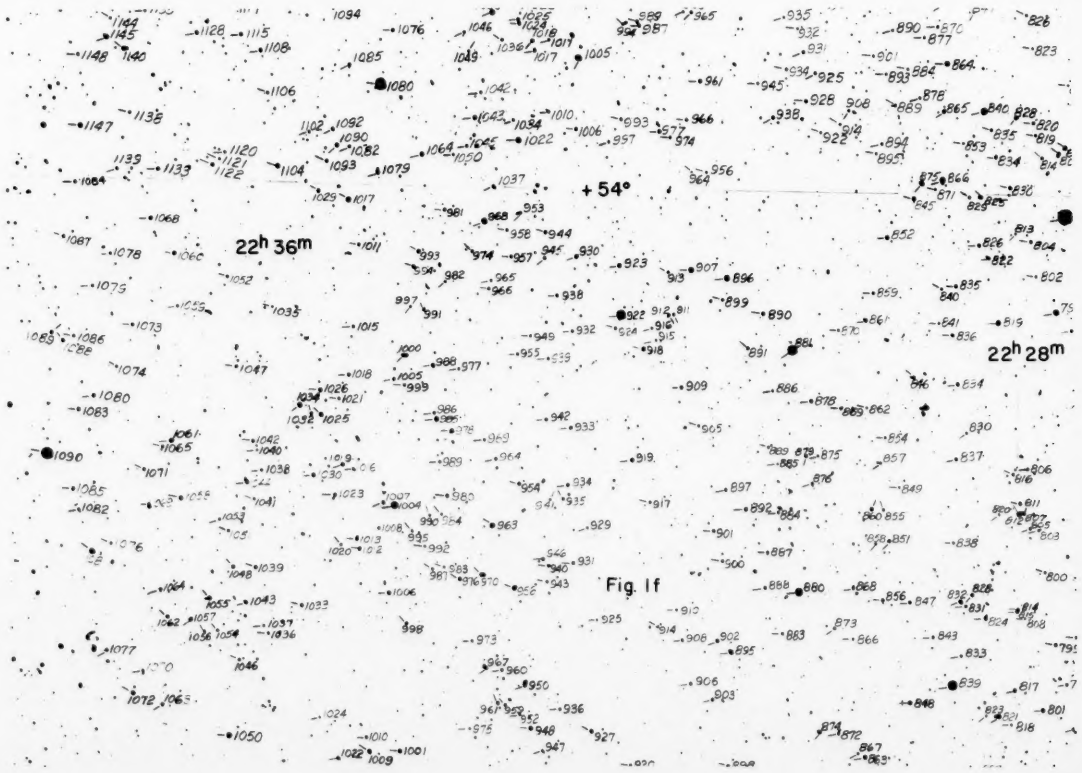

FIG. 1f.—Identification chart for LF4

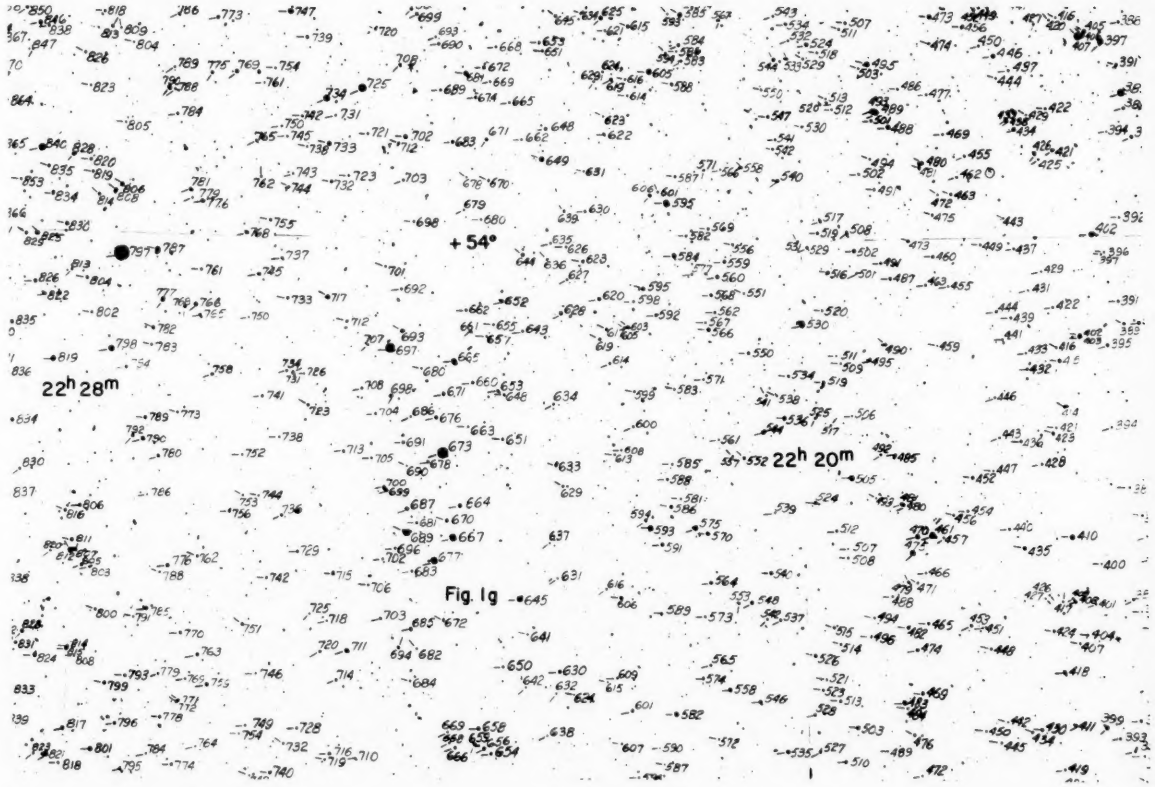

FIG. 1g.—Identification chart for LF4

FIG. 1g.—Identification chart for LF4

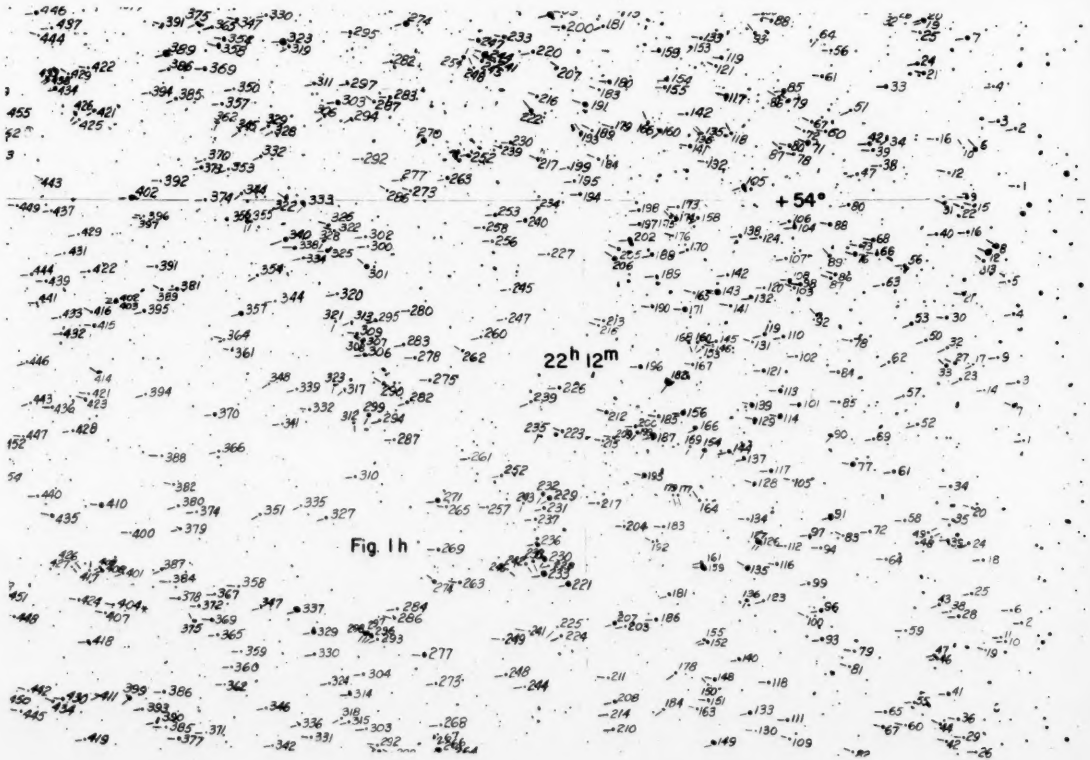

FIG. 1*h*.—Identification chart for LF4

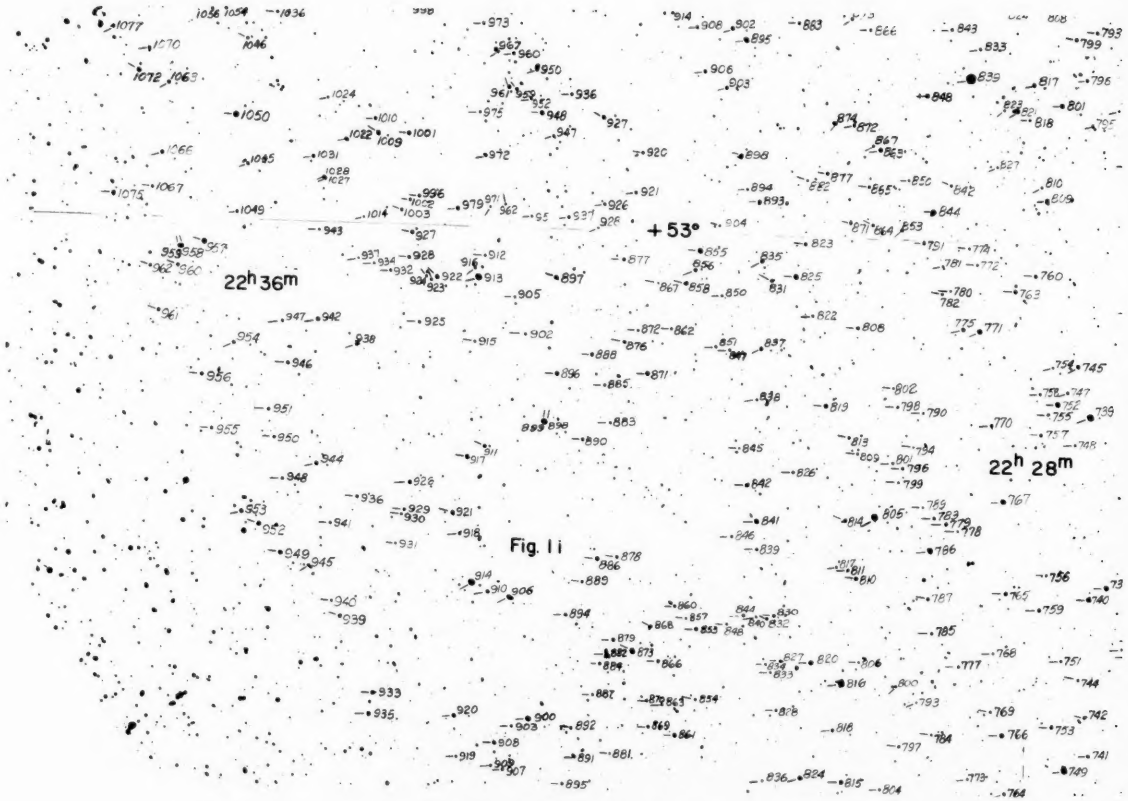

FIG. 1*i*.—Identification chart for LF4

FIG. 1*i*.—Identification chart for LF4

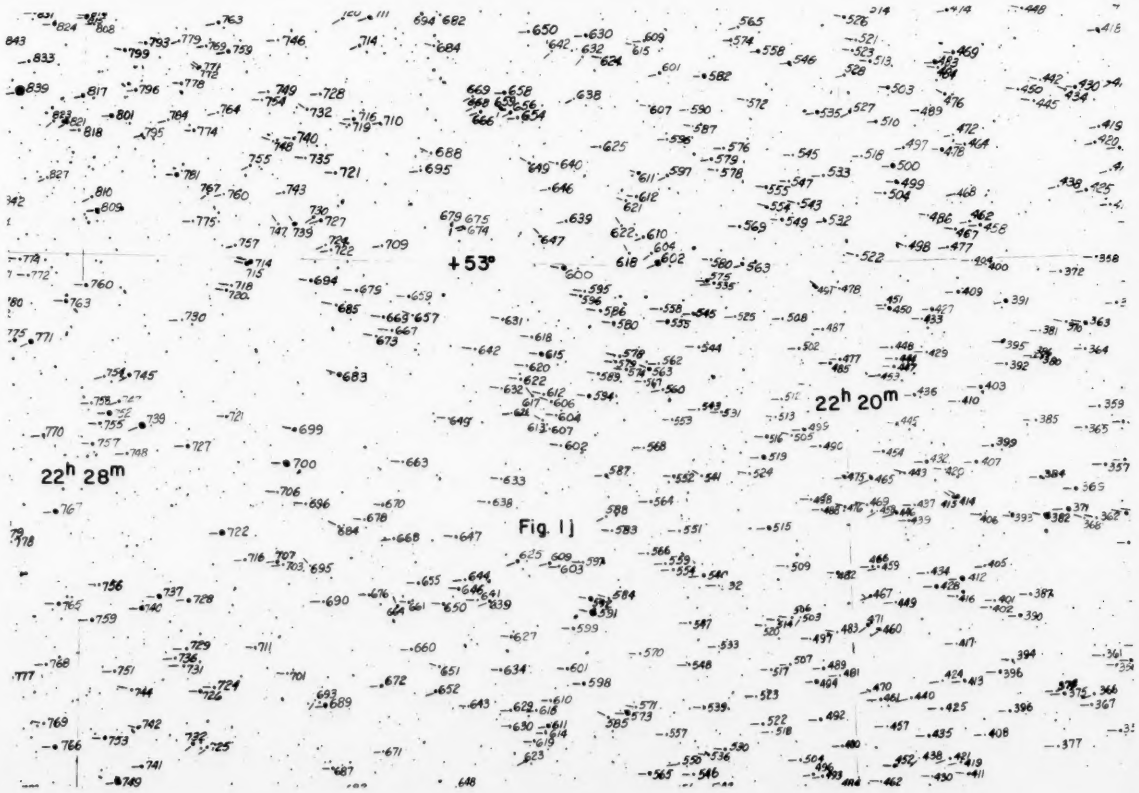

FIG. 1*j*.—Identification chart for LF4

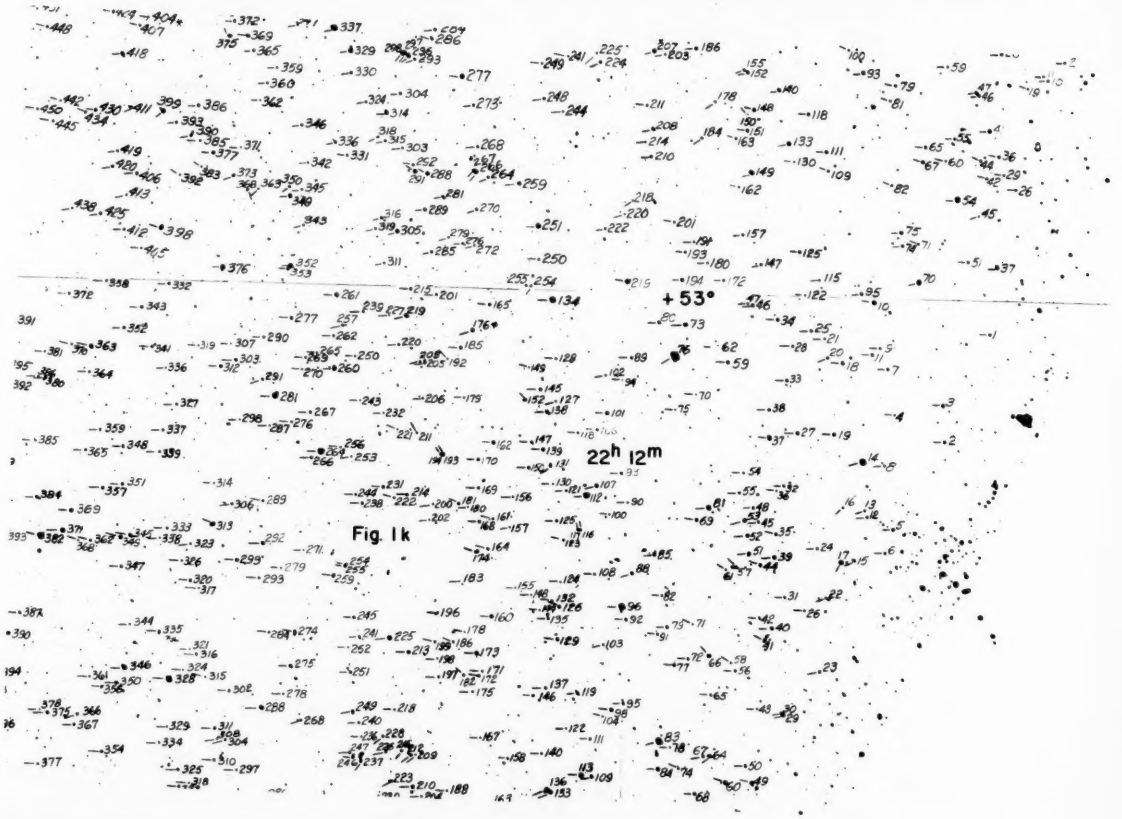

FIG. 1*k*.—Identification chart for LF4

FIG. 1k.—Identification chart for LF4

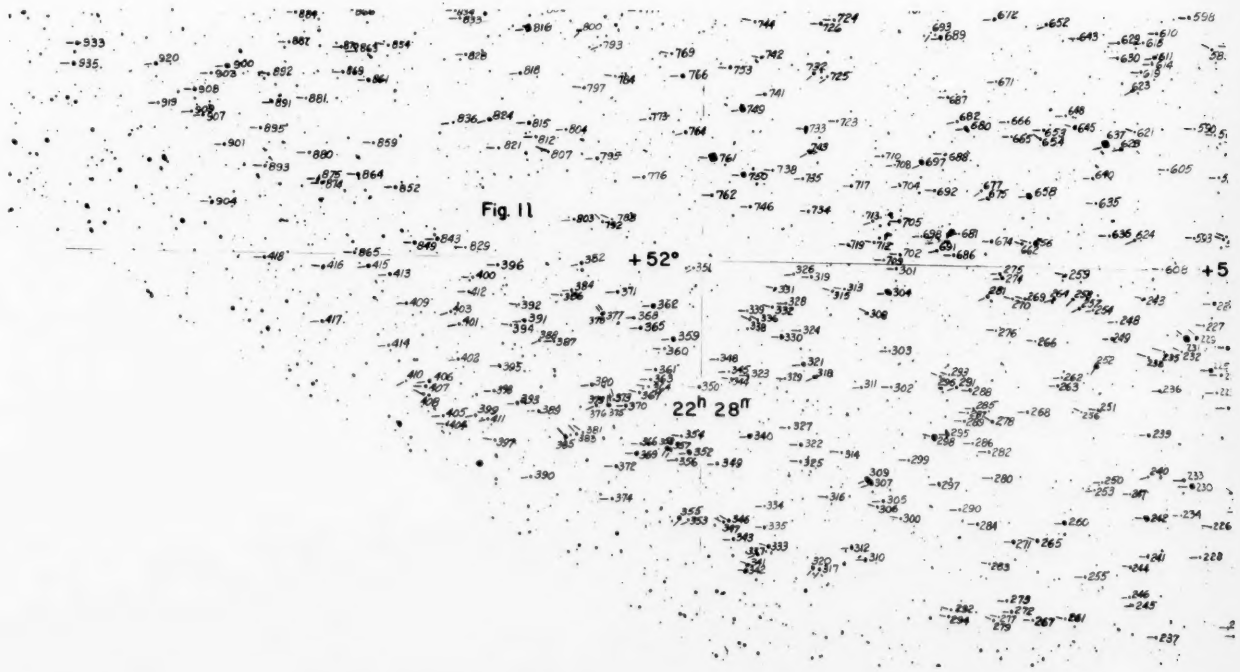

FIG. 1l.—Identification chart for LF4

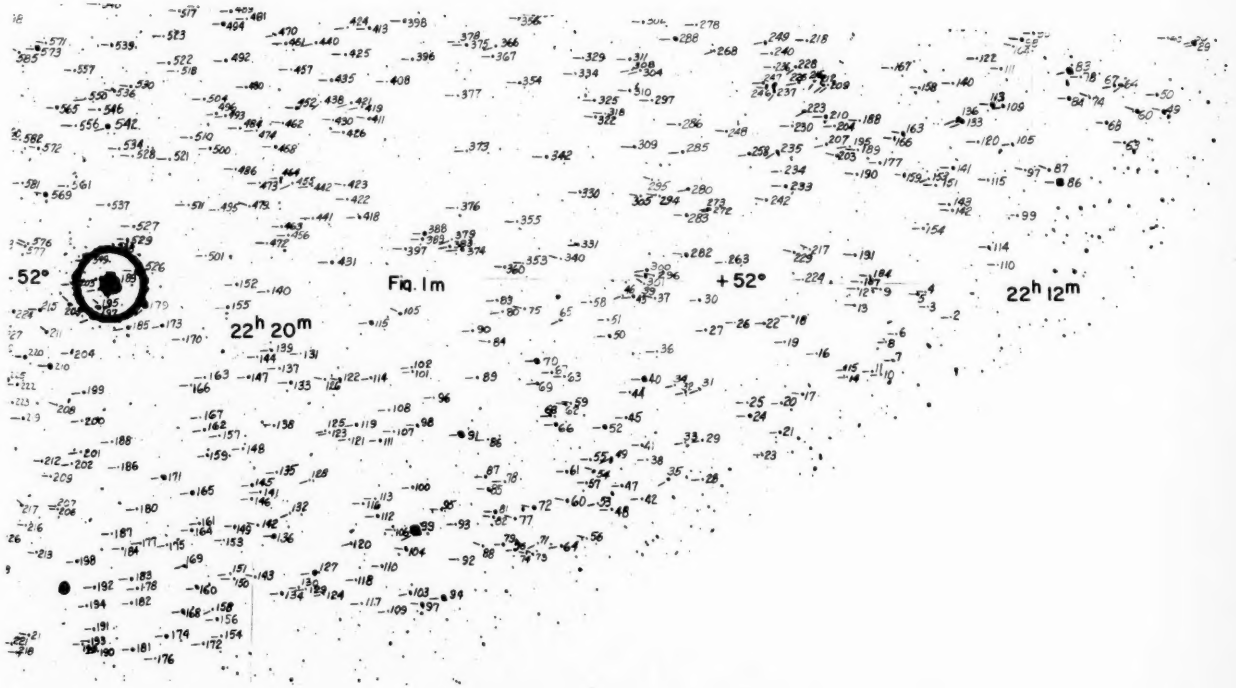

FIG. 1*m*.—Identification chart for LF4

Table 1

Observational Data for Region LF4

Zone +51°

No.	m_{pg}	R.I.	Sp.	No.	m_{pg}	R.I.	Sp.	No.	m_{pg}	R.I.	Sp.
1	12.52	...	B5	51	12.40	...	B9	101	12.57	...	B8:
2	12.95	...	A2-F0	52* R	11.14	...	F0V	102	12.83	+0.44	A2
3	12.87	...	A2	53	12.40	...	G0	103	11.74	...	F0
4	12.99	...	B5:	54	12.61	...	B5	104	11.97	...	G2V
5	12.15	...	A0	55	12.17	...	B8	105	12.18	...	B8
6	12.65	...	B5:	56	12.23	...	B8	106	12.95	...	A3:
7	12.14	...	F8	57	12.83	...	A0	107	12.56	+0.26	B5
8	13.01	...	A0:	58	12.36	...	G0V	108	12.28	+1.28	G5III
9	12.24	...	F0:	59	12.40	...	B5	109	12.52	...	B5
10	12.15	...	G0:	60	10.86	...	B5:	110 R	11.36	...	B5
11	12.12	...	G8IV	61*	11.22	...	G8III	111	12.89	+0.39	F0
12	12.47	...	G2:	62	11.97	...	G0:	112*	10.83	...	G0V
13	11.84	...	A5	63	12.12	...	G0III	113	12.41	-0.05	A2
14	12.61	...	B9	64*	11.20	...	K0IV	114	12.17	...	F0III
15	12.32	...	B:	65	12.55	+0.06	A0	115*	9.87	-0.03	A0
16	12.32	...	B5	66*	10.00	...	G8III	116	12.35	+0.05	B9
17	12.01	...	A2	67	12.37	...	G5V	117	13.34	...	G8III
18	11.97	...	K2III	68	12.05	...	F0	118	12.39	...	G2
19	12.19	...	K3:	69	11.11	-0.30	B5	119*	10.68	+0.18	A3-F0
20	11.86	...	B9	70*	8.82	-0.30	B1k	120	12.05	+0.07	A0
21*	11.08	...	F5	71	12.55	+0.25	A0	121	12.85	...	G0
22	11.88	...	G8IV	72*	9.88	...	K3III	122	12.09	+0.34	A3
23	12.34	...	A5	73	12.01	-0.10	B8	123	12.52	+0.10	B9
24*	10.00	...	B9	74	12.38	...	G2:	124	12.53	+0.09	B8
25	12.44	...	K2	75	12.42	-0.04	B9	125	12.57	...	K0III
26	12.87	...	B5	76	12.57	...	A2	126	12.07	+0.27	B5k
27	11.88	...	A0	77	11.77	+0.23	A5	127*	9.93	-0.15	B8
28	12.26	...	B8	78	12.63	+0.18	B5	128	12.85	...	M0III
29	12.95	...	K2:	79	11.28	-0.30	B9	129	12.53	...	G0:
30	11.56	...	B5	80	12.16:	...	G8:	130	12.11	...	G0
31	12.19	...	B5	81*	10.69	...	F5V	131	12.69	-0.07	B9
32	12.40	...	G5	82	11.68	+0.30	B5:	132	12.40	...	G0
33	12.79	...	G8:	83	12.32	+0.07	A0	133 R	10.59	-0.13	B8
34	12.52	...	B2	84	12.43	+0.29	A0	134	11.22	...	F0V
35	12.01	...	K0V	85	10.95	-0.02	B8	135	12.26	...	G2
36	12.56	...	A3	86	12.57	-0.15	A0	136*	10.08	-0.18	B8
37	12.27	...	A2-F0	87	11.45	+0.05	A0	137	11.99	+0.09	B8
38	12.76	...	K0	88	12.15	...	G0V	138	12.76	+0.08	B8
39	12.32	...	A0:	89	11.40	+0.11	A0	139	11.92	...	F0
40*	9.06	...	B8	90	11.59	...	G8III	140	12.49	-0.18	A0
41	12.01	...	G0V	91*	8.29	...	F2V	141	12.05	+0.25	A0
42	12.17	...	A0	92	12.68	+0.44	A3	142	11.58	...	G0
43	11.19	...	B9	93	12.83	+0.19	A3	143	11.82	+0.24	A2
44	12.36	...	F0:	94* R	9.01	-0.25	B5	144	12.38	+0.16	A3-F0
45	12.00	...	B8	95	12.15	+0.38	A0	145	10.65	-0.24	B8
46	12.57	...	B8:	96	12.97	...	G2:	146	11.42	-0.09	B8
47	11.58	...	F0III	97*	10.38	...	F0II	147	12.19	+0.13	B9
48	12.00	...	A0	98	11.71	+0.15	A2	148	12.44	...	B9
49	12.70	...	B8:	99*	6.57	+0.03	B2	149	11.42	...	K0III
50	12.47	...	B8:	100*	11.45	...	K0V	150	12.34	...	F0

Table 1

Observational Data for Region LF4 (Cont'd.)

Zone +51° (Cont'd.)

No.	m_{pg}	R.I.	Sp.	No.	m_{pg}	R.I.	Sp.	No.	m_{pg}	R.I.	Sp.	No
151	12.27	+0.67	B8	201	12.34	+0.12	A0	251	12.01	...	G0	301
152	11.26	-0.22	B9	202	12.51	...	G2V	252	11.85	+0.43	A5	302
153	12.47	...	G0	203	12.32	...	G0	253	12.69	+0.29	A2-F0:	303
154	12.31	-0.04	B8	204	12.36	...	G0	254	12.81	...	G0	304
155	11.04	+0.48	G0V	205	11.70	-0.06	A0	255	12.32	...	G8III	305
156	11.08	-0.25	B5	206	12.68	0.00	A3	256	12.84	+0.20	B9	306
157	12.70	...	K0V	207	12.94	+0.41	A2	257	11.13	+0.01	B9	307
158	12.53	+0.10	A2	208	12.73	+0.14	B9	258	11.98	+1.04	K0V	308
159	12.34	+0.20	A0	209	12.40	...	F0	259	12.04	+0.10	A0	309
160	12.00	+0.11	A0	210*	9.07	-0.14	B8	260*	9.85	-0.09	B9	310
161	12.32	...	F0	211	12.85:	...	A2	261	12.30	...	G0	311
162	11.29	+0.17	A3	212	11.91	...	F0	262	12.44	...	G5III	312
163	12.26	...	G5III	213	12.14	-0.08	A0	263 R	11.84	-0.03	A0p	313
164*	11.08	...	K2IV	214	12.41	+0.07	B9	264	11.05	0.00	A0	314
165*	9.63	...	K0IV	215	11.50	...	G5IV	265	11.58	...	B8	315
166	12.40	...	G0	216	12.74	+0.22	B9	266	12.89	...	K0III	316
167	13.01	...	G5:	217	12.93	...	K0	267	12.22	...	G2	317
168*	10.46	...	F0V	218	12.66	...	A0	268*	11.35	...	K2III	318
169	12.22	...	G2	219	11.53	+0.55	G0V	269	11.88	...	G8V	319
170	12.26	+0.30	A3	220* R	10.31	+0.24	A5	270	12.52	+0.06	A2	320
171* R	9.53	-0.20	B9	221	12.93	...	K0III:	271*	10.60	...	K0IV	321
172	11.86	-0.16	B5	222	12.10	-0.07	B8	272*	11.48	...	G5III	322
173	11.32	-0.31	B5	223	12.16	0.00	B8	273	12.93	...	K2	323
174*	10.30	...	K0IV	224*	10.65	...	K0V	274* R	10.72	+0.09	A0p	324
175	12.15	...	F8	225*	9.46	+0.38	A5	275	11.60	-0.04	B5k	325
176	12.47	...	G0:	226	12.74	...	G8	276	12.61	...	F0V	326
177	12.51	...	K2	227	12.68	+0.04	B9	277	13.24	...	K0III	327
178	11.64	-0.02	B9	228	12.40	+0.12	B9	278	11.22	...	F0V	328
179*	9.78	+0.44	F8V	229	10.91	...	F0V	279	12.24	...	G5V	329
180	12.12	...	F5	230* R	8.77	+0.19	A3	280	12.91	...	M0	330
181	11.26	...	G0III	231* R	8.26	-0.37	B3k	281	10.70	+0.50	F8V	331
182	11.93	...	G8	232	12.95	+0.27	A0	282	11.78	...	K0IV	332
183	11.02	-0.11	B9	233	11.64	...	G0V	283	12.82	+0.09	B9	333
184	12.15	...	G0V	234	12.77	...	G0	284	11.52	...	F2III	334
185	11.49	...	G2	235	12.34	...	G0	285	12.84	0.00	B9	335
186	12.91	...	F0	236	11.99	-0.05	B9	286	12.44	...	G5III	336
187	12.41	+0.23	A3-F0	237	11.63	-0.09	B9	287	12.90	+0.04	B9	337
188	12.44	...	G5III	238	12.14	...	F0	288	11.13	...	F0V	338
189*	(4.4)	...	G5III	239*	10.61	+0.17	A2-F0	289	12.87	...	K0	339
190	13.00	+0.40	A3	240	12.12	...	G0	290	12.01	...	K0III	340
191	12.28	...	G0	241	12.32	...	G0	291	12.00	+0.09	A0	341
192	12.66	...	F0:	242* R	8.91	-0.03	B9	292	12.22	...	G5III	342
193	12.70	...	K0III	243	12.22	...	G8III	293	12.62	+0.08	B9	343
194	12.05	+0.43	A5	244	12.53	+0.11	A0	294	12.58	-0.08	B5	344
195 R	10.53	+0.19	A5	245	12.79	...	K2	295	12.36	...	G5III	345
196	12.32	...	G2V	246	12.43	+0.04	A0	296	12.17	+0.35	A5	346
197	12.34	...	G5	247	12.61	-0.03	B5	297	11.62	...	G5III	347
198	11.41	...	F5V	248	12.94	...	A0	298* R	8.83	...	G0IIIp	348
199	12.15	...	G5III	249	11.25	+0.11	A0	299	12.75	+0.03	A0	349
200	12.30	+0.44	A3	250	12.53	...	G0	300	12.28	...	G0	350

Table 1

Observational Data for Region LF4 (Cont'd.)

Zone +51° (Cont'd.)

No.	m_{pg}	R.I.	Sp.	No.	m_{pg}	R.I.	Sp.	No.	m_{pg}	R.I.	Sp.
301	12.00	...	G0	351	12.28	...	K3:	401	12.39	...	G5III
302	12.44	...	G0	352*	9.65	...	A0	402	12.61	...	G5:
303	12.63	+0.13	B9	353	12.61	...	A0	403	12.56	...	F0
304*	8.78	0.00	B9	354	12.39	...	F0V	404	12.17	...	A3
305	11.41	+0.19	A2-F0	355*	10.25	...	A3	405	12.70	...	G5III
306	12.57	-0.05	B9	356	12.62	+0.52	G0	406*	11.08	...	B9
307*	8.96	-0.05	B9	357	12.24	...	B5	407	12.06	...	G0
308	12.09	+0.30	A5	358	11.49	...	B5	408	12.26	...	F0:
309*	10.08	-0.10	B9	359*	9.65	...	B8	409	12.15	...	G5V
310	12.85	...	G0	360	11.84	...	G0III	410	13.17	...	A0
311	12.54	+0.38	B5	361	11.75	...	K0III	411	12.61	...	G8III
312 R	11.58	+0.24	A2	362*	10.21	...	F8V	412	12.44	...	B8
313	12.98	-0.22	B8:	363	12.17	...	K2III	413	11.60	...	A5
314	12.39	...	F0	364	12.39	...	A2	414	12.66	...	G2
315	12.32	+0.04	B9	365	11.05	...	A0	415	11.80	...	G2V
316	12.24	+0.41	A5	366	12.61	...	G0	416	12.54	...	B9
317	11.38	+0.65	G0V	367	12.12	...	F0	417	12.34	...	F8:
318	12.85	...	A0:	368	12.17	...	G8V	418	12.07	...	A2
319 R	12.17	...	G8:	369*	10.74	...	G0V				
320*	10.48	...	G0III	370	11.26	...	B5				
								Zone +52°			
321*	10.34	-0.18	B5	371*	11.03	...	G5III	1	12.36	...	A3
322	10.74	+0.01	A0	372	11.68	...	A2	2	11.91	...	K0IV
323	12.61	...	K0:	373	12.81	...	A0	3	11.57	...	A0
324	12.73	+0.25	A0	374	12.00	...	B8	4	12.61	...	B5:
325	12.42	+0.27	A0:	375	12.28	...	G5V	5	11.86	...	A0
326	12.21	+0.21	A0	376	12.39	...	G0III	6	12.47	...	M0III
327	12.26	...	M2V	377	12.70	...	K5III	7	11.96	...	B8
328	12.34	...	G0	378	13.09	...	K0	8	12.28	...	B8
329	12.59	+0.02	B9	379	12.24	...	A2	9	12.26	...	A2-F0
330*	11.62	...	G8III	380*	10.95	...	F8V	10*	10.29	...	F8IV
331	12.15	...	A5	381	12.89	...	A2	11*	11.07	...	M0III
332	11.67	...	K3III	382*	10.98	...	G0III	12	11.92	...	B5
333*	10.55	...	F8III	383	12.08	...	G8III	13	12.40	...	F0
334	13.07	...	A0	384	12.28	...	G0	14*	8.07	...	F0V
335	12.08	...	G5	385	11.83	...	F0	15	12.40	...	G0
336	12.36	...	G2III	386	12.65	...	F5:	16	12.30	...	F0
337	11.83	...	F0	387	12.44	...	F0:	17*	10.08	...	B8
338	12.10	...	G8III	388	12.29	...	G0V	18	11.53	...	B5
339	12.61	...	A0	389	11.92	...	K2III	19	10.65	...	F8V
340*	10.13	...	B9	390	12.12	...	G2V	20	12.12	...	G8III
341	12.29	...	A2	391*	10.90	...	G5III	21	12.51	...	B5
342 R	11.67	...	A0	392	13.04	...	K0III	22	12.77	...	A0
343	11.68	...	A2	393	11.83	...	G0III	23	11.97	...	G5V
344	12.47	...	G0:	394	12.75	...	B5	24	12.15	...	G8III
345	12.95	...	B8	395	12.05	...	G0	25	11.71	...	G0V
346	11.21	...	A0	396	12.15	...	B5	26	12.57	...	A0
347	12.27	...	A0	397	12.47	...	G0:	27	10.96	...	B9
348	12.47	...	G5III	398	12.75	...	K3	28	12.09	...	A0
349	11.17	...	B9	399	12.22	...	A5	29*	10.50	...	A0
350	11.62	...	G0III	400	12.70	...	K0V	30	12.57	...	A3

Table 1

Observational Data for Region LF 4 (Cont'd.)

Zone +52° (Cont'd.)

No.	m_{pg}	R.I.	Sp.	No.	m_{pg}	R.I.	Sp.	No.	m_{pg}	R.I.	Sp.
31	12.44	...	A0	81*	9.04	...	K0III	131	11.95	...	K3III
32	12.40	...	F8	82	12.30	...	A2	132	12.66	...	A0
33	12.06	...	G0	83*	8.14	...	B8	133*	10.57	...	B5
34	10.82	...	K0III	84*	10.42	...	A0	134*	8.70	...	A5
35	12.34	...	B9	85	11.92	...	A5	135	12.36	...	K0
36	12.79	...	G0	86*	7.71	...	B8	136	10.21	...	G0IV
37*R	10.42	...	A0	87	11.25	...	A0	137	11.20	...	G0III
38	11.75	...	G2V	88	10.96	...	B8	138	11.63	...	A5
39*	10.86	...	G5IV	89	11.71	...	B8	139	10.61	...	A2
40	10.87	...	B9	90	12.52	...	B5	140	12.23	...	G0
41*	11.00	...	K0IV	91	12.40	...	G0	141*	10.46	...	G8IV
42	13.03	...	G5	92	11.96	...	B9	142	11.93	...	G2
43	12.66	...	B5:	93	12.65	...	A5:	143	11.84	...	B8
44	11.09	...	F5IV	94	13.25	...	B8	144	12.76	...	G5
45	12.58	...	B9	95	11.85	...	G8V:	145	10.87	...	B8
46*	10.91	...	G5IV	96*	8.45	...	B8	146	12.61	...	G5III
47	12.23	...	A2-F0	97	12.40	...	A0	147	12.11	...	G0
48	12.40	...	A2	98*R	10.46	...	B9	148	12.75	...	A2
49 R	10.73	...	B5	99	12.15	...	A0	149	13.01	...	A0
50	12.15	...	A0	100	12.93	...	A0	150	11.30	...	B8
51*	11.04	...	B9	101	10.96	...	A0	151	11.97	...	K0III
52	10.90	...	G5IV	102	12.36	...	A2	152	12.47	...	A0
53*	9.76	...	F0V	103	12.36	...	G8III	153	12.36	...	B8
54	12.44	...	B5:	104	12.47	...	B8	154	12.09	...	B5
55	11.91	...	F5V	105	12.47	...	G5III	155	13.08	...	B8
56	11.72	...	B5	106	12.21	...	G0:	156	12.65	...	G0
57	12.56	...	G5III	107	10.54	...	B8	157	12.51	...	G0
58	12.40	...	B5	108	12.06	...	A0	158	12.18	...	B8
59	10.73	...	B8	109	11.87	...	K0V	159	12.11:	...	A0
60*	10.38	...	B5	110	12.91	...	B9	160*	10.50	...	A3
61	12.65	...	A0	111	11.83	...	G2Ib:	161	12.22	...	F0
62	11.93	...	A5	112*	8.40	...	K2III	162	10.90	...	F0IV
63	12.07	...	A2	113*	8.66	...	K2IV	163*	10.65	...	A0
64	12.05	...	A0	114	12.19	...	F0	164	12.53	...	G5
65	12.75	...	K0III:	115	12.19	...	G8III	165	12.17	...	G5V
66*	11.26	...	F2V	116	12.23	...	F8	166	12.15	...	B9
67	12.19	...	F2	117	12.48	...	G0	167	12.62	+0.06	A0
68	11.35	...	A2	118	12.40	...	K0V	168	11.31	...	A5
69	10.95	...	B8	119	12.12	...	B5:	169	11.45	-0.09	A0
70	13.54	...	A0	120	11.87	...	G0V	170	11.36	-0.04	A0
71	12.48	...	G5III:	121	12.21	...	K2III	171*	11.48	...	G8III
72	12.21	...	B9	122	12.74	...	G5III	172	11.67	...	G0
73*	10.80	...	G0V	123	12.15	...	K0V	173*	10.25	...	F8IV
74	12.35	...	G5III	124	12.48	...	A0	174	12.38	...	G8
75	12.97	...	A0	125	12.26	...	G0	175	12.05	-0.05	A3
76*	7.16	...	A5	126*	10.63	...	A3	176*	10.47	+0.46	A3
77 R	11.35	...	A2	127	12.76	...	A0	177	11.27	...	G5III
78	12.57	...	K0III	128	12.22	...	A0	178	12.79	-0.08	B8:
79	11.63	...	A3	129	12.16	...	A0	179	12.34	+0.14	A0
80	12.00	...	G5III	130	12.51	...	A2	180	13.02	+0.14	A2

Table 1

Observational Data for Region LF4 (Cont'd.)

Zone +52° (Cont'd.)

No.	m_{pg}	R.I.	Sp.	No.	m_{pg}	R.I.	Sp.	No.	m_{pg}	R.I.	Sp.
181	11.40	. . .	G5IV	231*	10.77	. . .	K5III	281	12.29	. . .	A0
182	11.50	. . .	G0	232	13.03	+0.21	A0	282*	10.09	+0.51	F8V
183	13.25	+0.06	A0	233	11.64	+0.96	G5V	283*	10.78	-0.22	B9
184	11.88	+0.04	A0	234	12.87	+0.21	A0	284	12.11	+0.02	A0
185	10.96	-0.16	B9	235	11.46	-0.08	A0	285*	11.17	. . .	K0IV
186	11.84	+0.25	A2	236	12.69	+0.36	A0	286	12.02	. . .	F0V
187	12.68	+0.17	A0	237	12.13	. . .	G0	287	12.79	-0.09	B5
188	12.31	+0.09	A0	238	11.58	+1.29	K2V	288*R	10.21	-0.24	B8
189	12.11	. . .	F0:	239	11.79	-0.15	B8	289	12.12	. . .	F8
190	12.08	. . .	F8	240	12.13	. . .	K0III	290	11.60	-0.28	B8
191	11.91	-0.25	B8	241	12.31	-0.04	A0	291	12.12	-0.12	A0
192	13.05	0.00	A0	242	11.33	-0.10	B9	292	11.63	+0.24	A2
193*	10.37	. . .	G8IV	243	12.97	+0.17	B8	293	12.24	+0.26	B8
194	12.39	. . .	G5	244	12.31	+0.25	A2	294	12.22	. . .	G5III
195	12.89	+0.20	A0	245	11.75	. . .	G0	295	12.72	+0.02	A0
196	12.56	. . .	G0	246	12.29	-0.05	A0:	296	12.42	+0.14	A0
197	11.83	. . .	G8III	247	12.22	. . .	G5V	297	12.18	. . .	G0
198	12.48	. . .	K3:	248	12.48	-0.01	A2	298	12.57	. . .	G2
199	12.15	+0.11	A3	249	12.01	-0.05	A0	299	11.26	. . .	F5V
200	12.36	. . .	G5V	250	12.72	. . .	G0	300	10.68	-0.37	B8
201	12.07	-0.09	B9	251	11.67	+0.07	A2	301	10.70	-0.20	A0
202	12.90	+0.16	A0	252	12.93	+0.35	A3:	302	12.19	. . .	F0III
203	12.30	. . .	G2III	253	12.99	+0.27	A5:	303*	10.99	. . .	G5III
204	12.15	-0.27	B5	254	12.65	. . .	G5:	304	11.79	. . .	K0III
205	12.96	-0.06	A0	255	12.44	+0.05	B8	305	12.01	+0.03	A0
206	12.41	+0.23	A0	256	12.79	-0.01	B8	306	12.19	. . .	K0III
207	12.08	+0.31	A0	257	12.30	-0.03	A0	307	12.96	+0.18	A0
208	12.21	+0.22	B8	258	12.43	+0.21	A0	308	12.30	-0.18	B8
209	12.80	. . .	F0	259	11.75	. . .	G5IV	309	11.68	. . .	F0III
210*	10.00	. . .	M5III	260*	10.42	. . .	F0V	310*	11.88	. . .	G5III
211	12.74	. . .	K2III	261*	10.41	+0.11	A2	311 R	11.91	. . .	A0
212	11.64	+0.01	A0	262	12.15	. . .	F5	312 R	11.08	+0.17	A3p
213	11.12	-0.18	B8	263	13.38	+0.17	A0:	313 R	11.05	-0.24	B8
214	12.32	. . .	G5V	264*	8.45	-0.13	A0	314	12.85	+0.13	A2
215	11.84	+0.18	A0	265	12.52	-0.14	A0	315	12.50	. . .	G0
216	12.15	+1.10	K0V	266 R	12.09	+0.18	A2p	316	12.95	+0.20	A2
217	12.27	. . .	G0	267	11.57	+0.19	G5V	317	12.81	-0.10	B9
218	12.22	-0.07	A0	268	12.26	+1.09	K2V	318	12.62	+0.08	A0
219	11.33	-0.04	A0	269	12.15	. . .	G8V	319	12.61	-0.11	B5
220	12.62	. . .	G5III	270	12.44	. . .	K2	320	12.06	+0.30	A3
221	12.95	. . .	K2	271	13.13	+0.10	A0	321	13.18	+0.10	A0
222	12.23	. . .	G8V	272	12.44	. . .	G8:	322	11.50	-0.22	B8
223	12.05	. . .	K0III	273	12.17	+0.21	A2	323	12.21	-0.20	B8
224	12.35	+0.36	A0	274	12.17	. . .	G2	324	12.62	. . .	G5III
225*	9.56	+0.20	A2	275	11.39	-0.35	B9	325	12.31	+0.05	A0
226*	11.83	. . .	K0III	276	12.17	. . .	K0III	326	12.23	. . .	G2V
227	13.07	+0.07	A0	277*	10.97	+0.70	G5V	327	11.62	. . .	G0
228*	11.66	. . .	K0III	278	12.33	-0.19	A0	328*	8.13	. . .	G2III
229	11.50	. . .	G5III	279	12.58	. . .	G5III	329	12.46	+0.07	A0
230	12.31	+0.21	B8	280	11.55	+0.28	A5	330	12.41	-0.01	A0

Table 1

Observational Data for Region LF4 (Cont'd.)

Zone +52° (Cont'd.)

No.	m_{pg}	R.I.	Sp.	No.	m_{pg}	R.I.	Sp.	No.	m_{pg}	R.I.	Sp.
331*	10.95	. . .	K0III	381	12.50	. . .	G5III	431*	10.62	+0.52	G2V
332	11.46	+0.20	A5	382*	8.25	-0.25	B9	432 R	10.62	-0.18	B9
333	12.19	. . .	A5	383*	11.34	. . .	K3III	433	12.56	. . .	G0
334	12.78	+0.03	A3	384	11.79	-0.13	A0	434	12.53	-0.25	B9
335	12.39	+0.17	A5	385	12.48	-0.25	A0	435	12.38	. . .	G8V
336	12.76	+0.18	A3	386	12.28	. . .	K2III	436	11.90	-0.10	B8
337	11.71	. . .	F8	387	12.12	. . .	G5IV	437	12.30	-0.08	A0
338	12.73	+0.03	A0	388*	9.61	. . .	G2III	438	12.93	-0.03	A5
339	12.03	+0.23	A2	389	11.47	-0.09	B9	439	12.27	. . .	G0
340	12.46	+0.22	A5	390*	10.55	. . .	G5IV	440	11.53	. . .	F0V
341	11.79	. . .	K0III	391*	9.95	-0.11	B9	441	12.64	. . .	G8III
342*	10.62	-0.08	B8	392	12.12	. . .	G0	442	12.96	+0.04	A0
343	11.59	-0.13	B9	393	12.12	. . .	G0:	443	12.52	. . .	F2
344	12.46	+0.44	B8:	394	12.19	. . .	G5V	444	12.26	. . .	G0
345 R	11.96	. . .	A2	395	11.65	+0.01	A0	445	12.55	-0.32	B8:
346*	9.45	. . .	K0IV	396	11.56	. . .	G5IV	446	11.26	. . .	K2III
347	11.62	. . .	G8III	397	11.56	. . .	F5III	447 R	11.69	-0.07	A0
348	12.60	. . .	A0	398	11.71	-0.08	A0	448	12.38	. . .	G5
349*	10.30	-0.33	B5	399	11.40	. . .	G0III	449	12.74	. . .	F0
350	11.54	. . .	G0V	400	13.02	. . .	G0	450	10.35	-0.13	A0
351	11.54	-0.14	A0	401	12.35	-0.10	A0	451	12.65	+0.49	F0
352	11.40	. . .	G8IV	402	12.36	. . .	F8	452	11.95	. . .	G5III
353	12.95	+0.07	A0	403	10.69	-0.15	B8	453	12.70	+0.14	F0
354	11.75	. . .	K2IV	404	13.12	+0.12	A5	454	12.19	. . .	B9
355	12.15	. . .	G5IV	405	12.47	-0.26	A0	455	12.51	+0.03	A3
356	12.44	. . .	F2	406	12.35	-0.15	A0	456	12.17	. . .	G0
357	11.03	-0.14	B9	407 R	10.86	-0.28	B8	457	12.61	-0.11	A2
358	12.53	+0.19	G5	408	12.70	. . .	F2	458	13.40	-0.02	A0:
359	11.16	. . .	K3III	409	11.51	-0.07	B9	459	12.19	. . .	K3III
360	11.53	+0.15	A2-F0	410	12.30	. . .	F0	460	11.92	. . .	G2III
361	12.59	-0.31	A0	411	13.18:	. . .	K0:	461	11.41	+0.55	G0V
362	11.89	+0.12	A2	412*	9.06	-0.20	B9	462	12.28	. . .	F0
363*	9.79	+0.03	A0	413	12.23	. . .	A3	463	11.93	-0.07	A2
364	11.96	. . .	G5:	414	10.17	-0.23	B8	464	12.30	. . .	K0
365	11.88	-0.09	B8	415	12.19	. . .	G0III	465	10.84	-0.06	B9
366*	11.40	. . .	K5III	416	12.32	. . .	A0	466	11.99	+0.20	A5
367	11.84	-0.06	A0	417	12.69	+0.08	A0	467*	10.78	. . .	G0V
368	12.48	+0.09	B8	418	11.26	-0.14	A0	468	10.90	. . .	F2V
369	10.43	-0.21	B8	419	12.12	. . .	F0V	469	12.09	-0.19	B8
370	12.15	. . .	M0III	420	13.22	+0.02	A0	470	12.28	. . .	K0III
371*	9.03	. . .	K5III	421	11.85	. . .	F0	471*	10.09	. . .	G5IV
372	12.40	. . .	F2	422	11.92	. . .	G8IV	472	12.28	. . .	G5III
373	12.13	. . .	F0	423	12.23	. . .	G0	473	12.62	-0.05	A0
374*	9.88	. . .	F2V	424	12.23	. . .	A0	474	12.40	. . .	G0
375	11.73	. . .	A2	425	11.68	+0.38	B5	475	11.05	+0.03	A0
376	12.95	-0.05	A0	426*	11.71	-0.03	A3	476	11.61	+0.15	A0
377	12.88	+0.03	A0	427	10.73	. . .	F0IV	477 R	11.62	+0.14	A3
378	12.83	. . .	F0	428*	9.92	-0.22	B9	478	12.79	-0.05	A0
379	12.47	+0.05	A0	429	12.38	-0.32	A0	479	12.89:	. . .	A2
380	12.31	+1.09	K2V	430	12.85	+0.21	A0	480	12.52	. . .	F0

Table 1

Observational Data for Region LF4 (Cont'd.)

Zone +52° (Cont'd.)

No.	m_{pg}	R.I.	Sp.	No.	m_{pg}	R.I.	Sp.	No.	m_{pg}	R.I.	Sp.
481	12.69	...	F0	531	12.18	...	K0III	581	12.21	-0.09	B9
482	11.28	0.00	A0	532	13.08	+0.17	A2	582	12.60	...	F0:
483	12.34	+0.12	A2	533	13.17	...	B8	583	12.65	+0.07	A0
484	11.92	...	F0	534	12.40	...	G5V	584	12.44	...	G5III
485	11.44	...	F0IV	535	11.69	-0.27	B5	585	12.15	...	G0
486	12.12	...	G0V	536	11.91	-0.23	B8	586	12.57	...	G5III
487	12.30	+0.17	A2	537	12.02	...	K0III	587	11.20	-0.07	B9
488	12.34	...	F2	538	11.96	...	F8V	588	12.28	...	F0
489*	11.10	...	K2V	539	12.64	+0.16	A5	589	11.76	+0.08	A0
490	12.91	-0.07	A0	540*	10.56	+0.03	A2	590	12.97	0.00	A0
491	12.67	+0.31	A2	541	12.30	...	G0	591*	8.48	-0.22	A0
492	11.03	-0.21	B8	542*	9.01	+0.20	A5	592*	9.66	+0.22	A3
493	11.71	...	F0V	543	12.23	...	F2	593	12.61	...	G0:
494*	9.85	-0.03	B9	544	11.96	...	K3III	594 R	10.84	-0.28	B5
495	12.95	...	G0	545	12.12	-0.12	B5	595	12.40	+0.05	B9
496	11.39	...	F2V	546	12.21	-0.13	B9	596	12.15	...	G5IV
497	12.91	+0.27	A3	547	12.27	+0.07	A0	597	12.36	-0.01	B9
498	12.34	...	G2	548	12.21	...	K2III	598*	10.87	+1.13	G5V
499	12.43	...	K0III	549	11.96	-0.02	A0	599	11.92	...	F0III
500	11.60	...	G0III	550	12.57	-0.05	A0	600*	9.37	-0.12	B9
501	12.83	-0.01	A0	551	12.03	-0.08	A0	601	11.42	...	B8
502	11.72	...	G0	552	12.56	...	K3	602	12.68	-0.13	A0
503	12.95	...	G0	553	12.78	+0.04	A0	603	12.29	+0.03	B9
504	11.91	+0.15	A5	554	12.17	-0.09	B8	604	12.40	...	F0
505	12.44	...	G5III	555 R	11.25	+0.21	A3p	605	12.56	...	F5
506	12.30	...	G0	556	12.47	-0.07	A0	606	12.26	+0.08	A0
507	12.18	...	F5V	557	12.63	+0.13	A2	607	12.63	+0.06	B9
508	12.36	...	F5	558	12.26	...	G5III	608	13.06	+0.07	A3
509	13.15	+0.06	A0	559	12.33	+0.17	A3	609	11.15	+0.30	F8V
510	12.26	-0.18	A0	560*	12.30	...	M0III	610	12.38	-0.12	B9
511	12.30	...	G5III	561	12.56	+0.22	A5	611	12.81	-0.04	A0
512	12.42	...	G8V	562	12.27:	...	F0	612	12.34	...	G0
513	12.94	-0.20	A0	563	10.86	+0.01	A0	613	12.28	...	G5V
514	12.11	...	G5III	564	11.95	+0.03	A0	614	12.64	-0.11	A0
515*	10.24	-0.18	B8	565	12.23	...	K0III	615*	9.75	...	F0IV
516	10.85	...	F0IV	566	12.55	...	G8III	616	12.32	...	F0
517	11.95	-0.05	A0	567	12.48	...	F0	617	12.16	...	G8V
518	13.11	+0.24	A2:	568	12.65	...	G0	618	12.14	+1.06	K2V
519*	9.62	-0.16	B8	569*	9.39	-0.23	B8	619	12.34	...	K0
520	12.55	...	F0	570	12.40	...	F0	620	12.54	+0.13	A2
521	12.10	...	K0:	571	12.63	+0.39	A3:	621	12.61	...	G2:
522	11.34	...	G5IV	572	12.32	...	F0	622	12.64	+0.03	B9
523	12.48	...	F5	573*	9.08	...	F0V	623	12.89	+0.31	A0
524	12.12	...	G8V	574	12.70	...	F0	624	11.16	...	G0III
525	12.60	...	G0	575	10.82	-0.16	B8	625*	10.41	...	G8IV
526	10.78	...	G8III	576	12.33	+0.07	A0	626	13.10	+0.06	A2
527	12.01	-0.01	B9	577	11.96	...	G0	627	12.08	...	G5III
528	12.59	+0.27	A5	578	11.96	+0.22	A5	628	11.95	+0.15	A0
529	12.53	-0.11	B9	579	12.16	...	F8	629	12.48	...	G0
530	11.53	-0.21	A0	580	11.67	-0.07	A0	630	12.30	...	G0:

Table 1

Observational Data for Region LF4 (Cont'd.)

Zone +52° (Cont'd.)

No.	m_{pg}	R.I.	Sp.	No.	m_{pg}	R.I.	Sp.	No.	m_{pg}	R.I.	Sp.
631	13.14	+0.22	A0	681	13.09	+0.15	B8:	731	12.23	...	K0III
632	12.78	...	B8	682	11.96	...	G0V	732*	10.78	-0.04	B9
633	12.61	...	G0	683*	9.62	...	G5IV	733 R	10.39	-0.13	B8
634	11.61	+0.14	A0	684	12.05	...	F0	734	12.47	-0.09	A0
635	12.21	...	F0	685	12.21	...	G0	735	12.27	...	F0
636	12.30	...	F0	686	11.83	-0.05	B8	736	12.30	...	G0
637*	7.73	-0.15	B5	687	11.88	...	G0V	737*	9.43	...	K2IV
638	12.21	...	G0V	688	12.51	...	F8	738	12.21	...	G8III
639	11.49	-0.07	B8	689*R	10.45	-0.21	B8	739*	8.46	...	F0IV
640	12.40	...	F0	690	12.70	...	K0III	740	11.12	+0.11	A2
641	12.74	...	G2III	691	12.21	...	G0	741	12.56	+0.15	A2
642	12.28	...	G0	692	12.36	-0.11	A0	742	12.65	...	G8III
643	12.56	...	F8	693	13.17	-0.05	B5	743	12.08	-0.10	B8
644	12.67	-0.02	B8	694	11.49	...	M5V	744	12.18	...	F0
645	10.57	-0.01	A0	695	13.04	+0.18	A0	745*	10.57	+0.07	B9
646	11.35	...	F5IV	696	12.74	...	G2	746	11.83	...	K0III
647	11.55	-0.05	B8	697*	9.59	-0.18	B9	747	11.84	-0.04	B9
648	12.64	...	G5:	698	13.11	+0.07	A0	748	12.40	...	K0III
649	12.93	...	G5:	699	10.59	-0.05	B8	749*	8.42	...	G0IV
650	11.23	+0.02	B9	700*	8.41	+0.01	B9	750*	9.00	+0.88	G8V
651	12.35	+0.03	A0	701	12.71	+0.14	B5	751	12.18	+0.20	A0
652	11.10	+0.02	A0	702 R	11.89	-0.06	B5	752*	9.61	+0.06	B8
653	11.39	+0.17	A5	703	12.32	...	G0	753	12.35	+0.01	B9
654	12.01	...	F0	704	12.32	...	G2V	754	12.62	+0.20	A0
655	11.53	-0.25	B5	705*	11.49	...	K0	755	12.58	+0.30	A0
656	12.60	...	F0	706	12.51	...	G8III	756	12.57	...	F0
657	12.73	+0.59	A0:	707*	11.39	...	M0III	757	11.59	-0.13	B9
658*	8.74	...	G5III	708	12.98	+0.28	B8	758	12.37	+0.25	A0
659	11.61	...	G5IV	709	12.51	+0.36	A2	759 R	11.30	+0.32	A5
660	12.89	+0.29	A2	710	12.51	...	G0	760	11.40	...	G5III
661	12.63	+0.15	B5:	711	12.91	...	F2	761*	7.39	...	G5III
662	12.05	...	G2	712	12.14	-0.04	B5:	762	11.96	...	F0V
663	13.21	+0.20	B9	713	11.91	-0.01	B5	763	11.12	...	G5III
664	11.92	...	G0V	714*R	10.41	+0.21	B8	764 R	11.93	-0.11	B9
665	12.37	-0.03	B8	715	10.57	+0.06	A0	765 R	10.94	-0.16	B5
666	12.40	...	G5III	716	12.60	...	M0	766*	10.11	+0.01	A0
667	12.10	...	A0	717	12.13	+0.18	A0	767	10.80	+0.20	A3
668	12.23	-0.15	B8	718	12.35	+0.38	A3	768	12.32	...	G0
669	11.47	+0.09	A0	719	11.43	+0.09	A0	769	12.32	...	F0
670	12.73	...	G0	720	11.79	...	F5III	770	11.61	...	F0V
671*	12.51	...	F0	721	12.30	...	F8	771*	9.95	+0.15	A0
672	11.43	+0.15	A0	722*	8.71	...	K2III	772	12.43	...	G0
673	12.23	...	F0	723	13.08	+0.18	A0	773	12.49	+0.35	B8
674 R	11.01	-0.11	B9	724	12.55	+0.15	A3	774	12.40	+0.26	A2
675	12.21	...	K2III	725	12.65	-0.03	B9	775	11.09	...	F2V
676	12.28	...	G0	726*	10.80	...	G5III	776	12.30	...	G8III
677	12.12	...	F0	727	10.46	-0.15	B8	777	12.21	...	G0
678	12.71	+0.10	B9	728*	10.48	+0.46	G0V	778	12.79	...	G2
679	11.96	...	G5III	729	11.88	+0.26	A3	779	11.96	...	F0IV
680*	10.05	+0.48	F8V	730	12.83	...	G5III	780	12.66	+0.18	A0

Table 1

Observational Data for Region LF4 (Cont'd.)

Zone +52° (Cont'd.)

No.	m_{pg}	R.I.	Sp.	No.	m_{pg}	R.I.	Sp.	No.	m_{pg}	R.I.	Sp.
781	13.20	+0.28	A5:	831 R	11.79	+0.09	B9	881*	13.31	...	F0:
782	12.16	...	G0	832	12.51	...	G0	882	13.02	...	A2
783	12.09	...	F8	833	12.56	+0.12	A0	883	12.91	...	A3
784	13.21	...	B8	834	12.66	+0.17	B8	884	12.26	...	F8
785	12.12	...	K2V	835	12.17	+0.45	A0	885	12.32	...	G2V
786*	9.87	+0.03	B8	836	13.06	+0.30	A2	886	10.77	...	K0V
787	11.52	...	F0	837	11.49	+0.32	A0	887	13.11	...	M0III
788	12.87	+0.40	A0	838	12.88	...	K5III	888	11.71	...	F5III
789	13.02	...	F8	839	12.05	...	G8:	889	13.08	...	A0
790	12.76	+0.17	A0	840	12.95	+0.44	A0	890	12.17	...	K0V
791	12.19	...	G2V	841*R	10.14	+0.04	B8	891	12.51	...	B9
792	12.36	...	G0V	842	12.44	...	G0	892	12.26	...	K0III
793	13.17	+0.34	B5:	843	12.07	+0.25	A0	893	13.16	...	A0:
794	13.05	+0.06	A2	844	12.04	+0.30	A0	894	12.65	...	B5
795	11.57	+0.05	A2	845	13.28	+0.48	A0:	895	13.16	...	A2
796	11.91	+0.03	B9	846	12.79	...	G0:	896*	10.58	...	B9
797	12.70	...	K2III	847	12.43	...	G0III	897	11.83	...	A0
798	13.19	+0.40	B5	848	12.64	+0.21	A0	898*	10.82	...	F0V
799	12.94	+0.42	F0	849 R	11.36	-0.04	B8	899	9.77	...	A5
800	12.70	+0.32	A0	850	12.75	...	G8	900*	10.29	...	A0
801	12.30	+0.02	B9	851	12.53	+0.11	B9	901	12.79	...	A2
802	13.11	+0.15	A0	852	11.55	+0.77	G0V	902	12.65	...	K0III
803	12.40	...	G5III	853*	10.98	+1.22	G5V	903	12.61	...	A3
804	12.34	...	F0	854	12.55	...	G0	904	12.56	...	A5
805*	8.64	+0.04	A0	855*	9.77	+0.09	A0	905	12.74	...	A2
806	12.79	...	F0	856	11.94	0.00	B8	906	10.60	...	A3
807	12.79	...	G2V	857	12.79	+0.45	B3:	907	12.65	...	F0
808	11.87	...	F0	858	12.28	+0.41	A5	908	12.34	...	G5III
809	12.40	...	G2III	859	12.82	+0.18	A0	909	12.65	...	G5V:
810*	11.79	...	K0III	860	12.54	+0.36	A3	910	12.23	...	A3
811	12.30	...	F8	861	10.89	+0.12	B8	911	11.78	...	F8V
812	11.88	+0.06	A0	862	12.60	+0.32	A0	912	12.69	...	B8
813	11.89	+0.07	B8	863	12.58	+0.12	A0	913*	8.44	...	G0IV
814	12.02	+0.26	B9	864	11.39	...	F2IV	914*R	9.05	...	B8
815	10.88	+0.80	G5V	865	12.21	+0.16	A0	915	13.11	...	A2
816*	8.94	+0.03	B8	866*	11.58	+0.66	G0V	916	12.65	...	B8
817	12.53	+0.47	B5:	867	13.36	...	F0	917	11.34	...	A2
818	11.76	+0.42	A3	868	13.00	+0.27	A2	918	12.34	...	A2-F0
819*	10.11	...	K2III	869	11.94	+0.30	A2	919	12.57	...	A0
820 R	11.12	+0.13	B9	870	12.08	+0.26	A0	920	12.08	...	G2IV
821	12.51	...	K0IV	871*	10.41	...	F0IV	921*	11.82	...	K0III
822	12.35	+0.03	B9	872	12.74	...	G0	922	11.17	...	B9
823	11.13	...	G8IV	873*	9.23	+0.13	B9	923	12.30	...	B8
824	12.05	...	G8III	874	12.32	...	B9	924	12.61	...	F0:
825*	11.44	...	M5III	875	12.74	...	A5	925	12.35	...	K3III
826	12.28	...	G0:	876	12.88	...	A0	926	11.05	...	A0
827	12.67	+0.27	A0	877	11.92	...	B8	927	10.97	...	F8V
828	12.30	...	F8	878	12.32	...	A3	928	11.72	...	K0III
829	13.10	+0.36	A0:	879*	11.12	...	K5III	929	12.40	...	F0
830	11.96	...	G0	880	12.65	...	B9	930	12.85	+0.66	F0

Table 1

Observational Data for Region LF 4 (Cont'd.)

Zone +52° (Cont'd.)

No.	m_{pg}	R.I.	Sp.	No.	m_{pg}	R.I.	Sp.	No.	m_{pg}	R.I.	Sp.
931	13.36	...	A5:	16	12.36	...	B5:	66	11.58	...	A0
932	12.65	...	G5V	17	13.11	...	G0	67	10.96	...	F8
933	11.92	...	F0V	18	12.23	...	B9	68	10.77	...	F0V
934	13.05	...	A0	19	12.44	...	G5	69	12.44	...	G0:
935	11.75	...	A5	20	12.32	...	F2	70*R	9.96	...	B3
936	12.30	...	G0III	21	12.23	...	A5	71	12.51	...	A3
937	13.40	...	A2	22	12.28	...	G0	72	11.74	...	B9
938	12.65	...	G5III	23	12.40	...	G5III	73	12.73	...	G5V
939*	11.21	...	G5III	24	12.21	...	B9	74	12.37	...	A0
940	13.42	...	A0	25	12.64	...	B8:	75	11.41	...	F0V
941	12.77	...	A0	26	12.34	...	A2	76	11.09	...	F8III
942	11.20	...	A0	27	11.44	...	F0V	77*	10.00	...	B9
943	12.84	...	M0	28	11.44	...	B8	78	12.60	...	A0
944*	11.37	...	G5IV	29	13.54	...	K0	79	12.83	...	A0
945	13.10	...	A0:	30	11.57	...	A0	80	12.09	...	G5
946	12.34	...	G0III	31	12.68	...	A0	81	12.52	...	B5:
947	12.43	...	B8	32	11.91	...	K0:	82	13.02	...	G5:
948	12.40	...	G0	33	10.99	...	B2:	83	12.56	...	G8
949	11.79	...	A0	34	12.19	...	B8	84	11.92	...	A0
950	12.56	...	G0	35	12.36	...	A0	85	12.28	...	A0
951	13.02	...	F0	36	11.75	...	G5III	86	12.19	...	A0
952	11.63	...	A0	37 R	11.44	...	A0	87	12.32	...	B9
953	11.34	...	A0	38	12.86	...	K3III:	88	11.09	...	B5
954	11.95	...	B8	39	12.04	...	A0	89	12.05	...	A0
955	12.40	...	A3-F0	40	12.40	...	G5III	90	12.32	...	K0III
956	12.48	...	A0	41	10.55	...	F2V	91 R	10.93:	...	A2:
957*	9.75	...	F0IV	42	12.36	...	A0	92	12.52	...	K0III
958	12.05	...	K0IV	43	12.64	...	G8	93	10.62	...	A0
959	12.01	...	A2	44	12.18	...	G5III	94	12.42	...	F8
960	12.23	...	A2	45	12.83	...	A0	95	11.41	+0.23	A3
961	12.36	...	G5IV	46*	12.12	...	G8III	96*	10.79	...	G5III
962	12.76	...	A2	47	11.92	...	K0III	97	12.35	...	G0:
				48	12.91	...	A0:	98	11.44	...	G0V
				49	12.60	...	K0III	99	12.44	...	A2
	Zone +53°			50	12.12	...	G5V	100	12.65	...	A2
1	12.56	...	A0	51	11.96	...	B8	101	11.39	...	B5
2	12.28	...	B8	52	12.32	...	B9	102	12.47	...	G8:
3	12.25	...	B9	53*	11.07	...	K0III	103	12.60	...	B8
4	12.05	...	K0III	54*	8.85	...	B9	104	11.00	...	B8
5	12.39	...	A0	55	12.19	...	G8III	105	13.02	...	A0
6	12.26	...	G0	56	12.25	...	B5	106	12.36	...	A0
7	12.30	...	A2	57	12.47	...	A0	107	12.51	...	B5
8*	9.41	...	G0IV	58	12.36	...	G5V	108	11.57	...	B5
9	12.35	...	B8	59	12.42	...	G8III	109	12.31	...	G2
10	12.30	...	A0	60	12.40	...	G8III	110	12.04	...	B8
11	12.47	...	G0	61	10.90	...	F8V	111	11.18	...	B5
12*	8.39	...	G8III	62	12.39	...	F2:	112	12.79	...	G0
13	11.77	...	G8V	63	12.69	...	A5	113	10.78	...	A0
14	13.08	...	B8	64	12.23	...	G5IV	114	10.37	...	B9
15	12.35	...	A:	65	11.70	...	G5III	115	12.44	...	K0III

Table 1

Observational Data for Region LF4 (Cont'd.)

Zone +53° (Cont'd.)

No.	m_{pg}	R.I.	Sp.	No.	m_{pg}	R.I.	Sp.	No.	m_{pg}	R.I.	Sp.
116	12.52	...	A0	166	11.46	+0.21	A0	216	12.50	-0.12	B8
117	10.86	...	B8	167	12.07	...	F0	217	12.10	+0.20	A0
118	11.74	...	F2III	168	12.63	+0.23	B9	218	12.81	+0.22	B8:
119	11.79	...	F0	169	12.25	-0.01	B8	219*	8.89	...	K5III
120	13.07	...	A0	170	12.23	+0.25	B9	220	13.08	...	M0
121	11.00	...	A0	171*	9.50	...	F0V	221*	9.54	-0.18	B5
122	12.70	...	B9	172	12.16	+0.22	A2	222	12.40	...	G0
123	12.56	...	A0	173	12.26	...	G5	223 R	11.43	+0.07	A0
124	12.60	...	G0:	174	11.06	+0.10	A0	224	11.63	+0.22	A0
125	11.54	...	A2	175	11.44	+0.17	A2-F0	225	12.83	...	K2III
126	12.19	...	G5	176	13.03	...	M2	226	11.44	...	G0IV
127	10.90	...	A0	177	12.27	+0.10	B9	227	12.79	+0.33	A2
128	11.39	...	A0	178*	11.35	...	G5IV	228	12.35	...	G0
129*	10.33	...	B8	179	12.66	+0.48	A0	229*	10.13	...	G0V
130	12.99	...	A0	180	12.17	+0.09	B8	230*R	9.57	-0.07	B2:
131	12.52	...	A0	181	12.36	+0.16	A0	231	11.39	+0.19	A0
132	12.49	...	A0	182*	8.32	-0.28	B8	232	10.79	-0.09	A0
133	10.33	...	F8V	183	12.60	+0.10	B8	233*R	8.80	-0.03	B2:
134	12.19	...	A0	184	12.56	+0.36	A2	234	12.60	...	G0
135*R	9.81	...	B8s:	185	10.98	+0.02	B9	235	12.94	+0.29	A0
136	11.65	...	B8:	186*	10.49	...	M2III	236	11.83	...	G8III
137	12.51	...	B8:	187*	8.94	-0.07	A0	237	12.04	+0.43	A5:
138	11.65	...	B8	188	11.33	-0.17	B8	238	12.34	0.00	A0
139	10.95	...	B9	189	12.50	+0.05	B5:	239	11.90	+0.03	B8:
140	12.21	...	B9	190	11.87	...	B8	240	11.42	+0.65	G2V
141	12.15	...	G8V	191	12.38	+0.18	A0	241	12.96	+0.38	A0
142	12.31	...	G8III	192	12.35	...	F8	242	11.52	+0.06	B5
143*	8.79	...	B8	193	12.00	...	A2	243	12.40	...	B5
144*	10.42	...	G8IV	194	10.68	...	G0V	244	12.91	...	G8III
145	12.23	...	G5III	195*R	10.82	...	F5V	245	13.24	+0.35	A0
146	11.83	...	B5	196	10.48	-0.04	B9	246	12.87	+0.27	A2
147	11.87	...	G0V	197	11.60	+0.12	B9	247	13.29	...	K0III
148	10.94	...	B5	198	11.75	...	G0	248	12.21	...	F0
149	12.87	...	A0	199*	10.49	...	K2III	249	12.61	...	G8III
150	12.44	...	A0	200	11.23	-0.09	B8	250	12.10	-0.09	A0
151	12.21	...	A0	201	12.44	...	G0	251*	9.79	-0.06	B5
152 R	11.54	...	B9	202*	10.28	-0.04	B8	252	11.78	...	F0
153	12.36	-0.05	B5	203	12.44	...	G0	253	11.01	+0.22	A3
154	10.74	-0.06	B9	204	12.34	+0.05	A0	254	12.58	+0.26	A0
155	11.80	...	G8IV	205	11.45	-0.01	A0	255	12.30	+0.18	A0
156*	9.78	-0.02	B9	206	10.87	-0.11	B5	256	11.83	+0.15	B8
157	11.87	...	F8V	207*R	10.16	-0.20	B5k	257	12.28	...	G8V
158 R	11.54	-0.08	B8	208*	11.07	...	K2III	258	12.22	+0.42	A5
159*	9.34	-0.18	B5	209	11.90	-0.09	A0	259	11.03	-0.17	B9
160	11.81	+0.02	B9	210	11.71	...	K0III	260	12.51	+0.19	B9
161	11.52	-0.12	B8	211	12.19	...	F5	261	12.75	+0.06	A0
162	12.62	+0.24	B8	212	12.40	...	G8:	262	12.50	+0.30	A0
163	12.19	...	G0	213	13.24	+0.20	B8:	263	11.62	+1.46	G0Ib:
164	11.85	-0.05	B9	214	12.60	...	G0:	264	12.01	+0.13	A0
165	12.37	+0.23	B9	215	12.82	+0.22	A0	265	12.13	-0.05	B8

Table 1

Observational Data for Region LF4 (Cont'd.)

Zone +53° (Cont'd.)

No.	m_{pg}	R.I.	Sp.	No.	m_{pg}	R.I.	Sp.	No.	m_{pg}	R.I.	Sp.
266	10.96	...	G5	316	12.22	+0.06	A0	366	12.14	+0.10	A0
267	12.64	+0.17	A3	317	12.38	...	G0	367	12.05	...	G0
268	12.10	+0.08	B9	318	12.96	+0.18	A0	368	12.69	+0.09	A0
269	11.27	...	F5	319	11.88	-0.14	B8	369	11.65	+0.37	A3
270 R	11.61	+0.19	A5	320	11.98	+0.14	B9	370 R	10.76	+0.11	B8
271*R	9.66	+0.52	A3	321	12.26	...	G0	371	13.14	+0.06	A0
272	12.52	...	G5	322	12.17	+0.37	A2	372	12.24	...	G0
273	12.28	...	F0	323	12.32	...	G5III	373	12.55	...	F0:
274*	10.72	+0.33	A2	324	12.21	...	B8	374	12.60	+0.32	A2
275	11.80	+0.06	B3	325	12.44	...	G8	375	12.31	...	F8
276	12.48	...	G0:	326	12.09	+0.03	B3	376*	9.93	-0.03	B8
277*	10.49	...	F0V	327	11.49	...	G8III	377	10.96	-0.18	B5
278	11.85	+0.19	B5	328	12.40	+0.02	B9	378	11.76	+0.04	A0
279	12.68	+0.18	A2	329*	9.83	+0.09	A5	379 R	11.95	+0.47	A5
280	12.94	+0.38	B9	330	11.72	-0.03	A0	380	11.72	...	G5III
281	12.21	-0.31	B5	331	12.06	+0.16	A0	381 R	10.88	-0.02	B8
282	12.13	+0.28	A3-F0	332	12.11	+0.27	A0	382	12.17	...	G0
283	12.84	...	G5IV	333	11.87	-0.17	B5	383	12.92	+0.10	A0
284	11.66	-0.06	B5	334	13.11	+0.39	A2	384*	12.66	...	G5III
285 R	11.69	+0.37	A0	335	12.82	...	F0V	385	12.39	+0.35	A0
286	12.28	...	F0	336	11.94	...	G0	386	11.14	+0.08	A3
287	12.36	+0.54	B5	337*R	8.81	+0.31	B5	387	12.41	-0.09	B9
288	11.49	...	F0	338*	11.71	...	K2III	388	12.33	+0.41	A5:
289	11.73	-0.23	B5	339	12.30	+0.10	A0	389	11.95	...	G8IV
290	11.51	-0.09	B2	340*R	10.10	+0.06	B5	390	12.87	...	G8III
291	10.29	-0.03	B9	341	12.52	+0.34	F0	391	11.92	+0.02	A0
292	12.19	...	K2	342	12.52	...	K0:	392	12.44	...	G0
293 R	11.92	-0.12	B3	343	12.43	+0.47	B5:	393	11.88	...	F0
294	11.79	+0.22	A0	344	12.40	...	A0	394	12.60	...	G0
295	11.79	...	G0	345	12.33	+0.09	A0	395	11.13	+0.43	F8V
296	11.93	+0.10	B8	346	12.32	...	F0	396	12.48	...	G0
297*	10.59	+0.01	B9	347	12.82	+0.22	A0	397	12.79	+0.28	A3
298	10.86	...	F0IV	348	12.65	+0.11	A0	398*	10.66	+0.20	A0
299*	10.30	...	K2IV	349*R	10.68	+0.09	A3	399*R	9.93	+0.08	A2
300	12.47	...	K0III	350	11.92	...	G0:	400	12.65	-0.05	B8
301*R	9.99	-0.16	B2	351	12.05	...	G0V	401	12.52	...	G0
302	12.13	+0.21	A0	352*	10.34	+0.14	A2	402	11.93	+0.02	B9
303	12.32	+0.10	B5	353	11.87	...	G8III	403	12.49	+0.07	B8:
304	11.53	...	K0	354	12.14	-0.02	B5	404	12.42	+0.10	A2
305	10.68	-0.04	B8	355	12.41	+0.21	B9	405	13.05	+0.56	B9
306*	10.81	...	K5III	356	11.47	+0.47	F8V	406	11.88	...	F0
307	12.44	+0.38	A0	357*	10.13	+0.79	G5V	407	12.22	+0.13	B8
308	12.47	...	A0	358	11.96	...	K3III	408*R	11.19	+0.23	A2
309	12.46	...	G0	359	12.77	+0.24	F0	409	12.21	...	F0:
310	12.22	+0.11	B9	360	12.59	+0.14	B8	410	10.00:	...	B8
311	12.35	...	G0	361	12.53	+0.07	B9	411	12.38	+0.27	A2
312	11.88	...	G5III	362	12.81	-0.19	B8	412	12.19	+0.03	A2
313	12.83	+0.15	A0	363	12.49	0.00	A0	413	12.36	...	G8III
314	12.27	...	G8:	364	12.47	...	K0III	414	12.35	+0.11	B8
315	12.05	...	F8	365	11.91	...	G8V	415 R	10.95	+0.07	B8

Table 1

Observational Data for Region LF4 (Cont'd.)

Zone +53° (Cont'd.)

No.	m_{pg}	R.I.	Sp.	No.	m_{pg}	R.I.	Sp.	No.	m_{pg}	R.I.	Sp.
416	12.38	+0.13	A0p	466	12.67	+0.02	B8	516	12.32	. . .	F0
417	12.36	+0.18	B8	467	11.83	+0.07	A0	517	12.47	. . .	F0
418*	10.46	. . .	M0III	468	12.68	-0.06	A0	518	12.49	+0.21	A5
419	11.95	+0.57	G0:	469	12.70	. . .	F8:	519	11.23	-0.05	B9
420	12.08	+0.04	B9	470*R	10.15	-0.36	A0	520	12.47	+0.05	A0
421	12.46	+0.32	B2:	471	12.56	. . .	G0	521	12.38	. . .	F0III
422	12.11	. . .	G5IV	472	12.68	+0.22	A0	522	12.64	+0.04	A0
423	11.65	+0.02	B8	473	12.40	. . .	G0:	523	11.83	+0.27	A2
424	12.32	-0.09	B8	474	11.22	. . .	F2IV	524	12.06	. . .	F8
425	11.04	. . .	F0V	475*	9.21	-0.05	A0	525	12.56	. . .	G0:
426	12.48	. . .	G0	476	11.26	. . .	G5III	526	10.76	-0.21	B8
427	12.70	. . .	G0:	477	12.36	. . .	K0III	527	11.59	-0.37	B5:
428	12.02	+0.38	A2	478*	10.62	-0.10	B8	528	11.78	0.00	A0:
429	12.83	. . .	F0	479	11.78	+0.30	A3	529	11.81	-0.15	B9
430	10.92	+0.07	A0	480	12.41	-0.13	B5	530*	8.70	. . .	F2V
431	12.71	+0.23	B8	481	11.48	. . .	F0V	531	12.31	. . .	F0
432	12.51	+0.16	B8	482	11.09	+0.11	B8	532	11.30	. . .	G8III
433	12.52	. . .	F8:	483*	10.02	. . .	B9	533	11.81	. . .	A2
434	12.92	+0.05	A0	484	12.27	+0.32	A2	534	12.17	-0.10	A0
435*	10.46	. . .	F0V	485	12.44	. . .	F2	535*	10.43	+0.11	A2
436	11.67	. . .	G0	486	12.87	+0.18	B8	536	10.99	. . .	F0V
437	12.51	. . .	F0	487	11.30	. . .	F0V	537	11.45	-0.07	B9
438	12.52	+0.04	B8	488	12.12	-0.14	A0	538	12.91	. . .	G0
439	12.26	. . .	F0	489	12.57	. . .	A5	539	12.58	-0.04	B9
440	11.92	. . .	F8V	490	12.17	-0.05	A0	540*	10.58	+0.28	A5
441	12.74	+0.23	B9	491	11.99	+0.35	A3	541	12.09	-0.05	A0
442	12.60	. . .	F0	492	12.21	. . .	G8III	542	12.32	. . .	F2
443	12.27	+0.26	A2:	493	12.97	+0.48	A0	543	12.75	. . .	G2
444	12.87	+0.21	B9	494	12.32	. . .	G0	544	13.22	. . .	A0
445	13.13	. . .	G8III	495	12.47	. . .	G5:	545	12.35	. . .	G8III
446	12.56	. . .	A5	496	12.26	. . .	K5III	546*	11.08	. . .	G8III
447	12.88	+0.30	A2	497 R	11.76	+0.21	A2:	547	12.40	-0.09	A0
448 R	11.98	+0.32	A3-F0	498	12.70	-0.08	B5	548*	10.49	-0.07	B9
449	12.27	+0.14	A0	499	10.51	-0.11	B8	549	11.00	-0.21	B2
450	12.14	+0.16	A0	500*	9.75	-0.03	A0	550	11.48	+0.12	A3
451	12.74	+0.14	A0	501	12.48	. . .	G0	551	12.47	. . .	K2
452	11.16	+0.14	A2	502	10.60	-0.22	B5	552	11.23	-0.19	B9
453	11.29	+0.38	A3-F0	503	11.17	-0.27	B5	553	12.51	+0.40	A2
454	12.09	+0.10	B8	504	11.95	. . .	F8	554	11.70	-0.29	A0
455	12.63	+0.36	A0	505*	9.27	-0.15	A2	555	11.21	+0.02	B9
456	12.38	. . .	G8IV	506	12.64	-0.07	A0	556	12.52	. . .	G0
457	12.28	. . .	G0	507	12.74	+0.28	B5:	557	12.55	-0.17	B8
458	11.36	-0.02	A0	508	12.21	. . .	F0	558*	10.82	. . .	G5IV
459	12.94	+0.14	A0	509	12.50	+0.14	A2	559	10.70	. . .	G8IV
460	12.12	. . .	K0III	510	11.67	-0.33	B5	560*	10.56	0.00	B9
461*R	8.76	+0.83	A0p	511	13.16	+0.18	A0	561	12.40	. . .	F8:
462	12.63	+0.22	A0	512	11.68	+0.16	A2	562	12.15	+0.61	A0
463	12.46	+0.04	B8	513	11.49	. . .	K0III	563	11.06	+0.12	A0
464	12.44	+0.23	B9	514	11.89	+0.03	A0	564	11.28	. . .	G0
465	11.23	. . .	K0III	515	11.72	-0.02	B8	565	12.12	-0.08	A0

Table 1

Observational Data for Region LF4 (Cont'd.)

Zone +53° (Cont'd.)

No.	m_{pg}	R.I.	Sp.	No.	m_{pg}	R.I.	Sp.	No.	m_{pg}	R.I.	Sp.
566	10.58	-0.38	B5	616	12.30	...	G5V	666	11.56	-0.08	B8
567	12.30	+0.18	A2	617	12.69	+0.26	A0	667*	7.95	...	K2III
568	12.87	+0.17	A2:	618	12.30	...	G0	668	12.35	...	G0
569	11.77	-0.19	A0	619	11.51	-0.07	A0	669	12.42	+0.07	A2-F0
570*	10.81	...	K0III	620	10.96	+0.14	A0	670*	10.67	...	K3III
571	12.52	...	F0:	621	12.19	+0.15	A2	671	12.00	...	G5III
572	12.61	...	F5:	622	12.80	...	G5	672	12.40	+0.36	A5:
573	11.86	-0.08	B8	623	11.66	+0.15	A3	673*	7.34	...	F0V
574	12.00	...	G8III	624	12.80	...	G8:	674	12.43	...	K0III
575*	10.25	-0.19	B8	625	12.13	...	G0	675	12.51	...	G8
576	12.34	...	G5	626	12.35	+0.17	A0	676	11.07	-0.46	B3
577	12.28	+0.21	A0:	627	12.30	...	G0	677*R	8.45	+0.22	A0
578	12.32	...	G0	628	10.58	...	B9	678	12.74	+0.31	A0
579 R	11.10	+0.15	A2	629	12.30	...	G0	679	12.09	+0.29	A0
580	12.44	0.00	A0	630*	10.59	...	F2V	680	13.08	+0.09	B9
581	12.65	+0.25	A0	631	12.50	-0.10	A2	681	12.10	...	G5III
582*	9.82	...	B8	632	12.44	...	G2V	682	12.36	+0.32	B8:
583	12.56	+0.06	B9	633	12.13	...	K0III	683	11.32	-0.04	B9
584	10.11	-0.12	B8	634	12.48	...	F0	684	12.47	-0.07	A2
585	12.61	-0.09	A0	635	12.25	+0.09	A0	685	11.66	-0.22	A0
586	11.07	...	F0III	636	12.77	+0.18	A3	686	12.36	...	G0:
587	12.78	...	K0:	637	12.66	...	K0III	687	11.77	+0.17	B8
588	11.87	...	G5V	638	13.00	...	K0	688	12.46	+0.10	A0
589	12.12	-0.30	B5	639	12.21	-0.11	A0	689*	8.78	...	F0III
590	13.22	+0.33	A3:	640	12.23	+0.03	A0	690	12.76	...	F2
591	10.80	-0.04	A0	641	13.02	+0.12	A0	691*	11.39	...	K3III
592	11.93	+0.11	A0	642	12.47	...	G0:	692	12.23	...	G0:
593*	9.26	...	F8IV	643	11.99	...	G2V	693 R	11.02	...	F0III
594	11.49	...	G5IV	644	11.10	+0.05	A2	694	11.83	...	F8
595 R	11.06	-0.19	B8	645*	8.85	...	G0IV	695	12.47	...	K0
596	12.40	...	K0	646	12.42	+0.08	A0	696	12.02	0.00	A0
597	12.19	...	G5	647	12.70	+0.12	A5	697*	7.63	-0.18	B8
598	12.51	-0.19	B8	648	12.01	-0.01	B9	698	12.47	...	K0III
599	12.48	+0.12	A3	649	11.71	...	M2III	699	11.62	...	F0
600	12.17	...	G0	650	11.70	-0.10	B9	700	12.43	+0.13	B8
601	11.29	-0.02	A2	651	11.95	-0.04	B9	701	12.44	+0.26	A0
602*	8.72	-0.08	B9	652	11.75	-0.02	A3	702	12.35	...	G2
603	11.94	-0.24	B5	653	12.03	+0.04	A0	703	12.44	...	F0
604	12.36	...	G5III	654 R	11.67	...	F0V	704	12.36	...	G0
605	12.51	+0.05	A0	655	12.16	-0.07	B8	705	12.40	...	G0
606*	12.28	...	G0	656*	10.99	-0.25	B8	706	12.35	-0.19	A0
607	12.45	+0.03	A0	657	12.44	...	F5	707	12.44	...	K3III
608	12.57	-0.13	A2	658	10.72	-0.30	B8	708	12.17	-0.08	B8
609	12.30	...	G8III	659	10.89	-0.29	B8	709	12.48	...	F0
610	11.97	+0.10	A3	660	12.30	...	A2	710	12.52	+0.20	A2
611	11.54	-0.04	A0	661	12.57	+0.21	G8III	711*R	10.43	-0.46	B5
612	11.87	...	K2	662	11.94	...	A0	712	12.30	...	G5V
613	12.44	...	G0	663	12.47	...	F2	713	12.41	+0.06	A0
614	12.32	+0.29	A5	664*	10.64	-0.12	B8	714	12.56	...	G8
615	13.11	+0.12	A0	665*	9.04	...	F5IV	715	12.61	-0.15	B9

Table 1

Observational Data for Region LF 4 (Cont'd.)

Zone +53° (Cont'd.)

No.	m_{pg}	R.I.	Sp.	No.	m_{pg}	R.I.	Sp.	No.	m_{pg}	R.I.	Sp.
716*	11.53	. . .	M0III	766*	10.54	. . .	F0V	816	12.18	. . .	K0III
717*R	10.28	-0.34	B2k	767	12.60	. . .	G5	817	12.32	. . .	A0
718	12.47	. . .	G0	768 R	11.09	-0.38	B8	818	12.33	+0.33	A3
719	12.44	. . .	F5	769	12.56	+0.02	B5	819*	11.12	. . .	F0V
720	12.65	. . .	G0	770	11.96	. . .	G5III	820	13.02	. . .	G2
721	11.54	. . .	G0IV	771	12.35	+0.15	A0	821*	9.85	-0.09	B9
722	12.32	. . .	G5V	772	12.44	. . .	F0	822	12.20	-0.14	A0
723	11.57	+0.10	A2	773	12.28	. . .	F8	823	12.51	. . .	G0
724	12.40	. . .	G8V	774	11.69	-0.14	B9	824	10.76	. . .	G2IV
725	12.77	. . .	G5V	775	12.83	. . .	K0III	825	11.88	. . .	G5III
726	12.97	+0.07	B9	776	11.15	+0.23	A5	826	11.26	. . .	F5V
727	10.91	+0.15	A0	777	11.70	. . .	G5V	827	12.93	+0.09	A0
728	11.99	. . .	G5III	778	12.04	. . .	G0	828*	10.99	. . .	F5III
729 R	11.94	-0.10	B8	779	12.56	+0.16	B8	829	12.04	+0.08	A0
730	11.97	+0.31	A0	780	12.81	. . .	A2	830	12.49	+0.12	A0
731	12.02	. . .	F0	781*	10.25	. . .	F0V	831	12.40	. . .	F5
732	12.30	. . .	K0III	782*	11.08	. . .	K2III	832	11.86	. . .	G0
733	11.79	. . .	F0V	783	12.30	. . .	G5	833	11.92	-0.16	A0
734	12.27	. . .	G5V	784	12.79	+0.04	A0	834	11.63	+0.01	B9
735	12.47	. . .	G8III	785	10.95	. . .	F2V	835	11.07	. . .	F0V
736	11.87	. . .	F8	786	13.05	+0.13	A0	836	12.75	+0.10	B9
737	13.17	+0.14	A2	787*R	10.10	-0.20	B8	837	11.72	. . .	F0V
738	12.48	. . .	G0	788	12.90	+0.11	B9	838	12.66	. . .	G0
739	10.82	-0.02	B5	789	11.52	+0.02	A0	839*	7.26	. . .	F0IV
740	12.93	+0.32	B8	790*	10.46	. . .	G2III	840	12.51	. . .	K2III
741	11.82	. . .	G5V	791	13.01	+0.13	A0:	841	12.57	. . .	G5V
742	12.59	+0.03	B8	792	11.58	-0.02	A0	842	12.31	. . .	G0
743	12.32	. . .	G5V	793 R	11.82	-0.18	B9	843	12.12	. . .	G8V
744	12.77	-0.03	B9	794	12.04	. . .	G0V	844*	9.99	-0.17	B8
745	12.20	-0.05	B9	795	12.22	+0.10	B9	845*	10.74	+0.52	F8V
746	12.47	. . .	G0	796	11.59	-0.11	B8	846	12.03	-0.05	A0
747	12.85	+0.08	A0	797*	6.36	-0.25	B5	847 R	11.61	+0.15	A3
748	13.02	+0.18	A0	798*	9.16	-0.13	B9	848	11.26	. . .	F0V
749	12.52	+0.16	A0	799	11.09	-0.17	B8	849	12.95	+0.11	B8
750	13.41	. . .	A2	800	12.30	. . .	F5	850	12.53	-0.11	A0
751	11.89	. . .	A2	801*R	10.20	-0.40	B3k	851	11.54	-0.20	B9
752	12.68	+0.06	B8	802	12.52	. . .	G8III	852*	10.45	. . .	G8III
753	12.44	. . .	K0III	803	12.95	-0.01	A0	853	12.38	+0.18	B8
754	12.95	. . .	G5III	804	11.92	. . .	G5IV	854	12.87	. . .	G5III
755	12.24	+0.39	A3-F0	805	11.91	. . .	G8V	855	12.24	. . .	K0V
756	12.41	. . .	F0	806	12.00	. . .	G8III	856	11.67	-0.03	B9
757	12.88	. . .	G2	807	12.15	-0.18	A0	857	13.00	. . .	K0III
758	12.30	. . .	G0	808	13.02	+0.10	A5	858	12.52	. . .	A5
759*	10.58	. . .	F0IV	809 R	10.89	-0.13	B8	859	11.95	0.00	A2
760	12.97	+0.28	A0	810	12.23	+0.23	A2	860	10.84	-0.11	B9
761	11.99	-0.19	B8	811*	11.09	+0.23	A2	861	12.15	. . .	K0III
762	12.15	-0.13	B8	812*	9.52	-0.25	B8	862	13.03	. . .	F8
763*	10.75	. . .	K2III	813	12.88	+0.12	A0	863*	10.44	. . .	G5III
764	12.92	+0.22	A0	814	12.18	. . .	F0:	864	12.05	. . .	F5III
765	12.16	+0.20	B8	815	12.38	. . .	K0:	865	11.99	. . .	F0

Table 1

Observational Data for Region LF4 (Cont'd.)

Zone +53° (Cont'd.)

No.	m_{pg}	R.I.	Sp.	No.	m_{pg}	R.I.	Sp.	No.	m_{pg}	R.I.	Sp.
866	12.72	+0.45	B5	916	12.60	...	G0	966	12.78	...	G0
867	12.52	...	F8:	917	12.65	+0.33	B9	967	12.25	...	G8III
868	12.39	-0.08	B9:	918*	10.58	+0.46	G0V	968*	9.05	...	G5IV
869	12.12	+0.29	A0	919*	11.01	+0.37	F8V	969	12.70	...	G5III
870	12.48	+0.14	B8	920	12.10	+0.16	B9	970	11.17	+0.23	B8
871	12.64	+0.04	A0	921	11.99	...	F0V	971	13.27	+0.37	A5
872	12.44	...	K0	922*	7.60	0.00	A0	972	11.96	+0.62	B8
873	12.08	+0.10	A0	923	10.73	...	G5IV	973	12.59	...	G0
874	11.80	+0.25	A2	924	12.82	+0.52	A0	974	12.42	...	F5
875	12.56	...	G8	925	13.17	+0.35	A0	975	12.99	...	G5V
876	12.27	+0.07	A0	926	12.29	...	K0III	976	11.10	+0.46	A3
877 R	11.83	...	F2V	927	11.17	+0.02	B8	977	12.68	+0.64	B0:
878	11.17	-0.27	A3	928	13.05	...	K0III	978	12.16	+0.24	A2
879*R	11.10	+0.34	A5	929	13.11	...	G8	979	12.35	...	F2
880*	8.42	-0.21	B9	930	11.69	...	G5III	980 R	11.35	-0.03	B8
881*	7.10	...	G8III	931	11.91	...	G0V	981	12.16	-0.06	B5
882	12.73	+0.31	B8	932	12.56	...	G0	982	13.17	+0.33	A0
883	12.10	+0.18	B9	933	12.64	...	G5III	983	12.88	+0.34	A0
884	12.01	+0.10	B8	934	12.00	...	G0	984	13.07	...	F0
885	13.18	0.00	B8	935	12.74	...	G2	985*R	10.64	-0.04	B9
886	13.30	+0.18	B5:	936	12.30	...	G5III:	986	12.16	+0.34	B9
887	12.73	+0.30	A0	937	12.00	...	G0V	987	12.44	+0.24	A3
888	11.92	...	G5III	938	12.19	...	K0IV	988	12.52	...	G8:
889	12.67	+0.01	A0	939	12.35	...	G0	989	12.51	+0.33	A2
890	11.19	+1.01	G5V	940	12.78	+0.11	A0:	990	12.73	...	K0III
891	11.87	...	G5IV	941	12.85	+0.33	B8	991	12.32	+0.08	B9
892*	11.35	+1.76	K5V	942*	12.00	...	K0III	992	12.80	+0.40	A2
893	10.95	...	G5III	943	12.36	...	G5III	993*	11.03	...	G8III
894	12.74	+0.15	A0	944	11.77	+0.47	A5	994	11.39	0.00	B8
895*	10.26	+0.20	A3	945	12.00	+0.28	A0	995	13.14	+0.44	A0
896*	9.11	-0.07	B8	946	11.90	+0.23	B8	996	11.96	...	G8III
897	11.91	...	G8III	947	12.80	+0.24	B9	997	13.32	...	M2
898	11.82	+0.34	A5	948	10.45	...	A0	998	11.95	+0.43	A2
899	12.34	+0.14	B5	949	12.97	...	K0	999	12.36	...	G0:
900*	12.22	...	M2III	950	12.05	+0.07	B8:	1000	12.65	+0.32	A3
901	11.64	+0.15	A2	951	12.87	...	G5	1001	10.55	0.00	B8
902	11.16	+0.03	B8	952	12.78	+0.12	A0	1002	12.34	...	K3III
903	11.79	...	G0III	953	12.66	-0.02	B5	1003	12.22	...	A2-F0
904	13.03	...	K3III	954	11.27	-0.19	B8	1004*	8.63	...	B9
905	12.40	...	G0	955	12.44	+0.44	A3	1005	12.44	...	B8:
906 R	11.68	+0.64	G0:p	956*	10.25	...	G5III	1006*	10.50	...	G8IV
907*	9.57	+0.15	A0	957	12.36	...	G2V	1007	12.00	...	G0:
908	12.43	...	K3	958	13.05	...	G8III	1008	12.25	+0.39	A3
909 R	11.49	-0.14	B9	959	12.03	+0.09	A0	1009*	10.62	+0.12	B9
910	13.03	+0.35	A0	960	12.03	-0.01	A0	1010	11.96	...	K0III
911	12.34	+0.18	A0	961 R	11.06	+0.08	A0	1011	12.36	...	B9
912	12.64	-0.15	B3	962	13.14	+0.19	A0	1012	12.78	...	G8
913	12.47	...	F8	963	11.21	-0.09	A0	1013	11.83	-0.04	B8
914	13.54	...	G0:	964	11.98	+0.12	A0	1014	13.22	...	B8
915	13.07	+0.49	A0	965	12.90	...	F0	1015	12.36	...	A2

Table 1

Observational Data for Region LF4 (Cont'd.)

Zone +53° (Cont'd.)

No.	m_{pg}	R.I.	Sp.
1016	12.90	+0.18	A0
1017*	10.62	...	B9
1018	12.36	...	A0
1019 R	11.17	...	B8
1020	12.51	...	B9
1021	12.69	...	G2
1022	12.05	...	G0
1023	12.19	...	G8V
1024	13.11	...	G8III
1025*	10.58	...	A0
1026*	10.58	...	K0:
1027	12.44	...	A2
1028	12.40	...	F2
1029	12.83	...	A0
1030*	10.67	...	G2III
1031	11.82	...	A2
1032	13.00	...	G8III
1033	11.12	...	B9
1034*	10.08	...	G5III
1035	13.31	...	A0
1036	12.30	...	B9
1037	12.56	...	A5
1038	12.44	...	B8
1039	11.44	...	A0
1040	13.57	...	A2:
1041	12.87	...	A0:
1042	12.15	...	F8V
1043*	11.70	...	G8III
1044*R	11.03	...	B8
1045	12.36	...	F2
1046	12.35	...	A0
1047	12.44	...	A0
1048	11.72	...	B9
1049	12.73	...	A0
1050*	9.81	...	B8
1051	12.40	...	G8IV
1052	12.70	...	K0III
1053	12.93	...	G8III
1054	12.27	...	A3
1055*	10.32	...	K2III
1056	12.65	...	G0
1057	12.13	...	A5
1058	10.72	...	A3-F0
1059	12.89	...	G0
1060	11.45	...	F8V
1061	11.70	...	A0
1062	12.01	...	A0
1063	11.53	+0.43	F8V
1064	12.28	...	G0:
1065	12.52	...	G8III
1066*	11.71	...	K0IV
1067	12.70	...	G5V
1068	12.59	...	A0
1069	13.34	...	G5:
1070	13.50	...	A0
1071	12.18	...	G0
1072*	11.51	...	G0V
1073	12.30	...	A3
1074	13.11	...	F0
1075	11.44	...	B9
1076	13.07	...	K0III
1077	12.30	...	A0
1078	12.35	...	G8III
1079	12.52	...	A2
1080	12.00	...	K2V
1081*	9.53	...	B9
1082	12.97	...	G0
1083*	11.51	...	K0III
1084	12.44	...	K0III
1085	13.32	...	B9
1086	12.32	...	B8
1087	13.19	...	B8
1088	12.90	...	G5III
1089	12.30	...	F5
1090*	6.95:	...	K0III

Zone +54°

No.	m_{pg}	R.I.	Sp.
1	12.41	...	F0
2	12.11	...	B9
3	12.11	...	A0
4	12.46	...	B9
5	12.40	...	G2III
6*	10.14	...	G5III
7	11.71	...	B5
8	12.72	...	A0
9	12.99	...	G0:
10	12.57	...	A2
11	12.18	...	G5V
12	12.42	...	F8
13	12.18	...	G0V
14	12.41	...	A:
15	12.46	...	G8III
16	12.38	...	B9
17	10.77	...	G8III
18	10.48	...	B5k
19	13.65:	...	B8:
20	12.12	...	B8
21 R	11.40	...	A0
22	13.01	...	B5
23*	7.18	...	A0
24 R	11.40	...	B9
25	12.62	...	A2:
26	12.46	...	G0
27	12.29	...	F8
28	12.50	...	A0
29	11.81	...	A5
30	13.22	...	A0
31	13.17	...	B9
32	12.58	...	G8III
33 R	11.74	...	B8
34	13.09	...	A5:
35	12.83	...	G5:
36	13.17	...	A0
37	11.74	...	A2
38	12.54	...	G2:
39	12.46	...	F5
40	12.21	...	A2
41*R	11.21	...	G0V
42 R	10.56	...	B8
43*	10.60	...	K3III
44	12.32	...	A2
45	12.78	...	B9
46	12.58	...	G2V
47	11.85	...	G8III:
48	12.95	...	B8
49	11.80	...	A0
50	12.62	...	A0:
51	12.36	...	A0
52	12.86	...	A3
53	13.46	...	A0
54	12.56	...	A0
55	10.83	...	G2V
56	12.50	...	A0
57 R	11.12	...	B8
58	12.36	...	A2
59	12.50	...	B8:
60	12.11	...	B9
61	12.01	...	A0
62	11.59	...	G5V
63	12.84:	...	B8:
64	12.74	...	A0
65	12.41	...	A0
66	12.24	...	M2III
67	12.28	...	B8
68	11.80	...	F0
69	11.64	...	B9
70	12.96	...	G0
71*	10.02	...	G5III
72	12.46	...	B9
73	12.81	...	G8III
74	12.50	...	A0
75	12.62	...	K0III

Table 1

Observational Data for Region LF4 (Cont'd.)

Zone +54° (Cont'd.)

No.	m_{pg}	R.I.	Sp.	No.	m_{pg}	R.I.	Sp.	No.	m_{pg}	R.I.	Sp.
76	12.72	...	B8	126	12.46	...	K0	176	12.66	...	A0
77	12.28	...	B9	127 R	10.70	...	B8	177	12.81	...	K0
78	12.48	...	K0IV	128*	10.55	...	K2	178	12.95	...	G5:
79*R	12.53	...	G8III:	129	12.66	...	A0	179*	13.09	...	A0
80	11.10	...	G0III	130	12.53	...	B9	180	10.87	...	F8V
81	12.66	...	A0	131 R	12.10	+0.46	F5:	181	12.61	...	A0
82	12.58	...	G5	132	12.72	...	A5	182*R	10.02	...	B5
83	12.38	...	B9	133	12.46	...	G0	183	12.81	...	A0
84	12.38	...	B8	134	11.88	...	B9	184	12.50	...	M0
85	10.48	...	A3	135	13.60	...	A0	185	11.60	...	B9
86	12.27	...	A0	136	13.44	...	A3	186	11.45	...	K0III
87	12.40	...	B9	137	11.68	...	A0	187	12.66	...	B9
88	12.52	...	A0	138	12.76	...	F2	188	11.81	...	G5IV
89	11.62	...	A0	139*R	9.79	...	B5	189	12.34	...	F8
90	12.58	...	G5	140	13.14	...	G8III	190	11.73	...	B5k
91	11.62	...	B8	141	10.79	...	A3-F0	191*R	9.91	...	B2k
92	12.15	...	G8	142	12.38	...	G0:	192	12.95	...	B9
93	12.25	...	G5III	143	12.29	...	G0	193	12.46	...	B8
94	12.11	...	K0	144	13.09	...	A0:	194	11.59	...	G8V
95	11.01	...	A0	145 R	11.97	...	B8	195	12.19	...	K2III
96	12.32	+0.47	F8:	146	12.67	...	G5V	196	11.81	...	A5
97	11.65	...	B5	147	12.46	...	A5	197	11.86	...	A2
98	11.06	...	A0	148	13.29	...	K0	198*	11.50	...	K0V
99	12.54	...	G5	149	12.02	...	B8	199	12.54	...	G5
100*	10.67	...	K0III	150	12.13	...	G8IV	200	10.78	...	G2V
101	12.46	...	B8	151	12.71	...	G0	201	12.50	...	B9
102	11.32	...	F0V	152	12.15	...	K2	202	12.72	...	B5:
103	11.55	...	B8	153	12.50	...	B8	203	10.19	...	A5
104	12.15	...	G5III	154	11.40	...	G2V	204	11.81	...	A0
105	10.15	...	A0	155	11.89	...	K0III	205	12.72	...	B9
106	12.02	...	B8	156	12.25	...	A2	206	12.42	...	B9
107	12.54	...	B9	157	11.37	...	A0	207	12.59	...	B8
108	13.01	...	K0	158	12.29	...	K0	208	13.31	...	A0
109	12.41	...	G0	159*	10.83	...	K3III	209*	8.99	...	B8
110	12.60	...	B8	160	10.65	...	A0	210	12.99	...	A0
111	12.41	...	A0	161*R	9.37	...	A0	211	13.21	+0.19	A0
112	12.38	...	G2	162	11.46	...	B8	212	10.38	+0.21	B9
113	12.25	...	A0	163	12.18	...	F8V	213	12.70	+0.19	A2
114	11.60	...	B8	164	12.25	...	G0	214	13.14	...	F0
115*	7.94	...	K2III	165	11.36	...	B5	215	12.57	...	A2:
116	12.36	...	B8	166	11.76	...	A0	216	12.76	...	A0
117*	9.40	...	K0III	167	13.09	...	A0	217	12.58	...	G5III
118	12.86	...	G8:	168	12.67	...	B5	218	12.11	-0.21	B8
119	11.93	...	B8	169	12.06	...	B5k	219 R	10.99	+0.14	A0p
120	12.72	...	G5	170	12.50	...	A0	220	11.55	...	A0
121	12.95	...	B8	171	10.92	...	F2III	221	10.73	+0.09	A2
122	11.00	...	B8	172	10.79	...	G5III	222 R	10.11	+0.20	A0
123	12.50	...	A0	173*R	9.52	...	A0	223	10.92	...	F5V
124	11.37	...	F0V	174	12.25	...	A2	224	12.39	-0.19	B5:
125	10.92	...	G5V	175	12.06	...	B8	225	12.46	...	G0

Table 1

Observational Data for Region LF4 (Cont'd.)

Zone +54° (Cont'd.)

No.	m_{pg}	R.I.	Sp.	No.	m_{pg}	R.I.	Sp.	No.	m_{pg}	R.I.	Sp.
226	11.05	-0.35	B2	276*	7.97	+0.85	K0V	326	10.49	-0.19	B5k
227	12.45	-0.13	B8:	277	12.84	+0.24	A2	327	11.76	+0.06	A0
228	12.84	+0.37	A2	278 R	12.10	-0.12	B2	328	12.81	. . .	K0
229	13.38	+0.19	A0	279	11.81	. . .	F0V	329	12.59	+0.07	A0
230	11.95	-0.13	B5	280*	9.41	. . .	G5III	330 R	11.75	+0.11	A0
231	12.87	+0.17	B8	281 R	11.50:	. . .	B5	331	12.71	+0.19	A0
232	13.17	. . .	G8	282	12.36	. . .	F0	332	11.74	+0.07	A0
233 R	11.06	-0.24	B9	283	11.63	-0.26	B5:	333*	10.09	. . .	B8
234	10.91	-0.07	A0	284*	7.97	+0.02	A5	334	12.61	+0.41	A2
235	12.31	-0.11	B8:	285	11.71	+0.07	A0	335	10.67	-0.05	B9
236	11.10	. . .	B8:	286	12.21	. . .	F2	336	11.34	-0.10	A0
237	11.59	-0.32	B5:	287	12.33	-0.11	B5	337	12.52	+0.12	A0
238	12.05	+0.57	A3:	288	12.41	+0.09	A0	338	10.23	-0.06	B9
239	12.06	+0.38	A2	289	10.65	. . .	K0IV	339	10.85	. . .	G2IV
240	12.95	. . .	G0	290	11.18	+0.66	G5V	340	12.42	. . .	G0
241	12.67	+0.29	A5	291	12.68	-0.14	A2	341	11.19	-0.09	B9
242	12.53	. . .	G2	292	12.56	+0.04	A0	342	12.39	+0.21	B8
243	12.26	+0.29	A0	293	13.02	. . .	G5III	343	12.46	. . .	G5V
244*	8.91	-0.22	B9	294	12.60	+0.12	B8	344	12.03	+0.15	A0
245	11.50	. . .	K2III	295	11.88	. . .	G5V	345	12.46	-0.18	B9
246 R	10.56	-0.08	A2p	296	11.41	. . .	G8III	346	12.72	. . .	G5:
247*	10.39	. . .	G5III	297	12.22	+0.16	A0	347	10.93	-0.21	B5
248	12.59	+0.09	A0	298	12.58	. . .	G0	348*	10.15	-0.23	B8
249	12.79	+0.23	A0	299	12.43	+0.19	A2	349	12.57	. . .	G5III
250	12.86	. . .	G8III	300	12.57	+0.19	A2	350	12.48	-0.04	A3:
251 R	11.91	-0.01	A2	301	11.88	+0.36	A2	351	10.74	-0.03	B8
252	11.72	+0.48	G0V	302	10.83	. . .	F8V	352	12.23	+0.08	B5
253	11.88	-0.17	B5	303*	10.07	+0.03	A2	353	12.34	. . .	G0
254*	10.66	+0.50	G0V	304	12.21	+0.09	B9	354 R	11.67	+0.33	A0
255	11.73	. . .	F8V	305	12.36	. . .	G0	355	12.13	+0.01	B5
256	12.44	. . .	G5III	306	12.10	+0.04	B8	356	12.28	+0.13	B8
257	10.92	. . .	G8IV	307 R	10.20	-0.29	B3	357 R	11.79	-0.15	A2p
258	12.52	. . .	G0:	308	12.53	. . .	G0:	358	11.07	-0.01	B8
259	12.44	. . .	K0III	309	12.30	+0.14	A0	359	12.46	-0.10	B5
260	12.02	. . .	G0	310	12.28	. . .	B8	360	12.49	. . .	F8
261	12.29	-0.15	B8	311	12.16	-0.06	A2	361	12.26	+0.32	A5
262	13.07	+0.15	A0	312	12.72	+0.28	A2-F0	362	12.36	. . .	G5III
263*	10.62	. . .	A2	313	12.42	. . .	F0	363	12.70	+0.25	A0
264	12.62	+0.26	A0	314	12.69	+0.52	A5	364	12.46	. . .	G5V
265	11.99	-0.05	B5	315	11.10	. . .	G0	365	11.54	-0.02	B5k
266	12.43	. . .	G0	316	12.72	+0.12	A0	366	13.05	+0.36	B9
267	12.54	. . .	F0	317	12.20	+0.50	B9	367	11.65	. . .	G8V
268	12.41	. . .	G5V	318*	8.85	-0.15	B9	368	12.96	+0.16	A0
269	12.34	-0.14	A2	319	12.99	+0.07	A0	369 R	10.77	+0.11	B2:
270*	8.95	. . .	F5V	320	12.17	. . .	G0	370	12.56	+0.15	B8
271	12.47	+0.17	B2:	321	11.68	. . .	G0III	371	13.01	+0.35	A0
272	12.55	-0.05	B3	322	11.02	-0.12	B5	372	11.93	. . .	F0V
273	12.19	+0.05	B8	323*R	8.58	-0.16	B0k	373	11.23	+0.77	G5V
274*	8.67	. . .	K0III	324	12.74	+0.40	A3-F0	374	12.40	. . .	A0
275	12.23	. . .	A2-F0	325*	10.19	. . .	F0V	375	11.33	-0.07	B5

Table 1

Observational Data for Region LF4 (Cont'd.)

Zone +54° (Cont'd.)

No.	m_{pg}	R.I.	Sp.	No.	m_{pg}	R.I.	Sp.	No.	m_{pg}	R.I.	Sp.
376	11.89	+0.33	A2	426	12.33	...	F0III	476	12.42	...	G0
377	11.28	-0.05	B9	427	12.79	+0.07	B8	477	12.46	+0.24	A0
378	12.05	...	G8III	428*	10.91	-0.01	B5k	478	12.09	+0.33	A2
379*	10.55	-0.12	B3	429	12.58	-0.06	B5k:	479*	7.20	...	F5V
380	11.10	+0.04	A2	430	12.07	...	F0	480	10.98	-0.06	B5k
381	12.22	-0.04	B8	431	12.08	0.00	B8	481	12.36	...	G0:
382	12.20	...	F0	432	12.10	-0.10	B2	482	11.19	+0.15	A0
383	12.06	...	A0	433	12.35	...	G8III	483	12.31	+0.08	A2
384	12.41	+0.11	B9	434	11.01	...	F0V	484	12.17	...	G2V
385	11.28	+0.25	A5	435	12.25	...	G5V	485	12.62	+0.74	G0Ib:
386	12.66	...	G0	436	13.11	+0.37	A0	486	12.55	+0.37	A0
387	12.67	+0.26	B9	437	12.17	+0.13	A0	487	11.93	...	G0V
388	12.32	+0.33	A2	438	12.05	+0.16	B5	488*	9.48	...	K0IV
389*	8.67	+0.06	A2	439	12.55	+0.37	B9	489*	9.46	-0.12	A0
390	11.81	...	G8IV	440	12.68	+0.54	A0	490	9.39	+0.03	A5
391	12.35	-0.08	A0	441	12.64	+0.02	B9	491	12.70	...	G8
392	12.71	...	K0III	442	12.02	+0.32	A3	492	12.80	...	G0
393	12.25	...	F2V	443	12.86	...	G2:	493*R	9.96	+0.10	A0
394	12.83	+0.09	A0	444	13.10	+0.12	B9	494	12.76	+0.12	A0
395	12.62	-0.02	B5:	445	12.50	-0.39	A0	495*	8.94	...	G5III
396	12.62	...	G0	446*	10.39	-0.09	B5k	496	12.47	+0.10	A0
397*	8.77	-0.14	B8	447	11.91	-0.01	B2:	497	11.42	+0.36	G0V
398	11.34	-0.16	B9	448	12.30	...	F0	498	12.26	+0.17	B0:
399	11.15	-0.65	B5	449	11.74	+0.06	B9	499	11.80	...	F0III
400	12.46	+0.45	A0	450	12.34	...	G8V	500	12.25	...	F8
401	12.10	+0.11	B5	451	11.92	+0.24	A3	501	11.62	...	M5
402*R	9.50	-0.06	B0k	452	11.57	+0.09	B9	502	13.03	...	F0
403	12.97	+0.12	B8	453	13.46	+0.42	A0	503	13.08	...	F8
404	11.27	+0.30	G0V	454	12.37	+0.27	A0	504	11.97	...	F5V
405	10.58	-0.26	B5	455	12.76	...	F0:	505*	9.67	...	G5III
406	11.11	+0.31	A5	456	12.24	...	K2:	506	12.25	+0.11	A0
407*	8.28	+0.40	A5	457	12.35	-0.07	A0	507 R	11.96	+0.20	A3-F0
408	12.40	...	K0III	458	11.64	...	G8V	508	11.89	...	F8V
409	13.10	+0.30	A0:	459	12.38	...	G0	509	11.95	...	A0
410	12.02	...	G8IV	460	11.73	+0.34	A0	510	10.56	...	F2V
411	12.70	+0.29	A2:	461	11.40	+0.09	G5V	511	12.50	...	K0
412	12.36	+0.01	B5	462	12.58	...	G0	512	12.59	+0.17	B9
413	11.88	+0.28	A0	463	11.85	...	G0V	513	13.17	...	F2:
414	12.50	+0.26	B9	464	12.80	...	F0	514	12.29	...	G0
415 R	11.87	-0.21	B8	465*	10.58	+0.16	A5	515*	8.89	-0.31	B3
416	11.79	+0.25	A0	466	12.46	-0.04	B8	516	12.70	...	G5:
417	12.38	+0.10	A0	467	11.75	-0.09	B3	517	12.46	+0.40	A3
418	12.20	...	G0	468	12.97	+0.40	B5	518	12.39	+0.27	A3-F0
419	12.49	...	K0	469	12.43	...	G0:	519	11.61	...	G5V
420	12.66	...	F2	470	11.07	-0.07	B8	520	12.58	+0.18	A0
421	12.58	...	G5III	471	11.17	...	F8V	521	12.22	...	A3:
422	12.60	+0.24	A0	472	12.58	...	G0	522	12.87	+0.41	A0
423	12.31	...	G8III	473*	10.08	-0.01	B9	523	12.36	...	K0III
424	11.47	-0.04	B8	474	12.42	...	G5:	524	11.14	-0.24	B8
425	12.61	+0.08	A0	475	12.44	...	K3	525	12.51	+0.21	B8:

Table 1

Observational Data for Region LF4 (Cont'd.)

Zone +54° (Cont'd.)

No.	m_{pg}	R.I.	Sp.	No.	m_{pg}	R.I.	Sp.	No.	m_{pg}	R.I.	Sp.
526	11.88	+0.22	A0	576	12.17	+0.31	B8	626	11.19	-0.17	B8
527	12.58	...	F0	577	10.85	-0.03	B8	627	12.47	+0.15	A2
528	12.43	+0.06	B9	578	12.55	-0.02	B5:	628	13.15	+0.09	B9
529	12.27	...	G2V	579	11.53	+0.21	A2-F0	629	12.35	+0.19	B9
530	12.76	+0.10	B9	580	12.00	+0.12	B8	630	12.15	...	G8III
531	12.21	+0.51	A2-F0	581*	10.79	...	G8III	631	13.17	...	G8III
532	12.58	+0.56	B5	582	12.62	...	K5	632*	10.36	-0.34	B5
533	12.72	+0.28	A5:	583	12.37	+0.01	B8	633	12.32	+0.30	A3
534	12.36	+0.25	A0	584	11.06	-0.03	B8	634	12.86	+0.14	A0
535	12.73	+0.35	A2	585*	9.86	-0.14	B8	635	12.42	...	G5V
536	11.12	+0.32	F8V	586	12.62	...	F5:	636	12.06	+0.10	B9
537	12.84	+0.30	A0	587	11.95	-0.19	B5	637	11.10	-0.18	B8
538	12.94	+0.24	A0	588	11.20	+0.29	A3-F0	638	11.70	...	B8
539	12.46	+0.25	A2	589*	9.67	...	G5V	639	12.01	0.00	B8
540	11.18	-0.60	B9	590	12.68	+0.37	A0	640*	11.54	...	M0III
541	12.50	...	K0III	591	10.49	+0.19	A3	641*	8.13	-0.29	B9
542	12.38	...	K0III	592	13.11	...	G8	642	12.97	...	A0
543	12.59	...	B8	593	12.74	...	F2	643	12.27	+0.09	A0
544	11.83	...	K0III	594	12.50	...	F0	644	13.28:	...	B9:
545	13.10	+0.30	A0	595*	8.50	+0.07	A3	645	12.24	...	G0
546	12.42	...	G0	596	12.11	...	G8III:	646*	9.31	-0.08	A0
547	11.51	+0.55	G2V	597	12.36	...	G0	647	12.06	-0.06	B8
548	11.73	-0.05	A0	598	11.89	+0.05	B9	648	11.41	+0.19	A5
549*R	8.74	-0.11	B0k	599	12.45	+0.02	B5	649*	9.45	...	K0IV
550	13.04	...	A2	600	12.33	0.00	B8	650	12.46	...	K5
551	12.66	...	G0	601	12.36	...	K0III	651	12.03	+0.17	A3
552	12.62	...	F8:	602*R	9.14	-0.22	B0k	652	12.27	...	G8III
553	12.66	+0.08	B5	603	12.09	+0.39	A5	653	13.06	...	G0
554	12.15	+0.43	A5	604	12.84	+0.24	A2	654	11.00	...	G0III
555	12.37	+0.23	A0	605*R	9.87	...	B9	655	13.05	+0.23	A0
556	12.86	+0.14	B5:	606 R	11.25	+0.25	B3k	656	12.34	+0.20	A0
557	12.26	-0.09	B5	607	11.67	...	F5V	657*R	8.08	-0.24	B9
558	12.45	...	G0	608	11.68	0.00	A0	658	10.99	+0.57	A3
559	13.10	+0.34	A0	609*	8.71	...	F0V	659	11.76	-0.02	B8
560	12.58	...	G0	610	12.79	+0.09	B8	660	12.42	+0.26	F0:
561	12.50	...	G5	611	12.93	+0.17	B9	661*	8.59	-0.22	B9
562*	10.78	...	M0III	612	12.87	+0.27	B9	662	12.53	...	G0
563	12.37	...	F8	613*	11.31	...	G5III	663	11.31	+0.24	A3
564	12.85	+0.05	B9	614	12.66	...	K0III	664	12.50	...	G5III
565	12.61	...	F0	615	11.06	+1.44	G8V	665	12.41	+0.07	B8
566	13.02	+0.23	A0	616	12.79	...	A0	666	12.42	...	G5III
567	12.62	+0.05	B9	617	11.53	+0.03	A0	667	12.66	...	G0
568	12.85	+0.25	B9	618*	9.88	-0.15	B5k	668	12.32	+0.35	A5
569	11.68	-0.24	B5	619	12.82	-0.06	B8	669	12.96	+0.10	B8
570*	11.20	+1.48	K0V	620	12.67	+0.08	A2	670	12.84	...	G0
571	12.73	+0.21	A0	621	12.89	...	A0	671	11.13	-0.09	B8
572*R	7.83	+0.13	B2k	622	12.46	...	G0	672	11.98	...	F0V
573	12.38	...	G5III	623	13.02	...	A0	673	11.73	-0.15	B8
574	12.29	+0.46	A5:	624	12.59	...	A3	674	12.04	-0.15	B8
575	12.66	...	F2	625	10.29	-0.15	B8	675	12.46	...	A0

Table 1

Observational Data for Region LF4 (Cont'd.)

Zone +54° (Cont'd.)

No.	m_{pg}	R.I.	Sp.	No.	m_{pg}	R.I.	Sp.	No.	m_{pg}	R.I.	Sp.
676	12.53	+0.17	A0	726	12.94	+0.28	B8	776	11.38	-0.07	B8
677	12.42	+0.17	A0	727	12.51	+0.35	A2-F0	777	10.55	-0.01	A0
678	13.11	+0.23	B8	728*	10.56	...	K0IV	778	12.88	+0.16	A0
679	12.60	-0.16	B8	729	12.42	+0.16	A0	779	12.80	+0.02	B8
680	12.80	+0.13	B9	730	12.23	+0.35	A2	780	11.57	...	K0III
681*	10.35	...	F0V	731	12.57	...	F8	781	11.48	-0.02	A0
682	13.01	+0.19	B8	732	11.67	...	G8III	782	12.93	+0.07	A0
683	11.27	+0.01	B9	733*	10.11	-0.16	B8	783	12.98	+0.20	A0
684	13.00	+0.43	B9	734*	9.26	+0.04	A2	784	12.19	-0.05	B9
685	10.76	+0.02	A2	735 R	10.90	-0.26	B8	785	12.02	...	F8V
686	12.10	0.00	A0	736*	11.05	...	G8III	786	12.74	+0.22	A0
687*	9.18	-0.29	B9	737	12.72	...	G2:	787	12.51	+0.14	B8
688	12.54	+0.36	A2-F0	738	12.88	+0.16	B9	788	12.37	...	K0
689	12.46	+0.36	A5	739	11.45	...	G8IV	789	12.75	+0.19	A0
690	11.63	+0.45	F8V	740	11.41	...	F0IV	790*	10.52	+0.37	A2-F0
691	12.80	...	G8	741	11.55	...	G8III	791	11.98	-0.06	B9
692	12.84	+0.30	A0	742	12.48	...	G5V	792	12.36	...	G5III
693	12.76	...	G5	743	12.62	...	G5III	793 R	11.17	-0.27	A0
694	12.51	+0.35	B9	744	12.32	+0.19	A0	794	10.99	-0.31	A0
695	12.51	+0.19	A2	745	13.12	+0.47	B9	795	12.20	...	F2
696*	10.08	+0.24	A3	746	12.19	...	G0:	796	12.52	...	G5III
697	12.42	...	B5	747*	10.16	+0.54	G0V	797	12.81	+0.07	B8
698	12.05	+0.13	A2	748	12.25	...	A2	798	12.58	...	G0
699	11.53	0.00	A0	749	12.36	+0.18	A2	799*	11.00	...	K5III
700*	11.45	...	K2III	750	13.02	+0.32	A5	800	12.33	...	G8III
701	12.83	+0.53	A2-F0	751	13.03	...	K0	801	12.12	+0.04	A0
702*	10.42	+0.30	A5	752	12.34	+0.03	B8	802	12.67	+0.01	A0
703	12.25	...	G5V	753*	10.29	-0.09	B8	803*	10.39	+2.45	M0III:
704	11.80	...	F0V	754	12.54	+0.12	B8	804	13.21	+0.42	A0
705	12.94	+0.12	B8	755	11.59	-0.05	A2	805	13.05	+0.13	B8
706	13.01	+0.19	A2	756	12.10	0.00	A0	806	11.12	-0.08	A0
707	11.00	...	F8V	757*	10.16	-0.10	B9	807	12.61	+0.33	A2-F0
708 R	11.94	+0.19	A0	758	12.20	...	F0V	808	11.38	+0.28	A3
709	12.32	...	K0III	759	11.71	+0.09	A0	809	13.03	...	A2:
710	12.47	...	G0:	760	11.77	...	G0	810	12.92	+0.22	A0
711	12.38	...	F5	761	12.98	+0.30	A0	811	11.14	+0.08	A0
712	12.38	...	G5III	762	12.47	+0.21	A0	812	11.97	+0.33	A0
713	13.05	...	G8	763 R	11.88	+0.12	A0	813	11.76	-0.04	A0
714	12.44	...	G8III	764	13.06	+0.10	B5:	814	11.78	+0.13	A0
715	12.54	...	G2	765	12.53	...	K0III	815	12.00	...	G5III
716*	10.73	...	K2III	766	11.69	...	G8II	816*	9.20	-0.14	B9
717*	9.29	...	F5IV	767	10.27	-0.15	B5	817	12.27	...	G0V
718	12.31	...	G5V	768	12.36	...	K3III	818	12.36	...	K0III
719	12.58	...	G0	769*	10.72	+0.08	A2	819	12.36	...	G5
720	12.41	...	F0V	770	12.27	-0.07	B5	820	12.05	+0.29	A2
721	12.36	...	G0	771	12.20	...	F0	821	11.77	+0.14	A2
722	12.38	...	K0III	772	12.81	+0.09	A0	822	12.82	...	G8III
723	12.43	...	G5V	773	12.06	...	F2	823	13.04	+0.27	A2
724	13.24	+0.30	B8	774*	11.08	...	G5III	824	12.16	...	B9
725*R	8.37	-0.09	B8	775	11.43	+0.54	G0V	825	12.23	+0.15	A0

Table 1

Observational Data for Region LF4 (Cont'd.)

Zone +54° (Cont'd.)

No.	m_{pg}	R.I.	Sp.	No.	m_{pg}	R.I.	Sp.	No.	m_{pg}	R.I.	Sp.
826	12.30	+0.20	A3	876	10.70	+0.05	A0	926	12.57	+0.31	A0
827	11.63	...	A0	877	12.85	+0.13	B9	927	13.02	+0.26	B9
828	11.84	-0.12	A0	878	12.48	+0.15	B8	928	11.36	+0.59	G2V
829	11.67	+0.99	K0V	879	11.59	...	F0V	929	12.93	...	F0
830	11.92	+0.01	A0	880	12.32	...	G0	930	12.57	+0.23	B5
831 R	10.47	-0.21	B8	881 R	11.20	-0.24	B2k	931	11.81	+0.33	A0
832	12.61	+0.15	B9	882	12.78	+0.28	A0	932	13.15	+0.35	B8
833	13.11	+0.24	B9	883	12.74	+0.44	A0	933	12.78	+0.38	A0
834	12.92	+0.01	A0	884	12.58	...	F5	934	12.29	+0.13	A2
835	11.95	-0.01	A0	885	12.58	...	G0:	935	13.19	+0.21	B9
836	12.71	...	G8III	886	12.33	...	G8III	936	12.79	...	G5III
837*R	9.61	-0.16	B2k	887	12.10	...	G2V	937*	7.95	...	F0V
838	12.66	+0.18	B9	888	12.42	...	F0	938	11.24	0.00	B9
839	12.64	+0.28	B8	889	12.29	...	F8	939	12.43	+0.45	B0:
840*	8.65	-0.11	B9	890	13.14	+0.27	A0	940	13.17	...	G8
841*	9.57	-0.19	B9	891	13.22	...	B8	941	12.93	...	B0:
842*	11.09	...	G5III	892	10.83	-0.17	B2	942	12.41	...	G0
843	12.99	+0.24	B9	893	13.05	...	G0	943*	11.04	...	G5IV
844	12.00	+0.04	B8	894	12.06	...	F8	944	12.32	...	F0
845	11.56	+0.42	A5	895	12.50	...	K2III	945	12.90	+0.44	A0
846	10.76	...	F2V	896	12.02	-0.05	B3	946	12.99	+0.18	B9
847	13.14	+0.20	A0	897 R	11.61	-0.03	A0	947	12.96	...	G0
848	12.42	...	F0	898	11.50	+0.01	A0	948	12.24	+0.02	B8
849	12.38	...	F2	899	11.41	+0.01	A0	949	12.33	+0.41	A0
850 R	11.77	...	A2	900	11.54	...	G8III	950	12.35	-0.01	A0
851	12.17	+0.09	B8	901	12.60	-0.01	B8	951*	12.15	+0.04	B9
852	13.02	+0.24	B8	902	11.49	+0.09	A2	952	10.81	+0.05	B8
853	12.86	-0.02	A0	903	12.32	+0.20	A0	953	12.62	...	G8:
854	12.88	...	K0III	904	12.43	+0.16	A0	954	12.38	+0.19	B9
855	12.71	...	F8	905	11.53	+0.28	A0	955	11.53	...	F0IV
856	10.56	-0.04	B2	906	12.02	...	G0V	956	12.94	...	F0
867	12.11	...	G5III	907	12.33	-0.02	B8	957	8.65	...	F0III
868	12.53	...	G5III	908	12.66	...	G5III	958	12.48	-0.04	B5
869	12.57	...	F8	909	12.50	...	F5:	959*	11.56	...	G8V
860	11.48	+0.04	B9	910	13.01	...	K0III	960*	8.91	-0.13	B8
861	13.15	+0.33	B9	911	12.34	...	G0	961	11.45	...	K0IV
862	12.02	+0.14	B5	912	11.95	...	F0	962*	12.06	...	G8IV
863	12.46	...	G0	913*	9.68	...	G8III	963*	10.11	+0.05	B8
864*	9.23	...	A0	914	12.53	...	F0	964	12.95	+0.21	A0
865	11.82	...	A0	915*	10.44	-0.02	B9	965	11.44	...	G5III
866*	8.92	+0.92	G5V	916	12.46	...	A3:	966	12.18	...	F2
867	12.14	+1.50	G51b	917	12.38	...	F0	967	12.58	...	G0
868	12.75	...	K0III	918	12.63	...	G8III	968	12.10	+0.30	A2
869	13.01	+0.43	A0	919	11.35	+0.01	B9	969	12.98	+0.16	A0
870	12.88	...	G0	920	12.13	+0.30	B9	970	12.62	...	F0
871	12.45	...	F0	921	12.50	...	F0	971*	10.49	+0.11	A0
872*	10.27	...	M2III	922	12.83	+0.45	F0	972	11.27	+0.37	G0V
873	12.32	+0.08	A0	923	11.89	...	G0III	973*R	10.42	+0.36	A3
874	12.81	...	A0	924	12.85	+0.19	A0	974	12.58	...	F0
875*	10.35	...	F0V	925	12.28	+0.14	B9	975	12.12	...	B0:

Table 1

Observational Data for Region LF4 (Cont'd.)

Zone +54° (Cont'd.)

No.	m_{pg}	R.I.	Sp.	No.	m_{pg}	R.I.	Sp.	No.	m_{pg}	R.I.	Sp.
976*	10.88	+0.18	B5	1026*	9.99	...	B9	1076	11.93	...	F2V
977 R	11.04	+0.02	B9	1027	11.68	...	A0	1077 R	11.17	...	B8
978*	10.21	+0.16	A0	1028	11.59	...	B8	1078	12.12	...	G0
979	12.98	+0.39	B8	1029	12.21	...	A0	1079	11.10	...	B5
980	12.40	+0.56	A5	1030	11.50	...	A0	1080*	7.17	...	B8
981	12.23	+0.31	A0	1031	12.83	...	A0	1081	12.44	...	G5
982	13.25	+0.38	B9	1032	12.62	...	A2	1082	12.52	...	A3
983	10.93	...	G5IV	1033	12.74	...	B9	1083	12.06	...	A0
984	11.97	...	G2III	1034	12.17	...	G5V	1084	12.53	...	G8III
985	12.69	+0.15	A0	1035	12.17	...	A0	1085	12.23	...	G0
986	11.37	...	F0III	1036	12.62	...	A0	1086	12.27	...	F0:
987	11.67	+0.15	B9	1037	12.34	...	G5IV	1087	11.81	...	A0
988	12.17	...	G8IV	1038	12.62	...	A0	1088 R	11.47	...	B9
989	12.01	...	F0	1039*	9.36	...	F2V	1089	12.58	...	G5:
990	11.36	...	G5III	1040	12.58	...	A0	1090*	10.52	...	K0III
991	12.98	+0.20	B3	1041	12.01	...	K0III	1091	12.77	...	B9
992	11.66	+0.22	A0	1042	12.45	...	B8	1092	12.24	...	K0IV
993	12.46	+0.42	A0	1043*	10.35	...	F0III	1093*	11.93	...	K0III
994	12.86	+0.50	B9	1044	12.38	...	A0	1094	12.48	...	F8
995	12.35	-0.06	B8	1045	12.40	...	F8	1095	12.42	...	B8
996	12.95	+0.49	B5	1046	12.62	...	A0	1096	10.88	...	F0V
997	12.54	+0.12	A0	1047	12.19	...	A3	1097	12.63	...	A0
998	10.74	...	G5III	1048	13.08	...	A2	1098	12.47	...	G0
999	11.53	+0.43	A2	1049	13.05	...	F0	1099	12.42	...	B5
1000*	11.47	...	K0III	1050	12.84	...	B8	1100*R	10.31	...	B5k
1001	12.17	...	G8V	1051	11.08	...	B9	1101*	10.02	...	G5III
1002	11.74	...	F0	1052*	11.08	...	G5IV	1102	12.70	...	A0
1003	11.93	...	F8	1053*	11.23	...	K3III	1103	12.67	...	F0
1004	12.70	...	K0III	1054	11.32	...	B8	1104*	10.17	...	F0III
1005*R	9.24	+0.26	A3	1055	12.53	...	B:	1105	12.49	...	A0
1006	11.69	+0.03	B5	1056*	10.19	...	B8	1106	12.58	...	A0
1007 R	11.85	+0.09	B9	1057	13.11	...	B9	1107	12.03	...	G0
1008	11.48	...	A5	1058*	10.60	...	K3III	1108	12.25	...	G8V
1009	12.93	...	G0	1059	11.97	...	G5V	1109	11.88	...	F8
1010	12.37	...	G8III	1060	12.29	...	B8	1110	12.55	...	A0
1011	12.48	...	G8III	1061*	8.69	...	G0IV	1111	12.58	...	F0
1012	12.66	...	K0	1062*	10.51	...	K0III	1112*R	11.25	...	G0Ib:
1013	12.42	...	G0:	1063	11.05	...	B0	1113*	10.47	...	A3
1014	9.92	...	B9	1064*	10.86	...	G5III	1114	11.37	...	B8
1015	12.50	...	G0	1065	12.36	...	G0	1115	11.18	...	B9
1016	12.29	...	G5V	1066	12.36	...	F0	1116	11.24	...	B8
1017	12.33	...	G5V	1067*	9.06	...	A3	1117	12.36	...	G0
1018*	9.99	...	B9	1068	11.74	...	A0	1118	12.58	...	F0
1019	12.93	...	B8	1069	12.53	...	B8	1119*	10.06	...	B9
1020	13.14	...	A0	1070	12.84	...	B9	1120	12.62	...	B8
1021*	10.73	...	F2IV	1071	11.32	...	A0	1121	13.08	...	B8:
1022*	9.32	...	F8IV	1072	13.20	...	K0III	1122*	11.24	...	G0:
1023	12.58	...	A0	1073	11.23	...	F2V	1123	12.97	...	B9
1024	11.76	...	A0	1074	12.24	...	B8	1124	11.28	...	A2
1025	11.73	...	A0	1075	11.85	...	A0	1125	12.54	...	B8

Table 1

Observational Data for Region LF4 (Cont'd.)

Zone +54° (Cont'd.)

No.	m_{pg}	R.I.	Sp.	No.	m_{pg}	R.I.	Sp.	No.	m_{pg}	R.I.	Sp.
1126	12.48	...	G2	26	12.71	...	K3	76	11.23	...	G0V
1127	13.08	...	B5	27	12.82	...	K2III	77*	10.89	...	A0
1128	11.93	...	B9	28	11.38	...	B5	78	11.95	...	B8
1129*	8.32	...	A2	29*	10.79	...	M0III	79	12.77	...	K0:
1130	12.36	...	B8	30*	10.98	...	K3III	80	12.29	...	B5k
1131	10.88	...	F0V	31	12.31	...	B9	81	11.76	...	G8IV
1132	11.93	...	B5k	32	11.46	...	B9	82 R	12.03	+0.11	B5p
1133	12.58	...	G8III	33	11.51	...	F8	83 R	11.42	...	nova
1134	11.96	...	G0	34	11.91	...	B5	84*R	9.46	...	B2k
1135	12.02	...	A0	35*	8.47	...	A0	85	12.52	...	G0
1136	12.29	...	A0	36*	9.69	...	F0V	86	12.36	...	G2
1137	12.41	...	G8III	37	12.38	...	B8	87	10.83	...	G5IV
1138	13.22	...	B9	38	12.46	...	K0III	88	12.73	...	F0:
1139	12.11	...	A0	39	12.12	...	B9	89	12.60	...	A0
1140*	10.56	...	A0	40 R	11.90	+1.00	B2p	90	12.60	...	B8
1141	12.66	...	G5V	41	12.86	...	A0	91	12.00	...	F0V
1142	12.83	...	B8	42	12.86	...	G0	92	11.33	...	A0
1143	13.21	...	B9	43	12.86	...	A2	93	11.81	...	A0
1144	12.67	...	A2	44	12.91	...	B5	94	10.29	-0.13	A3:
1145*	10.56	...	A0	45	12.78	...	B5	95*	9.21	-0.58	A0
1146*R	9.36	...	A3-F5	46	11.79	...	F8V	96	12.28	+0.33	A0
1147*	10.27	...	B9	47*R	10.20	...	B2k	97	12.46	...	K0III
1148	12.38	...	G8V	48*	8.96	...	A0	98 R	11.83	+0.41	A2-F0
				49*	10.10	...	G0III:	99*	9.97	...	F2V
	Zone +55°			50	12.94	...	A0	100	11.83	...	F0V
1*	9.81	...	M0III	51	12.67	...	B9	101	11.88	+0.32	A0
2	12.16	...	G0III:	52	11.87	...	B5	102	12.95	+0.49	B8
3	12.90	...	A3	53	12.52	...	G5	103	10.94	-0.02	A3
4	12.56	...	A0	54	11.95	...	G0	104	10.38	-0.36	B5
5	12.39	...	B8:	55	12.68	...	K0IV:	105	12.69	...	G8III
6 R	10.46	...	B8	56	12.56	...	B9	106	12.50	...	G0V
7	11.91	...	A3	57	13.45	...	A0:	107	12.42	+0.20	A0
8	11.83	...	B8	58	12.18	...	G0	108	12.41	...	G0:
9	12.68	...	B5:	59	12.56	...	B5:	109	11.84	...	F0V
10	12.41	...	F0V	60*	6.99	...	B8	110	12.53	...	G0:
11	12.60	...	B5	61	10.53	...	B5k	111 R	10.74	-0.06	A0
12	12.63	...	G0	62	12.25	...	G8V	112	10.87	...	F0V
13	11.55	...	A5	63	11.78	...	B9	113	12.05	...	K0III
14	12.52	...	A2	64	12.77	...	B9	114 R	11.59	+0.01	B8
15	12.52	...	A3-F0	65	12.76	...	K0	115	12.97	+0.27	A0
16	11.87	...	F0V	66	12.38	...	G0:	116*	8.82	-0.15	B9
17	11.87	...	F8III	67 R	10.46	...	B2k	117 R	10.63	+0.12	B0k
18*	7.14	...	B9	68	11.43	...	A0	118	12.51	...	K2III
19	12.09	...	B9	69	12.63	...	A2	119	12.25	...	F0
20*	7.95	...	K2III	70	13.21	...	B8	120 R	11.40	-0.06	B5k
21	12.52	...	B9	71 R	10.11	...	B9	121	12.22	...	G0:
22	11.81	...	A2	72	11.74	...	G5III	122	12.52	...	F0
23	12.60	...	G0:	73	12.16	...	B8	123	12.60	...	G0
24	12.76	...	A2	74	12.51	...	F8III	124*	10.62	...	G5III
25	11.91	...	B9	75	12.18	...	G5III:	125	12.38	...	G0V

Table 1

Observational Data for Region LF4 (Cont'd.)

Zone +55° (Cont'd.)

No.	m_{pg}	R.I.	Sp.	No.	m_{pg}	R.I.	Sp.	No.	m_{pg}	R.I.	Sp.
126	12.88	+0.27	B9:	176	12.59	+0.21	B5:	226	12.71	...	A0
127	11.87	...	F2V	177	12.94	+0.17	B2	227	12.34	+0.10	A3
128	12.23	+0.21	A0	178	12.92	+0.16	B8	228*	9.89	...	G8IV
129	12.95	+0.18	A0	179	12.21	...	G0	229 R	9.73	-0.07	A2p
130*	9.58	...	G0V	180	12.43	...	G5	230	11.98	...	K0III
131	11.63	-0.11	B9	181	11.25	-0.23	B5	231	11.95	...	G5V
132*	10.53	...	F2V:	182	11.75	...	M0III	232	12.91	+0.23	B9
133	10.44	-0.38	B8	183	11.91	+0.03	B5	233	11.91	...	G5V
134	12.60	...	G0:	184	11.60	-0.08	B8	234	12.78	+0.20	A0
135	13.35:	...	G8	185	12.30	-0.06	B3	235	12.41	...	G2V
136*	10.98	...	K0III	186 R	10.81	+0.41	O8	236	12.63	...	G5III
137	12.76	+0.15	A0:	187	12.83	+0.19	B8	237	10.94	...	B8
138 R	11.96:	+0.11	B3k	188*	9.57	...	A0	238	12.19	-0.01	A0
139	12.61	+0.15	A2	189	12.41	...	F8	239	12.33	+0.05	B9
140	12.81	+0.13	B8:	190	12.65	+0.15	B9	240	12.38	+0.27	B9
141	12.59	+0.07	A3	191*	7.93	-0.57	B9	241	12.81	...	G5III
142	11.50	+0.04	A0	192	12.68	...	G2:	242	10.77	...	G0III
143	12.60	...	G0:	193	12.72	+0.31	B0	243	12.24	+0.12	B9
144	12.24	...	G0	194	12.67	...	G5:	244	13.15	...	M5III
145	11.06	+0.06	B3	195*	8.65	-0.03	A3	245	11.01	+0.06	A3
146*R	9.71	...	B0k	196	12.73	+0.55	G5:	246	12.89	-0.08	B0:
147	12.67	...	F2	197*R	10.25	-0.07	A0	247*	8.93	...	F0IV
148	11.47	...	G2V	198	10.02	-0.25	B8	248	12.56	+0.53	A3
149	12.42	-0.02	B5	199	10.39	-0.15	B9	249	10.77	-0.26	B2:
150	13.18	...	B9	200	12.05	-0.09	B3	250 R	11.60	+0.18	A3
151	12.50	...	G0	201	11.12	...	F5V	251	13.16	+0.18	B5
152	11.70	+0.28	A0	202*	8.90	...	G2V	252	12.60	...	G0V
153	12.84	+0.01	B8	203	11.42	+0.04	A0	253	12.10	...	G0
154	12.65	+0.05	A0	204	11.92	+0.36	B0:	254	10.53	-0.05	B8
155	11.07	...	K0IV	205*	9.62	...	F8V	255	10.89	...	F0V
156	11.91	...	K0:	206	10.68	-0.02	A0	256	12.84	+0.26	B5
157	11.95	+0.05	A5	207	12.63	+0.36	A0:	257*	11.41	...	K0III
158	12.27	...	B5	208	12.41	...	G0	258	12.48	...	G8III
159	12.81	+0.05	B9	209	11.19	+0.02	B9	259	11.76	+0.29	A3
160	11.74	+0.04	B9	210*	7.49	-0.07	B8	260	12.46	...	G8
161	11.83	-0.08	B9	211*R	9.94	-0.26	B8	261	11.96	-0.04	B9
162	12.87	+0.19	B2:	212*R	9.40	-0.27	B2k	262	12.54	+0.10	B8:
163*R	10.45	-0.21	B3p:	213	11.91	...	G0V	263	12.63	...	K0:
164	13.17	+0.22	B9	214	12.25	+0.01	B8	264	12.70	+0.42	A2
165	12.70	+0.46	A2	215	10.80	+0.04	A0	265*R	10.57	-0.07	B9
166	11.91	...	G5III	216	12.07	...	F0V	266	12.71	...	K0:
167	12.81	...	G0:	217	11.46	+0.20	A0	267	11.93	...	G2V
168	11.95	...	F0V	218	12.55	...	K0V	268*	9.00	-0.40	B9
169	12.96	+0.25	A0	219	12.13	...	G0V	269	10.68	-0.02	A0
170	12.47	+0.36	B0:	220	12.53	-0.18	A3	270	11.85	+0.07	A2
171	11.91	+0.11	B9	221	12.18	...	K5III	271	12.82	...	G5
172	10.98	...	G0III	222	12.52	...	F0	272	12.20	-0.02	A0
173	10.69	-0.16	B8	223	12.04	...	G0V	273	12.61	+0.05	A:
174	12.71	+0.21	A0	224*	10.07	-0.05	A0	274	12.98	+0.43	A0
175	10.71	...	F0III	225	11.87	...	G5III	275	12.56	...	G2

Table 1

Observational Data for Region LF4 (Cont'd.)

Zone +55° (Cont'd.)

No.	m_{pg}	R.I.	Sp.	No.	m_{pg}	R.I.	Sp.	No.	m_{pg}	R.I.	Sp.
276	12.28	-0.12	B0	326	12.35	...	K0III	376*	9.25	-0.21	A2
277	12.34	...	G0V	327	12.09	+0.20	B3:	377	12.69	+0.24	B5:
278	12.13	+0.13	A0	328	12.63	...	K0III	378	12.40	+0.22	A0
279	11.58	+0.34	A5	329	11.55	...	F0III	379	12.44	+0.06	B5
280	12.40	+0.13	A0	330	12.54	...	F0III	380	13.03	+0.33	A2:
281	12.45	+0.10	B5	331	11.38	+0.13	A0	381	11.99	...	F5:
282	12.52	...	G0	332	11.72	+0.18	B9	382	12.44	...	G5III
283	12.22	+0.24	B2	333	10.59	...	B8	383	12.70	+0.19	A0
284*	10.29	...	G0V	334*R	9.47	-0.17	B2	384	12.61	+0.08	B9
285	11.36	+0.02	A0	335	12.39	+0.28	A5:	385	12.72	+0.08	B9
286	12.67	...	G8	336*R	10.02	-0.35	B8	386	10.84	-0.06	B8
287	12.17	+0.17	B8	337	12.53	...	K3III	387	12.28	...	F2V
288	11.97	+0.27	A3	338	12.54	+0.17	B8	388	12.52	...	K0III
289 R	10.36	-0.10	B0	339	12.82	+0.56	A0	389	12.88	+0.17	B8
290*	9.44	-0.12	B9	340	12.21	+0.29	A2	390	12.44	...	K2III
291	12.22	-0.02	B3	341	12.64	...	B9	391	12.48	+0.48	A2-F0
292	11.16	...	G8III	342	12.71	...	K0	392	12.96	+0.47	A2:
293 R	10.21	-0.05	B0	343	12.52	...	G0	393	12.15	+0.01	B9
294	11.55	-0.13	B8	344	11.69	-0.08	B2	394*	8.98	+0.40	G2V
295	11.91	...	K3V	345	12.80	+0.06	B8	395	12.01	...	G8III
296	12.46	...	G0	346	11.90	...	K0III	396	12.46	...	G8V
297	12.62	-0.10	B3	347	13.14	+0.52	A3	397 R	10.95	-0.07	B5
298	12.81	+0.25	B5	348	11.54	-0.11	B9	398	12.68	...	G0:
299*R	(7.75v)	...	M01a	349	11.91	...	G0	399	12.28	...	K3III
300	12.79	+0.23	A2	350*R	10.21	...	O8	400	11.63	...	K5III
301	12.60	...	G0:	351	11.75	+0.05	B8	401*R	9.64	0.00	B3
302	13.03	+0.29	B5k	352	11.73	+0.10	A0	402	12.69	+0.15	B8
303 R	10.81	+0.07	B5k	353*	10.21	...	F0V	403	12.11	+0.20	B9
304	11.71	+0.11	A2	354	12.85	+0.29	A0:	404	12.91	+0.32	B8
305 R	10.49	...	O8	355	12.67	...	K2III	405	11.95	...	K0III
306	10.12	...	F0V	356*	9.30	-0.26	B8	406	12.22	+0.04	B9
307	11.73	...	G2V	357	12.18	+0.04	A0	407	12.48	...	G2
308	13.73	...	G0V:	358	11.83	...	B8	408	12.14	+0.06	B5
309	12.50	+0.16	B8	359*	11.64	...	G5III	409	12.67	...	G5V
310	12.76	+0.26	A3	360*	10.17	...	G5III	410	12.56	...	K3
311	11.63	+0.10	B8	361	12.41	...	G8III	411	12.63	...	G0
312*R	10.45	-0.05	B9	362 R	10.98	-0.09	B3k	412	12.26	...	A0:
313	11.93	-0.07	B8	363*R	10.00	-0.26	B8	413	11.36	+0.40	A5
314	12.41	+0.05	A0	364	11.67	+0.11	A0	414	12.86	...	K0III
315	12.59	+0.11	A0	365	12.46	...	F2	415	12.48	...	F8
316	11.15	-0.23	B5	366	10.72	-0.04	B8	416	12.58	-0.05	B2:
317	12.46	...	F0III	367	12.81	+0.23	B5	417	12.87	+0.32	B0:
318*	10.23	-0.22	B8	368	12.56	-0.02	B3:	418	12.71	+0.26	B8
319	12.08	...	G0	369	12.54	+0.18	B0:	419	12.98	+0.62	A2-F0
320	11.37	+0.07	A2	370	12.70	+0.48	A0	420	12.36	+0.08	B9
321*	11.19	+0.15	A3	371	11.55	...	G5V	421 R	10.98	0.00	B2
322*R	10.08	...	O8	372	12.44	-0.04	B5	422	12.44	...	K0V
323*	10.48	-0.03	A2	373	12.68	+0.48	A2	423	12.73	...	K0III
324	11.02	...	G0V	374	12.17	...	G0	424*	11.04	...	B2
325	12.86	...	G8	375	12.40	+0.13	A0	425	12.56	...	G2

Table 1

Observational Data for Region LF4 (Cont'd.)

Zone + 55° (Cont'd.)

No.	m_{pg}	R.I.	Sp.	No.	m_{pg}	R.I.	Sp.	No.	m_{pg}	R.I.	Sp.
426*	9.61	...	F8V	476	11.18	...	G8III	526	11.72	...	G2IV
427	13.30	+0.40	B9	477	12.41	+0.13	B9	527*	8.84	...	B5
428	12.34	...	G0	478	12.50	+0.47	B9	528	11.74	+0.12	B9
429	11.99	...	G8III	479 R	11.29	-0.01	B8	529	13.04	...	K3
430 R	11.02	+0.04	B9	480	11.17	+0.12	B8	530	12.62	...	K0
431	11.31	-0.01	B5k	481	12.74	...	G8III	531	11.22	+0.23	A2
432	12.50	...	G0	482	12.47	+0.31	B9	532	11.35	+0.13	B9:
433	12.25	+0.21	A0	483	11.94	+0.34	A3	533*	9.10	-0.08	B8
434	11.92	+0.14	B9	484	11.92	+0.32	A5	534	12.46	...	F0III
435	12.91	...	G5III	485	12.67	...	G0	535	12.90	...	A5
436	12.62	+0.34	B8	486	12.27	+0.49	A0	536	13.21	...	A2
437	12.12	+0.52	A3	487	12.12	...	F0V	537	11.47	...	A3-F0
438	12.94	+0.13	B9	488	12.48	...	K3III	538	12.96	...	F0
439	11.92	+0.28	A0	489	12.23	...	G5V	539	13.12	...	K0
440	10.76	-0.02	B8	490	12.43	...	G5III	540	11.46	...	B5
441 R	10.90	...	B0	491	10.99	+0.24	B9	541	12.33	...	B5
442	11.87	...	G5IV	492*R	11.22	+0.04	B0k	542*	10.78	...	F0V
443*R	9.87	+0.07	A0	493	11.37	+0.15	B8	543	12.62	...	A0
444	12.68	+0.39	B5	494	11.39	+0.32	B0	544	12.45	...	F0
445	12.09	+0.25	B5	495	12.68	...	G2	545	12.46	...	F0V
446	12.21	+0.13	B9	496	13.12	+0.45	A5	546	12.68	...	A3:
447	12.35	+0.15	B5	497	12.51	+0.56	B8	547	12.60	...	A3
448	12.28	+0.28	B9	498	11.79	+0.24	B0k	548	12.58	...	A2
449*	10.98	...	K2III	499	12.34	-0.02	B0:	549	12.01	...	G8III
450	12.24	+0.36	A0	500	12.42	...	G0V	550	11.36	...	B9
451*	10.00	-0.14	B9	501 R	11.51	+0.15	B5	551	12.81	...	A2
452	11.69	...	F0V	502	12.53	+0.33	A3	552	12.37	...	M8III
453*	10.74	+0.19	A5	503	12.64	...	G8III:	553	12.01	...	G5III
454	12.82	...	K0	504	12.93	+0.49	A0	554	11.38	...	A2
455	12.87	+0.59	A2	505	12.46	...	G8III	555	12.63	...	A0
456	13.01	...	K0	506	12.61	+0.55	A5	556	12.59	...	G8III
457	12.67	...	G0:	507	12.52	...	K0III	557	12.72	...	F0
458	11.19	-0.01	B8	508	11.80	+0.08	B8	558*	10.18	...	F8V
459	12.98	+0.30	B8	509	12.12	+0.35	B8	559	11.64	...	A0
460	12.81	...	B5	510	12.71	...	G8:	560	11.59	...	G0V
461	12.63	+0.08	B9	511	12.22	+0.11	B5	561	11.99	...	B8
462*	11.25	...	G5V	512	11.46	+0.06	B8	562	12.63	...	B8
463	11.81	+0.05	B5	513*	10.69	-0.49	A2	563	12.99	...	K2
464	12.84	+0.10	B8	514	13.32	+0.38	B9	564	12.43	...	A2
465	12.69	...	G0	515	10.85	...	B9	565	12.50	...	G0:
466*	9.24	...	F0III	516	12.59	...	K0:	566	12.25	...	G0
467	12.60	+0.68	B5:	517	12.78	+0.50	A0	567	11.74	...	A3-F2
468	11.89	+0.29	A2	518*	10.32	+0.23	B0k	568	11.64	...	F5V
469	11.41	...	G0V	519	12.59	...	G0V	569	12.59	...	G5III
470	11.93	+0.29	A0	520	12.72	...	G2V	570	11.67	...	B8
471*R	11.02	...	O5	521	12.46	...	G0	571	12.62	...	F2V
472	12.46	...	G2V	522	12.34	+0.24	A0	572	13.13	...	B8
473	11.02	...	K0III	523	11.75	+0.10	B8	573*	10.04	...	F0V
474	12.35	+0.46	A2	524	13.06	+0.37	A2	574	11.76	...	B9
475	12.71	...	G8III	525	12.37	...	K2III	575	11.14	...	B8

Table 1

Observational Data for Region LF4 (Cont'd.)

Zone +55° (Cont'd.)

No.	m_{pg}	R.I.	Sp.	No.	m_{pg}	R.I.	Sp.	No.	m_{pg}	R.I.	Sp.
576	12.09	...	B8	586	13.21	...	B9	596	12.92	...	B8
577	12.37	...	A5	587	11.78	...	K2III	597	11.98	...	A5
578	12.72	...	A2:	588	12.82	...	G5III	598	12.72	...	A0
579*R	10.29	...	B8	589	12.76	...	B2:	599*	10.01	...	B8
580*R	10.57	...	B9	590	12.50	...	A3	600	12.46	...	G0:
581	12.50	...	G5III	591	12.50	...	F0V	601	12.59	...	B8
582	11.65	...	K0III	592	12.50	...	B5	602	12.86	...	B8
583*	10.08	...	B8	593	11.83	...	G5III	603*	10.32	...	A2
584	11.87	...	B9	594	12.91	...	B8	604	12.86	...	A2
585	12.52	...	A2	595	10.88	...	B5				

Remarks Concerning Spectra in Table 1

Zone +51°

No.

52 Spectral type is for the close pair. BD +51°3322
94 Interstellar K suspected. BD +51°3337
110 Interstellar K suspected.
171 λ4128 strong. BD +51°3356
230 Hydrogen lines have sharp cores and broad wings. BD +51°3368
231 Trace of interstellar λ4430. BD +51°3369
242 Hydrogen lines sharp; suspect presence of λ3820 but other He lines are absent. BD +51°3371
263 Class OB star? Hydrogen lines very sharp; λ4233 present.
274 Metallic lines prominent; hydrogen lines sharp. BD +51°3377
298 K line weak for class G; UV has characteristics of an A star. BD +51°3381
319 Spectrum of the pair is given.

These stars in Zone +51° have hydrogen lines sharper than usual: 133, 195, 220 (BD +51°3364), 312, 342.

Zone +52°

37 Spectral class is for the brighter of an unresolved pair. BD +52°3137
49 Class OB star.
77 Possibly variable spectrum A0 to F0.
98 Possibly class OB star; λ3820 present. BD +51°3297
266 Possibly metallic line A star; λ4174 very conspicuous.
312 λ4077 and λ4174 present; no G band.
345 Close double; spectra not separable.
447 Hydrogen lines have very sharp cores.
555 Possibly variable spectrum A2 to F0; metallic lines appear on some plates.
702 Surrounding No. 702 is a cluster of 12th mag. B5, B8 stars.
764 Trace of metallic lines; prominent line at λ4010.
765 λ3820 unusually strong.
849 Strong λ3860; hydrogen lines sharp.
914 Variable RZ Lacertae. BD +51°3420

These stars in Zone +52° have hydrogen lines sharper than usual: 288 (BD +51°3319), 311, 313, 407, 432, 477, 594, 674, 689 (BD +51°3380), 714 (BD +52°3215), 733, 759, 820, 831, 841 (BD +52°3238).

Zone +53°

70 Interstellar K suspected; λ4430 (interstellar) present; class Bi star. BD +52°3129
91 Overlap makes spectrum peculiar; on 2° prism plate the companion appears to be of type about M0.
135 Class OB star; hydrogen lines very sharp. BD +52°3135
152 λ4033 strong.
195 Spectrum of brighter star given. BD +53°2816
207 May possibly be A0I; overlap gives spurious lines. BD +52°3147
230 Class OB star probably; overlap makes classification uncertain. BD +53°2823
233 Class OB star probably; overlap makes classification uncertain. BD +52°3153
293 Class Bi star probably; overlap makes classification uncertain.
301 Class OB star. BD +53°2833
337 Class OB star. BD +52°3167
340 Class OB star. BD +53°2837
461 Strong lines at λ4400 and 4310. Hydrogen lines sharp. Metallic lines present. Color high for A0. BD +53°2849
497 Spectrum possibly variable, B5 to A3.
654 Spectrum possibly variable; A2 to F0.
677 Class OB star. BD +53°2877
693 λ4174 unusually strong.
711 Class OB or Bi star. BD +52°3210
717 Class OB star. BD +53°2885
801 Class Bi star. BD +52°3224
847 Prominent lines at λ3870 and λ4050.
877 λ4226 unusually strong.
906 Hydrogen lines in UV strong; H and K weak; possible G0Ib
1044 λ4033 prominent. BD +53°2941

These stars in Zone +53° have hydrogen lines sharper than usual; 37, 158, 223, 270, 271 (BD +53°2828), 285, 349 (BD +52°3170), 370, 379, 381, 399 (BD +52°3176), 408 (BD +52°3178), 415, 448, 470 (BD +53°2850), 579, 595, 729, 768, 787 (BD +53°2894), 793, 809, 879 (BD +53°2909), 909, 961, 980, 985 (BD +53°2927), 1019.

Remarks Concerning Spectra in Table 1 (Cont'd.)

Zone +54°

No.

21 λ4226 prominent for class A0.
41 λ4226 unusually strong. BD +54° 2696
79 Close double; spectral class of brighter component given. BD +53° 2806
127 Hγ and Hδ unusually sharp.
131 Spectral type appears to vary from F0 to F8.
139 Trace of interstellar K and λ4430. BD +54° 2705
191 Class OB star; λ4686 prominent.
219 Possibly class 0B star; some metallic lines present; hydrogen lines sharp.
246 Class OB star; λ4033 prominent; hydrogen lines very sharp.
278 2' southeast of No. 278 is a very faint N or R star.
281 Very close pair; spectral class of brighter component given.
307 Suspect interstellar K and λ4430.
323 Class OB star. BD +53° 2838
330 Cluster of A stars in this area.
357 Hydrogen lines sharp; λ4033 very strong.
369 AW Lacertae (?); overlap makes spectral class uncertain.
402 Class OB star; strong λ3860. BD +53° 2843
493 λ4033 prominent. BD +53° 2854
507 λ4226 very strong.
549 Class OB star. BD +54° 2751
572 Class OB star; interstellar K and λ4430 present. BD +54° 2756
602 Class OB star; interstellar λ4430 present. BD +54° 2758
605 λ4128 prominent; hydrogen lines sharp; possibly OB star. BD +53° 2867
606 λ4026 weak and λ4471 strong for class B3.
708 λ4033 very strong.
793 λ4033 present; metallic lines present.
837 Class OB star. BD +54° 2790
850 TW Lacertae.
881 Class OB (?) interstellar λ4430 present; K line appears too strong for interstellar.
1007 Hydrogen lines very broad.
1088 Hydrogen lines very broad.
1112 Peculiarity possibly due to overlap. BD +54° 2823
1146 G band very strong; UV too strong for class F. BD +53° 2945

These stars in Zone +54° have hydrogen lines sharper than usual for their class: 24, 33, 42, 57, 145, 161 (BD +54° 2706), 173 (BD +53° 2819), 182 (BD +54° 2711), 222, 233, 251, 354, 415, 657 (BD +53° 2870), 725 (BD +53° 2884), 735, 763, 831, 897, 973 (BD +54° 2803), 977, 1005 (BD +53° 2920), 1077, 1100 (BD +54° 2821).

Zone +55°

40 Hydrogen lines very weak; interstellar λ4430 and K suspected; spectrum strong in the ultraviolet.
47 Class Bi star. BD +54° 2718
67 Class OB star; λ4686 prominent; λ4430 (interstellar) suspected.
82 λ4143 unusually strong; marked blend at λ4240; interstellar K and λ4430 present.
83 Nova Lacertae 1936.
84 Class OB star. BD +54° 2726
98 Predominantly A2 but metallic lines and trace of G band are present.
111 Trace of λ4174, G band, λ4226.
117 Class OB star.
120 Interstellar λ4430 present.
138 Interstellar λ4430 present.
146 Class Bi star; interstellar λ4430 present. BD +55° 2722
163 Hydrogen lines very sharp; metallic lines present; class Bi. BD +54° 2737
186 Class OB star.
212 Class Bi star. BD +54° 2745
229 Metallic line A star; hydrogen lines sharp; λ4226 prominent.
250 λ4033 prominent; trace of G band.
289 Class OB star.
293 Class OB star.
299 RW Cephei. BD +55° 2737
303 Hydrogen lines very sharp; interstellar λ4430 present.
305 Class OB star.
322 Class OB star. BD +54° 2761

Remarks Concerning Spectra in Table 1 (Cont'd.)

Zone +55° (Cont'd.)

No.

334 Class OB star. BD +54° 2764
350 Class OB star. BD +54° 2766
362 λ4430 (interstellar) suspected.
397 Interstellar K suspected.
401 Class OB star. BD +54° 2775
421 Possibly class OB; trace of λ4686 (?).
471 Strong continuum but all lines very weak. BD +55° 2754
492 There is a cluster of early B stars near No. 492. BD +54° 2789
501 Interstellar K suspected.

These stars in Zone +55° have hydrogen lines sharper than usual for their class: 6, 71, 114, 197, (BD +54° 2743), 211 (BD +54° 2744), 265 (BD +55° 2734), 312 (BD +54° 2759), 336 (BD +55° 2742), 363 (BD +55° 2745), 430, 443 (BD +54° 2782), 479, 579,(BD +54° 2807), 580 (BD +54° 2808).

STELLAR SPECTRA AND COLORS IN A MILKY WAY REGION IN CASSIOPEIA

ALICE H. FARNSWORTH

John Payson Williston Observatory, Mount Holyoke College, South Hadley, Massachusetts

Received March 25, 1955

ABSTRACT

Spectral types, photographic magnitudes, and blue-red color indices are given for a thousand stars brighter than 12.4 mag. within a circular field 11.3 square degrees in area, centered at R.A. = 1^h40^m, Dec. = $+60°.2$ (1945). Table 1 lists the data, and identification charts appear in Figure 1*a*–Figure 1*d*. Table 3 gives photoelectric magnitudes of a sequence of twenty-five stars used as a basis for the determinations of magnitude.

The region here catalogued is designated LF5 in the series of regions along the Milky Way under study at the Warner and Swasey Observatory of the Case Institute of Technology on plates taken with the Schmidt-type 24–36-inch telescope (McCuskey and Seyfert 1947). The field is circular and covers 11.3 square degrees, centered at R.A. 1^h40^m, Dec. $+60°.2$; $l = 97°$, $b = -1°$ (1945). All stars for which it was possible to determine the spectral type are included. Stars omitted had overlapping or dense spectra impossible to evaluate. Many of the former occur in the five open clusters found in the field. The faint limit is approximately 12.4 mag. photographic.

The photometric measures were made with a graduated scale of images. Photoelectric magnitudes (listed in Table 3) of a sequence of standard stars, obtained as described in a paper (Farnsworth and McCuskey 1955) which deals with the analysis of LF5, served as the basis for the catalogue magnitudes. Each photographic magnitude given is the average obtained from measures on four Kodak II*a*-O plates with exposures of 30 seconds, taken in pairs. Each pair includes one plate taken with the telescope east, the other with the telescope west, of the piers. The red magnitudes used for finding the listed red color indices depend on 60-second exposures made on two pairs of Kodak 103*a*-E plates used with Wratten No. 22 filter. The average probable error for both a blue and a red magnitude rounds off at ± 0.04 mag., with the agreement of the red magnitudes systematically better.

Spectral types and luminosities were estimated by Dr. J. J. Nassau and the writer on objective-prism plates chiefly of 4° dispersion, using the criteria of Nassau and van Albada (1947). The luminosity classes are designated according to the system of Morgan, Keenan, and Kellman (1943). The class OB indicates early-type stars of high luminosity, as in the work of Nassau and Morgan (1951).

DESCRIPTION OF THE TABLES AND CHARTS

In Table 1, the catalogue, the first column gives the serial number of the star as it appears on the charts of Figure 1*a*–Figure 1*d*. The bright star just west of the field is δ Cassiopeiae. The charts are printed north up, in four sections according to the key given as an inset on Figure 1*a*. The numbers are approximately in order of right ascension in 1° zones of declination, as indicated for 1950 on the charts. An asterisk marks each BD star, and the letter "R" denotes a remark following the table.

The remaining three columns of Table 1 give, respectively, the photographic magnitude, the blue-red color index, and the spectral type with (where possible) the luminosity class of the star. The latter "m" following the spectral class designates an A-type star

which shows the G band. The letter "p" indicates the occurrence of features not normal for a star of its class.

Table 2 gives equivalent designations of stars in Table 1 and the *BD* catalogue.

Table 3 lists photoelectric magnitudes (blue and red) for the sequence of stars used as a basis for the catalogue magnitudes. Designations for the two brightest stars are *BD* numbers; for the three faintest stars, letters as shown in Figures 1*a*, 1*b*, and 1*d* near the center; and for the rest, the catalogue numbers of Table 1.

A comparison of spectral types with those listed in the *Henry Draper Catalogue* is possible for 68 stars and is shown graphically in the lower part of Figure 2. Two discrepant cases are 61°53, listed here as B3, and 61°107, an F2 supergiant. A plot of 43 stars in common with the *Henry Draper Extension* appears in the upper part of Figure 2.

Grateful acknowledgment is made to Dr. J. J. Nassau for his help in numerous consultations at the Warner and Swasey Observatory and for the opportunity to work on the Schmidt plates taken there. This investigation has been carried out with the assistance of a contract made with Mount Holyoke College by the Office of Naval Research, and of a grant to the college from the National Science Foundation.

REFERENCES

Farnsworth, A. H., and McCuskey, S. W. 1955, *Ap. J.*, **121**, 643.
McCuskey, S. W., and Seyfert, C. K. 1947, *Ap. J.*, **106**, 1.
Morgan, W. W., Keenan, P., and Kellman, E. 1943, *An Atlas of Stellar Spectra* (Chicago: University of Chicago Press).
Nassau, J. J., and van Albada, G. B. 1947, *Ap. J.*, **106**, 20.
Nassau, J. J., and Morgan, W. W. 1951, *Pub. U. Michigan Obs.*, **10**, 43.

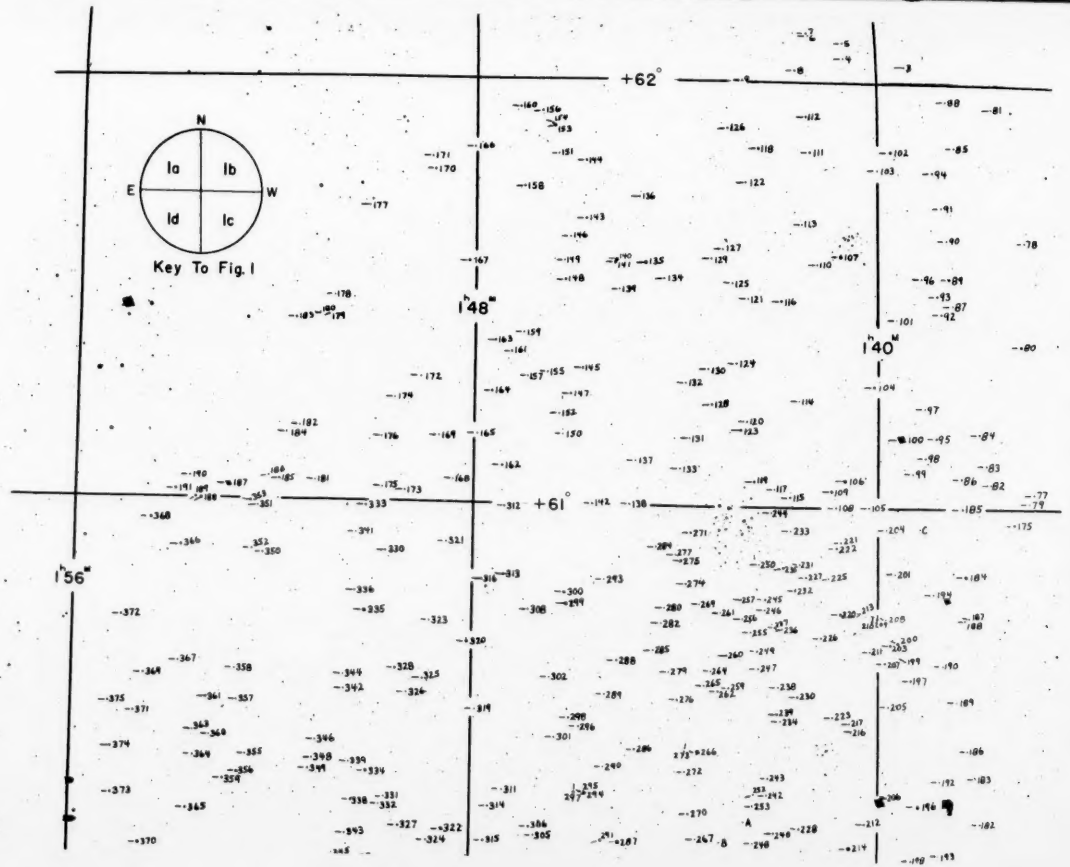

FIG. 1*a*.—Identification chart for LF5

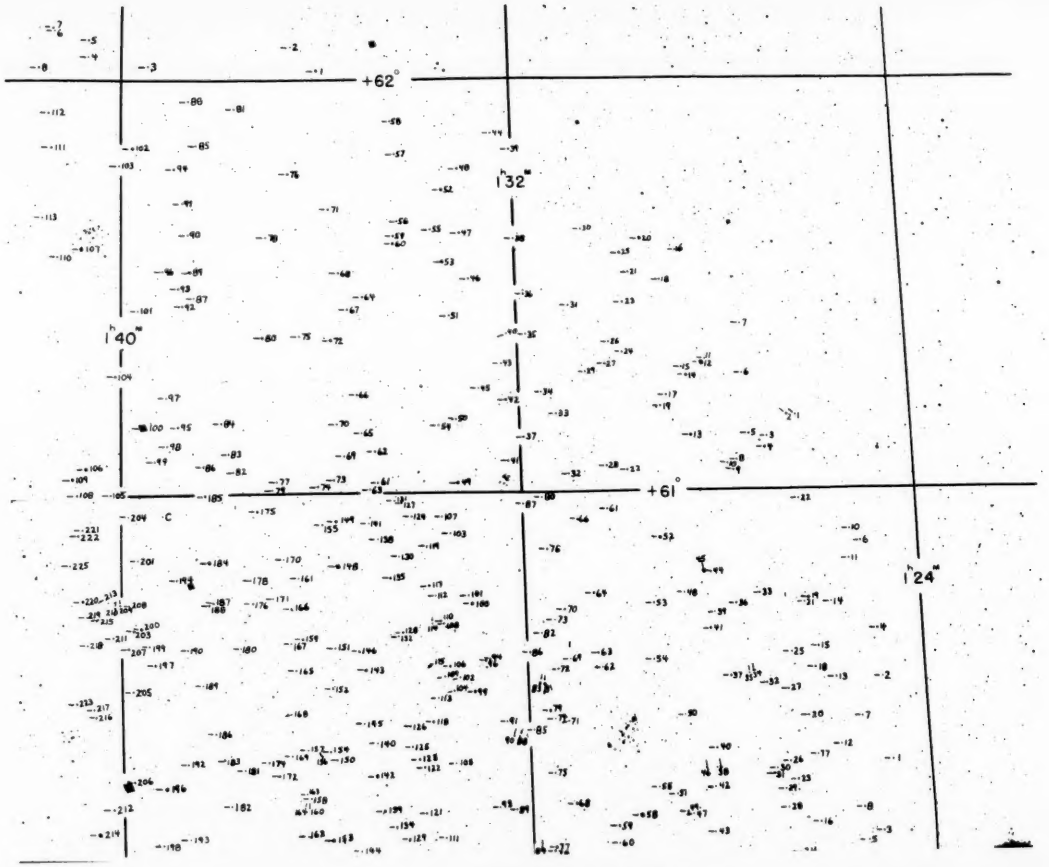

FIG. 1*b*.—Identification chart for LF5

FIG. 1*b*.—Identification chart for LF5

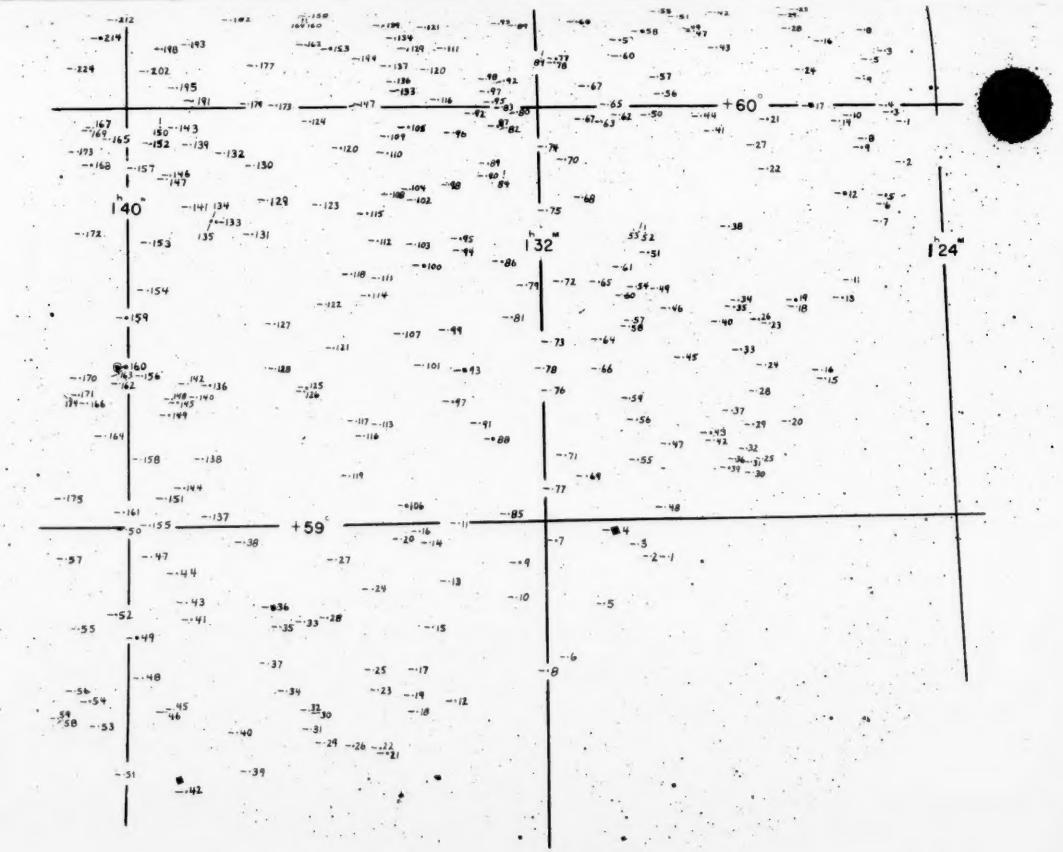

FIG. 1*c*.—Identification chart for LF5

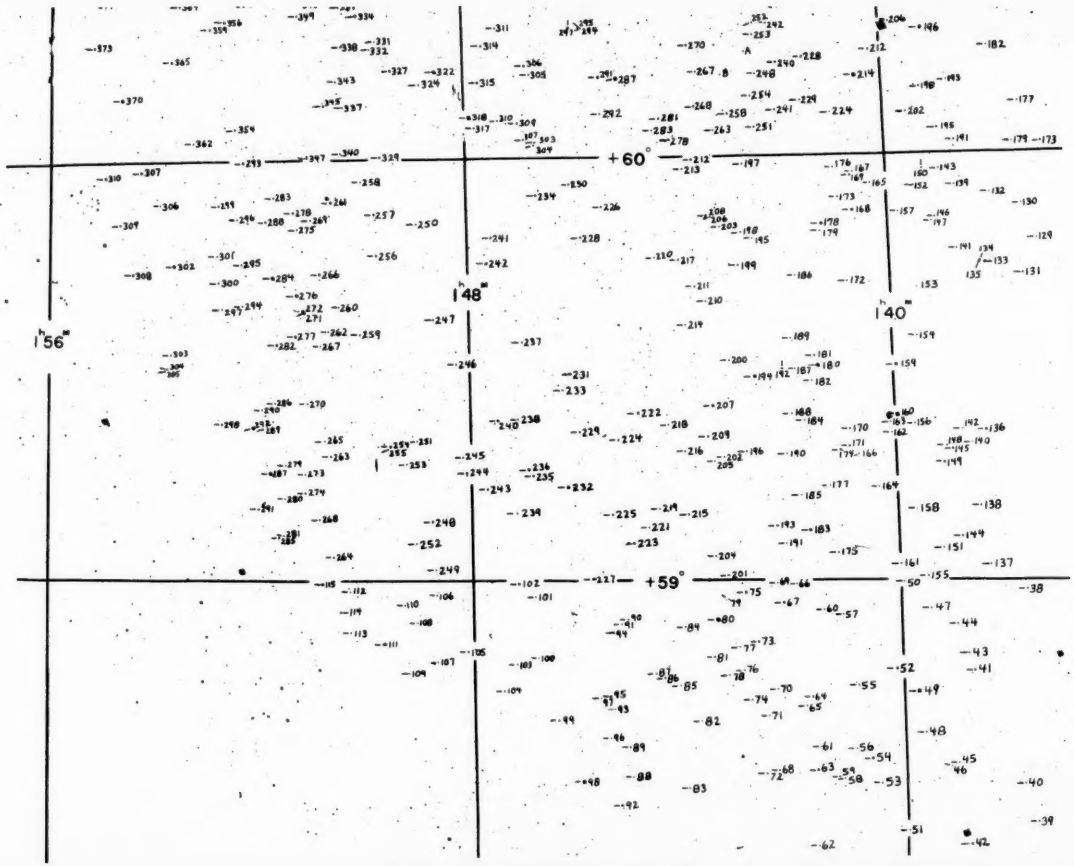

FIG. 1*d*.—Identification chart for LF5

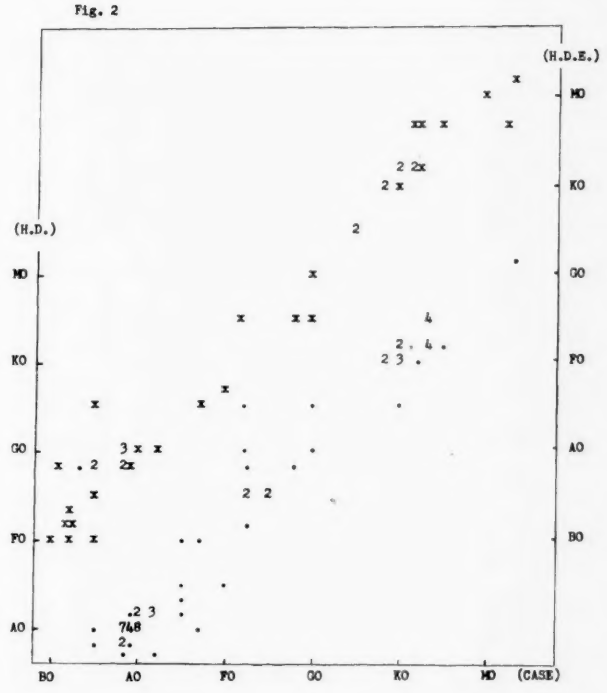

FIG. 2.—Comparison of Case spectral classes (*horizontal scale*) with the *HD* system (*circles, vertical scale at left*) and with the *HDE* (*crosses, scale at right*). Numerals indicate number of cases falling at same point on the plot; symbols represent single cases.

Table 1

Observational Data for Region LF5

Zone + 58°

No.	m_{pg}	R.I.	Sp.
1	12.01	+0.93	F8
2	12.32	+1.71	G8
3	12.28	+0.88	G0V
4*R	5.6	+1.4	K0III
5*	11.30	+1.80	G8III
6	12.47	+0.85	B8
7*	9.78	+0.22	A0
8	12.12	+1.00	A5m
9*	9.15	+0.05	B8
10	11.87	+0.75	B5
11	11.68	+0.49	A2
12	11.96	+0.43	B8
13	12.34	+0.71	F8
14	11.72	+0.88	G0
15	12.07	+0.87	G5
16	11.53	+0.80	G0
17	11.42	+0.65	F5V
18	12.16	+0.51	A2
19	11.71	+0.95	G0
20	12.38	+0.63	B8
21*	9.56	+0.37	F0III
22*	10.30	+0.16	B5
23	11.84	+0.36	A0
24	11.56	+0.38	B9
25	12.35	+0.63	A0
26*R	10.80	+0.83	G0V
27	12.00	+0.78	F8
28*	10.74	+0.25	B5
29	11.96	+0.48	B8
30	10.94	+0.14	B5
31	11.98	+0.24	B5:
32	11.66	+1.08	G5
33	11.86	+0.48	A0
34	12.06	+0.40	B5
35	11.51	+1.50	K0III
36*	7.00	-0.20	B8
37	12.39	+0.65	F5
38	11.32	+0.60	F2
39	11.71	+0.53	F0
40	11.76	+0.19	A2
41*	10.50	+0.14	B5
42	11.62	+0.40	A0
43	11.58	+0.37	B9
44	11.85	+0.65	F0
45	12.32	+1.22	F8
46	12.45	+0.63	A2
47	12.11	+1.76	G5III
48	11.64	+0.58	A5m
49*	8.52	-0.13	B9
50	12.06	+0.85	F0
51	12.12	+0.40	A3
52*	10.29	+1.49	G8III
53	11.98	+0.69	F5
54*	10.01	+1.08	G5III
55	11.52	+0.77	F0V
56	12.18	+1.74	G5III
57*	12.24	+2.74	K3
58	12.16	+0.50	B8:
59*	11.48	+1.50	G2III
60	11.74	+0.55	F0
61 R	12.48	+0.79	A2
62	11.76	+0.72	G0
63*	9.78	+1.36	K0III
64	11.54	+0.74	F2
65	12.03	+0.83	G2
66	12.41	+0.43	A3
67*	10.04	+0.26	B3
68	11.58	+0.78	F8
69	12.32	+0.98	G2
70	12.40	+0.74	F0
71	12.34	+0.62	A0
72	11.42	+0.30	B9
73*	10.80	+0.56	F2V
74	12.12	+2.05	K0III
75*	9.74	+1.37	K2III
76	12.32	+0.58	A2
77	12.21	+0.73	A5
78	12.29	+0.77	A5
79	12.32	+0.54	A0
80*	7.94	+0.66	G0V
81	11.58	+0.78	F5
82	12.36	+0.59	A0
83	11.99	+0.37	B3
84	11.99	+0.80	A5
85	12.46	+0.60	A2
86*	11.45	+0.44	A0
87	11.68	+0.62	A5m
88	12.34	+0.62	A3
89	11.44	+0.21	B3
90	11.94	+0.78	F8
91	12.34	+1.63	G5
92*	10.26	+0.36	A2
93	12.28	+0.44	B5
94*	10.46	+1.88	K3III
95*	10.46	+0.45	A7m
96	12.37	+0.69	A3
97	12.35	+0.64	A0
98*	8.80	+0.16	A0
99	11.39	+0.31	B3
100	12.40	+0.48	B5
101	12.20	+0.39	B9
102*	10.51	+0.31	B2
103	12.06	+0.61	A3m
104	11.26	+1.49	G8V
105	11.02	+0.14	B2
106	12.07	+0.94	F2:
107	12.38	+0.92	G0:
108	12.06	+0.86	G0
109	12.25	+0.47	F:
110	11.68	+0.34	B3
111*	9.16	+0.12	A0
112	12.15	+0.35	B8
113	11.77	+0.35	A2
114	12.18	+0.44	B9
115*	9.48	+0.26	A2v

Zone + 59°

No.	m_{pg}	R.I.	Sp.
1	12.27	+0.60	B5
2	12.09	+0.71	F5
3*	10.54	+0.10	A2
4	11.30	+0.36	B5
5	10.97	+0.22	A2
6	12.10	+0.37	A3
7	12.38	+0.71	A5
8	12.24	+0.84	G0
9*	10.34	+1.22	G8III
10	11.98	+0.32	B5
11	12.55	+1.81	K2III
12*	7.85	+1.02	F2II
13*	10.03	+0.67	G0V
14	12.04	+0.94	G2
15*	10.85	+0.65	F5V
16	12.27	+0.54	B5
17*	7.22	-0.20	OB
18	12.17	+0.95	G :
19*	8.28	+1.96	K3III
20	11.59	+0.39	B8
21*	9.94	+0.18	B5
22 R	11.44	+0.30	B5
23	11.04	-0.02	B5
24	12.08	+1.05	G2:
25	12.41	+0.54	A5
26*	9.68	+0.04	B2
27	12.50	+0.48	B5
28	12.22	+1.20	G0
29*	10.57	+0.57	G0V
30	12.46	+0.51	A0
31	11.22	+0.64	G0V
32*	11.23	+0.75	G2V
33*	10.90	+0.64	G0V
34	11.88	+1.62	G5III
35*	10.06	+0.02	OB

Table 1

Observational Data for Region LF5 (Cont'd.)

Zone +59° (Con'd.)

No.	m_{pg}	R.I.	Sp.	No.	m_{pg}	R.I.	Sp.	No.	m_{pg}	R.I.	Sp.
36	12.19	+0.45	A3	86*	9.84	+0.22	B5	136*	9.70	+0.19	B2
37	11.32	+0.11	B8	87*	9.50	+2.03	K5III	137	11.60	+0.46	A2
38*	10.86	+2.44	K3III	88*	8.27	+0.57	F5III	138*R	10.82	+0.57	A5
39*	9.58	+0.04	B3	89	10.84	+0.09	B5	139	11.86	+0.61	B9
40	12.32	+0.81	A5	90	11.61	+0.16	A2	140	12.35	+0.46	B8
41	12.16	+0.79	F5	91	12.08	+0.92	F5	141	12.10	+0.42	A0
42	12.06	+0.30	A2	92	11.98	+0.28	B9	142	12.24	+0.37	B:
43*	9.34	-0.04	B8	93*	7.31	+0.09	F0III	143	11.55	+0.23	B9
44	11.29	-0.07	B3	94	12.42	+0.54	A0	144*	10.82	+0.29	B8
45	11.30	+0.08	B8	95*	9.64	+0.04	B0	145*	10.57	+0.14	B1
46	11.39	+0.20	B5	96	12.12	+2.18	G2	146	11.81	+0.35	B9
47	11.01	+0.19	B2	97*	9.62	+0.14	B5	147	12.29	+0.68	G2
48	12.17	+2.01	G8III	98	11.81	+0.29	A5	148	11.68	+0.78	F2V
49	12.14	+0.30	B5	99	11.84	+0.78	A7	149*	10.06	+0.31	B5
50 R	12.02	+0.22	B5:	100*	8.28	+0.00	B5	150	11.36	+0.10	B3
51*	10.02	-0.08	B8	101	12.06	+0.78	A5	151	11.66	+1.24	F2V
52	11.96	+0.81	F5	102	12.34	+0.51	A3	152	11.29	+0.03	B3
53*	11.50	+1.51	G5III	103	12.38	+0.73	F2	153	12.09	+0.58	B:
54	11.81	+0.09	B3	104	11.84	+0.22	B5	154	11.94	+0.86	F5
55	10.79	+0.47	B9	105*	9.48	-0.08	B9	155*	11.40	+2.25	K2III
56	10.97	+0.39	B3	106*	8.24	+0.27	A5	156	11.76	+0.19	Bp
57	12.26	+0.53	B9	107	11.58	+0.86	F2	157	12.16	+0.26	B8
58	11.60	+0.62	F0V	108	11.88	+0.58	A2	158	12.47	+0.78	F8
59	11.95	+0.80	G0	109	12.00	+1.10	F5:	159*	9.02	+0.00	B9
60	12.54	+0.86	G0	110*	10.81	+0.82	F2	160*	7.68	+1.52	K0III
61	12.30	+0.34	B3	111	12.19	+1.97	K0:III:	161	11.37	+0.71	F8V
62	12.24	+0.78	F0:	112	10.68	+0.31	B9	162	12.02	+0.68	B9
63*	10.65	+0.27	A2	113	11.86	+1.07	F5	163	11.74	+0.72	F
64*	10.48	+0.36	A7	114	11.13	+0.38	B0	164	12.22	+0.64	B8
65 R	11.41	+0.35	B8	115	11.80	+0.76	F8:	165 R	12.23	+0.48	B0:
66	12.48	1.78	K2:III:	116	11.79	+0.68	F8	166	11.98	+1.25	F8
67	12.12	0.23	B3	117	12.03	+1.81	G5	167	11.97	+1.11	G2:
68	11.53	0.35	A3	118	11.35	+0.26	B5	168*	9.90	+0.19	OB
69	10.88	0.76	F8V	119	11.58	+0.82	F8	169	10.68	+0.12	B8
70	10.79	0.05	B3	120	11.29	+0.73	F8V	170*	11.29	+1.69	G2:
71*	10.92	2.80	M3III	121	11.54	+0.79	F2V	171*	10.72	+1.02	G0
72	11.28	0.67	F8V	122	12.18	+0.82	B9	172	11.73	+0.64	A5
73	12.22	0.34	B3	123	12.13	+0.54	A3	173	11.76	+2.21	K0III
74	12.22	0.84	G2	124	11.08	+0.14	B5	174*	10.61	+0.19	B9
75	11.03	0.21	B5	125*	9.41	+0.80	G0V	175	11.52	+0.31	B5
76	12.36	0.75	A2	126	10.80	+0.12	B3	176	11.90	+0.61	A0
77	12.12	+0.92	A3	127	12.00	+0.65	A5	177	12.32	+0.75	A3
78	11.74	+0.90	F5	128	12.14	+0.77	F8	178*	9.23	+0.11	B8
79	11.48	+0.27	B5	129	12.16	+0.89	G0	179	12.14	+0.76	F5
80	11.56	+0.78	F2	130	12.12	+0.25	B5	180*	8.46	+0.16	A0
81*	10.44	+0.18	B9	131*	10.67	+0.27	B3	181	10.86	+0.75	F0p
82	11.49	+0.03	B5	132	12.10	+0.92	A3	182	12.16	+1.51	G0
83	12.38	+0.71	A2	133*	9.20	+0.18	B8	183*	9.27	-0.02	B8
84	11.94	+0.72	G0	134	11.66	+0.41	A	184	11.45	+0.40	OB
85	11.01	+0.35	A0	135*	10.00	+1.72	K0III	185	12.28	+0.56	A3

Table 1

Observational Data for Region LF5 (Cont'd.)

Zone +59° (Cont'd.)

No.	m_{pg}	R.I.	Sp.	No.	m_{pg}	R.I.	Sp.	No.	m_{pg}	R.I.	Sp.
186	12.24	+0.42	A0	236*	9.39	+1.23	G8III	286	12.52	+0.50	B8
187	12.46	+0.48	B9	237	12.00	+0.44	B5	287*	8.42	+0.20	A5m
188	11.68	+0.94	A3	238*	11.71	+1.97	K3III	288	11.05	+0.47	B8
189	12.30	+1.07	G0:	239	11.77	+0.33	B9	289	11.42	+0.60	B5:
190	12.08	+0.84	F5	240*R	10.16	+0.12	B9	290	12.02	+0.76	G0:
191	12.19	+0.53	B8	241*	11.13	+0.29	B2	291*	10.76	+0.39	A5
192*	11.62	+1.74	G5V	242*	10.86	+0.28	B2	292*	8.58	-0.13	B9
193*	10.52	+0.12	A0	243	11.00	+0.37	A2	293*	9.97	+0.16	B3
194*	8.70	+1.36	K0III	244*	10.45	+1.31	G8III	294	11.87	+0.28	B5
195	12.34	+0.39	A0	245	12.20	+0.84	G0	295	11.83	+0.49	A2
196	11.52	+0.34	B9	246	11.99	+0.38	A0	296	12.03	+0.35	B5
197	11.78	+0.69	F5V	247	11.56	+0.50	B5	297	12.20	+0.52	B9
198	11.94	+1.02	G5V	248*	10.98	+0.31	A0	298	11.02	+0.37	A3
199	11.48	+0.55	B5	249	12.05	+2.03	G8III	299	11.13	+0.17	B3
200	11.70	+0.26	B8	250	12.08	+0.65	B8	300	11.71	+1.06	G2
201	11.92	+0.24	B9	251	12.02	+0.62	F5	301	12.40	+1.99	G5:
202	11.97	+0.67	OB	252	11.46	+0.18	B8	302*	9.18	+0.32	B5
203	12.45	+1.93	K5:	253	12.03	+0.31	B9	303	11.53	+0.75	A2
204	11.64	+0.32	B0:	254*	10.15	+0.17	OB	304	11.08	+0.68	A5
205	12.28	+1.69	G0	255	12.03	+0.31	A5	305*	10.82	+1.56	K0III
206	12.14	+0.50	A0	256*	10.79	+0.37	B9	306	12.25	+0.61	B3
207*	9.58	+0.82	G5V	257*	10.41	+0.19	B8	307*	9.67	+2.71	K3III
208*	10.78	+1.70	G5III	258	12.52	+0.75	-	308	10.59	+0.53	A3Ib
209*	10.64	+0.11	B8	259	11.70	+0.58	A0:	309	11.04	+0.38	B5
210	12.02	+0.59	F8	260	12.16	+0.84	A2	310*	9.55	+0.06	B9
211	11.80	+0.64	A5	261*	9.75	+2.58	M3III				
212*	11.04	+0.43	B9	262	11.92	+0.42	B2				
213	11.84	+0.60	A3	263*	10.86	+1.46	K5V				
214	12.28	+0.96	F8	264*	11.08	+2.30	K5III				
215	10.96	+0.64	F2V	265	12.10	+0.27	A2				
216	11.56	+0.36	B8	266*	9.92	+0.88	A7m				
217	11.14	+0.28	A0	267	12.43	+0.45	A3				
218	12.33	+0.48	A2	268	11.50	+0.22	A2				
219	12.30	+1.12	K0:	269	11.90	+0.64	OB				
220 R	12.23	+0.69	A3:	270	12.12	+1.64	K0				
221	12.26	+0.36	B1	271	11.04	+0.30	A0:				
222*	9.79	+2.06	K2III	272*	8.62	+0.17	B8				
223*	10.55	+0.74	F8V	273	12.13	+0.71	F2				
224*	11.41	+2.43	M0III	274	11.10	+0.56	F8				
225	11.13	+0.99	G2V	275	12.01	+0.66	F5				
226	11.52	+0.30	B5	276*R	8.84	+0.46	F5III				
227	12.24	+0.87	G2	277*	9.68	+1.42	K0III				
228*	11.10	+0.82	G2III	278*	10.53	+2.49	K2III				
229	11.10	+0.62	F2	279	12.12	+0.37	B5				
230	11.84	+0.88	G0V	280	12.34	+0.37	B2:				
231*	10.24	+0.64	G0V	281*	11.48	+2.34	K3III				
232*	9.28	+0.12	B8	282*	10.14	+0.52	F2				
233	12.11	+2.53	K2	283	11.85	+0.46	B0				
234*	10.90	+0.24	B5	284*R	8.30	-0.02	B9				
235*	10.89	+0.36	A2	285	11.02	+0.57	A5				

Zone +60°

No.	m_{pg}	R.I.	Sp.
1 R	12.00	+0.78	G0
2	12.20	+0.77	G0
3	12.35	+1.61	G5III
4*	10.50	+0.40	A5
5	12.02	+0.76	F2
6	12.04	+0.32	B3
7	12.10	+0.82	G0
8	11.40	+0.40	A5
9	11.34	+0.41	B8
10 R	12.12	+0.56	A
11	12.02	+0.62	F5:
12	12.18	+0.25	B5:
13	11.82	+0.75	G2
14	12.12	+0.28	B1
15*	11.00	+0.77	A5
16	11.28	+0.60	F5
17	12.10	+0.24	B8
18*	11.02	+0.04	B8
19*R	9.6	+0.1	B3
20	12.05	+0.24	B5:
21	12.24	+0.90	F2:
22	11.71	+0.81	G2
23	10.76	+0.08	B5
24	12.06	+0.32	B5
25	12.32	+0.52	A0

Table 1

Observational Data for Region LF5 (Cont'd.)

Zone +60° (Cont'd.)

No.	m_{pg}	R.I.	Sp.	No.	m_{pg}	R.I.	Sp.	No.	m_{pg}	R.I.	Sp.
26	11.26	+0.28	B3	76*	11.50	+1.95	G8III	126	12.16	+1.82	G8:
27	11.66	+0.36	A3	77*	9.37	+0.18	A7m	127	12.12	+0.28	B8:
28	11.88	+0.12	B3	78*	10.60	-0.04	B8	128	10.75	+0.39	G0III
29	12.13	+0.24	B3	79*	9.72	-0.04	B1	129	11.57	-0.06	B3:
30	11.96	+0.30	B2	80	12.18	+0.48	A5	130	12.34	+1.67	G5III
31*	10.56	0.00	B3	81*	9.00	+0.48	F8V	131	11.52	+0.01	B3:
32*	11.46	+1.98	K2III	82	12.20	+0.54	F0	132	11.56	+0.86	F8
33	11.92	+0.06	F2	83*	9.41	+0.23	F8V	133	11.83	+0.05	B8:
34	12.16	+0.51	A0	84	12.35	+1.90	G8III	134	11.66	+0.08	B5
35	12.20	+0.62	F5	85	12.12	+0.51	A5	135*	11.05	+2.83	K3III
36*	10.95	+0.48	F5V	86	10.88	-0.04	B1	136	11.96	+0.34	A2
37*	10.42	+0.38	B5	87	11.18	+0.19	B2	137*	10.53	-0.01	B2
38*	9.72	+0.16	B2	88	11.76	+0.06	B2:	138	12.34	+0.44	B5:
39	12.37	+0.48	B9	89	12.23	+1.75	G8:	139*	9.68	+0.10	B1
40*	10.66	+0.35	B2	90	11.41	+0.04	B9	140	11.86	+0.22	B8
41*	9.60	+1.84	K3III	91	11.62	+0.12	B5	141	12.32	+0.42	A0
42	11.97	+0.87	F5	92*	11.10	+2.04	K0III	142*	8.96	+0.26	OB
43	11.76	+0.16	B9	93	12.22	+1.90	G8:	143*	9.26	+2.08	K3III
44*R	11.22	+0.24	A2	94	10.40	+0.96	F0	144	12.40	+1.00	F5
45*R	8.31	-0.11	B5	95	11.20	+0.22	A2	145	12.28	+0.34	B5:
46	10.95	+0.05	B8:	96*	11.58	+0.32	G0:	146	11.35	+0.15	B3:
47	12.32	+0.35	B8	97	11.60	+0.36	A3	147	11.42	+0.42	A0
48	12.05	+0.20	A7	98	12.42	+0.52	A2	148*	7.69	+0.95	F2Ia
49*	10.53	+1.07	K0III	99*	9.18	-0.10	A0	149*	9.31	+1.37	K0III
50	12.30	+0.28	B5:	100*	9.10	-0.14	B0	150	11.18	+0.49	A5
51	11.94	+0.15	B5	101	11.35	+0.25	A3	151	12.20	+0.32	A3:
52*	8.75	+0.11	OB	102*	11.70	+2.04	K2III	152	11.74	+0.26	A0:
53*	11.36	+0.57	A5	103	11.35	+0.83	G5V	153*	8.76	+0.19	OB
54*	11.56	+2.35	K3III	104 R	11.50	+0.27	A0	154	11.86	+0.20	B5:
55	12.30	+0.71	F0	105	12.29	+0.41	A0	155	11.43	+0.61	F5
56	11.66	+1.52	G5III	106*	9.96	-0.11	B2	156	11.27	+0.09	B3
57	11.59	+0.03	B3	107	11.98	+0.30	A0	157	11.84	+1.58	G5
58*	7.69	-0.09	B8	108	11.01	-0.19	B2	158	11.61	+0.23	B2
59*	10.07	+0.49	F8V	109	11.17	+0.69	F5	159*	9.78	+2.92	M2III
60	12.19	+1.43	K2III	110	11.56	-0.06	B1	160*	12.06	+2.74	K:
61	11.53	+0.43	A3	111	11.80	+0.69	F5	161	12.32	+1.46	G5:
62	12.12	+0.46	A0	112	12.36	+0.47	A2	162	11.96	+0.40	B9
63	10.70	-0.12	B5	113	12.17	+0.88	F8	163	12.22	+0.54	A0
64*	10.48	+0.50	F2III	114	12.15	+1.66	K0III	164	12.37	+0.55	B9
65	12.30	+0.66	B9	115	12.22	+1.55	G0:	165	11.14	+0.15	B1
66*	11.21	+0.27	A3Ib	116	12.04	+0.38	B3	166	11.30	+0.14	B1
67	11.18	0.00	B5	117*	10.38	+0.42	A7m	167	11.82	+0.16	B5:
68*	9.86	+0.10	B2	118*R	9.86	+1.94	K2III	168	12.26	+0.40	A0:
69	12.28	+0.44	G2:	119	12.26	+0.78	G0	169	11.86	+0.20	A0
70	11.14	+0.24	B8	120	12.37	+0.69	F5	170	12.28	+0.42	B5:
71	12.41	+0.71	F2	121	10.90	-0.13	B5	171	12.30	+0.67	F2
72	11.68	+0.30	A2	122*R	10.92	+0.78	F5	172*	10.52	-0.08	B8
73	12.20	+0.22	B5	123*	10.36	+0.47	A5m	173	10.52	+0.83	A5m
74	12.28	+0.65	A3	124	11.64	+0.28	B5	174*	10.68	+0.05	B5
75	12.29	+0.56	A0:	125*	11.03	+0.57	F5	175*	10.50	+0.40	B2

Table 1

Observational Data for Region LF5 (Cont'd.)

Zone +60° (Cont'd.)

No.	m_{pg}	R.I.	Sp.	No.	m_{pg}	R.I.	Sp.	No.	m_{pg}	R.I.	Sp.
176	11.09	+0.07	B8	226	11.06	+0.50	B9	276	11.62	+0.76	OB:
177	11.66	+1.50	G5III	227	11.02	+0.52	B5	277	11.88	+0.67	OB:
178	12.19	+0.75	A7	228	11.34	+0.66	A3	278	10.96	+0.22	B2
179	12.32	+0.44	A2	229	11.92	+0.39	B9	279	12.24	+0.53	F2:
180	12.10	+0.22	B8:	230*	10.03	+0.51	OB	280	11.90	+0.38	B5
181	11.78	+0.20	B1	231	11.87	+0.55	B3	281*	11.10	+0.34	B5
182	11.47	+0.26	A0	232*	10.55	+0.21	A0	282	11.96	+0.55	B9
183	12.25	+0.21	B1	233	11.78	+0.45	B1	283	12.32	+0.42	A5
184*	8.69	+0.02	B9	234	11.68	+0.41	B3	284	11.62	+0.52	B5
185*	11.08	+1.44	G5III	235*	10.41	+0.60	OB	285	11.86	+0.99	G0
186	11.48	+0.40	A3	236	11.96	+0.54	OB:	286*	10.64	+0.26	B1
187*	11.46	+0.68	F5	237*	12.19	+0.57	A5	287*R	8.95	+0.23	A5
188	11.47	+0.65	F8V	238	11.47	+0.39	B3:	288*	10.40	+0.48	A7
189	12.41	+0.65	F8	239	10.16	+0.49	B2:	289	11.56	+0.46	A3
190	12.07	+0.73	F5	240*	10.44	+1.46	K0III	290	12.35	+0.65	A2
191*	11.09	+0.37	A3	241	11.17	+0.31	A3	291*	9.87	+0.18	A0
192	11.92	+0.49	B9	242*	11.39	+0.46	A2	292	12.06	+0.39	B3:
193	12.40	+0.73	A3	243	11.26	+1.78	K0III	293	12.20	+0.66	OB:
194	11.82	+0.73	F5	244	12.02	+0.68	A2	294	12.26	+0.68	F0:
195*	10.42	+0.57	F8III	245*	10.38	+2.96	K0:III:	295*	11.44	+2.32	K3III
196*R	8.18	+1.60	K1III	246	11.64	+0.34	B8:	296	10.64	+0.26	B5
197*	10.27	+0.22	B1	247	11.32	+0.28	B3:	297*	9.99	+0.12	B9
198 R	11.00	+0.81	G0V	248	11.94	+0.33	A5:	298*	10.86	+0.15	B9
199	11.40	+0.24	A0	249*	11.00	+0.36	A5	299*	8.70	+0.08	A0
200*	9.51	+0.04	B9	250	11.98	+0.71	F2:	300*	9.46	+0.16	B5
201	11.91	+0.29	B3	251	11.34	+0.22	B3	301	11.70	+0.49	B5:
202	12.31	+0.42	A3	252	11.92	+0.49	B3:	302	12.15	+0.67	A2:
203*R	10.17	+1.17	G2comp	253	11.36	+0.34	B9	303	12.32	+0.67	A0
204	12.32	+0.50	A3	254	12.16	+0.32	B8:	304	12.02	+0.42	B9
205*	11.44	+1.50	G2	255	12.00	+0.45	B5:	305	11.88	+0.44	B8
206 R	12.23	+1.75	G2	256*	11.37	+3.13	M2III	306*	10.83	+0.41	A2
207*	10.38	+0.10	B9	257	12.09	+0.87	F2	307	11.88	+0.49	B5
208	12.10	+0.42	B5	258	11.30	+0.71	F2V	308	11.34	+0.36	B2
209	11.18	+0.18	B3	259*	11.32	+0.53	B2	309	11.37	+0.27	B3
210	11.54	+0.24	B3	260	10.99	+0.21	B8	310	12.08	+0.98	F8
211	11.18	0.00	B5	261	12.42	+0.71	B9	311	12.08	+0.60	A0
212	11.02	+0.32	OB	262	10.80	+0.16	A2	312*	11.00	+0.30	B8
213	12.02	+0.36	A0	263	12.28	+2.32	K5III	313*R	10.63	+0.54	F5V
214*	8.17	+0.29	A2	264	12.20	+0.63	B1	314	10.88	+0.44	A5
215	12.06	+0.24	B3:	265	11.84	+0.50	OB	315*	10.66	+0.20	OB
216	11.94	+0.26	B5	266*	8.02	+0.47	OB	316*	10.95	+0.87	B3
217	11.60	+0.60	A2	267	11.91	+0.72	F5	317	11.74	+0.47	A5
218	12.28	+0.64	B5:	268*	11.00	+3.21	M2III	318*R	8.20	+0.10	B8
219	12.00	+0.53	A3	269	12.16	+0.53	B3	319	12.16	+0.56	B:
220*	10.20	+0.34	B5	270*	10.68	+0.23	A2	320*	9.18	+0.40	F2III
221	11.66	+0.72	F8	271*	10.27	+0.81	OB	321	11.84	+0.66	B8
222*	10.52	+0.30	A3	272	11.62	+0.30	B5:	322*	8.98	-0.09	A0
223	10.86	+0.18	B8	273	12.03	+0.35	B5:	323 R	12.00	+1.88	OB
224	12.43	+0.56	A0	274*	10.72	+0.42	B5	324	11.91	+0.75	F0
225	11.98	+0.53	B5:	275*	9.72	+0.64	OB	325*	11.19	+0.58	OB

Table 1

Observational Data for Region LF5 (Cont'd.)

Zone +60° (Cont'd.)

No.	m_{pg}	R.I.	Sp.
326	12.13	+0.67	F5
327*	10.20	+0.28	B5
328*	10.21	+0.63	OB
329*	10.98	+0.27	B5
330*	10.95	+0.43	A2
331	12.43	+0.64	B9
332	12.24	+0.58	B9
333*R	10.79	+1.21	A3
334*	9.58	+0.30	A7m
335*	8.64	+0.47	F2III
336	11.50	+0.44	A2
337	12.25	+0.65	A0
338*	11.16	+0.58	B2
339	12.24	+0.53	A3
340	12.19	+0.51	B5
341	12.24	+0.56	A3
342*	11.45	+0.70	F0
343	11.46	+0.58	G0
344	12.32	+0.84	G0:
345*	10.31	+0.16	A0
346	12.14	+0.62	B2:
347*	11.06	+0.43	B5
348	11.57	+0.23	B1
349*	11.06	+0.28	B5
350	11.83	+0.79	OB
351	12.02	+0.52	F5
352	11.86	+0.46	B1
353*R	10.52	+0.30	A2
354	11.25	+0.47	F5III
355	12.16	+0.58	A3
356 R	10.84	+0.56	G0
357	11.89	+0.45	A0
358*	12.18	+0.77	B5:
359*	10.28	+0.31	OB
360*	12.32	+1.67	G5
361*	10.87	+0.29	A0
362	12.14	+0.46	B2:
363	11.88	+0.54	B3
364*	11.43	+0.33	A0
365*	10.12	+0.20	A2
366*	9.77	+0.53	OB
367*	11.52	+0.58	A7
368*	9.28	+1.76	K3III
369*	10.71	+2.37	K5III
370*	8.86	+1.27	A5Ia
371*	10.88	+0.79	A7
372*	10.47	+1.27	G8III
373*	10.24	+0.50	OB
374	10.82	+0.92	OB
375*	11.05	+0.78	G0V

Zone +61°

No.	m_{pg}	R.I.	Sp.
1	12.12	+0.46	B9
2*	10.12	+0.13	B3
3	11.76	+0.27	B5
4*	10.24	+0.10	B5
5*	10.94	+0.70	B1
6	12.28	+0.49	A2
7	12.20	+0.46	B8
8	11.27	+0.25	B5
9	11.30	+0.27	B9
10	11.32	+0.68	F5
11	12.26	+0.69	F5
12*R	7.81	-0.01	A0
13*	9.02	+1.39	G8III
14*	9.16	+1.19	F2IV
15*	11.74	+0.53	B8
16	12.28	+1.80	G2:
17 R	12.00	+0.39	B5:
18	11.24	+0.61	G2V
19*	11.10	+1.44	F5III
20*	8.93	-0.16	B9
21*	11.28	+1.58	K2III
22	10.94	+0.70	G0V
23*	10.72	+1.31	G8III
24	11.16	+0.40	B2
25*	9.90	+0.25	A2
26	11.93	+0.55	F5
27*	10.87	+3.03	K3pIII
28	11.00	+0.01	B3
29	12.09	+0.24	B3:
30	11.74	+0.70	OB
31	11.52	+0.70	B2:
32	11.94	+0.26	B5
33 R	11.84	+0.38	B9
34	12.07	+0.72	G2
35	11.26	+0.48	B2
36*R	11.04	+1.48	B5
37	11.08	+0.20	B1
38*	11.36	+0.41	F5III
39*R	11.04	+1.06	A5
40	11.98	+0.56	F0
41	11.62	+0.34	B:
42*	9.95	+1.81	K0III
43 R	11.88	+0.56	B8
44	11.88	+0.42	B1
45	12.26	+0.51	B:
46	10.89	+0.65	F2III
47*	10.08	+0.17	A3
48*	10.19	+0.07	A0
49*	9.11	+0.19	B8
50*	10.94	+0.26	B2
51 R	11.40	+1.10	OB
52*	9.20	+0.08	A2
53*	8.89	+0.95	B3
54*	11.22	+0.12	A2
55	11.84	+0.55	B2
56	12.23	+0.63	F2
57	11.65	+0.62	OB:
58	11.90	+0.61	F5
59	10.98	+0.00	B8
60*	9.20	+1.79	K0III
61*	10.92	+0.32	F2V
62*	10.48	+0.36	OB
63	11.98	+0.38	B8
64*	10.48	+0.30	A7
65	12.24	+0.66	F2
66*R	10.88	+0.24	A5
67*	10.64	+0.09	A7
68*	10.88	+0.54	OB
69*	11.22	+0.50	B2
70	11.39	+0.56	F2
71	10.56	+0.00	A0
72*	9.06	-0.03	A3
73	10.58	+0.02	A5
74*	10.82	+0.44	A7
75	11.46	+0.20	A0
76*	10.40	+0.25	A2
77	11.58	+0.58	A0
78	11.91	+1.92	G8III
79	11.88	+0.34	B5
80*	9.87	+0.77	G5V
81	12.27	+0.75	G2
82	11.95	+1.21	G2
83	11.73	+0.51	B1
84*	11.08	+0.44	A7
85	12.31	+0.64	A0
86*	11.08	+0.49	OB
87	12.28	+0.70	B2
88	12.08	+0.51	B2
89*	9.80	+0.47	B3
90	12.20	+0.35	B9
91	11.92	+0.55	A0
92*	11.46	+1.26	G5
93	11.22	+0.64	G2III
94	11.12	+0.97	G2
95*R	10.90	+2.18	OB+M0
96	11.77	+0.91	OB
97	12.28	+0.56	B1
98	12.26	+0.42	B2
99	12.04	+0.23	B1
100*	6.32	-0.18	B8

Table 1

Observational Data for Region LF5 (Cont'd.)

Zone +61° (Cont'd.)

No.	m_{pg}	R.I.	Sp.
101	12.20	+0.64	B2
102*	9.34	-0.24	B5
103	12.18	+1.09	G5
104*	9.94	+0.28	A5
105	11.29	+0.19	B5
106*	8.95	+0.02	A0
107*	8.39	+1.55	F2I
108	11.43	+0.48	A5
109*	9.60	+1.58	K2III
110	11.80	+0.54	B1
111*	10.50	+0.16	B5
112	11.19	+0.50	A7
113	12.30	+0.78	F5:
114	12.24	+0.81	G0
115*	10.60	+0.28	A0
116*	9.97	+0.15	B9
117	11.92	+0.71	F2
118*	9.58	+0.26	A2p
119*	10.47	+0.51	OB
120	11.24	+0.48	F5
121	12.24	+1.10	G0
122	11.15	+0.63	OB
123*	9.80	+0.79	A2Ib
124*R	10.82	+1.04	B5
125	11.75	+0.67	A2
126*	11.06	+2.02	K2III
127	12.10	+0.78	F2
128*	10.16	+0.48	OB
129	11.31	+0.54	A3
130*	11.20	+1.52	G8III
131*R	11.88	+1.94	F8
132*	12.08	+1.67	G8III
133	11.29	+0.50	B3
134	12.05	+0.62	B8
135*	9.11	+0.01	A0
136	11.70	+0.63	F8
137	12.18	+0.68	A5
138	11.44	+0.54	OB
139	12.24	+0.76	G0
140*	8.99	+0.24	A2
141*	9.84	+0.93	F5+A
142*	11.10	+0.52	A7
143*	10.16	+0.15	B5
144*	10.54	+0.42	A3
145 R	12.24	+1.11	G2:
146	11.90	+0.61	A0
147*	10.60	+0.66	F5V
148*	10.30	+0.14	A3
149	12.24	+0.58	B3:
150	12.24	+0.80	G0
151	11.81	+0.63	F2
152	11.56	+0.38	OB
153*	8.82	+1.04	G0III
154	11.00	+0.78	G0V
155	12.15	+0.49	OB:
156*	10.48	+0.54	A5
157	12.15	+0.76	OB:
158	10.77	+0.61	F0
159	12.04	+0.50	B:
160*	10.95	+0.21	A2
161*	10.45	+0.61	F8
162*	10.13	+0.66	OB
163*	12.04	+1.43	F5
164*	10.20	+0.34	A5
165	11.86	+0.44	B3:
166*	11.00	+0.10	B9
167*	9.56	+0.22	A0
168	12.09	+0.63	A3
169	11.96	+1.64	G8III
170*	10.19	+0.14	B9
171*	11.40	+0.78	G0
172	12.12	+0.68	G2
173	11.99	+0.53	A7
174	11.91	+0.45	A0
175*	11.56	+0.53	B5
176	11.90	+0.56	B3
177	11.84	+0.69	G0
178	12.04	+0.70	F5
179	12.25	+0.70	F8
180	11.91	+0.35	A2
181	12.12	+0.57	A7
182	11.96	+0.46	B1
183*	10.16	+0.61	G2III
184*	11.20	+1.39	G5III
185*	11.40	+0.18	A5
186	11.99	+1.53	G5III
187*R	7.33	-0.02	B8
188*	9.26	+1.39	K0III
189*	10.26	+0.28	A7m
190	11.62	+0.68	F8
191*	9.86	+0.12	B8

Zone +62°

No.	m_{pg}	R.I.	Sp.
1*	10.50	+0.18	B8
2	12.30	+0.62	B3:
3	11.87	+0.77	F8
4	11.88	+0.54	A0:
5	11.50	+0.08	A2
6	12.26	+0.58	B8:
7	10.75	+0.63	B5
8	10.85	+0.10	B8
9	12.21	+0.36	A2

REMARKS

Zone +58°

4	X Cas
26	Spectrum suggests close companion
61	H lines very broad

Zone +59°

22	IL Cas
50	Spectrum indicates close double
65	ADS 1215, measured as one image
138	ADS 1324
165	ADS 1351, measured as one image
220	Spectrum indicates duplicity
240	ADS 1455
276	ADS 1509
284	ADS 1513

Zone +60°

1	ADS 1155, companion not in evidence
10	BU Cas
19	XX Cas shows variation 9.6 to 10.3 on blue and red plates
44	ADS 1196 B
45	ADS 1196 A
104	ADS 1251, companion not in evidence
118	H lines strong
122	ADS 1261
196	ADS 1337 A
198	ADS 1338, companion not in evidence
203	Spectrum composite
206	ADS 1344 C
287	ADS 1421 A
313	ADS 1452 A
318	ADS 1461
323	R. I. seems anomalous for spectral type
333	R. I. seems anomalous for spectral type
353	ADS 1524, companion not in evidence
356	ADS 1527 B

Zone +61°

12	ADS 1194, measured as one image
17	Spectrum indicates duplicity
33	ADS 1220, companion not in evidence
36	R. I. anomalous for spectral type
39	R. I. anomalous for spectral type
43	ADS 1239 A, companion not in evidence
51	R. I. anomalous for spectral type
66	ADS 1275 A
95	AZ Cas
124	R. I. anomalous for spectral type
131	Probably BY Cas
145	ADS 1433 B is given with magnitude 9.4 in ADS
187	ADS 1531

Table 2

BD Equivalents

BD	LF5
57°	
350	58° 21
351	58 22
356	58 26
400	58 92
58°	
248	59° 15
252	59 26
253	59 29
254	59 32
255	59 33
256	59 39
257	59 43
260	58 4
261	59 64
262	58 5
263	59 71
264	58 7
265	58 9
266	59 88
268	59 93
269	59 97
270	59 106
271	58 28
272	59 125
273	58 36
274	59 136
275	59 138
276	58 41
277	59 144
278	59 145
279	59 149
280	59 155
281	58 49
282	59 160
283	58 52
284	58 54
285	59 170
286	59 171
287	59 174
288	58 57
289	58 59
290	59 183
291	58 63
292	58 67
293	59 193
294	58 73
295	58 75
296	59 207
297	58 80
298	59 209
299	58 86
300	59 222
301	59 223
302	59 224
303	58 94
304	58 95
305	58 98
306	59 232
307	59 235

BD	LF5
58°	
308	59° 236
309	59 238
310	58 102
311	59 240
312	59 244
313	59 248
315	59 254
316	58 111
317	59 263
318	59 264
319	58 115
322	59 281
325	59 287
328	59 291
330	59 292
59°	
254	59° 3
257	59 9
258	59 12
259	59 13
260	59 17
261	59 19
262	60 31
263	59 21
264	60 38
265	60 40
266	59 35
267	59 38
268	60 49
269	60 58
270	59 51
272	59 53
275	60 59
277	59 63
278	60 68
279	60 77
280	60 79
281	60 78
282	59 81
283	60 92
284	59 86
285	59 87
286	59 95
287	60 118
288	60 122
289	60 123
290	59 100
291	60 125
292	59 105
293	60 137
294	59 110
295	60 139
296	60 142
297	60 153
298	60 160
299	60 172
300	60 174
301	59 131
302	59 133

BD	LF5
59°	
303	59° 135
304	60 191
305	60 195
306	60 196
308	59 159
309	60 214
310	59 168
311	59 178
312	59 180
313	60 240
314	60 242
315	59 192
316	59 194
317	59 208
318	60 266
319	60 268
320	59 212
321	60 270
322	60 281
323	60 286
324	60 287
325	60 291
326	60 295
327	59 228
328	60 297
329	59 231
330	59 234
331	60 306
332	59 241
333	59 242
334	60 315
336	60 318
337	60 322
338	60 327
339	60 329
340	59 256
341	59 257
342	60 334
343	60 338
344	59 261
345	60 345
346	59 266
347	60 347
348	59 272
349	60 349
350	59 276
351	59 277
352	59 278
353	59 282
354	59 284
355	59 293
357	60 359
358	60 360
359	60 364
360	59 302
361	60 365
362	59 305
363	59 307
364	60 370
365	59 310

BD	LF5
59°	
367	60° 373
60°	
241	60° 4
244	60 15
245	60 18
246	60 19
247	61 2
248	61 4
249	60 32
250	61 5
251	60 36
252	60 37
253	61 12
254	60 41
255	60 45
256	61 13
257	61 14
258	61 15
260	61 19
261	60 52
262	60 53
263	60 54
264	61 23
265	61 27
266	60 64
267	60 66
268	60 76
269	60 81
271	60 83
272	61 36
273	61 42
278	60 96
279	60 100
280	60 99
281	61 49
282	61 50
283	60 102
284	60 106
285	61 54
286	60 117
287	60 135
288	61 61
289	61 62
290	61 64
291	61 66
292	60 143
293	61 67
294	61 69
295	60 149
296	60 148
297	61 72
298	61 74
299	60 159
301	61 80
302	60 175
303	61 84
304	60 187
305	60 184
306	60 185

Table 2

BD Equivalents (Cont'd.)

BD	LF5	BD	LF5	BD	LF5	BD	LF5
60^{0}		60^{0}		60^{0}		61^{0}	
307	61^{0} 86	346	61^{0} 130	376	61^{0} 183	300	61^{0} 52
309	61 92	347	60 271	377	61 184	301	61 53
310	61 95	348	61 131	378	61 185	303	61 60
311	60 197	349	61 132	379	60 353	305	61 68
312	61 100	350	60 274	381	60 358	307	62 1
313	60 200	351	60 275	383	61 187	308	61 76
314	60 203	352	60 288	384	60 361	310	61 89
315	60 205	353	61 142	386	61 188	314	61 102
316	60 207	355	61 147	387	61 189	316	61 107
317	61 104	356	60 298	388	60 367	318	61 111
318	61 106	357	60 299	389	60 366	319	61 116
319	60 220	358	60 300	390	61 191	320	61 118
320	60 222	359	61 161	392	60 368	321	61 126
321	61 109	360	60 312	396	60 369	327	61 135
322	60 230	361	60 313	397	60 371	329	61 140
323	60 232	362	61 162	399	60 372	330	61 141
324	61 115	363	61 163	402	60 375	331	61 144
325	60 235	364	61 164			332	61 143
326	60 237	365	60 316	61^{0}		333	61 148
327	60 245	366	60 320	286	61^{0} 20	334	61 153
328	60 249	368	60 325	287	61 21	335	61 156
329	61 119	369	60 328	288	61 25	336	61 160
335	60 256	370	61 175	295	61 38	337	61 166
336	61 123	371	60 330	296	61 39	338	61 167
337	61 124	372	60 335	297	61 48	339	61 170
338	60 259	373	60 333	298	61 47	340	61 171
345	61 128	374	60 342				

Table 3

PHOTOELECTRIC MAGNITUDE SEQUENCE

Designation			m_{pg}	m_r
59°	307	(BD)	5.76	5.94
60°	308	(BD)	6.64	6.83
60°	214		8.00	7.90
60°	266		8.03	7.56
59°	180		8.32	8.28
60°	153		8.74	8.60
60°	142		8.92	8.74
59°	178		9.17	9.12
60°	291		9.78	9.64
60°	207		10.35	10.30
60°	122		10.69	10.14
60°	223		10.82	10.61
60°	198		10.98	10.31
60°	150		11.17	10.57
60°	295		11.44	9.04
60°	188		11.46	10.69
60°	217		11.48	10.98
60°	177		11.53	10.12
60°	267		11.82	11.11
60°	252		12.00	11.44
60°	160		12.11	9.11
60°	114		12.12	10.33
A			12.28	11.82
B			12.42	11.72
C			12.62	11.77

TOROIDAL OSCILLATIONS OF AN INCOMPRESSIBLE CONDUCTIVE FLUID SPHERE IN A DECAY FIELD

EBERHART JENSEN*
Yerkes Observatory
Received November 16, 1953; revised April 6, 1955

ABSTRACT

The decaying magnetic field in a conducting homogeneous fluid sphere which has the longest decay time is a dipole field outside the sphere. In this initial state it is assumed that no material motions are present. If this state is perturbed, hydromagnetic oscillations about the initial field will result. If periods short compared to the decay time are considered, it is shown how the eigen-value matrix for the characteristic frequencies can be found in the case of toroidal oscillations. The modes of the velocity field and of the perturbed magnetic field are asymmetrical in the sense that the associated Legendre functions involved have $m > 0$. The eigen-value matrix is symmetrical and thus gives only real values of ω^2. Since the matrix is nondiagonal, the exact values of the characteristic frequencies cannot be found. The approximate solution obtained by taking into account only the terms of lowest order in the matrix shows that both positive and negative values of ω^2 appear. In one of the cases considered, corresponding to a rigid boundary, the eigen-values apparently form a continuous spectrum. An application is made to the terrestrial field.

I. INTRODUCTION

An interesting problem in the theory of hydromagnetic oscillations occurs in connection with the secular variations in the earth's magnetic field. As is well known (see Bullard 1949*a*), these variations are quite substantial and take place in times of the order of a hundred to a thousand years. Since the time of decay of an initially prevalent magnetic field in a fluid sphere of the dimensions and conductivity of the earth's core is of the order of 15,000 years (Elsasser 1950), it is clear that, for the problem of the secular variations of the earth's field, we may treat the fluid core of the earth as an infinitely good conductor.

A problem which was suggested to the writer by S. Chandrasekhar in this connection was the following: Given a decay field in a large gravitating body of planetary or stellar dimensions, to investigate the periods of oscillations of the decay field during time intervals short compared to the decay time. On investigating this problem, it appeared that there must exist eigen-values corresponding to imaginary frequencies. This may have a bearing on the dynamo mechanism for the maintenance of the main field, as discussed in recent years by Elsasser (1946*a*, *b*, 1947, 1950) and Bullard (1949*b*, *c*). Now the decaying magnetic field in a conductor resulting from the Joule heating of a corresponding freely decaying current system has been investigated, particularly by Elsasser (1946*a*, *b*, 1947), along lines first set out by Lamb (1883).

In this paper we shall restrict ourselves to certain simple modes of the field in an incompressible fluid conductor of constant electrical conductivity. We shall set up the linearized equations which govern the oscillations of short period (short compared to the decay time) about the original field and try to evaluate by a numerical procedure the values of the characteristic frequencies of lowest order.

It may be stated here that the particular modes of oscillation which we shall consider are those which result from a velocity field which is toroidal in the sense of Elsasser. However, in treating the velocity field, we shall consider two cases: one in which the tangential components of the velocity are nonvanishing and the other in which the tangential components do vanish at the boundary. These two cases correspond, respectively, to the bounding surface being free or rigid. This paper is largely based on Elsasser's work, and his notations are mostly used. Electromagnetic units are used throughout.

* From the Institute of Theoretical Astrophysics, University of Oslo, Blindern, Oslo, Norway.

II. THE BASIC FUNCTIONS $\boldsymbol{T}$ AND $\boldsymbol{S}$

It is well known (Stratton 1941) that the equations governing the decaying magnetic field $\boldsymbol{H}$, in a homogeneous sphere with a constant electrical conductivity σ, is

$$\nabla^2 \boldsymbol{H} = 4\pi\sigma\mu \frac{\partial \boldsymbol{H}}{\partial t}. \tag{1}$$

The decay of the field predicted by equation (1) is by ohmic losses when there are no material motions. In terms of the vector potential $\boldsymbol{A}$, defined in the following manner,

$$\boldsymbol{H} = \operatorname{curl} \boldsymbol{A}\ , \tag{2}$$

equation (1) takes the form

$$\nabla^2 \boldsymbol{A} = 4\pi\sigma\mu \frac{\partial \boldsymbol{A}}{\partial t}. \tag{3}$$

In the subsequent discussion of this equation we will suppose that $\mu = 1$. Equation (3) is valid inside the conducting sphere. Outside the sphere the vector potential will be governed by Laplace's equation,

$$\nabla^2 \boldsymbol{A} = 0\ . \tag{4}$$

In solving equations (3) and (4) appropriately for the problem at hand, we seek solutions of the form

$$\boldsymbol{A} = \boldsymbol{A}_0 e^{-t/\tau}\ , \tag{5}$$

where τ is a constant of the dimension of a time—the decay time—which will be determined presently. For solutions of the form (5), equations (3) and (4) become, respectively,

$$\nabla^2 \boldsymbol{A}_0 + k^2 \boldsymbol{A}_0 = 0 \qquad \text{and} \qquad \nabla^2 \boldsymbol{A}_0 = 0\ , \tag{6}$$

where $k^2 = 4\pi\sigma/\tau$. As is well known (Stratton 1941; Elsasser 1946*a*), it is possible to construct three independent solutions satisfying equations (6) in terms of a scalar generating function ψ which satisfies the equations

$$\nabla^2 \psi + k^2 \psi = 0 \qquad \text{(inside the sphere)}\ , \tag{7}$$

$$\nabla^2 \psi = 0 \qquad \text{(outside the sphere)}\ . \tag{8}$$

Thus

$$\boldsymbol{U} = R\nabla\psi\ , \quad \boldsymbol{T} = \operatorname{curl}(\boldsymbol{r}\psi)\ , \quad \text{and} \quad \boldsymbol{S} = R \operatorname{curl}\operatorname{curl}(\boldsymbol{r}\psi) \tag{9}$$

represent solutions of equations (3) and (4). Here $\boldsymbol{r}$ is the radius vector from the center and R is the radius of the sphere. The functions $\boldsymbol{T}$ and $\boldsymbol{S}$ are related reciprocally by the equations

$$\boldsymbol{T} = (Rk^2)^{-1} \operatorname{curl} \boldsymbol{S} \qquad \text{and} \qquad \boldsymbol{S} = R \operatorname{curl} \boldsymbol{T}\ . \tag{10}$$

Elsasser calls these functions "toroidal" and "poloidal," respectively.

In the subsequent work we shall make use of the toroidal and poloidal functions only. But we shall find it necessary to distinguish two cases: one in which these functions do not vanish on the surface of the sphere and are derived from a solution ψ such that ψ and $\partial\psi/\partial r$ are continuous on this boundary, and the other in which the solutions vanish on the boundary and in the entire space outside. We shall distinguish this latter set of solutions by denoting them by $\mathfrak{T}$ and $\mathfrak{S}$ and their generating function by Φ. We shall refer to these two cases as "case I" and "case II," respectively.

a) CASE I

When equations (7) and (8) for ψ are solved with the boundary conditions that ψ and $\partial\psi/\partial r$ are both continuous at $r = R$, it is found that the solution inside the sphere is given by (cf. Elsasser 1946*a*)

$$\psi_{ns}^{m} = Z_n N_n^m \left(\frac{R}{r}\right)^{1/2} J_{n+1/2}(k_{ns} r)\, P_n^m(\theta)\, e^{im\phi}, \tag{11}$$

where Z_n and N_n^m are constants which we shall presently specify; $J_{n+1/2}$ is the spherical Bessel function of order $n + \frac{1}{2}$, which is regular at $r = 0$; and P_n^m is the associated Legendre function. The characteristic values, k_{ns}, of k are the zeros of the equation

$$R k_{ns} J_{n-1/2}(k_{ns} R) = 0\,. \tag{12}$$

The index s denotes the number of the zero, $s = 1$, corresponding to the smallest positive root, so that $s - 1$ will give the number of nodes in the interior $(0, R)$ of the function ψ_{ns}^m, and also of $\boldsymbol{T}_{ns}^m$ (cf. eq. [14]). Outside the sphere, ψ is clearly a multiple of $r^{-(n+1)} P_n^m(\theta) e^{im\phi}$; it will be convenient to write this solution in the following form (cf. eq. [11]):

$$\psi_{ns}^{m} = Z_n N_n^m \left(\frac{R}{r}\right)^{n+1} J_{n+1/2}(k_{ns} R)\, P_n^m(\theta)\, e^{im\phi}. \tag{13}$$

In accordance with equation (9), solutions $\boldsymbol{T}$ and $\boldsymbol{S}$ obtained from the foregoing generating function will have the following components in the r-, θ-, and ϕ-directions:

$$\boldsymbol{T}_{ns}^{m} = \left(0, \frac{1}{\sin\theta}\frac{\partial\psi_{ns}^m}{\partial\phi}, -\frac{\partial\psi_{ns}^m}{\partial\theta}\right) \tag{14}$$

and

$$\boldsymbol{S}_{ns}^{m} = \frac{R}{r}\left[n(n+1)\,\psi_{ns}^m, \frac{\partial}{\partial r}\left(r\frac{\partial\psi_{ns}^m}{\partial\theta}\right), \frac{1}{\sin\theta}\frac{\partial}{\partial r}\left(r\frac{\partial\psi_{ns}^m}{\partial\phi}\right)\right]. \tag{15}$$

Since ψ_{ns}^m and its derivatives are continuous at the surface, this will also be the case with the components of the functions $\boldsymbol{T}_{ns}^m$ and $\boldsymbol{S}_{ns}^m$.

Now it can be shown that the $\boldsymbol{T}$ and $\boldsymbol{S}$ functions form an orthogonal set, with the integral property,

$$\int \boldsymbol{T}(\beta)\cdot\boldsymbol{T}^*(\gamma)\, dv = 0\,, \qquad \int \boldsymbol{S}(\beta)\cdot\boldsymbol{S}^*(\gamma)\, dv = 0 \quad \text{if} \quad \beta \neq \gamma\,. \tag{16}$$

In equation (16) β or γ stands for a set of indices like n, s, and m. The functions $\boldsymbol{T}$ and $\boldsymbol{S}$ have another important property which will be used later and is expressed by the following relations:

$$\int \boldsymbol{S}(\alpha)\cdot\boldsymbol{T}^*(\beta)\, dv = 0\,, \qquad \int \boldsymbol{T}(\gamma)\cdot\boldsymbol{S}^*(\epsilon)\, dv = 0\,. \tag{17}$$

This is valid regardless of the values of the indices α, β, γ, and ϵ entering. To prove this, we use the definitions as expressed by equations (14) and (15). From these equations we get

$$\int \boldsymbol{S}(\alpha)\cdot\boldsymbol{T}^*(\beta)\, dv = R\int \frac{1}{r\sin\theta}\left\{\frac{\partial}{\partial r}\left[r\frac{\partial\psi(\alpha)}{\partial\theta}\right]\frac{\partial\psi^*(\beta)}{\partial\phi} - \frac{\partial}{\partial r}\left[r\frac{\partial\psi(\alpha)}{\partial\phi}\right]\frac{\partial\psi^*(\beta)}{\partial\theta}\right\} dv$$

$$= -R\int_0^R \frac{d}{dr}\left[r^{1/2}\Im\left(r \mid n_\alpha + \tfrac{1}{2}, n_\alpha - \tfrac{1}{2}, s\right)\right]\Im\left(r \mid n_\beta + \tfrac{1}{2}, n_\beta - \tfrac{1}{2}, s\right) r^{1/2} dr \tag{18}$$

$$\times\left\{im_\beta\int_0^\pi \frac{dP_{n_\alpha}^{m_\alpha}}{d\theta} P_{n_\beta}^{m_\beta} d\theta + im_\alpha\int_0^\pi P_{n_\alpha}^{m_\alpha}\frac{dP_{n_\beta}^{m_\beta}}{d\theta}\, d\theta\right\}\times\int_0^{2\pi} e^{i(m_\alpha - m_\beta)\phi} d\phi \times \text{constant}\,.$$

For convenience we have here introduced a new notation for the Bessel functions: $\mathfrak{J}(r|n, q, s)$ denotes a Bessel function of order n, with argument $r \times$ (scale factor), the scale factor being the sth zero of a Bessel function of order q divided by R. When $m_\alpha \neq m_\beta$, it is seen that expression (18) will vanish, since the integral over ϕ vanishes. When $m_\alpha = m_\beta = 0$, it will also vanish. In the case $m_\alpha = m_\beta > 0$ the factor containing the integrals over θ may be written

$$im_\alpha \int_0^\pi \frac{d}{d\theta}\left(P_{n_\alpha}^{m_\alpha} P_{n_\beta}^{m_\alpha}\right) d\theta = im_\alpha P_{n_\alpha}^{m_\alpha} P_{n_\beta}^{m_\alpha}\Big|_0^\pi . \tag{19}$$

But at points $\theta = 0$ and π, $P_n^m = 0$ when $m > 0$. The first integral in equation (17) will therefore vanish for all values of the indices. That the second integral, $\int \boldsymbol{T}(\gamma)\cdot\boldsymbol{S}^*(\epsilon)dv$, has the same property is shown in a similar way. We shall make use later of both the toroidal and the poloidal functions as a basis for series expansions. However, when both $\boldsymbol{T}$ and $\boldsymbol{S}$ are derived from the same generating function ψ, only one of them may be normalized at a time. We shall choose to normalize the $\boldsymbol{T}$ functions, and evaluate the integrals $K_\alpha^2 = \int \boldsymbol{S}(\alpha)\cdot\boldsymbol{S}^*(\alpha)dv$ and carry this factor along in the calculations.

Normalization of the $\boldsymbol{T}$ functions.—The constants Z_n and N_n^m in the solution given in equations (11) and (13) are now determined in such a way that the $\boldsymbol{T}$ functions are normalized, i.e.,

$$\int \boldsymbol{T}(\beta)\cdot\boldsymbol{T}^*(\beta)\, dv = 1 , \tag{20}$$

where the integration is effected over the relevant volume. In the subsequent work we shall make use of the $\boldsymbol{T}$ and $\boldsymbol{S}$ functions in expanding the vector potential of the perturbed magnetic field; and, since this will vanish at all points where the velocity is zero, it would appear natural to carry out this normalization (20) for integration over the interior of the sphere only. The $\boldsymbol{T}$ functions normalized over the whole space will differ from the functions we shall use, by the constant factor $[2n - 1/2n + 1]^{1/2}$.

Let $Y_n^m(\theta, \phi) = P_n^m(\theta)e^{im\phi}$ represent the general surface harmonic and $F(r)$ the r-dependent part of ψ_{ns}^m. According to equation (14), the integrand is

$$\boldsymbol{T}_{ns}^m\cdot\boldsymbol{T}_{ns}^{m*} = [F(r)]^2\left\{\frac{1}{\sin^2\theta}\frac{\partial Y_n^m}{\partial\phi}\frac{\partial Y_n^{m*}}{\partial\phi}+\frac{\partial Y_n^m}{\partial\theta}\frac{\partial Y_n^{m*}}{\partial\theta}\right\}. \tag{21}$$

First N_n^m is determined in such a way that

$$(N_n^m)^2\int_0^{2\pi}\int_0^\pi\left\{\frac{1}{\sin^2\theta}\frac{\partial Y_n^m}{\partial\phi}\frac{\partial Y_n^{m*}}{\partial\phi}+\frac{\partial Y_n^m}{\partial\theta}\frac{\partial Y_n^{m*}}{\partial\theta}\right\}\sin\theta\, d\theta\, d\phi = 1 . \tag{22}$$

As shown by Elsasser, this leads to

$$N_n^m = \left[\frac{(2n+1)(n-m)!}{4\pi n(n+1)(n+m)!}\right]^{1/2} . \tag{23}$$

Next we determine the normalization constant Z_n (cf. eq. [11]) from the equation

$$Z_n^2 R\int_0^R r\,[J_{n+1/2}(k_{ns}r)]^2 dr = 1 . \tag{24}$$

Using a well-known property of the Bessel functions (cf. Margenau and Murphy 1943, p. 117), we find that equation (24) gives

$$Z_n = \frac{2^{1/2}}{R^{3/2}J_{n+1/2}(k_{ns}R)} . \tag{25}$$

The generating function from which the normalized $\boldsymbol{T}$ functions can be derived is, therefore,

$$\psi_{ns}^{m}=\left[\frac{(2n+1)\,(n-m)\,!}{2\pi n\,(n+1)\,(n+m)\,!}\right]^{1/2}\frac{1}{RJ_{n+1/2}\,(k_{ns}R)}\,\frac{J_{n+1/2}\,(k_{ns}r)}{r^{1/2}}\,P_{n}^{m}\,e^{im\phi}. \tag{26}$$

The integral $K_a^2=\int \boldsymbol{S}(a)\cdot\boldsymbol{S}^{*}(a)dv$ when $\boldsymbol{S}$ is evaluated by using the generating function giving normalized $\boldsymbol{T}$ functions.—No attempt will be made to find analytical expressions for the integrals over Bessel functions which appear here. With the accuracy we want, it is a much faster procedure to calculate these integrals numerically.

Using the definition of the $\boldsymbol{S}$ functions (cf. eq. [15]), we have the following expression for K_a^2:

$$K_a^2=R^2\int\frac{1}{r^2}\Big\{n_a^2\,(n_a+1)^2\,|\,\psi\,(a)\,|^2+\left|\frac{\partial}{\partial r}\left[r\,\frac{\partial\psi\,(a)}{\partial\theta}\right]\right|^2 +\frac{1}{\sin^2\theta}\left|\frac{\partial}{\partial r}\left[r\,\frac{\partial\psi\,(a)}{\partial\phi}\right]\right|^2\Big\}dv. \tag{27}$$

For the generating function ψ we have

$$\psi\,(a)=M_a\,\frac{\Im\,(r\,|\,n_a+\tfrac{1}{2},\,n_a-\tfrac{1}{2},s)}{r^{1/2}}\,P_{n_a}^{m_a}e^{im_a\phi}, \tag{28}$$

where, according to equation (26), M_a is given by

$$M_a=\left[\frac{(2n_a+1)\,(n_a-m_a)\,!}{2\pi n_a\,(n_a+1)\,(n_a+m_a)\,!}\right]^{1/2}\frac{1}{R\,\Im\,(R\,|\,n_a+\tfrac{1}{2},\,n_a-\tfrac{1}{2},s)}. \tag{29}$$

The first term in the integral in equation (27) takes the form

$$\begin{aligned}&M_a^2R^2n_a^2\,(n_a+1)^2\int_0^R[\,\Im\,(r\,|\,n_a+\tfrac{1}{2},\,n_a-\tfrac{1}{2},s)\,]^2\,\frac{dr}{r}\times\int_0^{\pi}(P_{n_a}^{m_a})^2\sin\theta\,d\theta\times\int_0^{2\pi}d\phi\\ &=2\pi M_a^2R^2n_a^2\,(n_a+1)^2\,\frac{(n_a+m_a)\,!}{(n_a-m_a)\,!}\,\frac{2}{2n_a+1}\int_0^R[\,\Im\,(r\,|\,n_a+\tfrac{1}{2},\,n_a-\tfrac{1}{2},s)\,]^2\,\frac{dr}{r}\\ &=\frac{2n_a\,(n_a+1)}{[\,\Im\,(R\,|\,n_a+\tfrac{1}{2},\,n_a-\tfrac{1}{2},s)\,]^2}\int^R[\,\Im\,(r\,|\,n_a+\tfrac{1}{2},\,n_a-\tfrac{1}{2},s)\,]^2\,\frac{dr}{r}.\end{aligned} \tag{30}$$

In writing down this equation, we have made use of equation (29) and of the well-known result,

$$\int_0^{\pi}(P_n^m)^2\sin\theta\,d\theta=\frac{2}{2n+1}\,\frac{(n+m)\,!}{(n-m)\,!}. \tag{31}$$

The last two terms in equation (27) for K_a^2 have the r-dependent part in common, and we shall therefore treat these terms together. We get

$$\begin{aligned}M_a^2R^2\int_0^R\left\{\frac{d}{dr}\,[r^{1/2}\Im\,(r\,|\,n_a+\tfrac{1}{2},\,n_a-\tfrac{1}{2},s)\,]\right\}^2dr\\ \times\int_0^{\pi}\left\{\left(\frac{dP_{n_a}^{m_a}}{d\theta}\right)^2+\frac{m_a^2}{\sin^2\theta}\,(P_{n_a}^{m_a})^2\right\}\sin\theta\,d\theta\times\int_0^{2\pi}d\phi.\end{aligned} \tag{32}$$

The integral over θ will first be evaluated. Introducing the new variable $x=\cos\theta$, we get

$$\begin{aligned}&\int_0^{\pi}\left\{\left(\frac{dP_{n_a}^{m_a}}{d\theta}\right)^2+\frac{m_a^2}{\sin^2\theta}\,(P_{n_a}^{m_a})^2\right\}\sin\theta\,d\theta\\ &\qquad=\int_{-1}^{+1}\left\{(1-x^2)\left(\frac{dP_{n_a}^{m_a}}{dx}\right)^2+\frac{m_a^2}{1-x^2}\,(P_{n_a}^{m_a})^2\right\}dx.\end{aligned} \tag{33}$$

Integrating the first term by parts, the result is

$$P_{n_a}^{m_a}(1-x^2)\frac{dP_{n_a}^{m_a}}{dx}\Big|_{-1}^{+1}+\int_{-1}^{+1}P_{n_a}^{m_a}\left\{\frac{m_a^2}{1-x^2}P_{n_a}^{m_a}-\frac{d}{dx}\left[(1-x^2)\frac{dP_{n_a}^{m_a}}{dx}\right]\right\}dx. \tag{34}$$

The differential equation for $P_{n_a}^{m_a}$ gives

$$\frac{m_a^2}{1-x^2}P_{n_a}^{m_a}-\frac{d}{dx}\left[(1-x^2)\frac{dP_{n_a}^{m_a}}{dx}\right]=n_a(n_a+1)P_{n_a}^{m_a}. \tag{35}$$

Integrating this, we get, for the integral over θ,

$$n_a(n_a+1)\int_{-1}^{+1}(P_{n_a}^{m_a})^2dx=\frac{2n_a(n_a+1)}{2n_a+1}\frac{(n_a+m_a)!}{(n_a-m_a)!}. \tag{36}$$

For the integral over r in equation (32) we have the expression

$$\begin{aligned}&\int_0^R\left\{\frac{d}{dr}[r^{1/2}\Im(r\,|\,n_a+\tfrac{1}{2},\,n_a-\tfrac{1}{2},s)]\right\}^2dr\\&=\int_0^R\left\{\frac{1}{2r^{1/2}}\Im(r\,|\,n_a+\tfrac{1}{2},\,n_a-\tfrac{1}{2},s)+r^{1/2}\frac{d}{dr}[\Im(r\,|\,n_a+\tfrac{1}{2},\,n_a-\tfrac{1}{2},s)]\right\}^2dr.\end{aligned} \tag{37}$$

This is now further reduced by making use of the relation (cf. Margenau and Murphy 1943, p. 112)

$$\frac{d}{dz}J_{n+1/2}(z)=J_{n-1/2}(z)-\frac{n+\frac{1}{2}}{z}J_{n+1/2}(z). \tag{38}$$

When this is introduced, we finally get, for the integral over r in equation (32), the expression

$$\begin{aligned}&\int_0^R\left\{k_{n_a^s}r^{1/2}\Im(r\,|\,n_a-\tfrac{1}{2},\,n_a-\tfrac{1}{2},s)-\frac{n_a}{r^{1/2}}\Im(r\,|\,n_a+\tfrac{1}{2},\,n_a-\tfrac{1}{2},s)\right\}^2dr\\&=k_{n_a^s}^2\int_0^R[\Im(r\,|\,n_a-\tfrac{1}{2},\,n_a-\tfrac{1}{2},s)]^2r\,dr-2n_ak_{n_a^s}\int_0^R\Im(r\,|\,n_a-\tfrac{1}{2},\,n_a-\tfrac{1}{2},s)\\&\qquad\times\Im(r\,|\,n_a+\tfrac{1}{2},\,n_a-\tfrac{1}{2},s)\,dr+n_a^2\int_0^R[\Im(r\,|\,n_a+\tfrac{1}{2},\,n_a-\tfrac{1}{2},s)]^2\frac{dr}{r}.\end{aligned} \tag{39}$$

Combining equations (36), (29), and (39), we get, for expression (32),

$$\begin{aligned}&\frac{2}{[\Im(R\,|\,n_a+\tfrac{1}{2},\,n_a-\tfrac{1}{2},s)]^2}\left\{k_{n_a^s}^2\int_0^R[\Im(r\,|\,n_a-\tfrac{1}{2},\,n_a-\tfrac{1}{2},s)]^2r\,dr\right.\\&\qquad-2n_ak_{n_a^s}\int_0^R\Im(r\,|\,n_a-\tfrac{1}{2},\,n_a-\tfrac{1}{2},s)\,\Im(r\,|\,n_a+\tfrac{1}{2},\,n_a-\tfrac{1}{2},s)\,dr\\&\qquad\left.+n_a^2\int_0^R[\Im(r\,|\,n_a+\tfrac{1}{2},\,n_a-\tfrac{1}{2},s)]^2\frac{dr}{r}\right\}.\end{aligned} \tag{40}$$

Addition of the expressions given in equations (30) and (40) finally gives K_a^2 in the form we want, as follows:

$$\begin{aligned}K_a^2=&\frac{2}{[\Im(R\,|\,n_a+\tfrac{1}{2},\,n_a-\tfrac{1}{2},s)]^2}\left\{n_a(2n_a+1)\int_0^R[\Im(r\,|\,n_a+\tfrac{1}{2},\,n_a-\tfrac{1}{2},s)]^2\frac{dr}{r}\right.\\&-2n_ak_{n_a^s}\int_0^R\Im(r\,|\,n_a-\tfrac{1}{2},\,n_a-\tfrac{1}{2},s)\,\Im(r\,|\,n_a+\tfrac{1}{2},\,n_a-\tfrac{1}{2},s)\,dr\\&\left.+k_{n_a^s}^2\int_0^R[\Im(r\,|\,n_a-\tfrac{1}{2},\,n_a-\tfrac{1}{2},s)]^2r\,dr\right\}.\end{aligned} \tag{41}$$

b) CASE II

To be able to treat a velocity field which vanishes at the material boundary, we shall introduce a toroidal field with this property. This field is derived from a generating function Φ in the same way as $\boldsymbol{T}$ was derived from ψ, according to equation (14); thus

$$\mathfrak{T}_{ns}^{m}=\left(0,\frac{1}{\sin\theta}\frac{\partial\Phi_{ns}^{m}}{\partial\phi},-\frac{\partial\Phi_{ns}^{m}}{\partial\theta}\right). \tag{42}$$

The function $\mathfrak{T}$ is essentially equivalent to the solution given by Bullard (Bullard 1949*c*) for the toroidal decay field. The boundary condition is now $\mathfrak{T}=0$ at $r=R$. It may be readily verified from equation (42) that, if Φ vanishes at $r=R$, $\mathfrak{T}$ will also have this property. The corresponding characteristic values, which we shall now denote by l_{ns}, are clearly the zeros of $J_{n+1/2}$:

$$J_{n+1/2}\,(l_{ns}R)=0\,. \tag{43}$$

For Φ_{ns}^{m} we then have

$$\Phi_{ns}^{m}=Z_{n}N_{n}^{m}\left(\frac{R}{r}\right)^{1/2}J_{n+1/2}\,(l_{ns}r)\,P_{n}^{m}\,e^{im\phi}. \tag{44}$$

The normalization of the $\mathfrak{T}$ *functions.*—Since the part of Φ depending upon θ and ϕ is given, as before, by the same surface harmonic, we have expression (23) for N_{n}^{m}. The part of the normalization integral depending upon r is

$$Z_{n}^{2}R\int_{0}^{R}r\,[J_{n+1/2}\,(l_{ns}r)\,]^{2}dr=1\,, \tag{45}$$

the integration being carried out from 0 to R, since $\mathfrak{T}$ is identically zero outside the material boundary. To evaluate the integral in equation (45), we once more use the reduction formula referred to in connection with equation (24). We find

$$\int_{0}^{R}r\,[J_{n+1/2}\,(l_{ns}r)\,]^{2}dr=-\frac{R^{2}}{2}\,J_{n-1/2}\,(l_{ns}R)\,J_{n+3/2}\,(l_{ns}R)\,. \tag{46}$$

Hence

$$Z_{n}=\frac{2^{1/2}}{R^{3/2}[\,-J_{n-1/2}\,(l_{ns}R)\,J_{n+3/2}\,(l_{ns}R)\,]^{1/2}}. \tag{47}$$

The generating function for the normalized $\mathfrak{T}$ functions is

$$\Phi_{ns}^{m}=\frac{1}{R}\left[\frac{(2n+1)\,(n-m)\,!}{2\pi n\,(n+1)\,(n+m)\,!}\right]^{1/2}[\,-J_{n-1/2}\,(l_{ns}R)\,J_{n+3/2}\,(l_{ns}R)\,]^{-1/2}\times\frac{J_{n+1/2}\,(l_{ns}r)}{r^{1/2}}\,P_{n}^{m}\,e^{im\phi}. \tag{48}$$

The integral $\mathfrak{K}_{a}^{2}=\int\mathfrak{S}(a)\cdot\mathfrak{S}^{*}(a)dv$ *when* $\mathfrak{S}(a)$ *is evaluated by using the generating function giving normalized* $\mathfrak{T}(a)$ *functions.*—Using the definition of the $\mathfrak{S}$ function in terms of the generating function Φ, we get

$$\mathfrak{K}_{a}^{2}=R^{2}\int\frac{1}{r^{2}}\left\{n_{a}^{2}\,(n_{a}+1)^{2}\,|\,\Phi\,(a)\,|^{2}+\left|\frac{\partial}{\partial r}\left[r\,\frac{\partial\Phi\,(a)}{\partial\theta}\right]\right|^{2}+\frac{1}{\sin^{2}\theta}\left|\frac{\partial}{\partial r}\left[r\,\frac{\partial\Phi\,(a)}{\partial\phi}\right]\right|^{2}\right\}dv\,. \tag{49}$$

For the generating function Φ we now write

$$\Phi\,(a)=\mathfrak{M}_{a}\frac{\mathfrak{J}\,(r\,|\,n_{a}+\frac{1}{2},\,n_{a}+\frac{1}{2},\,s)}{r^{1/2}}\,P_{n}^{m}\,e^{im\phi}, \tag{50}$$

where, according to equation (48), $\mathfrak{M}_a$ is given by

$$\mathfrak{M}_a = \left[\frac{(2n_a+1)\,(n_a-m_a)\,!}{2\pi n_a\,(n_a+1)\,(n_a+m_a)\,!}\right]^{1/2} \times \frac{1}{R\,[-\Im\,(R\,|\,n_a-\frac{1}{2},\,n_a+\frac{1}{2},s)\;\Im\,(R\,|\,n_a+\frac{3}{2},\,n_a+\frac{1}{2},s)\,]^{1/2}}. \tag{51}$$

Proceeding in the same way as in case I, we arrive at the following expression for $\mathfrak{K}_a^2$:

$$\mathfrak{K}_a^2 = \frac{2}{[-\Im\,(R\,|\,n_a-\frac{1}{2},\,n_a+\frac{1}{2},s)\;\Im\,(R\,|\,n_a+\frac{3}{2},\,n_a+\frac{1}{2},s)\,]} \times \Big\{ n_a\,(2n_a+1)\int_0^R [\,\Im\,(r\,|\,n_a+\tfrac{1}{2},\,n_a+\tfrac{1}{2},s)\,]^2\,\frac{dr}{r} - 2l_{n_a s}n_a\int_0^R \Im\,(r\,|\,n_a-\tfrac{1}{2},\,n_a+\tfrac{1}{2},s)\;\Im\,(r\,|\,n_a+\tfrac{1}{2},\,n_a+\tfrac{1}{2},s)\,dr + l_{n_a s}^2\int_0^R [\,\Im\,(r\,|\,n_a-\tfrac{1}{2},\,n_a+\tfrac{1}{2},s)\,]^2\,r\,dr \Big\}. \tag{52}$$

III. THE INITIAL FIELD

As the initial field we shall choose the simplest possible poloidal decay field S_{11}^0. This is an axially symmetrical field and therefore does not depend upon the variable ϕ. Its generating function has no node inside the sphere, and outside the sphere the field is a dipole field.

For this case the generating function is

$$\psi_{11}^0 = C\left(\frac{R}{r}\right)^{1/2} J_{3/2}\,(k_{11}r)\,P_1\,(\theta) \tag{53}$$

inside the sphere, and

$$\psi_{11}^0 = C\left(\frac{R}{r}\right)^{2} J_{3/2}\,(k_{11}R)\,P_1\,(\theta) \tag{54}$$

outside the sphere. The constant C can be expressed in terms of the polar value of the field, H_p, at the surface of the sphere (that is, the field at the point $r = R$, $\theta = 0$); then

$$C = \frac{H_p}{2J_{3/2}\,(k_{11}R)} = \frac{\pi H_p}{2^{3/2}} \qquad \left(\text{since } J_{3/2}\,[k_{11}R] = \frac{2^{1/2}}{\pi}\right), \tag{55}$$

and the expression for ψ_{11}^0 becomes

$$\psi_{11}^0 = \frac{\pi H_p}{2^{3/2}}\left(\frac{R}{r}\right)^{1/2} J_{3/2}\,(k_{11}r)\,P_1\,(\theta) \qquad \text{(inside)} \tag{56}$$

and

$$\psi_{11}^0 = \frac{H_p}{2}\left(\frac{R}{r}\right)^{2} P_1\,(\theta) \qquad \text{(outside)}. \tag{57}$$

The corresponding expressions for the components of the initial field then are, according to equation (9), given by

$$(\boldsymbol{S}_{11}^0)_r = \frac{\pi}{2^{1/2}}\,H_p\left(\frac{R}{r}\right)^{3/2} J_{3/2}\,(k_{11}r)\cos\Theta, \tag{58a}$$

$$(S^0_{11})_\theta = -\frac{\pi}{2^{3/2}} H_p \frac{R^{3/2}}{r} \frac{d}{dr} [r^{1/2} J_{3/2}(k_{11} r)] \sin\theta , \tag{58b}$$

and

$$(S^0_{11})_\phi = 0 \tag{58c}$$

inside, and

$$S^0_{11} = \left[H_p \left(\frac{R}{r}\right)^3 \cos\theta , \frac{H_p}{2} \left(\frac{R}{r}\right)^3 \sin\theta , 0 \right] \tag{59}$$

outside the sphere.

IV. MATRIX ELEMENTS AND THE SELECTION RULES

In the following discussion of toroidal oscillations when the initial field is an S^0_{11} field, we shall encounter matrix elements of the following forms:

$$\int \boldsymbol{T}(\alpha) \times \boldsymbol{S}^0_{11} \cdot \boldsymbol{T}^*(\beta)\, dv , \qquad \int \boldsymbol{T}^0_{11} \times \boldsymbol{S}(\alpha) \cdot \boldsymbol{T}^*(\beta)\, dv , \tag{60a, b}$$

$$\int \mathfrak{T}(\alpha) \times \boldsymbol{S}^0_{11} \cdot \mathfrak{T}^*(\beta)\, dv , \qquad \int \boldsymbol{T}^0_{11} \times \mathfrak{S}(\alpha) \cdot \mathfrak{T}^*(\beta)\, dv , \tag{61a, b}$$

$$\int \boldsymbol{T}(\alpha) \times \boldsymbol{S}^0_{11} \cdot \boldsymbol{S}^*(\beta)\, dv = -\int \boldsymbol{S}^*(\beta) \times \boldsymbol{S}^0_{11} \cdot \boldsymbol{T}(\alpha)\, dv \tag{62a}$$

and

$$\int \mathfrak{T}(\alpha) \times \boldsymbol{S}^0_{11} \cdot \mathfrak{S}^*(\beta)\, dv = -\int \mathfrak{S}^*(\beta) \times \boldsymbol{S}^0_{11} \cdot \mathfrak{T}(\alpha)\, dv , \tag{62b}$$

where the integrations are to be carried out over the interior of the sphere. In Elsasser's notations these matrix elements are

$$\begin{aligned} &[\boldsymbol{T}(\alpha) \times \boldsymbol{S}^0_{11} \cdot \boldsymbol{T}^*(\beta)] , \qquad [\boldsymbol{T}^0_{11} \times \boldsymbol{S}(\alpha) \cdot \boldsymbol{T}^*(\beta)] , \\ &[\mathfrak{T}(\alpha) \times \boldsymbol{S}^0_{11} \cdot \mathfrak{T}^*(\beta)] , \qquad [\boldsymbol{T}^0_{11} \times \mathfrak{S}(\alpha) \cdot \mathfrak{T}^*(\beta)] , \\ &[\boldsymbol{T}(\alpha) \times \boldsymbol{S}^0_{11} \cdot \boldsymbol{S}^*(\beta)] , \qquad [\mathfrak{T}(\alpha) \times \boldsymbol{S}^0_{11} \cdot \mathfrak{S}^*(\beta)] , \end{aligned} \tag{63}$$

respectively.

Considering the first of these matrix elements, we have

$$\begin{aligned} [\boldsymbol{T}(\alpha) \times \boldsymbol{S}^0_{11} \cdot \boldsymbol{T}^*(\beta)] &= 2R \iiint \psi^0_{11} \left\{ \frac{\partial \psi(\alpha)}{\partial \phi} \frac{\partial \psi^*(\beta)}{\partial \theta} - \frac{\partial \psi(\alpha)}{\partial \theta} \frac{\partial \psi^*(\beta)}{\partial \phi} \right\} \\ &\times r\, dr\, d\theta\, d\phi = \frac{H_p}{R^{1/2} 2^{3/2}} \frac{1}{\Im(R \mid n_\alpha + \frac{1}{2}, n_\alpha - \frac{1}{2}, s)\, \Im(R \mid n_\beta + \frac{1}{2}, n_\beta - \frac{1}{2}, s)} \\ &\times \left[\frac{(2n_\alpha + 1)(2n_\beta + 1)(n_\alpha - m_\alpha)!\,(n_\beta - m_\beta)!}{n_\alpha (n_\alpha + 1)\, n_\beta (n_\beta + 1)(n_\alpha + m_\alpha)!\,(n_\beta + m_\beta)!} \right]^{1/2} \\ &\times \int_0^R r^{-1/2} J_{3/2}(k_{11} r)\, \Im(r \mid n_\alpha + \tfrac{1}{2}, n_\alpha - \tfrac{1}{2}, s)\, \Im(r \mid n_\beta + \tfrac{1}{2}, n_\beta - \tfrac{1}{2}, s)\, dr \\ &\times \int_0^\pi P_1 \left\{ i m_\alpha P^{m_\alpha}_{n_\alpha} \frac{dP^{m_\beta}_{n_\beta}}{d\theta} + i m_\beta P^{m_\beta}_{n_\beta} \frac{dP^{m_\alpha}_{n_\alpha}}{d\theta} \right\} d\theta \times \int_0^{2\pi} e^{i(m_\alpha - m_\beta)\phi} d\phi , \end{aligned} \tag{64}$$

on substituting for the different functions from equations (14) and (15) and using expressions (26) and (56) for the generating functions.

The integral over ϕ in equation (64) is seen to vanish if $m_\alpha \neq m_\beta$. We therefore have the selection rule $m_\alpha = m_\beta \neq 0$. Next, considering the integral over θ, we have

$$\int_0^\pi P_1 \left\{ P^{m_\alpha}_{n_\alpha} \frac{dP^{m_\alpha}_{n_\beta}}{d\theta} + P^{m_\alpha}_{n_\beta} \frac{dP^{m_\alpha}_{n_\alpha}}{d\theta} \right\} d\theta = \int_0^\pi P_1 \frac{d}{d\theta} (P^{m_\alpha}_{n_\alpha} P^{m_\alpha}_{n_\beta})\, d\theta . \tag{65}$$

After an integration by parts, the foregoing becomes

$$P_1 P_{n_\alpha}^{m_\alpha} P_{n_\beta}^{m_\alpha} \Big|_0^\pi - \int_0^\pi \frac{dP_1}{d\theta} P_{n_\alpha}^{m_\alpha} P_{n_\beta}^{m_\alpha} d\theta . \tag{66}$$

Since $m_\alpha > 0$, the first term will vanish, and, since $dP_1/d\theta = -\sin\theta$, the expression reduces to

$$\int_0^\pi P_{n_\alpha}^{m_\alpha} P_{n_\beta}^{m_\alpha} \sin\theta \, d\theta . \tag{67}$$

Because of the orthogonality of the functions P_n^m, this integral will vanish except when $n_\alpha = n_\beta$. The only nonvanishing matrix element of type (60a), therefore, is

$$\begin{aligned}[\boldsymbol{T}(\alpha) \times \boldsymbol{S}_{11}^0 \cdot \boldsymbol{T}^*(\alpha)] &= \frac{2\pi i m_\alpha H_p}{R^{1/2} 2^{3/2} [\Im(R \mid n_\alpha + \tfrac{1}{2}, n_\alpha - \tfrac{1}{2}, s)]^2} \frac{(2n_\alpha + 1)(n_\alpha - m_\alpha)!}{n_\alpha (n_\alpha + 1)(n_\alpha + m_\alpha)!} \\ &\times \int_0^R r^{-1/2} J_{3/2}(k_{11} r) [\Im(r \mid n_\alpha + \tfrac{1}{2}, n_\alpha - \tfrac{1}{2}, s)]^2 dr \times \int_0^\pi (P_{n_\alpha}^{m_\alpha})^2 \sin\theta \, d\theta \, d\theta \\ &= \frac{2^{1/2} \pi i m_\alpha H_p}{n_\alpha (n_\alpha + 1) R^{1/2} [\Im(R \mid n_\alpha + \tfrac{1}{2}, n_\alpha - \tfrac{1}{2}, s)]^2} \\ &\times \int_0^R r^{-1/2} J_{3/2}(k_{11} r) [\Im(r \mid n_\alpha + \tfrac{1}{2}, n_\alpha - \tfrac{1}{2}, s)]^2 dr .\end{aligned} \tag{68}$$

The matrix elements of type (60b) may be reduced similarly, and it will further appear that there exists a very simple relation between these two types of matrix elements. From the same equations as in the previous case, we have

$$\begin{aligned}[\boldsymbol{T}_{11}^0 \times \boldsymbol{S}(\alpha) \cdot \boldsymbol{T}^*(\beta)] &= n_\alpha (n_\alpha + 1) R \iiint \psi(\alpha) \left\{ \frac{\partial \psi_{11}^0}{\partial \phi} \frac{\partial \psi^*(\beta)}{\partial \theta} - \frac{\partial \psi_{11}^0}{\partial \theta} \frac{\partial \psi^*(\beta)}{\partial \phi} \right\} \\ &\times r \, dr \, d\phi \, d\theta = -n_\alpha (n_\alpha + 1) R \iiint \psi(\alpha) \frac{\partial \psi_{11}^0}{\partial \theta} \frac{\partial \psi^*(\beta)}{\partial \phi} \, r \, dr \, d\theta \, d\phi \\ &= \frac{\pi i m_\beta n_\alpha (n_\alpha + 1) H_p}{2^{3/2} R^{1/2}} \left[\frac{(2n_\alpha + 1)(2n_\beta + 1)(n_\alpha - m_\alpha)!(n_\beta - m_\beta)!}{4\pi^2 n_\alpha (n_\alpha + 1) n_\beta (n_\beta + 1)(n_\alpha + m_\alpha)!(n_\beta + m_\beta)!} \right]^{1/2} \\ &\times \frac{1}{\Im(R \mid n_\alpha + \tfrac{1}{2}, n_\alpha - \tfrac{1}{2}, s) \, \Im(R \mid n_\beta + \tfrac{1}{2}, n_\beta - \tfrac{1}{2}, s)} \\ &\times \int_0^R r^{-1/2} J_{3/2}(k_{11} r) \, \Im(r \mid n_\alpha + \tfrac{1}{2}, n_\alpha - \tfrac{1}{2}, s) \, \Im(r \mid n_\beta + \tfrac{1}{2}, n_\beta - \tfrac{1}{2}, s) \, dr \\ &\times \int_0^\pi P_{n_\alpha}^{m_\alpha} P_{n_\beta}^{m_\beta} \frac{dP_1}{d\theta} \, d\theta \times \int_0^{2\pi} e^{i(m_\alpha - m_\beta)\phi} d\phi .\end{aligned} \tag{69}$$

Again the integral over ϕ leads to a vanishing integral unless $m_\alpha = m_\beta \neq 0$. Similarly, for the integration over θ to lead to a finite result, it is necessary that $n_\alpha = n_\beta$. The nonvanishing matrix element of type (60b), therefore, is

$$\begin{aligned}[\boldsymbol{T}_{11}^0 \times \boldsymbol{S}(\alpha) \cdot \boldsymbol{T}^*(\alpha)] &= -\frac{\pi i m_\alpha H_p}{2^{1/2} R^{1/2} [\Im(R \mid n_\alpha + \tfrac{1}{2}, n_\alpha - \tfrac{1}{2}, s)]^2} \\ &\times \int_0^R r^{-1/2} J_{3/2}(k_{11} r) [\Im(r \mid n_\alpha + \tfrac{1}{2}, n_\alpha - \tfrac{1}{2}, s)]^2 dr .\end{aligned} \tag{70}$$

Comparing this with equation (68), we have the following relation:

$$[\boldsymbol{T}(a) \times \boldsymbol{S}_{11}^{0} \cdot \boldsymbol{T}^{*}(a)] = -\frac{2}{n_a(n_a+1)} [\boldsymbol{T}_{11}^{0} \cdot \boldsymbol{S}(a) \times \boldsymbol{T}^{*}(a)]. \tag{71}$$

We shall find this relation useful in the subsequent work.

Consider next the matrix element (61*a*). From equations (15) and (42) (cf. eq. [64]) we have

$$[\mathfrak{T}(a) \times \boldsymbol{S}_{11}^{0} \cdot \mathfrak{T}^{*}(\beta)] = 2R \iiint \psi_{11}^{0} \left\{ \frac{\partial \Phi(a)}{\partial \phi} \frac{\partial \Phi^{*}(\beta)}{\partial \theta} - \frac{\partial \Phi(a)}{\partial \theta} \frac{\partial \Phi^{*}(\beta)}{\partial \phi} \right\} r\, dr\, d\theta\, d\phi. \tag{72}$$

Introducing from equations (48) and (56) for the generating function, we obtain

$$\begin{aligned}
&[\mathfrak{T}(a) \times \boldsymbol{S}_{11}^{0} \cdot \mathfrak{T}^{*}(\beta)] \\
&= \frac{2\pi H_p}{2^{3/2} R^{1/2}} \frac{1}{[-\Im(R \mid n_a - \tfrac{1}{2}, n_a + \tfrac{1}{2}, s)\, \Im(R \mid n_a + \tfrac{3}{2}, n_a + \tfrac{1}{2}, s)]^{1/2}} \\
&\times \frac{1}{[-\Im(R \mid n_\beta - \tfrac{1}{2}, n_\beta + \tfrac{1}{2}, s)\, \Im(R \mid n_\beta + \tfrac{3}{2}, n_\beta + \tfrac{1}{2}, s)]^{1/2}} \\
&\times \left[\frac{(2n_a+1)(2n_\beta+1)(n_a - m_a)!\,(n_\beta - m_\beta)!}{4\pi^2 n_a (n_a+1)\, n_\beta (n_\beta+1)(n_a + m_a)!\,(n_\beta + m_\beta)!} \right]^{1/2} \\
&\times \int_0^R r^{-1/2} J_{3/2}(k_{11} r)\, \Im(r \mid n_a + \tfrac{1}{2}, n_a + \tfrac{1}{2}, s)\, \Im(r \mid n_\beta + \tfrac{1}{2}, n_\beta + \tfrac{1}{2}, s)\, dr \\
&\times \int_0^\pi P_1 \left\{ i m_a P_{n_a}^{m_a} \frac{dP_{n_\beta}^{m_\beta}}{d\theta} + i m_\beta \frac{dP_{n_a}^{m_a}}{d\theta} P_{n_\beta}^{m_\beta} \right\} d\theta \times \int_0^{2\pi} e^{i(m_a - m_\beta)\phi} d\phi.
\end{aligned} \tag{73}$$

Now, since the integrals over θ and ϕ are the same as in equation (64), the same selection rules apply, and the conditions for the matrix element not to vanish are $m_a = m_\beta \neq 0$ and $n_a = n_\beta$. The only nonvanishing matrix elements of type (61*a*) are therefore of the form

$$\begin{aligned}
[\mathfrak{T}(a) \times \boldsymbol{S}_{11}^{0} \cdot \mathfrak{T}^{*}(a)] &= \frac{2^{1/2} \pi i m_a H_p}{R^{1/2} n_a (n_a+1)} \\
&\times \frac{1}{[-\Im(R \mid n_a - \tfrac{1}{2}, n_a + \tfrac{1}{2}, s)\, \Im(R \mid n_a + \tfrac{3}{2}, n_a + \tfrac{1}{2}, s)]} \\
&\times \int_0^R r^{-1/2} J_{3/2}(k_{11} r) [\Im(r \mid n_a + \tfrac{1}{2}, n_a + \tfrac{1}{2}, s)]^2 dr.
\end{aligned} \tag{74}$$

Similarly, we find that the only nonvanishing matrix elements of type (61*b*) are

$$\begin{aligned}
[\boldsymbol{T}_{11}^{t} \times \mathfrak{S}(a) \cdot \mathfrak{T}^{*}(a)] &= -\frac{\pi i m_a H_p}{2^{1/2} R^{1/2}} \\
&\times \frac{1}{[-\Im(R \mid n_a - \tfrac{1}{2}, n_a + \tfrac{1}{2}, s)\, \Im(R \mid n_a + \tfrac{3}{2}, n_a + \tfrac{1}{2}, s)]} \\
&\times \int_0^R r^{-1/2} J_{3/2}(k_{11} r) [\Im(r \mid n_a + \tfrac{1}{2}, n_a + \tfrac{1}{2}, s)]^2 dr.
\end{aligned} \tag{75}$$

Between matrix elements (74) and (75) we have a relation analogous to equation (71), namely,

$$[\mathfrak{T}(a) \times \boldsymbol{S}^0_{11} \cdot \mathfrak{T}^*(a)] = -\frac{2}{n_a(n_a+1)} [\boldsymbol{T}^0_{11} \times \mathfrak{S}(a) \cdot \mathfrak{T}^*(a)]. \tag{76}$$

The last two types of matrix elements, as given in equations (62*a*) and (62*b*), are somewhat more complicated than the previous ones and lead to other selection rules. We shall now consider the properties of these elements in detail. Starting with elements of the form (62*a*), we have, according to the definitions given in equations (14) and (15),

$$\begin{aligned}
&[\boldsymbol{T}(i) \times \boldsymbol{S}^0_{11} \cdot \boldsymbol{S}^*(\beta)] \\
&\quad = n_\beta(n_\beta+1) R^2 \iiint \frac{\partial}{\partial r}\left(r \frac{\partial \psi^0_{11}}{\partial \theta}\right) \frac{\partial \psi(i)}{\partial \theta} \psi^*(\beta) \sin\theta \, d\theta \, d\theta \, d\phi \, dr \\
&\quad - 2R^2 \iiint \frac{\partial}{\partial r}\left[r \frac{\partial \psi^*(\beta)}{\partial \theta}\right] \frac{\partial \psi(i)}{\partial \theta} \psi^0_{11} \sin\theta \, d\theta \, d\theta \, d\phi \, dr \\
&\quad - 2R^2 \iiint \frac{\partial}{\partial r}\left[r \frac{\partial \psi^*(\beta)}{\partial \phi}\right] \frac{\partial \psi(i)}{\partial \phi} \psi^0_{11} \frac{1}{\sin\theta} \, d\theta \, d\phi \, dr .
\end{aligned} \tag{77}$$

We shall first evaluate the first term on the right-hand side and then treat the two following terms together. For the first term we get, using the generating functions given in equations (26) and (56) (see also eq. [29]),

$$\begin{aligned}
&n_\beta(n_\beta+1) R^2 M_\beta M_i M^0_{11} \int_0^R \frac{d}{dr}[r^{1/2} J_{3/2}(k_{11} r)] \, \Im(r \mid n_i + \tfrac{1}{2}, n_i - \tfrac{1}{2}, s) \\
&\times \Im(r \mid n_\beta + \tfrac{1}{2}, n_\beta - \tfrac{1}{2}, s) \frac{dr}{r} \times \int_0^\pi \frac{dP_1}{d\theta} \frac{dP^{m_i}_{n_i}}{d\theta} P^{m_\beta}_{n_\beta} \sin\theta \, d\theta \times \int_0^{2\pi} e^{i(m_i - m_\beta)\phi} d\phi .
\end{aligned} \tag{78}$$

We must at once add one important remark: In the following we are interested only in cases where $m \neq 0$. We thus exclude the cases of axial symmetry. Thus we find the selection rule $m_\beta = m_i \neq 0$. Using equation (38), we get, for the integral over r in equation (78), the expression

$$\begin{aligned}
&\int_0^R \frac{d}{dr}[r^{1/2} J_{3/2}(k_{11} r)] \, \Im(r \mid n_i + \tfrac{1}{2}, n_i - \tfrac{1}{2}, s) \, \Im(r \mid n_\beta + \tfrac{1}{2}, n_\beta - \tfrac{1}{2}, s) \frac{dr}{r} \\
&\quad = k_{11} \int_0^R J_{1/2}(k_{11} r) \, \Im(r \mid n_i + \tfrac{1}{2}, n_i - \tfrac{1}{2}, s) \, \Im(r \mid n_\beta + \tfrac{1}{2}, n_\beta - \tfrac{1}{2}, s) \frac{dr}{r^{1/2}} \\
&\quad - \int_0^R J_{3/2}(k_{11} r) \, \Im(r \mid n_i + \tfrac{1}{2}, n_i - \tfrac{1}{2}, s) \, \Im(r \mid n_\beta + \tfrac{1}{2}, n_\beta - \tfrac{1}{2}, s) \frac{dr}{r^{3/2}} .
\end{aligned} \tag{79}$$

The integral over θ in equation (78) becomes

$$\begin{aligned}
\int_0^\pi \frac{dP_1}{d\theta} \frac{dP^{m_i}_{n_i}}{d\theta} P^{m_i}_{n_\beta} \sin\theta \, d\theta &= \int_{-1}^{+1} \frac{dP_1}{dx} \frac{dP^{m_i}_{n_i}}{dx} P^{m_i}_{n_\beta} (1-x^2) \, dx \\
&= \int_{-1}^{+1} \frac{dP^{m_i}_{n_i}}{dx} P^{m_i}_{n_\beta} (1-x^2) \, dx .
\end{aligned} \tag{80}$$

Here we have introduced the new variable $x = \cos\theta$, making $dP_1/dx = 1$. For the associated Legendre functions we have the following recurrence relations (Bateman 1932, p. 360):

$$(1-x^2)\frac{dP_n^m}{dx} = -nxP_n^m + (n+m)P_{n-1}^m,$$
$$xP_n^m = \frac{1}{2n+1}[(n+m)P_{n-1}^m + (n-m+1)P_{n+1}^m]. \quad (81a, b)$$

When these are combined, we get

$$(1-x^2)\frac{dP_n^m}{dx} = -\frac{n}{2n+1}[(n+m)P_{n-1}^m + (n-m+1)P_{n+1}^m] + (n+m)P_{n-1}^m$$
$$= -\frac{n(n-m+1)}{2n+1}P_{n+1}^m + \frac{(n+m)(n+1)}{2n+1}P_{n-1}^m. \quad (82)$$

The integral over θ in equation (78) therefore reduces to

$$\int_{-1}^{+1}\frac{dP_{n_i}^{m_i}}{dx}P_{n_\beta}^{m_i}(1-x^2)\,dx = -\frac{n_i(n_i-m_i+1)}{2n_i+1}\int_{-1}^{+1}P_{n_i+1}^{m_i}P_{n_\beta}^{m_i}dx$$
$$+\frac{(n_i+m_i)(n_i+1)}{2n_i+1}\int_{-1}^{+1}P_{n_i-1}^{m_i}P_{n_\beta}^{m_i}dx. \quad (83)$$

From this we get the following selection rule for n, $n_\beta = n_i + 1$, or $n_\beta = n_i - 1$:
In case $n_\beta = n_i + 1$ the integral over θ becomes

$$\int_{-1}^{+1}\frac{dP_{n_i}^{m_i}}{dx}P_{n_i+1}^{m_i}(1-x^2)\,dx = -\frac{n_i(n_i-m_i+1)}{2n_i+1}\int_{-1}^{+1}(P_{n_i+1}^{m_i})^2dx$$
$$= -\frac{n_i(n_i-m_i+1)}{2n_i+1}\frac{2}{2n_i+3}\frac{(n_i+1+m_i)!}{(n_i+1-m_i)!} \quad (84)$$
$$= -\frac{2}{(2n_i+1)(2n_i+3)}\frac{n_i(n_i+m_i+1)!}{(n_i-m_i)!}.$$

When $n_\beta = n_i - 1$, we get

$$\int_{-1}^{+1}\frac{dP_{n_i}^{m_i}}{dx}P_{n_i-1}^{m_i}(1-x^2)\,dx = \frac{(n_i+m_i)(n_i+1)}{2n_i+1}\frac{2}{2n_i-1}\frac{(n_i-1+m_i)!}{(n_i-1-m_i)!}$$
$$= \frac{2}{(2n_i-1)(2n_i+1)}\frac{(n_i+1)(n_i+m_i)!}{(n_i-m_i-1)!}. \quad (85)$$

The last two terms in equation (77) have the integral over r in common, and they are therefore treated together. For the sum we obtain

$$-2R^2\iiint\left\{\frac{\partial}{\partial r}\left[r\frac{\partial\psi^*(\beta)}{\partial\theta}\right]\frac{\partial\psi(i)}{\partial\theta}\psi_{11}^0 + \frac{1}{\sin^2\theta}\frac{\partial}{\partial r}\left[r\frac{\partial\psi^*(\beta)}{\partial\phi}\right]\frac{\partial\psi(i)}{\partial\phi}\psi_{11}^0\right\}$$
$$\times\sin\theta\,d\theta\,d\phi\,dr = -2M_\beta M_i M_{11}^0 R^2$$
$$\times\int_0^R\frac{d}{dr}[r^{1/2}\Im(r\mid n_\beta+\tfrac{1}{2},\, n_\beta-\tfrac{1}{2},\, s)]\,\Im(r\mid n_i+\tfrac{1}{2},\, n_i-\tfrac{1}{2},\, s)J_{3/2}(k_{11}r)\frac{dr}{r} \quad (86)$$
$$\times\int_0^\pi\left\{\frac{dP_{n_\beta}^{m_\beta}}{d\theta}\frac{dP_{n_i}^{m_i}}{d\theta} + \frac{m_i m_\beta}{\sin^2\theta}P_{n_\beta}^{m_\beta}P_{n_i}^{m_i}\right\}P_1\sin\theta\,d\theta\times\int_0^{2\pi}e^{i(m_i-m_\beta)\phi}d\phi.$$

Here we have written M_{11}^0 instead of $R^{1/2}C$ (cf eq. [53]). The integral over r is reduced in the same way as before, and the result is

$$\int_0^R \frac{d}{dr}\left[r^{1/2}\Im\left(r \mid n_\beta+\tfrac{1}{2}, n_\beta-\tfrac{1}{2}, s\right)\right]\Im\left(r \mid n_i+\tfrac{1}{2}, n_i-\tfrac{1}{2}, s\right)J_{3/2}(k_{11}r)\frac{dr}{r}$$

$$= k_{n_\beta s}\int_0^R \Im\left(r \mid n_\beta-\tfrac{1}{2}, n_\beta-\tfrac{1}{2}, s\right)\Im\left(r \mid n_i+\tfrac{1}{2}, n_i-\tfrac{1}{2}, s\right)J_{3/2}(k_{11}r)\frac{dr}{r^{1/2}} \quad (87)$$

$$- n_\beta\int_0^R \Im\left(r \mid n_\beta+\tfrac{1}{2}, n_\beta-\tfrac{1}{2}, s\right)\Im\left(r \mid n_i+\tfrac{1}{2}, n_i-\tfrac{1}{2}, s\right)J_{3/2}(k_{11}r)\frac{dr}{r^{3/2}}.$$

The integral over θ in equation (86) takes the following form, when the selection rule $m_\beta = m_i$ is applied:

$$\int_0^\pi\left\{\frac{dP_{n_\beta}^{m_i}}{d\theta}\frac{dP_{n_i}^{m_i}}{d\theta}+\frac{m_i^2}{\sin^2\theta}P_{n_\beta}^{m_i}P_{n_i}^{m_i}\right\}P_1\sin\theta\, d\theta \quad (88)$$

$$= \int_{-1}^{+1}\left\{\frac{dP_{n_\beta}^{m_i}}{dx}\frac{dP_{n_i}^{m_i}}{dx}(1-x^2)+\frac{m_i^2}{1-x^2}P_{n_\beta}^{m_i}P_{n_i}^{m_i}\right\}x\,dx.$$

From the differential equation for P_n^m we get (cf. eq. [35])

$$\frac{m^2}{1-x^2}P_n^m = \frac{d}{dx}\left[(1-x^2)\frac{dP_n^m}{dx}\right]+n(n+1)P_n^m. \quad (89)$$

When this is introduced for $P_{n_i}^{m_i}$, the result is, after one integration by parts,

$$\int_{-1}^{+1}\left\{\frac{dP_{n_\beta}^{m_i}}{dx}\frac{dP_{n_i}^{m_i}}{dx}(1-x^2)+\frac{d}{dx}\left[(1-x^2)\frac{dP_{n_i}^{m_i}}{dx}\right]P_{n_\beta}^{m_i}+n_i(n_i+1)P_{n_i}^{m_i}P_{n_\beta}^{m_i}\right\}x\,dx$$

$$= \int_{-1}^{+1}\left\{\frac{d}{dx}\left[(1-x^2)\frac{dP_{n_i}^{m_i}}{dx}P_{n_\beta}^{m_i}\right]+n_i(n_i+1)P_{n_i}^{m_i}P_{n_\beta}^{m_i}\right\}x\,dx \quad (90)$$

$$= (1-x^2)\,x\frac{dP_{n_i}^{m_i}}{dx}P_{n_\beta}^{m_i}\Big|_{-1}^{+1}-\int_{-1}^{+1}(1-x^2)\frac{dP_{n_i}^{m_i}}{dx}P_{n_\beta}^{m_i}dx$$

$$+ n_i(n_i+1)\int_{-1}^{+1}P_{n_i}^{m_i}P_{n_\beta}^{m_i}x\,dx.$$

Applying the recurrence relation as expressed in equation (82) in the first integral on the right-hand side and equation (81*b*) in the second, we get

$$-\int_{-1}^{+1}P_{n_\beta}^{m_i}\left\{-\frac{n_i(n_i-m_i+1)}{2n_i+1}P_{n_i+1}^{m_i}+\frac{(n_i+m_i)(n_i+1)}{2n_i+1}P_{n_i-1}^{m_i}\right\}dx$$

$$+ n_i(n_i+1)\int_{-1}^{+1}P_{n_\beta}^{m_i}\left\{\frac{n_i+m_i}{2n_i+1}P_{n_i-1}^{m_i}+\frac{(n_i-m_i+1)}{2n_i+1}P_{n_i+1}^{m_i}\right\}dx \quad (91)$$

$$= \frac{(n_i+1)(n_i-1)(n_i+m_i)}{2n_i+1}\int_{-1}^{+1}P_{n_\beta}^{m_i}P_{n_i-1}^{m_i}dx$$

$$+\frac{n_i(n_i+2)(n_i-m_i+1)}{2n_i+1}\int_{-1}^{+1}P_{n_\beta}^{m_i}P_{n_i+1}^{m_i}dx.$$

The selection rules are thus the same as in the previous case, $n_\beta = n_i + 1$ or $n_\beta = n_i - 1$. When $n_\beta = n_i + 1$, we have, for the integral over θ in equation (86),

$$\int_{-1}^{+1}\left\{\frac{dP_{n_i+1}^{m_i}}{dx}\frac{dP_{n_i}^{m_i}}{dx}(1-x^2)+\frac{m_i^2}{1-x^2}P_{n_i+1}^{m_i}P_{n_i}^{m_i}\right\}dx$$

$$=\frac{n_i(n_i+2)(n_i-m_i+1)}{2n_i+1}\int_{-1}^{+1}(P_{n_i+1}^{m_i})^2dx \quad (92)$$

$$=\frac{2n_i(n_i+2)}{(2n_i+1)(2n_i+3)}\frac{(n_i+m_i+1)!}{(n_i-m_i)!},$$

and, for $n_\beta = n_i - 1$,

$$\int_{-1}^{+1}\left\{\frac{dP_{n_i-1}^{m_i}}{dx}\frac{dP_{n_i}^{m_i}}{dx}(1-x^2)+\frac{m_i^2}{1-x^2}P_{n_i-1}^{m_i}P_{n_i}^{m_i}\right\}x\,dx$$

$$=\frac{(n_i+1)(n_i-1)(n_i+m_i)}{2n_i+1}\int_{-1}^{+1}(P_{n_i-1}^{m_i})^2dx \quad (93)$$

$$=\frac{2(n_i-1)(n_i+1)}{(2n_i-1)(2n_i+1)}\frac{(n_i+m_i)!}{(n_i-m_i-1)!}.$$

We have found that the only two types of matrix elements (62*a*) which do not vanish are

$$[\boldsymbol{T}_{ns}^m\times\boldsymbol{S}_{11}^0\cdot\boldsymbol{S}_{n+1,\,s}^{m*}] \quad \text{and} \quad [\boldsymbol{T}_{ns}^m\times\boldsymbol{S}_{11}^0\cdot\boldsymbol{S}_{n-1,\,s}^{m*}]\,. \quad (94)$$

Using equations (79), (84), (85), (87), (92), and (93) as well as (29) and (56), we can write down the explicit expressions for these two types of matrix elements. We have

$$[\boldsymbol{T}_{ns}^m\times\boldsymbol{S}_{11}^0\cdot\boldsymbol{S}_{n+1,\,s}^{m*}]=2\pi(n+1)(n+2)R^2M_{n+1,\,s}^mM_{n,\,s}^mM_{11}^0$$

$$\times\left\{k_{11}\int_0^R J_{1/2}(k_{11}r)\,\Im(r\,|\,n+\tfrac12,n-\tfrac12,s)\,\Im(r\,|\,n+\tfrac32,n+\tfrac12,s)\frac{dr}{r^{1/2}}\right.$$

$$\left.-\int_0^R J_{3/2}(k_{11}r)\,\Im(r\,|\,n+\tfrac12,n-\tfrac12,s)\,\Im(r\,|\,n+\tfrac32,n+\tfrac12,s)\frac{dr}{r^{3/2}}\right\}$$

$$\times\int_0^\pi\frac{dP_1}{d\theta}\frac{dP_n^m}{d\theta}P_{n+1}^m\sin\theta\,d\theta-4\pi R^2M_{n+1,\,s}^mM_{ns}^mM_{11}^0$$

$$\times\left\{k_{n+1\ s}\int_0^R J_{3/2}(k_{11}r)\,\Im(r\,|\,n+\tfrac12,n+\tfrac12,s)\,\Im(r\,|\,n+\tfrac12,n-\tfrac12,s)\frac{dr}{r^{1/2}}\right.$$

$$\left.-(n+1)\int_0^R J_{3/2}(k_{11}r)\,\Im(r\,|\,n+\tfrac32,n+\tfrac12,s)\,\Im(r\,|\,n+\tfrac12,n-\tfrac12,s)\frac{dr}{r^{3/2}}\right\} \quad (95)$$

$$\times\int_0^\pi\left\{\frac{dP_{n+1}^m}{d\theta}\frac{dP_n^m}{d\theta}+\frac{m^2}{\sin^2\theta}P_{n+1}^mP_n^m\right\}P_1\sin\theta\,d\theta$$

$$=-\frac{4\pi n(n+2)(n+m+1)!}{(2n+1)(2n+3)(n-m)!}M_{11}^0M_{ns}^mM_{n+1,\,s}^mR^2$$

$$\times\left\{(n+1)\,k_{11}\int_0^R J_{1/2}(k_{11}r)\,\Im(r\,|\,n+\tfrac12,n-\tfrac12,s)\,\Im(r\,|\,n+\tfrac32,n+\tfrac12,s)\frac{dr}{r^{1/2}}\right.$$

$$+2k_{n+1,\,s}\int_0^R J_{3/2}(k_{11}r)\,\Im(r\,|\,n+\tfrac12,n-\tfrac12,s)\,\Im(r\,|\,n+\tfrac12,n+\tfrac12,s)\frac{dr}{r^{1/2}}$$

$$\left.-3(n+1)\int_0^R J_{3/2}(k_{11}r)\,\Im(r\,|\,n+\tfrac12,n-\tfrac12,s)\,\Im(r\,|\,n+\tfrac32,n+\tfrac12,s)\frac{dr}{r^{3/2}}\right\}.$$

Similarly, we get

$$[\boldsymbol{T}^m_{ns} \times \boldsymbol{S}^0_{11} \cdot \boldsymbol{S}^{m*}_{n-1,\,s}] = \frac{4\pi (n-1)(n+1)(n+m)!}{(2n-1)(2n+1)(n-m-1)!} M^0_{11} M^m_{n-1\,s} M^m_{ns}$$
$$\times \Big\{ n k_{11} \int_0^R J_{1/2}(k_{11} r)\, \Im(r \mid n-\tfrac{1}{2}, n-\tfrac{3}{2}, s)\, \Im(r \mid n+\tfrac{1}{2}, n-\tfrac{1}{2}, s) \frac{dr}{r^{1/2}}$$
$$- 2 k_{n-1,\,s} \int_0^R J_{3/2}(k_{11} r)\, \Im(r \mid n-\tfrac{3}{2}, n-\tfrac{3}{2}, s)\, \Im(r \mid n+\tfrac{1}{2}, n-\tfrac{1}{2}, s) \frac{dr}{r^{1/2}} \tag{96}$$
$$+ (n-2) \int_0^R J_{3/2}(k_{11} r)\, \Im(r \mid n-\tfrac{1}{2}, n-\tfrac{3}{2}, s)\, \Im(r \mid n+\tfrac{1}{2}, n-\tfrac{1}{2}, s) \frac{dr}{r^{3/2}} \Big\}.$$

For matrix elements of type (62*b*) we get the following expression in terms of the generating function Φ:

$$[\mathfrak{T}(i) \times \boldsymbol{S}^0_{11} \cdot \mathfrak{S}^*(\beta)]$$
$$= n_\beta (n_\beta + 1) R^2 \iiint \frac{\partial}{\partial r} \left(r \frac{\partial \psi^0_{11}}{\partial \theta} \right) \frac{\partial \Phi(i)}{\partial \theta} \Phi^*(\beta) \sin\theta\, d\theta\, d\theta\, d\phi\, dr$$
$$- 2R^2 \iiint \psi^0_{11} \frac{\partial \Phi(i)}{\partial \theta} \frac{\partial}{\partial r} \left[r \frac{\partial \Phi^*(\beta)}{\partial \theta} \right] \sin\theta\, d\theta\, d\theta\, d\phi\, dr \tag{97}$$
$$- 2R^2 \iiint \psi^0_{11} \frac{\partial \Phi(i)}{\partial \phi} \frac{\partial}{\partial r} \left[r \frac{\partial \Phi^*(\beta)}{\partial \phi} \right] \frac{1}{\sin\theta}\, d\theta\, d\phi\, dr.$$

Since the integrals over θ and ϕ are the same as in the foregoing case, the selection rules are identical. The whole procedure in the evaluation of the matrix element is quite analogous to the case we have just discussed and will therefore not be repeated here; we write down only the results in the two cases corresponding to $n_\beta = n_i + 1$ and $n_\beta = n_i - 1$. For $n_\beta = n_i + 1$ we get

$$[\mathfrak{T}^m_{ns} \times \boldsymbol{S}^0_{11} \cdot \mathfrak{S}^{m*}_{n+1,\,s}] = -\frac{4\pi n (n+2)(n+m+1)!}{(2n+1)(2n+3)(n-m)!} M^0_{11} \mathfrak{M}^m_{ns} \mathfrak{M}^m_{n+1,\,s} R^2$$
$$\times \Big\{ (n+1) k_{11} \int_0^R J_{1/2}(k_{11} r)\, \Im(r \mid n+\tfrac{1}{2}, n+\tfrac{1}{2}, s)\, \Im(r \mid n+\tfrac{3}{2}, n+\tfrac{3}{2}, s) \frac{dr}{r^{1/2}}$$
$$+ 2 l_{n+1,\,s} \int_0^R J_{3/2}(k_{11} r)\, \Im(r \mid n+\tfrac{1}{2}, n+\tfrac{1}{2}, s)\, \Im(r \mid n+\tfrac{1}{2}, n+\tfrac{3}{2}, s) \frac{dr}{r^{1/2}} \tag{98}$$
$$- 3(n+1) \int_0^R J_{3/2}(k_{11} r)\, \Im(r \mid n+\tfrac{1}{2}, n+\tfrac{1}{2}, s)\, \Im(r \mid n+\tfrac{3}{2}, n+\tfrac{3}{2}, s) \frac{dr}{r^{3/2}} \Big\}.$$

In the case $n_\beta = n_i - 1$ the result is

$$[\mathfrak{T}^m_{ns} \times \boldsymbol{S}^0_{11} \cdot \mathfrak{S}^{m*}_{n-1\;\,s}] = \frac{4\pi (n-1)(n+1)(n+m)!}{(2n-1)(2n+1)(n-m-1)!} M^0_{11} \mathfrak{M}^m_{ns} \mathfrak{M}^m_{n-1,\,s} R^2$$
$$\times \Big\{ n k_{11} \int_0^R J_{1/2}(k_{11} r)\, \Im(r \mid n+\tfrac{1}{2}, n+\tfrac{1}{2}, s)\, \Im(r \mid n-\tfrac{1}{2}, n-\tfrac{1}{2}, s) \frac{dr}{r^{1/2}}$$
$$+ (n-2) \int_0^R J_{3/2}(k_{11} r)\, \Im(r \mid n+\tfrac{1}{2}, n+\tfrac{1}{2}, s)\, \Im(r \mid n-\tfrac{1}{2}, n-\tfrac{1}{2}, s) \frac{dr}{r^{3/2}} \tag{99}$$
$$- 2 l_{n-1,\,s} \int_0^R J_{3/2}(k_{11} r)\, \Im(r \mid n+\tfrac{1}{2}, n+\tfrac{1}{2}, s)\, \Im(r \mid n-\tfrac{3}{9}, n-\tfrac{1}{2}, s) \frac{dr}{r^{1/2}} \Big\}.$$

V. NUMERICAL VALUES OF SOME OF THE MATRIX ELEMENTS

In Table 1 we have listed the numerical values of some of the lowest-order matrix elements needed in the later discussion. The Bessel functions entering the integrand in the elements may all be expressed in terms of trigonometric functions, and it should be possible to evaluate the integrals analytically. However, the expressions are rather cum-

TABLE 1

NUMERICAL VALUES OF SOME MATRIX ELEMENTS OF LOWEST ORDER

$$[\boldsymbol{T}^1_{11}\times\boldsymbol{S}^0_{11}\cdot\boldsymbol{T}^{1*}_{11}]=0.8930iH_p \qquad [\mathfrak{T}^1_{11}\times\boldsymbol{S}^0_{11}\cdot\mathfrak{T}^{1*}_{11}]=1.1273iH_p$$
$$[\boldsymbol{T}^1_{21}\times\boldsymbol{S}^0_{11}\cdot\boldsymbol{T}^{1*}_{21}]=0.2839iH_p \qquad [\mathfrak{T}^1_{21}\times\boldsymbol{S}^0_{11}\cdot\mathfrak{T}^{1*}_{21}]=0.3495iH_p$$
$$[\boldsymbol{T}^2_{21}\times\boldsymbol{S}^0_{11}\cdot\boldsymbol{T}^{2*}_{21}]=0.5677iH_p \qquad [\mathfrak{T}^2_{21}\times\boldsymbol{S}^0_{11}\cdot\mathfrak{T}^{2*}_{21}]=0.6990iH_p$$
$$[\boldsymbol{T}^1_{31}\times\boldsymbol{S}^0_{11}\cdot\boldsymbol{T}^{1*}_{31}]=0.1390iH_p \qquad [\mathfrak{T}^1_{31}\times\boldsymbol{S}^0_{11}\cdot\mathfrak{T}^{1*}_{31}]=0.1652iH_p$$
$$[\boldsymbol{T}^2_{31}\times\boldsymbol{S}^0_{11}\cdot\boldsymbol{T}^{2*}_{31}]=0.2779iH_p \qquad [\mathfrak{T}^2_{31}\times\boldsymbol{S}^0_{11}\cdot\mathfrak{T}^{2*}_{31}]=0.3303iH_p$$
$$[\boldsymbol{T}^3_{31}\times\boldsymbol{S}^0_{11}\cdot\boldsymbol{T}^{3*}_{31}]=0.4169iH_p \qquad [\mathfrak{T}^3_{31}\times\boldsymbol{S}^0_{11}\cdot\mathfrak{T}^{3*}_{31}]=0.4955iH_p$$
$$[\boldsymbol{T}^1_{41}\times\boldsymbol{S}^0_{11}\cdot\boldsymbol{T}^{1*}_{41}]=0.0797iH_p \qquad [\mathfrak{T}^1_{41}\times\boldsymbol{S}^0_{11}\cdot\mathfrak{T}^{1*}_{41}]=0.0947iH_p$$
$$[\boldsymbol{T}^2_{41}\times\boldsymbol{S}^0_{11}\cdot\boldsymbol{T}^{2*}_{41}]=0.1595iH_p \qquad [\mathfrak{T}^2_{41}\times\boldsymbol{S}^0_{11}\cdot\mathfrak{T}^{2*}_{41}]=0.1895iH_p$$
$$[\boldsymbol{T}^3_{41}\times\boldsymbol{S}^0_{11}\cdot\boldsymbol{T}^{3*}_{41}]=0.2392iH_p \qquad [\mathfrak{T}^3_{41}\times\boldsymbol{S}^0_{11}\cdot\mathfrak{T}^{3*}_{41}]=0.2842iH_p$$
$$[\boldsymbol{T}^4_{41}\times\boldsymbol{S}^0_{11}\cdot\boldsymbol{T}^{4*}_{41}]=0.3190iH_p \qquad [\mathfrak{T}^4_{41}\times\boldsymbol{S}^0_{11}\cdot\mathfrak{T}^{4*}_{41}]=0.3789iH_p$$

$$[\boldsymbol{T}^1_{11}\times\boldsymbol{S}^0_{11}\cdot\boldsymbol{S}^{1*}_{21}]=-\,[\boldsymbol{S}^1_{21}\times\boldsymbol{S}^0_{11}\cdot\boldsymbol{T}^{1*}_{11}]=-1.9591\ H_p$$
$$[\boldsymbol{T}^1_{21}\times\boldsymbol{S}^0_{11}\cdot\boldsymbol{S}^{1*}_{11}]=-\,[\boldsymbol{S}^1_{11}\times\boldsymbol{S}^0_{11}\cdot\boldsymbol{T}^{1*}_{21}]=\ \ 0$$
$$[\boldsymbol{T}^1_{21}\times\boldsymbol{S}^0_{11}\cdot\boldsymbol{S}^{1*}_{31}]=-\,[\boldsymbol{S}^1_{31}\times\boldsymbol{S}^0_{11}\cdot\boldsymbol{T}^{1*}_{21}]=-2.3647\ H_p$$
$$[\boldsymbol{T}^2_{21}\times\boldsymbol{S}^0_{11}\cdot\boldsymbol{S}^{2*}_{31}]=-\,[\boldsymbol{S}^2_{31}\times\boldsymbol{S}^0_{11}\cdot\boldsymbol{T}^{2*}_{21}]=-1.8695\ H_p$$
$$[\boldsymbol{T}^1_{31}\times\boldsymbol{S}^0_{11}\cdot\boldsymbol{S}^{1*}_{21}]=-\,[\boldsymbol{S}^1_{21}\times\boldsymbol{S}^0_{11}\cdot\boldsymbol{T}^{1*}_{31}]=+0.0635\ H_p$$
$$[\boldsymbol{T}^2_{31}\times\boldsymbol{S}^0_{11}\cdot\boldsymbol{S}^{2*}_{21}]=-\,[\boldsymbol{S}^2_{21}\times\boldsymbol{S}^0_{11}\cdot\boldsymbol{T}^{2*}_{31}]=+0.0502\ H_p$$
$$[\boldsymbol{T}^1_{31}\times\boldsymbol{S}^0_{11}\cdot\boldsymbol{S}^{1*}_{41}]=-\,[\boldsymbol{S}^1_{41}\times\boldsymbol{S}^0_{11}\cdot\boldsymbol{T}^{1*}_{31}]=-2.4951\ H_p$$
$$[\boldsymbol{T}^2_{31}\times\boldsymbol{S}^0_{11}\cdot\boldsymbol{S}^{2*}_{41}]=-\,[\boldsymbol{S}^2_{41}\times\boldsymbol{S}^0_{11}\cdot\boldsymbol{T}^{1*}_{31}]=-2.2317\ H_p$$
$$[\boldsymbol{T}^3_{31}\times\boldsymbol{S}^0_{11}\cdot\boldsymbol{S}^{3*}_{41}]=-\,[\boldsymbol{S}^3_{41}\times\boldsymbol{S}^0_{11}\cdot\boldsymbol{T}^{3*}_{31}]=-1.7045\ H_p$$
$$[\boldsymbol{T}^1_{41}\times\boldsymbol{S}^0_{11}\cdot\boldsymbol{S}^{1*}_{31}]=-\,[\boldsymbol{S}^1_{31}\times\boldsymbol{S}^0_{11}\cdot\boldsymbol{T}^{1*}_{41}]=+0.0749\ H_p$$
$$[\boldsymbol{T}^2_{41}\times\boldsymbol{S}^0_{11}\cdot\boldsymbol{S}^{2*}_{31}]=-\,[\boldsymbol{S}^2_{31}\times\boldsymbol{S}^0_{11}\cdot\boldsymbol{T}^{2*}_{41}]=+0.0670\ H_p$$
$$[\boldsymbol{T}^3_{41}\times\boldsymbol{S}^0_{11}\cdot\boldsymbol{S}^{3*}_{31}]=-\,[\boldsymbol{S}^3_{31}\times\boldsymbol{S}^0_{11}\cdot\boldsymbol{T}^{3*}_{41}]=+0.0511\ H_p$$

$$[\mathfrak{T}^1_{11}\times\boldsymbol{S}^0_{11}\cdot\mathfrak{S}^{1*}_{21}]=-[\mathfrak{S}^1_{21}\times\boldsymbol{S}^0_{11}\cdot\mathfrak{T}^{1*}_{11}]=-2.9883\ H_p$$
$$[\mathfrak{T}^1_{21}\times\boldsymbol{S}^0_{11}\cdot\mathfrak{S}^{1*}_{11}]=-[\mathfrak{S}^1_{11}\times\boldsymbol{S}^0_{11}\cdot\mathfrak{T}^{1*}_{21}]=+1.8773\ H_p$$
$$[\mathfrak{T}^1_{21}\times\boldsymbol{S}^0_{11}\cdot\mathfrak{S}^{1*}_{31}]=-[\mathfrak{S}^1_{31}\times\boldsymbol{S}^0_{11}\cdot\mathfrak{T}^{1*}_{21}]=-3.6160\ H_p$$
$$[\mathfrak{T}^2_{21}\times\boldsymbol{S}^0_{11}\cdot\mathfrak{S}^{2*}_{31}]=-[\mathfrak{S}^2_{31}\times\boldsymbol{S}^0_{11}\cdot\mathfrak{T}^{2*}_{21}]=-2.8588\ H_p$$
$$[\mathfrak{T}^1_{31}\times\boldsymbol{S}^0_{11}\cdot\mathfrak{S}^{1*}_{21}]=-[\mathfrak{S}^1_{21}\times\boldsymbol{S}^0_{11}\cdot\mathfrak{T}^{1*}_{31}]=+2.2656\ H_p$$
$$[\mathfrak{T}^2_{31}\times\boldsymbol{S}^0_{11}\cdot\mathfrak{S}^{2*}_{21}]=-[\mathfrak{S}^2_{21}\times\boldsymbol{S}^0_{11}\cdot\mathfrak{T}^{2*}_{31}]=+1.7912\ H_p$$
$$[\mathfrak{T}^1_{31}\times\boldsymbol{S}^0_{11}\cdot\mathfrak{S}^{1*}_{41}]=-[\mathfrak{S}^1_{41}\times\boldsymbol{S}^0_{11}\cdot\mathfrak{T}^{1*}_{31}]=-3.8347\ H_p$$
$$[\mathfrak{T}^2_{31}\times\boldsymbol{S}^0_{11}\cdot\mathfrak{S}^{2*}_{41}]=-[\mathfrak{S}^2_{41}\times\boldsymbol{S}^0_{11}\cdot\mathfrak{T}^{2*}_{31}]=-3.4298\ H_p$$
$$[\mathfrak{T}^3_{31}\times\boldsymbol{S}^0_{11}\cdot\mathfrak{S}^{3*}_{41}]=-[\mathfrak{S}^3_{41}\times\boldsymbol{S}^0_{11}\cdot\mathfrak{T}^{3*}_{31}]=-2.6196\ H_p$$
$$[\mathfrak{T}^1_{41}\times\boldsymbol{S}^0_{11}\cdot\mathfrak{S}^{1*}_{31}]=-[\mathfrak{S}^1_{31}\times\boldsymbol{S}^0_{11}\cdot\mathfrak{T}^{1*}_{41}]=+2.3851\ H_p$$
$$[\mathfrak{T}^2_{41}\times\boldsymbol{S}^0_{11}\cdot\mathfrak{S}^{2*}_{31}]=-[\mathfrak{S}^2_{31}\times\boldsymbol{S}^0_{11}\cdot\mathfrak{T}^{2*}_{41}]=+2.1333\ H_p$$
$$[\mathfrak{T}^3_{41}\times\boldsymbol{S}^0_{11}\cdot\mathfrak{S}^{3*}_{31}]=-[\mathfrak{S}^3_{31}\times\boldsymbol{S}^0_{11}\cdot\mathfrak{T}^{3*}_{41}]=+1.6293\ H_p$$

bersome to handle, and for this reason it was found more convenient to evaluate them by numerical quadrature, using the *Tables of Spherical Bessel Functions* (1947). They are given to four decimal places.

In Table 2 are listed the values of the integrals K_a^2 and $\mathfrak{K}_a^2$ (see eqs. [41] and [52]), which are needed in the following calculations.

TABLE 2

NUMERICAL VALUES OF INTEGRALS K_a^2 AND $\mathfrak{K}_a^2$

$(K_{11})^2 = 7.8693$	$(\mathfrak{K}_{11})^2 = 20.1876$
$(K_{21})^2 = 16.1901$	$(\mathfrak{K}_{21})^2 = 33.2095$
$(K_{31})^2 = 27.2024$	$(\mathfrak{K}_{31})^2 = 48.8140$
$(K_{41})^2 = 40.8328$	$(\mathfrak{K}_{41})^2 = 66.9402$

VI. THE PERTURBATION EQUATIONS

In the initial state no material motions are present (see eq. [1]). We shall now consider the hydromagnetic oscillations about the equilibrium state defined by the field $\boldsymbol{S}_{11}^0$ (cf. Sec. III). The components of the velocity field, $\boldsymbol{u}$, set up, as well as the perturbations in the other field quantities, will be considered as small quantities of the first order.

The electromagnetic equations of the problem are

$$\operatorname{curl} \boldsymbol{H} = 4\pi \boldsymbol{J} \quad \text{with} \quad \boldsymbol{H} = \operatorname{curl} \boldsymbol{A} \quad \text{and} \quad \operatorname{div} \boldsymbol{H} = 0 , \tag{100}$$

$$\operatorname{curl} \boldsymbol{E} = -\frac{\partial \boldsymbol{H}}{\partial t} , \tag{101}$$

$$\boldsymbol{J} = \sigma (\boldsymbol{E} + \boldsymbol{u} \times \boldsymbol{H}) . \tag{102}$$

In equation (100) the displacement current $\partial \boldsymbol{E}/\partial t$ has been neglected; this is the customary hydromagnetic approximation.

The equation of motion is

$$\rho \frac{D\boldsymbol{u}}{dt} = \boldsymbol{J} \times \boldsymbol{H} - \nabla p - \rho \nabla V , \tag{103}$$

where p is the pressure and V is the gravitational potential. Substituting from equation (100) for $\boldsymbol{J}$ and writing

$$\nabla \pi = \frac{1}{\rho} \nabla p + \nabla V , \tag{104}$$

we obtain, for the equation of motion,

$$\frac{D\boldsymbol{u}}{dt} = \frac{1}{4\pi\rho} \operatorname{curl} \boldsymbol{H} \times \boldsymbol{H} - \nabla \pi . \tag{105}$$

As already stated, we shall consider the sphere to be homogeneous, making ρ a constant in this equation. We shall further assume that the fluid is incompressible, so that the equation of continuity takes the simple form

$$\operatorname{div} \boldsymbol{u} = 0 . \tag{106}$$

Let the quantities characterizing the initial state be denoted by a superscript zero. We then write,

$$\boldsymbol{H} = \boldsymbol{H}^0 + \boldsymbol{h}, \quad \boldsymbol{A} = \boldsymbol{A}^0 + \boldsymbol{a}, \quad \boldsymbol{E} = \boldsymbol{E}^0 + \boldsymbol{e}, \quad \pi = \pi^0 + \varpi, \quad \boldsymbol{J} = \boldsymbol{J}^0 + \boldsymbol{j} . \tag{107}$$

For the perturbations in the field variables the electromagnetic equations give

$$\text{curl } \boldsymbol{h} = 4\pi \boldsymbol{j}, \quad \boldsymbol{h} = \text{curl } \boldsymbol{a}, \quad \text{div } \boldsymbol{h} = 0, \quad \text{curl } \boldsymbol{e} = -\frac{\partial \boldsymbol{h}}{\partial t}, \quad \boldsymbol{j} = \sigma (\boldsymbol{e} + \boldsymbol{u} \times \boldsymbol{H}^0) . \tag{108}$$

Elimination of $\boldsymbol{j}$ and $\boldsymbol{e}$ between these equations results in the following equation for the perturbation in the magnetic field:

$$\frac{\partial \boldsymbol{h}}{\partial t} = \text{curl } (\boldsymbol{u} \times \boldsymbol{H}^0) + \frac{1}{4\pi\sigma} \nabla^2 \boldsymbol{h} . \tag{109}$$

Since we are interested only in oscillations with periods short compared to the decay time, the last term in this equation may be neglected. Also we shall consider $1/\tau \sim 1/4\pi\sigma$ to be a quantity of the first order.

Equation (109) therefore reduces to

$$\frac{\partial \boldsymbol{h}}{\partial t} = \text{curl } (\boldsymbol{u} \times \boldsymbol{H}^0) , \tag{110}$$

or, in terms of the vector potential, we have

$$\frac{\partial \boldsymbol{a}}{\partial t} = \boldsymbol{u} \times \boldsymbol{H}^0 . \tag{111}$$

The equation of motion (105) can be written in the following form, when second-order terms are neglected:

$$\frac{\partial \boldsymbol{u}}{\partial t} = \frac{1}{4\pi\rho} \{ \text{curl } \boldsymbol{h} \times \boldsymbol{H}^0 + \text{curl } \boldsymbol{H}^0 \times \boldsymbol{h} \} - \nabla \varpi , \tag{112}$$

where the magnetohydrostatic equation,

$$\frac{1}{4\pi\rho} \text{curl } \boldsymbol{H}^0 \times \boldsymbol{H}^0 - \nabla \pi^0 = 0 , \tag{113}$$

has been used in the reduction.

Here we must make the important assumption that, in spite of the "induction-drag" term, no appreciable deviation from the spherical form results.

Equation (112) can be brought into a more convenient form by applying the curl operator twice. The pressure term is eliminated, and, since the velocity is a solenoidal vector (see eq. [106]), we get

$$\frac{\partial (\nabla^2 \boldsymbol{u})}{\partial t} = -\frac{1}{4\pi\rho} \text{curl curl} \{ \text{curl } \boldsymbol{h} \times \boldsymbol{H}^0 + \text{curl } \boldsymbol{H}^0 \times \boldsymbol{h} \} . \tag{114}$$

Since we shall be interested only in times short compared to the decay time, we may treat $\boldsymbol{H}^0$ as a constant (cf. remarks after eq. [109]) in this equation. Consequently, a further differentiation of equation (114) with respect to time leads to the equation

$$\frac{\partial^2 (\nabla^2 \boldsymbol{u})}{\partial t^2} = -\frac{1}{4\pi\rho} \text{curl curl} \left\{ \text{curl } \frac{\partial \boldsymbol{h}}{\partial t} \times \boldsymbol{H}^0 + \text{curl } \boldsymbol{H}^0 \times \frac{\partial \boldsymbol{h}}{\partial t} \right\} . \tag{115}$$

We can eliminate $\partial \boldsymbol{h}/\partial t$ from this equation by making use of equation (110), but we shall not carry out this elimination explicitly.

From the equation of continuity (106) we obtain the following connection between ϖ and $\boldsymbol{h}$ by taking the divergence of equation (112); thus

$$\nabla^2\varpi = -\frac{1}{4\pi\rho}\{\boldsymbol{H}^0\cdot\nabla^2\boldsymbol{h}+\boldsymbol{h}\cdot\nabla^2\boldsymbol{H}^0+2\ \mathrm{curl}\ \boldsymbol{h}\cdot\mathrm{curl}\ \boldsymbol{H}^0\}. \tag{116}$$

VII. SOLUTION OF THE EQUATIONS IN THE CASE OF A TOROIDAL OSCILLATION

We shall now show how we can obtain approximate values for the characteristic frequencies of the toroidal oscillations in the special case of $\boldsymbol{H}^0 = \boldsymbol{S}^0_{11}$.

As we have already mentioned in connection with the definition of the functions $\boldsymbol{T}$ and $\mathfrak{T}$, we shall distinguish between two cases differing in the boundary conditions imposed on the velocity. We shall treat both the case when $\boldsymbol{u}$ has a value different from zero at the surface (free boundary) and the case when $\boldsymbol{u} = 0$ at the boundary (rigid boundary); the two cases correspond to the expansion of $\boldsymbol{u}$ in terms of $\boldsymbol{T}$ and $\mathfrak{T}$, respectively.

a) CASE I

In this case we expand the velocity in terms of toroidal functions, since we have limited ourselves to considering this special kind of oscillation. Once we have made this choice, we see from equation (111) that the corresponding vector potential $\boldsymbol{a}$ is neither a pure toroidal nor a pure poloidal function. In view of the "reciprocal orthogonality" valid for the $\boldsymbol{T}$ and $\boldsymbol{S}$ functions as expressed by equation (17), we may, however, use a more general expansion for $\boldsymbol{a}$ in the form of a sum of both toroidal and poloidal functions. Thus we write

$$\boldsymbol{u} = \sum_i a_i(t)\,\boldsymbol{T}(i)\,, \tag{117}$$

$$\boldsymbol{a} = \sum_\gamma \{\, c_\gamma(t)\,\boldsymbol{T}(\gamma) + d_\gamma(t)\,\boldsymbol{S}(\gamma)\,\}\,, \tag{118}$$

where the coefficients $a(t)$, $c(t)$, and $d(t)$ are functions of the time only. Inserting equations (117) and (118) in equation (111), we obtain the relation

$$\sum_\gamma \{\, \dot{c}_\gamma(t)\,\boldsymbol{T}(\gamma) + \dot{d}_\gamma(t)\,\boldsymbol{S}(\gamma)\,\} = \sum_i a_i(t)\,\boldsymbol{T}(i) \times \boldsymbol{S}^0_{11} \tag{119}$$

between the coefficients in the expansions for $\boldsymbol{u}$ and $\boldsymbol{a}$. Dots here indicate differentiation with respect to time. Scalar multiplication and integration, first with $\boldsymbol{T}^*(\gamma)$ and then with $\boldsymbol{S}^*(\gamma)$, give

$$\dot{c}_\gamma(t) = \sum_i a_i(t)\,[\boldsymbol{T}(i) \times \boldsymbol{S}^0_{11}\cdot\boldsymbol{T}^*(\gamma)]\,, \tag{120}$$

$$K^2_\gamma \dot{d}_\gamma(t) = \sum_i a_i(t)\,[\boldsymbol{T}(i) \times \boldsymbol{S}^0_{11}\cdot\boldsymbol{S}^*(\gamma)]\,, \tag{121}$$

where K^2_γ is the integral defined in equation (27). Next, consider equation (115). Since we are dealing with a toroidal velocity field, thus making the left-hand side a toroidal vector (cf. eqs. [10] and also [117]), we must expand the right-hand side in a similar series and then compare the coefficients. We start out with the expression in parentheses and write

$$\mathrm{curl}\,\frac{\partial\boldsymbol{h}}{\partial t}\times\boldsymbol{S}^0_{11} + Rk^2_{11}\boldsymbol{T}^0_{11}\times\frac{\partial\boldsymbol{h}}{\partial t} = \sum_j b_j(t)\,\boldsymbol{T}(\jmath)\,, \tag{122}$$

where we have replaced curl $\boldsymbol{S}_{11}^0$ by $Rk_{11}^2\boldsymbol{T}_{11}^0$ in accordance with equation (10). On the other hand, according to equations (118), (108), and (10), we have

$$\begin{aligned}\frac{\partial \boldsymbol{h}}{\partial t} &= \sum_\gamma \{\, \dot{c}_\gamma(t)\,\mathrm{curl}\,\boldsymbol{T}(\gamma) + \dot{d}_\gamma(t)\,\mathrm{curl}\,\boldsymbol{S}(\gamma)\,\} \\ &= \sum_\gamma \{\, \dot{c}_\gamma(t)\,R^{-1}\boldsymbol{S}(\gamma) + \dot{d}_\gamma(t)\,Rk_\gamma^2\boldsymbol{T}(\gamma)\,\}\end{aligned} \tag{123}$$

and

$$\mathrm{curl}\,\frac{\partial \boldsymbol{h}}{\partial t} = \sum_\gamma \{\, \dot{c}_\gamma(t)\,k_\gamma^2\boldsymbol{T}(\gamma) + \dot{d}_\gamma(t)\,k_\gamma^2\boldsymbol{S}(\gamma)\,\}. \tag{124}$$

Substituting the foregoing expression in equations (122), we obtain

$$\begin{aligned}\sum_j b_j(t)\,\boldsymbol{T}(j) = \sum_\gamma \{\, &\dot{c}_\gamma(t)\,k_\gamma^2\boldsymbol{T}(\gamma)\times\boldsymbol{S}_{11}^0 + \dot{d}_\gamma(t)\,k_\gamma^2\boldsymbol{S}(\gamma)\times\boldsymbol{S}_{11}^0 \\ &+ \dot{c}_\gamma(t)\,k_{11}^2\boldsymbol{T}_{11}^0\times\boldsymbol{S}(\gamma) + \dot{d}_\gamma(t)\,k_{11}^2k_\gamma^2R^2\boldsymbol{T}_{11}^0\times\boldsymbol{T}(\gamma)\,\}.\end{aligned} \tag{125}$$

Multiplication by $\boldsymbol{T}^*(j)$ and integration lead to the following expression for $b_j(t)$:

$$\begin{aligned}b_j(t) = \sum_\gamma \{\, &\dot{c}_\gamma(t)\,k_\gamma^2\,[\boldsymbol{T}(\gamma)\times\boldsymbol{S}_{11}^0\cdot\boldsymbol{T}^*(j)] + \dot{d}_\gamma(t)\,k_\gamma^2\,[\boldsymbol{S}(\gamma)\times\boldsymbol{S}_{11}^0\cdot\boldsymbol{T}^*(j)] \\ &+ \dot{c}_\gamma(t)\,k_{11}^2\,[\boldsymbol{T}_{11}^0\times\boldsymbol{S}(\gamma)\cdot\boldsymbol{T}^*(j)] + \dot{d}_\gamma(t)\,k_{11}^2k_\gamma^2R^2\,[\boldsymbol{T}_{11}^0\times\boldsymbol{T}(\gamma)\cdot\boldsymbol{T}^*(j)]\,\}.\end{aligned} \tag{126}$$

As is easily seen (cf. eq. [14]), the last matrix element in equation (126) vanishes identically, so we are left with three terms on the right-hand side.

Now, going back to equation (115), the equation of motion, we get, for the right-hand side of this equation,

$$-\frac{1}{4\pi\rho}\sum_j b_j(t)\,\mathrm{curl}\,\mathrm{curl}\,\boldsymbol{T}(j) = -\frac{1}{4\pi\rho}\sum_j b_j(t)\,k_j^2\boldsymbol{T}(j), \tag{127}$$

where $b_j(t)$ is given by equation (126). The expansion for the left-hand side of equation (115) is found from equations (117) and (10) to be

$$\frac{\partial^2(\nabla^2\boldsymbol{u})}{\partial t^2} = -\,\mathrm{curl}\,\mathrm{curl}\,\frac{\partial^2\boldsymbol{u}}{\partial t^2} = -\sum_i \frac{d^2a_i(t)}{dt^2}\,k_i^2\boldsymbol{T}(i). \tag{128}$$

A comparison between equations (128) and (127) shows

$$\frac{d^2a_j(t)}{dt^2} = \frac{1}{4\pi\rho}\,b_j(t), \tag{129}$$

where we have written j for the common index. Finally, inserting $b_j(t)$ from equation (126), we obtain

$$\begin{aligned}\frac{d^2a_j(t)}{dt^2} = \frac{1}{4\pi\rho}\sum_\gamma \{\, &\dot{c}_\gamma(t)\,(k_\gamma^2\,[\boldsymbol{T}(\gamma)\times\boldsymbol{S}_{11}^0\cdot\boldsymbol{T}^*(j)] + k_{11}^2\,[\boldsymbol{T}_{11}^0\times\boldsymbol{S}(\gamma)\cdot\boldsymbol{T}^*(j)]) \\ &+ \dot{d}_\gamma(t)\,k_\gamma^2\,[\boldsymbol{S}(\gamma)\times\boldsymbol{S}_{11}^0\cdot\boldsymbol{T}^*(j)]\,\}.\end{aligned} \tag{130}$$

Now, substituting for $\dot{c}_\gamma(l)$ and $\dot{d}_\gamma(l)$ from equations (120) and (121), we find the following infinite set of linear equations governing the a_j's:

$$\frac{d^2 a_j(l)}{dl^2} = \frac{1}{4\pi\rho}\sum_\gamma \sum_i \{ [\boldsymbol{T}(i) \times \boldsymbol{S}_{11}^0 \cdot \boldsymbol{T}^*(\gamma)] (k_\gamma^2 [\boldsymbol{T}(\gamma) \times \boldsymbol{S}_{11}^0 \cdot \boldsymbol{T}^*(j)] + k_{11}^2 [\boldsymbol{T}_{11}^0 \times \boldsymbol{S}(\gamma) \cdot \boldsymbol{T}^*(j)]) + k_\gamma^2 K_\gamma^{-2} [\boldsymbol{T}(i) \times \boldsymbol{S}_{11}^0 \cdot \boldsymbol{S}^*(\gamma)] [\boldsymbol{S}(\gamma) \times \boldsymbol{S}_{11}^0 \cdot \boldsymbol{T}^*(j)] \} a_i(l). \tag{131}$$

These equations admit solutions of the form

$$a_j(l) = a_j(0)\, e^{i\omega t} \tag{132}$$

where ω is a constant, provided that

$$\omega^2 a_j(0) = -\frac{1}{4\pi\rho}\sum_\gamma \sum_i a_i(0) \{ [\boldsymbol{T}(i) \times \boldsymbol{S}_{11}^0 \cdot \boldsymbol{T}^*(\gamma)] (k_\gamma^2 [\boldsymbol{T}(\gamma) \times \boldsymbol{S}_{11}^0 \cdot \boldsymbol{T}^*(j)] + k_{11}^2 [\boldsymbol{T}_{11}^0 \times \boldsymbol{S}(\gamma) \cdot \boldsymbol{T}^*(j)]) + k_\gamma^2 K_\gamma^{-2} [\boldsymbol{T}(i) \times \boldsymbol{S}_{11}^0 \cdot \boldsymbol{S}^*(\gamma)] [\boldsymbol{S}(\gamma) \times \boldsymbol{S}_{11}^0 \cdot \boldsymbol{T}^*(j)] \}. \tag{133}$$

$$\begin{bmatrix}
\times & \cdot & \times & \cdot & \cdot & \cdot & \cdot & \cdot & \cdot \\
\cdot & \times & \cdot & \times & \cdot & \cdot & \cdot & \cdot & \cdot \\
\times & \cdot & \times & \cdot & \times & \cdot & \cdot & \cdot & \cdot \\
\cdot & \times & \cdot & \times & \cdot & \times & \cdot & \cdot & \cdot \\
\cdot & \cdot & \times & \cdot & \times & \cdot & \times & \cdot & \cdot \\
\cdot & \cdot & \cdot & \times & \cdot & \times & \cdot & \times & \cdot
\end{bmatrix}$$

FIG. 1.—Crosses indicate terms different from zero

The condition that the $a(0)$'s do not all vanish identically is that the determinant of the foregoing linear system be zero. Using the selection rules valid for the matrix elements (60*a*) and (60*b*), we get the following system of equations (cf. eq. [71]):

$$\omega^2 a_j(0) = -\frac{1}{4\pi\rho}\{ [\boldsymbol{T}(j) \times \boldsymbol{S}_{11}^0 \cdot \boldsymbol{T}^*(j)] \}^2 \left\{ k_j^2 - \frac{n_j(n_j+1)}{2} k_{11}^2 \right\} a_j(0) - \frac{1}{4\pi\rho}\sum_\gamma \sum_i k_\gamma^2 K_\gamma^{-2} [\boldsymbol{T}(i) \times \boldsymbol{S}_{11}^0 \cdot \boldsymbol{S}^*(\gamma)] [\boldsymbol{S}(\gamma) \times \boldsymbol{S}_{11}^0 \cdot \boldsymbol{T}^*(j)] a_i(0). \tag{134}$$

Now, using the selection rules for the matrix elements of type (62*a*), we can get a picture of how the matrix which gives the characteristic values of ω will look. For a given value of the index j in the matrix, i.e., for a given line, we get two values of γ and four possible values of the index i. The right-hand side of equation (134) thus contains five terms different from zero, three of which are confined to the diagonal. How the matrix will finally look is indicated in Figure 1. It is further seen that the matrix is symmetrical; thus all characteristic values of ω^2 are real.

b) CASE II

The procedure for obtaining the approximate solution is just the same in this case as in case I, the only difference being the use of the $\mathfrak{T}$ and $\mathfrak{S}$ functions, which obey the correct set of boundary conditions for this case (cf. p. 160). In analogy with the first case we therefore write

$$\boldsymbol{u} = \sum_i a_i(t)\,\mathfrak{T}(i)\,, \tag{135}$$

$$\boldsymbol{a} = \sum_\gamma \{\, c_\gamma(t)\,\mathfrak{T}(\gamma) + d_\gamma(t)\,\mathfrak{S}(\gamma)\,\}\,. \tag{136}$$

In addition, using equation (111), we have

$$\sum_\gamma \{\, \dot{c}_\gamma(t)\,\mathfrak{T}(\gamma) + \dot{d}_\gamma(t)\,\mathfrak{S}(\gamma)\,\} = \sum_i a_i(t) \quad (i) \times \boldsymbol{S}_{11}^0\,, \tag{137}$$

from which we obtain

$$\dot{c}_\gamma(t) = \sum_i a_i(t)\,[\mathfrak{T}(i) \times \boldsymbol{S}_{11}^0 \cdot \mathfrak{T}^*(\gamma)\,] \tag{138}$$

and

$$K_\gamma^2 \dot{d}_\gamma(t) = \sum_i a_i(t)\,[\mathfrak{T}(i) \times \boldsymbol{S}_{11}^0 \cdot \mathfrak{S}^*(\gamma)\,]\,. \tag{139}$$

We also have, as before,

$$b_j(t) = \sum_\gamma \{\, \dot{c}_\gamma(t)\,(l_\gamma^2\,[\mathfrak{T}(\gamma) \times \boldsymbol{S}_{11}^0 \cdot \mathfrak{T}^*(j)\,] + k_{11}^2\,[\boldsymbol{T}_{11}^0 \times \mathfrak{S}(\gamma) \cdot \mathfrak{T}^*(j)\,]) + \dot{d}_\gamma(t)\,l_\gamma^2\,[\mathfrak{S}(\gamma) \times \boldsymbol{S}_{11}^0 \cdot \mathfrak{T}^*(j)\,]\,\}\,. \tag{140}$$

Using equations (135) and (136), we finally arrive at the following set of linear equations:

$$\omega^2 a_j(0) = -\frac{1}{4\pi\rho}\{\,[\mathfrak{T}(j) \times \boldsymbol{S}_{11}^0 \cdot \mathfrak{T}^*(j)\,]\,\}^2 \left\{ l_j^2 - \frac{n_j(n_j+1)}{2} \right\} a_j(0) - \frac{1}{4\pi\rho} \sum_\gamma \sum_i l_\gamma^2 \mathfrak{N}_\gamma^{-2}\,[\mathfrak{T}(i) \times \boldsymbol{S}_{11}^0 \cdot \mathfrak{S}^*(\gamma)\,]\,[\mathfrak{S}(\gamma) \times \boldsymbol{S}_{11}^0 \cdot \mathfrak{T}^*(j)\,]\,a_i(0)\,. \tag{141}$$

The analogy with case I (cf. eq. [134]) is thus complete.

VIII. NUMERICAL CALCULATION OF CHARACTERISTIC VALUES OF ω^2 IN DIFFERENT APPROXIMATIONS

The infinite sets of linear equations (134) and (141) do not, since the matrix is non-diagonal, admit of exact solutions. The next step in this investigation is therefore to find a suitable method by which the eigen-values may be determined in an approximate way. One procedure which seemingly would give the characteristic values for the lowest-order oscillations (lowest frequency, longest period) would be to cut down the order of the matrix and treat it as if it were finite. The first approximation would then be the zero of the equation obtained when only one term is retained, the second when a matrix of the second order is left over, and so on, as indicated in Figure 2. The result of the calculations when this procedure is used is given in Table 3.

From this table it appears that it is impossible to decide which of the frequencies is the fundamental one. As one goes to higher approximations, both lower and higher values of the frequency are added, and how close to zero the lowest frequency will lie cannot be found unless the infinite set of equations is solved completely. On the other hand, going to higher frequencies also means that the velocity field is getting more complicated. In an actual physical case this should lead to such velocity patterns being

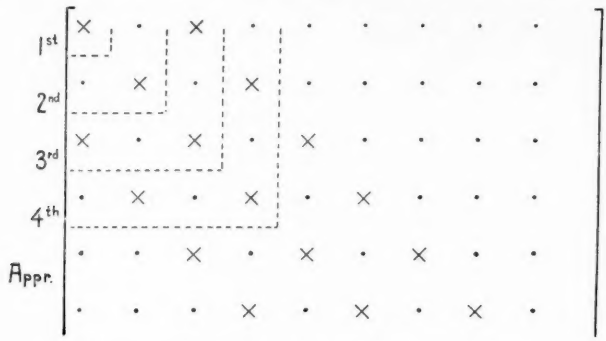

FIG. 2.—Terms retained in the various approximations

TABLE 3

CHARACTERISTIC FREQUENCIES, $\omega'^2 = \omega^2(H_p^2/4\pi\rho R^2)^{-1}$, IN DIFFERENT APPROXIMATIONS, CASE I

First	Second	Third	Fourth
0	+4.786	+6.070	+6.959
	−0.759	+4.791	+6.074
	−3.036	+1.232	+4.776
		−0.502	+1.238
		−2.005	−0.315
		−4.519	−1.045
			−1.269
			−2.005
			−2.850
			−5.073

damped out by viscosity more quickly. The positive eigen-values of ω'^2 seem to be converging in this case, giving the values +4.79, +6.07, and +1.23 for the most significant oscillations.

Some of the characteristic values of ω^2 are negative, corresponding to imaginary frequencies. The values of these frequencies seem to shift from one approximation to the next. It is difficult to draw any definite conclusions from this, but it seems possible that the negative eigen-values do not give a discrete spectrum at all.

In case II the coupling, as represented by the last term in equation (141), is stronger than in case I, and the convergence is doubtful. Here also one seemingly enters "in the middle of the array" of eigen-values. Fewer negative eigen-values are found for the lower modes than in case I. The result is given in Table 4.

IX. DISCUSSION

The main conclusion which may be drawn from the calculations presented here is that both positive and negative eigen-values of ω^2 are present.

From the solution given here it is not possible to decide which sign $i\omega$ will have or whether it corresponds to an exponential amplification with time or to a damping. We have not taken dissipation into account, since we have neglected both viscosity and dissipation due to ohmic losses. The amplification or damping is thus due to the interaction of the motion with the initial magnetic field, acting as the source of energy. Because of the coupling terms between the various modes in the velocity field, resulting in a nondiagonal matrix, it is not possible to investigate the stability properties of the various modes separately by using the equation of motion.

It is difficult to draw any definite conclusion regarding the eigen-value spectrum from the results of the approximate calculations given here, but in case II the eigen-values of ω^2 seem to form a continuous spectrum.

TABLE 4

CHARACTERISTIC FREQUENCIES, $\omega'^2 = \omega^2(H_p^2/4\pi\rho R^2)^{-1}$, IN DIFFERENT APPROXIMATIONS, CASE II

First	Second	Third	Fourth
+13.12	+22.05	+24.39	+27.69
	+ 3.966	+17.05	+21.63
	+ 1.763	+ 9.939	+14.23
		+ 2.504	+13.92
		+ 2.076	+ 4.314
		− 2.550	+ 1.259
			+ 0.819
			+ 0.092
			− 4.558

The simple model we have discussed is obviously not capable of explaining the phenomena encountered in magnetic variable stars. In the case of the earth's core, however, the condition should not be too far from the model we have considered. Case II ought to be used if the mantle is acting as a rigid boundary. If this is the case, our calculations indicate that periodic variations with any period may be present. If the surface of the highly conducting core is considered as free, corresponding to the discontinuity of the electrical conductivity lying inside the fluid core, we may apply case I. We shall assume 0.61 gauss as the polar value of the dipole component at the earth's surface. With the radius of the core $R_c = 3.5 \times 10^8$ cm (the data on the physical properties of the core are taken from Elsasser 1950), and an r^{-3} dependence on distance from the earth's center, we obtain $H_p = 3.7$ gauss as the appropriate polar field at the surface of the core. With $\rho = 10$ g cm^{-3}, we get

$$\frac{1}{R_c}\frac{H_p}{(4\pi\rho)^{1/2}} = 0.95 \times 10^{-9}\ \text{sec}^{-1}. \tag{142}$$

With the eigen-values of ω'^2, 4.79, 6.07, and 1.23, we get the following periods: 96, 85, and 189 years. This is within the range of periods found in the spectrum of the secular variations of the territorial field, according to recent investigations at Cambridge (Runcorn, private communication).

In conclusion I would like to express my sincere thanks to Professor Chandrasekhar for suggesting this problem and for his never failing encouragement and advice during the entire course of this work. I am indebted to the University of Chicago and to the Norwegian Research Council for Science and the Humanities for fellowships during the time when this work was carried out.

REFERENCES

Bateman, H. 1932, *Partial Differential Equations of Mathematical Physics* (Cambridge: At the University Press).
Bullard, E. C. 1949*a*, *M.N., Geophys. Suppl.*, **5**, 248.
———. 1949*b*, *Proc. R. Soc. London, A*, **197**, 433.
———. 1949*c*, *ibid.*, **199**, 413.
Elsasser, W. M. 1946*a*, *Phys. Rev.*, **69**, 106.
———. 1946*b*, *ibid.*, **70**, 202.
———. 1947, *ibid.*, **72**, 821.
———. 1950, *Rev. Mod. Phys.*, **22**, 1.
Lamb, H. 1883, *Phil. Trans.*, **174**, 519.
Margenau, H., and Murphy, G. M. 1943, *The Mathematics of Physics and Chemistry* (New York: D. Van Nostrand Co., Inc.), p. 117.
Stratton, J. A. 1941, *Electromagnetic Theory* (New York: McGraw-Hill Book Co., Inc.), chap. vii.
Tables of Spherical Bessel Functions (New York: Columbia University Press, 1947), Vols. 1 and 2.

NUCLEAR REACTIONS AND ELEMENT SYNTHESIS IN THE SURFACES OF STARS

W. A. FOWLER,* G. R. BURBIDGE, AND E. MARGARET BURBIDGE
Cavendish Laboratory, University of Cambridge
Received July 11, 1955

ABSTRACT

The astronomical evidence suggests that the anomalous overabundances, particularly of some heavy elements, in peculiar A stars with magnetic fields (Apm stars) are unlikely to be due to synthesis in the stellar interior. It is suggested in this paper that regions develop in which sufficient magnetic energy is available to accelerate particles on the stellar surface so that nuclear reactions can take place there. As a model it is supposed that the particles are accelerated in regions of changing magnetic field by the Swann betatron mechanism, modified to take account of the plasma and collision properties of the gas. The conditions necessary for element synthesis are plausible. They are, depending on the efficiency of the acceleration and nuclear processes, that the spot regions (assumed to have radii of 10^9–10^{10} cm) have densities of 10^{-8}–10^{-7} g/cc and local magnetic fields $H = 5 \times 10^5$–10^7 gauss and that average particle energies of $\sim$1 Mev are attained. One to 10 per cent of the spot is involved (or a much smaller fraction for the very large spots), and a fraction 0.01–0.5 of the magnetic energy is converted into kinetic energy. The anomalous abundances occur in a surface layer reaching down to $\rho = 10^{-4}$ g/cc. It is assumed that the time scales over which the mechanism is effective are 10^4–10^5 sec. Radiative effects may limit the time scale to the order of 1–10 sec, but favorable choices for the other parameters involved will compensate for this. Depending on the details of acceleration, energy loss, and energy-sharing mechanisms, we discuss two specific models.

a) An energy spectrum of the accelerated particles given by $f(E) \propto E^{-3}$, with about 1 per cent of the particles accelerated to 10–100 Mev. The still higher energy particles in the spectrum are to be identified with the observed high-energy cosmic radiation, probably after some additional acceleration in interstellar fields. Direct synthesis then takes place by $(\alpha, n) \ldots (\alpha, 3 \text{ nucleons})$ and by (d, p) and (d, n) reactions. This model can be criticized on the grounds of energy loss to electrons by the accelerated nuclei at $\rho = 10^{-8}$–10^{-7} g/cc, and it can be ruled out observationally if the D/H ratio in the Apm stars $\ll 0.01$, since theoretically it builds up to ~ 0.01.

b) A Maxwell-Boltzmann energy distribution in a "hot spot" within the magnetic spot, with $kT \sim 1$ Mev ($0.3 < kT < 1.5$), and all the particles involved. Synthesis then takes place by neutron production through (p, n) processes principally on the light nuclei, followed by (n, γ) capture processes on the metals. In the primary (p, n) process each stable target nucleus, X, serves catalytically to change protons into neutrons. The unstable residual isobar, Y, produced in the reaction $X + p \rightleftarrows Y + n$ decays back to X by positron-neutrino emission or electron capture, i.e., $Y \rightarrow X + \beta^+ + \nu$ or $Y + e^- \rightarrow X + \nu$. In this case the theoretical D/H ratio might be as low as $\sim 10^{-5}$.

These results are applied to the observed anomalies in α^2 CVn and HD 133029. By making plausible estimates about the spot activity and the amount of mixing, the overabundances of Sr, Y, Zr, La, the rare earths, and Pb can be reasonably explained if the activity has gone on for $\sim 5 \times 10^8$ years. Other anomalies, i.e., of O, Si, and Ca may also be explicable. Stellar surface synthesis of the cosmical D, Li, Be, and B is discussed, since these are unstable at the temperatures of stellar interiors. It is suggested that they are produced by spallation reactions on C, N, and O, either high up in the stellar atmospheres ($\rho \lesssim 10^{-9}$) or less probably in "hot spots" similar to case *b*, but where $kT \sim 5$ Mev. The postulated amount of magnetic activity in Apm stars is insufficient to produce reasonable abundances. If much smaller-scale activity on a larger number of stars (red dwarfs) is considered, then in $\sim 10^9$ years a D/H ratio of $\sim 10^{-6}$–10^{-9} and the cosmical abundances of Li, Be, and B can be produced, if a fairly high efficiency of production and ejection in these stars is assumed. The absolute upper limit on D/H is as high as 10^{-2} if equilibrium between stellar surfaces and interstellar material is reached. The natural radioactive elements may be produced by collisions between metal nuclei and the stable, heavy nuclei, such as lead and bismuth.

I. INTRODUCTION

It is well known that no nuclear reactions can take place as a result of thermal collisions at the temperatures of quiescent stellar surfaces. However, in this paper we shall attempt to discuss the special conditions under which surface reactions could take place. This problem seems worthy of consideration for the following reasons: (*a*) Certain

* Fulbright and Guggenheim Fellow on leave of absence from the California Institute of Technology.

groups of stars show large anomalous abundances relative to the cosmical abundances of the elements. (*b*) Recent work (Salpeter 1953; Cameron 1954, 1955*a*, *b;* Hoyle 1954; Fowler, Burbidge, and Burbidge 1955) has suggested that the synthesis of the elements in stars must be seriously considered as a theory of the origin of the elements. However, although this work has shown that the majority of the elements up to the natural α-emitters can be built in stellar interiors, D, Li, Be, and B are excluded because of their rapid rate of destruction at the temperatures in stellar interiors.

The stars which appear to show anomalous abundances of the heavier elements are the S stars, the Ba^+ stars, and the peculiar A and F stars. In the S stars the unstable element Tc is more abundant than in the more common M stars. There is also an apparent excessive abundance of Y, Zr, Ba, and La. In one particular star, R And (Bidelman 1953), the rare-earth elements Ce, Pr, Nd, Sm, Eu, Gd, Tb, Dy, Ho, and Er are present in appreciable quantities, and it is probable that these elements are increased in other S stars as well. A study of one S star (Buscombe and Merrill 1952) has shown that the anomalies in Y and Zr are probably quantitatively real, and Bidelman (1954) has also concluded that the S-star anomalies are real.

The Ba^+ stars, of which only nine are known at present (Bidelman 1955), have an apparent excessive abundance of Sr and Ba. Observations of a member of this group, ζ Cap (Garstang 1952), have shown that there are apparently increased abundances of Y, Zr, La, Ce, Pr, Nd, and Sm.

The peculiar A and F stars are characterized by apparently excessive abundances of some (but not necessarily all) of the elements Si, Mn, Cr, Sr, Y, Zr, and the rare earths (Eu in particular). Also in this group there is an apparent underabundance of O (Slettebak 1951) and usually Ca. A quantitative investigation of the peculiar A stars α^2 CVn and HD 133029 (Burbidge and Burbidge 1955, 1955*a*) has led to the following results relative to the cosmical abundances:

1. O is probably underabundant, although the factor could not be determined.
2. Ca is underabundant by a factor of about 30.
3. Si is overabundant by a factor of about 15.
4. The metallic group is overabundant by a factor of about 6; the effect is largest for Mn and Cr; the factor for Fe, which is the element contributing the major part of the metal peak, is only about 2, and this value is still subject to observational uncertainties.
5. Sr, Y, and Zr are overabundant by a factor of about 25.
6. La, Ce, Pr, Nd, Sm, Eu, Gd, and Dy have a mean excessive abundance ratio of the order of 600, while Ba is the only member of this group to have an apparently normal (solar) abundance.
7. Pb is probably overabundant by a factor of about 1500.
8. The presence of U cannot be ruled out. In addition, there are several unidentified lines in the spectra of these stars which may be attributable to other heavy elements.
9. Finally, one S star and thirty peculiar A and F stars have been shown by H. W. Babcock (Babcock and Cowling 1953) to have large photospheric magnetic fields of the order of 10^3–10^4 gauss.

In the work on element synthesis by Cameron (1955*a*, *b*) and by Fowler *et al.* (1955) it has been shown that the heavy elements may be synthesized in stellar interiors at an evolutionary stage which stars have reached when they have a helium core and a hydrogen-shell energy source surrounding it. Probably this stage is reached when the star appears as an S star, as has been assumed by Cameron, although this presupposes that mixing to the surface has taken place. Alternatively, the heavy elements may be synthesized in the giant stage without being mixed to the surface, in which case the stars will more reasonably be associated with the K and M giants. Thus there may not be any need to consider the possibility that surface nuclear reactions are responsible for the abundance anomalies in the S and Ba^+ stars (the latter are apparently giant stars and may perhaps represent a later stage in the evolution of an S star). However, it must be

remembered that one S star and four M stars have large magnetic fields, and therefore, in view of what follows in Sections II and III, surface reactions cannot be ruled out completely.

On the other hand, it is highly improbable that the peculiar A and F stars have reached a stage in their evolution when they can produce the observed anomalies internally. There are several arguments which lead us to conclude that they are still young stars, on or near the main sequence and hence without large helium cores. They are distinguished from normal main-sequence stars by their anomalous spectra. Their positions in the Hertzsprung-Russell diagram lie on or near the main sequence. Measurements of two color indices of a selection of them (Provin 1953) show that they lie well interspersed among the normal main-sequence B, A, and F stars, although they tend to be somewhat brighter and bluer than normal stars of the same spectral type and hence to be slightly hotter than their spectra would indicate. Peculiar A stars are found in at least two galactic clusters and belong to population I. For both the Coma cluster (Weaver 1952) and the Ursa Major stream (Roman 1949; Miczaika 1954), luminosity-temperature diagrams have been plotted. In both, the main sequence extends up to type A0, i.e., up to and including the region where the peculiar A stars lie. In the Ursa Major stream there are some red giants, but none cooler than K5. In the Coma cluster there are no red giants and only two yellow giants. A plot of the Coma cluster by Johnson (1954) shows that it is probably a relatively young system. Thus we conclude that the peculiar A stars are main-sequence stars, relatively young, without large helium cores and certainly without any production of neutrons from (α, n) reactions, which are necessary in the synthesis envisaged by Cameron (1955*a*, *b*) and by Fowler *et al.* (1955). Internal production of the heavy elements by these capture processes then does not appear possible.

Thus other mechanisms for producing the anomalous abundances must be considered. As has already been noted, many of the peculiar A and F stars have large variable magnetic fields. For example, α^2 CVn and HD 133029, in which the abundances have been measured, have variable fields with maxima of $+5000$ and $+10000$ gauss, respectively, α^2 CVn having a period of variation of about 5.5 days. This suggests the acceleration of ions in spots on the star's surface; the energetic particles which result may then produce nuclear reactions in the stellar surface. In Section II we shall discuss the mechanisms for ion acceleration and attempt to estimate their efficiency under certain conditions. In Section III we shall consider the general conditions for surface synthesis derived from the standpoint of nuclear physics.

II. ACCELERATION PROCESSES

In a previous paper (Burbidge and Burbidge 1955*a*) it has been suggested that acceleration processes are taking place in the atmosphere of α^2 CVn by the Swann betatron mechanism (Swann 1933; Riddiford and Butler 1952) for the acceleration of ions in growing or shrinking magnetic spots. This mechanism is the simplest one to discuss, mainly because Riddiford and Butler have applied it directly to sunspots. However, several other mechanisms have been proposed. That by Bagge and Biermann (1948, 1949) considers acceleration in the changing magnetic field produced by a pair of sunspots moving relatively to each other. Biermann (1953) has shown that the energies attained by both mechanisms are essentially similar. A mechanism of acceleration in solar flares has also been proposed by Kiepenheuer (1950). Unfortunately, the extension of the details of any of these theories to the surfaces of magnetic stars is beset with uncertainties. Our understanding of the form of the magnetic variations on the stellar surface is very sketchy. We can, however, put forward the following ideas.

a) The amount and the intensity of the magnetic activity on the surface of a magnetic star must be many orders of magnitude greater than that on the solar surface. This is indicated by the mean strengths of the order of 10^3–10^4 gauss over large parts of the

reversing layers of these stars, as compared with the mean strengths of the order of 5 gauss observed over the solar surface. Also the variation of the mean polarity of the fields in many cases indicates that large values of dH/dt are to be expected. Thus all the types of magnetic activity observed on the sun (Babcock and Babcock 1955) must be considered to be very much amplified in these stars.

b) By analogy with sunspots, stellar spots of great field intensity may be expected in magnetic stars. Sunspots have intensities, at the levels of observation, of about one thousand times the small general solar magnetic field. They are probably representative of the underlying magnetic field in the stellar interior; and for a magnetic star, therefore, fields of the order of 10^5–10^7 gauss in the spots are possible (the theoretical upper limit on the internal field strength is governed by the condition for stability of these stars [Chandrasekhar and Fermi 1953; Burbidge 1954]). Theories of the origin of sunspots as due to loops of internal field reaching the solar surface (cf. Bullard 1955) would suggest very large fields of this sort. We shall employ fields in the range 5×10^5–10^7 gauss, at levels below those at which the spectrum lines are formed, in the following calculations.

c) The time scale for the spot activity in the magnetic stars is of some importance in the following theory. A number of the magnetic stars (including both of those that will be discussed in Sec. IV) have probable or well-determined magnetic variation periods of the order of a few days (10^5–10^6 sec). In addition to this, some of these stars may have irregular variations of field superposed on the more regular magnetic oscillations, and these may have time scales of the order of 10^4 sec (cf. Burbidge and Burbidge 1955*a*, Sec. XIII). Also, although the total duration of sunspots is sometimes of the order of 10^6–10^7 sec, the periods of initial growth are about 10^4–10^5 sec. We shall therefore take 10^4–10^5 sec as the time during which acceleration processes are effective over energy loss by ionization and collision. However, see Section IV for a further discussion of the time scale. It will also be necessary in what follows to make some estimate of the size of the spots in magnetic stars, and we shall perforce use sunspot values (it should be borne in mind that, although spots in magnetic stars have an unknown form, magnetic-energy considerations suggest that they may be much larger than sunspots). We shall suppose that the activity takes place in spots at densities of between 10^{-8} and 10^{-7} g/cc. In a normal A0 star this corresponds roughly to a temperature range of 12000°–40000°.

d) It is reasonable to assume that general spot activity in a large proportion of otherwise quiescent, apparently nonmagnetic stars is continuously taking place. Activity similar to that occurring on the sun would not be observed even at the distance of the nearest stars. In other stars (some red dwarfs) flarelike characteristics are observed, so that there may be considerable magnetic activity in these. These general forms of activity are of importance when we consider the production of D, Li, Be, and B (Sec. V).

Bearing these arguments in mind, we can return to the acceleration mechanisms in a spot, as discussed by Riddiford and Butler (1952). They were concerned with relativistic velocities for cosmic-ray particles. In this paper we shall be primarily interested in energies in the range of 1–100 Mev, so that relativistic effects for ions can be neglected. We find in this case, from the results of Riddiford and Butler, that the kinetic energy gained by an accelerated ion of rest mass M_0 in time t is given by

$$\frac{E}{M_0 c^2} = \frac{1}{8}\frac{r_0^2 t}{c^2 t_0^3} \quad \text{for} \quad u_0 \ll \frac{r_0}{2t_0} \tag{1}$$

or

$$\frac{E}{M_0 c^2} = \frac{u_0^2 t}{c^2 t_0} \quad \text{for} \quad u_0 \gg \frac{r_0}{2t_0}, \tag{2}$$

where r_0 is the radius in the spot at which acceleration begins, u_0 is the injection velocity, and t_0 is the injection time relative to the time when H is zero. The derivation of this

expression assumes a uniform field varying linearly with time. It is important to note that the result is independent of the time rate of variation of the field and also of the charge of the ion, provided that $z_i > 10M_0/H_0l_0e \sim 10^{-3}M_0/H_0l_0$ for M_0 in atomic mass units. Here H_0 is the magnetic field at the time of injection t_0. This condition is fulfilled in all cases of interest. Also of importance is the fact that E is proportional to the rest mass of the accelerated nucleus, so that the energy per nucleon is the same for all ions.

From equation (1), if $r_0 = 2 \times 10^9$ cm, as at the periphery of sunspots, and $t = 10^4$ sec, the energy attained per nucleon for zero injection velocity is $5000/t_0^3$ Mev, so that, to achieve energies of 1, 10, or 100 Mev, the injection times are approximately 17, 8, and 4 sec after the spot begins to grow. These times are rather insensitive to the values chosen for r_0 and t. However, the final energy achieved is quite sensitive to the injection time. On the other hand, if the injection velocities correspond to energies of the order of tens of kilovolts, equation (2) applies, and the final energy achieved is not so sensitive to the injection time.

These considerations are of importance in regard to the energy spectrum of the accelerated particles. Riddiford and Butler show that if there is a source of ions which is constant during the relatively short injection time, then the number of particles with final energy between E and $E + dE$ is

$$f(E) \propto E^{-n}$$

where, by using equation (1) or (2), $n = \frac{4}{3}$ or 2, respectively, in the nonrelativistic case, and $\frac{5}{3}$ or 3 in the relativistic case. In the latter these extremes embrace the value of $\sim$2.5, which holds for the primary cosmic-ray spectrum at relativistic energies; however, it must be remembered that the mechanism for the acceleration of cosmic rays in the interstellar gas proposed by Fermi also gives a power-law spectrum of the observed form, and in this case the energy spectrum of the ions at the point when they are ejected from the star into the interstellar gas is not important. It can easily be shown that the same power laws hold for the energy spectrum averaged over the acceleration time, which is the spectrum of interest in connection with the nuclear processes occurring while the magnetic field is changing.

The density of the region in which ions can be accelerated has a considerable bearing on the extent to which nuclear processes occur in a magnetic spot both through the ρ^2 term in reaction rates and through the influence on the spectrum of the accelerated particles. This last point has been discussed by Riddiford and Butler, who argue as follows: *All* ions will be accelerated if the density is low enough that the maximum ionization energy loss per centimeter of path length, which occurs at about 0.1 Mev for protons, is less than the energy gain in the electric field. The effective energy gain for a particle which remains nonrelativistic throughout acceleration is very small, and the critical density will be much smaller than that occurring in spots. At the greater densities of interest, the injection of ions at energies greater than 0.1 Mev by other mechanisms, such as electric discharges, will be required, and equation (2) will be relevant. In general, only a few particles will be accelerated, and these will have a spectrum with $n = 2$. The secondary ions produced will not be accelerated because of their low injection velocities. Riddiford and Butler note that nonrelativistic particles are accelerated more slowly and are less able to overcome ionization losses, so that a cutoff in the spectrum near 10^2 Mev/nucleon might be expected. It is of some interest that the Fermi mechanism for acceleration of cosmic-ray particles requires injection energies of this order of magnitude.

It is probable that the energy losses produce a degraded spectrum in which there are a majority of low-energy particles and an inverse-power-law exponent somewhat greater than the upper limit given by Riddiford and Butler. The accelerating field must be thought of as maintaining the injected particles at a considerably greater energy and with a markedly different spectrum with respect to the main bulk of the particles in the Maxwell-Boltzmann distribution. This situation must be maintained at least long enough for each fast particle to undergo a nuclear process which will, in fact, be its fate

in a relatively short time. Inelastic losses will cease when ionization becomes complete. In a picture of this sort the large energy transfer between the accelerated and unaccelerated particles through collisions with electrons is not taken into consideration. Thus we shall consider in Section III that one feasible situation will be the acceleration of a small percentage of the particles in a spot with an inverse-power-law spectrum ($n = 2$ or somewhat greater) extending down to a nonrelativistic cutoff. In Section III it will be shown that the nuclear-physics requirements are met if $\sim$1 per cent of the particles are accelerated to 10–100 Mev.

As an extreme alternative we shall also consider the case in which ionization is completed early in the acceleration time so that no further inelastic collisions occur thereafter. We assume that the transfer of energy into radiation is negligible, even though this may be true only for periods considerably shorter than the spot lifetimes. The changing field accelerates the ions without requiring large injection velocities, and the large elastic collision cross-section with free electrons and other nuclei will lead to a general distribution in energy eventually approaching the Maxwell-Boltzmann distribution. That this is feasible can be seen by assuming that the ionization energy required comes from the magnetic field energy and that up to 10 per cent of the field energy can be extracted without disturbing the linear rise with time. The magnetic field, H_i, when ionization is complete in a medium of density ρ with mean rest mass $\bar{M}_0$ is then given by the equation

$$\frac{\rho\bar{w}}{\bar{M}_0} = F\left(\frac{H_i^2}{8\pi}\right),$$

where $\bar{w}$ is the mean energy loss per ion pair, $\sim$30 ev $= 5 \times 10^{-11}$ erg for all atoms, and F is the fraction of the field energy required. For $\rho = 10^{-7}$ g/cc, $\bar{M}_0 = 2 \times 10^{-24}$ g, and $F = 0.1$, the required field is $H_i \sim 2 \times 10^4$ gauss. If the field ultimately rises to 10^7 gauss in 10^4 sec, this field will occur at 20 sec, and the injection time for all ions will be of this order. The foregoing calculations then show that in such a "hot spot" an average energy per nucleon of about 1 Mev will be supplied by the field in the remaining period of acceleration without inelastic collisions. We shall discuss the feasibility of this in terms of the plasma properties of the gas in the latter part of this section.

Finally, at the end of the acceleration period, if f is the fraction of the magnetic energy which has been transformed into particle motion of average kinetic energy $\bar{E}$, we have

$$\frac{\rho\bar{E}}{\bar{M}_0} = f\left(\frac{H^2}{8\pi}\right).$$

If $\bar{E} = 1$ Mev $= 1.6 \times 10^{-6}$ erg in a region where $\rho = 10^{-7}$ g/cc and if f is only $\sim$0.01, then a maximum magnetic field, $H = 10^7$ gauss, is required. On the other hand, if this average energy is attained only in a region of lower density, $\sim 10^{-8}$ g/cc, and $f \sim 0.5$, then a field of only 5×10^5 gauss will be necessary.

Several criticisms of the acceleration mechanism under discussion have been made. These are not valid in our context, although they may be in connection with the production of cosmic-ray particles. It is often stated that a few particles will not be accelerated to relativistic energies but that the energy of an induced electric field will be dissipated over a great number of charged particles, each receiving only a small amount of the total available energy. The alternatives discussed here cover the extremes of the various schools of thought on this matter. We also note that extraction mechanisms are not required (except for some cases described in Sec. V). The particles will produce nuclear reactions on the spot, and even deceleration at the end of the spot life is irrelevant.

It is also worth noting that particles in the energy range which we shall find to be of interest in Section III are probably emitted by the sun. The experiments of Meinel and Fan (1952, 1953) on reproducing in the laboratory the features of the auroral spectrum

suggest that this is excited by protons and α-particles emitted from the sun in the energy range 80–250 kev, with the upper limit given as 500 kev (Das Gupta and Ghosh 1946) from the depth of penetration of the particles in the earth's atmosphere to the height of greatest auroral activity. Recently, Meredith, Gottlieb, and Van Allen (1955) have discussed the possibility of a large flux of 15-Mev protons as the source of the very soft component of cosmic radiation observed at high altitudes. In addition, the slowly varying "solar" component of cosmic rays consists of particles with a *mean* energy of only $2M_0c^2$ (Kiepenheuer 1954). Finally, particles with energy less than $\sim 10M_0c^2$ are emitted at the time of flares associated with sunspots (*ibid.*). These flares must be connected with some type of extraction mechanism for particles accelerated in the spot. At this point it might be asked why nuclear reactions should not go on in the sun's surface. According to the theory developed here, the reason for this is simply that the ratio of the efficiency of the process in magnetic stars to that in the sun is the ratio of the available amounts of magnetic energy, i.e., about 10^6.

It is necessary to say something about the acceleration mechanism from the point of view of the plasma properties of the gas. We have ignored so far the apparent tendency for the electric conductivity to short-circuit this whole induction mechanism. In recent years there have been numerous criticisms of the Swann mechanism based on arguments of this sort, and it is probable that some effects of this kind may take place. We may modify the argument given by Biermann (1953), following Schlüter (1952), as follows: Owing to the plasma properties of the gas, local changes of H must be accompanied by mass motions, whose velocity may be denoted by v'. Using the first of Maxwell's equations, he finds that the maximum density of accelerated ions is given by

$$\frac{\rho \bar{E}}{\bar{M}_0} \leq \left(\frac{H^2}{4\pi}\right)\left(\frac{L}{L'}\right)\left(\frac{v'}{c}\right),$$

where $\bar{E} = e\mathfrak{E}L$ is the average kinetic energy of the accelerated particle, $\mathfrak{E}$ is the induced electric field, L is the characteristic length for the acceleration, and L' is a second characteristic length such that curl $H \simeq H/L'$. For a stellar spot we do not have good estimates for either L, L', or v'. Schlüter gives examples for the solar corona and chromosphere, where observed values of v' may be used, and finds in this case an extremely low density of accelerated particles. However, if we suppose that in stellar spots, at the levels with which we are concerned, fields of the order of 3×10^6 gauss are present, and if $\bar{E} = 1$ Mev $= 1.6 \times 10^{-6}$ erg, and $\bar{M}_0 = 2 \times 10^{-24}$ g, then $\rho \sim 10^{-6}(L/L')(v'/c)$. Now, in general, we should expect that $L \gg L'$ (cf. the detailed discussion by Schlüter); L' will depend on the geometry of the field. If, for example, $v'/c = 10^{-3}$ and $L/L' = 10^2$, $\rho = 10^{-7}$ g/cc. For large values of L/L' it is not necessary to assume that there are such large mass motions at this depth. From the argument based on energy considerations, given earlier, $f = \frac{1}{2}(L/L')(v'/c)$.

The arguments given by Schlüter for the corona and chromosphere suggest that when a limiting density of accelerated particles is achieved, there is rough equipartition of energy between the very fast ions and the material taking part in the mass motions. However, this treatment completely ignores the collision effects mentioned earlier. These will tend to transfer energy from the high-energy component of the gas to the slower component, which will be further accelerated. Since the initial tendency is for all the ions in the spot to be accelerated, we can therefore see, in a qualitative fashion, what will be the sequence of events. When the spot first appears and begins to grow, the material high in the atmosphere of the star (density perhaps $\leq 10^{-14}$ g/cc) will tend to be accelerated, and a small fraction of the ions will reach very high relativistic energies (perhaps a fraction $\leq 10^{-10}$ by analogy with the solar corona). Because of the very low density and the decrease in cross-section with increasing energy, the effect of collisions will be very small, so that the tendency for atomic equipartition to take place can be

neglected. However, at lower levels in the spot (perhaps $\rho \leq 10^{-6}$ g/cc), a much larger proportion or, indeed, all the ions will initially tend to be accelerated, and the equivalent temperature of the region will rise. Small mass motions will develop, and only that fraction of the ions which can move relative to the changing magnetic field will be further accelerated. The rapid rate of collisions will continuously deplete this fraction while increasing the energy in the mass motions in the plasma, until finally the mechanism for further acceleration will break down when only a very small fraction of the ions have velocities different enough from those of the mass of material to be further accelerated. At this point the acceleration mechanism may be supposed to have effectively short-circuited itself, so that a natural cutoff in particle energy in the resulting spot is produced. At lower levels (perhaps $\rho \leq 10^{-4}$ g/cc) the densities are so great that any change in the magnetic field is followed immediately by corresponding mass motions, so that little or no acceleration by this process can be achieved.

Thus the two alternative conditions which we shall see are necessary from the standpoint of nuclear physics, i.e., that about 1 per cent of the material is accelerated to high energies or that the whole of the material in localized regions is accelerated to slightly lower energies, are both plausible at the densities which we wish to consider, i.e., 10^{-8}–10^{-7} g/cc. It is difficult to develop the argument further without detailed models involving the geometry and field strengths in spot regions on magnetic stars.

III. NUCLEAR PHYSICS

In this section we shall attempt to delineate in some detail the nuclear processes which might lead to the production of anomalous abundances of some elements. We shall also try to indicate the stellar surface conditions necessary for a transmutation of the elements comparable to that observed.

As far as the light elements are concerned, the stars which we are considering have normal cosmical abundances (with the possible exception of oxygen), so that light hydrogen and helium are the predominant constituents of the stellar surface, though the possibility that $\sim$1 per cent of deuterium is present also cannot be excluded (cf. Sec. IV). It is reasonable to assume that particular nuclei are not selectively accelerated by the mechanisms discussed in Section II, and, at the moderately high energies at which synthesis predominates over spallation, barrier factors will prevent reactions between pairs of nuclei, both of which have large Z-values. For these reasons, therefore, any nucleus will experience nuclear reactions primarily with protons, α-particles, and possibly deuterons.

Direct synthesis of heavier elements from lighter ones by primary collisions with protons requires that the (p, γ) capture processes dominate over all other nuclear processes. This is true only at certain resonances at low energies, where the rates of the reactions are hopelessly inadequate because of the Coulomb barrier factor at the low density and temperature of the quiescent stellar surface or because of the limited extent of the active areas. Therefore, we must look to secondary processes for synthesizing reactions. The most promising of these are (n, γ) neutron-capture processes on the intermediate and heavy nuclei, after the neutrons have been produced in (p, n) reactions chiefly on the light nuclei. The primary (p, n) reaction is neutral as far as synthesis is concerned, and so the ultimate result of the two reactions is an increase in atomic weight of the final capturing nucleus with no change for the nucleus involved in the primary (p, n) process. This double mechanism will be discussed in part *b* of this section. The conditions for synthesis are then, in this case, that all the particles in a "hot spot" must be accelerated and, through collisions, attain approximately a Maxwell-Boltzmann distribution in energy such that $kT \sim 1$ Mev, without, however, reaching equilibrium with radiation.

Direct synthesis of heavier elements from lighter ones is possible by primary collisions with deuterium through the (d, p) and (d, n) reactions and with α-particles through the (α, n) reaction and, in fact, through any α-reaction in which three nucleons or less are

produced. These primary mechanisms will be discussed in part *a* of this section. In this case the condition for synthesis is, then, that a small percentage of the particles are accelerated to energies in the range 10–100 Mev, with an energy distribution giving still fewer particles at higher energies to avoid spallation effects. The energy distributions required for *a* and *b* are the extreme cases of what might reasonably occur in stellar surfaces, as discussed in Section II, and we conclude that synthesis will occur in both cases and thus presumably in intermediate situations. We consider that these reactions take place in regions of density 10^{-8}–10^{-7} g/cc, and in Section IV a quantitative discussion of the amount of material synthesized is given.

a) Synthesis through Reactions Involving α-Particles and Deuterons

The energy dependence of α-particle and deuteron-induced reactions has been discussed and summarized by Blatt and Weisskopf (1952), who have given references to original papers. We shall first discuss the α-particle processes. The (α, n) reaction has a threshold energy of the order of 5 Mev, the energy equivalent of the mass excess of the neutron over that of the α-particle. However, the reaction does not approach its maximum value until the Coulomb barrier energy is reached at $2Ze^2/R_0A^{1/3} \simeq 2Z/A^{1/3}$; this is approximately equal to 14 Mev for intermediate nuclei like Fe^{56} and 28 Mev for heavy nuclei like Pb^{208}. The maximum value of the cross-section is roughly equal to the geometrical value,

$$\sigma_g = \pi R^2 \simeq \pi R_0^2 A^{2/3} = 0.06\, A^{2/3} \text{ barns}$$

so that, for Fe^{56}, $\sigma_{\max}(\alpha, n) \sim 1$ barn. The cross-section decreases at higher energy from its maximum value because of the competition from additional reactions, principally (α, pn), $(\alpha, 2n)$, $(\alpha, p2n)$, and $(\alpha, 3n)$. These reactions begin at higher threshold values, rise to maxima such that the total cross-section remains comparable to the geometrical cross-section, and then decrease. They, as well as the (α, n) reaction, result in synthesis; the increase in the atomic weight of the nucleus involved varies from $\Delta A = 1$ to $\Delta A = 3$. At still higher energies spallation processes set in and become comparable to the decreasing rates of synthesis at approximately 100 Mev. Because of the effect of nuclear transparency, the spallation reactions rise to a total cross-section of only half the geometrical value. These spallation reactions result in the emission of He, Li, Be, B, and even heavier nuclei, as well as copious numbers of neutrons and protons. The result is the breakup of the heavier nuclei rather than synthesis, with a negative value of ΔA which increases in magnitude roughly linearly with energy. Near 300 Mev, $\Delta A \simeq -12$.

Thus synthesis with $\Delta A \simeq 2$ is predominant with approximately the geometrical cross-section over the energy range from ~10 to 100 Mev, while spallation with $\Delta A \simeq -12$ and $\sigma \simeq 0.5\sigma_g$ predominates above 100 Mev. For over-all synthesis to occur, the energy spectrum of the accelerated α-particles must thus exhibit a greater flux of the lower-energy particles. Possible energy spectra have been discussed in Section II. The Maxwell-Boltzmann distribution for all particles requires too high an average energy ($kT \sim 10$ Mev) for the direct synthesis by α-particles, and so we are here interested in the inverse-power-law spectrum. For such a spectrum the synthesis to spallation ratio, β, is given by

$$\beta = \frac{|\sigma \Delta A|_{\text{syn}}}{|\sigma \Delta A|_{\text{spall}}} \frac{\int_{10}^{100} vE^{-n}dE}{\int_{100}^{\infty} vE^{-n}dE} \sim 10^{n-2},$$

so that $n \simeq 3$ is required if synthesis is to exceed spallation by an order of magnitude. This value is a possible one, as has been shown in Section II.

It is interesting to note that since the energy of the accelerated particle is proportional

to its atomic weight (cf. Sec. II), the relative number and flux of protons from 10 to 100 Mev is equal to that for the α-particles from 40 to 400 Mev. If the hydrogen to helium ratio is about 10, the flux of α-particles from 10 to 100 Mev is $0.1 \times 4^{n-1.5}$ times that for protons in this range. This ratio is about unity for $n \sim 3$. Fast-proton and α-reactions have been compared by Ghoshal (1950) and have been shown to be independent of the nature of the incident particle for the same compound nucleus at the same excitation. This independence holds roughly, on the average, for the same target nuclei and the same proton and α-particle energies. The average ΔA for the (p, n), (p, pn), $(p, 2n)$, and $(p, 3n)$ reactions is -1 compared to $+2$ for the corresponding α-particle reactions. Thus the effect of the fast protons is to decrease the synthesis produced by the fast α-particles by a factor of 2. A small increase in n will make this factor negligible.

The proportionality of energy with atomic weight means that the velocity spectra are identical for all particles. Thus the relative velocity and the energy in the rest-mass system are the same for a collision between an accelerated heavy nucleus and an unaccelerated light particle as for the opposite case, which we have discussed (we can neglect collisions between pairs of accelerated nuclei). This essentially doubles the synthesis rate, canceling the factor discussed in the previous paragraph.

We next consider the extent of the synthesis arising from the reactions of the accelerated α-particles with the remainder of the material, which is at a temperature not much different from that of the quiescent stellar surface ($\sim 10^4$ degrees). Most of the interactions will be with the C, N, O, and Ne group, which has a normal abundance relative to hydrogen, $a \sim 2 \times 10^{-3}$, and a geometrical cross-section equal to 0.35 barn. The mean lifetime for a fast α-particle is shown in Appendix I to be

$$\tau = \frac{2.2}{a \rho \sigma v} \simeq 10 \text{ sec},$$

where v, the α-particle velocity, has been taken as 3×10^9 cm/sec and ρ as 10^{-7} g/cc. The mean free paths, $\tau v \sim 3 \times 10^{10}$ cm, are quite long, but the radii of curvature in the magnetic field are considerably smaller ($\sim 10^6$ cm). Thus the fast α-particles rapidly interact, and essentially all those accelerated will produce reactions in the spot acceleration times of 10^4 sec.

Spallation will play an important role in the interaction of 10–100-Mev α-particles with the C, N, O, and Ne group, and it is doubtful whether any synthesis of heavier elements from this group will occur. In fact, it is highly probable that this group will be reduced in abundance with some production of He, Li, Be, and B. This may explain the possible observed underabundance of O. The main synthesis will be built upon the nuclei from Mg through the metal group, which have a total $a \sim 10^{-4}$ and an average geometrical cross-section of ~ 0.7 barn. The number of interactions which each of these nuclei will have is given by $0.7 a_\alpha / (0.35 \times 2 \times 10^{-3} + 0.7 \times 10^{-4}) \sim 10^3 a_\alpha$, where a_α is the number of fast α-particles relative to hydrogen. A reasonable estimate of the spallation in the C, N, O, and Ne group will increase this by a factor of 2. For an increase in atomic weight of 100 (50 interactions) by the intermediate nuclei, it is necessary that $2000 a_\alpha = 50$, or $a_\alpha = 0.025$. This means that about one-quarter of the normal helium abundance must be accelerated and eventually expended to synthesize the heavy nuclei from the intermediate group. It will be shown in Section IV that it is reasonable to suppose that all the surface material has been through a region of intense nuclear activity about four times, so that in each such spot about 6 per cent of the α-particles must reach energies in the range 10–100 Mev and then have a reaction with nuclei leading to an average $\Delta A \sim +2$. For an E^{-3} spectrum with an appropriate low-energy cutoff below which the remaining particles are unaccelerated, this implies an energy averaged over *all* the α-particles of ~ 2 Mev and, since $E \propto M_0$, an energy averaged over all particles (mostly protons) in the spot of ~ 0.7 Mev. About 1 per cent of all the particles are accelerated to 10–100 Mev.

It must be emphasized that *all* the particles must not be accelerated to high energy. This is because in such a case the neutrons emitted in the (p, n), (α, n), and other reactions will then remain at energies where they will induce copious spallation through $(n, 2n)$ and more complicated reactions.

When the bulk of material remains unaccelerated, the neutrons will be thermalized to energies $\sim$1 ev, corresponding to the temperature of the spot material, which is not too different from that in the quiescent stellar surface. They will be captured by the low-energy nuclei through the (n, γ) reaction, and the greatest proportion of the captures will be by hydrogen to form deuterium (cf. case *b*). The deuterium will increase in concentration until its destruction rate by the fast particles primarily through the D(p, n)2H reaction balances the formation by neutron capture, following their production by fast particles interacting principally with the C, N, O, and Ne group. The abundance ratio of D to C, N, O, and Ne is thus equal to the ratio of the formation to destruction cross-sections. The effective formation cross-section is $4 \times 0.35 = 1.4$ barns (the factor 4 occurs because both α-particles and protons produce, on the average, 2 neutrons in each interaction), while the destruction cross-section by D(p, n)2H is 0.13 barn at 10 Mev (Thomson 1952). Hence the deuterium concentration builds up to ten times that of the C to Ne group or to 1 or 2 per cent of that for hydrogen in each spot and eventually in all the surface material. The pickup reaction (p, d) will also synthesize deuterium directly. This buildup is unavoidable in the synthesis by fast particles, and this point may eventually serve as a test of the existence of this process.

The deuterium concentration builds up in the time required for one surface layer of material to be processed through active regions, i.e., about 10^8 years (Sec. IV), so that synthesis by the (d, p) and (d, n) stripping reactions occurs thereafter. The total cross-section for these two processes is given by $\sigma_{str} \simeq \pi R d \simeq 0.1 A^{1/3}$ barn, where $d \simeq 2 \times 10^{-13}$ cm is the diameter of the deuteron; σ_{str} then has a value for fast deuterons of about 0.5 barn on all intermediate and heavy nuclei. The next most important reaction, (d, pn), is neutral in regard to element synthesis. The stripping reactions are effective at relatively low energies, so that it is the flux of deuterons in the 5–50-Mev range which will be important. In percentage relative to the total number of deuterons, this is the same as the flux of 10–100-Mev α-particles. However, the total number of deuterons is, at most, 2 per cent on the basis of our earlier arguments, so that only a small ($\sim$20 per cent) increase in synthesis arises from the deuterium reactions.

The transfer of the intermediate nuclei to the heavy nuclei by the α- and deuteron reactions involves cross-sections which increase smoothly but slowly with atomic weight A. This has the consequence, if the cross-sections are taken, for ease of calculation, to be independent of A, that the original nuclei uniformly advance in atomic weight with a spread over A, after m reactions, given approximately by $(2\pi m)^{1/2}\Delta A$ (Appendix II), where ΔA is again the increase in A per process. For $m = 50$ and $\Delta A = 2$, this means that the metal group ($A \simeq 56$) will be moved into a group from $A = 138$ to $A = 174$, centered at $A = 156$. There is some indication that this may correspond to the observations on La to Dy (Burbidge and Burbidge 1955, 1955*a*). The original spread in A, differences in σ, and fluctuations in m and ΔA will tend to give a greater final spread and a different grouping from that indicated by this calculation.

b) Synthesis through (p, n) Processes in Light Nuclei Followed by (n, γ) Processes in Heavy Nuclei

Neutrons are produced in high-energy material containing hydrogen by reactions of the type

$$X + p \rightleftarrows Y + n\,, \tag{3}$$

where X is the initial nucleus and Y is the final nucleus with $A(X) = A(Y)$ and $Z(Y) = Z(X) + 1$. Both the (p, n) reaction and its inverse, the (n, p) reaction, are indicated here. The primary (p, n) reaction on stable nuclei is neutral with respect to synthesis and dis-

integration, since, if it is not followed by the (n, p) process, the nucleus Y decays to X by positron-neutrino emission or electron capture, i.e.,

$$Y \rightarrow X + \beta^+ + \nu$$

or

$$Y + e^- \rightarrow X + \nu \,. \tag{4}$$

Each target nucleus catalytically changes protons into neutrons; a neutron flux is established, and capture of some of these neutrons eventually synthesizes heavy nuclei. Those neutrons which do not interact in some way decay to protons according to

$$n \rightarrow p + \beta^- + \nu \,, \tag{5}$$

with a mean lifetime of 1100 sec.

We shall estimate the neutron flux resulting from these processes. It is clear from equations (3) and (4) that the (p, n) reactions on stable nuclei are always endoergic, with thresholds given by the maximum positron energy available in the decay of Y plus 1.80 Mev $(m_\beta c^2 + M_n c^2 - M_p c^2)$. Representative thresholds among the light nuclei are $|Q| = 18.5$, 3.0, 6.0, and 3.5 Mev for C^{12}, C^{13}, N^{14}, and N^{15}, respectively. Little experimental evidence is available on the cross-sections for the (p, n) reactions in light nuclei. However, the threshold energies are, in general, greater than the Coulomb barrier energies for protons and light nuclei, and thus it is reasonable to suppose that the cross-sections approach the geometrical values, discussed previously, within a relatively small energy interval above the absolute threshold. On an empirical basis we shall take the effective threshold as $|Q| + 1$ Mev.

The excitation energies in the compound nuclei are, in general, greater than 10 Mev, so that resonance effects will not be very marked. We shall thus consider the cross-section to be zero below $|Q| + 1$ Mev and equal to $0.06A^{2/3}$ barns above this value, up to energies where competition from other processes begins. These competitive processes are successively (p, d), $(p, 2n)$, (p, pn), $(p, 3n)$, and so on. It will be noted that most of these processes produce additional neutrons but that the thresholds are quite high, and thus these reactions can be neglected at the kinetic energies under consideration here. In the intermediate and heavy nuclei, barrier-penetration effects increase the effective threshold energies even for the (p, n) reaction, so that we can neglect this reaction on these nuclei in what follows.

Below the threshold for the (p, n) reactions the most important proton processes in the light nuclei are (p, γ) and (p, α) reactions. These lead to cyclic reactions among the CN isotopes, the NeNa isotopes, the MgAl isotopes, etc., with some very slow synthesis by leakage from the cycle to heavier nuclei. The OF isotopes are transmuted into the CN group primarily through the $O^{17}(p, \alpha)N^{14}$ and $O^{18}(p, \alpha)N^{15}$ reactions, both of which are exoergic. Thus, except for O and F, which will disappear if the reaction rates are high enough, the abundances of the light nuclei will not be markedly influenced by the (p, γ) and (p, α) processes. Some shifting of the abundances within each group will be expected, but this will not strongly affect the rates of the (p, n) reactions with this group of nuclei.

The (n, p) reactions with the unstable products, Y, are, of course, exoergic. The cross-sections will thus be the geometrical ones above about 1 Mev, except for competition by reactions such as (n, γ), (n, d), (n, pn), $(n, 2n)$, (n, α), and so on. In general, this competition will not be severe and can be neglected. The (n, γ) and $(n, 2n)$ reactions with heavy nuclei can be neglected in the neutron flux calculations because of the rarity of these nuclei and can be calculated later as a perturbation.

For reasons which will become clear, the conditions under which synthesis occurs through the (p, n) and (n, γ) processes require an acceleration of all the particles to an average energy of about 1 Mev. Thus we assume a Maxwell-Boltzmann distribution with $kT \sim 1$ Mev. This will hold for times 10^4–10^5 sec in "hot spots" with densities of 10^{-8}–10^{-7} g/cc. Because of the short time scale and the low density, complete equilibrium be-

tween the various nuclear species will not be reached. The previous discussion shows that only the equilibrium between (p, n) and (n, p) processes in light nuclei need be considered, along with the decay of the neutrons and the unstable nuclei.

Without a detailed mathematical approach, it can be seen that the reactions $Y(p, n)$ and $X(n, p)$ can be neglected; $Y(p, n)$ will be very endoergic; $X(n, p)$ will also be endoergic and can be neglected because of the low concentration of X to be expected at equilibrium. The neutron density will be small, and the great excess of protons will thus drive reaction (3) toward the right in such a way as to convert all the stable X nuclei into the proton-rich isobars, Y. After the spot activity has ceased, these will then decay back to the stable isobars.

If X, Y, n, and p now represent the number per cubic centimeter of X and Y nuclei, neutrons, and protons, respectively, then the following equations govern the time rate of change of X, Y, n, and p:

$$\frac{dY}{dt} = -\frac{dX}{dt} = \lambda_p p X - \lambda_n n Y - \gamma_Y Y , \tag{6}$$

$$\frac{dn}{dt} = -\frac{dp}{dt} = \lambda_p p X - \lambda_n n Y - \gamma_n n , \tag{7}$$

with the subsidiary conditions

$$X + Y = X_0 , \tag{8}$$

$$n + p = p_0 . \tag{9}$$

In these equations λ_p and λ_n are the reaction-rate parameters for the (p, n) and (n, p) processes, respectively. These can be calculated by the methods discussed in Appendix I, case 2*c*. Here γ_Y and γ_n are decay constants or reciprocals of the mean lifetimes for the β-decay processes involving nucleus Y and the neutron, respectively; X_0 and p_0 are the original cosmic abundance densities of X nuclei and protons; and $X_0 \ll p_0$.

The solution of equations (6)–(9) leads to the following conclusions. During the early stages of the reactions the β-decay terms in Y and n can be neglected and $n \sim Y \sim X_0$. The excess of protons converts all the X nuclei into Y, and for each Y nucleus one neutron is produced. This is true as long as $\lambda_p/\lambda_n > 4X_0/p_0$, i.e., as long as the rate of the (p, n) process is not too small compared with that of the (n, p) process, as is found to be the case. However, the ultimate equilibrium values, found by setting dY/dt and $dn/dt = 0$, yield

$$n = \frac{\gamma_Y}{\gamma_n} Y \approx \frac{(\gamma_Y/\gamma_n) X_0}{1 + (\gamma_Y/\gamma_n)(X_0/p_0) + \gamma_Y/\lambda_p p_0} \sim \frac{\gamma_Y}{\gamma_n} X_0 .$$

The latter approximation is obtained by neglecting the last two terms in the denominator. When $\gamma_Y > \gamma_n$, the decay of Y, being more rapid than that for the neutron, yields a multiplication factor γ_Y/γ_n in the neutron density. In the lifetime of a neutron a number γ_Y/γ_n of the Y nuclei decay to X nuclei, and these are then available to produce additional neutrons by the (p, n) process. The buildup to this enhanced abundance thus requires a time of the order of 1100 sec, which is an order of magnitude smaller than the acceleration times in the spots.

The application of these results to the various light nuclei indicates that the greatest number of neutrons is released by the reaction $N^{14}(p, n)O^{14}$. The reasons for this are that N^{14} is relatively abundant and the threshold is not too high and O^{14} has a short mean lifetime (104 sec). In this case $X_0/p_0 = 4.6 \times 10^{-4}$, $\gamma_Y = 0.01$ sec^{-1}, and $\gamma_n = 0.0009$ sec^{-1}; $\gamma_Y/\gamma_n = 11$ and $(\gamma_Y/\gamma_n)(X_0/p_0) = 5 \times 10^{-3} \ll 1$. From the calculations given in Appendix I, case 2*c*, when $kT = 1$ Mev, $\lambda_p p_0 = 0.2$ sec^{-1} at $\rho = 10^{-7}$ g/cc and 0.02 sec^{-1} at $\rho = 10^{-8}$ g/cc. The approximations are thus justified at 1 Mev, albeit roughly

for the lower density, and the neutron abundance relative to hydrogen becomes ~11 times the N^{14} abundance, or $a_n = n/p_0 = 5 \times 10^{-3}$. Moreover, kT cannot be lowered too much without reducing this value considerably. The neutron flux is nv_T, where $v_T = 1.4 \times 10^9$ cm/sec.

We estimate that other (p, n) reactions and the (α, n) reactions will together make a similar contribution to a_n, but, all approximations considered, the figure given is probably the most reliable one that can be obtained. The major approximation is the neglect of the competitive reaction $N^{14}(p, \gamma)$, which, as indicated in Appendix I, is about one hundred times slower than the $N^{14}(p, n)$ reaction. However, the mean lifetime of N^{14} in this process is 600 sec at $\rho = 10^{-7}$ g/cc and 6000 sec at $\rho = 10^{-8}$ g/cc. Thus, if $\rho = 10^{-7}$ g/cc, the full buildup of the neutron abundance given above, which requires about 1100 sec, will not quite be reached. It should be noted that the (p, γ) reactions in the CN isotopes are slow, as has been illustrated for N^{14}, and no appreciable energy generation from the CN cycle occurs at the low densities under consideration here.

The production of neutrons by exoergic (α, n) reactions on such nuclei as C^{13} and Ne^{21} will be of some importance in the "hot spots" under discussion, since the temperatures are high enough for proton and α-particle reactions to occur simultaneously. An interesting case in this connection is the cycle which incorporates the following reactions:

$$N^{14}(p, \gamma)(\beta^+, \nu)N^{15}(p, \alpha)C^{12}(p, \gamma)(\beta^+, \nu)C^{13} \begin{cases} \xrightarrow{(p, \gamma)} N^{14} \\ \xrightarrow{(\alpha, n)O^{16}(p, \gamma)(\beta^+, \nu)O^{17}(p, \alpha)} N^{14} \end{cases}$$

The upper branch is just the ordinary CN cycle in which $4p \rightarrow \alpha$, while the lower branch is a CNO cycle in which $5p \rightarrow \alpha + n$. Rough calculations show that in "hot spots" of somewhat longer duration than the average previously discussed, this branch will reach equilibrium, and neutrons will be produced, essentially from hydrogen, with the CNO isotopes serving as catalysts. The $Ne^{21}(\alpha, n)$ reaction will be important only in spots of higher-than-average energy, and in this case the production of the neutrons is accompanied by the transmutation of the NeNa isotopes into Mg.

The production of neutrons will be followed by their interaction with the nuclei in the spot material. The neutrons will be produced with energies somewhat greater, on the average, than 1 Mev. Since the scattering cross-section for neutrons in hydrogen is larger than the capture cross-section at all energies, the neutrons will, in general, be thermalized by collisions with protons in the "hot spot" before being captured. The diffusion lengths of the neutrons are comparable to sunspot dimensions, and we have neglected neutron escape from the spots in equations (6) and (7). The spots in Apm stars are probably larger than sunspots, and neutron escape is indeed negligible.

Once the neutron energy distribution is established, various reactions besides the (n, n) scattering process will take place. The neutrons may decay before being captured, but this has been considered in the derivation of the neutron flux. At energies up to several Mev the capture (n, γ) process is the most probable. As the energy is increased, inelastic scattering (n, n') and the $(n, 2n)$, $(n, 3n)$, and similar processes successively attain large cross-section values.

As long as the emitted neutrons are ultimately captured, these processes do not prevent over-all synthesis and contribute, in fact, to the neutron flux. However, it is essential in the interaction of the intermediate and heavy nuclei that the (n, γ) processes should be more probable than the processes which lead to a decrease in atomic weight. From this point of view, the (n, n') processes can be ignored, and the main competition comes from $(n, 2n)$ processes, particularly for those nuclei which have low thresholds for this reaction. The case of Zn^{67} is a critical one. The effective cross-section $\sigma(n, 2n)$ is just λ/v_T. The actual cross-section reaches the geometrical value $\simeq$1.0 barn about 1.5 Mev above the

threshold at 7.0 Mev. Using the methods given in Appendix I, case 2*c*, we find that $\lambda/v_T = 0.002$ barn at $kT = 1$ Mev and 0.075 barn at $kT = 2$ Mev. From the fast-neutron-capture cross-section measurements of Hughes, Garth, and Levin (1953), $\sigma(n, \gamma) \sim 0.005$ barn for nuclei with A near 67 at energies in the vicinity of 1 Mev. Thus $kT \sim 1$ Mev is an upper limit on the Maxwell-Boltzmann energy, if over-all synthesis is to occur in the interaction of the intermediate nuclei with neutrons. More detailed considerations indicate a definite upper limit of 1.5 Mev for kT. We note that the $(n, 2n)$ reaction, though less frequent than (n, γ), will produce the so-called "shielded" isobars.

The nuclei in the spots capture neutrons of a particular energy in proportion to $\sigma_A a_A$, where σ_A is the capture cross-section at the given energy and a_A is the relative abundance of the element. We assume that the original material has the cosmical abundances. The large metal peak centered around Fe (Fe^{56} is $\sim 10^4$ times as abundant as elements outside this peak) means that the metals and their capture products will capture more neutrons than other intermediate and heavy nuclei. Cameron (1954, 1955*a*, *b*) has shown that synthesis of the heavy nuclei to abundances $\sim 10^3$ times normal will occur if suffi-

TABLE 1

RELATIVE PRODUCTS OF CROSS-SECTIONS *times* ABUNDANCES

	Abundance (a_A)	Thermal $\sigma(n, \gamma)$ ($T = 300°$) (0.025 ev) (Barns)	Fast $\sigma(n, \gamma)$ ($T \sim 10^{10}$) (~ 1 Mev) (Barns)	$\sigma_A a_A$ (Normalized)	
				Thermal (300°)	Fast (10^{10} deg)
H	1	0.313*	3×10^{-5}†	100.0	99.7
Metals (mainly Fe^{56})	2.2×10^{-5}	3.1*	4.8×10^{-3}‡	0.02	0.3

* Measured (Feld 1953).
† Calculated (Blatt and Weisskopf 1952, pp. 604 ff.).
‡ Interpolated for $A = 56$ from smooth curve through data of Hughes, Garth, and Levin (1953).

cient neutrons are supplied so that each metal nucleus captures about 20 neutrons. We are thus primarily concerned with the competition between the metals and the lighter, more abundant, elements for neutron capture. Hydrogen will compete most strongly in this way. The abundances, cross-sections, and their products are given in Table 1.

The thermal (room-temperature) cross-sections can be extrapolated from $T = 300°$ to $T \sim 10^4$ degrees (the quiescent-surface temperature) by using a $1/v$ law. In the Mev region a $1/v$ law holds very approximately. It is clear, therefore, that both for case *a*, in which the major proportion of the material in the spot remained at low energies corresponding to 10^4 degrees, and in the present case, in which the whole of the material in "hot spots" has energies corresponding to 10^{10} degrees, the hydrogen captures practically all the neutrons, and the result of the initial neutron capture is the synthesis of deuterium rather than of the heavy elements. In fact, for element-building processes which rely on a neutron flux, i.e., this present case, the amount of synthesis of the heavy elements in the initial capture stage is not sufficient to compensate for the disintegration of these elements by the small proportion of protons having high energies. Thus, for heavy-element synthesis, a mechanism must be available to return the neutrons captured by the initial process to their free state. Since the majority of the collisions which the deuterium will make will be with protons, the main reaction which fulfils this requirement is

$$d + p \rightarrow n + 2p \,, \tag{10}$$

which is endoergic by 2.23 Mev. The deuteron-stripping processes on heavier elements will also be effective, but these will be neglected because of the comparative rarity of these nuclei. The buildup of deuterium will then be governed by the equation

$$\frac{dD}{dt} = \lambda_\gamma p n - \lambda_p D p , \tag{11}$$

where λ_γ and λ_p are the rates for the (n, γ) and (p, n) processes, respectively, and D, p, and n are now the number densities of deuterons, protons, and neutrons. Equilibrium will be reached when

$$\frac{dD}{dt} = 0 , \qquad \text{and hence} \qquad \frac{D}{n} = \frac{\lambda_n}{\lambda_p} .$$

At 1 Mev, $\sigma(n, \gamma) = 3 \times 10^{-5}$ barn and $\sigma(p, n) = 0.13$ barn above the threshold (Thomson 1952). Using the methods outlined in Appendix I, we find that the deuterium concentration reaches 2×10^{-3} of the neutron concentration or 10^{-5} of the hydrogen abundance. Thus under these conditions the neutrons are rapidly captured and lost by hydrogen in the spots, and the metallic elements and their capture products ultimately capture them. Neutrons which diffuse from the spots will produce deuterium, and D/H may build up to 10^{-2} as in case *a*.

The number of neutrons captured per metallic nucleus during the period of spot activity ($t = 10^4$–10^5 sec) can be computed. This number, N, is given by

$$N = \frac{t}{\tau} ,$$

where τ is the mean lifetime of a metallic nucleus for neutron capture, i.e.,

$$\tau = \frac{2.2}{a_n \rho v \sigma (n, \gamma)} .$$

For Fe^{56}, $a_n v \sigma(n, \gamma) = 3.4 \times 10^4$, so that

$$N = 1.5 \rho t \times 10^4 .$$

Thus, either for a time of spot activity $t = 10^4$ sec at $\rho = 10^{-7}$ g/cc, or for $t = 10^5$ sec at $\rho = 10^{-8}$ g/cc, $N = 15$. Therefore, the densities and lifetimes of active regions in stellar spots are such that anomalous abundances of the heavy elements $\sim 10^3$ times the normal abundances will be built up in the material of the active region during the lifetime of the spot. If shorter periods of nuclear activity are assumed, then the anomalous abundances will be reached only after the surface material has been processed through a greater number of spots.

As has been mentioned previously, Cameron, in connection with interior production of neutrons and anomalous abundances in giant stars, has solved the equations governing the sharing of neutrons in capture processes by nuclei, starting with those in the metal peak. Cross-sections for capture reactions for 10-kev neutrons were used by him, but since these were extrapolated smoothly from the experimental data for 1-Mev neutrons, the results should hold approximately in our case. Cameron has shown that saturation values for the abundance ratios relative to the normal cosmic abundances are reached successively among the heavy elements as 10–60 neutrons per metal nucleus are supplied and some 30–65 per cent of the metals have been converted. These ratios decrease only slowly after their maximum values are reached.

It should be emphasized that our calculations have been made here primarily for $kT =$ 1 Mev. The energy cannot be much higher if spallation by $(n, 2n)$ reactions is to be avoid-

ed, and it cannot be much lower if the flux of neutrons is to be sufficient to synthesize heavy elements from (n, γ) reactions. We estimate that, for our general conclusions to be valid, kT must fall within the limits 0.3–1.5 Mev.

We may sum up this section, therefore, by stating that the processes described in cases *a* and *b* can both produce anomalous overabundances of the heavy nuclei. Both cases *a* and *b* may occur in appropriate circumstances (though not simultaneously in a single active region), and the observed effects may be a result of both, acting over long time scales in the star's history. Also other subsidiary nuclear processes may take place. A comparison between the theoretical predictions and the observed anomalies will be given in Section IV.

IV. THE ANOMALOUS ABUNDANCES IN α^2 CANUM VENATICORUM AND HD 133029

a) The Nature of the Observed Anomalies

The observed anomalies in the magnetic stars α^2 CVn and HD 133029 (which will hereafter be called the "Apm stars") are summarized in Section I.

The magic-number isotopes of Sr, Y, and Zr have neutron-capture cross-sections only 1–10 per cent of those of their neighbors. The results of Cameron, which we have shown can be taken over for the neutron fluxes described in Section III*b*, suggest that the abundance of these isotopes can be built up to about forty-five times the cosmic abundance. This theoretical ratio is in reasonable agreement with the observed value of about 25 for this group.

For the group of elements from Ba to Dy, the neutron-capture-curves of Cameron suggest that the magic-number isotopes of Ba to Sm may attain anomalous overabundance ratios of about 10^4, while the rare earths Eu, Gd, and Dy, which do not have magic-number isotopes, should reach overabundance ratios of about 10^3. Alternatively, Section III*a* has shown that a sufficient number of charged-particle reactions may move a proportion of the metal peak into this region of atomic weight, which would again give an overabundance ratio of about 10^3. The observed mean overabundance ratio of the elements from La to Dy is about 600, while Ba apparently has no more than the normal cosmic abundance. From the point of view of Section III*b*, therefore, there are discrepancies between observation and theory. These might be explained by some moderation of the anomalous abundances expected from 1-Mev neutron capture alone by charged-particle reactions (Sec. III*a*) or by neutron reactions at higher energies, which are not so sensitive to magic-number effects.

The theoretical results for production by neutron capture of Pb, which, along with Bi, has magic isotopes, are consistent with the observations (overabundance ratio $\sim$ 1500), even though saturation is not reached in this case.

If a neutron flux is produced in material in which the metal abundance peak is absent, synthesis of the intermediate elements from the light ones by neutron capture can take place (Fowler, Burbidge, and Burbidge 1955). However, in the Apm stars the metal abundances have at least the normal cosmic values, so that practically no neutrons will be available to be captured by the lighter elements. The matter is further complicated in the Apm stars because the neutron-production processes by charged-particle interactions primarily deplete the light nuclei. It would be interesting, nonetheless, to see some reasons for the anomalous abundances of Ca, Si, and O in these stars.

The underabundance of Ca may be due to the fact that Ca^{40}, the most abundant isotope, is not synthesized directly in the neutron-capture process in stellar spots but is subsequently produced in the decay of K^{40} in quiescent regions. The mean lifetime of K^{40} is 2×10^9 years, so that, on the basis of a reasonable time scale, $\sim 10^9$ years, the Ca^{40} should be about as abundant as K^{40}. The normal cosmic abundance ratio of Ca^{40} to K^{40} is about 10^4. This large abundance of Ca^{40} is really the difficult matter to under-

stand, and it may arise from the charged-particle processes in stellar interiors discussed by Hoyle (1954). The "anomalous" low abundance in Apm star surfaces is thus seen not to be at all unreasonable, especially in view of the complicated effects of neutron emission and neutron capture in the light elements. This argument assumes that there are enough charged-particle and neutron interactions to scour out any Ca^{40} originally present.

The overabundance of Si may be attributable to the effects of the $S^{33}(n, \alpha)Si^{30}$ reaction for fast neutrons. This reaction is the most exoergic (n, α) process among intermediate nuclei and may well be more probable than the $S^{33}(n, \gamma)S^{34}$ reaction for fast neutrons, since the α-particles will have enough energy to surmount their mutual Coulomb barrier with the Si^{30}. Thus this may be a mechanism for piling up Si^{30} in the over-all capture process, and it would then be this isotope rather than Si^{28} which would constitute the overabundant Si, the observed overabundance ratio being about 15.

The observed underabundance of O may be attributable to the operation of (p, γ) and (p, α) reactions, which will occur in the light nuclei at the temperatures in active regions, even though they are not important in energy generation. The reactions $O^{16}(p, \gamma)F^{17}$-$(\beta^+)O^{17}$ and $O^{17}(p, \alpha)N^{14}$ transmute O into N^{14} and thus into CN isotopes. The CN isotopes are cyclic and stable under such processes.

We can see no simple explanation for the small overabundance ratios of Cr and Mn or for the probably greater overabundance of Mn in some other Apm stars. The only way of synthesizing the metal peak in stellar interiors appears to be that described by Hoyle (1954). The explanation of the results for Cr and Mn would require some rearrangement within the metal peak by nuclear reactions in the spots, using a small proportion of the Fe.

The results from Section III*a* and *b* suggest that a deuterium abundance relative to hydrogen of between 10^{-5} and 2×10^{-2} may be built up. Burbidge and Burbidge (1955*a*) suggested that certain faint lines in the wings of the hydrogen lines in one of the Apm stars (α^2 CVn) might be due to D, and roughly estimated from their strengths that the relative abundance was, in this case, 3×10^{-6}. However, Dr. Greenstein[1] has pointed out to us that the identification of a narrow line as due to D is suspect, because D lines will be subject to the same Stark-effect broadening as H and should appear as very broad features. If this is the case, it is difficult to set an upper limit to the amount of D which might be present without causing a measurable wave-length shift in the H lines, but it is probable that a D to H ratio of 0.01 might not be detectable. It is thus impossible at present to deduce from the abundance of D the relative importance of the two methods of synthesis discussed in Section III.

The occurrence of a large neutron flux (Sec. III*b*) does suggest that if some of the very heavy elements are originally present in the early stages of the star's history, then abundance anomalies of some of these elements may occur in the spots. We recall in this connection that the presence of U in α^2 CVn could not be ruled out; and, if definite spectroscopic identification could ever be made, it would almost certainly follow that U would be found observationally to be overabundant. The observational possibilities for the detection of transuranic elements, in particular Am, have been discussed elsewhere (Burbidge and Burbidge 1955*b*).

b) The Extent of the Activity

In order to see whether the amount of nuclear activity which may have taken place is sufficient to explain the observed abundance anomalies, it is necessary to discuss mixing in the outer layers of the Apm stars. It is probable that normal main-sequence A stars do not have large outer convective zones, so that the material will not be thoroughly mixed to great depths. It has been pointed out to us by Dr. Strömgren[2] that con-

[1] Private communication.

[2] Private communication; cf. also Rudkjøbing (1942) and Vitense (1951).

vective instability sets in high in the photosphere at optical depths around 0.25. However, the energy transport through turbulent convection currents is relatively much smaller than for the solar atmosphere. Consequently, it is likely that the structure of the outer atmosphere is close to that of an atmosphere in radiative equilibrium. In this case the convective instability will terminate at a depth where the temperature is under 20000° and the thickness of this hydrogen convective zone is only about 1000 km. Dr. Strömgren adds, however, that there is some uncertainty as to the possible effects of a helium convection zone. In the stars which have large general photospheric magnetic fields the convection effects will be very complex, the pattern of convection will be changed (the layer can best be described as being in a state of highly anisotropic hydromagnetic turbulence), but there is no reason to suppose that the general result will be a deepening of the convective, and hence mixing, zone. If anything, the tendency will be to inhibit the mixing effects except in the case of violent electromagnetic disturbance. This latter exception will be most probable in spot regions, which may allow some material to travel up and down to greater depths. We shall, however, be overestimating the total mass of the outer layer of the star, which has become thoroughly mixed, if we suppose that it comprises a layer of mean density 10^{-4} g/cc and thickness 10^4 km. In this case, if we take the radius of the star equal to $2R_\odot$, the total mass involved is 2.5×10^{28} g or only about 3×10^{-6} of the total mass of the star.

The conditions necessary for heavy-element synthesis in spots at densities of 10^{-8}–10^{-7} g/cc depend on field values, injection energies, ionization losses, etc. The frequency with which these conditions are met throughout a stellar spot will determine the overall efficiency of the spot mechanism. It does not seem unreasonable to assume that this efficiency is as high as 1–10 per cent. In a spot of radius 10^9 cm with equivalent height 10^8 cm and a mean density 10^{-7} g/cc, the mass contained is 3×10^{19} g. Let us suppose that the magnetic activity of the star has extended over a time scale of 5×10^8 years or 1.6×10^{16} sec and that, on the average, two spots having an average duration of 10^5 sec are present at any one time. Then some 3×10^{11} spots containing about 10^{31} g of material have occurred. At an efficiency of 1 per cent, this means that 10^{29} g of material have been processed. Roughly the same value is obtained at a density of 10^{-8} g/cc if an efficiency of 10 per cent is assumed. This amount of mass is four times that of the surface layer previously estimated and would indicate that all material in this layer has been processed several times.

All the individual estimates involved in this comparison are subject to considerable uncertainty, but we feel that, in general, our values are conservative ones. For example, we are almost certainly underestimating spot volumes in the Apm stars by supposing that the spot radii have the dimensions only of average sunspots. If radii of the order of 10^{10} cm were involved, then the total efficiency need be only 0.01–0.1 per cent to give the same results.

We conclude, therefore, that more than enough nuclear activity can have occurred in surfaces of the Apm stars to lead to the observed abundance anomalies.

There is one aspect of the problem in which our treatment has not been so conservative. Professors R. F. Christy and J. L. Greenstein have pointed out that electrons will lose energy rapidly by radiative collisions and by centrifugal acceleration in the magnetic field and that the particle energy will be transferred to radiation in a time short compared to the spot lifetimes. A rough estimate indicates that a 1-Mev electron will lose its energy by radiative processes in hydrogen at 10^{-7}–10^{-8} g/cc in 1–10 sec. Similar times hold for motion in magnetic fields of the order of 10^4 gauss. This result then requires that the rise of the magnetic field occur in periods of this order so that the nuclei and hence the electrons will acquire energy before it is lost to radiation. In order to reach the conclusion of the previous paragraph, it is then also necessary to assume high efficiency for the nuclear acceleration process and the larger value for the spot radii mentioned above, namely, 10^{10} cm.

If other Apm stars show abundance anomalies which vary from star to star, although they involve the same elements (we have taken means of the results for α^2 CVn and HD 133029, but some of the differences are real), this would suggest that the amount of magnetic activity will be different in different stars. We should expect, however, that the general trends of the anomalies would follow the theoretical discussion of Section III.

Finally, mention must be made of the magnetic stars which are not peculiar A or F stars, i.e., four M and one S star, which have been mentioned previously. We must suppose that the same sort of magnetic activity is going on in the surfaces of these stars. However, the difference between these stars and the Apm stars is probably in the extent of their mixing zones. The overabundance ratios in the Apm stars are produced only when about 3×10^{-6} of the total mass of the star is being mixed. Using the figures derived previously, we see that if a proportion $\sim 10^{-3}$ of the mass were involved, no overabundances, even in the heavy elements, would be expected. Since the cool giant stars apparently have large outer convective zones, it is more plausible, as has been shown elsewhere, to suppose that the overabundance of the heavy elements in the S stars is due to internal production and mixing right through the envelope.

V. THE SYNTHESIS OF D, Li, Be, AND B

In the previous sections we have considered the conditions of magnetic activity in a star having a strong general magnetic field. In this section the argument will be made more general. All discussions of the details of magnetic activity have been extrapolated from the observations of the sun, but there is every reason to suppose that this type of activity is widespread in normal, apparently quiescent, stars. Thus, if we wish to try to account for the cosmical abundances of D, Li, Be, and B, we can, as two extreme cases, assume either that a comparatively small number of particularly active stars has been responsible for the whole production of these elements or that the majority of stars throughout part of their evolutionary path contribute to the total production.

These elements and isotopes are all unstable at high temperatures, so that synthesis on the surface will be balanced by destruction in the deep interior, in suitable time scales, if any of the synthesizing stars have deep convective zones. Salpeter (1955) has calculated the rates of destruction in the sun. Thus stars passing through evolutionary stages in which they have large outer convective zones can be excluded from consideration if we are looking for stars to redistribute material into the interstellar medium by rare, large-scale outbursts, provided that the time spent in a convective stage is long enough for destruction to be fairly complete. Although stars lying on the main sequence above solar type may not have large outer convective zones, it appears probable that any such star, before reaching an explosive stage, will have passed through a giant stage when it had such a zone (Hoyle and Schwarzschild 1955).

On the other hand, stars having convective zones will contribute if the material which is synthesized on the surface is ejected almost immediately, before it has had time to mix in regions away from the active areas. Apart from the Apm stars, possible stars in which this latter process is taking place are the red dwarfs. Stars cooler than M4.5 appear generally to show emission lines in their spectra (Joy 1947), which are suggestive of flare mechanisms (Kron 1950) and hence of magnetic activity, although the attribution of this activity to magnetic fields is an extrapolation of the solar evidence. There are also, of course, the stars called "flare stars," in which the activity is very much larger; but these are not numerous enough for our purpose. Red dwarfs slightly earlier in spectral type than M4.5 have deep convective zones (Osterbrock 1953), and it is probable that the same applies to the cooler dwarfs in which other effects may also operate; for Kruger 60 A, Osterbrock could not derive a satisfactory model, even with convection. Red dwarfs are very numerous, since the form of the luminosity function in the solar neighborhood suggests that they contribute a considerable fraction of the galactic mass. We shall suppose that there are 10^{11} of these stars. Biermann (1955) has suggested that

solar-type stars may lose enough material from active regions to contribute about $1M_\odot$/year all together to the interstellar medium. However, this may be an overestimate. We shall suppose that the red dwarfs with average mass $\frac{1}{2}M_\odot$ contribute all together $0.005M_\odot$/year in corpuscular emission. As yet, there appears to be no spectroscopic evidence concerning the presence or absence of D, Li, Be, and B in red dwarf atmospheres.

We also need an estimate of the total number of Apm stars. From the value of 0.34/1000 pc^3 for the mean density of A stars near the sun (Malmquist and Hufnagel 1933) and the work of Morgan (1935) and Deutsch (1947), which indicates the proportion of A stars which are spectroscopically peculiar, we estimate that the total number of Apm stars is $\sim 10^7$ (we assume a one-to-one correspondence between spectroscopically peculiar A stars and stars with large magnetic fields). Another estimate may be obtained from the fact that the peculiar A stars brighter than 6.0 mag. and accessible at Yerkes total 61 (Deutsch 1947). Assuming an average absolute magnitude of +1, the volume surveyed is 10^{-5} of the total galactic volume, so that the total number is again 10^7.

In the Apm stars, among Li, Be, and B, only Be is likely to be spectroscopically observable, from the Be II lines. Dr. P. Swings has very kindly sent us tracings and enlargements of some Mount Wilson spectrograms of α^2 CVn in the ultraviolet and some wave-length measures made by Dr. L. Neven. He has indicated two lines which fall near the wave lengths of Be II λ 3130.42 and λ 3131.06, and we have estimated their strengths. By assuming that these lines are wholly due to Be II, we obtain[3] an upper limit to the relative abundance of Be, $a_{\mathrm{Be}}/a_{\mathrm{H}}$, of 10^{-10}. We note that this is similar to the ratio on the earth and in the sun (Greenstein and Tandberg-Hanssen 1954).

a) Deuterium

On the earth the abundance of D relative to H is about 10^{-4}, while, in the interstellar gas, attempts to detect the 327-Mc/sec line emitted by neutral D suggest[4] that the abundance is less than 10^{-3}–10^{-2}. In Section III*a* and *b* we showed that a D/H ratio lying between 2×10^{-2} and 10^{-5} might build up in the surface layers of the Apm stars. If smaller-scale nuclear activity occurs generally in regions of magnetic activity in stars like the M dwarfs, then any production of neutrons will always tend to lead to the formation of D. For example, high up in stellar atmospheres (perhaps $\rho < 10^{-9}$ g/cc), where a very small number of neutrons may be produced at higher energies than those considered in Section III, sufficient moderation of these will lead to D formation.

If we suppose that a "cosmical" abundance of D in the interstellar gas and dust is produced completely by the Apm stars in a time scale $\sim 10^9$ years, then the ratio R of the abundance in the surfaces of these stars to the cosmical abundance is $\sim(m \times 10^7 \times 10^9)/10^{11} = 10^5 m$, where m is the mass (in units of $1M_\odot$) ejected per year from a single star. We have previously suggested that a fraction of $\sim 10^{-5}M_\odot$ is contaminated by surface nuclear activity. Therefore, R must be $\ll 1$, since this value would imply that the whole outer layer is ejected from the star annually; this is clearly not the case, and the spectroscopic evidence does not indicate any large-scale ejection from these stars. If, for example, the whole skin of $10^{-5}M_\odot$ were ejected in about 10^8 years, then the interstellar abundance would be only $\sim 10^{-10}$–10^{-13}. Rare and remarkable emission-line magnetic stars like AG Pegasi (Burbidge and Burbidge 1954) might produce D and also eject large amounts of material, but such stars would be too few to affect the interstellar abundance.

Thus it seems more probable that more general ejection processes would be respon-

[3] A theoretical Milne-Eddington curve of growth with $B_0/B_1 = \frac{1}{3}^0$ and $\log a = -3.0$ was assumed for this region of the spectrum. The *f*-values have been listed by Greenstein and Tandberg-Hanssen (1954); cf. Burbidge and Burbidge (1955*a*) for the atmospheric parameters.

[4] We are indebted to Dr. L. R. O. Storey for information concerning his work and also that of the Australian radio astronomers.

sible for D in the gas and dust. Let us suppose that D is produced in red dwarfs and ejected in flarelike outbursts. Then, using the figures given previously for these stars, we find by an argument similar to that for the Apm stars that $R = 5 \times 10^{-5}$. If, in these stars, therefore, the equilibrium production of D is the same as calculated for the Apm stars, we derive an interstellar abundance of $\sim 10^{-6}$–10^{-9} of hydrogen. This can be increased only by assuming even more widespread surface activity in stars. This may indeed be the case, and the absolute upper limit would then be $D/H \sim 10^{-2}$ when the interstellar abundance reached equilibrium with the stellar surface abundance.

b) Li, Be, and B

The total terrestrial and meteoritic abundance of Li, Be, and B is only about 5×10^{-9} times that of H and about 3×10^{-6} times that of C, N, and O. Spitzer and Field (1955) have shown that the apparent abundance of interstellar Be is an order of magnitude less than that in the solar system; they suggest that this may be because an excessive amount of Be is locked up in grains. However, in the primary cosmic radiation it is found that the ratio (Li, Be, B)/(C, N, O) is near to unity (Gottstein 1954; Kaplon, Noon, and Racette 1954; Noon and Kaplon 1955), although Biswas, Peters, and Rama (1955) have maintained that it may not be so high as this and quote possible values of the order of 0.05. The results for the heavy cosmic-ray primaries suggest that there is rough agreement with the cosmical abundances up to Fe. This result has previously been interpreted by supposing that the presence of Li, Be, and B nuclei is indicative of nuclear collisions between the primary accelerated particles and the interstellar gas. Then, under stationary conditions, about as many Li, Be, and B nuclei are to be expected as C, N, and O nuclei, since their probability of production in a single nuclear encounter is large ($\sim \frac{1}{2}$). This argument, originally pointed out by Bradt and Peters (1950), is of considerable importance in connection with Fermi's theory of the origin of cosmic rays. It is assumed that cosmic-ray particles diffuse around the Galaxy for times long compared with the average time of escape along straight-line paths, but of the same order of magnitude as the mean life for nuclear collisions.

We consider it plausible, however, to suppose that a proportion, and perhaps the majority, of nuclear collisions of the primaries take place in the early stages of the acceleration process, before the particles are injected into the interstellar medium, where they gain further energy by the Fermi mechanism. Thus we suppose that the primary sources of cosmic radiation are the active regions on the surfaces of some types of stars.

There appear to be two possibilities. The first is that Li, Be, and B are produced in spots under conditions similar to those described in Section III*b*, but where $kT \sim 5$ Mev. In this case it can be shown that the (Li, Be, B)/(C, N, O) ratio becomes about unity. Such an origin would help to explain the fact that Fe is found in the primary cosmic radiation and has not been spallated, since it is not affected in spots at these comparatively low energies. However, if this type of activity were going on in the Apm stars, we should expect to find a large atmospheric abundance of these elements, and the small observed abundance of Be mentioned earlier argues against this possibility in these stars.

Alternatively, the Li, Be, and B can be produced by spallation reactions from C, N, and O at energies >100 Mev higher in the atmospheres ($\rho < 10^{-9}$ g/cc). At 10^{-9} g/cc a proton will make a nuclear collision with C, N, or O in about 100 sec. This type of spallation at very high energies poses exactly the same problems as those arising if it is supposed that the nuclear collisions take place in the interstellar gas, i.e., a sufficient number of collisions have to be made to produce the large (Li, Be, B)/(C, N, O) ratio but not enough further to spallate the Li, Be, and B or to spallate all the Fe.

In our picture a small fraction of the Li, Be, and B injected from a stellar atmosphere into the interstellar medium will be accelerated to form primary cosmic radiation, while the majority will be below the acceleration threshold and will eventually form part of the low-energy gas and dust.

Using these ideas, we can now make estimates of the possible "cosmical" abundance of Li, Be, and B. For the Apm stars, by the same argument as that used for D, we have $R = 10^5 m = 10^{-8}$ if a star loses the equivalent of its whole outer mixing shell, in which abundance anomalies occur, in 10^8 years. If Li, Be, and B are ejected without mixing from flares where they have a maximum abundance equal to that of C, N, and O, i.e., 2×10^{-3}, then a maximum cosmical abundance of 10^{-11} would be produced. If, on the other hand, Li, Be, and B are ejected from the mixed material of the outer layer, we shall take the upper limit of 10^{-10} for the abundance of Be in α^2 CVn as representative of the whole group. Then a cosmical abundance of only 10^{-18} would be produced.

However, the M dwarfs, being so much more numerous, provide a better chance of producing the observed interstellar abundance. Using the same figures as before, we have $R = 5 \times 10^{-5}$; if these elements are produced by spallation in active regions with maximum efficiency, an interstellar abundance ratio of 10^{-7} could therefore be produced. This is two or three orders of magnitude greater than the observed values, so that an efficiency of between 0.1 and 1 per cent, i.e., a (Li, Be, B)/(C, N, O) ratio of 10^{-3}–10^{-2} in the ejected material, is necessary to produce a cosmical abundance of the right order. However, the magnetic activity postulated in red dwarfs is orders of magnitude less than that in the Apm stars, so that we cannot say without some observational evidence —for example, on the composition of the material ejected from the sun—whether an efficiency as high as 0.1–1 per cent could ever be achieved.

Finally, mention should be made of three N-type stars in which Li appears strongly; these are the only stars which have so far been observed to have an unusual abundance of any of these elements. Spitzer (1949) has estimated that the abundance of Li may be about forty times the terrestrial abundance in one of these stars. Apparently, such stars form only a small proportion of all carbon stars, but the possibility cannot be ruled out that they contribute appreciably to the total amount of Li in the Galaxy. Whether the excessive abundance could have been produced by nuclear reactions in the surfaces of giant stars of this type, with convective outer regions, or whether it could have been produced internally, as suggested by Cameron (1955*a*), is uncertain.

Note added in proof.—A note on the production of light nuclei by cosmic radiation at the surfaces of stars by S. Hayakawa (1955) has come to our attention since our paper was submitted for publication.

c) The Natural Radioactive Elements

The difficulties in the synthesis of the natural radioactive elements from lighter elements are well known. The rapid emission of α-particles with $\Delta A = -4$ counteracts any synthesis mechanism which involves small increments in atomic weight per nuclear reaction. It is essentially necessary to bridge the gap from ${}_{83}Bi^{209}$, the heaviest stable nucleus, to the parent of a given radioactive series, e.g., ${}_{92}U^{238}$, in one nuclear process. Allowing for some spallation, it is clear that this will require a collision of the Bi^{209} with a nucleus of intermediate atomic weight. The most probable case will be ${}_{26}Fe^{56}$. Barrier factors will prevent the interaction at the average energy of stellar interiors, but there is some possibility that the reactions will occur on stellar surfaces in the less dense regions of magnetic spots, primarily because the energies of the interacting nuclei are proportional to their atomic weights. Thus a reasonable reaction on the basis of present experiments with heavy ions could be

$$ {}_{26}Fe^{56} + {}_{83}Bi^{209} \rightarrow {}_{92}U^{238} + {}_{4}Be^{7} + 2\alpha + 9p + 3n \, . $$

The relatively large charge carried away by the spallation fragments is somewhat higher than one would expect in the most probable spallation process but is not to be considered impossible.

Quantitatively, it is difficult to see how such reactions could account for the cosmical

abundances of the natural radioactive elements. Furthermore, if reactions of this type are important, then interactions between two Fe^{56} nuclei ought to be even more probable and should be evident in the synthesis of nuclei with $A \sim 100$. This may be the case, as has been suggested previously by Burbidge and Burbidge (1955*a*). No general conclusion can be drawn at the present time except that the synthesis of the natural radioactive elements by the mechanism here proposed would require very widespread surface activity in stars.

VI. CONCLUSION

We have discussed the possible occurrence of nuclear processes on the surfaces of stars, both in an attempt to explain the anomalous abundances of some elements observed in some peculiar A stars and also in order to see how far the "cosmical" abundances of D, Li, Be, and B can be explained by stellar synthesis.

As far as the first problem is concerned, the very uncertain state of our knowledge concerning the conditions in the atmospheres of the magnetic stars led us in our original approach to consider the problem first from the standpoint of nuclear physics, i.e., we derived the conditions for synthesis demanded by nuclear physics and attempted to show that these were plausible in a particular model. The discussion of the acceleration mechanisms was then put ahead of nuclear physics for clarity of presentation. The many unsolved problems of plasma physics and the limitations of observational techniques as far as the details of electromagnetic activity on stars other than the sun are concerned make such an approach inevitable. We wish to emphasize, therefore, that although we have restricted ourselves to the Swann mechanism when discussing the occurrence of spots and have invoked large local magnetic fields, we do not wish to imply that this is the only possibility. Other mechanisms, which are less well understood, e.g., neutral-point acceleration theories (Dungey 1953) or the acceleration of ions moving ahead of hydromagnetic shock waves (cf. Babcock and Babcock 1955), which can transform magnetic into kinetic energy, might also be effective in providing the energy for some nuclear reactions to take place. However, it is satisfactory that many of the anomalous abundances can be accounted for in the models which we have used.

To discuss the production of the "cosmical" abundances of D, Li, Be, and B has involved a more speculative approach as far as astrophysics is concerned. However, in view of the previous work on stellar evolution and the synthesis of the elements, which has shown that all the elements up to the natural α-emitters and excluding those unstable at high temperatures can be synthesized in stars, this attempt seemed worth while. The results show that even if a large number of fairly active stars are supposed to be ejecting material, only a low over-all abundance of D can be expected. The absolute upper limit on D/H is, however, of the order of 10^{-2}. It is promising, moreover, that the Li, Be, and B synthesis can produce the observed "cosmical" abundances if a fairly high efficiency of production through spallation is assumed. It may be that we have considerably overestimated this efficiency. If so, this might suggest that these elements were produced at an earlier stage in the evolution of the Galaxy, when the stars then present might have traveled through their evolutionary paths more rapidly and might also have been more effective, both in surface nuclear activity and in the ejection of material.

One of us, W. A. Fowler, wishes to express his thanks to Professors N. F. Mott and O. R. Frisch and many other members of the Cavendish Laboratory for hospitality during his stay in Cambridge. G. R. Burbidge is indebted to the Smithson Fund of the Royal Society for financial support.

APPENDIX I

Rates of Nuclear Reactions

In this appendix we derive expressions for the rates of nuclear reactions under certain conditions which have not been extensively treated in the literature. The number of nuclear reactions per cubic centimeter per second between two kinds of interacting nuclei can be written as follows:

$$p = n_a n_b \lambda \text{ cm}^{-3} \text{ sec}^{-1} ,$$

where n_a and n_b are the numbers per cubic centimeter of the two kinds of nuclei, and the reaction-rate parameter, λ, is given by

$$\lambda = \sigma v \text{ cm}^3 \text{ sec}^{-1} ,$$

where σ is the reaction cross-section and v is the relative velocity of the interacting nuclei. The mean lifetimes of particles of types a and b are then, respectively,

$$\tau_a = \frac{n_a}{p} = \frac{1}{n_b \lambda} = \frac{1}{n_b \sigma v} = \frac{2.2}{a_b \rho \sigma v} \tag{12}$$

and

$$\tau_b = \frac{n_b}{p} = \frac{1}{n_a \lambda} = \frac{1}{n_a \sigma v} = \frac{2.2}{a_a \rho \sigma v} . \tag{13}$$

The last expressions in equations (12) and (13) give the lifetimes in terms of the cross-sections in barns and the densities, ρ, in grams per cubic centimeter, for a material having normal cosmical abundances a. By number relative to hydrogen, we take $a_{\text{He}} = 0.10$, $a_{\text{CNONe}} = 2 \times 10^{-3}$, $a_{\text{Mg-A}} = 7 \times 10^{-5}$, $a_{\text{metals}} = 2.2 \times 10^{-5}$, and $a_{\text{atomic weight} > 64} = 10^{-8}$. The mean atomic weight is thus 1.34.

When the nuclei have a distribution in relative velocities, then these quantities must be averaged over this distribution, to give, for example,

$$\lambda = \int v \sigma (v) \phi (v) \, dv ,$$

where $\phi(v)$ represents a properly normalized velocity-distribution function. In terms of the energy of interaction E and with $\psi(E)dE = \phi(v)dv$, this becomes

$$\lambda = \int \left(\frac{2E}{M}\right)^{1/2} \sigma (E) \psi (E) \, dE ,$$

where M is the reduced rest mass of the interacting nuclei. We shall now consider several cases of interest in this paper.

Case 1

We take an inverse-power-law spectrum of the form $\psi(E) \propto E^{-n}$, with $n > \frac{3}{2}$, and with $\sigma = \sigma_0$ a constant over the energy range from E_1 to E_2. Then, for particles *in this energy range*,

$$\lambda = \sigma_0 v_1 \frac{n-1}{n-\frac{3}{2}} \left[\frac{1 - (E_1/E_2)^{n-1/2}}{1 - (E_1/E_2)^n}\right] . \tag{14}$$

For $n \gtrsim 3$ and $E_2 > E_1$, we have, to a good approximation,

$$\lambda \approx \sigma_0 v_1 .$$

Case 2

We take a Maxwell-Boltzmann distribution,

$$\phi (v) \, dv = \frac{4}{\pi^{1/2}} \frac{v^2}{v_T^3} \exp\left(-\frac{v^2}{v_T^2}\right) dv ,$$

where

$$v_T = \frac{2kT}{M},$$

or

$$\psi(E)\,dE = \frac{4}{\pi^{1/2}} \frac{E^{1/2}}{(kT)^{3/2}} \exp\left(-\frac{E}{kT}\right) dE.$$

a) If $\sigma \propto 1/v$, as is the case for slow-neutron reactions, then, averaging over all the particles, we have

$$\lambda = \sigma_T v_T, \tag{15a}$$

where

$$\sigma_T = \sigma(kT).$$

This result is independent of moderate departures from the $1/v$ law.

For σ = constant and $\sigma \propto 1/v^2$, we find

$$\lambda = \frac{2}{\pi^{1/2}} \sigma_T v_T. \tag{15b}$$

Thus the reaction rate depends primarily on the cross-section at energy kT.

b) For resonance reactions in which barrier-penetration factors (Coulomb or centrifugal) vary only slowly over the resonance,

$$\sigma = \frac{\sigma_r}{1 + [(E - E_r)/(\Gamma_r/2)]^2},$$

where σ_r is the cross-section and Γ_r is the width at the resonance energy E_r. Then

$$\lambda \approx \pi^{1/2} \sigma_r v_T \left(\frac{\Gamma_r}{kT}\right)\left(\frac{E_r}{kT}\right) \exp\left(-\frac{E_r}{kT}\right), \tag{16}$$

for $\Gamma_r < kT$. For slow-neutron resonances the cross-section should contain a factor $(E_r/E)^{1/2}$, and a term $\sigma_T v_T$ should be added to λ.

c) For high-energy threshold reactions in which $\sigma \approx \sigma_0$ is approximately constant above an effective threshold energy, E_t, averaging over all particles, we obtain

$$\lambda \approx \frac{2}{\pi^{1/2}} \sigma_0 v_T \left(\frac{E_t}{kT} + 1\right) \exp\left(-\frac{E_t}{kT}\right). \tag{17}$$

This expression represents the contribution to the integral for λ from all interactions exceeding E_t in energy. In the cases under consideration in this paper we can empirically take $E_t \sim |Q| + 1$ Mev, where $|Q|$ is the magnitude of the negative Q-value for the reaction. For positive Q, $E_t \sim 1$ Mev. In the case of charged-particle reactions in which the barrier height, E_b, is greater than $|Q|$ and $|Q|$ in turn exceeds the energy at which the product of the Maxwell-Boltzmann and barrier factors reaches a maximum, we can take $E_t \sim E_b + 1.5$. This is the case for some (α, n) reactions. The cross-sections usually decrease at energies well above the threshold, but this will only slightly decrease our estimate for λ.

As an example we will calculate λ_p for the $N^{14}(p, n)O^{14}$ reaction and λ_n for the $O^{14}(n, p)N^{14}$ reaction at $kT = 1$ Mev, $v_T = 1.4 \times 10^9$ cm/sec, using $\sigma_0 \approx \sigma_g \approx 0.06\, A^{2/3} = 0.35$ barn. For the (p, n) process, $Q = -6.0$ Mev, and the effective threshold is 7 Mev. Thus, substituting in equation (17), we obtain

$$\lambda_p = 4.0 \times 10^{-18}\ \text{cm}^3\ \text{sec}^{-1}.$$

Then

$$\tau(N^{14}) = \frac{1}{n_p \lambda_p} = \frac{5.5 \times 10^{-7}}{\rho} = 5.5\ \text{sec}$$

if $\rho = 10^{-7}$ g/cc. For comparison, using equation (16) and the results of Duncan and Perry (1951), we find that the mean lifetime of N^{14} for the $N^{14}(p, \gamma)$ reaction is 600 sec.

For the $O^{14}(n, p)N^{14}$ reaction, the Q is positive and the effective threshold is 1 Mev, so that

$$\lambda_n = 1.5 \times 10^{-16} \text{ cm}^3 \text{ sec}^{-1} ,$$

whence $\lambda_p/\lambda_n = 0.027$.

APPENDIX II

Synthesis of Nuclei through Successive Reactions

We consider in this appendix the synthesis of nuclei through successive reactions, all of one type, in which the cross-section can be taken to be at least approximately independent of atomic weight. Reactions in this category are the deuteron-stripping reactions, where $\sigma \propto A^{1/3}$, and even such reactions as (α, n), (α, pn), etc., where $\sigma \propto A^{2/3}$. It will be assumed in what follows that β-decay processes occur rapidly enough between reactions to produce the stable isobar for each atomic weight A.

Let n be the total supply of particles of the type which initiate the reaction and let ΔA be the change in atomic weight from the target to the residual nucleus. Let N_0 be the initial number of the original nuclei with atomic weight A_0. Then if N_A is the number of nuclei of atomic weight A,

$$\frac{dN_A}{dn} = \frac{-\sigma_A N_A + \sigma_{A-\Delta A} N_{A-\Delta A}}{\sum_A \sigma_A N_A} ,$$

with $N_A = 0$ for $A < A_0$.

If σ is independent of A, then

$$\frac{dN_A}{dn} = \frac{N_{A-\Delta A} - N_A}{\sum_A N_A} = \frac{N_{A-\Delta A} - N_A}{N_0} .$$

These are just the equations of radioactive decay from a parent-nucleus of atomic weight A_0, with n replacing the time and N_0 replacing the mean lifetime, which is the same for the parent- and all daughter-products. The solutions are well known and are

$$N_A = \frac{N_0}{m!} \left(\frac{n}{N_0} \right)^m \exp \left(- \frac{n}{N_0} \right),$$

where $m = (A - A_0)/\Delta A$ is the number of reactions required to transform A_0 into A. For a given n this expression reaches a maximum when $m = n/N_0$, given by

$$N_A \text{ (max)} = \frac{N_0}{m!} \, m^m \exp(-m) \qquad \text{with} \qquad m = \frac{n}{N_0} .$$

For large m this becomes

$$N_A \text{ (max)} \sim \frac{N_0}{(2\pi m)^{1/2}} .$$

A simple calculation shows that the nuclei are then spread over a range in A equal to $\sim(2\pi m)^{1/2}\Delta A$ centered on $A = A_0 + m\Delta A$.

REFERENCES

Babcock, H. W., and Babcock, H. D. 1955, *Ap. J.*, **121**, 349.

Babcock, H. W., and Cowling, T. G. 1953, *M.N.*, **113**, 357; see also *Carnegie Institution of Washington Year Book*, No. 53, p. 17, 1953–1954.

Bagge, E., and Biermann, L. 1948, *Naturwissenschaften*, **35**, 120.
———. 1949, *Zs. f. Naturforsch.*, **4a**, 303.
Bidelman, W. P. 1953, *Ap. J.*, **117**, 377.
———. 1954, *Mém. Soc. r. sci. de Liège*, **14**, 402; *Comm. du colloque d'ap. de Liège*, 1953.
———. 1955, *Vistas in Astronomy* (London: Pergamon Press).
Biermann, L. 1953, *Ann. Rev. Nuclear Sci.*, **2**, 335.
———. 1955, *Gas Dynamics of Cosmic Clouds* (Amsterdam: North Holland Pub. Co.), p. 212.
Biswas, S., Peters, B., and Rama. 1955, *Proc. Indian Acad. Sci., A*, **41**, 154.
Blatt, J. M., and Weisskopf, V. F. 1952, *Theoretical Nuclear Physics* (New York: John Wiley & Sons), chap. 9.
Bradt, H. L., and Peters, B. 1950, *Phys. Rev.*, **80**, 943.
Bullard, E. C. 1955, *Vistas in Astronomy* (London: Pergamon Press).
Burbidge, E. M., and Burbidge, G. R. 1955, *Ap. J.*, **122**, 396.
Burbidge, G. R. 1954, *Ap. J.*, **102**, 589.
Burbidge, G. R., and Burbidge, E. M. 1954, *Ap. J.*, **120**, 76.
———. 1955*a*, *Ap. J. Suppl.*, **1**, 431.
———. 1955*b*, *Observatory*, **75**, 116.
Buscombe, W., and Merrill, P. W. 1952, *Ap. J.*, **116**, 525.
Cameron, A. G. W. 1954, *Phys. Rev.*, **93**, 932.
———. 1955*a*, *Ap. J.*, **121**, 144.
———. 1955*b*, *Bull. Amer. Phys. Soc.*, **30**, 4, 27, and private communications.
Chandrasekhar, S., and Fermi, E. 1953, *Ap. J.*, **118**, 116.
Das Gupta, N. N., and Ghosh, S. K. 1946, *Rev. Mod. Phys.*, **18**, 225.
Deutsch, A. J. 1947, *Ap. J.*, **105**, 283.
Duncan, D. B., and Perry, J. E. 1951, *Phys. Rev.*, **82**, 809.
Dungey, J. W. 1953, *Phil. Mag.*, **44**, 725.
Feld, B. T. 1953, *Experimental Nuclear Physics*, Vol. **2**, ed. E. Segré (New York: John Wiley & Sons).
Fowler, W. A., Burbidge, G. R., and Burbidge, E. M. 1955, *Ap. J.*, **122**, 271.
Garstang, R. H. 1952, *Pub. A.S.P.*, **64**, 227.
Ghoshal, S. N. 1950, *Phys. Rev.*, **80**, 939.
Gottstein, K. 1954, *Phil. Mag.*, **45**, 347.
Greenstein, J. L., and Tandberg-Hanssen, E. 1954, *Ap. J.*, **119**, 113.
Hayakawa, S. 1955, *Prog. Theoret. Phys.*, **13**, 464.
Hoyle, F. 1954, *Ap. J. Suppl.*, **1**, 121.
Hoyle, F., and Schwarzschild, M. 1955, *Ap. J. Suppl.*, **2**, 1.
Hughes, D. J., Garth, R. C., and Levin, J. S. 1953, *Phys. Rev.*, **91**, 1423.
Johnson, H. L. 1954, *Ap. J.*, **120**, 325.
Joy, A. H. 1947, *Ap. J.*, **105**, 96.
Kaplon, M. F., Noon, J. H., and Racette, G. W. 1954, *Phys. Rev.*, **96**, 1408.
Kiepenheuer, K. O. 1950, *Phys. Rev.*, **78**, 809.
———. 1954, *The Sun*, ed. G. P. Kuiper (Chicago: University of Chicago Press), chap. 6.
Kron, G. E. 1950, *Pub. A.S.P.*, **62**, 141.
Malmquist, K. G., and Hufnagel, L. 1933, *Ann. Stockholm Obs.*, Vol. **11**, No. 9.
Meinel, A. B., and Fan, C. Y. 1952, *Ap. J.*, **115**, 330.
———. 1953, *ibid.*, **118**, 205.
Meredith, L. H., Gottlieb, M. B., and Van Allen, J. A. 1955, *Phys. Rev.*, **97**, 201.
Miczaika, G. R. 1954, *Lick Obs. Bull.*, No. 527.
Morgan, W. W. 1935, *Pub. Yerkes Obs.*, Vol. **7**, Part 3.
Noon, J. H., and Kaplon, M. F. 1955, *Phys. Rev.*, **97**, 769.
Osterbrock, D. E. 1953, *Ap. J.*, **118**, 529.
Provin, S. S. 1953, *Ap. J.*, **118**, 489.
Riddiford, L., and Butler, S. T. 1952, *Phil. Mag.*, **43**, 447.
Roman, N. G. 1949, *Ap. J.*, **110**, 205.
Rudkjøbing, M. 1942, *Zs. f. Ap.*, **21**, 254.
Salpeter, E. E. 1952, *Ap. J.*, **115**, 326.
———. 1955, *Phys. Rev.*, **97**, 1237.
Schlüter, A. 1952, *Zs. f. Naturforsch.*, **7a**, 136.
Slettebak, A. 1951, *Ap. J.*, **113**, 437.
Spitzer, L. 1949, *Ap. J.*, **109**, 548.
Spitzer, L., and Field, G. B. 1955, *Ap. J.*, **121**, 300.
Swann, W. F. G. 1933, *Phys. Rev.*, **43**, 217.
Thomson, D. M. 1952, Ph.D. thesis, University of Cambridge.
Vitense, E. 1951, *Zs. f. Ap.*, **28**, 81.
Weaver, H. F. 1952, *Ap. J.*, **116**, 612.

A CATALOGUE OF HIGH-VELOCITY STARS*

NANCY G. ROMAN
Yerkes and McDonald Observatories
Received September 21, 1955

ABSTRACT

The catalogue contains new spectral types, photoelectric magnitudes and colors, and spectroscopic parallaxes for about 600 high-velocity stars. For most of these, the space velocities and the eccentricities and semimajor axes of their galactic orbits are also given.

In recent years our increasing knowledge of the role of the high-velocity stars in problems of galactic structure and galactic evolution has led to a renewed interest in these objects. Therefore, it has seemed useful to prepare a new catalogue of such stars in which the available radial velocities, proper motions, and trigonometric parallaxes are supplemented by modern spectroscopic parallaxes, spectral types, and photoelectrically determined colors and magnitudes.

As a basis for the new catalogue, all nonvariable stars north of declination $-20°$, brighter than 9.5 m_v, and not later than M0, were selected from Miczaika's catalogue of high-velocity stars (1940). To these were added other stars from radial-velocity lists published since 1938 (see "Sources of Radial Velocity" in list of references), a few stars from a list of space motions of the bright stars (Roman 1952), nineteen stars whose velocities were measured at the David Dunlap Observatory but which have not been published, and a number of stars from the Yale catalogues[1] of proper motions. For the latter source, tangential velocities were estimated from the proper motions, magnitudes, and published spectral types, with the assumption that all stars were dwarfs.

Although, on the basis of modern data, an appreciable number of stars from Miczaika's catalogue have velocities smaller than the 63-km/sec limit which he set, these have been included in the present catalogue also, as were some stars selected from other lists whose large velocities later provied to be spurious. For selecting stars from the proper-motion catalogues, a lower limit of about 100 km/sec was used. Thus there is no definite limit above which the catalogue is complete or below which all stars are omitted. Nevertheless, the catalogue should provide a source of data for a large group of typical high-velocity stars, from which smaller groups can be selected for further investigation.

The classification spectra were taken with either the small spectrograph on the Yerkes 40-inch refractor or the 110-mm camera on the Cassegrain spectrograph on the McDonald 82-inch reflector. The dispersion of both combinations is near 120 A/mm at Hγ. A few of the Yerkes spectrograms were taken by other observers, primarily Guido Münch, while W. A. Hiltner took several of the McDonald spectrograms. The types are on the MK system (Johnson and Morgan 1953), with the following additional notations: For stars earlier than G0, "sd" has been used to indicate that the star has very weak lines and belongs to the group of F-type subdwarfs, whose absolute magnitude is assumed to be +5.0. For stars later than G0, "VI" indicates that the star appears to be below the main sequence, probably by about 1 mag. A few spectral types which have been published by Morgan (Johnson and Morgan 1953) are denoted by a superscript "M" following the type.

As is well known, the spectra of many high-velocity stars are not normal, and some compromise must be made in their classification. In the present catalogue the practice

* *Contributions from the McDonald Observatory of Texas*, No. 262.

[1] *Trans. Yale Astr. Obs.*, 1925–1953, Vols. **4, 5, 7, 9–12, 16–22, 24.**

has been to use the strength of the ionized strontium line, λ 4077, to determine the luminosity of all stars later than F5. For stars with decidedly weakened lines, the type has been determined from the usual line ratios whenever possible; among the A- and F-type stars, the strength of the hydrogen lines has been given high weight. Usually, this procedure leads to luminosities and predicted colors in agreement with the measured parallaxes and observed colors. The exceptions are indicated in the notes to the catalogue, as are extreme peculiarities in the spectra. Except for these stars, no attempt has been made to indicate weak cyanogen, a strong G band, or weakened metallic lines, as these effects are present to some extent in the spectra of almost all high-velocity stars. An indication of the weakness of the metallic lines in the F- and G-type spectra can be found from a comparison of the $B - V$ and $U - B$ colors for each star. An ultraviolet excess, ranging from 0.0 to more than 0.2 mag., which is found in most high-velocity stars is well correlated with the weakness of the lines. Moreover, both anomalies are correlated with velocity, in the sense that the stars with the weakest lines also have the largest ultraviolet excesses and the largest space velocities.

Most of the photometric observations were made with the 13-inch reflector at the McDonald Observatory; a few were made with the 24-inch reflector at Yerkes, while those with a superscript "J" following the visual magnitude are from the list by Johnson and Morgan (1953). The data on o^2 Eridani are from observations by W. A. Hiltner. All material was reduced immediately to the B, V, U system, and no systematic difference is noticeable between various seasons or telescopes. Except in the cases specifically mentioned in the notes, at least two observations were obtained for each star; the average number is $2\frac{1}{2}$. The average internal mean errors per star are: V, $\pm 0^m022$; $B - V$ $\pm 0^m018$; and $U - B$, $\pm 0^m027$. Since the observations were made with a small telescope, magnitudes fainter than 11.0 were difficult to measure accurately with the available equipment. Therefore, the $U - B$ colors of the faint red stars are somewhat uncertain. This probably accounts for the unusually large average mean error for the $U - B$ colors.

As far as possible, the radial velocities are from the *General Catalogue of Radial Velocities* (Wilson 1953). The remainder are from the radial-velocity lists from which the stars were taken or from the author's measurements of David Dunlap Observatory plates (Roman 1955). The sources of the proper motions are indicated in Table 1 by the standard abbreviations (see Kruse and Imgart 1936). In addition, "Y" refers to the *Transactions of the Yale Astronomical Observatory;* "C.C." to the *Astrographic Catalogue*, and "GFH" to motions computed from positions in the *Geschichte des Fixsternhimmels* (1922–1952), in the *Index der Sternörter* (Schorr and Kruse 1928), and in the Yale catalogues. The trigonometric parallaxes are from the 1950 parallax catalogue.

U, V, and W are the velocities relative to the centroid of motions of the near-by stars in the directions ($l = 57°.5$, $b = 0°$), ($l = 147°.5$, $b = 0°$), and ($b = 90°$); and Q is the vectorial sum of these components. On the assumption that this local centroid represents a circular velocity of rotation of 216 km/sec at a distance of 8.2 kpc from the center of the Galaxy, U and V have been used to compute the eccentricities and semimajor axes of the Newtonian orbits described by the projection of the star's motion on the galactic plane. At best, these orbits are only approximations, since we have ignored both the W component of the velocity and the lack of an exact inverse-square force field near the center of the Galaxy. However, their size and shape should provide more useful parameters for statistical discussions of these stars than Q alone.

It seems fairly definite that four of the stars in Table 1 move in hyperbolic orbits. These are BD+21°607, sd F5; BD+6°2932, G6 V; BD+2°3375, sd F5; and HD 134439, K0 VI, with orbits whose eccentricities are 1.10, 1.19, 1.15, and 1.37, respectively. A circular velocity near the sun of 270 km/sec would be necessary to account for the motions of these stars by elliptical orbits.

Visual double stars and spectroscopic binaries have been indicated in the notes to the catalogue. If both components of a visual double were observed as one star photo-

metrically, the measured magnitude was corrected to give the true magnitude of the brighter one. In these cases the magnitude difference is from Aitken's *New General Catalogue of Double Stars* (1932) and is given in the notes. Among the spectroscopic binaries, only the one with double lines was corrected for the presence of a second component; in this case it was assumed that the stars were equally bright. When either the spectral type or the photometric data were obtained for the fainter component of a double-star system, this component has been given a separate number in the table, but the data shared by both components are not repeated.

In Table 1, column 1 contains a running number; an asterisk after this number refers to a note at the end of the table. The name HD number or BD number of the star is given in column 2. Columns 3 and 4 give the 1900 right ascension and declination of the star, and column 5 gives its spectral type. The visual magnitude is in column 6, with the blue-yellow and ultraviolet-blue colors in columns 7 and 8. Columns 9 and 10 give the trigonometric and spectroscopic parallaxes. The running number from column 1 is repeated in column 11, on the second page of the table. Column 12 contains the radial velocity, and columns 13 and 14 the proper motion in right ascension and declination, respectively. The source of the proper motion is indicated in column 15. Columns 16, 17, and 18 give the components of the space velocity. The total space velocity is in column 19. The eccentricity and semimajor axis of the Newtonian orbit are in columns 20 and 21. Table 2 contains stars which do not fall within the limits of the catalogue but of which new observations have been made. This table contains all stars earlier than B6 or later than M0 which were observed, as well as other stars for which complete observational data are not available. The arrangement of the material is the same as in columns 1–14 of Table 1, except that columns 1 and 11 are omitted and the asterisk indicating a note is placed after the name of the star.

The author has benefited from discussions with many of her colleagues, particularly at the Yerkes and David Dunlap Observatories and by the use of their unpublished material.

REFERENCES

Aitken, G. R. 1932, *New General Catalogue of Double Stars* (Washington, D.C.: Carnegie Institution of Washington).
Duke, D. 1951, *Ap. J.*, **113**, 100.
Johnson, H. L., and Morgan, W. W. 1953, *Ap. J.*, **117**, 313.
Keenan, P. C., and Keller, G. 1951, *Ap. J.*, **113**, 700.
Kruse, W., and Imgart, B. 1936, *Bergedorfer Eigenbewegungs-Lexicon* (Bergedorf).
Miczaika, G. 1940, *A.N.*, **270**, 249.
Ramsey, J. F. 1950, *Ap. J.*, **111**, 434.
Roman, N. G. 1952, *Ap. J.*, **116**, 122.
———. 1953, *ibid.*, **117**, 467.
———. 1955, *Pub. David Dunlap Obs.*, **2**, 97.
Schorr, R., and Kruse, W. 1928, *Index der Sternörter* (Bergedorf).
Wilson, R. E. 1953, *General Catalogue of Radial Velocities* (Washington, D.C.: Carnegie Institution of Washington).
1922–1952, *Geschichte des Fixsternhimmels* (Karlsruhe).

SOURCES OF RADIAL VELOCITIES

Joy, A. H. 1947, *Ap. J.*, **105**, 96.
Joy, A. H., and Mitchell, S. A. 1948, *Ap. J.*, **108**, 234.
Kuiper, G. P. 1939, *Ap. J.*, **89**, 548.
———. 1940*a*, *ibid.*, **91**, 269.
———. 1940*b*, *ibid.*, **92**, 126.
———. 1942, *ibid.*, **95**, 201.
Merrill, P. W. 1947, *Pub. A.S.P.*, **59**, 256.
Moore, J. H., and Paddock, G. F. 1950, *Ap. J.*, **112**, 48.
Neubaurer, F. J. 1943, *Ap. J.*, **97**, 300.

Popper, D. M. 1942, *Ap. J.*, **95**, 307.
Popper, D. M., and Seyfert, K. 1940, *Pub. A.S.P.*, **52**, 401.
Wilson, R. E. 1943, *Pub. A.S.P.*, **55**, 282.
———. 1948, *Ap. J.*, **107**, 119.
Wilson, R. E., and Joy, A. H. 1950, *Ap. J.*, **111**, 221.
———. 1952, *ibid.*, **115**, 157.
Young, R. K. 1939, *Pub. David Dunlap Obs.*, **1**, 71.
———. 1945, *ibid.*, p. 311.

No.

1*
2
3
4
5

6
7
8
9*
10

11*
12*
13
14
15

16
17
18*
19
20

21
22
23
24
25

26
27
28
29
30

31
32
33*
34
35

36
37
38
39
40

41
42
43
44
45

46
47
48*
49
50

51
52*
53*
54
55

(1)

TABLE 1

Catalogue

No.	Name	α(1900)	δ(1900)	Sp.	V	B-V	U-B	π tr	π sp
1*	26	$0^h\ 0^m.2$	+ 8° 14'	K0 III p	8.22	+1.09	+ 0.53	0".000	+0".0032
2	245	0 2.2	+86 14	G2 V	8.37	+0.65	-0.07	+0.011	+0.0175
3	417	0 3.7	+24 54	K0 III	6.23	+0.97	+ 0.72		+0.0079
4	613	0 5.4	+32 35	K4 III	6.82	+1.44	+ 1.65		+0.0042
5	1368	0 12.7	- 0 11	F9 V	8.86	+0.53	0.00		+0.011
6	1918	0 18.4	+44 31	G9 III	7.61	+0.96	+ 0.68		+0.0035
7	2126	0 20.4	+33 34	K0 III-IV	8.22	+1.02	+ 0.74		+0.0044
8	2589	0 24.5	+76 28	K0 IV	6.21	+0.84	+ 0.55	+0.021	+0.029
9*	2774	0 26.2	+52 17	K2 III	5.60	+1.15	+ 1.12	+0.005	+0.0115
10	2925	0 27.4	+22 38	K0 III	6.82	+0.92	+ 0.60		+0.0060
11*	3266	0 30.7	+29 28	G2 V	7.94	+0.70	+ 0.08	+0.027	+0.017
12*				G5 V					
13	+53°104	0 31.2	+54 5	A0 V	10.55	+0.15	+ 0.01		+0.0009
14	3457	0 32.4	+ 2 35	K4 III	6.98	+1.32	+ 1.52		+0.0038
15	3512	0 33.0	- 1 3	K2 III	6.68	+1.26	+ 1.37		+0.0069
16	ε And	0 33.3	+28 46	G8 III	4.37	+0.88	+ 0.46	+0.031	+0.013
17	3556	0 33.4	+ 5 29	G0 V	8.77	+0.59	+ 0.10		+0.0125
18*	3567	0 33.5	- 8 51	F5 V	9.27	+0.45	-0.14		+0.0063
19	3628	0 34.0	+ 2 34	G2 V	7.30	+0.63	+ 0.12	+0.014	+0.029
20	3765	0 35.3	+39 40	K2 Vm	7.35	+0.93	+ 0.71	+0.071	+0.063
21	+ 71°81	0 37.2	+71 38	sd F5	10.27	+ 0.36	-0.16	+0.004	+0.0087
22	3989	0 37.4	+45 21	K5 III	7.03	+ 1.52	+ 1.74		+0.0036
23	47144	0 44.4	+29 54	G8 IV	7.62	+ 1.07	+ 0.77	-0.006	+0.015
24	5351	0 50.4	+68 31	K4 V	9.10	+ 1.03	+ 0.88	+0.048	+0.046
25	5780	0 54.3	+ 0 15	K4 III	7.61	+ 1.42	+ 1.69		+0.0029
26	5916	0 55.6	+44 55	G8 III-IV	6.84	+ 0.90	+ 0.45		+0.0079
27	25 Cet	0 58.0	- 5 22	K0 III-IV	5.44	+ 1.11	+ 1.04		+0.016
28	+63°137	1 0.4	+63 24	K7 V	8.94	+ 1.31	+ 1.18	+0.069	+0.083
29	6497	1 0.9	+56 24	K2 III	6.43	+ 1.18	+ 1.27		+0.0079
30	μ Cas	1 1.6	+54 26	G5 VI	5.20	+ 0.71	+ 0.11	+0.136	+0.150
31	78 Psc	1 2.4	+31 29	F5 IV	6.25	+ 0.40	-0.01		+0.013
32	29 Cet	1 2.9	+ 1 28	K0 IV	6.44	+ 0.87	+ 0.48	+0.022	+0.026
33*	6755	1 3.2	+61 1	F9 V	7.68	+ 0.72	+ 0.08	-0.001	+0.019
34	80 Psc	1 3.2	+ 5 7	F2 V	5.51	+ 0.34	+ 0.04	+ 0.033	+0.034
35	6833	1 3.9	+54 13	K1 III	6.73	+ 1.18	+ 0.88	+ 0.001	+0.0066
36	34 Cet	1 6.6	- 2 47	K4 III	5.95	+ 1.40	+ 1.66		+0.0060
37	7983	1 14.0	- 9 27	G2 V	8.90	+ 0.58	-0.02	+ 0.033	+0.014
38	8262	1 16.9	+18 10	G3 V	6.96	+ 0.62	+ 0.09	+ 0.040	+0.036
39	μ Psc	1 24.9	+ 5 38	K4 III	4.86	+ 1.37	+ 1.48	+ 0.021	+0.010
40	9166	1 25.2	+67 54	K3 III	6.76	+ 1.23	+ 1.39	-0.001	+0.0046
41	9407	1 27.3	+68 26	G6 V	6.53	+ 0.68	+ 0.24	+ 0.036	+0.058
42	9670	1 29.7	+ 0 26	F8 V	6.90	+ 0.52	-0.02	+ 0.003	+0.025
43	10015	1 32.7	+29 4	K0 IV-V	8.66	+ 0.83	+ 0.57	+ 0.009	+0.016
44	10126	1 33.9	+27 36	G8 V	7.70	+ 0.74	+ 0.28	+ 0.018	+0.038
45	10145	1 34.1	+66 25	G5 V	7.66	+ 0.68	+ 0.21	+ 0.039	+0.030
46	10436	1 36.8	+63 22	K5 V	8.40	+ 1.22	+ 1.10	+ 0.066	+0.076
47	10975	1 42.7	+37 27	K0 III	5.94	+ 0.97	+ 0.71		+0.0091
48*	11397	1 46.9	-16 48	G8 III	8.93	+ 0.68	+ 0.10	+ 0.016	+ 0.0017
49	11592	1 48.7	+10 8	F5 V	6.78	+ 0.46	-0.05		+ 0.020
50	56 And	1 50.2	+36 46	K0 III	5.67	+ 1.06	+ 0.91		+ 0.010
51	13043	2 2.5	- 1 5	G2 V	6.92	+ 0.61	+ 0.16	+ 0.036	+ 0.035
52*	13530	2 7.0	+50 36	K0 III	5.32	+ 0.93	+ 0.62	+ 0.006	+ 0.012
53*	19 Ari	2 7.6	+14 49	M0 III	5.74	+ 1.54	+ 1.90		+ 0.0063
54	13721	2 8.6	-10 13	F0 V	8.55	+ 0.28	+ 0.00		+ 0.0076
55	13783	$2^h\ 9^m.2$	+64°30'	G8 V	8.29	+ 0.66	+ 0.12	+ 0".020	+ 0".029
(1)	(2)	(3)	(4)	(5)	(6)	(7)	(8)	(9)	(10)

TABLE 1 (continued)

No.	ρ	$\mu\alpha$	$\mu\delta$	Source of μ	U	V	W	Q	e	a
1*	-213	+0.251	-0.058	GC	-346	+266	+140	458	0.98	67.6r
2	- 80	+0.334	-0.007	GC	- 96	+ 58	- 41	119	0.71	5.1
3	+ 15	+0.110	+0.033	GC	- 3	+ 87	- 9	88	0.40	9.5
4	- 14	-0.042	-0.037	GC	+ 3	- 44	- 13	46	0.21	8.8
5	+ 44	+0.339	+0.093	Y 21	- 14	+169	- 33	173	0.74	15.7
6	+ 36	+0.089	+0.012	GFH	- 21	+140	0	142	0.61	10.7
7	- 36	-0.128	-0.022	GFH	+ 41	-125	+ 13	132	0.80	32.9
8	+ 19	+0.339	-0.022	GC	- 5	+ 75	+ 5	75	0.34	8.9
9*	- 52	-0.056	-0.018	GC	- 26	- 29	+ 10	40	0.26	6.8
10	-112	+0.112	+0.012	GC	-109	+ 54	+ 81	146	0.76	4.8
11*	- 49	+0.184	-0.403	GC	-105	+ 6	- 63	123	0.75	4.7
12*										
13	- 12	-0.025	+0.036	AGK_2-Y4	+ 89	- 85	+205	239	1.14	54.1
14	+ 4	+0.090	-0.055	GC	-114	+ 82	- 35	145	0.74	5.2
15	- 55	-0.047	-0.004	GC	0	- 24	+ 55	60	0.11	8.3
16	- 83	-0.232	-0.249	GC	- 49	-118	- 21	129	0.59	7.6
17	+ 30	+0.135	-0.092	Y 22	+ 24	- 32	- 35	53	0.25	10.8
18*	- 50	+0.012	-0.564	Y 16	-350	-196	+199	448	0.79	9.5r
19	- 29	+0.779	+0.293	GC	- 85	+110	+ 53	149	0.71	6.0
20	- 62	+0.344	-0.669	GC	- 71	- 2	- 16	73	0.55	5.3
21	-114	+0.328	+0.107	Grw.	-191	+104	+ 45	224	0.99	4.6
22	- 21	+0.042	+0.015	GC	+ 24	- 37	+ 33	55	0.32	11.4
23	-163	+0.215	-0.025	GC	-149	- 5	+ 87	173	0.90	4.3
24	- 46	+0.691	-0.208	GC	- 69	+ 53	- 16	88	0.56	5.6
25	-103	-0.032	-0.102	GC	-125	-136	+ 15	185	0.86	5.8
26	- 71	+0.106	-0.021	GC	- 88	+ 29	+ 19	95	0.65	5.0
27	+ 15	-0.112	-0.101	GC	+ 7	- 21	- 21	31	0.12	8.9
28	- 3	+1.52	+0.29	Cl 20	- 45	+ 85	+ 30	101	0.49	6.7
29	- 96	+0.110	-0.128	GC	-118	+ 17	- 55	131	0.79	4.6
30	- 97	+3.416	-1.575	GC	-140	+ 49	- 21	150	0.88	4.4
31	+ 14	+0.200	-0.034	GC	- 31	+ 80	- 4	86	0.41	7.3
32	- 95	+0.133	-0.420	GC	- 99	- 31	+ 54	117	0.71	4.9
33*	-320	+0.619	+0.069	GC	-349	- 61	+ 35	356	0.66	5.0r
34	+ 7	-0.267	-0.176	GC	+13	- 25	+ 15	32	0.10	9.3
35	-245	+0.028	+0.046	GC	-195	-109	+ 74	235	1.00	4.8
36	- 9	-0.066	-0.020	GC	+22	- 36	+ 3	42	0.28	10.8
37	- 4	-0.198	-0.460	GC	-106	-149	- 47	189	0.81	6.2
38	+ 2	+0.541	-0.010	GC	- 35	+ 73	+ 17	83	0.42	6.9
39	+ 35	+0.291	-0.043	GC	- 78	+132	+ 22	155	0.71	6.7
40	- 14	+0.102	-0.052	GC	- 69	+100	- 29	125	0.62	6.2
41	- 31	-0.370	+0.123	GC	0	- 26	+ 7	27	0.12	8.3
42	- 18	+0.200	-0.268	GC	- 58	+ 15	+ 6	60	0.47	5.6
43	- 3	+0.418	-0.245	Y 9	-108	+ 95	- 26	146	0.78	5.3
44	+ 55	+0.510	+0.160	GC	+ 10	+105	+ 6	106	0.52	12.3
45	+ 16	+0.693	-0.241	GC	- 50	+118	- 7	128	0.59	7.4
46	- 49	-0.39	-0.58	Cl 20	- 23	- 25	- 36	49	0.23	6.9
47	+ 36	+0.112	-0.027	GC	- 13	+ 82	- 5	83	0.37	8.4
48*	+ 38	+0.135	-0.327	Y 12	-939	-229	-133	976	10.9	0.78r
49	- 21	-0.177	-0.288	GC	- 21	- 70	- 30	79	0.32	7.4
50	+ 58	+0.181	+0.008	GC	- 9	+119	+ 11	120	0.53	10.5
51	- 40	-0.234	-0.349	GC	- 15	- 49	- 5	51	0.23	7.5
52*	+ 27	+0.346	-0.167	GC	- 87	+139	- 14	165	0.77	6.6
53*	+ 23	+0.099	-0.022	GC	- 43	+ 79	+ 10	90	0.46	6.7
54	+ 1	+0.031	-0.118	Y 11	- 67	- 3	- 11	68	0.51	5.3
55	- 31	-0.366	-0.329	GC	+ 13	- 29	- 65	72	0.19	9.6
(11)	(12)	(13)	(14)	(15)	(16)	(17)	(18)	(19)	(20)	(21)

TABLE 1 (continued)

No.	Name	α (1900)	δ(1900)	Sp.	V	B-V	U-B	π tr	π sp
56	-1°306	2h 9m.5	- 1 40	G2 V	9.09	+0.57	-0.07	+0".013	+0".0125
57*	14214	2 12.8	+ 1 17	F9 V	5.56	+0.61	+0.09	+0.036	+0.051
58	+70°169	2 14.0	+70 43	K2 V	8.90	+0.86	+0.64	+0.034	+0.032
59	25 Ari	2 22.1	+ 9 45	F5 V	6.49	+0.46	-0.08	+0.021	+0.023
60	27 Ari	2 25.4	+17 16	K0 III	6.23	+0.90	+0.55		+0.0079
61	+4°415	2 29.4	+ 5 1	K3 V	9.87	+0.88	+0.56	+0.025	+0.025
62	16031	2 29.4	-12 49	sd F4	9.75	+0.45	-0.22	-0.009	+0.011
63	16141	2 30.3	- 3 59	G5 IV	6.82	+0.66	+0.21	+0.030	+0.019
64	16160	2 30.6	+ 6 25	K3 V	5.82	+0.99	+0.77	+0.147	+0.165
65	16397	2 32.7	+30 24	G1 V	7.32	+0.60	0.00	+0.037	+0.026
66	16505	2 33.8	+67 38	K3 III	7.02	+1.24	+1.38		+0.0042
67*	17647	2 44.9	+45 34	G5 V	8.62	+0.72	+0.11	+0.012	+0.014
68	18702	2 55.3	+ 5 36	K0 V	8.12	+0.85	+0.53	+0.017	+0.038
69	18757	2 55.7	+61 21	G4 V	6.60	+0.62	+0.17	+0.027	+0.046
70	19165	2 59.9	+27 18	F6 V	8.45	+0.49	-0.01		+0.011
71	19305	3 1.2	+ 1 36	M0 V	9.10	+1.35	+1.24	+0.059	+0.105
72	ε Per	3 1.8	+49 14	G0 V[M]	4.04[J]	+0.60	+0.10	+0.084	+0.115
73	19445	3 2.5	+25 58	sd F7	8.06	+0.46	-0.24	+0.021	+0.024
74	19618	3 4.4	+15 1	K0 IV-V	9.05	+0.84	+0.51		+0.014
75	19637	3 4.6	+26 31	K3 III	6.02	+1.28	+1.28		+0.0066
76	19735	3 5.5	+47 22	K5 III	6.33	+1.43	+1.64		+0.0050
77	20084	3 8.6	+84 34	G8 II-III	5.61	+0.92	+0.49	+0.022	+0.0048
78*	95 Cet	3 13.3	- 1 18	K1 IV	5.37	+1.04	+0.81	+ 0.006	+0.032
79	20709	3 15.1	+72 51	K3 III	7.02	+0.32	+1.42		+0.0042
80	21197	3 20.1	- 5 42	K5 V	7.85	+1.16	+1.16	+0.061	+0.100
81	21543	3 23.4	- 6 52	G2 V-V1	8.22	+0.62	+0.03	+0.022	+0.024
82	21910	3 26.9	+74 26	K0 III	7.46	+1.03	+0.75		+0.0044
83	+26°595	3 34.1	+26 40	G8 III	8.34	+1.05	+0.84		+0.0022
84	22879	3 35.3	- 3 32	F9 V	6.68	+0.55	-0.09	+0.032	+ 0.030
85	23050	3 36.9	+42 18	G2 V	7.47	+0.59	+0.03	+0.029	+ 0.026
86*	14 Tau	3 38.0	+19 21	K0 III	6.14	+1.01	+0.74		+0.0083
87*	23439	3 40.1	+41 9	K1 V	7.65	+0.81	+0.29	+0.037	+0.042
88	23841	3 43.1	+ 9 21	K2 III	6.68	+1.21	+1.16		+0.0069
89*	24000	3 44.3	+ 29 26	A2 V	8.76	+0.34	+0.24		+0.0044
90	24002	3 44.4	+ 1 4	K1 V	8.59	+0.84	+0.42	+0.025	+0.033
91	25178	3 55.0	+74 54	F8 V	7.16	+0.54	-0.08	+0.020	+0.022
92	25329	3 56.4	+35 2	K1 V	8.52	+0.88	+0.36	+0.054	+0.035
93	25532	3 58.2	+23 8	F6 IV-V	8.18	+0.70	+0.15		+0.0083
94	49 Per	4 1.6	+37 28	K1 III	6.09	+0.95	+0.75	+ 0.022	+ 0.0087
95	26298	4 4.5	-16 40	F2 V	8.14	+0.34	-0.05		+ 0.0105
96	26659	4 8.0	+85 6	G8 III	5.46	+0.87	+0.46	+ 0.012	+0.0081
97	+21°607	4 8.6	+22 6	sd F5	9.22	+0.44	-0.19	-0.003	+0.0145
98*	32 Eri	4 9.6	-10 30	K3 III	4.86	+1.18	+1.14	+ 0.011	+0.011
99*	α Eri	4 10.7	- 7 49	K1 V	4.48	+0.82	+0.45	+ 0.200	+0.220
100	27821	4 18.4	+ 6 8	A7 V	8.69	+0.32	+0.00		+0.0060
101	+24°659	4 21.8	+24 13	K3 V	9.37	+0.94	+0.51		+0.032
102	28424	4 23.9	+13 41	K2 III	7.72	+1.22	+1.08		+0.0043
103	55°900	4 27.9	+55 13	K2 V	8.33	+0.89	+0.65	+0.056	+0.042
104	29038	4 29.2	+16 47	K3 III	7.22	+1.18	+1.32		+0.0038
105	29065	4 29.4	- 9 11	K4 III	7.27	+1.46	+1.70	+ 0.007	+0.0083
106	29400	4 32.7	+66 33	G8 V	8.26	+0.75	+0.20	+ 0.020	+0.029
107	29587	4 34.5	+41 57	G2 V	7.27	+0.64	+0.05	+ 0.024	+0.029
108*	+29°734	4 40.3	+29 7	B9 V	9.88	+0.29	-0.08		+0.0017
109*	30455	4 42.8	+18 33	G2 V	6.97	+0.61	+0.09	+ 0.012	+0.0033
110	30604	4 44.1	+70 28	G0 V	8.85	+0.57	0.03	+ 0.013	+0.0125
111	30649	4 44.4	+45 41	G1 V-V1	6.97	+0.60	+0.23	+ 0.038	+0.038
112	30812	4 45.7	0 0	K1 III	7.26	+1.06	+0.96		+0.0050
113	31312	4 49.6	+74 7	K5 III	6.06	+1.57	+1.83		+0.0055
114	31501	4 51.3	+34 7	G8 V	8.18	+0.75	+0.33	+ 0.018	+0.030
115	31782	4 53.5	+25 47	K0 III	7.29	+0.80	+0.43		+0.0048
(1)	(2)	(3)	(4)	(5)	(6)	(7)	(8)	(9)	(10)

TABLE 1 (continued)

No.	ρ	$\mu\alpha$	$\mu\delta$	Source of μ	U	V	W	Q	e	a
56	+19	+0.993	-0.080	GC	-256	+270	+104	386	0.99	20.3r
57*	+27	+0.372	+0.381	GC	+16	+72	+14	75	0.44	11.7
58	-26	+0.574	-0.146	GC	-70	+67	+13	98	0.58	5.7
59	-41	-0.288	-0.201	GC	+6	-64	-11	65	0.28	9.4
60	-116	+0.029	-0.085	GC	-77	-69	+50	115	0.62	5.5
61	-72	-0.31	-0.61	Ci 20	-52	-115	-27	129	0.57	7.2
62	+63	+0.078	-0.155	Y 11	-75	+14	-60	97	0.53	5.3
63	-53	-0.150	-0.427	GC	-51	-93	-9	106	0.53	6.7
64	+23	+1.807	+1.459	GC	+8	+83	+34	90	0.41	10.6
65	-100	-0.483	-0.381	GC	-22	-122	-42	131	0.54	9.4
66	-50	-0.001	-0.012	GC	-31	-12	-12	35	0.27	6.5
67*	+16	+0.489	-0.319	GC	-145	+142	-14	203	0.62	5.6
68	+66	+0.649	-0.192	GC	-58	+100	-12	116	0.57	6.6
69	-7	+0.726	-0.679	GC	-70	+80	-17	108	0.60	5.8
70	+85	+0.060	-0.050	Y 24	+8	+99	-32	104	0.50	11.7
71	-22	+0.394	-0.890	Y 20	-35	-8	+13	38	0.30	6.3
72	+50	+1.267	-0.081	GC	-1	+87	+25	91	0.40	9.7
73	-139	-0.199	-0.796	GC	-117	-139	-68	194	0.84	5.8
74	-23	-0.069	-0.297	Y 19	-54	-42	-56	88	0.44	5.7
75	-16	+0.005	+0.073	GC	+35	+12	+53	65	0.36	12.7
76	-36	+0.074	-0.074	GC	-96	+39	-13	104	0.70	4.9
77	+33	+0.071	-0.129	GC	-25	+155	-37	161	0.67	11.7
78*	+28	+0.252	-0.047	GC	-24	+52	+4	57	0.30	7.1
79	-20	+0.057	-0.058	GC	-67	-37	+6	77	0.54	5.5
80	-12	-0.243	-0.773	GC	-19	-19	-13	30	0.19	7.1
81	+59	+0.353	-0.205	GC	-77	+68	-11	103	0.61	5.4
82	-104	+0.001	+0.053	GFH	-66	-85	+29	111	0.59	6.0
83	-199	+0.105	+0.102	GC	-347	-79	+60	361	0.67	5.5r
84	+114	+0.701	-0.213	GC	-113	+114	-23	162	0.79	5.9
85	+32	+0.367	+0.244	GC	-50	+81	+9	96	0.50	6.5
86*	+78	+0.118	-0.054	GC	-49	+109	-5	120	0.56	7.1
87*	+50	+0.595	-1.238	GC	-104	+110	-65	165	0.78	5.6
88	-80	+0.072	+0.013	GC	-21	-27	+85	92	0.22	7.0
89*	+12	-0.041	+0.000	GFH	+39	+11	-25	48	0.40	13.6
90	-16	+0.263	-0.635	Y 20	-80	-22	+3	83	0.61	5.1
91	+36	+0.179	-0.291	GC	-14	+96	+1	97	0.43	8.8
92	-30	+1.745	-1.348	GC	-282	+87	+40	298	0.91	4.8r
93	-113	+0.103	-0.120	GC	-99	-75	+40	130	0.72	5.0
94	-40	-0.107	-0.192	GC	-41	-28	-101	113	0.36	6.2
95	+82	+0.044	+0.182	Y 12	+18	+133	-9	135	0.68	18.0
96	-38	-0.053	+0.106	GC	+16	-63	+7	65	0.35	10.8
97	+339	+0.455	-0.283	GC	-121	+369	-59	393	1.10	7.2
98*	+7	-0.009	-0.160	GC	-41	-22	-25	53	0.35	6.2
99*	-42	-2.225	-3.418	GC	-4	-72	-30	78	0.33	8.9
100	+130	-0.019	+0.007	BAN 274	+5	+27	-7	28	0.14	8.7
101	+63	+0.367	+0.100	Y 10	-9	+93	+39	101	0.40	9.0
102	+96	+0.155	+0.026	Lei 15	-128	+141	+65	201	0.88	5.8
103	+50	+0.65	-0.28	Ci 20	-34	+93	+45	108	0.46	7.4
104	+43	0.000	-0.078	GC	-70	+37	-63	101	0.56	5.4
105	-27	-0.037	-0.109	GC	-14	-46	-32	58	0.24	7.6
106	-52	+0.378	+0.072	GC	-55	-16	+48	75	0.45	5.7
107	+113	+0.546	-0.417	GC	-62	+158	+25	172	0.70	9.2
108*	+12	-0.025	-0.042	Y 9-C.C.	-44	-1	-127	134	0.37	6.0
109*	+55	+0.196	-0.388	GC	-56	+66	-18	88	0.51	6.0
110	+45	+0.149	-0.265	GC	-51	+126	+8	136	0.61	7.6
111	+27	+0.385	-0.558	GC	-63	+69	-8	94	0.55	5.9
112	-9	+0.004	-0.062	Lei 15	-37	-17	-15	43	0.32	6.3
113	-52	+0.025	+0.036	GC	-24	-37	+22	49	0.26	6.9
114	+40	+0.587	-0.151	GFH	-60	+74	+62	114	0.54	6.0
115	-68	-0.092	-0.105	Bgd	-26	-69	-116	137	0.33	7.2
(11)	(12)	(13)	(14)	(15)	(16)	(17)	(18)	(19)	(20)	(21)

TABLE 1 (continued)

No.	Name	α(1900)	δ(1900)	Sp.	V	B−V	U−B	π tr	π sp
116	32023	$4^h55^m.2$	+ 0°52	F8 V	9.10	+0.57	+0.04		+ 0".0091
117	+55°960	5 0.2	+55 18	G2 V	9.33	+0.63	−0.01		+ 0.0115
118	32963	5 1.8	+26 12	G5 IV	7.58	+0.66	+0.21		+ 0.0135
119*	+29°847	5 9.4	+29 21	G2 V	8.83	+0.67	+0.20		+ 0.014
120	λ Aur	5 12.1	+40 1	G0 V^M	4.71^J	+0.67	+0.10	+0.066	+ 0.083
121*	34673	5 14.1	− 3 11	K3 V	7.77	+1.05	+0.82	+0.071	+ 0.066
122	35783	5 22.1	+78 18	F6 V	7.69	+0.46	−0.02	+0.013	+ 0.015
123*	35961	5 23.3	+54 35	G1 V	7.53	+0.64	+0.13	+0.018	+ 0.022
124	36003	5 23.5	− 3 34	K5 V	7.62	+1.09	+1.19	+0.071	+ 0.110
125	36283	5 25.6	+15 43	G5 V	8.64	+0.67	+0.12		+ 0.020
126*	36443	5 26.6	+ 0 2	G5 V	8.37	+0.66	+0.16	+0.032	+ 0.0022
127	36542	5 27.3	−10 5	B9 V	8.66	+0.00	−0.12		+ 0.0018
128	37008	5 30.4	+51 23	K2 V	7.71	+0.85	+0.45	+0.034	+ 0.055
129	ϕ^2 Ori	5 31.4	+ 9 14	K0 III	4.09	+0.95	+0.65	+0.024	+ 0.021
130*	37171	5 31.5	+10 58	K5 III	5.98	+1.55	+1.88		+ 0.0058
131	51 Ori	5 37.3	+1 26	K1 III	4.92	+1.16	+1.05	+0.011	+ 0.015
132	38847	5 43.6	+84 59	G0 V	8.86	+0.58	+0.12	+0.015	+ 0.012
133	39099	5 45.2	+14 1	K1 III	6.60	+1.06	+0.92		+ 0.0069
134	39853	5 50.1	−11 48	K5 III	5.66	+1.53	+1.84		+ 0.0066
135*	40460	5 53.8	+27 17	K1 III	6.59	+1.02	+0.84		+ 0.0069
136	38 Aur	5 56.1	+42 55	K0 III	6.10	+0.97	+0.78	+0.014	+ 0.0083
137	+19°1185	5 57.3	+19 23	G0 V	9.32	+0.62	−0.08	+0.033	+ 0.010
138	+26°1067	5 59.7	+26 34	K2 V	9.42	+0.88	+0.66	+0.017	+ 0.025
139	41636	6 1.3	+41 04	K0 III	6.36	+1.05	+0.82		+ 0.0072
140	42618	6 6.6	+ 6 49	G4 V	6.87	+0.63	+0.13	+0.033	+ 0.040
141	42855	6 8.0	+86 46	K3 III	6.60	+1.20	+1.20	−0.002	+ 0.0050
142	κ Aur	6 9.0	+29 32	G8 III	4.34	+1.03	+0.77	+0.016	+ 0.013
143	43147	6 9.6	+44 45	G9 V	9.10	+0.80	+0.29	+0.026	+ 0.022
144	43318	6 10.5	− 0 28	F6 V	5.65	+0.50	0.00	+0.034	+ 0.040
145	43 Aur	6 10.8	+46 24	K2 III	6.39	+1.11	+1.12		+ 0.0079
146*	43624	6 12.1	+27 15	K1 III	6.66	+1.09	+1.12		+ 0.0066
147*	44007	6 14.2	−14 48	G2 III	8.08	+0.86	+0.22		+ 0.0029
148	44030	6 14.4	+25 39	K4 III	7.58	+1.48	+1.75		+ 0.0029
149	6 Lyn	6 22.1	+58 14	K0 IV	5.88	+0.94	+0.66	+0.028	+ 0.033
150	+27°1124	6 22.9	+27 5	K2 V	8.63	+0.92	+0.62	+0.024	+ 0.036
151	ψ^2 Aur	6 32.2	+42 35	K3 III	4.80	+1.22	+1.28	+0.0038	+ 0.0115
152	ψ^4 Aur	6 35.8	+44 37	K5 III	5.02	+1.48	+1.83	+0.018	+ 0.0090
153*	49409	6 43.2	+ 7 45	G0 V	7.93	+0.60	+0.10	+0.012	+ 0.019
154	ψ^7 Aur	6 43.7	+41 54	K3 III	5.02	+1.27	+1.35	−0.005	+ 0.0102
155	+50°1359	6 44.6	+50 46	A5 V	10.04	+0.20	+0.12		+ 0.0026
156	+40°1758	6 49.5	+40 13	K5 V	9.08	+1.15	+1.09	+0.032	+ 0.055
157	θ CMa	6 49.6	−11 55	K4 III	4.08	+1.43	+1.69	+0.021	+ 0.0145
158	51219	6 51.4	+ 1 18	G8 V	7.42	+0.70	+0.22	+0.026	+ 0.014
159	62 Aur	6 52.3	+38 12	K2 III	5.99	+1.23	+1.16		+ 0.0096
160	51866	6 54.0	+48 32	K3 V	8.01	+0.99	+ 0.88	+0.032	+ 0.060
161	52071	6 54.7	+27 18	K2 III	7.12	+1.25	+1.28		+ 0.0057
162	20 Mon	7 5.3	− 4 5	K0 III	4.93	+1.03	+ 0.77	+0.021	+ 0.014
163	55458	7 7.8	+25 11	K1 V	8.41	+0.85	+ 0.38	+0.037	+ 0.036
164	55575	7 8.4	+47 25	G0 V	5.58	+0.58	+ 0.03	+0.037	+ 0.055
165	56224	7 11.1	+26 33	K1 III	7.25	+1.17	+ 1.18		+ 0.0052
166	56274	7 11.3	−12 53	G2 V	7.73	+0.63	−0.01	+0.034	+ 0.024
167*	57435	7 16.1	−14 41	K3 III	8.59	+1.23:	+1.12:		+ 0.0020
168	+46°1264	7 17.7	+46 18	K0 V	9.16	+0.82	+0.46	+0.012	+ 0.023
169	+50°1435	7 22.3	+50 11	G2 V	9.49	+0.68	+0.14		+ 0.0105
170	59374	7 24.6	+19 10	F8 V	8.50	+0.53	−0.10	+0.007	+ 0.012
171*	60298	7 28.7	+25 9	G2 V	7.34	+0.67	+0.11		+ 0.029
172	60778	7 31.0	+ 0 4	A1 V	9.10	+0.10	+0.14		+ 0.0022
173	−1°1792	7 34.8	− 1 17	G6 V	9.26	+0.82	+0.25	+0.012	+ 0.016
174	62301	7 38.1	+39 49	F8 V	6.76	+0.54	−0.04	+0.023	+ 0.026
175*	81 Gem	$7^h40^m.3$	+18 45	K5 III	4.90	+1.45	+1.73	+0".016	+ 0".0096
(1)	(2)	(3)	(4)	(5)	(6)	(7)	(8)	(9)	(10)

TABLE 1 (continued)

No.	ρ	$\mu\alpha$	$\mu\delta$	Source of μ	U	V	W	Q	e	a
116	+106	+0.066	+0.017	Bgd	- 28	+25	- 3	128	0.59	9.6
117	-121	-0.049	-0.366	GC	-136	- 27	-117	181	0.86	4.4
118	- 62	-0.065	-0.065	Bgd	0	- 48	- 17	51	0.22	8.6
119*	- 65	-0.006	-0.052		- 10	- 48	- 1	49	0.23	7.9
120	+ 66	+0.528	-0.659	GC	- 26	+ 22	+ 13	96	0.44	7.9
121*	+ 85	+0.726	+0.128	GC	- 50	+ 98	+ 25	113	0.54	6.8
122	+ 19	+0.070	-0.269	GC	- 36	+ 92	0	99	0.45	7.2
123*	+ 26	-0.121	-0.390	GC	- 26	+ 68	- 52	89	0.36	7.3
124	- 58	-0.324	-0.796	GC	+ 15	- 50	+ 2	52	0.29	10.2
125	+ 49	-0.038	-0.374	GC	- 69	+ 45	- 54	98	0.54	5.4
126*	- 9	+0.182	-0.472	Y 21	- 81	- 50	- 5	95	0.63	5.2
127	- 2	-0.014	+0.008	GFH	+ 4	+ 26	+ 46	53	0.14	8.5
128	- 44	-0.534	+ 0.107	GC	+ 25	- 27	- 36	51	0.28	11.1
129	+ 99	+0.093	-0.305	GC	- 86	+ 88	- 28	126	0.68	9.6
130*	-112	+0.047	-0.013	GC	+ 6	- 93	+ 52	107	0.45	10.8
131	+ 88	-0.054	-0.014	GC	- 22	+ 94	- 30	101	0.44	8.2
132	- 70	+0.091	+ 0.152	GC	- 31	- 74	+ 22	83	0.40	7.1
133	- 48	+0.015	+ 0.009	GC	+ 19	- 28	+ 23	41	0.23	10.3
134	+ 87	+0.065	+ 0.040	GC	- 49	+ 99	+ 35	116	0.54	6.9
135*	+ 96	-0.005	-0.078	GC	- 42	+111	- 17	120	0.54	7.5
136	+ 38	+0.119	-0.146	GC	- 91	+ 68	+ 35	119	0.79	5.2
137	-190	+0.673	-0.633	Y 19	-369	-246	+136	464	0.95	40.8*
138	- 92	-0.174	-0.366	Y 9	- 29	- 74	- 62	101	0.39	7.2
139	- 87	-0.013	-0.056	GC	- 34	- 60	- 34	77	0.39	6.8
140	- 54	+0.192	-0.266	GC	- 8	- 47	+ 16	51	0.22	8.0
141	+ 26	+0.013	-0.106	GC	- 32	+114	+ 15	119	0.53	8.2
142	+ 20	-0.067	-0.264	GC	- 68	+ 42	- 56	98	0.56	5.5
143	- 35	-0.242	-0.351	GC	- 41	+ 12	- 79	90	0.35	6.1
144	- 36	-0.162	-0.222	GC	+ 14	- 29	- 18	37	0.14	9.5
145	0	+0.023	-0.131	GC	- 65	+ 40	- 30	82	0.53	5.6
146*	- 49	+0.012	-0.074	GC	- 40	- 34	- 16	55	0.36	6.3
147*	+167	+0.051	-0.056	Y 12	-195	+ 64	+ 6	205	0.99	4.3
148	-104	+0.009	-0.042	GC	- 48	- 92	- 25	107	0.52	6.8
149	+ 36	-0.019	-0.337	GC	- 18	+ 72	+ 3	74	0.34	7.8
150	- 47	-0.230	-0.436	GC	- 25	- 25	- 53	64	0.22	6.8
151	+ 17	+0.008	-0.061	GC	- 15	+ 37	+ 6	40	0.26	7.1
152	- 73	-0.041	-0.032	GC	- 11	- 42	- 41	60	0.21	7.7
153*	- 87	-0.042	-0.372	Y 22	- 24	- 92	- 51	108	0.43	8.0
154	+ 61	-0.020	-0.134	GC	- 41	+ 90	- 7	99	0.49	7.1
155	- 17	-0.033	+0.014	AGK_2-Y 4	+ 55	+ 39	- 31	74	0.61	20.4
156	+ 49	+0.103	-0.457	GC	- 30	+ 67	+ 18	76	0.37	7.1
157	+ 97	-0.140	-0.018	GC	- 48	+ 96	- 42	115	0.52	7.0
158	- 12	-0.007	-0.567	GC	- 33	- 21	- 23	45	0.29	6.4
159	+ 25	-0.038	-0.125	GC	- 48	+ 52	- 27	76	0.44	6.1
160	- 23	+0.553	-0.443	GC	- 46	- 6	+ 27	54	0.38	5.9
161	+ 95	+0.001	-0.007	GC	- 13	+106	+ 30	111	0.48	9.4
163	+ 79	-0.004	+ 0.215	GC	+ 9	+117	+ 46	126	0.57	13.2
163	- 51	-0.414	-0.100	GC	+24	- 12	- 61	67	0.24	10.8
164	+ 85	+0.034	-0.187	GC	+ 4	+ 96	+ 40	104	0.45	10.7
165	+110	-0.039	+ 0.006	Y 9	+ 2	+116	+ 12	117	0.62	13.6
166	+ 60	-0.500	+ 0.177	GC	+14	+115	- 62	131	0.58	14.1
167*	+129	-0.013	+ 0.018	Y 12	- 56	+140	+ 17	152	0.66	8.0
168	+ 8	-0.251	-0.275	GFH	- 30	+ 59	- 47	81	0.35	6.9
169	- 77	+0.050	+ 0.009	Y 4	- 10	- 60	- 9	61	0.26	8.1
170	+ 80	+0.038	-0.452	GC	-185	+ 48	- 24	193	0.98	4.2
171*	-134	+0.146	-0.364	GC	- 23	-120	- 42	129	0.52	8.8
172	+ 39	-0.036	-0.116	Y 21	-182	- 38	-179	258	0.975	4.1
173	+ 45	+0.137	-0.235	GC	- 83	- 1	+ 24	86	0.62	5.0
174	- 3	+0.046	-0.687	GC	-139	+ 26	- 14	142	0.87	4.3
175*	+ 81	-0.075	-0.062	GC	- 40	+ 98	- 6	106	0.51	7.2
(11)	(12)	(13)	(14)	(15)	(16)	(17)	(18)	(19)	(20)	(21)

TABLE 1 (continued)

No.	Name	α (1900)	δ (1900)	Sp.	V	B-V	U-B	π tr	π sp
176	62902	$7^h14^m.1$	- 6°32'	K5 III	5.48	+ 1.38	+ 1.67		+0.0072
177	63410	7 43.6	+26 31	G8 III	6.78	+ 0.95	+ 0.59		+0.0044
178*	64090	7 47.2	+30 55	G2 VI	8.34	+ 0.60	-0.12	+0.042	+0.029
179	64259	7 47.8	-13 36	K2 III	6.61	+ 1.10	+ 1.00	-0.007	+0.0072
180	64606	7 49.6	- 1 10	G8 V	7.44	+ 0.73	+ 0.15	+0.047	+0.044
181	14 CMi	7 53.2	+ 2 29	K0 III	5.28	+ 0.91	+ 0.72	+0.024	+0.012
182	65430	7 53.7	+21 8	K0 V	7.69	+ 0.81	+ 0.48	+0.033	+0.046
183	65583	7 54.3	+29 31	G8 V	7.00	+ 0.70	+ 0.18	+0.056	+0.052
184	66141	7 57.1	+ 2 37	K2 III	4.40	+ 1.25	+ 1.24	+0.018	+0.020
185	66171	7 57.2	+72 13	G2 V	8.20	+ 0.61	+ 0.05	+0.017	+0.019
186	68017	8 5.5	+32 47	G4 V	6.80	+ 0.07	+ 0.13	+0.043	+0.042
187	68744	8 8.7	+73 39	G0 V	8.50	+ 0.60	+ 0.05	-0.002	+0.0145
188	68788	8 8.8	+73 44	K1 V	8.38	+ 0.84	+ 0.53	+0.012	+0.036
189	+ 54°1216	8 11.7	+54 25	sd F5	9.69	+ 0.48	-0.19	+0.008	+0.0115
190	+ 31°1781	8 12.1	+30 56	K4 V	8.80	+ 1.14	+ 1.11	+0.046	+0.052
191	69830	8 13.7	-12 18	G8 V	6.00	+ 0.76	+ 0.32	+0.075	+0.083
192	70352	8 16.3	+66 48	K2 V	8.91	+ 0.88	+ 0.68	+0.017	+0.032
193	70523	8 17.4	-17 16	K1 III	5.77	+ 1.05	+ 0.99		+0.010
194	71377	8 22.0	-12 12	K2 III	5.54	+ 1.19	+ 1.14		+0.012
195	71597	8 23.2	+ 0 36	K2 III	7.30	+ 1.16	+ 1.13	+0.008	+0.0052
196	71881	8 24.6	+50 57	G1 V	7.43	+ 0.63	+ 0.14	+0.017	+0.026
197	72184	8 26.4	+38 22	K2 III	5.90	+ 1.11	+ 1.17	+0.013	+0.010
198	ν^2 Can	8 27.1	+24 25	G9 III	6.36	+ 1.02	+ 0.88	+0.023	+0.0063
199	72614	8 28.8	+42 6	K2 V	8.78	+ 0.92	+ 0.71	+0.037	+0.033
200	73393	8 33.1	+56 2	G3 V	8.04	+ 0.68	+ 0.22	+0.009	+0.023
201*	73668	8 34.4	+ 6 8	G1 V	7.24	+ 0.60	+0.08	+0.009	+0.028
202	74000	8 36.2	-15 59	sd F6	10.26:	+ 0.32:	-0.07:	+0.016	+0.0089
203	+ 25°1981	8 38.5	+25 10	sd F2	9.35	+ 0.30	-0.12		+0.013
204*	74462	8 39.1	+67 49	G5 IV	8.74	+ 0.97	+ 0.53	+0.017	+0.0079
205	74721	8 40.4	+13 38	A0 V	8.72	+ 0.03	+ 0.13		+0.0021
206	75530	8 45.4	- 5 09	G8 V	9.18	+ 0.74	+ 0.22	+0.014	+0.019
207*	75632	8 46.0	+71 11	K5 V	8.06	+ 1.39	+ 1.21	+0.089	+0.063
208	76291	8 50.1	+46 1	K1 IV	5.74	+ 1.09	+ 1.06		+0.028
209	76932	8 54.0	-15 45	F9 V	5.86	+ 0.53	+ 0.08	+0.020	+0.044
210	77236	8 56.2	- 2 10	K2 III	7.54	+ 1.15	+ 1.02	+0.014	+0.0048
211	77353	8 56.9	- 0 6	K0 III	5.68	+ 1.14	+ 1.04		+0.010
212	77408	8 57.2	+33 16	F7 V	7.03	+ 0.50	-0.04		+0.023
213	77729	8 59.2	+26 34	K4 III	7.64	+ 1.38	+ 1.58		+0.0028
214	77818	8 59.7	+59 17	K1 IV	7.65	+ 1.01	+ 0.82		+0.0115
215	78249	9 2.1	+59 32	K1 IV	7.09	+ 0.99	+ 0.82		+0.0145
216	78479	9 3.4	+17 52	K3 III	7.19	+ 1.21	+ 1.33		+0.0038
217	78558	9 3.8	-14 44	G2 V	7.32	+ 0.61	+ 0.01	+0.032	+0.029
218*	79210	9 7.5	+53 7	M0 V	7.60	+ 1.38	+ 1.21	+0.163	+0.210
219*	79211			M0 V	7.70	+ 1.34	+ 1.22		
220	79452	9 9.1	+35 3	G6 III	5.97	+ 0.86	+ 0.37		+0.0066
221*	81192	9 19.1	+20 13	G8 III	6.56	+ 0.94	+ 0.55		+0.0048
222	82309	9 26.1	+20 27	K3 III	7.46	+ 1.28	+ 1.49		+0.0033
223*	θ UMa	9 26.2	+52 8	F6 IV^{bs}	3.16	+ 0.47	+ 0.02	+0.052	+0.056
224*	+ 58°1199	9 29.5	+58 21	G3 V	9.96	+ 0.63	+ 0.03		+0.0069
225	83186	9 31.5	+72 12	F9 V	7.48	+ 0.52	0.00	-0.006	+0.021
226	83425	9 33.2	+ 5 6	K3 III	4.66	+ 1.30	+ 1.46	+0.005	+0.012
227	83632	9 34.8	+26 28	K2 III	8.10	+ 1.35	+ 1.50		+0.0036
228	84453	9 40.3	+45 35	K0 IV	6.82	+ 0.95	+ 0.74		+0.022
229	84987	9 43.5	+14 14	sd F2	8.24	+ 0.41	-0.25	+ 0.025	+0.023
230	7 Sex	9 47.1	+ 2 55	A1 V	6.02	-0.04	-0.09	+0.009	+0.0091
231	86322	9 52.6	+75 14	K1 III	6.90	+ 1.05	+ 0.94		+0.0060
232	20 LMi	9 55.3	+32 26	G4 V	5.35	+ 0.66	+ 0.28	+0.053	+0.083
233	86986	9 57.1	+15 02	A1 V	7.99	+ 0.12	+ 0.16	-0.016	+0.0036
234*	87998	$10^h 3.6$	-19 15	G2 V	7.28	+ 0.61	+ 0.04	+0.015	+0.029
235	88371	$10^h 6^m.3$	+24°15'	G2 V	8.43	+ 0.63	+ 0.12	+0.019	+0.017
(1)	(2)	(3)	(4)	(5)	(6)	(7)	(8)	(9)	(10)

TABLE 1 (continued)

No.	ρ	$\mu\alpha$	$\mu\delta$	Source of μ	U	V	W	Q	e	a
176	- 32	+0.055	-0.095	GC	- 21	- 56	+ 1	60	0.33	7.5
177	+ 81	-0.035	-0.018	GC	- 20	+104	+ 4	106	0.47	8.7
178*	-240	+0.725	-1.836	GC	-365	-110	- 84	390	0.63	6.5r
179	- 29	-0.035	-0.080	GC	- 6	- 45	- 5	46	0.21	8.1
180	+ 93	-0.265	-0.058	GC	- 52	- 60	+ 4	79	0.47	6.1
181	+ 46	-0.160	+0.097	GC	+ 22	+100	- 15	103	0.57	15.1
182	- 28	+0.185	-0.553	GC	- 40	- 27	+ 4	48	0.35	6.2
183	+ 12	-0.146	-1.168	GC	- 95	+ 29	- 27	103	0.69	4.9
184	+ 71	-0.031	+0.102	GC	- 15	+ 83	+34	91	0.39	8.4
185	+ 37	-0.206	-0.459	GC	- 60	+130	0	143	0.62	7.8r
186	+ 27	-0.465	-0.657	GC	- 60	+ 67	- 39	98	0.53	5.9
187	+ 53	-0.063	-0.255	GC	- 31	+107	+ 35	117	0.50	8.0
188	- 3	-0.301	-0.481	GC	- 40	+ 70	- 15	82	0.43	6.7
189	+ 59	-0.010	-0.648	Y 4	-227	+138	+ 37	268	1.00	5.2r
190	+ 12	-0.291	-0.824	GC	- 64	+ 37	- 25	78	0.52	5.6
191	+ 30	+0.269	-0.981	GC	- 52	- 9	- 3	53	0.42	5.8
192	+ 18	+0.008	-0.533	GC	- 56	+ 62	+ 29	88	0.51	6.0
193	+ 68	-0.094	-0.016	GC	- 48	+ 71	- 19	88	0.47	6.4
194	+ 65	-0.092	-0.021	GC	- 45	+ 68	- 9	82	0.49	6.8
195	+110	-0.021	-0.050	Y 21	- 97	+ 78	+13	125	0.72	5.2
196	+ 17	-0.074	-0.329	GC	- 47	+ 51	+ 8	70	0.43	6.2
197	+ 15	-0.095	-0.169	GC	- 67	+ 57	- 28	92	0.55	5.6
198	+ 75	-0.066	-0.053	GC	- 47	+ 99	- 1	110	0.53	7.0
199	+ 58	-0.297	-0.736	GFH	- 93	+ 96	+ 1	134	0.71	5.4
200	+ 37	-0.251	-0.377	GC	- 39	+105	- 4	112	0.52	7.6
201*	- 18	-0.180	-0.317	GC	- 29	- 37	0	47	0.29	6.7
202	+203	+0.358	-0.475	Y 12	-317	-167	+70	365	0.86	6.9r
203	+ 47	-0.103	-0.334	GC	-119	+ 29	- 23	125	0.80	4.5
204*	-168	+0.049	-0.082	Grw.	-112	- 96	- 82	169	0.80	5.2
205	+ 9	-0.043	-0.142	GC	-271	- 21	-175	323	0.93	4.2r
206	+ 40	-0.209	-0.519	Y 17	-107	+ 5	- 81	134	0.74	4.6
207*	+ 48	-1.341	-0.354	GC	+ 11	+126	- 33	131	0.62	14.8
208	+ 58	-0.124	-0.042	GC	+ 5	+ 75	+30	81	0.36	9.8
209	+122	-0.027	-0.015	GC	- 92	+ 47	+75	128	0.65	5.2
210	+142	-0.142	-0.050	GC	-123	+164	- 51	211	0.88	6.6
211	+ 73	-0.051	+ 0.074	GC	- 17	+ 91	+42	102	0.40	8.6
212	+ 70	-0.406	-0.002	GC	- 2	+ 124	- 7	124	0.56	11.7
213	+104	+ 0.002	-0.039	Y 9	- 84	+ 75	+66	131	0.67	5.6
214	- 39	-0.021	-0.105	Lei 15	- 45	+ 6	- 17	48	0.37	6.0
215	+ 46	-0.164	-0.036	GC	+ 10	+ 89	+19	92	0.44	11.1
216	+ 76	-0.043	-0.038	GC	- 68	+ 92	+ 4	114	0.61	6.1
217	+ 60	-0.535	-0.206	GC	- 61	+ 81	- 52	114	0.51	6.4
218*	+ 10	-1.569	-0.590	GC	- 4	+ 51	- 9	52	0.24	8.4
219*										
220	+ 56	-0.147	+ 0.046	GC	+ 32	+134	- 25	140	0.90	27.6
221*	+135	-0.089	-0.120	GC	-156	+130	+13	203	0.94	5.3
222	- 11	-0.041	-0.132	GC	-169	+ 1	- 84	189	0.95	4.2
223*	+ 15	-0.950	-0.542	GC	- 40	+ 90	- 27	102	0.50	7.1
224*	- 16	+ 0.219	-0.310	Y 7	-191	- 78	+149	254	0.86	4.3
225	- 27	-0.221	-0.097	GC	- 30	+ 45	- 33	63	0.28	6.6
226	+ 45	-0.163	-0.057	GC	- 43	+ 79	- 15	91	0.46	6.3
227	+ 90	-0.038	-0.048	Y 9	- 82	+ 95	+34	130	0.63	5.8
228	- 44	+ 0.046	-0.138	GC	- 24	- 22	- 16	36	0.23	6.8
229	- 18	+ 0.380	-0.790	GC	-120	-111	- 7	164	0.80	4.6
230	+ 97	-0.183	+0.089	GC	- 28	+155	+34	161	0.67	11.3
231	+ 6	-0.055	-0.043	GC	- 24	+ 64	+ 3	68	0.34	7.3
232	+ 56	-0.522	-0.436	GC	- 30	+ 67	+35	81	0.37	7.1
233	+ 6	+ 0.139	-0.227	GC	-233	-230	+39	330	1.00	9.3r
234*	+ 12	-0.123	-0.332	GC	- 33	+ 4	- 34	48	0.28	6.4
235	+ 93	-0.388	+ 0.067	GC	- 18	+152	+18	154	0.66	12.3
(11)	(12)	(13)	(14)	(15)	(16)	(17)	(18)	(19)	(20)	(21)

TABLE 1 (continued)

No.	Name	α(1900)	δ(1900)	Sp.	V	B−V	U−B	π tr	π sp
236	88725	10h 8m9	+ 3°39'	G1 V	7.76	+0.60	−0.02	+ 0".047	+0".021
237*	γ Leo	10 14.5	+20 21	K0 III	1.84	+1.08	+ 1.04	+ 0.019	+0.053
238	89668	10 15.7	− 0 58	K3 V	9.41	+1.09	+ 1.00	+ 0.019	+0.032
239*	89707	10 16.0	−14 59	F8 V	(7.01)			+ 0.041	+0.024
240	89777	10 16.5	−16 33	G8 V	9.39	+0.73	+ 0.34	+ 0.008	+0.017
241	90250	10 20.0	+35 56	K1 III	6.49	+1.09	+ 0.99		+0.0072
242	90362	10 20.8	− 6 33	M0 III	5.55	+1.52	+ 1.83		+0.0066
243	90508	10 21.9	+49 19	G1 V	6.42	+0.60	+ 0.05	+ 0.051	+0.040
244	90711	10 23.2	− 6 5	K0 V	7.90	+0.81	+ 0.46	+ 0.033	+0.042
245	+30°2022	10 23.8	+30 10	K1 III	8.80	+1.11	+ 0.92		+0.0025
246	+46°1635	10 25.5	+46 3	K7 V	8.86	+1.33	+ 1.29	+ 0.064	+0.085
247	48 Leo	10 29.6	+ 7 28	G8 II-III	5.08	+0.93	+ 0.64	+ 0.027	+0.0059
248	91889	10 31.6	−11 42	F8 V	5.72	+0.52	0.00	+ 0.040	+0.044
249	92095	10 32.9	+54 12	K3 III	5.52	+1.27	+ 1.34		+0.0085
250	92538	10 35.9	+66 32	G0 V	8.30	+0.58	+ 0.11	+ 0.010	+0.016
251	+47°1806	10 38.1	+46 49	G1 IV	9.12	+0.62	+ 0.09		+0.0052
252	94028	10 46.1	+20 49	sd F8	8.23	+0.47	−0.19	+ 0.023	+0.023
253*	94084	10 46.5	+53 3	K2 III	6.44	+1.11	+ 1.01		+0.0078
254	94669	10 50.5	+42 33	K2 III	6.03	+1.13	+ 1.08	+ 0.016	+0.0095
255	+42°2163	10 51.4	+42 25	K1 V	9.72	+0.82	+ 0.39	+ 0.006	+0.020
256	α Crt	10 54.9	−17 46	K0 III	4.09	+1.10	+ 0.99	+ 0.024	+0.021
257*	97561	11 8.4	+20 41	G7 IV	6.92	+0.75	+ 0.33		+0.014
258	97916	11 10.7	+ 2 38	F5 V	9.22	+0.42	−0.13		+ 0.0066
259	75 Leo	11 12.2	+ 2 34	M0 III	5.18	+1.52	+ 1.82	+ 0.006	+ 0.0078
260	98281	11 13.2	− 4 31	G8 V	7.32	+0.73	+ 0.27	+ 0.049	+ 0.046
261	98824	11 17.3	+17 59	K1 III	7.04	+1.05	+ 0.96		+ 0.0058
262	99196	11 19.8	+11 59	K4 III	5.79	+1.38	+ 1.57		+ 0.0066
263	+51°1664	11 20.6	+50 55	K2 V	10.09	+0.83	+ 0.40		+ 0.018
264	100363	11 27.8	−11 29	F2 V	8.64	+0.30	+ 0.02		+ 0.0083
265	100470	11 28.6	+37 23	K0 III	6.40	+1.05	+ 0.93	−0.014	+ 0.0072
266	102158	11 40.3	+48 14	G2 V	8.05	+0.61	+ 0.05	−0.016	+ 0.021
267	ν Vir	11 40.7	+ 7 5	M0 III	4.00	+1.51	+ 1.76	+0.013	+ 0.014
268*	+ 51°1696	11 41.4	+51 27	G0 V1	(9.5)			−0.004	+ 0.014
269	102326	11 41.6	+77 36	G8 IV-V	8.75	+0.73	+ 0.45	+0.006	+ 0.014
270	103095	11 47.2	+38 25	G8 V1M	6.49V	+0.75	+ 0.17	+0.116	+ 0.105
271	104556	11 57.4	+43 34	G8 V	6.64	+0.86	+ 0.49	+0.010	+0.063
272	104800	11 59.0	+ 3 55	G0 V	9.27	+0.55	−0.07	+0.008	+0.010
273*	104817	11 59.1	+ 2 01	A7 m	7.68	+0.22	+ 0.08		+0.0096
274	104985	12 0.2	+77 28	K0 III-IV	5.80	+1.01	+ 0.85	+0.011	+0.013
275	104988	12 0.2	− 0 58	G8 V	8.19	+0.76	+ 0.26	+0.003	+0.030
276	105043	12 0.6	+63 30	K2 III	6.13	+0.17	+ 1.15		+0.0091
277	+22°2442	12 3.9	+22 21	G2 V	9.49	+0.66	+ 0.04		+0.0105
278	105791	12 5.6	+66 13	F8 V	8.68	+0.56	−0.02	+0.002	+0.011
279*	106038	12 7.0	+13 50	F6 V-V1	10.18	+0.48	−0.18	+0.038	+0.0066
280	106116	12 7.5	− 2 32	G4 V	7.46	+0.69	+ 0.24	+0.042	+0.030
281	106156	12 7.8	+10 37	G8 V	7.92	+0.79	+ 0.42		+0.035
282	106210	12 8.1	+11 24	G3 V	7.58	+ 0.66	+ 0.14	+0.021	+0.0275
283*	106365	12 9.1	+33 20	K2 III	6.87	+ 1.13	+ 1.07		+0.0083
284*				F9 V	8.77	+ 0.59	+ 0.06		
285	106516	12 10.0	− 9 43	F6 V	6.12	+ 0.45	−0.14	+0.028	+0.032
286	16 Vir	12 15.3	+ 3 53	K1 III	4.95	+ 1.13	+ 1.14	−0.005	+0.0145
287*	107452	12 16.0	−10 55	F0p(Sr)	8.25	+ 0.29	+ 0.10		+0.0058
288	107582	12 16.8	+62 19	G2 V	8.20	+ 0.61	+ 0.03		+0.019
289*	107760	12 17.9	+73 48	G7 V	8.00	+ 0.73	+ 0.26	+0.032	+0.022
290	107813	12 18.2	− 6 29	F2 V	9.41	+ 0.35	−0.11		+0.0058
291	108076	12 19.9	+38 52	G0 V	8.03	+ 0.56	−0.06	+0.021	+0.018
292	108177	12 20.5	+ 1 51	sd F5	9.68	+ 0.44	−0.25	+0.031	+0.0115
293	108754	12 24.6	− 2 46	G8 V	9.03	+ 0.70	+ 0.13	+0.046	+ 0.021
294	108910	12 25.7	− 3 31	K4 III	6.88	+ 1.43	+ 1.64		+ 0.0039
295*	109628	12h31m0	+11°57'	G2 V	8.43	+ 0.60	+ 0.04		+ 0".012
(1)	(2)	(3)	(4)	(5)	(6)	(7)	(8)	(9)	(10)

TABLE 1 (continued)

No.	ρ	$\mu\alpha$	$\mu\delta$	Source of μ	U	V	W	Q	e	a
236	- 24	+0.236	-0.413	GC	- 42	- 78	- 21	91	0.46	6.7
237*	- 37	+0.307	-0.152	GC	+ 12	- 27	- 11	32	0.19	9.3
238	+ 35	-0.667	-0.188	Y 21	- 56	+ 95	- 33	115	0.56	6.5
239*	+ 79	-0.225	+0.277	GC	- 35	+ 96	+ 64	121	0.48	6.9
240	+ 45	-0.486	+0.142	Y 12	- 35	+157	- 13	161	0.68	10.6
241	+ 11	-0.110	-0.071	GC	- 69	+ 71	- 17	100	0.51	6.1
242	+ 32	-0.143	+0.118	GC	+ 18	+152	+ 23	155	0.78	24.8
243	- 7	+0.081	-0.892	GC	- 94	- 6	+ 32	99	0.68	4.9
244	+ 28	-0.361	-0.294	GC	- 44	+ 41	- 12	61	0.40	6.2
245	+102	+0.003	-0.004	Lei 15	- 17	+ 58	+ 98	115	0.29	7.6
246	+ 25	-0.60	-0.58	Ci 20	- 46	+ 44	+ 6	64	0.41	6.1
247	+ 5	-0.106	+0.056	GC	+ 21	+110	- 13	113	0.60	15.3
248	- 9	+0.254	-0.676	GC	- 23	- 45	- 31	59	0.24	6.9
249	+ 45	-0.096	-0.084	GC	- 41	+ 83	+ 34	99	0.46	6.9
250	+ 3	+0.183	-0.073	GC	+ 3	- 27	+ 45	53	0.13	8.6
251	- 15	+ 0.001	-0.158	GFH+ AGK_2	-132	- 16	- 37	138	0.85	4.4
252	+ 62	-0.279	-0.477	GC	-117	+ 51	+ 22	130	0.79	4.6
253*	- 3	-0.071	-0.059	GC	- 39	+ 48	- 1	62	0.40	6.3
254	- 54	+ 0.013	-0.098	GC	- 41	- 24	- 30	56	0.36	6.2
255	- 26	-0.74	-0.31	Ci 20	-117	+137	- 81	198	0.84	5.9
256	+ 47	-0.461	+0.123	GC	- 47	+121	+ 14	131	0.60	7.8
257*	+ 45	-0.382	-0.136	GC	- 90	+122	- 3	152	0.74	6.1
258	+ 55	+ 0.218	-0.011	GC	+ 25	-119	+ 103	159	0.65	17.8
259	- 59	+ 0.054	-0.148	GC	- 20	- 60	-101	119	0.31	7.5
260	+ 10	+ 0.790	-0.149	GC	+ 19	- 61	+ 33	72	0.36	11.1
261	+ 5	-0.118	-0.022	GC	- 46	+ 95	- 21	108	0.51	6.9
262	+ 38	-0.106	-0.014	GC	- 44	+ 86	+ 15	98	0.48	6.8
263	- 80	-0.454	+0.074	Y 4	- 37	+ 96	-107	148	0.47	7.2
264	+131	+ 0.038	-0.149	Y 11	-126	- 51	+ 56	147	0.81	4.6
265	+ 18	-0.128	-0.063	GC	- 64	+ 81	+ 7	103	0.57	6.0
266	+ 24	-0.583	-0.299	GC	-103	+117	+ 21	157	0.78	5.7
267	+ 51	-0.018	-0.188	GC	- 68	- 6	+ 29	74	0.53	5.4
268*	+ 61	-0.832	-0.530	Bgd	-243	+ 222	+ 65	336	0.99	9.9r
269	- 93	+0.180	-0.101	GC	- 47	- 84	- 14	99	0.49	6.6
270	- 98	+3.994	-5.800	GC	-158	-272	- 8	315	0.99	24.0
271	- 13	-0.356	-0.518	GC	- 41	+ 21	+ 1	46	0.35	6.1
272	+ 11	+0.075	-0.601	GC	-202	-152	- 94	270	1.00	5.5
273*	+ 12	-0.114	-0.029	Y 20	- 35	+ 58	+ 3	68	0.39	6.4
274	- 20	+0.148	-0.094	GC	- 2	- 47	+ 28	55	0.22	3.4
275	+ 14	-0.518	+0.052	GC	- 32	+ 91	+ 10	97	0.45	7.5
276	- 26	-0.050	-0.079	GC	- 48	+ 18	+ 5	52	0.40	5.9
277	- 9	-0.394	+0.014	Y 10	- 58	+181	- 25	192	0.76	10.5
278	+ 69	-0.311	-0.042	GC	- 35	+155	+ 54	168	0.66	10.3
279*	+ 95	-0.184	-0.430	Y 19	-347	- 38	- 7	349	0.66	4.8r
280	+ 11	-0.604	+0.401	GC	+ 1	+128	+ 36	133	0.26	13.2
281	- 9	+ 0.211	-0.384	GC	- 18	- 32	- 13	39	0.21	7.2
282	- 30	+ 0.031	-0.605	GC	- 67	- 37	- 50	91	0.54	5.5
283*	- 10	-0.112	-0.016	GC	+ 36	- 39	- 10	54	0.38	13.1
284*										
285	+ 6	+ 0.031	-1.024	GC	- 94	- 56	- 80	136	0.65	5.0
286	+ 35	-0.292	-0.072	GC	- 72	+ 84	+ 20	112	0.61	5.8
287*	- 16	-0.019	-0.034	GC	- 10	+ 22	- 25	35	0.13	7.8
288	- 82	-0.282	-0.266	GC	-113	+ 16	- 30	118	0.76	4.7
289*	- 98	-0.457	+ 0.160	GC	- 77	+ 71	- 94	141	0.62	5.5
290	- 25	+ 0.110	-0.071	Y 16	+ 24	- 81	- 38	93	0.48	13.1
291	- 1	-0.578	+0.041	2 Grw	- 60	+153	- 3	164	0.70	8.4
292	+159	-0.012	-0.473	Y 20	-217	-116	+ 52	251	1.00	4.5r
293	- 4	-0.335	-0.583	GC	-125	+ 12	- 68	143	0.82	4.5
294	+ 84	-0.072	-0.001	GC	- 79	+ 71	+ 74	129	0.63	5.5
295*	+ 23	-0.301	-0.090	GC	- 90	- 64	+ 15	111	0.68	5.2
(11)	(12)	(13)	(14)	(15)	(16)	(17)	(18)	(19)	(20)	(21)

TABLE 1 (continued)

No.	Name	α(1900)	δ(1900)	Sp.	V	B-V	U-B	π tr	π sp
296	10 CVn	12h40m3	+39°49'	G0 V	5.95	+ 0.54	-0.01	+0".065	+0".046
297	33 Vir	12 41.3	+10 6	K1 1V	5.67	+ 0.99	+0.74	+0.021	+0.028
298	111515	12 44.6	+ 1 45	G8 V	8.17	+ 0.69	+0.14	+0.019	+0.030
299	111980	12 47.9	-17 57	F8 V	8.38	+ 0.53	-0.11	+0.008	+0.013
300	9 Dra	12 56.2	+67 8	K2 111	5.32	+ 1.29	+1.29	+0.004	+0.013
301	113101	12 56.2	- 7 54	G8 V	9.02	+ 0.74	+0.25	+0.006	+0.021
302*	113984	13 2.3	+ 1 8	F5 V	7.05	+ 0.49	-0.05		+0.018
303*	114060	13 2.9	+24 32	G5 V	8.14	+ 0.69	+0.20		+0.024
304*				G7 V	8.55	+ 0.77	+0.29		
305	114174	13 3.8	+ 5 46	G5 1V	6.80	+ 0.67	+0.17	+0.042	+0.019
306	114606	13 6.4	+10 9	G3 V	8.73	+ 0.62	+0.04	+0.052	+0.017
307	114703	13 7.0	+68 2	K2 V	8.88	+ 0.92	+0.67	+0.003	+0.032
308	114762	13 7.5	+18 3	F9 V	7.32	+ 0.54	-0.08		+0.023
309*	114960	13 8.8	+ 1 59	K5 111	6.59	+ 1.40	+1.72		+0.0044
310*	115046	13 9.5	+11 52	M0 111	5.67	+ 1.50	+1.86		+0.0063
311	115539	13 12.7	+14 18	G8 111-1V	7.21	+ 0.96	+0.62		+0.0066
312	116012	13 15.8	+ 4 39	K2 V	8.60	+ 0.94	+0.75	+0.025	+0.036
313	68 Vir	13 21.4	-12 11	M0 111	5.26	+ 1.53	+1.76		+0.0076
314	117246	13 24.1	-18 13	K4 111	6.89	+ 1.38	+1.57		+0.0040
315	117635	13 26.6	- 1 49	G9 V	7.37	+ 0.76	+0.31	+0.023	+0.048
316*	117876	13 28.1	+24 52	K0 111	6.11	+ 0.96	+0.70		+0.0083
317	117880	13 28.1	-18 00	A0 V	9.08	+ 0.04	+0.06		+0.0017
318*	118328	13 31.2	+68 17	G1 V	8.56	+ 0.61	+0.07	+0.003	+0.0115
319*	118742	13 33.7	+37 41	G5 V	7.78	+ 0.67	+0.24	+0.027	+0.0275
320	+13°2698	13 35.0	+13 06	F9 V	9.36	+ 0.58	-0.06		+0.0087
321*	84 Vir	13 38.0	+ 4 3	K2 111	5.37	+ 1.10	+1.05	+0.004	+0.012
322	120348	13 43.9	+42 33	K1 111	6.59	+ 1.09	+1.02		+0.0069
323	+34°2476	13 54.8	+34 23	sd F3	10.04	+ 0.42	-0.21	+0.020	+0.010
324	122563	13 57.6	+10 11	G0 V1	6.20	+ 0.90	+0.38		+0.069
325	123977	14 5.7	+59 49	K0 111	6.46	+ 1.02	+0.83		+0.0069
326*	124425	14 8.5	- 0 22	F6 1V	5.93	+ 0.47	+0.02	+0.020	+0.016
327	α Boo	14 11.1	+19 42	K2 111	0.06J	+ 1.23	+1.26	+0.090	+0.155
328	126681	14 21.9	-17 57	G2 V	9.33	+ 0.60	-0.07	0.000	+0.0115
329	126778	14 22.5	+29 2	K0 111	8.18	+ 0.92	+0.67		+0.0032
330	127339	14 25.7	- 8 12	K7 V	9.45	+ 1.42	+1.20	+0.047	+0.063
331*	127356	14 25.8	-15 11	G5 V	8.00	+ 0.72	+0.17	+0.035	+0.022
332	127871	14 28.7	+ 9 47	K2 V	8.82	+ 0.91	+0.68	+0.019	+0.033
333	128429	14 31.7	-11 53	F6 1V-V	6.18	+ 0.49	-0.04	+0.034	+0.021
334	128902	14 34.5	+44 4	K4 111	5.70	+ 1.48	+1.69		+0.0069
335	129245	14 36.4	+80 6	K3 111	6.26	+ 1.30	+1.46	+0.018	+0.0058
336	+14°2771	14 36.7	+14 02	G2 V	8.40	+ 0.59	+0.06		+0.0175
337	32 Boo	14 36.9	+12 5	G8 111	5.56	+ 0.94	+0.67		+0.0077
338	+6°2932	14 38.6	+ 6 15	G6 V	10.46	+ 0.70	+0.11	-0.020	+0.0091
339*	130145	14 41.4	+10 4	G2 V	7.26	+ 0.62	+0.10		+0.025
340	+17°2785	14 41.7	+16 56	K5 V	9.24	+ 1.28	+1.16	+0.067	+0.052
341*	130669	14 44.4	+10 38	K2 V	8.43	+ 0.88	+0.63		+0.0275
342	+26°2606	14 44.6	+26 8	sd F4	9.74	+ 0.42	-0.22		+0.0115
343	130871	14 45.5	+ 7 14	K2 V	9.10	+ 0.97	+0.72		+0.029
344	11 Lib	14 45.8	- 1 53	G8 111-1V	4.95	+ 0.98	+0.70	+0.015	+ 0.018
345	131111	14 46.6	+37 41	K0 111-1V	5.48	+ 1.02	+0.84	+ 0.026	+ 0.015
346*	131334	14 47.9	+19 9	G0 V	8.29	+ 0.62	+0.04	+ 0.005	+ 0.0145
347	131507	14 48.9	+59 42	K4 111	5.46	+ 1.36	+1.60		+ 0.0076
348	131582	14 49.3	+23 45	K3 V	8.64	+ 0.97	+0.70	+ 0.050	+ 0.046
349	132142	14 52.4	+54 4	K1 V	7.73	+ 0.79	+0.33	+ 0.044	+ 0.050
350*	+30°2611	15 2.7	+30 23	G8 111	9.13	+ 1.24	+1.13		+ 0.0015
351	134063	15 2.8	+22 57	G8 111	7.82	+ 0.92	+0.54		+ 0.0027
352	134088	15 2.9	- 7 31	G2 V	8.00	+ 0.59	-0.05		+ 0.021
353	134113	15 3.0	+ 9 16	F9 V	8.27	+ 0.57	-0.06	+ 0.018	+ 0.0145
354	+25°2874	15 3.1	+25 18	K7 V	10.12	+1.42	+1.01:	+ 0.075	+ 0.050
355	134439	15h 4m7	-15°54'	K0 V1	9.06	+ 0.80	+0.15	+ 0".040	+ 0".038
(1)	(2)	(3)	(4)	(5)	(6)	(7)	(8)	(9)	(10)

TABLE 1 (continued)

No.	ρ	$\mu\alpha$	$\mu\delta$	Source of μ	U	V	W	Q	e	a
296	+ 81	-0.355	+ 0.132	GC	+ 13	+ 63	+ 83	105	0.33	10.4
297	+ 52	+ 0.275	-0.452	GC	- 43	- 80	+ 33	97	0.44	6.5
298	- 4	-0.069	-0.658	GC	- 76	- 23	- 43	90	0.58	5.2
299	+144	+ 0.315	-0.798	GC	-187	-245	-106	326	0.99	11.5
300	- 30	-0.140	-0.017	GC	- 43	+ 47	- 9	64	0.43	6.2
301	- 30	-0.455	-0.111	GC	- 54	+102	- 25	118	0.56	6.8
302*	- 90	-0.101	-0.123	GC	- 3	+ 52	- 85	100	0.19	8.3
303*	- 5	-0.271	+ 0.151	GC	0	+ 78	+ 9	79	0.36	9.4
304*										
305	+ 22	+0.084	-0.638	GC	-119	- 92	- 40	156	0.82	5.1
306	+ 23	-0.517	+ 0.260	GC	- 24	+166	+ 66	180	0.71	13.2
307	- 12	-0.727	-0.052	GC	- 67	+ 96	+ 14	118	0.61	6.2
308	+ 50	-0.575	-0.018	GC	- 75	+ 85	+ 37	119	0.61	6.1
309*	+ 7	-0.050	-0.057	GC	- 72	+ 28	- 7	78	0.56	5.3
310*	+ 12	+0.072	-0.058	GC	+ 3	- 52	0	52	0.24	9.0
311	- 8	-0.096	-0.003	GC	- 34	+ 73	+ 7	81	0.41	7.0
312	- 24	-0.510	+ 0.174	GC	- 10	+ 90	+ 3	91	0.41	8.9
313	- 29	-0.135	-0.024	GC	- 42	- 58	- 11	72	0.41	6.4
314	+ 19	+ 0.040	-0.022	GC	+ 10	- 39	- 7	41	0.20	9.4
315	- 54	-0.831	+ 0.254	GC	- 8	+115	- 12	116	0.52	10.4
316*	+ 6	+ 0.048	-0.213	GC	- 72	- 79	0	107	0.61	5.8
317	- 45	-0.061	-0.135	Y 12	-309	+ 52	-260	407	0.88	4.4r
318*	+ 20	-0.188	+ 0.014	GC	- 25	+ 84	+ 19	90	0.41	7.7
319*	- 21	-0.225	-0.163	GC	- 43	+ 30	0	52	0.37	6.1
320	- 21	+ 0.127	-0.286	Y 19	- 73	-130	- 30	152	0.68	6.7
321*	- 42	-0.293	-0.077	GC	- 79	+106	- 17	133	0.67	6.0
322	- 1	+ 0.028	-0.066	GC	- 13	- 33	+ 17	39	0.18	7.5
323	-162	+ 0.105	-0.438	AJ 1001	-153	-134	-146	250	0.93	5.4
324	- 22	-0.199	-0.069	GC	- 5	+ 33	- 11	35	0.36	8.0
325	+ 11	-0.121	-0.028	GC	- 50	+ 62	+ 52	95	0.47	6.2
326*	+ 18	+ 0.204	-0.147	GC	+ 10	- 55	- 19	59	0.25	9.6
327	- 5	-1.098	-2.003	GC	- 61	+ 3	+ 3	71	0.49	5.5
328	- 47	-0.052	-0.306	Y 12	- 75	+ 26	-112	137	0.58	5.3
329	-130	+ 0.059	-0.157	Y 9	-134	-165	-153	262	0.90	6.4
330	- 27	-1.260	-0.217	Y 16	- 61	- 56	+ 16	84	0.55	5.7
331*	+ 29	+ 0.212	-0.376	GC	- 27	- 57	- 45	80	0.33	7.0
332	+ 28	+ 0.165	-0.517	GC	- 32	- 55	- 3	64	0.35	6.8
333	- 70	-0.876	+0.859	GC	- 48	+218	+ 92	241	0.88	20.0
334	- 49	-0.116	+0.028	GC	- 59	+ 85	- 6	104	0.55	6.2
335	- 23	-0.096	+ 0.083	GC	- 47	+105	- 19	117	0.54	7.1
336	- 18	-0.382	-0.087	Y 19	- 74	+ 80	+ 29	113	0.61	5.6
337	- 23	-0.159	-0.123	GC	-116	+ 44	+ 7	124	0.79	4.7
338	-138	-0.94	-0.03	Ci 20	-330	+ 387	+102	519	1.19	5.5r
339*	+ 25	+0.074	-0.268	GC	- 20	- 34	+ 5	40	0.23	7.1
340	+ 48	-0.126	-0.928	GC	- 55	- 53	+ 35	84	0.48	5.9
341*	- 92	-0.122	-0.194	GC	- 39	+ 61	- 70	101	0.40	6.6
342	+ 34	-0.031	-0.347	Y 9	- 92	- 91	+ 30	133	0.79	5.4
343	- 31	-0.605	-0.053	GC	- 66	+ 89	+ 24	113	0.59	6.1
344	+ 83	+0.081	-0.130	GC	- 11	- 67	+ 41	79	0.31	8.2
345	- 66	-0.213	+ 0.087	GC	- 48	- 58	- 22	78	0.45	6.2
346*	- 48	-0.021	+ 0.193	GC	+ 38	+ 85	- 18	95	0.60	17.7
347	+ 11	-0.124	+ 0.132	GC	- 3	- 96	+ 19	98	0.44	9.9
348	- 30	-0.837	+ 0.019	GC	- 57	+ 30	+ 22	101	0.53	6.2
349	- 15	-0.975	+ 0.468	GC	- 43	+106	+ 25	117	0.53	7.3
350*	-278	+0.010	-0.015	Lei 15	-109	+ 69	-248	280	0.77	5.0
351	-108	-0.007	-0.050	Lei 15	- 92	+ 12	- 93	131	0.67	4.9
352	- 59	-0.161	-0.456	GC	- 87	+ 41	- 70	119	0.65	5.1
353	- 60	-0.512	-0.057	GC	-132	+116	+ 33	179	0.86	5.6
354	- 64	-0.875	+ 0.490	GC	- 37	+123	+ 1	128	0.57	8.3
355	+ 292	-1.023	-3.533	GC	-454	-266	- 49	529	1.37	11.2r
(11)	(12)	(13)	(14)	(15)	(16)	(17)	(18)	(19)	(20)	(21)

TABLE 1 (continued)

No.	Name	α(1900)	δ(1900)	Sp.	V	B-V	U-B	π tr	π sp
356*	135101	15h 8m3	+19°40'	G5 V	6.68J	+0.68	+0.25	+0".025	+0".048
357*					7.53J	+0.73	+0.33		
358	135204	15 8.8	- 0 58	K0 V	6.60	+0.77	+0.33	+0.056	+0.076
359	-3°37146	15 8.8	- 3 26	K4 V	9.88	+1.15	+1.10	+0.036	+0.032
360	136064	15 13.5	+67 44	F8 V	5.10	+0.54	+0.09	+0.046	+0.057
361*	136161	15 14.0	- 1 48	A3 V	8.88	+0.32	+0.19		+0.0050
362	5 Ser	15 14.2	+ 2 9	F8 1V-V	5.06J	+0.54	+0.06	+0.037	+0.038
363	136257	15 14.6	- 8 18	F9 V	7.56	+0.55	+0.01	+0.004	+0.020
364*	136274	15 14.7	+26 4	G8 V	7.95	+0.74	+0.27	+0.005	+0.033
365	o CrB	15 16.0	+29 59	K0 III	5.51	+1.02	+0.77	+0.003	+0.011
366	136834	15 17.7	+ 1 47	K3 V	8.32	+1.00	+0.84	+0.031	+0.052
367	137704	15 22.4	+34 41	K4 III	5.46	+1.40	+1.64		+0.0076
368	137826	15 23.1	+66 54	G6 V	8.72	+0.69	+0.15	+0.019	+0.021
369	138367	15 26.6	+57 47	F6 1V-V	6.87	+0.49	+0.01	+0.024	+0.015
370	37 Lib	15 28.7	- 9 43	K1 III	4.63	+1.01	+0.86	+0.024	+0.017
371	41 Lib	15 33.1	-18 58	G8 III	5.38	+0.86	+0.54		+0.0084
372	139457	15 33.2	+10 35	F6 V	7.10	+0.50	-0.06	+0.015	+0.020
373*	140283	15 37.8	-10 37	sd F5	7.20	+0.48	-0.10	+0.013	+0.036
374	θ Lib	15 48.1	-16 26	K0 III-1V	4.16	+1.01	+0.81	+0.030	+0.028
375*	39 Ser	15 48.5	+13 31	G2 V	6.10	+0.60	0.00	+0.035	+0.050
376	X Her	15 49.2	+42 44	F9 V	4.60J	+0.56	+0.01	+0.056	+0.079
377	142574	15 50.2	+20 36	K4 III	5.44	+1.59	+1.94	+0.034	+0.0079
378	142575	15 50.2	+ 5 23	F0 V	8.62	+0.38	-0.08	+0.006	+0.0076
379	γ Ser	15 51.8	+15 59	F6 1V-V	3.85J	+0.48	-0.02	+0.069	+0.063
380	φ Ser	15 52.6	+14 42	K1 1V	5.54	+1.14	+1.16		+0.030
381	143291	15 54.4	+28 1	K0 V	8.00	+0.77	+0.30	+0.043	+0.040
382	49 Lib	15 54.7	-16 14	F8 V	5.48	+0.52	+0.02	+0.028	+0.048
383	143393	15 55.0	+29 44	K2 III	7.10	+1.13	+1.07		+0.0058
384	5 Her	15 56.8	+18 6	K0 III	5.12	+0.98	+0.74	-0.008	+0.013
385	ρ CrB	15 57.2	+33 36	G2 V	5.42	+0.60	+0.07	+0.042	+0.068
386	144287	15 59.9	+25 31	G8 V	7.11	+0.77	+0.32	+0.041	+0.050
387*	144515	16 1.2	+10 57	G8 V	8.28	+0.78	+0.29	+0.024	+0.029
388	144872	16 2.9	+38 55	K3 V	8.60	+0.96	+0.71	+0.056	+0.046
389	144889	16 3.0	+22 6	K4 III	6.14	+1.37	+1.51		+0.0057
390	145148	16 4.3	+ 6 41	K0 1V	5.98	+1.02	+0.76	+0.026	+0.032
391*	r CrB	16 5.3	+36 45	K0 III-1VM	4.74	+1.00	+0.85	+0.027	+0.022
392	146470	16 11.4	+32 25	K4 III	8.43	+1.35	+1.51		+0.0020
393	148530	16 23.6	+ 3 29	G9 V	8.82	+0.76	+0.36	+0.030	+0.025
394	148816	16 25.6	+ 4 26	F9 V	7.28	+0.54	-0.07	+0.028	+0.023
395	149105	16 27.4	+48 11	G0 V	7.00	+0.57	+0.07	-0.001	+0.029
396	29 Her	16 27.9	+11 42	K4 III	4.85	+1.50	+1.82	-0.011	+0.010
397	149890	16 32.6	+31 9	F8 V	7.12	+0.54	-0.02	+0.021	+0.023
398	150275	16 34.9	+77 39	K1 III	6.34	+1.00	+0.71	+0.016	+0.0079
399*	151199	16 40.9	+55 53	A5 p	6.16	+0.07	+0.11		+0.010
400*	151937	16 45.3	+30 8	K1 II-III	6.58	+1.25	+1.17		+0.0033
401	152391	16 48.0	+ 0 12	G6 V	6.64	+0.77	+0.31	+0.065	+0.055
402	152792	16 50.4	+43 0	G0 V	6.81	+0.65	+0.08	+0.029	+0.0315
403*	54 Her	16 51.0	+18 35	K4 III	5.35	+1.41	+1.66	+0.016	+0.0081
404	153344	16 53.8	+62 16	G5 1V	7.06	+0.67	+0.21		+0.017
405*	153472	16 54.7	+42 39	K3 III	6.34	+1.28	+1.41		+0.0057
406	154276	16 59.3	+17 20	G2 V	9.13	+0.67	+0.10	-0.005	+0.0125
407	154278	16 59.4	+13 42	K1 III	6.09	+1.02	+0.85		+0.0087
408	154363	16 59.9	- 4 53	K5 VM	7.74J	+1.16	+1.05	+0.083	+0.105
409					10.07J	+1.44	+1.09		
410*	154712	17 2.0	+59 43	K4 V	8.43	+1.10	+0.92	+0.040	+0.060
411	154733	17 2.1	+22 13	K4 III	5.55	+1.30	+1.52	+0.013	+0.0074
412	154759	17 2.4	+47 6	K3 III	8.15	+1.20	+1.19	+0.005	+0.0024
413	156681	17 13.9	+10 58	K4 II-III	5.03	+1.55	+1.90	-0.002	+0.0062
414	156802	17 14.5	- 7 55	G2 V	7.97	+0.68	+0.07	+0.010	+0.021
415	156968	17h15m4	+ 9°34'	G0 V	7.97	+0.60	+0.06	+0".009	+0".018
(1)	(2)	(3)	(4)	(5)	(6)	(7)	(8)	(9)	(10)

Table 1 (continued)

No.	ρ	μa	$\mu\delta$	Source of μ	U	V	W	Q	e	a
356*	- 37	-0.591	+ 0.284	GC	- 22	+ 85	+14	89	0.40	7.9
357*										
358	- 70	-1.284	-0.494	GC	- 69	+ 94	- 14	117	0.61	6.1
359	-108	-0.744	+ 0.177	Y 17	- 44	+165	+ 6	171	0.71	10.5
360	- 47	+0.218	-0.394	GC	- 22	- 27	- 21	41	0.18	6.9
361*	+ 6	+0.091	-0.101	Y 21	- 4	- 80	- 91	121	0.36	9.0
362	+ 54	+0.369	-0.521	GC	- 7	- 76	- 9	77	0.32	8.6
363	+ 29	+0.092	-0.199	GC	- 22	- 51	- 21	59	0.14	7.2
364*	- 29	-0.571	-0.129	GC	- 70	+ 57	+26	94	0.57	5.6
365	- 53	-0.124	-0.053	GC	- 64	+ 46	- 9	79	0.53	5.6
366	- 30	-0.358	-0.382	GC	- 43	+ 37	- 11	58	0.38	6.2
367	- 48	-0.108	+ 0.048	GC	- 43	+ 90	+ 7	100	0.49	6.9
368	- 34	-0.280	-0.014	GC	- 60	+ 40	+21	75	0.50	5.7
369	- 32	-0.266	+ 0.152	GC	- 55	+ 97	+17	113	0.56	6.6
370	+ 48	+0.301	-0.242	GC	+ 10	- 84	- 54	100	0.42	10.9
371	+ 47	+0.083	-0.094	GC	- 4	- 55	- 32	64	0.25	8.4
372	- 38	+0.142	-0.370	GC	- 25	- 77	- 17	83	0.36	7.4
373*	-171	-1.145	-0.320	GC	-117	-178	- 15	214	0.88	7.4
374	+ 3	+0.098	+ 0.126	GC	+ 34	+ 13	+12	38	0.38	13.1
375*	+ 36	-0.153	-0.564	GC	- 29	- 36	+25	53	0.29	6.7
376	- 55	+0.437	+ 0.629	GC	+ 9	+ 55	- 54	78	0.24	9.5
377	- 61	-0.082	+ 0.039	GC	- 33	+ 87	0	93	0.44	7.3
378	- 65	-0.289	+ 0.034	GC	-108	+146	+ 91	203	0.82	6.3
379	+ 7	+0.307	-1.292	GC	- 42	- 61	- 31	80	0.40	6.3
380	- 68	-0.123	+ 0.080	GC	- 19	+ 76	- 23	82	0.36	7.9
381	- 70	-0.761	+ 0.306	GC	- 63	+112	+ 21	130	0.62	6.7
382	- 25	-0.630	-0.400	GC	- 61	+ 53	+ 13	82	0.50	5.6
383	+ 18	+0.020	-0.051	GC	+ 2	- 31	+ 4	31	0.14	8.5
384	- 19	-0.053	+ 0.145	GC	+ 23	+ 72	+ 21	78	0.43	12.3
385	+ 18	-0.200	-0.774	GC	- 16	- 39	+ 25	49	0.22	7.4
386	- 41	-0.529	+ 0.667	GC	- 5	+105	+ 23	108	0.48	10.1
387*	- 61	-0.488	-0.053	GC	- 69	+ 82	+ 19	109	0.60	5.9
388	+ 24	+0.238	-0.546	GC	+ 11	- 48	+ 7	50	0.26	9.7
389	+ 57	-0.015	-0.048	GC	- 2	- 42	+ 45	62	0.19	8.4
390	- 4	+0.235	-0.744	GC	- 51	- 54	- 63	97	0.46	6.1
391*	- 18	-0.060	+ 0.322	GC	+ 23	+ 87	+ 6	90	0.49	13.1
392	-165	+0.013	-0.009	GPH	- 74	- 29	-134	156	0.57	5.3
393	+ 22	+0.013	-0.544	GC	- 62	- 55	- 28	87	0.52	5.7
394	- 52	-0.443	-1.398	GC	-273	- 72	- 77	293	0.93	4.4r
395	- 46	-0.095	-0.293	GC	- 51	- 14	- 10	54	0.35	6.1
396	+ 3	-0.179	-0.084	GC	- 72	+ 11	+ 57	92	0.56	5.3
397	- 8	-0.018	-0.481	GC	- 50	- 62	- 11	80	0.47	6.2
398	- 32	-0.101	+ 0.271	GC	- 70	+173	- 21	188	0.70	7.3
399*	- 46	+0.048	+ 0.079	GC	- 8	+ 53	- 43	69	0.20	7.9
400*	- 43	-0.071	+ 0.072	GC	- 29	+144	+ 79	167	0.54	8.3
401	+ 41	-0.723	-1.508	GC	-116	- 69	+ 12	136	0.80	4.9
402	+ 7	+0.114	-0.331	GC	+ 5	- 34	- 6	35	0.17	8.8
403*	+ 12	-0.112	+ 0.008	GC	- 23	+ 24	+ 66	74	0.22	6.9
404	- 82	-0.330	-0.055	GC	-112	+ 14	+ 31	117	0.77	4.6
405*	+ 28	-0.012	-0.059	GC	+ 4	- 37	+ 28	47	0.18	8.8
406	- 51	-0.218	-0.191	Y 18	-113	+ 10	+ 21	115	0.77	4.6
407	+ 46	+0.017	-0.135	GC	- 13	- 67	- 5	68	0.31	8.0
408	+ 28	-0.929	-1.130	GC	- 50	- 23	+ 34	65	0.42	5.9
409										
410*	- 74	-0.355	+ 0.239	GC	- 59	+ 46	- 16	77	0.50	5.7
411	- 96	-0.101	-0.047	GC	-104	+ 63	0	122	0.75	5.0
412	- 52	-0.006	+ 0.008	2 Grw	- 37	+ 46	- 14	61	0.36	6.5
413	+ 40	+0.001	-0.096	GC	- 22	- 60	- 7	64	0.32	7.3
414	- 89	-0.010	-0.222	GC	- 56	+ 82	- 40	107	0.53	6.3
415	- 12	-0.029	-0.314	GC	- 59	- 24	- 25	68	0.48	5.6
(11)	(12)	(13)	(14)	(15)	(16)	(17)	(18)	(19)	(20)	(21)

TABLE 1 (continued)

No.	Name	α(1900)	δ(1900)	Sp.	V	B-V	U-V	π tr	π sp
416	157089	17h16m1	+ 1°32'	G0 V	6.95	+ 0.60	-0.02	+ 0".036	+0".029
417	72 Her	17 16.9	+32 36	G2 V	5.39[J]	+ 0.62	+0.07	+ 0.069	+0.069
418	+ 31°3025	17 22.9	+31 9	G8 V	9.59	+ 0.84	+ 0.18	+ 0.036	+0.016
419	158226	17 23.0	+31 10	G1 V	8.50	+ 0.59	+ 0.01	+ 0.020	+0.015
420	158855	17 26.5	+ 1 45	K3 III	7.19	+1.35	+ 1.39		+0.0038
421	159329	17 29.1	+63 56	F9 V	7.63	+ 0.59	+ 0.02	+ 0.011	+0.020
422*	159482	17 29.9	+ 6 4	G0 V	8.38	+ 0.57	-0.04	+ 0.026	+0.015
423*	27 Dra	17 32.4	+68 12	K0 III	5.05	+ 1.08	+ 0.92	+ 0.018	+0.0135
424	+ 18°3423	17 33.9	+18 37	F6 V	9.79	+ 0.48	-0.10	+ 0.006	+0.0058
425	+ 2°3375	17 34.8	+ 2 28	sd F5	9.95	+ 0.44	-0.20		+0.010
426*	160538	17 35.4	+74 17	K2 III	6.55	+1.05	+ 0.81		+0.0072
427	160693	17 36.2	+37 16	G0 V	8.37	+ 0.61	-0.01	+ 0.032	+0.015
428	83 Her	17 38.4	+24 37	K4 III	5.51	+1.46	+ 1.68	+ 0.022	+0.0076
429	161198	17 39.0	+21 40	K0 V	7.51	+ 0.77	+ 0.31	+ 0.047	+0.050
430*	161817	17 42.6	+25 48	sd A2	6.98	+ 0.16	+ 0.10		+0.0125
431	161848	17 42.8	+ 4 59	K1 V	8.92	+ 0.85	+ 0.46	+ 0.040	+0.029
432*	162756	17 47.6	- 7 53	G0 V	7.64	+ 0.62	+ 0.07	+ 0.013	+0.021
433*	163810	17 53.0	-13 4	sd F8	9.62	+ 0.62	-0.06	+ 0.020	+0.011
434	164922	17 58.4	+26 25	K0 V	6.99	+ 0.80	+ 0.47	+ 0.048	+0.063
435	165401	18 0.7	+ 4 39	G2 V	6.79	+ 0.63	+ 0.04	+ 0.043	+0.036
436	165687	18 2.0	-17 10	K1 III	5.52	+1.11	+ 1.08		+0.0115
437	166229	18 4.6	+36 23	K2 III	5.47	+1.17	+ 1.21	+ 0.010	+0.012
438	167042	18 8.4	+54 15	K1 III	5.94	+ 0.94	+ 0.72	+ 0.020	+0.0095
439	167163	18 8.9	+ 0 11	A0 V	9.36	+ 0.37	+ 0.13	+ 0.001	+0.0024
440	167193	18 9.0	+21 51	K4 III	6.12	+1.47	+ 1.72		+0.0058
441	167768	18 11.6	- 3 2	G8 III	6.00	+ 0.89	+ 0.55	+ 0.005	+0.0063
442	168322	18 13.9	+40 54	K0 III	6.10	+1.00	+ 0.70	+ 0.010	+0.0083
443	η Ser	18 16.1	- 2 55	K0 III-1V[M]	3.26[J]	+ 0.94	+ 0.65	+ 0.054	+0.042
444	109 Her	18 19.4	+21 43	K2 III	3.82	+1.18	+ 1.16	+ 0.016	+0.026
445	169822	18 21.4	+ 8 44	G7 V	7.85	+ 0.68	+ 0.17	+ 0.032	+0.033
446	169957	18 22.0	+ 8 2	G2 IV	8.82	+ 0.66	+ 0.24		+0.0066
447	170357	18 23.9	+46 1	G1 V	8.31	+ 0.62	+ 0.06	+ 0.016	+0.017
448*	170737	18 25.9	+26 36	G8 III-IV	8.08	+ 0.82	+ 0.35		+0.0044
449	α Sct	18 29.8	- 8 19	K3 III	3.81	+1.34	+ 1.56	+ 0.013	+0.018
450	172310	18 34.4	+28 51	G5 V	8.42	+ 0.70	+ 0.21	+ 0.042	+0.022
451*	172323	18 34.5	+63 37	F9 V	8.07	+ 0.56	+ 0.06	+ 0.017	+0.016
452*	+ 31°3330	18 37.1	+31 28	K3 V	8.50	+ 0.94	+ 0.65	+ 0.031	+0.046
453*	175305	18 49.7	+74 37	G5 III	7.17	+ 0.78	+ 0.16	-0.008	+0.0040
454	175518	18 50.6	- 5 52	K0 IV-V	7.47	+ 0.75	+ 0.40	+ 0.031	+0.028
455	η Sct	18 51.7	- 5 58	K2 III	4.80	+1.80	+ 1.02	+ 0.037	+0.017
456	177758	19 0.9	-12 2	G0 V	7.24	+ 0.57	-0.02	+ 0.006	+0.026
457	177808	19 1.2	+31 36	M0 III	5.54	+1.54	+ 1.90	+ 0.014	+0.0069
458	178126	19 2.3	+ 7 29	K5 V	9.24	+1.07	+ 0.93	+ 0.026	+0.052
459*	179484	19 7.7	+38 37	G5 V	7.57	+ 0.76	+ 0.34	+ 0.007	+0.026
460*	179558	19 8.0	+16 41	G5 V	7.94	+ 0.76	+ 0.34	+ 0.019	+0.024
461	179626	19 8.2	- 0 45	F8 V	9.12	+ 0.53	-0.06	+ 0.011	+0.0091
462*	179958	19 9.5	+49 39	G4 V	6.57[J]	+ 0.65	+ 0.21	+ 0.041	+0.044
463*	179957			G4 V	6.75[U]	+ 0.64	+ 0.17		
464	+ 41°3306	19 15.7	+ 41 28	K0 V	8.84	+ 0.85	+ 0.34	+ 0.027	+0.0275
465	182293	19 18.9	+ 20 05	K3 III	7.14	+1.15	+ 1.20		+0.0039
466	31 Aql	19 20.2	+ 11 44	G8 IV	5.15	+ 0.79	+ 0.40	+ 0.059	+0.047
467	182807	19 21.3	+ 24 44	F6 V	6.19	+ 0.52	-0.03	+ 0.027	+0.030
468	α Vul	19 24.5	+ 24 28	M0 III	4.45	+1.51	+ 1.76	+ 0.012	+0.011
469*	+ 17°3992	19 27.2	+ 17 34	G2 V	8.26	+ 0.64	+ 0.06		+0.018
470	+ 35°3659	19 27.6	+ 35 58	sd F7	10.20	+ 0.48	-0.12	+ 0.005	+0.0091
471	+ 26°3578	19 28.4	+26 9	sd F4	9.36	+ 0.37	-0.23		+0.013
472*	184360	19 28.9	+ 20 12	A5p	7.28	+ 0.26	+ 0.12	-0.001	+0.0063
473*				F5 V					
474	μ Aql	19 29.2	+ 7 10	K3 III	4.44	+1.17	+ 1.27	+ 0.038	+0.0135
475	184467	19h29m4	+58°23'	K1 V	6.58	+ 0.88	+ 0.52	+ 0".038	+0".083
(1)	(2)	(3)	(4)	(5)	(6)	(7)	(8)	(9)	(10)

TABLE 1 (continued)

No.	ρ	μ_α	μ_δ	Source of μ	U	V	W	Q	e	a
416	-162	-0.157	+ 0.267	GC	- 36	+180	- 5	184	0.76	13.4
417	- 78	+ 0.126	-1.047	GC	- 75	- 8	- 56	94	0.57	5.2
418	- 73	-0.412	+ 0.085	Ci 18	-101	- 47	+ 79	137	0.73	4.9
419	- 70	-0.324	+ 0.138	GFH	- 79	+ 95	+ 69	142	0.66	5.8
420	- 16	-0.019	-0.037	Y 20	- 46	+ 8	+ 1	47	0.38	6.5
421	- 29	-0.009	-0.206	GC	- 24	- 50	- 12	57	0.15	7.1
422*	-144	-0.459	+ 0.389	GC	- 53	+208	+ 138	255	0.85	19.0
423*	- 73	-0.015	+ 0.131	GC	- 61	+ 54	- 31	87	0.52	5.8
424	-240	-0.161	-0.195	GC	-303	+ 66	- 35	312	0.85	4.7r
425	-389	-0.368	+ 0.069	Y 20	-229	+367	+ 69	438	1.15	9.2r
426*	- 9	-0.073	+ 0.035	GC	- 30	+ 37	+ 40	62	0.30	6.7
427	+ 40	-0.516	-0.843	GC	-141	-244	+ 104	300	0.96	13.6
428	- 27	-0.060	-0.108	GC	- 67	- 21	+ 6	70	0.52	5.4
429	+ 20	-0.140	-0.645	GC	- 20	+ 77	+ 5	80	0.37	7.8
430*	-363	-0.064	-0.016	GC	-270	+206	-165	378	0.98	9.1r
431	- 93	-0.575	-0.212	Y 20	-110	+ 75	+ 48	142	0.78	5.0
432*	-124	-0.052	-0.258	GC	- 86	+112	- 28	144	0.71	6.0
433*	+191	-0.473	-0.673	Y 11	-290	-276	+ 44	403	0.98	17.2r
434	+ 23	+0.385	-0.596	GC	+ 17	- 30	- 26	43	0.22	10.0
435	-124	+ 0.018	-0.309	GC	- 87	+ 93	- 32	135	0.70	5.7
436	- 32	-0.100	+ 0.056	GC	0	- 14	+ 51	53	0.07	8.2
437	- 7	-0.100	-0.187	GC	- 41	- 51	+ 17	68	0.39	6.4
438	- 16	+ 0.113	+ 0.248	GC	+ 24	+148	- 27	152	0.80	27.7
439	- 2	-0.028	-0.029	Y 21	- 62	- 15	+ 29	70	0.49	5.5
440	- 66	+ 0.058	+ 0.046	GC	+ 1	- 60	- 39	72	0.28	9.0
441	+ 2	+ 0.007	-0.270	GC	-146	- 71	- 94	188	0.90	4.6
442	- 73	-0.168	+ 0.066	GC	- 89	+ 62	+ 74	131	0.68	5.2
443	+ 9	-0.556	-0.700	GC	- 78	- 35	+ 31	91	0.60	5.2
444	- 58	+ 0.194	-0.250	GC	- 43	+ 25	- 57	76	0.37	6.1
445	- 22	-0.189	-0.486	Y 22	- 65	- 11	- 4	66	0.51	5.4
446	+ 42	-0.056	-0.102	Y 22	- 34	- 65	+ 15	75	0.39	6.8
447	- 86	-0.350	+ 0.205	GC	-103	+ 75	+ 76	148	0.75	5.1
448*	-137	+ 0.111	-0.084	Y 9	- 67	+ 85	-148	183	0.60	6.0
449	+ 36	-0.018	-0.314	GC	- 47	- 46	- 29	72	0.45	6.1
450	+ 28	-0.025	-0.467	Y 24	- 13	- 31	- 22	85	0.37	8.4
451*	- 11	-0.037	-0.251	GC	- 4	- 75	- 10	76	0.24	8.9
452*	+ 33	+0.076	-0.792	GFH	- 9	- 76	- 24	80	0.35	8.6
453*	-131	+ 0.320	+ 0.080	GC	- 32	+180	-392	433	0.76	14.1
454	- 77	-0.204	-0.390	GC	- 95	+ 48	+ 14	107	0.70	5.0
455	- 93	+ 0.061	-0.037	GC	- 39	+ 99	- 4	106	0.50	7.3
456	- 2	-0.214	-0.394	GC	- 68	- 16	+ 10	71	0.53	5.4
457	+ 6	+ 0.070	-0.071	GC	+ 13	- 10	- 57	59	0.13	9.4
458	+ 12	-0.354	-0.766	GC	- 43	- 43	+ 2	61	0.39	6.2
459*	+ 28	-0.245	-0.097	GC	+ 15	- 23	+ 44	52	0.18	9.7
460*	+ 37	+ 0.122	-0.210	GC	+ 21	- 17	- 33	43	0.25	10.5
461	- 71	-0.33	-0.43	Ci 20	-264	-110	+ 53	291	0.99	4.4r
462*	- 39	-0.200	+ 0.633	GC	- 34	+ 73	+ 41	94	0.42	7.1
463*										
464	-124	+ 0.06	-0.64	Ci 20	-125	- 44	- 78	154	0.83	4.6
465	-110	+ 0.016	+ 0.092	GC	- 28	+154	+ 75	174	0.67	10.6
466	-100	+ 0.719	+ 0.636	GC	- 15	+148	- 19	149	0.65	12.3
467	- 4	-0.184	-0.631	GC	- 48	- 67	- 17	84	0.43	6.3
468	- 86	-0.128	-0.107	GC	-102	+ 4	+ 29	106	0.72	4.3
469*	- 58	-0.020	-0.126	GC	- 58	+ 26	- 7	64	0.47	5.7
470	-172	-0.019	-0.549	AJ 1001	-256	-179	-152	333	1.00	5.6r
471	-128	-0.004	-0.174	Y 9	-130	+ 29	- 29	136	0.84	4.4
472*	- 52	+ 0.033	+ 0.046	GC	- 21	+ 64	- 47	82	0.35	8.2
473*										
474	- 24	+ 0.211	-0.157	GC	- 26	+ 34	- 81	92	0.28	6.7
475	+ 11	-0.523	-0.395	GC	+13	- 16	27	34	0.15	9.4
	(11)	(12)	(13)	(14)	(15)	(16)	(17)	(18)	(19)	(20)	(21)

TABLE 1 (continued)

No.	Name	α(1900)	δ(1900)	Sp.	V	B-V	U-B	π tr	π sp
476	184499	19h29m7	+32 59	G0 V	6.60	+0.59	+ 0.01	+ 0.034	+ 0.035
477	184700	19 30.6	- 0 26	G2 V	8.83	+0.67	+ 0.09	+ 0.014	+ 0.0145
478*	184860	19 31.0	-10 39	K2 V	8.40	+1.01	+ 0.82	+ 0.047	+ 0.036
479	σ Dra	19 32.6	+69 29	K0 V	4.68J	+0.79	+ 0.39	+ 0.179	+ 0.180
480	187923	19 47.4	+11 23	G2 V	5.78	+0.53	+ 0.21	+ 0.024	+ 0.058
481	188326	19 49.5	+38 30	G8 1V	7.56	+0.78	+ 0.35	+ 0.017	+ 0.015
482	189340	19 54.4	-10 13	G0 V	5.87	+0.58	+ 0.05	+ 0.037	+ 0.048
483	189558	19 55.5	-12 31	F9 V	7.72	+0.52	-0.02	-0.013	+ 0.019
484	190360	19 59.5	+29 38	G6 1V	5.70	+0.72	+ 0.38	+ 0.046	+ 0.033
485	190404	19 59.7	+23 5	K1 V	7.29	+0.82	+ 0.40	+ 0.050	+ 0.060
486	27 Cyg	20 2.6	+35 42	K0 1V	5.33	+0.85	+ 0.54	+ 0.030	+ 0.044
487	191046	20 2.8	+35 57	K0 111	7.04	+1.15	+ 1.03	+ 0.020	+ 0.0055
488	191069	20 2.9	-16 00	G5 V	8.11	+0.67	+ 0.22	+ 0.012	+ 0.025
489	191615	20 5.7	+25 15	G8 1V	7.80	+0.94	+ 0.83		+ 0.014
490	191785	20 6.5	+15 54	K1 V	7.33	+0.85	+ 0.50	+ 0.036	+ 0.060
491	192031	20 7.7	-15 43	G8 V	8.66	+0.72	+ 0.16	+ 0.026	+ 0.024
492	39 Cyg	20 19.9	+31 52	K3 111	4.40	+1.31	+ 1.47	+ 0.010	+ 0.014
493	194598	20 21.4	+ 9 9	F6 V	8.36	+0.49	-0.14	+ 0.003	+ 0.011
494	194960	20 23.3	-18 12	K1 111	6.54	+1.07	+ 0.87	+ 0.011	+ 0.0071
495	195506	20 26.7	+45 35	K2 111	6.40	+1.12	+ 1.07	+ 0.007	+ 0.0079
496*	195987	20 29.4	+41 32	G9 V	7.10	+0.81	+0.86	+ 0.036	+ 0.055
497	196348	20 31.7	-15 30	K3 111	6.76	1.25	+ 1.29		+ 0.0046
498	κ Del	20 34.3	+ 9 44	G5 1V	5.02	+0.74	+ 0.19	+ 0.022	+ 0.043
499	196795	20 34.6	+ 4 37	K5 V	7.89	+1.22	+ 1.17	+ 0.054	+ 0.096
500*	196882	20 35.1	+21 22	K3 111	8.49	+0.94	+ 0.60	+ 0.013	+ 0.0019
501	196892	20 35.1	-19 8	F6 V	8.21	+0.51	-0.13	+ 0.018	+ 0.012
502*	30 Vul	20 40.6	+24 55	K2 111	4.92	+1.17	+ 1.18	+ 0.004	+ 0.016
503	η Cep	20 43.3	+61 27	K0 1VM	3.43J	+0.92	+ 0.62	+ 0.071	+ 0.105
504	198273	20 44.1	- 9 01	G2 V	8.42	+0.60	0.00	+ 0.018	+ 0.0175
505	199191	20 50.4	+54 8	K0 111	7.12	+0.96	+ 0.61	+ 0.006	+ 0.0052
506	199476	20 52.4	+74 23	G8 V	7.76	+0.72	+ 0.16	+ 0.043	+ 0.036
507	199580	20 53.1	+42 30	K1 1V	7.18	+0.97	+ 0.73	+ 0.006	+ 0.014
508	200580	20 59.2	+ 2 36	F9 V	7.32	+0.54	-0.03	+ 0.004	+ 0.023
509	200779	21 0.4	+ 6 41	K7 V	8.34	+1.21	+ 1.12	+ 0.045	+ 0.110
510*	61 Cyg	21 2.4	+38 15	K5 VM	5.19J	+1.19	+ 1.10	+ 0.292	+ 0.330
511*				K7 VM	6.02J	+1.38	+ 1.23		
512*	201889	21 7.4	+23 45	G1 V	8.04	+0.58	+ 0.01		+ 0.017
513	201891	21 7.4	+17 20	F9 V1	7.38	+0.51	-0.09	+ 0.041	+ 0.032
514	202123	21 8.8	+73 18	K1 V	8.70	+0.81	+ 0.51	+ 0.027	+ 0.032
515	203344	21 16.6	+23 26	K0 111-1V	5.57	+1.05	+ 0.91	-0.005	+ 0.0145
516	1 Peg	21 17.6	+19 23	K1 111	4.09J	+1.10	+ 1.05	+ 0.013	+ 0.022
517					9.14J	+ 0.86	+ 0.52		
518	203842	21 19.6	+ 9 44	F5 111	6.34	+ 0.47	+ 0.13		+ 0.0055
519*	204129	21 21.5	+79 55	F6 V	7.32	+ 0.50	-0.04	+ 0.007	+ 0.018
520	204587	21 24.5	-12 56	M0 V	9.15	+1.24	+ 1.26	+ 0.056	+ 0.100
521	204814	21 26.0	+45 27	G8 V	7.89	+ 0.76	+ 0.31	+ 0.020	+ 0.035
522	205027	21 27.3	+ 0 34	G2 V	8.29	+ 0.61	+ 0.06	+ 0.005	+ 0.018
523	72 Cyg	21 30.7	+38 05	K1 111	4.91	+1.04	+ 1.02	+ 0.009	+ 0.015
524	205855	21 33.0	- 2 45	K0 V	8.63	+0.84	+ 0.55	+ 0.031	+ 0.030
525	206078	21 34.5	+ 61 51	G3 111	7.11	+ 0.97	+ 0.68		+ 0.0038
526	+24°4460	21 39.7	+ 24 53	K0 V	9.41	+ 0.85	+ 0.29	+ 0.033	+ 0.021
527	207134	21 41.8	+ 25 6	K3 111	6.28	+1.21	+ 1.25	+ 0.002	+ 0.0058
528	+4°4762	21 49.1	+ 4 30	G3 V	9.30	+ 0.64	+ 0.03		+ 0.0125
529	208776	21 53.4	+ 3 18	G0 V	6.94	+ 0.60	+ 0.08	+ 0.022	+ 0.030
530	ν Peg	22 0.6	+ 4 34	K4 111	4.85	+1.42	+ 1.81	+ 0.009	+ 0.010
531	210144	22 3.1	+ 52 39	G8 V	7.78	+ 0.80	+ 0.41	+ 0.033	+ 0.036
532	25 Peg	22 3.1	+ 21 13	B7 V	5.78	-0.10	-0.41		+ 0.0050
533*	+22°4567	22 5.9	+ 22 19	K3 V	9.23	+ 0.90	+ 0.68	+ 0.015	+ 0.035
534*	+17°4708	22 6.7	+ 17 36	sd F6	9.47	+ 0.43	-0.21	+ 0.015	+ 0.0125
535*	211076	22h9m6	+ 16 42	K4 111	6.42	+1.21	+1.15		+ 0.0048
(1)	(2)	(3)	(4)	(5)	(6)	(7)	(8)	(9)	(10)

TABLE 1 (continued)

No.	ρ	$\mu\alpha$	$\mu\delta$	Source of μ	U	V	W	Q	e	a
476	-163	-0.464	+0.207	GC	-151	+ 75	+59	179	0.92	4.6
477	- 22	-0.077	-0.336	GC	- 96	- 38	- 19	105	0.70	4.9
478*	+ 68	-0.280	-0.270	GC	- 2	- 68	+ 5	68	0.31	8.9
479	+ 27	+0.575	-1.745	GC	+ 47	- 9	- 15	50	0.48	15.9
480	- 17	-0.341	-0.320	GC	- 28	- 1	+ 20	34	0.23	6.6
481	- 71	-0.039	+ 0.340	GC	- 44	+119	+ 68	144	0.57	7.7
482	+ 23	-0.278	-0.398	GC	- 20	- 42	+ 6	47	0.25	7.2
483	- 15	-0.305	-0.364	GC	-100	- 55	+ 34	119	0.67	4.9
484	- 46	+0.676	-0.530	GC	- 43	+ 28	-115	126	0.37	6.1
485	- 3	-1.017	-0.918	GC	- 42	- 75	+ 34	92	0.45	6.7
486	- 34	-0.232	-0.438	GC	- 40	- 24	0	47	0.35	6.2
487	-100	-0.087	-0.065	2 Grw	-115	- 37	+ 36	126	0.79	4.7
488	- 2	+0.168	-0.412	Y 12	- 58	+ 15	- 47	76	0.47	5.6
489	- 94	+0.027	+0.026	Y 9	- 69	+ 75	+ 12	103	0.60	5.8
490	- 51	-0.418	+0.400	GC	- 25	+ 47	+ 60	80	0.29	7.0
491	+ 20	-0.350	-0.272	Y 12	- 44	- 51	+ 35	76	0.39	6.1
492	- 15	+0.037	-0.002	GC	+23	+ 32	- 3	40	0.28	10.9
493	-246	+0.113	-0.549	Y 22	-331	+ 34	- 89	344	0.67	4.9r
494	+ 4	+0.039	-0.117	GC	- 59	+ 11	- 42	73	0.49	5.5
495	- 31	+0.067	+0.152	GC	- 15	+116	+ 29	121	0.56	10.4
496*	- 10	-0.165	+0.447	GC	0	+ 40	+42	58	0.19	8.5
497	+ 18	+0.061	-0.038	GC	- 13	+ 32	- 66	74	0.19	7.4
498	- 52	+0.313	+0.015	GC	- 29	+ 68	- 2	74	0.37	7.1
499	- 43	+0.858	+0.085	GC	- 17	+ 70	- 7	72	0.33	7.8
500*	-111	+0.020	+0.012	GC	- 68	+102	+ 12	123	0.62	6.3
501	- 30	+0.057	-0.440	GC	-163	+ 11	- 46	170	0.94	4.2
502*	+ 31	-0.035	-0.178	GC	+ 13	- 36	- 23	45	0.24	9.7
503	- 87	+0.090	+0.320	GC	- 90	+ 41	+ 44	108	0.67	5.1
504	+ 28	-0.341	-0.150	Y 16	- 18	- 77	+ 46	91	0.34	7.8
505	-196	+0.021	+0.178	GC	-204	+140	+ 81	260	1.00	5.2
506	- 30	+0.406	+0.562	GC	- 51	+ 94	+ 1	107	0.53	6.2
507	- 19	+0.225	+0.220	GC	- 2	+125	+ 12	126	0.57	12.0
508	- 6	-0.294	-0.372	GC	- 53	- 60	+ 16	85	0.46	5.9
509	- 66	+0.078	-0.563	GC	- 58	+ 39	+ 22	73	0.48	5.7
510*	- 64	+4.120	+3.179	GC	- 48	- 64	+ 3	80	0.44	6.1
511*										
512*	-102	+0.423	+0.126	GC	- 72	+153	- 24	171	0.73	7.8
513	- 45	-0.116	-0.896	GC	-106	- 77	- 52	121	0.72	4.9
514	+ 10	-0.329	-0.390	GC	+ 41	- 51	+ 7	66	0.50	15.5
515	- 89	+0.235	-0.126	GC	- 93	+ 70	- 43	124	0.70	5.2
516	- 76	+0.105	+0.065	GC	- 54	+ 65	+ 28	89	0.49	6.1
517										
518	- 33	+0.068	+0.023	GC	- 10	+ 84	- 5	85	0.38	8.7
519*	+ 28	+0.155	+0.106	GC	+ 15	+ 74	+ 7	76	0.37	10.9
520	- 87	+1.021	-0.265	GC	- 49	+ 97	+ 29	112	0.53	6.8
521	- 84	+0.440	+0.360	2 Grw.	- 77	+ 93	+ 11	121	0.65	5.9
522	+ 16	-0.290	-0.322	Y 21	- 42	- 87	+ 8	97	0.46	6.8
523	- 66	+0.120	+0.098	GC	- 55	+ 70	+ 17	91	0.51	6.1
524	+ 7	-0.444	-0.281	Y 17	- 17	- 60	+ 28	68	0.30	7.6
525	- 75	+0.039	+0.124	GC	-106	+133	+ 83	189	0.80	6.0
526	- 51	-0.374	-0.507	Y 10	- 78	-108	+ 1	133	0.67	6.1
527	- 45	+0.163	+0.044	GC	- 33	+150	- 33	157	0.65	10.2
528	- 44	+0.280	-0.008	Y 20	- 45	+124	- 31	136	0.59	7.9
529	+ 25	-0.259	-0.137	GC	+ 15	- 34	+ 4	37	0.22	9.9
530	- 16	+0.105	+0.108	GC	+ 21	+ 86	+ 14	90	0.48	12.9
531	- 36	-0.542	-0.334	GC	- 14	- 71	+ 12	73	0.33	8.0
532	- 52	-0.052	-0.068	GC	- 60	- 52	+ 14	81	0.54	5.6
533*	- 25	-0.584	-0.051	GC	- 5	- 49	+ 58	76	0.27	8.4
534*	-296	+0.510	+0.071	Yk	-260	+241	+ 74	367	0.98	11.3r
535*	- 35	-0.091	-0.087	GC	- 50	- 98	+ 11	111	0.52	6.7
(11)	(12)	(13)	(14)	(15)	(16)	(17)	(18)	(19)	(20)	(21)

TABLE 1 (continued)

No.	Name	α(1900)	δ(1900)	Sp.	V	B-V	U-B	π tr	π sp
536	211476	22^h12^m3	+12°24'	G2 V	7.03	+ 0.60	+0.08	+0".040	+0".033
537	35 Peg	22 22.8	+ 4 12	K0 III	4.81	+ 1.05	+0.89	+0.021	+0.015
538	213893	22 29.5	+ 0 5	K5 III	6.70	+ 1.52	+1.84		+0.0042
539	214059	22 30.5	+ 4 52	G4 V	8.24	+ 0.68	+0.18		+0.022
540	215549	22 41.0	+ 29 55	K1 III-IV	6.37	+ 0.92	+0.68	+ 0.025	+0.0095
541*	215812	22 42.7	- 4 45	G5 V	6.66	+ 0.65	+0.12	+ 0.026	+0.038
542	77 Aqr	22 49.5	-16 48	K2 III	5.56	+ 1.14	+1.09	+ 0.014	+0.0115
543	216777	22 50.5	- 8 21	G6 V	8.02	+ 0.64	+0.12	+ 0.044	+0.029
544	+68°1345	22 55.1	+ 68 29	K0 V	8.74	+ 0.78	+0.42	+ 0.018	+0.029
545	218101	23 0.2	+ 16 2	G8 IV	6.44	+ 0.83	+0.55	+ 0.031	+0.026
546	218347	23 2.2	+ 15 44	F7 V	8.90	+ 0.51	+0.02		+0.0095
547	6 And	23 5.8	+ 43 0	F5 IV	5.95J	+ 0.44	-0.05	+ 0.025	+0.016
548*	219175	23 8.8	- 9 28	F9 V	7.56J	+ 0.56	-0.04	+ 0.014	+0.020
549*				G3 V	8.19J	+ 0.69	+0.09		
550	γ Psc	23 12.0	+ 2 44	G8 III M	3.68	+ 0.92	+0.58	+ 0.025	+0.017
551*	219617	23 12.0	-14 27	sd F8	8.17	+ 0.47	-0.20	+ 0.024	+0.023
552	219829	23 13.8	+ 4 52	K0 V	8.00	+ 0.82	+0.43	+ 0.018	+0.040
553	219962	23 15.0	+ 47 50	K2 III	6.32	+ 1.12	+1.05	-0.004	+0.0083
554	219953	23 15.0	+ 28 19	K1 V	8.87	+ 0.81	+0.36	+ 0.039	+0.029
555	221148	23 24.4	- 5 5	K3 III	6.26	+ 1.08	+1.14	+ 0.016	+0.0058
556*	221170	23 24.6	+ 29 53	G2 IV	7.66	+ 1.13	+0.64		+0.011
557	221354	23 26.4	+ 58 37	K0 V	6.75	+ 0.83	+0.50	+ 0.023	+0.071
558	14 And	23 26.4	+ 38 41	G8 III	5.22	+ 1.02	+0.86	+ 0.014	+0.0091
559	221585	23 28.2	+ 62 36	G8 IV	7.42	+ 0.74	+0.38		+0.016
560	221830	23 30.4	+ 30 27	G2 V	6.85	+ 0.59	+0.07	+ 0.008	+0.036
561	221914	23 31.0	+ 17 53	G5 V	7.63	+ 0.70	+0.22	+ 0.036	+0.032
562*	λ And	23 32.7	+ 45 55	G8 III-IV M	3.88J	+ 1.02	+0.68	+ 0.043	+0.029
563*	222455	23 35.6	- 0 8	K3 III	7.40	+ 1.17	+1.16		+0.0035
564	222794	23 38.4	+ 57 31	G2 V	7.10	+ 0.66	+0.02	+ 0.001	+0.032
565	222935	23 40.0	+ 29 0	K1 V	8.40	+ 0.86	+0.55	+ 0.017	+0.036
566	223238	23 42.7	+ 3 36	G2 V	7.70	+ 0.65	+0.15		+0.024
567	223498	23 44.9	+ 2 19	G7 V	8.32	+ 0.73	+0.38	+ 0.035	+0.026
568	224383	23 52.3	-10 12	G2 V	7.88	+ 0.63	+0.14	+ 0.016	+0.022
569	224618	23 54.2	-17 30	K0 V	8.92	+ 0.77	+0.25	+ 0.017	+0.026
570*	85 Peg	23 57.0	+ 26 32	G3 V M	5.75J	+ 0.66	+0.04	+ 0.086	+0.066
571	225239	23^h59^m6	+ 34 °7'	G2 V	6.12	+ 0.62	+0.09	+ 0".034	+0".050
(1)	(2)	(3)	(4)	(5)	(6)	(7)	(8)	(9)	(10)

TABLE 1 (continued)

No.	ρ	$\mu\alpha$	$\mu\delta$	Source of μ	U	V	W	Q	e	a
536	- 30	+ 0.845	+ 0.099	GC	- 31	+131	- 31	138	0.58	9.1
537	+ 54	+ 0.078	-0.308	GC	- 29	- 23	- 93	100	0.27	6.6
538	- 88	-0.027	-0.070	GC	-100	- 26	+49	114	0.71	4.8
539	- 7	+ 0.420	-0.202	Y 20	- 50	+ 74	- 53	104	0.49	6.3
540	- 1	-0.265	-0.352	GC	- 18	-187	- 73	202	0.81	21.0
541*	- 23	-0.206	-0.300	GC	- 28	- 17	+21	39	0.25	6.6
542	- 36	-0.225	-0.086	GC	- 9	- 67	+69	97	0.31	8.3
543	- 24	+ 0.577	-0.062	Y 16	- 55	+ 90	- 15	107	0.54	6.4
544	- 26	+ 0.589	+ 0.299	GC	- 67	+100	+10	121	0.61	6.3
545	- 27	-0.190	-0.193	GC	- 23	- 31	+13	41	0.24	6.9
546	- 22	-0.110	-0.041	GC	- 7	- 36	+27	46	0.15	7.9
547	- 43	-0.197	-0.188	GC	- 22	- 67	- 11	71	0.31	6.9
548*	- 32	+0.552	-0.035	GC	- 59	+133	- 12	146	0.65	7.5
549*										
550	- 14	+0.756	+ 0.022	GC	- 71	+205	- 49	222	0.84	12.6
551*	+ 10	-0.513	-1.186	GC	-163	-185	- 29	248	0.96	6.7
552	- 14	+ 0.472	-0.106	GC	- 30	+ 60	- 7	67	0.35	6.9
553	+ 23	+ 0.205	+ 0.032	GC	- 11	+133	- 19	135	0.49	9.7
554	- 51	+ 0.745	-0.062	GC	- 83	+110	- 14	139	0.70	6.0
555	- 25	+ 0.176	-0.225	GC	-205	+ 59	- 91	232	1.00	4.3
556*	-120	+ 0.011	-0.045	Y9	-104	- 12	+49	116	0.72	4.8
557	- 25	+ 1.095	+ 0.111	GC	- 54	+ 57	- 5	79	0.50	6.1
558	- 59	+ 0.285	-0.079	GC	-112	+115	- 50	168	0.81	5.5
559	+ 8	+ 0.434	+ 0.043	2 Grw	- 37	+137	- 16	143	0.61	9.0
560	-103	+ 0.547	+ 0.259	GC	- 96	+ 70	+66	136	0.71	5.2
561	- 25	+ 0.680	+ 0.212	GC	- 34	+117	+16	123	0.54	8.2
562*	+ 7	+ 0.158	-0.421	GC	- 5	+ 20	- 66	69	0.10	8.7
563*	- 2	-0.090	-0.017	Lei 15	+ 37	-100	+28	110	0.66	19.8
564	- 67	+ 0.383	+ 0.485	GC	- 80	+ 57	+67	119	0.63	5.3
565	+ 51	+ 0.945	+ 0.015	GC	- 2	-105	- 47	115	0.48	10.5
566	- 16	+ 0.335	-0.036	GC	- 35	+ 71	+ 2	79	0.41	6.9
567	- 27	+ 0.474	+ 0.168	GC	- 22	+105	+27	111	0.48	8.6
568	- 28	+ 0.461	-0.159	GC	- 75	+ 88	+ 4	116	0.62	5.7
569	- 43	+ 0.171	-0.048	Y 12	-106	+202	+10	228	0.88	9.5
570*	- 36	+ 0.837	-0.988	GC	- 80	+ 32	- 40	95	0.61	5.2
571	+ 4	+ 0.755	+ 0.100	GC	- 19	+ 84	+ 2	86	0.39	8.1
(11)	(12)	(13)	(14)	(15)	(16)	(17)	(18)	(19)	(20)	(21)

Notes to Table 1

HD 26	See Keenan and Kellar, (1951). The spectroscopic parallax is computed with $M_v = +0.7$; this assumes that the star is a normal giant.
HD 2774	Spectroscopic binary
HD 3266	ADS 497, $\Delta m = 0.8$
HD 3567	The proper motion depends entirely on Yale for the only modern position.
HD 6755	CH strong; metallic lines very weak.
HD 11397	Very weak CN. The data for the star is discordant and the high tangential velocity is probably spurious.
HD 13580	Spectroscopic binary, orbit.
19 Ari	Spectroscopic binary.
HD 14214	Spectroscopic binary, orbit.
HD 17647	ADS 2173, $\Delta m = 1.5$
95 Cet	ADS 2459
14 Tau	Spectroscopic binary.
HD 28439	ADS 2757 $\Delta m = 0.6$. The spectral type of the secondary is K2 V.
HD 24000	Reddened. $m_o = 7.95$
39 Eri	ADS 3079 $\Delta m = 3$
o^2 Eri	ADS 3093
BD +29°734	Reddened. $m_o = 8.88$
HD 30455	Spectroscopic binary, orbit.
BD +29°847	ADS 3835 $\Delta m = 3.9$; Proper motion from Wilson and Joy (1952)
HD 34673	ADS 3900 $\Delta m = 4$
HD 35961	ADS 4099 $\Delta m = 1.7$
HD 36443	Data are discordant. The spectrum may be of the wrong star.
HD 37171	Spectroscopic binary.
HD 40460	Spectroscopic binary.
HD 43624	Spectroscopic binary.
HD 44007	The color indicates a later spectral type. All lines are very weak.
HD 49409	ADS 5469 $\Delta m = 0.8$
HD 57435	Photometric data are means of four discordant observations.
HD 60298	Only one photometric observation.
81 Gem	Spectroscopic binary.
HD 64090	Very weak lines.
HD 73668	ADS 6913
HD 74462	Very weak lines and strong CH.
HD 75632	ADS 7067 $\Delta m = 0.1$
HD 79210 and HD 79211	ADS 7251
HD 81192	Strong CH and very weak lines.

θ	UMa	ADS 7420
BD	+58°1199	ADS 7447. Triple star; 9.1, 9.8, and 10.7.
HD	87998	ADS 7655 $\Delta m = 3.7$
γ	Leo	ADS 7724 $\Delta m = 1.5$
HD	89707	No photometric observations. The magnitude is from the Henry Draper catalogue.
HD	94084	Spectroscopic binary.
HD	97561	ADS 8094 $\Delta m = 0$
BD	+51°1696	No photometric observations. The magnitude is from the BD catalogue.
HD	104817	A metallic line star. The K-line indicates the type A3.
HD	106038	The spectroscopic parallax assumes $M_v = +4.3$
HD	106365	ADS 8470
HD	107452	ADS 8523
HD	107760	Two-line spectroscopic binary, orbit.
HD	109628	ADS 8606 $\Delta m = 0$
HD	113984	ADS 8786
HD	114060	Double star
HD	114960	Spectroscopic binary
HD	115046	ADS 8832
HD	117876	ADS 8937
HD	118328	ADS 8959 $\Delta m = 0.5$
HD	118742	ADS 8981 $\Delta m = 2.4$
84	Vir	ADS 9000 $\Delta m = 2.4$
HD	124425	Spectroscopic binary, orbit
HD	127356	ADS 9291 $\Delta m = 0.9$
HD	130145	ADS 9380 $\Delta m = 1.0$
HD	130669	ADS 9397 $\Delta m = 0$
HD	131334	ADS 9428 $\Delta m = 1.7$
BD	+30°2611	CN very weak λ4290 strong
HD	135101	ADS 9535
HD	136161	Reddened. $m_o = 8.28$
HD	136274	Spectroscopic binary
HD	140283	Only one observation of the magnitude
39	Ser	Spectroscopic binary
HD	144515	Spectroscopic binary, orbit
τ	CrB	ADS 9939. Also spectroscopic binary
HD	151199	A chromium, strontium star similar to ιCas.
HD	151937	Weak CN. Very strong feature near λ4172
54	Her	ADS 10262
HD	153472	Spectroscopic binary

HD 154712	ADS 10329 $\Delta m = 1.2$
HD 159482	ADS 10638
27 Dra	Spectroscopic binary
HD 160538	Strong emission at H and K
HD 161817	The spectroscopic parallax assumes $M_v = +2.5$
HD 162756	ADS 10858 $\Delta m = 3.5$
HD 163810	ADS 10938 $\Delta m = 1.3$
HD 170737	Very weak lines and weak CN. CH strong
HD 172823	ADS 11503
BD +31°3330	ADS 11576 $\Delta m = 2.6$
HD 175305	Very weak lines
HD 179484	ADS 12145 $\Delta m = 0.5$
HD 179558	ADS 12160 $\Delta m = 1.3$
HD 179957 and HD 179958	ADS 12169
BD +17°3992	ADS 12557 $\Delta m = 3$
HD 184360	ADS 12594 $\Delta m = 2.5$
HD 184860	ADS 12664
HD 195987	Spectroscopic binary
HD 196882	ADS 14123 $\Delta m = 1.8$
30 Vul	Spectroscopic binary
61 Cyg	ADS 14636
HD 201889	ADS 14738 $\Delta m = 2.0$
HD 204129	ADS 14916
BD +22°4567	Spectroscopic binary
BD +17°4708	The proper motion is from a Yerkes parallax series.
HD 211076	ADS 15768 $\Delta m = 3.2$
HD 215812	ADS 16270 $\Delta m = 0.5$
HD 219175	ADS 16611
HD 219617	ADS 16644
HD 221170	The color indicates a much later spectral type, but the strength of the hydrogen lines makes this unlikely. CH is strong. All other lines are very weak.
λ And	Spectroscopic binary, orbit
HD 222455	ADS 16919
85 Peg	ADS 17175

TABLE 2

ADDITIONAL STARS

Name	α(1900)	δ(1900)	Sp.	V	B-V	U-B	π tr	π sp	ρ	μα	μδ
+15°28	0 11.1	+16°05	G0 V	9.76	+0.55	-0.02		+0.0079		+0.321	-0.074
1879	0 18.0	-16 36	M2 III	6.47	+1.60	+1.85		+0.0042	- 22	+0.065	+0.036
3950	0 37.0	+51 48	B1 III	6.91	+0.12	-0.68			- 92	-0.011	-0.012
4442*	0 38.8	+47 19	B5 V	5.68	-0.13	-0.56			- 60	-0.030	+0.016
10097	1 33.7	+ 4 37	G5 V	9.14	+0.67	+0.32		+0.016		+0.242	+0.047
-14°368*	1 51.8	-14 40	G5 V	9.66	+0.68	+0.04		+0.012		+0.233	+0.231
-17°484	2 26.7	-17 25		10.42	+0.47	-0.17	0.000		+234	+0.381	-0.068
+48°739	2 36.1	+48 34		9.31	+0.97	+0.70:	+0.067		- 97	+0.078	-0.398
+32°719	3 59.7	+32 42		9.99	+0.98	+0.70	+0.029		+112	+0.68	-0.85
28595	4 25.4	+14 53	M3 III	6.34	+1.70	+2.01		+0.0046	+ 38	+0.048	-0.046
o°873	4 45.8	+ 0 24		10.12	+0.54	+0.03			+108	+0.082	+0.017
36395	5 26.4	- 3 42	M1 V	7.96J	+1.48	+1.20	+0.163	+0.220	+ 11	+0.771	-2.098
39045	5 44.9	+32 6	M3 III	6.28	+1.74	+1.96		+0.0044	+103	+0.005	+0.004
39225	5 46.0	+33 53	M1 II	5.98	+1.59	+1.97		+0.0021	+101	+0.011	+0.003
+25°1120	6 0.6	+25 34	B9 V	10.02	+0.02	-0.15		+0.0010		0.000	+0.020
48228	6 37.3	+40 44	M4 III	6.84	+1.59	+1.79	+0.002	+0.0035	+ 40	-0.014	-0.159
52 Gem	7 8.6	+25 4	M1 III	5.82	+1.56	+1.83		+0.0058	+ 47	+0.052	-0.095
+9°1627	7 17.0	+ 9 6	K2 V	9.42	+0.89	+0.68		+0.025		+0.186	-0.326
+12°1624	7 33.2	+12 39		10.20	+1.10	+1.04				-0.313	-0.030
61606	7 35.0	- 3 22	K2 V				+0.085		- 21	+0.075	+0.288
-4°2150	7 51.8	- 4 20	G2 V							-0.105	+0.028
+25°1858	8 2.9	+24 55	G3 V	9.63	+0.69	+0.16		+0.011		+0.015	-0.392
+8°2015	8 10.3	+ 7 56		10.44	+0.67	+0.15				-0.193	-0.177
+33°1694	8 18.9	+32 58		10.04	+1.07	+0.86	+0.036		- 78	0.000	-0.64
76830	8 53.5	+18 31	M4 III	6.38	+1.55	+1.69	-0.006	+0.0042	+ 21	-0.41	-0.075
77586	8 58.4	+29 41	M3 III	7.60	+1.61	+1.76		+0.0024	+ 88	-0.015	-0.019
83162	9 31.4	-12 1		10.58	+0.12	+0.09				+0.019	-0.109
-0°2304	10 6.4	- 0 41	F4 V	9.76	+0.38	+0.04		+0.0050		-0.116	+0.008
+53°1395	10 7.5	+53 1		9.54	+1.10	+0.94	+0.047		- 25	+0.093	-0.771
41 UMa	10 40.2	+57 53	M1 III	6.34	+1.56	+1.90		+0.0046	- 2	-0.051	-0.069
95129	10 54.0	+36 38	M2 III	6.00	+1.59	+1.92	+0.016	+0.0052	- 26	+0.071	-0.056
+44°2051	11 00.5	+44 02	M2 V	8.66	+1.52	+1.16	+0.173	+0.190	+ 64	-4.434	+0.936
96574	11 2.4	+14 24	F9 V	7.32	+0.55	+0.04		+0.023		-0.374	+0.087
96884	11 4.0	+43 45	M2 III	5.89	+1.57	+1.90		+0.0055	+ 18	-0.065	-0.018
97503	11 8.1	+ 5 1	K5 V	8.73	+1.17	+1.09		+0.066		-0.293	-0.030
+66°717	11 14.8	+66 23	M1 VM	9.32J	+1.42	+1.08	+0.113	+0.120	+ 47	-2.947	+0.149
100041	11 25.6	+29 0	M4 III	6.72	+1.51	+1.81		+0.0036	+ 87	-0.086	0.000
101093	11 32.8	- 1 3	F9 V	7.62	+0.55	-0.01		+0.020		-0.306	+0.106
104216	11 55.1	+81 25	M2 III	6.17	+1.61	+1.90		+0.0048	+ 32	-0.069	-0.038
105281*	12 2.2	-10 7	F5 m	8.23	+0.41	+0.16		+0.0105		-0.072	-0.018
+9°2636	12 26.3	+ 9 22		9.69	+1.43	+1.22	+0.066		+ 21	-0.633	-0.521
114094	13 3.2	+ 4 19		9.70	+0.67	+0.18	+0.027		- 58	-0.45	-0.31
+18°2776	13 40.2	+18 20		9.68	+1.38	+0.94	+0.086		+ 27	+0.434	-1.848
119850	13 40.7	+15 26	M4 V	8.47	+1.44	+1.11	+0.193	+0.365	+ 15	+1.778	-1.457
87 Vir	13 42.0	-17 21	M1 III	5.44	+1.61	+1.93		+0.0069	+ 64	+0.057	-0.041
ε Boo B*	14 12.7	+51 50	K1 V	8.19	+0.80	+0.34	+0.044	+0.040	- 17	-0.147	+0.088
+32°2547	15 3.6	+32 47		11.13	+0.69	+0.14	+0.017		- 63	-0.17	-0.48
τ1 Ser	15 21.0	+15 47	M1 III	5.17	+1.66	+1.95	+0.015	+0.0076	- 20	-0.017	-0.013
φ Boo	15 34.2	+40 41	G8 III-IV	5.24	+0.88	+0.53	+0.019	+0.017	- 10	+0.059	+0.053
+67°922*	16 1.1	+67 3		9.44	+0.88	-0.68			-138	-0.017	+0.004
147117	16 14.8	-12 34		10.02	+0.41	+0.26				-0.105	+0.012
149363*	16 29.1	- 5 56	B0.5 V	7.80	+0.01	-0.87			+115	+0.009	0.000
154143	16 58.6	+14 14	M3 III	4.98	+1.63	+1.92	+0.005	+0.0079	+ 43	+0.019	-0.70
156966	17 15.4	+27 23	M1 III	6.70	+1.65	+1.94		+0.0038	+ 73	-0.004	-0.035
176029	18 53.1	+ 5 48	M2 V	9.25	+1.45	+1.31	+0.080	+0.150	+ 19	-0.209	-1.221
(1)	(2)	(3)	(4)	(5)	(6)	(7)	(8)	(9)	(10)	(11)	(12)

TABLE 2 (continued)

Name	α(1900)	δ(1900)	Sp	V	B-V	U-B	π tr	π sp	ρ	$\mu\alpha$	$\mu\delta$
178140	19 2.3	-15 23		9.54	+0.63	-0.03	+0.037			-0.137	-0.269
69 Dra	20 2.4	+76 13	M3 III	6.20	+1.61	+1.89		+0.00146	- 68	-0.028	-0.057
195137	20 24.4	-16 34		9.90	+0.65	+0.00				-0.284	-0.095
195686	20 27.4	- 9 42	sd GO	9.54	+0.65	+0.00		+0.0125		-0.067	-0.116
+24°4182	20 31.0	+25 02	G5 V	9.90	+0.62	+0.24	-0.003	+0.011		-0.243	-0.213
+12°4499	20 50.3	+12 48		8.81	+1.05	+1.05			- 32	+0.558	+0.371
+54°3090	20 54.8	+54 45	A1 V	10.22	+0.13	+0.09		+0.0013		-0.012	-0.007
(1)	(2)	(3)	(4)	(5)	(6)	(7)	(8)	(9)	(10)	(11)	(12)

Notes for Table 2

HD 4142 Spectral type from Ramsey (1950)

HD -14°363 Very weak lines

HD 105281 A metallic-line star. The K-Line type is A3.

ι Boo B ADS 9198

HD +67°922 Peculiar spectrum. See Roman (1953)

HD 149363 Spectral type from Duke (1951)

REVISED LIST OF ABSORPTION LINES IN THE SPECTRUM OF R ANDROMEDAE

PAUL W. MERRILL AND JESSE L. GREENSTEIN
Mount Wilson and Palomar Observatories
Carnegie Institution of Washington, California Institute of Technology
Received, September 30, 1955

ABSTRACT

Spectrograms, dispersion 4.5 A/mm in the blue region, 6.8 A/mm in the visual, obtained with the 200-inch telescope, form the basis of this article. A list of 1500 absorption lines and band heads from 4000 to 6900 A is in Table 7. The behavior of lines of the rare earths and of other heavy elements including technetium is briefly described. The displacements of lines of 6 neutral metals increase algebraically with excitation potential of the lower level. This work is preliminary to a discussion of chemical abundances in the atmosphere of R Andromedae.

Previous investigations (Merrill 1947*a*, 1952; Keenan 1954) have indicated that the spectrum of R Andromedae, 001838, a red variable star of period 407 days, magnitude range 5.6–11.7, is an excellent example of type S. Several spectrograms of R Andromedae near maximum light, obtained by Greenstein with the 200-inch telescope in the summer of 1954 (Table 1), form the basis of this article. They have higher dispersion than earlier

TABLE 1

SPECTROGRAMS OF R ANDROMEDAE

Plate No. Pb	Date 1954	Mag.	Phase (Days)	Range of λ (A)	Disp. (A/mm)	Rad. Vel. (km/sec)
1606	July 19	6.4	−15	4000–5070	4.5	− 9.6
1613	July 20	6.4	−14	4010–5080	4.5	−·9.8
1620*a*	July 21	6.3	−13	4930–6930	6.8	−10.4
1620*b*	July 21	6.3	−13	5430–6880	6.8	−10.4
1667	Aug. 18	6.4	+15	3690–5060	4.5	−10.2

photographs and make possible a list of lines more accurate and more complete than those previously published (Merrill 1948, 1952).

Shortward of 3760 A, virtually the only new data of value are wave lengths of lines in the band near 3700 A (Table 2). Nearly all these band lines are actually close doubles not resolved in the stellar spectrum. The laboratory values in Table 2 were computed from the individual wave lengths and intensities given by Herbig (1949). The new measurements strengthen the identification with ZrO announced by Herbig.

Between 3760 and 4000 A the new data are fragmentary. Longward from 4000 A, improvement over the old list is substantial; longward from 4800 A, additional material is extensive. The revised list (Table 7) is based on all available measurements. Lines obviously of molecular origin, as well as many weak lines measured on only one plate, have been omitted. More complete data could be obtained from microphotometer tracings.

For good lines the measured wave lengths are accurate to about 0.01 A. The estimated intensities in Table 7 are on an arbitrary scale: "1" indicates a well-marked line with good intensity for accurate measurement; "0" indicates the weakest observable trace of a line. A question mark in the intensity column indicates that the intensity is doubtful

because of blending with other atomic lines or with band structure; "s" means sharp; "w," wide.

The behavior of lines of various chemical elements in the absorption spectrum of R Andromedae has been previously described (Merrill 1947*a*). Additional remarks on some of the heavier elements follow. A discussion of the relative abundance of numerous elements, based on measures of line intensities, will be presented later by Greenstein.

ADDITIONAL REMARKS ON ELEMENTS IDENTIFIED IN R ANDROMEDAE (MERRILL 1947*a*)

Ga I.—The strong ground-level line 4172.05 A is present.

Y I.—Multiplets (12), (13), and possibly (14) (*Revised Multiplet Table*, Moore 1945) are present in moderate intensity.

TABLE 2

WAVE LENGTHS OF LINES IN THE ZrO BAND NEAR 3700 A

R And (A)	Lab.	R And (A)	Lab.	R And (A)	Lab.
3689.86*	.84	3694.4	.38	3699.70	.71
90.32*	.37	94.86	.83	3700.22	.22
90.75	.74	95.27	.28	00.8	.77
91.13	.11	95.83*	.74	01.4	.34
91.53	.48	96.23	.21	01.91	.89
91.89	.88	96.68	.69	02.36*	.46
92.27*	.27	97.17	.19	02.99	.03
92.70	.68	97.74*	.65	03.57*	.61
93.09	.08	98.16	.16	04.2	.21
93.51	.51	98.69	.66		
93.96*	.93	99.19	.17		

* Probably blended with an atomic line.

Zr I.—In addition to lines in the *Revised Multiplet Table*, more than 100 lines listed by Kiess and Kiess (1930) and in the Massachusetts Institute of Technology wave-length tables (Harrison 1939) have been identified.

Nb I.—Lines from the ground level a^6D (Humphreys and Meggers 1945), including a few not listed in the *Revised Multiplet Table*, are present in moderate intensity.

Tc I.—Observed lines are listed in Table 3. The identification appears to be well established.

Rare earths.—An investigation by Bidelman (1953) extended previous identifications of lines of rare earths in the spectrum of R Andromedae and emphasized the fact that these lines are more intense here than in the spectrum of R Leonis, type M8e. The higher dispersion of our recent spectrograms has allowed the probable identification of many more lines of these elements. A summary of our conclusions concerning the presence of lines of rare earths in the spectrum of R Andromedae is given in Table 4.

Hf I.—Lines 3682.24 and 3777.64 A of multiplet (1) are probably present.

Re I.—Two or three lines, notably 4889.14 and 5275.54 A, may be present in low intensity.

Os I.—Lines 4260.85 and 4420.47 A of multiplet (1) may be present in low intensity.

Pb I.—An extremely weak line may correspond to 4057.81 A of multiplet (1).

DISPLACEMENTS OF LINES

The new measurements confirm the earlier conclusion (Merrill 1947*a*) that displacements of lines of neutral atoms increase algebraically with excitation potential of the

lower atomic-energy level. A few very strong lines from the ground levels of certain atoms have especially large negative displacements, but the relationship of displacement to excitation potential seems more general than that to intensity. Data for numerous multiplets of six metallic atoms are collected in Table 5; normal places, Table 6, are plotted in Figure 1.

TABLE 3

LINES OF Tc I IN SPECTRUM OF R ANDROMEDAE

Lower Term	E.P. (ev)	Laboratory*		R Andromedae		Remarks
		λ (A)	Int.	λ (A)	Int.	
$a^6S_{2\,1/2}$	0.00	4297.06	500	0.01	5	1
		4262.26	400	.26	4	
		4238.19	300	.20	2	
$a^6D_{4\,1/2}$	.34	4031.63	300	.70	2	2
		3984.97	150	.98	1	
$a^6D_{3\,1/2}$	.40	4145.02	80	.99	0.5	3
		4095.68	150	.56	1	4
		4049.10	150	.14	0.5	
$a^6D_{2\,1/2}$	0.46	4172.52	80	.....	.....	5
		4088.70	100	0.72	1	

* W. F. Meggers, *Bureau Stand. J. Res.*, **47**, 7, 1951.

NOTES TO TABLE 3

1. Stronger component of a blend; weaker component measured at 4296.77 A.
2. Blended with Ti I (185) 4031.75 A.
3. $a^6D_{3\,1/2}$–$z^6D^0_{1\,1/2}$; also $a^6D_{0\,1/2}$–$z^6D^0_{0\,1/2}$.
4. Blended with V I (41) 4095.49 A.
5. Could be lost in the wings between Ga I (1) 4172.05 and Fe I (19) 4172.75 A.

TABLE 4

LINES OF RARE EARTHS IN SPECTRUM OF R ANDROMEDAE

Atomic No.	Element	Numerous Lines	Few Lines	No Evidence	Atomic No.	Element	Numerous Lines	Few Lines	No Evidence
57	La	.....	.....	?	64	Gd I	.....	×	.....
58	Ce	.....	.....	×		Gd II	.....	×	.....
59	Pr I	.....	.....	×	65	Tb II	.....	?	.....
	Pr II	.....	×	.....	66	Dy I	.....	×	.....
						Dy II	.....	×	.....
60	Nd I	.....	.....	×	67	Ho	.....	.....	?
	Nd II	×	.....	.....	68	Er	.....	×	.....
61	Pm	.....	.....	×	69	Tm I	.....	×	.....
62	Sm I	.....	?	.....		Tm II	.....	.....	×
	Sm II	×	.....	.....					
					70	Yb I	.....	×	.....
63	Eu I	.....	.....	?		Yb II	.....	.....	×
	Eu II	.....	×	.....	71	Lu	.....	.....	×

TABLE 5

DISPLACEMENTS OF MULTIPLETS

Mult.	Resid. (km/sec)	Wt.*
	Ti I: E.P. = 0.0 ev	
1	−2.9	2
2	−1.9	5
3	−0.6	6
4	−1.7	6
5	−1.6	4
6	−1.7	5
7	−2.6	1
8	−1.3	2
9	+0.7	1
10	+0.7	1
11	0.0	0.5
12	−2.0	3
13	−0.8	2
14	−1.8	1.5
15	−0.5	4
16	+0.8	0.5
17	−2.4	3
18	−1.8	3
19	−0.7	4
20	−1.4	1
21	−2.5	0.5
	E.P. = 0.8 ev	
35	+0.7	3
36	+1.1	1.5
37	+1.3	8
38	+0.5	11
39	−0.5	4
41	+1.7	3
42	−0.4	10
43	+0.8	6
44	−0.6	9
45	+1.4	1
	E.P. = 0.9 ev	
48	+0.9	1
52	+0.3	2
53	−0.6	1
56	+0.8	1
57	+4.8	0.5
59	−1.7	0.5
	E.P. = 1.0 ev	
69	+1.1	3
71	+4.0	1
72	+2.4	5
74	+1.2	4
75	+0.5	4
76	+0.6	1
78	+1.0	2
79	+1.0	2
80	0.0	2
83	−0.7	0.3

Mult.	Resid. (km/sec)	Wt.*
	Ti I; E.P. = 1.4 ev	
102	+0.8	3
106	+1.6	1
107	+1.6	1
108	+1.2	2
109	+1.3	1.5
110	+1.0	5
113	+0.7	6
	E.P. = 1.5 ev	
126	+1.2	1
129	+0.7	1
	E.P. = 1.7 ev	
145	+1.6	2
146	−0.3	5
148	−0.4	2
	E.P. = 1.9 ev	
154	+1.2	3
157	+0.6	3
159	+2.0	1
160	+1.1	4
161	+1.4	1.5
162	+2.1	1
	E.P. = 2.0 ev	
173	+1.9	6
175	+3.8	1
	E.P. = 2.1 ev	
185	+0.1	4
200	+2.1	2
206	+1.8	0.5
	E.P. = 2.2 ev	
218	+3.7	1
231	+1.4	3
233	+2.3	3

Mult.	Resid. (km/sec)	Wt.*
	V I; E.P. = 0.0 ev	
1	−3.6	2
2	−1.8	1.5
3	−1.2	8
4	−0.3	6
5	−0.3	8
6	−0.7	3
7	−1.9	6
8	+0.2	2
9	−2.0	4
10	0.0	1.5
11	−2.4	0.5
	E.P. = 0.3 ev	
19	−0.1	6
20	+0.8	6
21	+0.1	7
22	−0.5	11
23	+1.0	2
24	+1.1	4
26	0.0	1.5
27	−0.4	7
28	0.0	6
29	−0.4	1
	E.P. = 1.1 ev	
31	+3.1	3
34	+2.2	8
35	+0.7	6
36	−1.0	2
37	+0.8	6
40	0.0	3
42	+1.9	2
44	+0.4	2
	E.P. = 1.2 ev	
48	+2.8	2
50	+0.8	1.5
52	+1.8	2
	E.P. = 1.4 ev	
66	+2.3	0.5
	E.P. = 1.8 ev	
87	+1.3	2
88	+0.4	3
89	+3.4	2

TABLE 5—*Continued*

Mult.	Resid. (km/sec)	Wt.*
	V I; E.P. = 1.9 ev	
101	0.0	1
	E.P. = 2.0 ev	
109	+3.3	2
112	+0.7	1
	E.P. = 2.1 ev	
120	+2.1	2
121	+1.5	1
	Cr I; E.P. = 0.0 ev	
1	−2.8	2
2	−2.2	1
3	−0.8	0.3
4	0.0	0.2
	E.P. = 0.9 ev	
6	−0.9	1
7	−3.0	2
8	+1.3	2
9	−0.6	2
10	−0.9	3
	E.P. = 1.0 ev	
18	+1.7	9
20	+1.8	1
21	0.0	9
22	+0.1	10
23	+0.8	5
24	0.0	0.7
	E.P. = 2.5 ev	
38	+2.5	1.5
	Fe I E.P. = 0.0 ev	
1	−1.6	8
2	−1.7	10
3	−1.7	5
4	−0.9	3
5	−1.2	2
	Fe I; E.P. = 0.9 ev	
13	−0.9	2
15	+0.7	10
16	+1.5	8
18	+1.7	1.5
19	+0.3	5
20	+0.4	6
21	−0.7	3
22	+0.8	1.5
23	−0.6	4
24	+1.0	1
	E.P. = 1.5 ev	
36	+0.2	4
37	+2.0	2
39	+1.6	2
41	+0.6	4
42	+0.1	6
43	+1.3	5
45	+1.4	4
	E.P. = 2 2 ev	
68	+1.9	4
	E.P. = 2.4 ev	
114	+2.6	2
152	+1.5	6
318	E.P. = 2.8	
354	+3.1	4
355	+2.2	2
	+1.4	2
	E.P. = 2.9 ev	
383	+1.7	1
	Co I; E.P. = 0.0 ev	
1	−0.4	3
2	+0.4	4
3	−1.5	2
4	+0.8	1
5	0.0	0.5
6	−1.8	1
	Co I; E.P. = 0.5 ev	
15	+1.9	1
16	+0.9	2
18	0.0	2
19	+1.6	2
20	−0.8	0.2
21	+0.3	2
22	−0.1	1
23	+1.6	0.3
	E.P. = 1.0 ev	
28	+1.2	1.5
30	0.0	1
31	+2.6	2
33	+3.6	0.2
34	+2.3	1
	E.P. = 1.9 ev	
62	+2.4	0.3
	E.P. = 3.0 ev	
150	+2.7	1
	Zr I; E.P. = 0.0 ev	
1	−1.5	2
2	−2.2	5
3	−2.5	2
4	−1.7	3
5	−1.9	3
6	−0.8	4
8	−0.2	2
9	0.0	1
10	−1.7	4
11	0.0	1
12	−1.8	1
13	−0.1	0.3
15	−1.1	1
16	+1.9	0.3
	E.P. = 0.5 ev	
24	−1.2	4
25	−1.3	2
26	+2.2	1
27	+1.6	5
28	−0.6	1
29	0.0	1
31	+0.3	2
32	+0.7	1

TABLE 5—*Continued*

Mult.	Resid. (km/sec)	Wt.*	Mult.	Resid. (km/sec)	Wt.*	Mult.	Resid. (km/sec)	Wt.*
	Zr I; E.P. = 0.7 ev			Zr I; E.P. = 0.6 ev *Cont.*			E.P. = 1.5 ev	
43	+0.3	8	50	+2.9	0.5	62	+0.6	2
44	+0.5	5	51	+1.4	1	64	+1.3	0.5
45	+0.7	12	52	+1.7	1		E.P. = 1.6 ev	
46	−0.6	6		E.P. = 1.4 ev		65	+0.9	1
	E.P. = 0.6 ev		61	+0.3	4		E.P. = 1.8 ev	
47	−0.5	1				66	+0.6	1
48	−0.6	1						
49	−0.7	1						

* Weight 1 is assigned to the residual from a single good line measured on several plates. It corresponds to weight 3 or 4 in Tables 4 and 5 in *Ap. J.* **105,** 360, 1947.

TABLE 6

MEAN DISPLACEMENTS OF MULTIPLETS FROM VARIOUS ENERGY LEVELS

E.P. (ev)	Resid. (km/sec)	Wt.*	E.P. (ev)	Resid. (km/sec)	Wt.*	E.P. (ev)	Resid. (km/sec)	Wt.*
	Ti I			Cr I			Co I	
0.0	−1.4	56						
0.8	+0.3	56				0.0	−0.3	12
1.0	+1.1	30	0.0	−2.3	4	0.5	+0.6	12
1.4	+1.0	22	1.0	+0.3	45	1.0	+1.8	6
1.9	+1.1	30						
2.2	+1.8	14		Fe I			Zr I	
	V I					0.0	−1.3	29
0.0	−1.1	43	0.0	−1.5	28	0.5	+0.2	18
0.3	0.0	52	0.9	+0.5	43	0.6	+0.5	6
1.1	+1.3	38	1.5	+0.9	26	0.7	+0.3	30
1.9	+1 7	14	2.5	+2.0	20	1.5	+0.5	9

* Weight 1 is assigned to the residual from a single good line measured on several plates. It corresponds to weight 3 or 4 in Tables 4 and 5 in *Ap. J.*, **105,** 360, 1947.

The measured shortward displacement of lines of low excitation potential may be connected with a slight asymmetry of these lines. On tracings of our recent spectrograms certain ground-level lines appear less sharp on the shortward side than on the longward; examples are two lines of multiplet (1) of Zr I, 6762.38 and 6832.93 A. The circumstances suggest that the true radial velocity of the star is yielded by lines of higher excitation potential.

Relative displacements similar to those in the spectrum of R Andromedae have been found in the spectra of several long-period variables of type Me: *o* Ceti (Adams 1941; Joy 1954); R Hydrae (Merrill 1946*a*); R Leonis (Merrill 1946*b*); χ Cygni (Merrill 1947). Judged by the measurements published by Dorothy N. Davis (1947), similar relative displacements (at least of lines of *Fe* I and *Ti* I) are not present in the spectrum of β Pegasi, type gM2. The slight negative displacements of the ground-level lines in spectra of the long-period variable stars may represent a mild exhibition of the more extreme effects well known in cM spectra (Spitzer 1939). The structure of the lines will have to be taken into account in the interpretation of curves of growth derived from lines at various excitation potentials and, more generally, in discussions of excitation temperature, turbulence, and stratification in the atmospheres of red giant stars. Systematic outward motions in the outermost layers of the atmospheres, together with variation of

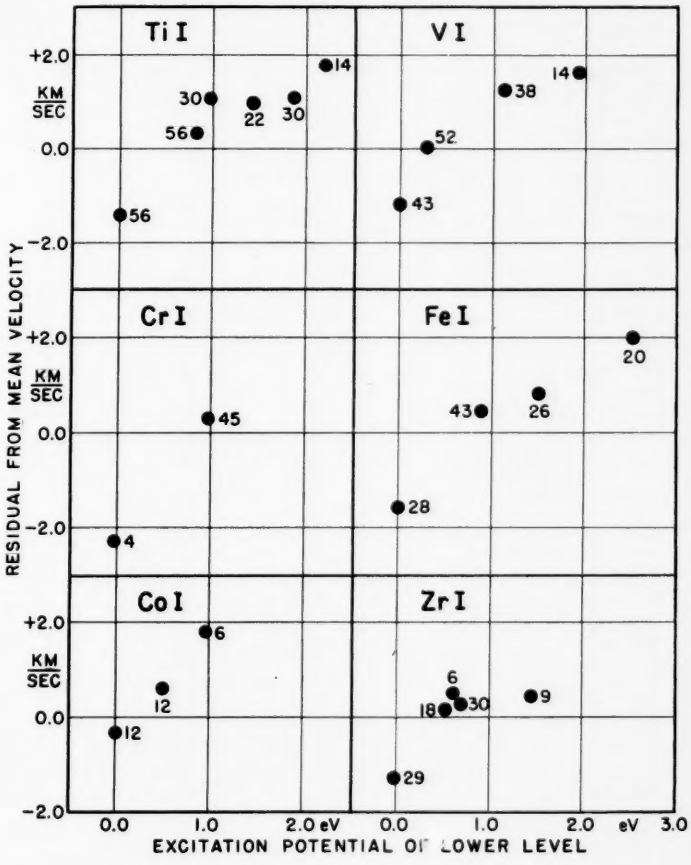

FIG. 1.—Displacement of absorption lines in the spectrum of R Andromedae plotted against excitation potential of lower level. Normal places with numbers of lines. See Tables 5 and 6.

excitation potential with level, may account for the small displacements observed in the spectrum of R Andromedae. Larger effects in line structure and curves of growth in spectra of supergiants may similarly have their origin in systematic atmospheric motions. The structure of lines in spectra of red giant and supergiant stars deserves further study, preferably with very high dispersion.

We express our appreciation to the American Academy of Arts and Sciences for a grant in support of this investigation.

REFERENCES

Adams, W. S. 1941, *Ap. J.*, **93**, 11.
Bidelman, W. P. 1953, *Ap. J.*, **117**, 377.
Davis, D. N. 1947, *Ap. J.*, **106**, 28.
Harrison, G. R. 1939, *M.I.T. Wavelength Tables* (New York: John Wiley & Sons).
Herbig, G. H. 1949, *Ap. J.*, **109**, 109.
Humphreys, C. J., and Meggers, W. F. 1945, *Bureau Stand. J. Res.*, **34**, 477.
Joy, A. H. 1954, *Ap. J. Suppl.*, **1**, 39.
Keenan, P. C. 1954, *Ap. J.*, **120**, 484.
Kiess, C. C. and H. K. 1930, *Bureau Stand. J. Res.*, **5**, 1205.
Merrill, P. W. 1946*a*, *Ap. J.*, **103**, 6.
———. 1946*b*, *ibid.*, p. 275.
———. 1947*a*, *ibid.*, **105**, 360.
———. 1947*b*, *ibid.*, **106**, 274.
———. 1948, *ibid.*, **107**, 303.
———. 1952, *ibid.*, **116**, 21.
Moore, C. E. 1945, *Princeton U. Obs. Contr.*, No. 20.
Spitzer, L., Jr. 1939, *Ap. J.*, **90**, 494.

TABLE 7

ABSORPTION LINES AND BANDS IN THE SPECTRUM OF R ANDROMEDAE

4000 – 6900 A

For wave lengths shorter than 4000 A, see Ap. J., 107,303,1948, Table 2

λ	Int.	IDENTIFICATION El.	Mult.	λ
4000				
00.53	1	?Dy II	..	.45
		Nd II	64	.49
01.15	1.5	Zr	0.2*	.09
		Zr	1.5*	.23
02.57	1	Zr	46	.55
03.15	0.5	Zr	1.4*	.09
04.00	1	Nd II	..	.01
04.74	0	..	..	..
05.27	1	Fe	43	.25
06.0	0.4	..	..	..
06.57	0.3	..	..	..
06.84	0.6	Fe	320	.77
07.51	1	Nd II	..	.44
		Zr	1.8*	.59
07.98	1.2	Er	..	.97
08.91	3	Ti	12	.93
09.65	2	Ti	11	.65
11.09	1	Co	2	.09
11.54	1	Ti	10	.53
12.32	0	Zr	1.9*	.25
		Nd II	10	.25
12.67	1	Nd II	..	.70
13.24	0.3	..	..	..
14.52	0.6	Sc II	8	.49
15.35	0.6	Ti	185	.38
17.05	0	Zr	1.5*	.00
17.31	0	..	..	..
17.77	0.5	Ti	185	.77
18.14	1.5	Mn	5	.10
18.83	1	?Nd II	19	.83
19.32	0.5	Co	16	.29
19.78	0	Nd II	..	.79
20.38	3	Sc	7	.40
20.92	1	?Nd II	19	.87
		Co	16	.90
21.33	0.7	Nd II	36	.33
21.80	1	Ti	185	.81
22.11	0	..	..	..
23.16	0.4w	Zr	..	.04
		?Sm II	4	.23
		Zr	1.4*	.29
23.68	1.5	Sc	7	.69
23.96	0.8	Zr	46	.99
24.55	1.5	Ti	12	.57
24.88	1	Zr	46	.92
26.22	0.3	Cr	37	.17
26.57	0.8	Ti	185	.54
27.13	2w	Co	3	.03
		Zr	46	.20
28.57	0.3	..	..	..
28.96	2s	Zr	0.5*	.95
29.93	4w	..	..	..
		Zr	46	.03
30.63	10w	Mn	2	.76
31.70	1w	Tc	0.3*	.63
		Ti	185	.75
32.95	10w	Ga	1	.98
		Mn	2	.07
34.46	10w	Mn	2	.49
35.85	4	Mn	5	.73
		Zr	0.2*	.89
37.41	0.3	..	..	..
38.15	0.4	?Nd II	31	.12
38.47	1	..	..	..
39.38	0.3	?Pr II	15	.36
39.81	4	Y	5	.83
40.80	1s	Nd II	30	.80
41.06	0s	?Nd II	..	.06
41.38	1.5	Mn	5	.36
41.72	0.4	Sm II	22	.68
42.33	1w	Zr	1.4*	.23
		?Cr	36	.25
		..	..	..
42.86	0.6w	Sm II	4	.72
		Sm II	9	.90
43.58	1.5s	Zr	32	.57
43.95	0.3?	?Fe	276	.90
44.10	1.5	K	3	.14
44.58	1.5s	Zr	46	.57
44.9	1w	..	..	..
45.43	0.3	Co	31	.39
45.85	4	Fe	43	.82
47.21	1?	K	3	.21
47.73	4w	?Y	6	.64
		Sc	7	.79
48.68	3w	?..	..	..
		Mn	5	.76
49.14	0.7	Tc	Ω 4*	.10
49.50	0.6	?Gd II	50	.43
49.87	0.4	?Gd II	..	.86
50.49	2	Zr	0.5*	.48
50.96	0	V	121	.96
51.14	0.4	Nd II	66	.14
51.37	0	?V	121	.35
52.45	2	..	..	..
53.61	0.5	Gd	5	.64
53.88	0.3?	?Ho	..	.92
54.51	4	Zr	0.2*	.43
		Sc	6	.56
55.03	2.5	Ti	80	.01
		Zr	46	.03
55.62	1.5	Mn	5	.54
		Zr	1.6*	.71
56.58	1	Fe	320	.53
		?Pr II	26	.54
57.19	2	Co	3	.20
57.83	0.4s	Pb	1	.83
58.23	2s	Co	16	.18
		Gd	5	.22
58.94	4	Nb	1	.93
		Mn	5	.93
59.33	2	Co	2	.32
59.97	0.8	Nd II	63	.96
60.25	2	Ti	80	.26
60.77	0.5	..	..	..
61.10	2	Nd II	10	.08
61.53	2	Zr	0.5*	.53
62.83	1.5w	Pr II	26	.82
63.28	0.3	?Zr	0.5*	.32
63.60	4s	Fe	43	.60
64.18	4	Zr	46	.16
		Ti	80	.20
64.58	0.5	Sm II	24	.58
65.10	3	Ti	80	.09
66.36	1.5	Co	30	.36
66.82	1w	Zr	..	.71
		Sm II	28	.74
		..	..	..
67.35	1?	Fe	217	.28
67.78	0.7?	..	..	..
67.93	3	?..	..	..
		Mn	5	.00
68.39	0.5	Sm II	42	.33
68.86	2	Zr	1.3*	.72
		..	..	..
69.27	3	?..	..	..
		Nd II	20	.27
70.30	1w	Mn	5	.28
70.75	2s	..	..	..
71.17	1.5	..	..	..
71.76	4	Fe	43	.74
72.68	3	Zr	46	.71
73.75	0.5w	..	..	..
74.05	0.3?	..	..	..
74.38	0.3	?Zr	2.3*	.35
74.97	2	Zr	0.5*	.93
		Zr	1.8*	.05
75.23	1.5	?Nd II	62	.12
		?Nd II	19	.27
76.13	0.3?	Co	16	.12
76.40	4w	Ti	9	.37
		?..	..	..
77.62	10w	Y	7	.38
		Sr II	1	.71
		Dy II	..	.97
78.64	3?w	Ti	80	.47
		Gd	5	.70
79.32	0.5w	Mn	5	.24
		Mn	5	.42
79.75	3	Nb	1	.73
80.24	1.5	Nd II	18	.23
80.57	1	Ru	7	.60
81.24	3	Zr	46	.22
81.47	1?	..	..	..
81.95	0.5	Pr II	..	.90
82.42	4w	Sc	6	.40
		Ti	80	.46
83.00	1	Mn	5	.94
		Zr	1.4*	.08
83.32	0.3	?Pr II	..	.34
83.70	4	Mn	5	.63
		Y	6	.71
84.47	2w	Zr	1.8*	.30
		..	..	..
84.91	0.5	..	..	..
85.42	0	..	..	..
85.82	1	Nd II	16	.82
86.66	1.5	?La II	10	.72
87.64	0.5	Er	..	.65
88.00	1	..	..	..
88.31	0.7	Co	2	.29
88.72	0.5	Tc	0.5*	.70
89.23	0.3	?Fe	422	.22
90.51	3	?Zr II	29	.52
		V	41	.58
90.93	0.3	..	..	..
91.99	1.5	V	52	.94
92.32	1?w	Sm II	1	.27
		Co	29	.39
92.71	2.5	V	27	.69
93.19	1	?Zr	0.5*	.16
93.57	2w	?Ni	1	.62
94.22	1.5	Tm	..	.19
		Zr	1.5*	.26
94.99	2	Ca	25	.93
		?Pr	..	.97
95.56	3w	V	41	.49
		Tc	Ω 4*	.68
96.24	1?	Fe	18	.21
96.42	1?w	..	..	..
98.19	1w	..	..	..
98.53	1?	..	..	..
99.26	3	..	..	..
99.78	3	V	27	.80

*Excitation potential of lower level in electron volts. This line is not in the Revised Multiplet Table (Moore 1945).

λ	Int.	IDENTIFICATION El.	Mult.	λ
4100				
00.34	3	Si H	..	.33
00.83	2	Fe	18	.74
		Nb	1	.92
01.77	3?	In	1	.76
02.32	5?	..	..	..
		Y	7	.38
02.91	1	Si	2	.93
		?Si H	..	..
03.29	2	?Dy II	..	.31
		?Si H	..	..
03.78	0.5	?Si H	..	..
		?Ho	..	.84
04.1	0.5?	?Si H	..	.11
04.34	1	Si H	..	.32
04.79	1.5	V	112	.78
05.19	3	V	27	.17
05.86	1	Si H	..	.82
		Tm	..	.84
06.28	1.5	?Fe	217	.27
		Si H	..	.30
06.65	1	Si H	..	.62
07.44	1.5	Si H	..	.41
		?Fe	354	.49
		?Zr	1.5*	.50
07.85	1	Si H	..	.76
		Si H	..	.87
08.45	2	Zr	32	.39
		Co	2	.49
09.08	1.5s	Si H	..	.05
		Nd II	17	.07
09.50	2?	Nd II	10	.46
		Si H	..	.60
09.77	2.5	Co	1	.71
		V	27	.79
		Si H	..	.82
10.60	2w	Co	29	.53
		Si H	..	.72
11.10	0	Si H	..	.09
11.39	0.8	Si H	..	.43
11.83	2w	V	27	.78
12.43	1?	Si H	..	.42
12.72	3	Ti	9	.71
13.52	1.5	V	52	.52
13.86	0.7	?Sm II	16	.90
14.14	0.6	Si H	..	.13
14.56	0.7	Si H	..	.51
15.16	2	V	27	.18
15.71	1?w	Si H	..	..
16.53	1.5	V	27	.47
16.81	1.5	V	27	.70
		..	..	..
17.51	1	Si H	..	.47
17.95	1.5	Si H	..	.91
18.52	1.5	?Fe	801	.55
18.78	0.5?	Co	28	.77
19.1	0.3?	Si H	..	.08
19.54	1?	Si H	..	.48
		Si H	..	.64
20.22	0.5s	Si H	..	.21
20.60	2w	V	41	.54
		?Si H	..	.61
21.39	2?	Co	28	.32
		Zr	32	.45
21.68	0.5?	Zr	1.5*	.67
22.04	0	..	..	..
22.70	1?w	Si H	..	.72
23.09	0.3	Si H	..	.02
23.49	2.5s	..	..	..
		V	27	.57
23.83	2	Nb	1	.81
24.95	1.5	Y II	14	.91
25.38	1.2	Si H	..	.35
26.54	0.5	Cr	35	.52
27.1	0.3	..	..	..
27.56	0.5	Y II	15	.57
28.05	3	Si H	..	.06
		V	27	.07
28.29	4	Y	5	.31
28.99	1	Si H	..	.93
29.40	0.3	..	..	..
29.75	2	Eu II	1	.73
		Si H	..	.81
30.4	0.3	?Zr	1.7*	.46
30.6	1	Ba II	4	.65
		Si H	..	.66
31.26	2w	Si H	..	.12
		Si H	..	.31
		Si H	..	.37
32.02	3	V	27	.02
		Si H	..	.05
		Fe	43	.06
32.43	0.3	..	..	..
32.8	0.5w	Si H	..	..
33.43	1	?Nd II	19	.36
		Si H	..	.44
33.83	0.5	..	..	..
34.25	3	Si H	..	.17
		Fe	3	.34
34.48	3	V	27	.49
34.92	0.5	Si H	..	.91
35.30	1s	?Rh	..	.27
		?Nd II	..	.33
35.72	1.5s	Zr	50	.68
		Si H	..	.70
36.08	0	..	..	..
36.46	2w	?V	26	.39
		Si H	..	.53
37.09	1	Nb	1	.09
37.59	1w	?Si H	..	..
39.70	3w	..	..	..
		Nb	1	.70
		..	..	..
40.63	1.3w	Si H	..	.54
		Si H	..	.72
41.27	0.5w	Pr II	10	.26
41.8	1w	Si H	..	.9
42.3	?	Si H	..	..
42.79	3	?V	26	.66
		Y	5	.86
43.1	?	Si H	..	.11
		?Pr	4	.14
43.89	1	Fe	43	.87
		Si H	..	.89
44.5	0.5	Si H	..	.54
		Si H	..	.70
44.99	0.7	Si H	..	.86
		Tc	0.4*	.02
45.36	0.5	Si H	..	.31
45.71	0.3	Si H	..	.68
46.28	2w	Si H	..	.19
		Si H	..	**.35**
46.70	2w	Si H	..	.62
47.27	1	Si H	..	.22
		?Zr	1.5*	.37
47.71	1.5s	Fe	42	.67
		Si H	..	.68
48.41	1.5w	Si H	..	.22
		Si H	..	.40
48.88	1s	?V	26	.86
		Si H	..	.91
49.40	0?	Si H	..	.40
49.77	2.5s	Fe	3	.76
50.35	0.7	Si H	..	.27
		?Co	16	.43
51.12	1w	Er	..	.10
52.08	1.5w	..	..	..
		Fe	18	.17
		?Sm II	16	.21
52.61	1s	?Si H	..	.56
		Nb	1	.58
		?Zr	1.4*	.64
53.02	0.6s	?Si H	..	.98
		?Cr	35	.07
53.32	0.7s	?V	26	.33
53.79	0.7?w	?Zr	1.6*	.75
		Cr	35	.82
54.54	0.4?	Fe	355	.50
55.03	1w	Si H	..	.87
		Si H	..	.06
55.7	1.5	Si H	..	.72
56.18	2	Nd II	10	.08
		Zr II	29	.24
		?Nd II	14	.26
56.83	0.5?	Fe	354	.80
57.05	0.5?	..	..	..
57.27	1	Si H	..	.24
57.79	1	Si H	..	.74
		Si H	..	.82
58.41	0.5	..	..	..
58.90	0.7	Si H	..	.88
59.64	2	V	25	.69
59.98	0	?Si H	..	.91
60.50	1w	..	..	..
61.17	0.3	..	..	..
61.7	0.4?	..	..	..
61.99	2w	Si H	..	.03
62.3	0.5?	Si H	..	.3
63.09	1.5	?Ho	..	.03
63.66	2	Nb	1	.66
64.21	2w	?Ti	163	.13
		?Si H	..	.33
64.73	2	Nb	1	.66
		Si H	..	.80
65.17	1w	Sc	20	.16
		?Si H	..	.20
65.98	1	Ba II	4	.00
66.38	2	?Ti	163	.31
		Zr	45	.37
66.9	0.3	Si H	..	.67
		Si H	..	.84
		Si H	..	.98
67.50	3	Y	7	.52
68.10	1.5	Nb	1	.12
68.50	0.7	Si H	..	.44
		? Zr	..	.45
68.94	0.5w	..	..	..
69.5	0.7w	Sm II	24	.48
69.8	0.5w	..	..	..
71.07	0.3	Ti	206	.02
71.53	0.5?	Zr	1.3*	.47
		Si H	..	.63
72.03	3	Ga	1	.05
72.74	2	Fe	19	.75
73.10	0	?Zr	0.6*	.13
73.39	0	Nd II	16	.38
74.09	4	Fe	19	.93
		Y	6	.14
74.93	2	Fe	19	.92
75.58	1	Gd	5	.54
		?Nd II	39	.61
		Fe	354	.64
76.08	0.3	..	..	..
76.33	0	Tc	..	.28
76.78	1.5	V	6	.79
77.49	3	..	..	..
		?Nd II	10	.32
		Y II	14	.54
		Co	2	**.59**
		Fe	18	.60
78.02	0	Sm II	16	.02
78.26	0	Si H	..	.25
78.64	1s	..	..	..
79.08	0.3?	..	..	..
79.47	3w	V	25	.42
		Pr II	4	.42
		?....	..	..
81.19	0.7w	Si H	..	.13
81.79	0.5	Fe	354	.76
82.60	1.5s	V	24	.59
83.33	1.5s	Zr	51	.31
83.77	1	?Sm II	4	.76
84.37	0.7w	?Gd II	15	.25
		..	..	..
84.90	1.5s	Fe	355	.90
85.13	0.3	..	..	..
85.38	0.3	..	..	..
86.13	2s	Ti	129	.12
86.83	1s	Dy	..	.81
87.09	1.5s	Fe	152	**.04**
87.55	2s	Zr	45	.56

TABLE 7 (Cont'd)

λ	Int.	IDENTIFICATION El.	Mult.	λ
87.84	1	Fe	152	.80
88.80	0.7	Si H	..	.78
		?..	..	..
89.49	1	Co	2	.50
89.86	1.3	V	24	.84
90.29	0.3	Si H	..	.24
90.73	4w	Co	1	.71
91.56	1.4	V	24	.56
92.11	1	Zr	1.6*	.10
93.5	0	Si H	..	.46
94.10	0.3	Zr	1.6*	.01
		?..	..	..
94.49	0	Zr	1.4*	.46
94.80	1.3	Zr	1.4*	.76
		Dy	..	.83
95.09	1.7w	..	..	..
96.23	0.7	Zr	1.6*	.14
		..	..	..
97.18	1w	?Fe	18	.10
		?SiH	..	.23
97.57	0.5?	?SiH	..	.62
98.23	0.4?	..	..	..
		Fe	152	.31
98.47	2w	Co	2	.42
99.21	2.5w	Zr	0.6*	.08
		Y II	5	.27
99.99	2	Fe	3	.97

4200

λ	Int.	IDENTIFICATION El.	Mult.	λ
00.89	1.3	V	6	.89
01.45	1.2s	Zr	45	.45
02.05	1.5	Fe	42	.03
02.64	0	..	..	..
03.10	0.5?	Sm II	42	.05
03.56	1	Fe	19	.57
		?Cr	35	.59
04.3	0.3?	..	..	..
04.66	1s	Y II	1	.69
05.03	0.8	Eu II	1	.05
05.29	0.3	..	..	..
05.68	0.4	?Nd II	19	.60
06.2	0.5	?Sm II	38	.13
06.68	3.5	Fe	3	.70
08.21	1w	..	..	..
09.05	0.4w	..	..	..
09.89	2	V	24	.86
10.38	1	Fe	152	.35
11.34	0	Zr	1.8*	.34
11.74	0.5	Dy	..	.72
		Ti	279	.73
13.88	1.5	Zr	45	.86
15.44	10	Sr II	1	.52
16.07	6	Fe	3	.19
..	..	..	..	..
26.7	50	Ca	2	.73
..	..	..	..	..
32.6	0.5	Fe	3	.72
34.01	0.7	Co	1	.00
		V	6	.00
34.55	1	V	6	.52
		?Sm II	42	.57
		Zr	0.6*	.63
35.88	1.5w	Y II	5	.73
		Y	5	.94
		Fe	152	.94
36.57	1	?Zr II	110	.56
37.07	0.3	Fe	19	.08
38.20	1.4	Tc	0.0*	.19
38.90	0	Fe	693	.82
39.32	2	Zr	45	.31
39.86	0.7	Fe	18	.85
40.36	2	Zr	45	.35
41.20	2	Zr	45	.20
		?Al H	..	.0
41.67	1	Zr	45	.68
42.04	1	?Zr	0.0*	.01
		..	..	..
42.47	0.3	..	..	..
43.01	0.7	?Ru	..	.06
43.38	0.3?	..	..	..
43.60	0.7	Zr	1.5*	.56
44.02	0.5	..	..	..
45.23	2w	..	..	..
46.47	0.7	..	..	..
46.85	2	Sc II	7	.83
47.43	2w	Nd II	8	.37
		?..	..	..
47.96	0.3	..	..	..
48.44	0.5	Fe	19	.40
49.20	0	..	..	..
49.56	0.8	?Sm II	..	.54
50.20	2.5w	Fe	152	.12
		?..	..	..
50.80	1.3	Fe	42	.79
51.29	0.4	?Al H	..	..
51.74	0	Gd II	15	.73
52.29	2	Co	1	.30
54.31	15w	Cr	1	.35
56.02	1.3	Ti	252	.02
		Zr	0.0*	.04
56.45	1	Sm II	37	.39
		Zr	0.5*	.44
56.88	0	..	..	..
57.26	0.3	?Zr0	..	.1
58.31	4	Fe	3	.32
59.29	2.5	V	6	.31
59.67	0.6?	?Al H	..	.5
60.05	1?	?Al H	..	..
60.48	1.3	Fe	152	.48
60.88	1.3	Os	1	.85
61.21	0.3	Zr	0.7*	.20
61.66	1	Ti	252	.61
62.26	5	Tc	0.0*	.26
63.16	1?	Ti	162	.13
63.41	1	?Al H	..	..
64.08	1w	?Zr	..	.02
		?Ho	..	.07
64.47	1s	?Al H	..	..
65.19	0.3?	..	..	..
65.73	2	Ti	162	.72
		Zr	0.1*	.75
66.18	0	..	..	..
66.65	1	Nd II	58	.72
67.09	1.2	?Al H	..	..
68.04	2.5	Zr	45	.01
		Co	1	.03
68.68	1.3	V	88	.64
69.15	0.7	..	..	..
69.76	0	..	..	..
70.17	0	?Ti	251	.14
70.57	0.5	Nd II	12	.56
71.16	1	Fe	152	.16
71.76	3	Fe	42	.76
72.44	2	Ti	44	.44
72.74	1	Nd II	11	.79
74.76	10w	Cr	1	.80
76.42	0.5	Ti	148	.44
76.70	1	?Zr	0.5*	.71
76.93	0.4	V	88	.96
77.59	0.7	?Al H	..	..
78.55	0.4w	Tb II	..	.54
79.69	0.4	Sm II	27	.68
79.95	0.4?	..	..	..
80.53	1	Gd II	15	.49
		?...	..	..
81.37	2	Ti	44	.37
82.23	1.5	Zr	45	.20
82.6	1.3?	?Ti	162	.70
83.02	3	Ca	5	.01
83.58	0.3?	?Al H	..	..
83.81	1.5	?Fe	19	.87
84.06	0.5	V	88	.06
84.55	0.4w	Nd II	10	.52
85.00	1	Ti	148	.99
85.47	0	Sm II	27	.50
85.77	0.3	Co	1	.78
86.01	3	Ti	44	.01
86.59	0.3	?Er	..	.56
		?Sm II	42	.64
87.05	1.5	?La II	75	.97
		..	..	..
87.45	3.5	Ti	44	.40
88.17	1.5	Ti	43	.16
89.05	2	Ti	44	.07
89.59	12	Ca	5	.36
		Cr	1	.72
90.55	0.8	..	..	..
90.91	1.4	Ti	44	.93
91.42	4	Zr	0.5*	.34
		Fe	3	.47
91.88	2	V	120	.82
92.69	0.8	Ti	79	.68
93.4	0.6w	..	..	..
94.14	2	Fe	41	.13
94.79	2	Sc II	15	.77
		Zr	45	.78
95.75	3s	Ti	44	.75
96.11	0.5?	V	120	.11
96.77	2?	?Sm	3	.74
		?Zr II	98	.74
97.01	5	Tc	0.0*	.06
97.76	1	V	120	.68
		Pr II	7	.76
97.98	0.8	?Al H	..	..
		?V	120	.03
98.66	3s	Ti	44	.66
98.9	2	Ca	5	.99
99.2	3	Ti	148	.23
		?Fe	152	.24
99.64	3s	Ti	43	.64

4300

λ	Int.	IDENTIFICATION El.	Mult.	λ
00.11	0	Ti II	41	.05
00.54	4	Ti	44	.57
01.08	4	Ti	44	.09
01.58	0.4?	Zr	1.6*	.58
02.04	1w	..	..	..
02.52	3	Ca	5	.53
02.90	1.5	Zr	45	.88
03.25	0.8	Co	1	.24
03.59	2	Nd II	10	.57
04.73	2	Zr	0.5*	.68
05.5	0.5 ?	..	..	..
05.85	3	Sc II	15	.72
		Ti	44	.91
06.23	2.5	V	5	.21
06.96	1?	Ti	43	.94
07.15	2	V	5	.18
07.86	2.5	Fe	42	.91
08.61	2	Dy II	..	.62
09.05	1	Sm II	15	.01
		Zr	..	.10
09.73	5w	Y II	5	.62
		?V	5	.80
		Zr	0.5*	.82
10.40	0.3	?Ti	79	.37
		?Zr	1.4*	.48
10.6	0.5w	?Ir	..	.59
11.25	0	..	..	..
12.45	0.5	..	..	..
12.89	0.5?	?Ti II	41	.86
13.0	bh?	Zr0	..	..
13.36	bh?	Zr0	..	.3
13.92	0.5w	Gd	4	.84
		Zr	..	.97
		Sc II	15	.08
14.38	1.5	Ti	45	.36
14.79	1.7	Ti	43	.80
15.50	0	..	..	..
18.64	2s	Ca	5	.65
19.04	2	Sm II	27	.94
		Zr	0.2*	.05
20.49	0	?Gd	..	.53
20.78	0	Sc II	15	.74
21.16	1.6	Zr	0.2*	.17
21.72	0	..	..	..
23.4	0.6w	?Sm II	8	.28
		?Ti	79	.44
24.06	0.2	Zr	1.8*	.03
25.08	1?	Sc II	15	.01
25.47	1?	Zr	0.7*	.44

TABLE 7 (Cont'd)

λ	Int.	IDENTIFICATION El.	Mult.	λ
25.74	4	Fe	42	.76
26.38	2	Ti	43	.36
27.05	1.7	Ti	43	.99
28.00	0.7w	..	..	..
28.67	0	..	..	..
29.06	0.7?	Sm II	15	.02
29.56	1.5	Zr	0.1*	.56
		Gd	..	.58
30.02	3	V	5	.02
30.76	0	..	..	..
31.82	1	..	..	..
32.82	4s	V	5	.82
34.0	0.5?w	..	..	..
34.85	1	Ti	43	.84
35.74	0.3	?Pr	..	.75
36.12	0.5	Zr	0.6*	.11
36.45	0	..	..	..
37.07	2	Fe	41	.05
37.54	3	Cr	22	.57
38.11	0.7w	?Zr	1.6*	.11
		?..	..	..
38.4	0.3	?Tb	..	.45
38.7	0.3?w	?Nd II	68	.70
39.45	2s	Cr	22	.45
39.72	1	Cr	22	.72
41.02	3?	V	5	.01
41.48	1.6?	..	..	..
42.11	1.5w	..	..	..
		?Gd II	15	.18
42.51	0	?Tb	..	.50
43.02	3	..	..	..
		?Zr	0.0*	.04
44.49	3	Cr	22	.51
45.20	0.5w	..	..	..
46.53	1.5	Gd	4	.46
		Zr	1.7*	.53
47.20	3s	Zr	0.1*	.23
		Fe	2	.24
47.89	2	Zr	1.0*	.89
48.8	1w	?Y	..	.79
		Zr	0.7*	.93
50.45	0	Sm II	46	.46
51.12	1.5w	Cr	22	.05
		?Nd II	10	.30
51.77	2s	Cr	22	.77
52.85	4	V	5	.87
	bh?	..	..	..
53.14	0.4?	..	..	..
53.79	0.3	..	..	..
54.11	0.2?	..	..	..
54.8	0.8	?Eu	..	.79
55.0	0.8	?Pr	..	.91
		?Eu II	22	.10
55.95	3	V	5	.94
		?..	..	..
56.56	1.5w	..	..	..
57.25	0	..	..	..
57.75	0	..	..	..
58.22	1	Nd II	10	.17
58.74	2	Y II	5	.73
		Zr	0.5*	.74
59.64	1.5s	Cr	22	.63
60.81	1.3	Zr	31	.80
61.97	2w	Co	1	.91
		Zr	0.1*	.94
63.52	1	V	23	.52
66.0	0.3	..	..	..
66.43	0.7	Zr	61	.45
67.03	0.3	..	..	..
68.03	1.5	V	5	.04
	bh	Zr0	..	.2
68.30	0.4?	Pr II	5	.33
68.66	0.4	Nd II	11	.63
71.29	2s	Cr	22	.28
72.38	1w	..	..	..
73.28	0.7s	Cr	22	.25
73.87	0.4	?Gd	..	.84
74.44	0.3	Sc II	14	.46
74.96	3	Y II	13	.94
75.71	3	?Fe	2	.93
75.91	4	Fe	2	.93
79.21	4	V	22	.24
79.74	0.6	..	..	..
83.52	4	Fe	41	.55
84.20	1	..	..	..
84.68	4	V	5	.72
84.96	3	Cr	22	.98
85.68	1.7	Nd II	50	.66
87.23	0.5w	?V	40	.21
88.10	0.6	..	..	..
89.21	4	Fe	2	.24
89.97	3	V	22	.97
90.85	0.3	Sm II	15	.86
91.75	0.8	Cr	22	.75
92.10	1.3	V	23	.07
93.27	1w	..	..	..
93.92	1w	?V	40	.84
		?Ti	244	.92
94.42	3w	?Re	..	.38
		Zr	0.1*	.49
94.91	0.5?	Zr	61	.94
95.21	3	Zr	0.5*	.20
		V	22	.23
98.03	2.5	Y II	5	.02
98.98	1.5w	..	..	..
99.86	0	?Ti II	51	.77

4400

λ	Int.	IDENTIFICATION El.	Mult.	λ
00.25	0.3	Zr	0.7*	.23
00.56	3	V	22	.58
00.82	2	Nd II	10	.83
01.58	0.3	?Ni	86	.55
01.86	0.5	?Gd	..	.85
02.99	1.3	Zr	0.5*	.96
03.36	0.5	Sm II	22	.36
03.75	0	?Ir	..	.78
04.37	2	Ti	218	.28
		?Ti	78	.40
04.79	2?	Fe	41	.75
04.98	4	V	23	.01
		Fe	2	.02
05.26	1?	..	..	..
05.73	1	Ti	78	.69
06.12	0.7	V	40	.15
06.64	4s	V	22	.64
07.11	0.7	..	..	..
07.64	4s	V	22	.64
08.18	3s	V	22	.20
08.51	3s	V	22	.51
08.84	3s	Pr II	4	.84
		?..	..	..
09.36	1	?Sm II	..	.34
09.69	0.2	Zr	0.7*	.63
10.69	0.3	..	..	..
11.11	2	Nd II	8	.05
12.24	3w	?Pr II	8	.16
		Cr	22	.25
		?Nd II	9	.26
13.06	1	Zr	61	.04
13.75	1	?Pr II	26	.76
14.15	2	Zr	0.2*	.14
		?..	..	..
14.44	0.3?	?Nd II	3	.43
14.73	0.5	?Gd	..	.74
15.14	2	Fe	41	.12
15.58	0.8	Sc II	14	.56
16.48	4	V	22	.47
17.31	1	Ti	161	.27
18.40	0.3	..	..	..
18.77	0.3	..	..	..
19.58	0.5	?Pr	..	.67
19.94	2.5s	V	21	.94
20.51	2w	Zr	61	.45
		?Os	1	.47
		?Sm II	32	.53
21.15	0.7	Sm II	37	.14
21.58	3s	V	22	.57
21.77	0.5?	Ti	218	.75
22.51	3	?V	79	.48
		?Y II	5	.59
22.81	2.5	Ti	78	.82
23.22	1	V	40	.21
24.38	1w	Sm II	45	.34
		?Nd	..	.34
25.43	3s	Ca	4	.44
26.01	3	V	22	.00
		Ti	161	.05
26.76	0.5	..	..	..
27.24	6	Fe	2	.31
28.52	3s	V	21	.52
29.16	2.5w	Zr	0.6*	.09
		?Pr II	2,4	.24
29.81	3	V	22	.80
30.38	1	Ti	113	.37
30.63	2	Fe	68	.62
31.50	1	Zr	61	.48
32.26	0.3	..	..	..
32.94	0.5	?La II	11	.95
33.98	2.5	Sm II	41	.88
		Ti	113	.00
34.33	0.4	Sm II	36	.32
35.06	7w	Ca	4	.96
		Fe	2	.15
35.66	3	Eu II	4	.58
		Ca	4	.69
36.14	3s	V	21	.14
36.63	0.8	Ti	160	.59
37.37	1	..	..	..
37.91	6w	V	21	.84
		Zr	0.5*	.04
39.02	0.5	..	..	..
39.50	0.4w	..	..	..
40.37	2	Ti	159	.34
41.30	1s	Ti	160	.27
41.69	5s	V	21	.68
42.36	2?	Fe	68	.34
43.28	0.5?	?Fe	350	.20
43.74	2	?Ti II	19	.80
44.21	5s	V	21	.21
45.47	5	Fe	2	.48
46.39	0.7?	?Nd II	49	.39
46.64	3	..	..	..
47.19	0	..	..	..
47.75	2	Fe	68	.72
48.89	0.5?	?Zr	0.6*	.94
49.13	3w	Ti	160	.14
49.79	2.5w	..	..	..
		Pr II	4	.87
50.34	1	Zr	1.3*	.27
50.52	0.3?	?Ti II	19	.49
50.92	3s	Ti	160	.90
51.59	3	Nd II	50	.57
		?Mn	22	.59
52.02	3	Nd II	6	.98
		V	87	.01
52.75	1.5	Sm II	26	.73
53.31	3s	Ti	113	.31
53.72	2s	Ti	160	.71
54.40	0.5?	?Pr II	5	.38
54.76	5s	Ca	4	.78
55.33	4s	Ti	113	.32
55.89	4s	Ca	4	.89
56.4	0.3?	?Zr	1.8*	.30
		Nd II	50	.39
56.63	2w	Ca	4	.61
57.45	5s	Ti	113	.43
		V	21	.48
57.76	0.5?	V	101	.76
58.53	2	Sm II	7	.52
59.06	3	?Zr	0.2*	.02
		Fe	68	.12
59.75	5s	V	21	.76
60.30	5	V	21	.29
		Zr	0.6*	.33
	bh	Zr0	..	.4
61.62	5	Fe	2	.65
62.06	4.5	Ti	8	.10
62.39	1?	V	87	.36
		?Nd II	54	.41
62.98	2.5	Nd II	50	.98
63.48	1w	Ti	160	.39
		Ti	160	.54

TABLE 7 (Cont'd)

λ	Int.	IDENTIFICATION El.	Mult.	λ
65.06	1s	Nd II	5	.08
		?Pr	..	.08
65.55	0.4?	?Nd II	13	.60
65.79	2	Ti	146	.81
66.54	4	Fe	2	.57
66.92	1	Co	150	.88
68.71	2	?Pr II	20	.71
		Zr	0.5*	.78
69.45	bh	Zr0	..	.4
71.27	0.5?	Ti	146	.24
71.65	2?w	Fe	2	.68
	bh	Zr0	..	.5
74.87	0.5	Ti	113	.85
79.68	0.5	Ti	146	.72
80.55	0.3	?Ti	146	.60
81.27	1	Ti	146	.26
82.15	3	Fe	2	.17
82.72	1	?Ti	113	.69
89.08	2w	Ti	146	.09
89.73	4	Fe	2	.74
93.82	bh	Zr0	..	.8
96.19	2?	Ti	146	.15
		?V	8	.24
	bh	Zr0	..	.2
96.84	1.5	Cr	10	.86
4500				
07.17	3	Zr	31	.11
		?Zr	0.1*	.26
12.72	2s	Ti	42	.73
18.01	3s	Ti	42	.02
19.63	1?	?Sm II	49	.63
	?bh	Zr0	..	.3
22.79	3	Ti	42	.80
23.42	0.5?	?Nb	..	.41
23.94	1?	Zr	0.6*	.91
		?Sm II	41	.91
27.36	5	Ti	42	.30
		?..	..	..
27.83	1?	?Y	14	.80
28.67	2?	Fe	68	.62
33.22	5s	Ti	42	.24
34.3	bh	Zr0	..	.4
34.74	4?	Ti	42	.78
35.59	3?	Ti	42	.57
35.94	5	Ti	42	.92
		Ti	42	.05
37.7	1w	V	82	.66
40.02	1	Zr	0.6*	.98
		?V	100	.01
40.48	3	Ti	8	.48
41.29	0.5	Nd II	58	.27
42.21	2	Zr	49	.22
44.68	3	Ti	42	.69
45.45	0.5	V	109	.39
45.95	2.5	Cr	10	.96
48.75	2.5	Ti	42	.76
52.46	3	Ti	42	.45
52.61	0	Sm II	23	.66
53.01	1	Zr	31	.01
53.98	7	Ba II	1	.03
55.13	1	Zr	1.5*	.12
55.49	3	Ti	42	.49
		Zr	1.5*	.52
56.17	1	Nd II	6	.14
57.68	1	..	..	..
59.92	1	..	..	..
60.75	1	V	109	.71
61.20	1.2	..	..	..
62.60	3	Ti	7	.64
63.20	1	?Pr	..	.13
		?Nd	..	.22
65.51	2	Cr	21	.51
66.22	0.7	Sm II	32	.21
71.10	4	Mg	1	.10
75.48	5	Zr	5	.52
77.16	4.5	V	4	.17
77.72	0.8	Sm II	23	.69
78.60	1	Ca	23	.56
78.91	1.3	?Nd	..	.88

λ	Int.	IDENTIFICATION El.	Mult.	λ
80.05	3	Cr	10	.06
80.38	4	V	4	.39
81.36	2.5w	?..	..	..
		Ca	23	.40
85.84	3?w	Ca	23	.87
86.35	4s	V	4	.36
90.53	2s	Zr	0.5*	.55
91.41	2.4s	Cr	21	.39
92.67	1	Fe	39	.66
94.09	5	V	4	.10
4600				
00.75	3s	Cr	21	.75
02.57	0.5	Zr	1.9*	.57
02.98	1	Fe	39	.94
04.16	1?	?Sm II	..	.18
04.42	2	Zr	29	.42
06.14	3s	V	4	.15
06.57	1?	Sm II	1	.51
06.76	1?	?Nb	..	.77
07.29	8	Sr	2	.33
09.82	0.5?	Zr	0.6*	.83
10.12	0.5?	Zr	0.5*	.11
12.21	1	?Dy	..	.28
13.38	3s	Cr	21	.37
15.71	1?	Sm II	22	.69
16.13	4s	Cr	21	.14
16.92	1?	..	..	..
17.29	3s	Ti	145	.27
18.48	1w	..	..	..
19.75	bh	Zr0	..	.8
23.13	2	Ti	145	.10
26.16	2	Cr	21	.19
26.4	1?	Zr	1.8*	.42
32.86	2?	..	..	..
33.95	4	Zr	5	.99
35.20	3	V	4	.18
37.77	bh	Zr0	..	.8
43.66	2	Y	4	.69
46.16	0.7	Cr	21	.17
51.28	3	Cr	21	.28
52.18	3.5	Cr	21	.16
56.45	3	Ti	6	.47
67.55	2	Ti	6	.58
74.78	3	Y	4	.84
76.94	1	Sm II	3	.91
81.87	4	Ti	6	.91
87.22	1	Sm II	3	.18
87.80	2s	Zr	43	.80
88.44	3	Zr	5	.45
90.84	0.8	Ti	76	.83
91.34	2	Ti	75	.34
91.77	0.7	Zr	0.6*	.73
93.65	4	?Sm II	14	.63
		Ti	6	.67
98.13	2w	?Eu	..	.14
98.77	3	Ti	75	.77
4700				
00.18	1.5w	Zr	..	.09
		Zr	0.5*	.18
03.5	1	..	..	..
04.38	1.2	Sm II	1	.40
06.57	1.5s	Nd II	3	.54
		V	119	.57
09.70	1	Nd II	7	.71
10.13	4	Zr	43	.08
		Ti	75	.19
11.93	1	Zr	64	.91
15.28	4	Ti	6	.30
17.64	2.5	Zr	0.6*	.62
		V	119	.69
19.13	1	Zr	66	.12
19.87	1	Sm II	3	.84
22.62	2.5	Ti	75	.60
23.18	2	Ti	75	.17
28.70	1	Sc	14	.77
29.23	1.5	Sc	14	.23
31.15	0.7	Zr	0.6*	.14
32.33	2	Zr	48	.34

λ	Int.	IDENTIFICATION El.	Mult.	λ
34.10	1	Sc	14	.09
36.93	bh	Zr0	..	.9
39.47	3	Zr	43	.48
41.04	1s	Sc	14	.02
41.90	1.5w	Sr	5	.92
42.81	1w	Ti	233	.79
43.82	1.5s	Sc	14	.81
53.16	2.3s	Sc	5	.15
54.04	1	Mn	16	.04
55.92	0.7w	?Eu	..	.94
56.23	0.5?	..	..	..
58.17	0.7	Ti	233	.12
58.88	2	Ti	41	.91
59.31	1	Ti	233	.27
60.98	5	Y	4	.98
63.9	0.5	Nd II	6	.86
71.12	1	Ti	41	.10
72.31	3s	Zr	43	.32
72.91	0.5	..	..	..
73.76	0.4	..	..	..
75.34	0.4	..	..	..
76.19	0.8w	..	..	..
77.84	1	Sm II	3	.85
79.35	4	Sc	5	.35
81.04	1	Y	13	.04
81.73	2	Ti	41	.72
82.64	0.3	Zr	0.2*	.60
83.40	1.5	?Ti	41	.31
		?Pr	..	.35
		Mn	16	.42
83.90	0.4	..	..	..
84.45	3	V	3	.48
84.93	1.5	Zr	44	.94
86.51	0.5	?V	113	.52
88.69	1	Zr	43	.69
89.15	1	Zr	0.6*	.12
89.39	1	?Cr	31	.35
		Nd	..	.43
89.85	0.3	Ti	41	.80
91.52	2	Sc	5	.50
99.38	2	Y	13	.30
99.78	4	V	3	.79
4800				
01.62	0.7?	..	..	..
01.96	1	..	..	..
05.47	0.4	..	..	..
05.88	2	Zr	43	.88
06.42	0.3?	..	..	..
06.75	1	?Zr	1.6*	.68
09.52	0.7	Zr	1.6*	.48
11.35	1	Nd II	3	.34
15.06	2.5	Zr	44	.05
15.66	4	Zr	43	.62
17.4	bh	Y0	..	.4
19.68	0.4	Y	13	.64
20.43	2	Ti	126	.41
21.72	0.4	?Gd	..	.71
23.52	2w	Mn	16	.52
24.30	2.5	Zr	43	.29
25.16	0.5?	..	..	..
25.49	1.5	?Ti	250	.44
		Nd II	3	.48
26.55	0.5	..	..	..
27.04	0.7?	..	..	..
27.43	4	V	3	.46
	bh	Zr0	..	.5
28.05	2	Zr	44	.05
29.34	0.5	Cr	31	.38
31.62	4	V	3	.64
32.41	4	V	3	.43
33.29	0.5w	?Sm II	..	.33
34.17	0.7w	..	..	..
35.7	bh?	..	..	..
39.87	1	Y	13	.87
40.86	3	Ti	53	.87
41.44	0.5	?Zr	0.6*	.45
45.67	1	Y	13	.67
46.4	bh	Zr0	..	7.1
48.2	bh	?Zr0	..	..

λ	Int.	IDENTIFICATION El.	Mult.	λ
50.6	bh?	?Zr0	..	..
51.45	3	Zr	43	.36
		V	3	.48
52.72	0.7	Y	13	.69
56.02	0.6	Ti	231	.01
56.76	0	?Gd	..	.74
57.19	0	..	..	..
57.65	0	..	..	..
58.04	0	..	..	..
58.90	0.8	Nd II	3	.03
59.8	0.5?	Y	13	.84
64.70	3	V	3	.74
65.32	0.3	..	..	..
66.08	1	Zr	44	.07
67.8	0.3	..	..	..
68.30	0.5	Ti	231	.26
70.15	1	Ti	231	.13
71.44	0.4w	?Fe	318	.32
		?Gd	..	.52
72.21	0.4	Fe	318	.14
73.60	0	..	..	..
75.47	3	V	3	.46
78.12	0.7	?Ca	35	.13
81.28	1?	Zr	44	.25
81.53	3	V	3	.55
83.67	2	Zr	44	.61
		Y II	22	.69
84.62	0.4	..	..	..
85.07	1	Ti	157	.08
89.11	0.5	?Re	1	.15
90.78	1	Fe	318	.76
91.53	1	Fe	318	.50
4900				
00.00	2w	Ti	157	.91
		Ba II	3	.93
		Y II	22	.13
05.11	0.3	Zr	43	.09
08.23	0.5w	Zr	..	.10
		Zr	1.9*	.29
09.10	1.5	Ti	39	.10
10.84	0	Zr	0.7*	.78
11.66	0	Zr	..	.60
13.62	1	Ti	157	.62
14.46	0	?Nd II	52	.38
15.28	0	Ti	157	.24
19.06	0.5	Fe	318	.00
19.89	0.5	Ti	200	.87
20.64	2	..	..	..
		Nd II	2	.69
21.84	1	Ti	200	.77
		?La II	7	.80
24.54	0.6	..	..	..
25.67	0.7?	V	50	.66
26.17	1	Ti	39	.15
27.12	0.6	..	..	..
28.37	0.3	Ti	200	.34
34.04	9	Ba II	1	.09
37.72	1.5	Ti	39	.72
39.71	3	Fe	16	.69
40.95	1	..	..	..
41.26	1.5	Ti	39	.32
42.50	2	Cr	9	.50
43.06	0.4?	?Ti	52	.07
43.95	0.7	..	..	..
46.09	0.5	..	..	..
46.78	0	..	..	..
47.66	1?	..	..	..
47.96	2	Ti	39	.99
48.76	2	Zr	28	.77
49.80	0.8w	?La	4	.76
		?Zr	..	.94
50.29	0.7w	..	..	..
51.08	0.4?	..	..	..
51.34	0.7	?Pr	..	.36
53.0	0.8w	..	..	..
53.23	1w	?Co	14	.18
54.4	bh	Ti0	..	.6
58.28	0.4	Ti	52	.26
59.15	1	Zr	..	.12
		Nd II	1	.13
64.91	1	Cr	9	.93
67.29	2	Ti	5	.30
72.65	0.5	..	..	..
73.03	0.4	Ti	173	.05
77.81	0.4	Ti	173	.73
78.27	0.5	Ti	173	.19
79.9	0.6w	..	..	..
81.73	3	Ti	38	.73
87.86	0.4	Zr	2.0*	.83
		?Co	14	.85
89.09	1.5w	?..	..	..
		Ti	173	.14
91.06	3	Ti	38	.07
94.13	2	Fe	16	.13
96.7	0.5?	..	..	..
97.06	5	Ti	5	.10
99.49	3	Ti	38	.50
5000				
01.00	0.3	Ti	173	.99
06.24	0.3	?Fe	318	.13
07.22	3	Ti	38	.21
09.25	0.8?	..	..	..
09.63	4w	Ti	5	.65
12.09	3w	Fe	16	.07
		?..	..	..
13.32	0.7	Ti	173	.28
		?Cr	60	.32
14.19	4w	Ti	5	.18
		Ti	38	.28
15.10	0.3	..	..	..
15.75	0.3	..	..	..
16.18	2	Ti	38	.16
20.03	2	Ti	38	.03
21.93	0.4	Cr	8	.90
22.88	2	Ti	38	.87
24.5	0.7?	..	..	..
24.85	2	Ti	38	.84
25.59	0.8?w	Cr	20	.54
		Ti	173	.57
35.92	3	Ti	110	.91
36.48	2.5	Ti	110	.47
37.94	0.4	..	..	..
38.40	2	Ti	110	.40
39.03	0.6	?Nb	..	.04
39.94	6w	Ti	5	.96
40.61	2s	Ti	38	.64
41.13	1	Fe	16	.07
41.73	2w	Fe	36	.76
43.09	0.5w	..	..	..
43.62	3	Ti	38	.58
45.07	0.4?	..	..	..
45.46	1.5	Ti	38	.40
		?Pr	..	.53
46.63	0.5	Zr	62	.61
49.84	0.5w	Fe	114	.82
51.66	3w	Fe	16	.64
51.87	2?	Cr	8	.90
58.02	0.5	..	..	..
60.05	4	Fe	1	.08
63.65	0.5	..	..	..
64.59	7w	Ti	5	.65
66.02	0.6s	Ti	110	.98
70.20	2	Sc	13	.25
		?Zr	1.8*	.27
71.50	2	Ti	110	.48
72.96	1	Cr	8	.92
74.02	1	?Zr	0.5*	.00
75.82	0.8s	Sc	13	.81
78.28	0.8	Zr	62	.28
79.0	0.5	?Nb	..	.96
79.74	1	Fe	16	.74
81.58	2	Sc	13	.55
83.33	1	Fe	16	.34
83.71	1.3	Sc	13	.71
85.48	2w	?Ti	109	.33
		Sc	13	.55
86.99	3	Sc	13	.95
		?Ti	109	.06
89.9	bh?	..	..	..
91.92	0.5	Cr	20	.89
92.89	0.5	?Nd II	48	.80
95.33	1.2w	?Nb	..	.30
96.76	1	Sc	13	.72
98.81	0.5	Fe	66	.70
99.22	1	Sc	13	.23
5100				
00.19	0.5	?Nb	..	.16
		?Sm II	..	.20
		?Sm	..	.30
01.17	1.5	Sc	13	.12
07.58	2w	Fe	16	.45
		Fe	36	.64
10.32	4	Fe	1	.41
13.47	1	Ti	109	.45
20.38	1	?Nb	..	.30
		?Ti	288	.42
		?Zr	2.0*	.42
23.80	1.5w	Fe	16	.72
		?..	..	..
27.54	4	Fe	16	.36
		Fe	1	.68
33.42	1.2	Zr	27	.42
34.84	0.7	?Nb	..	.75
37.12	1	..	..	..
38.40	0.5	..	..	..
39.56	1.5w	..	..	..
43.0	1.5w	Fe	16	.93
		..	..	..
45.49	1.7	Ti	109	.46
		Zr	2.1*	.46
47.46	5	Ti	4	.48
50.85	2	Fe	16	.84
52.14	5	?Fe	16	.92
		Ti	4	.18
53.34	0.5	..	..	..
55.47	0.5	Zr	1.6*	.46
56.52	0.6	..	..	..
66.18	5	Fe	1	.29
67.40	3w	Mg	2	.32
		Fe	37	.49
68.89	2	Fe	1	.90
71.66	0.6	Fe	36	.60
72.72	2s	Mg	2	.68
73.69	5	Ti	4	.74
75.69	1.5	Fe	1	.71
83.66	3	Mg	2	.60
85.0	bh	Zr0	..	.0
88.8	0.7	..	..	..
91.49	0.7	Nd II	45	.45
		?Fe	383	.46
92.98	4	Ti	4	.97
94.94	0.7	Fe	36	.94
5200				
00.3	1w	..	..	..
01.18	1	Zr	0.5*	.17
02.48	0.5	?Fe	66	.34
04.51	4	Cr	7	.52
		Fe	1	.58
05.97	4	Cr	7	.04
08.40	3	Cr	7	.44
10.34	4	Ti	4	.39
11.26	0.6	Ti	37	.22
12.42	1	?Nd II	44	.36
14.26	0.4	..	..	..
14.91	0.8	..	..	..

TABLE 7 (Cont'd)

λ	Int.	IDENTIFICATION El.	Mult.	λ
15.7	0.5	..	..	..
16.29	1	Fe	36	.28
17.59	0.7	..	..	..
19.65	4	Ti	4	.70
21.03	0.6	..	..	..
24.19	1.5	..	..	..
24.98	1.3	Zr	27	.94
25.55	3	Fe	1	.53
27.22	2	Fe	37	.19
28.23	1w	..	..	..
32.98	1	Fe	383	.95
33.83	1	Ti	37	.82
35.04	3	?Zr	0.0*	.07
37.23	1w	..	..	..
38.56	3	Ti	37	.56
39.95	1	Ti	37	.94
46.53	2	Ti	37	.57
47.03	4s	Fe	1	.05
47.57	2s	Cr	18	.56
50.18	3	Fe	1	.21
50.97	1	Ti	37	.95
51.57	0.7	?Ti	37	.49
52.09	3	Ti	4	.10
54.95	3	Fe	1	.96
55.55	1	Nd II	43	.51
61.73	1.3	Ca	22	.71
62.22	1	Ca	22	.24
64.17	4	Cr	18	.15
		?Ca	22	.24
65.78	4w	?Ca	22	.56
		Cr	18	.72
		?..	..	..
68.12	0.6	..	..	..
68.70	0.4	..	..	..
69.56	4	Fe	15	.54
70.32	2.5	Ca	22	.27
		Fe	37	.36
71.64	1	..	..	..
72.93	0.7	..	..	..
73.45	0.5s	Fe	114	.38
75.48	0.5	?Re	1	.54
76.94	1s	..	..	..
77.44	2s	Zr	27	.40
80.06	1w	Zr	1.6*	.06
81.31	0.4?	..	..	..
81.99	0.4?	..	..	..
82.42	2s	Ti	74	.38
83.52	1.7	..	..	..
84.39	1	Ti	74	.38
85.35	0.4	..	..	..
86.85	0.7	..	..	..
88.13	1	..	..	..
88.95	0.5?	..	..	..
89.31	2	?Ti	36	.28
90.55	1	..	..	..
93.2	bh	..	..	..
94.88	0.5	Zr	1.0*	.82
95.81	2	Ti	74	.78
96.71	3.5	Cr	18	.69
97.36	1	..	..	..
98.30	4	Cr	18	.27
99.62	0.4	..	..	..

5300

λ	Int.	IDENTIFICATION El.	Mult.	λ
00.02	1	Ti	74	.01
00.76	3	Cr	18	.75
01.97	3	Sc	4	.94
03.19	0.5s	..	..	..
03.78	0.7w	?Zr	1.7*	.80
		?Eu	..	.87
04.6	bh	Zr0	..	.6
05.9	bh	Zr0	..	.0
11.44	1	Zr	27	.42
19.87	0.5	Nd II	75	.82
23.94	1.5w	Ti	36	.96
28.01	3	Fe	15	.04
28.57	1	Fe	37	.53
30.89	2	?Zr	0.1*	.83
32.4	bh	Zr0	..	.5
38.36	0.5	Ti	35	.33
41.18	0.5	?Fe	37	.03
		..	..	..
43.00	1.3	Sc	4	.96
45.83	3	Cr	18	.81
48.34	2	Cr	18	.32
49.1	bh?	..	..	..
49.69	1	Sc	4	.70
60.5	bh	Zr0	..	.7
62.60	0.8	Zr	27	.56
64.3	bh	Zr0	..	.3
66.26	0.5	..	..	..
66.66	1	Ti	35	.65
69.68	2w	..	..	..
71.47	3	Fe	15	.49
75.3	bh	Zr0	..	.7
76.62	1	Ti	3	.59
79.0	bh	Zr0	..	.5
85.18	2s	Zr	26	.14
86.66	0.6	Zr	0.6*	.65
87.88	0.6w	..	..	..
89.18	1.5w	Ti	35	.18
	bh?	Zr0	..	.3
94.69	4	Mn	1	.67
96.54	3.5	Ti	3	.60
97.14	3	Fe	15	.13

5400

λ	Int.	IDENTIFICATION El.	Mult.	λ
00.14	1w	..	..	..
01.46	1	..	..	..
02.71	1w	?..	..	..
		?Eu	..	.79
04.1	bh	Zr0	..	.4
05.80	2	Fe	15	.78
07.68	1	Zr	0.7*	.63
	bh	Zr0	..	..
08.92	2.5	Ti	3	.94
09.88	2s	Cr	18	.79
26.26	4	Ti	3	.26
29.72	3	Fe	15	.70
32.53	5	Mn	1	.55
	bh	Zr0	..	3.2
34.55	2.5	Fe	15	.53
36.8	bh	Zr0	..	7.0
37.75	1	Zr	0.2*	.74
46.75	5w	Ti	3	.59
		Fe	15	.92
48.44	2w	?Zr	0.6*	.55
	bh	?TiO	..	..
51.21	0.6	?Zr	..	.21
53.66	0.5	Ti	108	.65
55.63	2.5	Fe	15	.61
56.5	bh	Zr0	..	.5
60.51	4	Ti	3	.50
61.8	bh	Zr0	..	.6
		Zr0	..	2.2
65.4	bh	Zr0	..	.4
66.51	1.3	Y	12	.46
74.23	1	Ti	108	.23
80.89	1	?Sr	9	.86
81.93	1.4	Sc	16	.99
84.62	0.6	Sc	16	.62
85.7	bh	Zr0	..	.7
89.64	0.8?	..	..	..
90.18	1	Ti	107	.15
	bh	Zr0	..	.3
90.84	2.5	Ti	3	.84
95.95	2w	V	2	.02
97.54	2	Fe	15	.52

5500

λ	Int.	IDENTIFICATION El.	Mult.	λ
00.81	0.8w	V	2	.82
01.51	2	Fe	15	.47
02.22	0.8	Zr	1.0*	.16
03.47	1	..	..	..
06.72	4w	?Mo	4	.51
		Fe	15	.78
11.89	1.5	?Ti	108	.80
		?..	..	..
12.56	4	Ti	106	.53
14.41	4?	Ti	106	.35
		Ti	106	.54
	bh	Zr0	..	5.3
15.12	2	V	2	.08
	bh?	Zr0	..	.3
17.20	2s	?V	2	.20
19.7	bh	Zr0	..	.6
27.56	4	Y	12	.54
30.43	1.5w	..	..	..
32.39	1?	?Zr	0.6*	.30
33.09	1.5	?Mo	4	.01
35.36	5w	?V	1	.38
		Ba	2	.48
38.7	bh	Zr0	..	.8
42.70	3	V	2	.72
45.3	bh	Zr0	..	.2
51.7	bh	Zr0	..	.7
53.2	bh	Zr0	..	.1
56.1	bh	Zr0	..	.1
75.0	bh	Zr0	..	.7
80.2	bh	Zr0	..	.1
81.8	bh	Zr0	..	.7
92.45	0.5	V	37	.41
92.86	1	V	1	.96
94.48	0.3	Nd II	79	.42
		?Ca	21	.47
96.5	bh	Zr0	..	.5
98.49	1	Ca	21	.49

5600

λ	Int.	IDENTIFICATION El.	Mult.	λ
01.26	0.5	Ca	21	.28
02.89	0.7w	Ca	21	.85
05.00	1	V	37	.94
06.40	1	..	..	..
08.83	1w	..	..	..
10.2	bh	Zr0	..	.1
12.05	1	..	..	..
20.14	0.6	Zr	25	.16
23.59	0.5	Zr	0.5*	.56
24.74	2w	V	37	.60
		V	37	.90
26.03	1	V	37	.01
27.63	2	V	.37	.63
28.9	bh	Zr0	..	9.0
		Zr0	..	9.5
32.41	0.7	V	1	.47
33.9	bh	Zr0	..	.9
58.1	bh	Zr0	..	.1
63.1	bh	Zr0	..	.1
64.54	1	Zr	47	.55
68.31	1	V	37	.37
70.85	1.5	V	36	.83
71.83	2	Sc	12	.80
80.90	2	Zr	25	.93
82.59	2w	?Na	6	.63
86.81	3	Sc	12	.83
87.6	bh	Zr0	..	.4
88.14	1	?Na	6	.20
92.4	bh	Zr0	..	.3
96.3	2	Gd	3	.22
98.53	3	V	35	.51

5700

λ	Int.	IDENTIFICATION El.	Mult.	λ
00.16	2	Sc	12	.14
03.57	3	V	35	.56
06.99	3	V	35	.97
08.84	4	Sc	12	.60
		Zr	0.0*	.88
11.78	3	Sc	12	.75
17.31	2	Sc	12	.30
18.1	bh	Zr0	..	.1
23.8	bh	Zr0	..	4.1
26.98	1	V	35	.02
31.20	1.5	V	36	.26
35.64	3	Zr	4	.70
37.09	0.8	V	35	.04
43.46	1	V	35	.44
47.9	bh	Zr0	..	8.1
53.7	bh	Zr0	..	.8
76.74	1	V	36	.67
		?Re	..	.81
78.4	bh	Zr0	..	.5
86.9	bh	Zr0	..	.8
91.32	1	?Zr	0.1*	.34
		?Gd	3	.38
97.72	4	Zr	4	.76

TABLE 7 (Cont'd)

λ	Int.	IDENTIFICATION El.	Mult.	λ
5800				
09.0	bh	ZrO	..	.2
14.4	bh	ZrO	..	.5
34.59	3w	..	..	..
39.02	bh	?ZrO	..	9.8
49.3	bl	..	..	..
51.80	0.7	..	..	..
53.70	2	Ba II	2	.68
57.45	1	Ca	47	.45
60.1	bh	ZrO	..	.1
66.48	2	Ti	72	.45
68.30	2w	?Zr	0.2*	.26
	bh?	ZrO	..	.0
79.79	2	Zr	4	.79
85.56	3	Zr	2	.61
89.9	15	Na	1	.95
93.0	bh?	..	..	..
95.8	10	Na	1	.92
99.36	2	Ti	72	.30
5900				
00.62	1?	?Nb	..	.59
01.06	2	Zr	0.1*	.09
08.7	bh?	ZrO	..	.5
11.3	bh?	ZrO	..	.5
13.68	3	Ti	2	.73
16.2	bh	ZrO	..	.4
18.63	1	Ti	71	.55
22.16	2	Ti	72	.11
25.12	0.5	Zr	0.6*	.17
35.17	3	Zr	2	.23
37.88	1	Ti	72	.81
40.62	2	Ti	2	.68
41.79	1.5	Ti	72	.76
43.22	1	?Re	..	.24
44.66	4	Ti	2	.65
		?..	..	..
46.8	bh	ZrO	..	7.0
53.19	0.7	Ti	154	.16
55.32	4	Zr	3	.37
56.79	0.5	..	..	..
65.85	1.3	Ti	154	.83
72.0	bh	YO	..	.2
77.7	bh	ZrO	..	.7
78.56	1	Ti	154	.54
84.52	3w	Ti	2	.59
87.7	bh	YO	..	.7
6000				
02.65	0.8	V	34	.60
03.8	bh?	YO	..	.6
20.0	bh?	YO	..	.0
21.3	bh	ZrO	..	.3
23.42	3	Y	3	.41
25.39	1.5w	Zr	0.2*	.41
31.66	3	Ti	2	.68
32.59	1	Zr	1.5*	.62
36.2	bh	ScO	..	.2
39.71	2	V	34	.69
53.8	bh	ZrO	..	.8
58.20	0.8	V	34	.11
		?..	..	..
59.2	bh?	ZrO	..	.3
62.83	3	Zr	3	.88
64.65	2	Ti	69	.63
69.4	bh	ZrO	..	0.0
79.36	1w	..	..	..
81.46	3	V	34	.42
82.58	1	..	..	..
85.25	3	Ti	69	.23
86.8	bh	ZrO	..	.9
90.21	3	V	34	.18
6100				
02.70	4	Ca	3	.72
11.67	2	V	34	.62
19.55	2	V	34	.50
20.3	bh	ZrO	..	.1
20.81	1?	Zr	24	.86
22.18	5	Ca	3	.22
24.86	1.6	Zr	24	.86
26.25	2	Ti	69	.22
27.45	4	Zr	2	.49
32.1	bh	YO	..	.1
34.53	5	Zr	2	.58
35.38	2	V	34	.36
36.8	bh	ZrO	..	7.2
38.43	1.2	Y	3	.44
40.46	2w	Zr	24	.50
41.72	2	Ba II	2	.72
43.21	4	Zr	2	.23
48.4	bh	YO	..	.4
50.18	2	V	20	.13
54.2	bh	ZrO	..	3.9
62.16	3	Ca	3	.17
70.38	1	V	20	.34
	bh?	ZrO	..	.2
91.69	3	Y	2	.73
93.02	0.8	Zr	24	.96
93.73	1	Sc	3	.67
99.17	3	V	19	.20
6200				
00.9	bh	ZrO	..	.9
03.8	bh	ZrO	..	.9
10.67	3	Sc	2	.68
13.01	1	Zr	24	.06
13.90	1	V	20	.87
16.36	2	V	19	.37
17.99	0.8	..	..	..
22.57	2	Y	2	.59
24.49	1.5	V	20	.51
29.4	bh	ZrO	..	.4
30.78	1	V	19	.74
33.19	1	V	20	.19
35.2	bh	ZrO	..	.1
39.6	1w	ZrO	..	8.9
		Sc	3	9.78
42.98	3w	V	19	.80
		V	19	.11
51.82	1	V	19	.83
58.84	2w	V	19	.60
		Sc	3	.96
61.1	bh	ZrO	..	0.9
66.32	0.7	?V	20	.32
		ZrO	..	.5
68.7	1w	?V	20	.84
		?ZrO	..	..
73.34	2w	?ZrO	..	.0
		Ti	1	.39
74.68	2	V	19	.67
76.34	0.7	Sc	2	.31
80.61	0.3	Fe	13	.62
85.17	2	V	19	.18
92.78	2	V	19	.85
	bh	ZrO	..	.8
95.16	1w	..	..	..
		Ti	1	.25
96.56	3	V	19	.52
		Ti	1	.65
98.2	bh	ZrO	..	9.0
6300				
05.69	3	Sc	2	.67
14.4	0.7	..	..	..
25.1	1	?ZrO	..	4.6
		?Ti	1	5.22
30.08	1	Cr	6	.10
36.29	0.7	..	..	..
44.8	bh	ZrO	..	.9
51.1	bh	ZrO	..	.2
59.84	0.4?	Ti	1	.90
78.4	bh	ZrO	..	.3
84.3	bh	ZrO	..	.6
6400				
00.31	0.5	Fe	13	.34
02.00	0.8	Y	2	.00
12.4	bh	ZrO	..	.3
13.25	2	Ti	1	.13
		Sc	1	.35
18.2	bh	ZrO	..	9.3
35.00	4s	Y	2	.02
39.07	2	Zr	1.5*	.01
		Ca	18	.07
45.74	1	Zr	57	.76
46.4	bh	ZrO	..	.5
48.02	0.5	Sc	1	.10
49.80	1	Ca	19	.81
51.66	0.5	Zr	0.6*	.62
52.41	0.8	V	48	.35
		?ZrO	..	.5
62.61	3w	Ca	18	.57
70.27	0.8	Zr	65	.25
71.65	0.8	Ca	18	.66
73.6	bh	ZrO	..	.3
80.4	bh	ZrO	..	.7
91.59	1	..	..	..
93.8	1	Ca	18	.78
95.18	bh	ZrO	..	.4
6500				
07.9	bh	ZrO	..	8.2
42.8	bh	ZrO	..	3.0
46.33	0.5	Ti	102	.28
49.4	bh	ZrO	..	.7
53.44	0.7	..	..	..
54.27	0.4	Ti	102	.23
56.03	1	Ti	102	.07
57.36	1.5	Y	1	.40
72.76	7	Ca	1	.78
75.69	1	..	..	..
76.53	2	Zr	0.0*	.57
77.7	bh	ZrO	..	8.2
84.5	bh	ZrO	..	.9
98.7	2	?Zr	0.1*	.84
99.0	2	Ti	49	.11
6600				
06.04	0.8	V	48	.98
13.1	bh	ZrO	..	.1
24.92	0.8	V	48	.86
31.19	1	..	..	..
49.1	bh	ZrO	..	.5
76.9	bh	?ZrO	..	..
80.7	bh	?ZrO	..	..
87.0	bh	ZrO	..	6.6
87.54	6s	Y	1	.57
6700				
07.7	0.5	Li	1	.74
09.7	bh	?ZrO	..	..
11.1	?	?ZrO	..	10.9
14.2	bh	..	..	..
17.76	2	Ca	32	.68
41.6	bh	?ZrO	..	..
42.4	?	?ZrO	..	2.5
43.14	4	Ti	48	.12
53.06	2w	V	31	.00
58.7	1w	..	..	..
62.34	10	Zr	1	.38
66.57	1	V	31	.49
69.19	1	Zr	1.5*	.16
70.53	0.7	..	..	..
75.93	0.8	..	..	..
77.2	bh	ZrO	..	.2
85.05	0.7	V	31	.98
93.70	5	Y	1	.71
6800				
12.55	1	?V	31	.40
		?ZrO	..	.5
		?Zr	..	.64
32.90	5	Zr	1	.93
40.1	bh	ZrO	..	.2
46.0	bh	?ZrO	..	7.3
86.5	bh	?ZrO	..	4.8
		?ZrO	..	7.8
92.64	1s	Sr	1	.58

PHOTOMETRY OF SOLAR FLARES

HELEN W. DODSON, E. RUTH HEDEMAN, AND ROBERT R. MCMATH
McMath-Hulbert Observatory of the University of Michigan
Received August 15, 1955

ABSTRACT

On the basis of photometric light-curves for 194 flares and subflares, the following data have been derived.

1. Hα intensity often varies differently in different parts of the same flare.

2. The change of Hα intensity with time in a flare can be well represented by the series of curves given by the equation

$$\log \frac{I_t}{I_0} = \left(\log \frac{I_{\max}}{I_0}\right) 10^{\pm a(t-t_{\max})},$$

where t is measured in minutes and a is positive for the ascending branch, negative for the descending branch, and takes values between 0.40 and 0.00313. For the descending branch of the light-curve, a is always smaller than for the ascending branch. The most usual value of a for the ascending branch is 0.10; for the descending branch a is $\gtrsim 0.025$ for 87 per cent of the cases.

3. Hα flare intensities have been measured in units of both the local and the central continuum at λ 6590. In the former, average Hα intensity at flare maximum ranged from 0.66 for subflares and 0.88 for flares of importance 1 to intensity 1.17 and 1.28 for flares of importance 2 and 3, respectively. In units of the central continuum the average values are about 0.1 lower. The brightest measured maximum was 1.9 times the local continuum for a flare at CMD 72°.

4. No convincing relationship has been found between rate of increase of intensity and maximum intensity attained by the flare. However, the slowest rate of increase apparently diminishes the chances of attaining a maximum as bright as the continuous spectrum.

5. There is evidence for center-to-limb variation in numerous characteristics of the Hα flares in this study. The slowest rates of rise and decline were observed only for flares within 55° of the central meridian, and the fastest rates of decline only for flares within 40° of the solar limb. Average intensity in units of the local continuum increased with increasing central meridian distance of the flares. In units of the central continuum, the average intensity diminished from center to limb. "Limb-darkening" equations for the flares and subflares are as follows:

$$\text{Flares: } I_c = 0.63 + 0.34 \cos \theta ,$$

$$\text{Subflares: } I_c = 0.36 + 0.26 \cos \theta .$$

For flares of the same importance, average duration diminished with increasing distance from the center of the disk. Near the center of the disk, the Hα flare usually lasted as long as, or longer than, the associated ionospheric disturbance, but for flares near the limb the reverse was true.

6. For the flares in this study, area and intensity increase together, but the correlation coefficient of these two measures is only 0.58 ± 0.03 p.e.

7. Flare duration was associated more closely with flare area than with maximum intensity. The duration of flares as measured by photometric light-curves is much longer than the average duration of flares reported in the *Quarterly Bulletin of Solar Activity*.

8. The reported starting times of SID's usually fall during the period of increasing intensity in the flare. Except in unusual cases, SID's were not reported unless the flare intensity was at least 0.8 of the local continuum and the area was of the order of 200 millionths of the solar disk. Near the limb the SID often lasts longer than the Hα flare.

9. There is apparently less diminution from center to limb in the ionizing radiation from flares than in Hα.

10. The ionospheric disturbances were unusually small for certain large and relatively bright flares associated with the onsets of 200-Mc/s noise storms.

11. Examination of ionospheric records for the times of the flares and subflares in this study has provided evidence for a new type of flare-associated ionospheric effect, a gradual ionospheric disturbance, in contradistinction to the sudden SID or Dellinger effect. The 45 reported SID's have been augmented by 19 additional, well-confirmed ionospheric disturbances and by 23 less certain events.

12. There is no evidence to indicate that subflares are not just smaller, fainter examples of the flare phenomenon. Flares and subflares in this study have similar disk distributions and rates of increase and decrease of intensity. Ionospheric disturbances accompanied at least four of the brightenings here classified as subflares.

INTRODUCTION

During the last decade there has been significant improvement in world-wide reporting of the occurrence of solar flares and in estimates or evaluations of certain of their features. Quantitative measurements relating to the physical aspects of flares are still very limited. Since 1949 the program of the McMath-Hulbert Observatory has included as one of its objectives the recording and measurement of photometrically standardized Hα spectroheliograms of solar flares throughout the course of their development. The spectroheliograms for this program were secured in the 50-foot solar tower, which gives solar images with diameters of either 2.2 or 4.4 inches. The photometric measurements were made with a densitometer especially designed for the flare program. Photometric light-curves for 194 flares and subflares are now available, and their study constitutes the present paper.

OBSERVATIONAL MATERIAL

For this investigation, flare intensities were measured in units of the undisturbed Hα background of the spectroheliogram, adjacent to the flare or at the same heliocentric distance as the brightening. Such intensity measures are designated I/I_0. Intensities so measured have been converted into units of the continuous spectrum at λ 6590 through a series of photometric studies of (1) spectroheliograms taken in the center of Hα and in the continuous spectrum at λ 6590 and (2) limb darkening of the undisturbed background of the Hα spectroheliograms. The value 0.32, adopted as the ratio at the center of the solar disk between the intensity of the undisturbed Hα background and that of the continuous spectrum at λ 6590, corrects for the major effects of scattered light within the spectrograph. Limb darkening of the Hα spectroheliograms is such that the ratio of the intensity of the Hα background to the local continuous spectrum is practically constant at value 0.32 across the entire solar disk. The nearly fixed ratio from center to limb between the intensity of the Hα background of the spectroheliograms and that of the continuum near Hα is consistent with the nearly constant values found by de Jager (1952) for the intensity in the center of Hα in units of the local continuum (see Fig. 1).

In the present paper flare intensities are expressed in two systems of units. In the first, the unit is the intensity of the continuous spectrum at λ 6590 at the distance of the flare from the center of the solar disk. It is designated I_{Local} or I_L and differs from the directly measured intensity in units of the adjacent undisturbed Hα background only by the constant factor 0.32. Measures of flare intensities in units of the continuous spectrum published up to this time have been expressed in units of the local continuum (Ellison 1952; Dodson 1953*a*, *b*).

The second system of intensities used in this study is designated I_{Center} or I_C and expresses flare intensities in a constant unit independent of the position of the flare on the disk. It has been derived by multiplying I_{Local} by the limb-darkening factor for the continuum near Hα at the heliocentric distance of the flare. For flares at or beyond the limb, intensities are expressed in terms of disk intensities at central meridian distances of approximately 85°.

All spectroheliograms were made with slit-widths of 0.10 mm. The scale of the spectrum is such that 0.10 mm is equivalent to 0.4 A. The width of the instrumental profile at half-intensity is of the order of 0.1 A.

Flare light-curves give essentially the variations with time of the central intensity of Hα for chosen points of the flare. For any one flare, light-curves for numerous points have usually been determined. For each flare in the study an area measurement has been made for the time of maximum intensity. Exact measurement of flare areas is a difficult photometric problem and has not been attempted by the authors for this investigation. The areas here reported are based on visually determined outlines of the bright, well-defined flare regions. The outlines were drawn from a projected image of the flare, in which 1 mm in the projected image corresponded to 2000 km at the center of the solar disk (solar diameter = 70 cm). Areas were measured by planimeter. They are

reported in two systems: (1) millionths of the solar hemisphere and (2) millionths of the solar disk. The former have been corrected for projection effects by multiplication by the secant of the central meridian distance of the flare. The reported areas are not necessarily the maximum areas of the flares, because many flares spread during the period of decreasing intensity.

The time interval most suitable for designating the duration of a flare is subject to uncertainty even when complete photometric records are available. The light-curve for a single part of the flare gives the duration of the physical change in a fixed region on the sun. For many flares this is identical with the duration of the entire phenomenon, and there is no problem. However, for certain flares, as one region fades, other adjacent regions brighten, and the total, complex flare phenomenon lasts considerably longer than

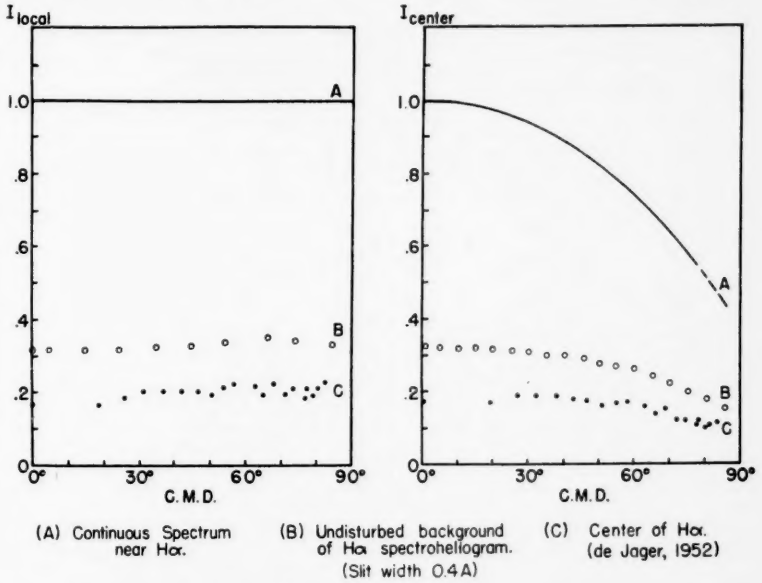

FIG. 1.—Relationships between intensity at the center of Hα and in the adjacent continuous spectrum for the undisturbed solar disk in units of the local and central continuum.

its individual components. In this study "duration" refers to the total interval between the initial brightening of the flare and the time when all parts of the flare either have returned to their preflare intensity or have stabilized at an intensity comparable to that of a plage rather than that of a flare.

In this study the position of a flare has been considered as determined by its distance from the central meridian, viz., the difference between the heliographic longitudes of the center of the solar disk and of the flare. This practice facilitates the study of flares in equal areas of the solar surface. The flares studied here occurred during the period in the solar cycle in which the average heliographic latitude of active areas was small and the central meridian distance could be used when needed as an approximation to the "heliocentric angle" or angular distance of a flare from the center of the apparent solar disk. In the present investigation no distinction has been made between flares on the basis of their location east or west of the central meridian.

At the present time the "importance" assigned a flare is an estimate of the greatness of the phenomenon, based on both intensity and area, and is reported on a scale of 1–3,

3 being the greatest. In this paper the term "subflare," or flare of importance 1−, is used to designate the many sudden monochromatic brightenings that can be seen and photographed in active solar regions but which are either smaller or fainter than the phenomena usually reported as flares of importance 1 in the *Quarterly Bulletin of Solar Activity*. The importance designations in this paper were assigned in most cases on the basis of visual estimates of area and intensity. It is hoped that certain standards may evolve by which future importance designations may be based on quantitative measures and may more nearly indicate circumstances of physical significance than mere adherence to arbitrary practice.

Hα observations of the flares have been supplemented by data on associated sudden ionospheric disturbances (SID's) as reported by the National Bureau of Standards in the F-series publications of the Central Radio Propagation Laboratory. Furthermore,

TABLE 1

DISK DISTRIBUTION OF FLARES AND SUBFLARES

CMD	In Photometric Study						Percentage Distribution for 2295 Flares in *Quarterly Bull.* (Jan., 1949–June, 1952)
	Number			Per Cent			
	Subflares	Flares	Total	Subflares	Flares	Total	
0°	(4)	(1)	(5)	(4)	(1)	(3)	(0.5)
1–10	17	19	36	16	22	19	14.8
11–20	10	9	19	9	10	10	12.1
21–30	21	17	38	20	19	19	13.1
31–40	17	12	29	16	14	15	12.5
41–50	12	11	23	11	12	12	11.9
51–60	11	9	20	11	10	10	12.0
61–70	4	2	6	4	2	3	10.7
71–80	6	4	10	6	4	5	7.0
81–90	3	5	8	3	6	4	5.4
Total	105	89	194	100	100	100	100.0

for the dates of all the flares and subflares in this study, intensity records of the 5-Mc/s WWV signal as received in Ithaca, New York, have been made available for our use through the generous co-operation of Dr. Charles R. Burrows, director of the School of Electrical Engineering of Cornell University. Finally, in order to extend the investigation beyond the usually reported SID's, the staff at CRPL was good enough to re-examine the ionospheric data at the National Bureau of Standards for all dates under consideration in the present study.

The flares included in this study are those for which we were fortunate enough to secure continuous records of photometric quality. Tables 1 and 2 summarize certain general facts for the flares in the investigation. The generality of the study can be evaluated on the basis of these facts.

AUXILIARY STUDIES

In order to test the implications of this study of photometric measurements of a relatively small number of flares against information from a much larger number of cases, three auxiliary studies have been prepared. The first is the tabulation of the disk distribution of all flares (2295) reported in the *Quarterly Bulletin of Solar Activity* from January, 1949, to June, 1952. The second is the determination of the duration of all

completely reported flares (1238) in the *Quarterly Bulletin* between January, 1948, and June, 1953, as a function of position on the disk and of importance. For this study the adopted time of start was that of the earliest underscored time; for the end, the latest underscored time was used. The importance adopted was the highest given by any observer. The third auxiliary study is the gathering-together of all reported data for all flares betweeen January, 1946, and September, 1954, known to have been in progress at the time of reported sudden ionospheric disturbances. This tabulation provides complete or partial data for 632 flares associated with sudden ionospheric disturbances.

FORMS OF LIGHT-CURVES FOR DIFFERENT PARTS OF SAME FLARE

The forms of the photometric light-curves for flares are varied and complex. A single light-curve gives the variation with time of the central intensity of Hα for a selected point within a flare. For any one flare, several light-curves are usually determined in order to give a representative sample of the types of variation that are in progress during the flare. For many flares, even relatively distant points start to brighten simultaneously

TABLE 2

DISTRIBUTION OF IMPORTANCE CLASSIFICATIONS AND SID'S FOR FLARES AND SUBFLARES IN PHOTOMETRIC STUDY

IMPORTANCE	NUMBER	WITH REPORTED SID'S		WITH DISTINCT IONOSPHERIC DISTURBANCE	
		No.	Per Cent	No.	Per Cent
Subflares	105	0	0	4	4
1	54	16	30	28	52
2	31	25	81	28	90
3	4	4	100	4	100
Total	194	45	.....	64	.....

and reach maximum intensity at very nearly the same time. The different parts of these flares seem to differ primarily in the intensity of their respective maxima (see Fig. 2, *a* and *b*).

Certain flares show brightenings that precede the onset of the principal increase in intensity. In some cases the region that brightens first continues to increase in intensity and becomes part of the primary flare. In others the region of initial brightening fades completely before the onset of the main flare, and it may or may not participate in the principal increase in intensity. Examples of such light-curves can be seen in our earlier publications (Dodson 1953) and in Figure 2, *b*.

The large number of light-curves now available makes it possible to recognize still another general pattern. Two parts of the flare start to brighten simultaneously, but at quite different rates (see Fig. 2, *c* and *d*). The more slowly increasing member may reach a maximum intensity equal to, greater than, or less than that of the more rapidly brightening part of the flare. In most cases the slow component reaches maximum at a later time than the fast component. This gives the appearance of a spreading of the flare with time. There are other flares in which brightenings actually begin at significantly later times in distant parts of the flare and suggest a true spreading with time of the flare disturbance—(see Fig. 2, *e* and *f*). In the majority of cases the slow components and the parts that start to brighten after the principal onset of the flare reach lower maxima than the rapidly increasing and early parts of the flare, and the superposed light-curves present a series of successive maxima, diminishing in intensity with time.

FORMS OF LIGHT-CURVES FOR DIFFERENT FLARES

I. LINEAR APPROXIMATIONS

In order to discuss the principal photometric differences between flares, it has been necessary to select for each flare the light-curve that seems best to represent the phenomenon in question. In general, we have selected the light-curve of the brightest portion of the flare. If two parts of the flare reached equally bright maxima but at different rates, we selected the light-curve with the fastest increase.

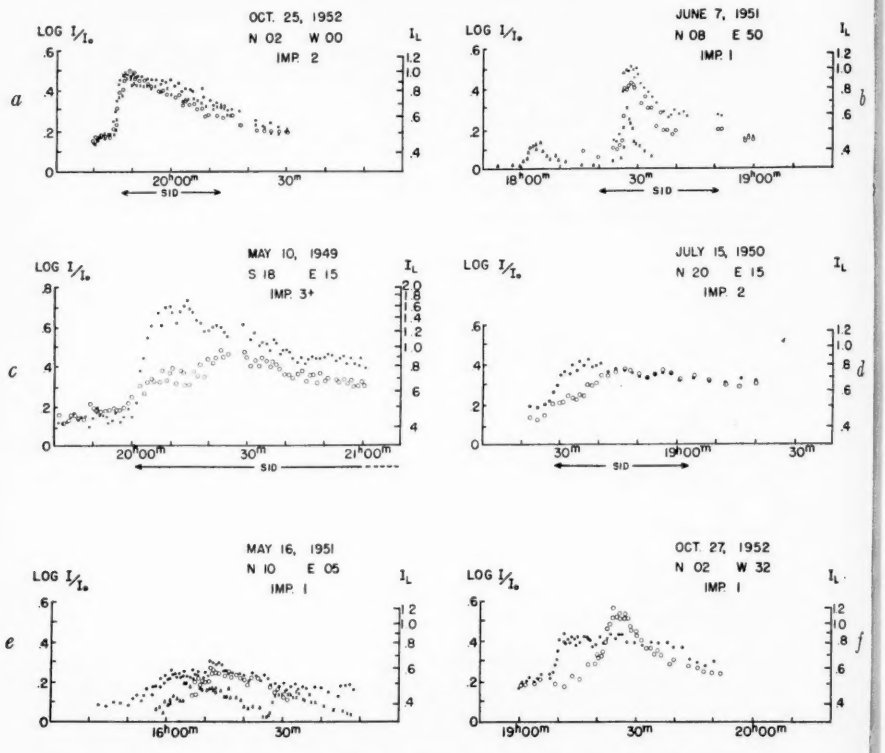

Fig. 2.—Comparison of light-curves for different parts of same flare

The appearance and shape of the light-curves depend in part upon the type of intensity measurement that is used in the graph. Choice must be made between the use of intensity and log intensity or some measure of difference in intensity of flare and background. For this paper the light-curves are plots of the directly measured quantities $\log I/I_0$ and $\log I_L$ versus time.

For the first survey of the shapes of light-curves, the discussion is limited to the brightenings classified as flares. The rates of increase and decrease of intensity are measured by the inclinations of two straight lines fitted to the ascending and descending parts of the curve of $\log I/I_0$ or $\log I_{\text{Local}}$ versus time. For some flares the straight lines give excellent approximations; for others the fit is less good. The linear scales of all the light-curves for which inclinations are discussed are such that 0.1 in the ordinate scale for $\log I/I_0$ is equal in length to 5 minutes in the abscissa or time scale.

An examination of all the light-curves gives a general impression of great similarity in shape for many of the curves and wide departure from these norms for the remainder. As has been indicated in earlier reports from this observatory, the rise to flare maximum is, in general, exponential (Mohler 1947), and there appear to be three "preferred" rates of increase in intensity (Dodson 1953). The fastest of the three rates of increase is such that the Hα intensity of the flare increases by about 2.5 times (1 mag.) in 4–5 minutes. This rate of increase corresponds to a change of about 0.1 in log intensity per minute. In the scale of the plotted light-curve it gives an angle of inclination for the ascending branch of about 80°. Flares increasing at this rate generally require from 2 to 5 minutes

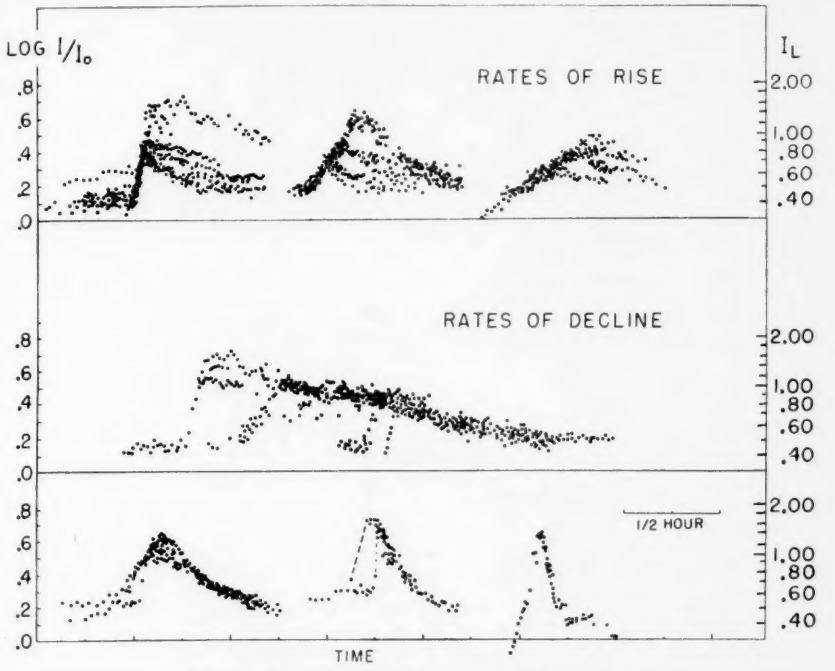

FIG. 3.—Comparison of light-curves for different flares

to reach their maximum, depending upon their final brightness and the intensity level from which they originated. The second "preferred" rate corresponds to a change of 1 mag. in 10–15 minutes or an angle of inclination of about 60° for the ascending branch of the light-curve. Some very large bright flares reach their maxima at this slower rate. The third rate is such that an increase of 1 mag. requires from $\frac{1}{2}$ to $\frac{3}{4}$ hour (angle of inclination 25°–30° in plotted light-curves). This very slow rise is relatively rare, and we have only one example in which an intensity equal to that of the continuous spectrum was attained at this rate.

It is not clear whether the three "preferred" rates of rise represent separate physical phenomena or are statistical peculiarities in a basically continuous distribution. Each of the original light-curves falls readily into one of the three groups. The three rates of rise are illustrated in the upper part of Figure 3, where the ascending portions of the light-curves of numerous flares have been superposed. The frequency distribution of the angles of inclination of the ascending branches of the light-curves is shown in Figure 4. The three "preferred" rates of rise are differentiated by different shading.

The most frequent or "preferred" rate of decline from maximum is very slow, about 1 mag. in $1\frac{1}{2}$–2 hours. This rate of decrease in intensity appears, in the scale of the plotted light-curves, as a descending branch that cuts the time axis at an acute angle less than 20° (this angle will be referred to as the "angle of inclination of the descending branch"). Many flares decline more rapidly. The wide range of rates of decline is illustrated by examples in Figure 3, and the frequency distribution for the inclination of the descending branch of the light-curve is given in Figure 4.

For every flare, the rate of increase in intensity to maximum is faster than the decline from maximum. Nevertheless, some flares decline as fast as others rise. These facts are clearly shown in the plot of inclination of rise versus inclination of decline (Fig. 5). The points for all flares lie within half the square. It is also apparent from this diagram that there is no other obvious relationship between rates of rise and decline. The fastest rises to maximum were followed by both slow and rapid declines.

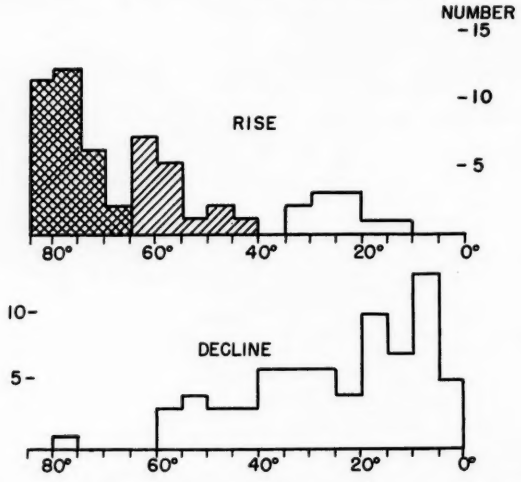

FIG. 4.—Inclinations of ascending and descending branches of light-curves for the flares in this study

Identification of the extreme cases in Figure 5 reveals the fact that the position of the flare on the apparent solar disk is playing some part in the observed rates of change of Hα intensity. All the flares with the fastest decline (inclination of the descending branch $\geq 50°$) were located at least 50° from the central meridian of the solar disk. At the other extreme, all the flares with the slowest rates of rise (inclination $\leq 40°$) lay within 55° of the central meridian.

The influence of the position of the flare on the disk upon the shape of the light-curve can be seen directly when the inclinations of the ascending and descending branches of the light-curve are plotted against the central meridian distance of the flare, as in Figure 6. In addition to the afore-mentioned relationships, this diagram shows that all flares for which the inclination of the descending branch was less than 30° lay within 55° of the central meridian. The results so far indicate that the slowest rates of rise and decline are observed only for flares within 55° of the central meridian, and the fastest rates of decline only for flares within 40° of the solar limb.

II. NONLINEAR APPROXIMATION

As can be seen from the illustrative examples in Figures 2 and 3, a straight line is generally a good approximation to the ascending branch of the light-curve but is sometimes far from satisfactory for the descending curve. It is possible to fit the plotted light-

curves by expressions that take into account the principal departures from linearity. The most satisfactory of these expressions, from the point of view of the ease with which all the light-curves can be represented, is the family of curves given by

$$\log \frac{I_t}{I_0} = \left(\log \frac{I_{\max}}{I_0}\right) 10^{\pm a(t-t_{\max})},$$

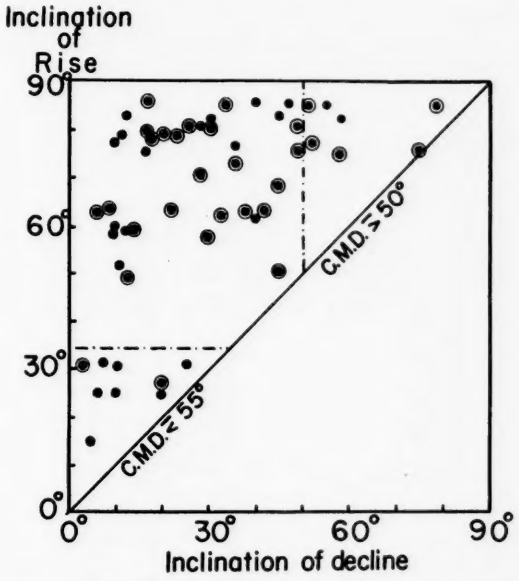

FIG. 5.—Comparison of rates of rise and decline for individual flares. (Circle indicates that SID was reported for time of flare.)

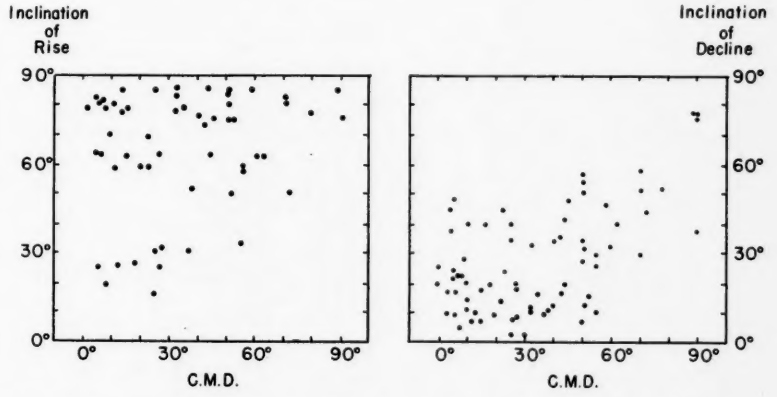

FIG. 6.—Inclinations of ascending and descending branches of light-curves plotted against central meridian distance of the flare.

where t is the time in minutes and a is positive for the ascending branch and negative for the descending branch of the light-curve. The parameter a can be considered to be a measure of the rate of increase or decrease of the Hα central intensity. The magnitude of a is generally different from the ascending and descending branches of the curve.

Graphs showing the variation of log I_L and log I/I_0 versus time were prepared for eight values of the parameter a for each of six values of maximum intensity. The chosen maxima covered the range 0.5–1.6 times the intensity of the local continuous spectrum (0.2–0.7 in log I/I_0). The values of a decreased by factors of 2 from 0.4 to 0.003125. The largest values of a describe the steepest curves. Figure 7 shows the graphs for maxima 1.6, 1.0, and 0.64 times the local continuous spectrum. A horizontal line is drawn to indicate average intensity for a plage. It should be pointed out that the intensities of the plages in which flares originate and to which they usually return cover a wide range (0.35–0.50 of I_{Local}).

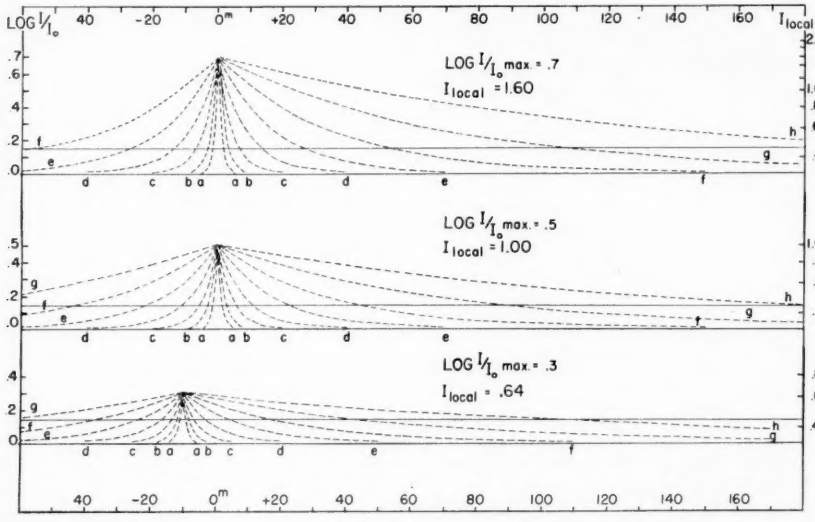

FIG. 7.—Examples of plots of log $(I_t/I_0) = [\log (I_{max}/I_0)]10^{\pm a(t-t_{max})}$ used for nonlinear approximation to flare light-curves. Parameters are as follows: *a*, 0.400; *b*, 0.200; *c*, 0.100; *d*, 0.050; *e*, 0.025; *f*, 0.0125; *g*, 0.00625; *h*, 0.00313.

The most representative light-curve for each flare and subflare was compared with the family of curves for the corresponding maximum intensity. In practically all cases it was possible to determine unambiguously values of a that gave satisfactory curves of descent. In a number of cases the ascending branch of the computed curves provided a somewhat poorer fit than did the straight-line approximation. The measures were carried out for both flares and subflares and are summarized in Table 3.

The frequency distributions of parameter a for both ascent and decline are very similar for the flares and subflares. Even though these two groups of brightenings differ greatly in the intensity of their maxima, the frequency distributions of rates of rise and decline as measured by parameter a are similar for both.

For more than a third of the flares and subflares, $a = 0.1$ for the ascending branch. For the descending branch, $a \leq 0.25$ for 87 per cent of all flares and subflares, with the most frequent value for flares at 0.0125. There are no cases where a was greater for the descending than for the ascending branch of the light-curve and very few where they were judged to be equal. This again shows that flares consistently rise to maximum intensity more rapidly than they decline.

These more detailed studies of the shapes of the light-curves again indicate that the position of the flare on the disk influences the observed rate of decline of a flare. The increase in the value of a for the descending branch of the light-curve, as the central meridian distance increases, is definite for the flares and can be discerned in the less accurate data for subflares (see Fig. 8). Flares far from the center of the disk appear to

TABLE 3

VALUES OF PARAMETER a FOR FLARES AND SUBFLARES

Parameter	Ascending Branch		Descending Branch	
	No. Flares	No. Subflares	No. Flares	No. Subflares
0.400 (steep)	5	3	.....	.....
.200	8	12	.....	1
.100	22	25	2	9
.050	11	18	4	5
.025	6	9	21	25
.0125	3	7	27	23
.00625	.....	.....	13	10
0.00313 (gradual)	1	.....	16	9
Total no.	56	74	83	82
Incomplete data	33	31	6	23

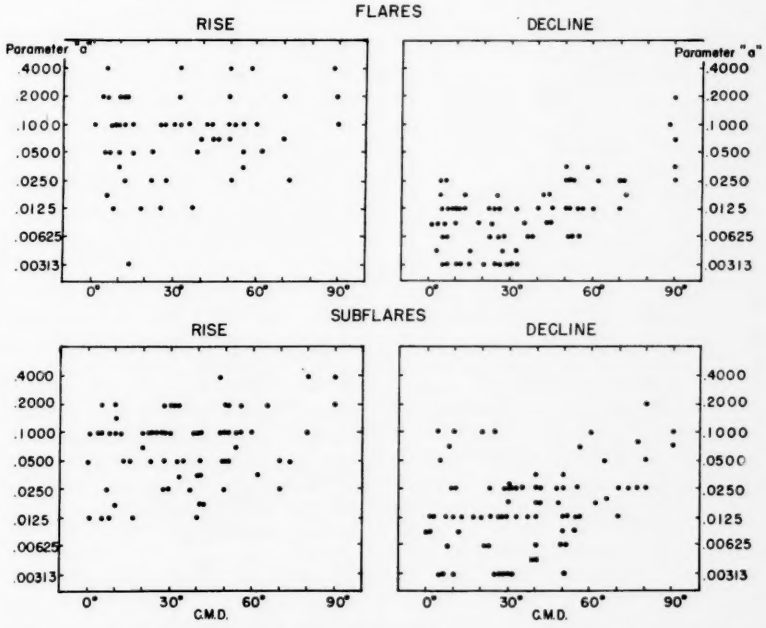

FIG. 8.—Parameters for rates of increase and decrease of intensity plotted against central meridian distance.

decrease in intensity more rapidly than those close to the center. Values of a for the ascending branch again show that very slow rates of rise are found only in the central part of the disk.

Although the actual rates of rise and decline of intensity depend in part on the type of intensity measure plotted, the foregoing systematic differences in the shapes of the light-curves for flares near the center and near the limb of the sun are independent of the choice of intensity measurement. They persist when log intensities are replaced by intensities. They are still present when curves are plotted in units of the central, instead of the local, continuum and when differences between the flare and background intensities replace the combined intensity.

TABLE 4

MAXIMUM INTENSITY OF FLARES IN UNITS OF CONTINUOUS SPECTRUM

Intensity	Local Continuum					Central Continuum				
	No. of Flares in Each Importance Category				Total	No. of Flares in Each Importance Category				Total
	Subflares	1	2	3		Subflares	1	2	3	
1.85–1.94	.....	.....	1	.....	1	.....	.....	.....	.....	.....
1.75–1.84	.....	.....	.....	.....	.....	.....	.....	.....	.....	.....
1.65–1.74	.....	.....	.....	.....	.....	.....	.....	.....	.....	.....
1.55–1.64	.....	.....	2	1	3	.....	.....	.....	1	1
1.45–1.54	.....	.....	3	.....	3	.....	.....	2	.....	2
1.35–1.44	.....	2	2	.....	4	.....	.....	1	.....	1
1.25–1.34	.....	.....	.....	1	1	.....	.....	2	.....	2
1.15–1.24	.....	2	3	.....	5	.....	2	.....	.....	2
1.05–1.14	.....	4	7	2	13	.....	1	5	1	7
0.95–1.04	.....	5	3	.....	8	.....	4	7	1	12
0.85–0.94	4	13	3	.....	20	.....	8	4	1	13
0.75–0.84	13	12	4	.....	29	1	10	6	.....	17
0.65–0.74	32	7	.....	.....	39	26	10	1	.....	37
0.55–0.64	39	4	.....	.....	43	32	12	.....	.....	44
0.45–0.54	15	.....	.....	.....	15	34	1	.....	.....	35
0.35–0.44	.....	.....	.....	.....	.....	7	1	.....	.....	8
0.25–0.34	1	.....	.....	.....	1	4	.....	.....	.....	4
Total	104	49	28	4	185	104	49	28	4	185
Incomplete data	1	5	3	.....	9	1	5	3	.....	9
Mean intensity	0.66	0.88	1.17	1.28	.....	0.56	0.76	1.02	1.13	.....

INTENSITY OF FLARES

The many pitfalls inherent in photometric work make the intensity of a flare a physical measurement most difficult to determine with precision. Measures of maximum flare intensity here reported have been read from photometric light-curves. If, for any flare, the period of maximum was not well covered by observations, the maximum intensity for the flare in question has been omitted. Measured maximum intensities in units of both the local and the central continuum are summarized in Table 4 and Figure 9. The data are subdivided according to the importance categories assigned by us on the basis of visual estimates of area and intensity.

This study makes clear the often overlooked fact that the central intensity of Hα for most flares is less than that of the continuous spectrum. If the subflares be admitted as lesser representatives of the same type of physical phenomenon as the flares, the pre-

ponderance of brightenings with maximum intensity less than that of the continuous spectrum is significantly augmented.

The highest intensities measured for flares in our photometric program are 1.9 times the local continuous spectrum for a flare at CMD 72° and 1.6 times the central continuum for a flare at CMD 15°. These maximum values are lower than certain intensities reported by Ellison (1952), viz., intensities two and three times the local continuum. The intensity measures in the present paper have been corrected for stray light but not for seeing conditions within the spectrograph and small departures from optimum observing conditions at the time of the flare. It is possible that such corrections or adjustments, if they could be made, might change the reported intensity by as much as 10 per cent or

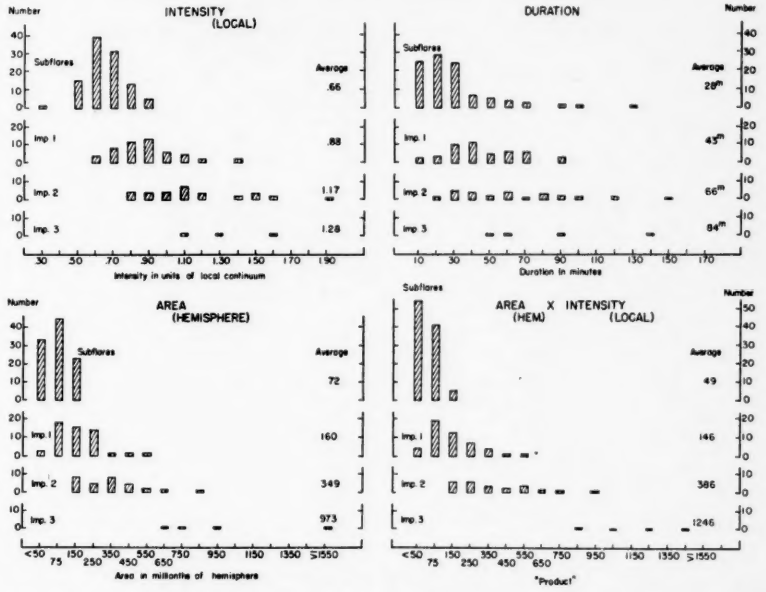

FIG. 9.—Summary of data on intensity, area, and duration for flares in different importance categories.

more in a few cases. We know that flares both larger and brighter than any for which we have photometric measures do occur, e.g., the unusual flare of July 25, 1946. Furthermore, if the saddle-shaped contours of Hα emissions in flares as reported by Ellison (1952) are general, spectroheliograms taken in the center of Hα might be expected to yield somewhat lower intensities than the maximum values recorded in the spectrum. Nevertheless, the present study of photographic records of flares leads us to conclude that flares with central Hα intensity greater than twice that of the *central* continuous spectrum near Hα must be extraordinarily rare phenomena. Spectra of major flares very near the solar limb may be expected to show intensities in units of the *local continuum* considerably higher than those reported in this paper.

In this study the average Hα intensity at flare maximum increases from 0.66 times the local continuous spectrum for the subflares and 0.88 for flares of importance 1, to 1.17 and 1.28 times the local continuum for flares of importance 2 and 3, respectively. The small number of flares of importance 3 in this study should be noted. From Table 4 and

Figure 9 the wide range of intensity within each importance category is at once apparent. Furthermore, there is a broad overlap of intensity values with successive importance categories. The same comments apply when intensities are expressed in units of the central, rather than the local, continuum (see Table 4).

It has often been suggested that the area and intensity of a flare are related quantities. It was hoped that careful measurements of photographic data would confirm and sharpen this relationship. Such is not the case. The measurements here reported confirm the fact that, *in general*, the intensity and area of flares increase together. However, the correlation coefficient of I_{Local} and area in units of hemisphere for the flares and subflares in this

TABLE 5

RELATION BETWEEN AREA AND INTENSITY

Area in Millionths of Hemisphere (Corrected for Projection)	Average Intensity		No. of Cases	Area in Millionths of Disk	Average Intensity		No. of Cases
	I_{Local}	I_{Center}			I_{Local}	I_{Center}	
0– 49	0.61	0.58	34	0– 49	0.61	0.56	27
50– 99	0.70	0.63	62	50– 99	0.68	0.57	41
100–199	0.80	0.70	44	100–199	0.75	0.66	54
200–299	0.98	0.82	16	200–299	0.79	0.74	16
300–699	1.19	1.03	18	300–699	1.09	0.96	29
≳700	1.15	1.10	4	≳700	1.10	1.05	11

TABLE 6

RELATION BETWEEN RATE OF INCREASE AND MAXIMUM INTENSITY

Rate of Increase of Intensity of Flares	Intensity at Maximum (I_L) (Subflares Excluded)						
	Number				Per Cent		
	≳1.3	1.0–1.2	<1.0	Total	≳1.3	1.0–1.2	<1.0
I (fastest, incl. ≲65°)	8	12	11	31	26	39	35
II (incl., 40°–64°)	2	6	7	15	13	40	47
III (slowest, incl. ≳40°)	0	1	9	10	0	10	90

study is only 0.58 ± 0.03 p.e. For log intensity and log area, the coefficient of correlation is 0.67 ± 0.03 p.e. The scatter of points is so very great that those who infer the intensity of individual flares from measured areas do so "at their own risk." The correlation between area and intensity is clearest for the small, faint brightenings. For flares in this study with areas as large as 200 millionths of the solar hemisphere, the correlation coefficient between area and intensity is only 0.30, and for areas of 300 millionths or more, it is reduced to 0.03, or no systematic increase of intensity with area (see Table 5 and Fig. 10).

Detailed examination of the data fails to reveal any clear-cut and convincing relationships between rates of rise or decline of intensity and the maximum intensity of Hα for the flare. However, there is some evidence that the slowest rate of increase (III) discourages, and the fastest rate of increase (I) favors, a bright maximum (see Table 6). The same tendency can be seen in the data when parameter a rather than the inclination of the ascending branch is used to measure the rate of increase of intensity. It must be

FIG. 10.—Relationship between area and intensity of flares. (Cross indicates that SID was reported with flare.)

pointed out, however, that, for almost half of the much fainter subflares, the inclination of the ascending branch gave a rate of increase of intensity as great as the fastest rate of rise (I) for the flares. There is no obvious, general relationship between rate of decline and intensity at maximum.

Measurements of intensity in this study indicate that the position of the flare on the disk influences in some degree the observed maximum intensity. The simple arithmetic average of the maximum values of I_{Local} for the flares in each 10° lune of the solar surface shows a tendency toward greater intensity with increasing central meridian distance (see Table 7 and Fig. 11). Within 40° of the central meridian the average value is slightly

TABLE 7

AVERAGE INTENSITY OF FLARES IN UNITS OF CONTINUOUS SPECTRUM AS FUNCTION OF POSITION OF FLARES ON SOLAR DISK

Position on Disk	Flares			Subflares		
	I_{Local}	$I_{Central}$	No.	I_{Local}	$I_{Central}$	No.
0°– 9°	0.95	0.95	14	0.60	0.60	15
10 –19	0.98	.96	12	.61	.60	13
20 –29	0.94	.90	15	.64	.60	18
30 –39	0.92	.84	10	.66	.61	13
40 –49	1.04	.90	8	.66	.57	14
50 –59	1.03	.83	13	.66	.53	17
60 –69	1.07	.75	3	.69	.48	4
70 –79	1.33	.77	4	.70	.41	6
80 –89	1.35	0.59	1	0.77	0.36	2

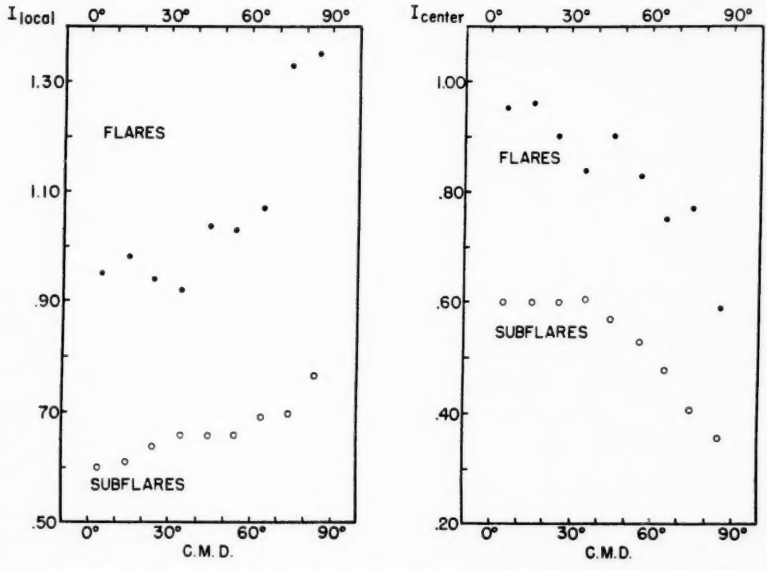

FIG. 11.—Relationship between average intensity of flares and position on the solar disk

less than that of the local continuum. For flares with central meridian distance greater than 40°, the average is greater than that of the local continuum. The same general trend is shown by the average values of I_{Local} for the subflares in this study. The increase in I_{Local} with increasing meridian distance is, of course, shown also by the intensity, I/I_0, as originally measured in units of the adjacent undisturbed Hα background.

The increase in the average value of I_L from center to limb can be interpreted as a difference in limb darkening in the center of Hα for the undisturbed parts of the solar disk and for the flare phenomenon. Limb darkening in the center of Hα for flares is apparently less than for the undisturbed parts of the solar disk. It is also less than for the continuous spectrum near Hα. The following equations, expressing the limb darkening for flares and subflares in this study, have been derived from graphs of the average value of I_c plotted against the cosine of the central meridian distance:

$$\text{Flares:} \quad I_c = 0.63 + 0.34 \cos\theta \,,$$

$$\text{Subflares:} \quad I_c = 0.36 + 0.26 \cos\theta \,.$$

It should be recalled that a previous publication has pointed out that the average of reported widths of Hα at flare maximum increases steadily from center to limb (Goldberg, Dodson, and Müller 1954).

AREA OF FLARES

The area of a flare is a quantity subject to at least two grave uncertainties. The first stems from the fact that the determination of flare area is basically a photometric problem, with all the difficulties inherent in such measurements. The observer must decide whether the flare area should include all regions that showed change, no matter how slight, or be confined to the brighter regions of the flare. If the latter, which intensity should be used as the limiting isophote? As previously stated, areas here reported are based on planimeter measurements of the visually determined outlines of the bright, well-defined flare regions on photographic records. Future studies may modify the values.

The second uncertainty in the determination of flare areas reflects the difficulty of deriving homogeneous area measurements for phenomena of unknown and probably different shapes observed in projection against different parts of a sphere. Because of this problem, flare areas are reported in two systems: (1) in units of the hemisphere, with correction for projection through multiplication by the secant of the central meridian distance or (2) in units of the disk, with no correction for projection. In the first system the average area for flares assigned to the successive importance categories steadily increased from 72 millionths of the hemisphere for subflares to 160, 349, and 973 millionths for flares of importance 1–3, respectively. As with intensities, there is a wide range of area within each importance category and a broad overlap of values for successive importance classes. In millionths of the disk the corresponding average values for the successive importance classes are 102, 248, 563, and 1535 (see Table 8 and Fig. 9).

The present study indicates that the range in area of flares and subflares is far greater than the range in Hα intensity. In area the extreme cases differed by a factor of the order of 100, whereas the Hα intensity of the brightest flare in the group was about six times that of the faintest subflare. For importance 3, the average area of flares is about fourteen times that of the subflares, but the average intensity in units of the local continuum is only twice as great.

For both flares and subflares in this study, a plot of uncorrected areas in units of the disk versus central meridian distance reveals a diminution of area with distance from the center of the disk. A similar plot of the same measures, corrected for projection by multiplication by the secant of the central meridian distance and in units of the hemisphere, presents a considerably more random appearance (see Fig. 12). However, there is evidence that the secant correction is too great, especially for the subflares. The aver-

age values of the area in units of the hemisphere, within 20 lunes, increases from center to limb (see Table 9). It is possible that the overcorrection results from a certain elevation of the phenomenon, an elevation that is small in comparison with the average lateral extent of flares but comparable to that of the much smaller subflares.

DURATION OF FLARES

"Duration" as here measured refers to the interval between the initial brightening of the flare and the time when all parts of the flare have returned to their original brightness or have stabilized at plage intensity. Duration, so measured, is the period during

TABLE 8

AREA OF FLARES AT TIME OF MAXIMUM INTENSITY

Area	Millionths of Hemisphere*					Millionths of Disk				
	No. of Flares in Each Importance Category				Total	No. of Flares in Each Importance Category				Total
	Subflares	1	2	3		Subflares	1	2	3	
≤1500				1	1				2	2
1000–1499								3	1	4
900– 999				1	1		1	2		3
800– 899			1		1		1	1		2
700– 799				1	1			3		3
600– 699			1	1	2			3		3
500– 599		1	3		4		2	3	1	6
400– 499		1	4		5		2	5		7
300– 399		1	8		9		9	6		15
200– 299		13	5		18	6	8	3		17
100– 199	22	15	8		45	33	21	2		56
50– 99	46	17			63	39	6			45
<50	33	2			35	26	2			28
Total	101	50	30	4	185	104	52	31	4	191
Excluded* or incomplete data	4	4	1		9	1	2			3
Mean area	72	160	349	973	160	102	248	563	1535	247

* All flares with CMD ≤ 85° are excluded from this tabulation.

TABLE 9

AVERAGE AREA OF FLARES IN UNITS OF MILLIONTHS OF HEMISPHERE AND DISK

Position on Disk CMD	Area		No. of Cases	Position on Disk CMD	Area		No. of Cases
	Hemisphere (Corrected)	Disk (Uncorrected)			Hemisphere (Corrected)	Disk (Uncorrected)	
Flares:				*Subflares:*			
0°–19°	226	437	28	0°–19°	54	106	28
20 –39	282	480	27	20 –39	66	114	30
40 –59	269	362	23	40 –59	77	101	32
60 –79	313	211	7	60 –79	111	70	10

which the Hα intensity is changing rather than the interval in which regions brighter than certain specific intensities are visible on the solar disk. The data are summarized in Figure 9.

The light-curves show that Hα intensity often continues to diminish long after regions bright enough to be recognized on a single spectroheliogram as of flare intensity have disappeared. It is not surprising, therefore, that the duration of flares is significantly longer when based on photometric light-curves than when reported on the basis of visual

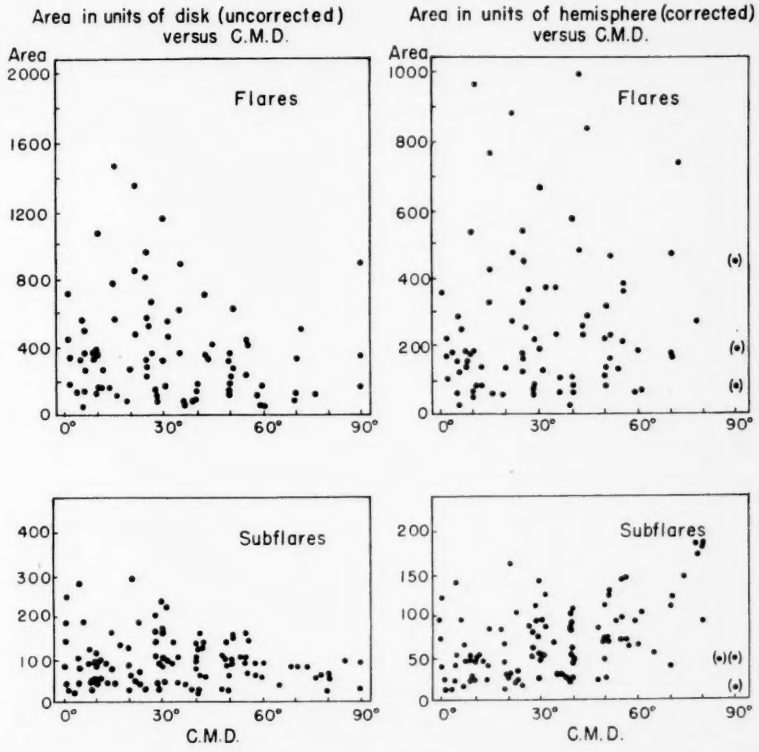

FIG. 12.—Area versus central meridian distance of flare. (Parentheses indicate that no correction was made for projection effects.)

observations. The long, slow decline of many flares makes the terminal time very difficult to ascertain without photographic records. Furthermore, even with photographic and photometric data, the determination of duration is a matter of judgment. The problem is especially difficult when the flare spreads with time to adjacent regions.

Table 10 summarizes the average duration of flares in different importance categories, as given by the photometric light-curves, by the auxiliary studies of data in the *Quarterly Bulletin* from January, 1948, to June, 1953, and by two earlier investigations (Waldmeier 1948; Ellison 1949).

The difference between duration as based on photographic, photometric light-curves and duration as determined visually is very large but is understandable. The difference between the two earlier studies of *Quarterly Bulletin* data and the present stems perhaps

from the policy in the later investigation of using the earliest and latest reports for start and end, respectively, and from the more complete observational programs of recent years.

The measurements here assembled indicate that the duration of a flare is associated much more closely with the area of the phenomenon than with the intensity attained by the brightest part of the flare. The values in Table 11 show that the average area is greater for flares of longer duration. There is no corresponding increase in average intensity with increasing average duration.

Additional evidence for the relation between area and duration can be found from the shape of the photometric light-curves for flares and subflares within 35° of the central meridian. For flares of the same intensity at maximum, there is a systematic increase in area as the rate of decline from maximum becomes slower (see Table 12). This type of relationship is not shown clearly by flares in this study for which the central meridian distance is greater than 35°. The increase in average area with average duration shown

TABLE 10

DURATION OF FLARES (MINUTES)

IMPORTANCE	PHOTOMETRIC LIGHT-CURVES		*Quart. Bull.* 1948–1953		WALDMEIER (1948) *Quart. Bull.* 1935–1944		ELLISON (1949) 1940–1948	
	Mean	No.	Mean	No.	Mean	No.	Mean	No.
Subflares	28	94	.....	.....	.....	.....	.....	.....
1	43	49	22	1000	20.3	683	17	41
2	66	28	48	211	33.4	209	29	18
3	84	4	93	27	62.4	35	62	21
3+					.....	.....	~3h	29

TABLE 11

RELATION BETWEEN DURATION, AREA, AND INTENSITY

DURATION (MINUTES)	AVERAGE AREA (MILLIONTHS)		AVERAGE INTENSITY		APPROXIMATE NO. OF CASES
	Hemisphere*	Disk	I_{Local}	I_{Center}	
Flares:					
0–19	82	125	1.00	0.74	4
20–39	204	283	1.07	0.91	24
40–59	193	306	0.93	0.80	21
60–79	355	573	0.93	0.85	14
80–99	441	777	0.93	0.89	8
≥100	557	934	1.38	1.24	4
Subflares:					
0–19	65	86	0.61	0.52	37
20–39	68	105	0.67	0.59	41
40–59	91	141	0.70	0.62	7
≥60	93	139	0.69	0.58	9

* All flares with CMD ≥ 85° excluded from this tabulation.

by the data in this paper is in agreement with the dependence between area and duration at half-maximum intensity, as reported for 22 flares by Severny and Shaposhnikova (1954).

Study of the shapes of the light-curves has indicated that there is a general tendency for flares to decline more quickly, the farther they are from the central meridian. If this is true and if other things are equal, the duration should be less for flares near the limb than for those near the center of the disk. It is not easy to select flares for which "other things are equal," but the importance designations provide approximate groupings of this kind. When the durations of flares in the light-curve study are distributed according to both importance and position on the disk, the diminution in duration with increasing central meridian distance is clearly evident (see Table 13).

TABLE 12

AVERAGE AREA AS FUNCTION OF BOTH INTENSITY AND RATE OF DECLINE FOR FLARES AND SUB-FLARES WITH CMD $\gtrless 35°$

PARAMETER OF DECLINE	AVERAGE AREA IN MILLIONTHS OF HEMISPHERE		
	$I_L =$ 0.60–0.79	$I_L =$ 0.80–0.99	$I_L = \leqslant 1.00$
0.40 (steep)	.....	.....	.....
.20	.....	.....	.....
.10	34	.....	.....
.05	41	.....	.....
.025	76	252	218
.0125	71	232	740
.00625	107	570	1028
0.00313 (gradual)	119	634	1057
No. of flares and sub-flares	46	20	16

TABLE 13

AVERAGE DURATION OF FLARES VERSUS CENTRAL MERIDIAN DISTANCE (MINUTES)

CMD	IMPORTANCE			
	1–	1	2	3
Light-curve study (170 cases):				
1°–30°	30	50	72	115
31 –60	30	41	64	60
61 –90	23	26	34	45
"Quarterly Bulletin" (1238 cases):				
1°–30°	.....	23	50	109
31 –60	.....	23	43	90
61 –90	.....	17	49	63

In order to test the generality of the results against a larger number of cases, the duration figures for 1238 flares from the *Quarterly Bulletin* were broken down in the same way. For importance 1 and importance 3 the average duration is lower for flares with CMD 61°–90° than for those with CMD 1°–30°. For importance 2 there is no difference. What evidence there is in the *Quarterly Bulletin* study points in the same direction as that indicated by the light-curve analysis (see Table 13).

SUDDEN IONOSPHERIC DISTURBANCES

Many flares are accompanied almost simultaneously by disturbances of the earth's ionosphere which are generally thought to result from an increase in the ultraviolet radiation falling upon the earth's ionosphere. Such ionospheric disburbances are detected in numerous ways, ranging from enhancement of atmospherics at long wave lengths to partial or complete fades of signal over long transmission paths for short wave lengths. The principal ionospheric information to which the authors have had access for the entire period of this study is the summary prepared by CRPL of the National Bureau of Standards of the major fades of high-frequency signals, classified as sudden ionospheric disturbances (SID).

The authors know of no SID reported for a time when the sun was under observation at the McMath-Hulbert Observatory for which a flare or subflare was not in progress on the sun. The converse is not true. There are numerous flares, some of them both large and bright, for which sudden ionospheric disturbances have not been *reported.*

I. SOLAR FACTORS AFFECTING FLARE-ASSOCIATED IONOSPHERIC DISTURBANCES

In order to gain insight into this problem, the flares in the photometric study have been divided into two groups, viz., those with and those without *reported* SID's. The flares in the two groups have been compared on the basis of intensity (both I_L and I_C), area (in units of hemisphere and disk), and the two products $A_H \times I_L$ and $A_D \times I_C$. The first product attempts to evaluate the flare as a solar phenomenon; the second more nearly describes the flare as viewed from, or experienced by, the earth. The product of area and intensity would be proportional to the energy of the flare in the center of Hα if the maximum intensity existed throughout the entire area or if all flares had the same distribution of intensities within the measured area of the flare. Comparison of the two groups of flares is shown in Figure 13 by a series of charts in which each flare is represented by a point, with the quantity under consideration as ordinate and the sine of the central meridian distance of the flare as abscissa. The position of the flare on the disk is introduced in these comparisons because it seemingly plays some part in the situation.

The comparisons show that, in general, SID's were not *reported* unless the central intensity of Hα in the flare was at least 0.8 of the local continuum. In units of the central continuum, the intensity "necessary" for an SID was systematically lower for flares near the limb. The minimum flare area for which SID's were reported ranged from 100 millionths of the hemisphere near the center to about 200 millionths near the limb. Unless a flare was at least 200 millionths of the disk in area, an SID was seldom reported.

When the product $(A_H \times I_L)$ is considered with respect to *reported* SID's, there is a center-to-limb effect. All flares with *reported* SID's and $(A_H \times I_L) < 200$ occurred within 35° of the central meridian. All flares without reported SID's and with $(A_H \times I_L) > 200$ took place in the limbward portion of the disk. (Flares at the extreme limb, for which A_H cannot be determined, are excluded from these statements.) The product $(A_D \times I_C)$ tends to remove this effect and proves to be the most successful of the six criteria in relating the Hα phenomenon to *reported* SID's. The value of $(A_D \times I_C)$ equal to 250 correctly separates 90 per cent of the flares in this study into the groups with and without reported SID's. The discordant cases are so few in number that it seems wise to consider them individually.

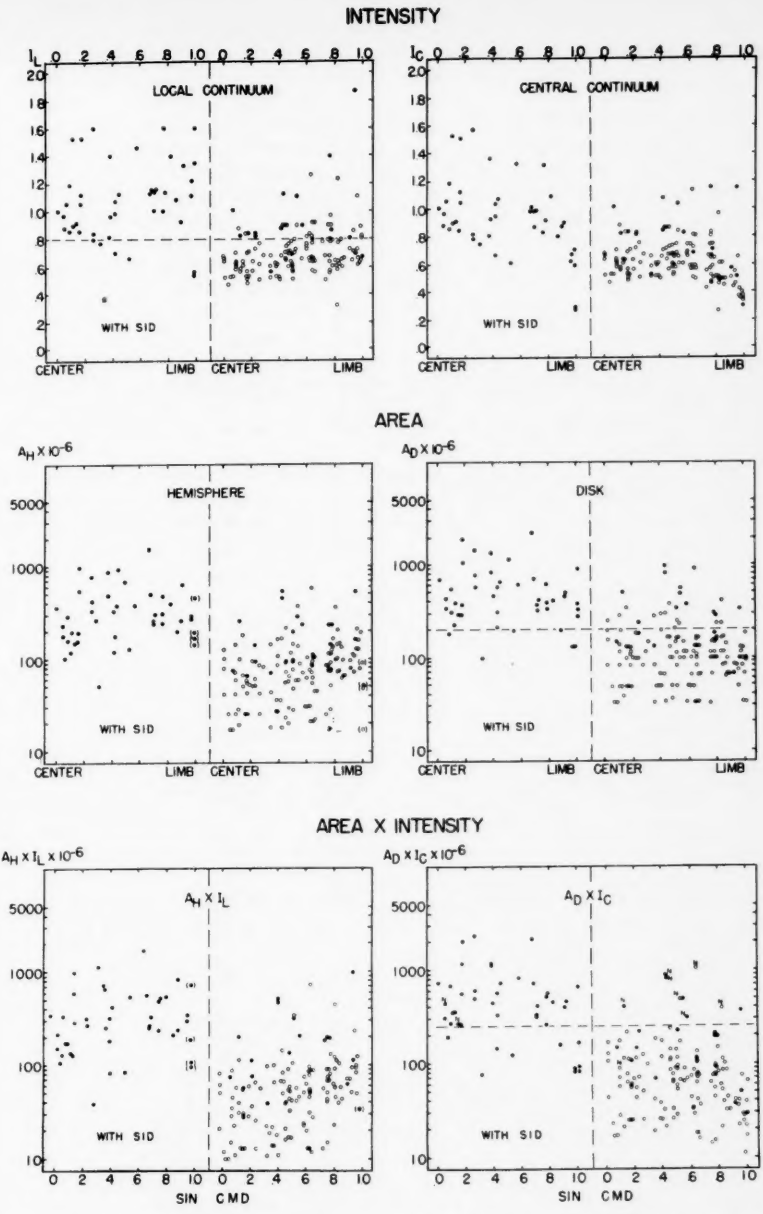

FIG. 13.—Comparison of flares with and without reported SID's. Filled circle in right half of each diagram indicates unreported ionospheric disturbance. *N* indicates onset of noise storm.

Of the ten flares with $(A_D \times I_C) < 250$, for which SID's were reported, two were cases in which we had difficulty with the photometric calibration. Two were flares in which the area increased greatly after the time of maximum intensity, and hence the area here used may not be representative. Five more were flares very close to the limb, where photometric measures are exceedingly difficult and the circumstances are often atypical.

There were nine flares discordant in the opposite sense. For these large bright flares it is difficult to allow errors of measurement or photometry sufficiently large to bring them into accord. It is therefore necessary either to consider them as constituting a different type of Hα brightening or to question the ionospheric data. There seems to be evidence for both lines of approach.

Of the nine large, bright flares without *reported* SID's, seven were associated with the onsets of noise storms at 200 Mc/s. Only three other flares in the entire study have this type of 200-Mc/s classification. The noise-storm flares are indicated by the letter *N* in Figure 13. A general study, by the authors, of flares associated with the onsets of noise storms has shown that such flares include a high proportion of large, "stringy" flares that spread with time rather than the more usual hard, sharp, well-defined brightenings. The intensity distribution in the flares associated with noise storms may be quite atypical, or the solar circumstances that favor the onset of noise storms may tend to inhibit the ionizing radiation of a flare.

A questioning of the inospheric data has led to the recognition of a new type of flare-associated ionospheric disturbance, an effect that can perhaps be called a "gradual ionospheric disturbance" in contradistinction to the well-recognized Dellinger effect, or SID, with its very sudden beginning.[1] The existence of many distinct ionospheric disturbances, coincident in time with flares but not included in the published lists of SID's, first became clear to the authors from records of variations in the intensity of the WWV 5-Mc/s signal as recorded at our observatory between May, 1953, and December, 1954. Through the generosity of Dr. Charles R. Burrows, director of the School of Electrical Engineering at Cornell University, the authors had the privilege of examining similar records of the 5-Mc/s WWV signal as received at Ithaca, New York, for the times of practically all flares in the photometric study. It was at once apparent that major ionospheric disturbances had accompanied a number of flares for which SID's had not been reported. Some of these disturbances began more gradually than the usually reported SID's. These findings and problems were discussed with Mr. Alan Shapley of CRPL of the National Bureau of Standards, who very kindly arranged for a complete re-examination of the ionospheric records of the National Bureau of Standards for all dates in the flare study. This examination confirmed the existence of the gradual ionospheric disturbance as a flare-associated phenomenon. It indicated that distinct disturbances had accompanied most, but not all, of the large bright flares without reported SID's. Furthermore, some of the originally reported SID's had been gradual fades. As a result of the re-examination, 19 well-defined ionospheric disturbances have been added to the 45 SID's originally reported. In Figure 13 the circles representing these new cases have been filled in. In addition, there is evidence, but less conclusive, for associated ionospheric effects with 23 other flares and subflares in this study.

It is possible that the sudden and gradual ionospheric disturbances represent two quite different types of phenomena. However, inspection of the Hα light-curves suggests that the differences in the ionospheric effects may primarily reflect differences in the rates of development of the flares. The ionospheric disturbances associated with flares for which the inclination of the ascending branch is less than 50° are now all classified as gradual, rather than sudden, fades. Furthermore, those ionospheric disturbances for which the rates of decline and recovery are unusually similar are associated with flares with nearly symmetrical light-curves. In most cases there is marked similarity between the development of the ionospheric disturbances and that of the Hα flare.

[1] Since November, 1955, the ionospheric disturbances reported in the F-series of CRPL are classified as S-SWF (Sudden short-wave fade) or G-SWF (Gradual short-wave fade).

These considerations suggest that there is probably no hard and fixed separation between flares that do and those that do not cause some change in the ionosphere. Increased precision in the detection of ionospheric disturbances will probably reduce the magnitude of the Hα phenomena with which such disturbances can be definitely associated. On the basis of ionospheric data now available for the flares in this study, it appears that, except in unusual cases, a maximum Hα intensity of the order of 0.8 of the local continuum was both necessary and sufficient for the occurrence of a concomitant ionospheric disturbance that satisfied standards of certainty as to the generality of the effect. This statement can be made if one allows errors only slightly more than 10 per cent in the measured Hα intensities.

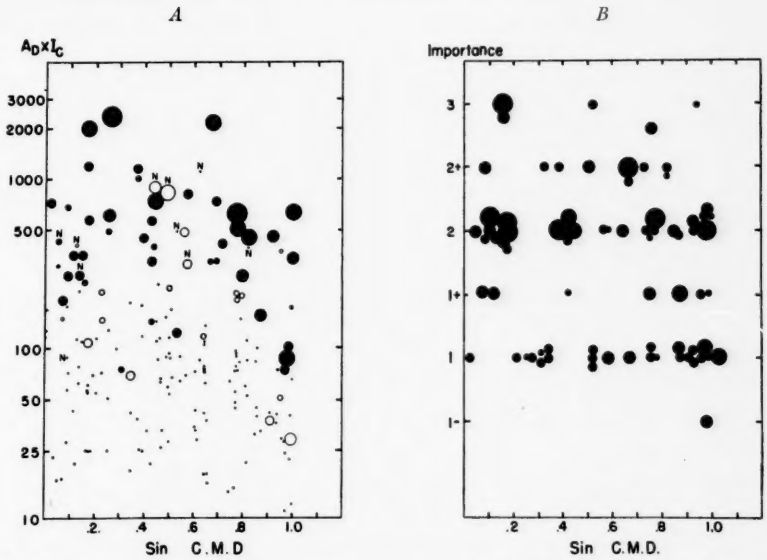

FIG. 14.—Comparison of importance of Hα flare and associated ionospheric disturbance. *A*, flares in light-curve study. Size of circle increases with magnitude of ionospheric disturbance. Dot signifies no recognizable ionospheric effect. Open circles indicate new ionospheric disturbance. *N* identifies flares associated with onset of noise storm. *B*, flares with total ionospheric fade as reported by CRPL (1949–1951) (solar data from *Quarterly Bulletin*). Size of circle increases with duration of ionospheric disturbance.

It is more difficult to generalize with respect to flare areas. Either the area is less critical in this matter, or its measurement is much less precise. If one allows an uncertainty of a factor of 2 in the measurement, one can say that, except in unusual cases, areas of the order of 200 millionths of the disk are both necessary and sufficient for the causation of ionospheric effects of the type here considered. These statements are based entirely on solar and terrestrial circumstances observed during the postmaximum phase of the sunspot cycle. The present study shows clearly that improvement in the understanding of the relationships between solar flares and concomitant ionospheric effects will depend as much upon improved ionospheric data as upon better solar observations.

II. COMPARISON OF MAGNITUDES OF Hα FLARE AND ASSOCIATED IONOSPHERIC DISTURBANCES

During the re-examination of the ionospheric records, the staff at CRPL was good enough to estimate the extent or magnitude of the ionospheric disturbances on an importance scale of 1− to 3+. The results of the re-examination of the records are presented graphically in Figure 14, *A*. In this diagram each flare is represented by a dot

or a circle. The importance of the ionospheric disturbance is indicated by the size of the circle. The small dot stands for "no clear-cut ionospheric disturbance." Filled circles are originally reported SID's. Open circles identify the 19 definite disturbances added as a result of the re-examination of the records. The letter *N* identifies flares associated with onsets of 200-Mc/s noise storms. The ordinate is the product, $A_D \times I_C$, for the flare, and the abscissa is its central meridian distance. This diagram shows clearly the fact that great ionospheric disturbances occur with flares in all parts of the solar disk. In general, the larger and brighter the Hα flare, as seen from the earth, the greater the associated ionospheric disturbance. The disparity between the magnitude of the ionospheric disturbance and that of the Hα flare associated with the onset of 200-Mc/s noise storms is again apparent.

The unusual greatness of the ionospheric disturbances caused by certain of the relatively small, faint flares near the limb suggests that the ionizing radiation from the flare is less subject to "limb darkening" or diminution than is Hα. Other lines of evidence tend to confirm this point of view. The *Quarterly Bulletin of Solar Activity* for the years 1949–1951 provides flare data for the times of 75 SID's with zero residual intensity. If the duration of these major SID's can be used as a basis for estimating their relative greatness, the foregoing material again shows that, for Hα flares of comparable importance (especially in importance class 1), the ionospheric disturbances tend to be greater for flares near the solar limb (see Fig. 14, *B*).

III. TIME RELATIONSHIPS OF FLARES AND IONOSPHERIC DISTURBANCES

Further evidence for a difference between the ionizing and the Hα radiation for flares near the limb stems from a study of the time relationships of Hα flares and associated ionospheric disturbances. The start of the ionospheric disturbance is either coincident with the start of the Hα brightening or follows closely within several minutes. Direct comparison of the photometric light-curves with ionospheric data sharpens this relationship. Three minutes was the most frequent time interval between the observed start of the Hα brightening and the reported start of SID's for the flares in the present study. For only five flares did Hα reach maximum intensity before the reported start of the SID. The ionospheric disturbance thus generally begins during the period of increasing intensity of the Hα flare.

It has been pointed out that many ionospheric disturbances last longer than the associated Hα flare (Bracewell and Straker 1949; Ellison 1953). This effect is apparently less pronounced when flare duration is based on photographic, photometric measures than on visual observations. There are 49 cases in the present study for which the ends of the ionospheric disturbance and flare are both well determined. For 22 of these cases the flares and SID's ended within 5 minutes of each other (ending times cannot be determined with an accuracy greater than 5 minutes). Twenty of the Hα flares lasted significantly longer than the ionospheric disturbances associated with them, and for only 7 cases did the SID continue more than 5 minutes after the apparent end of the Hα phenomenon (see Fig. 15, *A*). The photometric study thus indicates that, in general, the ionospheric disturbance continues during the period in which the Hα intensity in the region of the flare is changing, even though the residual intensity may no longer be very great.

A plot of the 49 well-determined differences in ending times for flares and SID's in this study shows that the ionospheric disturbance lasted longer than the visible Hα flare only when the flare was relatively close to the solar limb (CMD $\gtrsim 60°$). It is of interest to note that, in the references stated, the central meridian distance was greater than 65° for 4 of the 6 flares used to illustrate the greater duration of the ionospheric phenomenon. For the fifth flare there is evidence for an additional, later flare in another region. In the

last case the ending times of the Hα and ionospheric phenomena are similar, but the maxima are displaced. This may reflect the fact that the maximum area of a flare is sometimes attained after the time of maximum intensity.

In an effort to check these findings by data from a larger number of cases, we have determined the differences in ending times of flares and SID's for the 438 cases between January, 1946, and September, 1954, for which the two ending times have been reported

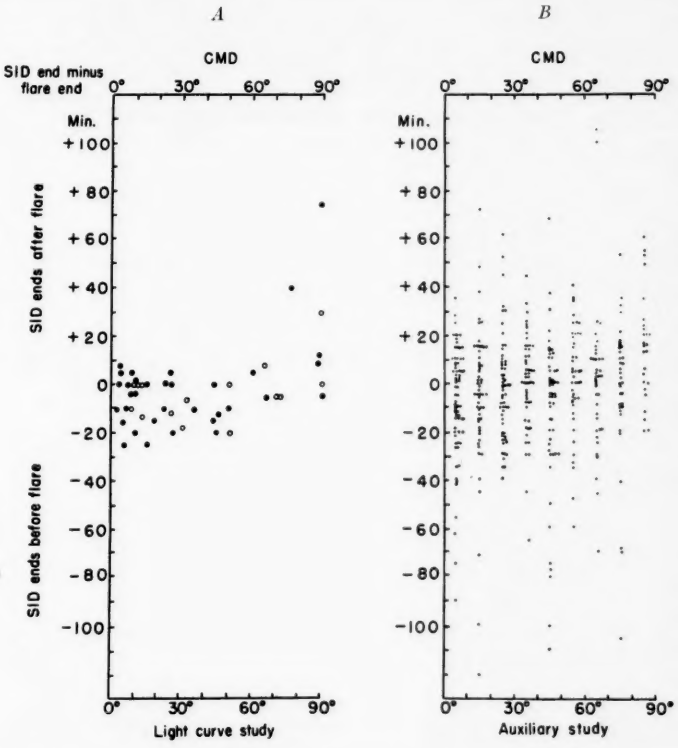

FIG. 15.—Comparison of ending times of *Hα* flares and associated SID's. (Open circle indicates unreported ionospheric disturbance.)

in the *Quarterly Bulletin of Solar Activity* and in the F-series publications of CRPL, respectively. A plot of these differences shows, first, the great uncertainty in the usually available data. It also indicates that the proportion of cases in which the SID continues after the apparent end of the Hα phenomenon increases with the central meridian distance of the flare and is greatest at the limb (see Fig. 15, *B*, and Table 14).

The foregoing considerations suggest that future investigations of Hα flares and their associated ionospheric disturbances probably will be focused more on the types and relative magnitudes of the two phenomena than on their mere occurrence. More extensive quantitative data are needed for both the ionospheric and the solar phenomena.

FLARES NEAR THE SOLAR LIMB

The material in this study has shown that flares near the solar limb present a number of abnormalities. Flares near the limb show a very great range in maximum intensity. The faintest and the second brightest flares in this study, those of April 29, 1949, and May 8, 1951, respectively, were at the limb, and both were associated with sudden ionospheric disturbances. The light-curves for these two flares are shown in Figure 16. Furthermore, both the rising and the declining branches of light-curves for flares near the limb are often exceedingly steep. The only flares in this study for which the inclination of the declining branch of the light-curve was as great as 60° occurred at central meridian distances of 80° or more. Five such light-curves are shown in the lower line of Figure 16.

TABLE 14

PER CENT OF FLARES IN 30° LUNES OF SOLAR SURFACE FOR WHICH SID ENDS AFTER Hα FLARE

CMD	Light-Curve Study (49 Cases)	Flares in *Quarterly Bulletin* (438 Cases)
0°–29°	19	42
30 –59	00	46
60 –90	58	57

TABLE 15

DISK DISTRIBUTION OF FLARES AND SUBFLARES WITH RAPID DECLINE IN INTENSITY
(Angle of Inclination of Decline >30°)

CMD	No. of Flares	No. of Subflares	Total
0°–29°	7	7	14
30 –59	13	8	21
60 –90	9	8	17

The same diagram brings together for comparison examples of light-curves separated according to rate of decline and the portion of the solar disk in which the flares were observed. The top line of Figure 16 shows the slow rate of decline (inclination 20° or less). We have no examples of flares that declined in intensity at this slow rate for meridian distances greater than 55°. The second line of Figure 16 gives examples of light-curves for which the angle of inclination is between 30° and 50°. Flares with this more rapid rate of decline were observed from center to limb. However, the more usual form of light-curve for flares at CMD 80°–90° was the still steeper decline illustrated in the bottom of the diagram.

The distribution on the disk of flares and subflares in this study for which the angle of inclination of the declining branch of the light-curve is >30° is almost uniform (see Table 15). The usual marked diminution in number of flares for central meridian distances

greater than 60° does not occur. If certain flares are elevated, it is probable that they would be visible closer to the limb than low-level flares. The almost uniform distribution of flares for which the angle of inclination of the declining branch of the light-curve is >30° suggests that the relatively rapid decline in intensity may refer to an elevated phenomenon. The very slow rate of decline, observed only for flares in the central part of the disk, may refer to low-level flares which would be visible only when the line of sight could penetrate to great depths in the solar atmosphere. A small number of direct observations confirm this interpretation. The flare of May 8, 1951 (Dodson and McMath 1952), with its rapid decline in intensity, was observed only as a feature extending beyond the solar limb. Careful search of the photographic records of the visible Hα disk provided no evidence whatsoever for a brightening of any portion of the disk during the major period of this flare and associated ionospheric disturbance. On April 29, 1949, the ionospheric disturbance began with the sudden brightening of an elevated part of a prominence and not with the earlier brightening of the plage at its base.

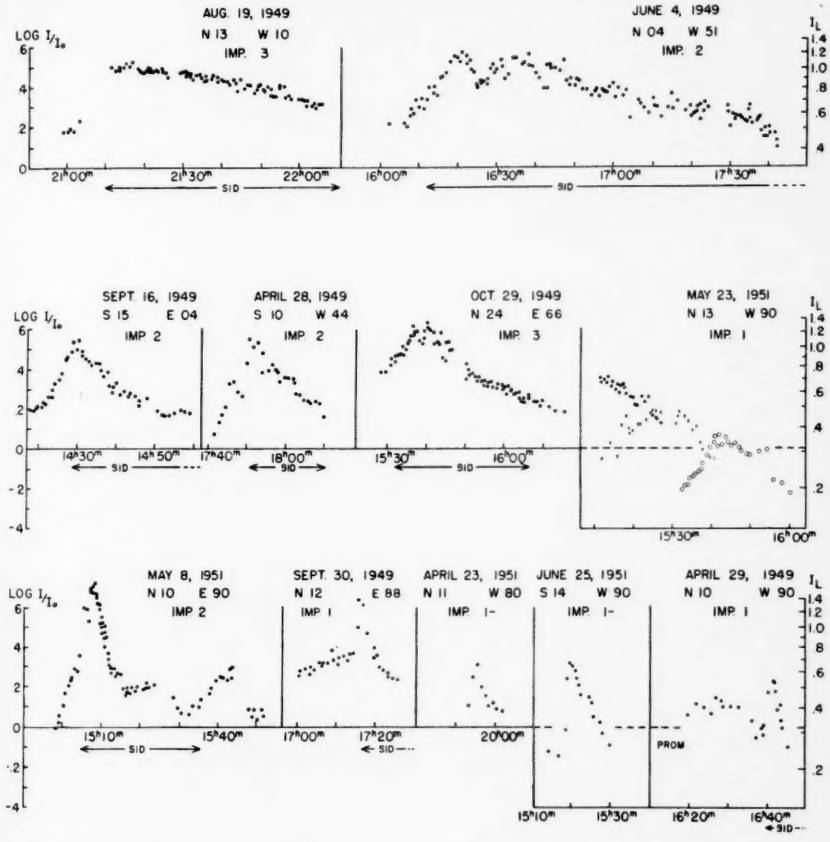

FIG. 16.—Examples of rates of decline for flares in different parts of solar disk. *Top:* Slow decline; CMD ≳ 55°. *Center:* More rapid decline; all parts of disk. *Bottom:* Very fast decline; CMD ≲ 80°.

If these interpretations are correct, the marked diminution in the number of flares observed and reported at central meridian distances greater than 60° stems from the lack of visibility in Hα of low-level phenomena when so near the limb that the line of sight must penetrate through a great extent of the sun's atmosphere.

The authors acknowledge with gratitude the part played by their colleagues at the McMath-Hulbert Observatory in the long observational program on which this study is based and in helpful discussions of the resultant data. They also wish to thank Dr. Charles R. Burrows, director of the School of Electrical Engineering at Cornell University, and Mr. Alan Shapley and Miss Virginia Lincoln, of the Central Radio Propagation Laboratory of the National Bureau of Standards, for making available original ionospheric records and for providing new measurements of ionospheric disturbances.

REFERENCES

Bracewell, R. N., and Straker, T. W. 1949, *M.N.*, **109**, 28.
Dodson, H. W. 1949, *Ap. J.*, **110**, 382.
———. 1953, *The Sun*, ed. G. P. Kuiper (Chicago: University of Chicago Press), pp. 692–703.
Dodson, H. W., and McMath, R. R. 1952, *Ap. J.*, **115**, 78.
Ellison, M. A. 1949, *M.N.*, **109**, 3.
———. 1952, *Pub. R. Obs. Edinburgh*, **1**, 75.
———. 1953, *Report, Accademia nazionale dei Lincei Fondazione Volta, Convegni 11*, p. 97.
Goldberg, L., Dodson, H. W., and Müller, E. A. 1954, *Ap. J.*, **120**, 83.
Jager, C. de. 1952, *Rech. Astr. Obs. Utrecht*, Vol. **13**, Part 1.
Menzel, D. H. 1931, *Lick Obs. Bull.*, **17**, Part 1.
Mohler, O. C. 1947, *Pub. A.S.P.*, **59**, 266.
Severny, A. B., and Shaposhnikova, E. F. 1954, *Astr. J., Moscow*, **31**, 124.
Waldmeier, M. 1948, *Astr. Mitt. Zürich*, No. 153.

STELLAR SPECTRA IN MILKY WAY REGIONS. V. A REGION IN MONOCEROS

S. W. McCuskey
Warner and Swasey Observatory, Case Institute of Technology
Received December 29, 1955

ABSTRACT

Spectra and photographic magnitudes are given for 2290 stars in LF9, an area of 16.4 square degrees in Monoceros at R.A. 6^h51^m; Dec. $-1°.3$ (1950). Blue-red color indices are listed for a majority of the early-type stars. Identification charts are presented in Figures 1*a*–1*f*.

INTRODUCTION

An analysis of spectral types, magnitudes, and colors for a study of the galactic structure in Monoceros was published recently by McCuskey (1954). This circular region, designated as LF9 in the program of the Warner and Swasey Observatory, is centered at R.A. 6^h51^m; Dec. $-1°.3$ (1950); $l = 182°$, $b = +2°$; it covers 16.4 square degrees of the sky. The present paper contains identification charts and a catalogue of the observational data for LF9. Preceding papers of this series have given similar data for regions LF1 Aquila (McCuskey 1949), LF2 Cygnus (McCuskey and Seyfert 1950), LF3a Cygnus (Annear 1953), LF3b Cygnus (Nassau and MacRae 1949), LF4 Cepheus-Lacerta (McCuskey 1955), and LF5 Cassiopeia (Farnsworth 1955).

OBSERVATIONAL DATA

All the observations were made with the 24–36-inch Schmidt telescope. Sectional charts covering LF9 are presented in Figures 1*a*–1*f*. A key to the sectioning appears in the upper left-hand corner of Figure 1*a*. The arrangement of numbering is similar to the *Bonner Durchmusterung*. In each zone of declination the stars are numbered approximately in order of right ascension. The co-ordinate lines on the charts are *approximate only*, and the printing reads correctly when north is up.

Table 1 gives the observational data for 2290 stars in LF9. The serial number in column 1 corresponds to the number for the star on the charts. An asterisk denotes a *BD* or an *SD* star, and an "R" indicates a remark following Table 1. In the Remarks, *BD* or *SD* numbers for a few stars in each zone are given, so that orientation with respect to the *BD* or *SD* charts may be made quickly.

Column 2 of Table 1 gives the apparent photographic magnitudes of the stars. These have been measured on four Kodak II*a*-O plates with the Eichner iris-diaphragm photometer. As determined from the internal agreement of the measures on four plates, the probable error of a final magnitude is ± 0.05 mag.

The photographically established magnitude sequence for this photometry was checked photoelectrically by Dr. D. A. MacRae on two nights. The visual magnitude, V, for one star of the sequence was determined by comparison with two standard stars, β Cnc and η Hya, of the list published by Johnson and Morgan (1953). The values of V observed on two nights differed by only 0.01 mag. Nine stars of the sequence were measured on the two nights to check the scale. The photoelectric yellow magnitudes Y_0, measured by MacRae, were converted to the International Photovisual System by the relation $V = Y_0 - 0.054C_0 +$ constant, where C_0 is our color index, reduced to outside the atmosphere. The V magnitudes and the colors, $P - V = 0.335 + 1.137C_0$, are essentially on the system defined by Stebbins, Whitford, and Johnson (1950). These two data yielded the photographic magnitudes and the colors for the sequence stars.

Column 3 of Table 1 gives the blue-red color indices for the early-type stars and for a few dwarf stars of later spectral type. The red magnitudes from which these were derived were measured on three Kodak 103*a*-E plates with the Eichner photometer. The plates were taken in combination with a Wratten No. 22 filter. The photoelectric colors $P - V$ for the sequence stars were converted into the blue-red system by the relation R.I. = $1.33(P - V)$. From this relation photored magnitudes were provided and were used in calibration of the plates measured with the Eichner photometer. Internal agreement among the three plates indicates a probable error of ± 0.05 mag. for a final red magnitude. The color indices, therefore, have a probable error of ± 0.07 mag.

The last column of Table 1 presents the spectral types and luminosity classes. For the most part these depend upon estimates made on three plates taken with the 4° objective prism attached to the 24–36-inch telescope. For the faintest stars only two plates were used. The luminosity nomenclature is that of Morgan, Keenan, and Kellman (1943). For the stars F0 and later and brighter than $m_{pg} = 11.0$, it was generally possible to distinguish four luminosity classes, viz., I (supergiant), III (giant), IV (intermediate), V (dwarf). For the fainter stars, and only for those of class later than F8, in general, luminosity classes III and V could be used. In many cases poorly exposed or overlapping spectra precluded the assignment of a luminosity class.

In the table of remarks, peculiarities noted in the spectra are given, together with th *BD* or *SD* numbers of stars where available. OB stars are those of high luminosity and early type, according to the designation by Nassau and Morgan (1951). Stars having hydrogen lines sharper than usual for their class are also listed.

I am greatly indebted to Dr. D. A. MacRae, now of the David Dunlap Observatory, for making the photoelectric observations on which the present photometry is based.

REFERENCES

Annear, P. R. 1953, *Ap. J.*, **118**, 77.
Farnsworth, A. H. 1955, *Ap. J. Suppl.*, Vol. **2**, No. 15.
Johnson, H. L., and Morgan, W. W. 1953, *Ap. J.*, **117**, 313.
McCuskey, S. W. 1949, *Ap. J.*, **109**, 426.
———. 1954, *ibid.*, **120**, 139.
———. 1955, *Ap. J. Suppl.*, Vol. **2**, No. 15.
McCuskey, S. W., and Seyfert, C. K. 1950, *Ap. J.*, **112**, 90.
Morgan, W. W., Keenan, P. C., and Kellman, E. 1943, *An Atlas of Stellar Spectra* (Chicago: University of Chicago Press).
Nassau, J. J., and MacRae, D. A. 1949, *Ap. J.*, **110**, 478.
Nassau, J. J., and Morgan, W. W. 1951, *Pub. U. Michigan Obs.*, **10**, 43.
Stebbins, J., Whitford, A. E., and Johnson, H. L. 1950, *Ap. J.*, **112**, 469.

Table 1

Observational Data in LF9

Zone 0°

No.	m_{pg}	R.I.	Sp.	No.	m_{pg}	R.I.	Sp.	No.	m_{pg}	R.I.	Sp.
1*	8.40	-0.53	B8	51	11.47	+0.06	A0	101	11.35	+0.08	A2
2*R	9.91	-0.53	B3	52*	10.08	-0.32	A0	102*	10.65	-0.17	A0
3	9.57	-0.58	A0	53	10.39	-0.21	A2	103	10.72	-0.20	B8
4	11.46	...	B5	54	11.85	...	A2	104	12.15	-0.04	A0
5	11.50	...	A0	55	11.59	-0.16	A0	105R	10.83	-0.02	A2
6	11.39	...	F8V	56*R	9.70	-0.12	A0p	106	11.44	...	B8
7*R	10.03	+0.07	A2-F2	57	11.56	-0.21	B9	107*	11.32	+0.30	A2
8	12.26	...	K0:	58R	11.49	-0.23	B:	108	11.30	+1.21	G8V:
9*	10.35	-0.11	F0V	59*R	9.13	-0.29	B3	109	10.87	-0.10	A0
10	11.60	...	B9	60R	9.81	-0.17	B5	110	10.05	...	F0V
11	11.70	-0.11	A0	61	11.59	...	K0III	111	11.36	...	G0III:
12	11.27	...	G2	62	10.84	...	F5III	112	11.60	...	G2
13	11.67	...	K0III	63	11.87	+0.08	B8	113	11.16	...	G0
14*	6.83	-0.13	F0V	64*	11.04	...	K0III	114*	10.48	...	G2III
15	11.33	...	B5:	65	12.01	+0.16	A2:	115	11.22	+0.11	B9
16*R	9.75	+1.77	G8Ib:	66*	9.58	...	G8III	116	11.84	-0.06	B9
17*	10.59	...	G5III	67*	9.87	+0.12	F8V	117	10.47	-0.10	A0
18*R	8.02	+0.17	A2III	68*	10.18	...	G5III	118	10.80	-0.19	A5
19*	9.20	-0.37	B3	69	11.59	-0.02	B9	119	11.68	+0.05	A3
20*	7.53	+0.59	G0V	70*	11.33	...	F0	120	11.38	...	F0
21	11.68	...	F0:	71R	11.71	+0.69	G8p	121	12.12	-0.05	A0
22	10.84	...	F0V	72*	9.62	-0.51	B8	122	11.80	+0.06	A0
23*	10.12	-0.20	A2	73*	11.28	...	G2	123R	11.63	...	K3p
24	11.52	...	G0	74	11.40	-0.03	B9	124	11.55	+0.04	A0
25	11.40	...	G0:	75	11.38	-0.19	A0	125*	11.63	...	G0:
26*	9.54	-0.39	B5	76	10.90	+0.05	B5	126*R	8.96	-0.58	B9
27	12.00	+0.02	A0	77	11.98	...	B8	127	12.31	...	A0
28*	10.26	+0.29	G0V	78*	8.14	-0.58	B8	128	11.41	...	A0
29	11.16	...	F8	79	10.80	...	B8:	129	11.50	+0.06	A0
30	11.06	-0.29	B8	80	10.58	+0.33	G0V	130	11.41	-0.02	A0
31*	9.50	-0.65	B8	81	10.76	+0.04	B9	131	12.00	-0.05	A0
32	10.92	...	G8III	82	11.35	-0.05	A0	132*	10.61	-0.19	A0
33	11.36	...	A0	83	10.25	-0.35	A2	133*	9.96	...	M5III
34	11.21	...	G0:	84	10.86	-0.24	B9	134	11.15	...	G0
35	11.16	...	F8V	85*	8.11	...	F5V	135	11.10	...	A0
36*	10.43	-0.25	B9	86*R	9.90	+0.03	O8	136	11.88	...	A5:
37R	11.60	-0.13	A0p	87*	9.80	-0.41	B9	137	11.30	...	G0
38	12.06	...	A0	88	11.96	...	G2:	138*R	8.65	+0.87	G0III:
39	11.09	...	G0:	89	10.42	...	A5	139*	10.44	...	G5III
40	11.72	...	A0	90	11.68	+0.09	A0	140*R	8.48	-0.17	B9
41	11.45	...	A0:	91*	9.49	-0.07	A0	141	11.52	-0.08	A0
42	11.21	+0.02	B8:	92	11.72	...	K0III	142*	8.95	-0.12	B8
43	11.28	...	F0	93	10.75	-0.33	A0	143*R	8.00	-0.29	B8
44	10.88	...	G0Ib:	94	12.17	...	K0:	144*	8.61	...	K0III
45*R	8.78	-0.32	B1	95	11.68	+0.11	A0	145*	10.98	...	G5III:
46*	9.50	-0.05	A5	96	10.21	...	A3	146	10.17	-0.38	B8
47*	9.49	-0.46	B8	97	11.50	...	G0	147	10.18	-0.22	B8
48	11.19	-0.24	A0	98*	11.10	...	F2V	148	10.60	-0.24	B9
49	11.34	...	B5	99	11.75	...	A0	149	11.86	-0.19	A0
50*R	10.73	+0.24	B0:	100	11.43	...	F8	150	10.60	...	A5

Table 1

Observational Data in LF9 (Cont'd.)

Zone 0° (Cont'd.)

No.	m_{pg}	R.I.	Sp.	No.	m_{pg}	R.I.	Sp.	No.	m_{pg}	R.I.	Sp.
151	9.82	-0.35	B8:	201	11.30	+0.14	B5	251	11.92	+0.29	A0
152*	9.75	+0.01	B9:	202	11.82	+0.10	B2:	252	12.24	-0.13	A0
153	12.00	+0.09	A0	203	11.22	...	G0:	253	10.75	+0.64	G2V
154	11.70	+0.07	A0	204	11.78	+0.02	A0	254	12.29	+0.43	A0
155*	9.88	-0.38	B9	205*	11.15	...	F0:	255	11.95	...	G0:
156	11.41	...	F0	206	11.49	...	F0	256	11.95	...	G0
157	11.67	+0.24	B9	207	11.98	+0.24	A0	257	10.92	+0.09	A3
158	11.31	...	G5	208	11.95	...	K3	258	10.51	-0.02	A0
159	11.27	+0.08	A0	209*	9.34	+0.02	A0	259	11.70	0.00	A0:
160	11.91	...	F2	210	12.13	...	K0III	260*	11.28	...	F0
161	11.18	-0.12	A0	211*	10.89	...	K0III	261* R	8.69	+0.04	B0
162	11.41	-0.17	B9	212	11.88	...	A0	262	11.20	-0.06	A0
163	10.92	-0.12	A0	213	11.66	...	G0:	263	11.78	-0.02	B8
164*	9.92	-0.19	A2	214* R	9.99	...	F0V	264R	10.76	+0.20	A0
165	10.39	-0.19	A0	215	11.00	...	G0:	265* R	9.68	-0.30	B5
166	10.68	-0.15	B9:	216	11.83	...	K5	266	11.97	...	K0
167*	10.89	-0.10	B8:	217	11.93	...	A5:	267*	10.09	+0.61	G2IV
168	10.77	-0.13	B8:	218*	9.86	-0.32	B8	268	11.81	...	G0
169	11.39	+0.18	F0	219	11.62	+0.26	B8	269	11.92	-0.03	A0
170	10.40	...	F2V	220	11.27	...	F8	270*	10.06	-0.23	B8
171	11.72	+0.02	A0	221	11.11	...	F0	271	11.73	...	K0
172*	9.38	...	G8III	222	11.05	...	G0:	272	11.40	...	G0
173	11.50	-0.03	B8	223	11.86	-0.18	B9	273*	10.72	-0.06	A0
174*	9.75	-0.27	B9	224	10.57	-0.08	B9	274	11.42	...	F5
175	11.00	-0.16	A0	225*	9.28	+0.26	G0V	275	10.67	-0.08	A0
176* R	10.29	-0.19	A0	226	11.75	...	G5	276	11.83	-0.10	A0
177*	10.27	...	F8V	227	11.62	-0.21	B9	277*	9.55	+0.28	G0V
178	11.93	+0.35	A:	228	11.21	...	G5IV	278	11.23	...	F8
179	11.29	...	G8III	229	11.26	-0.10	A0	279	11.92	...	K0:
180	11.17	...	F2	230	11.57	...	G5V	280	11.79	...	A0
181	11.55	...	K0	231	11.23	...	B5	281*	10.04	-0.02	A0
182	11.45	+0.52	G0:	232*	9.83	+0.05	A2	282	11.81	...	G8
183*	10.61	-0.22	A0	233	12.21	...	G0:	283	11.38	...	F2
184	11.88	+0.11	A0	234*	10.02	-0.28	B9	284	11.21	+0.35	F8V
185	11.07	-0.25	A0	235*	8.33	+0.12	A7	285*	10.68	+1.01	G8III
186	11.37	-0.03	A5	236	11.98	+0.39	A0	286	11.31	...	A2
187	12.06	...	G2:	237	10.95	+0.05	B8	287	11.27	...	K5:
188*	9.85	...	B9	238	11.60	...	B9	288	12.07	...	K0
189	11.75	...	F8	239R	11.71	+0.34	A5p	289	11.92	...	G2
190	11.04	-0.15	A0	240	11.11	+0.07	B5	290	12.57	+0.04	B8:
191* R	11.25	-0.25	B8	241	11.29	-0.14	A0	291	11.19	-0.01	A5
192R	11.58	-0.04	A2	242	11.40	+0.13	A0	292	10.29	-0.12	A2
193	11.51	+0.05	A0	243	11.88	...	A0	292aR	10.47	-0.23	B3
194	10.65	-0.36	B9	244*	9.20	...	G0IV	293	10.47	-0.05	A2
195	11.20	...	G0	245	9.90	-0.26	B5	294	11.53	+0.03	A3
196	12.19	...	G0:	246	11.97	+0.37	A0	295* R	9.68	-0.36	B9
197	11.55	...	M0	247*	10.02	...	K2III	296	12.17	-0.16	A0
198	11.14	-0.13	A0	248	11.50	-0.27	B9	297*	9.25	...	G8IV
199	12.15	-0.03	A0	249	11.65	...	G0	298	11.53	...	F2:
200*	9.27	-0.35	A0	250*	11.37	...	M5III	299*	10.25	...	G5V
								300	11.53	+0.19	A2

Table 1

Observational Data in LF9 (Cont'd.)

Zone 0° (Cont'd.)

No.	m_{pg}	R.I.	Sp.	No.	m_{pg}	R.I.	Sp.	No.	m_{pg}	R.I.	Sp.
301	11.28	...	F2	351	10.59	...	G5III	401*R	8.29	-0.16	A2
302	11.90	+0.02	A0	352	11.38	...	K0	402	11.66	...	K2
303	11.57	...	G0	353	10.73	-0.13	B8	403	11.59	0.00	A0
304	11.22	+0.07	G0	354R	11.02	+0.01	B8	404*	9.26	...	G5IV
305	10.63	...	A0	355	11.79	+0.15	A2	405	11.45	...	G2
306	12.68	...	K0	356	11.26	...	K5	406*	9.23	+0.04	A5
307	11.00	+0.55	G8IV	357*	9.69	-0.06	A0	407*	7.64:	...	F2V
308*	11.84	...	G0:	358*	10.15	-0.14	A0	408	11.18	...	G8III
309	11.71	+0.06	A0	359	11.46	-0.07	A3	409*	10.55	-0.04	A2
310	10.87	-0.09	A0	360*	11.48	+0.25	A0	410	11.76	+0.08	A0
311*	9.13	...	K0III	361	11.47	+0.12	B8	411*	8.95	-0.42	B8
312*	11.13	...	K21b	362	10.39	...	F5IV				
313	11.62	+0.17	A3	363	10.80	-0.18	B8				
314*	10.17	-0.34	A0	364	12.28	...	K0				
315	11.05	+0.38	G0	365*	10.46	-0.01	A0				
316*	10.28	...	K2IV	366R	11.59	+0.09	A3p				
316a	10.27	-0.19	B8	367*	10.96	...	K0III				
317*	10.42	...	G8III	368*	10.83	+1.00	G8V				
318	11.43	...	G8III	369	11.23	...	G0				
319	11.35	...	K0III	370	11.99	...	G2:				
320	11.72	+0.21	B5								
321	12.27	...	K2	371	11.44	...	G0				
322	11.91	...	G5:	372	11.32	+0.06	A0				
323	11.72	+0.08	A0	373*	9.12	-0.52	B8				
324	11.33	...	G0	374	11.69	...	F8:				
325	11.98	+0.16	A0	375	12.09	...	K0				
326	11.84	...	G0:	376*	9.65	...	G8III				
327	11.94	+0.15	A2:	377	9.75	-0.24	A2				
328*	10.60	+0.46	F8V	378	11.45	...	F0:				
329	12.00	+0.09	A0	379	11.32	+0.49	G2V				
330*	10.83	...	K5III	380	10.63	+0.84	G5III				
331	11.61	...	K0	381*R	7.48:	...	A5				
332*	8.57	-0.42	B9	382	10.27	-0.25	A2				
333	10.98	+0.07	B8	383	11.13	...	G2				
334	11.99	...	A0	384	11.33	...	G0				
335*	11.26	...	F8:	385	11.54	...	G0:				
336	11.25	+0.18	F0	386*	10.74	-0.38	B5				
337	11.72	-0.14	A2	387	10.34	-0.07	A7V				
338*	10.03	+0.11	A5	388	10.83	-0.05	F0V				
339*	8.33	...	K0III	389	11.87	...	G0				
340	12.24	...	K0	390	10.94	+0.25	G2V				
341	11.83	+0.11	A0	391*	8.97	...	K0III				
342	11.05	-0.10	A0	392*	9.41	...	K2III				
343	11.24	...	K0:	393	12.37	+0.13	A0				
344*	9.08	+1.40	G8IV	394	12.03	+0.26	A2				
345*	10.03	-0.31	B9	395	11.58	...	F0:				
346	10.80	-0.06	A3								
347	11.16	...	F5	396	10.76	-0.08	A5				
348	12.02	+0.31	A0	397	11.01	-0.05	B5				
348a	12.26	+0.37	B9	398	12.09	+0.19	A0				
349	11.58	...	G2:	399	11.47	-0.10	A0				
350*	10.28	-0.09	A3	400	11.31	...	G0				

Zone -1°

No.	m_{pg}	R.I.	Sp.
1*	10.31	...	F0V
2	10.68	-0.31	B9
3	11.92	...	K0:
4	11.75	...	G0:
5*	10.10	+0.23	G01b
6	11.62	...	G0
7	11.60	...	G8III
8	10.73	...	G0
9*	10.47	-0.65	B5
10*R	6.83	...	B8
11	11.32	...	K0III
12	11.80	...	A0
13	11.23	-0.18	A0
14*	8.94	...	F0IV
15	11.41	-0.34	A0
16	10.63	...	G0V
17*	9.70	-0.46	F0V
18	12.05	...	G5:
19	11.22	...	G8III
20	11.88	...	G0
21	10.16	-0.49	A0
22	11.58	...	G0
23	10.92	...	A5
24	10.25	...	F2III
25	11.99	...	K0
26	12.05	-0.03	A2
27	11.86	...	G5:
28	11.64	-0.03	A0
29*R	9.97	-0.76	B8
30*	9.75	-0.71	B8
31*R	6.58	-0.43	B8
32	10.85	...	F8
33	11.31	...	G8III
34R	10.48	-0.22	A5
35	11.05	-0.30	A0

Table 1

Observational Data in LF9 (Cont'd.)

Zone -1° (Cont'd.)

No.	m_{pg}	R.I.	Sp.	No.	m_{pg}	R.I.	Sp.	No.	m_{pg}	R.I.	Sp.
36	10.69	...	G0	86*	10.00	-0.58	B9	136	11.87	...	A0
37	11.39	...	G0:	87	11.10	-0.06	A3	137*	10.72	...	F8III
38	10.56	-0.18	A0	88	11.32	-0.11	A5	138	11.58	+0.24	F0
39	11.34	...	F8	89*	11.82	...	K0	139	11.75	+0.15	A0
40	10.88	...	G8III	90* R	9.49	...	A3	140	12.18	+0.61	A0
41*	10.87	...	G8III	91	10.75	...	G0	141*	11.62	...	K0
42	10.82	-0.36	A0	92	10.77	...	K01b:	142	12.24	+0.35	A0
43	11.44	...	F0:	93	12.10	+0.35	A0	143	11.58	...	G5
44	10.86	...	G2	94	11.30	+0.04	A0	144	11.57	+0.36	B0;
45	11.62	...	G0	95*	10.76	...	G5III	145	11.56	...	K2
46	10.17	...	F01b	96	11.27	-0.06	B9	146*	9.73	...	K3III
47	11.52	...	G0	97	11.25	...	B:	147* R	9.12	-0.28	B8
48	11.57	...	G8:	98*	10.25	-0.29	B9	148	11.76	...	K0III
49	11.15	...	K0III	99	12.00	+0.06	A0:	149*	9.25	+0.59	F8V
50	11.90	...	K0:	100*	9.29	...	G8III	150	11.27	+0.06	B5
51*	9.14	...	F5V	101*	9.92	...	F5V	151	12.17	+0.20	A0:
52	10.96	...	F8V	102	10.94	...	G8V	152	11.45	+0.13	A0
53	9.14	...	K0III	103	11.65	+0.05	B5:	153R	10.52	+0.23	B8
54*	10.60	...	A5	104*	9.51	...	G5III	154	11.93	...	G0
55	11.93	+0.34	A0	105	11.96	...	G5:	155	10.51	...	F5III:
56*	10.56	...	K0III	106	12.34	+0.28	A0:	156	10.68	-0.07	B9
57	11.40	...	F0	107	11.89	+0.20	A0	157	11.08	+0.24	A2
58* R	9.02	...	A2-F0	108*	11.23	...	G5	158*	10.50	...	G5III
59	11.83	...	G0	109*	8.44	...	G5III	159*	10.31	+0.06	A0
60	11.50	-0.19	B8	110	9.98	+0.96	G5IV	160	11.62	+0.17	A2:
61	10.61	...	G0	111*	10.67	...	G0	161	11.52	...	G0
62*	10.56	-0.16	B9	112	11.04	+0.03	B9	162	11.12	-0.09	B8
63*	9.87	...	F5V	113	11.45	...	G0	163	11.84	...	G8III
64	11.27	+0.08	A0	114*	9.34	-0.44	B5	164*	10.98	...	M2III
65* R	8.85	-0.67	B5	115	10.60	...	G01b	165*	6.20:	...	F0V
66*	10.64	...	G8III	116	10.84	+0.12	A0	166	11.97	...	K0:
67	11.42	-0.13	A0	117	12.04	+0.19	A0	167	11.46	+0.12	A2
68	11.36	-0.07	B9	118R	10.67	+0.14	B3	168*	10.62	+0.71	G5V
69	11.59	-0.07	B9	119*	9.45	-0.43	B9	169	11.60	...	F8
70	11.74	...	F2	120	10.63	...	F0V	170*	10.84	+1.24	G01b
71	11.94	-0.02	A0	121	11.53	...	G0	171	11.28	...	G8III
72	10.98	-0.05	A0	122*	10.28	...	G8III	172	10.86	...	F5V
73*	9.62	...	G5III	123* R	8.60	-0.49	B8	173*	10.02	...	K2III
74* R	8.66	-0.27	B2	124	11.41	...	G2	174	11.07	-0.15	B9
75	11.12	...	G0	125R	11.43	-0.12	B3:	175	11.07	+0.29	B9:
76	11.68	...	G0:	126	11.35	...	F2	176	11.09	...	K0III
77	11.21	...	G8III	127R	10.54	+0.06	B0:	177	10.47	+0.34	F0V
78	10.81	-0.05	A0	128	11.62	...	G0	178*	9.48	-0.34	B9
79*	9.78	...	A2	129	11.78	-0.05	B5:	179	10.80	+0.31	B8:
80R	10.98	...	B3	130*	10.57	-0.07	A0	180	10.86	+0.13	A3
81	11.88	...	G8	131*	10.38	+0.11	F0V	181	10.94	+0.08	A2
82	11.55	...	F8	132	11.52	...	G0	182	10.85	-0.09	B5
83	11.95	+0.28	A0	133	12.00	...	K2	183	10.82	+0.56	G2V
84* R	9.73	-0.31	A0	134	11.39	...	G2	184	11.64	...	G8III
85	11.04	...	G0	135	11.11	+0.16	A0	185	11.42	...	K0III

Table 1

Observational Data in LF9 (Cont'd.)

Zone -1° (Cont'd.)

No.	m_{pg}	R.I.	Sp.	No.	m_{pg}	R.I.	Sp.	No.	m_{pg}	R.I.	Sp.
186	11.45	0.00	B9	236	11.79	...	G5	286	12.27	+0.10	A3:
187	11.33	...	G0	237	11.48	-0.18	B8:	287	11.96	...	G8
188	10.96	+0.05	B9	238*	10.31	-0.17	A0	288*	9.09	-0.29	B9
189	11.00	+0.16	A0	239	12.16	+0.39	B9	289	11.68	...	K0
190	11.63	+0.13	B8	240	11.68	+0.04	A0	290	11.63	-0.09	A0
191	11.45	...	G5III	241	12.05	-0.02	B8:	291	11.10	...	G0
192	11.92	...	K0	242	11.79	...	G0	292*	11.59	+0.29	A0
193	12.06	...	G0:	243* R	9.84	0.00	B8	293	10.67	-0.12	B8
194	11.15	...	F8	244	12.11	+0.12	A0:	294*	11.60	...	G2:
195	11.43	+0.10	A0	245	11.41	+0.09	B8	295	10.76	+0.25	B9
196	11.88	...	G5:	246	11.10	-0.01	B8	296	11.98	...	G5:
197	11.05	+0.53	F2	247	11.25	+0.39	A3	297	11.58	...	G5:
198	11.86	-0.05	A2	248	10.16	-0.10	B8	298	12.09	...	G8
199	10.46	+0.14	B9	249	11.33	+0.07	A0	299*	9.33	-0.05	A5
200*	10.95	...	K0III	250* R	10.34	-0.25	B9	300R	10.22	-0.32	B8
201	12.15	+0.10	A2:	251	11.45	-0.05	A3	301*	11.19	...	M0III
202*	9.33	-0.18	B8	252*	9.61	...	F0IV	302	11.30	+0.27	F0
203	11.17	...	G0II	253	11.01	-0.01	B5:	303	12.16	...	K0
204	12.12	...	A0	254	12.09	...	G0:	304	11.74	...	G0
205* R	8.32	-0.01	B8	255	11.43	...	G0	305	11.29	...	G0
206	10.90	+0.25	A2	256* R	9.96	-0.19	B2	306	11.26	...	G0
207*	9.94	-0.07	B9	257	11.87	...	F0:	307	11.63	+0.06	A0
208	11.42	+0.24	A5	258	11.17	...	F8	308	11.48	0.00	A0
209*	10.91	...	G8III	259	11.04	...	G8III	309	11.74	+0.07	A0
210	11.97	+0.34	B9	260*	10.89	...	K0:	310	10.67	-0.11	A0
211	12.27	+0.37	A0	261R	11.66	-0.10	B8p	311	10.48	+0.39	G0V
212	11.76	...	K0	262	11.83	...	G8	312	11.58	+0.19	A3
213* R	8.75	-0.23	B3	263	10.52	-0.21	A0	313	12.23	-0.04	A0
214	11.62	0.00	B5	264	11.41	-0.15	A0	314	11.23	-0.23	B8
215	11.01	+0.23	B9	265	11.63	-0.02	B9	315*	10.04	+0.57	G2V
216	11.67	...	K0	266	10.90	+0.60	G2V	316	11.41	+0.29	B5
217	11.48	+0.07	B8	267*	9.56	...	K0IV	317	11.38	+0.70	G2V
218	12.05	...	G8	268	11.29	+1.15	G8V	318R	11.18	+0.19	A5:
219	11.65	+1.59	K5	269*	9.65	...	G5III	319	11.57	+0.05	B9
220	12.06	-0.02	A0	270* R	8.60	-0.39	B9	320	12.21	...	G2
221	11.88	...	G0:	271* R	9.31	-0.39	B5	321	11.25	+0.14	B8
222R	11.49	...	B:	272	11.74	...	G8	322*	10.40	0.00	A0
223	11.64	...	A0	273	11.89	...	K0:	323*	11.18	+0.93	G8V
224	11.47	+0.09	B8	274	11.30	...	G2:	324*	11.58	...	K0
225	11.46	...	G5	275* R	7.95	-0.45	B8	325	11.40	...	F5:
226	12.14	...	F0:	276	11.27	+0.23	A5	326	10.85	-0.05	B8
227	12.00	...	G0	277*	9.53	...	F5V	327	11.75	...	K0
228*	10.04	...	K0IV	278*	8.98	-0.26	A0	328	11.55	...	G2
229	11.68	-0.02	B8	279	11.52	-0.10	A0	329	12.19	...	G8:
230	11.83	...	K0:	280	10.96	-0.20	B5	330	11.78	...	G0:
231R	10.02	-0.23	B9	281* R	10.13	-0.22	B8	331	11.91	+0.23	A0:
232R	11.70	+0.11	A0	282*	9.18	-0.35	A0	332	11.68	...	G5:
233	12.03	+0.18	A0	283R	10.44	-0.33	A0p	333*	8.97	-0.35	B8
234	11.92	...	G5:	284*	10.59	+0.64	G0II:	334	12.25	+0.35	A0
235	11.23	-0.12	B5	285	11.75	-0.12	A0	335	11.47	+0.03	A2

Table 1

Observational Data in LF9 (Cont'd.)

Zone -1° (Cont'd.)

No.	m_{pg}	R.I.	Sp.	No.	m_{pg}	R.I.	Sp.	No.	m_{pg}	R.I.	Sp.
336	10.21	-0.15	A0	386	11.25	+0.03	A0	436*	10.30	-0.28	B8
337*	11.37	...	G8III	387	11.13	...	F8	437	12.23	...	K0:
338*	10.87	...	G2V:	388R	11.05	+0.09	B2	438	11.87	+0.12	B9
339	11.80	+0.13	B5:	389	12.19	...	K0	439	12.23	+0.21	A0:
340	11.29	...	G0	390	11.52	+0.05	B9	440* R	8.74	-0.32	B9
341	12.18	...	A0	391*	8.62	-0.40	B8	441*	10.92	...	G0
342	10.19	-0.13	A2	392	12.02	...	A0	442	12.44	...	G0
343	12.33	...	A0	393	11.43	...	G0	443	12.54	+0.17	A0
344	11.31	-0.01	A2	394*	11.38	...	G8	444	12.35	...	G5:
345	10.28	+0.91	G8IV	395	11.76	+0.19	A3	445	11.60	...	G5:
346*	11.19	-0.02	A0	396	11.42	+0.05	A2	446*	11.39	+0.15	B8
347*	9.95	-0.03	A0	397*	9.55	...	F5IV	447	12.05	+0.12	B5:
348	11.31	...	K0III	398*	10.67	-0.16	B9	448	11.91	+0.12	A0
349*	10.80	0.00	B8	399	12.11	...	G0	449*	10.27	...	F0V
350	11.80	+0.12	B9	400	12.20	...	G5:	450	11.11	-0.10	B5
351	11.97	...	K0	401R	11.17	+0.08	B8	451*	10.71	-0.31	B8
352	11.10	-0.04	B8	402	10.67	...	G0V	452	11.36	+0.02	A0
353	11.45	...	G2IV	403	10.93	-0.07	A0	453	11.69	-0.05	A3
354	10.83	+0.47	G0V	404	11.60	...	F2	454	11.94	+0.15	A0
355*	9.14	+0.14	A7V	405	12.22	+0.21	A0	455	11.07	-0.07	F0
356	10.95	...	F0V	406	12.27	...	K0	456	11.91	...	G5
357	10.99	+0.07	B9	407	12.06	...	K0:	457* R	10.66	-0.04	A3
358	11.74	...	F0	408	10.62	-0.10	A0	458*	11.83	...	G8
359*	9.03	...	K3IV:	409	11.94	...	A0:	459	12.27	...	K0
360*	8.72	-0.14	A0	410	11.57	-0.03	B5	460	11.76	+0.10	B9
361R	10.74	-0.14	A0	411	12.27	+0.40	A3:	461	10.92	-0.06	B8
362	12.31	+0.20	A2	412	12.03	...	G0:	462	11.91	...	K0
363	11.96	+0.20	A0	413	11.67	...	G0	463*	9.71	...	F0IV
364*	9.02	-0.13	A0	414	11.29	...	G0	464* R	8.47	-0.18	A0
365	11.87	...	M5III	415	11.55	+1.14	G8	465	10.22	...	F0V
366	11.65	...	G0	416*	10.14	+0.94	G5IV	466*	10.21	...	K0IV
367	10.36	-0.08	A2	417	12.40	+0.39	A0:	467	11.14	+0.01	B8
368	11.98	+0.05	B8	418	12.35	...	F0	468	11.56	...	G0
369	11.83	+0.08	A0	419R	10.80	+0.24	A2-F0	469	11.62	...	G8
370*	10.13	-0.23	A0	420	11.67	+0.22	A2	470	11.81	...	A2:
371	11.30	-0.09	A0	421* R	9.36	-0.29	B9	471	11.00	...	F8
372*	9.64	-0.01	A5	422	11.87	+0.01	A0	472	11.12	-0.14	B5
373	11.64	...	G5	423*	9.28	-0.15	A3	473	12.27	...	K0:
374*	9.04	-0.30	B8	424	12.11	...	G2:	474	12.41		
375	12.45	...	G8:	425	11.59	+0.09	A2	475	11.62	...	F0
376	12.34	+0.03	B9	426*	10.38	+0.47	G2V	476*	10.40	-0.27	A0
377R	10.47	-0.13	B8	427	12.06	...	G8	477	12.00	+0.22	B8
378	11.31	-0.09	A0	428	12.05	...	G0	478*	9.38	+0.32	G5V
379	10.76	+0.06	B9	429	10.99	+0.71	G8V:	479*	9.18	-0.52	B8
380*	10.47	...	F0V	430*	9.28	+0.56	G5V	480	9.69	-0.03	A5
381*	9.00	-0.18	B9	431*	9.68	...	G0IV	481	11.40	+0.24	A5:
382	11.12	...	F0	432	11.97	...	K0	482*	10.03	-0.27	B8
383	12.31	+0.19	A0:	433* R	8.59	-0.34	B8	483	11.95	+0.16	A2:
384*	10.04	...	K0III	434	11.54	...	G0:	484	11.73	+0.06	B5:
385	12.12	+0.19	A0	435	11.33	-0.02	B9	485	10.62	-0.13	B9

Table 1

Observational Data in LF9 (Cont'd.)

Zone -1° (Cont'd.)

No.	m_{pg}	R.I.	Sp.	No.	m_{pg}	R.I.	Sp.	No.	m_{pg}	R.I.	Sp.
486	11.77	+0.05	A0:	536*	8.87	-0.49	B9	41*	8.93	...	K2IV
487	10.70	-0.10	B9	537	11.47	-0.10	A0	42	11.17	-0.19	B8
488R	11.29	+0.09	A0	538	11.67	-0.36	B9	43	11.43	...	F5
489	10.42	-0.41	B8	539	11.90	...	G0:	44	11.52	...	G0
490	11.97	+0.07	A0	540*	11.09	...	K0IV	45	11.15	+0.86	G8V
491	11.41	...	F8	541	11.06	...	G0	46	11.85	...	G8
492	10.32	-0.13	A5	542	11.61	...	A3:	47	11.12	-0.23	A0
493*	8.78	+0.28	G0V	543	12.59	...	K0:	48*	9.77	...	F2:
494	9.40	+0.39	F8V					49	10.87	...	G8
495	11.68	...	K2					50	12.20	-0.15	A0:
				Zone -2°							
496*	9.67	...	G8III	1	10.52	...	G0	51	11.13	...	F8
497	10.77	+0.32	G0V	2*	9.29	...	F0IV	52	10.96	-0.08	B5
498	11.21	-0.07	A0	3	11.36	...	F0	53	11.71	...	G5
499*	9.79	...	F5IV	4	11.52	+0.02	B5	54*	11.13	...	G8
500	11.44	...	F2	5*	9.39	...	F8V	55	11.39	...	G0
501	11.92	+0.19	A2	6	11.49	-0.19	A2	56	11.04	...	G0
502* R	9.21	-0.49	B8	7	11.16	-0.38	A3	57*	9.68	-0.61	B8
503*	10.38	...	A0	8	11.78	...	G0:	58	10.85	...	F8
504	11.83	+0.07	A0	9	10.41	...	G0	59*	10.19	...	G0V
505*	10.32	...	K0IV	10	11.82	...	K0	60*	9.37	-0.76	B8
506*	10.20	...	G5III	11	10.33	...	F8	61* R	10.60	-0.23	A3
507R	11.65	+0.30	pec.	12*	8.96	-0.30	A5	62	12.20	+0.28	A0:
508*	7.19:	...	A2	13	10.64	-0.20	B9	63	11.88	...	B8
509	11.87	...	K0	14	11.44	-0.30	B9	64*	9.23	+0.06	G0V
510*	10.17	...	K0IV	15*	9.78	-0.36	F0V	65	11.92	...	G0
511	11.22	-0.12	A3	16*	9.37	...	B8	66	11.50	...	G8
512	11.43	...	F0:	17* R	8.78	...	F5IV	67*	8.57	-0.40	A0
513*	10.32	-0.32	A2	18	11.72	...	A2	68	11.54	...	G0
514	11.58	+1.47	K0III	19	11.76	...	G5:	69*	9.41	...	F5IV
515	11.06	...	F2	20	11.56	...	F5	70	11.73	+0.21	A5
516*	10.05	-0.39	B9	21	11.84	...	G0	71	11.16	...	F8
517	10.45	+0.34	F8V	22	10.60	...	F5IV	72	12.00	-0.02	A0:
518*	9.60	...	K2III	23*	10.24	...	K0III	73	11.25	-0.11	A2
519	11.22	...	K0	24	11.91	...	F0:	74	12.05	...	K0
520	11.90	...	A2	25	10.42	-0.50	B9	75	11.62	...	G0:
521	11.02	-0.12	B9	26	12.14	...	G8	76	12.10	...	A0
522	10.68	...	G0III	27	11.73	...	G2:	77* R	8.96	-0.47	A0
523*	10.36	-0.19	A0	28	10.89	-0.54	B9	78	11.89	...	G0
524* R	8.36	-0.41	B9	29	11.85	...	K5	79	12.06	-0.09	A0
525	11.96	...	G8	30	11.61	-0.12	A3	80*	10.43	-0.18	A2
526	11.50	...	F0	31	11.61	-0.20	A3	81*	9.81	-0.50	B5
527	11.35	...	M0V	32*	7.39	-0.68	B8	82*	10.03	...	K0III
528*	9.13	-0.46	B8	33	11.64	...	G8	83	11.79	+0.05	A0
529	10.78	...	F2	34* R	10.11	-0.70	B8	84	11.64	...	G5
530	11.98	...	G8:	35	11.53	-0.22	B9	85*	10.83	...	G8III
531*R	9.71	...	A5	36* R	8.87	-0.72	B3	86*	11.42	...	K5
532*	9.85	...	M5III	37*	8.59	-0.48	A3	87* R	9.57	...	A3-F8
533	11.90	...	G0:	38	11.88	...	K0	88*	9.69	-0.55	B9
534	11.93	...	G8	39	11.79	...	G0	89	11.25	...	G0II
535	11.90	...	G0:	40	10.14	...	G0V	90	11.33	-0.14	A0

Table 1

Observational Data in LF9 (Cont'd.)

Zone -2° (Cont'd.)

No.	m_{pg}	R.I.	Sp.	No.	m_{pg}	R.I.	Sp.	No.	m_{pg}	R.I.	Sp.
91	11.18	. . .	F8	141	11.13	+0.42	G5V	191	11.60	. . .	G8
92*	8.90	-0.45	A2	142R	10.55	-0.22	B8	192	11.55	+0.14	B9
93	10.50	. . .	G0V	143R	11.13	-0.26	B8	193*	8.10	-0.37	A0
94*	5.69	. . .	F0V	144	11.05	-0.15	A0	194*	9.19	-0.29	B5
95	10.84	. . .	F8	145*	10.41	. . .	K0III	195	10.71:var?		K5III:
96*	8.71	. . .	K5III	146*	11.69	+0.07	A0	196*R	9.81	-0.14	A0
97	11.44	-0.08	A0	147	11.21	. . .	K0III	197*	9.91	. . .	F5III
98	11.60	. . .	G0	148	11.75	-0.15	B9	198	11.58	. . .	G8III
99*	8.36	+1.05	K0III	149	11.17	+1.13	G8V	199	12.07	. . .	G0:
100	11.66	+0.11	B9	150	10.59	. . .	G8III	200	11.70	. . .	F0
101	11.28	. . .	F2	151	12.32	. . .	K5:	201	11.88	+0.13	A0
102	12.04	+0.09	A0	152	12.31	. . .	K0	202	11.80	+0.01	A2
103	11.82	. . .	G0	153	11.19	. . .	F2V	203*R	8.70	-0.30	A0
104	11.88	-0.18	B5	154*	9.34	-0.31	A0	204	11.87	. . .	A0:
105	11.58	+0.10	A2:	155*	10.90	. . .	K0III	205	11.92	-0.13	B9
106*	11.01	+0.92	G5IV	156	11.91	. . .	K3	206	11.89	. . .	G0
107*	10.36	. . .	F5IV	157	11.95	. . .	F5V	207*	9.74	. . .	F0IV
108	11.38	. . .	F2	158	11.25	+0.02	B5:	208	12.12	. . .	G8III
109	11.52	. . .	F0:	159	10.87	. . .	B8	209	12.06	+0.05	A0
110	11.12	. . .	G0	160*	10.57	+0.19	F8V	210	10.82	. . .	G5III
111	11.91	. . .	G2:	161	11.13	. . .	G0:	211	10.97	+0.35	G2V
112	11.54	. . .	G2:	162*R	9.43	+0.05	A5p	212*	8.74	-0.28	B9
113	10.90	-0.27	B9	163*	10.77	-0.07	A0	213*	11.10	. . .	M0III
114	11.64	. . .	M2	164	11.89	+0.02	A0	214	11.89	-0.13	A0
115	11.55	+0.24	F0:	165	11.74	. . .	K0	215	11.89	-0.17	A0
116	11.74	+0.18	F0	166*	10.04	. . .	G2IV	216*R	10.25	+0.25	A2-F0
117	12.37	. . .	G8	167	10.31	-0.08	A0	217*	9.65	-0.19	A2
118	11.32	. . .	G2	168	11.72	-0.08	B5:	218*	10.90	. . .	F2
119	11.31	+0.15	A2	169	10.60	-0.28	A0	219	11.13	. . .	F2
120	11.39	+0.21	F01b	170	10.91	-0.11	B8	220	11.67	+0.11	F0
121R	10.35	-0.13	A3-F0	171	11.89	+0.19	A3	221	10.39	+0.29	F8V
122*	10.29	-0.14	B8	172	12.18	. . .	K0	222*	9.44	. . .	G8IV
123	11.05	-0.15	B8	173*R	8.94	-0.33	B9	223	11.48	. . .	G0
124	11.62	. . .	F8:	174	11.38	+0.10	A0	224*	10.31	. . .	K2III
125	11.96	+0.14	B8:	175R	9.87	-0.52	B9	225	11.75	-0.07	B9
126	12.36	. . .	K3	176	11.43	. . .	F0	226	11.35	. . .	G8
127*	9.96	. . .	G8IV	177	12.16	. . .	G0:	227	11.48	-0.06	A0
128*R	10.08	-0.47	B8	178	11.06	. . .	G2	228*	9.93	-0.32	A0
129	11.79	. . .	G0	179	11.52	. . .	F0	229	11.63	. . .	G0
130	11.60	. . .	G0	180*	9.57	-0.10	A3	230	11.81	. . .	G0
131*R	9.60	-0.42	B8	181	12.04	+0.08	B9	231	11.02	+0.07	B5:
132	12.03	-0.01	B9	182	11.70	+0,06	A3	232	11.65	-0.16	A2
133	11.82	. . .	G0	183	11.26	. . .	B8:	233	11.59	-0.13	B9
134	11.54	. . .	F8:	184*	9.76	-0.67	B5	234	10.78	+0.15	A2
135*R	7.26:	. . .	B8	185*R	9.94	-0.35	B9	235*	8.97	. . .	F0III
136*	10.34	. . .	K2IV	186	11.78	. . .	G5	236	10.59	+0.22	G0V
137	11.74	. . .	G0	187	10.60	-0.38	B9	237	11.86	+0.10	A0
138	11.36	+0.01	A0	188	11.77	. . .	A5:	238	11.49	. . .	F8
139	12.01	+0.09	A0:	189	11.60	+0.38	A0	239	10.92	. . .	G8III
140	11.19	-0.03	B9	190	10.92	-0.12	A0	240	10.75	. . .	F2

Table 1

Observational Data in LF9 (Cont'd.)

Zone -2° (Cont'd.)

No.	m_{pg}	R.I.	Sp.	No.	m_{pg}	R.I.	Sp.	No.	m_{pg}	R.I.	Sp.
241*R	8.24	-0.56	B8	291	11.81	...	G0	341*	9.04	+0.05	A5
242	11.54	+0.11	A0	292	10.80	...	G0V	342*	8.74	...	G8III
243	10.60	...	G0	293*	9.90	...	K0III	343	10.81	...	G8III
244	11.94	+0.34	A0	294*	10.17	-0.39	B9	344	11.81	...	F0:
245	12.03	...	B8:	295	11.38	...	B8	345	11.58	-0.12	A0
246*	10.04	+0.36	F8V	296*R	9.22	-0.61	B5	346*	9.62	...	G8III
247	11.08	+0.01	A5	297	11.38	-0.28	B8	347	11.07	...	A0
248	11.01	...	F8	298	12.16	-0.08	A2:	348*	7.97	-0.32	B5
249	9.94	-0.39	B8	299	11.09	...	F8V	349	12.10	...	K2
250	11.57	-0.07	A0	300	11.68	-0.03	A0	350R	11.26	+0.04	A2
251*	8.96	-0.35	A0	301	11.69	-0.14	A0	351*	10.02	...	G8III
252	11.64	-0.11	A0	302*	9.18	...	G8IV	352	11.71	...	F8
253*R	9.14	-0.33	B5	303	11.03	...	K0:	353	11.27	...	G0
254	11.85	+0.01	B8:	304	11.35	-0.21	A0	354	11.57	...	G5III
255	12.01	-0.01	A0	305	10.87	-0.21	A0	355	11.73	...	G0
256	11.06	...	G5IV	306	11.76	-0.16	A0	356	12.24	+0.28	A0:
257	12.11	...	K0	307	12.08	+0.05	A2	357	11.14	...	F0:
258	12.05	-0.02	B8:	308	12.06	-0.09	A0	358	12.33	+0.02	A2
259*	11.05	...	K0V	309	11.57	...	G0	359	11.63	...	G0
260*	9.89	...	K0III	310	12.16	...	K2	360	10.59	...	G5V
261*	10.70	+1.27	K0IV	311	12.41	...	K5	361	11.39	+0.08	A3:
262R	10.24	-0.05	A0	312	11.90	+0.05	A0	362	11.32	-0.14	B8
263*R	9.76	+0.03	A5	313	11.57	-0.21	A3	363*	9.71	...	F0IV
264*	10.20	-0.40	B8	314	11.45	-0.20	A0	364	10.77	-0.21	A0
265*R	9.81	-0.28	B5	315	11.25	...	F0	365	11.22	...	G8III
266	11.02	...	B9	316*	5.42:	...	A3:	366*	8.62	-0.39	A2
267	11.77	...	K2:	317	10.87	...	G8	367	9.33	...	A0
268	11.61	...	F0:	318	11.49	...	G0	368R	11.59	+0.01	B:
269	11.44	...	K3	319	10.86	-0.16	A0	369	11.79	-0.09	B9
270	10.61	...	G5IV	320	11.94	...	K0	370	11.84	...	G0:
271	11.79	...	G8:	321*	8.54	-0.41	B9	371*	10.52	...	G8III
272*	9.60	-0.35	B8	322*R	8.28	-0.43	B8	372	11.54	...	G8III
273	10.90	...	F0	323	10.66	...	A0:	373	10.95	-0.23	B8
274	11.81	+0.05	A0	324R	11.07	...	A3-F0	374	10.96	-0.03	F0
275	11.66	...	A0:	325	11.74	+0.04	A2	375	12.16	...	A0:
276	12.00	...	K0:	326	9.83	+0.40	F8V	376	11.97	...	K0
277	10.92	-0.23	B9	327	11.14	-0.07	A0	377	11.10	-0.17	B9
278	11.18	+0.34	B9	328	11.63	...	B5:	378	11.52	...	G0V
279	11.29	...	K0	329	11.97	...	F0:	379*	10.01	+0.14	F0V
280	10.35	-0.41	B8	330	11.69	+0.13	B9	380	11.87	-0.02	B9
281	11.86	...	G2:	331	11.89	-0.07	A0	381	11.62	-0.10	A0
282	12.15	+0.04	A0	332	12.18	0.00	A2:	382	11.21	...	G0
283	11.83	...	F5:	333	11.05	-0.26	B8	383	11.58	...	B:
284	11.45	...	G5	334	11.75	+0.18	A0:	384	11.21	+0.02	A2
285	11.34	-0.25	A2	335	10.49	-0.26	A0	385*	9.26	-0.36	B9
286	11.35	...	G2:	336	10.67	-0.29	A0	386	12.10	...	G8III
287	11.71	-0.06	A0	337	12.39	+0.09	A0	387	12.35	...	G8:
288	12.42	...	G0:	338	11.51	...	G2V	388	10.65	...	F8V
289	11.28	...	G0	339*R	5.91:	...	B3	389	11.71	-0.32	A0
290	11.59	...	G0:	340R	10.47	...	A3p	390R	10.48	+0.04	A2-F0

Table 1

Observational Data in LF9 (Cont'd.)

Zone -2° (Cont'd.)

No.	m_{pg}	R.I.	Sp.	No.	m_{pg}	R.I.	Sp.	No.	m_{pg}	R.I.	Sp.
391	12.18	-0.08	A0	441	12.19	+0.12	A2:	491	11.00	+0.03	A0
392	11.32	...	F2	442	11.78	...	G8	492	11.07	-0.35	B8
393*	9.50	-0.23	B9	443R	11.05	-0.08	B8	493	10.98	-0.22	B5
394	11.64	-0.10	A0	444*	8.77	+0.01	A5	494	12.37	-0.03	B9:
395	11.31	...	G8V	445	12.51	+0.42	A0:	495	12.19	+0.01	A0
396	11.97	+0.01	A2	446	11.71	...	G5III	496	11.12	+0.82	G5V
397	11.66	...	A0:	447*	7.81	-0.21	A0	497	10.76	-0.20	B9
398* R	7.51	+0.40	A3	448	11.42	...	G0	498	11.92	+0.21	B8
399	11.28	...	G8III	448a	11.38	-0.16	B5:	499	10.63	-0.25	B9
400*	10.43	...	F0	449	12.14	...	A2	500	11.82	-0.01	A0
401	11.63	-0.06	B9	450	10.19	-0.23	A0	501	11.68	...	K0III
402	11.94	+0.04	A0	451	12.12	...	G5	502*	9.30	...	K2III
403	12.26	+0.11	A2:	452	11.09	-0.15	A0	503	12.16	+0.33	A5:
404* R	10.07	-0.35	B8	453	12.08	+0.15	A0	504*	9.14	+0.03	A2
405	10.71	-0.18	B8	454	11.75	...	K0	505	11.12	-0.08	B5:
406	11.30	-0.33	B9	455	11.58	0.00	A2	506	11.07	-0.13	A0
407	11.39	...	G8III	456	11.65	+0.26	B9	507	11.51	...	G0
408*	11.05	...	G8III	457	12.33	-0.06	A0:	508	11.99	...	F5
409	11.68	...	G5III	458	12.28	...	A0:	509	11.95	-0.15	A0:
410	11.37	+1.08	G5V	459	11.73	...	G0	510	11.84	+0.02	A2:
411	11.71	...	G0	460	11.67	...	K3:	511	11.99	+0.07	A0
412	11.50	...	K0III	461	11.92	+0.53	G0	512	10.75	-0.22	A0
413	12.03	...	K0	462	11.55	+0.18	A3	513	11.81	-0.12	A2
414	11.49	-0.07	A0	463R	11.70	+0.05	B9	514	11.11	...	F2
415*	10.82	...	F5	464	11.40	+0.22	A5:	515	10.66	+0.25	G0V
416	11.30	-0.14	A0	465*	10.12	...	G0IV	516	12.08	...	K0
417	10.31	-0.23	B9	466* R	10.50	-0.03	A0	517	11.62	...	A0:
418	11.29	+0.19	A0	467	11.23	...	A5	518	11.62	-0.11	B5
419	10.14	-0.04	A3	468	10.87	-0.39	B8:	519	10.94	-0.24	A0
420	12.57	+0.16	A0:	469	11.79	...	G0	520R	11.06	-0.12	A0
421	11.95	...	G0	470	10.96	...	F0II	521*	9.35	...	G8IV
422*	10.20	-0.09	A0	471	11.21	...	G0	522	11.13	-0.15	A0
423*	10.79	...	K0III	472*	9.40	-0.23	A2	523*	10.06	+0.16	A5
424	11.62	-0.05	A2	473	10.24	-0.11	B9	523aR	10.36	...	A2-F0
425	11.98	-0.11	A0:	474	12.13	...	G8:	524	11.60	...	G8III
426	11.38	...	F5	475	10.76	+0.64	G2V	525* R	9.22	-0.44	B5
427	12.00	...	F0:	476*	9.89	-0.22	A0	526	10.13	-0.52	B5
428	10.80	+0.14	F0	477	12.08	...	G2	527	11.63	+0.20	A0
429	12.10	+0.08	A0:	478	12.16	...	G0:	528	11.05	...	G0Ib:
430*	9.85	...	A2:	479	11.76	...	G8III	529	11.48	...	K0III
431* R	9.90	+0.33	O8	480	11.44	-0.12	B5	530	11.30	-0.06	B5
432*	9.16	-0.24	A0	481	11.77	+0.19	A0	531	12.19	...	K0:
433	12.39	...	G8	482	11.11	...	G0V	532R	10.87	-0.05	B8
434R	10.87	-0.21	A0I	483	11.62	0.00	A2	533	11.75	+0.11	A0
435	11.40	+0.18	A0	484	11.59	...	G5III	534	11.78	+0.03	A0:
436*	11.12	...	K0:	485	11.80	...	G2:	535	11.44	...	G0:
437	10.80	...	G5V	486	11.84	+0.18	A0	536	10.92	+0.06	A3
438R	10.38	-0.32	B8	487*	10.64	...	A3	537	11.23	...	G0
439	11.49	-0.01	A0	488R	10.62	-0.06	A0	538	11.36	...	G0
440	11.06	...	F8	489	11.37	+0.08	A0	539	10.35	-0.12	A0
				489a* R	8.70	+0.12	A5	540	12.18	...	G0:
				490* R	9.84	-0.22	A3				

Table 1

Observational Data in LF9 (Cont'd.)

Zone -2° (Cont'd.)

No.	m_{pg}	R.I.	Sp.	No.	m_{pg}	R.I.	Sp.	No.	m_{pg}	R.I.	Sp.
541	11.49	...	G0:	591	12.02	+0.03	A5:	641	11.11	-0.07	B8
542	11.05	+0.08	B9	592	11.94	+0.01	A3	642	11.62	+0.15	B9
543	10.66	...	F5V	593	12.20	...	K0:	643	10.63	...	F2V
544*	10.50	...	F5III	594	10.10	-0.28	B8	644	10.66	...	K0III
545	11.46	-0.01	A2	595*	9.87	-0.01	F0V	645	11.52	-0.23	B9:
546	10.39	-0.09	A0	596	12.22	...	G0	646	11.08	+0.14	A5:
547	12.03	...	K0	597	11.44	...	K0III	647	11.46	+0.05	A0
548	11.24	...	K2:	598	11.08	-0.03	B8	648	11.21	-0.13	B9
549*	9.95	...	G5III	599	11.45	-0.05	A0	649	12.51	...	K5:
550*	10.08	...	K0III	600	11.51	...	M0	650	10.83	...	G0
551*	10.85	...	K0III	601	11.91	...	G8	651	11.96	...	G0
552*	10.17	...	G8III	602	11.28	...	G5III	652	11.60	...	G0
553	12.18	+0.23	A2:	603	11.96	...	K0	653	11.12	...	G0
554	11.00	-0.11	B8	604	11.82	...	G8:	654	11.42	...	G2:
555	11.35	...	G2V	605	11.16	...	G0III	655	11.23	...	G0
556R	10.50	+0.15	B3	606	10.87	...	F0	656	11.45	...	G2:
557	12.20	+0.19	A0	607	11.27	-0.25	A0	657*	9.66	...	K0IV
558	11.85	0.00	A0	608	12.00	...	G0				
559	12.23	...	K5:	609	11.24	+0.13	A2:				
560	11.39	...	G2	610*	9.64	...	F5V				

Zone -3°

561*	8.98	...	F0V
562	12.15	+0.23	A0:
563*	11.18	+0.03	A0
564	10.95	...	G0
565*	10.08	...	F2V
566*	10.17	-0.31	B5
567R	10.65	-0.45	B5
568	10.92	...	F2
569	11.79	...	G0
570	11.60	+0.24	B5:
571	11.36	...	G0
572	11.45	+0.24	B5
573	11.30	...	F0
574	11.78	+0.08	A0
575	11.46	0.00	B8
576*	9.51	0.00	A2
577	12.04	+0.25	A0
578*	9.73	-0.21	A5
579	11.31	+0.18	B5
580	11.98	+0.11	A0:
581	11.89	+0.11	A0
582	11.85	+0.11	B9
583R	10.53	-0.21	B5
584	12.00	+0.20	A2:
585	10.51	...	G0V
586	11.58	+0.21	A3
587	12.27	...	G0:
588*	9.75	...	G8III
589	11.85	...	G0:
590	11.45	-0.08	B8
591	12.02	+0.03	A5:
592	11.94	+0.01	A3
593	12.20	...	K0:
594	10.10	-0.28	B8
595*	9.87	-0.01	F0V
596	12.22	...	G0
597	11.44	...	K0III
598	11.08	-0.03	B8
599	11.45	-0.05	A0
600	11.51	...	M0
601	11.91	...	G8
602	11.28	...	G5III
603	11.96	...	K0
604	11.82	...	G8:
605	11.16	...	G0III
606	10.87	...	F0
607	11.27	-0.25	A0
608	12.00	...	G0
609	11.24	+0.13	A2:
610*	9.64	...	F5V
611	10.11	+0.53	A5
612	11.77	+0.14	B9
613*	10.07	...	F2V
614	11.51	+0.15	A0
615	12.03	...	G0:
616	11.62	...	G0:
617*	9.83	0.00	A5
618	11.47	+0.06	A3
619	12.19	+0.23	A0:
620	11.61	-0.09	A0
621	11.41	...	G8III
622* R	10.27	+0.14	A3-F0
623	12.07	+0.23	B8:
624	11.12	+0.04	A0
625	11.45	...	G0
626	12.23	...	K0
627	10.51	...	F8
628*	7.08	...	K2III
629*	9.59	-0.31	A2
630	10.72	-0.41	A0
631*	8.67	...	F0V
632	11.37	...	G2:
633	12.19	...	F8:
634* R	10.02	-0.38	B8
635	11.27	-0.12	B8:
636	12.27	...	K0
637	11.37	...	G0
638	10.29	-0.16	A0
639	11.29	...	K0III
640R	11.28	+0.15	A3
641	11.11	-0.07	B8
642	11.62	+0.15	B9
643	10.63	...	F2V
644	10.66	...	K0III
645	11.52	-0.23	B9:
646	11.08	+0.14	A5:
647	11.46	+0.05	A0
648	11.21	-0.13	B9
649	12.51	...	K5:
650	10.83	...	G0
651	11.96	...	G0
652	11.60	...	G0
653	11.12	...	G0
654	11.42	...	G2:
655	11.23	...	G0
656	11.45	...	G2:
657*	9.66	...	K0IV
1	9.76	-0.65	A0
2*	9.28	-0.16	F5III
3*	9.24	...	F0V
4	11.35	...	G5
5* R	8.32	...	B5
6	11.98	+0.03	A0
7*	10.37	...	F5V
8*	9.57	-0.41	A0
9*	9.42	...	F0IV
10*	11.53	...	M0III
11	11.14	+0.03	B5
12	10.67	...	G0
13	11.89	...	G0:
14	11.47	...	G0
15	12.10	-0.08	A0:
16	11.53	+0.03	B9
17	11.45	...	A0
18*	10.13	-0.23	A5
19*	10.46	...	G5III
20*	8.88	-0.45	B8
21	11.83	...	G0
22*	10.01	+0.04	F8V
23	11.83	...	G0
24	11.18	-0.03	A2
25	11.81	...	G8:
26*	9.64	-0.53	A0
27	11.78	+0.04	A3
28* R	9.89	-0.64	B3
29*	9.02	-0.58	B8:Var?
30	11.86	-0.09	A0

Table 1

Observational Data in LF9 (Cont'd.)

Zone -3^{o} (Cont'd.)

No.	m_{pg}	R.I.	Sp.	No.	m_{pg}	R.I.	Sp.	No.	m_{pg}	R.I.	Sp.
31	11.34	+0.15	A0	81	10.90	-0.18	A0	131	11.64	-0.11	B5:
32*	11.22	...	K2III	82	12.00	+0.16	B9	132	12.08	...	G8III
33	11.88	...	K0:	83*	10.28	+0.10	G0V	133	11.59	...	K0III
34*	9.52	-0.61	B8	84	12.02	...	G0:	134	10.42	...	F2
35*	8.57	-0.63	A2	85	11.80	...	G0	135*	9.86	-0.60	B8
36*	10.40	-0.39	A0	86*	11.19	...	G8III	136*R	9.26	-0.72	B8
37*	10.56	...	G0V	87*	11.71	...	K0III	137	10.18	-0.52	A0
38	11.05	+0.46	B5	88	11.32	-0.24	B8	138*	10.68	...	K0III
39	11.92	...	G0	89*	5.53:	...	B8	138a	11.81	...	K0
40	12.20	...	G0:	90*	9.41	-0.38	A2	139	11.75	...	G0
41	11.81	...	F0:	91	12.11	...	G0:	140R	10.09	...	A3
42	11.56	+0.01	A2	92R	11.11	+0.02	A3-F5p	141	12.13	...	K0
43	11.84	...	F2:	93*R	9.64	-0.84	B8	142	10.92	...	G5V
44	11.05	-0.14	B9	94	12.01	+0.16	A2:	143	11.40	-0.15	A0
45*	8.75	-0.28	A5	95	12.34	+0.05	A0:	144	11.94	...	G0
46	11.23	+0.01	A0	96	10.92	+1.00	G8IV	145*R	10.02	-0.47	A0
47*	10.17	-0.48	B9	97	11.50	0.00	A3	146	11.83	...	K0
48	11.37	+0.14	A0	98	11.81	...	G2:	147*	10.09	...	F5IV
49	11.60	+0.21	A2	99	10.24	-0.52	B8	148*	9.98	-0.35	A0
50	11.72	...	A5	100	11.81	...	G0:	149	12.29	...	K0
51*	8.55	-0.30	A5	101	11.94	-0.17	B5	150	11.42	...	K3
52	12.29	...	K0	102R	10.86	-0.32	A0	151	11.98	...	F0
53	11.88	...	G0	103	11.45	-0.06	A0	152	11.44	...	G8
54*	10.96	-0.24	B8	104*R	9.99	-0.66	B3	153*	9.61	+0.07	G5V
55	12.12	...	K0:	105*	10.45	...	F5III	154	12.22	+0.15	B9
56*	9.79	...	F8III	106	11.88	...	K0III	155*	7.52	-0.16	A5
57	11.56	-0.23	B8:	107	11.14	-0.32	B9	156	12.03	+0.33	A0:
58	11.73	-0.04	A0	108	11.76	...	G0	157	11.75	+0.02	A0
59	11.28	...	G8III	109	12.05	...	G5	158	11.26	-0.07	A0
60	10.94	...	F8	110	12.00	-0.08	B9	159	11.36	...	F2
61	11.44	...	G0	111	11.71	-0.12	B5	160	10.82	-0.28	A0
62	11.78	...	G5V	112	11.73	...	G5:	161	12.11	+0.14	A0
63	12.01	+0.25	A0	113*	9.59	...	G8III	162	11.38	-0.11	B9
64	11.78	+0.19	F5	114	10.88	-0.21	A3	163	11.88	+0.15	A0
65	11.68	+0.04	A5	115	11.87	+0.12	A0:	164	10.90	...	F8V
66*R	9.11	-0.73	B9	116*R	9.50	-0.61	B8	165	11.81	+0.07	B8
67	10.30	-0.37	A2	117*	9.99	-0.38	A2	166	11.55	-0.03	B9
68	11.48	-0.14	A0	118	10.66	-0.23	A0	167	10.88	...	G5V
69	12.03	...	K0	119*	8.21	-0.53	B9	168*	9.75	-0.18	F0V
70	11.76	...	K0III	120	11.39	...	G0:	169	11.29	-0.25	A0
71	11.54	...	K0III	121	11.06	...	G8III	170	11.21	...	G5:
72	10.48	-0.39	A0	122	11.98	-0.09	A0	171*	8.26	-0.53	A2
73	11.22	...	G8III	123	11.79	-0.15	A0	172*R	8.78	-0.44	B8
74*	8.72	...	B8	124	11.55	-0.12	A0	173	10.92	-0.03	B8
75	11.69	-0.11	A0:	125	11.82	...	G5:	174	11.91	-0.03	B9
76	11.61	...	G0	126	11.04	...	G0	175	10.39	...	F2V
77	11.60	-0.05	A0	127	11.45	...	G0:	176	10.39	+0.64	G5IV
78	11.80	...	K0III	128	10.80	...	G5V	177	11.66	...	G0
79	11.11	...	F0	129	11.32	-0.10	A0	178*	7.61	...	K5III
80*	10.39	+0.20	F8V	130	11.50	...	G0	179*	9.62	...	F2V
								180R	10.94	-0.18	B8

Table 1

Observational Data in LF9 (Cont'd.)

Zone -3° (Cont'd.)

No.	m_{pg}	R.I.	Sp.	No.	m_{pg}	R.I.	Sp.	No.	m_{pg}	R.I.	Sp.
181R	10.06	-0.53	A0I	231	11.75	...	K0III	281	10.41	-0.31	B9
182	10.86	...	G8IV	232	12.14	...	G8III	282	11.60	...	G8III
183*	7.06	...	G8IV	233	12.01	+0.08	A0	283	11.22	...	G2V
184	11.43	...	G5:	234	11.62	+0.01	A0	284	10.37	-0.47	B5
185	11.96	+0.13	A0	235	10.37	-0.11	A3	285*	9.42	...	F0V
186	10.95	...	G0	236	11.36	...	G0	286	11.04	-0.01	A5
187	10.06	...	F5III	237	11.37	...	K0	287	11.65	...	G8III
188*	9.12	...	G5IV	238R	10.14	-0.25	A0	288	11.43	+0.48	G0:
189*	9.19	+0.45	G0V	239*	9.56	...	F0V	289	12.13	...	G8
190	11.72	-0.14	A0	240	11.16	...	F5:	290	12.31	...	M0:
191	11.15	...	G8III	241	11.39	...	G8:	291R	10.82	-0.24	B9
192	11.60	...	K0III	242*	9.10	-0.16	A2	292* R	8.84	-0.57	B5
193*	10.39	+1.01	G8III	243	10.70	-0.17	A3	293	11.06	-0.16	A3:
194	11.66	...	G8	244	12.14	...	A0	294*	9.82	...	G8III
195	10.82	+0.15	B8	245	11.58	+0.11	A0	295*	6.89	...	K0III
196	11.85	...	G0	246*	9.81	+0.06	A5	296*	9.04	-0.52	B8
197	11.78	...	G2:	247	11.86	...	G0	297	12.08	...	F0
198	10.12	-0.20	A2	248	12.09	...	G0	298	11.67	...	G0
199	11.03	...	F2	249	11.79	...	F5:	299	11.44	-0.29	B8:
200* R	9.98	-0.16	A2	250*	10.58	...	F2	300	11.75	...	F0
201	10.63	...	G0II:	251	11.51	+0.07	A0	301*	7.91	...	G8III
202	10.96	...	A0	252R	10.96	-0.02	A3	302	11.46	...	A5
203*	8.84	-0.28	B9	253	11.90	...	G0	303	11.21	...	B9
204	12.08	0.00	A0	254	11.94	...	G0	304	10.92	...	G8:
205	12.03	...	G0	255	11.50	+0.38	F0	305	10.56	-0.42	A0
206*	10.50	...	G5V	256	11.96	...	K0	306	11.43	...	F2:
207	11.76	...	G8	256a	11.71	-0.11	B9	307	11.96	...	G8:
208	12.09	...	K0	257*	9.87	...	F8V	308	11.99	-0.11	B9
209	11.56	...	K0	258	11.28	...	G0	309	10.68	-0.41	B5
210	11.57	...	K0III	259	11.84	+0.28	B5:	310	11.34	...	G5V
211	11.29	+0.10	A0	260	11.91	-0.13	A0	311*	9.47	+1.10	G5Ib
212	12.31	...	K0	261	11.49	...	G0	312	11.08	...	B9
213	10.48	-0.37	B8	262*	8.89	...	K2III	313	10.97	...	G0
214*	9.98	...	K0III	263	11.82	...	G8:	314*	9.93	...	G8IV
215	11.77	...	G0	264	12.17	...	G2	315	11.76	...	K0III:
216	11.29	...	F8	265	11.79	...	G0	316* R	9.56	-0.59	B9
217	11.86	+0.26	A0	266	10.86	...	F2	317	11.40	...	G0:
218	12.10	...	G5	267	11.64	-0.02	B9	318	10.61	...	K0III
219	11.12	+0.21	A0	268	10.39	...	F5V	319	11.64	-0.12	B8:
220	11.88	+0.01	A0	269*	10.45	...	F5	320	11.55	...	G8
221*	8.84	+0.81	G8V	270	10.67	+0.01	A5	321	11.20	...	G8III
222	11.76	+0.31	A0	271* R	10.02	-0.21	B2	322	11.62	-0.14	B8
223	11.42	...	G0:	272*	9.64	...	G8III	323	11.72	...	G8III
224	11.25	-0.14	A0	273* R	8.33	-0.57	B3	324	10.03	-0.49	B9
225	11.31	+1.36	G5III	274	11.01	...	F2III	325	10.83	-0.37	B8
226*	10.52	+0.57	F8V	275*	10.27	+1.25	K0V	326R	10.64	-0.40	A0I
227	11.52	...	F5:	276*	10.10	...	K3IV	327*	10.33	+0.39	G2V
228	11.52	0.00	A0	277	11.92	...	G8:	328	11.05	...	G0
229*	10.84	...	G0	278*	11.34	...	G8III	329	11.60	...	F0
230	11.10	+0.15	B5:	279*	10.33	...	G0II	330	10.95	...	F0
				280*	10.60	...	K0III				

Table 1

Observational Data in LF9 (Cont'd.)

Zone -3° (Cont'd.)

No.	m_{pg}	R.I.	Sp.	No.	m_{pg}	R.I.	Sp.	No.	m_{pg}	R.I.	Sp.
331*	10.78	...	G8III	381*	8.85	...	F2V	431	11.36	...	G0
332	11.14	...	G5III	382*	10.37	-0.28	B9	432	11.64	-0.38	B8
333*	9.30	-0.41	A2	383	11.83	...	G5:	433	12.13	...	A0:
334	11.36	-0.06	A0	384	12.13	...	G0:	434	10.97	...	G0:
335	10.11	-0.28	A3	385	11.62	...	G0	435	10.35	...	F0V
336*R	10.50	-0.40	B8	386*	10.65	+0.46	G0V	436	11.60	-0.17	A0
337*	10.28	...	K0III	387*	9.81	...	G5IV	437	11.98	+0.22	A0:
338	11.87	...	G0	388	11.80	-0.06	A2	438	11.35	...	G0
339	11.22	...	G5:	389	10.88	...	F0III	439	11.30	...	G2
340R	11.18	-0.13	B5	390*	10.21	...	G8III	440	11.27	-0.11	A0
341	11.96	...	G0	391*	10.43	...	G8III	441	10.78	...	G0
342	10.27	-0.29	B5	392	10.25	-0.39	A0	442*	10.25	...	K3III
343	10.83	-0.13	A5	393*R	9.79	-0.67	B8	443	11.57	-0.03	A0
344*	9.19	...	G8III	394	10.47	-0.18	A5	444*	10.72	+0.29	G0V
345	10.84	-0.27	B8	395	11.86	...	K3	445	11.49	...	G0
346*	10.39	+0.09	F8V	396*	10.19	...	M5III	446	11.33	-0.06	A3
347R	11.20	-0.28	A0	397*	8.83	-0.60	B8	447	10.54	-0.49	A0
348	10.78	-0.22	B8	398	10.91	...	F8V	448	9.54	...	F0V
349	11.34	+0.06	A0	399	11.38	...	G0	449	10.63	-0.40	A2
350	11.29	...	G0	400	12.26	...	F0:	450	11.66	...	K0
351	11.84	0.00	B9	401	11.95	+0.06	A0	451	9.95	-0.74	B8
352	11.94	...	F8	402	11.36	-0.36	B8	452*	10.72	...	F8III
353	11.18	-0.11	A2	403R	11.02	-0.45	B8	453	11.56	...	G8
354	11.34	...	M2III	404	11.89	...	G2	454	12.31	...	G8
355*R	9.83	-0.35	A3	405	11.94	...	A0	455R	10.34	-0.69	B5
356	11.15	...	G5III	406	11.99	...	G0	456	11.34	-0.25	A0
357*	10.00	...	G5III	407	11.94	+0.07	A0	457	11.56	-0.27	B5
358	11.36	...	F0	408	11.59	...	G0	458	12.15	-0.01	A0
359*	10.31	-0.27	B8	409*R	10.41	-0.05	A5	459*	11.08	...	G8III
360	10.81	-0.36	B8	410R	10.27	+0.12	B9	460*	8.79	-0.59	B9
361	11.42	-0.30	A5:	411	11.41	-0.11	A0	461	11.70	...	K2
362	10.88	+0.03	A5:	412	11.97	+0.06	A0	462	11.71	...	G8
363	12.27	0.00	A0	413*	9.41	...	G5IV	463	11.79	...	F8:
364	12.33	...	G8	414	12.15	...	G0	464	11.78	...	G0
365	9.85	-0.70	B5	415	11.27	-0.35	B9	465	10.54	-0.52	B8
366	12.44	...	K0:	416	12.13	-0.15	A0	466	10.80	-0.27	B8
367	10.95	...	F0	417	12.19	...	G0:	467	11.79	...	F8
368	11.16	...	A5	418	10.36	...	F2V	468	10.16	...	F5V
369	11.69	-0.15	A0	419*R	6.48:	...	B0	469*	9.63	-0.33	A3
370	11.85	-0.09	A0	420	11.55	-0.33	A0	470	11.38	-0.25	A0
371	12.43	-0.19	A0	421	12.09	...	A0:	471	12.36	...	K0
372	10.45	-0.22	A2	422*	9.83	-0.58	A2	472	11.86	...	G0
373*	8.69	-0.20	A5	423	11.78	-0.23	A0	473	11.59	...	A5:
374*	11.15	...	G8III	424*R	9.04	-0.89	B5	474	11.93	...	G0
375	12.00	...	G0	425	11.78	...	F8:	475	11.96	...	G2:
376	12.11	...	K0								
377	11.86	...	G5III	426	12.49	...	K0:	476	11.47	...	G0
378	11.47	...	G8III	427*	9.90	-0.53	B5	477	11.79	...	G2
379	11.69	-0.23	A0	428	11.46	...	F0:	478	12.05	...	K0:
380*	9.48	-0.45	B9	429	11.21	...	G8	479	11.53	-0.29	B5
380a	12.13	...	G0:	430	11.66	+0.01	A5	480	11.56	-0.23	A0

Table 1

Observational Data in LF9 (Cont'd.)

Zone -3° (Cont'd.)

No.	m_{pg}	R.I.	Sp.	No.	m_{pg}	R.I.	Sp.	No.	m_{pg}	R.I.	Sp.
481	11.31	-0.39	B5	6*	9.09	...	A3	56	10.83	-0.27	A0
482	12.02	...	G3	7*	9.09	...	F0V	57*	10.27	...	F2V
483* R	8.77	...	B8	8	11.01	-0.07	A5	58	11.86	-0.13	A0:
484	11.08	-0.29	B9	9	11.30	...	G0:	59	12.02	+0.03	A0
485*	8.44	-0.31	A5	10*	10.49	+0.23	G5V	60	12.06	...	G0
486* R	8.61	...	A2-F5	11	11.32	-0.06	B9	61	11.79	...	G8
487	11.92	-0.05	A0:	12* R	9.16	-0.78	A0	62	12.18	...	G0:
488*	10.68	...	G5III	13	11.74	-0.03	A5	63	11.71	-0.05	A0
489R	10.67	-0.35	B9	14*	9.31	...	K0III	64	11.54	...	K0
490	11.88	-0.08	A0	15	11.09	-0.39	B5	65	11.09	...	G0V
491	11.52	...	A5	16*	10.23	...	G0V	66	12.27	...	G8
492*	7.94	...	K0IV	17	11.45	...	G0	67*	7.91	-0.38	B9
493	12.10	0.00	A0	18	12.11	+0.09	A0:	68	11.16	-0.26	A0
494	12.35	...	G0	19	11.04	...	A0	69R	11.38	+0.16	pec.
495	11.94	...	G0	20*	11.76	...	K0III	70	10.86	-0.32	B8
496* R	9.20	-0.72	B0	21*	10.22	...	F5III:	71*	9.36	...	G0V
497	12.21	...	G0	22	11.45	-0.09	A0	72	11.24	...	F5
498	11.69	...	F8	23	10.27	-0.47	A0	73	12.06	...	G0:
499	11.41	...	G5	24	11.24	...	G8	74	11.06	...	G8III
500	11.54	...	F0	25R	10.61	-0.05	F51b	75	11.84	...	G5
501	11.07	-0.14	A2	26	11.49	-0.14	A0	76*	9.89	-0.40	A0
502	11.48	...	G0	27*	8.47	+0.05	A5	77*	9.11	...	K2III
503*	9.56	...	K0III	28*	9.83	-0.64	B5:	78	11.44	...	F8V
504	11.69	...	K0III	29*	10.20	...	F5V	79	11.95	-0.15	A2
505	11.52	...	G0	30* R	8.94	-0.69	B8	80*	11.65	...	M2III
506	12.35	...	K0	31	11.58	...	G0	81	11.63	...	K0
507	12.21	...	K0:	32	11.41	...	A0:	82	11.40	-0.10	B5:
508	11.71	-0.09	B5	33R	10.31	-0.71	B2	83	11.35	+0.89	G5V
509	11.10	-0.36	A0	34	12.32	+0.08	A3:	84	10.52	-0.32	A0
510	11.62	-0.21	A0	35	10.33	...	A5	85*	10.45	...	G8IV
511	10.50	...	F0III	36	10.76	...	G8III	86	11.21	+0.01	A0
512	11.88	...	G0:	37	11.97	...	K3	87	10.78	...	F0III
513*	9.39	-0.55	A0	38	10.76	-0.20	F0V	88	11.56	-0.02	B9
514*	9.74	...	M5III	39	11.29	-0.23	A0	89	11.90	+0.16	A0:
515	10.35	...	G0V	40	11.64	...	G0	90	10.61	-0.12	A0
516	11.13	-0.29	B5	41	11.78	-0.19	A0	91	11.64	-0.12	A5
517	11.93	-0.18	A3:	42R	11.06	-0.09	O:pec	92	11.67	...	G0:
518	11.77	...	G2:	43*	7.3:	...	B8	93* R	8.61	-0.74	B9
519*	9.25	-0.80	B5	44	10.99	...	F0	94	11.22	-0.37	B8
520	9.69	-0.81	B8	45* R	8.96	...	B8	95*	10.60	...	M0III
521*	11.63	+0.02	B5:	46	12.15	+0.11	A2:	96	10.97	-0.47	B5
522	10.81	-0.43	B5	47	11.18	-0.02	A3	97* R	9.83	-0.74	B5
523	10.81	-0.59	B5	48	11.43	...	A5	98	10.76	...	G0
				49	11.45	...	G2:	99	11.34	-0.23	A2
	Zone -4°			50	12.10	...	G0:	100	12.14	...	A0:
1	11.71	...	G0:	51R	10.12	-0.35	A2	101*	10.75	...	G5V
2	10.71	-0.43	A0	52	10.88	...	F0V	102*	8.46	-0.49	F0IV
3	11.85	...	K0	53	11.75	+0.07	A0	103	11.94	-0.20	A2:
4	10.64	-0.38	A2	54	11.71	...	A0	104	11.51	...	G0:
5	11.07	...	G0	55*	8.72	-0.29	A3	105	10.23	-0.65	B9

Table 1

Observational Data in LF9 (Cont'd.)

Zone -4° (Cont'd.)

No.	m_{pg}	R.I.	Sp.	No.	m_{pg}	R.I.	Sp.	No.	m_{pg}	R.I.	Sp.
106	11.06	-0.28	B3:	126	10.48	-0.36	A5	146	10.36	. . .	G0V
107	11.99	. . .	G5III	127	11.74	0.00	A3	147	11.71	+0.11	A2
108	9.98	. . .	G8III	128	11.69	. . .	G5III	148	10.60	-0.40	B9
109	11.00	. . .	G8III	129	10.86	. . .	F2	149	11.88	. . .	G0:
110	11.77	+0.10	A0	130*	10.77	. . .	G5	150	12.15	. . .	K0:
111	11.28	. . .	G8III	131	10.66	-0.33	A0	151	11.02	-0.36	B8
112	11.86	-0.07	A3-F2:	132	12.01	. . .	G0:	152	10.58	-0.42	A0
113	11.41	-0.20	A0	133	10.44	-0.63	B8	153	10.21	-0.71	B5
114	11.03	. . .	F5	134*	10.47	. . .	M0III	154* R	9.14	. . .	B2
115	10.48	-0.46	B5	135	11.19	+0.03	A2	155	11.56	. . .	K0
116	9.85	-0.98	B5	136	11.17	-0.17	A0	156* R	9.03	. . .	A0
117	11.50	. . .	G8III	137R	10.84	-0.25	A2				
118*	9.59	. . .	F8V	138	11.34	. . .	G0				
119	11.69	-0.07	B8	139* R	9.62	-0.58	B8				
120* R	7.43	-0.83	B3	140*	10.38	. . .	A:				
121* R	7.67	-0.23	A5	141	11.86	+0.05	B5				
122	11.67	-0.30	B5:	142	11.74	-0.04	A0:				
123	10.74	. . .	F5	143	11.16	. . .	A0				
124	10.57	-0.52	B9	144* R	9.64	-0.69	B8				
125R	11.21	-0.01	A0	145	11.48	-0.37	B8:				

Remarks Concerning Spectra in LF9

Zone 0°

No.	
2	Class OB? λ4026 strong. BD +0°1592.
7	λ4174 conspicuous; K weak for class F; metallic lines prominent. BD +0°1596.
16	K line weak; red end of spectrum very strong; G band weak. BD +0°1605.
37	λ4174 very strong; trace of G band; UV hydrogen very strong.
45	Class OB star. BD +0°1622.
50	Class OB star. BD +0°1624.
58	Class OB?
59	Class OB star. BD +0°1627.
60	Strong line λ3863 (Si II?).
71	UV weak; sharp break in spectrum at G band.
86	Class OB star. BD +0°1638.
105	Metallic lines present and trace of G band.
123	Possibly K supergiant.
138	Class OB star. BD +0°1651.
140	Cluster of early A type stars (NGC 2103). BD +0°1653.
191	Near No. 191 is a faint emission object (M2 star?). BD +0°1672.
214	λ3840, λ4036 unusually strong for class F. BD +0°1678.
239	Metallic line A star (?); K line too weak for class F.
261	Class OB star. BD +0°1691.
292a	Class OB star.
366	Metallic line A star (?).
	Stars having hydrogen lines sharper than usual for their class are: Nos. 18 = BD +0°1608; 56 = BD +0°1626; 126 = BD +1°1549; 143 = BD +0°1655; 176 = BD +0°1668; 192; 264; 265 = BD +0°1692; 295 = BD +0°1700; 354; 381 = BD +0°1737; 401 = BD +0°1744.

Zone -1°

34	Metallic line A star.
58	Hydrogen lines sharp; metallic lines and G band present. BD -0°1426.
74	Class OB star. BD -0°1433.
118	Class OB star.
125	Class OB star.
127	Class OB star.
153	Class OB (?); hydrogen lines very sharp.
205	Class OB star. BD -0°1468.
222	Strong UV; no lines visible.
232	Metallic line A star; λ4226 prominent for class.
256	Class OB star. BD +0°1682.
261	Trace of emission (?); spurious lines not due to overlap.
283	Class OB (?); K line present; UV hydrogen lines too strong for B5.
318	Hydrogen lines very sharp.
361	Trace of metallic lines; hydrogen lines sharp.
388	Class OB star (?).
419	K line weak for class F; λ4174 prominent.
457	Metallic lines suspected. BD -0° 1527.
507	Trace of emission at Hβ; λ4200 strong.
524	Trace of metallic lines. BD -0°1547.
531	K line too weak for class F; more like A3. BD -0°1550.
	Stars having hydrogen lines sharper than usual for their class are: Nos. 10 = BD -0°1416; 29 = BD -0°1420; 31 = BD -0°1421; 65 = BD -0°1428; 80; 84 = BD -0°1439; 90 = BD -0°1437; 123 = BD -0°1449; 147 = BD -0°1457; 213 = BD -0°1470; 231; 243 = BD +0°1676; 250 = BD -0°1473; 270 = BD -0°1478; 271 = BD +0°1686; 275 = BD -0°1479; 281 = BD +0°1690; 300; 377; 401; 421 = BD -0°1516; 433 = BD -0°1521; 440 = BD +0°1742; 464 = BD -0°1531; 488; 502 = BD -0°1537.

Remarks Concerning Spectra in LF9 (Cont'd.)

Zone -2^{o}

No.	
17	H and K very sharp; hydrogen lines very sharp. BD $-1^{o}1359$.
36	Class OB star. BD $-1^{o}1368$.
61	Trace of metallic lines. BD $-1^{o}1376$.
87	K line much too weak for F8; spectrum appears composite. BD $-1^{o}1384$.
121	K line weak for class F; hydrogen lines sharp.
162	UV hydrogen lines strong for F0; K line too strong for A5; trace of G band. BD $-1^{o}1404$.
203	Hydrogen lines very broad. BD $-1^{o}1413$.
216	K line weak; UV hydrogen lines sharp; trace of G band. BD $-1^{o}1417$.
262	UV hydrogen lines very sharp.
263	K line sharp; hydrogen lines sharp for normal A5. BD $-1^{o}1435$.
322	Close double; dominant spectrum given. BD $-1^{o}1443$.
324	Trace of G band; metallic lines present; K weak for class F.
340	Spectrum possibly variable A3 to F5.
350	Trace of metallic lines; hydrogen lines sharp.
368	UV continuum strong; all lines weak.
390	K line weak for class F; hydrogen lines sharp; G band present.
431	Class OB star. BD $-1^{o}1471$.
434	Class OB star.
523a	K line weak for class F; metallic lines and G band present.
556	Class OB star.
622	K line very weak; trace of G band. BD $-1^{o}1508$.
634	Hydrogen lines very broad. BD $-1^{o}1510$.
640	Metallic line A star.
	Stars having hydrogen lines sharper than usual for their class are:
	Nos. 34 = BD $-1^{o}1366$; 77 = BD $-1^{o}1379$; 128 = BD $-1^{o}1393$; 131 = BD $-1^{o}1394$;
	135 = BD $-1^{o}1395$; 142; 143; 173 = BD $-1^{o}1406$; 175; 185 = BD $-1^{o}1408$; 196 = BD $-1^{o}1411$;
	241 = BD $-1^{o}1424$; 253 = BD $-1^{o}1429$; 265 = BD $-1^{o}1434$; 296 = BD $-1^{o}1439$;
	339 = BD $-1^{o}1446$; 398 = BD $-1^{o}1459$; 404 = BD $-1^{o}1462$; 438; 443; 463; 466 = BD $-1^{o}1475$;
	488; 489a = BD $-1^{o}1480$; 490 = BD $-1^{o}1481$; 520; 525 = BD $-1^{o}1487$; 532; 567; 583.

Zone -3^{o}

5	Class OB star. BD $-1^{o}1362$.
92	Hydrogen lines sharp; K weak; G band prominent.
104	Class OB star. SD $-2^{o}1779$.
140	Trace of metallic lines.
145	Hydrogen lines have sharp cores. SD $-2^{o}1790$.
181	Class OB star.
200	Trace of metallic lines. SD $-2^{o}1804$.
271	Class OB star. BD $-1^{o}1441$.
273	Class OB star. SD $-2^{o}1820$.
292	Class OB star. BD $-1^{o}1450$.
326	Class OB star.
340	Strong line of HeI λ3926. Double?
347	Class OB (?).
409	Trace of metallic lines. BD $-1^{o}1478$.
419	Class OB star. SD $-2^{o}1856$.
424	Class OB star. SD $-2^{o}1857$.
486	Weak K line; strong G band; UV hydrogen lines strong. SD $-2^{o}1870$.
489	Hydrogen lines have sharp cores.
496	Class OB star. SD $-2^{o}1875$.
	These stars have hydrogen lines sharper than usual for their class:
	Nos. 28 = SD $-2^{o}1758$; 66 = SD $-2^{o}1770$; 93 = BD $-1^{o}1391$; 102; 116 = SD $-2^{o}1781$;
	136 = SD $-2^{o}1788$; 172 = SD $-2^{o}1797$; 180; 238; 252; 291; 316 = SD $-2^{o}1832$;
	336 = SD $-2^{o}1838$ = BD $-1^{o}1461$; 355 = SD $-2^{o}1842$; 393 = SD $-2^{o}1852$; 403; 410;
	455; 483 = BD $-1^{o}1494$.

Remarks Concerning Spectra in LF9 (Cont'd.)

Zone -4°

No.	
25	All hydrogen lines exceedingly sharp; H and K very sharp.
33	Class OB star.
42	No lines visible; UV strong; red end of spectrum strong.
51	Metallic line A star.
69	All lines very weak; UV strong.
97	Class OB star. SD -3°1639.
120	Class OB star. SD -2°1835.
125	Metallic line A star.
137	Trace of metallic lines.
154	Class OB star. SD -2°1860.
156	Spectrum for brighter of the double. SD -2°1861.

Spectra with hydrogen lines sharper than usual for their class are:
Nos. 12 = SD -3°1602; 30 = SD -2°1786; 45 = SD -3°1623; 93 = SD -3°1638;
121 = SD -3°1650; 139 = SD -3°1661; 144 = SD -3°1667.

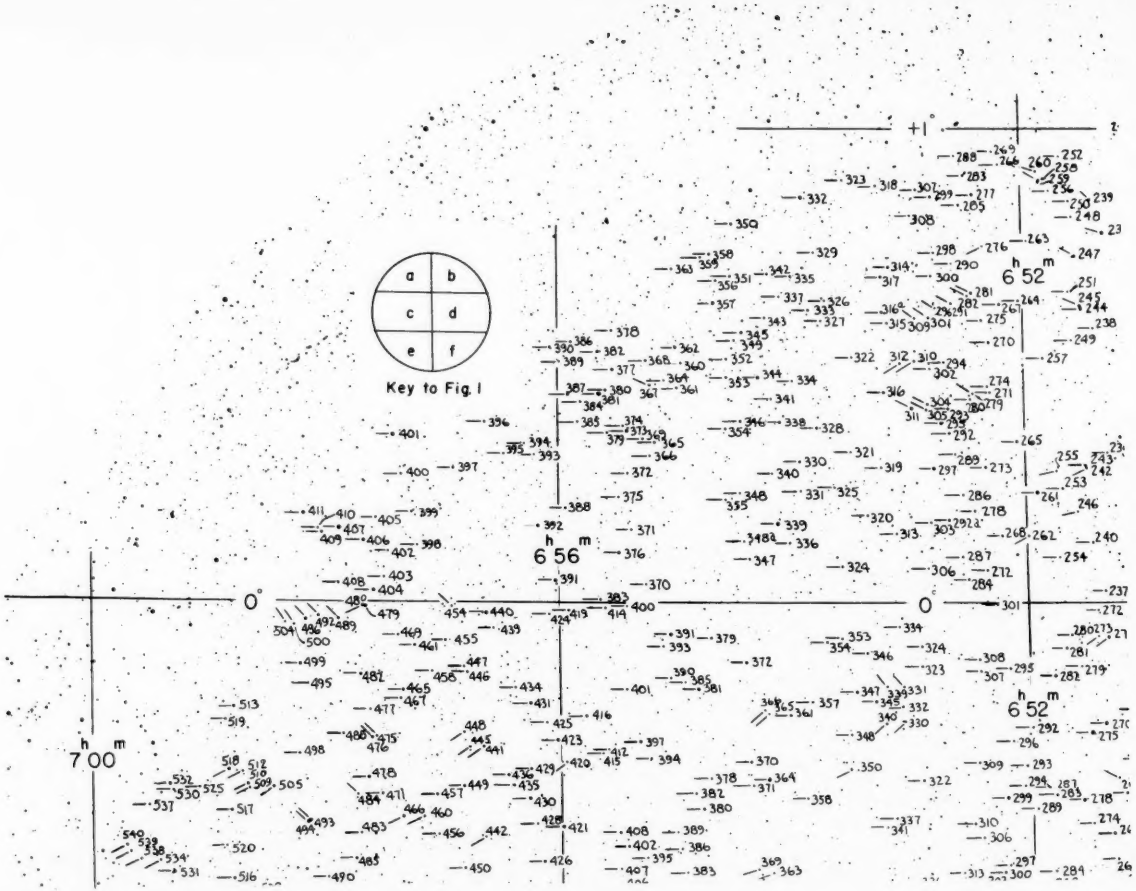

FIG. 1*a*.—Identification chart for LF9

FIG. 1*a*.—Identification chart for LF9

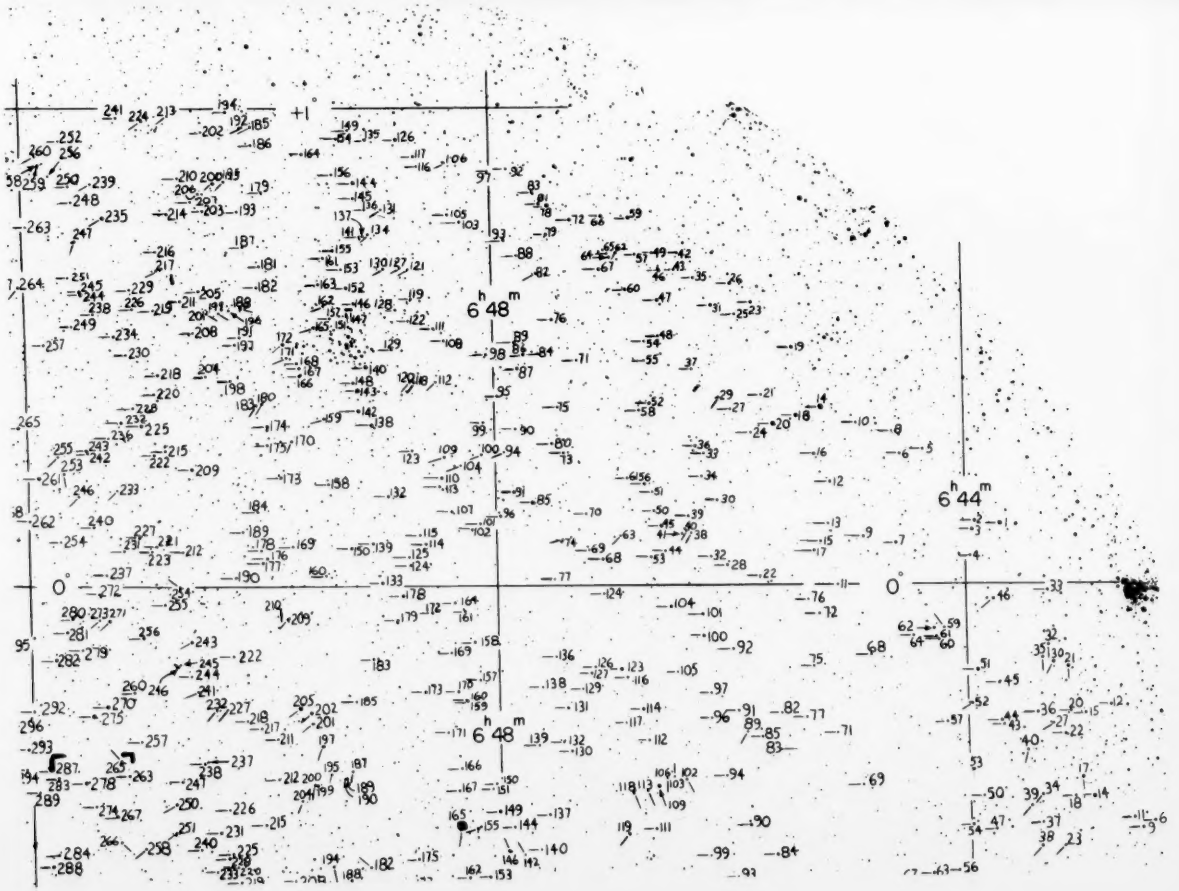

FIG. 1*b*.—Identification chart for LF9

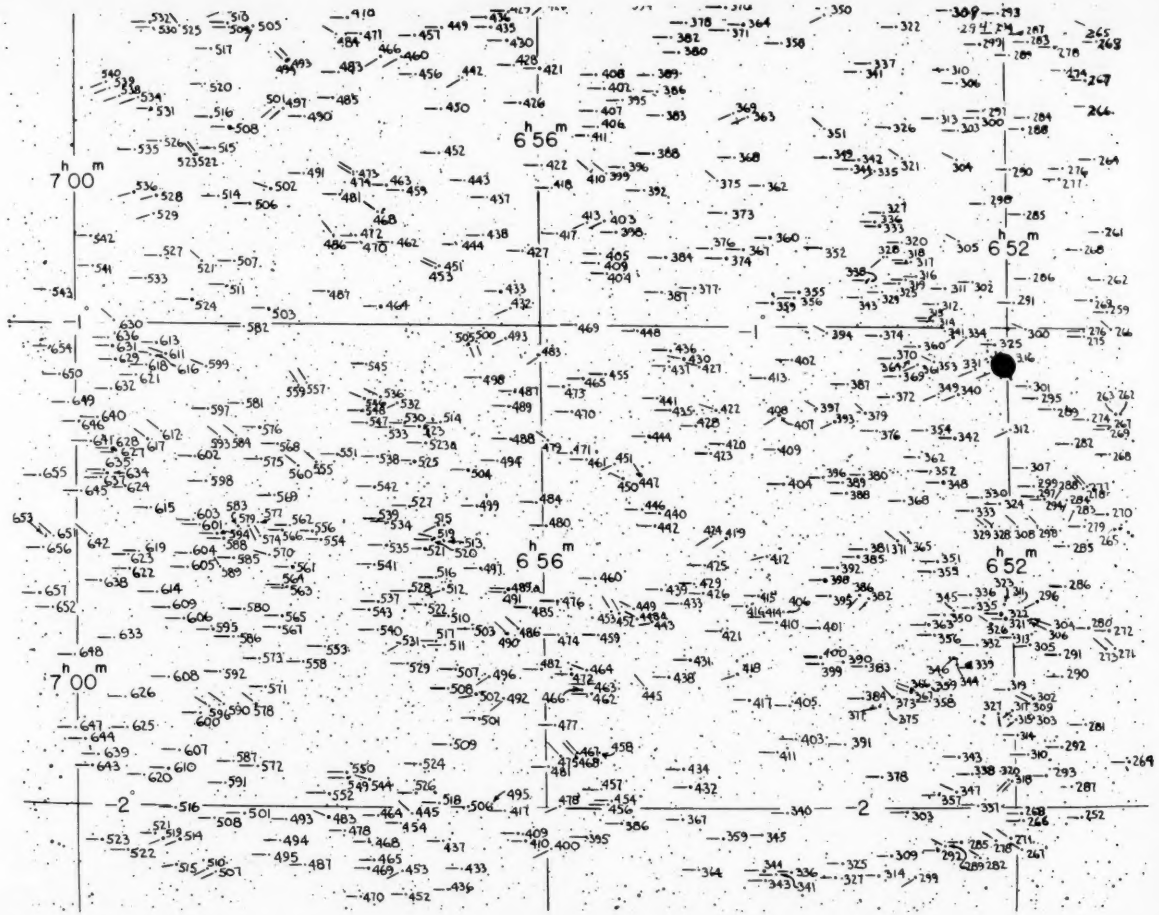

FIG. 1c.—Identification chart for LF9

FIG. 1c.—Identification chart for LF9

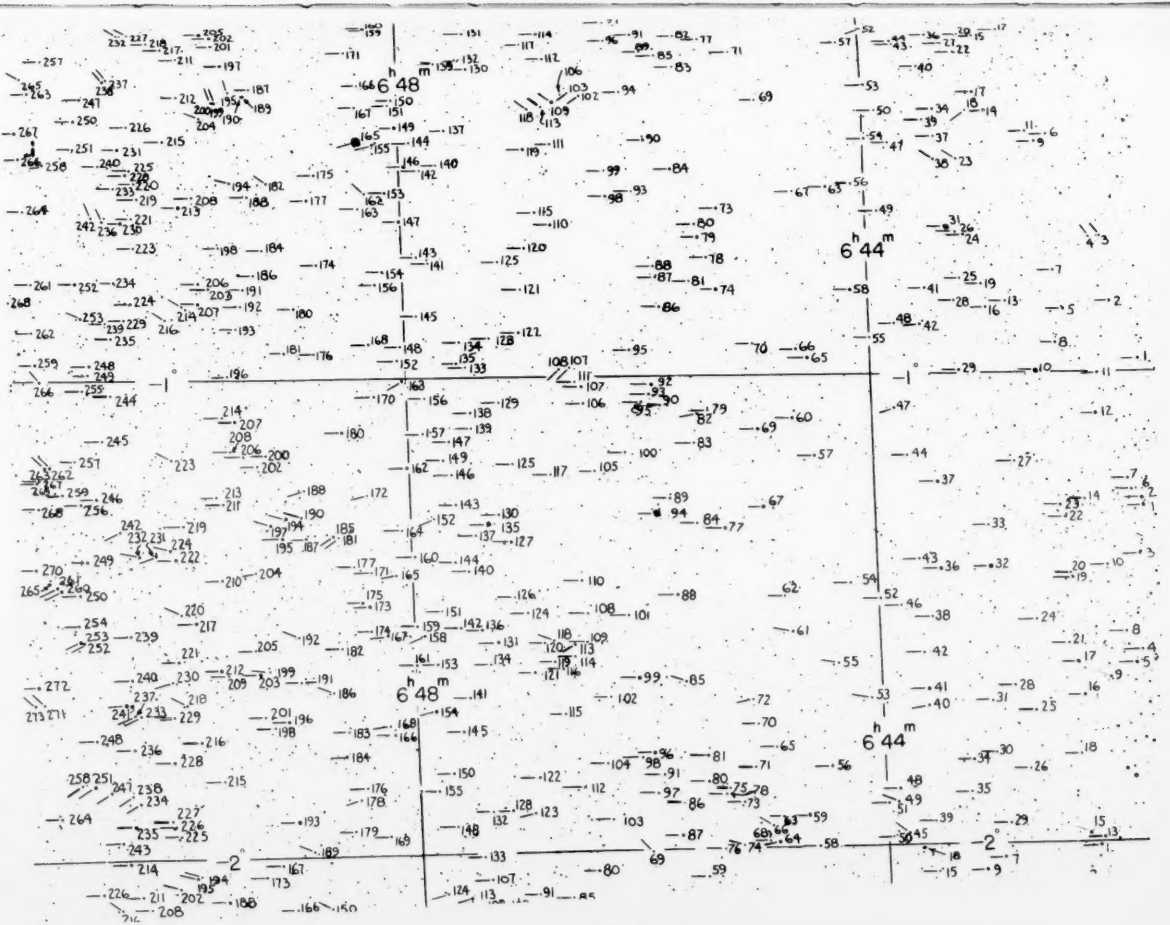

FIG. 1d.—Identification chart for LF9

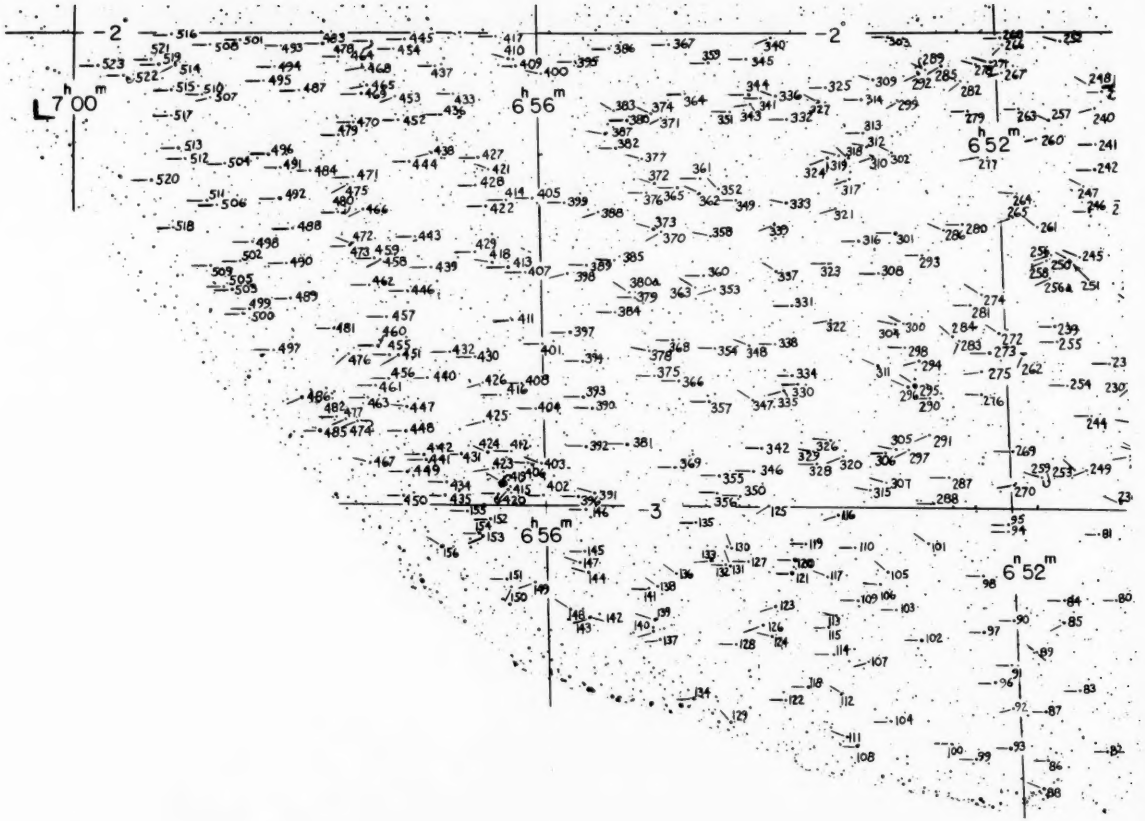

FIG. 1e.—Identification chart for LF9

FIG. 1*e*.—Identification chart for LF9

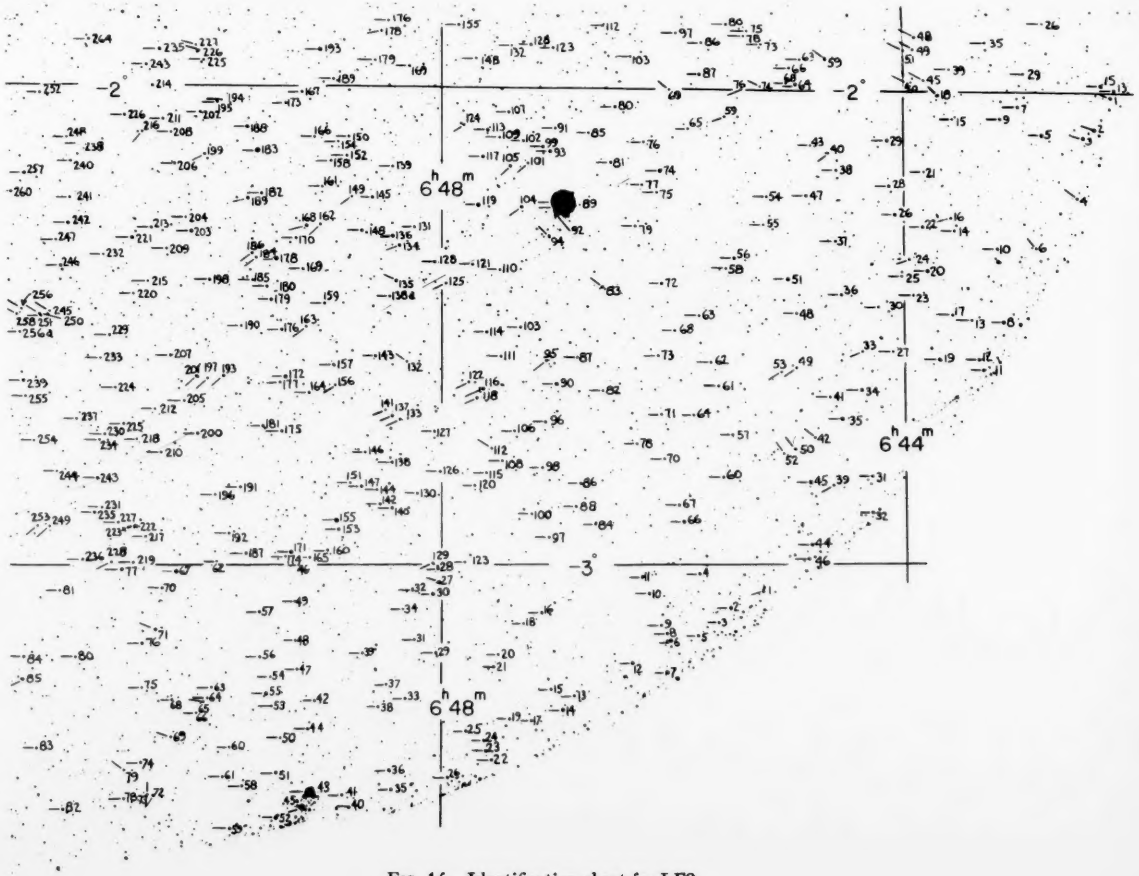

FIG. 1*f*.—Identification chart for LF9

STELLAR SPECTRA IN MILKY WAY REGIONS. VI. A REGION IN CAMELOPARDALIS

S. W. McCuskey
Warner and Swasey Observatory, Case Institute of Technology
Received December 29, 1955

ABSTRACT

Observational data on spectral class, photographic magnitudes, and red color indices are given for an area of 16.2 square degrees in Camelopardalis. The center of the field is R.A. 3^h51^m; Dec. $+56°.8$; $l = 114°$, $b = +4°$. These data are given for 929 stars. Identification charts are included.

INTRODUCTION

The spectral-class data, photographic magnitudes, and colors which comprise the contents of this paper refer to region LF6 in the general observing program (McCuskey and Seyfert 1947) of the Warner and Swasey Observatory. Similar catalogues for other areas have been published by McCuskey (1949, 1955), Nassau and MacRae (1949), McCuskey and Seyfert (1950), Annear (1953), and Farnsworth (1955). Co-ordinates of the center of the field are R.A. 3^h51^m; Dec. $+56°.8$ (1945); $l = 114°$, $b = +4°$. LF6 is one of 11 regions in the galactic plane for which studies of the variation of the stellar luminosity function are being made. An analysis of the data for LF6 has appeared elsewhere (McCuskey 1952). The field is circular and covers an area of 16.2 square degrees.

OBSERVATIONAL DATA

All the observations of spectral type have been made with the 4° prism attached to the 24–36-inch Schmidt-type telescope of this observatory. The photographic photometry was likewise done with this telescope, supplemented by photoelectric magnitudes and colors of the sequence stars and of a few additional field stars, obtained with the 10-inch refractor and the Schmidt telescope.

Sectional charts covering the area of LF6 are given in Figures 1*a*–1*f*. A key to the sectioning of the field is given in the upper left-hand corner of Figure 1*a*. The co-ordinates are approxmate, and the printing on each section reads correctly when north is up.

Table 1 contains the observational data for 929 stars in the region. A zone-numbering scheme similar to that of the *BD* catalogue has been employed; the numbers in Table 1, column 1, increase in order of right ascension in each zone. The network of co-ordinates refers approximately to the epoch 1950. An asterisk following a star number denotes a *BD* star, while "R" denotes a remark to be found in Table 2. A colon following the number indicates that the star is slightly outside the field of 16.2 square degrees used in the analysis. A few *BD* number equivalents to our zone numbers are also indicated in Table 2, to provide quick orientation with the *BD* catalogue and charts.

The second and third columns of Table 1 give, respectively, the apparent photographic magnitudes for all stars in the field and the red color indices for a majority of the stars. Colors have been determined from the given m_{pg} and from red-magnitude data based upon the North Polar Sequence as given by Nassau and Burger (1946). Four Kodak 103*a*-E plates and a No. 22 Wratten filter were used for the red magnitudes, while four Kodak II*a*-O plates were used for the blue. By comparison with the North Polar Sequence, sequences for the photometry were obtained both photographically and photoelectrically. In the photoelectric work, NPS stars 1, 4, 6, 10, 2r, and 4r were used to fix the zero point of the sequences in LF6. The probable errors for the tabulated photo-

graphic magnitudes and the colors are ± 0.04 and ± 0.06 mag., respectively. All measures of the plates were made with the iris-diaphragm astrophotometer of this observatory.

Table 1, column 4, gives the spectral class and, for the stars F0 and later, the luminosity class. A colon indicates uncertainty in the classification. The nomenclature for the luminosity class is that of Morgan, Keenan, and Kellman (1943), while criteria appropriate to our spectra have been published by Nassau and van Albada (1947). For stars fainter than $m_{pg} = 11.5$, only giant (III) and dwarf (V) classification has been attempted in most instances. In a few cases, overlapping spectra precluded the assignment of a luminosity class.

Remarks concerning individual spectra are given in Table 2. When a star is classed as OB, reference is made to the highly luminous objects listed by Nassau and Morgan (1951) in their recent survey of the Milky Way. Attention is drawn to a few of the interesting objects in LF6, such as the Oep star 55°124 and the B0p star 55°123.

It is a pleasure to record my thanks to Dr. D. A. MacRae for making the majority of the photoelectric observations of sequence stars on which the present photometry is based.

REFERENCES

Annear, P. R. 1953, *Ap. J.*, **118**, 77.
Farnsworth, A. H. 1955, *Ap. J. Suppl.*, Vol. **2**, No. 15.
McCuskey, S. W. 1949, *Ap. J.*, **109**, 426.
———. 1952, *ibid.*, **115**, 479.
———. 1955, *Ap. J. Suppl.*, Vol. **2**, No. 15.
McCuskey, S. W., and Seyfert, C. K. 1947, *Ap. J.*, **106**, 1.
———. 1950, *ibid.*, **112**, 90.
Morgan, W. W., Keenan, P. C., and Kellman, E. 1943, *An Atlas of Stellar Spectra* (Chicago: University of Chicago Press).
Nassau, J. J., and Albada, G. B. van. 1947, *Ap. J.*, **106**, 20.
Nassau, J. J., and Burger, V. 1946, *Ap. J.*, **103**, 25.
Nassau, J. J., and MacRae, D. A. 1949, *Ap. J.*, **110**, 478.
Nassau, J. J., and Morgan, W. W. 1951, *Ap. J.*, **113**, 141.

Table 1

Observational Data for Region LF6

Zone +54°

No.	m_{pg}	R.I.	Sp.
1:R	11.39	...	B8
2	12.50	...	K0:
3:*	6.86	...	A5
4*	11.33	...	G0
5:	11.57	...	F8IV
6:*	9.73	...	F0III
7*	8.73	...	A2
8R	11.57	...	A2
9R	12.10	...	B3
10	12.01	...	G0
11:	12.48	...	K0III:
12:*	8.46	...	F2III
13:	12.56	...	B9
14:	12.69	...	G0:
15	12.44	...	B8
16*	8.66	...	F8V
17	12.09	...	A0
18	12.98	...	K0
19:	12.43	...	A0
20:*	8.50	...	B9
21	13.02	...	B9
22	12.91	...	A0:
23:	12.32	...	K0
24:R	12.26	...	A0:
25:	12.65	...	A0
26	12.36	...	F0III
27R	12.14	...	B8
28:	12.19	...	A0
29	11.78	...	G8V
30	12.54	...	K0
31	12.39	+0.77	G0
32*	10.32	...	F8V
33	12.56	+1.96	G8III
34	11.58	...	F5V
35R	11.59	...	A3
36:	12.44	...	B8
37	12.04	+0.77	G0
38:	12.68	...	B9:
39:	11.89	...	G0V
40*	10.71	+0.56	B9
41*	11.58	...	G5V
42R	11.86	...	B9
43	12.52	+2.00	K0:
44	12.60	...	G0
45	11.23	...	B8
46:	12.45	...	A0
47* R	9.95	...	B8
48	12.58	...	B9
49*	10.89	...	G0V
50	12.32	+1.88	K0
51	12.65	...	K0:
52	12.20	...	A2
53:	11.93	...	B8
54:	11.83	...	B8
55:	12.65	...	B8
56	13.02	...	K0
57:	12.59	...	A0
58	12.74	...	G5
59:	11.59	...	K3V
60:	11.78	...	B8
61:*	11.15	...	G5IV
62	12.55	...	K0
63R	11.87	...	A0
64	12.67	...	B9
65:R	11.92	...	A0
66* R	10.64	...	B5
67:*	6.64	...	F2IV
68:*	9.25	...	F2V

Zone +55°

No.	m_{pg}	R.I.	Sp.
1:	12.08	...	B8
2:*	10.00	...	A3
3:*	8.83	...	A0
4:	11.86	...	G2
5*	11.21	...	F0
6	12.34	...	B8
7:*	11.17	...	G5V
8:	12.30	...	G0
9:	12.71	...	B9
10R	11.57	...	G0III
11*	10.29	...	G5IV
12:	13.02	...	B9:
13R	11.63	...	A0
14*	11.41	...	K3III
15*	10.48	...	G5III
16*	11.28	...	G5III
17	12.73	...	B8
18:	12.71	...	A0
19R	12.18	...	A0
20*	9.24	...	B8
21	12.36	+0.74	B5:
22	11.31	...	B8
23	12.38	...	A0
24:*	11.34	...	G8IV
25	12.38	...	A0:
26	11.45	...	A0
27*	11.09	...	A0
28	12.35	+0.74	G0
29	13.26	...	A0
30	13.08	+0.48	A0
31R	12.10	...	A0
32	11.53	...	F0
33	11.30	+0.54	B9
34	12.22	+0.76	G0
35	12.45	+0.48	B5
36	12.15	...	F0
37*	8.73	+0.39	A0
38R	12.10	+1.38	G0p
39R	11.98	...	A2
40	11.67	+0.92	F8
41	12.11	...	G0
42	11.77	...	B8
43	12.18	+0.57	B8
44	12.64	+0.68	A0
45	12.20	...	G0
46	12.32	...	B9:
47	11.40	...	F2III
48*	11.45	...	K2III
49	12.54	+0.65	A2
50	12.38	+0.64	A0
51*	5.76	-0.38	B9
52	11.63	+0.51	B9
53* R	10.61	+0.66	A2
54	12.18	+1.97	K0
55	12.09	+0.74	G2:
56*	8.94	+0.60	G2IV
57	11.69	+0.95	G2V
58*	8.95	+0.51	B8
59	12.42	+0.73	A5
60	11.60	+1.11	F0V
61	12.73	+0.88	A0
62*	8.58	+0.27	F8V
63*	9.85	+0.46	F8IV
64*	12.13	+2.18	G8III
65* R	11.38	...	K0III
66*	9.79	...	A3
67	12.34	+0.89	A0
68	13.20	+0.67	A0
69	12.89	+2.95	K5
70	12.30	+1.41	G0
71	12.22	+2.76	K3:
72*	11.01	+0.66	F0V
73	12.61	+0.65	B9
74*	10.05	+0.82	F2V
75	12.37	+0.74	A0
76	11.97	+0.57	B5
77	12.27	+0.57	A0
78	12.37	+0.40	A0
79	11.71	+0.88	G2III
80* R	11.62	+0.66	B0:

Table 1

Observational Data for Region LF6 (Cont'd.)

Zone +55° (Cont'd.)

No.	m_{pg}	R.I.	Sp.
81	13.18	+0.86	A0
82R	12.00	+0.70	A3
83	12.24	+0.70	F5
84*	11.07	+0.88	G0III
85	12.38	+0.43	B5
86	12.62	+1.09	G2
87	12.23	+2.22	K2
88*	10.18	+0.76	A0
89	12.14	+0.31	B9
90	12.29	+0.97	F0:
91	12.61	+0.27	B9
92	12.05	+0.36	G0:
93	11.80	+0.64	B9
94*	10.15	+0.71	G0V
95	12.63	+1.67	G8
96	12.92	...	K5
97	12.70	+0.56	A0
98	13.27	+2.74	M0
99* R	10.21	+0.84	B0
100	12.38	+0.48	A2
101	11.47	+0.75	F8V
102	12.65	+0.37	B8
103*	11.85	+2.07	G5III
104R	11.75	+0.93	Be:
105	12.68	+0.39	A0
106	12.58	+0.52	B5
107	11.62	+0.52	A0
108	12.36	+0.59	B9
109	12.16	+0.49	A0
110	12.23	+0.49	B8
111* R	10.78	+0.35	B8
112	12.69	+0.48	A0:
113	11.60	+0.38	B5:
114R	11.59	+0.70	B8
115	11.89	+1.26	F2
116	11.98	+0.59	A0
117R	11.96	+0.62	O5:
118	12.67	+1.44	K0
119	12.33	+0.69	A5
120	12.50	+0.41	B8
121	12.46	+1.00	G5
122	13.28	+0.48	B8
123* R	10.07	+1.01	B0p
124* R	11.30	+1.21	Oep
125	11.89	+0.50	B9
126	13.48	+4.06	M0
127*	7.52	+0.22	A0
128R	12.37	+0.47	B5
129	11.94	+0.26	B8
130	11.47	+2.03	G8:
131*	10.10	+1.82	G0III
132	12.92	+0.53	A0
133	12.75	...	A2
134* R	10.38	+0.25	B5
135	12.34	+0.62	G0:
136	12.21	+0.42	B5:
137	12.26	+0.92	G0
138	12.18	...	G0:
139R	12.22	+0.60	B9
140	12.31	+0.60	F0
141	12.02	+1.55	G8V
142R	11.63	+0.88	F0IIIp
143	11.03	+1.18	G5IV
144	12.42	+0.29	A0
145* R	9.42	+0.92	B1
146	11.92	...	G0
147*	9.61:	+1.72	K0III
148R	11.86	...	A0
149	11.47	+0.64	G0
150R	11.37	+0.47	B0:
151	11.90	+0.90	G0
152	12.40	...	A5:
153	11.14	+0.85	F0V
154	12.24	...	A2
155	12.27	+0.93	G0
156	12.06	...	A0
157	11.81	...	F0
158	12.10	...	B8
159	12.36	+0.19	A0
160	12.62	...	K0
161	11.72	+0.35	B9
162	12.58	...	B9
163	12.65	...	K0
164	10.80	...	B9
165	12.30	...	A0
166	12.61	...	G5
167R	11.63	+0.22	B0
168	11.97	...	B9
169	11.95	...	G5V
170:*	11.30	...	G0Ib:
171	12.00	...	G0
172	12.32	...	B9
173*	11.20	...	K2V
174	11.77	...	B:
175	11.51	...	G0
176:	11.62	...	A0
177:	11.80	...	G8III

Zone +56°

No.	m_{pg}	R.I.	Sp.
1:* R	7.52	...	B1
2:	12.95	...	A0
3:* R	10.04	...	B8
4:	12.21	...	A0
5:	12.60	...	G0
6:	12.23	...	F0
7:	11.33	...	B8
8:* R	[6.12]	...	B8
9:	12.61	...	K0
10:R	11.95	...	A2p
11*	10.48	...	F8V
12	12.45	...	G0
13*	10.66	...	F2V
14	12.47	...	K0
15	11.94	...	A0
16	12.46	...	G2III
17	11.62	...	A0
18	12.38	...	A0
19*	6.36	...	A0
20	11.16	...	G5IV
21*	11.81	...	K0:
22	11.89	...	G0
23	13.47	...	A0
24	13.08	...	G5
25	12.21	...	B8
26	12.24	...	G0
27	11.90	...	A2
28*	10.67	...	G0V
29	13.14	+0.56	B9
30* R	9.50	+0.41	B8
31*	9.95	+0.83	F0V
32	12.43	+0.47	B5:
33*	10.94	+0.72	A0
34	12.52	+0.80	B5
35	12.26	+0.69	B9
36*	11.88	+0.96	A3
37*	9.26	+0.61	B9
38*	8.91	+1.16	G5III
39*	11.17	+2.30	K0III
40	13.20	+0.36	A2
41	13.24	+0.48	A3
42	12.62	+0.52	A0
43	12.11	+0.51	B8
44	13.78	+3.06	M0
45	12.68	+0.57	A0
46	12.34	+2.16	K0III
47	12.77	+1.02	G2
48*	10.68	+0.65	B9
49	13.06	+0.51	B8
50*	11.19	+1.08	G0IV

Table 1

Observational Data for Region LF6 (Cont'd.)

Zone +56° (Cont'd.)

No.	m_{pg}	R.I.	Sp.	No.	m_{pg}	R.I.	Sp.	No.	m_{pg}	R.I.	Sp.
51	13.28	+0.47	A0	101	11.10	+0.47	B8	151*	10.27	+0.61	G0V
52	12.32	+1.50	K0:	102	11.83	+0.73	G0	152	12.50	+0.62	F0:
53	12.38	+1.63	K0:	103	12.73	+1.12	G0	153*	9.59	+0.82	G8IV
54	11.94	+1.91	K0V	104	12.30	+0.52	A0	154	10.82	+0.62	F8V
55	12.92	+0.54	B9	105	11.57	+0.54	B9	155* R	10.46	+0.27	B1
56	12.34	+0.50	B8	106	11.10	+0.58	B9	156	12.67	+0.58	A0
57	11.87	+1.16	G0	107	11.96	+0.51	A3	157	12.83	+0.55	A0
58*	10.38	+0.75	F0V	108	12.33	+0.46	A3:	158	12.25	+0.63	A0
59* R	10.78	+0.55	B8	109	12.53	+0.36	A0	159*	10.05	+0.63	B9
60*	8.97	+0.68	F2III	110	12.13	+1.92	G5III	160* R	9.23	+0.17	B2
61	11.57	+0.89	G0	111	10.72	+0.72	G0V	161	12.40	+0.52	F2
62	12.40	+0.59	A0	112R	10.75	+1.07	O8	162	12.05	+0.35	B9
63* R	9.17	+0.41	B5	113	11.83	+0.47	B8	163	12.76	+0.34	A0
64R	10.31	+0.55	B5	114	12.57	+0.55	A2	164	11.94	+0.79	A2
65*	10.07	+1.71	G2III	115	11.35	+0.75	F0	165	12.26	+2.45	G8:
66	11.26	+2.31	K0III	116*	11.16	+0.51	B9	166	12.40	+0.74	G0:
67	12.13	+0.85	G0	117	11.21	+0.99	G2V	167	11.65	+0.98	G0
68*	11.17	+2.61	K2III	118	12.32	. . .	B9	168	11.81	+0.76	G0
69* R	10.81	+0.70	B8	119R	10.93	+0.55	B8	169	12.26	+1.00	G8V
70	12.66	+1.81	G5III	120	12.82	+0.40	A0	170	12.05	+1.83	G5III
71	11.77	+0.68	B8	121R	11.46	+0.27	B8	171	11.29	+0.63	A2
72*	10.71	+1.83	G5III	122*	9.22	+1.25	G0II	172	12.08	+0.49	B9
73	11.71	+1.06	G0	123*	11.38	+0.96	G0V	173	12.31	+1.75	G0:
74R	12.28	+0.78	A2	124	12.40	+0.58	A0	174	11.73	+0.47	A0
75	11.84	+1.28	G0	125	12.17	+0.12	B5:	175	11.84	+0.78	G0
76* R	10.81	+1.32	A2	126*	7.24	+0.26	A3	176	12.12	+0.53	B9
77	11.07	+0.86	F5V	127	11.76	+0.30	B8	177	12.30	+0.28	B8
78* R	8.63	+0.18	B2	128	11.51	+0.94	A2-F0	178	11.91	+0.47	B8
79*	6.41	-0.01	B8	129*	9.69	+0.39	A2	179	10.84	+0.59	F0V
80	12.52	+1.00	G0	130R	11.01	+0.63	A3p	180*	11.76	+2.26	K0III
81*	7.23	+0.02	B9	131	11.89	+0.48	A0	181*	10.11	+0.51	A3
82	11.92	+0.98	G0	132	12.43	+0.57	G0	182*	11.69	+0.76	G0IV
83	12.40	+0.99	G0	133	12.52	+1.05	A2	183*	9.30	+1.42	G8III
84	12.28	+0.61	A3	134	13.18	+2.09	K0	184	12.24	+1.07	G0
85	12.32	+2.20	K0III	135	12.47	+0.58	A0	185	11.90	+2.07	G8III
86	11.94	+0.81	A2:	136	12.37	+1.77	G5III	186*	8.18	+0.46	F0III
87	12.11	+0.29	A0	137	12.52	+0.92	G0	187* R	9.29	+0.47	O5
88*	10.90	+2.01	G8III	138*	9.93	-0.01	B5	188	11.93	+0.48	B9
89	13.17	. . .	A0	139	12.87	+0.69	A3	189	12.07	+0.51	A0
90	12.66	+1.87	G8	140	12.30	+1.05	G0	190	12.39	+0.72	A0
91	11.69	+0.70	B5:	141	11.93	+1.37	G5III	191R	11.11	+0.88	A3
92	12.98	+0.41	A0	142	11.86	+1.76	G5V	192	11.98	+0.62	B8
93	12.38	+1.05	G0	143*	10.40	+0.76	F2V	193*	10.22	+0.66	G0V
94	12.38	+0.53	A0	144* R	10.51	+2.34	K3IIp	194	12.32	+0.55	B9
95	12.66	+0.69	A0:	145	12.68	+0.89	G5	195	12.69	. . .	A3
96	12.37	+0.72	A5:	146	12.22	+2.19	K2III	196	12.31	+0.78	G0
97	12.48	+2.05	K0	147	13.07	+0.27	A0:	197	12.60	+0.44	B9
98	12.40	+0.89	G8:	148	11.87	+0.36	B5	198*	9.01	+1.41	G5III
99R	11.89	+0.45	B3p	149	11.32	+0.69	F5III	199	12.25	+0.78	G0
100	12.18	+0.57	B8	150	12.40	+1.90	K0	200	12.45	+0.20	B5

Table 1

Observational Data for Region LF6 (Cont'd.)

Zone +56° (Cont'd.)

No.	m_{pg}	R.I.	Sp.
201*	10.14	+0.35	B9
202	11.38	+1.04	G2V
203R	11.96	+0.41	B0p
204	11.83	+0.72	G0
205	11.87	+0.50	A0
206	12.36	+2.06	K0
207*	9.95	+1.40	G5IV
208R	12.35	+0.25	B8:
209	11.42	+0.45	A0
210	12.55	+0.60	G0
211R	12.37	+1.53	A5p
212*	10.98	+1.89	K0III
213	11.71	+1.05	G0III
214	12.44	+1.87	G8III
215	12.60	+1.14	K0
216R	11.44	+0.74	B5
217*	8.00	+1.25	K0IV
218R	11.33	+0.73	A0
219	12.24	+1.08	K0III
220R	12.18	+0.56	A0
221	13.06	+0.47	B8
222	12.19	+1.73	G8V
223	12.68	+2.73	M2
224	12.60	+0.50	A0
225*	10.03	+2.39	K3III
226	12.46	+0.52	B8
227*	10.95	...	A0
228	12.38	...	G0
229	11.50	+0.69	F0III
230	11.47	+0.57	F0
231*	11.33	+2.42	K0IV
232	12.37	+0.48	B8:
233	11.57	+0.15	B9
234	12.02	+0.35	A2:
235* R	8.45	...	O9
236R	11.81	...	A3
237*	9.64	...	K5III
238	12.54	...	K0III
239	12.20	...	G0
240	12.93	...	A0
241	12.55	...	B5:
242	12.02	...	G5III
243	11.96	...	G0
244	12.12	...	G0
245	12.71	...	G0
246	11.91	...	B9
247	12.14	...	B9
248	11.51	...	A0
249:	12.30	...	B8
250	11.71	...	B5
251:	12.12	...	B8:
252	12.28	...	A0
253:*	11.70	...	G0
254:	11.89	...	G5III
255:	11.60	...	B9

Zone +57°

No.	m_{pg}	R.I.	Sp.
1:	12.80	...	A2
2:	13.38	...	A0
3:* R	9.64	...	B5
4:* R	10.94	...	B8
5:	12.20	...	G8III
6:	12.26	...	G0
7:	11.30	...	A0
8*	11.17	...	K2V
9:	12.13	...	A0
10	13.14	...	A0
11:	12.76	...	G0
12	12.02	...	B5
13	11.93	...	G5III
14	12.62	...	K0
15	12.03	...	G2:
16*	9.64	...	K0III
17*	10.49	+0.69	B9
18R	11.04	...	B9
19	12.62	...	B9
20	12.43	+2.44	K0
21* R	8.47	+0.34	B5
22*	10.76	+1.02	F5V
23	12.38	+1.79	G8III
24	12.46	+0.73	G0
25	12.18	+0.47	A0
26	11.89	...	G0V
27R	12.04	+0.71	pec
28	12.82	+0.90	B8
29	12.58	+0.39	A0
30	11.93	+1.16	F0
31	12.71	+1.05	G0
32R	11.69	+0.74	B5
33	12.08	+0.82	A2-F2
34	12.47	+1.92	G5
35	11.35	+0.84	G0V
36	11.54	...	K2III
37	12.52	+0.69	B9
38	12.40	+0.65	B8
39	12.22	+1.91	G5III
40	12.33	+0.83	G0
41*	8.82	+0.60	F5V
42*	9.51	+0.30	B8
43	12.34	+0.64	A0
44	12.02	+0.75	F0
45*	10.80	+0.85	G0V
46	13.19	+0.57	A0
47	12.10	+0.63	A0
48*	9.57	+0.23	B5
49	11.35	+0.61	B8
50	12.14	+0.46	A2
51	12.46	+0.38	A0
52	11.90	+0.96	G5V
53*	10.27	+2.81	K5III
54* R	10.13	+0.49	B9
55	12.75	+0.40	A3
56	12.46	+0.85	F0
57	13.19	+0.37	A0
58	11.10	+0.51	A0
59	12.90	+0.48	B8:
60	11.97	+1.85	G5V
61	11.98	+2.96	M0III
62	11.92	+0.93	F0
63	12.41	+0.35	A0
64	12.83	+0.46	A0
65	12.55	+1.03	G0
66	12.83	+0.54	A0
67	12.06	+0.71	F0V
68	12.84	...	B9:
69	12.21	+0.84	F8:
70R	11.37	+0.83	A3
71	11.62	+1.70	G5IV
72*	10.70	+1.22	G0III
73*	9.05	+0.87	G5V
74	11.66	+0.63	A0
75	12.38	+2.91	K2III
76	12.50	+0.44	A0
77	12.45	+0.46	B8
78	12.07	+0.57	B8
79	12.31	+1.97	K0III
80	12.76	...	G2:
81	10.86	+0.71	F0V
82	12.44	+1.82	K0III
83* R	10.73	+0.21	B5
84	12.58	+0.48	B9
85	11.63	+0.70	A5
86* R	11.35	+0.45	B3p
87	12.72	+0.53	A0
88*	11.54	+2.04	G8III
89*	9.59	+0.47	F2V
90*	10.65	+0.23	B8
91R	11.26	+0.65	A3
92	11.69	+0.73	F0V
93*	9.55	+0.50	F0V
94	12.56	+0.85	G0
95	12.21	+1.00	G5III

Table 1

Observational Data for Region LF6 (Cont'd.)

Zone +57° (Cont'd.)

No.	m_{pg}	R.I.	Sp.	No.	m_{pg}	R.I.	Sp.	No.	m_{pg}	R.I.	Sp.
96	12.27	+1.77	G5III	146*	9.65	+1.46	K0III	196R	11.29	+0.75	B9
97	11.56	+0.51	B9	147*R	9.72	+0.10	O8:p	197*	10.53	+0.78	G0V
98	12.90	+0.20	A0	148	12.20	+0.52	B8	198R	12.30	. . .	G5p
99*	5.76	. . .	A2	149	12.34	+0.55	A0	199	12.38	+2.20	G8III
100R	10.39	+0.43	B9	150	12.25	+0.70	A5	200	11.85	+0.70	B9
101	13.16	+0.63	A0	151R	11.57	+0.21	B9	201	12.07	+0.40	B8
102	11.95	+1.03	F0	152R	11.13	+0.22	B0:	202	13.00	+0.34	B8:
103	12.35	+0.74	A5	153	11.28	. . .	A2	203	11.49	+0.55	G0
104*	10.10	+0.85	G0IV	154	11.66	+0.43	A0	204	12.70	+0.68	A0
105	11.91	+1.25	G5V	155*	9.24	+0.48	F0IV	205	11.53	+0.97	F0III
106	11.54	+0.29	B9	156	12.06	+0.82	G0	206	12.62	+0.45	A2
107	11.51	+0.41	B9	157	11.63	+0.72	F0III	207	12.30	+0.27	B9
108*	11.37	+2.38	K2III	158	12.20	+1.88	G8	208	11.57	+1.80	G5III
109*	7.95	+0.25	A5	159	11.29	+1.82	G5III	209	12.22	+0.35	A0
110	12.23	+0.68	A0	160	12.01	+1.83	G5IV	210	13.18	+0.87	A0:
111	12.02	+1.97	G8III	161	12.78	+0.23	B9	211	11.50	+0.51	A0
112	11.39	+0.85	F5III	162	12.25	+0.69	F2	212*	10.29	+0.43	F2IV
113	12.19	+0.37	B9	163	11.57	+0.68	A3	213	12.74	+0.37	B9
114	12.28	+0.85	G0	164	11.53	+0.34	A0	214	12.31	+0.39	A0
115*	10.56	+2.69	M8III	165	12.34	+0.46	F0	215	12.43	+0.42	A0
116	12.10	+0.35	A2	166	12.64	+0.34	A0	216	11.77	+0.66	G2V
117*	9.13	+1.43	G5III	167	12.26	+1.90	K0III	217	12.15	+0.31	A5:
118	11.20	+0.50	B8	168	11.17	+0.42	A2	218	11.13	. . .	F8III
119R	11.01	+0.27	B0:p	169	11.80	+0.41	A0	219R	10.77	+0.36	B9
120*	10.38	+2.28	G8III	170*	10.06	+0.61	F5V	220	12.31	+0.45	G0
121	11.24	+0.72	A3	171*R	10.05	+0.16	B9	221*	9.54	+0.57	G0V
122	12.36	+0.40	A3	172	11.29	+0.78	G0V	222	12.28	. . .	A3
123	11.35	+0.62	A3	173*	10.36	+1.80	K0IV	223	12.39	+1.51	G8:
124R	10.81	+0.67	A3	174	12.63	+1.89	K0	224	11.66	+0.46	A2
125	11.82	+0.38	B9	175	12.44	+0.65	B5:	225	12.06	+1.70	K0III
126	11.94	+0.80	A3	176	12.92	. . .	K0	226*	10.81	. . .	A2
127*	10.91	+0.66	A2	177	12.67	+0.38	A0	227	12.36	. . .	F0
128	11.93	+0.71	F0	178	12.88	+2.65	M5	228	11.87	+0.84	G0
129	11.87	+0.77	G0	179	12.42	+1.63	G8	229	11.04	+0.81	F0V
130	11.94	+0.70	G5IV	180*	9.98	+0.23	B8	230*	11.93	. . .	G8III
131	11.24	. . .	B5	181	12.84	+2.06	K0	231*	10.87	+1.63	G5IV
132*	10.50	+1.88	G5III	182	12.40	+0.18	B8:	232	12.00	. . .	F2
133	12.35	+1.66	G5	183	11.80	+0.78	B9	233R	11.36	. . .	B5
134	12.58	+0.81	A0	184	11.99	+1.55	G5III	234	11.15	. . .	B8
135	12.43	+0.47	A0	185	12.20	+0.35	A0	235	12.02	. . .	B9
136	10.98	+0.33	B8	186	12.61	+0.56	B8	236	12.58	. . .	G5:
137	12.35	+0.44	B9	187*	9.08	+0.37	B9	237	11.61	. . .	B9
138	12.36	+0.45	B9	188	12.60	+1.18	G0	238	11.10	. . .	B9
139	11.77	+0.88	G0	189*	8.15	+0.24	A2	239*R	11.63	. . .	K2:
140R	11.30	+0.18	B2p	190*	10.88	+1.97	G8IV	240	11.85	. . .	G8V
141*	7.04	+0.06	A2	191*	10.90	+1.95	K0III	241	11.51	. . .	G0III
142R	11.90	+0.71	A3	192	12.15	+1.18	G0:	242*	11.93	. . .	B5:
143R	11.17	+0.52	B8	193	12.62	+0.47	B9	243	11.18	. . .	B9
144R	10.08	+0.14	O8:p	194	11.54	+0.41	B8:	244	12.42	. . .	A0
145	12.24	+0.80	G2	195	11.86	+1.88	G8:	245	11.06	. . .	G0IV

Table 1

Observational Data for Region LF6 (Cont'd.)

Zone +57° (Cont'd.)

No.	m_{pg}	R.I.	Sp.
246*	9.43	...	A3
247	12.22	...	B8
248:*	10.51	...	B8
249	12.04	...	A2-F0

Zone + 58°

No.	m_{pg}	R.I.	Sp.
1:R	11.16:	...	A0
2:*	11.16:	...	F2V
3R	11.94	...	F2p
4	12.38	...	B9
5:	12.86	...	B5
6:	12.98	...	K0
7:	12.38	...	B5
8	11.95	...	B9
9	12.42	...	B8:
10	9.66	...	A2
11:	12.36	...	F5
12:R	11.82	...	B9
13:	11.69	...	G01b
14R	11.99	...	B8p
15	12.31	...	B9
16R	11.95	...	B8
17	12.15	...	A0
18:*	11.14	...	A0
19:*	10.55	...	F5V
20	12.42	...	A0
21	11.65	+1.04	F8III
22	12.15	...	F0
23:	12.11	...	A5
24	12.89	...	B8
25R	12.62	+0.50	A2p
26R	12.40	...	A0p
27	11.87	+1.19	G8V
28	12.31	...	G0
29:R	12.10	...	A2-F0
30*	7.94	...	F5V
31	11.84	...	K0III
32	12.46	...	G0
33*	10.85	+2.12	G8III
34	10.40	+0.47	B5
35	13.22	+0.26	B8
36R	12.22	...	B9
37*	9.96	...	B5
38:	11.63	...	G5V
39*	10.15	+0.26	B8
40	12.13	+0.46	A0
41	11.29	...	B8
42	12.65	...	F0:
43	11.98	+0.27	B9
44:	12.36	...	B8
45*	10.00	...	G8II
46*	10.91	...	G5III
47	11.22	+0.92	F0III
48:	11.70	...	A2
49:R	11.95	...	B3
50R	12.05	...	A0
51	10.69	...	B9
52*	11.11	...	K2II
53:	11.88	...	B3
54	11.38	+0.77	A3-F0
55	12.98	+0.39	A0
56	11.96	...	A0
57*	10.48	+0.78	F2V
58	11.96	...	G0
59	12.08	...	F5
60* R	10.71	...	B8
61	12.82	...	A0
62*	10.92	...	F0
63	11.43	+0.36	B8
64*	10.81	...	G5
65	13.02	...	A0
66	12.89	...	B8
67	11.52	...	A2
68* R	10.37	+0.36	B2
69	10.92	+0.52	B8
70*	9.41	...	G2V
71	11.33	+0.44	A2:
72	11.82	+0.98	G0
73*	11.61	+2.11	K0III
74	12.33	...	A3
75	12.45	+0.40	A0
76*	11.19	...	B9
77	11.92	+0.80	A2-F0
78	12.79	+1.56	G5
79	12.08	+1.91	G5III
80	12.59	...	A2
81	12.66	...	A0:
82	10.95	+0.31	B8
83	12.32	+0.95	F0
84	12.78	+0.52	A5
85	11.57	+0.74	A0
86*	10.91	+0.54	B8
87	12.09	+0.67	A0:
88	11.75	+0.83	A0:
89	12.63	...	A2
90	12.20	...	F5
91	12.34	+1.22	G0
92	12.66	+0.62	A0
93	12.84	+2.15	K0:
94	11.62	+0.57	A0
95*	10.79	+0.49	B9
96	12.58	+0.36	A0
97*	11.30	...	G0V
98* R	10.17	+2.09	F81b
99	11.31	+0.34	B9
100	12.37	+1.06	G0
101*	10.09	+1.18	G8V
102*	10.13	...	F5III
103*	11.53	...	B5
104	11.21	+0.67	F2IV
105* R	10.39	+0.60	A2
106	12.37	...	A0
107*	10.98	+0.68	A3
108	12.08	...	F0
109	12.26	+1.73	G8V
110	12.22	...	A2
111*	10.26	+1.46	G5III
112	12.53	+0.64	A0
113	12.04	+0.81	F5V
114	13.02	...	A0
115	11.83	+0.81	G2V
116*	8.67	+0.53	F8IV
117	12.12	+0.30	B9
118	11.46	+0.62	A5
119	12.57	+2.00	K0
120	11.16	...	K0III
121	12.21	...	G2
122	12.04	+0.71	F0
123*	9.04	+0.48	F0V
124	12.24	+0.79	G2V
125	12.36	+0.55	A2
126*	10.77	+0.48	F8V
127	12.70	+0.49	B9
128	11.84	...	B9
129	11.85	...	G0
130	12.50	...	G8
131	12.59	+0.86	A3
132	11.64	+1.58	G2III
133	11.85	+0.51	B5
134*	10.57	+0.78	G2V
135	12.00	...	F0
136	11.87	...	G5V
137*	11.17	+0.97	G5IV
138:	13.00	...	K0
139	11.52	...	B8
140	12.12	+1.79	G8V
141	11.89	+0.18	B9
142	11.67	+0.69	A0
143* R	7.22	...	B5
144*	9.10	...	G0II
145*	10.78	+0.51	A3-F0

Table 1

Observational Data for Region LF6 (Cont'd.)

Zone +58° (Cont'd.)

No.	m_{pg}	R.I.	Sp.	No.	m_{pg}	R.I.	Sp.
146* R	10.64	+0.49	A0	161	11.67	+0.48	B9
147	12.38	+0.20	B5:	162	12.28	...	K0:
148	12.21	...	K0III	163	12.12	...	A0
149	11.63	...	F8	164	11.95	...	F5
150	12.04	...	A0	165*	11.05	...	G5V
151	12.17	...	G0	166	11.91	...	A5
152	12.54	+0.10	B8	167	12.57	...	G0
153*	11.18	...	F5V	168	11.69	...	F8V
154* R	8.05	...	G21b	169R	12.13	...	B9
155	12.04	...	A0	170	11.87	...	A3
156	11.88	...	B8	171:	12.44	...	B8:
157	11.98	...	G0:				
158*	10.46	...	A2				
159:*	10.22	...	A0				
160* R	10.31	...	A2				

Zone +59°

No.	m_{pg}	R.I.	Sp.
1:R	12.10	...	A3
2	11.46	...	A0
3	12.38	...	B8
4:	11.78	...	A0
5	12.05	...	B8
6*	10.11	...	G0V
7:R	12.30	...	B2:
8	11.77	...	B9
9:R	11.70	...	F0p

Table 2

Remarks concerning the spectra in LF6

Zone +54°

No.	
8	Metallic line A star.
9	Class OB star; trace of faint lines other than H and He.
27	Hydrogen lines have sharp cores.
35	Metallic lines suspected.
42	Possibly a class OB star.
47	λ3863 prominent.
63	Class OB; H lines very sharp; He absent; K visible.
65	Class OB; spectrum similar to No. 63.
66	Class OB: BD +54° 731.

Stars having hydrogen lines sharper than usual for their class are: Nos. 1; 24.

Zone +55°

10	Possibly G0Ib; λ4174 very strong.
13	Hβ, Hγ, Hδ unusually sharp; UV hydrogen lines appear normal.
19	Trace of λ4077 and λ4128.
31	Class OB.
38	H and K as in class G0; red end of spectrum strong and trace of bands; hydrogen lines weak.
65	Close double; combined spectrum given. BD +55° 829.
80	Class OB; strong UV continuum. BD +54° 718.
82	Metallic line A star.
99	Class OB. BD +55° 837.
104	Class OB; Hβ in emission (?).
117	Possibly class OB; overlap makes class uncertain.
123	Many spurious lines as in very close double but duplicity not evident on our chart plates; possibly class OB. BD +55° 838.
124	Strong continuum but very weak lines; suspect λ4200 (HeII); Hβ in emission; class OB. BD +54° 728.
142	Strong line at λ4030; K line weak; hydrogen lines sharp.
145	Class OB. BD +55° 845.
150	Class OB (?); overlap makes class uncertain.
167	Class OB.

Stars having hydrogen lines sharper than usual are: Nos. 39; 53 = BD +55° 825; 111 = BD +54° 726; 114; 128; 134 = BD +55° 841; 139; 148.

Zone +56°

1	Class OB. BD +56° 824.
8	m_{pg} obtained from Harvard Mimeo III; m_V reduced to photographic. BD +56° 826.
10	Metallic lines present; K line weak for class F; G band trace.
74	Possibly metallic line A star.
99	Trace of many lines other than H and He; interstellar K?
112	Class OB; very weak hydrogen lines.
130	K weak for class A5 or F0; hydrogen lines have very sharp cores.
144	Peculiarity in UV due to close companion. BD +56° 862.
155	Class OB star; Classification uncertain due to overlap. BD +56° 866.
160	Class OB. BD +56° 868.
187	Class OB. BD +56° 873.
191	Metallic line A star.
203	Class OB; strong UV but no lines visible.
208	Class OB (?); hydrogen lines very sharp; no helium.
218	Metallic line A star.
235	Class OB; strong interstellar K. BD +56° 884.
236	Hydrogen lines sharp; metallic lines suspected.

The following stars have hydrogen lines sharper than usual for their class: Nos. 3 = BD +56° 825; 30 = BD +56° 830; 59 = BD +56° 836; 63 = BD +55° 822; 64; 69 = BD +56° 841; 76 = BD +56° 843; 78 = BD +56° 845; 119; 121; 211; 216; 220.

Table 2

Remarks concerning the spectra in LF6 (Cont'd.)

Zone +57°

No.

21 Class OB. BD +57° 739.
27 Trace of Balmer series in UV; Hβ present; no other lines.
86 Class OB; background of unresolved lines. BD +56° 850.
91 Metallic line A star; λ4077 and 4128 prominent.
119 Class OB.
140 Class OB; spurious lines due to overlapping spectra.
142 Metallic line A star; trace of G band.
144 Class OB; overlap makes class uncertain; small cluster here.
147 Class OB; overlap makes class uncertain; small cluster here.
152 Class OB; class uncertain due to overlap.
171 Hydrogen lines sharp; λ3860 and 4128 prominent. BD +57° 764.
198 Red end of spectrum very strong; trace of G band; supergiant (?).
239 Very close double; companion star has R.I. = +0.63. BD +57° 778.

Stars having hydrogen lines sharper than usual for their class are: Nos. 3 = BD +57° 734; 4 = BD +57° 735; 18; 32; 54 = BD +57° 745; 70; 83 = BD +56° 849; 100; 124; 143; 151; 196; 219; 233.

Zone +58°

1 Metallic line A star; λ4174 conspicuous.
3 G-band unusually broad; K weak for class F; many metallic lines.
12 Trace of metallic lines.
14 Spurious lines may be due to overlapping spectrum.
16 Hydrogen lines very broad.
25 λ4174 strong; G-band suspected; strong line at λ4060; possibly A2-F0 but hydrogen too strong for class F.
26 Hydrogen lines very broad; conspicuous group at λ4040; λ4226 is conspicuous.
29 λ4226 conspicuous; K line weak for class F; hydrogen lines very broad.
36 Trace of metallic lines.
49 Cluster of stars near No. 49.
50 Metallic line A star; λ4045 conspicuous.
68 Class OB. BD +58° 658.
98 RW Cam. Cepheid with period 16.41 days; amplitude 1.41 mag. BD +58° 663.
105 Trace of λ4077 and other metallic lines. BD +58° 667.
154 RX Cam. Cepheid with period 7.91 days; amplitude 1.66 mag. BD +58° 694.
160 Metallic line A star. BD +57° 773.
169 Metallic line A star.

Stars having hydrogen lines sharper than usual for their class are: Nos. 60 = BD +58° 654; 143 = BD +58° 685; 146 = BD +57° 767.

Zone +59°

1 λ4174 strong; metallic line A star.
7 Suspect trace of emission at λ4600; class OB.
9 H and K weak; λ4077 and 4128 prominent; hydrogen lines very sharp.

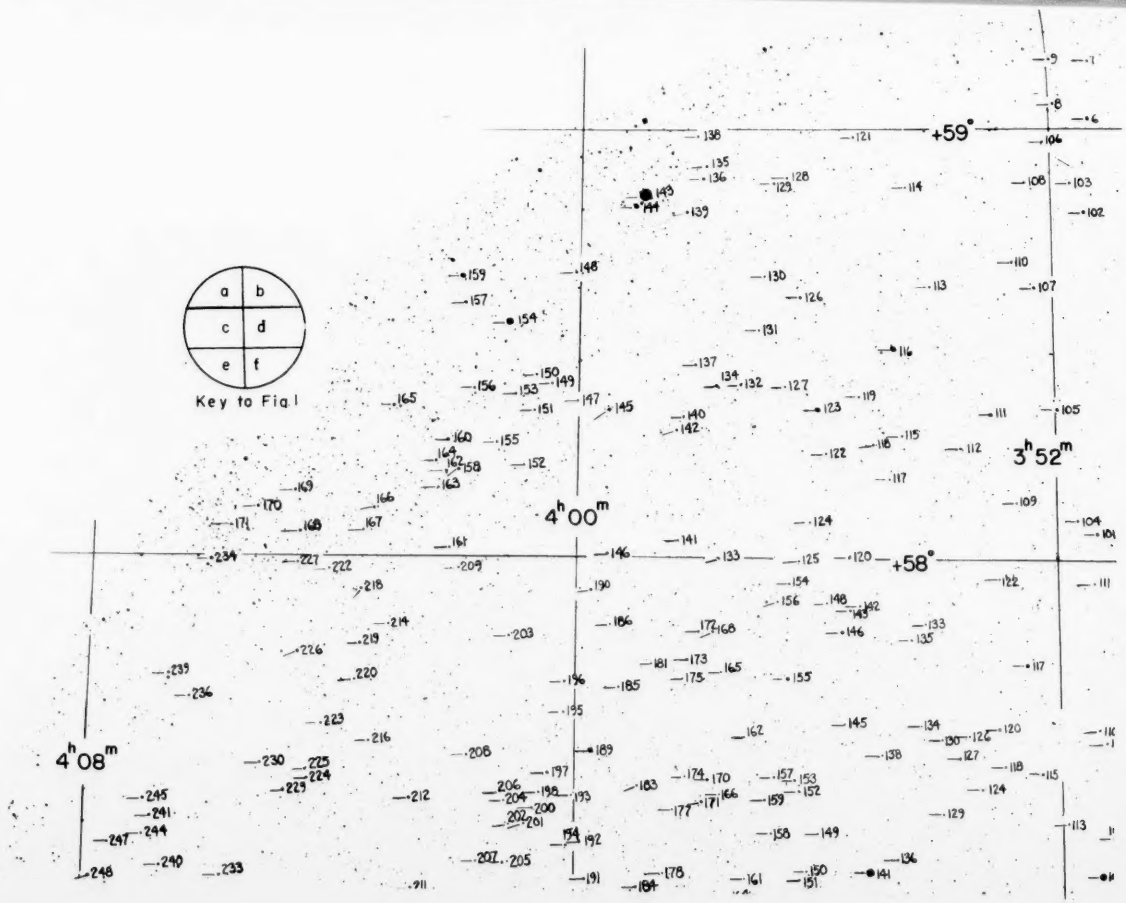

FIG. 1*a*.—Identification chart for LF6

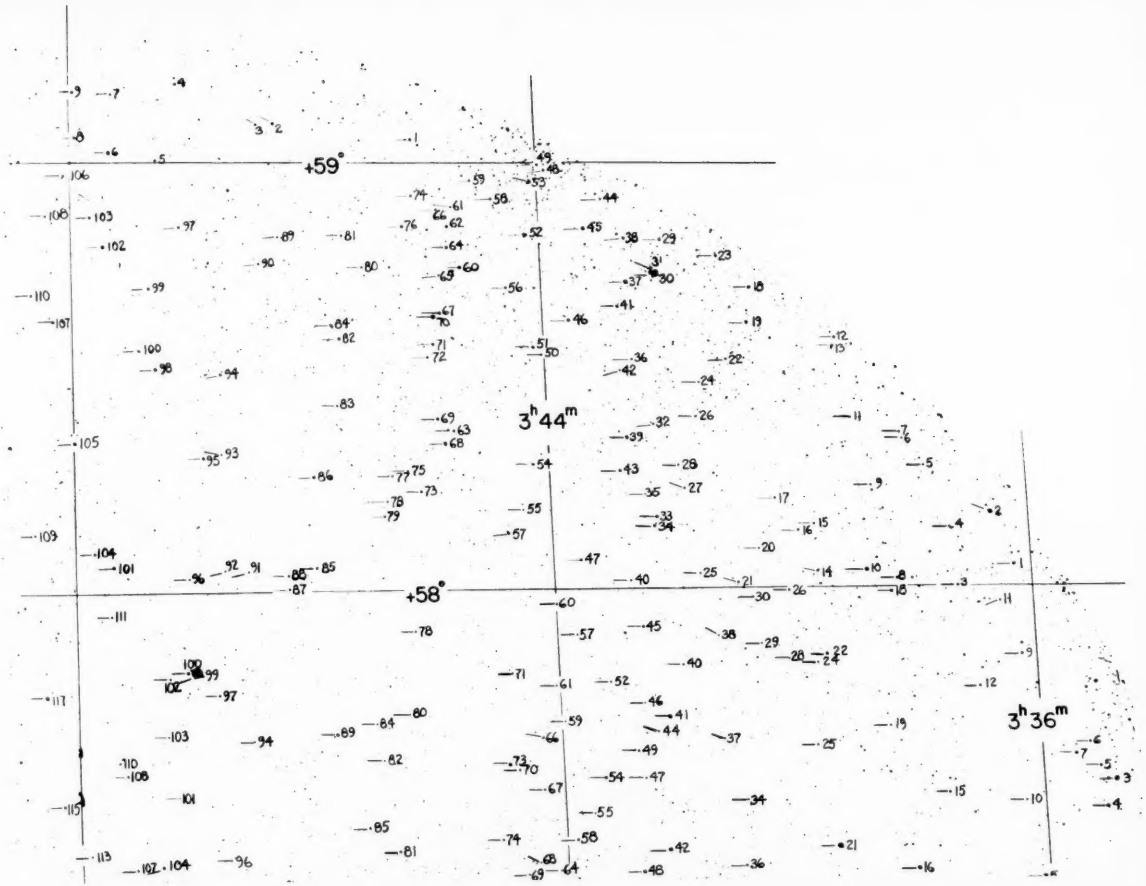

FIG. 1*b*.—Identification chart for LF6

FIG. 1*b*.—Identification chart for LF6

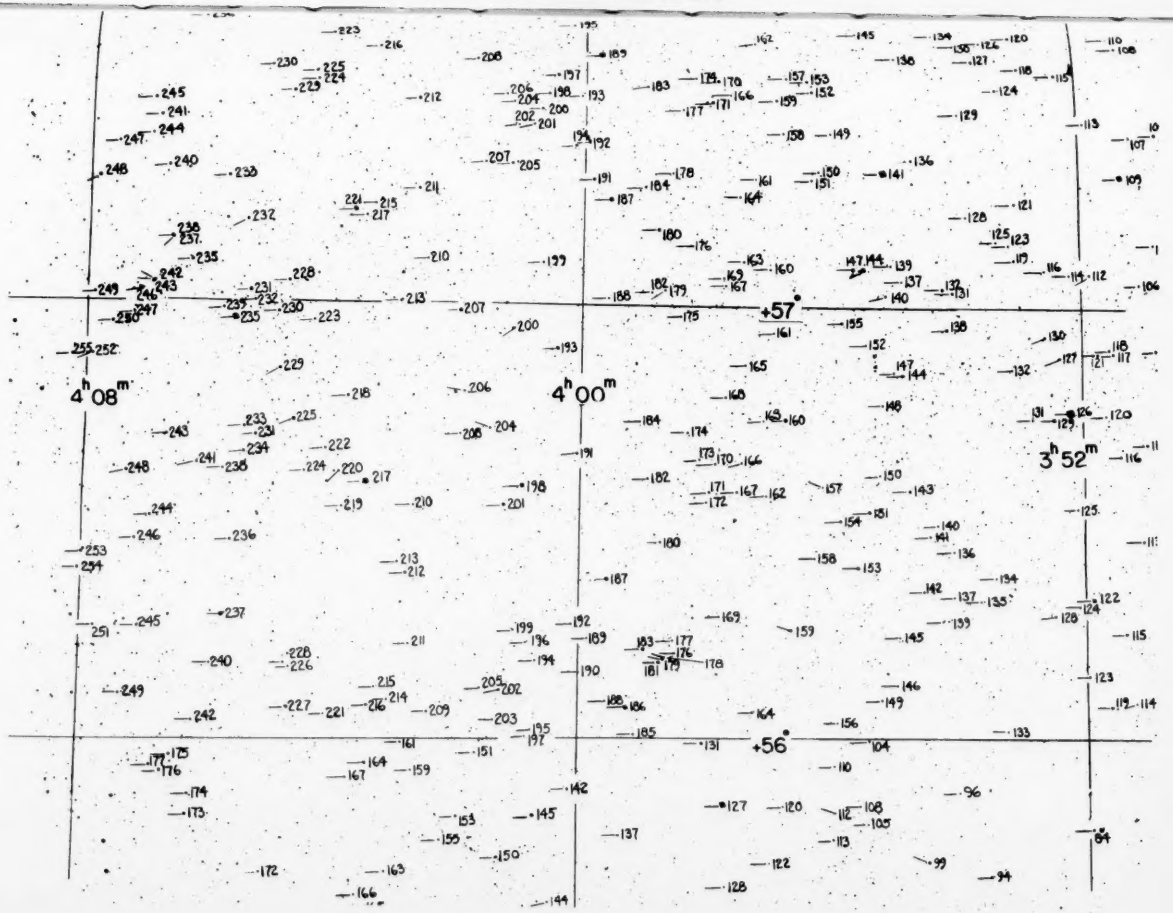

FIG. 1*c*.—Identification chart for LF6

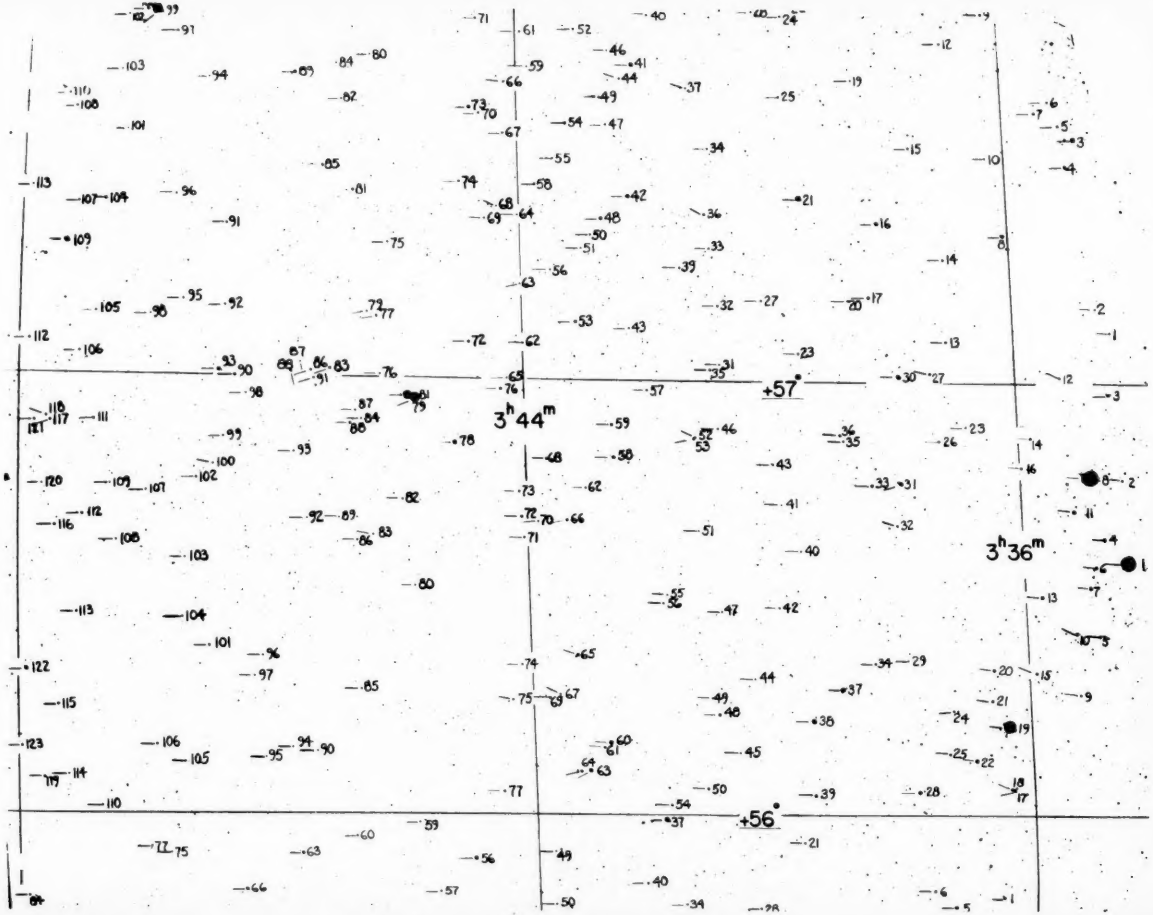

FIG. 1d.—Identification chart for LF6

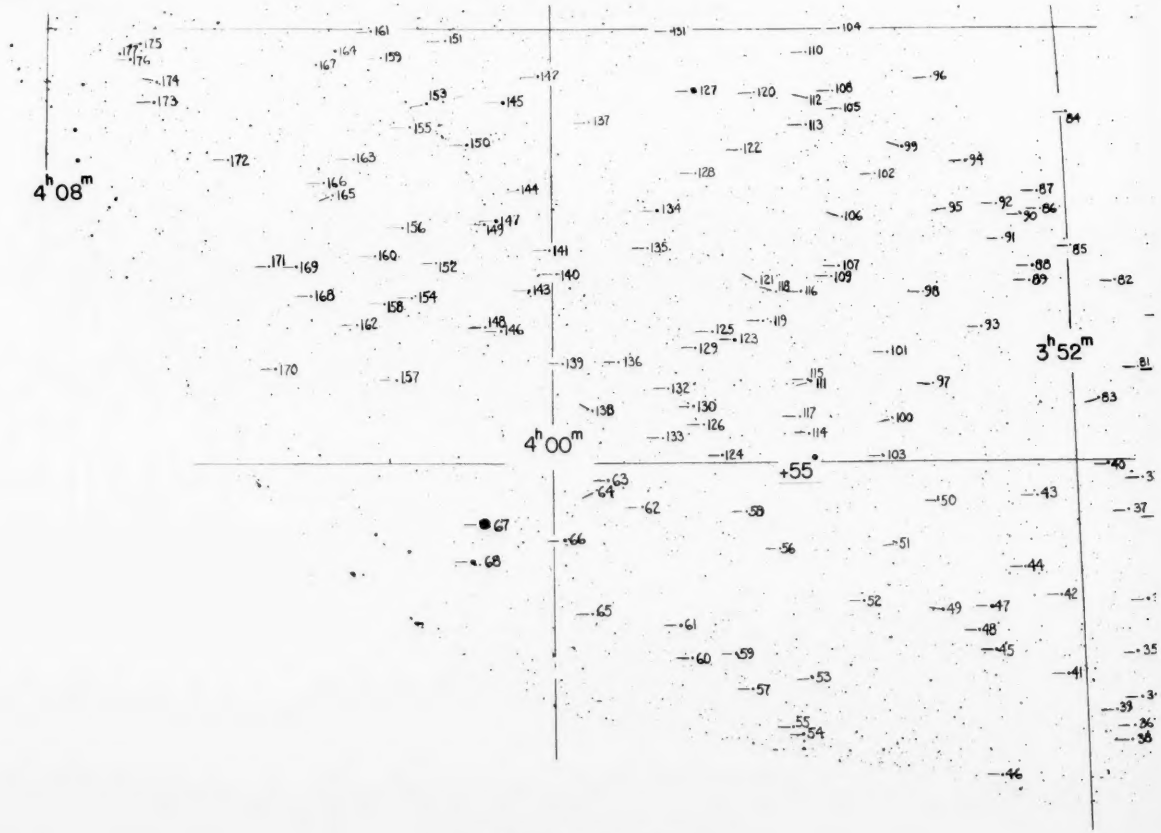

FIG. 1e.—Identification chart for LF6

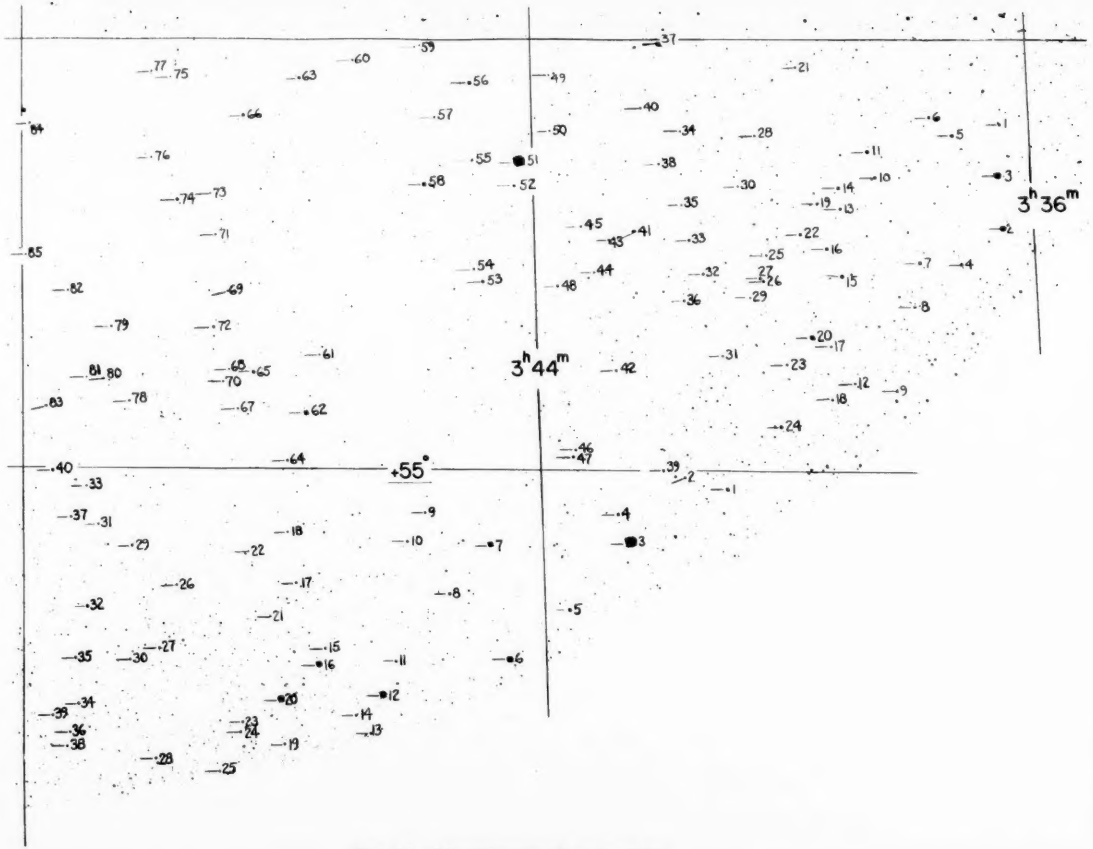

FIG. 1*f*.—Identification chart for LF6

CATALOGUES OF Hα-EMISSION STARS AND NEBULAE IN THE MAGELLANIC CLOUDS*

KARL G. HENIZE†
University of Michigan Observatory
Received May 5, 1956

ABSTRACT

Catalogues of 236 emission-line stars and 532 emission nebulae discovered on objective-prism photographs of the Magellanic Clouds are presented in four tables. A fifth table lists exciting stars involved in the Large Cloud nebulae. Finding charts are provided for both Clouds.

I. INTRODUCTION

Hα objective-prism photographs, taken with the Mount Wilson 10-inch camera at the Lamont-Hussey Observatory of the University of Michigan, reveal numerous emission-line stars and nebulae in the Magellanic Clouds. The results of a survey of the first plates taken were reported and discussed in 1950 by Henize and Miller (1951). Although these original data have been slightly revised and extended by subsequent examination of plates of unwidened spectra, the conclusions reached in 1950 remain essentially unchanged. Additional investigations of the Magellanic Clouds have been undertaken, notably the study of the surface brightnesses (Doherty, Aller, and Henize 1956) and electron densities (Aller 1956) of the Large Cloud nebulae. The primary purpose of the present paper is to set forth the discovery data on which these discussions have been based and to provide observers with catalogues and charts of the emission-line objects.

II. THE OBSERVATIONS

The instrument used in this investigation, the red-corrected Mount Wilson 10-inch camera equipped with a 15° objective prism, has a plate scale of 159″/mm and gives a dispersion of 450 A/mm at Hα. All exposures were taken on Kodak 103*a*-E emulsion with a red Plexiglass filter. Photometric calibration of the plates was made with a tube sensitometer. The limiting photored magnitude for continuous spectra is approximately 13.5, which, with the revised distance modulus of 19.0 for the Magellanic Clouds (Shapley and Nail 1954), corresponds to an absolute magnitude of −5.5. The survey covers an area 15° square centered on each Cloud. Two plates of widened spectra (width = 0.2 mm) and one plate of unwidened spectra on each region have been thoroughly searched and intercompared.

The material has been divided into five tables:

Table 1, "The Catalogue of Emission-Line Stars in the Large Cloud"
Table 2, "The Catalogue of Emission Nebulae in the Large Cloud"
Table 3, "The Catalogue of Exciting Stars Involved in the Large Cloud Nebulae"
Table 4, "The Catalogue of Emission-Line Stars in the Small Cloud"
Table 5, "The Catalogue of Emission Nebulae in the Small Cloud"

In the Small Cloud the objects are generally listed in the order of the *X*-co-ordinate defined by Miss Leavitt (1908). The Large Cloud has been divided into three zones of declination, and, with a few exceptions, the objects are listed consecutively in each zone according to the *X*-co-ordinate, beginning with the northernmost zone.

Positions are given in both the Harvard rectangular co-ordinate system (Leavitt

* Published by a grant from the Horace H. Rackham Fund of the University of Michigan.

† Currently Carnegie Postdoctoral Fellow at the Mount Wilson Observatory.

FIG. 1.—Identification chart for LF6

1908) and the equatorial system. Because of the high declination of the Magellanic Clouds, the Harvard rectangular system is more convenient for work with wide-angle photographs, and, as a consequence, most of the Harvard data are published on this system. In a finding list, however, it is also necessary to give equatorial co-ordinates to facilitate the setting of telescopes. The Harvard co-ordinates were transformed to equatorial co-ordinates by standard procedures, the plate constants being based on data given by Miss Leavitt (1908, Tables I and II). Within the main bodies of the Clouds the probable error introduced by the transformation amounts to about $\pm 10''$. The probable errors of the rectangular co-ordinates given in the present catalogues are about $\pm 10''$ in the Small Cloud and $\pm 20''$ in the Large Cloud.

Inasmuch as this survey is closely linked with the Michigan–Mount Wilson survey of the Milky Way for Be stars, a system of nomenclature similar to that used for the galactic Be stars has been adopted for the Magellanic Clouds. In this system the serial number of the object is preceded by the number of the plate on which it appears. In the Magellanic Clouds it is necessary to distinguish stars from nebulae by adding an "S" or "N" to the designation. Consequently, emission star 15 in the Large Cloud will be referred to as LHα 120-S 15, while nebula 80 in the Small Cloud will be designated LHα 115-N 80. The same plate numbers—LHα 120 and LHα 115—will be used throughout this work for the Large and Small Clouds, respectively.

III. THE CATALOGUES OF EMISSION-LINE STARS

One hundred and seventy-one emission-line stars in the Large Cloud and 65 in the Small Cloud are listed and described. It should be noted that the data discussed in 1950 have been revised by the reclassification of the point sources of Hα emission that show no underlying continuous spectrum. Whereas they were originally included among the emission-line stars, they will now be found in the list of nebulae. As a result, the present lists of emission-line stars contain only those objects that show a continuous spectrum underlying the Hα emission.

The sixth and seventh columns of Tables 1 and 4 give the intensities of the continuous spectrum and of the Hα emission, respectively. The intensity of the continuous spectrum is estimated on a scale from 1 to 5, in which 5 represents an overexposed spectrum and 3 a spectrum of optimum exposure. The additional symbol "*T*" denotes a trace of continuum too faint to be classed as intensity 1. The intensity of the Hα emission, on a similar scale, is relative to the background continuum.

The eighth column gives an estimate of the diffuseness of the Hα emission. Here 0 denotes a very sharp line; 1, a line neither very sharp nor appreciably widened; 2, a line of appreciable diffuseness; and 3, a line which is very diffuse. In most cases diffuseness indicates actual broadening of the emission line and implies that the star may be a Wolf-Rayet star. In a few spectra, however, the diffuseness may be due to fuzziness of the star image and possibly indicates that the emission star is multiple or that the emission arises from a barely resolved nebulosity which surrounds the star.

The ninth column gives the photographic magnitude. For stars whose spectral type is given in the tenth column, this magnitude is taken from the *Henry Draper Catalogue* or from *Harvard Bulletin*, No. 801 (Cannon 1924); otherwise it is estimated from the intensity of the red continuum on a system calibrated by the available *Henry Draper* magnitudes of the B stars. The adopted magnitudes equivalent to each intensity estimate are:

Intensity 4 = 10.5	Intensity 1 = 12
Intensity 3 = 11	*T* = 12.8
Intensity 2 = 11.5	

These may be considered as photographic magnitudes only in so far as they are applied to B stars of normal color. The data used for calibration indicate a maximum error of about ±0.6 mag., but, in application, even greater errors are to be expected.

References to the *Henry Draper Catalogue* and to the Mount Wilson catalogue of Be stars are given in the notes at the end of the tables. One star from the Harvard lists, the variable P Cygni star HD 269582 = MWC 112, shows no emission on LHα plates. Since the existence of emission in the spectrum of star 83 of the Large Cloud is extremely doubtful, this number has been omitted from Table 1.

IV. CATALOGUES OF EMISSION NEBULAE

The catalogues of emission nebulae include a total of 415 nebulae in the Large Cloud and 117 in the Small Cloud. Many of these objects are bright knots that lie in fainter patches of nebulosity. In view of the impossibility of making a significant distinction between isolated nebulae and knots imbedded in a faint nebulous background, all bright knots, whether or not they are associated with larger fields of nebulosity, are described as separate objects. An attempt has been made to indicate the close relationship between a group of knots involved in a nebulous background by assigning the knots the same number as the background nebulosity and designating the individual knots by letters of the alphabet assigned in the order of the brightnesses of the knots. In some instances groups of knots which seem to be physically related, even though no connecting background nebulosity is visible, have been assigned a group number.

In the present catalogue the appearance of the nebulae has been described in terms of four characteristics: intensity of the Hα image, irregularity of shape, elongation, and amount of internal structure. This system is closely related to that employed by Sharpless (1953) to describe the galactic diffuse nebulae. Although the Bok-Wade system of classification (Nail, Whitney, and Wade 1953) offers certain advantages in statistical discussions of nebular types, it is felt that for the purpose of identification it does not describe the individual nebulae with the precision of the Sharpless system.

The sixth and seventh columns of Tables 2 and 5 give the east-west and north-south diameters of the nebulae in that order. The measures are made on the Harvard rectangular co-ordinate system, and it must be remembered that the orientation of the measure will not be true north-south for objects near the east or west edge of the field. Those nebulae for which no diameters are given appear as point sources on LHα plates.

The eighth column gives the intensity of the continuum on a scale similar to that used for the emission stars. Positive data are given only if the continuum appears closely related to the nebulosity; that is, continua from isolated stars within a nebulosity are not considered. In general, the presence of a continuum probably indicates the existence of a cluster or group of stars whose extent is about equal to that of the nebulosity. Notes concerning the occurrence of emission lines other than Hα will be found at the end of Table 2.

The Hα intensity (ninth col. of Tables 2 and 5), which corresponds to the surface brightness for the extended nebulae, is estimated on a scale from 1 to 5, where 5 represents a strongly overexposed image, and the additional symbol "*T*" denotes a perceptible but extremely faint nebula. For those nebulae designated by an asterisk in the first column, photometric measures of the surface brightnesses of extended nebulae and of the integrated brightnesses of the compact nebulae are available in "A Photometric Catalogue of Emission Nebulae in the Large Magellanic Cloud" (Doherty *et al.* 1956). The photometric catalogue gives data for selected regions in all nebulae for which significant measures could be made.

Irregularity of outline (tenth col. of Tables 2 and 5) is estimated on a scale from 0 to 3, where 0 indicates a smooth boundary. A 4 or 5 listed in this column designates crescent-shaped nebulae or ring-shaped nebulae, respectively. Elongation (eleventh col.) is estimated on a scale from 0 to 3, with 0 denoting no elongation, and 3 a ratio of axes of at

least 3 to 1. Structure (twelfth col.) is given on a scale from 0 to 3, 0 indicating a smooth nebula with no visible structure.

In Table 2, thirteenth column, the number of early-type stars involved in each nebula of the Large Cloud is given. These stars are listed in Table 3 and include O and B stars from the *Henry Draper Catalogue* as well as the emission stars of Table 1. References to early-type *Henry Draper* stars found in the Small Cloud nebulae are given in the notes.

The present catalogue of Small Cloud nebulae has been compared with the catalogue of 152 emission nebulosities in the Small Cloud published by Nail *et al.* (1953). This comparison leads to the surprising result that the two catalogues share only 33 objects in common. Evidently this discrepancy must be attributed to differences in observing techniques, the Michigan observations having been made on objective-prism spectrum plates and the Harvard observations by a comparison of red and blue direct plates.

References to the Nail, Whitney, and Wade catalogue, to the *NGC*, and to early Harvard lists of emission nebulae are given in the notes at the end of the tables. Of the early Harvard discoveries, one—HB 891-26 = HD 269848—is not visible on our plates.

V. CHARTS

Identification charts for the Magellanic Cloud emission stars and nebulae are reproduced in Figures 1–13. These are copied from 5-hour direct-exposure plates taken with the Mount Wilson 10-inch camera on 103*a*-E emulsion through a red Plexiglass filter. The dates of these exposures were: Large Cloud, January 4, 1951; Small Cloud, November 22, 1949. The scale of all charts is 52″ per millimeter.

The approximate extent of faint nebulae is indicated on the charts by boundary lines, but these lines are not intended to define the limits of the nebulae or their shapes with great accuracy.

Small intense nebulae and point sources of Hα emission are indicated by a single line pointing to or touching the object. In order to distinguish the stars from the nebulae, the stars are marked with a caret ($\wedge$) and their numbers are preceded by an "S."

In crowded regions and in dense nebulosity it was not always possible to point out the fainter objects on the chart with complete certainty. However, reference to the rectangular co-ordinates and to the notes at the ends of the tables will help to resolve these uncertainties in most cases.

The positions of two novae which were discovered on LHα plates—N Mensae 1951 and N Tucanae 1951—are marked on the charts.

VI. DISCUSSION

In order to examine the differences between the nebulae of the Large and Small Clouds, it is useful to refer to the Bok-Wade classification of nebulae. The relation between this classification and the present descriptions has been determined by examination of those Small Cloud nebulae in the present catalogue that are also listed by Nail *et al.* The following close correlation is found between the two classifications: Type V of the Bok-Wade system is equivalent to objects in the present list that are stellar or that have diameters of less than 20 seconds of arc. Type IV is made up of the rings and crescents; type III contains only the nebulae with no irregularity, no elongation, and no structure; type II is made up of those objects with intensities of *T*, 1, 2, or 3, that show appreciable irregularity or elongation; and type I consists of irregular nebulae with intensities of 4 and 5.

The distribution of the Magellanic Cloud nebulae among the equivalent Bok-Wade types is given in Table 6. For the Small Cloud the results from the Nail-Whitney-Wade catalogue, as well as those from the present catalogue, are tabulated. Notwithstanding the afore-mentioned differences between these catalogues, the frequency distributions of the nebular types are in satisfactory agreement.

When the Large and Small Clouds are compared, one striking difference, previously

noted by Nail *et al.* (1953), is evident: whereas type I nebulae are abundant in the Large Cloud, they are almost entirely lacking in the Small Cloud. This is in contrast to the fact that the frequency of nebulae per unit area, irrespective of their types, is at least as great in the Small Cloud as in the Large. Thus it appears that nebulosity is as abundant in the Small Cloud as in the Large but that the surface brightnesses of the Small Cloud nebulae are not so great as those of nebulae of the Large Cloud. This phenomenon suggests that the interstellar medium of the Small Cloud does not attain such dense concencentrations as does the interstellar medium of the Large Cloud.

The relation of the emission stars and nebulae to the detailed structure of the Large Cloud was discussed by Henize and Miller (1951); the revised data do not change the conclusions reached in that paper. It should be pointed out that the outlying stars and nebulae show little correlation with the extended faint structure discovered by de Vaucouleurs (1954) in the outer regions of the Large Cloud.

TABLE 6

DISTRIBUTION OF MAGELLANIC CLOUD NEBULAE AMONG THE BOK-WADE NEBULAR TYPES

LHα DESCRIPTION	EQUIVALENT BOK-WADE TYPE	LARGE CLOUD		SMALL CLOUD			
		LHα		LHα		Harvard	
		No.	Per Cent	No.	Per Cent	No.	Per Cent
Stellar or diam. <20″	V	108	26	45	38	62	41
Rings and crescents	IV	20	5	3	3	3	2
Round, regular, and no structure	III	45	11	12	10	7	5
Irreg. with int. <4	II	165	40	57	49	79	51
Irreg. with int. =4 or 5	I	77	18	0	0	1	1
Total	.....	415	.....	117	.....	152	.....

The Large Cloud emission stars classed as type B or P Cygni in the *Henry Draper Catalogue* were also discussed by Henize and Miller (1951). It should be noted that revision of the distance modulus of the Magellanic Clouds to 19.0 increases the absolute magnitudes listed in Table 2 of that paper by 1.7 mag. Thus it is evident that the brightest emission B stars observed in the Large Magellanic Cloud are more luminous than the brightest stars so far observed among the galactic cB stars. The *Henry Draper Catalogue* assigns photographic magnitudes brighter than 10.0 (= −9.0 absolute magnitude) to four of the emission-line stars: LHα 120-S 86, -S 96, -S 155, and -S 171. One of these, LHα 120-S 96, is the variable star, S Doradus, which has strong hydrogen emission and an otherwise peculiar spectrum (Smith 1954). The remaining three stars are assigned to spectral class B and show moderate or weak emission. Their mean absolute magnitude is −9.4. Aside from their excessive luminosity, there is no reason at present not to class them as cBe stars. However, if these stars were found to vary in brightness, it might be possible to class them among the group of high-luminosity variables found by Hubble and Sandage (1953) in M31 and M33.

I wish to acknowledge my gratitude to Dr. Freeman D. Miller, who initiated this investigation of the Magellanic Clouds and has given me much advice and encouragement. The loan of the 10½-inch telescope by Dr. I. S. Bowen, director of the Mount Wilson and Palomar Observatories, and the generous financial support of the Horace H. Rack-

ham Fund of the University of Michigan made possible the observational program described here. I also wish to thank the National Science Foundation and the Carnegie Institution of Washington, whose fellowship grants have enabled me to complete the work.

REFERENCES

Aller, L. H. 1956, *Gaseous Nebulae* (New York: John W. Wiley & Son).
Cannon, A. J. 1924, *Harvard Bull.*, No. 801, p. 1.
———. 1933, *ibid.*, No. 891, p. 2.
Doherty, L., Aller, L. H., and Henize, K. G. 1956, *Ap. J. Suppl.*, No. 22.
Henize, K. G., and Miller, F. D. 1951, *Pub. Obs. U. Michigan*, **10**, 75.
Hubble, E., and Sandage, A. 1953, *Ap. J.*, **118**, 353.
Leavitt, H. S. 1908, *Harvard Ann.*, **60**, 87.
Nail, V. M., Whitney, C. A., and Wade, C. M. 1953, *Proc. Nat. Acad Sci.*, **39**, 1168.
Shapley, H., and Nail, V. M. 1954, *Proc. Nat. Acad. Sci.*, **40**, 1.
Sharpless, S. 1953, *Ap. J.*, **118**, 362.
Smith, H. J. 1954, *A.J.*, **59**, 332.
Vaucouleurs, G. de. 1954, *Observatory*, **74**, 158.

Table 1

EMISSION-LINE STARS IN THE LARGE MAGELLANIC CLOUD

Nr. LHα 120-	1950 R.A.	Dec.	Rect. Coords. X	Y	Int. C	Hα	Dif.	m	Sp.
			"	"					
S 1	$4^h48^m.1$	-67°30'	- 830	14720	T	2	0	12.8	
S 2	4 54.4	66 32	830	18540	T	2	0	12.8	
S 3	4 54.4	67 09	1140	16280	1	2	0	12.0	
S 4	4 55.3	66 36	1180	18350	T	3	0	12.8	
S 5	4 53.1	68 08	1200	12740	T	2	0	12.8	
S 6	4 53.2	68 08	1220	12700	T	2	1	12.8	
S 7	4 55.2	67 14	1460	16030	4	1	0	10.1	Pec.
S 8	4 55.6	67 34	1780	14850	T	2	3	12.9	Oa
S 9	4 57.6	66 37	2040	18380	1	3	0	12.0	
S 10	4 58.9	65 46	2130	21500	T	4	1	12.8	
S 11	4 57.4	67 25	2320	15460	T	2	1	12.8	
S 12	4 57.6	67 52	2600	13850	1	4	0	12.0	
S 13	5 00.2	67 12	3180	16380	1	2	0	12.0	
S 14	5 03.2	66 44	4070	18160	1	3	1	11.5	Oc
S 15	5 04.8	66 41	4640	18380	1	2	0	12.0	
S 16	5 06.1	65 43	4770	21970	T	1	0	12.8	
S 17	5 04.3	67 19	4680	16090	4	3	0	10.6	B
S 18	5 06.0	68 15	5560	12760	2	3	0	11.5	
S 19	5 08.0	66 55	5850	17650	T	2	0	12.8	
S 20	5 11.5	68 11	7380	13160	T	2	1	12.8	
S 21	5 13.2	67 17	7760	16470	1	2	0	12.0	
S 22	5 14.0	67 30	8080	15680	2	5	3	11.4	Pec.
S 23	5 16.0	66 21	8590	19880	1	1	1	12.0	
S 24	5 17.8	66 44	9290	18510	1	2	2	12.0	
S 25	5 20.2	65 12	9980	24140	1	2	2	12.0	
S 26	5 19.1	68 00	9920	13990	3	2	0	11.0	
S 27	5 19.3	68 08	10020	13450	1	1	1	12.0	
S 28	5 21.9	65 50	10680	21820	1	2	2	12.0	
S 29	5 22.2	65 45	10780	22130	T	1	1	12.8	
S 30	5 23.2	68 04	11320	13740	2	4	1	11.6	O
S 31	5 24.4	65 51	11610	21820	1	2	2	12.0	
S 32	5 24.8	67 28	11830	15930	1	2	2	12.0	
S 33	5 25.1	67 28	11920	15960	T	3	0	12.8	
S 34	5 26.9	67 31	12560	15770	2	2	1	11.7	B
S 35	5 27.3	66 23	12690	19880	2	4	1	11.5	
S 36	5 28.2	67 03	13010	17430	T	2	2	12.8	
S 37	5 28.1	67 33	12980	15610	T	2	1	12.8	
S 38	5 29.3	66 57	13390	17810	T	2	1	12.8	
S 39	5 29.5	66 58	13480	17780	T	1	1	12.8	
S 40	5 30.1	67 24	13670	16190	T	1	1	12.8	
S 41	5 30.4	67 28	13770	15930	T	1	2	12.8	
S 42	5 30.5	67 25	13830	16090	T	1	1	12.8	
S 43	5 30.6	67 19	13860	16500	2	2	1	11.5	
S 44	5 32.2	67 44	14370	14980	T	5	1	12.8	
S 45	5 32.3	66 25	14500	19720	3	3	0	11.6	B
S 46	5 32.4	67 01	14500	17550	2	4	0	11.5	

Table 1 (Cont'd)

Nr. LHα 120-	1950 R.A.	Dec.	Rect. Coords. X	Y	Int. C	Hα	Dif.	m	Sp.
			"	"					
S 47	$5^h32^m.5$	-67°43'	14500	15040	2	3	1	11.5	
S 48	5 33.3	67 39	14760	15260	1	2	0	12.0	
S 49	5 33.2	67 20	14760	16410	T	2	0	12.8	
S 50	5 34.1	66 57	15110	17810	1	1	1	12.0	
S 51	5 34.4	66 27	15260	19620	1	1	1	12.0	
S 52	5 35.1	66 56	15460	17810	2	1	1	11.5	
S 53	5 35.0	66 29	15490	19490	1	1	1	12.0	
S 54	5 36.3	67 08	15870	17110	1	2	0	12.0	
S 55	5 36.3	67 22	15840	16250	T	1	1	12.8	
S 56	5 41.2	67 21	17550	16220	1	2	0	12.0	
S 57	5 42.0	67 37	17780	15230	T	1	0	12.8	
S 58	5 42.7	67 20	18090	16280	T	1	1	12.8	
S 59	5 45.7	68 11	18890	13100	T	4	0	12.8	
S 60	5 46.2	67 35	19210	15260	T	2	1	12.8	
S 61	5 46.0	67 14	19240	16570	2	4	2	11.5	
S 62	5 46.8	67 33	19460	15420	T	1	1	12.8	
S 63	5 48.8	67 36	20130	15170	T	4	0	12.8	
S 64	5 50.6	67 39	20730	14880	T	2	1	12.8	
S 65	4 47.3	68 22	- 600	11610	1	2	1	12.0	
S 66	4 48.0	69 26	250	7820	1	2	0	12.0	
S 67	4 54.8	69 14	2290	8840	1	1	0	12.0	
S 68	4 52.6	68 26	1180	11580	T	2	1	12.8	
S 69	4 52.3	69 31	1650	7730	3	3	0	10.6	B
S 70	4 53.7	69 22	2000	8330	2	2	0	11.5	
S 71	4 54.4	69 10	2130	9060	1	4	0	12.0	
S 72	4 55.8	69 26	2700	8170	T	1	1	12.8	
S 73	4 57.2	69 55	3370	6460	4	4	0	10.4	B
S 74	4 58.9	68 56	3470	10110	1	3	1	11.6	B
S 75	5 00.3	68 31	3780	11610	2	2	1	11.5	
S 76	4 59.8	69 41	4100	7410	1	1	1	12.0	
S 77	5 02.7	68 41	4610	11100	1	3	0	12.0	
S 78	5 04.8	68 49	5370	10680	2	3	0	11.5	
S 79	5 05.1	69 03	5530	9890	1	2	1	12.0	
S 80	5 06.7	68 35	5920	11610	2	3	0	11.5	
S 81	5 07.2	68 26	6010	12150	1	3	0	12.0	
S 82	5 07.0	68 37	6010	11480	T	1	1	12.8	
S 84	5 06.3	70 02	6230	6360	T	2	0	12.8	
S 85	5 10.9	68 25	7250	12310	T	1	0	12.8	
S 86	5 10.6	68 50	7250	10780	4	2	1	9.8	B
S 87	5 10.7	68 46	7280	11040	T	1	1	12.8	
S 88	5 13.9	69 36	8490	8110	4	1	2	11.0	B
S 89	5 14.0	69 25	8480	8740	1	5	1	11.6	Pec.
S 90	5 14.0	69 24	8490	8810	3	1	2	11.4	B
S 91	5 14.3	69 35	8620	8140	3	2	1	11.6	Pec.
S 92	5 15.2	69 19	8840	9160	T	3	1	12.8	
S 93	5 16.7	68 25	9190	12400	1	2	0	12.0	

Table 1 (Cont'd)

Nr. LHα 120-	1950 R.A.	Dec.	Rect. Coords. X	Y	Int. C	Hα	Dif.	m	Sp.
			"	"					
S 94	$5^h16^m.5$	-69°44'	9320	7630	T	1	2	12.8	
S 95	5 18.2	69 54	9890	7060	4	2	0	10.8	B
S 96	5 18.7	69 19	9950	9220	5	4	1	9.5	Pec.
S 97	5 18.6	69 40	9980	7950	T	2	1	12.8	
S 98	5 18.7	69 40	10020	7950	T	1	0	12.8	
S 99	5 19.3	69 34	10180	8300	T	1	1	12.8	
S 100	5 20.6	69 14	10560	9510	1	2	3	12.0	
S 101	5 22.3	68 55	11100	10650	1	3	1	12.0	
S 102	5 22.3	69 36	11130	8200	T	1	2	12.8	
S 103	5 24.2	69 32	11730	8430	T	1	2	12.8	
S 104	5 24.6	69 41	11860	7930	T	2	1	12.8	
S 105	5 27.2	68 53	12690	10840	4	2	1	11.5	B
S 106	5 27.5	69 03	12780	10210	T	1	2	12.8	
S 107	5 27.8	69 16	12880	9410	T	2	1	12.8	
S 108	5 28.1	69 12	12970	9640	T	2	2	12.8	
S 109	5 28.2	69 14	13010	9570	1	3	0	12.0	
S 110	5 28.6	68 56	13130	10650	T	1	1	12.8	
S 111	5 28.7	69 11	13160	9700	1	5	1	12.2	Pec.
S 112	5 30.3	69 10	13670	9790	1	2	1	12.0	
S 113	5 30.7	69 02	13830	10240	T	1	2	12.8	
S 114	5 30.7	69 22	13800	9060	4	1	1	11.2	B
S 115	5 31.0	69 14	13900	9540	1	2	2	12.0	
S 116	5 31.2	69 05	13960	10050	4	1	1	10.8	B:
S 117	5 31.2	69 33	13960	8360	4	1	1	10.6	B
S 118	5 31.7	68 43	14150	11380	2	3	1	11.5	
S 119	5 31.8	69 08	14150	9920	2	3	2	11.4	B
S 120	5 31.8	69 08	14160	9920	T	1	3	12.8	
S 121	5 32.2	68 28	14340	12280	T	4	1	12.8	
S 122	5 34.1	68 41	14950	11510	T	1	1	12.8	
S 123	5 34.5	68 34	15100	11920	T	1	1	12.8	
S 124	5 35.7	69 42	15360	7820	4	4	1	10.5	Pec.
S 125	5 36.2	69 01	15610	10300	T	2	1	12.8	
S 126	5 36.4	68 58	15680	10430	1	1	1	12.0	
S 127	5 36.8	69 25	15740	8840	3	5	2	11.3	Pec.
S 128	5 37.2	69 31	15840	8460	2	4	3	11.1	Pec.
S 129	5 37.8	69 21	16060	9060	2	2	2	11.5	
S 130	5 38.2	68 56	16250	10560	3	1	1	11.3	B
S 131	5 38.7	69 31	16340	8460	1	3	0	12.0	
S 132	5 39.5	70 09	16470	6170	T	1	1	12.8	
S 133	5 39.3	69 03	16600	10110	3	3	2	10.6	Oa
S 134	5 40.6	69 24	16950	8840	2	5	2	12.0	Pec.
S 135	5 41.1	69 58	17010	6740	T	1	1	12.8	
S 136	5 41.9	69 26	17360	8710	2	1	1	11.5	
S 137	5 42.2	69 38	17400	7950	T	3	1	12.8	
S 138	5 41.8	68 42	17490	11350	T	1	0	12.8	
S 139	5 42.2	68 55	17550	10530	1	1	1	12.0	
S 140	5 42.7	68 19	17870	12690	T	2	1	12.8	

Table 1 (Cont'd)

Nr. LHα 120-	1950 R.A.	Dec.	Rect. Coords. X	Y	Int. C	Hα	Dif.	m	Sp.
			"	"					
S 141	$5^h44.^m5$	-69°15'	18220	9320	T	1	0	12.8	
S 142	5 44.8	69 20	18320	8970	1	3	0	12.0	
S 143	5 45.6	69 00	18640	10180	4	1	1	10.6	Bo:
S 144	5 48.9	70 08	19370	5980	T	2	3	12.8	
S 145	6 13.1	68 10	28070	11990	1	2	2	12.0	
S 146	4 43.4	70 38	- 380	3230	T	3	1	12.8	
S 147	4 54.6	71 04	3140	2260	T	3	1	12.8	
S 148	4 56.7	70 04	3280	5920	T	1	0	12.8	
S 149	4 59.9	70 17	4360	5280	3	4	1	10.4	Pec.
S 150	5 00.1	70 08	4360	5790	T	1	0	12.8	
S 151	5 00.2	70 07	4390	5850	T	1	2	12.8	
S 152	5 00.5	70 13	4520	5530	T	2	1	12.8	
S 153	4 59.7	70 50	4520	3240	T	1	1	12.8	
S 154	4 53.7	75 04	4900	-12240	T	2	1	12.8	
S 155	5 02.8	71 24	5660	1340	4	3	1	9.2	B
S 156	5 05.6	70 48	6260	3590	1	1	1	12.0	
S 157	5 05.4	71 16	6360	1910	T	1	1	12.8	
S 158	5 05.9	71 16	6520	1910	T	1	1	12.8	
S 159	5 07.1	71 32	6930	990	1	1	1	12.0	
S 160	5 12.8	71 10	8480	2390	T	2	1	12.8	
S 161	5 23.1	71 38	11540	830	1	2	1	12.3	Oa
S 162	5 24.8	71 12	11990	2420	2	1	0	11.5	
S 163	5 25.0	71 34	12080	1080	T	3	0	12.8	
S 164	5 26.8	71 38	12590	860	2	1	1	11.5	
S 165	5 28.6	71 50	13100	100	T	3	0	12.8	
S 166	5 28.7	70 37	13160	4550	T	1	1	12.8	
S 167	5 29.0	71 01	13230	3080	T	1	0	12.8	
S 168	5 41.7	70 54	17010	3370	T	1	1	12.8	
S 169	5 42.3	71 19	17080	1840	T	4	1	12.8	
S 170	5 55.3	73 01	20160	- 4550	T	2	1	12.8	
S 171	5 06.1	67 57	5500	13900	5	1	0	9.3	B
S 172	5 32.1	68 34	14310	11920	4	1	0	10.4	B

Notes to Table 1

LHα 120-

S 1 Presence of continuum doubtful because of overlapping spectrum.
S 3 Lies on south edge of cluster NGC 1735 directly west of bright star on southeast edge of cluster.
S 5 Lies on north edge of dense nebulosity.
S 6 Lies on east edge of dense nebulosity.
S 7 HD 32034. In cluster NGC 1747.
S 8 HD 32109. The emission line is very broad.
S 9 Western star of close pair.

Notes to Table 1 (Cont'd)

LHα 120-

S 95 HD 269327.
S 96 HD 35343. S Doradus. MWC 108.
S 105 HD 269551.
S 106 Western star of close pair.
S 107 Lies slightly east of the arrow tip.
S 111 HD 269599 = MWC 113. In cluster NGC 1994.
S 114 HD 269649.
S 115 Emission star is moderately bright and has two fainter stars slightly to the west.
S 116 HD 269662.
S 117 HD 269661. Emission is perhaps doubtful.
S 119 HD 269687.
S 121 Northern star of compact triangle.
S 123 Brightest member of a faint cluster.
S 124 HD 37836 = MWC 121.
S 127 HD 37974 = MWC 123.
S 128 HD 269858 = MWC 511. The emission line is broad. Central star of three in line.
S 129 Eastern star of close pair.
S 130 HD 269896.
S 132 Emission doubtful.
S 133 HD 38282.
S 134 HD 38489 = MWC 126. In very bright knot of nebulosity.
S 143 HD 270086. Emission doubtful.
S 144 Probably the northern star of close pair. Presence of continuum doubtful because of overlapping spectrum.
S 145 Patch of emission in cluster NGC 2214. The emission is superposed on a strong continuum and may arise from one or more closely grouped stars.
S 148 Lies between two brighter stars.
S 149 HD 32763 = MWC 97.
S 153 Western star of faint pair.
S 155 HD 269006.
S 156 Probably a single emission-line star involved in a small group of stars.
S 158 Probably northern star of close pair.
S 161 HD 36063.
S 162 Continuum appears reddish. Perhaps a late-type star?
S 164 Emission perhaps doubtful.
S 166 Western star of close pair.
S 171 HD 33579. A note in the HDC indicates the class may be Oe5.
S 172 HD 269700.

Notes to Table 1 (Cont'd)

LHα 120-

S 11 The emission is perhaps doubtful.
S 14 HD 33133.
S 15 Probably the fainter and southern star of close pair.
S 17 HD 268939.
S 22 HD 34664 = MWC 105. Three faint emission lines which probably correspond to Fe II λ6456, [O I] λ6364 and [O I] λ6300 are visible.
S 23 NGC 1887. Faint Hα emission is visible on a diffuse continuous spectrum. The Hα emission is somewhat doubtful.
S 24 The emission line and the continuum are somewhat diffuse. Perhaps a group of emission-line stars?
S 25 The emission line is broad. Perhaps a Wolf-Rayet star?
S 27 Northwest star of close pair. Hα emission somewhat doubtful.
S 29 Emission is clearly visible on only one plate.
S 30 HD 269445.
S 34 HD 269540.
S 35 Western star of close pair.
S 36 The emission line is very broad. Probably a Wolf-Rayet star.
S 39 Emission perhaps doubtful.
S 43 Lies on western edge of cluster NGC 2004.
S 45 HD 269722.
S 47 Imbedded in dense nebulosity. About 42" north and slightly east of bright star.
S 52 Faint star on southwest edge of small cluster.
S 53 Probably the northern star of close pair.
S 62 Emission perhaps doubtful.
S 66 Continuous spectrum diffuse. Perhaps a compact group.
S 69 HD 268718.
S 72 Probably southern star of close pair.
S 73 HD 268835.
S 74 HD 268840.
S 85 Emission perhaps doubtful.
S 86 HD 269128.
S 88 HD 269216. Probably variable. The red continuum seen on LHα plates is definitely brighter than that of a normal B star of magnitude 11.0. Further, the continuum appears to be stronger in January 1951 than in December 1949.
S 89 HD 269217 = MWC 106.
S 90 HD 269219.
S 91 HD 269227 = MWC 492.

Table 2

EMISSION NEBULAE IN THE LARGE MAGELLANIC CLOUD

Nr. LHα 120-	1950 R.A.	Dec.	Rect. Coords. X	Y	Diameter X	Y	Int. C	Hα	Ir.	El.	St.	Stars
			"	"	"	"						
N 1	$4^h42^m.3$	-66°17'	- 3657	18728				1				
N 2	4 43.1	68 01	- 2231	12606	91	95		1	0	0	0	
N 3	4 50.0	67 46	- 42	13853	469	573		T	1	2	1	1
N 4A	4 52.1	67 00	250	16741	53	50		5	0	0	0	
N 4B	4 52.1	66 59	264	16800	60	50		3	0	0	1	
N 4C	4 52.3	67 00	346	16763	24	31	T	1	0	0	0	
N 4D	4 53.2	66 59	635	16836	250	189		1	0	0	1	1
N 4E	4 52.5	67 00	415	16746	42	46		1	0	0	0	
N 4F	4 51.7	67 00	128	16742	72	70		1	1	0	0	
N 5	4 52.6	67 22	628	15437	199	202		2	0	0	1	
N 6	4 54.0	66 50	862	17411	17	13		1	0	0	0	
N 7	4 53.5	67 28	992	15126	54	61		2	0	0	1	
N 8	4 53.1	68 08	1199	12704	85	116		5	1	0	2	2
N 8A	4 53.0	68 09	1176	12673				2				
N 9	4 55.2	67 13	1474	16101	393	528		1	4	2	1	1
N 10								1			3	2
N 11	4 56.4	66 30	1541	18760	1277	1404		2	2	1	3	4
N 11A	4 57.2	66 27	1801	18935			1	5				
N 11B	4 56.8	66 28	1659	18851	262	212		5	1	2	2	3
N 11C	4 57.7	66 32	2009	18700	191	158		5	1	1	2	1
N 11D	4 57.7	66 33	2035	18629				3				
N 11E	4 58.1	66 25	2120	19096	119	127		4	5	0	2	
N 11F	4 56.5	66 36	1635	18394	199	97		4	3	3	3	
N 11G	4 55.4	66 27	1152	18868	79	69		3	1	1	1	
N 11H	4 55.8	66 33	1366	18531	27	26		3	1	0	1	
N 11I	4 55.8	66 39	1387	18204	110	51		3	0	2	0	
N 11J	4 57.4	66 23	1841	19230			T	1				
N 11K	4 57.6	66 19	1901	19436	61	52	1	1	0	0	0	
N 11L	4 54.7	66 30	936	18674	67	60		1	0	0	0	
N 12	4 58.6	66 16	2226	19672	238	288		1	1	0	1	
N 12A	4 58.8	66 18	2329	19587	32	37		1	0	0	0	
N 13	5 00.1	66 09	2729	20151	132	156		T	0	0	0	
N 14	5 00.0	66 19	2754	19523	168	172		1	0	0	1	
N 15	5 00.7	66 27	3082	19088	18	20		2	0	0	0	
N 16	4 58.1	67 46	2727	14255				3				
N 16A	5 00.0	68 03	3467	13305	214	110		T	0	1	0	1
N 17	5 03.8	67 23	4531	15871	110	75		T	1	0	1	
N 17A	5 03.9	67 23	4569	15845	23	22		5	0	0	0	
N 17B	5 03.7	67 22	4504	15880	57	57		4	5	0	1	
N 18	5 04.7	66 44	4624	18198				4				
N 19	5 03.5	68 01	4632	13536				T				
N 20	5 05.2	66 59	4893	17307	106	40		2	0	0	1	
N 21	5 04.9	67 38	4991	14983	221	139		1	1	0	1	
N 22	5 05.1	67 52	5145	14123			1	5				
N 23	5 05.8	68 12	5482	12990	817	596		1	2	2	2	2
N 23A	5 05.1	68 08	5215	13163	82	107		3	1	0	1	
N 24	5 06.2	67 50	5501	14300				2				
N 25	5 09.4	67 52	6597	14287				2				
N 26	5 10.7	67 09	6863	16911	27	30	1	4	0	0	0	
N 27	5 11.0	67 11	6972	16755	48	53	T	3	0	0	0	
N 28	5 11.1	67 52	7185	14303				2				
N 29	5 12.6	66 42	7411	18577			T	2				
N 30	5 13.8	67 28	8018	15798	456	564		T	1	2	1	
N 30A	5 14.0	67 27	8081	15899	30	41		4	0	1	1	
N 30B	5 14.0	67 31	8081	15640	25	17		3	0	1	0	
N 30C	5 13.9	67 31	8068	15616	317	132		2	4	2	0	2
N 30D	5 13.3	67 32	7868	15547	66	62		1	1	1	1	
N 31	5 15.1	66 31	8270	19275	60	90		T	0	1	0	
N 32	5 15.9	68 02	8830	13790	16	19		2	0	1	0	
N 33	5 16.9	67 23	9091	16154	81	69		4	5	0	1	
N 34A	5 17.5	66 47	9188	18373				3				
N 34B	5 17.5	66 47	9207	18351				2				
N 34C	5 17.5	66 47	9204	18342				2				
N 35	5 17.8	66 04	9199	20945	109	134		T	1	0	0	
N 36	5 18.0	67 57	9528	14117	65	78		T	1	0	1	
N 37	5 20.3	66 56	10204	17810	230	137		1	2	2	2	
N 38	5 20.6	66 50	10295	18209	64	52		5	0	0	1	
N 39	5 20.9	67 09	10451	17072				2				

Table 2 (Cont'd)

Nr. LHα 120-	1950 R.A.	1950 Dec.	Rect. Coords. X	Rect. Coords. Y	Diameter X	Diameter Y	Int. C	Int. Hα	Ir.	El.	St.	Stars
			"	"	"	"						
N 40	$5^h21.^m5$	-65°30'	10518	23063	80	80		2	1	1	1	
N 41	5 20.7	68 04	10463	13745	51	49		1	0	0	0	
N 42	5 21.6	67 03	10680	17420				2				
N 43	5 22.2	65 46	10779	22060	655	247		1	1	2	1	2
N 44	5 22.6	67 59	11121	14064	943	1163		4	2	2	3	2
N 44A	5 21.6	67 54	10775	14351				5				
N 44B	5 22.2	68 00	10956	13977	67	57		5	1	0	0	
N 44C	5 22.4	68 01	11043	13929	47	67		5	0	0	0	
N 44D	5 23.0	68 07	11247	13567	91	74		5	1	1	1	
N 44E	5 23.4	68 03	11387	13826	33	36		5	0	0	0	1
N 44F	5 21.8	67 58	10837	14126	66	59		5	1	0	1	
N 44G	5 22.5	68 07	11083	13555				4				
N 44H	5 23.0	68 04	11244	13760	44	47		4	0	1	0	
N 44I	5 22.7	67 57	11128	14145				2				
N 44J	5 21.8	67 49	10809	14625	43	41		4	0	0	0	
N 44K	5 22.5	68 07	11084	13567	56	51		4	0	0	0	
N 44L	5 23.3	68 03	11337	13826	35	36		3	1	0	1	
N 44M	5 23.8	68 03	11530	13800	49	40		2	0	0	0	
N 44N	5 24.0	67 59	11580	14072	25	24		2	0	0	0	
N 45	5 22.8	66 44	11082	18575	69	77		2	1	0	0	
N 45A	5 22.8	66 44	11096	18590				2				
N 46	5 23.1	66 25	11169	19707	59	64		3	0	0	1	
N 47	5 24.5	67 12	11725	16907				1				
N 48	5 25.4	66 23	12010	19840	739	913		1	1	3	2	
N 48A	5 25.8	66 18	12135	20179				4				
N 48B	5 25.6	66 20	12090	20034	35	52		4	0	1	1	
N 48C	5 25.8	66 17	12152	20218	20	25		4	1	0	0	
N 48D	5 25.4	66 24	12014	19777	56	50		2	0	0	0	
N 48E	5 24.9	66 30	11824	19431	33	36		1	1	2	0	
N 49	5 26.0	66 08	12203	20799	68	82		5	2	0	2	
N 50	5 26.0	67 12	12254	16884	153	193		1	1	0	0	
N 51	5 26.9	67 35	12549	15510	1171	1179		2	3	2	3	2
N 51A	5 28.0	67 28	12961	15960	18	25	1	4	0	1	0	
N 51B	5 26.4	67 40	12376	15233	29	31	1	4	0	0	0	
N 51C	5 27.8	67 30	12867	15837	84	92		4	1	1	2	
N 51D	5 26.0	67 32	12253	15691	508	586		3	5	0	3	2
N 51E	5 26.7	67 41	12502	15132	378	422		1	1	1	2	1
N 52	5 28.8	67 36	13218	15463				1				
N 53	5 29.4	67 35	13416	15520			1	3				
N 54	5 29.5	67 16	13455	16685				1				
N 55	5 32.3	66 28	14496	19549	278	434		3	3	3	3	1
N 55A	5 32.5	66 29	14575	19470	65	60		4	1	0	1	
N 56	5 34.3	67 36	15130	15426	1940	1452		1	2	2	2	6
N 57	5 32.5	67 43	14486	15022	652	645		3	1	2	2	3
N 57A	5 32.4	67 44	14467	14976	55	44		4	0	1	0	1
N 57B	5 32.3	67 48	14400	14712	26	25		4	0	0	1	
N 57C	5 33.3	67 44	14765	14926	94	94		3	5	0	1	1
N 57D	5 33.0	67 43	14657	15034				2				
N 57E	5 32.1	67 44	14343	14951	366	377		2	5	0	2	3
N 58	5 32.8	67 31	14598	15760	35	34		3	1	0	1	
N 59	5 35.6	67 35	15576	15458	561	456		3	3	1	3	
N 59A	5 35.5	67 36	15549	15437	152	174		5	3	1	3	
N 59B	5 36.3	67 35	15798	15464	117	118		4	1	1	2	
N 59C	5 35.8	67 38	15625	15273	90	87		3	0	0	1	
N 60	5 34.1	67 55	15017	14314				3				
N 61								T			1	1
N 62A	5 34.6	66 15	15374	20292	108	41		3	0	3	0	
N 62B	5 34.4	66 10	15276	20609	173	239		2	4	3	0	1
N 63	5 35.6	66 01	15755	21150	290	380		2	2	1	1	
N 63A	5 35.7	66 02	15770	21100	40	40		5	1	0	1	
N 64A	5 37.1	66 22	16235	19860	30	40		2	0	0	1	
N 64B	5 37.1	66 21	16235	19940	350	260		2	1	1	1	
N 64C	5 37.3	66 17	16330	20130	100	120		2	5	0	0	
N 65	5 37.3	66 38	16280	18860	760	440		T	1	2	0	
N 66	5 36.5	67 19	15900	16410				2				
N 67	5 38.9	64 41	17187	25949	15	15	T	1	0	1	1	
N 68	5 37.2	68 15	16040	13038	21	20	T	3	1	0	0	
N 69	5 40.5	66 17	17490	20100				3				
N 70	5 43.5	67 51	18235	14390	410	420		3	5	0	2	
N 71	5 43.9	67 27	18452	15812	48	47		4	0	0	1	

Table 2 (Cont'd)

Nr. LHa 120-	1950 R.A.	Dec.	Rect. Coords. X	Y	Diameter X	Y	Int. C	Hα	Ir.	El.	St.	Stars
			"	"	"	"						
N 72	5^h43^m6	-66°17'	18619	20034	32	32	1	5	0	1	0	
N 73	5 44.5	67 27	18667	15789	20	40	1	T	0	1	1	
N 74	5 45.8	67 09	19223	16870	795	286		1	1	3	1	1
N 74A	5 45.8	67 10	19191	16830	32	17	1	4	1	2	1	
N 74B	5 45.4	67 09	19080	16864	128	20		3	2	3	2	
N 75A	5 55.9	68 07	22339	13022	31	32		2	0	0	0	
N 75B	5 56.2	68 12	22411	12736	334	286		1	1	0	0	
N 76	4 49.2	68 29	103	11248	111	100		1	1	0	0	
N 77A	4 49.7	69 17	697	8411	30	32	1	5	0	0	0	
N 77B	4 50.0	69 18	804	8378	34	28	1	3	0	1	0	
N 77C	4 50.3	69 17	907	8447	23	25	1	3	0	1	1	
N 77D	4 49.1	69 15	497	8522	68	62		3	0	0	1	
N 77E	4 50.0	69 18	804	8368	299	370		2	1	1	1	
N 77F	4 48.7	69 13	354	8588	19	22		2	0	0	1	
N 78	4 50.5	69 39	1166	7153				2				
N 79	4 51.1	69 30	1263	7723	1038	814		1	1	2	2	
N 79A	4 52.1	69 29	1569	7852	78	75	1	5	1	1	0	
N 79B	4 52.3	69 29	1623	7846	21	20		5	0	0	0	
N 79C	4 52.3	69 26	1605	8029	51	46		4	0	0	1	
N 79D	4 52.7	69 27	1744	7986	75	61		4	0	0	0	
N 79E	4 52.5	69 25	1657	8053	180	154		3	1	1	1	
N 80	4 54.3	68 27	1758	11636	84	77		3	0	0	1	
N 81A	4 53.0	69 18	1773	8503	100	93		2	0	0	1	
N 81B	4 53.3	69 19	1873	8447	101	86		1	0	1	0	
N 82	4 53.8	69 23	2045	8256				5				
N 83	4 54.5	69 16	2218	8733	340	297		3	2	1	2	
N 83A	4 54.3	69 17	2160	8612	61	55		5	1	1	0	
N 83B	4 54.6	69 16	2269	8694	44	37		5	0	1	0	
N 83C	4 54.2	69 15	2129	8772	21	20	1	3	0	1	0	
N 83D	4 54.4	69 16	2203	8724	20	21		2	0	0	1	
N 84	4 55.7	68 31	2237	11471	113	108		2	0	0	1	
N 85	4 55.9	68 41	2399	10857	23	23	T	2	1	0	0	
N 86	4 55.9	68 45	2423	10653	223	222		1	5	0	2	
N 87	4 54.7	69 35	2436	7590	19	14		4	0	0	0	
N 88	4 55.1	69 29	2530	7983	36	21		2	0	1	1	
N 89	4 55.3	69 25	2548	8215				4				
N 90	4 55.7	69 21	2641	8441	25	27	1	4	0	0	1	
N 91	4 57.5	68 29	2816	11646	420	384		3	3	1	3	2
N 91A	4 57.3	68 31	2785	11487	41	32		5	1	1	0	
N 91B	4 57.4	68 31	2817	11554	47	48		4	1	0	2	1
N 92	4 57.3	68 50	2923	10383	169	163		1	1	0	1	
N 92A	4 57.5	68 50	2966	10391	28	30	T	4	1	1	1	
N 92B	4 57.2	68 50	2884	10356	40	48		2	1	1	1	
N 93	4 57.2	69 17	3096	8730	41	26		1	1	2	1	
N 94A	4 56.6	69 29	2975	7999	90	49		1	1	2	1	
N 94B	4 56.8	69 31	3061	7923	62	45		1	2	1	2	
N 94C	4 57.2	69 35	3244	7692	207	223		1	2	2	2	
N 95	5 02.8	68 33	4601	11614	16	13		1	1	1	1	
N 96	5 03.2	69 26	5048	8446				2				
N 97	5 05.1	68 44	5423	11004				3				
N 98	5 04.8	69 51	5694	6965				2				
N 99	5 06.3	69 44	6149	7419				1				
N 100	5 07.5	68 37	6193	11532	183	155		T	0	1	1	1
N 101	5 07.8	69 13	6450	9357				1				
N 102	5 08.3	68 45	6477	11042				2				
N 103A	5 08.9	68 50	6711	10746	205	332		3	2	2	2	
N 103B	5 09.6	68 50	6944	10746	97	82		3	1	1	1	
N 104A	5 10.3	68 34	7090	11746				2				
N 104B	5 09.7	68 33	6877	11796	193	154		1	1	1	1	
N 105	5 10.1	68 58	7135	10298	322	340		1	2	0	2	
N 105A	5 10.2	68 58	7160	10310	160	270		4	2	2	3	4
N 106	5 10.5	68 53	7247	10620				1				
N 107	5 10.9	68 41	7312	11364				1				
N 108	5 10.8	69 31	7476	8340	41	44		2	1	0	1	
N 109	5 12.1	69 32	7902	8298	24	29		1	0	0	1	
N 110	5 11.8	70 06	7949	6248				2				
N 111	5 13.1	69 08	8129	9792				1				
N 112	5 13.7	69 15	8363	9343	48	38		4	0	0	1	
N 113	5 13.8	69 24	8419	8800	371	556		3	1	1	2	4
N 113A	5 13.7	69 27	8408	8627	21	29		5	1	0	0	

Table 2 (Cont'd)

Nr. LHα 120-	1950 R.A.	Dec.	Rect. Coords. X	Y	Diameter X	Y	Int. C	Hα	Ir.	El.	St.	Stars
			"	"	"	"						
N 113B	$5^h13^m.7$	-69°27'	8390	8640				4				
N 113C	5 13.6	69 26	8366	8691	81	65		4	1	0	1	
N 113D	5 13.5	69 27	8328	8638	65	73		4	0	0	1	
N 113E	5 13.6	69 27	8374	8648				3				
N 113F	5 14.0	69 27	8479	8615	49	44		4	1	1	0	
N 114	5 15.1	69 31	8862	8446	336	528		2	2	3	2	
N 114A	5 14.9	69 34	8792	8220	45	45		3	1	2	1	1
N 115	5 14.5	70 12	8812	5962	38	37		1	0	0	0	
N 116	5 17.3	69 57	9611	6885	86	60		1	0	0	1	
N 117	5 17.4	69 38	9609	8054	28	27		4	0	0	1	
N 118	5 19.3	68 24	10052	12494	26	27		4	0	0	1	
N 119	5 18.7	69 15	9954	9437	800	932		3	3	1	3	4
N 119A	5 18.3	69 14	9824	9474				1				
N 120	5 19.3	69 43	10220	7756	520	365		3	1	3	2	
N 120A	5 19.5	69 41	10259	7855	38	43		5	1	1	1	
N 120B	5 19.5	69 42	10280	7834	37	51		5	0	1	0	
N 120C	5 19.8	69 42	10374	7806	86	97		5	2	1	2	2
N 120D	5 18.8	69 43	10062	7750	65	60		3	1	1	1	
N 121	5 19.7	69 50	10358	7316			T	5				
N 122	5 20.3	69 34	10504	8302				2				
N 123	5 20.6	69 57	10640	6947				2				
N 124	5 21.6	68 38	10842	11692				2				
N 125	5 21.4	70 12	10899	6000				1				
N 126	5 21.9	69 05	10972	10048	48	32		T	0	1	0	
N 127A	5 22.0	69 43	11059	7747	73	70		5	1	0	2	
N 127B	5 21.7	69 44	10974	7731	87	82		2	0	0	0	
N 128	5 22.5	68 41	11142	11517	75	53		T	1	1	0	
N 129	5 22.8	69 45	11317	7641	24	27	T	4	1	1	0	
N 130	5 23.0	70 13	11397	5981	54	69	2	2	1	2	0	
N 131	5 23.3	69 54	11485	7135	53	32		3	0	1	1	
N 132A	5 24.1	69 40	11705	7982	43	44		4	0	0	0	
N 132B	5 24.7	69 42	11908	7872	38	31		3	0	1	1	
N 132C	5 24.9	69 43	11978	7766	32	35	T	2	0	0	1	
N 132D	5 25.5	69 40	12141	7937	32	24		2	1	1	1	
N 132E	5 24.8	69 42	11943	7877				1				
N 132F	5 23.9	69 38	11655	8119	32	32		1	1	0	0	
N 132G	5 24.5	69 41	11830	7892	41	37		1	0	0	1	
N 132H	5 25.3	69 41	12102	7919	30	23		1	0	0	1	
N 132I	5 24.5	69 43	11826	7793	103	75		1	0	1	1	
N 132J	5 24.0	69 41	11665	7893	70	86		T	0	0	1	
N 133	5 24.8	70 07	11961	6314				2				
N 134	5 26.2	69 55	12393	7057	27	26		T	0	0	0	
N 135								2			3	45
N 136	5 23.8	69 07	11599	9976				1				
N 137A	5 24.3	68 58	11750	10488	27	23		1	0	1	1	
N 137B	5 24.5	68 58	11791	10516	42	32		T	0	2	0	
N 138	5 24.8	68 33	11877	12021	391	363		1	1	2	1	1
N 138A	5 25.3	68 31	12050	12171	46	47	1	5	0	0	0	
N 138B	5 24.4	68 32	11761	12051	26	26		4	1	0	0	
N 138C	5 24.9	68 31	11903	12138	35	41	T	2	1	0	0	
N 138D	5 24.5	68 32	11770	12070	21	22		2	1	0	0	
N 139	5 25.1	69 22	12009	9044				1				
N 140	5 25.5	69 14	12152	9569	516	430		T	1	3	1	
N 141	5 25.7	68 58	12199	10522				2				
N 142	5 25.9	69 28	12266	8722	131	210		1	1	1	1	
N 143	5 26.8	69 21	12570	9098	127	164		2	0	1	1	
N 144	5 26.9	68 52	12576	10887	528	479		4	2	1	3	4
N 144A	5 27.0	68 51	12627	10955	43	46		5	0	0	0	
N 144B	5 26.8	68 51	12555	10951				4				
N 145	5 27.9	69 11	12919	9715				2				
N 146	5 29.1	69 03	13289	10218	53	37		2	0	2	1	
N 147	5 29.4	69 25	13389	8885				1				
N 148A	5 33.0	68 25	14617	12458	24	25	T	5	0	0	0	
N 148B	5 31.9	68 36	14244	11807				3				
N 148C	5 32.0	68 34	14265	11959	125	117		3	1	0	1	1
N 148D	5 31.6	68 33	14133	12003	26	28		3	1	0	0	
N 148E	5 31.9	68 30	14216	12193	33	33		2	1	1	2	
N 148F	5 31.2	68 36	13990	11834	26	24		2	1	0	0	
N 148G	5 32.7	68 41	14483	11543				1				
N 148H	5 31.6	68 38	14133	11696	22	24	T	1	0	0	0	

Table 2 (Cont'd)

Nr. LHα 120-	1950 R.A.	Dec.	Rect. Coords. X	Y	Diameter X	Y	C	Hα	Ir.	El.	St.	Stars
			"	"	"	"						
N 148I	$5^h32.^m1$	-68°42'	14298	11467	213	229		1	5	0	0	
N 149A	5 33.3	69 48	14600	7471	25	27		5	1	0	1	
N 149B	5 33.3	69 48	14583	7483				1				
N 150	5 34.0	68 47	14901	11148	49	31		4	1	2	1	
N 151	5 34.0	68 38	14929	11701				2				
N 152	5 34.5	69 28	15000	8682				1				
N 153	5 34.7	69 00	15105	10362				2				
N 154	5 35.5	69 44	15291	7700	1054	888		3	1	2	3	4
N 154A	5 36.4	69 40	15568	7909	80	54		4	1	1	1	
N 154B	5 34.9	69 48	15102	7446				3				1
N 155	5 37.7	69 47	15974	7481	51	51		2	0	0	1	
N 156	5 38.1	69 36	16115	8174	27	36	1	3	1	1	1	
N 157	5 38.0	69 08	16161	9826	1849	1781		3	1	1	3	6
N 157A	5 38.9	69 06	16465	9916	922	1063		5	2	0	3	8
N 157B	5 38.0	69 12	16167	9601	200	182		4	1	0	2	
N 158	5 39.9	69 28	16733	8582	746	759		3	3	2	3	6
N 158A	5 40.6	69 24	16963	8854	53	47		5	1	0	1	1
N 158B	5 39.1	69 25	16479	8757	26	22		4	0	1	0	
N 158C	5 39.5	69 32	16571	8394	217	210		4	3	0	3	2
N 158D	5 39.7	69 34	16642	8222	40	39		4	0	1	2	
N 159	5 40.4	69 46	16816	7496	288	249		1	2	0	2	
N 159A	5 40.1	69 47	16728	7439	56	62		5	2	0	1	
N 159B	5 40.5	69 45	16861	7548				3				
N 159C	5 40.4	69 47	16829	7472	140	107		4	2	1	2	
N 159D	5 40.4	69 45	16827	7572	131	97		4	0	1	2	
N 159E	5 40.5	69 48	16835	7389	35	35		5	1	0	0	
N 159F	5 40.1	69 46	16726	7551	48	47		4	1	0	1	
N 159G	5 40.8	69 46	16935	7518	50	50		4	1	0	1	
N 159H	5 39.9	69 48	16672	7386				2				
N 159I	5 40.2	69 46	16758	7534				1				
N 159J	5 40.0	69 44	16703	7598				1				
N 159K	5 40.0	69 47	16684	7469	25	22		2	1	1	0	
N 159L	5 40.5	69 50	16850	7260	62	28		1	4	2	0	
N 160	5 40.8	69 38	16958	7983	678	787		3	1	1	3	
N 160A	5 40.2	69 40	16765	7888	94	94		5	1	0	0	
N 160B	5 40.6	69 41	16893	7796	60	38		5	1	0	0	
N 160C	5 40.8	69 41	16971	7805	44	40		5	0	0	0	
N 160D	5 40.0	69 40	16707	7859	55	58		4	1	0	1	
N 160E	5 40.9	69 42	16980	7720	51	37		3	0	1	1	
N 160F	5 41.2	69 44	17083	7614	58	49		3	0	0	1	
N 161	5 40.5	69 00	17003	10260	65	62		3	1	1	1	
N 162	5 41.3	69 17	17198	9245				1				
N 163	5 43.6	69 46	17811	7436	217	213		3	1	0	2	
N 164	5 42.9	69 05	17758	9928	293	310		3	2	2	3	
N 165	5 43.2	68 58	17885	10382	103	93		3	5	0	1	
N 166	5 44.7	69 25	18253	8666	14	30		1	0	2	0	
N 167	5 44.8	69 23	18301	8800	64	47		2	0	0	1	
N 168	5 45.8	69 46	18507	7409	127	191		2	1	2	1	
N 168A	5 45.9	69 47	18535	7358	23	24		4	0	1	0	
N 168B	5 45.7	69 47	18492	7346				1				
N 169A	5 46.9	69 34	18905	8077	64	64		2	1	0	0	
N 169B	5 46.8	69 35	18873	8029	32	31		2	0	0	0	
N 169C	5 46.5	69 34	18786	8133	80	80		1	1	0	1	
N 170	5 47.4	69 27	19096	8491				3				
N 171A	5 39.9	70 13	16605	5866	21	21		2	0	0	0	
N 171B	5 39.8	70 14	16555	5845	57	70		1	1	0	0	
N 172	5 40.6	69 56	16874	6916	53	52		2	0	0	1	
N 173	5 40.8	69 54	16933	7023	49	54		1	0	0	0	
N 174	5 40.9	69 58	16936	6778	22	25		1	0	1	0	
N 175	5 41.2	70 03	17020	6450	118	107		2	5	0	1	
N 176	5 41.3	70 11	17026	6003	41	37	T	3	0	0	0	
N 177	5 41.6	69 55	17183	6913	102	175		3	1	1	1	
N 178	5 43.1	70 10	17581	6019				2				
N 179A	5 48.4	69 53	19294	6877	47	48		3	1	0	1	
N 179B	5 48.4	69 53	19291	6928	24	24		2	0	0	1	
N 179C	5 48.3	69 52	19271	6980	32	32		1	1	0	0	
N 179D	5 48.6	69 52	19358	6948	48	48		T	1	0	0	
N 180	5 49.5	70 05	19573	6153	604	859		1	1	2	1	1
N 180A	5 49.1	70 06	19434	6149	24	24		4	1	0	0	
N 180B	5 49.4	70 03	19541	6296	286	318		3	0	1	3	2

Table 2 (Cont'd)

Nr. LHα 120-	1950 R.A.	Dec.	Rect. Coords. X	Y	Diameter X	Y	Int. C	Hα	Ir.	El.	St.	Stars
			"	"	"	"						
N 180C	$5^h48^m.7$	-70°02'	19326	6376	111	96		2	0	1	0	
N 181	5 49.9	69 09	20002	9508				2				
N 182	4 39.0	70 41	- 1670	2813				3				
N 183	4 46.4	70 55	660	2407				2				
N 184	4 48.5	72 30	2194	- 3180				2				
N 185	4 54.2	70 05	2528	5779	390	397		1	1	0	1	
N 186A	5 01.3	70 18	4801	5243				3				
N 186B	5 00.4	70 08	4454	5830	38	36		3	0	0	0	
N 186C	5 00.0	70 13	4380	5475	27	28		2	1	0	0	
N 186D	5 00.3	70 12	4452	5545	88	114		T	5	0	0	1
N 186E	5 00.1	70 15	4411	5375	538	510		T	5	0	0	1
N 187	5 02.5	70 46	5348	3590				1				
N 188	5 04.1	70 18	5656	5338				2				
N 189	5 05.3	70 12	5970	5750	90	76		1	1	2	1	
N 190	5 04.9	70 48	6057	3547	114	133		3	0	0	1	
N 191A	5 05.2	70 58	6203	2934	48	53	2	5	0	1	0	
N 191B	5 05.1	70 58	6168	2983	54	52		2	0	0	0	
N 192	5 10.1	70 53	7637	3405				2				
N 193A	5 13.0	70 28	8386	4944	29	25	1	5	0	0	0	
N 193B	5 12.7	70 32	8326	4716	32	36		2	0	0	0	
N 193C	5 13.0	70 28	8385	4929	38	52		2	0	1	1	
N 193D	5 12.8	70 31	8361	4756	29	35		T	1	0	0	
N 193E	5 12.6	70 32	8294	4683	29	35		T	1	0	0	
N 194	5 16.5	71 50	9685	51	16	19		3	1	0	0	
N 195	5 18.4	71 18	10138	2008	167	182		1	0	1	0	
N 195A	5 18.2	71 18	10087	2023	34	27		4	1	1	1	
N 195B	5 18.3	71 18	10116	1977	46	32		4	1	1	0	
N 196	5 20.7	70 28	10722	5026				1				
N 197	5 21.6	71 45	11133	381	21	21	1	3	0	0	0	
N 198	5 23.2	71 38	11549	856	339	441		1	5	1	1	1
N 199	5 23.4	71 21	11593	1850				2				
N 200	5 24.0	71 23	11767	1722	394	795		1	4	2	1	1
N 201	5 25.6	71 35	12262	1044				3				
N 202	5 25.8	71 30	12297	1349	53	59		T	1	0	0	
N 203	5 25.8	73 41	12360	- 6580				2				
N 204	5 28.0	70 36	12941	4596	242	193		3	1	1	3	
N 205A	5 28.3	71 26	13019	1563	100	175		1	1	1	1	
N 205B	5 26.9	71 38	12625	845	230	200		T	1	1	1	2
N 206	5 31.3	71 07	13895	2692	1038	935		3	2	0	3	3
N 206A	5 32.0	71 06	14101	2795	116	229		5	1	1	1	1
N 206B	5 31.4	71 10	13941	2559	38	37		4	1	1	0	
N 206C	5 29.6	71 11	13388	2482	24	24		1	0	0	0	
N 206D	5 33.0	71 15	14400	2237	27	25		1	1	0	0	
N 207	5 31.2	70 46	13878	3968				1				
N 208	5 31.9	70 42	14118	4203				3				
N 209	5 34.3	71 53	14709	- 101				2				
N 210	5 35.7	74 18	14820	- 8900				1				
N 211	5 36.6	73 54	15100	- 7430				1				
N 212	5 37.7	71 54	15662	- 181				1				
N 213	5 39.0	70 42	16222	4153	186	169		3	1	0	1	
N 213A	5 38.9	70 42	16213	4160	44	48	T	5	1	1	0	
N 214	5 41.6	71 16	16878	2055	600	831		T	0	3	0	
N 214A	5 40.6	71 10	16612	2428	35	35		5	1	1	0	
N 214B	5 40.6	71 11	16622	2395	44	27		4	1	1	1	
N 214C	5 42.3	71 20	17079	1784	198	179		4	1	0	2	1
N 214D	5 40.8	71 12	16681	2349	90	87		2	1	0	1	
N 214E	5 40.8	71 13	16682	2263	35	38	1	1	1	1	0	
N 214F	5 42.1	71 16	17045	2048	41	47	1	1	0	1	0	
N 214G	5 42.0	71 15	16997	2093	30	27		1	1	0	0	
N 214H	5 42.1	71 18	17036	1955	54	59		1	1	0	1	
N 215	5 42.1	72 42	16730	- 3121				3				
N 216	5 41.6	70 55	16963	3319	59	54		T	0	0	0	
N 217	5 41.3	70 29	16964	4923				2				
N 218	5 41.5	70 35	17000	4519	28	28		5	0	1	0	
N 219	5 41.7	70 24	17088	5194	40	36		4	0	0	0	
N 220	5 49.4	70 17	19462	5422	20	14	T	T	0	1	0	
N 221	6 19.5	71 35	27670	- 250				2				

Notes to Table 2

LHα 120-	
N 4A	NGC 1714 = HD 31606 Pd.
N 4B	NGC 1715.
N 4E	Very faint nebula about conspicuous central star.
N 6	Probably southern and brighter member of close pair.
N 8	HDE 268680. Probably = NGC 1736. The NGC description suits the object but the position is 1.0 minutes in error.
N 10	This region to the north and east of LHα 120-N 11 contains several extremely faint patches of nebulosity whose boundaries are very indefinite. It is probable that this region is a continuous field of faint nebulosity. The boundaries are too indefinite to record a position for the field.
N 11A	Probably IC 2116 = HD 32340 P (see Harv. Bull. 891). The position previously given for this object appears to be somewhat in error. It is not NGC 1769 as is noted in the HDC.
N 11B	Includes NGC 1763 = HD 32256 P (see Harv. Bull. 891) and IC 2115 = HD 32279 Pc.
N 11C	NGC 1769.
N 11E	NGC 1773.
N 11F	NGC 1760.
N 16A	This object is not related to N 16.
N 17B	NGC 1814.
N 23A	NGC 1829.
N 25	On southwest edge of cluster NGC 1852.
N 26	The continuum is diffuse.
N 30B	A very small nebulosity enclosed in a triangle of stars. Probably in cluster NGC 1871.
N 31	Very faint nebula about two stars. Hα emission perhaps doubtful.
N 33	NGC 1895.
N 37	In cluster NGC 1919.
N 38	NGC 1920 = Harv. Bull. 891-16 = HD 269372.
N 44	Includes NGC 1937. NGC 1934 is not visible on LHα plates.
N 40	Possibly NGC 1923.
N 44A	Harv. Bull. 891-17 = HD 269404.
N 44B	NGC 1935 = IC 2126 = HD 35814 Pec.
N 44C	NGC 1936 = IC 2127 = HD 35861 Pd.
N 44D	Harv. Bull. 891-19 = HD 269443. Probably part of IC 2128, which also probably includes 44E, 44H and 44L.
N 44F	NGC 1929 = Harv. Bull. 891-18 = HD 269407.
N 46	NGC 1941.
N 48	Includes NGC 1945.
N 48E	Lies at center of NGC 1945.
N 49	[O I] λ6300 shows strong emission. Harv. Bull. 891-20 = HD 271255.
N 51A	In cluster NGC 1974.
N 53	The continuum is probably due to an overlapping spectrum.
N 55A	Harv. Bull. 891-21 = HD 269730.
N 57A	In cluster NGC 2014. Probably Harv. Bull. 891-22 = HD 269725.
N 57C	NGC 2020.
N 59	Includes HD 269803 = NGC 2029.
N 59A	Consists of two bright knots: NGC 2032 = HD 37731 Pd and NGC 2035 = HD 269824 = Harv. Bull. 891-24.
N 59B	NGC 2040 = HD 269852.
N 61	This region, between LHα 120-N 63 and LHα 120-N 65, seems to have an extremely faint background of nebulosity connecting the brighter knots. The boundaries are too indefinite to record a position.
N 63	NGC 2030.
N 63A	Probably HD 271389. Shows [O I] λ6300 in emission.
N 73	A very faint nebula about a conspicuous central star. Central star possibly multiple.
N 75B	NGC 2147.
N 77A	IC 2105 = HD 31351 Pc.
N 79A	Probably IC 2111 = HD 31673 Pc.
N 79B	Possibly IC 2111?
N 79E	Contains the cluster NGC 1727.
N 82	Strong [N II] λ6584 visible.
N 83	Includes NGC 1745 and NGC 1737.
N 83A	NGC 1743 = HD 31947 Pc.
N 83B	NGC 1748 = IC 2114 = HD 32014 Pc.
N 87	A small emission patch on southeast edge of bright star image.
N 88	Lies 10" east of faint star.
N 90	The continuum is probably diffuse.
N 91	NGC 1770.
N 91A	IC 2117 = HD 32364 Pd.
N 94A	Possibly NGC 1767.
N 97	Strong [N II] λ6584 visible.
N 102	Eastern member of very close pair. Strong [N II] λ6584 visible.

LHα 120-	
N 103A	NGC 1850. Includes HD 34026 Cl, Con; and HD 34039 Neb., Con. The compact cluster is brighter than the nebulosity but wisps of Hα emission are unmistakably visible along the southern edge of the cluster.
N 104A	Lies 20" southwest of faint cluster.
N 105A	NGC 1858. Contains Harv. Bull. 891-11 = HD 269111.
N 107	Lies 15" west of star.
N 113	Contains NGC 1872 which is a cluster without Hα emission.
N 113A	113A, B and E form a chain of three small intense knots of nebulosity which, together, make up NGC 1877.
N 113C	Contains NGC 1876 and HD 34679 Cl, Con. The HD object seems to refer also to 113A, B, D, E and F.
N 113D	NGC 1874.
N 113F	NGC 1880.
N 120A	Part of NGC 1918.
N 120B	Part of NGC 1918. Harv. Bull. 891-13 = HD 269367.
N 121	NGC 1921 = Harv. Bull. 891-14 = HD 269379. A peculiar, small, ring-like object which shows no Hα emission lies 25" to the east.
N 122	Harv. Bull. 891-15 = HD 269390.
N 130	A fan-like nebula attached to the cluster NGC 1943. The continuum is probably due entirely to the cluster.
N 135	This is an extended region of about two square degrees in extent which is filled with faint nebulous wisps and filaments. The region is very complex and only the more conspicuous knots are listed. The associated stars listed for LHα 120-N 135 are those not otherwise listed for the conspicuous knots. This region contains several conspicuous clouds of blue supergiant stars whose members are too faint to appear in the Henry Draper Extension. NGC 2050 appears to be a part of this region.
N 138A	NGC 1949 = HD 36301 Pc.
N 144	Includes NGC 1962, NGC 1965, NGC 1970.
N 144A	NGC 1966.
N 145	On southwest edge of cluster NGC 1984.
N 151	Identification on chart uncertain. Maybe it is the object 20" to the north of the marked object.
N 152	This is a very faint object 35" southwest of bright star.
N 153	Probably northeast member of close pair.
N 154A	Harv. Bull. 891-25 = HD 269822.
N 154B	On southwest edge of cluster NGC 2033.
N 156	The continuum is diffuse.
N 157A	30 Doradus = NGC 2070 = HD 38268 Pd. Includes NGC 2069.
N 157B	NGC 2060.
N 158	Contains NGC 2081.
N 158C	NGC 2074. Harv. Bull. 891-27 = HD 269930.
N 159A	NGC 2079 = HD 38437 Pc.
N 159C	NGC 2084. Includes Harv. Bull. 891-28 = HD 269942 and Harv. Bull. 891-29 = HD 269950.
N 159D	NGC 2083.
N 159F	NGC 2078.
N 160A	NGC 2080 = HD 38436 Pd.
N 160B	NGC 2085 = HD 269952.
N 160C	NGC 2086. Probably = IC 2145 = HD 38540 Pc.
N 160D	NGC 2077 = HD 38416 Pd = HD 269937.
N 168A	In cluster NGC 2113.
N 181	Strong [N II] λ6584 visible.
N 186E	Listed in Harv. Circ. 271 as "Nebulous wisp about star." Contains NGC 1791.
N 190	NGC 1833.
N 191A	Harv. Bull. 891-10 = HD 33540 P.
N 193A	Harv. Bull. 891-12 = HD 269211.
N 195B	NGC 1914.
N 201	Northwest member of close pair.
N 203	Lies 5" east of star.
N 206A	NGC 2018.
N 213A	NGC 2075.
N 214C	NGC 2103.
N 217	Lies 20" south of bright star.
N 220	Probably is the faint object 20" east of faint star.

Table 3

EXCITING STARS IN THE LARGE MAGELLANIC CLOUD NEBULAE

Neb. Nr. LHα 120-	Star Nr.	Posi-tion	1900 R.A.	Dec.	m	Sp.
			$4^h50^m.3$	-67°50'		
N 3	HD 268605		4 53.4	67 05	11.0	B
N 4D	HD 268653		4 53.2	68 12	10.5	Bo
N 8	LHα 120-S 5		4 53.3	68 13	12.8	
	LHα 120-S 6		4 55.2	67 20	12.8	
N 9	HD 32034	C	5 00.8	66 05	10.1	Pec.
N 10	HD 270948		5 01.1	66 01	11.6	Con.
	HD 270952		4 56.4	66 38	11.5	Con.
N 11	HD 32228	C	4 56.9	66 44	10.2	Oa
	HD 268732		4 55.1	66 40	11.0	B
	LHα 120-S 4		4 57.5	66 41	12.8	
	LHα 120-S 9		4 56.5	66 34	12.0	
N 11B	HD 268715		4 56.8	66 33	11.5	B
	HD 268721		4 56.9	66 33	11.8	B
	HD 268726		4 57.5	66 37	11.3	B
N 11C	HD 268743		5 00.1	68 06	11.1	B
N 16A	HD 268847		5 05.4	68 13	13.9	O
N 23	HD 33486		5 06.1	68 19	8.1	B9
	LHα 120-S 18		5 14.0	67 34	11.5	
N 30C	HD 34664	C	5 14.1	67 34	11.4	Pec.
	HD 269195		5 21.5	65 51	11.1	B
N 43	HD 271191		5 22.0	65 48	10.2	B
	LHα 120-S 29		5 22.2	68 00	12.8	
N 44	HD 269412		5 23.3	68 07	11.4	B
	HD 269445		5 23.5	68 06	11.6	O
N 44E	HD 269449		5 27.0	67 34	14.1	O
N 51	HD 269540		5 28.2	67 36	11.7	B
	LHα 120-S 37		5 26.3	67 35	12.8	
N 51D	HD 36402		5 26.4	67 35	10.8	Oa
	HD 269525		5 27.1	67 44	11.5	B
N 51E	HD 269545		5 32.2	66 28	11.4	B
N 55	HD 269722		5 32.1	67 38	11.6	B
N 56	HD 269702		5 32.3	67 33	11.9	Con.
	HD 269713		5 32.5	67 35	11.9	Con.
	HD 269718		5 32.7	67 36	9.5	B*
	HD 269726		5 36.0	67 30	12.3	Con.
	HD 269841		5 36.1	67 31	11.6	Con.
	HD 269845		5 32.0	67 42	11.2	Con.
N 57	HD 269698		5 32.6	67 45	11.7	O
	LHα 120-S 47		5 33.4	67 41	11.5	
	LHα 120-S 48		5 32.6	67 45	12.0	
N 57A	HD 269717		5 33.4	67 46	11.8	B
N 57C	HD 269748	C	5 31.8	67 45	13.1	O
N 57E	HD 269692		5 32.4	67 45	13.9	O
	HD 269714				11.7	B

Table 3 (Cont'd)

Neb. Nr. LHα 120-	Star Nr.	Position	1900 R.A.	Dec.	m	Sp.
	LHα 120-S 44	C	$5^h32^m.2$	-67°46'	12.8	
N 61	HD 271363		5 34.0	66 18	11.5	Con.
N 62B	HD 271366	C	5 34.1	66 13	11.8	Con.
N 74	HD 270149		5 46.9	67 11	13.8	O
N 91	HD 268798		4 57.4	68 35	10.8	B:
	HD 268804		4 57.6	68 34	11.1	B:
N 91B	HD 32402		4 57.8	68 33	12.3	Oa
N 100	HD 269050	C	5 07.7	68 40	11.2	B
N 105A	HD 34169		5 10.2	69 00	13.2	Oa
	HD 34187		5 10.3	69 01	14.0	O
	HD 269113		5 10.4	69 00	14.5	O
	HD 269116		5 10.4	69 03	11.2	B:
N 113	HD 34783		5 14.8	69 25	13.8	Oa
	HD 269215		5 14.2	69 25	11.1	B:*
	HD 269217		5 14.3	69 28	11.6	Pec.
	HD 269219		5 14.3	69 27	11.4	B
N 114A	HD 269244	C	5 15.2	69 36	11.2	B
N 119	HD 35343		5 18.9	69 21	var.	Pec.
	HD 269321		5 18.6	69 22	10.9	B:
	HD 269333		5 18.9	69 18	11.2	Oe
	HD 269357		5 19.6	69 19	12.1	Con.
N 120C	HD 35517		5 20.1	69 45	11.5	Oa
	HD 269382	C	5 20.2	69 46	11.5	B5:
N 135	HD 37974		5 37.2	69 26	11.3	Pec.
	HD 38030		5 37.6	69 30	12.6	Oa
	HD 269549		5 27.3	69 12	14.8	O
	HD 269578		5 28.3	69 04	10.2	B:
	HD 269582		5 28.5	69 04	var.	Pec.
	HD 269599		5 29.0	69 13	12.2	Pec.
	HD 269604		5 29.1	68 58	11.0	B
	HD 269618		5 29.8	68 50	14.2	O:
	HD 269619		5 29.9	68 33	11.1	B
	HD 269624		5 30.1	68 59	15.0	O
	HD 269649		5 31.1	69 24	11.2	B
	HD 269651		5 31.2	69 13	11.0	B
	HD 269661		5 31.6	69 36	10.6	B
	HD 269662		5 31.5	69 07	10.8	B:
	HD 269665		5 31.5	68 49	10.6	B9
	HD 269668		5 31.6	68 58	11.8	B
	HD 269687		5 32.0	69 10	11.4	B
	HD 269705		5 32.7	69 23	11.6	B
	HD 269762		5 34.8	69 03	10.8	B
	HD 269832		5 36.8	69 27	11.0	B
	HD 269858		5 37.5	69 33	11.1	Pec.
	HD 269859		5 37.5	69 33	10.9	B

Table 3 (Cont'd)

Neb. Nr. LHα 120-	Star Nr.	Position	1900 R.A.	Dec.	m	Sp.
			$5^h39^m.4$	-69°26'		
	HD 269920		5 39.4	-69 26	11.3	B:
	HD 269982		5 41.7	69 18	11.1	B
	HD 269992		5 42.3	69 51	11.1	Con.
	HD 269997		5 42.0	69 08	11.1	B
	HD 270086		5 45.9	69 02	10.6	Bo:
	LHα 120-S 106		5 27.8	69 05	12.8	
	LHα 120-S 107		5 28.1	69 19	12.8	
	LHα 120-S 108		5 28.4	69 15	12.8	
	LHα 120-S 109		5 28.5	69 16	12.0	
	LHα 120-S 110		5 28.8	68 58	12.8	
	LHα 120-S 112		5 30.6	69 12	12.0	
	LHα 120-S 113		5 31.0	69 05	12.8	
	LHα 120-S 115		5 31.3	69 16	12.0	
	LHα 120-S 120		5 32.1	69 10	12.8	
	LHα 120-S 122		5 34.3	68 43	12.8	
	LHα 120-S 125		5 36.5	69 02	12.8	
	LHα 120-S 126		5 36.7	69 00	12.0	
	LHα 120-S 129		5 38.1	69 23	11.5	
	LHα 120-S 136		5 42.2	69 27	11.5	
	LHα 120-S 137		5 42.5	69 39	12.8	
	LHα 120-S 139		5 42.4	68 57	12.0	
	LHα 120-S 141		5 44.8	69 16	12.8	
	LHα 120-S 142		5 45.2	69 21	12.0	
N 138	HD 269485		5 24.8	68 37	14.3	O
N 144	HD 36521		5 27.1	68 55	11.4	Oa
	HD 269546		5 27.3	68 55	10.4	B
	HD 269548		5 27.3	68 52	13.6	O
	HD 269551		5 27.4	68 55	11.5	B
N 148	LHα 120-S 118		5 31.9	68 45	11.5	
	LHα 120-S 121		5 32.4	68 30	12.8	
N 148C	HD 269700		5 32.3	68 37	10.4	B
N 154	HD 37680		5 35.2	69 49	12.6	Oa
	HD 37836		5 36.2	69 44	10.5	Pec.
	HD 269784		5 35.8	69 47	14.2	O
	HD 269786		5 35.9	69 49	11.0	B
N 154B	HD 269769		5 35.4	69 50	11.5	Con.
N 157	HD 38029		5 37.6	69 15	11.3	Oa
	HD 269818		5 36.4	69 14	14.4	O
	HD 269826		5 36.6	69 13	11.4	B:
	HD 269828		5 36.7	69 15	13.6	Oc
	HD 269888		5 38.4	69 18	15.1	O
	HD 269896		5 38.4	68 58	11.3	B
N 157A	HD 38282		5 39.5	69 05	10.6	Oa
	HD 38344		5 39.9	69 05	12.6	O
	HD 269883		5 38.3	69 11	14.7	O
	HD 269891		5 38.5	69 08	11.5	Oc
	HD 269902		5 38.8	69 09	11.0	B

Table 3 (Cont'd)

Neb. Nr. LHα 120-	Star. Nr.	Posi-tion	1900 R.A.	Dec.	m	Sp.
	HD 269919		$5^h39^m.2$	-69°08'	13.7	O
	HD 269926		5 39.4	69 03	12.5	O
	HD 269928		5 39.6	69 09	11.8	O
N 158	HD 38448		5 40.7	69 27	13.1	Oa
	HD 38472		5 40.9	69 27	13.4	O
	HD 269908		5 39.2	69 33	14.8	O
	HD 269936		5 40.2	69 30	11.2	B
	HD 269956		5 41.0	69 27	11.6	O
	LHα 120-S 131		5 39.1	69 32	12.0	
N 158A	HD 38489		5 41.0	69 26	12.0	Pec.
N 158C	HD 269923		5 39.6	69 33	10.8	B
	HD 269927		5 39.7	69 32	11.1	B
N 180	LHα 120-S 144		5 49.4	70 09	12.8	
N 180B	HD 270145		5 49.8	70 05	11.8	Con.
	HD 270151		5 50.0	70 04	11.8	Con.
N 186D	LHα 120-S 152	C	5 00.9	70 17	12.8	
N 186E	HD 32763	C	5 00.3	70 20	10.4	Pec.
N 198	HD 36063	C	5 23.9	71 43	12.3	Oa
N 200	HD 36156	C	5 24.6	71 26	12.2	Oa
	HD 269547		5 27.6	71 38	11.5	B
N 205B	LHα 120-S 164		5 27.5	71 40	11.5	
N 206	HD 37248		5 32.0	71 06	12.2	Oa
	HD 269656		5 31.9	71 06	11.7	B:
	HD 269660		5 32.1	71 08	11.4	B
N 206A	HD 269676		5 32.5	71 08	11.4	B
N 214C	LHα 120-S 169		5 43.0	71 21	12.8	

Table 4

EMISSION-LINE STARS IN THE SMALL MAGELLANIC CLOUD

Nr. LHα 115-	1950 R.A.	Dec.	Rect. Coords. X	Y	Int. C	Hα	Dif.	m	Sp.
			"	"					
S 1	$0^h26^m.5$	-70°03'	4620	20051	2	2	1	11.5	
S 2	0 41.3	73 39	9881	7386	2	2	2	11.5	
S 3	0 41.8	73 43	9999	7184	1	2	1	12.0	
S 4	0 43.2	72 58	10239	9893	T	3	1	12.8	
S 5	0 43.9	72 14	10323	12595	1	1	0	12.0	
S 6	0 45.1	73 25	10808	8307	1	5	1	12.0	
S 7	0 45.4	73 31	10884	7968	1	2	0	12.0	
S 8	0 46.8	72 28	11136	11765	T	1	0	12.8	
S 9	0 46.6	73 00	11142	9812	1	2	1	12.0	
S 10	0 46.5	73 08	11146	9369	T	1	0	12.8	
S 11	0 48.7	73 47	11773	7020	T	1	2	12.8	
S 12	0 49.0	73 24	11820	8362	T	1	1	12.8	
S 13	0 49.6	73 33	11970	7831	1	1	1	12.0	
S 14	0 50.0	72 16	12016	12521	1	2	1	12.0	
S 15	0 50.5	72 25	12152	11950	1	2	1	12.0	
S 16	0 50.7	72 27	12208	11818	T	1	1	12.8	
S 17	0 51.9	73 26	12560	8255	T	3	0	12.8	
S 18	0 52.4	72 58	12692	9967	T	5	1	12.8	
S 19	0 52.6	72 46	12729	10726	1	2	2	12.0	
S 20	0 52.6	72 33	12737	11453	T	1	2	12.8	
S 21	0 53.3	73 13	12930	9087	1	1	3	12.0	
S 22	0 53.8	72 23	13051	12097	1	1	1	12.0	
S 23	0 54.2	72 25	13153	11948	1	2	0	12.0	
S 24	0 55.0	73 18	13352	8733	T	1	0	12.8	
S 25	0 55.7	72 18	13568	12395	1	3	0	12.0	
S 26	0 55.8	72 32	13598	11529	3	1	3	11.0	
S 27	0 57.2	72 13	13995	12695	2	1	2	11.5	
S 28	0 57.8	72 26	14138	11889	2	2	2	11.5	Oa
S 29	0 57.8	72 17	14155	12421	2	4	0	11.5	
S 30	0 59.0	72 27	14482	11839	2	1	1	11.5	
S 31	0 59.0	71 47	14524	14231	T	3	1	12.8	
S 32	0 59.8	72 40	14688	11064	T	1	0	12.8	
S 33	0 59.8	72 17	14703	12377	2	1	1	11.5	
S 34	0 59.9	72 25	14720	11915	T	1	1	12.8	
S 35	1 00.5	71 46	14931	14290	T	2	1	12.8	
S 36	1 01.4	72 42	15098	10914	T	2	1	12.8	
S 37	1 01.5	72 45	15123	10737	3	1	1	11.0	
S 38	1 02.1	72 30	15314	11627	1	3	1	12.0	
S 39	1 02.4	72 49	15366	10453	1	1	1	12.0	
S 40	1 02.3	72 10	15420	12802	2	1	2	11.5	
S 41	1 02.7	72 25	15502	11895	T	2	1	12.8	
S 42	1 03.3	73 03	15562	9621	1	2	1	12.0	
S 43	1 03.5	72 41	15682	10958	1	2	2	12.0	
S 44	1 04.1	72 42	15835	10864	1	2	3	12.0	
S 45	1 04.4	72 36	15915	11246	3	1	0	11.0	

Table 4 (Cont'd)

Nr. LHα 115-	1950 R.A.	Dec.	Rect. Coords. X	Y	Int. C	Hα	Dif.	m	Sp.
			m	m					
S 46	$1^h04.^m2$	-72°02'	15948	13269	1	3	0	12.0	
S 47	1 04.5	72 34	15966	11345	T	2	1	12.8	
S 48	1 05.2	73 26	15992	8179	1	2	1	12.0	
S 49	1 04.7	72 44	15993	10755	1	2	1	12.0	
S 50	1 05.0	72 33	16087	11384	2	2	0	11.5	
S 51	1 05.2	72 15	16210	12492	T	3	1	12.8	
S 52	1 05.8	72 44	16268	10728	4	2	1	10.8	B
S 53	1 07.3	73 31	16520	7889	1	2	0	12.0	
S 54	1 06.9	72 40	16589	10989	T	1	1	12.8	
S 55	1 09.6	73 34	17089	7652	T	2	0	12.8	
S 56	1 09.8	72 39	17389	10978	T	3	2	12.8	
S 57	1 12.1	73 36	17743	7487	4	1	0	10.5	B
S 58	1 13.9	73 44	18152	6949	T	2	0	12.8	
S 59	1 17.1	73 47	18952	6697	T	2	1	12.8	
S 60	1 17.0	73 25	19042	8044	2	1	0	11.5	
S 61	1 22.4	73 39	20329	7031	T	1	2	12.8	
S 62	1 29.1	73 34	22070	7145	1	3	0	12.0	
S 63	1 28.1	72 58	22126	9299	3	3	0	11.0	
S 64	1 30.1	73 04	22614	8867	2	3	0	11.5	
S 65	1 43.3	74 55	24660	1661	3	4	1	11.0	

Notes to Table 4

LHα 115-

S 3 A member of the close group NGC 242. This star lies at the extreme eastern edge of the group.
S 9 Probably northern-most star of close trio.
S 11 Emission perhaps doubtful.
S 16 Emission visible on only one plate.
S 19 Northern-most star of compact triangle of stars.
S 22 Emission doubtful. Probably southeast star of close pair.
S 26 The continuous spectrum is diffuse. Probably a cluster with one or more emission stars. Not in the NGC.
S 28 HD 5980. The magnitude is estimated from LHα plates.
S 31 Emission visible on only one plate.
S 39 Spectrum variable? Unmistakable emission on earliest plate seems weaker on later plates.
S 44 Northern star of close pair. Presence of continuum doubtful because of overlapping spectrum.
S 50 A fainter star lies 15" to the southwest.
S 52 HD 6884.
S 57 HD 7583. Emission doubtful.
S 58 Emission perhaps doubtful.
S 60 Emission perhaps doubtful. Continuum is rather red. Perhaps a late-type star?
S 61 Emission perhaps doubtful although strongly suspected on two plates.

Table 5

EMISSION NEBULAE IN THE SMALL MAGELLANIC CLOUD

Nr. LHα 115-	1950 R.A.	Dec.	Rect. Coords. X	Y	Diameter X	Y	C	Hα	Ir.	El.	St.
			"	"	"	"					
N 1	0^h21^m9	-73°54'	5045	6062				2			
N 2	0 30.5	71 58	6536	13288				2			
N 3	0 29.7	74 04	7061	5691	48	28		2	0	1	0
N 4	0 32.4	73 30	7543	7824				1			
N 5	0 39.4	73 02	9255	9642				2			
N 6	0 39.6	74 03	9526	5924				2			
N 7	0 41.5	72 55	9787	10090				2			
N 8	0 41.3	73 16	9802	8781	21	14		1	0	1	0
N 9	0 41.7	73 19	9916	8638	21	18		3	0	1	0
N 10	0 43.1	73 27	10294	8187	23	22		2	1	0	0
N 11	0 43.2	73 33	10340	7799	24	22	T	2	1	1	0
N 12	0 44.2	73 22	10552	8455	395	228		2	3	2	2
N 12A	0 44.7	73 23	10686	8434	112	113		2	5	0	2
N 12B	0 43.6	73 21	10417	8519	124	101		2	1	0	2
N 13A	0 43.6	73 39	10451	7421	35	27		3	0	1	0
N 13B	0 43.6	73 39	10439	7456	59	42		2	0	1	0
N 14	0 44.5	73 29	10650	8051	24	23		1	0	0	0
N 15	0 44.4	73 42	10657	7276	27	27		1	0	0	0
N 16	0 44.5	73 40	10679	7404	64	46		1	0	1	0
N 17	0 44.9	73 48	10807	6912	191	187		1	0	0	0
N 18	0 45.2	73 06	10778	9468				1			
N 19	0 45.9	73 24	11008	8350	311	419		1	1	1	1
N 20	0 46.0	73 32	11056	7903				1			
N 21	0 46.0	73 34	11056	7777	43	36		2	1	0	0
N 22	0 46.2	73 33	11104	7850	151	118		2	1	0	1
N 23	0 46.2	73 34	11110	7763	56	41		2	5	0	2
N 24	0 46.4	73 36	11165	7640	70	71		2	1	0	1
N 25	0 46.4	73 31	11147	7973	48	45		3	0	0	0
N 26	0 46.4	73 31	11146	7936				2			
N 27	0 46.6	73 22	11191	8477	51	34		2	1	2	2
N 28	0 46.8	73 32	11252	7897	121	114		2	1	0	2
N 28A	0 46.7	73 32	11231	7865	54	32		2	0	2	0
N 29	0 46.8	73 14	11231	8953				2			
N 30	0 47.3	73 25	11366	8335	152	156		2	1	0	1
N 30A	0 47.2	73 26	11344	8243	20	18		2	0	0	0
N 31	0 46.9	73 43	11310	7259				1			
N 32	0 47.9	73 05	11495	9521	33	27		2	0	0	1
N 33	0 47.7	73 43	11516	7244				2			
N 34	0 47.9	73 27	11546	8204				2			
N 35	0 48.4	72 49	11617	10504	35	49		1	4	1	0
N 36	0 48.8	73 09	11739	9285	263	238		1	1	0	1
N 37	0 49.0	73 03	11792	9630	319	291		1	1	1	1
N 38	0 48.2	74 01	11646	6176				2			
N 39	0 48.7	73 16	11722	8892				1			
N 40	0 48.9	73 59	11827	6261				1			
N 41	0 49.2	73 10	11856	9265	21	17		2	0	0	1
N 42	0 49.7	72 43	11942	10896				2			
N 43	0 49.5	74 14	11985	5386				2			
N 44	0 50.1	71 41	11999	14626				2			
N 45	0 50.0	73 30	12064	8035	36	31		2	0	0	1
N 46	0 50.1	73 07	12067	9412	19	16		3	0	1	0
N 47	0 50.3	73 37	12150	7620				2			
N 48	0 50.6	73 43	12240	7224	46	35		1	0	0	0
N 49	0 50.5	73 52	12230	6687	16	15		1	0	0	0
N 50	0 51.1	72 55	12326	10139	140	84		1	1	3	0
N 51	0 50.9	73 42	12326	7280	54	38		2	1	0	1
N 52A	0 51.9	72 56	12557	10090	19	16		2	0	0	0
N 52B	0 52.0	72 56	12565	10109	24	19		2	0	1	0
N 53	0 52.4	71 51	12655	14035	23	21		2	0	2	0
N 54	0 54.2	70 36	13180	18540				2			
N 55	0 53.5	72 19	12981	12300				2			
N 56	0 53.6	73 43	12994	7245				2			
N 57	0 54.0	72 33	13111	11507	35	35	1	1	0	1	0
N 58	0 54.5	72 34	13258	11433	60	70		1	0	1	0
N 59	0 55.5	73 50	13486	6819	88	81		1	0	0	0
N 60	0 55.6	74 29	13478	4456				2			
N 61	0 55.8	72 49	13593	10530				2			
N 62	0 56.3	72 56	13709	10112	65	50		1	0	1	0

Table 5 (Cont'd)

Nr. LHα 115-	1950 R.A.	Dec.	Rect. Coords. X	Y	Diameter X	Y	Int. C	Hα	Ir.	El.	St.
			"	"	"	"					
N 63	$0^h56^m.6$	-72°55'	13801	10140	35	27	T	3	0	0	0
N 64	0 56.7	72 56	13822	10072	80	66		1	0	0	1
N 64A	0 56.8	72 56	13844	10077	24	17		3	0	1	0
N 65	0 56.2	72 05	13729	13181				1			
N 66	0 57.5	72 27	14057	11863	584	491		3	2	0	3
N 66A	0 57.6	72 27	14082	11818				2			
N 66B	0 57.5	72 26	14067	11885	27	19		2	0	0	0
N 66C	0 57.5	72 26	14078	11915	19	11		2	0	1	0
N 66D	0 56.5	72 27	13782	11820	32	11	1	2	0	2	1
N 67	0 56.9	71 52	13924	13955	12	19		2	0	1	0
N 68	0 57.0	72 44	13926	10836				2			
N 69	0 57.5	72 41	14060	11015	27	24		2	0	0	1
N 70	0 57.6	72 18	14092	12366				2			
N 71	0 59.3	71 52	14595	13969	22	13		3	0	1	0
N 72	0 59.8	72 07	14736	13038	26	17	T	2	0	1	0
N 73	1 03.4	76 04	15150	- 1310				2			
N 74	1 00.6	72 07	14948	12994	53	35		1	1	0	0
N 75	1 00.8	72 13	14990	12667	63	41		1	0	2	0
N 76	1 01.9	72 20	15274	12220	258	322		2	1	1	0
N 76A	1 02.2	72 20	15355	12225	26	15		2	0	0	0
N 76B	1 01.5	72 23	15161	12072	31	22		2	0	1	0
N 76C	1 02.3	72 25	15374	11947				2			
N 77A	1 01.2	72 09	15099	12874	29	19		3	0	0	1
N 77B	1 01.1	72 10	15072	12862	19	19		1	0	0	0
N 78	1 03.8	72 17	15799	12376	260	365		2	3	2	2
N 78A	1 03.5	72 15	15722	12509	19	19		2	0	0	0
N 78B	1 03.5	72 16	15721	12482	24	13		2	1	2	0
N 78C	1 04.1	72 20	15887	12220	32	21	1	2	1	0	1
N 78D	1 03.6	72 14	15757	12545	33	17		2	0	2	1
N 79	1 06.1	72 51	16327	10317	18	8		1	2	3	1
N 80	1 06.9	72 16	16667	12437	154	198		1	1	0	1
N 80A	1 06.9	72 16	16669	12393	32	21		2	1	0	0
N 81	1 07.8	73 28	16653	8076	30	29	1	3	1	0	0
N 82	1 11.0	74 07	17315	5640				2			
N 83	1 12.4	73 33	17813	7650	198	165		2	1	0	0
N 83A	1 12.5	73 34	17834	7616	32	24		3	0	0	0
N 83B	1 12.5	73 32	17853	7748	19	24		2	1	1	0
N 83C	1 12.7	73 33	17893	7670	29	28		2	0	0	1
N 84	1 13.3	73 34	18046	7584	198	355		2	3	3	2
N 84A	1 13.3	73 34	18039	7577	30	19		3	0	2	0
N 84B	1 13.4	73 36	18075	7495	21	15		3	0	1	0
N 84C	1 12.9	73 32	17963	7741	33	32		2	0	0	0
N 84D	1 13.4	73 37	18059	7438	23	9		2	0	2	0
N 85	1 14.4	73 36	18325	7420			T	1			
N 86	1 14.4	73 26	18362	8066				2			
N 87	1 19.9	73 30	19764	7665				2			
N 88	1 22.9	73 24	20568	7918			T	3			
N 89	1 24.5	73 38	20862	7032	261	283		1	1	1	1
N 90	1 28.3	73 49	21747	6282	199	147		2	1	1	2

Notes to Table 5

LHα 115-

N 3 Nail 1 (Nail, Whitney and Wade 1953).
N 9 Harv. Bull. 891-1. Lies 25" south of bright star.
N 10 Nail 15. Lies 25" southwest of bright star and 20" northeast of fainter star.
N 11 Nail 16.
N 12 Includes Nail 21.
N 12A NGC 261. Harv. Bull. 891-4. Nail 25.
N 12B NGC 249. Harv. Bull. 891-3. Nail 18.
N 13A Harv. Bull. 891-2.
N 13B 13A and 13B make up NGC 248 = Nail 19.
N 18 Lies 20" northwest of bright star.
N 19 Nail 26.
N 22 Nail 28. Contains the cluster NGC 267.
N 25 Nail 30.
N 26 Harv. Bull. 891-5.
N 30 Includes Nail 34.
N 31 Probably the eastern member of close pair.
N 32 Nail 41.
N 33 Lies 30" northeast of bright star and 20" northwest of fainter star.
N 34 Nail 42.
N 35 Nail 45? Listed there as a "nebulous star." Shows unmistakable semicircle of nebulosity about central star on LHα plates.
N 36 Nail 49.
N 39 Somewhat doubtful.
N 45 Nail 59.
N 47 Possibly NGC 294.
N 50 Possibly excited by HD 5291.
N 52A Possibly Nail 75?
N 52B Nail 76.
N 53 Probably southwest member of close pair.
N 57 Shows a strong diffuse continuum. Probably a nebulosity about a bright cluster. Not in the NGC.
N 58 Includes Nail 88.
N 62 Part of Nail 93.
N 63 Nail 97.
N 64 Part of Nail 93.
N 64A Nail 99.
N 66 NGC 346. Harv. Bull. 891-6. Nail 101. Excited by HD 5980.
N 71. Nail 107.
N 72 Nail 110.
N 76 Nail 116. Contains the cluster NGC 371.
N 78 Contains NGC 395 = Nail 128 and IC 1624 = Nail 129. IC 1624, although well visible on red direct plates, shows no Hα emission on objective-prism plates.
N 78A Part of Nail 128 which also includes 78B and 78D.
N 78C Shows a strong continuum. Possibly two Hα emission stars close together.
N 81 IC 1644. Nail 136.
N 80 Nail 137. Includes Nail 142, an object not visible on our plates.
N 83 Nail 148. The "triangular group" referred to probably includes 83A, B and C. This group is possibly excited by HD 7583.
N 83A NGC 456. Harv. Bull. 891-7.
N 84 Includes Nail 151.
N 84A NGC 460. Harv. Bull. 891-8.
N 84B Harv. Bull. 891-9. Part of Nail 150. This is not NGC 460 as reported by Nail et al.
N 84C Nail 149.
N 90 NGC 356. Possibly excited by O star at $1^h28^m52^s$, $-73°56.'1$ (1900)(Harv. Bull. 891).

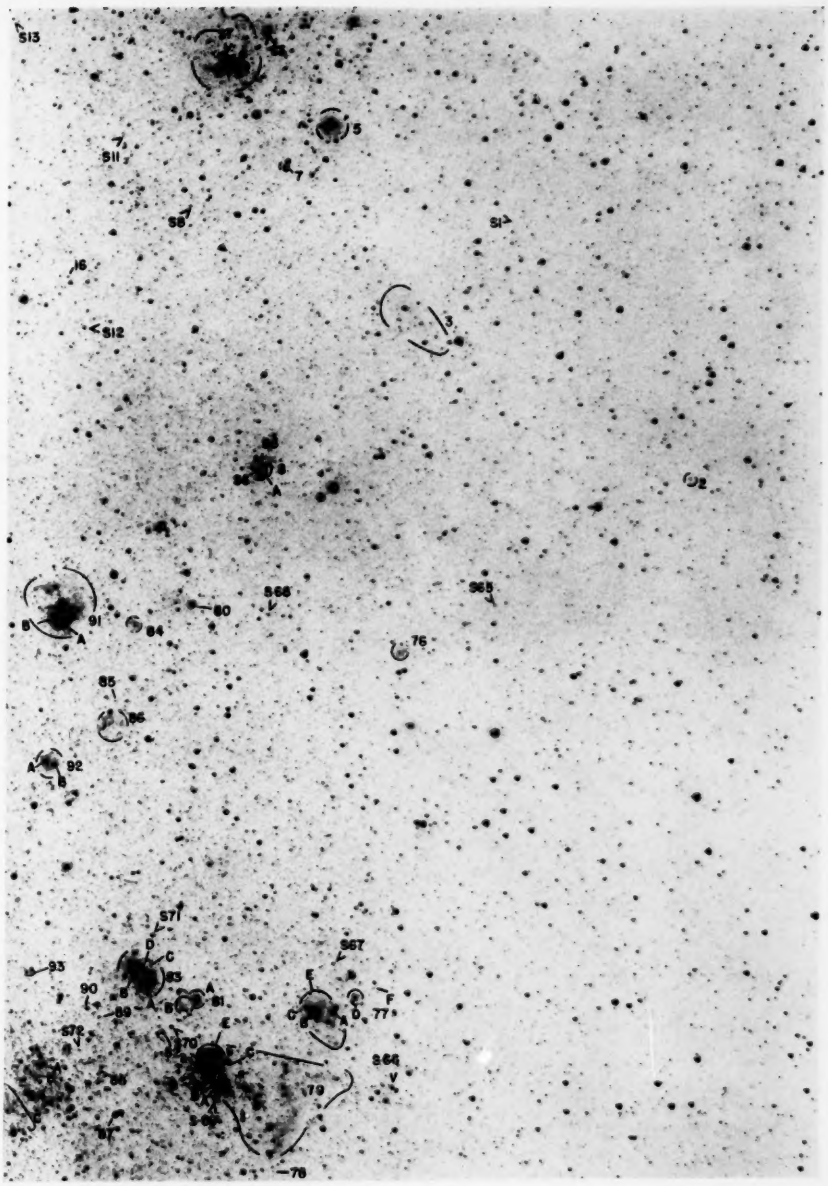

FIG. 1.—Emission stars and nebulae in the Large Magellanic Cloud. *Plate center:* $X = 40$, $Y = 11610$. North is at the top, east at the left.

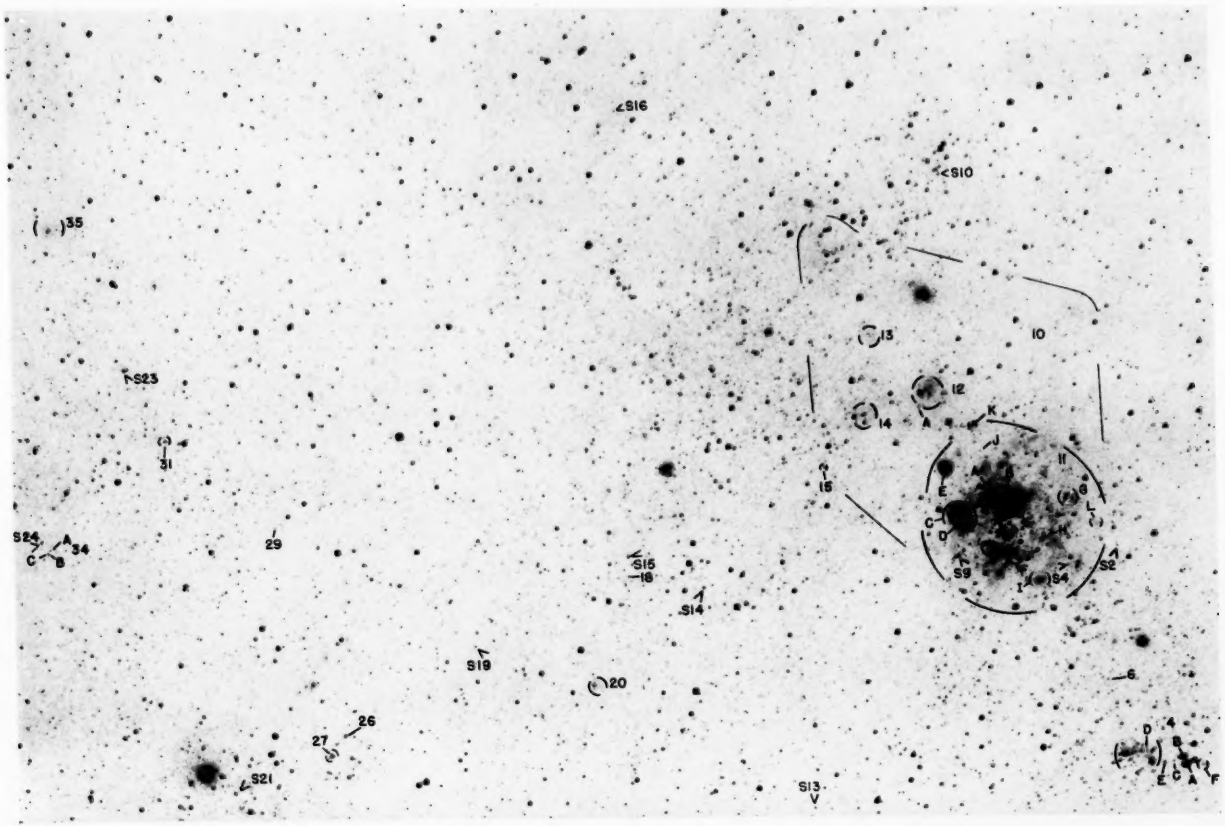

FIG. 2.—Emission stars and nebulae in the Large Magellanic Cloud. *Plate center:* $X = 4760$, $Y = 19520$. North is at the top, east at the left

FIG. 2.—Emission stars and nebulae in the Large Magellanic Cloud. *Plate center:* $X = 4760$, $Y = 19520$. North is at the top, east at the left

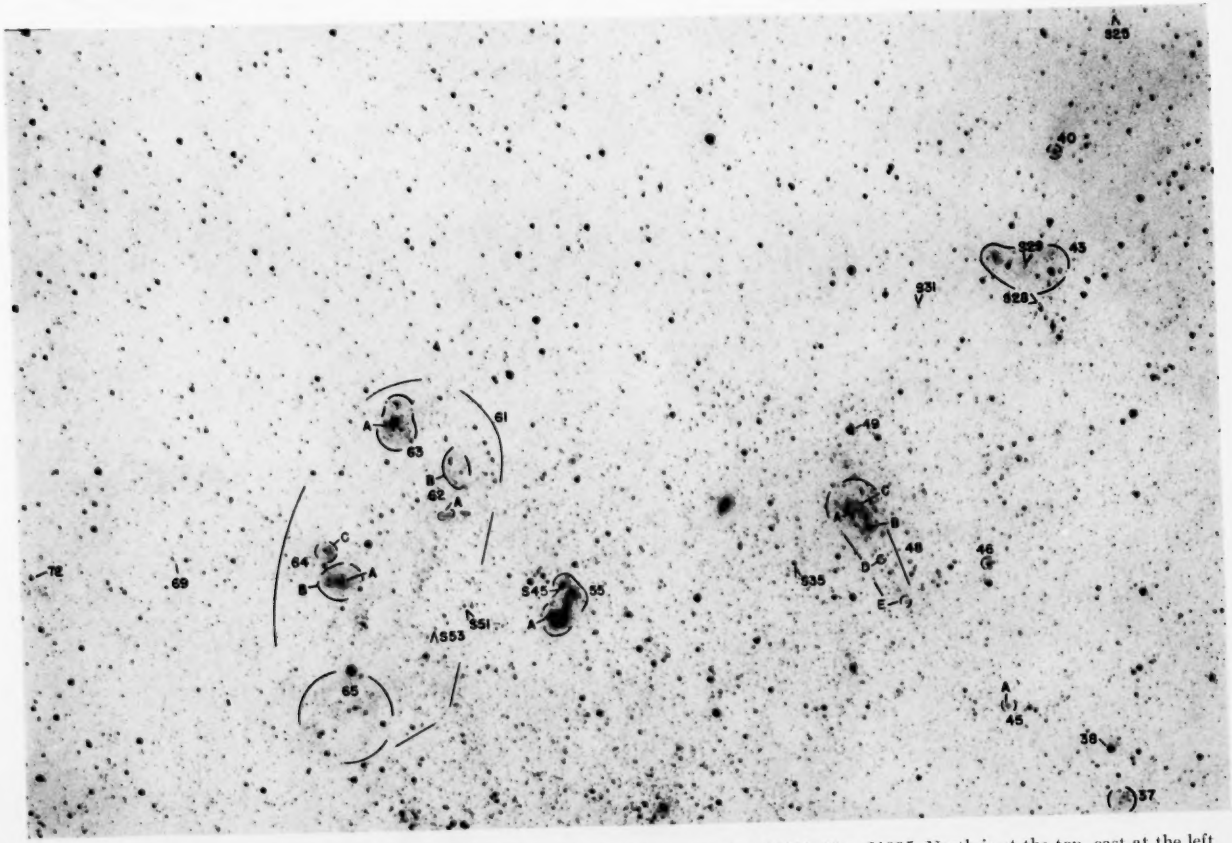

FIG. 3.—Emission stars and nebulae in the Large Magellanic Cloud. *Plate center:* $X = 14010$, $Y = 21005$. North is at the top, east at the left

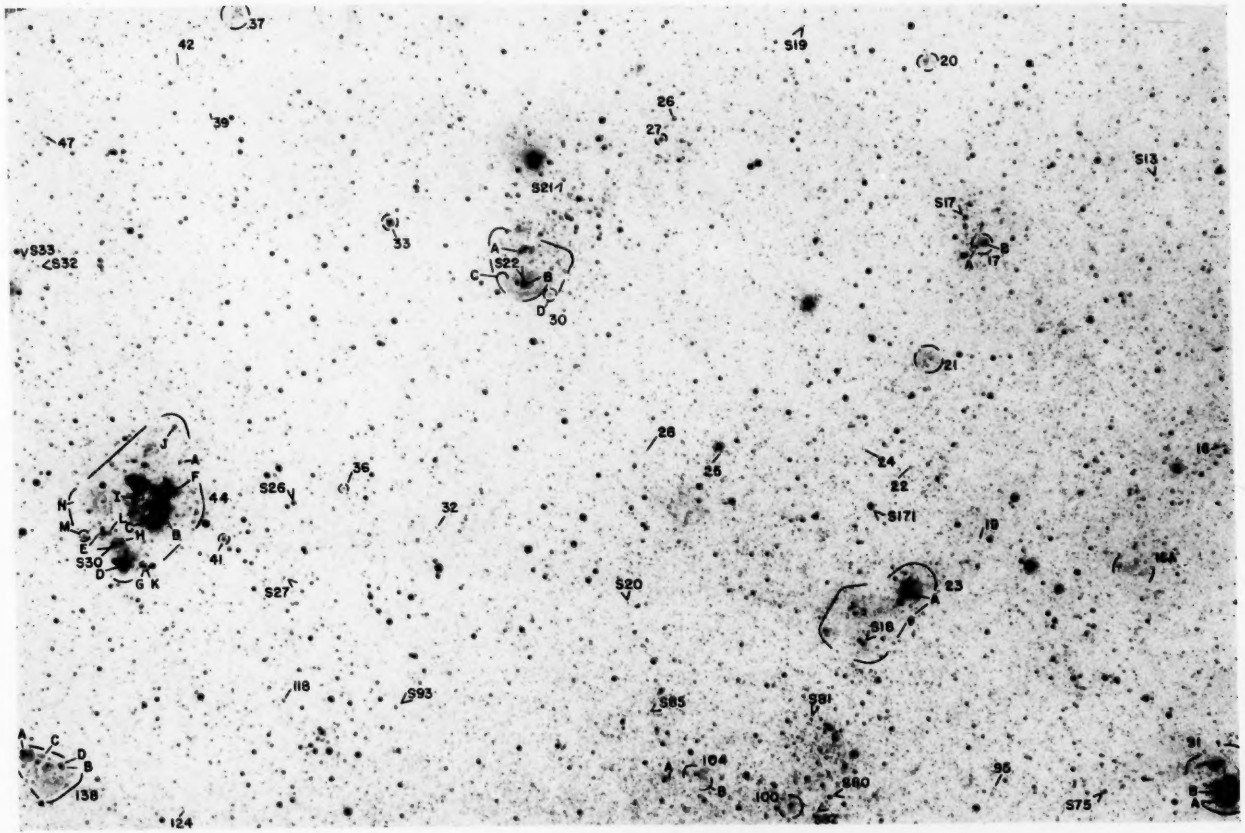

FIG. 4.—Emission stars and nebulae in the Large Magellanic Cloud. *Plate center:* $X = 7355$, $Y = 14605$. North is at the top, east at the left

FIG. 4.—Emission stars and nebulae in the Large Magellanic Cloud. *Plate center:* $X = 7355$, $Y = 14005$. North is at the top, east at the

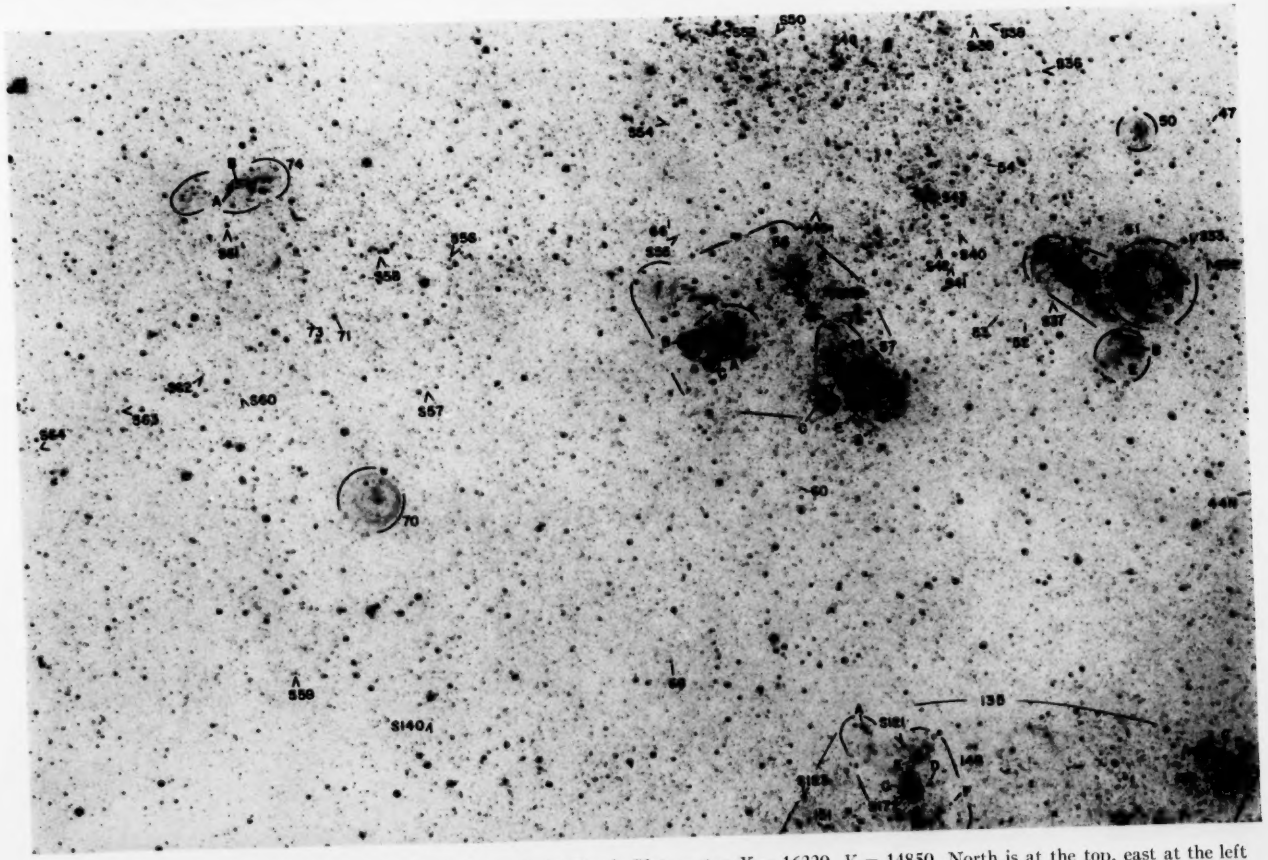

FIG. 5.—Emission stars and nebulae in the Large Magellanic Cloud. *Plate center:* $X = 16220$, $Y = 14850$. North is at the top, east at the left

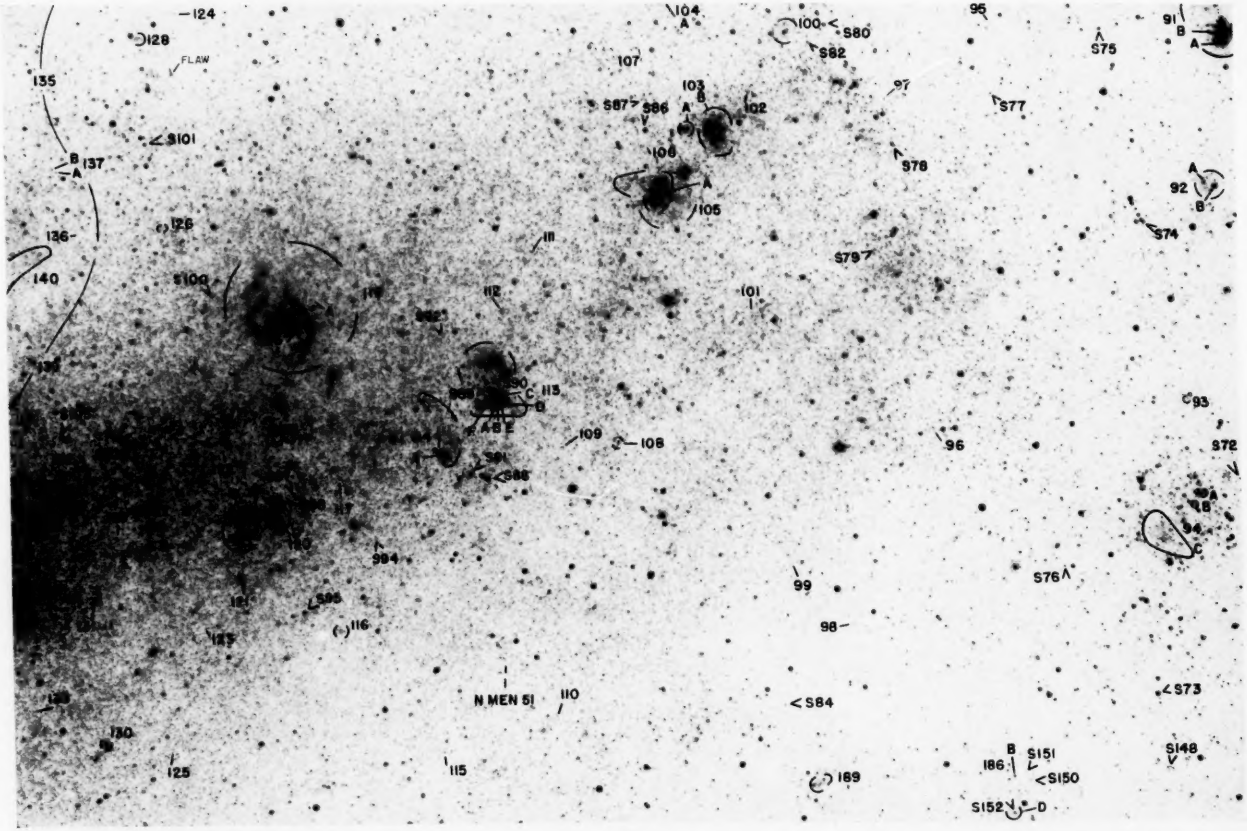

FIG. 6.—Emission stars and nebulae in the Large Magellanic Cloud. *Plate center:* $X = 7425$, $Y = 8545$. North is at the top, east at the left

FIG. 6.—Emission stars and nebulae in the Large Magellanic Cloud. *Plate center:* $X = 7425$, $Y = 8545$. North is at the top, east at the left

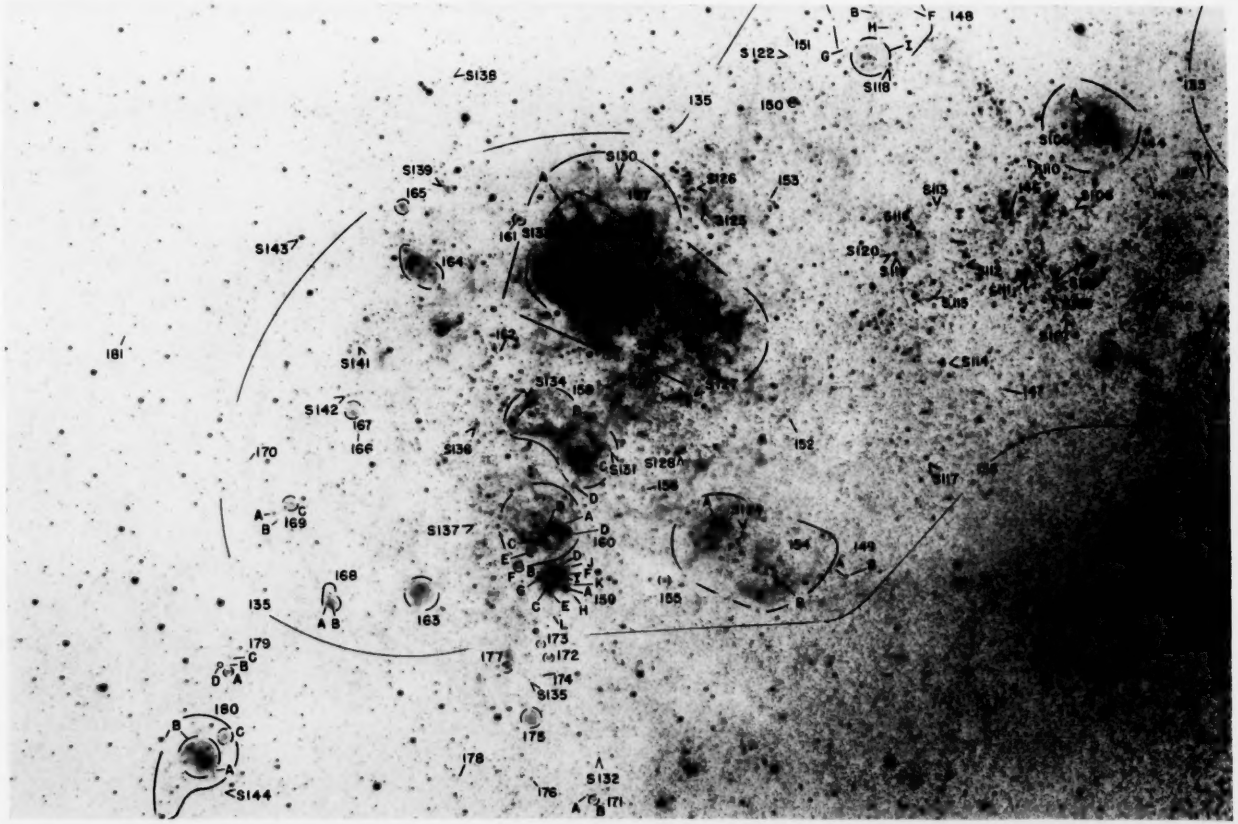

FIG. 7.—Emission stars and nebulae in the Large Magellanic Cloud. *Plate center:* $X = 16285$, $Y = 8785$. North is at the top, east at the left

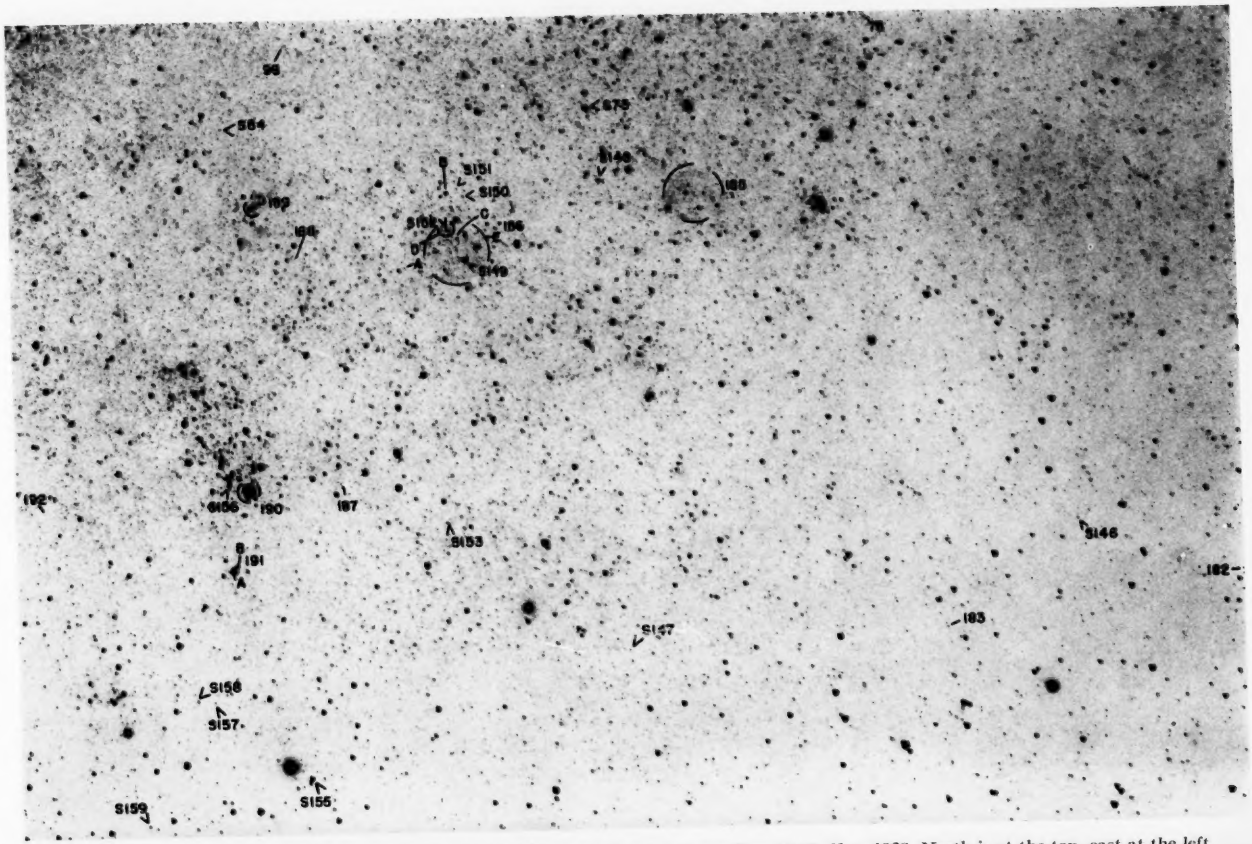

FIG. 8.—Emission stars and nebulae in the Large Magellanic Cloud. *Plate center:* $X = 3110$, $Y = 4020$. North is at the top, east at the left

FIG. 8.—Emission stars and nebulae in the Large Magellanic Cloud. *Plate center:* $X = 3110$, $Y = 4020$. North is at the top, east at the left

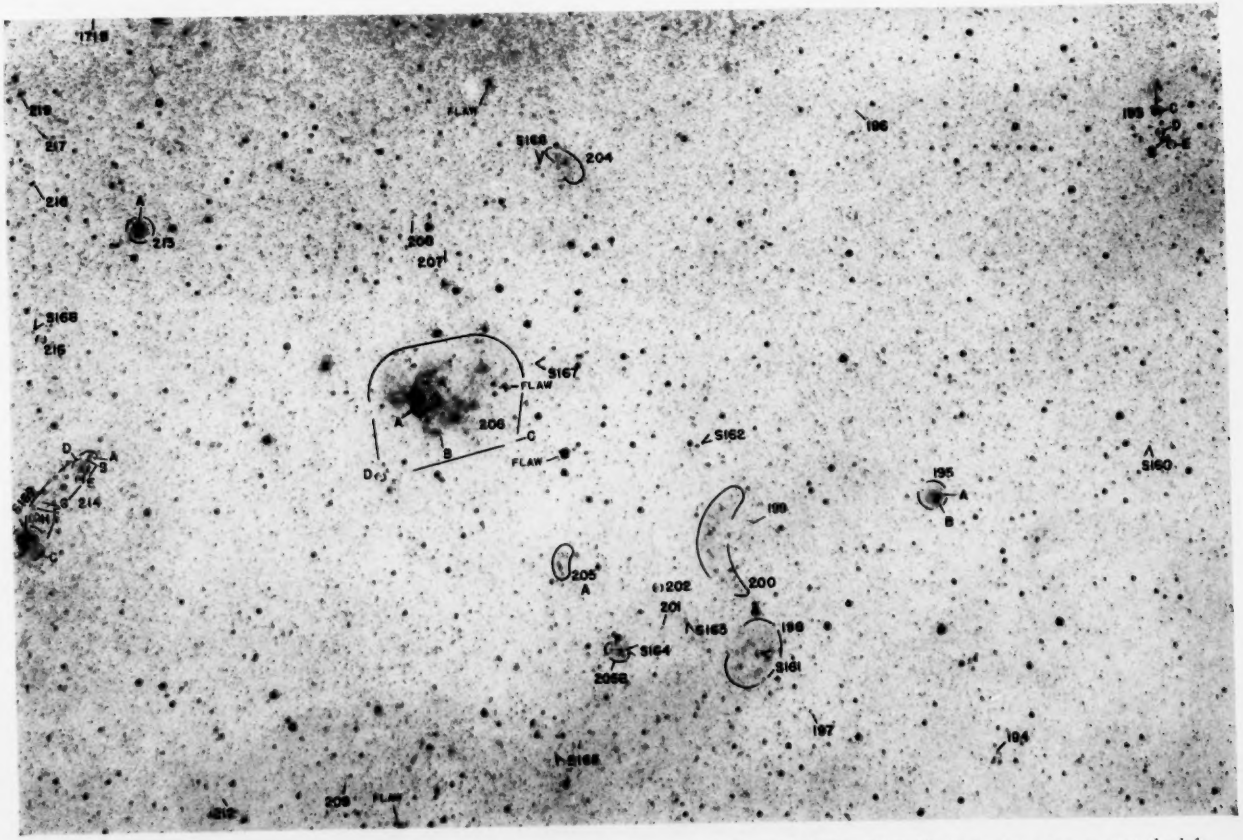

FIG. 9.—Emission stars and nebulae in the Large Magellanic Cloud. *Plate center:* $X = 12540$, $Y = 2650$. North is at the top, east at the left

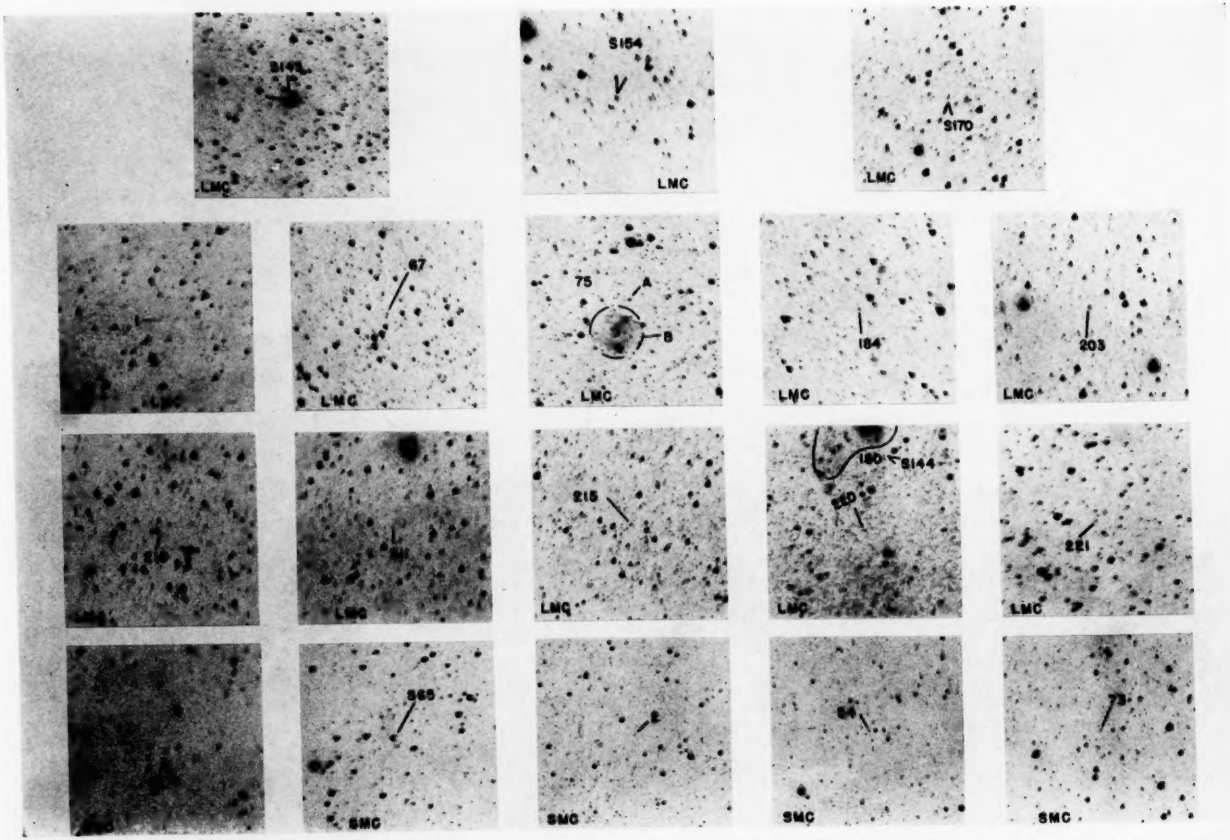

FIG. 10.—Outlying emission objects in the Magellanic Clouds. *LMC* indicates objects in the Large Cloud; *SMC*, objects in the Small Cloud. North is at the top, east at the left.

FIG. 10.—Outlying emission objects in the Magellanic Clouds. LMC indicates objects in the large [illegible]
is at the top, east at the left.

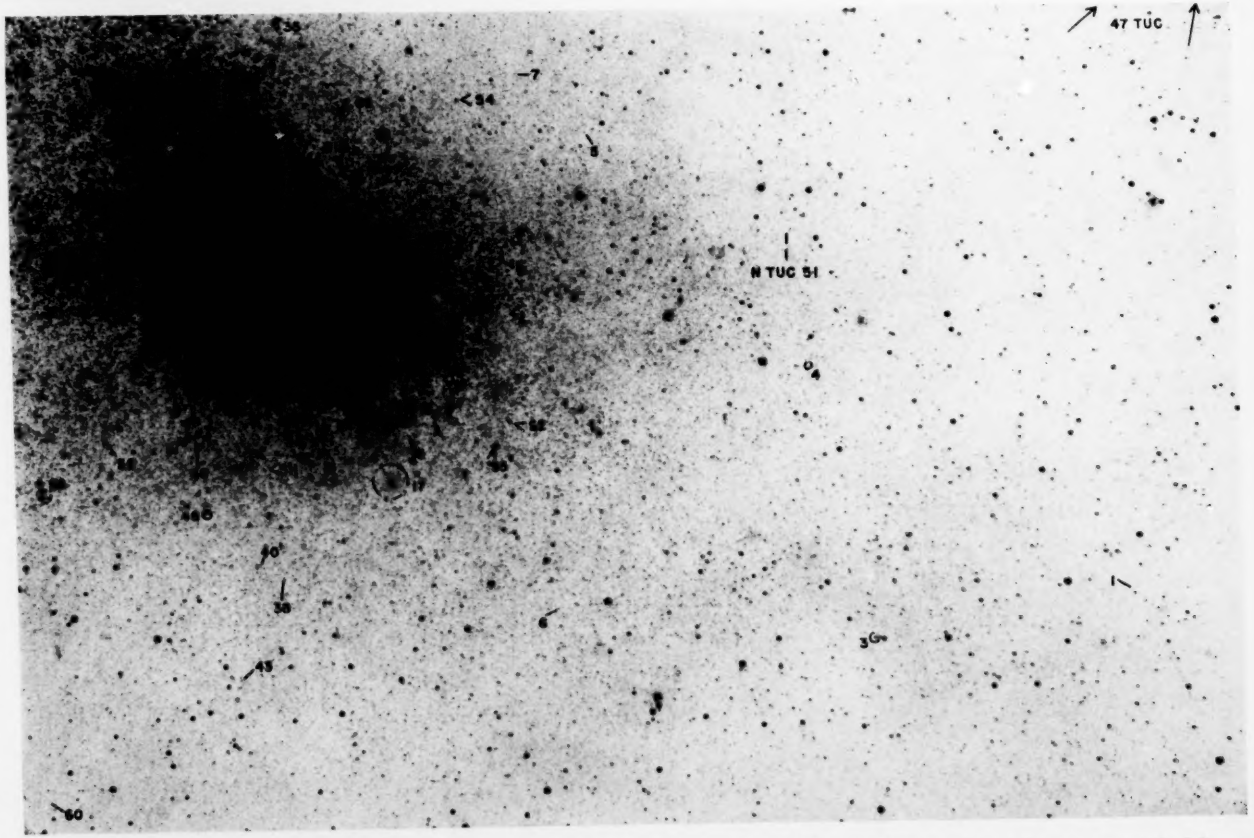

FIG. 11.—Emission stars and nebulae in the Small Magellanic Cloud. *Plate center:* $X = 8940$, $Y = 7430$. North is at the top, east at the left

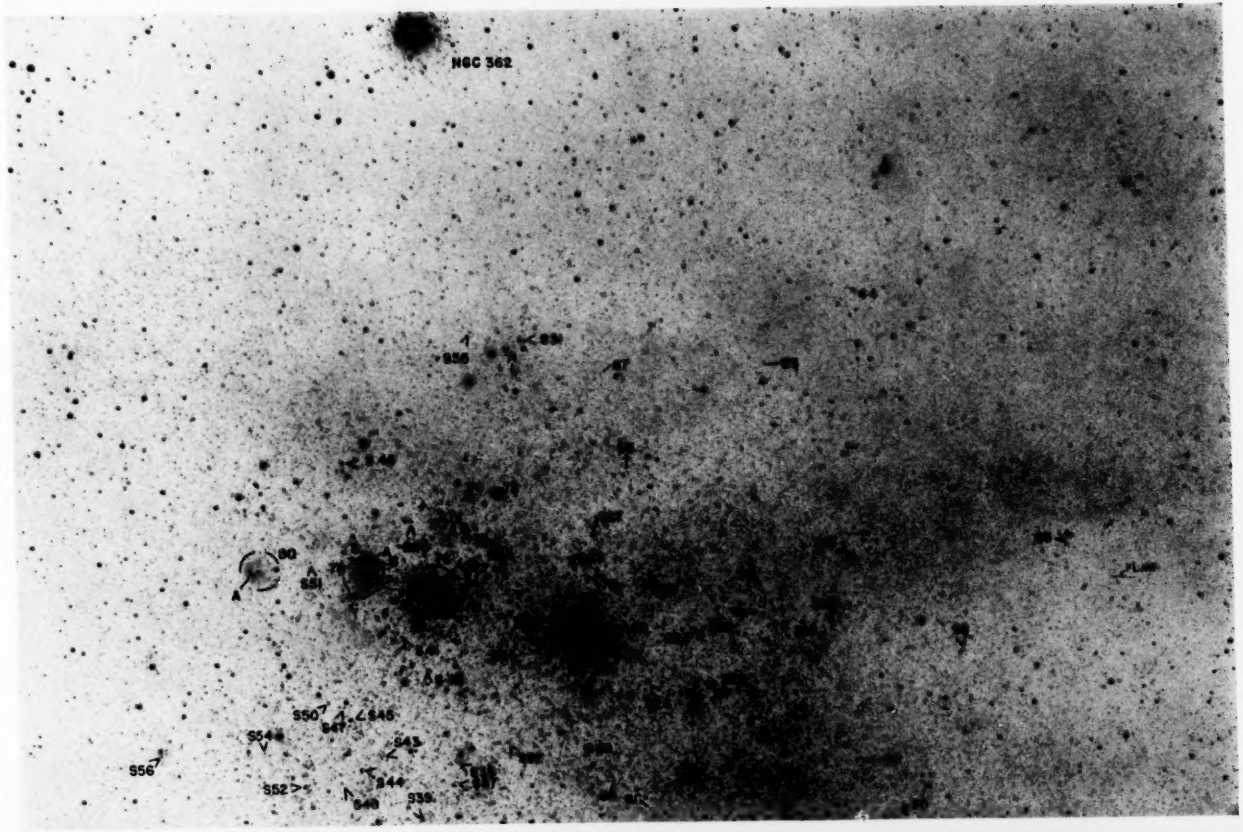

FIG. 12.—Emission stars and nebulae in the Small Magellanic Cloud. *Plate center:* $X = 13775$, $Y = 13635$. North is at the top, east at the left

FIG. 12.—Emission stars and nebulae in the Small Magellanic Cloud. *Plate center:* $X = 13775$, $Y = 13635$. North is at the top, east at the left

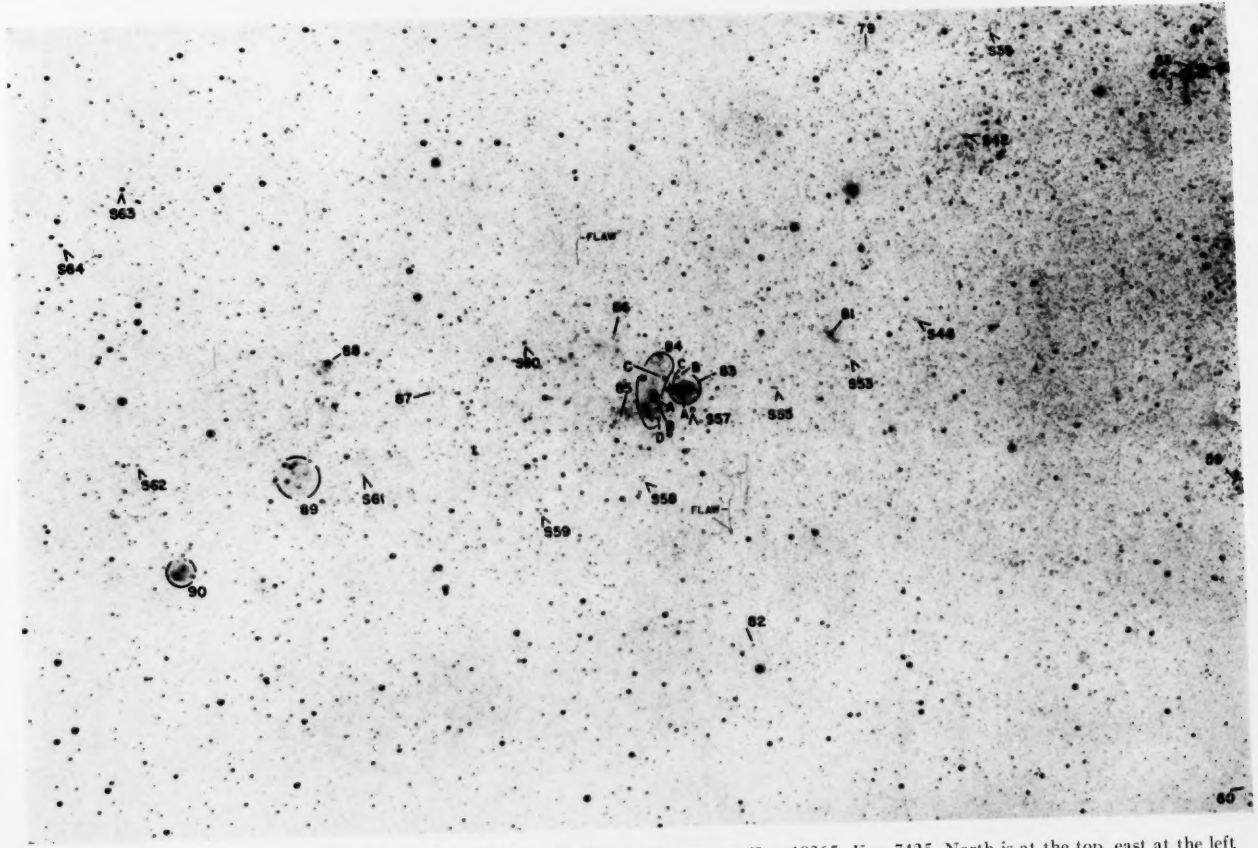

FIG. 13.—Emission stars and nebulae in the Small Magellanic Cloud. *Plate center:* $X = 18265$, $Y = 7425$. North is at the top, east at the left

A PHOTOMETRIC CATALOGUE OF EMISSION NEBULOSITIES IN THE LARGE MAGELLANIC CLOUD

LOWELL DOHERTY,* KARL G. HENIZE,† AND LAWRENCE H. ALLER
University of Michigan Observatory
Received May 5, 1956

ABSTRACT

Widened and unwidened objective-prism photographs covering a narrow wave-length band near Hα have been microphotometered to obtain 285 cross-sectional intensity profiles for selected nebulosities in the central region of the Large Magellanic Cloud. Stellar spectra on the widened plates permitted an approximate absolute brightness calibration of the nebular profiles by the method of Ambarzumian. The profiles have been represented by simple geometric figures, which are described in the catalogue by a system of letters and numerals. Profile widths are given in seconds of arc and peak intensities in ergs/cm²/sec/steradian. The position of each microphotometer trace is shown on accompanying charts. Equivalent Hα stellar magnitudes are given for six Hα-emission stars.

I. INTRODUCTION

The Magellanic Clouds have for many years been the subjects of astronomical investigation by reason of their relative nearness to our own Galaxy. Their characteristics, as galaxies, have been described by Shapley (1950), and, most recently, a new study of their structure has been undertaken by de Vaucouleurs (1955). Optical studies have been augmented by contour mapping of the Clouds in the radio wave lengths, both in the 21-cm line of hydrogen (Kerr, Hindman, and Robinson 1954) and in the continuous radiation at 3.5 meters (Mills 1955). A summary of knowledge of the individual constituents of the Clouds is given by Buscombe, Gascoigne, and de Vaucouleurs (1954). Although certain types of objects have been comparatively well studied, as, for example, the cepheid variables, others have yet to be examined in any great detail. The emission nebulae, which are contained primarily in the Large Cloud, fall into the latter category.

Nebulae in the Large Cloud appear in a rich variety of forms. Some 60 per cent of the nebulae have been classified as "irregular" by Henize (1956, Part I). To give for these emission nebulae an adequate specification of their structure and physical characteristics, more than a qualitative description is necessary. In order to derive the densities and temperatures of the gas, it is necessary to measure the monochromatic surface brightness of each nebulosity on an absolute scale, i.e., in units such as ergs/cm²/sec/steradian; we should also have the relative intensities of the various monochromatic radiations as derived from spectroscopic studies and, finally, the distribution of surface brightness in each image. If the distance and geometry of the nebulosity are known, the emission per unit volume can be estimated. Unfortunately, such detailed information has been obtained only for a few planetary nebulae, and even for these objects reliable distances are not available (Aller 1956).

The observing program described in Part I included a series of both widened and unwidened photometrically calibrated objective-prism plates. These observations are discussed in this paper.

Ideally, each nebula should be described by a set of isophotic monochromatic contours. For this catalogue a less complete, but more practical, method has been employed. We believe that this description is better suited to the complexity of these nebulosities and to their small linear scale on the available plates. We have made microphotometer

* National Science Foundation Fellow in Astronomy (1954–1956).

† Carnegie Fellow at Mount Wilson and Palomar Observatories (1954–1956).

tracings across selected parts of 115 nebulous regions and reduced them, to obtain descriptions in the form of cross-section intensity profiles. Each profile is represented in the catalogue by a combination of letters and digits which permits approximate reconstruction of the original profile by the use of simple geometric figures. The peak intensity is given in ergs/cm^2/sec/steradian, and the position of each tracing is indicated on a chart.

II. THE OBSERVATIONAL DATA

The telescope has been described in Part I. The plate scale was 159″/mm, while the 15° objective prism gave a dispersion of 450 A/mm at Hα. A Plexiglass 160 filter (red) combined with a 103*a*-E emulsion limited the spectrum to the immediate neighborhood of Hα and shortward about 500 A. The peak sensitivity of this particular plate-filter combination lies to the shortward of Hα at about λ 6400. In the photometric measurements we have used four plates exposed on a common center. The series included one unwidened and one widened plate at each of two exposure times, 300 and 75 minutes. The 300-minute exposures favored the fainter nebulosities; the 75-minute exposures brought out only the brighter features. Calibration exposures were impressed with a tube sensitometer built into the telescope and utilizing the same filter. The calibration exposures were impressed on a clear portion of the plate. Because of the narrow band pass of the plate-filter combination, we may suppose that the transmitted sky background has essentially the same color as the light registered in the spots.

If a pair of widened and unwidened plates is calibrated and developed under exactly the same conditions, the two spectrograms should be photometrically equivalent. In particular, widened stellar spectra on one plate should permit the absolute calibration of nebular surface brightnesses on the other by the method of Ambarzumian (1933). Since one of the plates is widened by a slow drifting, whereas the other is not, reciprocity failure may introduce a small zero-point error. Hence a photoelectric check on the surface brightnesses of a few objects would be desirable.

It was not possible to develop the four plates of the series together, but they were processed under as nearly similar conditions as possible. In order to test the photometric equivalence of the plates, we compared tracings made on both widened and unwidened plates on regions that appeared broad and uniform. That is, we selected portions of nebulosities whose surface brightnesses would not be much affected by widening. From the plate pair with the 300-minute exposure we selected six common regions of moderate density and measured surface brightness ratios ranging from 0.74 to 1.16, with an average of 1.03. Hence we may suppose that these plates are equivalent. The 75-minute exposures showed only the brightest features, which were generally compact knots, and the Loop Nebula, although quite extensive, has a sharp filamentary structure. There were no really satisfactory regions for comparison of the two plates, but the unwidened plate appeared systematically weaker. This conclusion was substantiated by the smaller γ of the characteristic curve of the unwidened plate, and it was concluded that, because of evident differences in development, the unwidened plate could not be calibrated by its companion. In order to make usable the profiles derived from the unwidened plate of shorter exposure, the latter was compared against the 300-minute unwidened plate. Three broad features whose intensities were such as to make them measurable upon both exposures gave a ratio between the intensity scales of the two plates of 7.6 ± 0.7. The ratio for equivalent plates, of course, should have been 4, barring reciprocity-law failure. In the catalogue, brightnesses derived from the shorter exposure are marked by asterisks. These form a "secondary" set of profiles, in that their calibration is based on nebulae (which were directly calibrated) rather than on a comparison to stellar spectra. The (*) system of intensities comprises about one-third the entries in the catalogue.

The Intensity Measurements

All the plates were traced with the photoelectric densitometer of the McMath-Hulbert Observatory. The reductions of the tracings were carried out in the conventional way. In each case it was necessary to subtract the night-sky background (which remains rather constant over a given plate) or, in the case of small condensations superposed on an amorphous background, the surface brightness of this diffuse background also. Specific examples of the latter situation will be given shortly.

In tracing the widened spectra, we made the length of the analyzing slit equal to the width of the stellar spectra. If we select stars of the same spectral class as the sun and also measure on the same plate a group of nebulosities, we may transform the arbitrary zero point of the scale of surface brightnesses to c.g.s. units by the method of Ambarzumian. That is, the spot sensitometer calibration establishes the scale of relative surface brightnesses, but the zero point must be fixed by comparison with stars of known magnitude and color.

Since the effects of differential extinction are negligible in such a small area of the sky in this region of the spectrum, we may employ directly the equation of Ambarzumian, viz.:

$$\log \frac{S}{S^0} = \log \frac{I}{I^*} - 0.4\,(m^* - m^0) + \log H\,,$$

where S and S^0 are the surface brightnesses of the nebula and sun, respectively, in a 1 A interval at Hα; I is the measured nebular intensity reduced to one square second of arc; I^* is the measured intensity at Hα in the widened stellar spectrum, reduced to an interval of 1 A; m^* and m^0 are the apparent magnitudes of the star and sun, respectively; and H is the area of the sun's disk in square seconds of arc.

In practice, since the plates are photometrically equivalent and the intensities are referred to the same calibration spots, the analyzing slits need not be identical for both plates, but the slit dimensions for the widened plate must be used in the reductions. For the 300-minute widened plate the average spectrum width was 30″, and the slit width used was 2″.8 or 7.9 A. Ten stars identified as G0 in the *Henry Draper Catalogue Extension* were traced to obtain I^*. Their photographic magnitudes ranged from 11.2 to 12.0. Since Hα fell on the steep slope of the photographic spectrum, it was difficult to measure accurately the intensity at this point. After correction for magnitude differences, seven stars fell into a group with about 5 per cent r.m.s. deviation; the remaining three departed considerably from the average and were discarded. The value $m(pv) = -26.84$ for the sun was taken from Kuiper's discussion (1938). With a color index of +0.50, we have $m^0(pg) = -26.34$. The solar surface brightnesses given by Mulders (1935) were interpolated graphically to obtain the Hα intensity 2.88×10^6 ergs/sec/cm^2/A per unit solid angle at the center of the disk. This value was corrected with the factor $I_0/F = 1.21$ taken from the limb-darkening values adopted by Minnaert (1953), so that $S^0(\text{H}\alpha) = 2.39 \times 10^6$.

Nebular Tracings

The tracing deflection associated with a given point on the photographic plate is determined by the plate density integrated over the area of the analyzing slit. Since the effect of averaging variations in plate density cannot easily be allowed for, it is necessary to make the slit sufficiently small that density variations can be treated as simple intensity variations, if it is desired to obtain an accurate profile. On the other hand, the plate grain sets a lower limit to the slit size for a desired amplitude fluctuation in the tracing. The slit dimensions finally chosen for both unwidened plates were 7″.8 × 13″. The use of a rectangle permits better resolution in one direction, which is desirable for narrow

filamentary structures. Since, for convenience, all tracings were run parallel to the dispersion, features were selected whose orientation permitted the rectangular shape to be used to advantage. That is, despite the smaller slit dimension in the direction of the tracing, the final effect of the smearing will be greater than in the other co-ordinate. In this direction the influence of the integration over the slit can be judged more accurately from the profile. In general, however, this effect is small; no corrections have been made to any of the catalogue objects for smearing by the slit or by "seeing." The latter can be estimated from the widths of the stellar spectra and is less than the slit area. Beyond the central region of the plate, coma and ultimately astigmatism affect the image quality, as can be seen by inspection of the stellar spectra.

In certain nebulosities the effect of the finite resolution of the microphotometer is significant. Many bright, symmetrical knots are only two or three slit-lengths in diameter. Some of their observed extent may be produced by seeing, so that the real nebula is appreciably smaller and of higher surface brightness. Those knots which had diameters between 20″ and 30″ and showed little change in size on plates of shorter exposure were considered as "extended" nebulae. The true surface brightnesses of such objects must necessarily be larger than the values we have listed, but observations with larger telescopes will be required to make the necessary corrections.

Intrinsically small objects, not much (if any) larger than stars on our plates, show smaller dimensions on the shorter exposures than on the longer ones. The integrated brightnesses of such essentially stellar nebulosities may be measured on the plates with widened images. For these objects we have given the apparent magnitude of a G0 star which would contribute an amount of energy in 1 A of its continuous spectrum at Hα equivalent to the integrated Hα brightness of the small nebulosity. Emission-line stars with weak continua may occasionally be mistaken for such nebulosities.

The measured intensities are affected by other errors that do not depend on the geometry of the nebulosity involved. Bright features that fall high on the shoulder of the deflection–log I curve can be estimated only with difficulty. A minimum value of the surface brightness is tabulated and is indicated by a colon (:).

The establishment of the zero point is difficult because of inaccuracies in the magnitudes, spectral types, and colors of the reference stars, on the one hand, and the previously mentioned influence of reciprocity failure, on the other. Reciprocity failure affects the widened stellar exposure but not the exposure of an extended nebula. A photoelectric check of the zero point with a red-sensitive cell should be easy, at least for some of the brighter objects.

Scale errors in the system of emission-line intensities could arise from inaccuracies in the calibration-curves and from the influence of sky fog. In his photometric investigations of external galaxies, Holmberg (1950) found that the spot calibrations did not agree with the calibration secured from out-of-focus images of stars in standard sequences. The interpretation placed on this discrepancy was that the spot exposures, which did not include the influence of the sky fog, gave false results. Holmberg's observations, however, embraced a large range in wave length, so that the color of the sky fog differed from that of the calibration spots. In our procedure this difficulty is minimized by a narrow band pass and filter combination. The color of the sky can differ only slightly from that of Hα or the calibration lamp.

III. THE CATALOGUE

Profile Representation

The unreduced tracing profile for each nebular cross-section is approximated by straight lines in such a way that the profile can be represented by groups of triangles and trapezoids. Where the background beneath a particular feature is sloping, widths are measured after projection onto the horizontal, unless the background is included in some

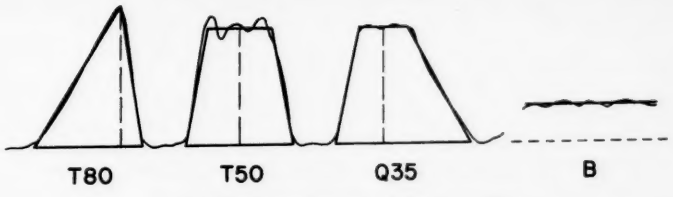

FIG. 1.—Representation of simple profiles

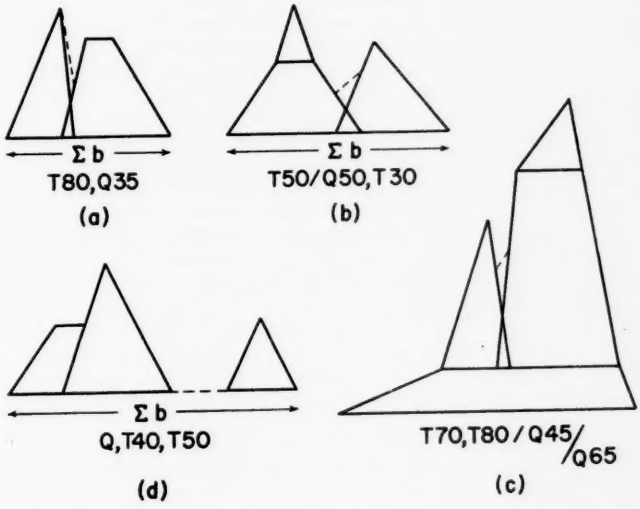

FIG. 2.—Methods of combining simple descriptions for the representation of complex profiles

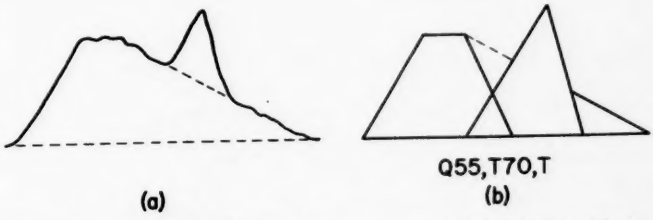

FIG. 3.—Comparison of an observed profile for two superposed nebulosities (*a*) with the chosen catalogue description (*b*).

larger description. All widths are given in seconds of arc, and the required vertical dimensions are given in units of surface brightness. After reconstruction, size and brightness at any point of the profile can then be read directly from the plotted curve.

The shape of each simple part of the synthesized profile is represented by a letter and number pair. Call this a "component description" or "CD." The components are then combined graphically according to the tabular grouping of the CD's into a total profile description or "PD." The letter *Q* indicates a trapezoid; if no other component is to be superposed, it is understood that the feature is not perfectly uniform but shows slight brightness variations. The letter *T* may be a triangle or trapezoid; it distinguishes features with sharper peaks. The brightness of a *T* feature with a large upper width will be an average of several peaks and valleys. *B* is a region of more or less uniform brightness without well-defined boundaries. The numerical part of a CD refers to the asymmetry of the component. If horizontal displacement is measured from one end of the base in the same direction as the tracing was run, then the asymmetry number is the ratio of the displacement of the center of the upper width to the base width. The ratios are given to two figures, rounded off to 0 or 5. *B*, of course, appears without a number. Figure 1 illustrates the representation of simple profiles.

Where the descriptions are combined, the following rules apply:

1. *CD's connected by commas.*—The components are constructed on the same base line and may or may not overlap. The displacement (from the first component) of the farther end of the base of each succeeding component is listed in the table as Σb (see Fig. 2, *a*).

2. *CD's connected by a slant bar* (/).—The components are to be superposed. The right side of the bar is the lower component, and the only part affected by rule 1 (Fig. 2, *b*).

3. *CD group followed by a slant extending to the line below.*—All components preceding the slant are superposed on the feature whose CD appears below (Fig. 2, *c*).

4. *CD consisting of T or Q without numerals.*—The component shares a side with the adjacent component, so that its shape is already determined. Actual cases in the catalogue leave no ambiguity, whether the preceding or following component is attached. The pair is taken as a single component for measuring displacement in a group (Fig. 2, *d*).

5. *CD is a dash* (—).—The component is an integral part of the PD, but the intensity is off-scale, and no shape is given.

After the construction of the figure from the PD, the ordinates are to be added for overlapping components, as is shown in the examples. The use of particular components is not meant to suggest that the actual synthesis of the observed profile occurs by the addition of physical components of those types. For example, the profile of Figure 3, *a*, would probably be the result of superposing a narrow filament and a broad region. For convenience, however, the catalogue representation would be as in Figure 3, *b*. The situation is usually clear from the charts.

The Charts

The photographs, Figures 4–11, are enlargements of selected areas of the unwidened 300-minute plate and show the positions of the tracings. Each nebula is identified by its Henize catalogue number, and Part I is to be used for finding purposes. A single chart is a composite of several sections of the cloud arranged to suit space requirements, so that, although natural grouping is followed as far as possible, it will usually be necessary to refer to the finding charts for relative positions of nebulae.

Each tracing is marked by an arrow. The central section of the arrow is not inked and defines the region in which the tracing was used. Where space does not permit a full arrow, only the arrowhead is shown, but the part traced should be evident. The faint rings 185 and 186 are outlined by dashed lines. If there are two or more tracings in one catalogue region, they are numbered 1, 2, . . . , in smaller figures than the nebula's catalogue designation. Two numbers may apply to one arrow, since the same feature may have been traced on both the long- and the short-exposure plate. Near plate center (see

Part I) the north-south line is defined by the direction of dispersion, and east is toward the top of the chart when it is held in reading position. The scale (roughly 30″/mm) is shown by the line at the bottom of each chart.

The Tables

The numerical section of the catalogue is contained in two tables. The first presents the data for the extended nebulae and has nine columns, three for identification and the remainder for description. The first column ("Ca") lists the Part I catalogue number of the nebula or region of nebulosity and is followed by the number of the tracing within the region ("Tr"). Next is the number of the chart on which the region is reproduced ("Ch"). The fourth column ("PD") describes the nebular cross-section. The succeeding three columns give the width of each component at the base (b) and at the top (t), and the displacement of the component (Σb), all in seconds of arc rounded off to the nearest 5″. In the eighth column is the surface brightness ("S") in units of 10^{-4} c.g.s., and the final column ("rem") contains both the asterisks which designate the secondary brightness system and references to the remarks which follow the tables.

For a complex PD, the b, t, and S values for each component are listed vertically in the same order as the CD's are arranged from left to right. In some cases a number of separated components have the same background and, although B appears several times in the PD, its brightness is given only once, usually on the last line. To save space, long PD's are split and appear on two lines; the situation should be apparent from the Σb values.

To clarify the use of the catalogue, Figure 2, *c*, has been taken directly from the tables as an illustration of the method of profile construction. Table 1 lists the description given in the accompanying table. The nebulosity as described here has four components, three

Cat.	Tr	Ch	PD	b	t	Σb	S
11*e*	2	8	T70, T80/Q45/Q65	50	0		5.4
				50	0		2.6
				90	50		7.1
				220	130		1.6

of which are superposed on the fourth, a broad, faint base whose width is 220″. Further, two of the remaining components are superposed, so that only two elements, T70 and Q45, rest on the lowest component. Since their combined base width, 140″, is greater than the 130″ width upon which they must rest, the two components will overlap slightly. However, no value of Σb is listed, so the components fit exactly on the 130″ given. The absolute surface brightness of the nebula at the point corresponding to the peak of the tracing is then the sum of the component intensities beneath the peak, or $S_{max} = (2.6 + 7.1 + 1.6) \times 10^{-4} = 11.3 \times 10^{-4} \cong 1.1 \times 10^{-3}$.

Table 2 lists the magnitudes, as defined elsewhere, of compact nebulae and Hα-emission stars.

We have not attempted a detailed analysis of the individual objects described in the catalogue. We have estimated electron densities and have discussed the application of the Strömgren theory for those nebulae associated with easily identified illuminating stars (Henize, Doherty, and Aller 1953). The total Hα emission of the Large Magellanic Cloud cannot be estimated accurately from the data presented herewith. Photometrically calibrated isophotic contours would have to be measured for all extended regions of nebulosity.

We are grateful to Director I. S. Bowen, of Mount Wilson and Palomar Observatories, for the loan of the 10.5-inch camera and to the Horace H. Rackham Fund of the University of Michigan which made a grant not only in support of the observational program but also for the cost of publication.

TABLE 2

EQUIVALENT STELLAR MAGNITUDES OF COMPACT NEBULAE AND EMISSION-LINE STARS IN THE LARGE MAGELLANIC CLOUD

Cat.	Ch	Tr	m_a
77*c*	5	5	9.2
82	5	.....	8.5
83*b*	5	2	7.4
89	5	.....	8.9
91*a*	8	4	7.3
113*a*	4	3	8.4
191*a*	5	1	7.8
197	4	.....	10.1
201	4	.....	9.5
218	2	.....	8.6

Cat.	Ch	Tr	m_a
S14	.....	.....	9.1
S44	.....	.....	9.1
S89	.....	.....	8.1
S124	.....	.....	7.4
S142	.....	.....	10.1
S163	.....	.....	9.7

REFERENCES

Aller, L. H. 1956, *Gaseous Nebulae* (New York: John Wiley & Sons, Inc.).
Ambarzumian, V. A. 1933, *Zs. f. Ap.*, **6**, 107.
Buscombe, W., Gascoigne, S. C. B., and Vaucouleurs, G. de. 1954, Suppl. to *Australian Jour. Sci.*, Vol. **17**, No. 3.
Henize, K. G. 1956, *Ap. J. Suppl.*, No. 22.
Henize, K. G., Doherty, L., and Aller, L. H. 1953, *A.J.*, **58**, 215; see also Aller, L. H. 1956, *Gaseous Nebulae*, p. 285.
Holmberg, E. 1950, *Lund Medd.*, ser. II, No. 128.
Kerr, F. J., Hindman, J. F., and Robinson, B. J. 1954, *Australian Jour. Phys.*, **7**, 297–314.
Mills, B. Y. 1955, *Australian Jour. Phys.*, **8**, 368.
Minnaert, M. 1953, *The Sun*, ed. G. P. Kuiper (Chicago: University of Chicago Press), p. 101.
Shapley, H. 1950, *Pub. Obs. U. Michigan*, **10**, 79–84.
Vaucouleurs, G. de. 1955, *A.J.*, **60**, 126–140.

Table 1

SURFACE BRIGHTNESSES AND INTENSITY PROFILES
OF EXTENDED NEBULAE IN THE LMC

Ca.	Tr.	Ch.	PD	b	t	Σb	$S_{(x10^{-4})}$	Rem.
4d	1	8	B				1.3	
e	2		B				0.61	
c	3		T60	45	0		1.5	
b	4		Q45	65	25		4.8	
b	5		T45	70	10		6.3	(1)
a	6		T40	35	0		150.	*
f	7		Q40	85	20		0.82	
f	8		Q35	35	5		1.2	
5		8	Q65	170	15		3.0	
7		8	T50	80	5		2.8	
8		8	T75,T35	35	5		13.	*
				35	0	65	27.	*
9		8	Q50	135	50		0.88	
11e	1	8	T50,T40	80	5		7.5	
				100	30	160	6.5	
e	2		T70,T80/Q45/Q65	50	0		4.5	
				50	0		2.2	
				90	50		5.9	
				220	130		1.3	
d	3		T,T70	55	0		11.	*
				125	0		34.	*
d	4		T55/Q25	45	0		25.	*
				170	45		17.	*
b	5		Q,T45,T40	35	15		12.	*
				45	10		28.	*
				85	25	155	22.	*
b	6		T55/Q80	15	0		22.	*
				125	15		51.	*
b	7		T65,Q	125	0		31.	*
				60	35		18.	*
	8		T30	110	15		3.4	
f	9		T30	105	0		9.0	
f	10		Q55	60	20		2.9	
	11		T40	60	0		4.2	
i	12		T50/Q60	60	10		2.9	
				195	60		1.1	
h	13		T60	35	0		2.8	
g	14		T35	75	5		5.4	
g	15		Q40	75	10		3.0	
13		8	Q60	195	90		0.58	
14		8	Q45	200	135		0.41	
16a		8	T40	160	30		0.76	
17a	1	8	T,T60	40	0		1.6	
				30	0		9.1	

Table 1 - Continued

Ca.	Tr.	Ch.	PD	b	t	Σb	S (x10^{-4})	Rem.
b	2		Q,Q40	25	10		2.2	
				55	10		4.3	
b	3		T65	100	30		3.2	
20		8	T30	70	10		2.5	
21		8	Q35	120	30		1.1	
23a	1	8	T,Q40	105	0		2.2	
				150	50		6.7	
a	2		Q,T45/Q60	20	20		1.9	
				60	20		1.2	
				165	60		4.4	
26		7	T50	35	0		6.7	
27		7	T50	60	0		4.4	
30c	1	7	Q50	60	15		1.1	
a	2		T50	50	5		9.6:	
c	3		T60	60	5		1.8	
d	4		T60	65	10		1.3	
d	5		Q60	40	5		1.2	
33	1	7	T50	80	25		7.2	
	2		T60,T45	50	5		8.9	
				40	5	75	8.9	
35		6	T70	135	20		0.90	
36		7	Q40	90	30		0.79	
37	1	6	T55	40	0		2.2	
	2		Q45	55	20		0.61	
38		6	T60	55	0		16.	*
40		6	Q60	125	30		2.2	
43		6	Q50	175	105		1.0	
44m	1	7	Q30	65	15		2.5	
	2		T65	25	0		0.93	
e	3		T45	35	0		22.	*
e	4		T45	55	10		5.6	
l	5		T50	45	15		5.0	
h	6		T50/Q55/B	45	0		9.3:	
				100	45		2.1	
							2.4	
d	7		Q50,Q	115	20		5.7	
				175	90		2.4	
	8		T50	110	50		3.4	
	9		T65/B	40	0		2.2	(2)
			T50/B	35	5	225	3.2	
			T65,T45/B	40	0	275	1.6	
				105	45	375	4.6	
							1.5	
k	10		T45,Q	35	0		18. :	
				15	10		6.9	

Table 1 - Continued

Ca.	Tr.	Ch.	PD	b	t	Σb	$S_{(x10^{-4})}$	Rem.
	11		T45,T45	115	15		11. :	
				220	105	305	9.0	
j	12		T45	50	10		5.9	
45		6	Q50/Q65	55	20		1.3	
				125	55		1.1	
46		6	T55	60	0		5.3	
48	1	6	Q50	225	35		3.6	
c	2		T40	40	0		5.7	
a	3		T45	30	5		4.7	
b	4		Q50/Q55	65	10		6.6	
				125	65		1.9	
d	5		T40	70	5		1.8	
49	1	6	T80/Q50	30	0		1.8	(3)
				65	30		5.1	
	2		Q50	60	20		24.	*
50	1	7	T40	180	0		1.9	
	2		Q50	245	90		1.4	
51c	1	7	Q50	110	20		19.	*
	2		T50/B	60	20		2.6	
							2.8	
	3		Q30	175	55		3.2	
	4		T30	75	5		1.6	
d	5		Q,T70,Q45,T	75	60		1.2	
				45	5		3.2	
				130	15		6.6	
				100	0	340	1.5	
e	6		Q55	60	25		1.4	
d	7		Q45,T55,-	125	15		4.8	
				130	15	220	7.7	
b	8		T40	30	0		15.	(4)*
d	9		T50,Q	40	5		2.6	
				30	25		0.73	
d	10		T80	50	0		1.3	
			T50,Q	90	0		2.1	
				50	50	195	0.88	
			T20	145	0	350	1.2	
d	11		Q65,Q45	190	75		4.2	
				105	20	265	5.1	
55a	1	6	Q40	80	15		20.	*
	2		T50,Q40,T50,T80/B	80	25		1.3	
				100	30	180	1.7	
				65	25	230	3.7	
				50	0	280	2.2	
							2.0	
	3		T50	130	50		4.1	
57c	1	7	T55/Q55,T60	35	0		2.8	
				110	35		2.1	
				65	0	155	3.8	

Table 1 - Continued

Ca.	Tr.	Ch.	PD	b	t	Σb	S (x10^{-4})	Rem.
c	2		T40	85	20		4.4	
			T45	40	0	110	3.5	
d	3		T40	30	0		2.2	
e	4		Q65,T55	75	30		4.4	
				65	35	130	4.6	
a	5		T45	40	0		23.	*
e	6		T50/B	60	5		4.4	
							2.0	
b	7		T45	35	0		6.5	
58		7	Q70	55	10		2.7	
59b	1	7	T65	110	5		21.	*
	2		Q,Q55	65	60		1.5	
				80	15		6.1	
c	3		Q55	90	15		4.9	
a	4		T70,T30	65	0		47.	*
				55	5	105	36.	*
a	5		T75	125	10		58.	*
	6		Q,T55/B	80	65		2.7	
				85	0		12. :	
							2.4	
62a	1	6	T55	30	0		2.7	
a	2		T40	40	0		3.2	
63a	1	6	T60	45	5		33.	*
	2		B				1.4	
64c	1	6	Q50	160	70		2.1	
b	2		T60	50	5		1.9	
70	1	6	T45,T45,Q65	70	0		1.1	
				185	95	255	0.79	
				145	65	375	0.70	
	2		Q,Q45,T45	55	45		1.3	
				90	10		2.5	
				175	65	295	1.8	
			T40,Q35	40	0	370	1.7	
				60	5	420	1.6	
	3		T40	105	50		1.3	
			T55	135	85		1.1	
	4		T50	180	15		3.1	
71		6	T60	45	0		8.0	
72		6	T50	40	0		14. :	
74a	1	6	T50	35	0		7.0	
b	2		T65	30	0		2.5	
76		5	T70	125	30		1.1	
77e	1	5	Q70,T60/Q35	115	10		2.3	
				20	5		1.2	
				85	20	175	1.8	
b	2		T75/Q60	90	0		4.0	
				265	90		3.8	
a	3		T35	20	0		80.	*

Table 1 - Continued

Ca.	Tr.	Ch.	PD	b	t	Σb	S ($\times 10^{-4}$)	Rem.
d	4		T60/Q55	30	0		2.3	
				100	30		2.3	
79e	1	5	Q,-				7.2	(5)
e	2		T55,Q,T	120	30		9.3	
				55	25		5.3	
				175	0		4.0	
c	3		T55	95	0		18.	*
	4		T50/B	40	5		5.5	(6)
							1.2	
			T40/B	45	5	110	2.7	(7)
							1.9	
	5		-,Q				3.4	(8)
a	6		T45	40	0		110.	*
a	7		Q30	90	15		7.8	
80	1	8	T65	85	10		5.7	
	2		T60	75	20		3.8	
81b	1	5	Q50	90	45		1.7	
a	2		T40,Q	60	5		6.4	
				35	20		3.1	
83	1	5	T25	255	0		6.0	(9)
d	3		T,T50	90	0		1.3	(10)
				85	5		2.9	
a,c	4		Q,T40,T50,T50	30	10		2.2	
				45	0		4.8	
				75	15	140	8.9	
				105	10	240	10. :	
84		8	Q50	75	20		1.6	
88		5	T50	35	5		3.0	
90		5	T40	35	0		7.6	
91	1	8	Q45	60	10		1.6	
	2		Q45	55	20		1.7	
			T50/B	30	5	195	3.0	
							1.2	
			T55/B	45	0	250	2.5	
							2.0	
			T50/B	45	10	315	1.2	
							2.3	
b	3		T50,T70,T	50	10		9.6	*
				65	10		30.	*
				60	0	165	16.	*
92a	1	5	T40,T50,Q	75	5		2.7	
				50	60		3.8	
				55	30	160	1.8	
b	2		Q,T50	100	40		2.2	
				80	15		4.1	
94a		5	T30/B	30	0		1.9	
							1.6	
103a	1	4	Q35,Q	75	10		5.1	

Table 1 - Continued

Ca.	Tr.	Ch.	PD	b	t	Σb	S (x10^{-4})	Rem.
				20	15		2.6	
b	2		T50	30	10		2.1	
105		4	T55/Q60,T35	60	25		50.	*
				100	60		25.	*
				45	0	145	36.	*
108		4	T55	45	10		1.7	
112		4	T50	35	0		10.	*
113	1	4	T45	90	5		6.0	
f	2		T65	55	0		23.	*
b,c	4		T45,T60	20	0		23.	*
				55	10	75	27.	*
e,c	5		T50/Q30	100	15		24.	*
				225	100		8.2	*
d,c	6		T45,Q	95	0		31.	*
				45	20		21.	*
d	7		T50,Q	65	5		7.0	
				20	10		5.5	
115		4	Q55	35	10		1.1	
116		3	T30	75	0		2.2	
119	1	3	T40,T15,T50	75	0		4.2	
				120	0	180	3.1	
				105	15	260	9.4:	
	2		T65,T	80	0		23.	*
				190	0		10.	*
120c	1	3	T55	125	25		31.	*
b	2		T50/Q30	25	0		36.	*
				85	25		25.	*
a	3		T50	30	0		35.	*
	4		Q,T50	15	15		4.6	
				125	5		6.0	
d	5		T50	90	35		11.	*
122		3	T50	25	0		5.8	(11)
127a	1	3	Q				4.6	(12)
a	2		T65/Q70	25	0		26.	*
				65	25		24.	*
b	3		T55,T30	20	0		3.9	
				105	40	120	3.4	
128		3	Q50	55	30		0.82	
132g	1	3	Q45	40	10		2.0	
f	2		T55	45	0		2.6	
138a	1	7	T40	35	0		80.	*
c	2		T40	50	5		3.1	
b	3		T65	25	0		15.	(13)*
140		3	Q40	95	25		1.1	
142		3	T,Q55	70	0		1.4	
				70	15		2.1	
143		3	Q50	235	45		2.9	

Table 1 - Continued

Ca.	Tr.	Ch.	PD	b	t	Σb	S (x10^{-4})	Rem.
144	1	3	T70,T45/B	40	0		2.2	
				50	0	85	2.3	
			T20/B	135	0	240	1.6	
							1.3	
b	2		T70	135	20		18.	*
	3		T60,T40,-/Q50	40	15		3.6	
				55	25	85	4.8	
				80		155		
				280	155		1.7	
148a	1	2	T50	35	0		11. :	
	2		Q55	60	25		1.1	
c	3		T,T30	130	0		3.4	
				215	0		7.6	
c,b	4		Q50/B	105	60		2.7	
							1.1	
			T45/Q35	20	0		5.0	
				85	20		2.1	
e	5		T50	30	0		3.2	
d	6		T40	35	5		3.4	
f	7		T45	35	5		3.0	
150		2	T65	30	0		20.	*
154	1	1	T40,T65	70	10		6.3	(14)
				60	0	105	5.6	
	2		T50	105	60		3.9	(14)
	3		B,T75,T15				3.7	
				105	5		7.2	
				120	0	205	5.6	
a	4		T65	35	0		69.	*
	5		Q45,T	70	35		2.8	
				115	90		1.2	
	6		T20,T70,Q	60	0		2.2	
				75	5		2.3	
				45	40	170	0.93	
155		1	T70	75	0		3.9	
156		1	T40	35	0		4.1	
157	1	1	T45/Q35	35	0		4.1	
				80	35		2.6	
a	2		T55,T	185	25		34.	*
				195	0		15.	*
a	3		T55	60	0		24.	*
			T,T40,T70,	65	0		27.	*
			T25,T45/B	75	0	190	83.	*
				55	0	230	130.	*
				45	0	265	110.	*
				55	5	310	35.	*
			T55/B	40	0	410	27.	*
							10.	*
	4		T25	80	0		1.9	

Table 1 - Continued

Ca.	Tr.	Ch.	PD	b	t	Σb	S (x10^{-4})	Rem.
			T50	55	0	190	3.1	
			T50	95	0	330	2.0	
			T45	60	0	380	1.7	
			T50	50	10	455	2.3	
			Q40/B	95	25	595	4.2	
							1.7	(15)
158	1	1	T65	85	10		4.9	
			T55	75	0	275	5.3	
a	2		T45	35	0		100.	*
c,d	3		Q70,T10	50	15		11.	*
				115	5	165	18.	*
			T55	35	0	285	23.	*
c	4		T35/Q45	80	0		52.	*
				325	80		19.	*
b	5		T45	30	0		25.	*
159b,c	1	1	Q35,T35	105	30		14.	*
				90	0	180	57.	*
b,c	2		Q,T55	65	55		18.	*
				30	0		44.	*
			T50,Q45	30	0	150	29.	*
				50	10	195	27.	*
b,c,e	3		T50	120	75		25.	*
			T55	85	5	215	32.	*
			T50	35	5	260	21.	*
a	4		T30	50	0		120.	*
k	5		T55	35	0		3.3	
160f	1	1	T55	60	25		2.7	
c	2		T45	40	0		96.	*
d	3		Q35/Q65	55	10		29.	*
				120	55		13.	*
161	1	1	Q45/Q45	50	10		4.3	
				105	50		1.8	
	2		T45	50	0		6.7	
163	1	1	Q50/Q60	80	30		2.8	
				260	80		2.0	
	2		T60,T60/Q55	75	15		1.9	
				55	0		3.2	
				250	130		2.4	
	3		T45,Q	165	0		5.1	
				40	40		1.5	
164	1	1	T35,Q50	70	0		4.0	
				135	25	200	3.6	
	2		T40,T60/Q50	80	10		4.3	
				100	10		4.2	
				250	155		2.1	
	3		T55,Q50,Q	95	25		4.0	
				95	30		4.8	

Table 1 - Continued

Ca	Tr.	Ch.	PD	b	t	Σb	S (x10^{-4})	Rem.
				90	35	255	4.0	
165		1	T60	100	40		2.6	
167		2	T,Q60	85	0		1.1	
				60	15		3.3	
168a	1	2	T55	30	0		26.	*
a	2		T,T60	135	0		3.0	
				85	15		8.7	
169a	1	2	T60	60	10		3.4	
b	2		T45	35	5		1.9	
c	3		T40	130	15		2.0	
171a	1	1	T35	30	0		2.2	
b	2		T75	100	0		2.1	
172		1	T65	50	0		3.8	
175	1	1	T60	165	60		2.5	
	2		T60	155	50		2.8	
176		1	T60	50	0		4.6	
177		1	Q40	50	15		4.6	
179a,b	1	2	T35,T55	40	0		2.7	
				55	0	95	5.9	
c	2		T40	40	0		1.5	
180b	1	2	B				7.5	*
b	2		T50,Q45	155	60		5.3	
				155	55	270	7.4	
a,b	3		Q,T75,T50	50	30		3.4	
				170	10		8.6	
				45	0	250	8.4	
c	4		T35	115	30		2.4	
c	5		T45	105	45		1.8	
185	1	5	T70	35	5		0.67	
	2		T50	60	50		0.44	
			T50	60	40		0.58	
186b	1	5	T45	40	5		5.3	
e	2		B				0.70	
			B				0.47	
189	1	4	T40/Q55	30	0		1.5	
				105	30		1.9	
	2		T70,T45	40	0		1.1	
				40	0	75	1.9	
190	1	5	Q60,Q	75	25		2.1	
				25	15		1.1	
	2		Q30	80	15		6.0	
	3		T45/B	55	0		3.6	
							1.4	
191a	2	5	T50	55	0		10. :	
b	3		Q50	70	15		2.5	
193a	1	4	T35	20	0		37.	(16)*
b	2		Q35	45	5		3.3	
195b		4	-,T30/Q15					

Table 1 - Continued

Ca.	Tr.	Ch.	PD	b	t	$\sum b$	S ($\times 10^{-4}$)	Rem.
				45	25		2.5	
				145	45		4.0	
198	1	4	Q50	110	15		1.0	
	2		B				1.0	
200		4	B				0.41	
202		4	T50	90	30		0.88	
204		2	Q,Q40	25	15		2.7	
				40	10		4.3	
205a		4	T35	145	15		1.7	
206	1	2	Q45	130	40		3.5	
a	2		T45	135	0		35.	*
a	3		T70,T50,	210	0		4.1	
			T25,T25	180	35	360	8.8	
				125	15	460	4.9	
				130	20	580	3.0	
	4		T,Q50,	115	0		2.4	
			Q35,T30	110	10		5.1	
				380	55	565	5.7	
				80	15	645	4.8	
b	5		T45	45	5		6.7	
213a	1	2	T35	45	0		75.	*
	2		T35/Q60	115	10		3.9	
				195	115		1.3	
214c	1	2	T30/Q35	40	0		32.	*
				185	40		13.	*
d	2		Q55	105	20		3.6	
b	3		T50/B	40	0		8.5	
							1.2	
219		2	T55	35	0		23.	*

Notes to LMC Photometric Catalog

(1) Edge of (b) only; the shape had to be estimated from the overlapping tracing profiles of (b) and (a).
(2) Average background intensity.
(3) O I image.
(4) Small knot; the peak intensity given is too low.
(5) Region north of the stellar spectrum only.
(6) Wisp joining (a) and (b), west of the stellar spectrum.
(7) Region west of the stellar spectrum.
(8) Nebulosity south of (a).
(9) The nebulosity extends south "under" the intense knot b; the profile does not include the knot.
(10) Region north of (a) only.
(11) Small knot; the peak intensity given is too low.
(12) South shoulder of (a) only.
(13) Small knot; the peak intensity given is too low.
(14) This region is not specifically numbered in the Henize catalog (Part I); but here it has been included under 154.
(15) Average background intensity.
(16) Small knot; the peak intensity given is too low.

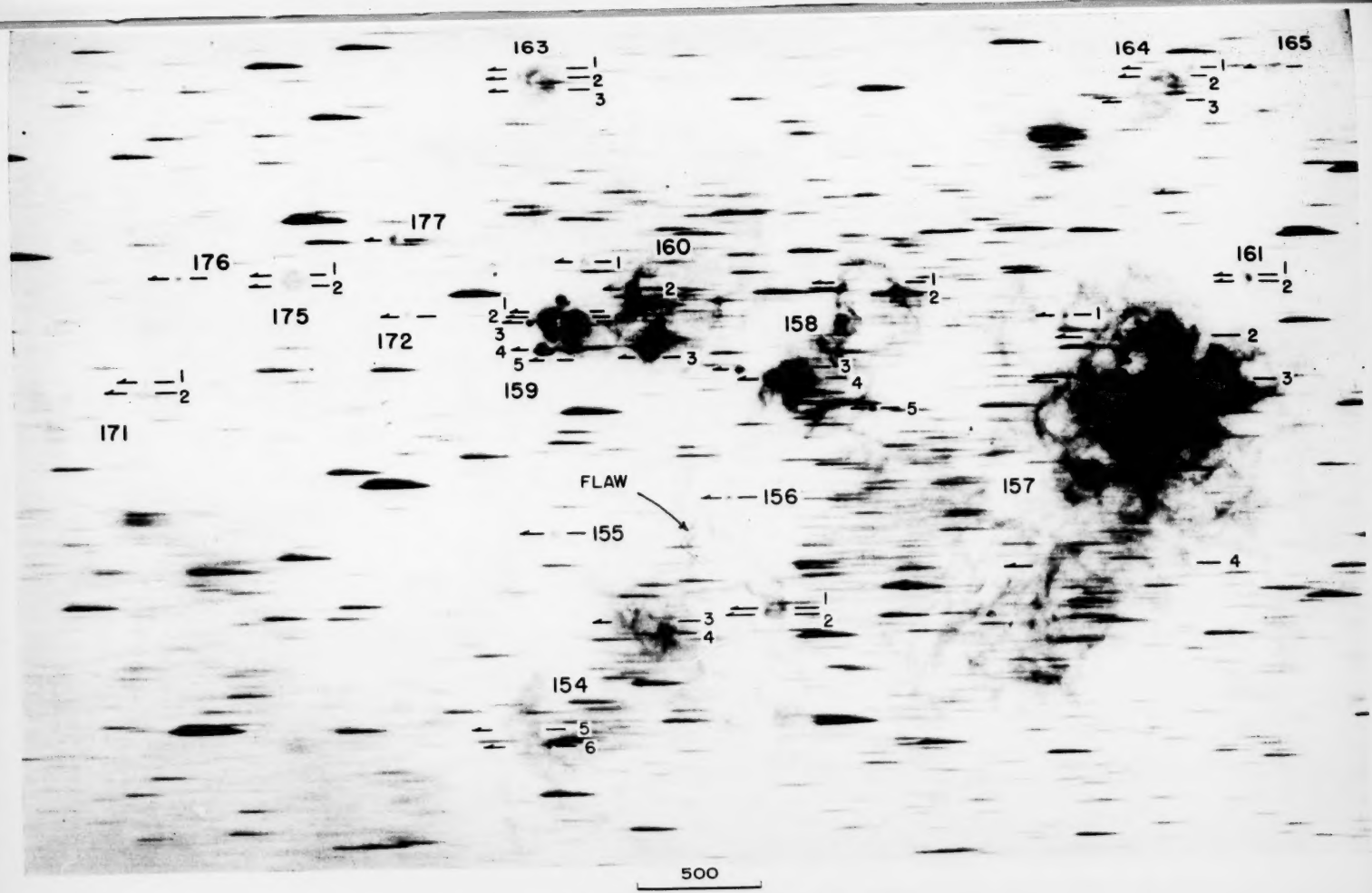

FIG. 4.—Positions of LMC microphotometer tracings. Chart 1

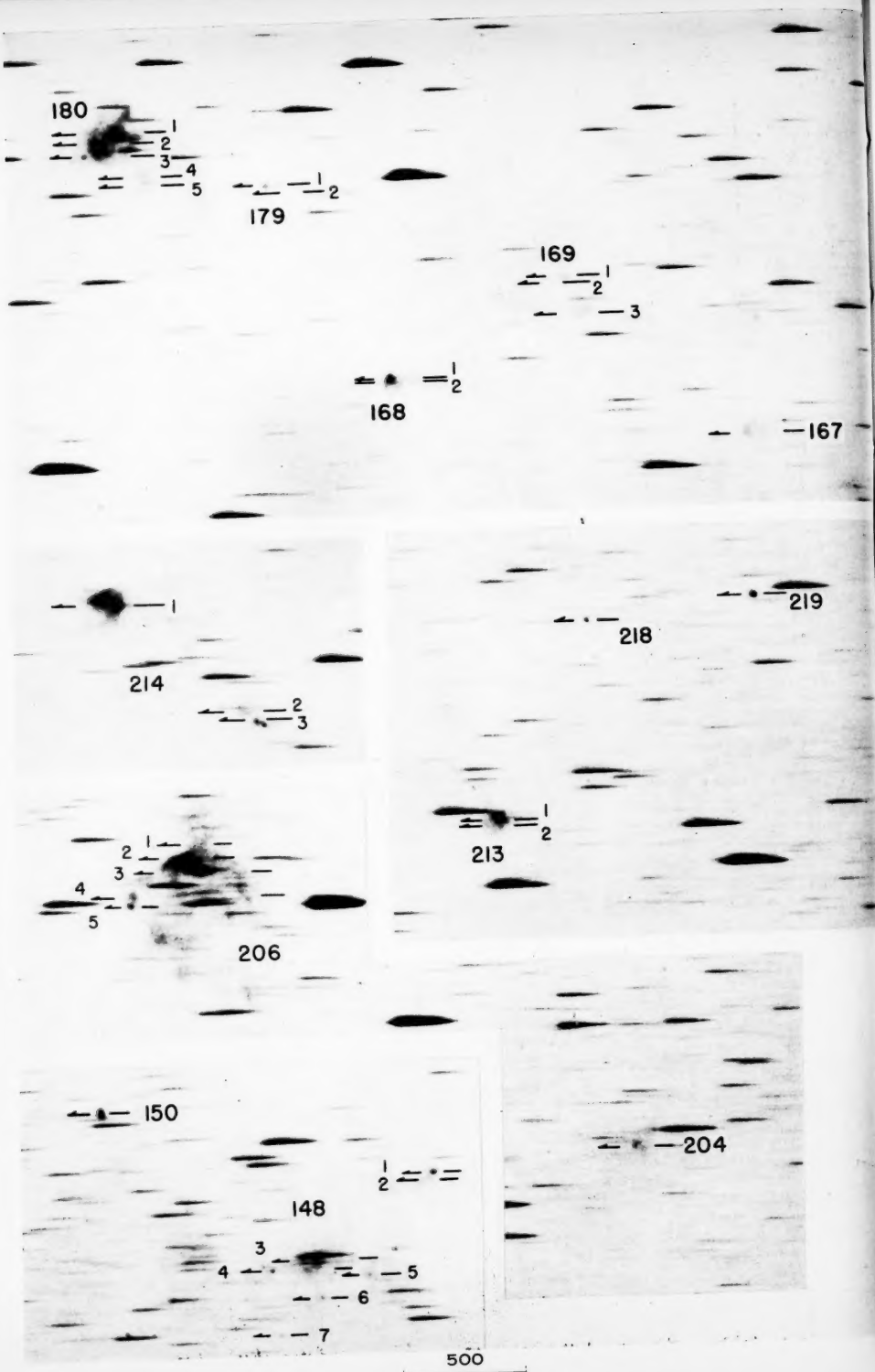

FIG. 5.—Positions of LMC microphotometer tracings. Chart 2

FIG. 6.—Positions of LMC microphotometer tracings. Chart 3

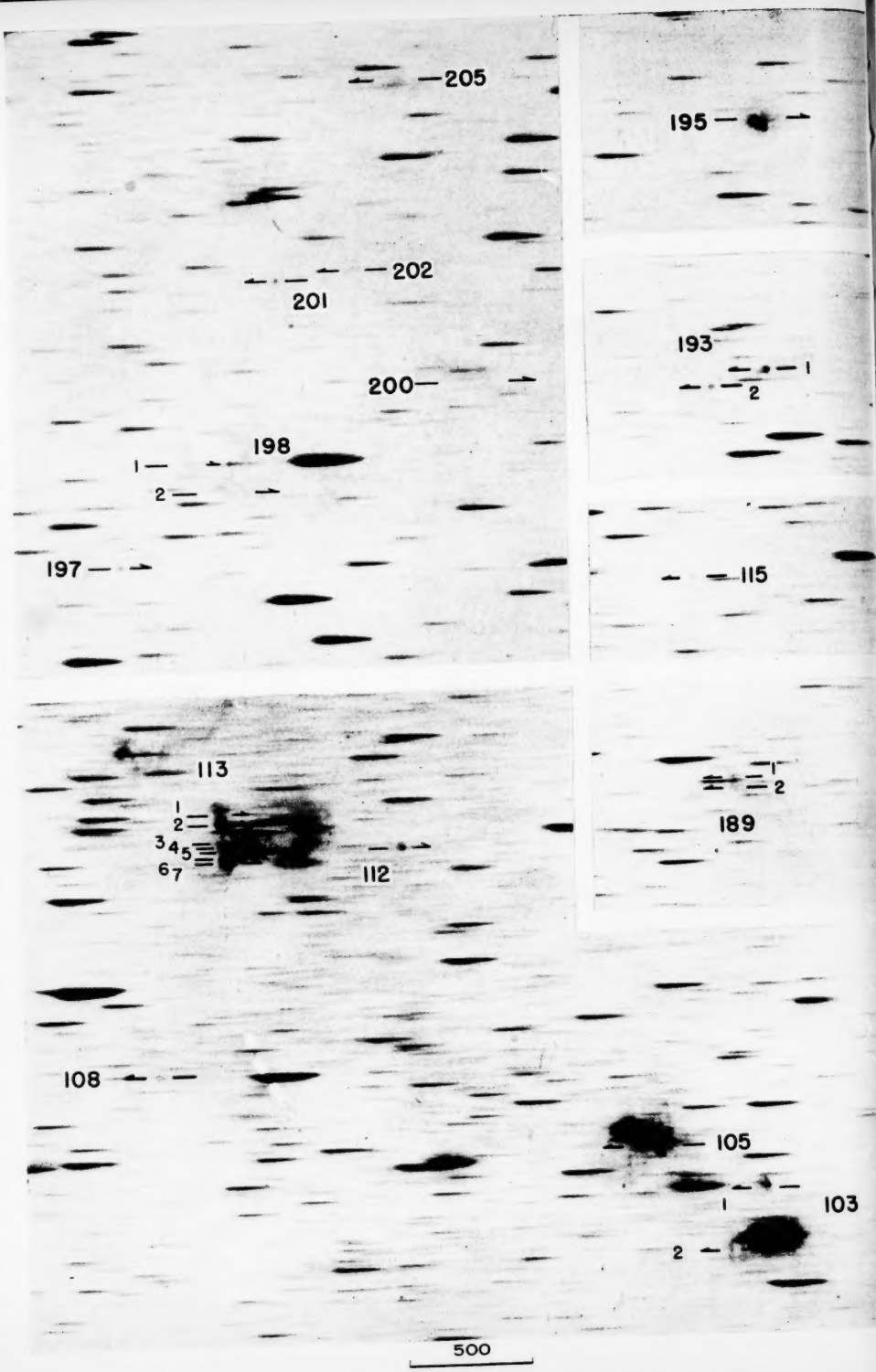

FIG. 7.—Positions of LMC microphotometer tracings. Chart 4

FIG. 8.—Positions of LMC microphotometer tracings. Chart 5

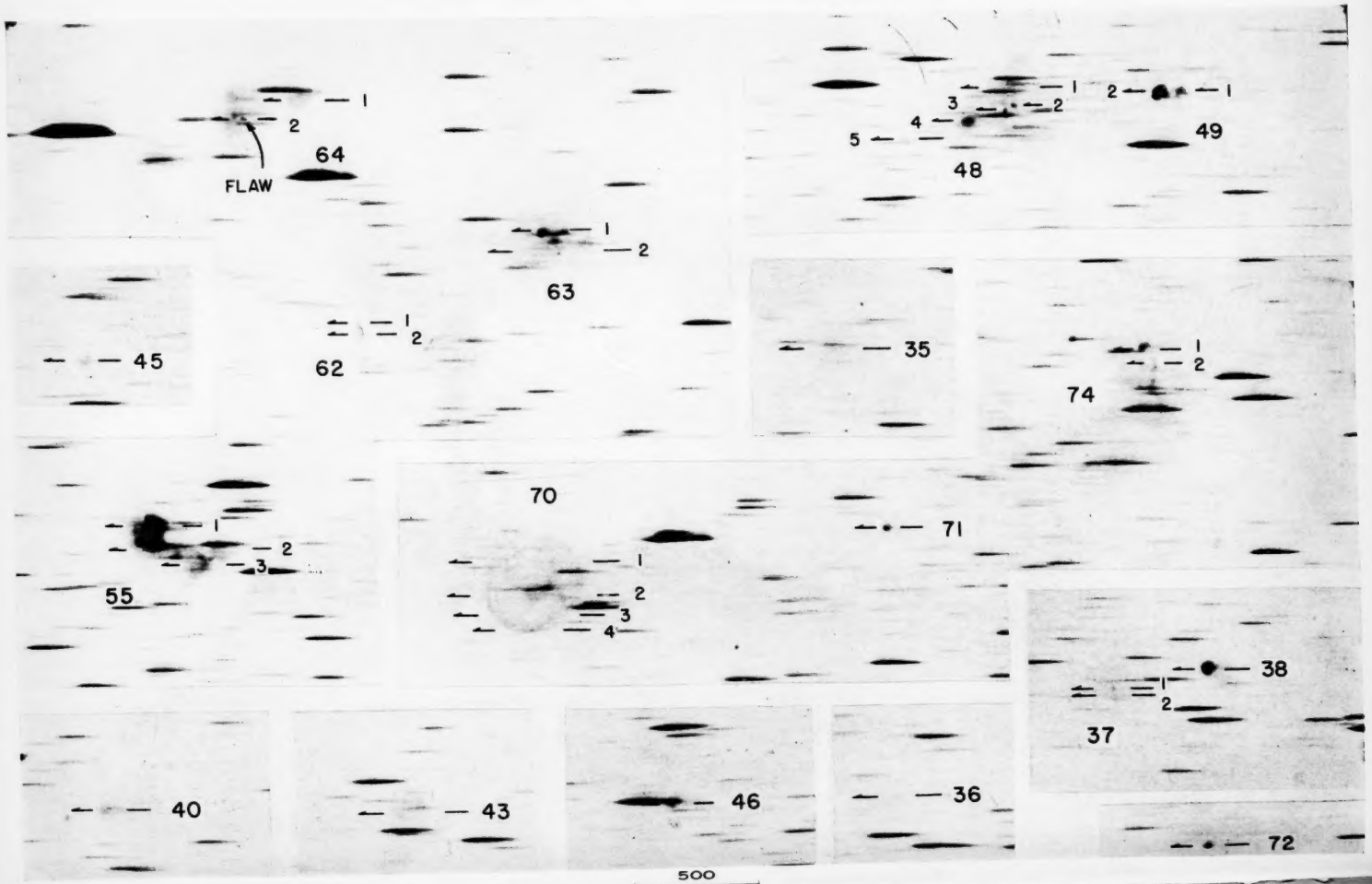
FLAW
64
63
62
48
49
45
35
74
70
71
55
38
37
40
43
46
36
72
500

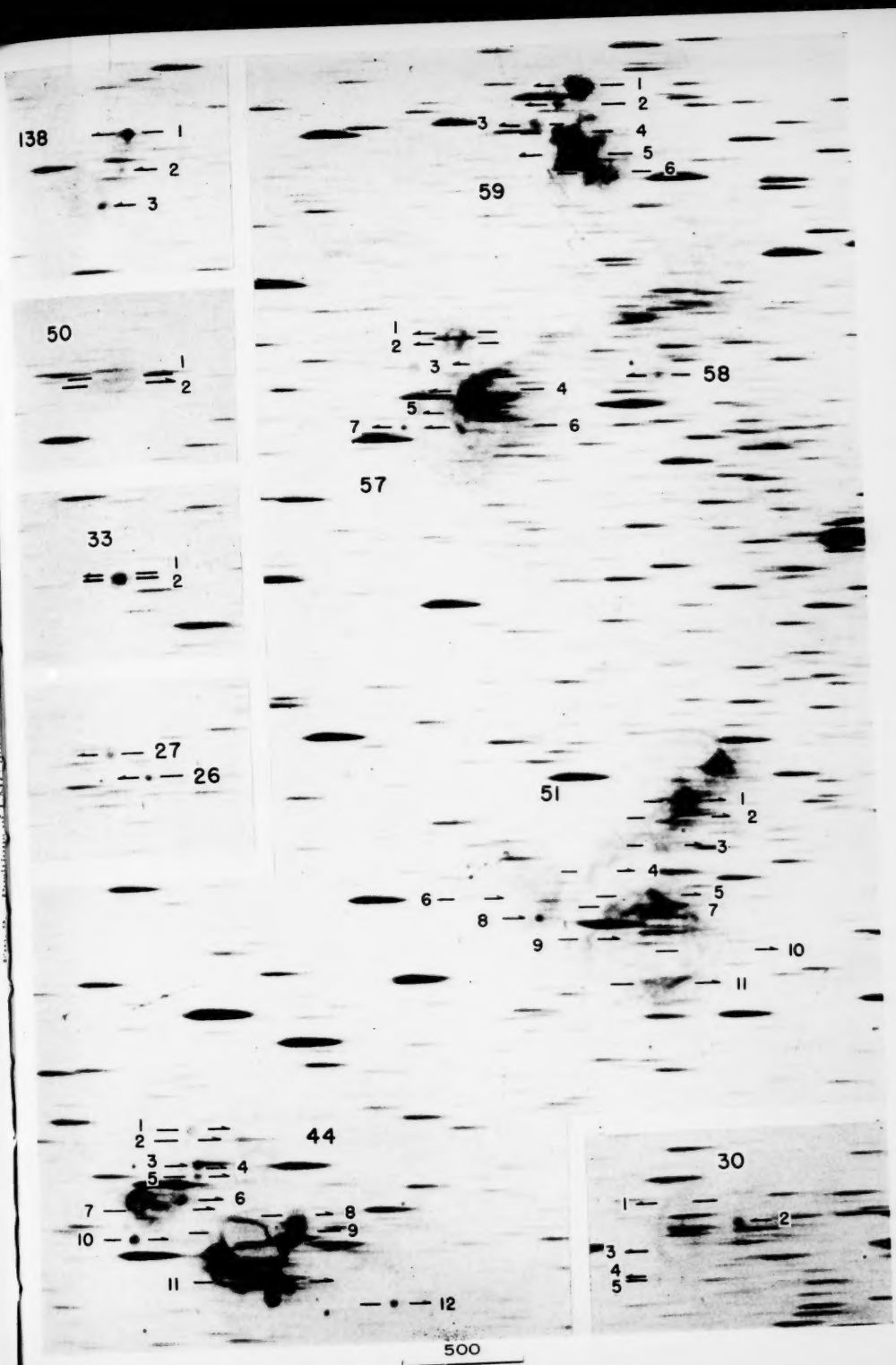

Fig. 10.—Positions of LMC microphotometer tracings. Chart 7

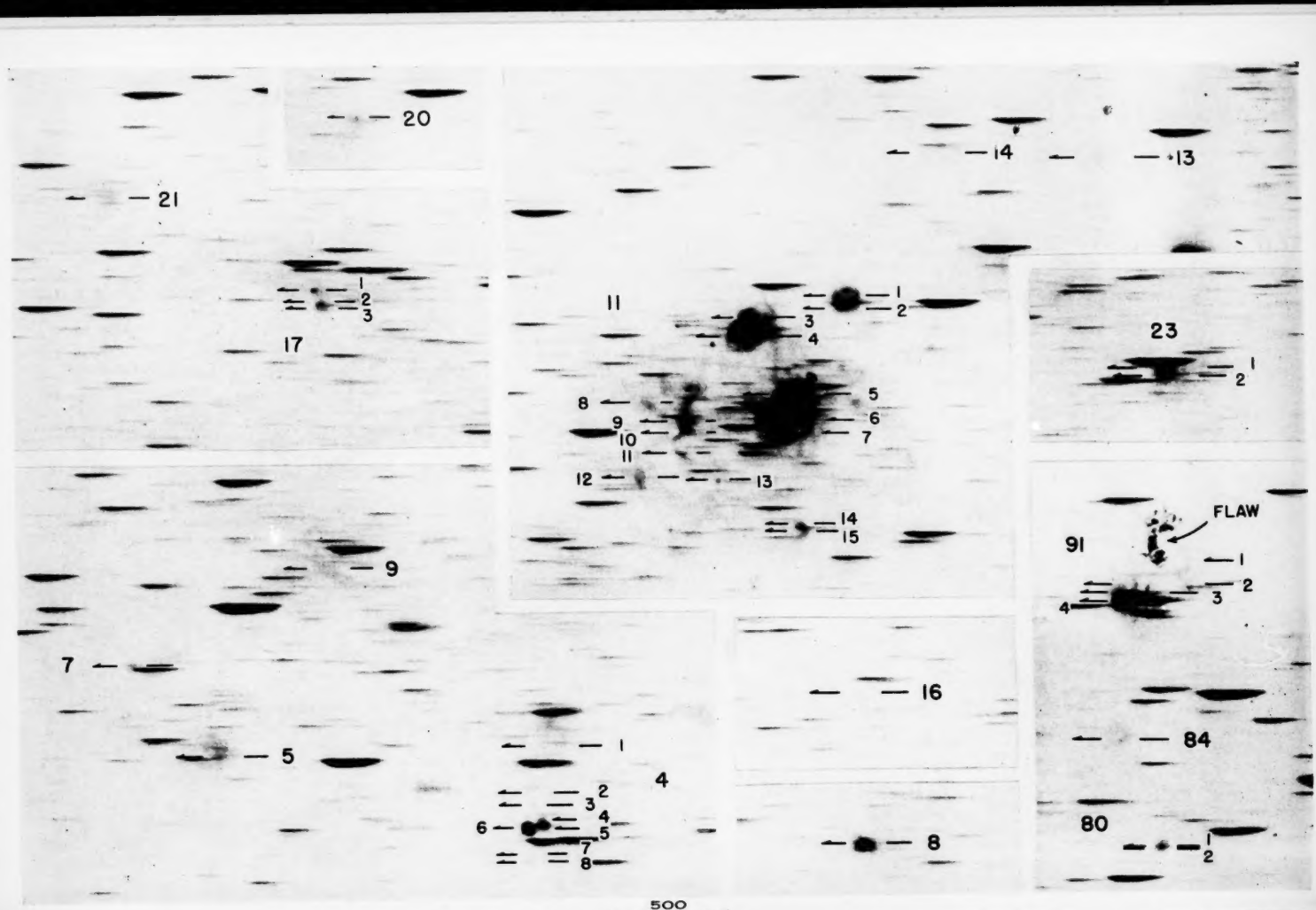
20
21
17
1
2
3
14
13
11
1
2
3
4
5
6
7
8
9
10
11
12
13
14
15
23
1
2
FLAW
91
1
2
3
4
84
80
1
2
9
7
5
1
4
2
3
4
5
6
7
8
16
8
500

STUDIES OF EXTREMELY YOUNG CLUSTERS. I. NGC 2264

MERLE F. WALKER*
Mount Wilson and Palomar Observatories
Carnegie Institution of Washington, California Institute of Technology
Received May 21, 1956

ABSTRACT

Three-color photoelectric and photographic observations of NGC 2264 have been obtained to $V = 17$, in order to investigate the color-magnitude diagram of an extremely young cluster of stars. The diagram indicates that the cluster possesses a normal main sequence extending from O7 to A0, below which the stars fall above the main sequence. The reality of this effect has been confirmed by spectroscopic observations. The shape of the color-magnitude diagram agrees approximately with that predicted theoretically for clusters which are so young that the fainter stars are still in the process of contracting gravitationally from the prestellar medium and have not yet reached the main sequence. The age of the cluster given by the point where the cluster stars depart from the main sequence is about 3×10^6 years.

In addition to luminosity effects, the spectra of the stars which lie above the main sequence show a number of peculiarities. One of the most striking is that later than F8 the rotational velocity of the stars appears to increase, suggesting that these stars have not yet had time to dissipate the original angular momentum of the material from which they have condensed.

The occurrence of T Tauri stars in the cluster and their location in the color-magnitude diagram indicate that stars of this type are extremely young and are still in the gravitational contraction state. Whether the T Tauri phenomenon represents a necessary stage in the gravitational contraction of all newly formed stars cannot be determined from the present observations. A number of new T Tauri variables was discovered during this investigation.

The luminosity function of the cluster is complete to $M_v = +8$ and appears to show a maximum at $M_v = +6$. Brighter than $M_v = +3$, the observed function agrees with the luminosity function which would be observed in the solar neighborhood if no evolution of stars away from the main sequence had taken place.

I. INTRODUCTION

While considerable observational work has now been done upon the problem of the later evolution of stars away from the main sequence, almost no observational investigations of the very early stages of stellar evolution have been made. Recent theoretical work by Salpeter (1953) and by Henyey, LeLevier, and Levée (1955) has indicated that in a group of stars which is only a few million years old the fainter members of the group will still be in the process of contracting gravitationally from the prestellar medium. The rate of contraction of an individual star depends upon its mass. As the configuration contracts, the decrease in the radiating surface is offset by the increasing temperature of the surface, so that the luminosity of the star remains nearly constant. As a result, the color-magnitude diagram of an extremely young cluster of stars should consist of a normal main sequence for the brightest stars, whose masses are greater than some critical value which depends upon the age of the cluster. Below this limit the cluster stars will fall above the main sequence and be displaced from it in the direction of lower temperatures.

The O and early B stars are known, from considerations of the rate of consumption of nuclear fuel, to have maximum lifetimes of only a few million years. Thus, to investigate the early stages of stellar evolution, we must determine the color-magnitude diagrams of clusters containing O or early B stars. At the present time, only one such group of stars has been investigated to a sufficiently faint absolute magnitude to show the divergence of the faint stars just discussed. This is the investigation of the Orion aggregate of stars by Parenago (1953). Unfortunately, Parenago did not have adequate observational ma-

* Carnegie Fellow, 1952–1954. Now at the Warner and Swasey Observatory of the Case Institute of Technology.

terial at his disposal to be able to prepare a really satisfactory color-magnitude diagram; the colors and magnitudes of his fainter stars had to be determined by measuring the images of these stars on published photographs of the field. However, his results do suggest that the fainter stars in the Orion aggregate depart from the main sequence in the direction predicted by the theory. His diagram consists of a normal main sequence extending from O to about A5. Below that, the main sequence appears to end, and one encounters a large cloud of subgiants.

This paper is the first of a series which will describe the photometric results for a number of extremely young clusters obtained during the last few years at the Mount Wilson Observatory. In order to investigate the fainter members of one of these clusters, it is necessary that the following five conditions be fulfilled as nearly as possible: (1) that the cluster contain both bright OB stars and faint stars; (2) that the cluster be relatively near, so that the intrinsically faint members will be accessible for observation; (3) that the cluster be in some manner recognizable as a group even to the faint stars, since most of the clusters are so far away that reliable proper motions cannot be obtained and since even for the few nearby groups, such as the Orion association, the proper-motion data do not extend to a sufficiently faint magnitude limit to enable one to determine the membership of the faint stars on this basis; (4) that the amount of emission nebulosity in the cluster be a minimum, since practical experience has shown that the observation of the faint stars in nebulous clusters is extremely difficult; and (5) that the amount of interstellar reddening should be small and uniform over the entire area of the cluster.

The Orion association is the nearest of these clusters of extremely young stars, and it possesses both bright and faint stars. However, it is extremely nebulous, so that the accurate observation of the faint members would be almost impossible. NGC 2264, on the other hand, is probably the most favorable of the young clusters for the purpose of investigating the faint members. It shows a very definite concentration of stars to the center of the cluster, and it is seen projected upon an extensive dark cloud (Herbig 1954), which effectively eliminates all or nearly all background stars from the central region of the cluster. While the cluster is farther away than Orion, the amount and intensity of emission nebulosity found in NGC 2264 is much smaller than is usually encountered in such objects, so that it is possible to observe accurately stars which are intrinsically much fainter than could be examined in the Orion association. Moreover, the reddening of the cluster is only 0.082 mag. in $B-V$ and appears to be uniform over the entire area of the cluster. The cluster contains a large number of faint stars which are either variable stars (Kukarkin and Parenago 1955; Wenzel 1955*a*, *b*) or which have been shown by Herbig (1954) to have bright Hα, or both. These are presumably T Tauri stars.

II. PHOTOMETRIC OBSERVATIONS

Photoelectric observations of NGC 2264 on the U, B, V system of Johnson and Morgan (1953) have been obtained with the instruments described below and listed in Table 5. Yellow, blue, and ultraviolet plates were also obtained, using the 60-inch reflector, for supplemental photographic photometry. In addition, other plates, mostly in the blue, were taken with the 60-inch in order to carry out a blink survey for the detection of additional variable stars.

In general, the instrument used for the photoelectric observations depended upon the magnitude of the star; the brighter stars were observed mainly with the 20-inch reflector at Palomar and with the 40-inch reflector at the Lowell Observatory. Fainter stars were observed with the 60-inch and 100-inch reflectors at Mount Wilson. The photometric equipment used at Mount Wilson, which has been described elsewhere (Walker 1954), employed an EMI end-on multiplier-tube type 5659 and the following filters: yellow, 1.7-mm Schott GG 11; blue, 1-mm Schott BG 12 plus 2-mm Schott GG 13; ultraviolet, 2.6-mm Corning 9863. For the observations reported here, the same multiplier tube and a similar set of filters were employed with the 20-inch at Palomar. The observations with

FIG. 1.—Northern section of NGC 2264. Stars for which photoelectric or photographic magnitudes and colors have been obtained. North is at the top, east to the left. The scale of the figure is 17'.6 mm.

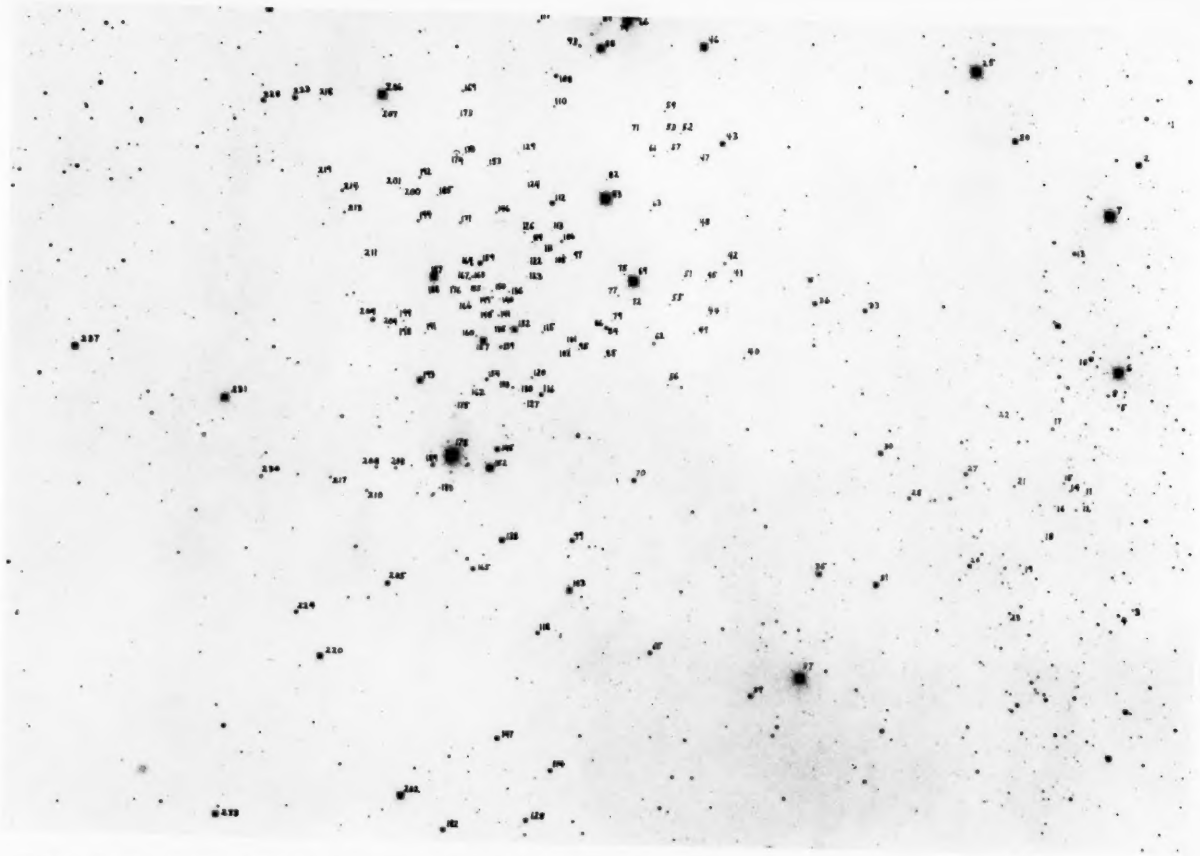

FIG. 2.—Southern section of NGC 2264. Stars for which photoelectric or photographic magnitudes and colors have been obtained. Orientation and scale as in Fig. 1.

the 40-inch at Lowell were made, using a 1P21 multiplier and the following filters: yellow, Corning 3384; blue, Corning 5030 plus Schott GG 13; ultraviolet, Corning 9863. A number of the brighter stars have also been observed by Johnson (1956); his measurements have been combined with the other observations in obtaining the final values of the magnitudes and colors.

The accuracy of a single observation for stars brighter than about $V = 14.0$ is: V, ± 0.026 mag.; $B-V$, ± 0.014 mag.; $U-B$, ± 0.016 mag. Below this the accuracy decreases, being about ± 0.10 mag. at $V = 17.0$ for both the magnitude and the color observations.

As indicated in the introduction, the difficulty in allowing for the effect of the irregular brightness of the emission nebulosity in which many of the cluster stars are situated is extremely great, for either photographic or photoelectric photometry. Experience has shown that if a photograph of the region in blue light which is exposed to the sky limit shows *any* trace of nebulosity, then difficulty is certain to be encountered in measuring the intensity of stars situated in it which are fainter than $V = 15$ or 16. Photoelectrically, a certain amount of background nebulosity can be handled by taking sky readings in four directions around the star; this has been done for all the faint stars in NGC 2264 in regions where any nebulosity was detectable. Such a technique, of course, increases considerably the amount of observing time required per star and limits the number of faint stars which can be observed. Even this method becomes unsuitable when only a very moderate amount of nebulosity is shown on the photograph; in such a case the difference in the sky readings may become several times larger than the intensity of the star. In the tables of the photoelectric observations, stars in which this difficulty was encountered have been marked as having lower weight due to the effect of the nebulosity.

In addition to observations of stars in the cluster proper, photoelectric observations were made of the brighter stars over the entire area shown in Figures 1 and 2, for the purpose of determining how far from the cluster center scattered members are still to be encountered. Also a photoelectric sequence has been set up in the area west and south of the cluster beyond the limits of the dark cloud, in a region where most of the stars are evidently background stars and thus are more likely to be constant than stars from the central area of the cluster. This sequence is intended for the use of photographic observers interested in obtaining three-color light-curves of the variable stars, who have instruments of sufficiently large field to obtain both the sequence and the cluster on a single plate. Little use was made of this sequence in the present investigation, since it lay outside the photometric field of the plates.

As indicated, the photographic observations were obtained with the 60-inch reflector, diaphragmed to 32 inches. In this way a photometric field 23′ in diameter was obtained, and, in addition, the entire area of the 5 × 7-inch plates could then be used for the detection of variable stars with the blink comparator. The following plate and filter combinations were used: yellow, Eastman 103*a*-D plus Schott GG 11 (1.4 mm); blue, Eastman 103*a*-O plus Schott GG 13 (1.9 mm); ultraviolet, Eastman 103*a*-O plus Schott UG 2 (2.0 mm). When plates for photometric measurement were taken, a set of three—yellow, blue, and ultraviolet—was taken on the same night so that false color effects would not be introduced by night-to-night variations in the brightness of the variable stars. Even so, there is still the possibility that some changes of brightness could have occurred between the different exposures of a set. The exposures of NGC 2264 were quite long, being 30 minutes in the blue, 60 minutes in the yellow, and 120 minutes in the ultraviolet. While little is known about the rapidity of the light-variations of the stars in NGC 2264, Haro and Morgan (1953) have found that changes in intervals of $\frac{1}{2}$ hour occur in some of the variables in the Orion Nebula. In view of the probability that many more of the stars in NGC 2264 are occasionally variable or are slowly variable over a long period of time, the photographic and photoelectric observations of the fainter stars in the cluster were made as near together in time as was possible. Three sets of yellow, blue, and ultraviolet

TABLE 1

PHOTOELECTRIC OBSERVATIONS OF NON-VARIABLE STARS

No.	van Maanen No.	V	B–V	U–B	No. Obs.	Inst.	Spectrum	Remarks
1		14.32	+0.93	+0.30	2	5		1
2		9.68	+0.27	+0.12	1	2	A7 III,IV	
3		14.58	+1.45	+1.13	1	5		1
4		13.46	+0.43	+0.01	1	5		1
5		14.11	+0.54	+0.09	3	5		1
6		8.17	+0.38	−0.08	2	2,3		2
7		7.74	−0.11	−0.65	2	2,3		
8		13.62	+1.26	+1.01*	3	5		1
9		11.98	+2.04	+2.16	2	5		3
10		11.24	+0.59	+0.20	2	5		1
11		16.04	+0.87	+0.07	1	5		1
12		15.47	+1.30	+0.19	1	5		1
13		12.04	+1.68	+1.46	2	5		1
14		14.82	+0.80	+0.21	1	5		1
15		14.64	+1.22	+0.68	2	5		1
16		16.10	+0.96	+0.36	3	5		1
17		12.87	+0.36	+0.27	2	5		1
18		15.20	+0.85	+0.24	2	5		1
19		15.51	+0.83	−0.02	1	5		1
20		10.27	+0.43	+0.10	2	2,3	F2 III	
21		14.06	+0.78	+0.26	2	5		1
22		17.06	+1.08	+0.20	3	5		1
23		13.72	+0.83	+0.52	2	5		1
24		8.56	−0.06	−0.35	2	3		
25		7.80	+0.39	−0.02	2	2,3		2
26		11.78	+0.48	−0.02	2	4,5		1
27		12.04	+0.53	+0.21	2	5	A0 III	4
28		12.28	+0.47	−0.10	2	5		1
29		10.12	+0.45	+0.01	1	3		1
30		10.75	+0.05	−0.02	2	5		
31		10.25	+0.34	−0.04	2	4,5	A7 IV (p?)	
32	5	12.99	+0.77	+0.09	1	3		1
33		11.67	+2.54	+2.45	1	5		3
34	6	10.91	+0.41	+0.09	1	3		1
35		10.32	+0.10	+0.00	2	4,5		
36		10.88	+0.03	+0.04	1	3		
37		8.08	+1.46	+1.72	3	2,3	K5 III	5
38	21	10.95	+1.04	+0.66	1	3		1
39		11.32	+0.13	+0.09	1	3		1
43	13	10.50	+0.21	+0.13	1	3	A7 III	
46	15	9.19	+0.21	+0.13	4	1,2,5	A5 III	6
50	16	8.11	−0.12	−0.73	3	1,2,5	B3 V (p?) ϕ	7
54†	17	14.25	+1.25	+1.03	1	4		
60	27	12.46	+1.03	+0.67	1	3		1
64	28	15.34	+0.94	+0.42	1	5		
65		11.71	+0.56	−0.08	1	3		
66	36	12.28	+0.70	−0.21†	1	4		
67	35	10.80	+0.62	−0.43†	1	4	B2 V	8
68	30	11.72	+0.67	+0.12	2	3,4	G0 IV,V	
69		8.26	+1.41	+1.56	Std		K3 II–III	
70*		11.06	+0.62	+0.08	2	3		
73	29	9.32	+0.85	+0.51	3	2,3,5	G5 III (p?)	
74	37	8.44	−0.13	−0.60	4	1,2,5		9
76†	34	14.11	+0.76	+0.41	1	4		
81		16.27	+1.26	+0.08	1	5		
83		7.93	−0.14	−0.84	3	2,3,5		10
85		14.98	+1.09	+0.78	1	5		
87		10.74	+0.23	+0.07	1	3		
88	40	9.02	−0.10	−0.66	2	1,5	B5 V ϕ	11
91*		12.32	+0.67	−0.05	2	3		
92	45	11.69	+0.86	+0.48	3	1,4,5	K0 IV p	
93†	41	13.22	+0.92	+0.65	1	4		
94		10.42	+0.43	−0.08	1	3		
98		11.75	+0.62	−0.07	1	3		
99		10.80	+0.29	−0.05	1	3		
100	48	9.98	+0.14	+0.07	2	1,5	A2 IV	12
103		10.03	+0.02	−0.16	1	3		13
104	50	11.36	+0.26	+0.14*	2	1,4	A5 IV	
106		13.28	+0.72	+0.41	1	4		
107	52	8.81	−0.06	−0.44	2	3,5		14
108	39	11.87	+0.55	+0.06	1	3	G0 III,IV(p?)	
109	49	9.08	−0.10	−0.56	2	1,5	B6 V ϕ	15
112		10.77	+0.01	−0.16	2	2,5	A0 V	
114		11.54	+0.52	+0.10	1	3		1
116		11.68	+0.59	−0.01	2	2,5	F5 III,IV	
117	72	13.52	+0.70	+0.18	1	4		
118		11.78	+0.56	−0.03	1	3		
121	59	10.80	+0.23	+0.08	1	1		16
125	68	12.29	+0.63	+0.02	1	4	F6–G0 III–Vp	
128		10.99	+0.21	0.00	1	3		1
131	60	4.62	−0.24	−1.08	3	1,2,3	O7 ϕ	17
132		10.23	−0.03	−0.32	2	5		
134†	56	12.38	+0.84	+0.05*	2	1,4		
136		15.16	+1.58	+1.07	1	5		
137	63	9.88	−0.06	−0.40	2	1,5		18
138		10.14	+0.07	−0.05	1	3		
141		14.70	+1.15	+0.87	1	5		
142	62	8.97	−0.07	−0.58	1	5		19
143†	61	10.59	+0.67	−0.14	1	5		20
144†	69	13.83	+1.38	+0.33	1	4		
145		10.64	+0.05	−0.03	3	2,3,5	A0 V	
147		10.96	+0.77	+0.47	1	3		1,2
148		13.60	+0.69	+0.09	1	5		
151	71	12.53	+0.52	−0.07	1	4		
152		9.10	−0.07	−0.38	3	2,3,5		
154		12.74	+0.71	+0.12	1	5	G2 III,IV p	
155		16.48	+1.43	+0.98	1	5		
156†	70	14.66	+1.25	+0.69	1	4		
157		10.06	−0.06	−0.35	2	3,5		
158	57	10.36	+0.36	+0.12	2	1,5	A7–F0 IV,V p	
159		10.97	+0.07	−0.09	1	5	A0 V	
165		10.94	+0.15	+0.01	1	3		
168	65	15.13	+1.26	+1.04	1	5		
172		10.04	−0.05	−0.45	1	3		
173		16.41	+1.29	+0.77	1	5		
176		15.79	+1.59	+0.85	1	5		
177		9.20	+0.77	+0.09	1	3		1
178		7.14	−0.20	−0.97	2	5		21
179	81	9.95	+0.01	−0.20	2	1,4		22
180	86	12.86	+0.51	−0.04	1	3		
181	80	10.03	−0.04	−0.32	2	1,4	B9–A0 IV–V	23
182		10.31	+0.08	+0.06	2	3,5	A2 V	
186		15.62	+1.56	+0.94	1	5		
187		9.21	−0.06	−0.40	2	2,3		24
189		11.20	+0.47	−0.21	1	3		
190	82	12.26	+0.68	+0.03	1	4		
193		9.77	+0.25	+0.06	2	2,3	A7 III p	
195	79	12.64	+0.53	−0.01	3	1,4,5		
196	83	11.46	+0.53	−0.05	2	3,4	F6–F8 IV (p?)	
202		8.98	+0.09	−0.63	2	3,5	B2 V	8
205		12.90	+0.76	+0.18	1	3		
205		10.60	+0.34	−0.04	1	3		
206	76	8.70	−0.08	−0.43	2	1,5		25
208		12.54	+0.81	−0.09	1	3		
209		11.29	+0.38	−0.05	1	3		
210		13.27	+0.77	+0.13	1	3		
212	98	7.47	−0.14	−0.76	Std		B2.5 V ϕ	26
215	100+101	9.29	+0.08	−0.15	2	1,5	A0 IV–V, A0 IV–V	13
216	97	11.69	+0.77	+0.18	1	3		
220		9.69	+0.48	−0.04	1	3		
221	92	12.12	+0.35	−0.04	1	3		1
222	99	9.88	+0.15	+0.12	2	1,5	A3 IV	
223	103	10.86	+0.37	−0.02	1	3		
224		11.49	+0.53	+0.17	1	3		
225*	128	13.19	+0.58	+0.03	2	3		1
226	112	9.59	+0.15	+0.12	3	3,5	A3–4 III	
227	127	11.77	+0.53	−0.11	1	3		1
228	107	11.07	+0.36	+0.02	1	3		
229	131	8.52	+1.20	+1.18	3	2,3,5	K2 II–III	
230		12.34	+1.33	+0.55	1	3		27
231		8.96	−0.13	−0.66	3	2,3,5		
232	130	9.78	+0.02	−0.08	2	3		
233		9.54	+0.58	+0.06	2	3,5	G0 V	28
234	123	12.39	+0.49	−0.04	1	3		1
235	125	13.44	+0.40	+0.06	1	3		1
236	114	11.35	+0.65	+0.18	3	3		1
237		9.44	+1.44	+1.27	3	2,3,5	K2 II–III	
238		9.94	+1.24	+1.53	1	3		1
239		9.33	+1.17	+1.05	1	3		1

plates were selected for measurement. These were taken on December 3, 5, and 6, 1953 (U.T.), while the photoelectric observations of the fainter stars were mainly secured in January, February, and March, 1954.

The photometric plates were measured in an Eichner iris-diaphragm photometer. Only the stars in a restricted area of the cluster which is quite free from nebulosity were measured, since, as mentioned, it appears to be even more difficult to allow properly for the effect of nebulosity in photographic photometry than in the photoelectric measurements. The plates were calibrated from the photoelectric observations of stars in the same area. Unfortunately, the number of such standards is not so large as it should be for really accurate work. For this reason, some weight was given in constructing the calibration-curves to photoelectric measurements of some of the emission Hα stars which had given no indication of variability on the blink plates secured during the same season. It is also possible that other stars which are not known to be variable may have varied slightly between the time that the photographic and photoelectric observations were made. However, it appears likely that the systematic effect upon the photographic magnitudes caused by the possible use of variable stars as standards is less than about 0.02 mag. So far as could be determined, no color equation exists between the photographic measurements and the U, B, V system. This is in agreement with the conclusions of Johnson and Sandage (1955).

The photometric observations are contained in Tables 1–4. Table 1 lists the photo-

* Measures discordant.

† Lower weight owing to uncertainty in determining the proper sky correction as a result of either the nebulous background or scattered light from a nearby bright star.

‡ Classified by Morgan (private communication).

REMARKS ON TABLE 1

1. Excluded from the color-magnitude and two-color diagrams on the basis of position outside the central area of the cluster.
2. Probably a foreground star.
3. Foreground dM star.
4. Reddened; in view of the spectral type and position in the cluster, probably a background star.
5. The ultraviolet measurement has low weight.
6. Trumpler: Sp. = A1n, V_r = +19.9 km/sec.
7. Trumpler: Sp. = B5n, V_r = +21.0 km/sec; double lines on some plates.
8. Reddened; correcting for the reddening, the star falls somewhat below the main sequence of the cluster and may be either a member or a background star; for No. 67, at least, the position of the star in the cluster renders the former alternative the more probable; omitted from the color-magnitude and two-color diagrams.
9. Trumpler: Sp. = B5, V_r = (+22.6) km/sec; double-line spectroscopic binary, orbit.
10. Trumpler: Sp. = B3s, V_r = +29.4 km/sec.
11. Trumpler: Sp. = B6n, V_r = +19.4 ± 4 km/sec; variable velocity.
12. Trumpler: Sp. = A0n, V_r = +25 ± 7 km/sec; variable velocity.
13. Visual double star; magnitude corrected by 0.70 in the color-magnitude diagram.
14. Trumpler: Sp. = B8n, V_r = +21.0 km/sec.
15. Trumpler: Sp. = B7n, V_r = +21 ± 6 km/sec; variable velocity.
16. Measured by Johnson only; Trumpler finds m_{pg} = 12.91 on the B system and suggests that the photoelectric measurement may refer to van Maanen No. 58.
17. S Mon. Trumpler: Sp. = O7, V_r = +32.2 km/sec.
18. Trumpler: Sp. = B9, V_r = +16.0 km/sec.
19. Trumpler: Sp. = B7n, V_r = +24.3 km/sec.
20. This star, together with No. 142, forms ADS 5325; Trumpler finds m_{pg} = 9.94 on the B system; the photoelectric measurement may be affected by scattered light from No. 142.
21. Trumpler: Sp. = B2s, V_r = +21.2 km/sec.
22. Trumpler: Sp. = A0n, V_r = +17 ± 8 km/sec; variable velocity.
23. Trumpler: Sp. = B9n, V_r = +23.0 km/sec.
24. Trumpler: Sp. = B8, V_r = +30.6 ± 3.5 km/sec; probably variable velocity; double lines on some plates.
25. Trumpler: Sp. = B8n, V_r = +22.9 ± 4 km/sec; close double, not separated.
26. Trumpler: Sp. = B3, V_r = +22.6 km/sec.
27. Low weight.
28. The spectral type shows this to be a foreground star.

electric observations of stars which are not known to vary, either from the present investigation or from work of other observers, and which do not have emission Hα. The first column in Table 1 gives the identification number of the star in Figure 1 or Figure 2, which identify all the stars for which photoelectric or photographic observations have been obtained. The second column gives the star numbers assigned by van Maanen (1930). The seventh column identifies the instruments used for the observations, accord-

TABLE 2

PHOTOGRAPHIC OBSERVATIONS OF NON-VARIABLE STARS

No.	V	$B-V$	$U-B$	Wt.	Remarks	No.	V	$B-V$	$U-B$	Wt.	Remarks
40.....	14.42	+1.10	+1.21	3		132.....	10.24	−0.08	.....	2	
41.....	14.06	+0.80	+0.36	3		135.....	14.93	+1.03	+0.07	1	6
42.....	13.24	+0.84	+0.49	3		136.....	15.22	+1.75	+ .91	3	
45.....	15.25	+0.94	+0.74	3		140.....	16.16	+1.59	+ .50	3	
47.....	16.64	+2.0	.....	1	1	141.....	14.70	+1.16	+ .86	3	
49.....	15.34	+1.00	+0.88	3		148.....	13.59	+0.69	+ .15	3	
51.....	15.95	+1.52	+1.2	2	2	154.....	12.73	+0.72	+ .13	3	
52.....	15.55	+1.26	+0.35	3		155.....	16.47	+1.43	+ .8	2	2
56.....	14.96	+1.48	+1.32	3		157.....	10.10	−0.03	.....	2	
57.....	14.84	+2.57	.....	3	3	159.....	10.96	+0.11	− .08	3	
59.....	15.11	+1.10	+0.35	3		160.....	14.85	+0.96	+ .67	2	5
61.....	15.01	+0.89	+0.23	3		162.....	15.28	+1.34	+ .84	3	
62.....	12.43	+0.58	−0.06	3		163.....	13.79	+0.92	+ .63	3	
63.....	14.66	+0.88	+0.43	3		167.....	14.04	+0.75	+ .38	3	
71.....	16.95	+1.03	.....	2	4	170.....	15.93	+1.47	− .01	3	
75.....	15.64	+1.38	+0.16	2	5	171.....	13.83	+0.68	+ .23	3	
84.....	12.01	+0.66	+0.09	3		173.....	.....	.....	.....	3	7
85.....	15.01	+1.08	+0.81	3		174.....	15.19	+1.08	+ .31	3	
97.....	16.77	+1.17	+0.5	2	4	176.....	15.83	+1.59	+ .81	3	
101.....	16.63	+1.72	.....	1	4	185.....	15.97	+0.94	+ .20	3	
102.....	15.67	+1.39	+1.26	3		188.....	15.96	+0.51	.....	1	6
106.....	13.30	+0.73	+0.25	3		192.....	13.84	+0.48	− .08	3	
111.....	16.81	+1.15	+0.37	1	4	194.....	13.15	+0.60	− .04	3	
112.....	10.84	−0.04	−0.18	3		198.....	15.32	+1.25	+ .89	3	
113.....	16.63	+0.41	−0.07	2		201.....	15.76	+1.04	+ .44	3	
116.....	11.65	+0.59	0.00	3		207.....	15.62	+0.93	.....	3	
119.....	15.49	+1.24	+0.39	3		211.....	16.10	+1.84	.....	3	
120.....	14.02	+1.48	+1.25	3		213.....	13.74	+0.85	+ .58	3	
124.....	16.66	+1.14	−0.55	1		214.....	13.25	+0.75	+ .26	3	
129.....	16.38	+1.26	−0.65	2		218.....	16.07	+1.21	+0.66	3	
130.....	16.43	+1.12	.....	1		219.....	15.78	+1.02	.....	2	

REMARKS

1. B near plate limit.
2. U near plate limit.
3. Foreground dM star?
4. Near plate limit.
5. Near bright star; observations scattered.
6. See remark 5; observations only on the night of best seeing used.
7. $B = 17.71$.

ing to their numbers in Table 5. Spectral types and radial velocities determined by Trumpler (1956) for a number of the stars are given in the Remarks to Table 1.

Table 2 lists the photographic observations of stars which are not known to be variable or to have Hα in emission. As in Table 1, the number of the star is its photometric identification number in Figures 1 and 2. The accuracy of the observations is indicated roughly by the weights given in the fifth column. The probable errors corresponding to the weights are: Wt. 3, $\leq \pm 0.05$ mag.; Wt. 2, ± 0.06 mag. to ± 0.10 mag.; Wt. 1, ± 0.11 mag. to ± 0.20 mag.

Table 3 lists all photometric observations, photographic and photoelectric, of the

TABLE 3

PHOTOMETRIC OBSERVATIONS OF KNOWN VARIABLE STARS

No.	Var. Star No.	Official Var. Star Name	LHa No.	Date	V	B-V	U-B	Inst. (Pe. Obs.)	Remarks
44	116	KY Mon	10	1	17.2	-----	-----		1
				2	15.74	+0.63	-0.13		
				3	15.95	+0.54	+0.26		
53	120	------	--	1	16.40	+1.04	-0.14		
				2	-----	-----	-----		2
				3	16.52	-----	-----		
55	121	S 5190	12	1	14.72	+1.28	+0.47		
				2	14.60	+1.32	+0.96		
				3	14.97	+1.49	+1.45		
72	---	S 5191	16	1	16.57	+1.68	-----		
				2	16.38	+1.52	-----		
				3	16.51	+1.63	-----		
77	---	S 5192	18	1	14.61	+1.14	+0.87		
				2	14.44	+1.21	+0.83		
				3	14.49	+1.16	+0.93		
				7	14.51	+1.19	+0.92	4	
78	W 6	LP Mon	20	9	15.40	+1.23	-0.42	5	3
79	127	S 5193	22	1	15.63	+0.32	-0.76		
				2	16.10	+0.43	-1.10		
				3	16.10	+0.71	-1.02		
				10	15.87	+0.56	-1.21	5	
80	W 7	GP Mon	--	9	15.25	+1.54	+0.72	5	
86	129	------	--	1	16.49	-----	-----		
				2	-----	-----	-----		4
				3	16.17	+1.51	-----		
89	W 8	LQ Mon	24	5	16.34	+1.05	-0.59	5	3
93	131	S 5194	26	1	15.68	+0.98	-0.11		
				2	15.65	+1.27	-0.19		
				3	15.60	+1.08	-0.24		
				10	16.05	+1.11	-0.01	5	
96	---	LR Mon	27	7	14.08	+1.10	+1.23	4	3
105	---	LT Mon	30	1	14.79	+0.92	-0.46		
				2	14.92	+0.72	-0.06		
				3	14.94	+0.86	-0.23		
				6	15.11	+1.07	-0.36	4	
110	---	S 5177	33	1	14.36	+1.04	+0.22		
				2	14.60	+0.95	+0.38		
				3	14.51	+1.08	-----		
115	---	S 5196	35	1	14.32	+1.03	+0.66		
				2	14.33	1.06	+0.67		
				3	14.45	+1.00	+0.64		
				10	14.42	+1.01	+0.40	5	
122	W 12	GQ Mon	38	1	15.19	+1.64	+0.55		
				2	16.46	-----	-----		
				3	16.29	+1.42	-----		
123	An 2	-------	40	1	16.26	+1.72	-0.66		
				2	16.88	-----	-----		
				3	16.49	+1.07	-0.05		
126	---	LU Mon	41	1	15.10	+1.13	-0.03		
				2	15.02	+1.01	+0.17		
				3	14.97	+1.31	-0.27		
127	W 13	-------	--	1	15.52	+1.69	----		
				2	15.77	+1.58	----		
				3	15.59	+1.38	+1.15		
				9	15.75	+1.50	+0.87	5	
133	S 4001	10 Mon	43	1	13.62	+1.08	+0.80		5
				2	13.80	+1.26	+0.71		
				3	13.83	+0.92	+0.98		
				11	13.83	+1.06	+0.64	5	
139	S 4002	IP Mon	47	1	13.19	+1.30	+0.74		
				2	13.21	+1.42	+0.92		
				3	13.22	+1.16	+0.95		
				10	13.39	+1.29	+0.65	5	
153	----	LW Mon	48	1	15.87	+1.04	-0.11		
				2	15.87	+1.15	-----		
				3	15.83	+1.15	-0.65		
				12	15.87	+1.24	+0.36	5	
161	----	LX Mon	51	7	14.96	+0.67	-0.61	4	3
164	----	S 5181	53	1	13.31	+0.76	+0.36		
				2	13.26	+0.80	+0.30		
				3	13.29	+0.82	+0.28		
				10	13.29	+0.84	+0.25	5	
175	W 17	----	58	9	16.12	+1.41	+0.48	5	
183	W 18	----	59	6	15.22	+0.97	+0.66	4	
184	S 4003	MM Mon	60	9	14.14	+1.00	-0.01	5	3
197	S 4004	IQ Mon	66	9	16.28	+0.93	-0.13	5	
199	----	S 5200	68	1	14.89	+1.15	+0.30		
				2	15.19	+0.87	+0.38		
				3	14.92	+1.24	+0.19		
200	148	-----	67	1	16.95	+1.40	-0.78		6
				2	-----	------	-----		2
				3	-----	------	-0.56		7
204	---	S 5201	70	1	15.22	-1.12	+0.37		
				2	15.38	----	----		8
				3	15.11	+1.19	+0.57		
217	---	MO Mon	72	13	13.54	+1.22	-0.16	3	

REMARKS ON TABLE 3

1. $U = 18.16$; V has low weight, being at the plate limit.
2. Too faint to measure.
3. Lower weight, owing to uncertainty in determining the proper sky correction as a result of the nebulous background.
4. Not measured on this night because of poor seeing and the nearness of the variable to a brighter star.
5. Herbig (1954): Spectral type G5 or K0 from the strength of the G band.
6. Low weight; star near plate limit.
7. $B = 18.17$.
8. $U = 16.51$; B not measured.

TABLE 4

PHOTOMETRIC OBSERVATIONS OF POSSIBLE VARIABLE STARS

No.	LHα No.	Date	V	$B-V$	$U-B$	Inst. (Pe. Obs.)	Remarks
48		1	15.05	+1.51	+1.14	.....	
		2	.....	.....	.....	.....	1
		3	15.23	+1.75	+1.02	.....	
58	13	8	15.50	+0.97	+0.63	5	2
82	23	1	15.37	+0.70	−0.49	.....	3
		2	15.62	+0.69	.....	.....	
		3	15.63	+0.56	−1.22	.....	
90	25	4	13.18	+0.22	+0.08	5	4
		5	13.05	+0.18	−0.05	5	
		8	12.88	+0.15	−0.06	5	
146		1	14.61	+1.16	+0.61	.....	
		2	14.65	+1.06	+0.62	.....	
		3	.....	.....	.....	.....	5
		12	14.46	+1.09	+0.77	5	
149		1	14.10	+0.95	+0.78	.....	
		2	14.20	+1.01	+0.64	.....	
		3	14.17	+1.00	+0.68	.....	
		11	14.35	+1.01	+0.64	5	
150		1	15.40	+1.18	+0.59	.....	
		2	15.23	+1.14	.....	.....	
		3	15.28	+1.20	+0.74	.....	
		11	15.44	+1.28	+1.22	5	
166		1	16.24	+1.54	.....	.....	6
		2	16.37	.....	.....	.....	
		3	16.18	+1.52	+0.40	.....	
169		1	13.46	+0.68	.....	.....	6, 7
		2	13.48	+0.61	+0.12	.....	
		3	13.59	+0.63	−0.43	.....	
		12	13.39	+0.78	+0.26	5	
191		1	15.35	+1.30	+0.88	.....	
		2	15.47	+1.39	.....	.....	
		3	15.29	+1.33	+1.09	.....	

REMARKS

1. $B = 16.58$; V, U not measured.
2. No evidence of variability on blink plates; the star is included here because it has bright Hα.
3. U affected by scattered light from star No. 83; this is probably the cause of the discordance in the U measures.
4. Van Maanen No. 43. Sp. = A2p; Trumpler (1930) gives $m_{pg} = 12.84$, while Herbig (1954) found $m_{pg} = 14.0$; Herbig points out that this discrepancy might have been caused by the effect of the nebulous background upon the measurements.
5. $U = 16.21$; V, B not measured.
6. Suspected of variability on one pair of blink plates.
7. This star is on the edge of the photometric field of the photographic plates; the systematic difference between the photographic magnitudes and the photoelectric measurement may thus be a distance-to-center effect.

known variable stars, including those discovered both in the present investigation and by other observers. Here, unlike Tables 1 and 2, where average values are given, the individual photographic and photoelectric observations for each date are presented. Since each photographic observation is thus based upon one plate, the accuracy of the photographic observations in this table is considerably lower than in Table 2. However, in view of the known variability of the stars, it is probably desirable to preserve these individual measurements rather than to form averages. The number of the star in the first column is again the photometric identification number in Figures 1 and 2. The second column gives the number of the star in Figure 3, which will be discussed in the following section. The third column identifies previously known variables. The letter designations are those assigned by Kukarkin and Parenago (1955), while the S-numbers are variables discovered at Sonneberg by Wenzel (1955*a*, *b*) which have not yet received official letter designations. The LHα numbers in the fourth column are the numbers given by Herbig

TABLE 5

INSTRUMENTS USED FOR PHOTOELECTRIC OBSERVATIONS

No. in Table	Description	No. in Table	Description
1.....	Unpublished observation by Johnson (1956) with Lowell 20-inch reflector or McDonald 82-inch reflector	2.....	20-inch reflector, Palomar
		3.....	40-inch reflector, Lowell
		4.....	60-inch reflector, Mount Wilson
		5.....	100-inch reflector, Mount Wilson

TABLE 6

DATES OF OBSERVATION REFERRED TO IN TABLES 3 AND 4

No. in Table	Date (U.T.)	No. in Table	Date (U.T.)	No. in Table	Date (U.T.)
1.....	Dec. 3, 1953	6.....	Feb. 2, 1954	11.....	Mar. 6, 1954
2.....	Dec. 5, 1953	7.....	Feb. 3, 1954	12.....	Mar. 7, 1954
3.....	Dec. 6, 1953	8.....	Feb. 24, 1954	13.....	Feb. 24, 1955
4.....	Jan. 5, 1954	9.....	Feb. 25, 1954		
5.....	Feb. 1, 1954	10.....	Feb. 26, 1954		

(1954) to those stars in which he has detected bright Hα. The fifth column gives the date of observation; the dates corresponding to the numbers in this column are given in Table 6. The ninth column gives the identification number (Table 5) of the instrument used in obtaining the photoelectric measurements. Where no number is given, the observation is photographic.

Where there was a variation of more than about 0.20 mag. in all three colors between the photographic measurements for the three dates or between the photographic and photoelectric observations, the star has been considered a possible variable and is listed in Table 4. The explanation of the various columns is the same as in Table 3. One star, No. 90 = LHα 25, is included here because, although the three photoelectric observations show a variation of 0.20 mag., the star is situated in a nebulous region of the cluster, so that the reality of a variation of this size may be open to some question. This star will be discussed in greater detail in a later section.

III. BLINK SURVEY FOR VARIABLE STARS

As indicated previously, additional plates were taken with the 60-inch reflector for the purpose of detecting new variable stars in NGC 2264. Four pairs of plates taken between

December, 1953, and April, 1954, were blinked for variables, and, in addition, one plate taken in December, 1955, was blinked with one taken in March, 1954, making a total of five pairs searched. The variables found in this survey are indicated in Figure 3, which shows the entire plate area examined. These new variables are numbered from 101; the other variables marked in Figure 3 are those which were known to be variable at the start of this investigation. The stars numbered W 1–W 20 are variables found by Wolf (1924). The four variables marked S 4001–S 4004 were discovered by Hoffmeister (1949), while the two stars marked An 1 and An 2 were discovered to be variable by Herbig

TABLE 7

IDENTIFICATION OF VARIABLE STARS IN FIGURE 3

Var. Star No.	Official Var. Star Name	LHα No.	No. Pairs	Var. Star No.	Official Var. Star Name	LHα No.	No. Pairs
W 1			0	115	KX Mon	9	2
W 2	KV Mon	3	0	116*	KY Mon	10	3
W 3	LL Mon	11	2	117			2
W 4		14	1	118	KZ Mon		3
W 5			2	119			4, *1*
W 6	LP Mon	20	4	120			4
W 7	GP Mon		3, *1*	121	S 5190	12	3
W 8	LQ Mon	24	4	122			2
W 9			0	123			1, *1*
W 10	LS Mon	28	2	124			4
W 11		37	2	125			2
W 12	GQ Mon	38	2	126	S 5172	15	4
W 13			0	127†	S 5193	22	1
W 14			0	128	LO Mon	19	2
W 15	LY Mon	49	1	129			2
W 16			2, *1*	130			2
W 17		58	3	131†	S 5194	26	1
W 18		59	0	132			2
W 19			4	133		29	2
W 20	MP Mon	78	1	134		36	2
S 4001	IO Mon	43	0	135		39	3, *1*
S 4002	IP Mon	47	1	136		44	2
S 4003	MM Mon	60	1	137		42	3
S 4004	IQ Mon	66	2, *1*	138			3
An 1	LM Mon		3	139			2
An 2		40	1	140			3
101			3	141			2
102			1, *1*	142			4
103			3	143			2
104			1, *1*	144			2
105	KU Mon	2	2	145			2
106			2	146			3
107			2	147	S 5204		2
108			2	148‡		67	2, *1*
109			2, *1*	149			2
110			2	150	S 5186	80	3, *1*
111			2	151			2
112		5	2	152			2
113			2	153			2
114			2				

* Noted as variable by Haro and Herbig (1955).

† Variability confirmed by the photometric measurements.

‡ Noted by Wenzel (1955*a*) as possibly having rapid variations of about 0.7 mag.; Wenzel could not confirm the reality of these variations.

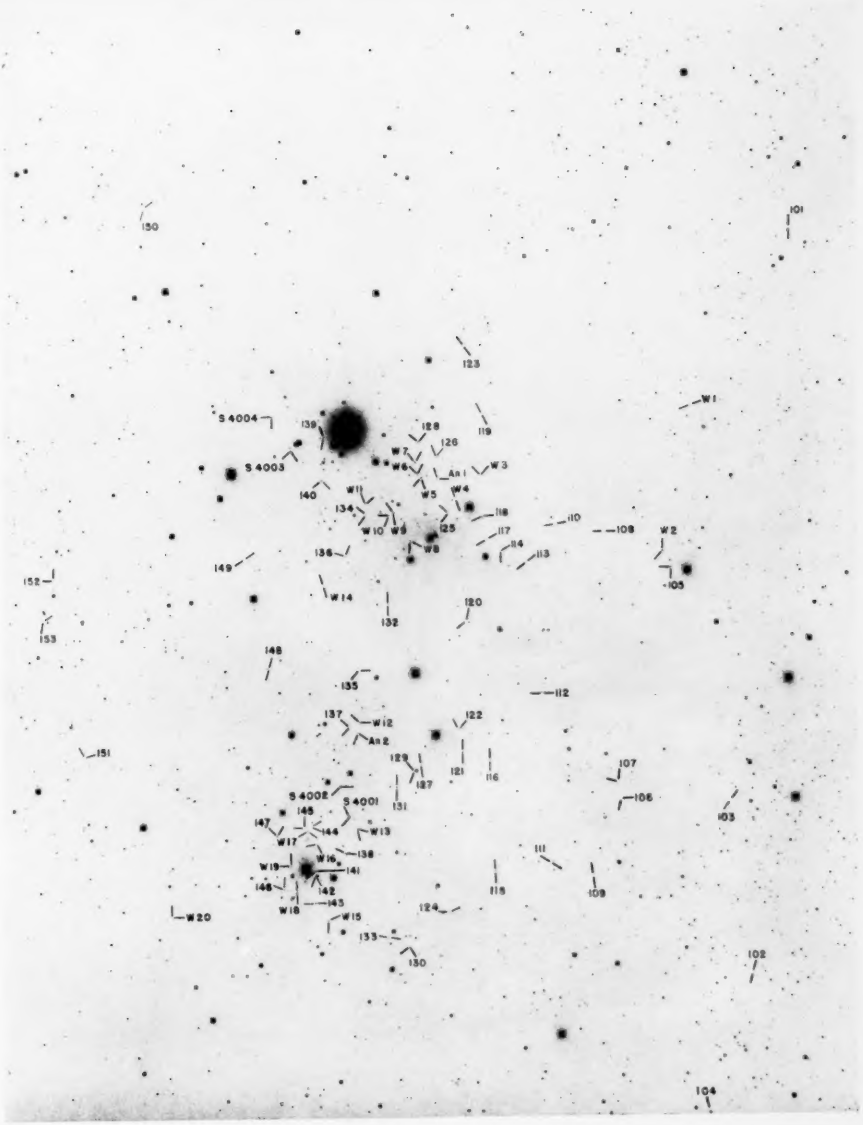

FIG. 3.—Field of NGC 2264 searched for variable stars. The figure shows the variables known prior to the present investigation and those (numbered from 101) found in this study. The scale is 24'.0/mm.

(1954). Since this investigation was begun, a number of the variables discovered in this program have been announced by other observers. However, it was felt desirable to indicate the stars whose variability was independently detected in the program, since this material provides a homogeneous sample of the variability of the stars in NGC 2264 at the time of the observations. Table 7 gives the identification number of the variables in Figure 3; the official variable-star designation of the variables which have been announced by other observers; the LHα number of the star; and the number of pairs of blink plates upon which the variability was detected. As in Table 3, the letter designations of the known variables are those assigned by Kukarkin and Parenago (1954), while the S numbers are by Wenzel (1954*a*, *b*). As can be seen from the fourth column in Table 7, the variability of the star was not considered established unless the star had been noted as variable on two independent pairs of plates. Two exceptions are variables Nos. 127 and 131, whose variability was confirmed by the photometric observations. The italicized number *1* indicates that the star was found to be variable on the plate taken in 1955, blinked with one taken in 1954. The variability of the stars known to be variable at the beginning of the survey is also shown in the fourth column. Of the other variables which have been announced since the present search was undertaken, only six—IP, MN, and MO Mon, S 5176, S 5177, and S 5184—were found to be variable on one pair of blink plates; no variability was detected for the remainder.

The percentage of the variable stars showing emission Hα at any one time can now be re-estimated from the number of variables found in this investigation and the number of bright Hα stars found by Herbig (1954). The percentage showing bright Hα turns out to be 42; using the total number of variables found by all observers, the percentage is 36. These values compare reasonably well with the value of 47 per cent found for the variable stars in the Orion Nebula (Herbig 1954), suggesting that the variable and bright Hα stars in the two clusters have similar characteristics.

IV. DISCUSSION OF PHOTOMETRIC OBSERVATIONS

The photometric observations of NGC 2264 are presented in Figures 4 and 5, which show the color-magnitude diagram and the $U-B, B-V$ diagram, respectively. In these figures the dots represent photoelectric observations and the circles photographic measurements. Vertical lines indicate known light-variables, while horizontal lines indicate stars having bright Hα. Small symbols indicate observations of lower weight. The positions of the variable stars represent some sort of average of the data available (usually only the photoelectric observation is plotted where both photographic and photoelectric measurements were made) and thus are to be regarded as *instantaneous* positions of the variables in the diagrams rather than *mean* positions. In Figure 5 the line represents the normal relationship between the colors of unreddened, main-sequence stars. From the displacement of the stars earlier than A0 from this line and computing the reddening path for the cluster from the formulae derived by Blanco (1956), we find the reddening of the cluster to be 0.082 mag. in $B-V$, and it appears to be uniform over the entire field of Figures 1 and 2. Since the reddening is both small and uniform, the observed colors and magnitudes of the stars have been plotted in Figure 4, and the lines, representing the standard main sequence and normal yellow giant branch as given by Johnson and Morgan (1953), have been shifted in $B-V$ by the amount of reddening determined from Figure 5.

The stars included in Figures 4 and 5 were selected from the photometric material in the following manner. For the stars earlier than A0, membership in the cluster can be unambiguously determined from the two-color diagram. A few such members are to be found scattered over nearly the entire area of Figures 1 and 2; all these stars have been included in the diagrams. For stars later than A0 the determination of membership from the two-color diagram becomes more difficult. Thus, for these stars, only those have been included (1) which lie well within the boundaries of the dark cloud against which the

cluster is seen projected or (2) for which spectral types and luminosities have been obtained which appear to confirm cluster membership.

It will be seen that the color-magnitude diagram is quite unusual. The diagram indicates that there is a continuous sequence of stars connecting the OB stars with the T Tauri stars, the latter appearing abruptly at $V = 13$. However, below A0 the sequence departs from the normal main sequence by first rising by 1.5 mag. and then extending as a broad band, 2 mag. wide, parallel to and about 2 mag. above the main sequence. Below $V = 13$, the *maximum* departure of the stars from the main sequence increases, reaching about 5.2 mag. at $B-V = 1.6$. Whether the mean line also diverges is not clear,

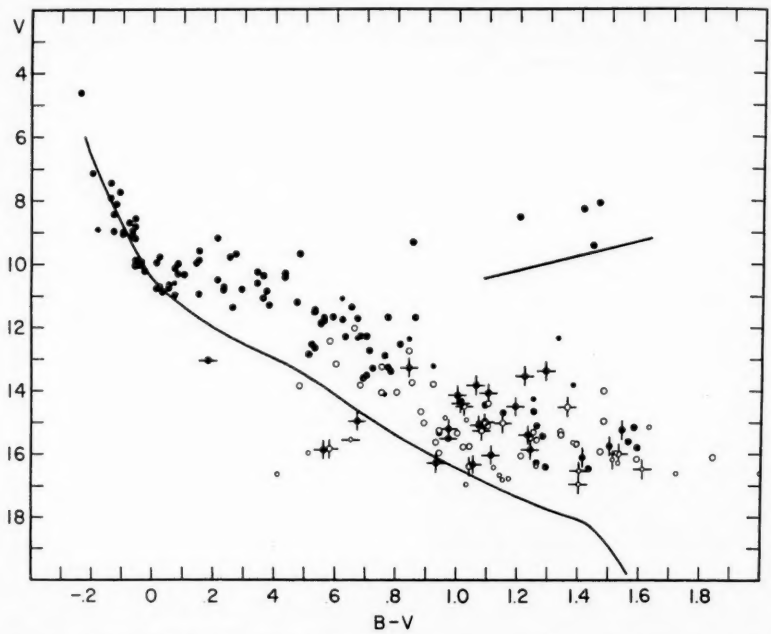

FIG. 4.—Color-magnitude diagram of NGC 2264. Dots represent photoelectric, and circles photographic, observations. Vertical lines indicate known light-variables; horizontal lines indicate stars having bright Hα. Small symbols indicate observations of lower weight. Observed values of the magnitudes and colors have been plotted. The lines represent the standard main sequence and giant branch of Johnson and Morgan (1953), corrected for the uniform reddening of the cluster.

owing to the incompleteness of the observations. Note that the cluster appears to contain five yellow giants; these will be discussed in a later section.

The distance of NGC 2264 was first determined by fitting the main sequence of the cluster above A0 to the standard main sequence of Johnson and Morgan (1953). In this manner the apparent distance modulus was found to be 10.2 mag. However, Johnson and Hiltner (1956) have recently shown that, for young groups of stars like NGC 2264, a correction of -0.5 mag. must be applied, at spectral type A0, to the distance moduli derived for such groups, using Johnson and Morgan's standard main sequence. This correction is necessary, since, on the average, stars of spectral type about A0 observed in the general field are sufficiently old that they have already begun to evolve away from the initial or "zero-age" main sequence. With this correction, the apparent distance modulus

of NGC 2264 is 9.7 mag. Using the ratio of total to selective absorption of 3.0 given by Johnson and Morgan (1953), we find the true distance modulus of the cluster to be 9.5 mag., or about 800 pc. Since Johnson and Hiltner's paper appeared after the diagrams for the present paper had been completed, the main sequences shown in Figures 4 and 9 have been left uncorrected and are the standard main sequence of Johnson and Morgan. The only errors resulting from this procedure are that the position of the giant branch should be 0.5 mag. higher than it is shown and that there are some minor changes in the shape of the main sequence which do not affect the present discussion. All the data discussed in the text and presented in the tables have been derived on the basis of the final distance modulus of 9.5 mag.

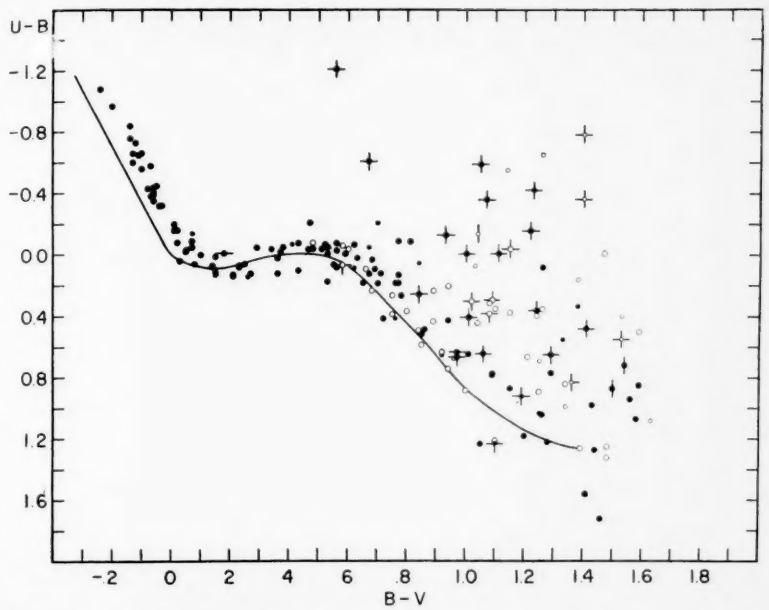

FIG. 5.—Two-color diagram of NGC 2264. The line represents the normal relationship between the color indices of unreddened main-sequence stars. Symbols as in Fig. 4.

There are three types of objects which might produce a spurious color-magnitude diagram which would resemble the one which we observe for NGC 2264. These are (1) background stars of high luminosity, (2) highly reddened early-type members of the cluster, and (3) foreground stars. We have already indicated that, for the central portion of the cluster, which lies well within the limits of the dark cloud, there should be no effect of background stars, since, as pointed out by Herbig (1954), the cloud is extremely opaque, the average penetration of the cloud being only 1 or 2 pc. For the same reason we would not expect to observe many reddened early-type member stars, since only those stars which lie in a very narrow zone 1–2 pc in depth would be observable. Furthermore, such stars should be recognizable from their location in the two-color diagram, provided that the reddening is not extreme. Three such stars were found and their reddened character confirmed by spectroscopic observations, which will be discussed in the following section. The two-color observations and the spectra of such stars that have been obtained con-

firm our conclusion that the effect of reddened early-type stars is negligible down to about $B-V = +0.8$. A few *very* highly reddened early-type stars with colors greater than $B-V = +0.8$ may be included in the diagram, since, as discussed later, many of the fainter stars are abnormally bright in the ultraviolet, which causes them to occupy the same region of the two-color diagram as would extremely reddened stars of early type. It can be seen from Figure 5 that below A0 it is very difficult to determine whether a star shows the general reddening of the cluster and hence is a member or whether it is an unreddened foreground star. However, the number of foreground stars to be expected over the central area of the cluster (0.17 sq. deg.) has been computed for each interval of apparent magnitude, by means of the luminosity function of van Rhijn (1936) and the luminosity functions derived by McCuskey (1949, 1954) for two areas near NGC 2264. Owing to the relatively small distance and small angular extent of the cluster, the number of foreground stars to be expected turns out to be very small, regardless of the luminosity function used. This result agrees with the appearance of the cluster; a zone can be traced around the cluster just within the boundaries of the dark cloud, where the density of stars is almost zero. We are therefore led to the conclusion that the color-magnitude diagram derived for NGC 2264 is not greatly influenced by the presence of non-members or reddened early-type member stars.

Perhaps the outstanding feature of Figure 5 is that, while the bright stars in the cluster fall along a sequence displaced slightly from the normal relationship between $U-B$ and $B-V$, many of the fainter stars depart widely from this normal relationship. This departure is in a direction which could indicate either that these faint stars are in reality very early O- and B-type stars which are heavily reddened or that the stars are intrinsically very much brighter in the ultraviolet than normal stars having the same $B-V$ color. We have already seen that, owing to the great opacity of the dark cloud, we would expect that very few heavily reddened O and B stars would be observed in the cluster. Since, in addition, Figure 5 shows that most of these stars are T Tauri stars—either known light-variables or emission Hα stars or both—it is evident that at least the great majority of these stars are actually abnormally bright in the ultraviolet. This unusual brightness in the ultraviolet has already been pointed out by Haro and Herbig (1955), who detected this anomaly in several of the stars in NGC 2264 and in the Orion Nebula. So far, no interpretation of this phenomenon has been found. There also appears to be a tendency for stars between $B-V = +0.4$ and $B-V = +0.6$ to be slightly brighter than normal in the ultraviolet; perhaps it is with these stars that the ultraviolet anomaly which becomes so pronounced for the fainter members of the cluster first sets in. It is to be noted that the very intensity of the ultraviolet excess in one star, No. 79 = LHα 22, shows that the effect must be intrinsic; if the position of this star in the two-color diagram were the result of reddening, then the temperature of the star would have to be far greater than has ever been observed for any other object.

The location of the T Tauri stars in the color-magnitude diagram of NGC 2264 confirms very clearly the conclusion of Herbig (1952) that T Tauri stars in the Taurus-Aurigae dark clouds tend to lie above the main sequence. Herbig found that, beginning at about spectral class K4 or K5, the T Tauri stars begin to fall more and more above the main sequence, their departure from the main sequence reaching about 2.5 mag. at type M2 or M3. The G-type T Tauri stars, on the other hand, tend to lie below the main sequence. The same trend is evident in Figure 4. With the possible exception of No. 90, the earliest of the variables have color classes of about F6–G0 and lie below the main sequence. At about $B-V = +0.8$ (color class about G8) the mean line of the variables crosses the main sequence, and the later variables lie progressively farther above the main sequence, reaching about 4 mag. by color class M3. In NGC 2264 the point at which the variables cross over the main sequence is earlier, and the average departure of the later variables from the main sequence is more rapid with color class than that found by Herbig in Taurus-Aurigae. This may result from a difference in the stars found in the

FIG. 6.—Spectra of stars in NGC 2264 and MK standards

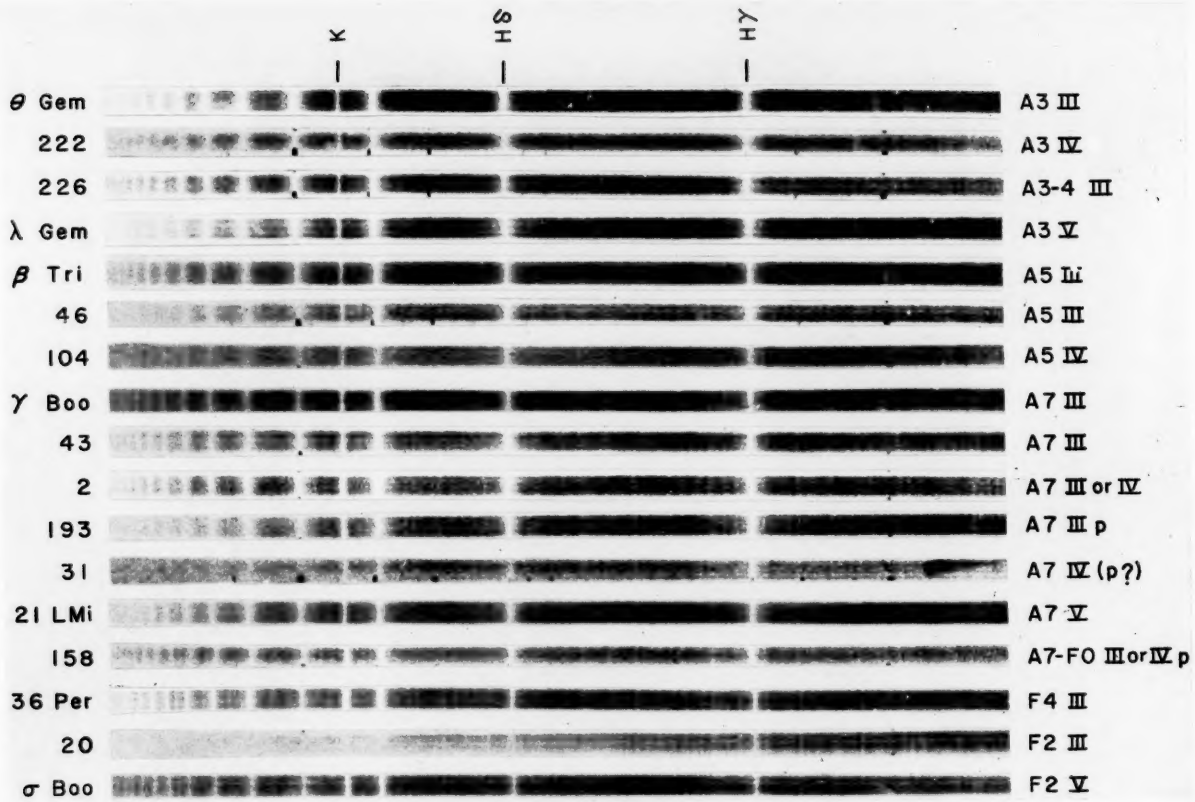

FIG. 7.—Spectra of stars in NGC 2264 and MK standards

FIG. 7.—Spectra of stars in NGC 2264 and MK standards

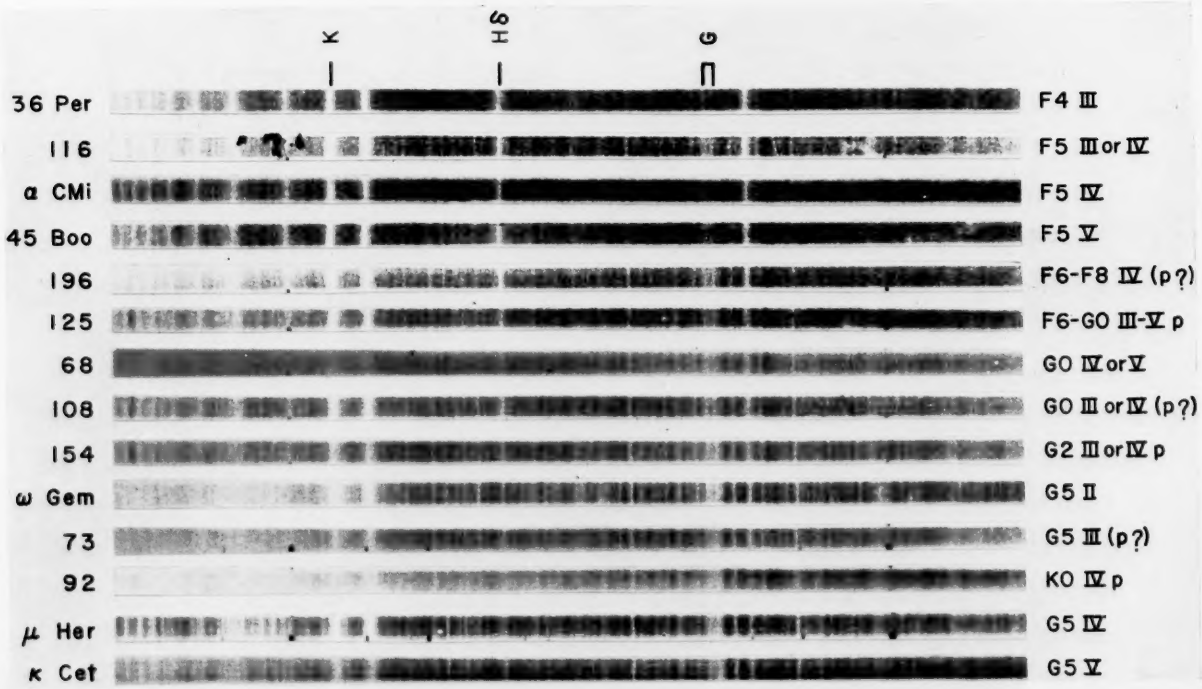

FIG. 8.—Spectra of stars in NGC 2264 and MK standards

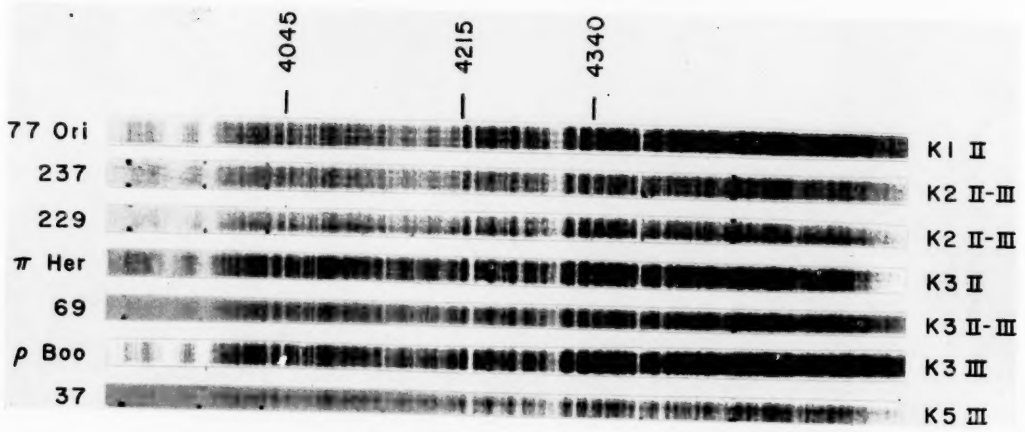

FIG. 9.—Spectra of stars in NGC 2264 and MK standards

two regions, but it is more probable that it is caused by the fact that the photometric observations at NGC 2264 extend only to $M_v = +7.5$. Also the entire light-ranges of most of the variables discussed by Herbig were available, so that he was able to plot mean light-positions, whereas in NGC 2264 it has been necessary to use "instantaneous" values of the brightness of the variables.

The photometric observations of the variable stars in NGC 2264 are not sufficiently numerous to permit us to draw any conclusions regarding the nature of their light-curves. Neither are they sufficiently exact to provide much indication of how the colors of the stars change with their brightness. If the variability of No. 90 indicated by the photometric observations is real, then in this star the $B-V$ and $U-B$ colors both decrease as the star brightens. However, this star is of much earlier type than the other variables in NGC 2264 and might thus show a different type of color variation than the T Taurus variables of later class. Considering only the known variables for which the largest changes in brightness have been observed, there is some indication that the stars tend to become redder in $B-V$ as they become brighter, but this is extremely uncertain in view of the limited number and low weight of the observations. Nos. 79 and 153 suggest that variations in $U-B$ may occur independently of the brightness in B and V. If this is correct, it would seem to indicate that the source of excitation of the ultraviolet excess in these stars is independent of the general source of radiation of the star. A careful study of the light- and color-variations of these stars would be very desirable.

V. SPECTROSCOPIC OBSERVATIONS

Following the discovery of the anomalous color-magnitude diagram of NGC 2264, spectroscopic observations were secured for as many as possible of the stars which appear to depart from the main sequence, in order to test the reality of this effect and to determine whether these stars exhibit any spectroscopic peculiarities. The observations were made with the Newtonian-focus grating-spectrograph on the 100-inch reflector. A grating and camera combination giving a dispersion of 83 A/mm was used. Both the stars in the cluster and a number of MK standards were observed on Eastman II*a*-O plates; baked plates were employed for the fainter stars in the cluster. Owing to the limited amount of observing time which could be devoted to this part of the program, only one plate was taken of each of the cluster stars. This fact must be kept in mind in the discussion which follows, since, working from single plates, some of the apparent peculiarities of the spectra may be only the result of local variations in the sensitivity of the plates.

The spectra of the cluster stars and of a number of MK standards are shown in Figures 6, 7, 8, and 9. A brief description of those spectra which appear to be abnormal is given below; the spectra of the remaining stars appear to be normal, showing only the luminosity effects as indicated by the spectral classifications given in the figures and listed in Table 1.

No. 90, LHα 25, A2p.—This star, as shown in Figure 4, falls below the main sequence of the cluster. The colors and spectral type show that it is not a reddened member or background star, so that its position in the color-magnitude diagram must reflect the intrinsic properties of the star. As pointed out in Section II and in the Remarks to Table 4, there is some evidence that the light is variable. The hydrogen lines are narrow, having moderately deep cores and shallow wings. It appears possible that the structure of these hydrogen lines is caused by a weak shell, although there is no decrement in the lines as one goes to the higher levels. The spectrum shows three emission lines of mercury, λ 3650, λ 4046, and λ 4358, produced by the lights of Los Angeles; these lines are to be found on the spectra of all the fainter cluster stars. In addition, [O II] λ 3727 appears in emission, as it does in a number of the fainter stars in NGC 2264, from the nebulosity in which the star is situated. The stellar emission lines have been tentatively identified as [Fe II] λ 4243, λ 4287, and λ 4413. The presence of these lines would appear to strengthen the supposition that the star possesses a weak shell. The only absorption lines in the

spectrum other than the Balmer lines are Ca II K, He I λ 4471, and Mg II λ 4481. He I λ 4026 may also be present weakly in absorption.

No. 193, A7 III p.—The ratio of λ 4030/λ 4128 gives a spectral type about A8, as does the strength of Ca I λ 4226 and the K line. However, λ 4300/λ 4385 gives A5. Apparently, λ 4385 is abnormally strong, as is λ 4351. The strength of the feature at λ 4290 suggests a type near F2. This last feature also appears abnormally strong in Nos. 2, 31, and 43.

No. 31, A7 IV (p?).—This spectrum is rather weak to classify accurately. Ca I λ 4226 appears to be weaker than in Nos. 2, 43, and 193. The ratio λ 4300/λ 4385 gives a spectral class about A3, while λ 4030/λ 4128 gives A7. In this star, λ 4300 appears to be abnormally weak. The hydrogen lines may also be weak. As mentioned previously, λ 4290 appears to be abnormally strong in this star, appearing stronger than λ 4272.

No. 158, A7–F0 IV, V p.—The ratio λ 4300/λ 4385 gives a spectral type near F4, apparently due to the abnormal strength of the blend at λ 4300. The strength of the K line would indicate a spectral type around F2 or F3. The ratio λ 4230/λ 4128 gives about F0, while Ca I λ 4226 appears to be weak and would indicate a spectral class about A5–A7. There appears to be an abnormal feature just to the violet of λ 4481. Owing to the weakness of the spectrum, only the ratio λ 4417/λ 4481 is available for the determination of the luminosity class, which could be either IV or V. However, the anomalous line strengths would seem to indicate that this is not a foreground star.

No. 196, F6–F8 IV (p?).—The ratios λ 4045/Hδ and λ 4325/Hγ give F6–F8; the strength of the G band indicates a type about G0. There may be a small amount of rotational broadening of the lines.

No. 125, F6–G0 III–V p.—The spectral class is difficult to estimate precisely, because the hydrogen lines appear to be weak. Excluding the hydrogen lines, the general appearance of the spectrum places it between F6 and G0. The luminosity criteria give λ 4045/λ 4077, about III, but λ 4045 appears to be abnormally weak, so that this determination has low weight; λ 4077/λ 4226, V; λ 4383/λ 4172, V; λ 4063/λ 4077, IV; λ 4172/λ 4272, IV. There may be a small amount of rotational broadening of the lines.

No. 68, G0 IV, V.—The spectrum appears fairly normal, except that the hydrogen lines may be slightly weak. The luminosity criteria give λ 4063/λ 4077, IV; λ 4144/λ 4077, V. There is some rotational broadening of the lines.

No. 154, G2 III, IV p.—The hydrogen lines are weak, as is λ 4045. Excluding the hydrogen lines, the general appearance of the spectrum is about G2. The lines show a very pronounced rotational broadening.

No. 73, G5 III (p?).—Hydrogen lines weak? The spectral type was determined from the ratios λ 4030/λ 4300 and λ 4325/λ 4340. There is little or no rotational broadening of the lines.

No. 92, K0 IV p.—The spectral type was determined from the ratios λ 4030/λ 4300 and λ 4325/λ 4340 and may be slightly uncertain, owing to a lack of adequate standards near K0. The lines λ 4045 and λ 4385 appear to be weak, and the intensities of several other features may also be anomalous. The spectrum of this star is remarkable, in that it has very diffuse lines, indicating a very large rotational velocity. A rough measurement of the width of the lines gives a value of $v \sin i$ between 100 and 150 km/sec.

The radial velocities of the stars have not been measured; these, together with a complete analysis of the spectral peculiarities, will be given later, when additional plates of the stars are available.

In general, the spectra appear to confirm the peculiar structure of the color-magnitude diagram. Figure 10 shows the color-magnitude diagram, together with the spectral class and luminosity of all the stars which have been observed spectroscopically, with the exception of those whose spectra have indicated that they are not members of the cluster (see Remarks, Table 1). The figure shows that at the point where the cluster sequence leaves the main sequence, the spectral type is A0 V and that, for stars later than A0, the

luminosity increases along the "hump" in the cluster sequence, reaching A5 III at the top with star No. 46. The cluster membership of this star is particularly well determined, because its radial velocity has been measured by Trumpler (1956) (see Remarks, Table 1) and agrees well with the mean radial velocity of the cluster. Below this point, most of the spectra again show indications of having luminosities greater than those of main-sequence stars. In general, the luminosities of the cluster stars derived from their spectra agree fairly well with the luminosities determined from the color-magnitude diagram. The disagreements which do exist between the spectroscopic and photometric absolute magnitudes

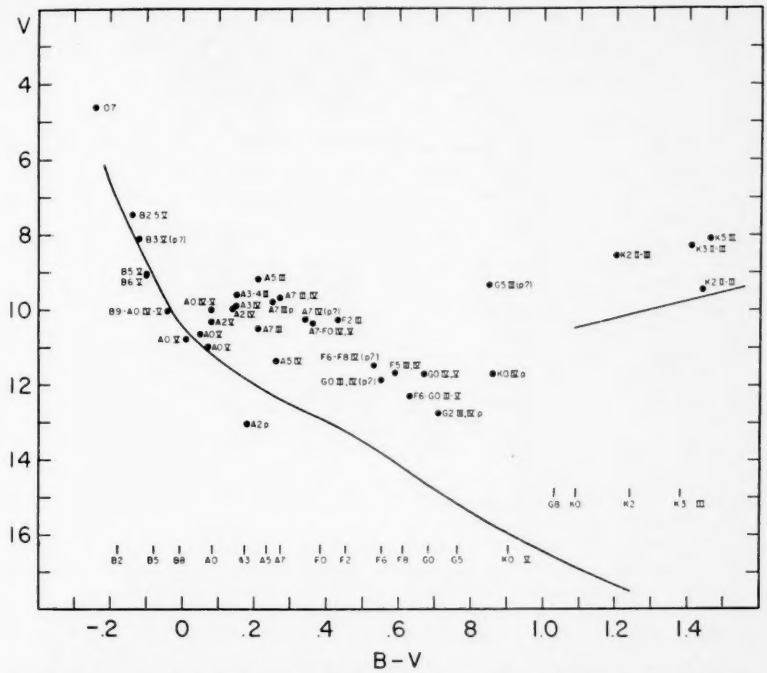

FIG. 10.—Color-magnitude diagram of NGC 2264 for those stars for which spectra have been obtained and whose spectral types show them to be members of the cluster. The five yellow giants in NGC 2264 are included, even though their cluster membership is not entirely certain. As in Fig. 4, the observed colors and magnitudes are plotted and the positions of the main sequence and giant branches have been corrected for the reddening of the cluster. The spectral classes corresponding to different values of $B-V$ have been plotted at the bottom of the figure, allowing for the reddening of the cluster.

are probably not serious, in view of the fact that only one plate of each star was available for classification and that a complete set of MK standards was not available.

As pointed out in Section IV, it is difficult to determine from the two-color diagram whether a star later than A0 shares the reddening of the cluster. In Figure 10 the spectral classes corresponding to different values of $B-V$ (Johnson and Morgan 1953) have been plotted, allowing for the reddening of the cluster. In general, the observed spectral types tend to agree with those predicted from the colors, indicating that these stars share the reddening of the cluster and thus are not unreddened foreground stars.

As mentioned previously, the spectra and colors of three stars which fall in the cluster sequence—Nos. 27, 67, and 202—indicate that they are reddened stars of earlier type.

In two cases the stars are located near the edge of the dark cloud and are evidently seen through its outer fringes. One of these two—No. 27—is probably a background star, on the basis of the spectral type and luminosity and the position of the star in the color-magnitude diagram when the effects of reddening have been removed. In the same way the other stars are probably members of the cluster, although they have not been included in the color-magnitude or two-color diagrams. One of these—No. 67—is interesting, in that it lies in the central part of the cluster and appears to be the only object in that part of the cluster which is located slightly inside the dark cloud. We have seen in the preceding section that we would expect to observe very few such objects, owing to the large opacity of the cloud.

One of the most unusual features of the spectra is that the stars of the cluster sequence having the latest spectral types show rotational broadening of their lines. In the general field, rapidly rotating stars are almost never encountered among spectral types later than about G0 (Herbig and Spalding 1955), while in NGC 2264 the effect of rotation first becomes noticeable at about F8 and increases with advancing spectral class. There is the possibility that these stars are variables of the W UMa type. However, no indication of variability was found on the blink plates, and the fact that all of the stars later than F8 show the effect militates against this explanation.

As mentioned earlier, five stars occur in NGC 2264 which fall into the region of the color-magnitude diagram normally populated by the yellow giants. The spectra of these stars indicate that they are, in fact, giants. Is it possible that, even though they are giants, they are field stars? McCuskey (1949, 1954) has published the observed distributions of stars of different spectral types and apparent magnitudes in two selected areas near NGC 2264. Taking the average of these two areas, the number of yellow giants encountered, down to the magnitudes of the giants observed in NGC 2264, is about 0.5 star per square degree for stars of spectral type G5 III and 0.3 star per square degree for all stars between spectral types K2 III and K5 III. The area covered by the yellow giants in NGC 2264 is about 0.47 square degree. The number of yellow giants observed in the cluster is thus about six and sixteen times, respectively, the number of field stars to be expected in the two spectral groups just mentioned, so that it would appear that these stars might be members of the cluster. That one of them is not a foreground star is suggested by its magnitude and color. No. 237 appears to be reddened about 0.27 mag. more than the other stars in $B-V$. Correcting for this differential reddening, we find the star to lie reasonably well along the sequence populated by the other giants in NGC 2264, and its position in the cluster suggests that it may be a star which is slightly imbedded in the outer edge of the dark cloud. Radial velocities of these stars must be obtained before their membership in the cluster can be considered to be definitely established.

VI. THE LUMINOSITY FUNCTION

For the purpose of determining the luminosity function of the cluster, it is necessary to know the magnitudes of the stars to only a few tenths of a magnitude. Consequently, distance-to-center corrections can be neglected, so that the faint standards established just beyond the boundaries of the dark cloud could be used to provide the calibration-curve of the plate. With some extrapolation of the calibration-curve, it was then possible to determine approximate magnitudes on one of the yellow plates of all stars between $10.99 < V \leq 18.00$ in an approximately rectangular area of 0.17 square degree in the central region of the cluster, well within the boundaries of the dark cloud. The brighter stars in this area have all been observed photoelectrically and were counted from the photometric measurements, rejecting the yellow giants occurring in this region. The number of stars in each 1-mag. interval is given in Table 8. The area covered by the star counts corresponds to about 33 pc^2. From considerations of reddening observed for the cluster stars, we may probably assume that all the cluster stars which were counted are located in front of the dark cloud. We do not know, however, what the exact spatial

relationship is between the cloud and the cluster. The occurrence of the T Tauri stars in NGC 2264 suggests that the cluster is not separated very far in space from the cloud. But whether we see only that fraction of a much larger aggregate of stars which have dispersed out of the cloud or whether the entire cluster lies in front of the cloud, we cannot tell. An upper limit to the volume of space occupied by the observed stars in NGC 2264 is given by supposing that the depth of the group is equal to its largest diameter, about 38′. At the distance of the cluster, this corresponds to a depth of 9 pc, so that the upper limit to the volume of the cluster is about 300 pc³. Using this value of the volume, the number of stars per cubic parsec in each magnitude interval is given in the fourth column of Table 8. The fifth column gives the number of stars per cubic parsec per magnitude interval near the sun, according to van Rhijn (1936). The comparison of the luminosity function for NGC 2264 and van Rhijn's function will be discussed in the following sec-

TABLE 8

LUMINOSITY FUNCTION FOR CENTRAL REGION OF NGC 2264

V	M_v	NGC 2264		LOG No.† STARS PER Pc³ NEAR SUN+10	LOG NGC 2264/ VICINITY OF SUN	LOG‡ ψ/ϕ	REDUCED LOG§ NGC 2264/ VICINITY OF SUN
		No. Stars per Mag. Interval	log No.* Stars per Pc³+10				
4.5	−5.0	1	7.52	2.77	4.75	.....	3.45
5.5	−4.0	0	.....	3.58	.....	2.98	.....
6.5	−3.0	0	.....	4.12	.....	2.60	.....
7.5	−2.0	3	8.00	4.71	3.29	2.13	1.99
8.5	−1.0	4	8.11	5.32	2.79	1.71	1.49
9.5	0.0	11	8.57	5.98	2.59	1.29	1.29
10.5	+1.0	14	8.67	6.59	2.08	0.88	0.78
11.5	+2.0	12	8.60	6.71	1.89	0.54	0.59
12.5	+3.0	10	8.52	6.98	1.54	0.15	0.24
13.5	+4.0	36	9.08	7.29	1.79	0.00	0.49
14.5	+5.0	50	9.22	7.40	1.82	0.00	0.52
15.5	+6.0	103	9.54	7.45	2.09	0.00	0.79
16.5	+7.0	72	9.38	7.45	1.93	0.00	0.63
17.5	+8.0	68	9.36	7.55	1.81	0.00	0.51

* Assuming the volume of the cluster to be 300 pc³.

† Van Rhijn (1936).

‡ Log of ratio of "original" to observed luminosity function (Salpeter 1955).

§ Assuming a star density in the cluster twenty times that in the solar neighborhood.

tion. It is to be noted, however, that the counts suggest that there is a maximum to the luminosity function in NGC 2264 at about $M_v = +6$, although this should be checked by counts going to fainter limiting magnitudes. That the maximum of the luminosity function has been passed is suggested by the fact that plates with the 60-inch reflector exposed to a limiting magnitude about 1 mag. fainter than those used in this investigation do not show a very large increase in the number of stars visible. It is interesting to note that Herbig (1954) found a frequency maximum in the number of emission Hα stars at $m_{pg} = 15$ or 16, which corresponds to an absolute visual magnitude of $M_v = +4.5$ or +5.5. However, Herbig points out that the magnitudes which he gives for his emission Hα stars are not consistent with their brightnesses at the time that their bright Hα was detected, since the plate from which the magnitudes were determined was taken nearly a year before the spectrograms, and that this may have produced a spurious frequency maximum at a brighter magnitude than the true maximum. Also it must be remembered that in both Herbig's work and in the present investigation "instantaneous" values of the

brightness of the variable stars have been used in determining the luminosity function and that this may have had some effect upon the results.

VII. INTERPRETATION FROM THE STANDPOINT OF STELLAR EVOLUTION

In the preceding sections we have seen that the color-magnitude diagram for NGC 2264 consists of an apparently normal main sequence extending from O7 to A0. For stars later than A0, the sequence departs from the normal main sequence by first rising by 1.5 mag. and then extending as a broad band of points 2 mag. wide parallel to and about 2 mag. above the main sequence. The reality of the 1.5-mag. rise has been checked spectroscopically, as has the membership of a number of the fainter stars. From the situation of the cluster against a dark cloud and from consideration of the number of foreground stars to be expected, we have concluded that the color-magnitude diagram is not badly affected by non-members and therefore represents with fair accuracy the stellar content of the cluster. As pointed out in the introduction, theoretical investigations predict that in an extremely young cluster of stars the fainter stars will still be in the process of contracting from the prestellar medium, since the contraction time depends upon the mass of the star. Consequently, the color-magnitude diagram of such a cluster should consist of a main sequence extending down to some point which depends upon the age of the cluster, below which the stars will lie to the right of the main sequence, departing more and more from it as one goes to fainter stars. Thus we see that, at least in a general way, the color-magnitude diagram of NGC 2264 agrees with the diagram predicted theoretically for an extremely young cluster of stars.

Salpeter (1953) has calculated that about 10^6 years are required for an A0 star to reach the main sequence, while the more refined calculations of Henyey *et al.* (1955) give 3×10^6 years as the time required for an A0 star to reach the main sequence by gravitational contraction from a starting configuration having a surface temperature of 4000°. It is evident that if the theory of gravitational contraction time is correct and if the turnoff of the cluster sequence is actually the result of the age of the stars, then the age of the cluster inferred from the maximum possible lifetime of the brightest star in the cluster should be greater than, or equal to, the age given by the turnoff. The age of the brightest star in NGC 2264, the O7 star S Mon, has been estimated from the rate of conversion of hydrogen to helium. If we assume that the star has a mass of $15\mathfrak{M}_\odot$ and that it has maintained its present luminosity throughout its lifetime, the time required for it to burn 10 per cent of its hydrogen is 2.1×10^6 years. However, it is possible that S Mon is somewhat older than this and has already begun to evolve away from the main sequence. An upper limit to the age of the star can be obtained by assuming that S Mon began its career on the main sequence with an absolute magnitude that was 1 mag. fainter than its present luminosity and that the star has just now reached the point where, having burned 10 per cent of its hydrogen, it is beginning to evolve away from the main sequence. In this manner the maximum possible age of S Mon is found to be 5.3×10^6 years. The true age of the star probably lies somewhere between 2 and 5×10^6 years and agrees well with the age inferred from the turnoff of the main sequence. Owing to the distance of NGC 2264, the proper-motion data available at the present time (van Maanen 1930) are not sufficiently accurate to permit the age of the cluster to be determined from any possible motions of expansion.

An interesting feature of the calculation by Henyey *et al.* (1955) of the evolutionary tracks of gravitationally contracting stars is that they indicate that the brightness of the star decreases just before it reaches the main sequence. For an A0 star, the amount of the decrease is about 0.6 mag. Thus, although the size and shape of the "hump" in the cluster sequence at A0 is not the same as predicted by the theory, it may be that this feature of the color-magnitude diagram is related to the predicted decrease in brightness.

Unfortunately, the theoretical work which has been done to date does not give us a good picture of the shape of the sequence in the cluster below the turnoff from the main se-

quence. However, it would appear that the sequence should continually diverge from the main sequence rather than run more or less parallel to it, as it is observed to do in NGC 2264. This disagreement is probably not too serious, since the theoretical work is still in a rather preliminary state. At the present time the most significant comparisons of the observations with the theory are probably the age determined from the point of turnoff and the *direction* of the divergence of the fainter stars.

At the same time it is worth noting that if the influence of foreground stars upon the color-magnitude diagram of NGC 2264 has been underestimated, the effect of these stars would be to make the cluster sequence appear to run more nearly parallel to the main sequence than it actually does. In addition, we have tacitly assumed that the ages of all the stars in the cluster are identical; if this is not the case, then this difference in age will also have the effect of making the cluster sequence run more nearly parallel to the main sequence than would a sequence composed of stars of the same age. Finally, we must remember that a large number of the fainter stars are variable, and, since "instantaneous" rather than mean positions of the variables have been used in the diagram, the shape of the cluster sequence may have been affected.

One feature of the color-magnitude diagram for which the present theory does not account is the occurrence of several stars *below* the position of the main sequence, discussed in Section IV. Another unexplained feature is the apparent existence of five yellow giants in the cluster. As pointed out in Section V, the membership of these stars is still not entirely certain. If they are members, this will be the first cluster in which yellow giants have been found together with OB stars. It will also differ from other galactic clusters, in that the giants in NGC 2264 are several magnitudes fainter than the brightest stars on the main sequence. According to our current ideas of stellar evolution, the giants in the somewhat older galactic clusters are stars which were once on the main sequence but have now evolved along almost horizontal tracks into the giant region (Johnson and Sandage 1955). In the case of NGC 2264, there has not been time for the observed giants to have been produced by stars evolving from the main sequence unless we suppose that these stars were formed much earlier than the other stars in the cluster. If these five stars are members of the cluster, then one possible explanation of their existence might be that they, too, are young stars which are in the process of contracting gravitationally to the main sequence.

It was pointed out in Section V that a rapid increase in the rotational velocity of stars belonging to the cluster sequence occurs between F8 and K0. As we indicated, this is the exact opposite of the variation of rotational velocity with spectral type found for ordinary stars. However, such a variation of rotation with spectral type might be expected in a group of stars such as this where the stars are in the process of contracting from the prestellar medium. While we still do not know very much about the manner in which the mutual gravitational attraction of a cloud of material becomes the dominant force acting upon it, it would seem reasonable to suppose that such a mass of material, when condensing to form a star, would possess some angular momentum. As the protostar continues to contract, the angular velocity will increase, and, if some mechanism did not act to diminish this rotational velocity, it is very probable that the star would exceed the limit of rotational stability long before it had reached the main sequence. The problem of the loss of angular momentum has been investigated by Lüst and Schlüter (1955). Making plausible assumptions regarding the density of interstellar material in the immediate neighborhood of a newly formed star, they find that if the star possesses a magnetic field of 100 gauss at its surface, the effect of magnetic braking is sufficiently great to cause a star rotating with a velocity at the limit of rotational stability to lose all its angular momentum in less than 10^6 years. It is difficult to determine the length of time required for the loss of angular momentum from the color-magnitude diagram of NGC 2264, since we cannot be sure to what extent the observed stars represent a homogeneous age or mass group. If we interpret those stars which show rotation as being stars of similar mass and

slightly different age, then the evolutionary tracks computed by Henyey *et al.* (1955) indicate that the angular momentum of these stars is being lost in about 10^6 years, in agreement with the order of the length of time predicted theoretically.

The occurrence of the T Tauri stars in NGC 2264 and their location in the color-magnitude diagram seem to indicate that stars of this type are extremely young and are in the process of contracting gravitationally to the main sequence. It is not clear from the observations of NGC 2264 whether the T Tauri phenomenon represents a particular stage in the gravitational contraction of all newly formed stars or whether it is only stars fainter than a certain absolute magnitude which show the effect. The fact that there is a rather sharp upper limit to the T Tauri stars in NGC 2264 at $M_v = +3.5$ gives us no information on this point, since the rate of evolution is a function of mass or luminosity, so that the stars brighter than this limit may all have passed through the T Tauri stage. Even for the stars fainter than $M_v = +3.5$, it is not clear whether the T Tauri phenomenon is a necessary result of the contraction process or whether, as is commonly suggested, the phenomenon results from the interaction of these stars with surrounding nebulosity, although the fact that the reddening of the cluster is small would seem to militate against the interaction theory. It is certain that the study of the T Tauri stars will be of great importance to our understanding of these early stages of stellar evolution.

Salpeter (1955) has computed an "original" luminosity function from the observed luminosity function for stars in the solar neighborhood and the known rates of evolution of stars away from the main sequence. This "original" luminosity function should represent the appearance of the luminosity function in an extremely young group of stars where no evolution away from the main sequence has yet occurred, provided that the distribution of masses in the group is the same as for stars in the vicinity of the sun. Plotting the evolutionary tracks calculated by Henyey *et al.* (1955) in terms of V and $B-V$, it turns out that, to a first approximation, the V magnitude of a gravitationally contracting star remains constant. Thus the luminosity function for a cluster containing gravitationally contracting stars can be compared with the luminosity function for main-sequence stars. A comparison of Salpeter's luminosity function with the observed luminosity function of NGC 2264 is given in Table 8. The sixth column of the table gives the logarithm of the ratio of the number of stars in NGC 2264 to the number in the neighborhood of the sun, for each magnitude interval. The seventh column gives $\log \psi/\phi$, where ψ/ϕ is the ratio of the number of stars in the "original" luminosity function to the number in the observed luminosity function for the solar neighborhood, calculated by Salpeter. The comparison with Salpeter's luminosity function is facilitated in the eighth column, which gives the observed ratio of the number of cluster stars to stars in the vicinity of the sun, reduced on the assumption that the density of stars in the cluster is twenty times the density in the solar neighborhood. It will be seen that the luminosity function for NGC 2264 agrees well with Salpeter's luminosity function for stars brighter than $M_v = +3$, although the comparison is not too exact because of the small number of bright stars in the cluster. Relative to the number of brighter stars, there is an excess of stars in the cluster fainter than $M_v = +3$, compared to the solar neighborhood. It is interesting to note that this is just the portion of the luminosity function populated by the T Tauri stars. The interpretation of the variations in the luminosity functions of different young clusters of stars and between those of the clusters and the solar neighborhood will be discussed in a later paper in this series.

Since the V magnitude of the contracting stars remains roughly constant, we may use the mass-luminosity law in connection with the observed luminosity function to estimate the total mass of the cluster. In this way the total mass of NGC 2264 is found to be about $450\mathfrak{M}_\odot$. Assuming that the volume of the cluster is 300 pc^3, the mass density of the cluster is $1.5\mathfrak{M}_\odot/\text{pc}^3$. The density required for stable configurations has been estimated (Bok 1934) to be $0.1\mathfrak{M}_\odot/\text{pc}^3$.

Most of the observational material presented in this paper was obtained at the Mount Wilson and Palomar Observatories under a Carnegie Fellowship. However, some additional photoelectric observations of the brighter stars were secured in February and March, 1955, during a visit to the Lowell Observatory, and I am indebted to Dr. A. G. Wilson for making the facilities of the observatory available to me. Also the spectra of a few of the fainter stars in NGC 2264 were observed during the winter of 1955 while a guest investigator at Mount Wilson, under a National Science Foundation grant, administered by the University of California, Berkeley.

I am also greatly indebted to Drs. H. L. Johnson, W. W. Morgan, and R. J. Trumpler for permission to include unpublished observations of NGC 2264 in this paper. It is likewise a pleasure to thank Dr. A. J. Deutsch for checking my classifications of the spectra of stars in NGC 2264 and Drs. W. Baade and G. H. Herbig for many stimulating discussions of the problem.

REFERENCES

Blanco, V. M. 1956, *Ap. J.*, **123**, 64.
Bok, B. J. 1935, *Harvard Circ.*, No. 384.
Haro, G., and Herbig, G. H. 1955, *Bol. Obs. Tonantzintla y Tacubaya*, No. 12, p. 33.
Haro, G., and Morgan, W. W. 1953, *Ap. J.*, **118**, 16.
Henyey, L. G., LeLevier, R., and Levée, R. D. 1955, *Pub. A.S.P.*, **67**, 154.
Herbig, G. H. 1952, *J.R.A.S. Canada*, **46**, 222; *Dom. Ap. Obs. Contr.*, No. 27 (Part 3).
———. 1954, *Ap. J.*, **119**, 483.
Herbig, G. H., and Spalding, J. F. 1955, *Ap. J.*, **121**, 118.
Hoffmeister, C. 1949, *Ergebn. A.N.*, **12**, A10.
Johnson, H. L. 1956, private communication.
Johnson, H. L., and Hiltner, W. A. 1956, *Ap. J.*, **123**, 267.
Johnson, H. L., and Morgan, W. W. 1953, *Ap. J.*, **117**, 313.
Johnson, H. L., and Sandage, A. R. 1955, *Ap. J.*, **121**, 616.
Kukarkin, B. V., and Parenago, P. P. 1955, Seventh Suppl. to *General Catalogue of Variable Stars* (Moscow).
Lüst, R., and Schlüter, A. 1955, *Zs. f. Ap.*, **38**, 190.
McCuskey, S. W. 1949, *Ap. J.*, **109**, 139.
———. 1954, *ibid.*, **120**, 139.
Parenago, P. P. 1953, *Astr. Zhur.*, **30**, 249.
Salpeter, E. E. 1953, *Symposium on Astrophysics* (Ann Arbor: University of Michigan).
———. 1955, *Ap. J.*, **121**, 161.
Trumpler, R. J. 1930, *Lick Obs. Bull.*, **14**, 154.
———. 1956, private communication.
van Maanen, A. 1930, *Mt. W. Contr.*, No. 405.
van Rhijn, P. 1936, *Groningen Pub.*, No. 47, p. 17.
Walker, M. F. 1954, *Pub. A.S.P.*, **66**, 71.
Wenzel, W. 1955*a*, *Mitt. veränderliche Sterne*, No. 190.
———. 1955*b*, *ibid.*, No. 193.
Wolf, M. 1924, *A.N.*, **221**, 379.

PHOTOMETRIC, POLARIZATION, AND SPECTROGRAPHIC OBSERVATIONS OF O AND B STARS*

W. A. HILTNER
Yerkes and McDonald Observatories
Received June 20, 1956

ABSTRACT

This paper consists primarily of a catalogue of O and B stars for which observations for polarization, magnitude, color, and spectral types are available. The magnitudes and colors are on the *U*, *B*, *V* system, and the spectral types on the two-dimensional MK system. In addition to the direct observations for magnitude, colors, spectral types, and polarization, the interstellar absorption, the distance modulus, and the ratio of interstellar polarization to absorption are also recorded in the catalogue. The maximum polarization, 0.22 mag., has been found in Cygnus, where the absorption is in excess of 10 mag. An inclination for the Orion-Perseus spiral arms is derived from the alignment of the planes of vibration. The longitude of the radius vector perpendicular to the spiral arm is 102°, in contrast to approximately 135° from 21-cm observations but is in fair agreement with the O association data. A maximum value for the ratio of polarization absorption, p/A_v, is determined. A value near 0.06 is indicated from the analysis of the data.

INTRODUCTION

This is the third catalogue of early-type stars for which interstellar polarization measurements have been made (Hiltner 1951 and 1954). This catalogue differs from the previous two. In addition to the polarization data, the stars were also observed for magnitude and color on the *U*, *B*, *V* system, and slit spectrograms were obtained for spectral classification on the MK system. These additional data, of course, greatly enhance the value of the catalogue not only for investigations on interstellar polarization but also for other galactic-structure studies. For example, a reliable maximum value for the ratio of interstellar polarization to total absorption can be determined. Distance moduli can now be computed. However, the accuracy for an individual star is not sufficiently great to assist materially in polarization studies, but these data should prove useful in other galactic-structure studies, where the average of a number of stars can give significant information—for example, the distances of associations. Many stars in this catalogue also appear in one or the other of the earlier ones. This is the case where the observed polarization was published previous to this catalogue and in the meantime spectroscopic and photometric observations were completed.

OBSERVATIONS

Polarization Measurements

The polarization observations in this paper consist of data previously published as well as new data. All interstellar polarization data published earlier (Hiltner 1951, 1954) and the new data published here were obtained with a photoelectric photometer attached to the 82-inch reflector of the McDonald Observatory. The polarization analyzer consisted of a Polaroid sheet mounted between glass plates. Relative to the photosensitive surface, this Polaroid occupied either of two positions differing by 90° in position angle. In addition to this rotation of 90°, the Cassegrain focus of the telescope is provided with a head that can be rotated to any position angle. Consequently, the Polaroid in either of the two positions separated by 90° could occupy any position angle. A series of observations, where the difference in intensity at the two positions of the Polaroid is measured at different settings of the Cassegrain head, yielded a sine-curve when the differ-

* *Contribution of the McDonald Observatory of the University of Texas*, No. 269.

ences in intensities were plotted against position angle. In the normal observing program an observation was made with the Cassegrain head set at some arbitrary position angle. An observation at this angle consisted of a deflection with the Polaroid in one of its two positions, a deflection in the other position 90° from the first and then a second deflection at the original position. The Cassegrain head was then rotated in position angle by 30°, and the same procedure was followed. That is, one deflection at position A of the Polaroid, a deflection at position B, 90° from A, and then a second deflection at A. From these two sets of observations the position angle was estimated at which the maximum polarization effect could be observed. An observation at this estimated position angle was then made. In this case the observation consisted of three deflections at position A of the Polaroid separated by two at position B. This observation near maximum polarization was then followed by two sets of observations with the position angle of the Cassegrain head set at 45° on either side. These two series of observations taken to determine the position angle of the plane of vibration consisted of three deflections each, two at position A, separated by one at B. All deflections had a duration of about 30 seconds.

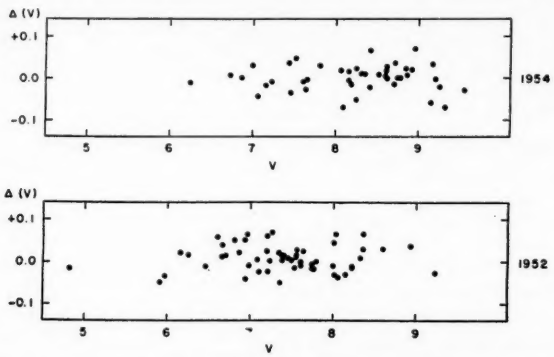

FIG. 1.—Comparison of magnitudes obtained with the 13-inch and the 82-inch reflectors of the McDonald Observatory.

The first two preliminary series of observations as well as the last three were entered into a least-squares solution for the amount of polarization and the plane of vibration. At some galactic longitudes the plane of vibration could be estimated (plane of the Galaxy) in advance with sufficient accuracy. Under such circumstances only the last three series of observations were necessary.

In the earlier observations an RCA 1P21 photomultiplier was employed. Later this was replaced by an EMI 5659 photomultiplier, since the latter has a photocathode normal to the optical axis of the telescope and hence should be insensitive to the plane of vibration of the exciting radiation. However, this photomultiplier was also sensitive to the plane of vibration of the exciting radiation. The radiation transmitted by the photocathode was free to be absorbed by the Venetian blind of the multiplier structure (Sommer and Turk 1950). Since the Venetian blinds are inclined to the optical axis and have photoelectric sensitivity, a residual polarization of about 0.01 mag. was present. This residual polarization, detected by observing nearby stars, was removed by a quartz depolarizer.

Magnitude and Color Measurements

The photometric observations in three colors were obtained over a period of 4 years. Two telescopes were employed—the 13-inch and the 82-inch reflectors of the McDonald

Observatory. Three amplifiers of three different designs were used during the four observing seasons. In all cases the amplifiers were checked for linearity and calibrated against standard laboratory potentiometers. The same RCA 1P21 photomultiplier and filters were employed with the 82-inch reflector throughout the series, and this same combination was used with the 13-inch reflector in 1954. However, a different set, but of the same type, of photomultiplier and filters was used on the 13-inch reflector in 1952.

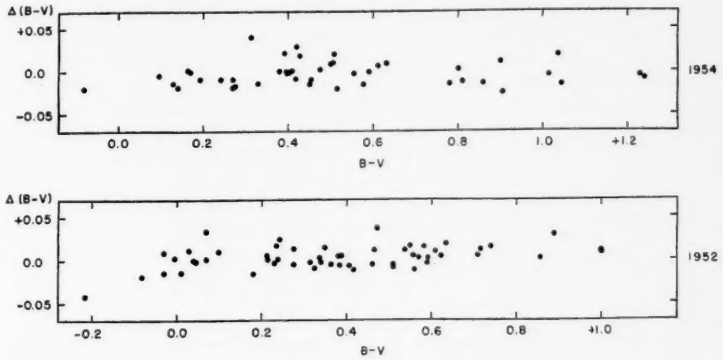

FIG. 2.—Comparison of $B-V$ colors obtained with the 13-inch and 82-inch reflectors of the McDonald Observatory.

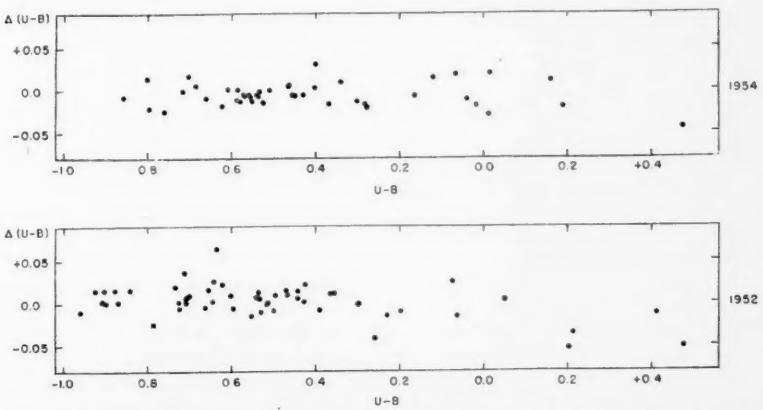

FIG. 3.—Comparison of $U-B$ colors obtained with the 13-inch and the 82-inch reflectors of the McDonald Observatory.

In all cases the same filter-photomultiplier combinations were used as were originally employed in defining the U, B, V color system (Johnson and Morgan 1953), to which all natural colors and magnitudes were transferred. No difficulty was encountered in transferring color systems, for all transformations were linear. A comparison of the 1952 and 1954 13-inch observations and the 82-inch observations for all seasons is shown in Figures 1, 2, and 3. For the 1952 13-inch reflector data no piece of equipment was in common with the 82-inch reflector data. Any systematic difference that may be present is less

than 0.01 mag., in magnitude as well as in color. The 1954 13-inch observations employed the same equipment as that used on the 82-inch reflector. Again any systematic error is less than 0.01 mag. The individual points in the figures are often represented by only one observation by either or both telescopes.

The extinction was determined on all nights when the run was long enough to permit such determination. However, a mean value was used, for the evidence supports the conclusion that, in general, if only photometric nights are used for photometry, the extinction is less variable than the accuracy with which it can be determined during a night when the extinction observations are interspersed with a significant number of observations on program stars. Nightly corrections were then added to the observations. These corrections are evaluated by observing standard stars at frequent intervals—about 1 hour. At the beginning of the photometric observations the extinction was given careful consideration. In August and September, 1952, the extinction was measured with great care. The results of these observations are recorded in Table 1. These data support the

TABLE 1

EXTINCTION MEASUREMENTS

Date 1952	k_y	k_{cy}	k_{cu}	Date 1952	k_y	k_{cy}	k_{cu}
August 19.....	0.151	0.090	0.307	September 6....	0.145	0.086	0.303
20.....	.159	.087	.310	7....	.163	.086	.312
21.....	.157	.089	.307	8....	0.168	0.088	0.315
22.....	0.151	0.090	0.314				

TABLE 2

STANDARD STARS

Star	V	$B-V$	$U-B$	Star	V	$B-V$	$U-B$
HD 14633....	7.44	−0.210	−1.067	δ Tri.....	4.87	+0.61	+0.02
10 Lac.....	4.87	− .200	−1.045	α Ori.....	1.99	+1.153	+1.12
η Hga.....	4.31	− .196	−0.74	HR 8832....	5.56	+1.013	+0.892
γ Her.....	3.89	− .155	−0.558	ϵ CrB.....	4.15	+1.227	+1.282
HR 875.....	5.17	+0.085	+0.05				

conclusion that, when only photometric nights are used for photometry, the extinction is indeed quite uniform from night to night. In the table, k_y represents the extinction for the yellow filter, k_{cy} the extinction for blue minus yellow color, and k_{cu} the extinction for ultraviolet minus blue color—all for zero natural color. The color extinctions were computed with the condition in the least-squares solution that the no-atmosphere colors of the extinction stars were constant from night to night.

Only nights of good quality were used for photometric observations. On nights of doubtful or non-photometric quality, the Cassegrain spectrograph was placed on the telescope to obtain classification spectrograms of program stars.

To transfer from the natural colors to the U, B, V system, the standard stars listed in Table 2 were employed. In addition to these stars, others with published U, B, V magnitudes and colors were observed to check the linearity of the transformation. The values given in Table 2 do not differ significantly from the more recent values published by Johnson (1956).

Spectroscopic Observations

In order to secure spectrograms for two-dimensional classification, a new camera was installed on the Cassegrain spectrograph of the McDonald Observatory. The lens, designed by Dr. F. E. Ross, consists of three elements, two of which are cemented. It has an aperture of 90 mm and a focal length of 118 mm. The dispersion is 86 A/mm at Hδ when used in conjunction with the two glass prisms. The exposure time for a twelfth-magnitude star is 1 hour for a spectrogram 0.7 mm wide on Eastman 103*a*-O emulsion. As mentioned earlier, the spectrographic observations were, in general, reserved for those nights when the sky was not of photometric quality. All spectrograms were developed under the same physical conditions.

Nearly sixteen hundred spectrograms of O and B stars have been obtained to date by the author with this spectrograph. The stars are distributed approximately as follows: 600 stars with *Henry Draper* numbers, 175 with *Henry Draper Extension* numbers, and 600 with *Bonner Durchmusterung* numbers only, and 200 stars not in these catalogues. Of the 1600, over 600 of the fainter stars in the Nassau and Morgan (1951) published list of OB stars were observed. These spectrograms were classified by Morgan and the classifications published (Morgan, Code, and Whitford 1955). The remaining spectrograms are of stars found in the various lists of early-type stars.

TABLE 3

O AND B STARS

Star	1855		Magnitude	Star	1855		Magnitude
	α	δ			α	δ	
1.....	0^h19^m8	+63° 18′	10.87	13.....	0^h46^m0	+62° 42′	11.21
2.....	20.0	+63 20	11.11	14.....	0 47.0	+63 13	11.06
3.....	21.6	+62 16	10.49	15.....	0 48.3	+62 29	11.67
4.....	24.1	+62 29	11.09				
5.....	34.5	+64 08	11.29	16.....	0 50.7	+63 51	11.00
				17.....	0 50.9	+63 02	11.73
6.....	35.6	+63 41	11.38	18.....	0 52.1	+63 09	11.10
7.....	36.5	+63 36	10.69	19.....	0 52.1	+63 10	10.92
8*.....	36.6	+63 36	9.50	20.....	0 52.2	+63 09	11.18
9.....	36.7	+63 11	11.22				
10.....	40.5	+63 25	11.15	21.....	0 53.7	+63 13	11.03
				22.....	2 12.9	+57 30	10.56
11.....	40.7	+63 06	10.71	23.....	2 44.9	+58 38	10.66
12.....	0 43.4	+63 46	11.31	24*.....	2 47.0	+57 18	10.24

* No. 8 = BD+63°89; star No. 24 can be found on chart for star 13, reference 2. It is 12 mm from the left edge and 3 mm from the top edge of the chart.

New Early-Type Stars

Earlier work (Hiltner 1951) had shown that high polarization was present in the region $\alpha = 0^h40^m$ and $\delta = +63°$. In order to investigate this region further, objective-prism plates of long exposure were obtained with the 26-inch Schmidt at the Tonantzintla Observatory, centered on this position. A large number of faint early-type stars were found. Those which have been observed for color, spectral classification, and polarization are recorded in Table 3. In addition, this table contains three early-type stars found by the Misses González at the Observatorio Tonantzintla. These three stars were in tentative lists of O and B stars kindly sent to the author by the Misses González but as yet do not appear in any of the published lists from Tonantzintla. For ease of identification Figures 4 and 5 give identification charts for all the stars in Table 3 except No. 24. This

star can be identified on the chart for star 13 in the *Boletín de los Observatorios Tonantzintla y Tacubaya* (González and González 1953). It is 12 mm from the left edge and 3 mm from the top edge of the chart. For further ease in identification a few *BD* stars are identified on each chart. These stars are listed in Table 4.

TABLE 4

IDENTIFICATION OF REFERENCE STARS IN FIGURES 4 AND 5

Chart A	Chart B	Chart G	Chart H
a) +63°52	*a*) +62°102	*a*) +62°164	*a*) +63°118
b) +63°55		*b*) +62°172	*b*) +62°175
Chart C	Chart D	Chart I	*c*) +63°114
a) +64°68	*a*) +63°81	*a*) +63°117	Chart J
b) +64°74		*b*) +63°122	*a*) +62°175
Chart E	Chart F	Chart K	*b*) +62°185
a) +62°147	*a*) +63°97	*a*) +57°553	Chart L
b) +62°152	*b*) +63°99	*b*) +57°551	*a*) +58°532
		c) +57°555	*b*) +58°529

THE CATALOGUE

This catalogue (Table 5) of O and B stars has 1259 entries. There is appreciable overlap with two previous catalogues on interstellar polarization published by the author. However, this catalogue gives not only polarization measurements but also the two-dimensional spectral types and the magnitudes and colors in the *U*, *B*, *V* system. Details of the catalogue follow.

Column 1.—This column gives running numbers to the stars observed in this program for which we have complete data. An asterisk after a number in this column and following columns refers to a footnote at the end of the table.

Column 2.—The *Henry Draper Catalogue* number is given whenever available. Stars in the *Henry Draper Extension* are prefixed with an *E*.

Column 3.—The *Bonner Durchmusterung* number is given also whenever available. For a few other stars the *Córdoba Durchmusterung* number is recorded.

Columns 4 and 5.—These columns give the position of the stars for the 1900 epoch.

Columns 6 and 7.—The galactic co-ordinates, referred to the pole at $\alpha = 12^h40^m$, $\delta = +28°$ (1900), are recorded in these columns. The co-ordinates were first computed with the help of the Lund tables (Ohlsson 1932) from the 1900 co-ordinates. The computations were checked graphically with charts constructed from the Lund tables.

Column 8.—The galactic parallactic angle is given in this column. It is the angle between the galactic-latitude circle and the declination circle. Again the Lund tables were employed.

Column 9.—This column gives the observed amount of polarization in magnitudes.

Column 10.—The position angle of the electric-vector maximum is given here in equatorial co-ordinates.

Column 11.—The position angle of the electric vector is given here in galactic co-ordinates. It is obtained by adding the observed position angle in equatorial co-ordinates to the parallactic angle.

Column 12.—This column gives the spectral-luminosity type. The spectral types were obtained from the literature when available (for example, Morgan, Code, and Whitford 1955). Many previously unclassified stars were kindly classified by W. W. Morgan from spectrograms obtained by the author. Also some spectral classifications were made by the author.

Columns 13, 14, and 15.—These columns give the photometric observations on the *U*, *B*, *V* system. All entries are represented by two or more observations per star obtained on different nights and, in many cases, different seasons.

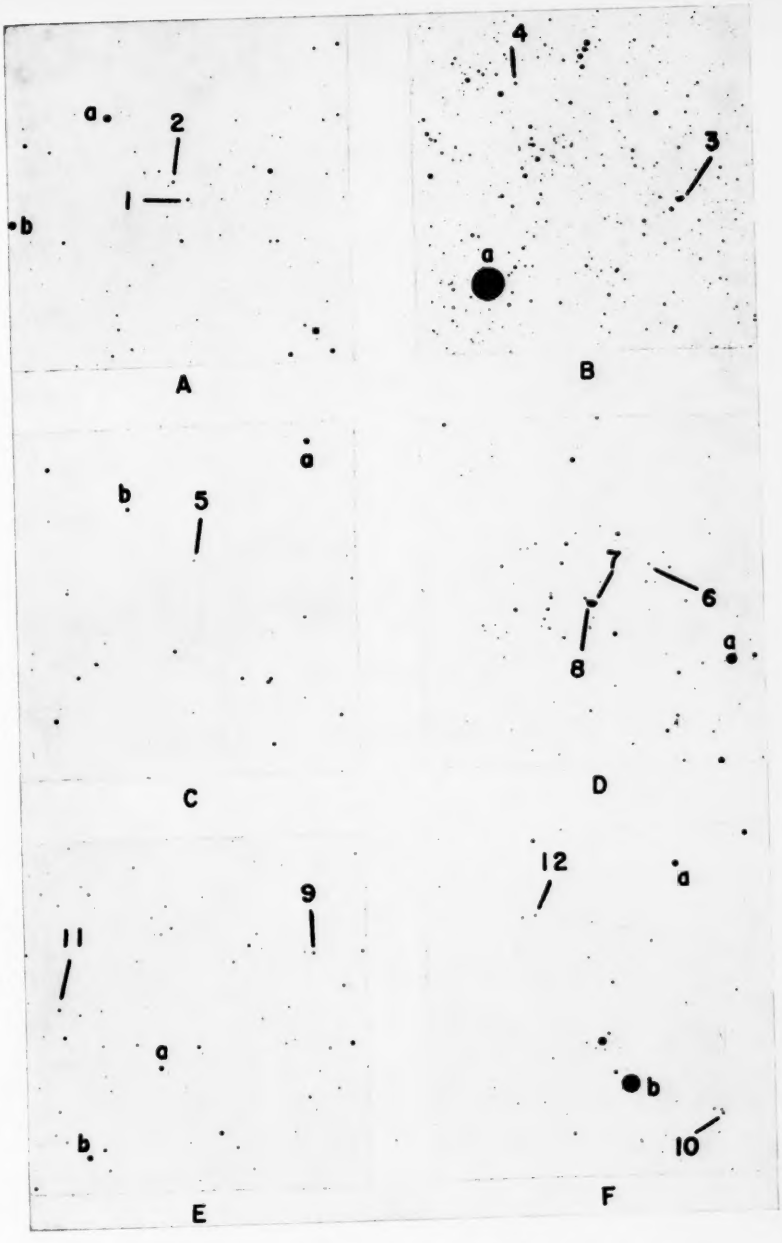

FIG. 4.—Finding charts for new OB stars

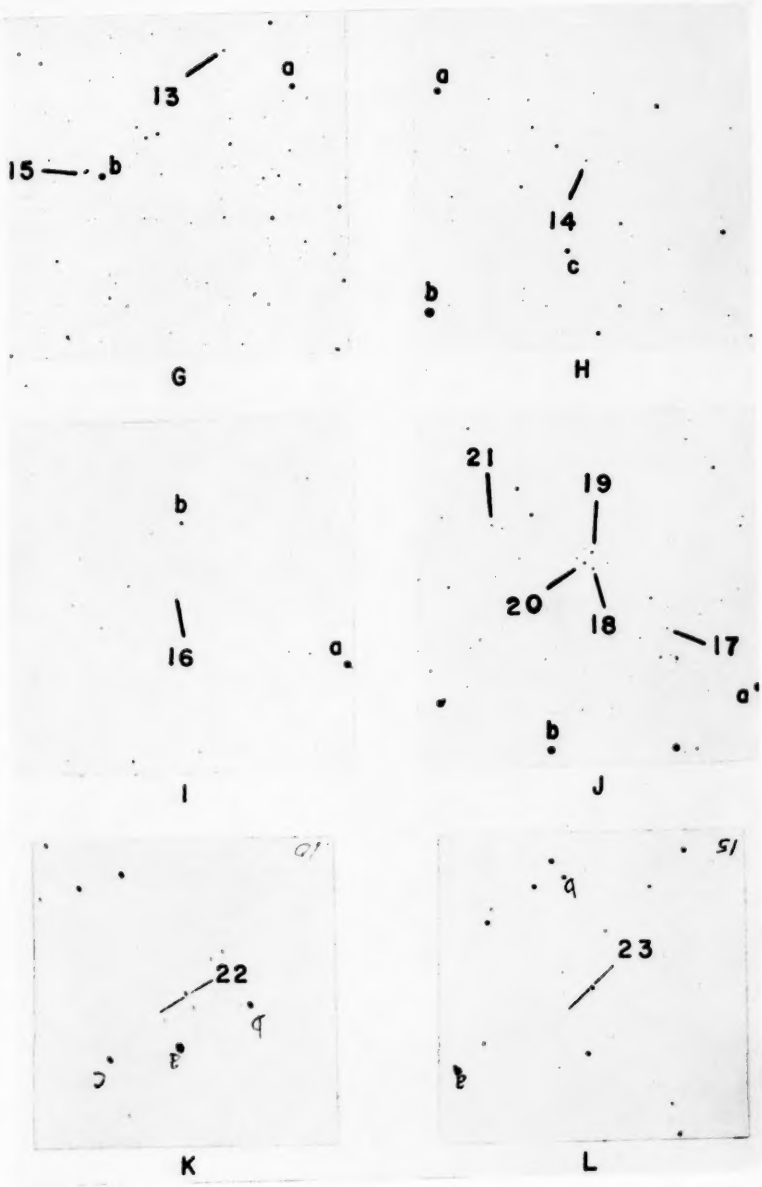

FIG. 5.—Finding charts for new OB stars

TABLE 5

TABLE 5

PHOTOMETRIC AND SPECTROGRAPHIC OBSERVATIONS OF O AND B STARS

No.	HD	BD	1900 α	1900 δ	l	b	φ	p	θ	θ'	Spectrum	V	B-V	U-B	$3E_{(B-V)}$	m	M	m-M	p/A_V
			h^m																
1		+60°2668	0 00.8	+60°19'	85.2	- 1.3	8.6	0.054	82	91	B1 III	8.95	+0.47	-0.48	2.19	6.76	-4.4	11.2	0.025
2	108	+62°2363	0 00.9	+63°07'	85.6	+ 1.4	8.6	0.035	81	90	O8 fp	7.40	+0.18	-0.79	1.47	5.93	-5.1	11.0	0.024
3*			0 01.1	+61°58'	85.4	+ 0.3	8.6	0.053	59	67	B1.5 e III-V	10.47	+0.26	-0.67	1.53	8.94	-3.4	12.3	0.035
4*			0 01.3	+59°45'	85.1	- 1.9	8.5	0.015	129	137	B8 II:	10.88	+0.55	+0.11	1.92	8.96	-4.4	13.4	0.008
5		+59°2829	0 01.6	+60°04'	85.2	- 1.6	8.5	0.030	74	82	B0: IV: pne	9.84	+0.40	-0.65	2.10	7.74	-4.6	12.3	0.014
6		+62°1	0 02.4	+62°31'	85.7	+ 0.8	8.3	0.076	71	80	B2 pe (IV-V)*	10.34	+0.34	-0.63	1.74	8.60	-2.4	11.0	0.044
7	593	+58°11	0 05.3	+59°06'	85.6	- 2.6	7.7	0.023	60	68	B1 V	6.69	+0.03	-0.75	0.87	5.82	-3.1	8.9	0.026
8	698	+57°28	0 06.3	+57°39'	85.5	- 4.1	7.5	0.034	63	70	B5 II:	7.07	+0.18	-0.40	1.02	6.05	-4.6	10.6	0.033
9	1070	+58°18	0 09.9	+59°15'	86.2	- 2.5	6.6	0.026	71	78	A5 II:	7.98	+0.59	+0.51	1.32	6.66			0.020
10	1383	+60°25	0 12.9	+61°10'	86.7	- 0.7	6.0	0.029	81	87	B1 II	7.63	+0.26	-0.68	1.56	6.07	-4.9	11.0	0.018
11		+62°49	0 13.4	+63°01'	87.0	+ 1.2	5.9	0.067	81	87	B0.5 III	8.94	+0.41	-0.52	2.07	6.87	-4.7	11.6	0.032
12	1544	+61°38	0 14.6	+61°31'	87.0	- 0.3	5.6	0.040	89	95	B0 III:	8.11	+0.17	-0.76	1.41	6.70	-5.0	11.7	0.028
13*		+61°39	0 14.8	+61°54'	87.0	0.0	5.6	0.059	91	97	B0.5 IV	8.52	+0.30	-0.75	1.74	6.78	-4.2	11.0	0.034
14		+61°40	0 15.0	+61°50'	87.0	0.0	5.5	0.068	58	63	B2 p (e?)*	9.55	+0.47	-0.51	2.13	7.42			0.032
15		+63°33	0 16.2	+64°03'	87.4	+ 2.2	5.3	0.084	103	108	B1 V	9.44	+0.57	-0.34	2.49	6.95	-3.1	10.1	0.034
16		+60°39	0 16.2	+61°10'	87.1	- 0.7	5.3	0.030	85	90	O9 V	9.46	+0.24	-0.70	1.65	7.81	-4.6	12.4	0.018
17		+62°68	0 18.1	+62°49'	87.5	+ 0.9	4.8	0.076	96	101	B1 II	9.61	+0.58	-0.38	2.52	7.09	-4.9	12.0	0.030
18	1976	+51°62	0 18.9	+51°28'	86.7	-10.4	4.7	0.018	72	77	B5 IV	5.56	-0.11	-0.61	0.15	5.41	-1.8	7.2	0.120
19		+63°41	0 19.6	+64°07'	87.8	+ 2.2	4.5	0.119	104	109	B0 III	10.46	+0.81	-0.27	3.33	7.13	-5.0	12.1	0.036
20	2083	+71°16	0 20.0	+71°15'	88.4	+ 9.3	4.5	0.032	92	96	B1 V	6.89	+0.03	-0.83	0.87	6.02	-3.1	9.1	0.037
21		+63°43	0 20.0	+64°11'	87.8	+ 2.3	4.4	0.088	103	107	B0.5 n (V)	10.73	+0.76	-0.30	3.12	7.61	-3.6	11.2	0.028
22		+61°74	0 20.4	+62°00'	87.7	+ 0.1	4.3	0.040	92	96	O9 V nn	9.55	+0.32	-0.66	1.89	7.66	-4.6	12.3	0.021
23		+61°77	0 20.8	+62°13'	87.8	+ 0.3	4.2	0.039	90	94	B1 IV	9.59	+0.19	-0.66	1.35	8.24	-3.8	12.0	0.029
24		+62°79	0 20.9	+62°53'	87.8	+ 1.0	4.2	0.062	73	77	O9.5 IV	9.22	+0.41	-0.56	2.13	7.09	-4.4	11.5	0.029
25		+63°48	0 21.0	+63°52'	87.9	+ 1.9	4.2	0.119	109	113	B1 (III:) nne	9.12	+0.88	-0.19	3.42	5.70	-4.4	10.1	0.035
26		+60°51	0 21.0	+60°52'	87.7	- 1.0	4.2	0.063	63	67	A2 Ib	9.23	+0.62	+0.23	1.68	7.55	-5.6	13.2	0.038
27		+62°81	0 21.8	+62°30'	87.9	+ 0.6	4.0	0.037	83	87	B2 III	11.05	+0.37	-0.51	1.83	9.22	-3.6	12.8	0.020
28	2329	+57°85	0 22.1	+58°00'	87.6	- 3.9	4.0	0.026	70	74	B3 V	7.43	+0.07	-0.52	0.81	6.62	-1.5	8.1	0.032
29*			0 22.3	+63°33'	88.0	+ 1.6	3.9	0.127	89	92	B7 (III):	10.87	+0.85	+0.23	2.91	7.96			0.044
30	E 236419	+59°61	0 22.3	+60°04'	87.8	- 1.9	3.9	0.047	81	85	B2 III	9.14	+0.31	-0.51	1.65	7.49	-3.6	11.1	0.028
31*			0 22.6	+63°35'	88.1	+ 1.7	3.8	0.112	89	92	B1 V	11.11	+0.99	-0.20	3.75	7.36	-3.1	10.5	0.030
32		+55°81	0 22.7	+55°51'	87.6	- 6.1	3.8	0.037	68	72	B1.5: V: nn (e)	10.07	+0.07	-0.64	0.96	9.11	-2.6	11.7	0.038
33*			0 23.2	+62°31'	88.1	+ 0.6	3.7	0.051	96	100	B0 (V) p (e)	10.49	+0.39	-0.60	2.07	8.42	-4.1	12.5	0.025
34	2451	+61°92	0 23.2	+61°57'	88.0	0.0	3.7	0.041	84	88	B0.5 IV	8.73	+0.19	-0.72	1.41	7.32	-4.2	11.5	0.029
35	2619	+64°52	0 24.7	+64°43'	88.4	+ 2.8	3.4	0.100	99	102	B0.5 III	8.31	+0.57	-0.44	2.55	5.76	-4.7	10.5	0.039

TABLE 5—Continued

No.	HD	BD	1900 α (h m)	1900 δ	l	b	φ	p	θ	θ'	Spectrum	V	B-V	U-B	3E(B-V)	m	M	m-M	p/A$_V$
36		+61°105	0 25.6	+61°53'	88.3	- 0.1	3.2	0.074	81	84	O9 V	9.29	+0.27	-0.69	1.74	7.55	-4.6	12.2	0.042
37*			0 26.8	+62°44'	88.5	+ 0.8	2.9	0.063	72	75	B2 V	11.09	+0.52	-0.23	2.28	8.81	-2.0	10.8	0.028
38	2905	+62°102	0 27.3	+62°23'	88.5	+ 0.4	2.8	0.032	83	86	B1 Ia	4.16	+0.14	-0.79	1.20	2.96	-6.9	9.9	0.027
39	2928	+61°113	0 27.5	+61°59'	88.5	0.0	2.8	0.070	67	70	A0 Iab	8.61	+0.62	+0.07	1.86	6.75	-6.5	13.3	0.038
40		+63°61	0 27.6	+63°27'	88.6	+ 1.5	2.7	0.150	94	97	B1 Iab	9.65	+0.91	-0.17	3.51	6.14	-6.5	12.6	0.043
41		+61°122	0 29.2	+61°53'	88.7	- 0.1	2.4	0.060	85	87	B2 pe (V)	10.39	+0.32	-0.59	1.68	8.71	-2.0	10.7	0.036
42	3191	+60°71	0 30.1	+60°55'	88.8	- 1.1	2.2	0.055	53	55	B1 IV: nn	8.57	+0.44	-0.44	2.10	6.47	-3.8	10.3	0.026
43		+60°73	0 31.3	+60°49'	88.9	- 1.2	1.9	0.086	60	62	B1 Ib	9.64	+0.57	-0.42	2.49	7.15	-5.8	13.0	0.034
44*			0 34.0	+60°25'	89.3	- 1.6	1.3	0.054	72	73	O9 IV	9.99	+0.37	-0.61	2.04	7.95	-5.4	13.4	0.026
45		+63°70	0 34.9	+63°22'	89.4	+ 1.4	1.1	0.105	105	106	B0 Ib	9.17	+0.72	-0.37	3.06	6.11	-6.2	12.3	0.034
46*			0 36.6	+63°30'	89.7	+ 1.5	0.8	0.135	106	107	B0 pe (III)?*	10.75	+0.87	-0.26	3.51	7.24	-5.0	12.2	0.038
47	3940	+63°81	0 36.9	+63°45'	89.7	+ 1.8	0.7	0.108	100	101	A1 Ia	7.26	+0.73	+0.05	2.10	5.16	-6.9	12.1	0.051
48*			0 37.1	+64°22'	89.7	+ 2.4	0.6	0.154	93	94	B0.5 IV	11.29	+0.63	-0.38	2.73	8.56	-4.2	12.8	0.056
49		+61°153	0 37.1	+61°41'	89.7	- 0.3	0.6	0.010	105	106	A0 Ib	9.33	+0.84	+0.33	2.52	6.81	-5.6	12.4	0.004
50	4004*	+63°83	0 37.5	+64°14'	89.7	+ 2.2	0.5	0.138	96	97	W R	10.18	+0.37	-0.27					
51*			0 38.3	+63°55'	89.8	+ 1.9	0.4	0.147	99	99	B1 p (e) (V)	11.38	+0.59	-0.34	2.55	8.83	-3.1	11.9	0.058
52		+63°87	0 38.8	+63°47'	89.9	+ 1.8	0.3	0.126	96	96	B0.5 IV	9.87	+0.52	-0.47	2.40	7.47	-4.2	11.7	0.052
53*			0 38.8	+63°22'	89.9	+ 1.4	0.3	0.104	105	105	B1 pe (IV-V)	10.60	+0.72	-0.43	2.94	7.66	-3.4	11.1	0.035
54		+64°76	0 38.9	+64°43'	89.9	+ 2.7	0.2	0.148	94	94	B1 Ib	9.10	+0.59	-0.39	2.55	6.55	-5.8	12.4	0.058
55*			0 39.2	+63°51'	89.9	+ 1.9	0.2	0.124	92	92	B1 IV p ?	10.69	+0.49	-0.46	2.25	8.44	-3.8	12.2	0.055
56*		+63°89	0 39.2	+63°51'	89.9	+ 1.9	0.2	0.117	89	89	B1 Ib	9.50	+0.60	-0.41	2.58	6.92	-5.8	12.7	0.045
57*			0 39.3	+63°25'	89.9	+ 1.4	0.1	0.115	98	98	B2 III	11.22	+0.65	-0.31	2.67	8.55	-3.6	12.2	0.043
58*			0 39.3	+63°10'	89.9	+ 1.1	0.2	0.126	104	104	B1 III	11.05	+0.70	-0.28	2.88	8.17	-4.4	12.6	0.044
59*			0 39.5	+62°48'	89.9	+ 0.8	0.1	0.084	106	106	B0.5 V	10.50	+0.66	-0.31	2.82	7.68	-3.6	11.3	0.030
60		+63°92	0 39.9	+63°51'	90.0	+ 1.9	0.0	0.129	91	91	B2 n (III)	10.68	+0.57	-0.35	2.43	8.25	-3.6	11.8	0.053
61*			0 40.5	+63°50'	90.1	+ 1.8	359.9	0.095	91	91	B2 III	10.50	+0.53	-0.36	2.31	8.19	-3.6	11.8	0.041
62*			0 40.7	+63°55'	90.1	+ 1.9	359.8	0.100	96	96	B3 III	11.04	+0.56	-0.26	2.28	8.76	-3.3	12.1	0.044
63*			0 42.2	+62°27'	90.2	+ 0.5	359.5	0.086	89	89	O7	11.40	+0.48	-0.53	2.40	9.00	-5.1	14.1	0.036
64	4613	+64°83	0 43.0	+65°02'	90.3	+ 3.0	359.3	0.110	96	95	B1 II	8.79	+0.58	-0.35	2.52	6.27	-4.9	11.2	0.044
65*			0 43.1	+63°39'	90.3	+ 1.7	359.3	0.111	98	97	B3 IV	11.15	+0.51	-0.26	2.13	9.02	-2.5	11.5	0.052
66*			0 43.4	+63°19'	90.4	+ 1.3	359.3	0.134	97	96	B2 V: pe	10.71	+0.66	-0.27	2.70	8.01	-2.0	10.0	0.050
67*			0 43.8	+60°27'	90.5	- 1.6	359.2	0.048	74	73	B2: V: pnne	9.89	+0.40	-0.51	1.92	7.97	-2.0	10.0	0.025
68	4694	+63°97	0 43.9	+64°05'	90.4	+ 2.1	359.1	0.148	98	97	B3 Ia	8.50	+0.72	-0.16	2.76	5.74	-6.9	12.6	0.054
69		+60°114*	0 44.3	+60°22'	90.5	- 1.6	359.0	0.035	78	77	B2 III: pe	9.87	+0.50	-0.49	2.22	7.65	-3.6	11.2	0.016
70		+61°175	0 44.5	+61°50'	90.5	- 0.2	359.0	0.063	76	75	B3 II	9.59	+0.76	-0.10	2.88	6.71	-4.6	11.3	0.022

TABLE 5—Continued

TABLE 5—Continued

No.	HD	BD	1900 α	1900 δ	l	b	φ	p	θ	θ'	Spectrum	V	B-V	U-B	$3E_{(B-V)}$	m	M	m-M	p/A_V
			h m																
71	4768	+58°119	0 44.6	+59°07'	90.6	- 2.9	359.0	0.049	82	81	B5 Ib	7.57	+0.38	-0.34	1.62	5.95	-5.8	11.8	0.030
72	4841	+62°160	0 45.4	+63°14'	90.6	+ 1.2	358.8	0.097	98	97	B5 Ia	6.86	+0.57	-0.30	2.19	4.67	-6.9	11.6	0.044
73		+63°102	0 46.1	+64°08'	90.7	+ 2.1	358.6	0.155	102	101	B1 II	10.00	+0.57	-0.41	2.49	7.51	-4.9	12.4	0.062
74*			0 46.2	+64°00'	90.7	+ 2.0	358.6	0.118	102	101	B2 V	11.31	+0.45	-0.39	2.07	9.24	-2.0	11.2	0.057
75		+63°108	0 47.6	+64°13'	90.8	+ 2.2	358.3	0.151	103	102	B3 III?	10.67	+0.68	-0.21	2.64	8.03	-3.3	11.3	0.057
76*			0 48.8	+62°57'	91.0	+ 1.0	358.1	0.075	97	95	B2 V	11.21	+0.36	-0.42	1.80	9.41	-2.0	11.4	0.042
77		+64°93	0 49.0	+64°42'	91.0	+ 2.7	358.0	0.090	99	97	B2 III	10.18	+0.45	-0.33	2.07	8.11	-3.6	11.7	0.043
78*			0 49.8	+63°27'	91.1	+ 1.5	357.8	0.112	98	96	B2 IV	11.06	+0.64	-0.25	2.64	8.42	-2.9	11.3	0.042
79*			0 51.1	+62°44'	91.2	+ 0.8	357.6	0.097	97	95	B1 V	11.67	+0.30	-0.47	1.68	9.99	-3.1	13.1	0.058
80		+64°106*	0 51.4	+64°20'	91.2	+ 2.3	357.5	0.115	99	96	B1 V	10.34	+0.69	-0.21	2.85	7.49	-3.1	10.6	0.040
81*			0 51.5	+61°22'	91.4	- 0.6	357.5	0.089	100	98	B1 pe	10.60	+0.72	-0.37	2.94	7.66			0.030
82	E 236589	+55°215	0 52.1	+55°54'	91.7	- 6.0	357.3	0.033	82	79	B1 II	9.32	+0.15	-0.69	1.23	8.09	-4.9	13.0	0.027
83	5551	+62°175	0 52.2	+63°11'	91.4	+ 1.2	357.3	0.085	93	90	B1.5 Ib	7.71	+0.62	-0.36	2.61	5.10	-5.8	10.9	0.032
84	5552	+61°187	0 52.2	+61°24'	91.5	- 0.6	357.3	0.068	101	98	B1 Ia	9.08	+0.71	-0.29	2.91	6.17	-6.9	13.1	0.023
85*			0 53.2	+62°30'	91.5	+ 0.5	357.1	0.108	95	92	B2 III	10.49	+0.49	-0.37	2.19	8.30	-3.6	11.9	0.049
86*			0 53.4	+64°08'	91.5	+ 2.2	357.0	0.132	110	107	B2 III	10.99	+0.72	-0.20	2.88	8.11	-3.6	11.7	0.046
87	5689	+62°178	0 53.5	+63°05'	91.5	+ 1.1	357.0	0.087	96	93	O6	9.13	+0.34	-0.68	1.98	7.15	-5.1	12.2	0.044
88*			0 53.6	+64°07'	91.5	+ 2.2	357.0	0.125	99	96	B1 V	10.99	+0.72	-0.21	2.94	8.05	-3.1	11.2	0.042
89*			0 53.7	+63°17'	91.6	+ 1.3	357.0	0.133	99	97	B1 V	11.72	+0.53	-0.34	2.37	9.35	-3.1	12.4	0.056
90	5776	+62°181	0 54.3	+62°30'	91.7	+ 0.6	356.8	0.113	93	90	A0 Ib	8.05	+0.52	+0.11	1.56	6.49	-5.6	12.1	0.072
91*			0 54.9	+63°23'	91.7	+ 1.4	356.7	0.109	100	97	B9 (III):	11.10	+0.55	-0.00	1.83	9.27			0.060
92		+62°183	0 54.9	+62°54'	91.7	+ 1.0	356.7	0.119	92	89	B1 V: p	8.96	+0.69	-0.24	2.85	6.11	-3.1	9.2	0.042
93*			0 55.0	+63°25'	91.7	+ 1.5	356.7	0.134	98	95	B1 V	10.92	+0.61	-0.29	2.61	8.31	-3.1	11.4	0.051
94*			0 55.1	+63°24'	91.7	+ 1.5	356.7	0.149	93	90	B2 V	11.18	+0.66	-0.22	2.70	8.48	-2.0	10.5	0.055
95		+62°186	0 56.2	+62°27'	91.9	+ 0.5	356.4	0.105	93	89	B1 V	9.89	+0.36	-0.50	1.86	8.03	-3.1	11.1	0.056
96*			0 56.6	+63°28'	91.9	+ 1.5	356.3	0.121	98	94	B3 III	11.03	+0.57	-0.19	2.31	8.72	-3.3	12.0	0.052
97*			0 57.6	+63°13'	92.0	+ 1.3	356.1	0.096	98	94	B1 IV	10.04	+0.65	-0.27	2.73	7.31	-3.8	11.1	0.035
98	6182	+61°200	0 57.8	+61°18'	92.1	- 0.6	356.1	0.084	100	96	B1 Ib p	8.23	+0.47	-0.46	2.19	6.04	-5.8	11.8	0.038
99	6675	+68°74	1 02.4	+69°10'	92.0	+ 7.3	355.0	0.036	123	118	B0.5 III	6.90	+0.31	-0.64	1.77	5.13	-4.7	9.8	0.020
100		+60°169	1 02.7	+60°56'	92.8	- 1.0	355.0	0.082	86	81	B1 V	9.98	+0.26	-0.53	1.56	8.42	-3.1	11.5	0.052
101		+62°212	1 02.8	+63°09'	92.6	+ 1.3	355.0	0.100	96	91	B0.5 V	9.62	+0.79	-0.17	3.21	6.41	-3.6	10.0	0.031
102*			1 02.8	+62°18'	92.6	+ 0.4	355.0	0.108	75	70	B0 III	10.42	+0.77	-0.31	3.21	7.21	-5.0	12.2	0.034
103	E 236633	+59°191	1 02.9	+60°06'	92.9	- 1.8	355.0	0.123	86	81	B0.5 III	9.16	+0.39	-0.59	2.01	7.15	-4.7	11.8	0.061
104		+61°220	1 05.1	+62°12'	92.9	+ 0.3	354.5	0.098	100	95	B7 Ib	9.68	+0.92	+0.13	3.12	6.56	-5.7	12.3	0.031
105		+60°180	1 05.8	+60°47'	93.2	- 1.1	354.3	0.092	89	83	B0: : pe	9.32	+0.25	-0.68	1.65	7.67			0.056

TABLE 5—Continued

No.	HD	BD	1900 α	1900 δ	l	b	φ	p	θ	θ'	Spectrum	V	B-V	U-B	$3E_{(B-V)}$	m	M	m-M	p/A_v
			h m																
106	7103	+61°223	1 06.2	+61°21'	93.1	- 0.5	354.2	0.071	84	78	B3 Ib	8.35	+0.53	-0.28	2.19	6.16	-6.5	12.7	0.032
107	E 236664	+58°195	1 07.5	+58°33'	93.6	- 3.3	353.9	0.053	98	92	B0.5 V	10.02	+0.21	-0.69	1.47	8.55	-3.6	12.2	0.036
108	7252	+60°188	1 07.7	+60°21'	93.4	- 1.5	353.9	0.078	99	93	B1 V	7.12	+0.09	-0.74	1.05	6.07	-3.1	9.2	0.074
109		+60°191	1 08.1	+60°48'	93.4	- 1.0	353.8	0.076	89	83	B2 IV	9.94	+0.61	-0.14	2.55	7.39	-2.9	10.3	0.030
110		+63°167	1 11.6	+63°47'	93.5	+ 2.0	353.0	0.106	85	78	B2 III	10.35	+0.53	-0.36	2.31	8.04	-3.6	11.6	0.046
111	7720	+61°240	1 11.9	+61°22'	93.8	- 0.4	353.0	0.071	107	100	B5 II	8.87	+0.58	-0.16	2.22	6.65	-4.6	11.2	0.032
112	E 236689	+57°240	1 12.3	+57°51'	94.3	- 3.9	352.9	0.059	91	84	B1.5 (V) pe*	9.46	+0.28	-0.50	1.59	7.87	-2.6	10.5	0.037
113		+57°243	1 12.5	+57°41'	94.4	- 4.0	352.8	0.096	94	87	B0: IV: e	9.49	+0.26	-0.55	1.68	7.81	-4.6	12.4	0.057
114		+57°252	1 13.2	+57°44'	94.4	- 4.0	352.7	0.057	98	91	B1 IV	9.50	+0.26	-0.56	1.56	7.94	-3.8	11.7	0.036
115	7902	+57°257	1 13.6	+57°40'	94.5	- 4.0	352.6	0.065	95	88	B6 Ib	6.93	+0.40	-0.39	1.62	5.31	-5.7	11.0	0.040
116*			1 14.1	+61°58'	94.0	+ 0.2	352.5	0.086	105	98	B0 V:	10.22	+0.50	-0.47	2.40	7.82	-4.1	11.9	0.036
117*			1 14.4	+62°01'	94.0	+ 0.3	352.4	0.090	104	96	B1 V	10.85	+0.52	-0.45	2.34	8.51	-3.1	11.6	0.038
118*			1 15.5	+64°04'	93.9	+ 2.3	352.2	0.101	101	93	B1: II:	11.08	+0.68	-0.35	2.82	8.26	-4.9	13.2	0.036
119*			1 16.3	+60°59'	94.4	- 0.7	352.0	0.105	148	140	B pe	10.76	+0.85	-0.26					
120		+64°156	1 16.9	+65°06'	93.9	+ 3.3	351.8	0.116	103	95	B0.5 III	9.54	+0.61	-0.36	2.67	6.87	-4.7	11.6	0.043
121		+63°180	1 17.6	+63°26'	94.2	+ 1.7	351.7	0.118	95	87	A0: Ia	10.01	+1.04	+0.30	3.12	6.87	-6.9	13.8	0.038
122		+62°245	1 17.7	+62°18'	94.4	+ 0.6	351.7	0.076	107	99	B1: pe (V)	10.15	+0.90	-0.14	3.48	6.67	-3.1	9.8	0.022
123*			1 17.8	+62°27'	94.4	+ 0.8	351.7	0.131	101	93	B1: V:	10.78	+0.72	-0.22	2.94	7.84	-3.1	10.9	0.044
124		+62°246	1 18.0	+62°16'	94.4	+ 0.6	351.6	0.118	115	107	B5 Ia	8.74	+0.91	+0.01	3.21	5.53	-6.9	12.4	0.037
125		+60°232	1 18.6	+60°17'	94.8	- 1.4	351.5	0.050	101	93	B2 III	9.97	+0.27	-0.49	1.53	8.44	-3.6	12.0	0.033
126		+62°249	1 19.5	+62°31'	94.5	+ 0.9	351.3	0.120	104	96	O9.5 V	10.04	+0.70	-0.34	3.00	7.04	-4.4	11.4	0.040
127	E 236740	+59°251	1 20.1	+59°46'	95.0	- 1.9	351.2	0.071	104	95	B3 Ia	7.90	+0.46	-0.36	1.98	5.92	-6.9	12.8	0.036
128	8768	+62°254	1 21.4	+62°45'	94.7	+ 1.1	350.9	0.085	100	91	O9.5 IV	8.69	+0.40	-0.60	2.10	6.59	-5.0	11.6	0.040
129		+58°241	1 21.4	+58°43'	95.4	- 2.9	350.9	0.081	101	92	B1 V	9.97	+0.26	-0.57	1.56	8.41	-3.1	11.5	0.052
130		+62°258	1 23.3	+63°04'	94.9	+ 1.5	350.5	0.111	103	93	B1 IV	9.87	+0.67	-0.25	2.79	7.08	-3.8	10.9	0.040
131	8965	+59°260	1 23.3	+59°44'	95.4	- 1.8	350.4	0.062	103	93	B0.5 V	7.28	+0.02	-0.82	0.90	6.38	-3.6	10.0	0.069
132		+61°277	1 23.7	+62°13'	95.1	+ 0.6	350.4	0.116	112	102	B0 IV: nn	9.63	+0.58	-0.39	2.64	6.99	-4.6	11.6	0.044
133	E 236762	+58°252	1 24.5	+59°13'	95.7	- 2.3	350.2	0.075	101	91	B1.5 III	9.57	+0.21	-0.56	1.38	8.19	-4.0	12.2	0.054
134	9105	+62°259	1 24.6	+62°51'	95.1	+ 1.3	350.2	0.072	104	94	B5 Iab	7.47	+0.55	-0.25	2.13	5.34	-6.5	11.8	0.034
135	E 236768	+58°256	1 25.2	+58°52'	95.9	- 2.6	350.0	0.073	104	94	B1: V: nnp	9.49	+0.29	-0.53	1.65	7.84	-3.1	10.9	0.044
136		+61°285	1 25.9	+61°27'	95.5	- 0.1	349.9	0.091	111	101	B0.5 III	9.42	+0.42	-0.48	2.10	7.32	-4.7	12.0	0.043
137		+60°261	1 25.9	+60°37'	95.6	- 0.9	349.9	0.080	111	101	O7	8.63	+0.31	-0.67	1.89	6.74	-5.1	11.8	0.042
138		+59°273	1 26.7	+60°07'	95.8	- 1.4	349.7	0.080	105	95	B2 III	9.08	+0.22	-0.56	1.38	7.70	-3.6	11.3	0.058
139		+60°274	1 28.9	+60°46'	96.0	- 0.7	349.2	0.083	106	95	B3 III	10.66	+0.33	-0.41	1.59	9.07	-3.3	12.4	0.052
140		+62°275	1 29.1	+63°08'	95.5	+ 1.7	349.2	0.091	102	91	B3 ? III	9.82	+0.84	-0.12	3.12	6.70	-3.3	10.0	0.029

TABLE 5—Continued

No.	HD	BD	1900 α	1900 δ	l	b	φ	p	θ	θ'	Spectrum	V	B-V	U-B	$3E_{(B-V)}$	m	M	m-M	p/A_v
			h m																
141		+60°279	1 29.7	+60°28'	96.1	- 1.0	349.0	0.070	104	93	B2 II	9.08	+0.19	-0.62	1.29	7.79	-4.7	12.5	0.054
142*			1 29.9	+61°48'	95.9	+ 0.4	349.0	0.076	111	100	B1 V	9.77	+0.52	-0.37	2.34	7.43	-3.1	10.5	0.032
143		+62°278	1 30.0	+63°15'	95.6	+ 1.7	349.0	0.068	96	85	B0.5 III	9.85	+0.65	-0.29	2.79	7.06	-4.7	11.8	0.024
144		+59°286	1 30.2	+59°26'	96.4	- 2.0	348.9	0.083	102	91	B1 III: n	9.56	+0.30	-0.55	1.68	7.88	-4.4	12.3	0.049
145		+60°289	1 31.5	+60°51'	96.2	- 0.5	348.7	0.119	102	91	B2 II-III	10.17	+0.52	-0.36	2.28	7.89	-4.2	12.1	0.052
146*			1 32.3	+61°13'	96.3	- 0.2	348.5	0.067	104	92	B2 V	10.37	+0.55	-0.27	2.37	8.00	-2.0	10.0	0.028
147	E 236810	+59°296	1 31.8	+60°04'	96.4	- 1.3	348.6	0.081	97	86	B2 III	8.67	+0.25	-0.54	1.47	7.20	-3.6	10.8	0.055
148*	9974		1 32.4	+57°39'	97.0	- 3.6	348.4	0.059	95	83	W R	10.69	+0.02	-0.86					
149	E 236815	+59°297	1 32.8	+59°54'	96.6	- 1.4	348.4	0.062	98	86	B0.5 III	8.52	+0.22	-0.69	1.50	7.02	-4.7	11.7	0.041
150		+57°359	1 33.0	+57°20'	97.1	- 3.9	348.3	0.067	92	80	B1: V:	9.91	+0.26	-0.54	1.56	8.35	-3.1	11.4	0.043
151	10063	+55°375	1 33.3	+55°17'	97.6	- 5.9	348.2	0.048	92	80	B8 Iab	7.39	+0.25	-0.33	1.02	6.37	-6.5	12.9	0.047
152	10125	+63°218	1 33.9	+63°40'	95.9	+ 2.3	348.1	0.078	101	89	O9.5 Ib	8.22	+0.31	-0.65	1.83	6.39	-6.6	13.0	0.043
153*			1 33.9	+62°04'	96.3	+ 0.7	348.1	0.093	102	90	B3: II:	10.58	+0.62	-0.27	2.46	8.12	-4.6	12.7	0.038
154		+62°292	1 35.0	+63°06'	96.2	+ 1.8	347.9	0.096	102	90	B1: pe	10.40	+0.55	-0.41	2.43	7.97			0.040
155		+60°311	1 35.9	+60°20'	96.9	- 0.9	347.7	0.064	102	90	B2 III: nn	9.96	+0.28	-0.48	1.56	8.40	-3.6	12.0	0.041
156		+62°296	1 36.1	+63°06'	96.3	+ 1.8	347.6	0.103	101	89	B1 IV	9.84	+0.54	-0.33	2.40	7.44	-3.8	11.2	0.043
157		+61°312	1 36.3	+61°57'	96.6	+ 0.7	347.6	0.112	110	98	B1 III	9.22	+0.53	-0.41	2.37	6.85	-4.4	11.2	0.047
158		+62°297	1 36.4	+63°05'	96.3	+ 1.8	347.6	0.103	100	88	B1 Ib	9.14	+0.63	-0.36	2.67	6.47	-5.8	12.3	0.038
159		+55°393	1 37.6	+55°40'	98.1	- 5.4	347.3	0.050	106	93	B1 V	10.50	+0.03	-0.70	0.87	9.63	-3.1	12.7	0.057
160		+62°300	1 38.1	+62°21'	96.7	+ 1.1	347.2	0.077	108	95	B1 V: pne	9.96	+0.33	-0.54	1.77	8.19	-3.1	11.3	0.044
161		+60°322	1 38.2	+60°18'	97.2	- 0.9	347.2	0.066	108	95	B2 III	9.73	+0.54	-0.33	2.34	7.39	-3.6	11.0	0.028
162		+60°331	1 39.0	+60°44'	97.2	- 0.4	347.0	0.115	98	85	B8 Iab	8.95	+0.85	+0.08	2.82	6.13	-6.5	12.6	0.041
163		+60°336	1 39.2	+60°56'	97.1	- 0.3	347.0	0.110	106	93	B9 Iab	9.09	+0.78	+0.20	2.52	6.57	-6.5	13.1	0.044
164*			1 39.2	+61°31'	97.0	+ 0.3	347.0	0.115	101	88	B1 II	10.55	+0.66	-0.27	2.76	7.79	-4.9	12.7	0.042
165		+60°333	1 39.2	+60°44'	97.2	- 0.4	347.0	0.110	100	87	B5 Iab	8.91	+0.77	-0.09	2.79	6.12	-6.5	12.6	0.039
166		+60°339	1 39.5	+60°45'	97.2	- 0.4	346.9	0.105	99	86	B6 Iab	8.50	+0.66	-0.18	2.40	6.10	-6.5	12.6	0.044
167		+60°343	1 39.6	+60°45'	97.2	- 0.4	346.9	0.130	103	90	B2 II	9.27	+0.59	-0.28	2.49	6.78	-4.7	11.5	0.052
168	E 232522	+54°372	1 39.6	+54°51'	98.6	- 6.2	346.8	0.035	103	90	B1 II	8.67	-0.01	-0.84	0.75	7.92	-4.9	12.8	0.047
169		+62°304	1 39.8	+62°35'	96.8	+ 1.4	346.8	0.082	104	91	B3 III n	10.25	+0.47	-0.32	2.01	8.24	-3.3	11.5	0.041
170		+60°345	1 39.8	+61°00'	97.2	- 0.2	346.8	0.104	103	90	B0 II:	9.74	+0.59	-0.45	2.67	7.07	-5.4	12.5	0.039
171	10756	+59°318	1 40.1	+60°10'	97.4	- 1.0	346.8	0.070	100	87	B8 Ia	7.54	+0.44	-0.27	1.59	5.95	-6.9	12.8	0.044
172	10898	+57°399	1 41.9	+57°58'	98.2	- 3.1	346.4	0.085	95	81	B2 Ib	7.40	+0.35	-0.52	1.77	5.63	-5.8	11.4	0.048
173		+63°247	1 42.3	+63°50'	96.8	+ 2.7	346.3	0.102	103	89	B0 III	9.73	+0.33	-0.63	1.89	7.84	-5.0	12.8	0.054
174		+58°310	1 43.7	+58°45'	98.2	- 2.2	346.0	0.092	99	85	B1 V	10.17	+0.25	-0.53	1.53	8.64	-3.1	11.7	0.060
175		+60°362	1 44.0	+60°51'	97.7	- 0.2	345.9	0.109	106	92	B2 II-III	9.58	+0.64	-0.29	2.64	6.94	-4.2	11.1	0.041

TABLE 5—Continued

No.	HD	BD	1900 α	1900 δ	l	b	φ	p	θ	θ'	Spectrum	V	B-V	U-B	3E(B-V)	m	M	m-M	p/A$_V$
176		+54°395	1^{h}45^m.2	+54°58'	99.3	- 5.8	345.6	0.045	102	88	B0 IV: p	9.91	+0.10	-0.79	1.20	8.71	-4.6	13.3	0.038
177		+60°368	1 45.4	+60°20'	98.0	- 0.7	345.6	0.073	109	94	B1: III:	10.62	+0.61	-0.35	2.61	8.01	-4.4	12.4	0.028
178	E 236894	+57°409	1 45.4	+57°57'	98.6	- 3.0	345.6	0.085	96	82	O8 V	9.37	+0.19	-0.76	1.50	7.87	-5.1	13.0	0.057
179	E 232552	+54°398	1 45.8	+54°51'	99.4	- 6.0	345.4	0.047	115	100	B0 p e	8.03	+0.37	-0.74	2.01	6.02			0.023
180		+63°253	1 46.1	+63°42'	97.2	+ 2.6	345.4	0.091	106	91	B0 III	9.32	+0.45	-0.49	2.25	7.07	-5.0	12.1	0.040
181		+61°342	1 46.1	+62°03'	97.7	+ 1.0	345.5	0.074	104	89	B0.5 II	9.56	+0.44	-0.53	2.16	7.40	-5.2	12.6	0.034
182		+54°404	1 46.5	+54°38'	99.6	- 6.1	345.2	0.046	119	104	B1 III	9.77	+0.21	-0.62	1.41	8.36	-4.4	12.8	0.033
183	11554	+57°425	1 48.4	+57°24'	99.1	- 3.4	344.9	0.092	96	81	B1 V p e	9.55	+0.27	-0.58	1.59	7.96	-3.1	11.1	0.058
184		+59°357	1 49.4	+60°05'	98.6	- 0.8	344.7	0.084	99	84	B0.5 IV	9.97	+0.47	-0.53	2.25	7.72	-4.2	11.9	0.037
185		+55°441	1 49.4	+56°04'	99.6	- 4.6	344.7	0.060	100	85	B1 (V) p e	9.68	+0.18	-0.75	1.32	8.36	-3.1	11.5	0.045
186		+63°261	1 50.0	+63°33'	97.7	+ 2.6	344.6	0.089	103	88	B pnne*	9.62	+0.51	-0.63					
187		+60°389	1 50.3	+60°38'	98.5	- 0.2	344.5	0.084	103	88	B3 Ib	9.28	+0.59	-0.29	2.37	6.91	-5.8	12.7	0.035
188*			1 50.8	+59°30'	98.9	- 1.3	344.4	0.116	95	80	B1 V	9.96	+0.43	-0.40	2.07	7.89	-3.1	11.0	0.056
189		+60°393	1 50.9	+61°05'	98.5	+ 0.2	344.4	0.084	107	92	B2 pe	10.66	+0.44	-0.43	2.04	8.62			0.041
190*			1 51.2	+61°27'	98.3	+ 0.6	344.4	0.168	102	86	B1 V: *	11.17	+0.79	-0.26	3.15	8.02	-3.1	11.1	0.053
191	11831	+59°364	1 51.1	+59°54'	98.8	- 0.9	344.4	0.113	97	81	A2 Ia	8.04	+0.88	+0.37	2.46	5 58	-6.9	12.5	0.046
192		+59°367	1 51.6	+60°02'	98.8	- 0.7	344.3	0.108	99	83	O9.5 Ib	9.77	+0.53	-0.52	2.49	7.28	-6.6	13.9	0.043
193*			1 51.7	+60°08'	98.8	- 0.6	344.2	0.092	99	83	B1 pe (V)	10.16	+0.75	-0.36	3.03	7.13	-3.1	10.2	0.030
194		+58°343	1 52.1	+58°27'	99.3	- 2.3	344.1	0.070	94	78	B2 III	9.64	+0.36	-0.41	1.80	7.84	-3.6	11.4	0.039
195		+61°362	1 52.9	+61°51'	98.5	+ 1.1	344.0	0.108	101	85	B2 III	10.29	+0.44	-0.46	2.04	8.25	-3.6	11.8	0.053
196		+59°374	1 53.0	+59°14'	99.2	- 1.5	343.9	0.102	97	80	B1 V	9.68	+0.40	-0.45	1.98	7.70	-3.1	10.8	0.052
197*			1 53.4	+62°25'	98.4	+ 1.6	343.9	0.085	97	81	B2 V	10.64	+0.41	-0.39	1.95	8.69	-2.0	10.7	0.044
198*			1 53.5	+62°32'	98.4	+ 1.7	343.8	0.105	106	89	B1 V	10.57	+0.50	-0.35	2.28	8.29	-3.1	11.4	0.046
199		+58°351	1 53.7	+58°29'	99.4	- 2.2	343.8	0.093	98	81	B1 III	10.00	+0.46	-0.42	2.16	7.84	-4.4	12.2	0.043
200*			1 54.0	+61°54'	98.6	+ 1.2	343.7	0.131	98	82	B2: V:	11.16	+0.52	-0.36	2.28	8.88	-2.0	10.9	0.057
201*			1 54.5	+61°23'	98.8	+ 0.7	343.6	0.103	109	93	B1 V:	10.49	+0.51	-0.45	2.31	8.18	-3.1	11.3	0.044
202		+60°416	1 54.6	+60°34'	99.1	- 0.1	343.6	0.115	99	82	B0.5 III	9.56	+0.67	-0.33	2.85	6.71	-4.7	11.4	0.040
203		+59°387	1 55.5	+59°36'	99.4	- 1.0	343.4	0.096	104	87	B3 II	9.59	+0.63	-0.30	2.49	7.10	-4.6	11.7	0.038
204	12301	+63°274	1 55.6	+63°54'	98.2	+ 3.1	343.4	0.051	110	93	B8 Ib	5.58	+0.38	-0.27	1.41	4.17	-5.6	9.8	0.036
205		+59°388	1 55.6	+59°30'	99.5	- 1.1	343.4	0.096	101	85	B3 II	9.62	+0.60	-0.23	2.40	7.22	-4.7	11.9	0.040
206	12302	+58°356	1 55.6	+59°12'	99.6	- 1.4	343.4	0.044	88	71	B1: V: pe*	8.06	+0.25	-0.46	1.53	6.53	-3.1	9.6	0.029
207	12323	+54°441	1 55.8	+55°08'	100.7	- 5.3	343.3	0.033	102	85	O9 V*	8.90	-0.02	-0.93	0.87	8.03	-4.6	12.6	0.038
208		+61°370	1 56.4	+61°24'	99.0	+ 0.9	343.2	0.165	103	87	O9 V	10.06	+0.70	-0.37	3.03	7.03	-4.6	11.6	0.054
209		+61°371	1 56.9	+61°56'	98.9	+ 1.3	343.1	0.100	109	92	B3: II: pe	11.09	+0.46	-0.25	1.98	9.11	-4.6	13.7	0.050
210	E 232588	+54°448	1 57.1	+54°38'	101.1	- 5.7	343.0	0.058	109	92	B1.5 III	8.63	+0.07	-0.71	0.96	7.67	-4.0	11.7	0.060

TABLE 5—Continued

No.	HD	BD	1900 α	1900 δ	l	b	φ	p	θ	θ'	Spectrum	V	B-V	U-B	$3E_{(B-V)}$	m	M	m-M	p/A_V
			h m																
211	E 236935	+57°469	1 57.2	+58°00	100.1	- 2.5	343.0	0.093	91	74	B1: V:ne	9.33	+0.40	-0.45	1.98	7.35	-3.1	10.4	0.047
212	12509	+63°281	1 57.6	+63°54'	98.4	+ 3.2	342.9	0.074	113	96	B1 III	7.09	+0.35	-0.54	1.83	5.26	-4.4	9.7	0.040
213		+61°375	1 57.8	+61°36'	99.1	+ 1.0	342.9	0.062	105	88	B0. 5 IV	9.55	+0.57	-0.44	2.55	7.00	-4.2	11.2	0.024
214	12567	+63°287	1 58.1	+63°49'	98.5	+ 3.0	342.9	0.094	107	90	B0. 5 III	8.30	+0.38	-0.56	1.98	6.32	-4.7	11.0	0.047
215*			1 58.6	+62°53'	98.8	+ 2.2	342.7	0.129	108	90	B0. 5: pe	10.24	+0.46	-0.60	2.22	8.02			0.058
216*			1 59.0	+62°52'	98.9	+ 2.2	342.6	0.135	107	90	B pe	10.28	+0.45	-0.61					
217		+58°372	1 59.4	+58°48'	100.2	- 1.6	342.6	0.087	111	93	B3 III	10.39	+0.35	-0.40	1.65	8.74	-3.3	12.0	0.053
218	12727	+56°425	1 59.6	+56°34'	100.8	- 3.8	342.5	0.075	105	87	B2 III	9.03	+0.08	-0.72	0.96	8.07	-3.6	11.7	0.078
219		+60°435	2 00.9	+60°55'	99.7	+ 0.4	342.2	0.084	113	96	B2 III	9.68	+0.47	-0.38	2.13	7.55	-3.6	11.2	0.039
220	12856	+56°429	2 00.9	+56°38'	101.0	- 3.6	342.2	0.029	107	89	B0 pe	8.53	+0.23	-0.77	1.59	6.94			0.018
221	12867	+57°492	2 01.0	+57°14'	100.8	- 3.1	342.2	0.076	101	83	B1 V	9.41	+0.15	-0.67	1.23	8.18	-3.1	11.3	0.062
222	12882	+64°295	2 01.1	+64°33'	98.6	+ 3.9	342.1	0.064	109	91	B6 Ia	7.50	+0.38	-0.53	1.56	5.94	-6.9	12.8	0.041
223		+61°382	2 01.2	+61°18'	99.6	+ 0.8	342.2	0.166	107	89	B1: V:	10.70	+0.83	-0.14	3.27	7.43	-3.1	10.5	0.051
224	12953	+57°494	2 01.7	+57°57'	100.7	- 2.4	342.0	0.074	108	90	A1 Ia	5.65	+0.60	+0.00	1.71	3.94	-6.9	10.8	0.043
225	12993	+57°498	2 02.1	+57°27'	100.9	- 2.8	341.9	0.089	91	73	O5	8.95	+0.21	-0.79	1.59	7.36	-5.1	12.5	0.056
226	13036	+58°384	2 02.5	+59°09'	100.4	- 1.2	341.9	0.078	114	96	B0. 5: III:	8.55	+0.53	-0.41	2.43	6.12	-4.7	10.8	0.032
227	13051	+56°432	2 02.6	+56°31'	101.2	- 3.7	341.8	0.048	100	82	B1 IV::	8.66	+0.13	-0.73	1.17	7.49	-3.8	11.3	0.041
228		+63°300	2 02.9	+63°36'	99.1	+ 3.1	341.8	0.106	108	90	B pe	9.69	+0.55	-0.55					
229	13256	+60°447	2 04.5	+60°14'	100.3	- 0.1	341.4	0.138	100	82	B1 Ia	8.61	+1.20	-0.01	4.38	4.23	-6.9	11.1	0.032
230	13267	+56°438	2 04.6	+57°11'	101.3	- 3.0	341.4	0.088	107	88	B5 Ia	6.33	+0.33	-0.43	1.47	4.86	-6.9	11.8	0.060
231	13268	+55°534	2 04.6	+55°41'	101.8	- 4.4	341.4	0.060	110	91	O8 V nn	8.18	+0.13	-0.83	1.32	6.86	-5.1	12.0	0.045
232	13338	+57°512	2 05.3	+57°28'	101.3	- 2.7	341.2	0.085	111	92	B1 V	9.03	+0.25	-0.55	1.53	7.50	-3.1	10.6	0.056
233*			2 05.4	+59°26'	100.7	- 0.8	341.3	0.105	94	75	O9 V	11.03	+0.97	-0.13	3.84	7.19	-4.6	11.8	0.027
234		+57°513	2 05.5	+57°38'	101.2	- 2.5	341.2	0.085	110	91	B1 III	9.50	+0.29	-0.56	1.65	7.85	-4.4	12.2	0.052
235		+57°515	2 05.7	+57°13'	101.4	- 2.9	341.2	0.093	111	92	B1: pe	9.69	+0.37	-0.63	1.89	7.80			0.049
236	13402	+58°396	2 05.9	+59°04'	100.8	- 1.1	341.1	0.116	104	85	B0. 5 I	8.07	+0.61	-0.42	2.67	6.03	-6.5	12.5	0.043
237		+58°400	2 06.4	+58°42'	101.0	- 1.5	341.0	0.140	110	91	B3 Ib-II	9.40	+0.65	-0.23	2.55	6.85	-5.2	12.0	0.055
238	13476	+57°519	2 06.6	+58°06'	101.2	- 2.0	341.0	0.090	109	90	A3 Iab	6.41	+0.61	+0.26	1.56	4.85	-6.5	11.4	0.058
239		+57°520	2 06.7	+57°58'	101.3	- 2.1	341.0	0.102	105	86	B1 II	9.62	+0.39	-0.51	1.95	7.67	-4.9	12.6	0.052
240	13494	+55°543	2 06.7	+56°06'	101.9	- 3.9	340.9	0.055	109	90	B1 III	9.30	+0.18	-0.65	1.32	7.98	-4.4	12.4	0.042
241	13544	+53°480	2 07.1	+53°27'	102.8	- 6.4	340.8	0.049	106	87	B0. 5 IV	8.88	-0.01	-0.82	0.81	8.07	-4.2	12.3	0.060
242	13561	+55°547	2 07.3	+56°02'	102.0	- 3.9	340.8	0.066	110	91	B0. 5 V: p?*	8.83	+0.09	-0.77	1.11	7.72	-3.6	11.3	0.059
243		+54°490	2 07.4	+54°35'	102.5	- 5.3	340.7	0.069	110	91	B1 V	9.52	+0.11	-0.67	1.11	8.41	-3.1	11.5	0.062
244	13590	+63°310	2 07.6	+63°34'	99.6	+ 3.2	340.7	0.096	118	99	B2 III	7.90	+0.35	-0.41	1.77	6.13	-3.6	9.7	0.054
245	13621	+54°494	2 07.8	+54°51'	102.5	- 5.0	340.6	0.050	107	88	B1 V	8.08	+0.06	-0.79	0.96	7.12	-3.1	10.2	0.052

TABLE 5—Continued

No.	HD	BD	1900 α	1900 δ	l	b	φ	p	θ	θ'	Spectrum	V	B-V	U-B	3E(B-V)	m	M	m-M	p/A$_V$
			h m																
246	13659	+56°462	2 08.1	+56°28'	102.0	- 3.5	340.6	0.080	104	85	B1 Ib	8.65	+0.56	-0.41	2.46	6.19	-6.5	12.7	0.032
247	13716	+57°525	2 08.6	+57°18'	101.8	- 2.7	340.5	0.088	112	93	B0.5 III	8.27	+0.32	-0.59	1.80	6.47	-4.7	11.2	0.049
248	13744	+57°526	2 08.9	+57°50'	101.6	- 2.2	340.5	0.092	109	90	A0 Iab	7.58	+0.75	+0.18	2.25	5.33	-6.5	11.8	0.041
249	13745	+55°554	2 08.9	+55°32'	102.4	- 4.3	340.4	0.063	110	90	B0 III	7.83	+0.16	-0.77	1.38	6.45	-5.0	11.4	0.046
250		+59°451	2 09.0	+59°13'	101.2	- 0.9	340.5	0.097	101	82	B1 II	9.30	+0.69	-0.29	2.85	6.45	-4.9	11.4	0.034
251	13758	+57°527	2 09.0	+57°17'	101.8	- 2.7	340.4	0.100	108	88	B1 V	9.05	+0.33	-0.53	1.77	7.28	-3.1	10.4	0.056
252*			2 09.7	+57°50'	101.7	- 2.1	340.3	0.084	117	98	B0.5 V	10.22	+0.55	-0.37	2.49	7.73	-3.6	11.3	0.034
253	13831	+56°469	2 09.7	+56°17'	102.2	- 3.6	340.3	0.066	105	85	B0 III p?	8.26	+0.10	-0.81	1.20	7.06	-5.0	12.1	0.055
254	13841	+56°470	2 09.8	+56°34'	102.2	- 3.3	340.3	0.073	111	91	B2 Ib	7.37	+0.23	-0.65	1.41	5.96	-5.8	11.8	0.052
255		+65°473	2 09.9	+56°40'	102.1	- 3.2	340.2	0.095	111	91	B1 II:	9.07	+0.24	-0.63	1.50	7.57	-4.9	12.5	0.063
256	13854	+56°471	2 09.9	+56°36'	102.2	- 3.3	340.2	0.083	112	92	B1 Iab	6.47	+0.28	-0.67	1.62	4.85	-6.5	11.4	0.051
257	13866	+56°475	2 10.0	+56°15'	102.3	- 3.6	340.2	0.073	115	95	B2 Ib	7.48	+0.19	-0.65	1.29	6.19	-5.8	12.0	0.056
258	13890	+56°478	2 10.2	+56°19'	102.3	- 3.5	340.2	0.075	107	87	B1 III: pe	8.47	+0.19	-0.63	1.35	7.12	-4.4	11.5	0.056
259*			2 10.2	+59°07'	101.4	- 0.9	340.2	0.102	104	84	B1 Ib	10.59	+0.64	-0.29	2.70	7.89	-5.8	13.7	0.038
260	13900	+56°479	2 10.3	+56°26'	102.3	- 3.4	340.2	0.075	116	96	B1 IV	9.17	+0.16	-0.66	1.26	7.91	-3.8	11.7	0.060
261*			2 10.4	+58°32'	101.6	- 1.4	340.2	0.127	102	82	B pe	10.15	+0.84	-0.30					
262		+56°482	2 10.6	+56°44'	102.2	- 3.1	340.1	0.104	116	96	B1 III? p	9.36	+0.30	-0.60	1.68	7.68	-4.4	12.1	0.062
263		+56°484	2 10.7	+56°26'	102.3	- 3.4	340.1	0.075	124	104	B0: V: ne	9.62	+0.32	-0.70	1.86	7.76	-4.1	11.9	0.040
264	13969	+56°485	2 10.8	+56°38'	102.3	- 3.2	340.0	0.096	114	94	B1 IV:	8.86	+0.29	-0.59	1.65	7.21	-3.8	11.0	0.058
265		+59°456	2 11.0	+59°20'	101.4	- 0.7	340.0	0.107	107	87	B0.5 V	9.88	+0.55	-0.41	2.49	7.39	-3.6	11.0	0.043
266	14010	+63°315	2 11.1	+63°58'	99.8	+ 3.7	340.0	0.092	112	92	B9 Ia	7.11	+0.60	-0.10	1.98	5.13	-6.9	12.0	0.046
267	14014	+55°567	2 11.1	+55°46'	102.6	- 4.0	340.0	0.056	114	94	B0.5 V	8.75	+0.14	-0.66	1.26	7.49	-3.6	11.1	0.044
268		+56°493	2 11.3	+56°24'	102.4	- 3.4	339.9	0.079	126	106	B1 V: pe:	9.62	+0.19	-0.66	1.35	8.27	-3.1	11.4	0.058
269	14052	+56°500	2 11.4	+56°45'	102.3	- 3.1	339.9	0.088	116	96	B1 Ib	8.18	+0.30	-0.58	1.68	6.50	-5.8	12.3	0.052
270	14053	+56°498	2 11.4	+56°33'	102.4	- 3.3	339.9	0.065	115	95	B0.5 III	8.43	+0.24	-0.62	1.56	6.87	-4.7	11.6	0.042
271	14092	+56°507	2 11.7	+56°18'	102.5	- 3.5	339.8	0.091	120	100	B1 V	9.23	+0.23	-0.59	1.47	7.76	-3.1	10.9	0.062
272		+59°461	2 12.1	+59°16'	101.5	- 0.7	339.8	0.110	104	84	B1 II	10.09	+0.51	-0.39	2.31	7.78	-4.9	12.7	0.048
273	14134	+56°522	2 12.1	+56°40'	102.4	- 3.1	339.8	0.084	114	94	B3 Ia	6.55	+0.47	-0.38	2.01	4.54	-6.9	11.4	0.042
274	14143	+56°530	2 12.2	+56°43'	102.4	- 3.1	339.7	0.086	117	97	B2 Ia	6.65	+0.52	-0.45	2.28	4.37	-6.9	11.3	0.038
275	14162	+56°535	2 12.4	+56°41'	102.5	- 3.1	339.7	0.091	115	95	B0.5 V	9.37	+0.38	-0.49	1.98	7.39	-3.6	11.0	0.046
276	14250	+56°545	2 13.2	+56°39'	102.6	- 3.1	339.5	0.079	109	89	B0.5 V: n	8.96	+0.32	-0.54	1.80	7.16	-3.6	10.8	0.044
277	14302	+55°587	2 13.6	+55°52'	102.9	- 3.8	339.4	0.068	115	94	B1 II-III	8.57	+0.26	-0.56	1.56	7.01	-4.6	11.6	0.044
278		+56°549	2 13.7	+57°00'	102.5	- 2.7	339.4	0.078	117	97	B1 V	9.82	+0.33	-0.50	1.77	8.05	-3.1	11.2	0.044
279	14322	+55°588	2 13.8	+55°27'	103.1	- 4.2	339.4	0.066	113	92	B8 Ib	6.74	+0.35	-0.33	1.32	5.42	-5.6	11.0	0.050
280	14331	+55°590	2 13.9	+55°22'	103.1	- 4.2	339.3	0.060	108	87	B0 III	8.41	+0..16	-0.75	1.38	7.03	-5.0	12.0	0.043

TABLE 5—Continued

No.	HD	BD	1900 α	1900 δ	l	b	φ	p	θ	θ'	Spectrum	V	B-V	U-B	$3E_{(B-V)}$	m	M	m-M	p/A_V
281		+58°451	$2^h14.1^m$	+59°00'	101.9	- 0.8	339.4	0.101	110	89	B1 III:	10.07	+0.52	-0.36	2.34	7.73	-4.4	12.1	0.043
282	14357	+56°555	2 14.1	+56°25'	102.8	- 3.3	339.3	0.096	113	92	B2 II	8.52	+0.31	-0.52	1.65	6.87	-4.7	11.6	0.058
283*			2 14.1	+59°00'	101.9	- 0.8	339.4	0.049	109	88	A	10.36	+0.35	+0.22					
284		+58°453	2 14.7	+58°51'	102.0	- 0.9	339.2	0.083	110	89	B1 V	10.53	+0.45	-0.45	2.13	8.40	-3.1	11.5	0.039
285	14422	+56°565	2 14.7	+56°56'	102.7	- 2.7	339.2	0.067	117	96	B1 V: pe	8.99	+0.51	-0.64	2.31	6.68	-3.1	9.8	0.029
286	14433	+56°568	2 14.8	+56°47'	102.7	- 2.9	339.2	0.086	112	91	A1 Ia	6.42	+0.57	+0.07	1.62	4.80	-6.9	11.7	0.053
287	14434	+56°567	2 14.8	+56°27'	102.8	- 3.2	339.2	0.084	116	95	O6	8.48	+0.16	-0.78	1.44	7.04	-5.1	12.1	0.058
288	14442	+58°455	2 14.9	+59°06'	101.9	- 0.7	339.2	0.090	113	92	O5.5	9.21	+0.41	-0.61	2.19	7.02	-5.1	12.1	0.041
289	14443	+56°570	2 14.9	+56°42'	102.8	- 3.0	339.1	0.082	117	96	B2 Ib	8.04	+0.35	-0.54	1.77	6.27	-5.8	12.1	0.046
290	14489	+55°598	2 15.3	+55°23'	103.3	- 4.2	339.0	0.049	114	93	A2 Ia	5.17	+0.37	-0.11	0.93	4.24	-6.9	11.1	0.053
291	14501	+57°551	2 15.4	+57°42'	102.5	- 2.0	339.1	0.080	111	90	B3 V: n	9.42	+0.40	-0.32	1.80	7.62	-1.5	9.1	0.044
292		+56°586	2 15.5	+56°37'	102.9	- 3.0	339.0	0.066	115	94	B1 V	9.94	+0.25	-0.59	1.53	8.41	-3.1	11.5	0.043
293		+56°589	2 15.6	+57°03'	102.7	- 2.6	339.0	0.080	117	96	B1 III	9.46	+0.41	-0.48	2.01	7.45	-4.4	11.8	0.040
294	14520	+56°588	2 15.6	+56°38'	102.9	- 3.0	339.0	0.087	115	94	B2 II	9.25	+0.32	-0.53	1.68	7.57	-4.7	12.3	0.052
295		+60°470	2 15.8	+60°22'	101.6	+ 0.5	339.0	0.068	116	95	O8 V	9.88	+0.70	-0.36	3.03	6.85	-5.1	12.0	0.022
296	14535	+56°591	2 15.8	+56°47'	102.9	- 2.8	339.0	0.077	111	90	A1 Ia p?	7.45	+0.71	+0.12	2.04	5.41	-6.9	12.3	0.038
297	14542	+56°593	2 15.9	+56°56'	102.8	- 2.7	339.0	0.067	116	95	B8 Ia	6.95	+0.61	-0.13	2.10	4.85	-6.9	11.8	0.032
298*			2 16.0	+57°43'	102.6	- 1.9	338.9	0.086	114	93	B1 V	10.56	+0.41	-0.44	2.01	8.55	-3.1	11.6	0.043
299		+58°458	2 16.3	+58°30'	102.3	- 1.2	338.9	0.102	115	94	B1 pe	9.80	+0.54	-0.59	2.40	7.40			0.042
300	14605	+55°605	2 16.5	+56°08'	103.2	- 3.4	338.8	0.089	116	95	B0.5 (V) pe*	9.34	+0.27	-0.75	1.65	7.69	-3.6	11.3	0.054
301*			2 16.7	+57°53'	102.6	- 1.7	338.8	0.085	109	88	B0 IV: nn	9.44	+0.43	-0.57	2.19	7.25	-4.6	11.8	0.039
302		+58°461	2 17.1	+58°46'	102.3	- 0.9	338.7	0.070	115	94	B0.5 III	9.76	+0.45	-0.51	2.19	7.57	-4.7	12.3	0.032
303		+57°558	2 17.3	+57°52'	102.7	- 1.7	338.7	0.076	115	94	B0.5 III	9.89	+0.55	-0.42	2.49	7.40	-4.7	12.1	0.030
304	14818	+55°612	2 18.2	+56°10'	103.4	- 3.3	338.4	0.081	114	92	B2 Ia	6.21	+0.31	-0.61	1.65	4.56	-6.9	11.5	0.049
305*			2 18.6	+59°32'	102.2	- 0.1	338.4	0.097	115	93	B0 IV:	10.66	+0.77	-0.26	3.21	7.45	-4.6	12.0	0.030
306		+61°411	2 19.0	+61°33'	101.5	+ 1.8	338.3	0.107	120	99	O8:	10.19	+0.99	-0.09	3.90	6.29	-5.1	11.4	0.027
307	14899	+56°621	2 19.2	+56°47'	103.3	- 2.6	338.2	0.070	116	94	B8 Ib	7.38	+0.44	-0.10	1.59	5.79	-5.6	11.4	0.044
308	14947	+58°467	2 19.5	+58°25'	102.7	- 1.1	338.2	0.100	122	100	O6 f	7.98	+0.46	-0.61	2.34	5.64			0.043
309*			2 19.6	+57°24'	103.1	- 2.1	338.2	0.073	118	96	B2 IV	10.49	+0.43	-0.41	2.01	8.48	-2.9	11.4	0.036
310	14956	+57°568	2 19.6	+57°14'	103.2	- 2.2	338.2	0.078	117	95	B2 Ia	7.17	+0.72	-0.28	2.88	4.29	-6.9	11.2	0.027
311*			2 22.2	+57°46'	103.3	- 1.6	337.6	0.089	113	91	B1 III	9.86	+0.48	-0.44	2.22	7.64	-4.4	12.0	0.040
312		+59°497	2 22.3	+61°24'	101.9	+ 1.8	337.6	0.126	116	94	B0 V:	10.47	+0.74	-0.32	3.12	7.35	-4.1	11.4	0.040
313	15316	+57°576	2 22.8	+57°22'	103.5	- 1.9	337.4	0.100	110	87	A3 Iab	7.21	+0.77	+0.45	2.04	5.17	-6.5	11.7	0.049
314	15325	+56°635	2 22.9	+56°48'	103.8	- 2.4	337.4	0.115	113	90	B1 IV	8.51	+0.42	-0.47	2.04	6.47	-3.8	10.3	0.056
315		+57°579	2 23.0	+57°13'	103.6	- 2.1	337.4	0.083	108	85	B1 V	10.09	+0.49	-0.40	2.25	7.84	-3.1	10.9	0.037

TABLE 5—Continued

No.	HD	BD	1900 α	1900 δ	l	b	ϕ	p	θ	θ'	Spectrum	V	B-V	U-B	$3E_{(B-V)}$	m	M	m-M	p/A_V
			h m																
316		+60°493	2 23.3	+60°44'	102.3	+ 1.2	337.4	0.091	111	88	B0.5 Ia	8.44	+0.79	-0.30	3.21	5.23	-6.9	12.1	0.028
317		+62°411	2 23.9	+62°58'	101.5	+ 3.3	337.2	0.083	113	90	B1 Ib-II	8.46	+0.32	-0.60	1.74	6.72	-5.4	12.1	0.048
318		+60°497	2 24.2	+61°11'	102.2	+ 1.7	337.2	0.125	116	93	O7	8.80	+0.57	-0.48	2.67	6.13	-5.1	11.2	0.047
319	15450	+56°642	2 24.2	+56°27'	104.1	- 2.7	337.2	0.084	122	99	B2: pe	8.84	+0.34	-0.64	1.74	7.10			0.048
320		+60°498	2 24.5	+61°07'	102.3	+ 1.6	337.1	0.134	123	100	O9 V	9.93	+0.54	-0.46	2.55	7.38	-4.6	12.0	0.052
321	15497	+57°582	2 24.6	+57°15'	103.8	- 2.0	337.1	0.096	109	86	B6 Ia	6.98	+0.79	-0.05	2.79	4.19	-6.9	11.1	0.034
322*			2 24.8	+59°36'	102.9	+ 0.2	337.1	0.104	107	84	B0.5 V	10.52	+1.08	+0.06	4.08	6.44	-3.6	10.0	0.025
323		+60°501	2 25.0	+61°02'	102.4	+ 1.6	337.0	0.120	122	99	O6.5	9.60	+0.46	-0.58	2.34	7.26	-5.1	12.4	0.051
324	15548	+56°647	2 25.0	+56°13'	104.2	- 2.9	337.0	0.108	125	102	B1 V	9.27	+0.28	-0.58	1.62	7.65	-3.1	10.8	0.067
325	15558	+60°502	2 25.1	+61°01'	102.4	+ 1.6	337.0	0.110	120	97	O6	7.81	+0.52	-0.56	2.52	5.29	-5.1	10.4	0.044
326		+60°503	2 25.1	+60°31'	102.6	+ 1.1	337.0	0.151	119	96	B1.5 V	9.95	+0.66	-0.31	2.73	7.22	-2.6	9.8	0.055
327	15570	+60°504	2 25.2	+60°56'	102.4	+ 1.5	337.0	0.131	117	94	O5 f	8.10	+0.70	-0.40	3.06	5.04			0.043
328	15571	+56°648	2 25.2	+56°59'	104.0	- 2.2	337.0	0.093	124	101	B1 II:	8.33	+0.57	-0.43	2.49	5.84	-4.9	10.7	0.037
329	15620	+57°584	2 25.6	+57°31'	103.8	- 1.6	336.9	0.111	111	88	B8 Iab	8.35	+0.92	+0.17	3.03	5.32	-6.5	11.8	0.037
330	15629	+60°507	2 25.7	+61°05'	102.4	+ 1.6	336.9	0.105	120	97	O5	8.42	+0.43	-0.62	2.25	6.17	-5.1	11.3	0.047
331	15642	+54°569	2 25.8	+54°54'	104.9	- 4.0	336.8	0.065	115	92	B0 III:	8.51	+0.07	-0.84	1.11	7.40	-5.0	12.4	0.058
332		+57°586	2 26.1	+58°09'	103.6	- 1.0	336.8	0.110	122	99	B1 II	10.11	+0.61	-0.33	2.61	7.50	-4.9	12.4	0.042
333	15690	+56°656	2 26.3	+57°05'	104.1	- 2.0	336.7	0.115	113	89	B1.5 Ib	8.02	+0.65	-0.25	2.70	5.32	-5.8	11.1	0.042
334		+60°512	2 26.4	+60°57'	102.6	+ 1.6	336.7	0.028	107	84	O6	9.41	+0.50	-0.53	2.46	6.95	-5.1	12.0	0.011
335*			2 26.4	+60°57'	102.6	+ 1.6	336.7	0.094	117	94		10.26	+0.68	+0.12					
336		+59°510	2 26.7	+59°34'	103.1	+ 0.3	336.7	0.097	117	94	B1 III	10.28	+0.56	-0.40	2.46	7.82	-4.4	12.2	0.039
337	15752	+57°589	2 26.8	+57°58'	103.8	- 1.2	336.6	0.112	121	98	B0 III	8.74	+0.49	-0.52	2.37	6.37	-5.0	11.4	0.047
338		+62°419	2 27.2	+63°09'	101.8	+ 3.6	336.5	0.100	114	91	B0: V?	9.72	+0.36	-0.59	1.98	7.74	-4.1	11.8	0.050
339	15785	+59°513	2 27.2	+60°06'	103.0	+ 0.8	336.5	0.104	121	98	B1 Iab	8.34	+0.57	-0.50	2.49	5.85	-6.5	12.4	0.042
340		+58°488	2 27.2	+59°06'	103.4	- 0.1	336.5	0.131	107	83	B0.5 V	9.85	+0.68	-0.26	2.88	6.97	-3.6	10.6	0.045
341	E 236971	+56°660	2 28.3	+57°03'	104.3	- 1.9	336.3	0.096	119	95	B1 IV	9.55	+0.50	-0.40	2.28	7.27	-3.8	11.1	0.042
342		+62°424	2 28.4	+62°31'	102.2	+ 3.1	336.2	0.080	112	88	O8	8.83	+0.45	-0.57	2.28	6.55	-5.1	11.6	0.035
343		+57°593	2 28.6	+57°22'	104.3	- 1.6	336.2	0.093	118	94	B1 III	9.92	+0.61	-0.31	2.61	7.31	-4.4	11.7	0.036
344	16243	+57°602	2 31.3	+57°23'	104.6	- 1.5	335.7	0.079	117	93	B2 II:	8.26	+0.56	-0.27	2.40	5.86	-4.7	10.6	0.033
345	16264	+56°676	2 31.5	+57°10'	104.7	- 1.7	335.6	0.063	121	97	B1: V:	9.25	+0.44	-0.44	2.10	7.15	-3.1	10.2	0.030
346	16310	+58°498	2 32.0	+58°38'	104.2	- 0.3	335.5	0.108	122	97	B1 II:	8.12	+0.65	-0.36	2.73	5.39	-4.9	10.3	0.040
347	16429	+60°541	2 33.1	+60°51'	103.3	+ 1.8	335.3	0.049	128	103	O9.5 III	7.67	+0.62	-0.38	2.76	4.91	-5.7	10.6	0.018
348	16691	+56°693	2 35.5	+56°28'	105.5	- 2.0	334.8	0.078	118	93	O5 f	8.71	+0.48	-0.55	2.40	6.31			0.032
349	16778	+59°535	2 36.3	+59°24'	104.3	+ 0.6	334.6	0.114	121	96	A2 Ia	7.68	+0.89	+0.36	2.49	5.19	-6.9	12.1	0.046
350	16779	+57°620	2 36.3	+57°24'	105.2	- 1.2	334.6	0.102	115	90	B2 Ib	8.85	+0.74	-0.26	2.94	5.91	-5.8	11.7	0.035

TABLE 5—Continued

No.	HD	BD	1900 α	1900 δ	l	b	φ	p	θ	θ'	Spectrum	V	B-V	U-B	$3E_{(B-V)}$	m	M	m-M	p/A_V
			h m																
351	16808	+57°622	2 36.7	+57°53'	105.0	- 0.7	334.5	0.104	123	98	B0. 5 Ib	8.60	+0.56	-0.47	2.52	6.08	-5.8	11.9	0.041
352	16832	+56°703	2 36.9	+56°14'	105.7	- 2.2	334.4	0.102	119	93	B0 p*	8.85	+0.40	-0.58	2.10	6.75			0.048
353		+57°626	2 37.6	+57°13'	105.4	- 1.2	334.3	0.072	120	94	B1 Ib	9.95	+0.65	-0.29	2.73	7.22	-5.8	13.0	0.026
354	17088	+57°632	2 39.5	+57°19'	105.6	- 1.0	333.9	0.085	116	90	B9 Ia	7.50	+0.82	+0.05	2.64	4.86	-6.9	11.8	0.032
355	17114	+58°518	2 39.7	+58°55'	104.9	+ 0.4	333.9	0.110	113	87	B1 V	9.17	+0.50	-0.45	2.28	6.89	-3.1	10.0	0.048
356	17145	+57°634	2 40.0	+57°15'	105.7	- 1.1	333.8	0.096	116	90	B8 Ia	8.12	+0.84	+0.00	2.79	5.33	-6.9	12.2	0.034
357	17378	+56°718	2 42.2	+56°40'	106.2	- 1.5	333.3	0.101	121	94	A5 Ia	6.25	+0.89	+0.50	2.49	3.76	-6.9	10.7	0.040
358	E 237007	+59°549	2 42.7	+59°59'	104.8	+ 1.5	333.2	0.075	113	86	B0 V	9.45	+0.33	-0.60	1.89	7.56	-4.1	11.7	0.040
359	17505	+59°552	2 43.4	+60°01'	104.8	+ 1.6	333.1	0.075	109	82	O7	7.06	+0.40	-0.64	2.16	4.90	-5.1	10.0	0.035
360	17520	+59°553	2 43.5	+59°59'	104.9	+ 1.6	333.1	0.071	111	84	O8 V	8.27	+0.32	-0.58	1.89	6.38	-5.1	11.5	0.038
361	17603	+56°728	2 44.4	+56°38'	106.5	- 1.4	332.8	0.106	114	87	O7 f:	8.45	+0.65	-0.42	2.91	5.54			0.036
362		+59°562	2 45.6	+60°03'	105.1	+ 1.7	332.6	0.077	113	86	O8 V	9.73	+0.47	-0.53	2.34	7.39	-5.1	12.5	0.033
363		+60°586	2 46.4	+60°14'	105.1	+ 2.0	332.4	0.053	114	86	O7	8.48	+0.30	-0.67	1.86	6.62	-5.1	11.7	0.028
364	17857	+63°367	2 47.0	+63°43'	103.5	+ 5.1	332.2	0.102	112	84	B8 Ib	7.66	+0.75	-0.02	2.52	5.14	-5.6	10.7	0.040
365		+56°739	2 47.4	+57°02'	106.7	- 0.8	332.2	0.100	115	87	O9. 5 Ib	9.96	+1.00	-0.07	3.90	6.06	-6.6	12.7	0.026
366*			2 48.3	+58°49'	106.0	+ 0.8	332.0	0.141	112	84	B1 V	10.66	+0.57	-0.34	2.49	8.17	-3.1	11.3	0.057
367		+60°594	2 49.1	+61°01'	105.0	+ 2.8	331.8	0.086	121	93	O9 V	9.30	+0.36	-0.64	2.01	7.29	-4.6	11.9	0.043
368	18076	+58°534	2 49.2	+58°41'	106.1	+ 0.7	331.8	0.128	112	84	B0 II-III	9.06	+0.58	-0.42	2.64	6.42	-5.2	11.6	0.048
369		+60°596	2 49.3	+60°16'	105.4	+ 2.2	331.8	0.086	115	87	B1 V: n	9.64	+0.37	-0.54	1.89	7.75	-3.1	10.8	0.046
370*			2 50.3	+57°29'	106.8	- 0.2	331.6	0.128	118	90	B2 III	10.25	+0.81	-0.16	3.15	7.10	-3.6	10.7	0.041
371*			2 51.1	+57°42'	106.8	0.0	331.4	0.121	116	87	B1 II-III	10.04	+0.80	-0.21	3.18	6.86	-4.6	11.5	0.038
372	18326	+59°578	2 51.6	+60°10'	105.7	+ 2.2	331.3	0.070	117	88	O8	7.82	+0.38	-0.63	2.07	5.75	-5.1	10.8	0.034
373		+51°659	2 51.6	+51°42'	109.8	- 5.2	331.2	0.078	103	74	B0 III nn	9.37	+0.40	-0.52	2.10	7.27	-5.0	12.3	0.037
374	18352	+60°608	2 51.9	+60°53'	105.4	+ 2.8	331.2	0.077	115	86	B1 V*	8.80	+0.23	-0.63	1.47	5.33	-3.1	8.4	0.052
375	18409	+62°504	2 52.4	+62°19'	104.7	+ 4.1	331.1	0.092	114	85	O9 Ib	8.36	+0.42	-0.59	2.19	6.17	-6.9	13.1	0.042
376	E 237056	+57°681	2 55.0	+57°13'	107.5	- 0.2	330.6	0.128	125	96	B0. 5: V:pe	8.27	+0.75	-0.38	3.09	5.18	-3.6	8.8	0.041
377		+57°687	2 58.7	+57°27'	107.8	+ 0.3	329.8	0.116	118	88	B1 Ib	9.99	+0.89	-0.18	3.45	6.54	-5.8	12.3	0.034
378	19243	+61°525	3 00.7	+62°00'	105.7	+ 4.3	329.3	0.050	130	99	B1 V:e	6.72	+0.22	-0.63	1.44	5.28	-3.1	8.4	0.035
379	19820	+59°609	3 06.2	+59°11'	107.8	+ 2.3	328.2	0.105	114	82	O9 IV	7.1*	+0.51	-0.51	2.46	4.62	-5.4	10.0	0.043
380	E 237090	+59°611	3 07.2	+59°33'	107.7	+ 2.7	328.0	0.111	104	72	B0. 5 IV: nn	8.86	+0.53	-0.43	2.43	6.43	-4.2	10.6	0.046
381	E 237091	+59°612	3 07.3	+59°33'	107.7	+ 2.7	328.0	0.105	112	80	B1: V: pnne	8.67	+0.66	-0.37	2.76	5.91	-3.1	9.0	0.038
382		+59°704	3 09.1	+51°38'	112.1	- 3.9	327.6	0.066	115	83	B1 V: nn	10.34	+0.43	-0.39	2.07	8.27	-3.1	11.4	0.032
383		+51°710	3 11.6	+51°40'	112.4	- 3.7	327.1	0.095	107	74	B5 Ib	9.75	+0.59	-0.18	2.25	7.50	-5.8	13.3	0.042
384	E 237121	+58°587	3 12.7	+58°30'	108.9	+ 2.2	326.9	0.106	110	77	B0. 5 V	8.94	+0.46	-0.51	2.22	6.72	-3.6	10.3	0.048
385	20898	+59°648	3 17.1	+60°08'	108.4	+ 3.8	325.9	0.047	108	74	B2 III	7.92	+0.45	-0.42	2.07	5.85	-3.6	9.4	0.023

TABLE 5—Continued

No.	HD	BD	1900 α	1900 δ	l	b	φ	p	θ	θ'	Spectrum	V	B-V	U-B	3E(B-V)	m	M	m-M	p/A_V
			h m																0.038
386		+49°916	3 17.1	+49°18'	114.5	- 5.2	325.9	0.046	130	96	B2 p Shell	9.53	+0.16	-0.43	1.20	8.33			0.067
387	20959	+58°600	3 17.8	+59°05'	109.1	+ 3.0	325.8	0.095	120	86	B3 III	8.00	+0.27	-0.46	1.41	6.59	-3.3	9.9	0.035
388	21212	+61°587	3 20.3	+62°09'	107.6	+ 5.7	325.2	0.088	135	100	B2 (V) e	8.13	+0.59	-0.42	2.49	5.64	-2.0	7.6	0.051
389	21291	+59°660	3 21.0	+59°36'	109.1	+ 3.7	325.1	0.075	117	82	B9 Ia	4.20	-0.43	-0.23	1.47	2.73	-6.9	9.6	0.045
390	21389	+58°607	3 21.9	+58°32'	109.8	+ 2.9	325.0	0.075	121	86	A0 Ia	4.53	+0.56	-0.12	1.68	2.85	-6.9	9.8	
												7.03	+0.35	-0.33	1.65	5.38	-3.3	8.7	0.018
391	21483	+29°566	3 22.7	+30°02'	127.0	-20.2	322.2	0.030	176	138	B3 III	6.40	+0.03	-0.73	0.81	5.59	-2.9	8.5	0.042
392	21803	+44°734	3 25.8	+44°32'	118.3	- 8.2	323.8	0.034	132	96	B2 IV	5.89	-0.06	-0.87	0.60	5.29	-3.1	8.4	0.030
393	21856	+34°674	3 26.3	+35°06'	124.3	-15.7	322.5	0.018	68	30	B1 V	6.53	+0.33	-0.56	1.83	4.70	-4.7	9.4	0.022
394	22253	+56°824	3 29.9	+56°23'	112.0	+ 1.8	323.4	0.040	127	90	B0.5 III	7.48	+0.11	-0.57	1.05	6.43	-2.0	8.4	0.010
395	23060	+33°704	3 37.0	+33°48'	127.0	-15.3	320.3	0.010	82	43	B2 Vp Veiled								
												3.84	+0.05	-0.75	0.93	2.91	-4.9	7.8	0.015
396	23180	+31°642	3 38.0	+31°58'	128.4	+16.6	319.8	0.014	29	169	B1 II	8.53	+0.68	+0.01	2.52	6.01	-0.9	6.9	0.010
397		+31°643	3 38.3	+31°51'	128.5	-16.7	319.7	0.024	150	110	B5 V	6.65	+0.09	-0.57	0.87	5.78	-2.5	8.3	0.040
398	23478	+31°649	3 40.4	+32°00'	128.7	-16.2	319.4	0.035	31	170	B3 IV	6.55	+0.08	-0.62	0.96	5.59	-2.0	7.6	0.017
399	23625	+33°717	3 41.5	+33°18'	128.0	-15.1	319.4	0.016	28	167	B2 V	6.72	+0.42	-0.56	2.10	4.62	-4.7	9.3	0.032
400	23675	+52°714	3 41.9	+52°21'	115.8	- 0.4	321.0	0.067	133	94	B0.5 III								
												6.94	+0.32	-0.54	1.74	5.20	-3.8	9.0	0.033
401	23800	+52°715	3 42.9	+52°11'	116.0	- 0.4	320.8	0.058	123	84	B1 IV	5.76	+0.01	-0.81	0.81	4.95	-3.1	8.0	0.027
402	24131	+33°728	3 45.5	+34°03'	128.2	-14.0	318.8	0.022	88	47	B1 V	7.43	+0.04	-0.63	0.84	6.59	-2.0	8.6	0.015
403	24190	+33°730	3 46.0	+33°53'	128.4	-14.1	318.7	0.013	95	54	B2 V	11.09	+0.75	-0.14	3.03	8.06	-3.1	11.2	0.010
404*			3 46.1	+52°56'	115.9	+ 0.5	320.2	0.030	124	84	B1 V	10.17	+0.39	-0.48	1.89	8.28	-2.9	11.2	0.022
405*			3 46.7	+46°35'	120.1	- 4.3	319.9	0.041	145	105	B2: IV: nne								
												6.72	+0.38	-0.61	2.07	4.65	-5.0	9.6	0.020
406	24431	+52°726	3 48.1	+52°21'	116.6	+ 0.2	319.8	0.041	118	78	O9 IV-V	6.82	+0.55	-0.17	2.25	4.57	-4.6	9.2	0.025
407	24432	+48°1019	3 48.1	+48°45'	118.9	- 2.5	319.7	0.056	135	95	B3 II	6.07	+0.31	-0.82					
408	24534	+30°591	3 49.1	+30°45'	131.1	-15.9	317.6	0.025	49	7	Ope (var)	9.57	+0.71	-0.27	2.85	6.72	-5.8	12.5	0.038
409		+55°837	3 50.0	+55°38'	114.6	+ 2.9	319.3	0.110	133	92	B2 Ib	5.48	-0.03	-0.75	0.63	4.85	-2.0	6.8	0.032
410	24640	+34°768	3 50.0	+34°47'	128.4	-12.8	318.1	0.020	99	57	B2 V								
												10.13	+1.06	-0.01	3.90	6.23	-6.5	12.7	0.022
411		+52°729	3 50.1	+52°25'	116.7	+ 0.5	319.4	0.085	124	84	B2 Iab	10.08	+0.27	-0.69	1.77	8.31	-5.1	13.4	0.038
412*			3 51.0	+56°56'	113.9	+ 4.0	319.1	0.067	134	93	O7.5	9.68	+0.28	-0.69	1.80	7.88	-5.1	13.0	0.047
413		+56°864	3 51.1	+56°56'	113.9	+ 4.0	319.0	0.084	136	95	O6 nn	10.28	+0.36	-0.60	2.01	8.27	-4.6	12.9	0.048
414		+56°866	3 51.4	+56°49'	114.0	+ 3.9	319.0	0.097	136	95	O9 V	9.14	+0.31	-0.57	1.77	7.37	-3.6	11.0	0.046
415	E 237204	+56°868	3 52.4	+56°37'	114.2	+ 3.9	318.8	0.082	134	93	B0.5 V								
												4.02	+0.04	-0.93	1.08	2.94	-5.1	8.0	0.025
416	24912	+35°775	3 52.5	+35°30'	128.3	-11.9	317.8	0.027	102	60	O7	9.29	+0.82	-0.11	3.06	6.23	-5.8	12.0	0.032
417		+55°838	3 52.8	+55°13'	115.2	+ 2.9	318.8	0.097	133	92	B3 Ib	8.86	+0.41	-0.43	2.07	6.79	-3.6	10.4	0.005
418	E 232874	+53°723	3 54.5	+53°27'	116.6	+ 1.7	318.5	0.011	95	54	B0.5 V	10.64	+0.87	-0.18	3.39	7.25			0.017
419*			3 54.7	+52°33'	117.2	+ 1.0	318.5	0.057	128	87	B1 ? p*	8.98	+0.49	-0.51	2.37	6.61	-6.6	13.2	0.032
420	E 237211	+56°873	3 55.3	+56°15'	114.8	+ 3.9	318.2	0.075	139	97	O9.5 I? p*								

420	E 237211	+56°873	3 55.3	+56 15	114.5															

TABLE 5—Continued

No.	HD	BD	1900 α	1900 δ	l	b	φ	p	θ	θ'	Spectrum	V	B-V	U-B	3E(B-V)	m	M	m-M	p/A_V
421	E 237213	+55°845	3h 56.5m	+55°43'	115.3	+ 3.6	318.0	0.079	138	96	B3 Ia	8.72	+0.77	-0.06	2.91	5.81	-6.9	12.7	0.027
422	25348	+52°752	3 56.6	+53°03'	117.1	+ 1.6	318.1	0.030	122	80	B1 V pnne	8.33	+0.21	-0.65	1.41	6.92	-3.1	10.0	0.021
423	25443	+61°669	3 57.4	+61°48'	111.2	+ 8.2	317.4	0.115	136	93	B0.5 III	6.74	+0.33	-0.62	1.83	4.91	-4.7	9.6	0.063
424	25517	+43°886	3 58.1	+44°00'	123.3	- 4.9	317.6	0.055	160	118	B1 V	9.27	+0.25	-0.57	1.53	7.74	-3.1	10.8	0.036
425	25914	+56°884	4 01.2	+56°50'	115.0	+ 4.8	317.0	0.102	141	98	B6 Ia	7.99	+0.60	-0.28	2.22	5.77	-6.9	12.7	0.046
426	E 232947	+53°765'	4 17.6	+53°11'	119.2	+ 3.9	314.0	0.137	149	103	B0 Ia	9.32	+0.64	-0.40	2.82	6.50	-6.9	13.4	0.048
427		+51°921	4 17.7	+51°48'	120.2	+ 2.9	314.0	0.097	140	94	B0 II	9.63	+0.73	-0.30	3.09	6.54	-5.4	11.9	0.031
428	E 232999	+50°1043	4 37.0	+50°23'	123.3	+ 4.2	310.5	0.082	158	108	B1 IV	9.37	+0.56	-0.31	2.46	6.91	-3.8	10.7	0.033
429	30353	+43°1069	4 41.8	+43°06'	129.4	+ 0.2	309.8	0.050	149	99	A pe	7.76	+0.46	-0.17					
430		+41°974	4 43.2	+41°30'	130.8	- 0.7	309.6	0.022	156	106	B pe	9.33	+0.17	-0.56					
431	31327	+35°930	4 49.7	+36°01'	135.9	- 3.1	308.4	0.010	102	50	B2 Ib	6.06	+0.41	-0.44	1.95	4.11	-5.8	9.9	0.005
432		+30°748	4 52.1	+30°33'	140.5	- 6.1	307.7	< .003			B1.5 V	9.66	+0.31	-0.41	1.68	7.98	-2.6	10.6	
433	31617	+43°1147	4 52.2	+43°11'	130.6	+ 1.7	308.1	0.040	163	111	B2 IV	7.42	+0.00	-0.77	0.72	6.70	-2.9	9.6	0.056
434		+43°1168	4 55.0	+43°42'	130.5	+ 2.4	307.6	0.124	137	85	B9 Iab	9.39	+0.92	+0.20	2.94	6.45	-6.5	13.0	0.042
435		+40°1189	5 03.3	+40°32'	133.9	+ 1.7	306.3	0.043	160	106	B2: III: nn	8.91	+0.06	-0.67	0.90	8.01	-3.6	11.6	0.048
436	33357	+41°1101	5 04.6	+42°02'	132.9	+ 2.8	306.1	0.047	154	100	B1: (V) n (e)	8.40	+0.00	-0.73	0.78	7.62	-3.1	10.7	0.060
437	33461	+41°1106	5 05.3	+41°06'	133.7	+ 2.4	306.0	0.037	167	113	B2: V: nne	7.78	+0.27	-0.55	1.53	6.25	-2.0	8.2	0.024
438		+39°1204	5 05.3	+39°26'	135.0	+ 1.4	306.0	0.054	153	99	B pe	10.26	+0.40	-0.55					
439	33604	+40°1213	5 06.3	+40°05'	134.6	+ 1.9	305.8	0.026	165	111	B2 V: pe	7.26	+0.05	-0.70	0.87	6.39	-2.0	8.4	0.030
440*			5 08.2	+36°36'	137.7	+ 0.2	305.6	0.063	137	83	B1 V: p(e)	10.97	+0.73	-0.30	2.97	8.00	-3.1	11.1	0.021
441		+39°1264	5 14.1	+39°13'	136.2	+ 2.7	304.7	0.062	156	101	B2 V	9.88	+0.34	-0.41	1.74	8.14	-2.0	10.1	0.036
442	34921	+37°1160	5 15.8	+37°35'	137.7	+ 2.0	304.5	0.079	147	92	B0 IV: pe	7.51	+0.14	-0.86	1.32	6.19	-4.6	10.8	0.060
443	E 242908	+33°1023	5 16.0	+33°25'	141.2	- 0.3	304.5	0.054	151	96	O5	9.04	+0.28	-0.72	1.80	7.24	-5.1	12.3	0.030
444	E 242926	+33°1024	5 16.1	+33°13'	141.4	- 0.4	304.5	0.042	146	91	O6	9.35	+0.34	-0.65	1.98	7.37	-5.1	12.5	0.021
445	E 242935	+33°1026	5 16.2	+33°19'	141.3	- 0.4	304.5	0.065	163	107	O8	9.43	+0.20	-0.73	1.53	7.90	-5.1	13.0	0.042
446*			5 16.7	+33°29'	141.2	- 0.2	304.4	0.062	154	98	B1 IV?*	10.64	+0.31	-0.62	1.71	8.93	-3.8	12.7	0.036
447	35215	+30°873	5 18.1	+30°06'	144.2	- 1.8	304.2	0.022	122	66	B1 V	9.40	+0.08	-0.66	1.02	8.38	-3.1	11.5	0.022
448	35347	+29°886	5 19.0	+29°32'	144.8	- 2.0	304.0	0.024	135	79	B1: (V:) e	8.93	+0.12	-0.74	1.14	7.79	-3.1	10.9	0.021
449		+42°1286	5 19.4	+42°56'	133.7	+ 5.6	303.6	0.079	143	87	B0.5 V	10.09	+0.28	-0.64	1.68	8.41	-3.6	12.0	0.047
450		+42°1288	5 20.1	+42°13'	134.4	+ 5.3	303.6	0.090	162	106	B8 Ib	9.48	+0.38	-0.23	1.41	8.07	-5.6	13.7	0.064
451	35619	+34°1046	5 21.0	+34°41'	140.7	+ 1.3	303.8	0.048	170	114	O7	8.60	+0.23	-0.69	1.65	6.95	-5.1	12.0	0.029
452	35633	+34°1049	5 21.1	+34°27'	140.9	+ 1.1	303.8	0.023	172	116	B0.5 IV	8.04	+0.32	-0.66	1.80	6.24	-4.2	10.4	0.013
453	35653	+33°1049	5 21.2	+33°52'	141.4	+ 0.8	303.8	0.045	162	106	B0.5 V	7.44	+0.12	-0.75	1.20	6.24	-3.6	9.8	0.038
454		+33°1056	5 21.6	+33°14'	142.0	+ 0.5	303.7	0.093	161	105	B0 III	10.61	+0.45	-0.50	2.25	8.36	-5.0	13.4	0.041
455		+34°1059	5 22.0	+34°56'	140.7	+ 1.6	303.6	0.055	153	97	B0 IV-V	9.22	+0.19	-0.76	1.47	7.75	-4.4	12.2	0.037

TABLE 5—Continued

No.	HD	BD	1900 α	1900 δ	l	b	φ	p	θ	θ'	Spectrum	V	B-V	U-B	3E(B-V)	m	M	m-M	p/A_V
			h m																
456		+34°1058	5 22.0	+34°35'	140.9	+ 1.4	303.6	0.063	160	104	O8 nn	8.78	+0.26	-0.73	1.71	7.07	-5.1	12.2	0.037
457	35921	+35°1137	5 23.0	+35°18'	140.4	+ 1.9	303.5	0.043	143	87	O9.5 III	6.81	+0.20	-0.78	1.50	5.31	-5.7	11.0	0.029
458	35952	+35°1139	5 23.2	+35°53'	140.0	+ 2.3	303.4	0.033	133	76	B5 II-III	8.84	+0.27	-0.32	1.29	7.55	-3.7	11.2	0.026
459		+35°1141	5 23.3	+35°07'	140.6	+ 1.9	303.4	0.031	152	95	B0. 5: V: n	9.59	+0.10	-0.74	1.14	8.45	-3.6	12.0	0.027
460	36212	+34°1077	5 25.1	+34°48'	141.1	+ 2.0	303.2	0.044	163	106	B3 II	7.77	+0.24	-0.52	1.32	6.45	-2.5	9.0	0.033
461		+39°1328	5 25.2	+39°59'	136.8	+ 4.9	302.9	0.096	163	106	O9 III?*	9.85	+0.57	-0.46	2.64	7.21	-6.4	13.6	0.036
462	36280	+34°1079	5 25.5	+34°52'	141.1	+ 2.1	303.1	0.027	154	97	B0. 5 IV n	8.85	+0.10	-0.77	1.14	7.71	-4.2	11.9	0.024
463	36483	+36°1177	5 26.9	+36°24'	140.0	+ 3.2	302.9	0.083	149	92	O9. 5 III	8.18	+0.43	-0.55	2.19	5.99	-5.7	11.7	0.038
464	36547	+23°942	5 27.4	+23°16'	150.9	- 3.9	302.8	0.037	144	87	B1 III	8.81	+0.38	-0.56	1.92	6.89	-4.4	11.3	0.019
465		+35°1169	5 27.6	+35°45'	140.6	+ 3.0	302.8	0.036	133	76	B1: V: pe	9.37	+0.45	-0.40	2.13	7.24	-3.1	10.3	0.017
466	E 244894	+27°797	5 28.3	+27°31'	147.6	- 1.4	302.8	0.035	19	141	B1 pe (III, V)	9.86	+0.45	-0.61	2.13	7.73	-3.8	11.5	0.016
467	36879	+21°899	5 29.7	+21°20'	153.0	- 4.4	302.4	0.045	152	94	O6	7.56	+0.22	-0.80	1.62	5.94	-5.1	11.0	0.028
468	E 245310	+21°901*	5 30.4	+21°08'	153.2	- 4.4	302.3	0.085	146	88	B1: V: nne*	8.87	+0.28	-0.67	1.62	7.25	-3.1	10.4	0.052
469	37032	+34°1118	5 30.5	+34°45'	141.7	+ 2.9	302.5	0.030	169	112	B0. 5 V	8.10	+0.10	-0.78	1.14	6.96	-3.6	10.6	0.026
470	E 245493	+33°1103	5 31.3	+33°54'	142.5	+ 1.6	302.4	0.024	165	107	B2: V: p(e)	8.63	+0.02	-0.73	0.78	7.85	-2.0	9.8	0.031
471	E 245770	+26°883	5 32.7	+26°16'	149.2	- 1.2	302.3	0.016	180	122	B pe	9.39	+0.45	-0.54					
472	37614-5	+38°1250	5 34.7	+38°08'	139.3	+ 5.4	301.7	0.044	170	112	B2 III	8.20	+0.13	-0.63	1.11	7.09	-3.6	10.7	0.040
473	37737	+36°1233	5 35.7	+36°09'	141.1	+ 4.6	301.7	0.021	133	75	B0 II:	8.00	+0.31	-0.62	1.83	6.17	-5.4	11.6	0.011
474		+37°1292	5 35.9	+37°56'	139.6	+ 5.5	301.5	0.025	5	127	B3 V: p(e)	9.08	+0.20	-0.52	1.20	7.88	-1.5	9.4	0.021
475	37767	+36°1236	5 35.9	+36°06'	141.2	+ 4.6	301.6	0.019	7	129	B3 V	8.94	+0.15	-0.48	1.05	7.89	-1.5	9.4	0.018
476		+34°1150	5 36.4	+34°18'	142.8	+ 3.7	301.7	0.016	41	163	B2 V	9.58	+0.20	-0.49	1.32	8.26	-2.0	10.3	0.012
477	38017	+30°992	5 37.6	+30°53'	145.8	+ 2.1	301.7	0.047	13	135	B3 III	8.08	+0.26	-0.47	1.38	6.70	-3.3	10.0	0.034
478	E 246878	+27°850'	5 38.2	+27°12'	149.0	+ 0.3	301.7	0.012	133	75	B0. 5 V: pe	9.38	+0.16	-0.59	1.32	8.06	-3.6	11.7	0.009
479	E 246901	+33°1138	5 38.3	+33°29'	143.7	+ 3.6	301.5	0.028	158	100	B1: +G5: Ib:	8.08	+1.24	-0.20					
480	38131	+35°1223	5 38.4	+35°08'	142.3	+ 4.5	301.4	0.018	169	110	B0. 5 V	8.19	+0.21	-0.69	1.47	6.72	-3.6	10.3	0.012
481		+34°1162	5 38.6	+34°03'	143.2	+ 4.0	301.4	0.024	176	117	B2 V: nn	8.93	+0.12	-0.58	1.08	7.85	-2.0	9.8	0.022
482	38191	+21°958	5 38.9	+21°25'	154.0	- 2.6	301.5	0.040	152	94	B1: (V) n (e)	8.73	+0.14	-0.69	1.20	7.53	-3.1	10.6	0.033
483	E 247176	+26°943	5 39.5	+26°32'	149.7	+ 0.2	301.5	0.020	131	72	B2 V	9.59	+0.18	-0.55	1.26	8.33	-2.0	10.3	0.016
484		+36°1261	5 41.7	+36°12'	141.7	+ 5.6	300.9	0.025	169	110	B2 III? p?	9.09	+0.28	-0.47	1.56	7.53	-3.6	11.1	0.016
485	38658	+28°902	5 42.3	+28°17'	148.6	+ 1.7	301.2	0.021	0	121	B3 II	8.35	+0.20	-0.59	1.20	7.15	-4.6	11.8	0.018
486	E 247754	+25°989	5 42.4	+25°04'	151.2	0.0	301.2	0.053	150	91	B1 V: nn	9.65	+0.26	-0.60	1.56	8.09	-3.1	11.2	0.034
487	38708	+29°1005	5 42.6	+29°06'	147.9	+ 2.1	301.1	0.025	167	108	B3: p(e) shell:	8.24	+0.01	-0.49	0.63	7.61			0.040
488	38909	+31°1115	5 44.0	+31°02'	146.4	+ 3.4	300.9	0.025	152	93	B3 II-III	8.16	+0.01	-0.62	0.63	7.53	-4.0	11.5	0.040
489	39136	+32°1111	5 45.4	+32°13'	145.5	+ 4.3	300.6	<.005			B3 III	8.66	+0.09	-0.45	0.87	7.93	-3.3	11.2	
490	E 248587	+19°1111	5 46.5	+19°07'	156.9	- 2.3	300.9	0.054	146	87	A0 Iab	7.94	+0.65	+0.12	1.95	5.99	-6.5	12.5	0.028

TABLE 5—Continued

No.	HD	BD	1900 α	1900 δ	l	b	φ	p	θ	θ'	Spectrum	V	B-V	U-B	$3E_{(B-V)}$	m	M	m-M	p/A_V
			h m																
491	E 248893	+22°1090	5 48.0	+22°06'	154.5	- 0.4	300.7	0.075	155	96	B0 II-III	9.69	+0.44	-0.56	2.22	7.47	-5.2	12.7	0.034
492	E 248894	+20°1158	5 48.0	+20°51'	155.6	- 1.1	300.6	0.049	146	87	O8: V: nn	9.29	+0.24	-0.73	1.65	7.64	-5.1	12.7	0.030
493	E 249071	+27°909	5 49.0	+27°54'	149.7	+ 2.7	300.4	0.070	168	108	B2 III:	9.47	+0.39	-0.47	1.89	7.58	-3.6	11.2	0.037
494	39680(A)	+13°1026	5 49.0	+13°49'	161.8	- 4.4	300 3	0.014	143	83	O6: pe	7.99	+0.02	-0.96	1.02	6.97	-5.1	12.1	0.014
495	39712	+30°1055	5 49.2	+30°41'	147.3	+ 4.2	300.3	0.014	162	102	B2 IV	8.38	+0.11	-0.56	1.05	7.33	-2.9	10.2	0.013
496	39746	+27°914	5 49.4	+27°42'	149.9	+ 2.7	300.4	0.040	178	118	B1 II	7.04	+0.22	-0.68	1.44	5.60	-4.9	10.5	0.028
497*			5 49.9	+25°23'	151.9	+ 1.6	300.4	0.070	162	102	B1 III	10.89	+0.68	-0.32	2.82	8.07	-4.4	12.5	0.025
498*			5 49.9	+20°04'	156.5	- 1.1	300.5	0.049	152	92	B1 IV	10.91	+0.33	-0.56	1.77	9.14	-3.8	12.9	0.028
499	39970	+24°1033	5 50.9	+24°14'	153.0	+ 1.2	300.4	0.035	161	101	A0 Ia	6.02	+0.39	-0.20	1.17	4.85	-6.9	11.8	0.030
500	40003	+23°1119	5 51.1	+23°25'	153.8	+ 0.9	300.3	0.062	167	107	B3 Ib	8.60	+0.82	-0.08	3.06	5.54	-5.8	11.3	0.020
501	40111	+25°1052	5 51.8	+25°57'	151.6	+ 2.3	300.2	0.023	164	104	B1 Ib	4.81	-0.06	-0.94	0.60	4.21	-5.8	10.0	0.038
502	E 249695	+30°1071	5 52.2	+30°12'	148.0	+ 4.1	300.0	0.023	176	116	B1: V: pnne	8.99	+0.17	-0.65	1.29	7.70	-3.1	10.8	0.018
503	40297	+27°938	5 52.8	+27°33'	150.4	+ 3.3	300.0	0.030	177	117	A0 Ib	7.27	+0.29	-0.07	0.87	6.40	-5.6	12.0	0.034
504	E 249845	+32°1146	5 53.0	+32°53'	145.8	+ 6.0	299.6	< .003			B2: V: nn*	8.79	+0.08	-0.53	0.96	7.83	-2.0	9.8	
505	E 250028	+25°1065	5 53.8	+25°06'	152.6	+ 2.2	300.1	0.093	164	104	B2: V: pnne*	9.09	+0.23	-0.61	1.41	7.68	-2.0	9.7	0.066
506	E 250163	+19°1166	5 54.4	+19°11'	157.8	- 0.6	300.1	0.036	136	76	B1. 5: V: pne	9.62	+0.58	-0.34	2.49	7.13	-2.6	9.7	0.014
507	40589	+27°945	5 54.7	+27°35'	150.6	+ 3.6	299.8	0.015	158	98	B9 Iab:	6.05	+0.25	-0.26	0.93	5.12	-6.5	11.6	0.016
508	E 250289	+23°1148	5 55.0	+23°20'	154 3	+ 1.6	300.0	0.064	162	102	B2 III: e	8.27	+0.56	-0.32	2.40	5.87	-3.6	9.5	0.027
509	E 250290	+23°1149	5 55.0	+23°18'	154.3	+ 1.6	300.0	0.073	163	103	B3 Ib	7.38	+0.61	-0.24	2.43	4.95	-5.8	10.8	0.030
510*			5 56.0	+20°12'	157.1	+ 0.2	299.9	0.044	170	110	B1 V	11.50	+0.61	-0.33	2.61	8.89	-3.1	12.0	0.017
511	40893	+31°1174	5 56.7	+31°02'	147.8	+ 5.7	299.4	0.030	140	79	B0 IV:	8.90	+0.16	-0.78	1.38	7.52	-4.6	12.1	0.022
512	40894	+28°991	5 56.7	+28°40'	149.8	+ 4.6	299.5	0.009	161	101	B2 V	7.56	-0.08	-0.74	0.48	7.08	-2.0	9.1	0.019
513	E 251117	+28°1001	5 58.7	+28°46'	150.0	+ 5.0	299.3	0.033	161	100	B0 IV	9.11	+0.17	-0.75	1.41	7.70	-4.6	12.3	0.023
514	E 251204	+23°1179	5 59.0	+23°24'	154.7	+ 2.4	299.6	0.101	155	95	B0 IV	10.28	+0.48	-0.55	2.34	7.94	-4.6	12.5	0.043
515	E 251311	+23°1183	5 59.4	+23°01'	155.1	+ 2.3	299.6	0.048	0	120	B1. 5: IV: n	8.81	+0.34	-0.50	1.77	7.04	-3.4	10.4	0.027
516	41398	+28°1008	5 59.8	+28°56'	149.9	+ 5.3	299.2	0.048	166	105	B2 Ib	7.46	+0.32	-0.65	1.68	5.78	-5.8	11.6	0.029
517	E 251726	+19°1210	6 01.0	+19°02'	158.7	+ 0.7	299.5	0.069	171	111	B1 V: e	9.37	+0.54	-0.54	2.40	6.97	-3.1	10.1	0.029
518	41690	+21°1120	6 01.6	+21°53'	156.3	+ 2.2	299.4	0.058	177	116	B1 V	7.71	+0.22	-0.62	1.44	6.27	-3.1	9.4	0.040
519	E 252325	+20°1278	6 03.1	+20°39'	157.5	+ 1.9	299.3	0.104	163	103	B1: V:	10.79	+0.57	-0.43	2.49	8.30	-3.1	11.4	0.042
520	41997	+15°1079	6 03.2	+15°44'	161.8	- 0.5	299.4	0.070	159	98	O7	8.42	+0.38	-0.61	2.10	6.32	-5.1	11.4	0.033
521	42087	+23°1226	6 03.7	+23°08'	155.4	+ 3.2	299.2	0.043	172	111	B2. 5 Ib	5.76	+0.20	-0.64	1.26	4.50	-5.8	10.3	0.034
522	42088	+20°1284	6 03.7	+20°31'	157.7	+ 2.0	299.3	0.052	178	117	O6	7.55	+0.07	-0.89	1.17	6.38	-5.1	11.5	0.044
523*			6 04.3	+13°08'	164.2	- 1.5	299.2	0.079	167	106	O9 V	10.23	+0.46	-0.56	2.31	7.92	-4.6	12.5	0.034
524*			6 05.1	+13°12'	164.3	- 1.3	299.2	0.087	161	100	O9 V	10.57	+0.46	-0.54	2.31	8.26	-4.6	12.9	0.038
525	42379	+21°1143	6 05.3	+21°36'	157.0	+ 2.8	299.1	0.060	170	109	B1 II	7.37	+0.35	-0.58	1.83	5.54	-4.9	10.4	0.033

TABLE 5—Continued

No.	HD	BD	1900 α	1900 δ	l	b	ϕ	p	θ	θ'	Spectrum	V	B-V	U-B	3E(B-V)	m	M	m-M	p/A$_V$
			h m																
526	42400	+20°1302	6 05.4	+20°56'	157.6	+ 2.5	299.1	0.047	169	108	B5 II	6.84	+0.18	-0.44	1.02	5.82	-4.6	10.4	0.046
527	E 252956	+13°1148	5 05.4	+13°09'	164.4	- 1.3	299.2	0.080	160	99	B0.5 IV	10.18	+0.42	-0.54	2.10	8.08	-4.2	12.3	0.038
528	E 253049	+20°1305	6 05.8	+20°10'	158.3	+ 2.2	299.1	0.040	176	115	B2 IV	9.56	+0.14	-0.54	1.14	8.42	-2.9	11.3	0.035
529	E 253214	+20°1309	6 06.4	+20°07'	158.4	+ 2.3	299.1	0.060	173	112	B1.5: V: nn	9.47	+0.24	-0.53	1.47	8.00	-2.6	10.6	0.041
530	E 253247	+18°1123	6 06.5	+18°03'	160.2	+ 1.4	299.1	0.032	3	122	B0 V	9.78	+0.34	-0.59	1.92	7.86	-4.1	12.0	0.017
531		+18°1124	6 06.9	+18°01'	160.3	+ 1.4	299.1	0.064	14	133	B0.5 V::	10.76	+0.58	-0.39	2.58	8.18	-3.6	11.8	0.025
532	42896	+20°1322	6 08.2	+20°13'	158.5	+ 2.7	298.9	0.018	7	126	B1: V: nn	8.59	-0.07	-0.85	0.57	8.02	-3.1	11.1	0.032
533	E 253683	+19°1265	6 08.2	+19°00'	159.6	+ 2.1	298.9	0.078	159	98	B0.5 IV	9.30	+0.34	-0.58	1.86	7.44	-4.2	11.6	0.042
534	43078	+22°1243	6 09.2	+22°20'	156.8	+ 3.9	298.7	0.070	165	104	B0 IV	8.78	+0.35	-0.57	1.95	6.83	-4.6	11.4	0.036
535	E 254042	+24°1176	6 09.8	+24°06'	155.3	+ 4.9	298.5	0.085	173	112	B0.5: IV: nn	8.93	+0.35	-0.58	1.89	7.04	-4.2	11.2	0.045
536	43384	+23°1275	6 10.8	+23°46'	155.7	+ 5.0	298.5	0.062	170	109	B3 Iab	6.23	+0.45	-0.37	1.95	4.28	-6.5	10.8	0.032
537	43582	+22°1267	6 11.9	+22°41'	156.8	+ 4.7	298.5	0.028	8	126	B0 III n*	9.12	+0.81	-0.19	3.33	5.79	-5.0	10.8	0.008
538	E 254647	+11°1100	6 12.0	+11°14'	166.8	- 0.8	298.8	0.024	11	130	B pe	10.01	+0.39	-0.68					
539	E 254699	+23°1286	6 12.3	+23°36'	156.0	+ 5.2	298.3	0.074	176	114	B1 V	9.04	+0.40	-0.46	1.98	7.06	-3.1	10.2	0.037
540	E 254755	+22°1273	6 12.5	+22°43'	156.8	+ 4.8	298.4	0.039	8	126	O9 V: p?	8.84	+0.60	-0.44	2.73	6.11	-4.6	10.7	0.014
541	43703	+23°1289	6 12.6	+23°03'	156.5	+ 5.0	298.4	0.037	143	81	B1 IV: p	8.62	+0.42	-0.53	2.04	6.58	-3.8	10.4	0.018
542	43753	+23°1297	6 12.9	+23°02'	156.6	+ 5.0	298.3	0.059	161	99	B0.5 III	7.90	+0.30	-0.64	1.74	6.16	-4.7	10.9	0.034
543*			6 13.1	+14°33'	164.0	+ 1.0	298.7	0.056	159	98	B0 V	10.89	+0.30	-0.64	1.80	9.09	-4.1	13.2	0.031
544	43818	+23°1300	6 13.2	+23°30'	156.2	+ 5.3	298.3	0.043	177	115	B0 II	6.92	+0.29	-0.69	1.77	5.15	-5.4	10.6	0.024
545	E 255055	+23°1304	6 13.6	+23°20'	156.4	+ 5.3	298.3	0.019	163	101	O9 V: p	9.38	+0.26	-0.70	1.71	7.67	-4.6	12.3	0.011
546	44139	+22°1291	6 15.1	+22°13'	157.5	+ 5.1	298.2	0.046	2	120	B0.5 V	8.78	+0.28	-0.57	1.68	7.10	-3.6	10.7	0.027
547	44498	+08°1296	6 17.0	+08°22'	169.9	- 1.1	298.5	0.008	179	118	B2.5 V	8.83	-0.08	-0.59	0.42	8.41	-1.8	10.2	0.019
548	44597	+20°1399	6 17.5	+20°27'	159.3	+ 4.8	298.1	0.047	170	108	O9 V	9.02	+0.26	-0.69	1.71	7.31	-4.6	11.9	0.027
549	E 256276	+22°1311	6 17.7	+22°27'	157.6	+ 5.7	298.0	0.033	9	127	B1.5: V: nn	9.24	+0.16	-0.69	1.23	8.01	-2.6	10.6	0.027
550	44637	+15°1176	6 17.7	+15°09'	164.0	+ 2.3	298.4	0.039	1	120	B2 V: pe	8.03	+0.24	-0.52	1.44	6.59	-2.0	8.6	0.027
551	E 256413	+19°1331	6 18.1	+19°58'	159.8	+ 4.7	298.1	0.054	168	106	B5 III	8.93	+0.35	-0.37	1.53	7.40	-2.8	10.2	0.035
552	E 256577	+08°1314	6 18.6	+08°21'	170.1	- 0.8	298.5	0.035	148	87	B2 IV: p (e)	9.48	+0.13	-0.75	1.11	8.37	-2.9	11.3	0.032
553	44811	+19°1335	6 18.8	+19°45'	160.1	+ 4.7	298.1	0.035	172	110	O7.5 V	8.42	+0.13	-0.80	1.35	7.07	-5.1	12.2	0.026
554	44965	+11°1162	6 19.6	+11°45'	167.2	+ 1.1	298.4	0.010	7	125	B3 II	7.82	+0.31	-0.44	1.53	6.29	-4.6	10.9	0.006
555	45166	+08°1332	6 20.8	+08°03'	170.7	- 0.4	298.4	0.018	162	100	B pe*	9.88	-0.07	-0.76					
556	45314	+14°1296	6 21.6	+14°57'	164.7	+ 3.0	298.2	0.031	170	108	O9 ? pe	6.64	+0.15	-0.88	1.38	5.26	-4.6	9.9	0.022
557	E 257971	+11°1191	6.23.1	+11°22'	168.0	+ 1.7	298.3	< .004			B0.5 III	8.90	+0.06	-0.79	1.02	7.88	-4.7	12.6	
558	45626	-04°1534	6 23.4	-04°23'	181.9	- 5.7	297.7	0.044	157	95	B7 pe shell	9.36	+0.05	-0.48	0.51	8.85			0.086
559	45910	+05°1267	6 25.2	+05°57'	173.0	- 0.5	298.2	0.017	2	120	B2: III: pe shell	6.77	+0.32	-0.68	1.68	5.09	-3.6	8.7	0.010
560	45995	+11°1204	6 25.6	+11°19'	168.3	+ 2.2	298.1	0.024	138	76	B2 V: nne	6.15	-0.08	-0.87	0.48	5.67	-2.0	7.7	0.050

TABLE 5—Continued

No.	HD	BD	1900 α	1900 δ	l	b	φ	p	θ	θ'	Spectrum	V	B-V	U-B	$3E_{(B-V)}$	m	M	m-M	p/A_V
561	46056	+04°1291	6h 26.0m	+04°54'	174.0	- 0.8	298.2	0.025	154	92	O8	8.15	+0.19	-0.74	1.50	6.65	-5.1	11.8	0.017
562	46149	+05°1282	6 26.6	+05°06'	173.9	- 0.6	298.2	< .004			O8	7.61	+0.19	-0.77	1.50	6.11	-5.1	11.2	
563	46150	+05°1283	6 26.6	+05°00'	174.0	- 0.6	298.2	0.016	7	125	O6	6.76	+0.13	-0.82	1.35	5.41	-5.1	10.5	0.012
564	E 259135	+04°1299	6 26.7	+04°55'	174.1	- 0.6	298.2	0.031	153	91	B1: V: n	8.57	+0.18	-0.70	1.32	7.25	-3.1	10.4	0.023
565	46223	+04°1302	6 27.0	+04°53'	174.2	- 0.6	298.2	0.030	169	107	O5	7.28	+0.22	-0.77	1.62	5.66	-5.1	10.8	0.018
566*			6 27.0	+03°38'	175.3	- 1.2	298.2	0.053	18	136		11.14	+0.82	-0.10					0.013
567	E 259431	+10°1172	6 27.6	+10°24'	169.4	+ 2.2	298.1	0.017	106	44	B6 pe	8.74	+0.28	-0.54	1.26	7.48			0.034
568	E 259440	+05°1291	6 27.6	+05°52'	173.4	+ 0.0	298.2	0.088	164	102	B0: pe	9.17	+0.55	-0.55	2.55	6.62			0.024
569	E 259597	+08°1388	6 28.1	+08°24'	171.2	+ 1.3	298.1	0.030	75	13	B0. 5: V: nne*	8.57	+0.14	-0.72	1.26	7.31	-3.6	10.9	0.024
570		+00°1472	6 28.1	+00°46'	177.9	- 2.3	298.1	0.017	148	86	B2 Ib	9.15	+0.70	-0.25	2.82	6.33	-5.8	12.1	0.006
571	46484	+04°1319	6 28.6	+04°44'	174.5	- 0.3	298.1	0.030	166	104	B1 V	7.74	+0.36	-0.61	1.86	5.88	-3.1	9.0	0.016
572	46485	+04°1318	6 28.6	+04°36'	174.6	- 0.4	298.1	0.039	157	95	O8	8.27	+0.33	-0.68	1.92	6.35	-5.1	11.4	0.020
573*			6 28.9	+11°14'	168.8	+ 2.8	298.0	0.050	161	99	B3 III	10.53	+0.58	-0.13	2.34	8.19	-3.3	11.5	0.021
574	46559	+02°1292	6 29.0	+02°28'	176.5	- 1.3	298.1	0.033	143	81	B8 I	8.15	+0.61	+0.03	2.10	6.05	-6.5	12.6	0.016
575	46573	+02°1295	6 29.1	+02°36'	176.4	- 1.2	298.1	0.022	154	92	O7	7.95	+0.33	-0.66	1.95	6.00	-5.1	11.1	0.011
576	E 259954	+08°1399	6 29.2	+08°26'	171.3	+ 1.6	298.1	0.014	145	83	B2 IV	9.21	+0.06	-0.64	0.90	8.31	-2.9	11.2	0.016
577	46660	+11°1232	6 29.5	+11°12'	168.9	+ 3.0	298.0	0.038	13	131	B1 V	8.04	+0.31	-0.61	1.71	6.33	-3.1	9.4	0.022
578	46711	+02°1299	6 29.8	+02°51'	176.3	- 0.9	298.1	0.064	37	156	B3 II	9.10	+0.87	+0.01	3.21	5.89	-4.6	10.5	0.020
579	46783	+09°1295	6 30.2	+09°56'	170.1	+ 2.5	298.0	0.027	5	123	B9 Ib	8.06	+0.31	-0.08	1.11	6.95	-5.6	12.6	0.024
580	46847	+02°1302	6 30.5	+02°47'	176.4	- 0.8	298.1	0.042	22	140	B0 III: p	8.96	+0.67	-0.37	2.91	6.05	-5.0	11.0	0.014
581	46867	+05°1315	6 30.6	+05°24'	174.1	+ 0.5	298.1	0.044	156	94	B0. 5 V	8.30	+0.22	-0.64	1.50	6.80	-3.6	10.4	0.029
582	46966	+06°1303	6 31.1	+06°10'	173.5	+ 0.9	298.1	0.011	136	74	O8	6.88	-0.04	-0.93	0.81	6.07	-5.1	11.2	0.014
583	47032	+04°1341	6 31.5	+04°46'	174.9	+ 0.4	298.1	0.038	161	99	B0 III	8.83	+0.45	-0.57	2.25	6.58	-5.0	11.6	0.017
584	47129	+06°1309	6 32.0	+06°13'	173.6	+ 1.2	298.1	0.022	144	82	O8	6.08	+0.06	-0.89	1.11	6.97	-5.1	12.1	0.020
585	47240	+05°1334	6 32.5	+05°03'	174.7	+ 0.7	298.0	0.023	173	111	B1 Ib	6.15	+0.14	-0.73	1.20	4.95	-5.8	10.8	0.019
586	E 261021	+03°1329	6 32.6	+03°42'	175.9	+ 0.1	298.1	0.020	169	107	B2 III	9.48	+0.66	-0.33	2.70	6.78	-3.6	10.4	0.007
587*			6 32.9	+02°28'	177.0	- 0.4	298.0	0.038	13	131	B1 V	10.68	+0.37	-0.40	1.89	8.79	-3.1	11.9	0.020
588	47360	+04°1360	6 33.1	+04°43'	175.0	+ 0.7	298.0	0.008	165	103	B0. 5 V	8.19	+0.13	-0.69	1.23	6.96	-3.6	10.6	0.006
589	47382	+04°1361	6 33.2	+04°42'	175.1	+ 0.7	298.0	0.017	153	91	B0 III	7.14	+0.17	-0.76	1.41	5.73	-5.0	10.7	0.012
590	47417	+07°1386	6 33.4	+07°00'	173.0	+ 1.8	298.0	0.005	91	29	B0 IV	6.97	+0.01	-0.86	0.93	6.04	-4.6	10.6	0.005
591*			6 33.9	+03°44'	176.0	+ 0.4	298.1	0.044	17	135	B2 V	10.70	+0.59	-0.33	2.49	8.21	-2.0	10.2	0.018
592	47761	-04°1607	6 35.1	-04°36'	183.5	- 3.2	297.9	0.048	169	107	B2 V: pe	8.63	+0.17	-0.62	1.23	7.40	-2.0	9.4	0.039
593		-00°1385	6 35.2	-00°16'	179.7	- 1.2	298.0	0.061	151	89	O8	9.87	+0.31	-0.67	1.86	8.01	-5.1	13.1	0.033
594	47887	+09°1344	6 35.7	+09°34'	171.0	+ 3.5	297.8	< .004			B2 III:	7.14	-0.18	-0.95	0.18	6.96	-3.6	10.6	
595	48099	+06°1351	6 36.6	+06°27'	173.9	+ 2.3	297.9	< .004			O6	6.38	-0.05	-0.95	0.81	5.57	-5.1	10.7	

TABLE 5—Continued

No.	HD	BD	1900 α	1900 δ	l	b	φ	p	θ	θ'	Spectrum	V	B-V	U-B	$3E_{(B-V)}$	m	M	m-M	p/A_V
			h m																
596	48279	+01°1472	6 37.5	+01°49'	178.1	+ 0.3	289.0	0.029	155	93	O8	7.97	+0.11	-0.81	1.26	6.71	-5.1	11.8	0.023
597	48282	-10°1651	6 37.5	-10°24'	188.9	- 5.4	297.5	0.018	169	107	B3 III	8.85	+0.30	-0.38	1.50	7.35	-3.3	10.6	0.012
598	48663	+12°1267	6 39.4	+12°21'	169.0	+ 5.7	297.5	0.031	2	119	B1 V	8.59	-0.01	-0.73	0.75	7.84	-3.1	10.9	0.041
599		+00°1576	6 39.7	+00°43'	179.3	+ 0.3	298.0	0.050	146	84	O9 III:	9.26	+0.43	-0.59	2.22	7.04	-6.4	13.4	0.022
600*			6 40.0	+02°12'	178.1	+ 1.0	298.0	0.032	164	102	B1 V	10.45	+0.18	-0.57	1.32	9.13	-3.1	12.2	0.024
601	49330	+00°1607	6 42.8	+00°53'	179.6	+ 1.0	298.0	0.037	133	71	B0: pnne	8.88	+0.26	-0.69	1.68	7.20			0.022
602	49585	+00°1624	6 44.0	+00°12'	180.3	+ 1.0	298.0	0.027	180	118	B0. 5: (V) nn	9.12	+0.10	-0.71	1.14	7.98	-3.6	11.6	0.024
603	49992	-05°1827	6 46.0	-05°13'	185.3	- 1.1	298.0	0.027	89	27	B1: pne	9.02	+0.11	-0.86	1.11	7.91			0.024
604	50064	+00°1651	6 46.4	+00°25'	180.4	+ 1.6	298.0	0.048	150	88	B6: Ia	8.21	+0.77	-0.26	2.73	5.48	-6.9	12.4	0.018
605		+01°1560	6 46.7	+10°30'	179.5	+ 2.2	298.0	0.013	89	27	O8:	9.66	+0.28	-0.68	1.77	7.89	-5.1	13.0	0.007
606	50696	+00°1691	6 49.2	+00°18'	180.8	+ 2.2	298.0	0.005	139	77	B1: (V) nne	8.91	-0.01	-0.83	0.75	8.16	-3.1	11.3	0.007
607		-01°1471	6 51.9	-01°37'	182.8	+ 1.9	298.1	0.076	155	94	B0. 5 III	9.92	+0.46	-0.49	2.22	7.70	-4.7	12.4	0.034
608	51756	-02°1856	6 53.5	-02°53'	184.1	+ 1.6	298.1	< .003			B0. 5 IV	7.23	-0.07	-0.91	0.63	6.60	-4.2	10.8	
609	52244	-16°1694	6 55.3	-16°03'	195.9	- 4.2	298.0	0.015	13	131	B2: III: pne	9.16	+0.31	-0.58	1.65	7.51	-3.6	11.1	0.009
610	52266	-05°1912	6 55.4	-05°40'	186.8	+ 0.7	298.2	0.012	141	79	O9 V	7.23	-0.01	-0.90	0.90	6.33	-4.6	10.9	0.013
611		+00°1769	6 57.3	+00°38'	181.5	+ 4.1	298.0	0.011	133	71	B3 III	9.35	+0.14	-0.62	1.02	8.33	-3.3	11.6	0.011
612	53032	-02°1898	6 58.4	-02°36'	184.5	+ 2.8	298.2	< .003			B6: (IV:)	9.32	+0.06	-0.50	0.60	8.72			
613	53367	-10°1848	6 59.7	-10°18'	191.4	- 0.5	298.4	0.011	27	145	B0 IV: e	6.97	+0.44	-0.59	2.22	4.75	-4.6	9.4	0.005
614	53428	-08°1729	6 59.9	-08°42'	190.0	+ 0.3	298.4	0.015	117	55	B2 Ib	8.35	+0.31	-0.56	1.65	6.70	-5.8	12.5	0.009
615	53649	-08°1733	7 00.7	-08°52'	190.2	+ 0.4	298.4	0.021	127	66	B0. 5 III	9.12	+0.25	-0.66	1.59	7.53	-4.7	12.2	0.013
616	53667	-08°1734	7 00.8	-08°34'	190.0	+ 0.5	298.4	0.025	127	65	B0. 5 III	7.75	+0.24	-0.71	1.56	6.19	-4.7	10.9	0.016
617	53754	-08°1737	7 01.1	-08°39'	190.1	+ 0.6	298.5	0.029	129	68	B1 II	8.16	+0.21	-0.66	1.41	6.75	-4.9	11.6	0.020
618	53756	-12°1777	7 01.1	-12°40'	193.6	- 1.4	298.4	0.005	123	61	B2 IV	7.32	-0.08	-0.78	0.48	6.84	-2.9	9.7	0.010
619	54439	-11°1812	7 03.7	-11°42'	193.1	- 0.3	298.6	0.018	136	74	B2 III n	7.71	+0.04	-0.77	0.84	6.87	-3.6	10.5	0.021
620	54464	-03°1762	7 03.8	-03°54'	186.3	+ 3.4	298.4	< .003			B2: (V) pe	8.32	-0.01	-0.63	0.69	7.63	-2.0	9.6	
621		-00°1618	7 05.9	-00°52'	183.6	+ 4.9	298.2	< .002			B1 V: ne	9.63	-0.05	-0.78	0.63	9.00	-3.1	12.1	
622	54786	-15°1672	7 05.1	-15°56'	197.0	- 2.1	298.6	0.017	116	55	B0: pe	8.98	+0.23	-0.87	1.59	7.39			0.011
623	54911	-15°1681	7 05.6	-15°31'	196.7	- 1.8	298.6	< .003			B2 II	7.32	-0.08	-0.82	0.48	6.84	-4.7	11.5	
624	55606	-01°1603	7 08.5	-01°54'	185.0	+ 5.4	298.4	0.012	60	178	B1: V: pnne	9.11	-0.04	-0.79	0.66	8.45	-3.1	11.6	0.018
625	56847	-15°1748	7 13.6	-15°27'	197.5	0.0	299.1	0.015	97	36	B7 Ib? shell?	8.91	+0.19	-0.47	0.93	7.98	-5.6	13.6	0.016
626	57386	-08°1856	7 15.9	-08°15'	191.5	+ 4.0	299.1	0.012	141	80	B1. 5: V: pnne	8.03	-0.02	-0.76	0.69	7.34	-2.6	9.9	0.017
627	57393	-23°5296	7 15.9	-23°55'	205.2	- 3.7	299.1	0.006	94	33	B pe	9.09	-0.01	-0.77					
628	59075	-18°1847	7 23.2	-18°17'	201.1	+ 0.5	299.9	0.024	3	123	B8 I:	7.65	+0.34	-0.27	1.29	6.36	-6.5	12.9	0.019
629	59094	-15°1837	7 23.3	-15°53'	199.1	+ 1.8	299.8	0.011	118	58	B2 V: nne	8.44	+0.15	-0.70	1.17	7.80	-2.0	9.8	0.009
630	60196	-28°4485	7 28.2	-28°31'	210.6	- 3.6	300.1	0.004	110	50	B0. 5 III	8.97	+0.02	-0.86	0.90	9.07	-4.7	13.8	0.004

TABLE 5—Continued

No.	HD	BD	1900 α	1900 δ	l	b	φ	p	θ	θ'	Spectrum	V	B-V	U-B	$3E_{(B-V)}$	m	M	m-M	p/A_V
630	60196	-28 4469																	
631	60284	-27°4205	7h28m.6	-27°39'	209.9	- 3.0	300.2	0.018	108	49	B1: II:	9.09	+0.15	-0.79	1.23	7.86	-4.9	12.8	0.015
632	60308	-15°1892	7 28.7	-15°14'	199.2	+ 3.2	300.2	0.028	149	89	B2 Iab	8.20	+0.42	-0.49	1.98	6.22	-6.5	12.7	0.014
633	60479	-27°4229	7 29.5	-27°45'	210.1	- 2.9	300.3	< .003			B0: II:	8.41	+0.34	-0.66	1.92	6.49	-5.4	11.9	
634	61347	-13°2143	7 33.7	-13°38'	198.4	+ 5.1	300.4	0.043	33	154	O9 Ib	8.43	+0.17	-0.76	1.44	6.99	-6.9	13.9	0.030
635	62532	-17°2120	7 39.3	-17°42'	202.6	+ 4.2	301.2	0.010	127	68	B1: V: pnne	8.41	+0.08	-0.68	1.02	7.39	-3.1	10.5	0.010
636		-29°4849	7 40.0	-29°05'	212.4	- 1.6	301.4	0.007	17	139	O9.5 II	10.00	+0.22	-0.72	1.56	8.44	-6.2	14.6	0.004
637	63005	-26°4925	7 41.6	-26°15'	210.2	+ 0.2	301.7	0.007	143	85	O7	9.11	-0.02	-0.95	0.90	8.21	-5.1	13.3	0.008
638	63290	-27°4533	7 43.0	-27°41'	211.5	- 0.3	301.8	0.061	130	72	B2 Iab	9.26	+0.50	-0.43	2.22	7.04	-6.5	13.5	0.027
639	63359	-26°4982	7 43.4	-26°27'	210.5	+ 0.4	301.9	0.008	25	147	B pe	9.48	+0.04	-0.88					
640	63964	-28°4950	7 46.4	-28°48'	212.9	- 0.3	302.2	0.028	124	66		8.18	+0.82	+0.49					
641	64315	-26°5115	7 48.2	-26°10'	210.9	+ 1.5	302.4	0.066	114	56	O6: nn (e)	9.21	+0.22	-0.74	1.62	7.59	-5.1	12.7	0.041
642	64399	-24°6101	7 48.6	-24°51'	209.8	+ 2.2	302.4	0.005	119	61	B5 II:	8.29	+0.01	-0.71	0.51	7.78	-4.6	12.4	0.010
643	147889	-24°12684	16 19.4	-24°14'	320.8	+15.7	48.6	0.069	179	48	B2 V	7.92	+0.86	-0.15	3.30	4.62	-2.0	6.6	0.021
644		-33°12155	17 25.7	-33°16'	322.5	- 1.3	56.8	0.054	180	57	B0 III	9.09	+0.79	-0.28	3.27	5.82	-5.0	10.8	0.016
645		-33°12242	17 29.6	-33°49'	322.4	- 2.3	57.4	0.118	52	109	B1 Ia	9.36	+1.16	+0.03	4.26	5.10	-6.9	12.0	0.028
646		-29°13809	17 31.7	-29°03'	326.7	- 0.1	57.6	0.098	158	35	O9 V	9.74	+0.68	-0.34	2.97	6.77	-4.6	11.4	0.033
647	159864	-17°4864	17 31.8	-17°46'	336.3	+ 5.9	58.1	0.036	60	118	B0.5 II	8.59	+0.24	-0.72	1.56	7.03	-5.2	12.2	0.023
648	160186	-18°4598	17 33.4	-18°21'	336.0	+ 5.3	58.2	0.043	61	119	B0.5 V	9.05	+0.19	-0.73	1.41	7.64	-3.6	11.2	0.030
649	160529	-33°12361	17 35.3	-33°27'	323.4	- 3.1	58.1	0.150	20	78	A2 Ia+	6.67	+1.28	+0.35	3.66	3.01			0.041
650	160704	-23°13515	17 36.3	-23°41'	331.8	+ 1.9	58.2	0.086	7	65		9.29	+0.72	-0.30	3.00	6.29	-4.7	11.0	0.029
651	160730	-24°13435	17 36.4	-24°15'	331.3	+ 1.6	58.2	0.078	2	60	O8	9.68	+0.66	-0.40	2.91	6.77	-5.1	11.9	0.027
652*			17 36.9	-28°37'	327.7	- 0.8	58.2	0.131	178	57	B1 nn (II-III)	10.56	+0.81	-0.20	3.21	7.35	-4.6	12.0	0.041
653	161061	-28°13519	17 38.3	-28°08'	328.2	- 0.8	58.3	0.131	173	52	B2 III	8.47	+0.77	-0.31	3.03	5.44	-3.6	9.0	0.043
654	161103	-27°11872	17 38.5	-27°12'	329.0	- 0.4	58.4	0.109	172	50	B2: pe (III-V)?	(8.69)	+0.44	-0.69	2.04	6.65	-2.9	9.6	0.053
655*			17 38.8	-29°53'	326.8	- 1.8	58.4	0.105	158	35	B0.5 Ib	10.75	+1.10	+0.02	4.14	6.61	-5.8	12.4	0.025
656	316204		17 39.0	-28°22'	328.1	- 1.1	58.4	0.087	168	46	B2 III	9.29	+0.32	-0.52	1.68	7.61	-3.6	11.2	0.052
657	316232		17 39.4	-29°11'	327.5	- 1.6	58.5	0.110	4	63	O9 IV	10.30	+0.68	-0.37	2.97	7.33	-5.4	12.7	0.037
658	161291	-27°11899	17 39.6	-27°11'	329.2	- 0.6	58.5	0.144	180	58	B1 Iab	8.89	+0.75	-0.25	3.03	5.86	-6.5	12.4	0.048
659	316332		17 41.1	-29°36'	327.3	- 2.1	58.7	0.040	16	75	B3 Ia	9.47	+1.38	+0.31	4.74	4.73	-6.9	11.6	0.008
660	316311		17 41.2	-28°55'	327.9	- 1.8	58.7	0.059	172	51	B1 Ib	10.24	+0.92	-0.14	3.54	6.70	-5.8	12.5	0.017
661*			17 41.2	-29°23'	327.5	- 2.0	58.7	0.072	13	72	B0 n III?	11.06	+0.70	-0.34	3.00	8.06	-5.0	13.1	0.024
662*			17 41.5	-29°30'	327.4	- 2.1	58.8	0.065	25	84	B1 Ib-II	10.87	+0.89	-0.11	3.45	7.42	-5.4	12.8	0.019
663	316326		17 41.7	-29°17'	327.6	- 2.1	58.8	0.066	6	64	B1 II	10.08	+0.62	-0.32	2.64	7.44	-4.9	12.3	0.025
664	316274		17 42.0	-27°43'	329.0	- 1.3	58.8	0.040	4	63	B2 II	10.41	+0.72	-0.14	2.88	7.53	-4.7	12.2	0.014
665	316325		17 42.0	-29°18'	327.7	- 2.1	58.8	0.069	3	61	B1 IV	10.60	+0.62	-0.29	2.64	7.96	-3.8	11.8	0.026

TABLE 5—Continued

No.	HD	BD	1900 α	1900 δ	l	b	φ	p	θ	θ'	Spectrum	V	B-V	U-B	3E(B-V)	m	M	m-M	p/A$_v$
			h m																
666	316341		17 42.2	-29°56'	327.1	- 2.5	58.9	0.049	180	58	B0. 5 V (pe)?	9.74	+0.42	-0.50	2.10	7.64	-3.6	11.2	0.023
667	316393		17 44.0	-28°28'	328.6	- 2.1	59.0	0.048	0	59	B3 II-III	10.71	+0.39	-0.38	1.77	8.94	-4.0	12.9	0.027
668*			17 44.0	-30°08'	327.2	- 2.9	59.1	0.034	169	48	B3 IV	11.31	+0.56	-0.13	2.28	9.03	-2.5	11.5	0.015
669	162168	-32°13411	17 44.5	-32°58'	324.8	- 4.5	59.3	0.050	161	40	B0 II	8.43	+0.62	-0.35	2.76	5.67	-5.4	11.1	0.018
670	316436		17 44.8	-30°08'	327.3	- 3.1	59.2	0.046	7	66	B3: pe (III-V)?	10.22	+0.59	-0.18	2.37	7.85	-2.5	10.4	0.019
671	316464		17 44.8	-30°37'	326.9	- 3.3	59.2	0.057	164	43	B1 V (e)?	10.59	+0.50	-0.44	2.28	8.31	-3.1	11.4	0.025
672	316409		17 45.1	-28°54'	328.3	- 2.5	59.2	0.062	179	58	B1 V	10.56	+0.46	-0.30	2.16	8.40	-3.1	11.5	0.029
673*			17 45.2	-29°54'	327.5	- 3.0	59.2	0.054	11	71	B8 IV?	11.60	+0.41	-0.02	1.50	10.10			0.036
674	316406		17 45.4	-28°46'	328.5	- 2.5	59.2	0.055	0	59	B2 IV	10.51	+0.26	-0.46	1.50	9.01	-2.9	11.9	0.037
675*			17 45.6	-28°07'	329.1	- 2.2	59.2	0.102	19	78	B1 Ib-II	11.07	+0.77	-0.23	3.09	7.98	-5.4	13.4	0.033
676	316520		17 45.7	-28°45'	328.6	- 2.5	59.2	0.051	1	60	B5: nn (e) (III-V)	10.79	+0.33	-0.28	1.47	9.32	-1.8	11.1	0.035
677	316587		17 45.8	-29°55'	327.6	- 3.2	59.3	0.011	155	35	B1: n (e) (V)	10.58	+0.33	-0.49	1.77	8.81	-3.1	11.9	0.006
678	316589		17 45.9	-30°02'	327.4	- 3.2	59.3	0.026	19	78	B2 nn (e) (III-V)	10.57	+0.31	-0.48	1.65	8.92	-2.9	11.8	0.016
679	162717	-24°13584	17 47.3	-24°15'	332.6	- 0.5	59.3	0.067	179	58	B2 III	9.35	+0.50	-0.38	2.22	7.13	-3.6	10.7	0.030
680	162718	-24°13585	17 47.3	-24°45'	332.2	- 0.8	59.3	0.077	7	66	B pe	8.73	+0.65	-0.44					
681	316569		17 48.1	-29°47'	327.9	- 3.5	59.5	0.027	12	71	B3 II	9.37	+0.30	-0.49	1.50	7.87	-4.6	12.5	0.018
682	316568		17 48.3	-29°43'	328.0	- 3.5	59.6	0.033	12	71	B2 pe (IV-V)	9.76	+0.25	-0.62	1.47	8.29	-2.4	10.7	0.022
683	162978	-24°13615	17 48.7	-24°52'	332.2	- 1.1	59.4	0.027	179	58	O8	6.20	+0.04	-0.89	1.05	5.15	-5.1	10.2	0.026
684	163065	-30°14934	17 49.1	-30°32'	327.4	- 4.1	59.7	0.039	43	102	B1 Iab	8.63	+0.37	-0.54	1.89	6.74	-6.5	13.2	0.021
685	316729		17 51.0	-29°34'	328.5	- 3.9	59.9	0.031	16	76	B1 n II:	9.94	+0.33	-0.59	1.77	8.17	-4.9	13.1	0.018
686	163453	-28°13895	17 51.1	-28°14'	329.6	- 3.3	59.8	0.041	16	75	B0. 5: pe (V)?	9.28	+0.65	-0.47	2.79	6.49	-3.6	10.1	0.015
687	163454	-30°14987	17 51.1	-31°00'	327.2	- 4.7	60.0	0.031	53	113	B0. 5: pe (V)?	8.24	+0.30	-0.72	1.74	6.50	-3.6	10.1	0.018
688	163667	-31°14893	17 52.2	-31°47'	326.6	- 5.3	60.2	0.027	18	78	B0. 5 III	8.76	+0.42	-0.53	2.10	6.66	-4.7	11.4	0.013
689	163777	-25°12523	17 52.8	-25°10'	332.4	- 2.1	59.9	0.019	163	43	B1 II	9.31	+0.44	-0.50	2.10	7.21	-4.9	12.1	0.009
690	316786		17 53.0	-27°15'	330.7	- 3.2	60.0	0.037	178	58	B5 IV	11.01	+0.31	-0.22	1.41	9.60	-1.8	11.4	0.026
691	164018	-23°13741	17 54.0	-23°07'	334.4	- 1.3	59.9	0.029	132	12	B0. 5 III	9.18	+0.65	-0.28	2.79	6.39	-4.7	11.1	0.010
692	164019	-28°13994	17 54.0	-28°36'	329.6	- 4.0	60.2	0.049	177	57	B0 Ia	9.31	+0.26	-0.71	1.68	7.63	-6.9	14.5	0.029
693	164032	-29°14322	17 54.1	-29°49'	328.6	- 4.7	60.3	0.013	29	90	B1 Ib	7.48	+0.14	-0.73	1.20	6.28	-5.8	12.1	0.011
694	164103	-14°4842	17 54.5	-14°47'	341.6	+ 2.8	60.1	0.014	38	98	B5 IV	8.12	+0.10	-0.45	0.78	7.34	-1.8	9.1	0.018
695	164188	-15°4767	17 54.9	-15°48'	340.8	+ 2.3	60.1	0.007	71	131	B0. 5 IV	8.70	+0.19	-0.71	1.41	7.29	-4.2	11.5	0.005
696	164384	-23°13789	17 55.7	-23°10'	334.5	- 1.7	60.1	< .004			B1. 5: V: nn	8.27	-0.03	-0.78	0.66	7.61	-2.6	10.2	
697	164438	-19°4800	17 56.0	-19°06'	338.1	+ 0.3	60.1	0.028	73	133	O9 IV	7.48	+0.34	-0.66	1.95	5.53	-5.4	10.9	0.014
698	164492	-23°13804	17 56.3	-23°01'	334.7	- 1.7	60.2	< .004			O7	7.63	-0.00	-0.86	0.96	6.67	-5.1	11.8	
699	164883	-22°4541	17 58.2	-22°30'	335.4	- 1.8	60.3	0.013	114	175	B0 V	7.28	+0.01	-0.83	0.93	6.35	-4.1	10.4	0.014
700		-22°4543	17 58.2	-22°29'	335.4	- 1.8	60.3	0.006	130	11	B1 V: n	8.87	+0.01	-0.76	0.81	8.06	-3.1	11.2	0.007

TABLE 5—Continued

No.	HD	BD	1900 α	1900 δ	l	b	φ	p	θ	θ'	Spectrum	V	B-V	U-B	$3E_{(B-V)}$	m	M	m-M	p/A_V
			h m																
701	165049	-15°4803	17 59.0	-15°22'	341.7	+ 1.6	60.4	0.015	49	109	B2 III	8.18	+0.37	-0.50	1.83	6.35	-3.6	10.0	0.008
702	165285	-19°4836	18 00.1	-19°58'	337.8	- 0.9	60.4	0.022	63	123	B0.5 V: nne	9.01	+0.31	-0.63	1.77	7.24	-3.6	10.8	0.012
703	165319	-14°4880	18 00.3	-14°12'	342.8	+ 1.9	60.5	0.029	58	119	B0 Ia	7.94	+0.59	-0.50	2.67	5.27	-6.9	12.2	0.011
704		-17°5020	18 00.7	-17°12'	340.3	+ 0.3	60.5	0.027	156	37	B0 III	9.35	+0.62	-0.43	2.76	6.59	-5.0	11.6	0.010
705	165516	-21°4855	18 01.2	-21°27'	336.6	- 1.9	60.6	0.006	146	26	B0.5 Ib	6.29	+0.12	-0.78	1.20	5.09	-5.8	10.9	0.005
706	165783	-19°4858	18 02.6	-19°52'	338.2	- 1.4	60.2	0.019	83	143	B1:V	8.41	+0.28	-0.49	1.62	6.79	-3.1	9.9	0.012
707	166125	-14°4908	18 04.1	-14°12'	343.3	+ 1.1	60.7	0.027	32	93	B3 II-III	9.08	+0.52	-0.31	2.46	6.62	-4.0	10.6	0.011
708	166167	-21°4879	18 04.3	-21°20'	337.1	- 2.5	60.8	0.036	75	136	B9 Ib	8.59	+0.56	+0.12	1.86	6.73	-5.6	12.3	0.019
709	166286	-16°4736	18 04.8	-16°46'	341.1	- 0.4	60.8	0.020	11	72	B1 II	8.46	+0.23	-0.63	1.47	6.99	-4.9	11.9	0.014
710		-19°4882	18 04.8	-19°12'	339.0	- 1.5	60.8	0.006	26	87	B1.5 V	9.06	+0.20	-0.53	1.35	7.71	-2.6	10.3	0.004
711	166304	-16°4739	18 04.9	-16°44'	341.2	- 0.4	60.8	0.029	53	114	B1 V	9.33	+0.19	-0.63	1.35	7.98	-3.1	11.1	0.021
712	166443	-20°5020	18 05.5	-20°44'	337.8	- 2.4	61.0	0.028	140	21	B1 V: e	8.74	+0.19	-0.77	1.35	7.39	-3.1	10.5	0.021
713	166524	-18°4826	18 05.9	-18°25'	339.8	- 1.4	60.9	0.011	105	166	B0? V pe	9.94	+0.48	-0.56	2.34	7.60	-4.1	11.7	0.005
714	166539	-15°4854	18 06.0	-15°37'	342.3	- 0.0	60.8	0.028	32	93	B0 IV	8.83	+0.25	-0.75	1.65	7.18	-4.6	11.8	0.017
715		-14°4922	18 06.3	-14°58'	342.9	+ 0.2	60.9	0.125	19	80	O9.5: II:	9.73	+0.85	-0.30	3.45	6.28	-6.2	12.5	0.036
716	166628	-19°4895	18 06.4	-19°28'	339.0	- 2.0	60.9	0.010	155	36	B3 Ia	7.17	+0.59	-0.29	2.37	4.80	-6.9	11.7	0.004
717		-15°4861	18 06.6	-15°36'	342.4	- 0.2	60.9	0.024	50	111	B1 (V) ne	9.21	+0.24	-0.63	1.50	7.71	-3.1	10.8	0.016
718	166734	-10°4625	18 06.9	-10°46'	346.6	+ 2.1	61.0	0.070	65	126	O8 f	8.42	+1.09	-0.12	4.20	4.22			0.017
719		-12°4949	18 08.0	-12°55'	344.9	+ 0.9	61.0	0.027	58	119	B9: IV:	10.78	+0.39	+0.13	1.35	9.43			0.020
720		-20°5043	18 08.1	-20°20'	338.4	- 2.8	61.1	0.075	62	123	O6	9.52	+0.85	-0.20	3.51	6.01	-5.1	11.1	0.021
721	167263	-20°5055	18 09.3	-20°25'	338.4	- 3.0	61.2	< .004			O9 II	5.98	+0.04	-0.88	1.05	4.93	-6.4	11.3	
722	167264	-20°5054	18 09.3	-20°46'	338.2	- 3.2	61.2	< .004			B0 Ia	5.38	+0.07	-0.87	1.11	4.27	-6.9	11.2	
723	167330	-12°4954	18 09.6	-12°34'	345.4	+ 0.7	61.1	0.040	74	135	O9 I-II	8.23	+0.66	-0.45	2.91	5.32	-6.6	11.9	0.014
724	167336	-18°4863	18 09.6	-18°24'	340.3	- 2.1	61.1	0.037	161	42	B0 II	8.71	+0.53	-0.48	2.49	6.22	-5.4	11.6	0.015
725		-20°5060	18 09.7	-20°23'	338.5	- 3.1	61.2	0.019	153	34	B0: IV:: pe	8.84	+0.24	-0.77	1.62	7.22	-4.6	11.8	0.012
726	167451	-13°4897	18 10.2	-13°36'	344.5	+ 0.1	61.1	0.021	37	98	B0.5 Ib	8.23	+0.79	-0.27	3.21	5.02	-5.8	10.8	0.007
727		-14°4957	18 10.4	-14°39'	343.6	- 0.5	61.1	0.054	126	7	B0.5 IV	9.81	+0.51	-0.49	2.37	7.44	-4.2	11.6	0.023
728	167543	-14°4959	18 10.6	-14°40'	343.7	- 0.6	61.1	0.052	122	3	B2 III	8.56	+0.43	-0.53	2.01	6.55	-3.6	10.2	0.026
729		-15°4906	18 11.1	-15°41'	342.8	- 1.2	61.2	0.007	30	91	B1 IV: n	9.46	+0.36	-0.52	1.86	7.60	-3.8	11.4	0.004
730	167659	-19°4944	18 11.1	-19°00'	339.9	- 2.7	61.3	0.034	27	88	O8	7.39	+0.22	-0.74	1.59	5.80	-5.1	10.9	0.021
731		-11°4579	18 11.2	-11°50'	346.2	+ 0.7	61.2	0.061	91	152	Bc: V::*	10.44	+1.08	-0.05	4.14	6.30	-4.1	10.4	0.015
732		-12°4964	18 11.8	-12°21'	345.8	+ 0.3	61.2	0.066	96	157	O8	9.82	+0.91	-0.22	3.66	6.16	-5.1	11.3	0.018
733		-11°4581	18 11.8	-11°47'	346.3	+ 0.6	61.2	0.051	83	144	B1: II:	11.32	+0.93	-0.10	3.57	7.75	-4.9	12.6	0.014
734	167838	-15°4911	18 11.9	-15°28'	343.1	- 1.2	61.2	< .004			B5 Ia	6.73	+0.46	-0.36	1.86	4.87	-6.9	11.8	
735		-12°4970	18 12.1	-12°32'	345.7	+ 0.2	61.2	0.054	88	150	B0.5 Ia	8.78	+1.02	-0.11	3.90	4.88	-6.9	11.8	0.014

TABLE 5—Continued

No.	HD	BD	1900 α	1900 δ	l	b	φ	p	θ	θ'	Spectrum	V	B-V	U-B	$3E_{(B-V)}$	m	M	m-M	p/A_V
736		-19°4955	$18^h 12^m.2$	-19°09'	339.9	- 3.1	61.3	0.061	179	61	B3: Ia:	8.90	+0.96	-0.05	3.48	5.42	-6.9	12.3	0.018
737		-12°4979	18 12.4	-12°17'	345.9	+ 0.2	61.2	0.021	118	180	O7 (f)	10.44	+0.68	-0.32	3.00	7.44			0.007
738		-11°4586	18 12.5	-11°20'	346.8	+ 0.8	61.2	0.062	92	153	O8 (I?)	9.40	+1.00	-0.14	3.93	5.47	-6.9	12.4	0.016
739	167971	-12°4980	18 12.5	-12°17'	346.0	+ 0.2	61.2	0.028	150	31	O8 f	7.50	+0.77	-0.32	3.24	4.26			0.009
740		-12°4982	18 12.6	-12°13'	346.0	+ 0.2	61.2	0.024	95	156	B0 II	9.26	+0.67	-0.42	2.91	6.35	-5.4	11.8	0.008
741		-12°4984	18 12.7	-12°00'	346.2	+ 0.3	61.3	0.050	103	164	O9 V	9.93	+0.83	-0.26	3.42	6.51	-4.6	11.1	0.015
742		-13°4929	18 13.0	-13°48'	344.7	- 0.7	61.3	0.061	78	139	B0 IV	9.85	+0.64	-0.44	2.82	7.03	-4.6	11.6	0.022
743		-13°4928	18 13.0	-13°49'	344.7	- 0.7	61.3	0.060	72	133	B0. 5: V: ne	10.12	+0.49	-0.56	2.31	7.81	-3.6	11.4	0.026
744	168112	-12°4988	18 13.1	-12°08'	346.2	+ 0.1	61.3	0.025	127	8	O6	8.52	+0.69	-0.40	3.03	5.49	-5.1	10.6	0.008
745		-13°4930	18 13.2	-13°52'	344.7	- 0.7	61.3	0.045	77	138	O9. 5 V	9.44	+0.30	-0.70	1.80	7.64	-4.4	12.0	0.025
746		-12°4994	18 13.4	-12°09'	346.2	+ 0.1	61.3	0.034	156	37	O9: II:	9.81	+0.70	-0.39	3.03	6.78	-4.6	11.4	0.011
747		-13°4936	18 13.4	-13°59'	344.6	- 0.8	61.3	0.035	101	162	B1: V: ne	9.71	+0.63	-0.59	2.67	7.04	-3.1	10.1	0.013
748	168206	-11°4593	18 13.5	-11°40'	346.6	+ 0.3	61.3	0.053	92	153	W R	9.14	+0.72	-0.26					
749	168302	-16°4812	18 13.9	-16°03'	342.8	- 1.9	61.4	0.020	76	137	B5 V	9.26	+0.20	-0.36	1.08	8.18	-0.9	9.1	0.018
750		-13°4941	18 14.4	-13°06'	345.4	- 0.4	61.3	0.040	29	90	O9. 5 IV	9.75	+1.08	-0.07	4.14	5.61	-5.0	10.6	0.010
751	168418	-17°5141	18 14.4	-17°02'	342.0	- 2.5	61.4	0.016	14	75	B2 III	9.43	+0.33	-0.43	1.71	7.72	-3.6	11.3	0.009
752		-12°5008	18 14.5	-12°41'	345.8	- 0.4	61.4	0.048	149	30	B0. 5 III	9.81	+1.01	-0.08	3.87	5.94	-4.7	10.6	0.012
753		-12°5009	18 14.7	-12°13'	346.3	- 0.2	61.4	0.015	3	65	O8	9.54	+0.68	-0.42	2.97	6.57	-5.1	11.7	0.005
754	168571	-17°5151	18 15.3	-17°26'	341.8	- 2.9	61.5	0.023	92	154	B1 Ib-II*	7.79	+0.53	-0.40	2.37	5.42	-5.4	10.8	0.010
755	168607	-16°4829	18 15.5	-16°25'	342.7	- 2.4	61.5	0.046	20	81	B9 Ia+p	8.29	+1.60	+0.40	4.98	3.31			0.009
756	168625	-16°4830	18 15.6	-16°25'	342.7	- 2.5	61.5	0.095	13	75	B8 Ia+?	8.41	+1.46	+0.38	4.65	3.76			0.020
757		-20°5108	18 16.4	-20°07'	339.5	- 4.4	61.7	0.032	39	100	B0. 5 II	9.16	+0.53	-0.41	2.43	6.73	-5.2	11.9	0.013
758		-14°5016	18 17.0	-14°42'	344.4	- 1.9	61.5	0.011	85	147	B1 II	9.38	+0.64	-0.39	2.70	6.68	-4.9	11.6	0.004
759	169034	-13°4958	18 17.6	-13°39'	345.4	- 1.6	61.5	0.042	66	128	B5 Ia	8.14	+1.25	+0.20	4.23	3.91	-6.9	10.8	0.010
760*			18 17.6	-13°49'	345.2	- 1.6	61.5	0.061	57	118	W R	12.02	+0.98	+0.54					
761		-11°4620	18 17.9	-11°58'	346.9	- 0.8	61.5	0.032	83	145	O5	10.17	+0.80	-0.31	3.36	6.81	-5.1	11.9	0.010
762		-14°5029	18 18.1	-14°12'	344.9	- 1.9	61.6	0.029	70	131	B1. 5 Ib	9.61	+1.15	-0.02	4.20	5.41	-5.8	11.2	0.007
763		-09°4713	18 18.4	-09°57'	348.7	+ 0.0	61.5	0.012	46	108	B2: V: pne	9.78	+0.45	-0.41	2.07	7.71	-2.0	9.7	0.006
764		-14°5030	18 18.6	-14°13'	345.0	- 2.0	61.6	0.029	3	65	B5 Ia	9.52	+1.03	+0.03	3.57	5.95	-6.9	12.8	0.008
765		-10°4682	18 18.8	-10°52'	347.9	- 0.5	61.6	0.049	72	133	O7	9.63	+0.56	-0.55	2.64	6.99	-5.1	12.1	0.018
766		-14°5037	18 19.4	-14°42'	344.6	- 2.4	61.7	0.065	177	58	B1. 5 Ia (+?)	8.24	+1.39	+0.19	4.92	3.32	-6.9	10.2	0.013
767	169454	-14°5039	18 19.6	-14°02'	345.2	- 2.2	61.7	0.046	12	74	B1 Ia+	6.61	+0.94	-0.18	3.60	3.01			0.013
768	169727	-13°4979	18 21.0	-13°43'	345.7	- 2.3	61.7	0.033	48	110	O6	9.28	+0.80	-0.36	3.36	5.92	-5.1	11.0	0.010
769	169754	-11°4631	18 21.1	-11°25'	347.7	- 1.2	61.7	0.015	44	106	B0. 5 Ia	8.38	+1.06	-0.01	4.02	4.36	-6.9	11.3	0.004
770		-14°5062	18 22.2	-14°46'	344.9	- 3.1	61.8	0.027	75	136	B0. 5: ne (V?)	9.30	+0.48	-0.61	2.28	7.02	-3.6	10.6	0.012

TABLE 5—Continued

No.	HD	BD	1900 α	1900 δ	l	b	φ	p	θ	θ'	Spectrum	V	B-V	U-B	$3E_{(B-V)}$	m	M	m-M	p/A_V
			h m																
771		-09°4742	18 22.9	-09°38'	349.5	- 0.8	61.7	0.017	147	29	B2: V:	10.44	+0.75	-0.24	2.97	7.47	-2.0	9.5	0.006
772	170159	-13°4992	18 22.9	-13°04'	346.5	- 2.4	61.8	0.025	117	179	B0.5 Ib	8.36	+0.59	-0.41	2.61	5.75	-5.8	11.6	0.010
773		-08°4617	18 23.8	-08°38'	350.5	- 0.5	61.7	0.042	138	19	O8.5 (V)	9.36	+0.91	-0.21	3.66	5.70	-5.1	10.8	0.011
774		-12°5083	18 25.8	-12°25'	347.4	- 2.7	61.9	0.017	169	51	B1 Ib	9.47	+0.42	-0.57	2.04	7.43	-5.8	13.2	0.008
775		-11°4667	18 26.8	-11°22'	348.4	- 2.4	61.9	0.050	145	27	B1: V: pe	9.8*	+0.86	-0.12	3.36	6.49	-3.1	9.6	0.015
776	170938	-15°5004	18 26.9	-15°46'	344.5	- 4.5	62.2	0.078	119	1	B1 Ia	7.87	+0.85	-0.25	3.33	4.54	-6.5	11.0	0.023
777		-14°5102	18 27.4	-13°59'	346.2	- 3.8	62.1	< .002			B1 V pe	9.01	+0.20	-0.70	1.38	7.62	-3.1	10.7	
778		-12°5104	18 28.3	-12°20'	347.7	- 3.2	62.0	0.046	148	30	O7	9.55	+0.58	-0.48	2.70	6.85	-5.1	12.0	0.017
779	172252	-12°5132	18 34.1	-11°58'	348.7	- 4.3	62.3	0.100	147	29	B2: npe (V)	9.48	+0.65	-0.36	2.67	6.81	-2.0	8.8	0.037
780	172275	-07°4645	18 34.2	-07°27'	352.7	- 2.2	62.0	0.083	1	63	O6	9.35	+0.77	-0.37	3.27	6.08	-5.1	11.2	0.025
781		-12°5133	18 34.4	-12°31'	348.3	- 4.6	62.3	0.094	148	31	B1 V	10.78	+0.70	-0.23	2.88	7.90	-3.1	11.0	0.033
782	172367	-07°4650	18 34.7	-07°20'	352.9	- 2.3	62.0	0.035	11	73	B0 V	9.50	+0.45	-0.50	2.25	7.25	-4.1	11.4	0.016
783		-13°5056	18 34.7	-13°30'	347.4	- 5.2	62.4	0.106	150	33	B0: V:	9.69	+0.78	-0.19	3.24	6.45	-4.1	10.6	0.033
784	172488	-08°4675	18 35.4	-08°49'	351.7	- 3.1	62.1	0.012	126	8	B0.5 V	7.62	+0.54	-0.40	2.46	5.16	-3.6	8.8	0.005
785		-13°5073	18 35.7	-13°57'	347.2	- 5.6	62.5	0.100	151	33	B1: (IV) pe	10.14	+0.86	-0.28	3.36	6.78	-3.8	10.6	0.030
786	173219	-07°4689	18 39.1	-07°13'	353.5	- 3.2	62.2	0.009	38	100	B1: V: pne	7.80	+0.22	-0.77	1.44	6.36	-3.1	9.5	0.006
787	173438	-04°4575	18 40.2	-04°42'	355.9	- 2.3	62.1	0.057	53	115	B0.5 Ia	8.23	+0.80	-0.26	3.24	4.99	-6.9	11.9	0.018
788		-12°5163	18 41.3	-12°24'	349.2	- 6.1	62.6	0.032	105	168	B9: IV:	9.38	+0.57	+0.25	1.89	7.49			0.017
789		-12°5166	18 41.5	-12°15'	349.3	- 6.0	62.6	0.027	129	12	B0.5 I	9.81	+0.70	-0.37	2.94	6.87	-6.5	13.4	0.009
790	174571	+08°3866	18 46.0	+08°35'	8.3	+ 2.7	62.1	0.066	80	142	B3 V: pe	8.89	+0.56	-0.25	2.28	6.61	-1.5	8.1	0.029
791		-00°3584	18 48.4	-00°41'	0.4	- 2.2	62.0	0.011	42	104	O8	9.98	+0.63	-0.45	2.82	7.16	-5.1	12.3	0.004
792	175514	+09°3928	18 50.6	+09°13'	9.4	+ 2.0	62.0	0.045	106	168	O8: V nn	8.59	+0.59	-0.45	2.70	5.89	-5.1	11.0	0.017
793	175544	+00°4055	18 50.7	+00°08'	1.4	- 2.3	62.0	< .004			B3 V	7.35	+0.10	-0.64	0.90	6.45	-1.5	8.0	
794		+11°3707	18 57.9	+11°07'	11.9	+ 1.3	61.7	0.019	164	46	B1 Ia:	10.57	+1.04	-0.10	3.90	6.67	-6.9	13.6	0.005
795	177284	2°4840	18 58.9	-02°10'	0.3	- 5.2	62.1	0.053	45	107	B0.5 p	8.60	+0.49	-0.51	2.31	6.29			0.023
796		+02°3771	18 59.2	+02°58'	4.8	- 2.9	61.8	0.013	96	158	B0 III	9.21	+0.63	-0.39	2.79	6.42	-5.0	11.4	0.005
797	E 230579	+10°3774	18 59.4	+10°58'	11.9	+ 0.9	61.6	0.040	99	160	B1.5: IV: ne	9.13	+0.53	-0.41	2.34	6.79	-3.4	10.2	0.017
798	177812	+03°3893	19 01.1	+03°06'	5.2	- 3.2	61.7	0.030	65	127	B1 Ib	8.60	+0.63	-0.36	2.67	5.93	-5.8	11.7	0.011
799	178124	+11°3738	19 02.3	+11°17'	12.6	+ 0.5	61.5	0.019	52	113	B1 V nn	9.45	+0.41	-0.36	2.01	7.44	-3.1	10.5	0.009
800	178129	+03°3902	19 02.3	+03°17'	5.5	- 3.4	61.7	0.010	48	110	B3 Ia	7.41	+0.50	-0.35	2.10	5.31	-6.9	12.2	0.005
801		+14°3887	19 17.0	+14°42'	17.3	- 1.0	60.6	0.056	3	63	B ep	9.90	+1.59	+0.37					
802	E 231285	+14°3898	19 18.9	+15°01'	17.8	- 1.3	60.5	0.014	53	114	B0 III	9.50	+0.75	-0.32	3.15	6.35	-5.0	11.4	0.004
803		+22°3687	19 20.5	+22°34'	24.5	+ 2.1	60.4	0.048	0	60	B2 (V) pe*	9.38	+0.63	-0.36	2.61	6.77	-2.0	8.8	0.018
804	183143	+18°4085	19 23.0	+18°05'	20.9	- 0.6	60.2	0.130	179	60	B7 Ia	6.87	+1.24	+0.15	4.08	2.79	-6.9	9.7	0.032
805	E 231564	+12°3927	19 24.8	+12°22'	16.2	- 3.8	60.2	0.060	35	95	B1 Ib	10.24	+0.79	-0.25	3.15	7.09	-5.8	12.9	0.019

TABLE 5—Continued

No.	HD	BD	1900 α	1900 δ	l	b	φ	p	θ	θ'	Spectrum	V	B-V	U-B	$3E_{(B-V)}$	m	M	m-M	p/A_V
			h m																
806	183561	+26°3566	19 25.1	+26°30'	28.5	+ 3.2	60.1	0.024	178	58	B2 III	8.05	+0.17	-0.54	1.23	6.82	-3.6	10.4	0.020
807	184943	+23°3706	19 31.7	+23°38'	26.8	+ 0.4	59.4	0.080	34	93	B9 Ib	8.20	+0.71	-0.06	2.31	5.89	-5.6	11.5	0.035
808		+34°3631	19 33.1	+35°01'	36.7	+ 5.9	59.8	< .003			B2 V	10.16	-0.11	-0.88	0.39	9.77	-2.0	11.8	
809	185418	+16°3928	19 33.9	+17°02'	21.3	- 3.4	59.3	0.015	13	72	B0.5 V	7.45	+0.22	-0.67	1.50	5.95	-3.6	9.6	0.010
810		+25°3912	19 35.7	+25°11'	28.6	+ 0.4	59.0	0.081	33	92	B2.5 V	10.21	+0.70	-0.08	2.76	7.45	-1.8	9.2	0.029
811		+23°3730	19 36.0	+23°47'	27.4	- 0.4	59.0	0.078	22	81	B8 Ib	9.28	+0.99	+0.11	3.24	6.04	-5.6	11.6	0.024
812	185859	+20°4218	19 36.1	+20°15'	24.4	- 2.2	59.0	0.040	8	67	B0.5 Ia	6.49	+0.39	-0.62	2.01	4.48	-6.9	11.4	0.020
813		+28°3434	19 37.3	+28°55'	31.9	+ 2.1	58.9	0.018	46	105	B1 Ib p	8.50	+0.20	-0.71	1.38	7.12	-5.8	12.9	0.013
814		+28°3438	19 38.1	+28°46'	31.9	+ 1.8	58.8	0.009	96	154	B2 IV	8.93	+0.01	-0.70	0.75	8.18	-2.9	11.1	0.012
815		+23°3745	19 38.6	+23°13'	27.2	- 1.2	58.7	0.132	26	85	B0.5 Ib	8.73	+0.66	-0.38	2.82	5.91	-5.8	11.7	0.047
816		+22°3781	19 38.8	+23°02'	27.1	- 1.3	58.7	0.059	10	69	B0 IV	9.75	+0.43	-0.55	2.19	7.56	-4.6	12.2	0.027
817		+23°3747	19 38.9	+23°12'	27.2	- 1.2	58.7	0.066	14	73	B1 III	10.37	+0.61	-0.39	2.61	7.76	-4.4	12.2	0.025
818		+22°3782	19 39.0	+23°03'	27.1	- 1.3	58.7	0.089	8	67	O7	9.34	+0.56	-0.52	2.64	6.70	-5.1	11.8	0.034
819		+25°3941	19 40.3	+25°59'	29.8	- 0.1	58.5	0.005	85	144	B1.5 V	10.41	+0.70	-0.19	2.85	7.56	-2.6	10.2	0.002
820		+23°3759	19 41.0	+23°48'	28.0	- 1.3	58.4	0.062	11	70	B0 II	8.77	+0.77	-0.34	3.21	5.56	-5.4	11.0	0.019
821		+23°3761	19 41.2	+24°04'	28.3	- 1.2	58.4	0.042	28	87	B0 II:	8.83	+0.66	-0.44	2.88	5.95	-5.4	11.4	0.014
822	186745-6	+23°3760	19 41.2	+23°41'	27.9	- 1.4	58.4	0.040	25	83	B8 Ia	7.03	+0.93	+0.05	3.06	3.97	-6.9	10.9	0.013
823		+23°3762	19 41.4	+23°44'	28.0	- 1.4	58.4	0.043	27	86	B0.5 III: nn	9.29	+0.76	-0.29	3.12	6.17	-4.7	10.9	0.014
824		+25°3952	19 41.5	+25°07'	29.2	- 0.7	58.4	0.025	38	96	O8	10.15	+0.63	-0.42	2.82	7.33	-5.1	12.4	0.009
825		+24°3866	19 41.5	+24°52'	28.9	- 0.9	58.4	< .003			O8 f	9.57	+1.18	+0.02	4.47	5.10			
826		+22°3800	19 41.5	+22°57'	27.3	- 1.9	58.4	0.012	19	77	B2 III: n	9.61	+0.33	-0.52	1.71	7.90	-3.6	11.5	0.007
827	186841	+23°3767	19 41.7	+23°50'	28.1	- 1.4	58.4	0.056	27	85	B1 Ia	7.85	+0.79	-0.29	3.15	4.70	-6.9	11.6	0.018
828	186943		19 42.2	+28°01'	31.7	+ 0.7	58.3	0.021	18	76	W N	10.23	+0.27	-0.64					
829	186980	+31°3765	19 42.4	+31°52'	35.0	+ 2.7	58.4	0.017	29	87	O7.5	7.48	+0.08	-0.84	1.20	6.28	-5.1	11.4	0.014
830		+27°3512	19 42.6	+28°00'	31.8	+ 0.6	58.2	0.008	17	75	O7.5	8.77	+0.20	-0.78	1.56	7.21	-5.1	12.3	0.005
831		+24°3881	19 42.8	+24°36'	28.9	- 1.3	58.2	0.021	37	95	O6 f*	9.12	+0.69	-0.43	3.03	6.09			0.007
832		+27°3513	19 42.9	+27°47'	31.6	+ 0.4	58.2	0.025	40	98	A2 Ia	8.31	+0.39	+0.01	0.99	7.32	-6.9	14.2	0.025
833		+34°3707	19 42.9	+34°24'	37.2	+ 3.9	58.4	0.023	67	125	B3: II:	10.59	-0.04	-0.81	0.48	10.11	-3.3	13.4	0.048
834	187282		19 44.1	+17°57'	23.4	- 5.0	58.4	0.026	4	62	W R	10.51							
835		+24°3893	19 44.6	+24°33'	29.1	- 1.6	58.1	0.014	29	87	B1.5 V	9.63	+0.40	-0.48	1.95	7.68	-2.6	10.3	0.007
836		+28°3485	19 44.8	+28°33'	32.5	+ 0.5	58.0	0.027	57	115	B2 V: n	9.40	+0.10	-0.57	1.02	8.38	-2.0	10.4	0.026
837	187459	+33°3602	19 45.0	+33°12'	36.5	+ 2.9	58.1	0.062	33	91	B0.5 Ib	6.44	+0.20	-0.74	1.44	5.00	-5.8	10.8	0.043
838	E 225985	+32°3583	19 45.7	+32°43'	36.1	+ 2.5	58.0	0.011	149	27	B1 V: pe shell	9.08	+0.10	-0.77	1.08	8.00	-3.1	11.1	0.010
839		+29°3772	19 46.7	+29°09'	33.2	+ 0.4	57.7	0.037	59	117	O7 f	10.10	+0.50	-0.53	2.46	7.64			0.015
840		+22°3836	19 46.8	+22°35'	27.7	- 3.1	57.9	0.046	35	93	B1 II	9.20	+0.49	-0.46	2.25	6.95	-4.9	11.8	0.020

TABLE 5—Continued

No.	HD	BD	1900 α	1900 δ	l	b	φ	p	θ	θ'	Spectrum	V	B-V	U-B	3E(B-V)	m	M	m-M	p/A$_V$
841		+29°3774	19h46.8m	+29°09'	33.2	+ 0.4	57.7	0.032	72	130	B2 Ib	9.93	+0.56	-0.36	2.40	7.53	-5.8	13.3	0.013
842		+33°3618	19 47.0	+33°24'	36.8	+ 2.7	57.8	0.071	41	99	B1 Ib	9.87	+0.55	-0.44	2.43	7.44	-5.8	13.2	0.029
843	187851	+27°3534	19 47.0	+27°27'	31.8	- 0.5	57.7	0.024	24	82	B2 V: nn	7.74	+0.13	-0.63	1.11	6.63	-2.0	8.6	0.022
844	187983	+24°3914	19 47.8	+24°44'	29.6	- 2.1	57.7	0.019	159	37	A1 Iab	5.58	+0.71	+0.13	2.04	3.54	-6.5	10.0	0.009
845		+21°3959	19 48.5	+21°59'	27.4	- 3.8	57.7	0.053	41	98	B2 V p(e)	9.85	+0.34	-0.36	1.74	8.11	-2.0	10.1	0.030
846		+22°3847	19 49.4	+22°21'	27.8	- 3.7	57.6	0.046	15	72	B5 III	9.58	+0.23	-0.45	1.17	8.41	-2.8	11.2	0.039
847		+27°3550	19 50.1	+28°04'	32.7	- 0.7	57.4	0.035	64	122	B9 Ia	8.94	+0.98	+0.30	3.12	5.82	-6.9	12.7	0.011
848		+29°3814	19 52.7	+29°43'	34.4	- 0.4	57.0	0.034	33	90	B0 V	10.18	+0.45	-0.51	2.25	7.93	-4.1	12.0	0.015
849	E 226868	+34°3815	19 54.6	+34°56'	39.0	+ 2.1	56.9	0.108	135	12	B0 Ib	8.89	+0.85	-0.24	3.45	5.44	-6.2	11.6	0.031
850		+35°3899	19 55.5	+35°51'	39.9	+ 2.5	56.8	0.047	147	24	B0.5 III	9.12	+0.16	-0.74	1.32	7.80	-4.7	12.5	0.036
851	E 227018	+34°3828	19 56.1	+35°02'	39.2	+ 1.9	56.6	0.048	120	177	O7	8.99	+0.38	-0.62	2.10	6.89	-5.1	12.0	0.023
852	189779	+29°3844	19 56.6	+29°37'	34.8	- 1.1	56.5	0.018	63	120	B2 III	8.22	+0.10	-0.63	1.02	7.20	-3.6	10.8	0.018
853		+29°3842	19 56.6	+30°06'	35.2	- 0.9	56.5	0.034	85	141	B1 V: e?	10.11	+0.49	-0.42	2.25	7.86	-3.1	11.0	0.015
854	190066	+21°4027	19 58.1	+21°52'	28.5	- 5.7	56.8	0.030	33	90	B1 Iab*	6.48	+0.18	-0.75	1.32	5.16	-6.5	11.7	0.023
855	E 227245	+35°3924	19 58.6	+35°24'	39.8	+ 1.7	56.3	0.049	135	11	O7	9.74	+0.62	-0.44	2.82	6.92	-5.1	12.0	0.017
856		+36°3827	19 58.6	+36°49'	41.0	+ 2.5	56.3	0.013	78	134	B0 IV:	10.59	+0.23	-0.69	1.59	9.00	-4.6	13.6	0.008
857		+28°3598	19 59.1	+28°25'	34.1	- 2.3	56.3	0.076	39	96	B0 III: np	9.43	+1.02	-0.05	3.96	5.47	-5.0	10.5	0.019
858		+25°4083	19 59.8	+25°59'	32.2	- 3.7	56.2	0.042	160	37	B1 III	8.94	+0.63	-0.31	2.67	6.27	-4.4	10.7	0.016
859	190467	+36°3841	20 00.0	+36°08'	40.6	+ 1.9	56.1	0.010	153	29	B5 II: n	8.21	+0.17	-0.46	0.99	7.22	-4.6	11.8	0.010
860		+31°3921	20 00.3	+31°52'	37.1	- 0.5	56.0	0.015	40	96	B1 Ib	8.70	+0.46	-0.45	2.16	6.54	-5.8	12.3	0.007
861		+33°3717	20 00.6	+33°25'	38.4	+ 0.3	56.0	0.034	75	131	O7:	10.28	+0.47	-0.54	2.37	7.91	-5.1	13.0	0.014
862	190603	+31°3925	20 00.7	+31°56'	37.2	- 0.6	56.0	0.018	76	132	B1.5 Ia+	5.65	+0.53	-0.46	2.34	3.31			0.008
863	190864	+35°3949	20 01.9	+35°19'	40.1	+ 1.1	55.8	0.020	168	44	O6	7.76	+0.20	-0.78	1.56	6.20	-5.1	11.3	0.013
864	E 227611	+35°3950	20 02.0	+35°37'	40.4	+ 1.3	55.8	0.035	14	69	B0 pe	8.82	+0.35	-0.70	1.95	6.87			0.018
865		+35°3956	20 02.2	+35°28'	40.3	+ 1.2	55.8	0.008	27	83	B0.5 V	8.85	+0.19	-0.62	1.41	7.44	-3.6	11.0	0.006
866	E 227634	+35°3957	20 02.3	+35°29'	40.3	+ 1.1	55.8	0.020	4	60	B0 Ib	7.91	+0.25	-0.66	1.65	6.26	-6.0	12.3	0.012
867*	190967	+34°3871	20 02.4	+35°06'	40.0	+ 0.9	55.8	0.022	104	160	B1 Ib-II	8.04	+0.41	-0.56	2.01	6.03	-5.4	11.4	0.011
868	190991	+39°4033	20 02.5	+39°47'	43.9	+ 3.5	55.9	0.027	100	156	B0 IV p	8.22	+0.14	-0.78	1.32	6.90	-4.6	11.5	0.020
869		+35°3961	20 02.7	+36°02'	40.8	+ 1.4	55.7	0.017	141	17	B3 II	9.68	+0.33	-0.46	1.59	8.09	-4.6	12.7	0.011
870	E 227704	+34°3874	20 02.9	+34°38'	39.7	+ 0.6	55.7	0.032	137	12	B0 III	8.60	+0.34	-0.63	1.92	6.68	-5.0	11.7	0.017
871	E 227757	+35°3967	20 03.5	+36°04'	40.9	+ 1.3	55.6	0.025	101	157	O9.5 V	9.20	+0.18	-0.75	1.44	7.76	-4.4	12.2	0.017
872		+36°3882	20 03.7	+36°16'	41.1	+ 1.3	55.6	0.046	130	6	B1 III:	9.89	+0.38	-0.52	1.92	7.97	-4.4	12.4	0.024
873	191396	+37°3783	20 04.6	+37°50'	42.5	+ 2.1	55.5	0.028	42	97	B0.5 II	8.13	+0.25	-0.66	1.59	6.54	-5.2	11.7	0.018
874	191423	+42°3599	20 04.7	+42°19'	46.2	+ 4.6	55.7	0.018	106	162	O9 V:	8.03	+0.16	-0.77	1.41	6.62	-4.6	11.2	0.013
875	E 227902	+37°3785	20 04.9	+37°13'	42.0	+ 1.7	55.4	0.033	3	59	B1 V	9.25	+0.26	-0.49	1.56	7.69	-3.1	10.8	0.021

TABLE 5—Continued

No.	HD	BD	1900 α	1900 δ	l	b	φ	p	θ	θ'	Spectrum	V	B-V	U-B	$3E_{(B-V)}$	m	M	m-M	p/A_V
876		+40°4032	20h04m.9	+40°57'	45.1	+ 3.8	55.6	0.025	79	135	B2 III	10.44	+0.25	-0.55	1.47	8.97	-3.6	12.6	0.017
877		+35°3986	20 05.1	+35°17'	40.5	+ 0.6	55.4	0.012	64	119	B pe	9.98	+0.57	-0.54					
878	191611	+36°3906	20 05.7	+36°12'	41.3	+ 1.0	55.3	< .004			B0.5 III	8.59	+0.37	-0.60	1.95	6.64	-4.7	11.3	
879	E 228041	+35°3998	20 06.2	+35°12'	40.5	+ 0.3	55.2	0.041	130	6	B0.5 V: e	8.97	+0.36	-0.66	1.92	7.05	-3.6	10.6	0.021
880	E 228052	+36°3914	20 06.3	+36°24'	41.5	+ 1.0	55.2	0.011	115	170	B1 II	8.82	+0.47	-0.48	2.19	6.63	-4.9	11.5	0.005
881	E 228053	+44°3365	20 06.6	+45°06'	48.7	+ 5.9	55.6	0.015	17	73	B0: Ib: p	9.54	+0.64	-0.41	2.82	6.72	-6.2	12.9	0.005
882	E 228101	+37°3804	20 06.9	+37°10'	42.2	+ 1.3	55.1	0.015	163	39	B1 V	8.44	+0.07	-0.65	0.99	7.45	-3.1	10.6	0.015
883	E 228104	+35°4004	20 06.9	+35°35'	40.9	+ 0.5	55.1	0.012	75	130	B1: IV: pe	8.84	+0.28	-0.70	1.62	7.22	-3.8	11.0	0.007
884	191978	+40°4050	20 07.5	+41°04'	45.5	+ 3.5	55.2	< .002			O8	8.02	+0.14	-0.78	1.35	6.67	-5.1	11.8	
885	192103	+35°4013	20 08.1	+35°54'	41.3	+ 0.4	54.9	< .004			W R	8.06	+0.05	-0.41					
886	E 228263	+37°3819	20 08.4	+37°21'	42.6	+ 1.2	54.9	0.012	141	16	B1 V	9.42	+0.16	-0.61	1.26	8.16	-3.1	11.3	0.010
887		+39°4076	20 08.4	+39°42'	44.5	+ 2.5	55.0	0.029	59	114	B pe	9.88	+0.58	-0.52					
888	192281	+39°4082	20 09.0	+39°58'	44.8	+ 2.6	55.0	0.015	9	64	O5 f	7.55	+0.38	-0.61	2.10	5.45			0.007
889	E 228368	+34°3920	20 09.5	+34°43'	40.5	- 0.5	54.7	0.046	174	49	O7	8.39	+0.49	-0.51	2.43	5.96	-5.1	11.1	0.019
890		+40°4061	20 09.5	+40°43'	45.4	+ 3.0	54.8	0.005	147	22	B1 V	10.02	+0.23	-0.68	1.47	8.55	-3.1	11.6	0.003
891	192422	+38°3956	20 09.7	+38°28'	43.6	+ 1.6	54.7	0.034	11	66	B0.5 Ib	7.09	+0.50	-0.47	2.34	4.75	-5.8	10.6	0.014
892		+32°3749	20 09.7	+32°15'	38.5	- 2.0	54.8	0.080	19	74	B0: pe	9.92	+0.86	+0.33	3.48	6.44			0.023
893	E 228452	+34°3929	20 10.2	+35°06'	40.9	- 0.4	54.6	0.075	1	56	B3 V	9.77	+0.66	-0.09	2.58	7.19	-1.5	8.7	0.029
894	192539	+31°4001	20 10.3	+31°41'	38.1	- 2.4	54.7	0.025	177	52	B2 III	7.29	+0.13	-0.63	1.11	6.18	-3.6	9.8	0.022
895	E 228456	+36°3948	20 10.3	+36°30'	42.1	+ 0.4	54.6	0.025	139	13	B2 IV	9.86	+0.25	-0.50	1.47	8.39	-2.9	11.3	0.017
896		+37°3837	20 10.3	+37°56'	43.1	+ 1.2	54.6	0.014	159	34	B2 II:	9.47	+0.40	-0.47	1.92	7.55	-4.7	12.2	0.007
897		+32°3752	20 10.4	+33°08'	39.3	- 1.6	54.6	0.076	76	131	B2 V n	9.88	+0.69	-0.23	2.79	7.09	-2.0	9.1	0.027
898	192641	+36°3956	20 10.8	+36°21'	42.0	+ 0.2	54.5	0.025	168	43	W R	7.93	+0.27	-0.45					
899	192639	+36°3958	20 10.8	+37°03'	42.6	+ 0.6	54.6	.004			O8 f	7.11	+0.35	-0.63	1.98	5.13			
900	192660	+39°4096	20 10.9	+40°01'	45.0	+ 2.3	54.6	0.022	140	15	B0 Ia	7.54	+0.63	-0.36	2.79	4.75	-6.9	11.6	0.008
901		+41°3670	20 11.2	+41°32'	46.3	+ 3.2	54.6	0.038	33	88	B0.5 II	10.20	+0.83	-0.22	3.33	6.87	-5.2	12.1	0.011
902	E 228548	+39°4098	20 11.4	+39°40'	44.8	+ 2.1	54.5	0.018	105	160	B0 pe	10.10	+0.69	-0.39	2.97	7.13			0.006
903	E 228587	+36°3966	20 11.7	+36°19'	42.1	+ 0.1	54.4	0.026	131	5	B1 II	10.07	+0.80	-0.14	3.18	6.89	-4.9	11.8	0.008
904	E 228602	+36°3968	20 11.8	+36°32'	42.3	+ 0.2	54.4	0.010	143	18	B1 III	9.84	+0.57	-0.30	2.49	7.35	-4.4	11.8	0.004
905	192832	+41°3675	20 11.9	+42°06'	46.8	+ 3.4	54.5	0.025	63	118	B5 Ia	8.62	+0.89	-0.02	3.15	5.47	-6.9	12.4	0.008
906		+34°3952	20 12.7	+34°48'	41.0	- 1.0	54.3	0.023	1	55	B3 II	9.96	+0.70	-0.13	2.70	7.26	-4.6	11.9	0.008
907	E 228690	+37°3861	20 12.8	+37°37'	43.3	+ 0.6	54.3	0.015	59	114	B0.5 V:	9.25	+0.27	-0.58	1.65	7.60	-3.6	11.2	0.009
908		+37°3862	20 12.8	+37°20'	43.0	+ 0.5	54.3	0.005	128	2	B0 V:	8.99	+0.38	-0.47	2.04	6.95	-4.1	11.0	0.002
909	193032	+38°3980	20 13.0	+38°35'	44.1	+ 1.2	54.2	0.035	38	92	B0 III	8.32	+0.35	-0.58	1.95	6.37	-5.0	11.4	0.018
910	E 228712	+40°4087	20 13.1	+40°34'	45.7	+ 2.3	54.3	0.034	7	62	B0.5 Ia	8.65	+1.13	+0.06	4.23	4.42	-6.9	11.3	0.008

TABLE 5—Continued

No.	HD	BD	1900 α	1900 δ	l	b	φ	p	θ	θ'	Spectrum	V	B-V	U-B	$3E_{(B-V)}$	m	M	m-M	p/A_V
			h m																
911	193076	+37°3866	20 13.3	+37°22'	43.1	+ 0.4	54.2	0.010	96	150	B0.5 II	7.62	+0.33	-0.57	1.83	5.79	-5.2	11.0	0.005
912	193117	+40°4090	20 13.5	+40°32'	45.7	+ 2.2	54.2	0.033	10	64	O9.5 II	8.70	+0.61	-0.42	2.73	5.97	-6.2	12.2	0.012
913	193182	+39°4115	20 13.8	+39°16'	44.7	+ 1.4	54.1	0.014	134	8	A: shell	6.52	-0.09	-0.18					
914	E 228766	+36°3991	20 13.8	+37°00'	42.9	+ 0.1	54.1	0.025	112	166	(O6 f or W R)	9.14	+0.65	-0.37	2.91	6.23			0.009
915	E 228779	+34°3961	20 14.0	+34°30'	40.9	- 1.4	54.1	0.045	0	54	O9.5 Ib	8.92	+1.31	+0.22	4.83	4.09	-6.6	10.7	0.009
916	193237	+37°3871	20 14.1	+37°43'	43.5	+ 0.5	54.1	0.023	37	91	P Cyg	4.83	+0.42	-0.58					
917		+39°4117	20 14.2	+39°43'	45.1	+ 1.7	54.1	0.017	156	30	B1 II	3.39	+0.87	-0.07	3.39	6.51	-4.9	11.4	0.005
918		+30°3980	20 14.4	+30°30'	37.7	- 3.8	54.2	0.099	13	67	B9 Ib-II	8.28	+0.76	+0.15	2.46	5.82	-5.0	10.8	0.040
919	E 228841	+38°4000	20 14.8	+38°34'	44.3	+ 0.9	54.0	0.028	174	48	O7.5 p	8.93	+0.57	-0.43	2.67	6.26	-5.1	11.4	0.010
920	E 228854	+35°4062	20 15.0	+36°02'	42.3	- 0.7	53.9	0.032	42	96	O8:	8.93	+0.71	-0.28	3.06	5.87	-5.1	11.0	0.010
921	E 228860	+36°4001	20 15.1	+36°39'	42.8	- 0.3	53.9	0.030	102	156	B0.5 IV	9.68	+0.60	-0.32	2.64	7.04	-4.2	11.2	0.011
922		+36°4000	20 15.1	+36°56'	42.9	- 0.2	53.9	0.054	81	135	B0.5 Ia	9.63	+0.81	-0.16	3.27	6.36	-6.9	13.3	0.016
923		+38°4002	20 15.1	+39°06'	44.7	+ 1.2	53.9	0.033	172	46	B1 V	9.22	+0.44	-0.45	2.10	7.12	-3.1	10.2	0.016
924	193443	+37°3879	20 15.2	+37°57'	43.8	+ 0.5	53.9	0.034	56	110	O9 III	7.24	+0.41	-0.54	2.16	5.08	-6.4	11.5	0.016
925		+36°4004	20 15.4	+37°05'	43.2	- 0.1	53.9	0.035	73	127	B0.5 III:	9.63	+0.90	-0.13	3.54	6.09	-4.7	10.8	0.010
926	E 228882	+40°4113	20 15.4	+40°23'	45.8	+ 1.9	53.9	0.039	136	10	B0.5 Ia	9.21	+1.15	+0.12	4.29	4.92	-6.9	11.8	0.009
927	193514	+38°4006	20 15.5	+38°57'	44.7	+ 1.0	53.9	0.030	48	102	O7 f	7.38	+0.45	-0.51	2.31	5.07			0.013
928	193576	+38°4010	20 15.8	+38°25'	44.3	+ 0.6	53.8	0.015	150	24	W R	8.0*	+0.50	-0.39					
929	E 228913	+35°4067	20 15.8	+35°54'	42.2	- 0.9	53.8	0.041	51	105	B0.5 III: nn	9.96	+0.60	-0.35	2.64	7.32	-4.7	12.0	0.016
930	E 228919	+39°4135	20 15.9	+40°08'	45.7	+ 1.6	53.8	0.017	89	143	B1 IV	9.68	+0.63	-0.28	2.67	7.01	-3.8	10.8	0.006
931	E 228928	+40°4117	20 16.0	+40°20'	45.8	+ 1.7	53.8	< .003			B2 Ib: nn	9.69	+0.89	-0.14	3.39	6.30	-5.8	12.1	
932	E 228929	+39°4136	20 16.0	+39°36'	45.3	+ 1.3	53.8	0.058	51	105	B0.5 Ib	9.63	+1.15	+0.07	4.29	5.34	-5.8	11.1	0.014
933	E 228943	+38°4016	20 16.1	+38°17'	44.2	+ 0.5	53.8	0.025	14	68	B0 II:	9.29	+0.91	-0.10	3.63	5.66	-5.4	11.1	0.007
934		+38°4017	20 16.4	+38°39'	44.5	+ 0.7	53.7	0.015	172	46		9.91	+0.41	-0.48					
935	E 228969	+38°4018	20 16.5	+38°21'	44.3	+ 0.5	53.7	0.026	174	48	B2 II:	9.50	+0.73	-0.21	2.91	6.59	-4.7	11.3	0.009
936	E 228989	+38°4025	20 16.7	+38°23'	44.4	+ 0.5	53.7	0.031	170	44	O9 V nn	9.72	+0.77	-0.20	3.24	6.48	-4.6	11.1	0.010
937	E 229033	+37°3898	20 17.2	+37°25'	43.6	- 0.2	53.6	0.019	82	135	B0 II-III	8.77	+0.72	-0.23	3.06	5.71	-5.2	10.9	0.006
938		+36°4022	20 17.3	+36°29'	42.9	- 0.7	53.6	0.057	65	119	O9.5 II	9.94	+0.83	-0.20	3.39	6.55	-6.2	12.8	0.017
939	E 229049	+38°4031	20 17.4	+38°42'	44.7	+ 0.5	53.6	0.033	14	68	B2 III: p	9.62	+0.48	-0.44	2.16	7.46	-3.6	11.1	0.015
940	E 229059	+36°4024	20 17.5	+37°05'	43.4	- 0.4	53.5	0.045	59	112	B1.5 Iap	8.70	+1.53	+0.43	5.34	3.36	-6.9	10.3	0.008
941	193928	+36°4028	20 17.8	+36°36'	43.0	- 0.8	53.5	0.038	68	122	W R	9.78	+0.82	+0.07					
942		+45°3149	20 17.9	+45°44'	50.4	+ 4.6	53.7	0.032	163	37	B1 V	9.45	+0.32	-0.49	1.74	7.71	-3.1	10.8	0.018
943		+38°4036	20 18.2	+38°18'	44.5	+ 0.2	53.4	0.032	23	76	B3 Ib-II	8.66	+0.61	-0.14	2.43	6.23	-5.2	11.4	0.013
944	E 229108	+38°4038	20 18.3	+39°08'	45.1	+ 0.7	53.4	0.093	51	105	B0.5 Ib	9.48	+0.81	-0.19	3.27	6.21	-5.8	12.0	0.028
945	194057	+44°3439	20 18.4	+44°30'	49.5	+ 3.8	53.6	0.082	73	127	B1 Ib	7.51	+0.86	-0.16	3.36	4.15	-5.8	10.0	0.024

TABLE 5—Continued

No.	HD	BD	1900 α	1900 δ	l	b	φ	p	θ	θ'	Spectrum	V	B-V	U-B	$3E_{(B-V)}$	m	M	m-M	p/A_V
946	E 229115	+34°3992	$20^h18.^m4$	+34°55'	41.8	- 1.9	53.4	0.065	24	78	B2 IV	9.92	+0.67	-0.06	2.73	7.19	-2.9	10.1	0.024
947	194092	+40°4137	20 18.6	+40°39'	46.4	+ 1.5	53.4	0.014	77	130	B0.5 III	8.26	+0.13	-0.73	1.23	7.03	-4.7	11.7	0.011
948		+38°4043	20 18.7	+38°24'	44.6	+ 0.2	53.4	0.030	50	103	O9 III	9.02	+0.59	-0.39	2.70	6.32	-6.4	12.7	0.011
949		+38°4044	20 18.7	+38°35'	44.7	+ 0.3	53.4	0.049	43	96	B1 V	10.03	+0.49	-0.42	2.25	7.78	-3.1	10.9	0.022
950	E 229153	+37°3910	20 19.0	+37°39'	44.0	- 0.3	53.3	0.022	169	42	B0 I	9.07	+1.17	+0.15	4.41	4.66	-6.5	11.2	0.005
951	E 229159	+38°4050	20 19.2	+38°53'	45.0	+ 0.4	53.3	0.035	79	132	B1.5 Ib	8.54	+1.00	0.00	3.75	4.79	-5.8	10.6	0.009
952*			20 19.2	+39°10'	45.3	+ 0.5	53.3	0.022	115	168	B pe*	10.56	+1.25	-0.19					
953	194205	+38°4053	20 19.3	+39°02'	45.2	+ 0.4	53.3	0.075	61	115	B2 III	9.04	+0.53	-0.32	2.31	6.73	-3.6	10.3	0.032
954	E 229171	+37°3913	20 19.4	+38°08'	44.5	- 0.1	53.2	0.017	20	73	B0.5 III: n	9.33	+0.55	-0.34	2.49	6.84	-4.7	11.5	0.007
955		+38°4054	20 19.5	+38°50'	45.0	+ 0.3	53.2	0.069	73	126	B1: III:	9.98	+1.02	+0.08	3.84	6.14	-4.4	10.5	0.018
956	E 229196	+40°4147	20 19.7	+40°34'	46.5	+ 1.3	53.2	0.043	156	29	O5	8.54	+0.90	-0.15	3.66	4.88	-5.1	10.0	0.012
957	194279	+40°4150	20 19.7	+40°26'	46.3	+ 1.2	53.2	0.061	177	50	B1.5 Ia	7.01	+1.03	-0.03	3.84	3.17	-6.9	10.1	0.016
958	194280	+38°4057	20 19.7	+38°37'	44.9	+ 0.1	53.2	0.094	65	118	B0 Ib	8.39	+0.76	-0.21	3.18	5.21	-6.2	11.4	0.030
959		+36°4049	20 19.8	+36°36'	43.3	- 1.1	53.2	0.008	81	134	B3 II	8.61	+0.72	-0.10	2.76	5.85	-4.6	10.4	0.003
960*			20 19.8	+39°02'	45.2	+ 0.4	53.2	0.121	56	109	B0 V	10.62	+1.19	+0.21	4.47	6.15	-4.1	10.2	0.027
961	E 229202	+39°4162	20 19.8	+39°50'	45.9	+ 0.8	53.2	0.011	109	162	O8 V:	9.53	+0.87	-0.12	3.54	5.99	-5.1	11.1	0.003
962		+36°4048	20 19.8	+36°59'	43.6	- 0.9	53.2	0.063	54	107	B0 Ib	9.66	+1.27	+0.21	4.71	4.95	-6.2	11.2	0.013
963	E 229214	+36°4050	20 20.0	+36°12'	43.0	- 1.4	53.2	0.037	38	91	B1 Ib	9.54	+0.70	-0.26	2.88	6.66	-5.8	12.5	0.013
964	E 229221	+38°4062	20 20.1	+38°11'	44.6	- 0.2	53.1	0.034	66	119	B pe	9.21	+0.92	-0.18					
965	E 229227	+38°4065	20 20.2	+38°08'	44.6	- 0.2	53.1	0.019	63	116	B0 II	9.38	+0.80	-0.15	3.30	6.08	-5.4	11.5	0.006
966	E 229232	+38°4070	20 20.3	+38°47'	45.1	+ 0.1	53.1	0.091	67	120	O5 f	9.53	+0.82	-0.17	3.42	6.11			0.027
967	E 229234	+38°4069	20 20.3	+38°12'	44.6	- 0.2	53.1	0.027	93	146	O9.5 III	8.92	+0.77	-0.19	3.21	5.71	-5.7	11.4	0.008
968	E 229238	+38°4071	20 20.4	+38°13'	44.6	- 0.2	53.1	0.030	86	139	B0 I	8.88	+0.90	-0.06	3.60	5.28	-6.5	11.8	0.008
969	E 229239	+38°4072	20 20.4	+38°11'	44.6	- 0.2	53.1	0.041	99	152	B0 II	8.92	+0.87	-0.15	3.51	5.41	-5.4	10.8	0.012
970*			20 20.5	+39°20'	45.6	+ 0.4	53.1	0.059	27	80	O7	9.86	+1.18	+0.11	4.50	5.36	-5.1	10.5	0.013
971		+39°4168	20 20.7	+39°26'	45.7	+ 0.5	53.0	0.043	4	57	O7	9.99	+1.07	+0.03	4.17	5.82	-5.1	10.9	0.010
972*			20 21.3	+39°08'	45.5	+ 0.2	53.0	0.089	55	108	B0.5: III:	10.63	+1.62	+0.65	5.70	4.93	-4.7	9.6	0.016
973		+37°3927	20 21.3	+37°09'	43.9	- 1.0	53.0	0.029	61	114	O8 f	10.15	+1.25	+0.23	4.68	5.47			0.006
974	194649	+39°4177	20 21.7	+39°54'	46.1	+ 0.6	52.9	0.014	22	75	O6.5	9.00	+0.95	-0.09	3.81	5.19	-5.1	10.3	0.004
975		+36°4063	20 21.9	+37°03'	43.9	- 1.2	52.9	0.099	49	102	O9.5 Ib	9.71	+1.14	+0.08	4.32	5.39	-6.6	12.0	0.023
976	194779	+40°4164	20 22.4	+41°01'	47.1	+ 1.2	52.8	0.010	57	110	B3 II	7.77	+0.23	-0.52	1.29	6.48	-4.6	11.1	0.008
977		+39°4189	20 22.7	+39°20'	45.8	+ 0.1	52.7	0.060	14	67	B2 p? e?*	9.33	+1.11	+0.09	4.05	5.28			0.015
978	194839	+40°4165	20 22.8	+41°03'	47.2	+ 1.1	52.7	0.026	171	44	B0.5 Ia	7.49	+1.00	-0.09	3.84	3.65	-6.9	10.6	0.007
979		+38°4098	20 23.8	+38°26'	45.2	- 0.6	52.6	0.048	68	121	B9 Ib	8.96	+0.88	+0.43	2.82	6.14	-5.6	11.7	0.017
980		+40°4179	20 24.1	+40°16'	46.7	+ 0.5	52.5	0.020	20	72	O8 V:	9.65	+0.57	-0.43	2.64	7.01	-5.1	12.1	0.008

TABLE 5—Continued

No.	HD	BD	1900 α	1900 δ	l	b	φ	p	θ	θ'	Spectrum	V	B-V	U-B	$3E_{(B-V)}$	m	M	m-M	p/A_V
			h m																
981		+37°3945	20 24.6	+38°02'	45.0	- 1.0	52.4	0.067	64	116	B0 II: nn	9.53	+0.77	-0.17	3.21	6.32	-5.4	11.7	0.021
982		+40°4185	20 24.7	+40°18'	46.8	+ 0.4	52.4	0.015	158	30	B0 V:	9.82	+0.84	-0.16	3.42	6.40	-4.1	10.5	0.004
983	195213	+40°4187	20 24.9	+40°28'	47.0	+ 0.4	52.4	0.019	68	120	O7	8.74	+0.85	-0.26	3.51	5.23	-5.1	10.3	0.005
984	195229	+41°3765	20 25.0	+41°40'	47.9	+ 1.2	52.4	0.032	52	104	B0.5 III	7.66	+0.16	-0.71	1.32	6.34	-4.7	11.0	0.024
985	195407	+36°4095	20 26.0	+36°39'	44.1	- 2.1	52.3	0.035	48	100	B0 IV: pe	7.80	+0.34	-0.66	1.92	5.88	-4.6	10.5	0.018
986		+46°2948	20 26.1	+46°19'	51.7	+ 3.9	52.4	0.046	6	58	B1 V: nne*	10.05	+0.28	-0.59	1.62	8.43	-3.1	11.5	0.028
987	195592	+43°3630	20 27.2	+43°59'	50.0	+ 2.3	52.1	0.027	117	169	O9.5 Ia	7.08	+0.87	-0.19	3.51	3.57	-6.9	10.5	0.008
988*			20 27.7	+41°10'	47.8	+ 0.5	51.9	0.040	72	123	B1 Ib?	10.84	+1.29	-0.12	4.65	6.19	-5.8	12.0	0.009
989		+40°4212	20 28.0	+40°52'	47.6	+ 0.2	51.9	0.130	106	158	O9 ?	10.29	+1.63	+0.54	5.82	4.47	-4.6	9.1	0.022
990		+40°4219	20 28.6	+41°06'	47.9	+ 0.3	51.8	0.051	78	130	O8	10.22	+1.19	+0.10	4.50	5.72	-5.1	10.8	0.011
991		+40°4220	20 28.8	+40°58'	47.8	+ 0.2	51.8	0.083	80	132	O7 f	9.20	+1.70	+0.58	6.06	3.14			0.014
992*			20 29.1	+40°55'	47.8	+ 0.1	51.7	0.218	119	171	O	11.51	+3.35		11.01	0.50			0.020
993*			20 29.2	+41°68'	48.0	+ 0.2	51.7	0.039	56	108	O8 (V)	10.67	+1.23	+0.15	4.62	6.05	-5.1	11.2	0.008
994	195965	+47°3136	20 29.3	+47°53'	53.3	+ 4.4	51.9	0.020	35	87	B0 V	6.98	-0.05	-0.90	0.75	6.23	-4.1	10.3	0.027
995*			20 29.6	+40°55'	47.9	0.0	51.6	0.056	51	103	O5 f	10.81	+1.93		6.75	4.06			0.008
996		+40°4227	20 29.6	+40°58'	47.9	+ 0.1	51.6	0.023	86	138	O6 f	9.05	+1.27	+0.16	4.77	4.28			0.005
997*			20 29.7	+41°00'	47.9	+ 0.1	51.6	0.079	94	146	O6 f	10.48	+1.45	+0.27	5.31	5.17			0.015
998		+37°3976	20 30.1	+37°56'	45.6	- 1.9	51.6	0.050	166	37	B1.5 V n	10.25	+0.76	-0.16	3.03	7.22	-2.6	9.8	0.016
999		+41°3804	20 30.2	+41°12'	48.2	+ 0.1	51.5	0.008	51	103	O9.5 Ia	9.89	+1.53	+0.41	5.49	4.40	-6.9	11.3	0.001
1000		+45°3216	20 30.5	+45°19'	51.4	+ 2.6	51.6	0.021	17	68	O8	9.07	+0.39	-0.57	2.10	6.97	-5.1	12.1	0.010
1001		+41°3807	20 30.6	+41°16'	48.3	+ 0.1	51.5	0.075	159	30	O6 f	10.05	+1.44	+0.29	5.28	4.77			0.014
1002		+36°4145	20 32.5	+37°04'	45.2	- 2.8	51.2	0.038	38	89	O9 V	8.95	+0.65	-0.37	2.88	6.07	-4.6	10.7	0.013
1003		+45°3230	20 33.9	+45°47'	52.2	+ 2.5	51.0	0.072	177	48	B0 III	9.40	+0.75	-0.27	3.15	6.25	-5.0	11.2	0.023
1004		+47°3162	20 36.7	+47°44'	54.0	+ 3.3	50.5	0.042	75	126	B1 Ib-II	9.80	+0.64	-0.33	2.70	7.10	-5.4	12.5	0.016
1005	197406	+52°2777	20 38.4	+52°14'	57.6	+ 6.0	50.5	0.020	101	152	W R ?*	10.30	+0.57	-0.45					
1006		+42°3835	20 38.6	+42°49'	50.4	- 0.1	50.1	0.029	16	66	O9 p?	9.20	+0.91	-0.19	3.66	5.54	-4.6	10.1	0.008
1007	197460	+35°4229	20 38.8	+36°02'	45.2	- 4.5	50.3	0.032	3	53	B0.5 Ib	8.14	+0.34	-0.55	1.86	6.28	-5.8	12.1	0.017
1008		+45°3246	20 39.1	+45°32'	52.5	+ 1.6	50.1	<.003			B1 V n	9.67	+0.17	-0.64	1.29	8.38	-3.1	11.5	
1009	197770	+56°2477	20 40.7	+56°46'	61.4	+ 8.6	50.5	0.088	130	0	B2 IV	6.32	+0.33	-0.48	1.71	4.61	-2.9	7.5	0.051
1010		+45°3260	20 42.2	+45°58'	53.2	+ 1.5	49.5	0.035	21	71	O9 V	9.06	+0.51	-0.50	2.46	6.60	-4.6	11.2	0.014
1011	E 235350	+50°3189	20 42.3	+50°49'	56.9	+ 4.6	49.7	<.004			B0.5 IV	9.27	+0.29	-0.61	1.71	7.56	-4.2	11.8	
1012		+35°4258	20 42.3	+35°11'	45.0	- 5.5	49.8	0.011	7	57	B0.5 V n	9.41	+0.01	-0.74	0.87	8.54	-3.6	12.1	0.013
1013	198478	+45°3291	20 45.5	+45°45'	53.4	+ 0.9	48.9	0.061	5	54	B3 Ia	4.83	+0.40	-0.46	1.80	3.03	-6.9	9.9	0.034
1014	198479	+45°3290	20 45.5	+45°16'	53.1	+ 0.6	48.9	0.057	15	64	B1 III	8.57	+0.38	-0.52	1.92	6.65	-4.4	11.0	0.030
1015	198512	+53°2495	20 45.7	+53°32'	59.4	+ 6.0	49.2	0.041	128	177	B1 V pnne	8.29	+0.37	-0.53	1.89	6.40	-3.1	9.5	0.022

TABLE 5—Continued

No.	HD	BD	1900 α	1900 δ	l	b	φ	p	θ	θ'	Spectrum	V	B-V	U-B	$3E_{(B-V)}$	m	M	m-M	p/A_V
			h m																
1016		+44°3594	20 45.8	+45°03'	52.9	+ 0.4	48.9	0.044	12	61	B1: V: pne*	9.78	+0.68	-0.37	2.82	6.96	-3.1	10.1	0.016
1017	198781	+63°1663	20 47.6	+63°40'	67.3	+12.3	50.1	0.030	157	27	B0.5 V	6.45	+0.07	-0.77	1.05	5.40	-3.6	9.0	0.028
1018*			20 48.2	+45°39'	53.7	+ 0.5	48.5	0.050	9	57	B0.5 n V	10.54	+0.41	-0.51	2.07	8.47	-3.6	12.1	0.024
1019	198895	+54°2429	20 48.4	+55°07'	60.8	+ 6.7	48.9	0.119	149	18	B1 V	8.30	+0.56	-0.31	2.46	5.84	-3.1	8.9	0.048
1020	198931	+43°3747	20 48.6	+44°03'	52.5	- 0.7	48.4	0.096	146	14	B1 V nne:	8.72	+0.59	-0.31	2.55	6.17	-3.1	9.3	0.038
1021		+47°3211	20 49.7	+47°33'	55.3	+ 1.5	48.2	0.068	10	58	B0 II-III	9.79	+0.77	-0.27	3.21	6.58	-5.2	11.8	0.021
1022		+37°4092	20 49.8	+37°48'	48.0	- 5.0	48.4	0.028	172	40	B1 III	9.66	+0.29	-0.57	1.65	8.01	-4.4	12.4	0.017
1023	199216	+48°3242	20 50.7	+49°09'	56.6	+ 2.5	48.1	0.040	135	3	B1 II	7.03	+0.48	-0.46	2.22	4.81	-4.9	9.7	0.018
1024		+44°3627	20 51.3	+44°28'	53.2	- 0.7	47.9	0.017	46	94	B3 V	9.85	+0.76	-0.10	2.88	6.97	-1.5	8.5	0.006
1025	199356	+39°4368	20 51.6	+39°55'	49.8	+ 3.7	48.0	0.051	151	19	B2 IV p:	7.12	+0.15	-0.76	1.17	5.95	-2.9	8.8	0.044
1026	199478	+46°3111	20 52.4	+47°02'	55.2	+ 0.8	47.7	0.040	11	59	B8 Ia	5.66	+0.47	-0.33	1.68	3.98	-6.9	10.9	0.024
1027		+42°3914	20 52.7	+42°44'	52.0	- 2.1	47.7	0.100	150	18	B0 III:	8.43	+1.05	+0.08	4.05	4.38	-5.0	9.4	0.025
1028	199579	+44°3639	20 53.1	+44°33'	53.4	- 0.9	47.6	0.020	55	103	O6	5.96	+0.05	-0.85	1.11	4.85	-5.1	10.0	0.018
1029		+45°3339	20 53.2	+45°58'	54.5	0.0	47.6	0.053	29	77	B1 IV	9.93	+0.42	-0.42	2.04	7.89	-3.8	11.7	0.026
1030		+45°3341	20 53.6	+46°09'	54.7	+ 0.1	47.5	0.068	50	98	B1 II	8.73	+0.48	-0.48	2.22	6.51	-4.9	11.4	0.031
1031		+44°3655	20 54.8	+44°45'	53.8	- 1.0	47.3	0.048	42	89	B1 IV	9.24	+0.31	-0.51	1.71	7.53	-3.8	11.3	0.028
1032		+45°3360	20 57.0	+45°51'	54.8	- 0.5	46.9	0.030	25	72	B3 V	10.00	+0.20	-0.43	1.20	8.80	-1.5	10.3	0.025
1033	200776	+45°3384	21 00.4	+45°56'	55.3	- 0.9	46.3	0.010	31	77	B1 IV: p	7.81	+0.01	-0.82	0.81	7.00	-3.8	10.8	0.012
1034	200857	+54°2470	21 01.0	+54°51'	61.8	+ 5.2	46.4	0.030	154	20	B3 III	9.66	+0.56	-0.23	2.28	7.38	-3.3	10.7	0.013
1035*			21 01.4	+47°33'	56.6	+ 0.1	46.1	0.039	33	79	B1 V nne	10.48	+0.48	-0.49	2.22	8.26	-3.1	11.4	0.018
1036		+45°3406	21 03.0	+45°27'	55.3	- 1.6	45.8	0.048	48	94	B5 Iab	9.52	+0.59	-0.17	2.25	7.27	-6.5	13.8	0.021
1037		+47°3302	21 05.0	+47°16'	56.8	- 0.5	45.4	0.026	0	46	B2 pne (V)	10.49	+0.38	-0.51	1.86	8.63	-2.0	10.6	0.014
1038		+44°3731	21 07.8	+45°05'	55.6	- 2.4	44.9	0.036	26	71	B5 III	9.50	+0.07	-0.45	0.69	8.81	-2.8	11.6	0.052
1039	202124	+43°3842	21 08.8	+44°07'	55.0	- 3.2	44.8	0.011	90	135	O9.5 Ib	7.80	+0.22	-0.69	1.56	6.24	-6.6	12.8	0.007
1040	202214	+59°2334	21 09.3	+59°35'	66.0	+ 7.7	45.1	0.017	143	8	B0 V	5.63	+0.11	-0.77	1.23	4.40	-4.1	8.5	0.014
1041	202253	+43°3850	21 09.5	+43°28'	54.7	- 3.8	44.7	0.015	50	95	B2 III	7.75	+0.14	-0.61	1.14	6.61	-3.6	10.2	0.013
1042*			21 10.1	+48°00'	58.0	- 0.6	44.5	0.044	10	55	B2 ne (V)	10.38	+0.65	-0.17	2.67	7.71	-2.0	9.7	0.016
1043		+41°4064	21 12.3	+42°07'	54.1	- 5.1	44.2	0.050	51	95	B3: pnn*	9.02	+0.29	-0.22	1.47	7.55			0.034
1044	203938	+46°3294	21 20.2	+46°44'	58.3	- 2.7	42.6	0.030	160	23	B0.5 IV	7.08	+0.46	-0.41	2.22	4.86	-4.2	9.1	0.014
1045		+43°3913	21 21.3	+44°01'	56.6	- 4.9	42.5	0.050	42	85	B1.5 V: pnne	8.86	+0.55	-0.35	2.40	6.46	-2.6	9.1	0.021
1046		+47°3421	21 25.0	+47°37'	59.5	- 2.6	41.7	<.005			A0 Iab	9.54	+0.58	+0.01	1.74	7.80	-6.5	14.3	
1047	204710	+44°3832	21 25.4	+44°29'	57.5	- 5.0	41.7	0.050	36	78	B8 Ib	6.95	+0.26	-0.24	1.05	5.90	-6.9	12.8	0.048
1048	204722	+43°3941	21 25.5	+43°54'	57.1	- 5.4	41.7	0.025	10	52	B2 V: nn (e)	7.67	-0.02	-0.85	0.66	7.01	-2.0	9.0	0.038
1049	204827	+58°2272	21 26.1	+58°18'	66.7	+ 5.3	41.6	0.122	59	101	B0 V	7.95	+0.81	-0.15	3.33	4.62	-4.1	8.7	0.037
1050	205196	+56°2589	21 28.6	+57°04'	66.2	+ 4.1	41.0	0.062	79	120	B0 Ib	7.45	+0.57	-0.45	2.61	4.84	-6.2	11.0	0.024

TABLE 5—Continued

No.	HD	BD	1900 α	1900 δ	l	b	φ	p	θ	θ'	Spectrum	V	E-V	U-B	$3E_{(B-V)}$	m	M	m-M	p/A_V
			h m																
1051		+47°3487	21 32.1	+47°28'	60.3	- 3.5	40.3	<.003			B pe*	9.12	+0.68	-0.24					
1052		+48°3437	21 32.6	+48°54'	61.3	- 2.5	40.2	0.028	179	39	B1 Iab	8.69	+0.16	-0.70	1.26	7.43	-6.5	13.9	0.022
1053	206183	+56°2614	21 35.3	+56°32'	66.5	+ 3.1	39.6	0.015	46	86	B0 V	7.40	+0.14	-0.79	1.32	6.08	-4.1	10.2	0.011
1054	206259	+51°3112	21 35.8	+51°54'	63.6	- 0.5	39.5	0.017	29	69	B3 III	7.54	+0.05	-0.57	0.75	6.79	-3.3	10.1	0.023
1055*			21 36.5	+49°56'	62.5	- 2.1	39.4	0.044	52	91	B0: pe	10.73	+0.52	-0.54	2.46	8.27			0.018
1056		+49°3591	21 36.7	+50°03'	62.6	- 2.0	39.3	<.004			O7.5	9.67	+0.52	-0.48	2.52	7.15	-5.1	12.2	
1057		+56°2626	21 38.4	+56°15'	66.7	+ 2.6	39.0	0.048	20	59	B0.5 III	10.47	+0.65	-0.35	2.79	7.68	-4.7	12.4	0.017
1058	206773	+57°2374	21 39.3	+57°17'	67.4	+ 3.4	38.8	0.039	170	29	B0 V: pe	6.91	+0.21	-0.82	1.53	5.38	-4.1	9.5	0.025
1059	E 239758	+58°2320	21 41.8	+58°36'	68.5	+ 4.2	38.4	0.046	51	89	B2 III: nn	9.50	+0.26	-0.54	1.50	8.00	-3.6	11.6	0.031
1060		+49°3615	21 42.2	+49°50'	63.1	- 2.7	38.2	0.082	90	47	B1 V:	9.07	+0.33	-0.47	1.77	7.30	-3.1	10.4	0.046
1061	207260	+60°2288	21 42.6	+60°40'	69.9	+ 5.7	38.3	0.037	46	84	A2 Ia	4.29	+0.52	+0.14	1.38	2.91	-6.9	9.8	0.027
1062		+56°2640	21 43.1	+56°27'	67.3	+ 2.4	38.1	0.034	23	61	B0.5 p V:	9.25	+0.70	-0.35	2.94	6.31	-3.6	9.9	0.012
1063	207329	+51°3144	21 43.1	+51°39'	64.4	- 1.4	38.0	0.038	1	39	B1.5 Ib? e	7.60	+0.29	-0.57	1.62	5.98	-5.8	11.8	0.023
1064		+54°2623	21 43.5	+54°52'	66.4	+ 1.1	37.9	0.059	23	61	B1 IV	9.66	+0.68	-0.31	2.82	6.84	-3.8	10.6	0.021
1065		+54°2629	21 44.2	+54°52'	66.5	+ 1.0	37.8	0.048	22	60	B1 II	10.54	+0.65	-0.31	2.73	7.81	-4.9	12.7	0.018
1066	207538	+59°2420	21 44.6	+59°14'	69.2	+ 4.4	37.8	0.046	61	99	B0 V	7.31	+0.33	-0.64	1.89	5.42	-4.1	9.5	0.024
1067	207793	+52°3043	21 46.5	+52°14'	65.1	- 1.2	37.3	0.017	6	43	B0.5 III	6.60	+0.38	-0.56	1.98	4.62	-4.7	9.3	0.009
1068		+47°3588	21 48.9	+47°33'	62.5	- 5.2	37.0	0.025	32	69	B1.5 V	9.61	+0.09	-0.66	1.02	8.59	-2.6	11.2	0.024
1069	208220	+42°4241	21 49.7	+43°01'	60.0	- 8.9	37.2	0.023	42	79	B1 IV e	9.49	+0.04	-0.75	0.90	8.59	-3.8	12.4	0.026
1070*			21 50.2	+53°45'	66.5	- 0.4	36.6	0.054	72	108	B2 p (IV, V)	11.16	+0.46	-0.30	2.10	9.06	-2.4	11.5	0.026
1071	208501	+55°2644	21 51.5	+56°08'	68.0	+ 1.4	36.3	0.035	43	79	B8 Ib	5.79	+0.74	-0.02	2.49	3.30	-5.6	8.9	0.014
1072	E 235673	+52°3071	21 54.1	+52°19'	66.1	- 1.9	35.8	0.052	28	64	O7	9.14	+0.21	-0.77	1.59	7.55	-5.1	12.6	0.033
1073	208905	+60°2320	21 54.3	+60°49'	71.1	+ 5.0	35.9	0.018	39	75	B1 V p?	6.98	+0.09	-0.73	1.05	5.93	-3.1	9.0	0.017
1074	E 235679	+53°2749	21 55.0	+53°59'	67.2	- 0.6	35.6	0.038	51	87	B2 II	8.86	+0.35	-0.55	1.77	7.09	-4.7	11.8	0.021
1075	209145	+59°2443	21 56.1	+59°50'	70.7	+ 4.1	35.5	<.004			B1 V	7.62	+0.33	-0.50	1.77	5.85	-3.1	9.0	
1076	209296	+56°2676	21 57.2	+56°14'	68.8	+ 1.0	35.1	0.020	59	94	B6: V: n	8.28	+0.26	-0.23	1.20	7.08	-0.5	7.6	0.017
1077		+58°2373	21 58.1	+59°01'	70.5	+ 3.3	35.0	0.075	41	76	B5 Ia	9.34	+0.92	-0.03	3.24	6.10	-6.9	13.0	0.023
1078		+54°2676	21 59.7	+54°37'	68.1	- 0.5	34.6	0.060	65	100	B1: nne (V)	10.29	+0.46	-0.38	2.16	8.13	-3.1	11.2	0.028
1079	209678	+52°3088	22 00.1	+52°43'	67.1	- 2.1	34.6	0.066	33	68	B2 I	8.42	+0.39	-0.47	1.89	6.53	-6.5	13.0	0.035
1080		+51°3239	22 00.3	+51°37'	66.5	- 3.0	34.6	0.045	30	65	B2 V	9.92	+0.09	-0.59	0.99	8.93	-2.0	10.9	0.045
1081	209900	+52°3095	22 01.6	+53°01'	67.4	- 2.0	34.3	0.048	39	73	A0 Ib-II	8.71	+0.45	+0.23	1.35	7.36	-5.0	12.4	0.036
1082	209975	+61°2246	22 02.1	+61°48'	72.4	+ 5.3	34.3	0.023	68	102	O9.5 Ib	5.10	+0.09	-0.84	1.17	3.93	-6.6	10.5	0.020
1083		+49°3735	22 02.2	+49°25'	65.5	- 5.0	34.3	0.036	35	69	B1.5 V: nn (e)?	9.72	+0.05	-0.64	0.90	8.82	-2.6	11.4	0.040
1084	210072	+54°2683	22 02.7	+54°46'	68.6	- 0.6	34.0	0.015	47	81	B2 V	7.65	+0.31	-0.36	1.65	6.00	-2.0	8.0	0.009
1085	210221	+52°3114	22 03.8	+52°49'	67.6	- 2.3	33.8	0.041	45	79	A3 Ib	6.14	+0.43	+0.24	1.02	5.12	-5.6	10.7	0.040

TABLE 5—Continued

No.	HD	BD	1900 α	1900 δ	l	b	φ	p	θ	θ'	Spectrum	V	B-V	U-B	$3E_{(B-V)}$	m	M	m-M	p/A_v
			h m																
1086		+53°2790	22 04.3	+54°02'	68.3	- 1.3	33.7	0.070	40	73	O9.5 III? p	9.86	+0.25	-0.71	1.65	8.21	-5.7	13.9	0.042
1087		+52°3122*	22 05.0	+53°28'	68.1	- 1.9	33.6	0.037	49	83	B1 V:	9.30	+0.30	-0.60	1.68	7.62	-3.1	10.7	0.022
1088	210478	+60°2348	22 05.6	+60°30'	72.1	+ 4.0	33.5	0.018	49	83	B1 V	7.33	+0.07	-0.71	0.99	6.34	-3.1	9.4	0.018
1089		+57°2465	22 05.9	+57°22'	70.4	+ 1.3	33.4	0.097	41	75	B0.5 n (V)	11.00	+0.73	-0.25	3.03	7.97	-3.6	11.6	0.032
1090	210628	+55°2695	22 06.9	+55°36'	69.5	- 0.2	33.2	0.027	59	92	B6: V:	6.92	+0.10	-0.37	0.72	6.20	-0.5	6.7	0.038
1091	210809	+51°3281	22 07.9	+51°56'	67.7	- 3.4	33.0	0.033	49	82	O9 Ib	7.54	+0.05	-0.89	1.08	6.46	-6.9	13.4	0.030
1092	210839	+58°2402	22 08.1	+58°56'	71.5	+ 2.5	32.9	0.024	59	92	O6 f	5.05	+0.25	-0.76	1.71	3.34			0.014
1093		+52°3135	22 08.4	+53°12'	68.4	- 2.4	32.9	0.043	40	73	B3 II:	9.62	+0.33	-0.50	1.59	8.03	-4.6	12.6	0.027
1094	E 239886	+56°2733	22 08.9	+56°46'	70.4	+ 0.6	32.8	0.110	49	82	B9 Iab	8.84	+0.85	+0.12	2.73	6.11	-6.5	12.6	0.040
1095*			22 09.4	+57°10'	70.7	+ 0.9	32.6	0.079	45	78	B1 III	10.32	+0.65	-0.34	2.73	7.59	-4.4	12.0	0.029
1096	E 239895	+56°2735	22 09.8	+57°10'	70.7	+ 0.8	32.6	0.066	51	84	B8 Ia	8.63	+1.02	+0.12	3.33	5.30	-6.9	12.2	0.020
1097		+53°2820	22 10.1	+53°55'	69.0	- 1.9	32.5	0.049	49	82	B0 IV: n	9.95	+0.10	-0.78	1.20	8.75	-4.6	13.4	0.041
1098*			22 10.7	+53°47'	69.0	- 2.1	32.4	0.028	68	100	B1 IV	10.33	+0.85	-0.17	3.33	7.00	-3.8	10.8	0.008
1099		+54°2718	22 11.3	+54°58'	69.7	- 1.1	32.3	0.060	56	89	B2 III	10.15	+0.19	-0.62	1.29	8.86	-3.6	12.5	0.046
1100*			22 11.7	+60°35'	72.7	+ 3.6	32.2	0.006	100	132	B2 V	10.68	+0.60	-0.17	2.52	8.16	-2.0	10.2	0.002
1101		+53°2833	22 12.4	+53°40'	69.1	- 2.3	32.0	0.053	50	82	B1 III	10.01	+0.22	-0.66	1.44	8.57	-4.4	13.0	0.037
1102		+54°2726	22 13.0	+54°59'	69.9	- 1.2	31.9	0.085	54	86	B1 II	9.38	+0.33	-0.54	1.77	7.61	-4.9	12.5	0.048
1103	E 235781	+52°3167	22 13.2	+53°13'	69.0	- 2.8	31.9	0.042	29	61	B6 Ib	8.59	+0.43	-0.26	1.71	6.88	-5.7	12.6	0.024
1104		+53°2837	22 13.3	+53°42'	69.3	- 2.4	31.9	0.040	45	77	B2 III:	9.97	+0.26	-0.54	1.50	8.47	-3.6	12.1	0.027
1105	E 235783	+53°2838	22 13.4	+53°59'	69.4	- 2.1	31.8	0.047	55	87	B1 Ib	8.68	+0.17	-0.71	1.29	7.39	-5.8	13.2	0.036
1106*			22 14.4	+55°25'	70.3	- 1.0	31.6	0.102	45	77	B0 III:*	10.45	+0.51	-0.51	2.43	8.02	-5.0	13.0	0.042
1107		+53°2843	22 14.9	+53°46'	69.5	- 2.4	31.5	0.058	51	83	O8	9.50	+0.21	-0.75	1.56	7.94	-5.1	13.0	0.037
1108	211853	+55°2721	22 15.0	+55°37'	70.4	- 0.9	31.5	0.089	44	75		9.02	+0.40	-0.55					
1109	211880	+62°2061	22 15.2	+62°43'	74.2	+ 5.2	31.6	0.010	52	84	B0.5 V	7.75	+0.32	-0.60	1.80	5.95	-3.6	9.6	0.006
1110	E 235795	+51°3330	22 15.2	+51°37'	68.4	- 4.3	31.5	0.019	40	72	B1: V: nne	9.14	+0.07	-0.78	0.99	8.15	-3.1	11.2	0.019
1111		+60°2380	22 15.6	+60°16'	73.0	+ 3.1	31.4	0.008	168	20	B2 III	9.04	+0.39	-0.50	1.89	7.15	-3.6	10.8	0.004
1112	E 239923	+58°2421	22 15.8	+58°27'	72.1	+ 1.5	31.3	0.069	54	86	B3 Ib	8.89	+0.33	-0.12	3.09	5.80	-5.8	11.6	0.022
1113	211971	+59°2506	22 15.9	+59°38'	72.7	+ 2.5	31.3	0.014	87	118	A2 Ib	6.89	+0.99	+0.42	2.79	4.10	-5.6	9.7	0.005
1114	212044	+51°3341	22 16.4	+51°21'	68.4	- 4.6	31.3	0.028	49	80	B1: V: pnne	6.98	+0.04	-0.91	0.90	0.90	-3.1	9.2	0.031
1115*			22 16.5	+55°53'	70.8	- 0.7	31.2	0.094	58	89	B1 pe (IV)	10.08*	+0.45	-0.53	2.13	7.95	-3.8	11.8	0.044
1116		+54°2745	22 17.4	+55°03'	70.5	- 1.5	31.0	0.069	53	84	B0.5 IV: n	9.56	+0.21	-0.67	1.47	8.09	-4.2	12.3	0.047
1117*			22 18.2	+59°47'	73.0	+ 2.5	30.8	0.060	114	145	B3 V	10.42	+0.87	0.00	3.21	7.21	-1.5	8.7	0.019
1118*			22 18.5	+55°08'	70.7	- 1.5	30.8	0.073	48	79	O5	10.29	+0.27	-0.73	1.77	8.52	-5.1	13.6	0.041
1119	E 235813	+54°2751	22 18.5	+54°18'	70.1	- 2.2	30.8	0.058	43	74	B0 III	8.84	+0.22	-0.74	1.56	7.28	-5.0	12.3	0.037
1120	212455	+54°2756	22 19.3	+54°44'	70.6	- 1.9	30.6	0.058	49	80	B5 Iab	7.87	+0.38	-0.36	1.62	6.25	-6.5	12.8	0.036

TABLE 5—Continued

No.	HD	BD	1900 α	1900 δ	l	b	φ	p	θ	θ'	Spectrum	V	B-V	U-B	$3E_{(B-V)}$	m	M	m-M	p/A_V
1121	E 235825	+54°2758	22h19.6m	+54°44'	70.6	- 1.9	30.5	0.071	54	85	O9 V	9.28	+0.24	-0.73	1.65	7.63	-4.6	12.2	0.043
1122		+54°2761	22 19.9	+55°11'	70.9	- 1.6	30.5	0.065	48	79	O5 f	9.98	+0.34	-0.68	1.98	8.00			0.033
1123		+54°2764	22 20.1	+54°53'	70.7	- 1.8	30.4	0.065	46	76	B1 Ib	9.54	+0.28	-0.62	1.62	7.92	-5.8	13.7	0.040
1124*			22 21.0	+61°03'	74.0	+ 3.4	30.3	0.033	94	125	B3 Vn *	10.60	+0.77	-0.12	2.91	7.69	-1.5	9.2	0.011
1125		+57°2525	22 21.3	+57°20'	72.1	+ 0.2	30.2	0.046	43	73	B1.5 pe (IV-V)	10.35	+0.25	-0.59	1.50	8.85	-3.0	11.8	0.031
1126		+55°2748	22 21.5	+55°47'	71.4	- 1.2	30.1	0.073	53	83	B0.5 V	9.96	+0.44	-0.52	2.16	7.80	-3.6	11.4	0.034
1127	212827	+53°2877	22 22.0	+53°16'	70.2	- 3.4	30.1	0.041	44	74	A0 II	8.30	+0.26	+0.12	0.78	7.52	-4.4	11.9	0.052
1128		+62°2078	22 22.2	+62°54'	75.0	+ 4.9	30.1	0.152	74	104	O7	9.72	+1.11	0.00	4.29	5.43	-5.1	10.5	0.035
1129		+54°2775	22 22.2	+54°57'	71.0	- 1.9	30.0	0.062	53	83	B1 V	9.57	+0.30	-0.49	1.68	7.89	-3.1	11.0	0.037
1130		+52°3210	22 23.0	+53°08'	70.2	- 3.6	29.9	0.040	54	84	B1 V	10.69	-0.02	-0.78	0.72	9.97	-3.1	13.1	0.056
1131		+53°2885	22 23.2	+53°40'	70.5	- 3.1	29.8	0.026	53	83	B2 III	10.46	+0.04	-0.76	0.84	9.62	-3.6	13.2	0.031
1132		+57°2536	22 23.7	+57°52'	72.7	+ 0.5	29.7	0.064	37	67	B1 II-III	10.32	+0.49	-0.43	2.25	8.07	-4.6	12.7	0.028
1133	213087	+64°1664	22 23.9	+64°37'	76.0	+ 6.4	29.8	0.017	33	63	B0.5 Ib	5.46	+0.37	-0.59	1.95	3.51	-5.8	9.3	0.009
1134*			22 23.9	+56°59'	72.3	- 0.3	29.6	0.078	37	66	B1 III	10.77	+0.53	-0.40	2.37	8.40	-4.4	12.8	0.033
1135	E 239967	+55°2756	22 25.1	+56°06'	72.0	- 1.1	29.4	0.055	46	76	B3 II	9.36	+0.33	-0.49	1.59	7.77	-4.6	12.4	0.034
1136	213405	+64°1672	22 26.0	+64°36'	76.2	+ 6.1	29.4	0.013	9	38	B0.5 V	7.95	+0.47	-0.44	2.25	5.70	-3.6	9.3	0.006
1137*			22 26.2	+56°30'	72.3	- 0.9	29.1	0.048	59	89	B0.5 III:	10.49	+0.56	-0.47	2.52	7.97	-4.7	12.7	0.019
1138		+54°2790	22 26.2	+54°17'	71.2	- 2.8	29.2	0.052	55	84	B0 IV n	9.69	+0.20	-0.67	1.50	8.19	-4.6	12.8	0.035
1139	213470	+56°2794	22 26.5	+56°43'	72.4	- 0.7	29.1	0.067	56	85	A3 Ia	6.65	+0.56	+0.24	1.41	5.24	-6.9	12.1	0.048
1140*			22 26.7	+56°07'	72.2	- 1.2	29.0	0.034	62	91	B0 IV	9.89*	+0.60	-0.39	2.70	7.19	-4.6	11.8	0.012
1141		+60°2405	22 27.5	+61°06'	74.7	+ 3.1	28.9	0.055	88	117	B3 nn (V?)	9.91	+0.54	-0.19	2.22	7.69	-1.5	9.2	0.025
1142	E 235874	+50°3748	22 28.9	+50°42'	69.8	- 6.1	28.7	0.029	42	71	B3 III	9.64	0.00	-0.70	0.60	9.04	-3.3	12.3	0.048
1143*		+55°2770	22 29.9	+56°01'	72.5	- 1.5	28.4	0.070	60	88	B1.5 II	10.10	+0.37	-0.54	1.86	8.24	-4.8	13.0	0.038
1144*		+55°2770	22 29.9	+56°01'	72.5	- 1.5	28.4	0.070	61	89	B1.5 III	9.70	+0.35	-0.54	1.80	7.90	-4.0	11.9	0.039
1145*			22 30.4	+57°50'	73.4	0.0	28.2	0.056	44	72	B2 III	10.45	+0.42	-0.46	1.98	8.47	-3.6	12.1	0.028
1146		+55°2771	22 30.4	+56°11'	72.7	- 1.4	28.3	0.075	63	91	B1 IV	9.70	+0.48	-0.45	2.22	7.48	-3.8	11.3	0.034
1147	214419	+56°2818	22 32.9	+56°23'	73.0	- 1.4	27.7	0.113	64	92	W R *	8.8*	+0.41	-0.53					
1148	E 240010	+55°2783	22 34.6	+55°19'	72.8	- 2.5	27.4	0.079	76	103	B1: IV: pnne	9.48	+0.38	-0.60	1.92	7.56	-3.8	11.4	0.041
1149		+57°2581	22 36.1	+57°54'	74.1	- 0.3	27.0	0.063	72	99	B0 III	10.04	+0.61	-0.42	2.73	7.31	-5.0	12.3	0.023
1150		+55°2795	22 38.7	+55°50'	73.5	- 2.3	26.5	0.050	49	76	B1 III	9.80	+0.31	-0.52	1.71	8.09	-4.4	12.5	0.029
1151		+53°2964	22 39.2	+53°33'	72.6	- 4.3	26.4	0.025	61	87	B2 IV: pnne	9.19	+0.15	-0.71	1.17	8.02	-2.9	10.9	0.021
1152		+54°2847	22 40.3	+55°13'	73.5	- 2.9	26.2	0.073	51	77	B1 II? nn	10.12	+0.39	-0.53	1.95	8.17	-4.9	13.1	0.037
1153	215605	+57°2597	22 41.3	+57°20'	74.5	- 1.1	25.9	0.031	40	66	B2: IV: nne	9.43	+0.25	+0.68	1.47	7.96	-2.9	10.9	0.021
1154	E 240047	+56°2852	22 41.4	+56°55'	74.3	- 1.5	25.9	0.048	62	88	B2 III	9.83	+0.35	-0.43	1.77	8.06	-3.6	11.7	0.027
1155		+55°2808	22 42.3	+55°48'	74.0	- 2.5	25.7	0.060	51	77	B2 III	10.01	+0.41	-0.46	1.95	8.06	-3.6	11.7	0.031

TABLE 5—Continued

No.	HD	BD	1900 α	1900 δ	l	b	φ	p	θ	θ'	Spectrum	V	B-V	U-B	$3E_{(B-V)}$	m	M	m-M	p/A_V
1156	215806	+57°2606	22h42m.7	+57°46'	74.9	- 0.8	25.6	0.040	71	97	B0 Ib	9.20	+0.42	-0.57	2.16	7.04	-6.2	13.2	0.018
1157	215835	+57°2607	22 42.9	+57°33'	74.8	- 1.0	25.6	0.060	63	89	O6 n	8.59	+0.33	-0.65	1.95	6.64	-5.1	11.7	0.031
1158	215836	+55°2809	22 42.9	+55°54'	74.1	- 2.5	25.6	0.073	56	82	B1 II	9.19	+0.50	-0.43	2.28	6.91	-4.9	11.8	0.032
1159		+57°2611	22 43.4	+57°58'	75.0	- 0.6	25.5	0.041	72	97	B0 III	9.64	+0.49	-0.52	2.37	7.27	-5.0	12.3	0.017
1160*			22 43.8	+56°45'	74.6	- 1.8	25.4	0.062	53	79	B0: III: pe	10.18	+0.45	-0.65	2.25	7.92	-5.0	12.9	0.028
1161	216014	+64°1717	22 44.2	+64°32'	77.9	+ 5.3	25.4	0.035	58	83	B0.5 V: nn	6.8*	+0.31	-0.62	1.77	5.03	-3.6	8.6	0.020
1162	216044	+54°2865	22 44.5	+54°36'	73.7	- 3.7	25.3	0.023	64	89	B0 II	8.51	+0.08	-0.82	1.14	7.37	-5.4	12.8	0.020
1163		+61°2352	22 46.0	+61°48'	77.0	+ 2.7	25.0	0.075	63	88	B5 Ib:	10.02	+1.43	+0.49	4.77	5.25	-5.8	11.0	0.016
1164	216248	+57°2625	22 46.3	+58°08'	75.5	- 0.7	24.9	0.034	55	80	B3 II	9.89	+0.44	-0.41	1.92	7.97	-4.6	12.6	0.018
1165	216411	+58°2492	22 47.6	+58°28'	75.7	- 0.4	24.6	0.059	46	71	B1 Ia	7.20	+0.60	-0.43	2.58	4.62	-6.9	11.5	0.023
1166	216438	+52°3315	22 47.8	+53°11'	73.6	- 5.2	24.6	0.031	56	81	B1 II	8.46	+0.06	-0.76	0.96	7.50	-4.9	12.4	0.032
1167	216532	+61°2356	22 48.6	+61°54'	77.3	+ 2.7	24.4	0.044	71	95	O8	8.00	+0.54	-0.47	2.55	5.45	-5.1	10.6	0.017
1168	216629	+61°2361	22 49.4	+61°36'	77.2	+ 2.4	25.2	0.111	105	130	B2 pe	9.30	+0.73	-0.20	2.91	6.39			0.038
1169	216658	+61°2363	22 49.6	+61°36'	77.3	+ 2.3	24.2	0.091	101	125	B0 V	8.89	+0.70	-0.29	3.00	5.89	-4.1	10.0	0.030
1170	216711	+61°2364	22 50.0	+62°04'	77.5	+ 2.7	24.1	0.047	86	110	B1 V	9.05	+0.62	-0.33	2.64	6.41	-3.1	9.5	0.018
1171		+55°2840	22 51.0	+55°51'	75.1	- 3.0	23.9	0.064	46	70	O7.5 p	10.01	+0.45	-0.56	2.31	7.70	-5.1	12.8	0.028
1172		+56°2903	22 51.6	+57°04'	75.7	- 1.9	23.7	0.063	59	83	B0.5: IV:	10.12	+0.22	-0.67	1.50	8.62	-4.2	12.8	0.042
1173	216898	+61°2370	22 51.8	+61°46'	77.6	+ 2.4	23.7	0.085	85	109	O8	8.00	+0.53	-0.48	2.52	5.48	-5.1	10.6	0.034
1174	216927	+58°2511	22 52.0	+58°22'	76.2	- 0.7	23.6	0.040	39	63	B9 Ia	8.31	+0.86	+0.05	2.76	5.55	-6.9	12.4	0.014
1175		+63°1907	22 52.5	+63°56'	78.5	+ 4.3	23.6	0.080	40	64	B1 Ia	9.08	+0.85	-0.21	3.33	5.75	-6.9	12.6	0.024
1176	217035	+62°2136	22 52.6	+62°19'	77.9	+ 2.9	23.5	0.037	91	115	B0 V	7.74	+0.46	-0.54	2.28	5.46	-4.1	9.6	0.016
1177	217061	+61°2372	22 52.8	+62°05'	77.8	+ 2.6	23.5	0.030	87	110	B1 V	8.77	+0.69	-0.25	2.85	5.92	-3.1	9.0	0.010
1178	217086	+61°2373	22 53.0	+62°12'	77.9	+ 2.7	23.4	0.024	93	116	O5	7.64	+0.63	-0.43	2.85	4.79	-5.1	9.9	0.008
1179	217312	+62°2147	22 54.8	+62°32'	78.2	+ 3.0	23.1	0.028	80	103	B0 IV	7.39	+0.39	-0.55	2.07	5.32	-4.6	9.9	0.014
1180	217463	+62°2152	22 55.8	+62°14'	78.2	+ 2.6	22.8	0.016	93	116	B2 V	8.99	+0.54	-0.35	2.34	6.65	-2.0	8.6	0.007
1181	217490	+58°2521	22 56.0	+59°05'	77.0	- 0.3	22.8	0.074	51	74	B0.5 Ia	8.73	+0.80	-0.27	3.24	5.49	-6.9	12.4	0.023
1182	E 240160	+56°2928	22 57.4	+56°27'	76.2	- 2.8	22.5	0.058	75	98	O9	10.02	+0.48	-0.52	2.37	7.65	-4.6	12.2	0.024
1183		+56°2929	22 57.5	+56°30'	76.2	- 2.8	22.5	0.049	63	86	B2 V: nn	10.32	+0.27	+0.43	1.53	8.79	-2.0	10.8	0.032
1184		+56°2930	22 57.8	+57°00'	76.4	- 2.3	22.4	0.080	76	98	B1 IV	9.68	+0.37	-0.51	1.89	7.79	-3.8	11.6	0.042
1185	E 240165	+56°2931	22 58.0	+56°39'	76.3	- 2.6	22.4	0.061	78	100	O9.5 V	10.13	+0.47	-0.53	2.31	7.82	-4.4	12.2	0.026
1186	E 240168	+55°2878	22 58.2	+56°04'	76.1	- 3.2	22.4	0.037	37	59	B1 III	9.17	+0.55	-0.39	2.43	6.74	-4.4	11.1	0.015
1187	E 240171	+56°2934	22 58.5	+56°36'	76.3	- 2.7	22.3	0.045	66	88	B1 V	9.90	+0.18	-0.65	1.32	8.58	-3.1	11.7	0.034
1188	217919	+62°2161	22 59.0	+63°10'	78.9	+ 3.3	22.2	0.015	64	86	B0 IV: n	8.24	+0.62	-0.30	2.76	5.48	-4.6	10.1	0.005
1189		+57°2678	22 59.4	+57°46'	76.9	- 1.7	22.1	0.063	64	86	B0.5 V	9.79	+0.48	-0.49	2.28	7.51	-3.6	11.1	0.028
1190	218066	+62°2163	23 00.0	+62°51'	78.9	+ 3.0	21.9	0.015	37	59	B1: V:	7.62	+0.40	-0.52	1.98	5.64	-3.1	8.7	0.008

TABLE 5—Continued

No.	HD	BD	1900 α	1900 δ	l	b	φ	p	θ	θ'	Spectrum	V	B-V	U-B	$3E_{(B-V)}$	m	M	m-M	p/A_v
			h m																
1191	216195	+57°2689	23 01.0	+57°43'	77.1	- 1.8	21.7	0.055	70	92	O8	8.34	+0.27	-0.70	1.74	6.60	-5.1	11.7	0.032
1192	218323	+63°1928	23 02.0	+63°46'	79.4	+ 3.8	21.5	0.041	68	90	B0.5 II	7.62	+0.59	-0.39	2.61	5.01	-5.2	10.2	0.016
1193	218342	+62°2170	23 02.1	+62°41'	79.0	+ 2.8	21.5	0.041	58	80	B0 IV	7.38	+0.41	-0.55	2.13	5.25	-4.6	9.8	0.019
1194	218376	+58°2545	23 02.4	+58°53'	77.7	- 0.8	21.4	0.019	71	92	B0.5 IV	4.84	-0.04	-0.87	0.72	4.12	-4.2	8.3	0.026
1195		+55°2899	23 02.7	+55°28'	76.5	- 4.0	21.4	0.027	63	84	B1 III p	10.21	+0.14	-0.67	1.20	9.01	-4.4	13.4	0.022
1196	E 236044	+53°3076	23 02.7	+54°13'	76.0	- 5.1	21.4	0.035	64	85	B1 V	9.60	+0.20	-0.66	1.38	8.22	-3.1	11.3	0.025
1197		+58°2549	23 04.5	+58°35'	77.8	- 1.2	20.9	0.097	75	96	B0 III	10.31	+0.72	-0.26	3.06	7.25	-5.0	12.2	0.032
1198		+60°2493	23 05.4	+60°56'	78.8	+ 1.0	20.8	0.070	106	127	B0.5 pe*	9.42	+0.84	-0.30	3.36	6.06			0.021
1199	218915	+52°3383	23 06.7	+52°31'	76.0	- 6.9	20.6	0.025	53	84	O9 I	7.20	+0.02	-0.90	0.99	6.21	-6.9	13.1	0.025
1200		+59°2664	23 07.0	+60°03'	78.6	+ 0.1	20.4	0.066	67	87	B1.5 II	9.71	+0.83	-0.20	3.24	6.47	-4.8	11.3	0.020
1201	219287	+58°2565	23 09.6	+58°51'	78.5	- 1.1	19.8	0.023	61	81	B0 Ia	8.91	+1.02	-0.13	3.96	4.95	-6.9	11.8	0.006
1202*			23 10.5	+59°01'	78.7	- 1.0	19.6	0.047	84	103	B0 III*	10.71	+0.68	-0.37	2.94	7.77	-5.0	12.8	0.016
1203	219460	+59°2683	23 10.8	+59°55'	79.0	- 0.2	19.6	0.055	74	94	W R	9.89	+0.62	-0.28					
1204		+61°2408	23 11.1	+61°32'	79.6	+ 1.3	19.5	0.072	93	112	B0 III? p?	9.7*	+0.79	-0.21	3.27	6.43	-5.0	11.4	0.022
1205		+61°2472	23 12.0	+62°12'	79.9	+ 1.9	19.3	0.062	64	83	B5 Ib	9.57	+1.12	+0.11	3.84	5.73	-5.8	11.5	0.016
1206		+63°1962	23 12.8	+63°15'	80.4	+ 2.9	19.2	0.053	63	82	B1 III	8.40	+0.32	-0.56	1.74	6.66	-4.4	11.1	0.030
1207*			23 12.8	+61°20'	79.7	+ 1.1	19.2	0.051	105	124	B0.5 Ib:	10.23	+1.00	-0.09	3.84	6.39	-5.8	12.2	0.013
1208*			23 13.0	+59°29'	79.2	- 0.7	19.1	0.008	39	58	B0.5 V	10.89	+0.46	-0.48	2.22	8.67	-3.6	12.3	0.004
1209		+63°1964	23 13.1	+63°34'	80.5	+ 3.2	19.1	0.089	63	82	B0 II	8.46	+0.71	-0.38	3.03	5.43	-5.4	10.8	0.029
1210	E 240250	+59°2695	23 13.6	+59°19'	79.2	- 0.9	19.0	0.067	90	109	B9 Iab	8.81	+0.65	+0.02	2.13	6.68	-6.5	13.2	0.031
1211		+62°2210	23 14.3	+62°56'	80.4	+ 2.5	18.8	0.144	74	93	B9 Ia	8.42	+1.15	+0.32	3.63	4.79	-6.9	11.7	0.040
1212	220116	+57°2724	23 16.1	+57°43'	78.9	- 2.5	18.5	0.090	81	99	B0.5 V pe	8.69	+0.59	-0.43	2.61	6.08	-3.6	9.7	0.034
1213		+60°2522	23 16.2	+60°38'	79.9	+ 0.3	18.4	0.033	63	81	O7 f	8.67	+0.41	-0.62	2.19	6.48			0.015
1214		+58°2580	23 16.7	+58°25'	79.3	- 1.9	18.3	0.094	75	93	B0.5 V:	10.10	+0.80	-0.27	3.24	6.86	-3.6	10.5	0.029
1215		+60°2525	23 17.3	+60°18'	79.9	- 0.1	18.2	0.029	62	80	B0 III-IV	9.64	+0.30	-0.64	1.80	7.84	-4.8	12.6	0.016
1216		+59°2707	23 17.7	+59°49'	79.8	- 0.6	18.1	0.028	77	95	B9: V:	9.84	+0.08	-0.11	0.42	9.42	+1.0	8.4	0.067
1217*			23 18.4	+61°35'	80.5	+ 1.1	17.9	0.065	86	104	O8 (f)	10.80	+0.75	-0.35	3.18	7.62			0.020
1218		+59°2719	23 20.9	+60°06'	80.3	- 0.4	17.4	0.037	136	154	B2 III:	10.63	+0.65	-0.28	2.67	7.96	-3.6	11.6	0.014
1219	220770	+60°2539	23 21.4	+60°53'	80.6	+ 0.3	17.3	0.048	69	86	A5 Ib	7.84	+0.80	+0.48	1.95	5.89			0.025
1220		+60°2542	23 22.6	+60°50'	80.7	+ 0.2	17.0	0.039	67	84	A2 Ib	8.81	+0.66	+0.19	1.80	7.01	-5.6	12.6	0.022
1221		+60°2553	23 24.1	+60°45'	80.9	+ 0.1	16.7	0.028	72	89	B2 II	10.08	+0.45	-0.43	2.07	8.01	-4.7	12.7	0.014
1222		+59°2735	23 25.5	+59°18'	80.6	- 1.3	16.4	0.100	63	80	B0 Ib	9.89	+1.16	-0.04	4.38	5.51	-6.2	11.7	0.023
1223		+60°2581	23 30.5	+60°51'	81.6	0.0	15.3	0.054	60	75	B3 V	10.60	+0.64	-0.09	2.52	8.08	-1.5	9.6	0.021
1224		+60°2582	23 30.9	+60°22'	81.6	- 0.5	15.2	0.068	73	88	B8 Iab	8.68	+0.77	+0.01	2.58	6.10	-6.5	12.6	0.026
1225		+60°2584	23 31.0	+60°38'	81.7	- 0.3	15.2	0.049	59	74	B1 pe (III-V)	10.29	+0.53	-0.58	2.37	7.92	-3.8	11.7	0.021

TABLE 5—Concluded

No.	HD	BD	1900 α	1900 δ	l	b	φ	p	θ	θ'	Spectrum	V	B-V	U-B	$3E_{(B-V)}$	m	M	m-M	p/A_V
1226*			$23^h38.^m6$	+60°57'	82.6	- 0.2	13.5	0.062	62	75	B0.5 IV	9.78	+0.53	-0.45	2.43	7.35	-4.2	11.6	0.026
1227		+61°2509	23 39.0	+61°36'	82.8	+ 0.4	13.4	0.048	77	90	B0.5 Ib	8.42	+0.46	-0.55	2.22	6.20	-5.8	12.0	0.022
1228		+60°2615	23 39.9	+61°07'	82.8	0.0	13.2	0.030	70	83	B0.5 Ib	9.10	+0.60	-0.45	2.64	6.46	-5.8	12.3	0.011
1229		+61°2515	23 40.9	+61°43'	83.1	+ 0.5	13.0	0.061	84	97	B0.5 V	9.95	+0.43	-0.51	2.13	7.82	-3.6	11.4	0.029
1230		+62°2296	23 42.4	+62°40'	83.4	+ 1.4	12.7	0.057	115	128	B3 Ia?	8.65	+1.09	+0.06	3.87	4.78	-6.9	11.7	0.015
1231		+61°2526	23 42.8	+61°29'	83.2	+ 0.2	12.6	0.024	90	103	B2 Ib	8.77	+0.39	-0.50	1.89	6.88	-5.8	12.7	0.013
1232		+62°2299	23 43.1	+62°50'	83.6	+ 1.5	12.5	0.023	174	7	O8	9.58	+0.61	-0.47	2.76	6.82	-5.1	11.9	0.008
1233		+61°2529	23 43.6	+61°26'	83.2	+ 0.2	12.4	0.034	88	100	B1 Ib	8.65	+0.53	-0.47	2.37	6.28	-5.8	12.1	0.014
1234	223387	+56°3094	23 44.0	+56°40'	82.3	- 4.5	12.4	0.051	68	80	B pe	8.80	+0.21	-0.79					
1235	223385	+61°2533	23 44.0	+61°40'	83.4	+ 0.4	12.3	0.026	57	69	A3 Ia+	5.42	+0.66	-0.02	1.71	3.71			0.015
1236		+62°2313	23 46.9	+62°45'	84.0	+ 1.4	11.7	0.035	79	91	B3 Ib	8.82	+0.49	-0.25	2.07	6.75	-5.8	12.6	0.017
1237		+61°2550	23 47.3	+61°34'	83.8	+ 0.2	11.6	0.029	62	74	B0 IV	9.29	+0.33	-0.63	1.89	7.40	-4.6	12.0	0.015
1238		+61°2559	23 48.6	+61°52'	84.0	+ 0.5	11.3	0.043	65	76	O9 V	9.72	+0.29	-0.66	1.80	7.92	-4.6	12.5	0.024
1239	223924	+56°3106	23 48.6	+56°16'	82.9	- 5.0	11.4	0.035	64	75	B1.5 V	8.24	+0.02	-0.71	0.81	7.43	-2.6	10.0	0.043
1240		+62°2320	23 48.8	+62°40'	84.2	+ 1.2	11.3	0.049	77	88	B2 V	10.08	+0.37	-0.49	1.83	8.25	-2.0	10.2	0.027
1241	223960	+60°2636	23 48.9	+60°18'	83.7	- 1.1	11.3	0.067	80	91	A0 Ia+	6.91	+0.71	-0.05	2.13	4.78			0.031
1242	223987	+60°2637	23 49.2	+61°03'	83.9	- 0.4	11.2	0.055	70	81	B1.5 Ib	7.54	+0.51	-0.49	2.28	5.26	-5.8	11.1	0.024
1243	224055	+61°2562	23 49.7	+61°17'	84.0	- 0.1	11.1	0.088	67	78	B3 Ia	7.17	+0.71	-0.22	2.73	4.44	-6.9	11.3	0.032
1244	224151	+56°3115	23 50.5	+56°53'	83.2	- 4.5	10.9	0.020	87	98	B0.5 II	6.00	+0.22	-0.72	1.50	4.50	-5.2	9.7	0.013
1245	224257	+55°3051	23 51.3	+55°26'	83.1	- 5.9	10.8	0.033	66	77	B0 IV	7.98	-0.06	-0.89	0.72	7.26	-4.6	11.9	0.046
1246*			23 51.7	+60°40'	84.1	- 0.8	10.7	0.054	89	100	B1 ne (V)	9.84	+0.43	-0.52	2.07	7.77	-3.1	10.9	0.026
1247		+62°2329	23 51.7	+62°56'	84.6	+ 1.4	10.7	0.077	70	81	B5 V	10.13	+0.40	-0.22	1.68	8.45	-0.9	9.4	0.046
1248		+66°1661	23 52.4	+67°00'	85.4	+ 5.4	10.5	0.087	89	100	O9 V	8.72	+0.81	-0.20	3.36	5.36	-4.6	10.0	0.026
1249	224424	+58°2676	23 52.7	+59°09'	84.0	- 2.3	10.4	0.044	48	58	B1 Iab	8.09	+0.73	-0.22	2.97	5.12	-6.5	11.6	0.015
1250	224425	+56°3119	23 52.7	+56°34'	83.5	- 4.9	10.4	.004			A2: V:*	7.30	+0.22	+0.15	0.48	6.82	+2.0	8.8	
1251*			23 53.7	+60°36'	84.3	- 0.9	10.2	0.046	85	95	B1 V	10.22	+0.29	-0.59	1.65	8.57	-3.1	11.7	0.028
1252	E 240464	+59°2799	23 53.7	+59°43'	84.2	- 1.8	10.2	0.032	73	83	O9 V	9.59	+0.31	-0.61	1.86	7.73	-4.6	12.3	0.017
1253	224599	+59°2801	23 54.1	+59°29'	84.2	- 2.0	10.1	0.030	21	31	B0.5: V: pnne	9.55	+0.42	-0.53	2.10	7.45	-3.6	11.0	0.014
1254	224905	+59°2813	23 56.6	+59°54'	84.6	- 1.7	9.6	0.024	101	111	B1 V n	8.47	+0.15	-0.56	1.23	7.24	-3.1	10.3	0.020
1255		+66°1675	23 57.0	+66°51'	85.8	+ 5.2	9.5	0.113	106	116	O7	9.05	+1.09	+0.04	4.23	4.82	-5.1	9.9	0.027
1256		+62°2353	23 57.2	+62°20'	85.1	+ 0.8	9.4	0.060	74	83	B3 II	9.87	+0.24	-0.60	1.32	8.55	-4.6	13.2	0.045
1257	225094	+62°2356	23 58.3	+63°05'	85.3	+ 1.5	9.2	0.050	75	84	B3 Ia	6.24	+0.33	-0.54	1.59	4.65	-6.9	11.6	0.031
1258	225146	+60°2663	23 58.8	+60°33'	85.0	- 1.1	9.1	0.068	72	81	B0 Ib p	8.60	+0.38	-0.64	2.04	6.56	-6.2	12.8	0.033
1259	225160	+61°2585	23 58.9	+61°40'	85.1	+ 0.1	9.1	0.053	92	101	O8 f	8.19	+0.27	-0.72	1.74	6.45			0.030

FOOTNOTES

Catalogue Number	
3	No. 40 Reference 1. May be variable in magnitude.
4	No. 41 Reference 1.
6	Strong Fe II emission.
13	A 1952, August 21 observation gave V = 9.01, B-V = +0.16, U-B = -0.71. A 1952, September 10 observation gave V = 8.80, B-V = +0.23, U-B = -0.80. The data in the table refers to three concordant 1954 observations.
14	Shell spectrum? Like 27 C Ma? He I 3964 very strong.
29	No. 1 Reference 9.
31	No. 2 Reference 9.
33	No. 3 Reference 9.
37	No. 4 Reference 9.
44	No. 1 Reference 5.
46	No. 89 Reference 8. Very strong Fe II emission.
48	No. 5 Reference 9.
51	No. 6 Reference 9.
53	No. 89 Reference 8.
55	No. 7 Reference 9.
56	Also No. 8 Reference 9.
57	No. 9 Reference 9.
58	No. 102 Reference 8.
59	No. 103 Reference 8.
61	No. 106 Reference 8.
62	No. 108 Reference 8.
63	No. 110 Reference 8. Strong 4430.
65	No. 10 Reference 9.
66	No. 11 Reference 9.
67	No. 2 Reference 5.
69	Five photometric observations gave extreme values in V of 9.79 and 9.94.
74	No. 12 Reference 9.
76	No. 13 Reference 9.
78	No. 14 Reference 9.
79	No. 15 Reference 9.
81	No. 2 Reference 6.
85	No. 1 Reference 2.
86	No. 3 Reference 6.
88	No. 16 Reference 9.
89	No. 17 Reference 9.
91	No. 18 Reference 9.
93	No. 19 Reference 9.
94	No. 20 Reference 9.
96	No. 21 Reference 9.
97	No. 2 Reference 2.
102	No. 5 Reference 6.
112	Shell

FOOTNOTES—Continued

Catalogue Number	
116	No. 10 Reference 6.
117	No. 11 Reference 6.
118	No. 12 Reference 6.
119	No. 13 Reference 6.
123	No. 14 Reference 6.
142	No. 20 Reference 6.
146	No. 21 Reference 6.
148	This star is recorded as No. 80, spectral type O6 f p, in Morgan, Code and Whitford (1955) and as anonymous No. 4 in Nassau and Morgan (1951).
153	No. 22 Reference 6.
164	No. 24 Reference 6.
186	B pnne or A pnne shell?
188	No. 3 Reference 2.
190	Moonlight on spectrogram.
193	No. 5 Reference 2.
197	No. 31 Reference 6.
198	No. 32 Reference 6.
200	No. 33 Reference 6.
201	No. 34 Reference 6.
206	Shell at Hδ? 4481 too strong.
207	Fainter than 10 Lac.
215	No. 6 Reference 2.
216	No. 36 Reference 6.
233	No. 7 Reference 2.
242	O II weak.
252	No. 8 Reference 2.
259	No. 39 Reference 6.
261	No. 40 Reference 6.
283	A type companion of BD +58°451.
298	No. 22 Reference 9.
300	H lines very broad.
301	No. 5 Reference 5.
305	No. 9 Reference 2.
309	No. 10 Reference 2.
311	No. 11 Reference 2.
322	No. 12 Reference 2.
335	Northern and preceeding companion of BD +60°512.
352	Luminosity V at 4650. I a-b at 4100.
366	No. 23 Reference 9.
370	No. 24 Reference 9.
371	No. 13 Reference 2.
374	K weak.
379	Variable, CC Cas.
404	No. 14 Reference 2.
405	No. 6 Reference 5.

Catalogue Number	
412	No. 7 Reference 5.
419	No. 15 Reference 2. Two line binary?
420	Ia from N III, C III weak.
440	No. 16 Reference 2.
446	No. 17 Reference 2. Moonlight on spectrogram.
461	4650 weak.
468	Fainter, following star is gG8.
497	No. 18 Reference 2.
498	No. 19 Reference 2.
504	Shell
505	Shell
510	No. 20 Reference 2.
523	No. 21 Reference 2.
524	No. 22 Reference 2.
537	Very strong H and K. K.
543	No. 23 Reference 2.
555	High excitation emission superposed on about O9.
566	No. 25 Reference 2.
569	Shell
573	No. 26 Reference 2.
587	No. 27 Reference 2.
591	No. 28 Reference 2.
600	No. 29 Reference 2.
652	No. 33 Reference 7.
655	No. 34 Reference 7.
661	No. 35 Reference 7.
662	No. 30 Reference 7.
668	No. 37 Reference 7.
673	No. 36 Reference 7.
675	No. 38 Reference 7.
731	Moonlight on spectrogram.
760	No. 2 Reference 10.
775	Probably variable 1952, August 22 V = 9.77, B-V = +0.86, U-B = -0.12. 1952, September 8 V = 9.92, B-V = +0.87, U-B = -0.12.
803	Strong H emission.
831	Weak K line.
854	Weak K line.
867	Probably variable 1954, July 30 V = 7.94, B-V = +0.40, U-B = -0.57. 1954 July 31 V = 8.14, B-V = +0.42, U-B = -0.56.
928	Variable. V 444 Cygni.
952	No. 14 Reference 3, MWC 342, very strong emission of H and Fe II.
960	No. 16 Reference 3.
970	No. 17 Reference 3.

FOOTNOTES—Concluded

Catalogue Number	
972	No. 19 Reference 3.
977	Similar to 27 C Ma?
988	No. 2 in VI Cyg, Reference 11.
992	No. 12 in VI Cyg, Reference 12. Faint companion not included in photometric observations.
993	No. 6 in VI Cyg, Reference 11.
995	No. 9 in VI Cyg, Reference 11.
997	No. 7 in VI Cyg, Reference 11.
1016	Probably 2-line binary.
1018	No. 44 Reference 1.
1035	No. 4 Reference 1.
1042	No. 7 Reference 1.
1043	Shell. May be variable in magnitude.
1051	P Cygni spectrum.
1055	No. 9 Reference 1.
1070	No. 47 Reference 1.
1095	No. 49 Reference 1.
1098	No. 50 Reference 1.
1100	No. 17 Reference 1.
1106	No. 52 Reference 1. Two line binary. 0.2 mag fainter on 1953, June 30.
1115	No. 18 Reference 1. May be variable in magnitude.
1117	No. 20 Reference 1.
1118	No. 21 Reference 1.
1124	No. 55 Reference 1. Moonlight on spectrogram.
1134	No. 25 Reference 1.
1137	No. 58 Reference 1.
1140	No. 59 Reference 1.
1143	Preceeding.
1144	Following.
1145	No. 62 Reference 1.
1147	Variable in magnitude and spectrum. CQ Cep.
1160	No. 65 Reference 1.
1161	Variable. A H Cep.
1198	All lines very weak.
1202	No. 30 Reference 1. H and K very strong.
1207	No. 32 Reference 1.
1208	No. 68 Reference 1.
1217	No. 70 Reference 1.
1226	No. 36 Reference 1.
1246	No. 38 Reference 1.
1250	This star was incorrectly recorded in Ap. J. 114, p 258 as HD 224436.
1251	No. 39 Reference 1.

REFERENCES FOR TABLE 5

Reference 1. Gonzalez, G. and Gonzalez, G. 1952, Bol. Obs. Ton.y Tac., No. 5, pp.1 - 7.
Reference 2. Gonzalez, G. and Gonzalez, G. 1953, ibid, No. 7, pp. 3 - 10.
Reference 3. Nassau, J. J., and Harris, Daniel III, 1952, Ap. J. 115, 459-474. Table I.
Reference 4. Munch, Luis. 1953, Bol. Obs. Ton. y Tac., No. 7, pp. 23 - 32.
Reference 5. Nassau, J. J. and Morgan, W. W. 1951, Ap. J. 113, 149.
Reference 6. Gonzales, G. and Gonzalez, G. 1954, Bol. Obs. Ton. y Tac., No. 9, pp. 26 - 27.
Reference 7. Morgan, W. W., Gonzalez, G. and Gonzalez, G. 1953, Ap. J. 118, 345 - 346.
Reference 8. Munch, Luis. 1954, Bol. Obs. Ton. y Tac., No. 10, pp. 28 - 40.
Reference 9. Hiltner, W. A. Table 1 of this publication.
Reference 10. Hiltner, W. A. and Iriarte, B. 1955, Ap. J. 121, 556.
Reference 11. Munch, Luis and Morgan, W. W. 1953, 118, 161.
Reference 12. Morgan, W. W., Johnson, H. L., Roman, Nancy G., 1954, PASP 66, 85.

Column 16.—This column is a computation of the interstellar absorption at that wave length corresponding to the V magnitude. The normal colors adopted are those given in Table 6. A uniform ratio of total to selective absorption of 3 (Hiltner and Johnson 1956) was assumed for all galactic longitudes and latitudes.

Column 17.—This gives the magnitude corrected for interstellar absorption found in column 16.

Column 18.—The absolute magnitudes assumed here are based on the tentative calibration published earlier (Johnson and Hiltner 1956). Blaauw (1956) has shown that the observed luminosity of the early-type stars, especially B2 and B3, is dependent upon whether the star is a member of an association or a field star. Here, however, we have made no corrections for such evolutionary effects.

Column 19.—This column gives the distance modulus of the individual stars.

Column 20.—The astrophysically important quantity—the ratio of interstellar polarization to interstellar absorption—is given in this column. It is, of course, the ratio of columns 9 and 16.

TABLE 6

NORMAL COLORS OF O AND B STARS

Spectral Type	$(B-V)_0$	Spectral Type	$(B-V)_0$	Spectral Type	$(B-V)_0$
O5	−0.32	B0.5	−0.28	B9	−0.06
O6	− .32	B1	− .26	B9.5	− .03
O7	− .32	B2	− .24	A0	.00
O8	− .31	B3	− .20	A1	+ .03
O9	− .31	B5	− .16	A2	+ .06
O9.5	− .30	B6	− .14	A3	+ .09
B0	−0 30	B7	− .12	A5	+0.15
		B8	−0.09		

DISCUSSION

Distribution of the Stars

The distribution of the stars in the catalogue is shown in Figures 6, 7, and 8. In the upper part of each figure the stars have been plotted in galactic co-ordinates. Only those stars in the catalogue with galactic latitude from −6° to +6° are on the diagram. Although these data are not free of observational selection, because of the available telescope time and other factors, the well-known regions where few early-type stars are known are well defined: galactic longitudes 350°–25° and from 110° to 130°. Also many associations can be identified, but a discussion of the associations will not be made here. On the lower sections of the three figures are plotted the stars for which distance moduli are available. In general, the observed stars have distance moduli from 10 to 13. To a first approximation the three diagrams appear to show little more than a general scattering, with a few exceptions, notably the double cluster in Perseus. This scatter for individual distance moduli is to be anticipated, since the probable error for the distance modulus of a single star is of the order of 0.5 mag. One interesting feature should be noted in passing: it is the concentration of stars at increasing distance modulus in passing from longitude 105° backward to, say, 70°. At the double cluster the distance modulus is 11.8, but at 70° it has increased to 12.7, corresponding to distances of 2.3 and 3.5 kpc, respectively. There is little doubt that this is evidence of the Perseus spiral arm (see Morgan, Whitford, and Code 1953).

For purposes of analysis the stars in Table 5 were placed in fifteen galactic-longitude groups. Because of the non-uniform distribution of stars in galactic longitude, the

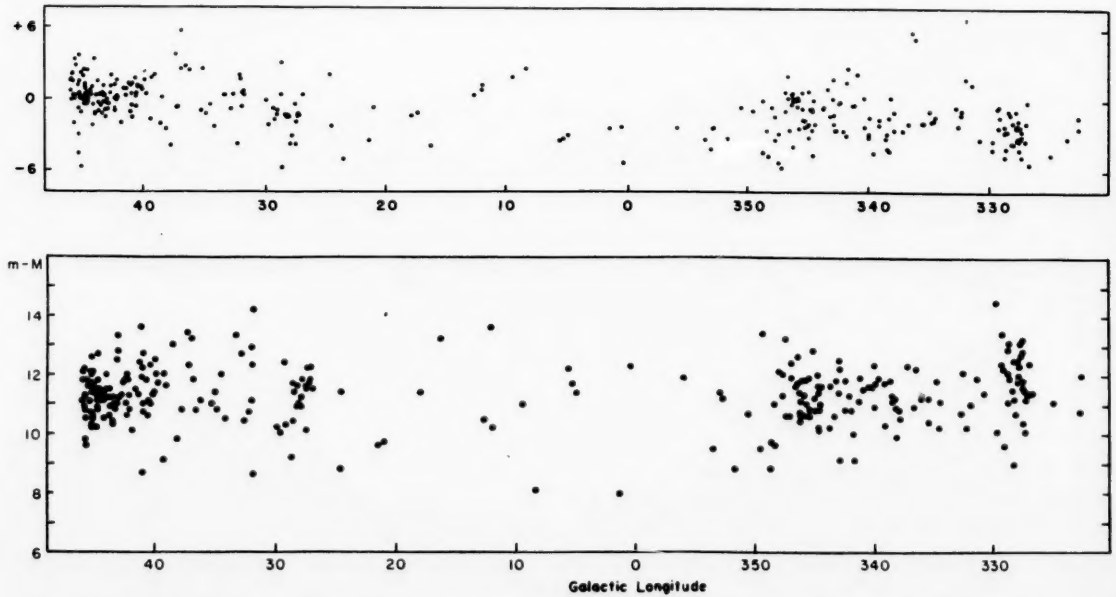

FIG. 6.—Distribution of the stars in the catalogue in galactic co-ordinates, and in galactic longitude and distance modulus. All stars in the catalogue from $l = -6°$ to $l = +6°$ are plotted in the upper figure. The lower figure contains only those stars from $l = -6°$ to $l = +6°$ for which distance moduli are recorded in the table.

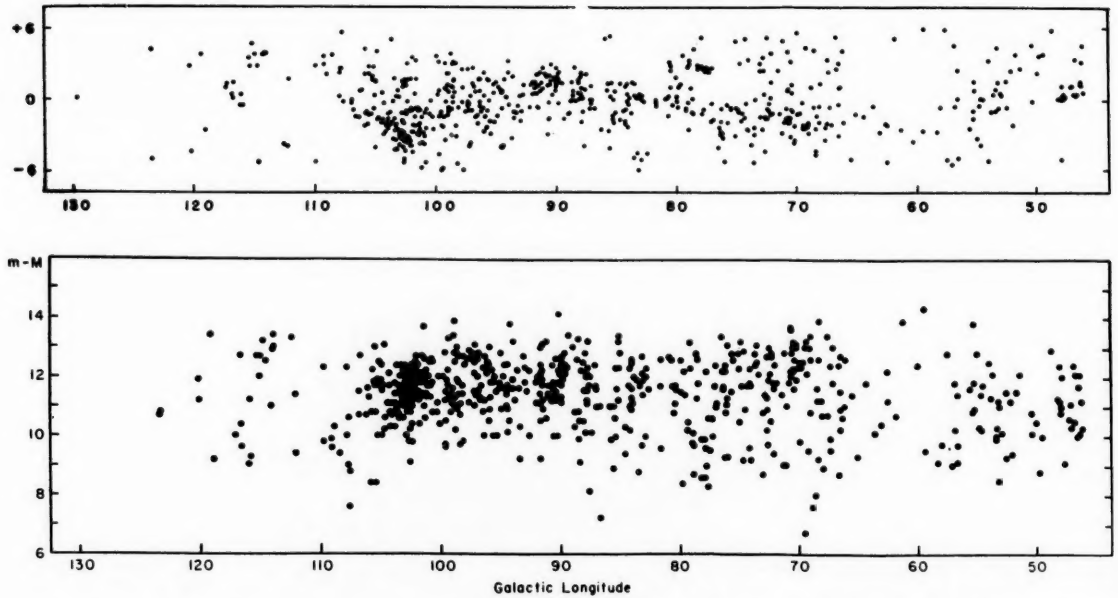

FIG. 7.—Distribution of the stars in the catalogue in galactic co-ordinates and in galactic longitude and distance modulus. All stars in the catalogue from $l = -6°$ to $l = +6°$ are plotted in the upper figure. The lower figure contains only those stars from $l = -6°$ to $l = +6°$ for which distance moduli are recorded in the table.

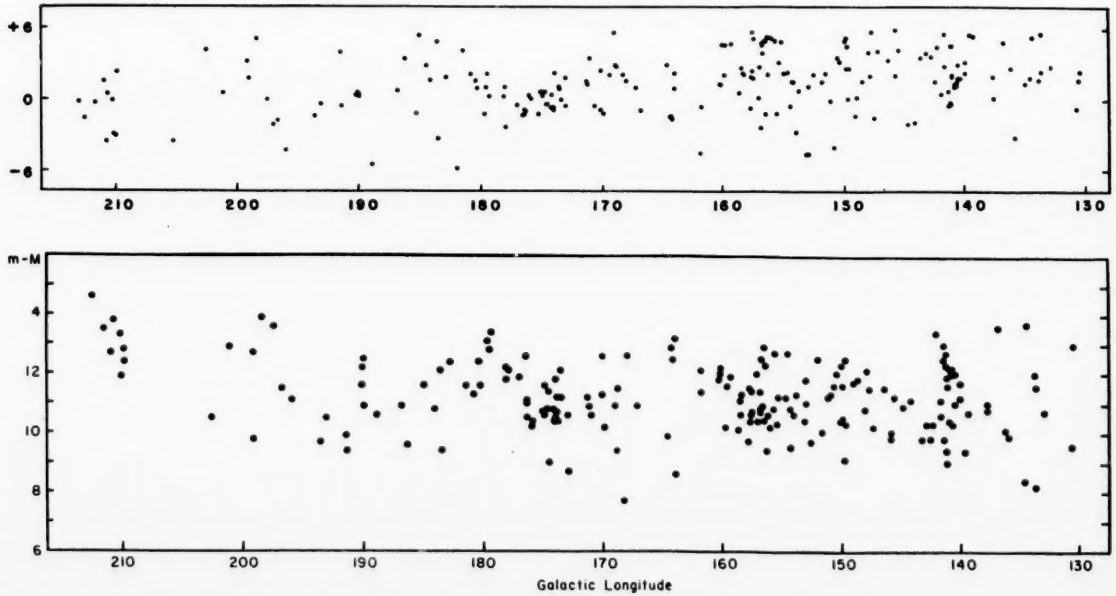

FIG. 8.—Distribution in stars in the catalogue in galactic co-ordinates and in galactic longitude and distance modulus. All stars in the catalogue from $l = -6°$ to $l = +6°$ are plotted in the upper figure. The lower figure contains only those stars from $l = -6°$ to $l = +6°$ for which distance moduli are recorded in the table.

boundary limits in longitude were defined in such a way as to avoid as much as possible large longitude intervals and still have a sufficiently large number of stars in each group to give the statistics some significance. The boundaries of the fifteen groups are given in Table 7, along with the number of stars in each group. In addition, the standard deviation, σ, of the alignment of the electric vector and the average value for the ratio of

TABLE 7

NUMBERS OF STARS, VALUES OF σ AND MEAN RATIOS p/A_v TO GALACTIC-LONGITUDE GROUPS

l	No. of Stars	σ	p/A_v	l	No. of Stars	σ	p/A_v
322°.5–335°	47	0.31	0.025	85° – 95°	130	0.22	0.038
335 –350	83	.88	.014	95 –102.5	158	.10	.045
350 – 25	22	.75	.014				
25 – 40	55	.62	.020	102.5–110	90	.11	.041
40 – 50	124	.77	.012	110 –140	43	.20	.034
				140 –160	87	.27	.028
50 – 65	44	.61	.022	160 –180	51	.43	.020
65 – 75	99	.27	.029	180 –213	34	0.56	0.016
75 – 85	89	0.35	0.023				

interstellar polarization to interstellar absorption are also given in the table for each group. For all groups the galactic-latitude limits were $-6°$ to $+6°$. The discussion of the data in the present paper will be limited to the more general aspects of interstellar polarization.

Alignment of the Electric Vector

The individual stars with galactic latitude between $-6°$ and $+6°$ are shown in Figures 9–21, where each star is represented by a line. The length of the line gives a measure of the relative amount of polarization, and the inclination of the line corresponds to the plane of vibration for that particular star. Few comments need be made regarding these plots. It is well known that the departure from uniform alignment of the electric vector varies appreciably with galactic longitude (Hiltner 1951). Also the average amount of polarization varies with longitude (Hall and Mikesell 1950; Hiltner 1951). In general, the highest polarization is observed in Perseus, and the lowest on either side of this region. However, there is one outstanding exception. The greatest amount of polarization observed thus far is in Cygnus, where normally the smallest average polarization is found. The star with the highest polarization is No. 12 in association VI Cyg. Its interstellar absorption is near 10 mag., and the polarization is 0.22 mag.

The alignment of the electric vector as a function of galactic longitude is illustrated in Figure 22. In this figure, histograms are shown for the fifteen longitude groups where the number of stars are plotted against the position angle. Two extremes are immediately noted, as well as intermediate cases: a flat-top distribution that shows little or no preference for any position angle and a strong concentration at position angle 90°, that is, the electric vector parallel to the galactic plane. The two extremes are well illustrated by the Cygnus region, $l = 40°$–$50°$ (flat-top distribution), and the Cassiopeia-Perseus region, $l = 95°$–$110°$ (concentration at 90°).

The variation in alignment of the electric vector with galactic longitude is also illustrated in Figure 23, where the standard deviation of the alignment, σ, from Table 7 is plotted against longitude. There are several features of this diagram that should be noted. First, there is a well-defined minimum at longitude 102°. Second, the slope from 40° to the minimum at 102° is greater than that from 102° to larger galactic longitudes.

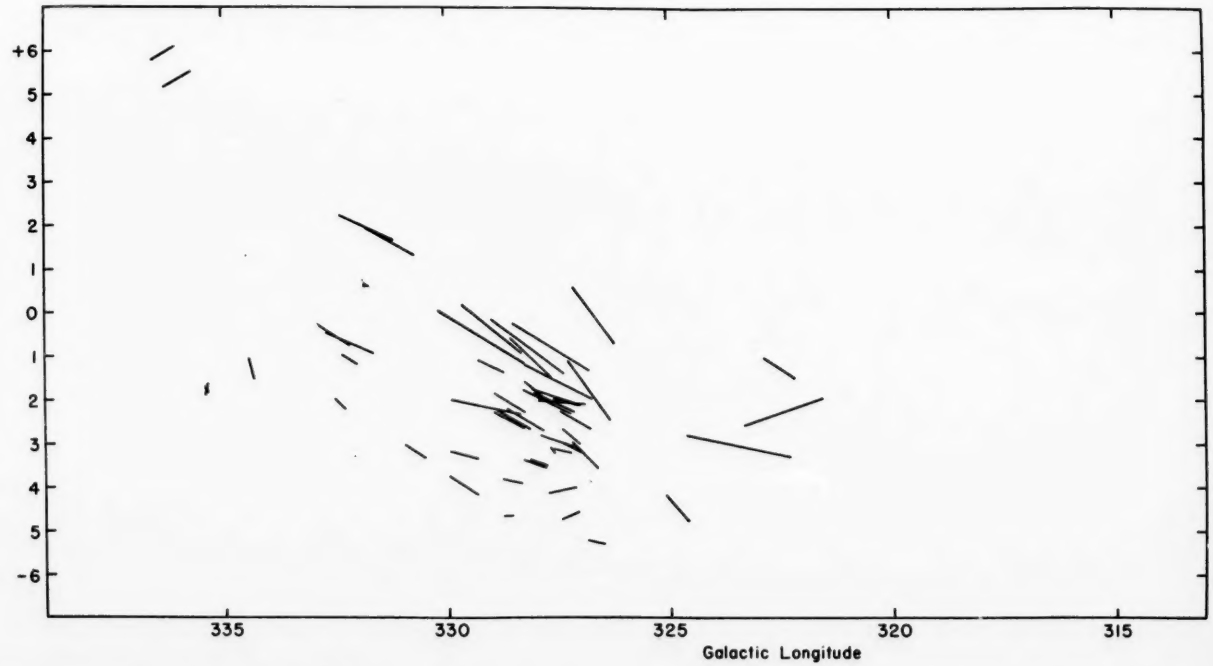

FIG. 9.—Polarization of stars in low galactic latitude. The length of the lines indicates the relative amounts of polarization, and the position angle indicates the plane of vibration.

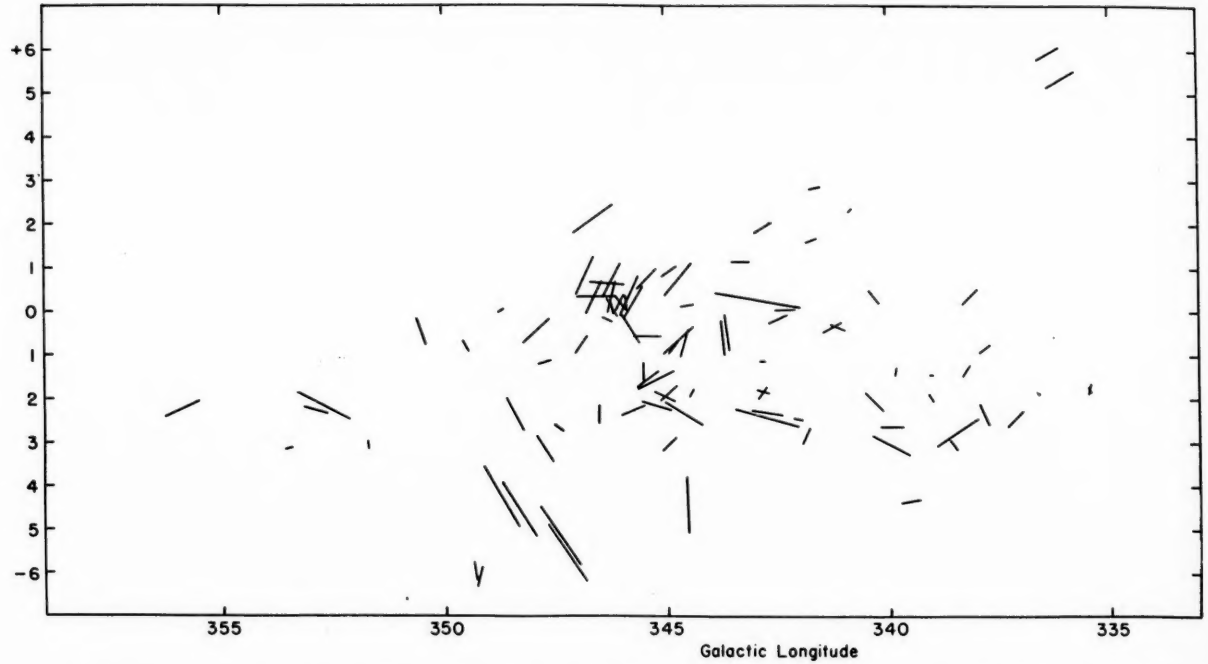

FIG. 10.—Polarization of stars in low galactic latitude. The length of the lines indicates the relative amounts of polarization, and the position angle indicates the plane of vibration.

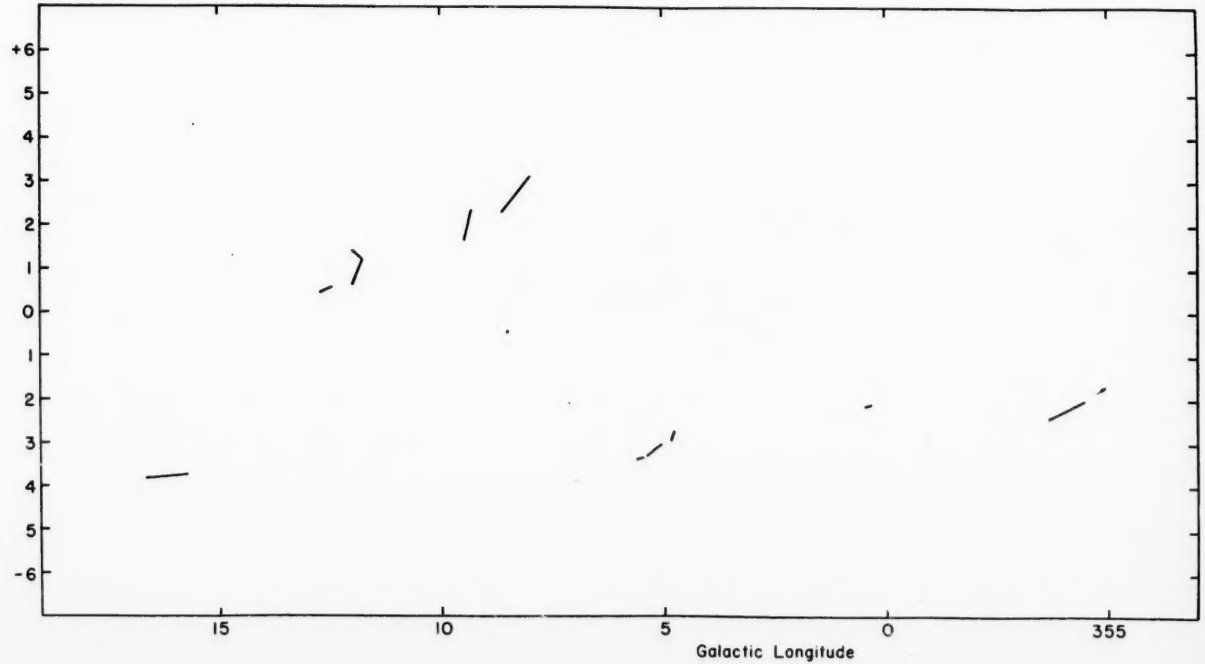

FIG. 11.—Polarization of stars in low galactic latitude. The length of the lines indicates the relative amounts of polarization, and the position angle indicates the plane of vibration.

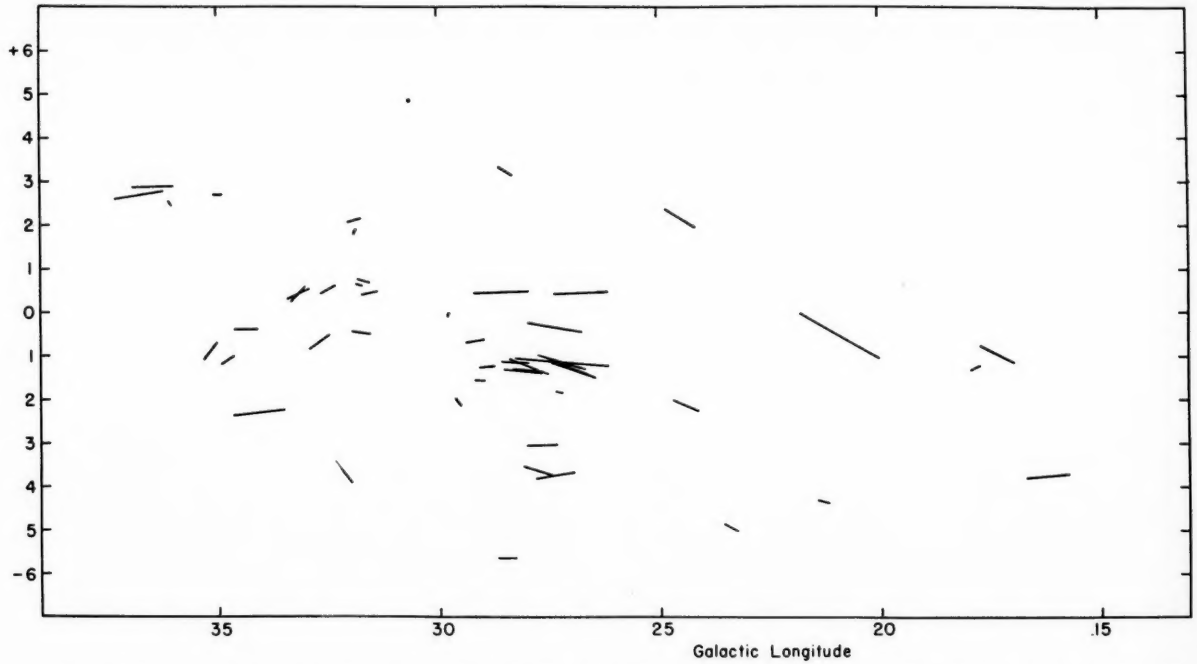

FIG. 12.—Polarization of stars in low galactic latitude. The length of the lines indicates the relative amounts of polarization, and the position angle indicates the plane of vibration.

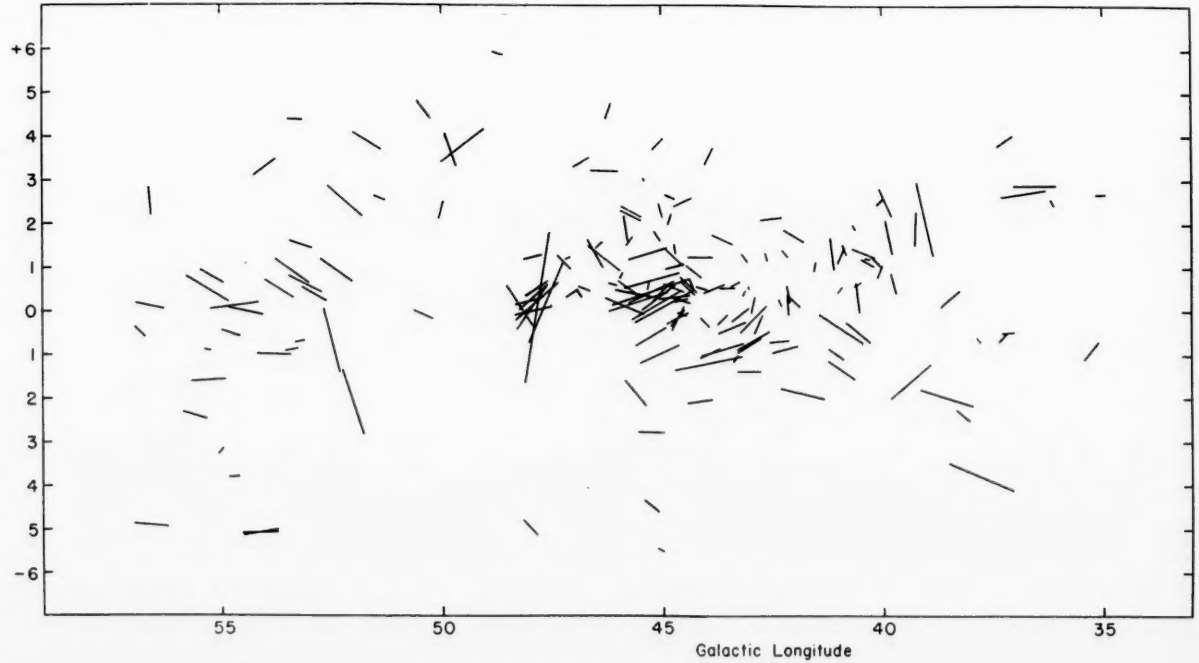

FIG. 13.—Polarization of stars in low galactic latitude. The length of the lines indicates the relative amounts of polarization, and the position angle indicates the plane of vibration. Note the randomness of the plane of vibration. Although, in general, this region has low polarization, the maximum polarization thus far observed is also found in this region.

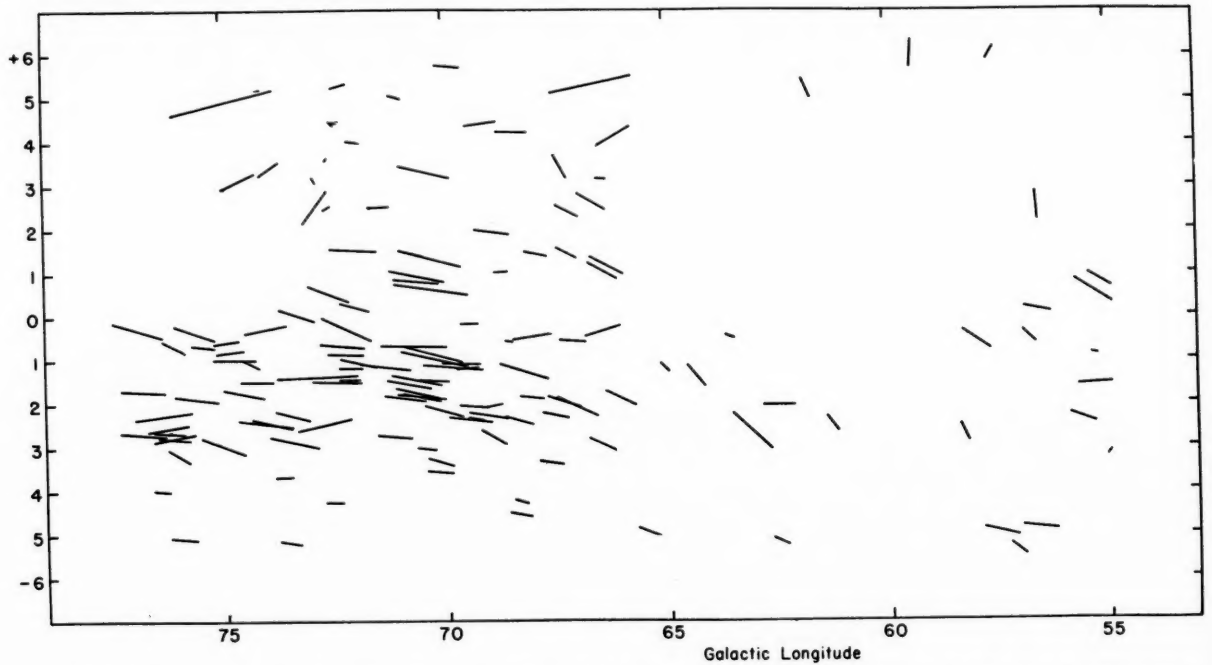

FIG. 14.—Polarization of stars in low galactic latitude. The length of the lines indicates the relative amounts of polarization, and the position angle indicates the plane of vibration.

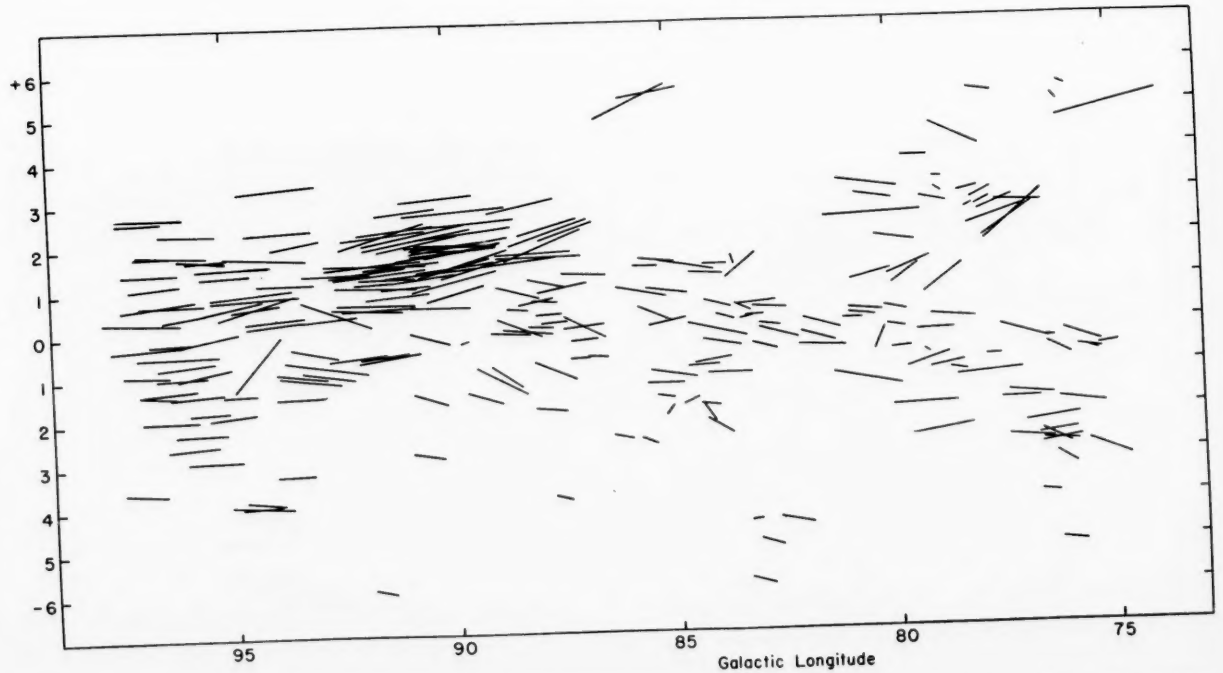

FIG. 15.—Polarization of stars in low galactic latitude. The length of the lines indicates the relative amounts of polarization, and the position angle indicates the plane of vibration.

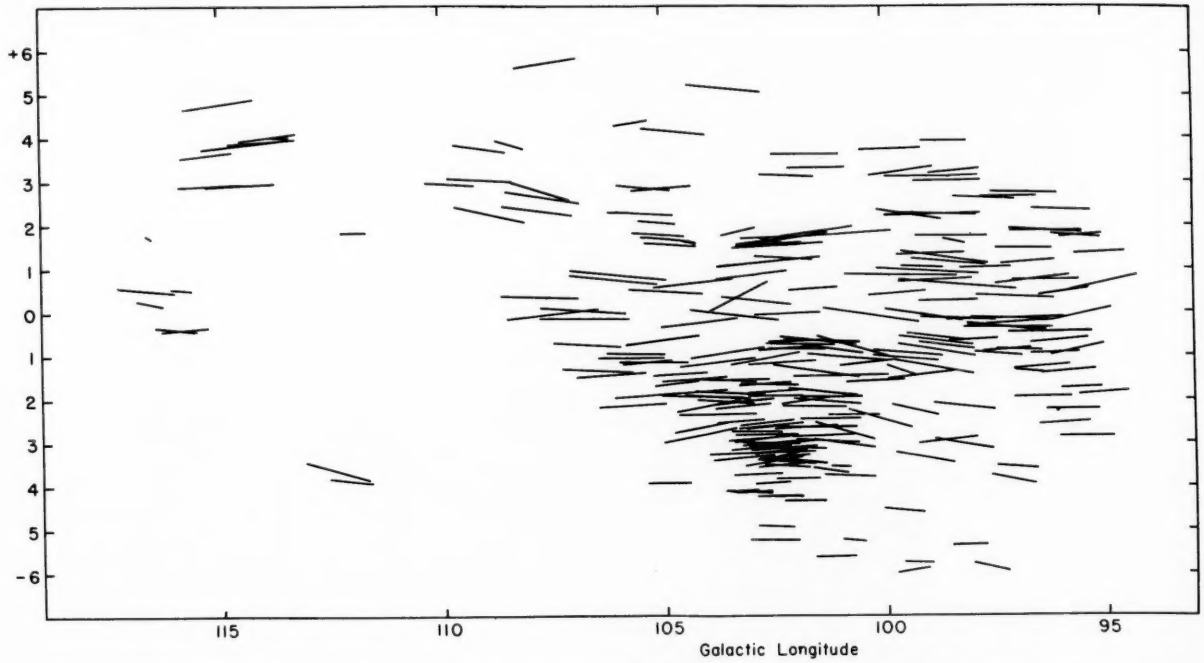

FIG. 16.—Polarization of stars in low galactic latitude. The length of the lines indicates the relative amounts of polarization, and the position angle indicates the plane of vibration. Not all the stars observed in this region are plotted, because of overlap, especially in h and κ Persei.

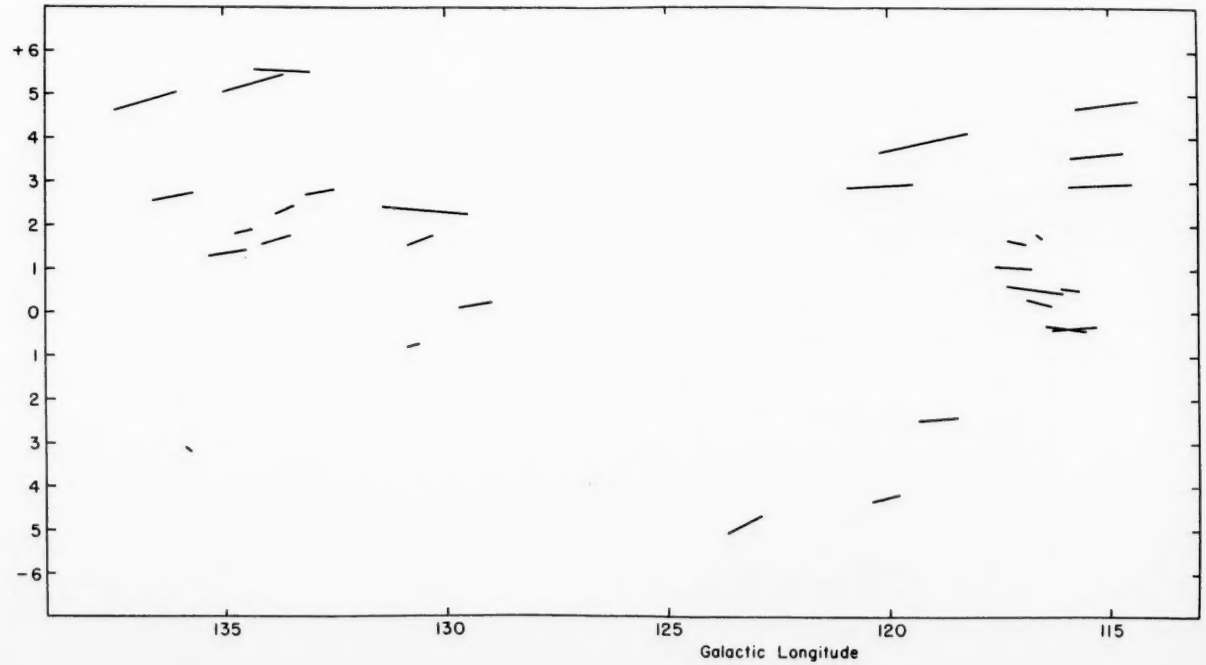

FIG. 17.—Polarization of stars in low galactic latitude. The length of the lines indicates the relative amounts of polarization, and the position angle indicates the plane of vibration.

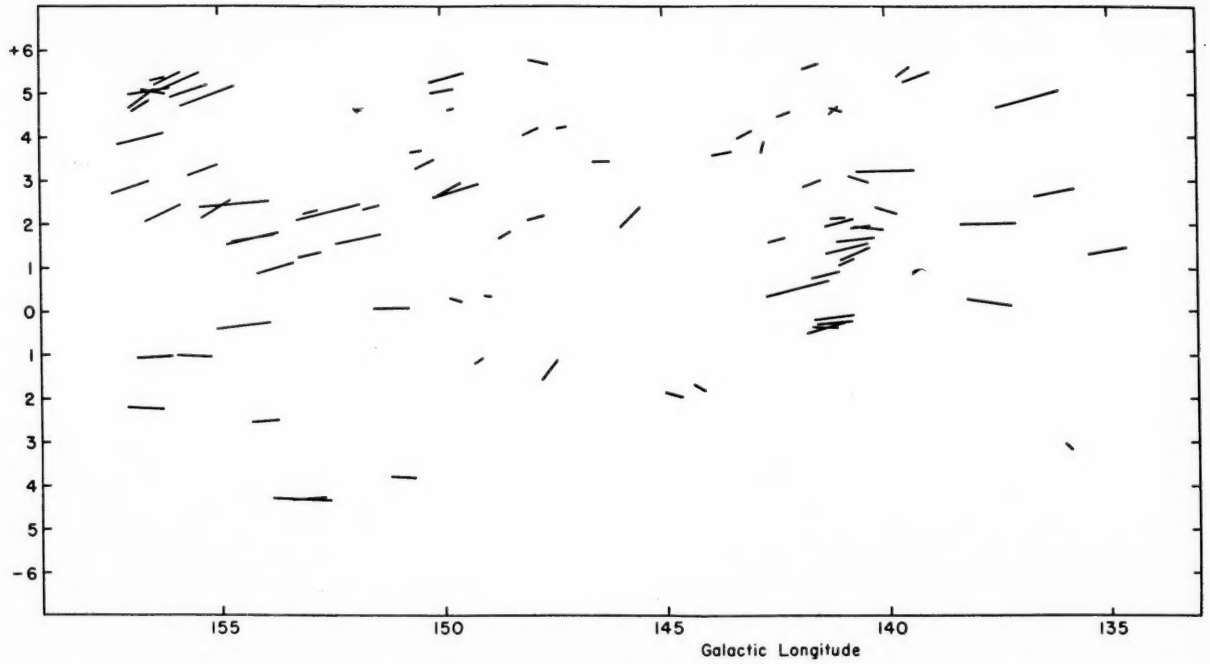

FIG. 18.—Polarization of stars in low galactic latitude. The length of the lines indicates the relative amounts of polarization, and the position angle indicates the plane of vibration.

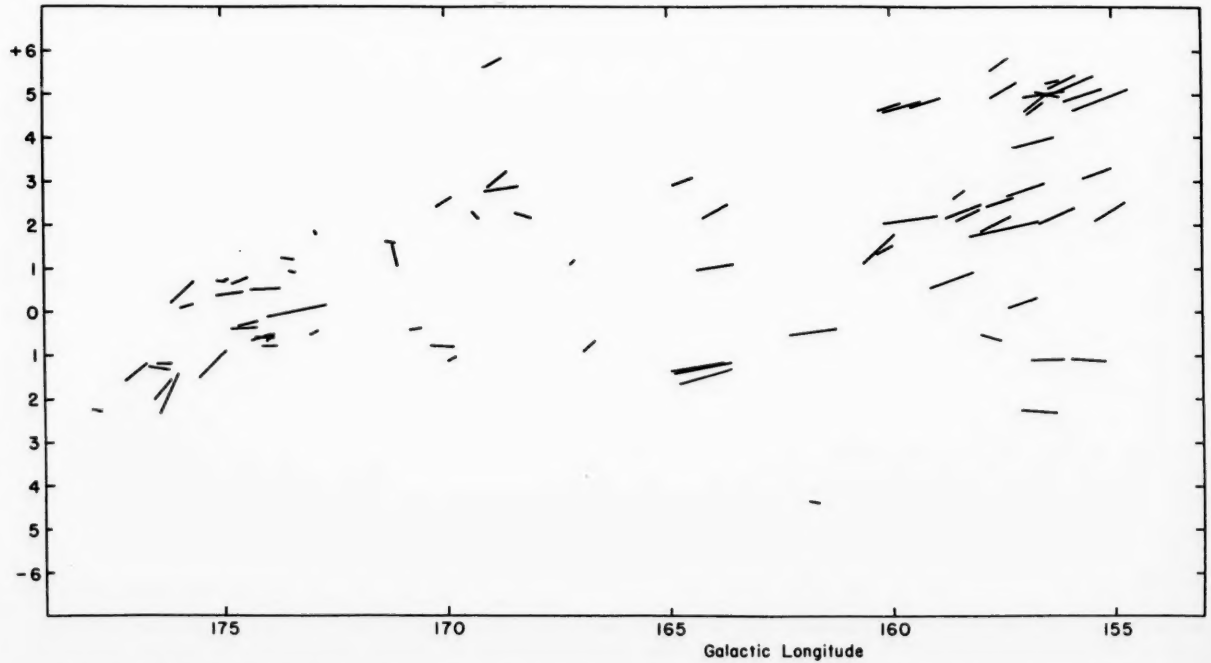

FIG. 19.—Polarization of stars in low galactic latitude. The length of the lines indicates the relative amounts of polarization, and the position angle indicates the plane of vibration.

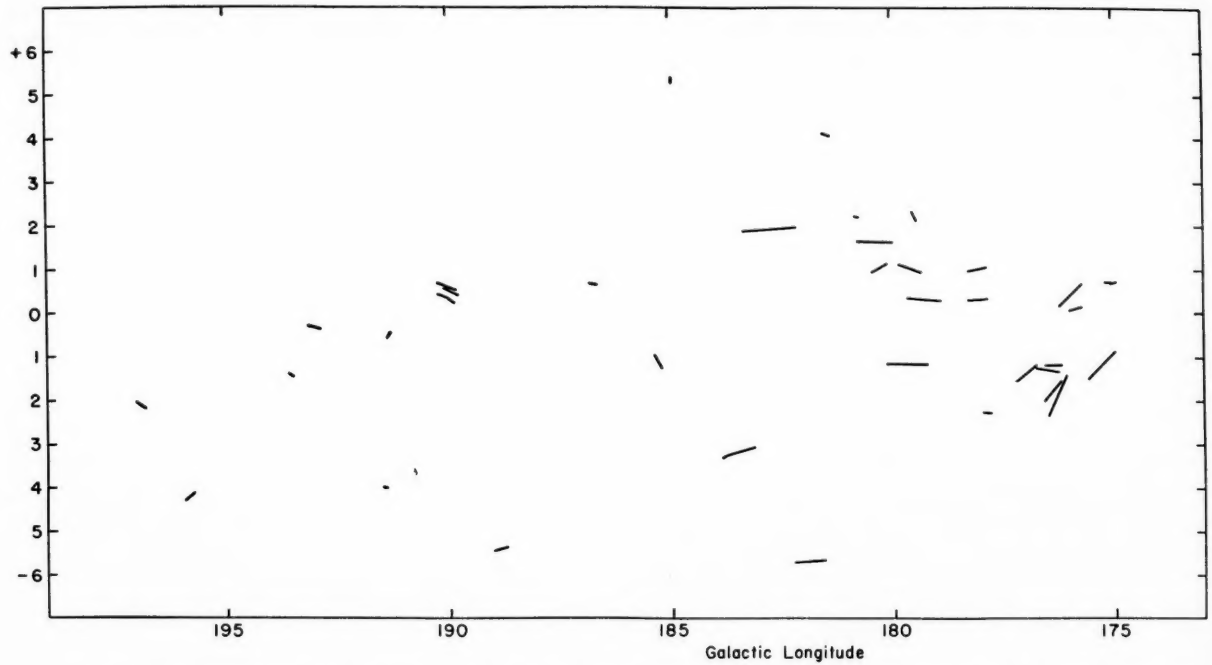

FIG. 20.—Polarization of stars in low galactic latitude. The length of the lines indicates the relative amounts of polarization, and the position angle indicates the plane of vibration.

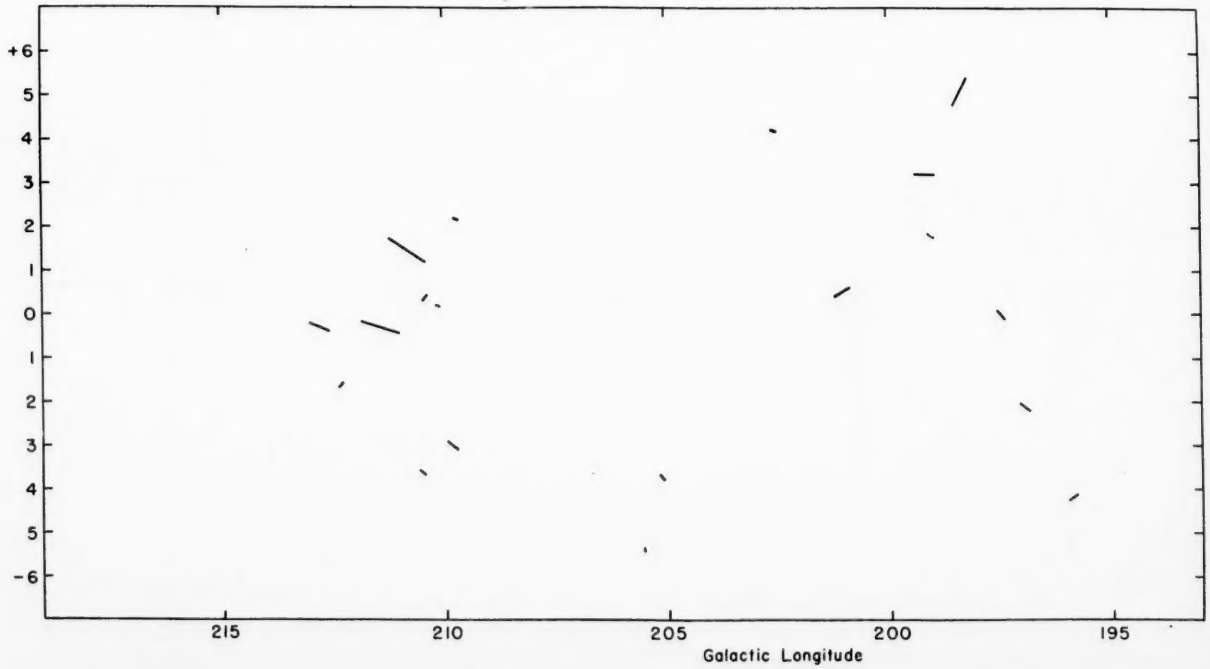

FIG. 21.—Polarization of stars in low galactic latitude. The length of the lines indicates the relative amounts of polarization, and the position angle indicates the plane of vibration.

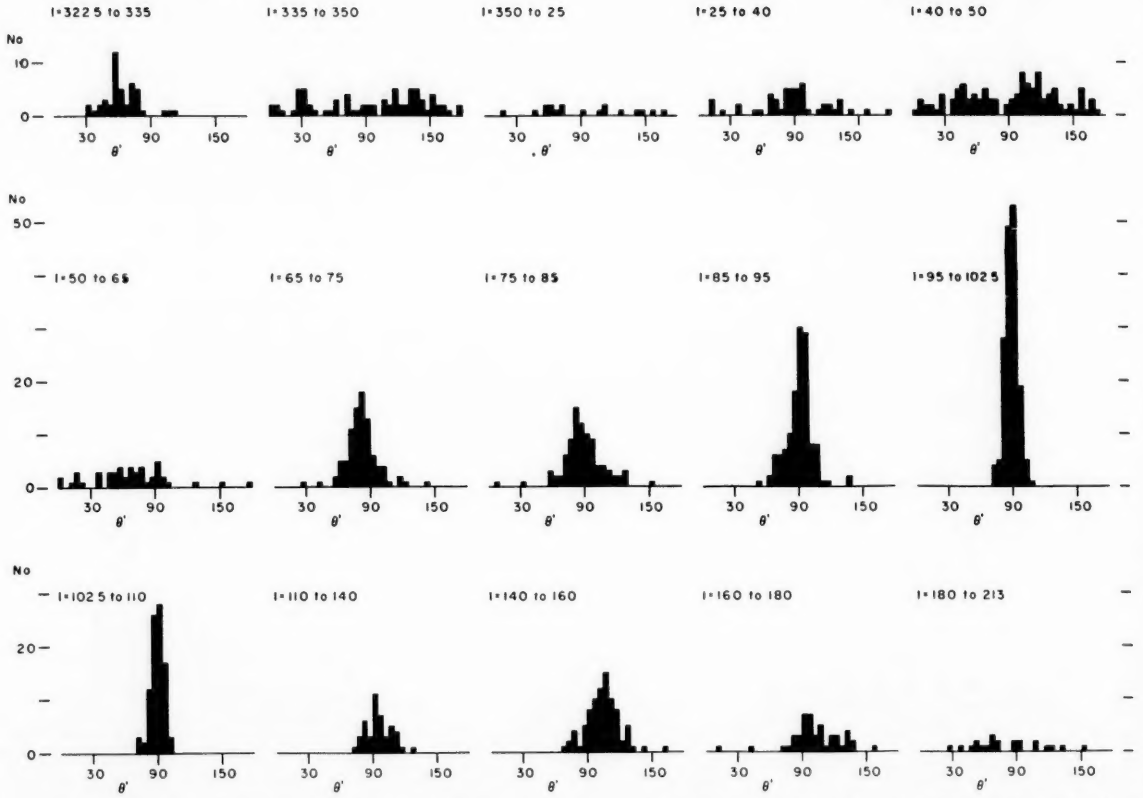

FIG. 22.—Histograms showing the distribution in the planes of vibrations for fifteen longitude groups. Compare the region from $l = 40°$–$50°$ with $l = 95°$–$102°5$.

These variations in alignment with galactic longitude can be interpreted on the assumption that, to a first approximation, the alignment force (magnetic field) is in the plane of the Galaxy more or less parallel to the spiral arms. This general picture of the alignment force has received further support from polarization measurements of the extragalactic nebula NGC 7331 by Elvius (1956). For the reddened part of this nebula the electric vector is approximately parallel to the galactic equator. In the Cassiopeia-Perseus region the line of sight is perpendicular to the axis of the spiral arm and hence perpendicular to the alignment force. Perfect alignment should be displayed. However, the dispersion in this region is about 0.1 radian. This dispersion has been interpreted by Chandrasekhar and Fermi (1953) and Davis (1951) as a "waviness" in the magnetic lines of force caused by the turbulent motions of the gas masses in the spiral arms. This same small dispersion will also introduce a random distribution in the planes of vibration for a line of sight parallel to the axis of a spiral arm, such as we observe in Cygnus; for then a small random waviness will present an apparent magnetic field of random direction. All the evidence thus far accumulated supports the conclusion that the alignment

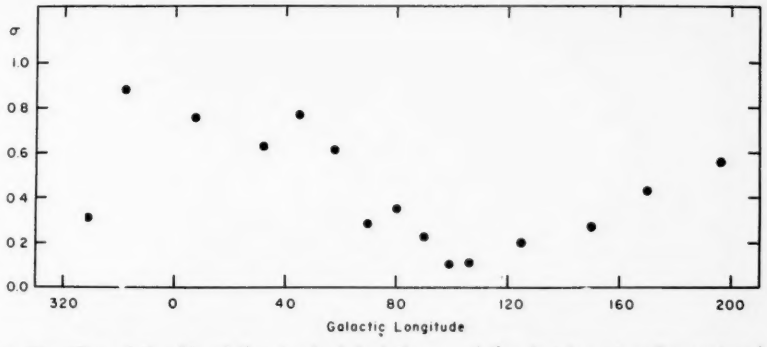

FIG. 23.—The relationship of the standard deviation, σ, of the electric-vector alignment and the galactic longitude. Note the minimum at $l = 102°$, which probably represents the longitude at which the spiral arm is observed normal to the axis of the arm.

force is associated with the Galaxy and that this alignment force is in all cases parallel to the galactic plane except for small local dispersions.

If the conclusion that the alignment force is parallel to the spiral arms is correct, it follows that the minimum in Figure 23 should represent that line of sight which is perpendicular to the spiral arms. This minimum at 102° can be compared directly with other data. Morgan, Whitford, and Code (1953) have published a model of the Galaxy based on their observations of early-type associations. From their Figure 1 the line of sight, which is perpendicular to the spiral arm, is estimated to be near 110°. A model of the Galaxy derived from 21-cm observations, published by van de Hulst, Muller, and Oort (1954), also gives us a value for the quantity in question. From their Figure 11 a value near 135° is estimated. The value $l = 102°$ is in fair agreement with that determined from the O-type associations but appears incompatible with the 21-cm observations.

One further step could be taken in the interpretation of Figure 23. If the spiral arms were linear over the distances considered here, the curve in Figure 23 should be symmetrical about the minimum. The curve is not symmetrical, for it has a smaller slope at greater longitudes. This can be interpreted as a curvature in the spiral arm. However, this point should not be belabored at this time, since the data at greater longitudes are limited and also the assumption is made in this interpretation that the turbulent velocities, the strength of the general magnetic field, and the density of the gas and dust are uniform.

Ratio of Polarization to Absorption

In the theoretical interpretation of interstellar polarization it is of great importance to have a reliable upper limit for the ratio of interstellar polarization to interstellar absorption. This observed value must then be attained by theory as a minimum condition. Up to now, several values have been used in the literature. For example, Greenstein (1951) suggested 0.04 for the ratio of polarization to photographic absorption, while van de Hulst (1950) used the value 0.055. The latter concluded from preliminary calculations that the computed amount of polarization for very long, perfectly aligned ice needles with an index of 1.25 is barely sufficient to explain this ratio.

The large quantity of data in Table 5 should permit an accurate evaluation of this ratio. Because of the danger of depolarization when large absorptions are employed and because of a possible systematic error in the ratio when small absorptions are used, a value based on the data in Table 5 will be derived in a somewhat arbitrary fashion. This ratio will then be examined in detail as to whether or not the value is a reasonable one.

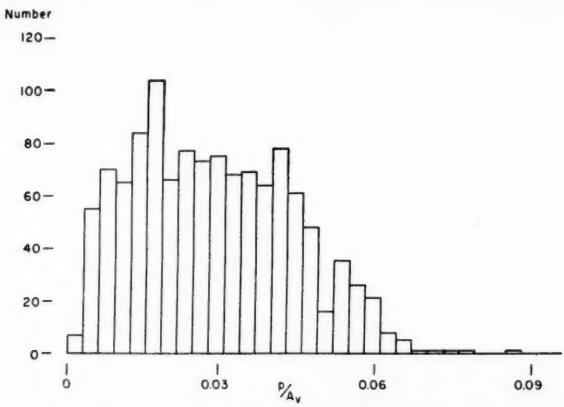

FIG. 24.—Histogram of the ratio of the interstellar polarization to interstellar absorption versus the number of stars. A value of $p/A_v = 0.06$ is estimated to be the minimum upper value for this ratio.

The ratio of polarization to absorption was computed for each star. A histogram was then constructed in which the number of stars was plotted against the ratio p/A_v. The mean value for all stars in this catalogue is 0.028. Note that the ratios given in the histogram refer to the polarization with respect to visual absorption at an effective wave length near 5400 A. Hence the two values given at the beginning of this section must be multiplied by 0.77 when compared with the values given in Table 5 and in the histogram. In setting a maximum value, four sources of error should be considered: (1) errors in the measured polarization; this should be negligible, since the polarization measurements have a probable error of 0.002 mag.; (2) errors in the measured color; here also the observational errors should be negligible, for the color observations have an accuracy of 0.01 mag.; (3) errors in the assumed intrinsic colors either because of errors in Table 6 or because of the presence of stars with a more blue intrinsic color; (4) error in the ratio of total to selective absorption. The more reliable data all support the conclusion that the value $A_v/E_{(B-V)} = 3$ is the best that can now be determined and that the error is not in excess of 10 per cent. The last two are the greater sources of error and, of course, the most difficult to evaluate. With these precautions in mind, the value 0.06 was selected with the aid of Figure 24. Twenty-five stars have a ratio equal to, or in excess of, this adopted value.

The reasonableness of 0.06, which is 40 per cent larger than the value considered by van de Hulst, can be checked by further consideration of the data in Table 5. First, the polarization was plotted against the absorption for the fifteen longitude intervals (Figs. 25 and 26). Note that, for the regions where the electric vector is well aligned, the value 0.06 for p/A_v forms an excellent upper envelope.

Figure 27 is a diagram in which the standard deviation is plotted as abscissa and the

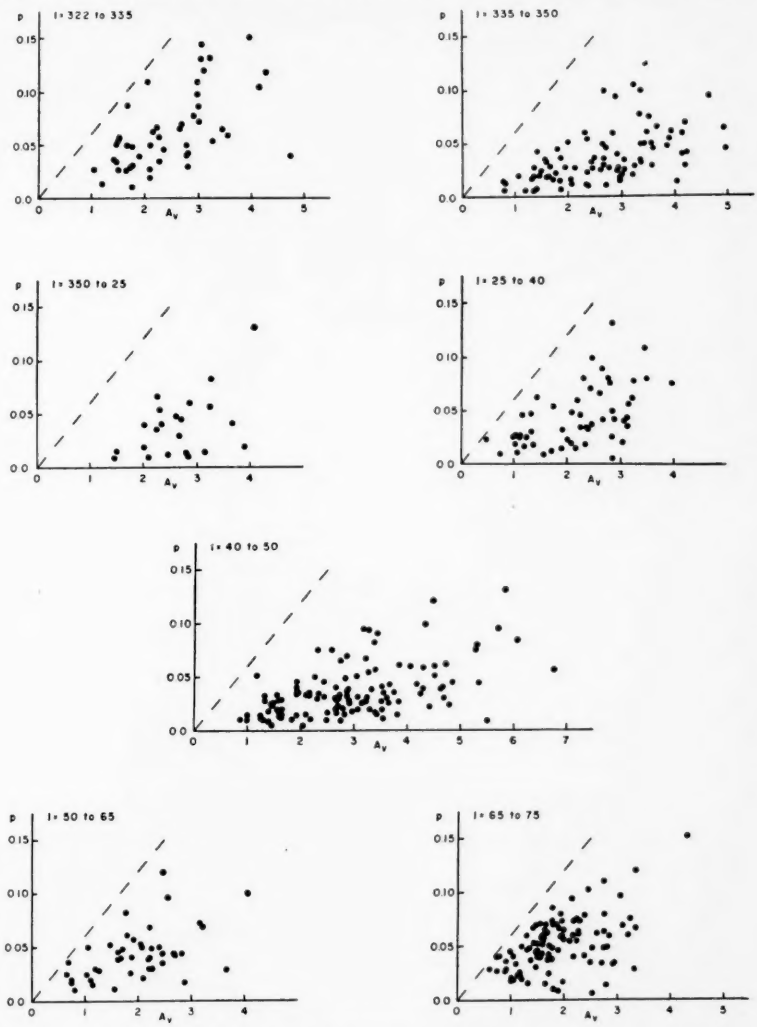

FIG. 25.—Relationship of polarization and absorption for seven galactic-longitude intervals. The absence of a one-to-one correspondence emphasizes that absorption is a necessary, but insufficient, condition for interstellar polarization. The dashed line represents a slope $p/A_v = 0.06$.

ratio p/A_v as ordinate. The general interpretation of this diagram is not immediately apparent, for the relationship of p/A_v and σ must contain many parameters, such as field strength, galactic longitude, turbulent gas velocities, and density. But an excellent correlation is present in which the ratio p/A_v increases as the standard deviation decreases. When this curve is extrapolated out to $\sigma = 0$ (perfect alignment), a value for p/A_v near 0.06 is indicated. It is to be noted that the average value of p/A_v is plotted

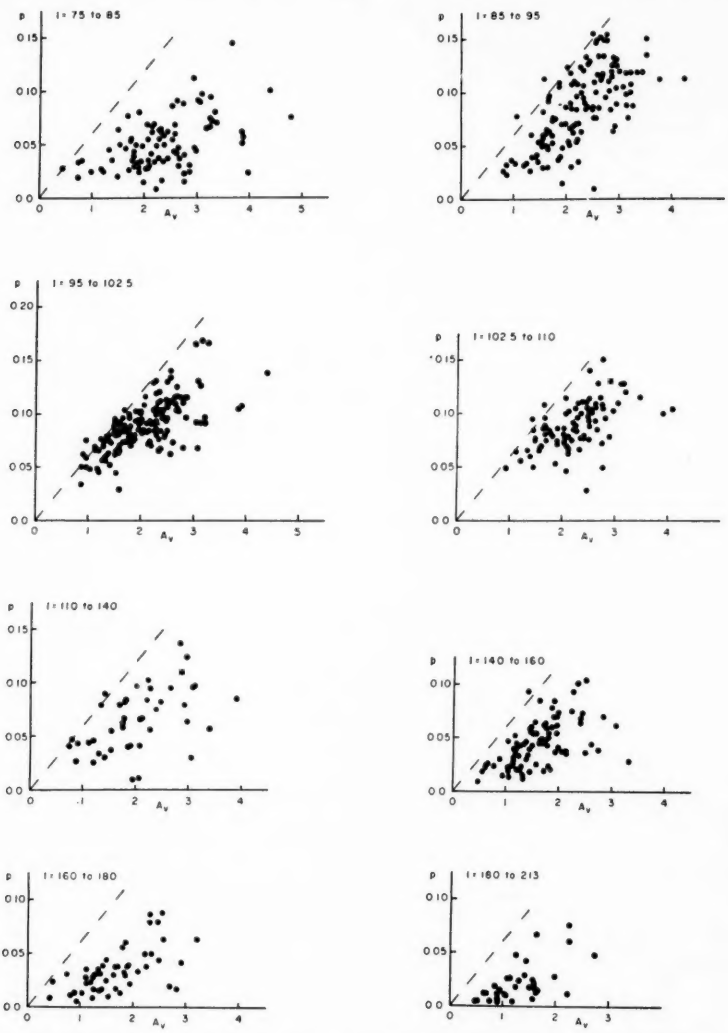

FIG. 26.—Relationship of polarization and absorption for eight galactic-longitude intervals. Note that the dashed line $p/A_v = 0.06$ represents an upper envelope.

in this curve. Hence there is no selection effect present where the larger values of p/A_v are given greater weight.

On the assumption that depolarization is always present because of the absence of perfect alignment even under the most favorable conditions, a correlation should exist between the ratio p/A_v and the amount of interstellar absorption. If this were so, then an upper limit for p/A_v could be obtained by extrapolating such a curve to $A_v = 0$. Such diagrams for the fifteen longitude intervals are shown in Figures 28 and 29. The diagrams do not show anything especially significant except for the Cassiopeia-Perseus

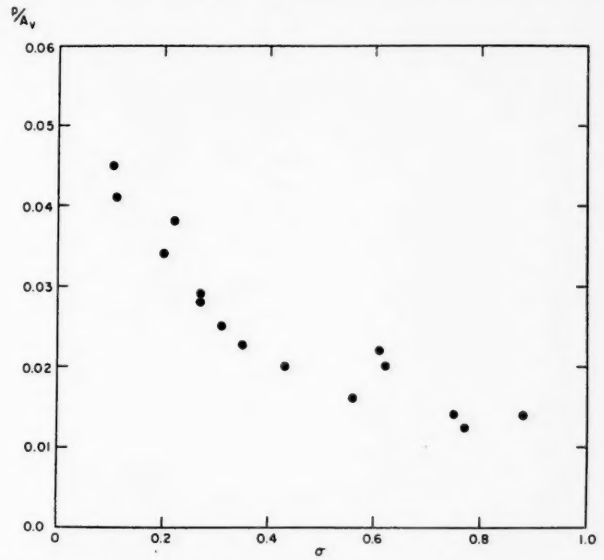

FIG. 27.—Relationship of the ratio of polarization to absorption and the standard deviation

region. Here a correlation is found with the anticipated sign. If the curves for $l = 95°$–$102°.5$ and $l = 102°.5$–$110°$ are extrapolated out to $A_v = 0$, the intersection will be near $p/A_v = 0.06$ or higher.

Variation of Polarization with Distance

In Figure 30 are four diagrams for two longitude intervals. The absorption is plotted against the distance in two of the four diagrams, and the polarization is plotted also against the distance in the other two. In all four cases little more than a scatter diagram is obtained. In the two diagrams of A_v versus distance, the upper right sections are devoid of stars because of selection. These diagrams emphasize the weak correlation of absorption with distance and the absence of any significant correlation of interstellar polarization with distance.

It is a pleasure to express my appreciation to those who assisted in the preparation of the O and B star catalogue. I wish especially to thank Misses Barbara Perkins and Gail Moeller, the former for contributing immeasurably in the photometric reductions and

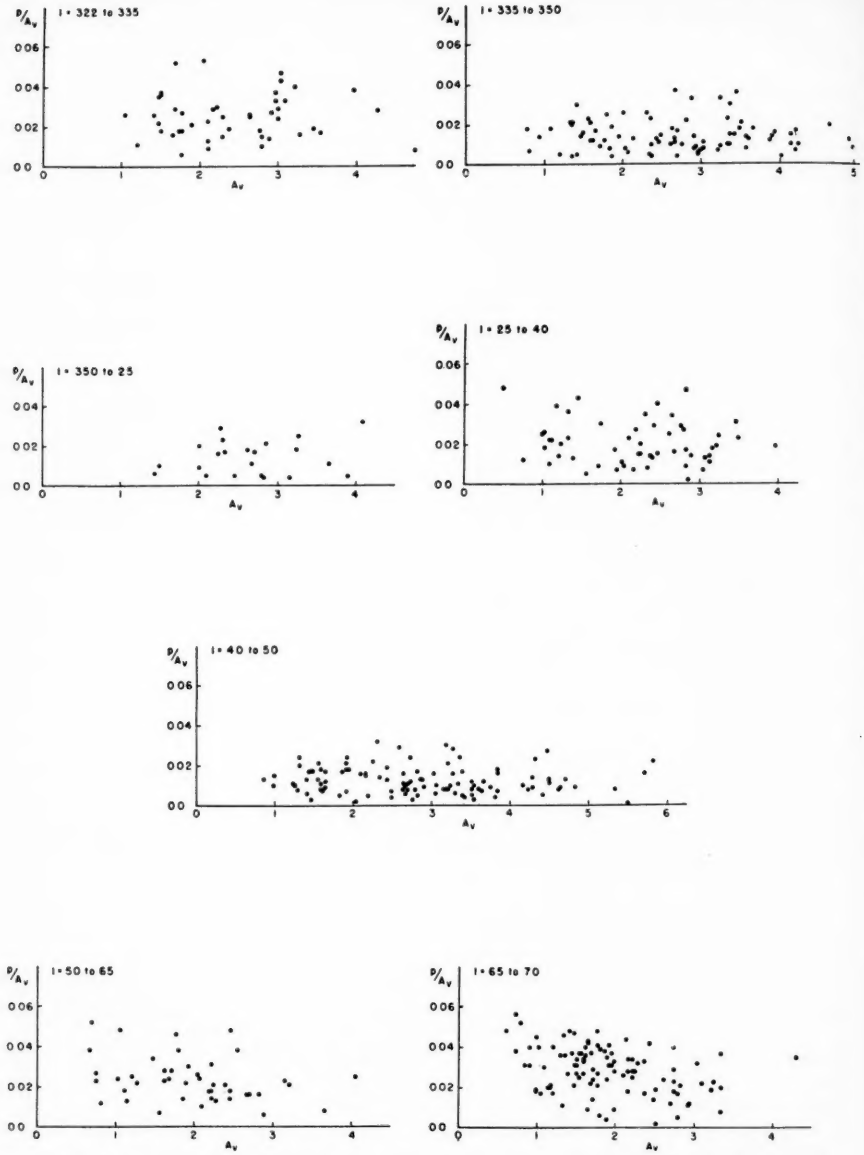

FIG. 28.—Relationship of the ratio of polarization to absorption and interstellar absorption for seven galactic-longitude intervals.

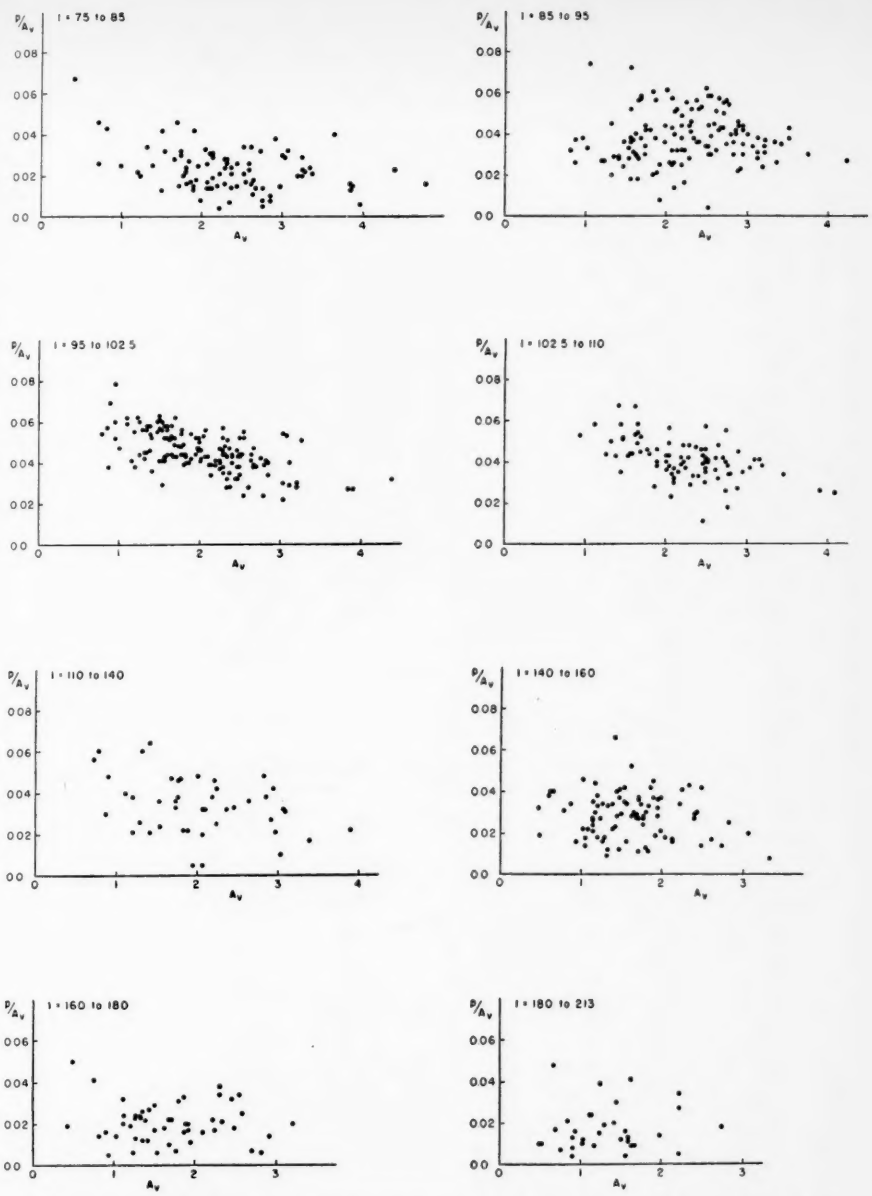

FIG. 29.—Relationship of the ratio of polarization to absorption and interstellar absorption for seven galactic-longitude intervals. Note that from $l = 95°$ to $l = 110°$ the ratio p/A_v increases with decreasing absorption, suggesting the presence of depolarization.

the latter for computational assistance and for preparing the catalogue for publication. My particular thanks are due Dr. W. W. Morgan for the classification of many spectrograms. The National Science Foundation gave financial assistance, for which appreciation is gratefully recorded.

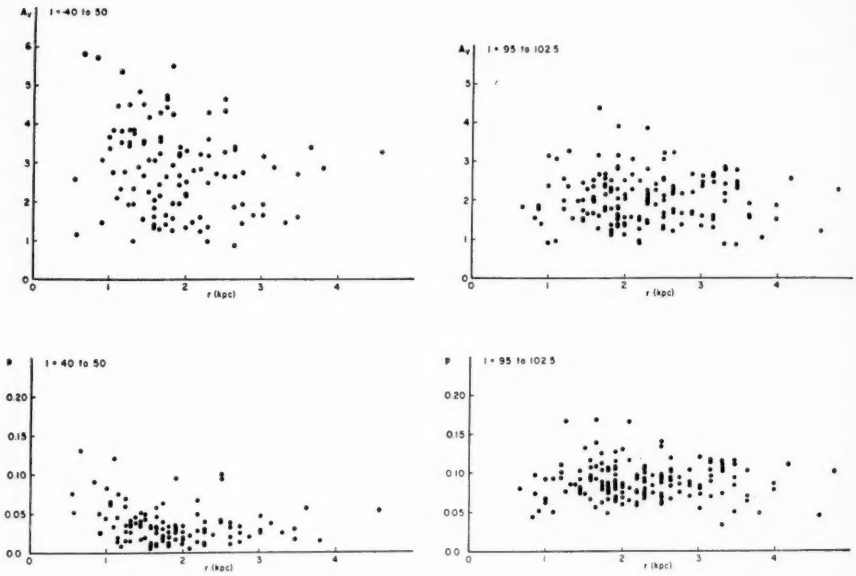

FIG. 30.—Correlation of interstellar absorption with distance and the interstellar polarization with distance. The upper right sections of the A_v versus r (kpc) plots are devoid of stars because of observational selection.

REFERENCES

Blaauw, A. 1956, private communication.
Chandrasekhar, S., and Fermi, E. 1953, *Ap. J.*, **118**, 113.
Davis, Leverett. 1951, *Phys. Rev.*, **81**, 890.
Elvius, Aina. 1956, *Stockholm Ann.*, **19**, 1.
González, G., and González, G. 1953, *Bol. Obs. Ton. y Tac.*, No. 7, p. 8.
Greenstein, J. L. 1951, *Astrophysics*, ed. J. A. Hynek (New York: McGraw-Hill Book Co.), chap. xiii.
Hall, J. S., and Mikesell, A. H. 1950, *Pub. U.S. Naval Obs.*, **17**, 1.
Hiltner, W. A. 1951, *Ap. J.*, **114**, 241.
———. 1954, *ibid.*, **120**, 454.
Hiltner, W. A., and Johnson, H. L. 1956, *Ap. J.*, **124**, 367.
Hulst, H. C. van de. 1950, *Ap. J.*, **112**, 1.
Hulst, H. C. van de, Muller, C. A., and Oort, J. H. 1954, *B.A.N.*, **12**, 117.
Johnson, H. L. 1956, *Ann. d'ap.*, **18**, 292.
Johnson, H. L., and Hiltner, W. A. 1956, *Ap. J.*, **123**, 267.
Johnson, H. L., and Morgan, W. W. 1953, *Ap. J.*, **117**, 313.
Morgan, W. W., Code, A. D., and Whitford, A. E. 1955, *Ap. J., Suppl.*, **2**, 41.
Morgan, W. W., Whitford, A. E., and Coce, A. D. 1953, *Ap. J.*, **118**, 318.
Nassau, J. J., and Morgan, W. W. 1951, *Ap. J.*, **113**, 141.
Ohlsson, John. 1952, *Ann. Obs. Lund*, No. 3, pp. 1–147.
Sommer, A., and Turk, W. 1950, *J. Scient. Instr.*, **27**, 113.